

Aage Niels Bohr | Abner Shimony | Adi Shamir | Akira Furusawa | Alain Aspect | Alain Ravex | Alain Sarlette | Alan Aspuru-Guzik | Alastair Abbott | Albert Einstein | Alberto Bramati | Alexander Andreev | Alexander Holevo | Alexander Prokhorov | Alexandre Blais | Alexandre Zagoskin | Alexei Bylinskii | Alexei Grinbaum | Alexei Kitaev | Alexia Auffèves | Alfred Kastler | Alfred Pérot | Alonzo Church | Amir Naveh | André Luiz Barbosa | Andrea Morello | Andrea Rodriguez Blanco | Andreas Wallraff | Andrew Childs | Andrew Cross | Andrew Gleason | Andrew Horsley | Andrew S. Dzurak | Andrew Steane | Andrew G. White | Andy Matuschak | Anne Broadbent | Anne Canteaut | Anne Matsuura | Anthony Leverrier | Antoine Browaeys | Anton Zeilinger | Aram Harrow | Arieh Warshel | Arthur Holly Compton | Arthur Leonard Schawlow | Artur Ekert | Astrid Lambrecht | Audrey Bienfait | Axel Becke | Benjamin Huard | Benoît Valiron | Bettina Heim | Bob Wiens | Boris Podolsky | Brian Josephson | Bruce Kane | Bruno Desruelle | Brydie D. Witt | Carl C. Pironi | Carlo Rovelli | Chad Rigetti | Charles Bennett | Charles Fabry | Charles Hard Townes | Charles Hermitage | Chien-Shiung Wu | Christa F. Hoffmann-Spörl | Christopher Monroe | Christine Silberhorn | Christophe Jurczak | Christophe Solomon | Christophe Valtot | Christopher Monroe | Christopher Papell | Claude Cohen Tannoudji | Claude Weisbuch | Clauss Jönsson | Clinton Davisson | Cornelis Dorsman | Craig Gidney | Cristian Calude | Cristina Escoda | Cyril Al-louche | Damien Stehlé | Daniel Esteve | Daniel Gottesman | Dave Wecker | David Bohm | David Deutsch | David DiVincenzo | David Gosset | David Hilbert | David J. Thouless | David Loss | David P. DiVincenzo | Derikis Dieks | Dieter Lehner | Dirk Bouwmeester | Don Coppersmith | Doron Meyer | Donald Stuckey | Doug Harlow | Douglas Leung | Douglas Stone | Edoardo M. Kessler | Edoardo S. Kessler | Edward Farrel | Edward Frenkel | Edward Teller | Eliahu G. Kalchauer | Eliahu G. Kalchauer | Eleni Diamantopoulou | Elliott H. Lieb | Eyal Shalev | Elvira Shishenina | Emanuel Knill | Emmy Noether | Enrico Fermi | Eric Cornell | Ernest Rutherford | Ernst Ising | Erwin Schrödinger | Etienne Klein | Ettore Majorana | Ewin Tang | Fabio Sciarrino | Faye Wattleton | Felix Bloch | Francesca Ferlino | Franck Balestro | Frank Wilczek | François Le Gall | Frédéric Grosshans | Frédéric Magniez | Freeman John Dyson | Friedrich Hund | Friedrich Paschen | Geordie Rose | George Uhlenbeck | Georges Paget Thomson | Georges Zweig | Georges-Olivier Reymond | Gerard Milburn | Gerrit Jan Flim | Gil Kalai | Gilles Goulet | Gilles Goulet | Gordon Baym | Gordon Gould | Guang-Can Guo | Haig Farris | Hans Albrecht Bethe | Hans Jürgen Briegel | Hantaro Nagaoka | Harald Fritzsche | Hartmut Neven | Heike Kamerlingh Onnes | Heinrich Hertz | Hélène Bouchiat | Hélène Perrin | Hendrik Anthony Kramers | Hendrik Casimir | Hendrik Lorentz | Hendrik van Loon | Immanuel Bloch | Iñigo Artundo | Iordanis Kerenidis | Irfan Siddiqi | Isaac Chuang | Isaac Newton | Itamar Sivan | Jacqueline Bloch | Jacques Salomon | James Clerk Maxwell | James Clarke | James Clerk Maxwell | James Park | Jared Cole | Jason Alicea | Jay Gambetta | Jean Dalibard | Jean Michel Raimond | Jean-François Roch | Jean-Michel Gérard | Jean-Philip Piquemal | Jian-Wei Pan | Jelena Krivošević | Jelena Krivošević | Jeremy O'Brien | Joannes van der Waals | Joe O'Gorman | Johann Balmer | Johannes Pollanen | Johannes Rydberg | John Bardeen | John Clauser | John Frank Allen | John Hall | John Levy | John Martinis | John Morton | John Preskill | John Robert Schrieffer | John Rowell | John Smolin | John Stewart Bell | John Von Neumann | John Watrous | John Wheeler | Jonathan Dowling | Jonathan Koomey | Jonathan P. Home | José Capmany | José David Domenech | Jose Ignacio Latorre | Joseph John Hopfield | Joseph John Thomson | Josh Nunn | Juan Ignacio Cirac | Julia Kempe | Julian Schwinger | Julien Bobroff | Jürgen Mlynek | Kenneth Appel | Kenneth Regan | Kevin Young | Kirill Tolpygo | Kohei Itoh | Kristel Michielsen | Krysta Svore | Lin Huang | Kurt Gödel | Le Si Dang | Lee Smolin | Léon Brillouin | Leon Neil Cooper | Leonard Adleman | Lester Germer | Lev Bishop | Lev Landau | Lieven Vandersypen | Linus Pauling | Llewellyn Thomas | Loïc Henriët | Louis Cauchy | Louis de Broglie | Lu Jeu Sham | Lucien Hardy | Ludwig Boltzmann | Luigi Frunzio | Magdalena Hauser | Marcus Doherty | Marcus Doherty | Marcus J. Heule | Markus Schuld | Marie-Anne Bouchiat | Marina Huerta | Martin Karplus | Masahide Sasaki | Masahiro Kimura | Masahito Hayashi | Mathieu Munsch | Matthew Hutchings | Matthias Troyer | Matthieu Desjardins | Maud Vinet | Max Born | Maximilian Schlosser | Mazyar Mirrahimi | Menno Verdhorst | Michael Ben-Or | Michael Frank | Michael Freedman | Michael Horne | Michael Levitt | Michael Nielsen | Michel Brune | Michel Devoret | Michelle Simmons | Mikhail G. Aleshin | Mikhail Lukin | Mio Murao | Murray Gell-Mann | Nathan Gemelke | Nathan Rosen | Nathanaël Cottet | Niccolò Pavesi | Nick P. Parker | Nicolas Gisin | Nicolas Roch | Niels Henrik Abel | Nikolay Basov | Nir Minerbi | Nobuyuki Imoto | Oleg Lobachev | Oliver G. Schmidt | Oskar Painter | Pascale Senellart | Pascual Jordan | Pascual Muñoz | Patrice Bertet | Patrice Bertet | Patrice Bertet | Paul Dirac | Paul Hiriart | Perola Milman | Pete Shadbolt | Peter Higgs | Peter Knight | Peter Knight | Peter Knight | Peter Knight | Peter Knight | Philip W. Anderson | Philipp Lenard | Philippe Duluc | Philippe Grangier | Pierre Hohenberg | Pierre Hohenberg | Pierre Hohenberg | Pranav Gokhale | Pyotr Kapitsa | Qingfeng Wang | Rainer Blatt | Raphaël Lescanne | Raymond Laflamme | Rebecca J. N. Young | Renée J. Outhamer | René Descartes | Richard Feynman | Richard Holt | Richard Karp | Richard Murray | Robert J. Simon | Robert J. Simon | Robert J. Simon | Robert Andrews Millikan | Robert Dennard | Robert König | Robert McDermott | Roy J. Glauber | Robert Raussendorf | Robert William Boyd | Robin Blume-Kohout | Roger Penrose | Roland Gähler | Roman Lutsiv | Ron Rivest | Roy G. Kleber | Ronald Walsworth | Rudolf Grimm | Ryan Babbush | Samuel Goudsmit | Sandu Popescu | Sara Ducci | Sarah Sheldon | Satyendranath Bose | Scott Aaronson | Sébastien Balibar | Serge Haroche | Sergey Bravyi | Seth Lloyd | Shengtao Wang | Shi Yaoyun | Shin'ichirō Tomonaga | Silvano de Franceschi | Simon Benjamin | Simon Perdris | Simone Severini | Sophia Economou | Stefanie Barz | Stephanie Wehner | Steve Girvin | Steve Lamoreaux | Taki Kontos | Théau Peronin | Theodor Hänsch | Theodore Lyman | Theodore Maiman | Thibault Jacqmir | Tommaso Offenberg | Tommaso Offenberg | Tommaso Offenberg | Tommaso Toffoli | Tracy Northup | Travis Humble | Urmila Mahadev | Urmila Mahadev | Urmila Mahadev | Valerian Giesz | Vasilis Armaos | Vincent Bouchiat | Virginia D'Auria | Vlad Anisimov | Vladan Vuletic | Vladimir Fock | Walter Brattain | Walter Kohn | Walter Houser Brattain | Walther Meissner | Walther Nernst | Wassim Estephan | Werner Heisenberg | Wilhelm Wien | William Rowan Hamilton | William Shockley | William Wootters | Willis Eugene Lamb | Winfried Hensinger | Wojciech Zurek | Wolfgang Haken | Wolfgang Lechner | Wolfgang Pauli | Wolfgang Pauli | Wolfgang Ketterle | Xavier Waintal | Yakov Frenkel | Yasuhiko Arakawa | Yasunobu Nakamura | Yehuda Naveh | Yoshihisa Yamamoto | Yuichiro Minato | Yuri Alexeev | Yuri Manin | Zaki Leghtas

Understanding

Quantum Technologies

Sixth edition - 2023

Volume 2/3: computing hardware, communication and cryptography, sensing

Olivier Ezratty



le lab quantique

le lab quantique

Le Lab Quantique is a supporter and promoter of this book, but not its publisher or editor.



Understanding Quantum Technologies

Sixth edition – Version 6.8

Volume 2/3

2023

Olivier Ezratty

About the author

Olivier Ezratty
consultant and author



[0000-0003-3944-2896](https://orcid.org/0000-0003-3944-2896)

[olivier \(at\) oezratty.net](mailto:olivier(at)oezratty.net), www.oezratty.net, [@olivez](https://twitter.com/olivez)
+33 6 67 37 92 41

Olivier Ezratty advises and trains various public and industry organizations in the development of their innovation strategies in the quantum technologies realm. He brings them a rare 360° understanding of the scientific, technology, market and ecosystems dimensions of this burgeoning and complex domain.

He covered many other topics since 2005, like digital television, Internet of things and artificial intelligence. As such, he carried out various strategic advisory missions of conferences or training in different verticals and domains such as **media and telecoms** (Orange, Bouygues Telecom, TDF, Astra), **finance and insurance** (BPCE, Société Générale, Swiss Life, Crédit Agricole, Crédit Mutuel-CIC, Generali), **industry and services** (Schneider, Camfil, Vinci, NTN-STR, Econocom, ADP, Air France, Airbus) and the **public sector** (CEA, Météo France, Bpifrance, Business France).

He became a quantum technologies specialist in 2018 with many complementary activities:

- **Author** of the reference book **Understanding Quantum Technologies** (September 2021, 2022 and 2023) following three previous editions in French in 2018, 2019 and 2020. The 2021, 2022 and 2023 editions are also available in paperback version on Amazon.
- **Trainer and teacher** on quantum technologies for **Cappgemini Institut** and for **CEA INSTN**. In September 2021, he took in charge an elective curriculum on quantum technologies for **EPITA**, an IT engineering school in France.
- **Speaker** in a large number of quantum technology events since 2018 such as the Q2B Paris organized by QC Ware, France Quantum and other events, on top of presentations at Société Générale, BNP, Crédit Agricole, Michelin, Adéo, L'Oréal, FIECC, IHEDN, Business France, CentraleSupélec, Avolta Partners, IHEDN, etc.
- **Producer** of two series of podcasts on quantum technologies along with Fanny Bouton (in French): a monthly « Quantum » on tech news (since September 2019) and Decode Quantum, with entrepreneurs and researchers since March 2020, with a total of over 100 episodes as of July 2023.
- **Cofounder** of the **Quantum Energy Initiative** with Alexia Auffèves (CNRS MajuLab Singapore), Robert Whitney (CNRS LPMCM) and Janine Splettstoesser (Chalmers University, Sweden).
- **Expert** for **Bpifrance** to evaluate quantum collaborative projects and startups.
- **Ambassador** for France 2030 since February 2022, the French government innovation strategy plan.

He also lectures in various universities such as CentraleSupélec, Ecole des Mines de Paris, Telecom Paristech, Les Gobelins, HEC, Neoma Rouen and SciencePo, on artificial intelligence, entrepreneurship and product management (until 2020) and on quantum technologies (since 2018), in French and English as needed. He is also the author of many open source ebooks in French on entrepreneurship (2006-2019), the CES of Las Vegas yearly report (2006-2020) and on artificial intelligence (2016-2021).

Olivier Ezratty started in 1985 at **Sogitec**, a subsidiary of the Dassault group, where he was successively Software Engineer, then Head of the Research Department in the Communication Division. He initialized developments under Windows 1.0 in the field of editorial computing as well as on SGML, the ancestor of HTML and XML. Joining **Microsoft France** in 1990, he gained a strong experience in many areas of the marketing mix: products, channels, markets and communication. He launched in France the first version of Visual Basic in 1991 and Windows NT in 1993. In 1998, he became Marketing and Communication Director of Microsoft France and in 2001, of the Developer Division, which he created in France to launch the .NET platform and promote it to developers, higher education and research, as well as to startups. Olivier Ezratty is a software engineer from **Centrale Paris** (1985), which became CentraleSupélec in 2015.

This document is provided to you free of charge and is licensed under a "Creative Commons" license.
in the variant "Attribution-Noncommercial-No Derivative Works 2.0".



see <http://creativecommons.org/licenses/by-nc-nd/2.0/> - web site [ISSN 2680-0527](http://www.oezratty.net)

Credits

Cover illustration: personal creation associating a Bloch sphere describing a qubit and the symbol of peace (my creation, first published in 2018) above a long list of over 400 scientists and entrepreneurs who are mentioned in the ebook.

This document contains nearly 1,000 illustrations. I have managed to give credits to their creators as much as possible. Most sources are credited in footnotes or in the text. Only scientists' portraits are not credited since it is quite hard to track it. I have added my own credit in most of the illustrations I have created. In some cases, I have redrawn some third-party illustrations to create clean vector versions or used existing third-party illustrations and added my own text comments. The originals are still credited in that case.

Table of contents

Volume 1/3	i
Foreword	vii
Why	1
A complex domain in search of pedagogy	3
A new technology wave	5
Reading guide	5
First and second quantum revolutions applications	7
Why quantum computing?	9
History and scientists	23
Precursors	26
Founders	33
Post-war	52
Quantum technologies physicists	55
Quantum information science and algorithms creators	72
Research for dummies	80
Quantum physics 101	98
Postulates	100
Quantization	103
Wave-particle duality	110
Superposition and entanglement	117
Indetermination	121
Measurement	122
No-cloning	123
Tunnel effect	124
Quantum matter	125
Extreme quantum	153
Gate-based quantum computing	163
In a nutshell	163
Linear algebra	165
Qubits	183
Bloch sphere	186
Registers	190
Gates	194
Inputs and outputs	205
Qubit lifecycle	207
Measurement	209
Quantum computing engineering	220
Key parameters	221
Quantum computers segmentation	224
Qubit types	228
Architecture overview	236
Processor layout	238
Error correction	240
Quantum memory	278
Quantum technologies energetics	284

Economics.....	300
Quantum uncertainty.....	303
Volume 2/3.....	319
Content.....	325
Quantum computing hardware	327
Quantum annealing	331
Superconducting qubits.....	349
Quantum dots spins qubits	414
NV centers qubits.....	440
Topological qubits.....	453
Trapped ions qubits.....	464
Neutral atoms qubits	489
NMR qubits.....	512
Photon qubits	515
Quantum enabling technologies.....	562
Cryogenics	562
Qubits control electronics	584
Thermometers	624
Vacuum	625
Lasers	625
Photonics.....	631
Fabs and manufacturing tools	636
Other enabling technologies vendors	655
Raw materials.....	658
Unconventional computing.....	668
Supercomputing and HPCs	669
Digital annealing computing.....	677
Reversible and adiabatic calculation.....	682
Superconducting computing	686
Probabilistic computing	693
Optical computing.....	693
Chemical computing	700
Quantum telecommunications and cryptography	702
Public key cryptography	703
Quantum cryptanalysis threats	705
Quantum Random Numbers Generators	717
Quantum Key Distribution.....	727
Post-quantum cryptography	750
Quantum computing cryptography	761
Quantum homomorphic cryptography	761
Quantum telecommunications.....	761
Quantum Physical Unclonable Functions	775
Vendors	777
Quantum sensing.....	327
Quantum sensing use-cases and market.....	797
International System of Measurement	799
Quantum sensing taxonomy.....	800
Quantum gravimeters, gyroscopes and accelerometers	803

Quantum clocks	809
Quantum magnetometers	815
Quantum thermometers.....	820
Quantum frequencies sensing	821
Quantum imaging.....	823
Quantum pressure sensors.....	832
Quantum radars and lidars	832
Quantum chemical sensors.....	836
Quantum NEMS and MEMS	837
Volume 3/3	847
Content.....	853
Quantum algorithms.....	855
Algorithms classes	860
Basic algorithms toolbox	867
Higher level algorithms.....	882
NISQ algorithms	910
Quantum inspired algorithms.....	934
Complexity classes.....	938
Quantum speedups	949
Quantum software development tools.....	956
Development tool classes.....	957
Research-originated quantum development tools	975
Quantum vendors development tools.....	981
Cloud quantum computing.....	994
Quantum software engineering	998
Benchmarking	1005
Quantum computing applications	1025
Case studies evaluation	1025
Market forecasts	1031
Healthcare	1037
Energy and chemistry.....	1048
Transportation and logistics	1065
Retail	1071
Telecommunications	1072
Finance.....	1073
Insurance	1082
Marketing.....	1083
Content and media	1084
Defense and aerospace.....	1085
Intelligence services	1088
Industry	1088
Climate change.....	1089
Science	1092
Software and tools vendors	1094
Service vendors	1123
Quantum technologies around the world.....	1127
Quantum computing startups and SMEs.....	1128
Global investments.....	1136

Patents	1140
North America.....	1143
South America.....	1157
Europe	1158
Russia.....	1199
Africa, Near and Middle East	1201
Asia-Pacific	1205
Corporate adoption.....	1227
Understand the imperative	1227
Technology screening	1229
Needs analysis.....	1230
Training	1231
Evaluation	1231
Quantum technologies and society	1233
Human ambition.....	1233
Science fiction.....	1234
Quantum foundations.....	1238
Responsible quantum innovation.....	1247
Religions and mysticism	1253
Public education.....	1254
Professional education	1255
Jobs impact.....	1260
Gender balance.....	1260
Quantum technologies marketing	1264
Quantum fake sciences	1266
Quantum biology	1266
Quantum medicine	1276
Quantum management	1284
Other exaggerations	1287
Conclusion.....	1293
Resources	1296
Events.....	1296
Websites and content sources.....	1299
Podcasts.....	1300
Books and ebooks	1300
Comics	1305
Presentations	1305
Training	1306
Reports	1306
Miscellaneous	1306
Glossary.....	1307
Index.....	1333
Table of figures	1350
Revisions history	1377

Content

This is the **second volume** of the book “Understanding Quantum Computing”, that is also downloadable from <https://www.oezratty.net/wordpress/2023/understanding-quantum-technologies-2023/>. The downloadable PDFs are available in a single volume A4 and Letter version, containing the three volumes in sequential order. You can also download compressed PDFs for the three volumes in A4 and Letter formats. Their size fits into the constraints of ebook readers like the Kindle from Amazon.

This book printed version separates volume 1, volume 2 and volume 3.

The **first volume** contains a history of quantum physics, some quantum physics 101 and everything about quantum computing basics and engineering.

This **second volume** contains the parts dedicated to quantum computing hardware, enabling technologies, unconventional computing solutions which are potential alternate routes between classical and quantum computing, quantum telecommunications, quantum cryptography, post-quantum cryptography and quantum sensing.

The **third volume** contains the parts dedicated to algorithms, software tools, case studies, an inventory of quantum investments per country, various societal topics, corporate adoption methodologies, quantum fake sciences, glossary, an index and bibliography.

The three-volume index and glossary are consolidated at the end of the third volume.

The book is split into three volumes to make its printing easier, some online printing services including Amazon being limited to a maximum of 600 pages. Here, we have three volumes of respectively 322, 530 and 532 pages, covers included.

You can order the printed version of this book in three volumes on all **Amazon** sites with searching for the book title, edition 2023.

Page intentionally left blank

Quantum computing hardware

In a bottom-up approach, we have covered successively the basics of quantum physics, the mathematical aspects of gate-based quantum computing, then quantum computing engineering and enabling technologies. Let us now move to the last stack, quantum computers, focusing on their specifics depending on the types of physical qubits they are using. We are dealing here with all sorts of players: public research laboratories, large established companies as well as startups.

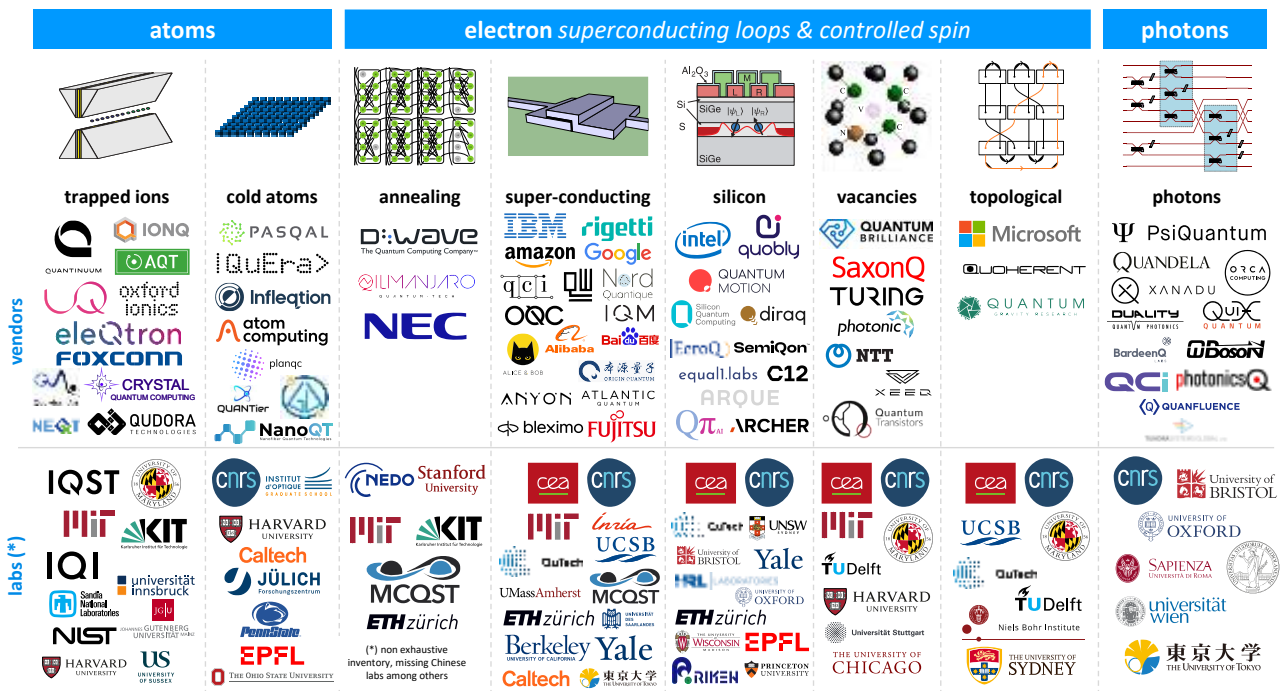


Figure 275: a map of key research lab and industry vendors in quantum computing hardware per qubit type. (cc) Olivier Ezratty, 2023. Qubits drawing source: [Scientists are close to building a quantum computer that can beat a conventional one](#) by Gabriel Popkin in Science Mag, December 2016. I consolidated the logos lists since 2018. It is incomplete for the research labs at the bottom but rather exhaustive for the vendors at the top. It doesn't list China academic labs.

The number of startups in this inventory keeps growing, in Figure 275. They do not shy away from Google and IBM. There are not many Chinese startups yet. For the moment, the country's investments in quantum computing are concentrated in well-funded public research like with Jian Wei-Pan's giant lab in Hefei and with large cloud companies like Baidu and Alibaba. Notice that Chinese labs are missing in the chart. There are eight main categories of quantum computers grouped into three categories:

Atoms:

- **Trapped ions** found in particular at IonQ, a spin-off from the University of Maryland, as well as at Quantinuum and Alpine Quantum Technologies (Austria).
- **Cold atoms** like rubidium, cesium and strontium are used by Pasqal, QuEra, ColdQuanta and Atom Computing to create both analog quantum computers and gate-based quantum computers.
- **Nuclear Magnetic Resonance**, which is nearly abandoned as a path for quantum computing, NISQ or beyond despite one China company selling a desktop version for educational use cases.

Electrons:

- **NV centers** with only a few industrial players like Quantum Brilliance, Turing and XeeQ. NV centers applications are also used in quantum sensing and quantum communications.

- **Superconducting** effect qubits are used in IBM's, Google, Rigetti, OQC and IQM quantum computers as well as in D-Wave quantum annealers. This is a broad category with Josephson qubits (transmon, fluxonium, coaxmon, unimon, ...) and photon cavities-based qubits using superconducting control qubits (cat-qubits, GKP) with Alice&Bob, Amazon, Nord Quantique and QCI.
- **Quantum dots spins qubits** pushed notably by Intel, Quantum Motion, SQC, C12, Archer and the consortium between CEA-Leti CNRS Institut Néel and CEA-IRIG in France. There are many variations there as well.
- **Topological qubits** with the hypothetical Majorana fermions from Microsoft whose existence is yet to be proven. Other topological qubits avenues are investigated in research laboratories at the fundamental research level.

Flying qubits:

- **Photon qubits**, with a lot of variations like boson sampling, coherent Ising machines and [MBQC](#) architectures to circumvents the difficulty to handle two-qubit gates and the limited computing depth of flying qubits. The current main photon qubit vendors are PsiQuantum, Xanadu, and Quandela.
- **Flying electrons**, a separate track of qubits, with no commercial vendor yet involved in it. It is a fundamental research field⁸⁶⁹.

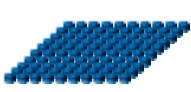
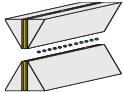
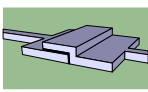
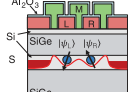
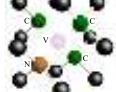
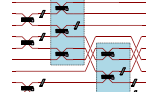
	atoms		electrons superconducting & spins			photons
						
	cold atoms	trapped ions	superconducting	silicon	NV centers	photons
qubit size	about 1 μm space between atoms	about 1 μm space between atoms	(100μ) ²	(100nm) ²	<(100nm) ²	nanophotonics waveguides lengths, MZI, PBS, etc
best two qubits gates fidelities	99.5%	99.94%	99.68% (IBM Egret 33 qubits)	>99% (SiGe)	99.2%	98%
best readout fidelity	95%	99.99%	99.4%	99% (SiGe)	98%	50%
best gate time	≈1 ns	0.1 to 4 μs	20 ns to 300 ns	≈5 μs	10-700 ns	<1 ns
best T ₁	> 1 s	0,2s-10mn	100-400μs	20-120μs	2.4 ms	∞ & time of flight
qubits temperature	< 1mK 4K for vacuum pump	<1mK 4K cryostat	15mK dilution cryostat	100mK-1K dilution cryostat	4K to RT	RT 4K-10K cryostats for photons gen. & det.
operational qubits	1,180 (Atom Computing)	32 (IonQ and Quantinuum)	433 (IBM) 176 (China)	12 (Intel) in SiGe	5 (Quantum Brilliance)-10	216 modes GBS (Xanadu)
scalability	up to 10,000	<100	1000s	millions	100s	100s-1M

Figure 276: figures of merit per qubit type. Best gate time covers only the electronics drive part but not the whole classical drive computing time. Best T₁ is the best qubit relaxation time. These are the best figures of merit, but it does not mean a single system in a column has them all! There are also some inconsistencies between the fidelities obtained in labs with a few qubits and with commercial systems with more qubits. Some of the data sources: cold atoms ([Neutral Atom Quantum Computing Hardware: Performance and End-User Perspective](#) by Karen Wintersperger et al, April-May 2023 (27 pages)), trapped ions ([Trapped Ion Quantum Computing: Progress and Challenges](#), 2019, [Materials Challenges for Trapped Ion Quantum Computers](#), 2020, [Infineon](#), IonQ and Quantinuum, [High-Fidelity Bell-State Preparation with ⁴⁰Ca+ Optical Qubits](#) by Craig R. Clark et al, PRL, September 2021 (7 pages)), silicon ([Roadmap on quantum nanotechnologies](#), 2020), superconducting (many IBM papers), NV centers ([Quantum computer based on color centers in diamond](#), 2021). I list only the most demanding two qubit gates and readouts fidelities. Cold atoms systems are usually simulators, but data pertains to gate-based implementations. (cc) Olivier Ezratty, 2020-2023.

⁸⁶⁹ See [Universal and ultrafast quantum computation based on free-electron-polariton blockade](#) by Aviv Karnieli et al, March 2023 (24 pages).

Solid-states qubits usually refer to the electron qubits category with superconducting and electron spin qubits. However, trapped ions and photon qubit also rely on semiconductor circuits for their operations. But the “ions” are flying above their control circuits and the photons are circulating in nanophotonic circuits.

Many of the commercial companies in this panorama are associated with American or European research laboratories. Google collaborates with the University of Santa Barbara in California, IBM and Microsoft with the University of Delft in the Netherlands, and IBM with the University of Zurich, among other publicly funded research organizations.

These categories of technologies have different levels of maturity. Superconducting qubits are the most proven to date. Trapped ions are best-in-class with regards to fidelity and connectivity but do not seem to scale well. Neutral atoms are starting to scale better. Linear optics and NV centers also have some difficulties to scale. Electron spin-based systems could scale but are less mature. Finally, Majorana fermions are still in limbo. But other qubit types are looming around and may become promising (other topological materials, Silicon Carbide, etc.). Creating assessment on the maturity of these technology pertains more to weather forecast than climate change predictions. Meaning, while you can forge some ideas on the relative maturity of these technologies with a short-term view, it is much harder to make sound predictions in the longer term. For example, scaling these various technologies face very different challenges. As such, the table in Figure 276 is a sketchy and probably highly questionable comparison between these different qubits, particularly with cold atoms which are so far, used in quantum simulation mode and not gate-based architectures.

Another way of comparing qubit classes is to look at where the industry bucks are going. I created the chart below in Figure 277 with doing some guesswork on how much was invested by the large IT companies (IBM, Google, Microsoft, Amazon, Intel). But again, investors are not necessary in a position to guess which technology will really scale.

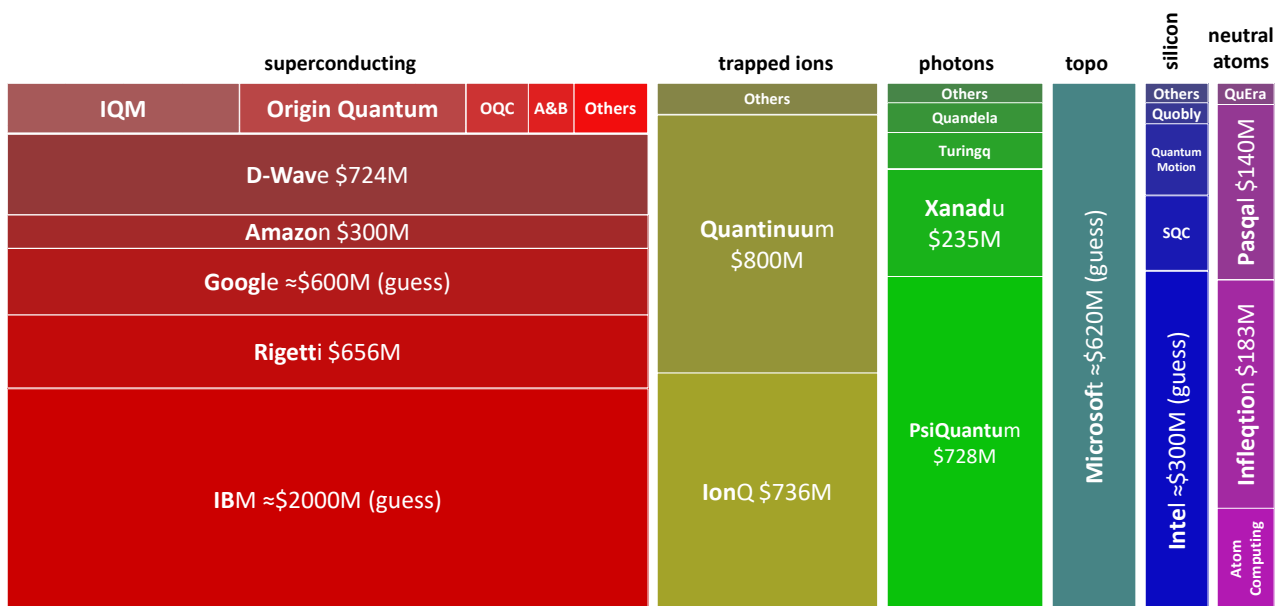


Figure 277: fuzzy logic assessment of industry investments per qubit type mixing capital investment for startups and internal investments for legacy companies is “life to date” (LTD). (cc) Olivier Ezratty, January 2024.

These numbers are approximate and if you have some information to correct or update it, I’ll take it! For startups, it is easier and consolidate the amount publicly raised either in venture capital or through a SPAC (for D-Wave, IonQ and Rigetti). What do you learn from this chart? That superconducting qubits are kings, followed by trapped ions and photon qubits. Therefore, silicon and cold atoms qubits seem under invested.

Both because it seems Intel has not yet invested much in silicon qubits that have a rather low TRL and since no large company invested in cold atoms. I would seriously advise not to determine future winners based on these amounts.

There is so much scientific and technological uncertainty! Some solutions even not in this chart could show up in the future, either in the topological qubits space, beyond Microsoft’s sole endeavor, or with SiC and other variations of spin cavities (beyond NV centers which don’t show up in the chart due to the very small amount raised by the couple startups from this field).

Another summary view, in Figure 278, shows how various qubit types have use cases beyond quantum computing and even, within the three paradigm of quantum computing with all qubit types being usable for quantum simulations although it seems it is only available with neutral atom qubits with commercial vendors⁸⁷⁰. Photons, cavity spins and cold atoms have the broadest use cases given they have many applications in quantum sensing. Silicon qubits seem to have a narrower usage scope but don’t discount them too soon. They may showcase one of the best scalability potential for quantum computing.

quantum objects	atoms		superconducting & controlled spin			photons
	trapped ions	cold atoms	super-conducting	quantum dots spins	cavity spins (NV, SiC)	photons
gate-based computing		possible			possible	
analog quantum simulation	tested		tested	tested		tested in CV mode
quantum annealing						
quantum memory	in repeaters	in repeaters			in repeaters	with cold atoms or delay lines
quantum telecoms & QKD					in repeaters	QKD protocols
quantum sensing		gravity, RF	SQUIDs, magnetism		magnetism	clocks

Figure 278: qubit types and their use cases in all quantum computing paradigms and on telecommunications and sensing. Orange means: less commonplace and/or harder to implement. (cc) Olivier Ezratty, 2022-2023.

At last, Figure 279 presents a summary of the scalability challenges faced by the main qubit types around (I left aside topological and NV centers qubits). Many of these topics are detailed in this part and others in the enabling technologies part⁸⁷¹. The table lists a lot of enormous challenges. For each of these, many research teams and vendors are proposing many different approaches and options. The upside is it is reassuring, the downside being that these options are still very immature, and you have to look at the details of their figures of merit to understand how it could scale. I make a broad inventory of the various envisioned solutions but am not in a position to assess their viability in most cases.

All in all, two overarching questions remain: how many entangled objects can be controlled in an efficient manner and with low noise, and how deterministic photon entanglement interconnectivity will scale without an exponential overhead that would kill any quantum advantage?

⁸⁷⁰ See the review [The Coming Decades of Quantum Simulation](#) by Joana Fraxanet, Tymoteusz Salamon and Maciej Lewenstein, ICFO, April-December 2022 (45 pages). It even mentions polaritons as a qubit type for quantum simulations.

⁸⁷¹ See [2022 Roadmap for Materials for Quantum Technologies](#) by Christoph Becher et al, February 2022 (38 pages) which provides an overview of many qubit types and their various challenges.

	superconducting	neutral atoms	trapped ions	silicon spins	photons
challenges	<ul style="list-style-type: none"> noise and crosstalk \nearrow with # of qubits. electronics energetic cost. scaling cabling, circulators. scaling cryostats. 	<ul style="list-style-type: none"> atom controls beyond 1000 qubits. harder to implement gate-based QC. SLM resolution. 	<ul style="list-style-type: none"> entanglement beyond 30 qubits. overall scaling beyond 40 qubits. slow gate speed. 	<ul style="list-style-type: none"> controlled electrostatic potential. error correction. qubits entanglement. fab cycle time. 	<ul style="list-style-type: none"> photon sources power. photon statistics. creating large cluster states of entangled photons.
solutions	<ul style="list-style-type: none"> materials improvement. 3D chipset stacking. cryo-CMOS or SFQ. microwave signals multiplexing. scale-out with photons. more powerful cryostats, JJ circulators. 	<ul style="list-style-type: none"> scale-out with atoms/photon conversion. more powerful lasers and SLMs. various atoms controls (microwaves, lasers). 	<ul style="list-style-type: none"> ions shuttling. switched to baryum (IonQ). Rydberg states ions (Crystal Quantum Computing). QPU photonic interconnect. 	<ul style="list-style-type: none"> material and interfaces improvement. integrated cryoelectronics. more powerful cryostats. more efficient fabs (GF). 	<ul style="list-style-type: none"> bright and deterministic photon sources (Quandela). deterministic sources of cluster states. MBQC. integrated nanophotonics.
caveats	<ul style="list-style-type: none"> photonic interconnect overhead and statistics. energetic cost of microwave multiplexing. SFQ backaction on qubits. 	<ul style="list-style-type: none"> gate control precision. losing the atom while computing. potential applicability limited to mid-scale simulations. 	<ul style="list-style-type: none"> photonic interconnect viability. photonic interconnect statistics and impact on speedups. 	<ul style="list-style-type: none"> scalability potential is capital intensive. two-qubit gates fidelities improving slowly. 	<ul style="list-style-type: none"> photon statistics. small cluster states so far.

(cc) Olivier Ezratty, 2023

Figure 279: the various pathways to scalability in quantum computing per qubit type. (cc) Olivier Ezratty, 2022-2023.

Quantum annealing

Quantum annealing is a particular quantum computing paradigm and technology that is also based on quantum physics and qubits but works entirely differently compared to gate-based quantum computing as we will detail here. It has characteristics and performance levels that are intermediate between traditional supercomputers and general-purpose (fault-tolerant) gate-based quantum computers (Figure 282) D-Wave is the main commercial player in this category. Some research laboratories are also involved in quantum annealing but not as many as those involved in the different types of gate-based quantum computers.

In the 2000s, the interest in Shor's factoring algorithm created more traction for gates-based quantum computing, at the expense of quantum annealing. Ironically, the largest integer factoring (of 6 digits: 376,289) by a quantum processor was achieved in 2018 on a D-Wave quantum annealer and not with Shor's algorithm on a gate-based system and it is still the record to date⁸⁷².

History

The quantum annealing paradigm (QA) is an optimization process for finding the global minimum of a given objective function by a process using quantum fluctuations and the tunnel effect⁸⁷³. It is mostly used for solving problems like combinatorial optimization problems where the search space is discrete, with many local minima. It is still usable for chemical simulations and non-discrete problems.

The idea to implement quantum annealing using quantum tunnelling effect came first in 1988 and 1989 in Italy and Germany⁸⁷⁴. It was then perfected in Japan by **Tadashi Kadowaki** and **Hidetoshi Nishimori** in 1998 with the "introduction of quantum fluctuations into the simulated annealing process of optimization problems, aiming at faster convergence to the optimal state. Quantum fluctuations cause transitions between states and thus play the same role as thermal fluctuations in the conventional approach. The idea is tested by the transverse Ising model, in which the transverse field is

⁸⁷² See [Quantum Annealing for Prime Factorization](#) by Shuxian Jiang et al, 2018 (9 pages).

⁸⁷³ Source: https://en.wikipedia.org/wiki/Quantum_annealing

⁸⁷⁴ See [A numerical implementation of quantum annealing](#) by S. Albeverio et al, University of Milan, July 1988 (10 pages) which refers to [Quantum stochastic optimization](#) by Bruno Apolloni et al, 1989 (12 pages).

*a function of time similar to the temperature in the conventional method. The goal is to find the ground state of the diagonal part of the Hamiltonian with high accuracy as quickly as possible*⁸⁷⁵.

As described in Wikipedia: “*Quantum annealing starts from a quantum-mechanical superposition of all possible states (candidate states) with equal weights. Then, the system evolves following the time-dependent Schrödinger equation [...]. The amplitudes of all candidate states keep changing, realizing a quantum parallelism, according to the time-dependent strength of the transverse field, which causes quantum tunneling between states. If the rate of change of the transverse field is slow enough, the system stays close to the ground state of the instantaneous Hamiltonian. The transverse field is finally switched off, and the system is expected to have reached the ground state of the classical Ising model that corresponds to the solution to the original optimization problem*”. In here, what is a “transverse field”? It is a transverse magnetic field that is applied in an homogenous way on qubits and then slowly decreased to control the evolution of the Ising model⁸⁷⁶.

A year after Tadashi Kadowaki and Hidetoshi Nishimori’s paper, **D-Wave** was created in Canada and it produced its first commercial annealer 13 years later, in 2012. But Japan did not surrender to the idea to create annealing industry solutions.

It took the form of a digital annealer created by **Fujitsu** and plans by **NEC** to create a quantum annealer. Also, many Japanese software startups are dedicated to quantum annealing.

At some point, John Martinis was working on creating a quantum annealer at **UCSB** but the idea was abandoned in favor of gate-based superconducting qubits when he started working at Google in 2004⁸⁷⁷. In Europe, **Qilimanjaro** (Spain) is in the process of creating a quantum annealer that would have greater capacities than the ones from D-Wave.

In 2000, **Edward Farhi** et al from the MIT created an algorithm to solve a SAT problem using adiabatic evolution which is considered an algorithmic cornerstone of quantum annealing⁸⁷⁸.

In 2013, Google and NASA set-up a joint quantum computing lab, **QUAIL**, and toyed with D-Wave systems. It drove some awareness on the first supposed and oversold “quantum advantage” in 2015. Quantum annealing and D-Wave drove relatively bad press in the quantum community. They oversold their capacity and didn’t explain well how it worked. Things fared better starting in 2017 and 2020 with their latest 2,000 and 5,000 qubit releases.

Science

We must start here with explaining Figure 280 which connects the (quantum) adiabatic theorem and the various forms of digital simulated and quantum annealing:

- The **adiabatic theorem** states if you are in the ground state of a slowly varying quantum system, you stay in the ground state. It was created by Max Born and Vladimir Fock in 1928.
- The **diabatic theorem** is related to quick Hamiltonian evolutions and can be implemented in gate-based quantum computing although a recent proposal emerged to implement it with a quantum annealer using a locally managed transverse field⁸⁷⁹.

⁸⁷⁵ See [Quantum annealing in the transverse Ising model](#) by Tadashi Kadowaki and Hidetoshi Nishimori, 1998 (9 pages).

⁸⁷⁶ An Ising model is a statistical physics model created to solve problems of simulation of ferromagnetic and para-magnetic materials associating particles having two state levels (a magnetic moment +1 or -1) which are linked together.

⁸⁷⁷ See the thesis [Superconducting flux qubits for high-connectivity quantum annealing without lossy dielectrics](#) by Christopher M. Quintana, 2017 (413 pages), directed by John Martinis who was then at Google.

⁸⁷⁸ See [Quantum Computation by Adiabatic Evolution](#) by Edward Farhi, Jeffrey Goldstone, Sam Gutmann and Michael Sipser, MIT and Northwestern University, 2000 (24 pages).

⁸⁷⁹ See [Locally Suppressed Transverse-Field Protocol for Diabatic Quantum Annealing](#) by Louis Fry-Bouriaux et al, UCL October 2021 (18 pages).

Implementations are based on:

- **Simulated annealers** working on a classical computer including Fujitsu’s digital annealers. Digitized simulated annealing can be used for more efficient integer factoring on NISQ QPUs than with Shor’s algorithm⁸⁸⁰.
- **Quantum annealers** (D-Wave) where a problem is converted into a generic **BQM** (binary quadratic model), from a **QUBO** optimization problems (Quadratic unconstrained binary optimization) or **Ising** problem (to solve some physics simulation problems like in ferromagnetism). It is faster than simulated digital annealing according to a 2022 benchmark⁸⁸¹.
- **Gate-based quantum computers**, using a time discretization of the system Hamiltonian evolution⁸⁸².
- **Reverse annealing** uses classical methods such as simulated annealing to find a trivial solution that initializes a quantum annealing process. This has been recently implemented with D-Wave annealers and seems more efficient than classical quantum annealing.
- **Diabatic quantum computing** is also running on gate-based quantum computers modeling a quick Hamiltonian change. It is used as part of the counter-diabatic technique promoted by ParityQC^{883 884 885}.

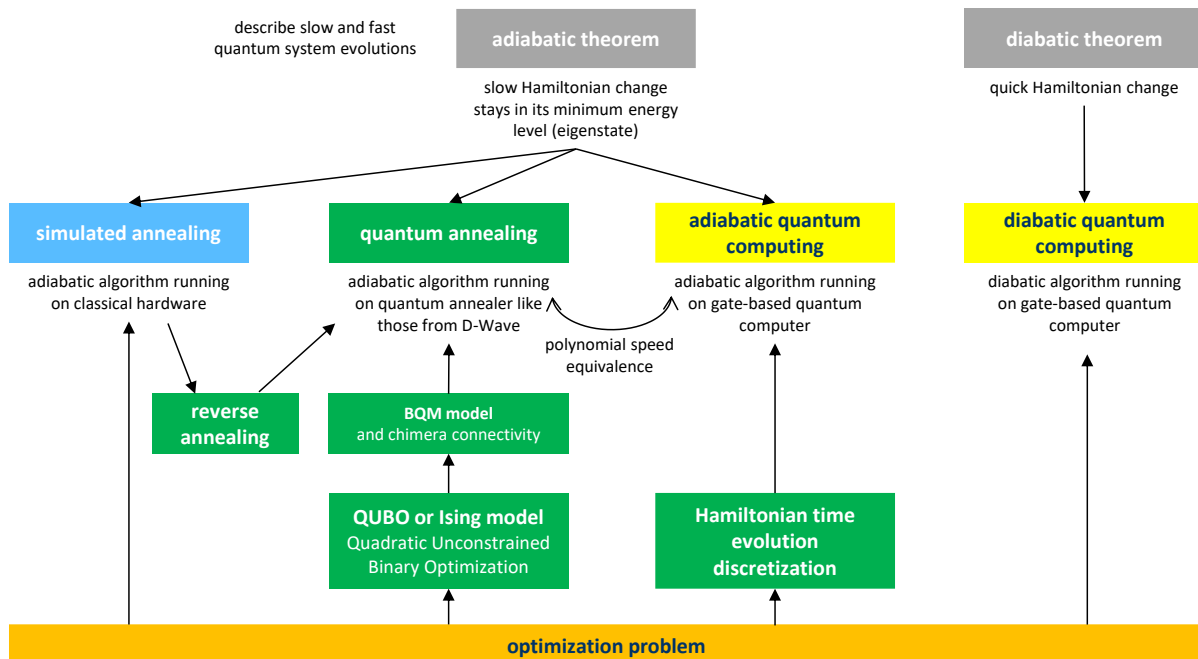


Figure 280: from the adiabatic theorem to quantum annealing. (cc) Olivier Ezratty, 2022-2023. And some references found in [Adiabatic quantum computation](#) by Tameem Albash and Daniel A. Lidar, 2018 (71 pages).

⁸⁸⁰ See [Digitized Adiabatic Quantum Factorization](#) by Narendra N. Hegade, Enrique Solano et al, November 2021 (10 pages).

⁸⁸¹ See [Benchmarking Quantum\(-inspired\) Annealing Hardware on Practical Use Cases](#) by Tian Huang et al, March 2022 (35 pages).

⁸⁸² See [On Quantum Annealing Without a Physical Quantum Annealer](#) by Ameya Bhave and Ajinkya Borle, University of Maryland, July 2023 (9 pages).

⁸⁸³ See [Rapid counter-diabatic sweeps in lattice gauge adiabatic quantum computing](#) by Andreas Hartmann and Wolfgang Lechner, New Journal of Physics, 2019 (14 pages).

⁸⁸⁴ See [Polynomial scaling enhancement in the ground-state preparation of Ising spin models via counterdiabatic driving](#) by Andreas Hartmann, Glen Bigan Mbeng, and Wolfgang Lechner, PRA, February 2022 (8 pages).

⁸⁸⁵ See [Many-body quantum heat engines with shortcuts to adiabaticity](#) by Andreas Hartmann, Victor Mukherjee, Wolfgang Niedenzu, and Wolfgang Lechner, Physical Review Research, May 2020 (13 pages).

Quantum annealing starts with preparing a system of interconnected qubits with establishing links between them using weights that are defined by couplers, a bit like in neural networks used in artificial intelligence. It sets the relative qubits connections energy in the longitudinal field (z) and the absolute qubits energy as a linear coefficient or bias on each qubit.

These values h_i and J_{ij} are discretized depending on the capabilities of the DACs integrated in the chip. It was using a 4 bit encoding in the first commercial D-Wave systems with values ranging from -1 to +1 by steps of 1/8. The precision of these DACs has since then improved with each new generation of D-Wave annealer.

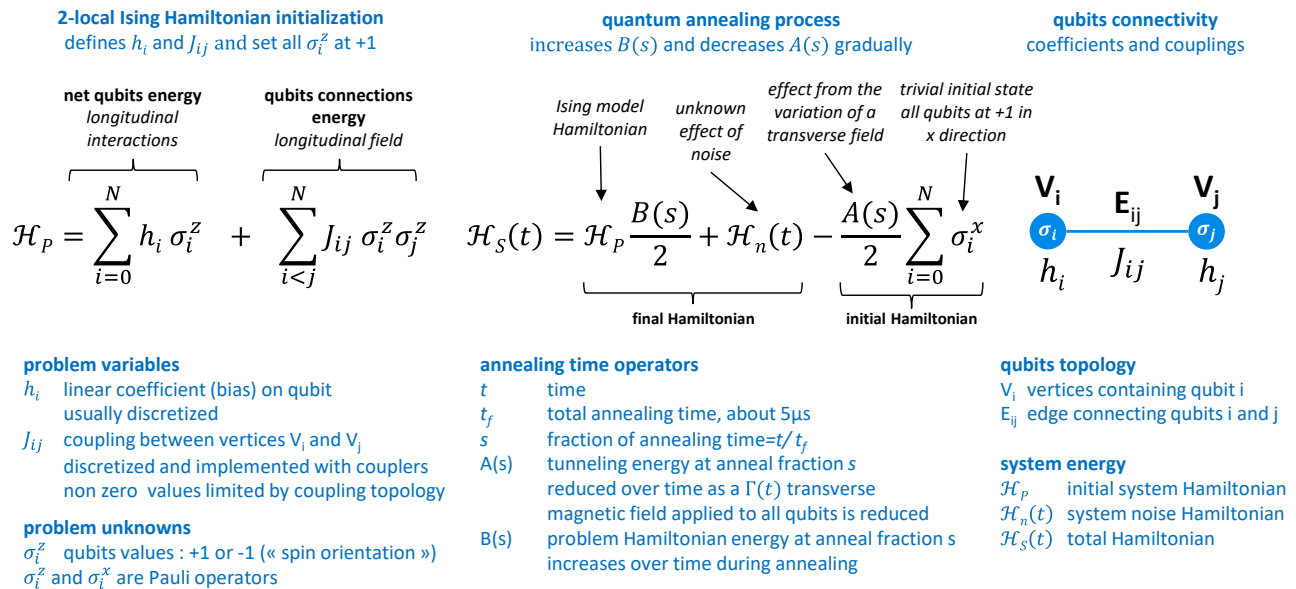


Figure 281: uncovering a quantum annealing Hamiltonian. (cc) Olivier Ezratty, 2022.

The minor embedding process consists in mapping the problem to solve to the quantum annealer qubit structure and connectivity. There are many optimizations available for this embedding process, particularly for solving optimization problems^{886 887 888 889}.

The system is then initialized with setting the qubits at $|+\rangle$, a perfect superposition between $|0\rangle$ and $|1\rangle$, corresponding to the lowest-energy state of the system, also called the tunneling Hamiltonian.

The annealing process then takes place progressively, reducing this magnetic transverse field down to zero, which, thanks to the quantum tunnel effect, will drive the system to an equilibrium state that corresponds to a minimum energy level. In the equations in Figure 281, it means reducing the value of scalar $A(s)$ and increasing the value of $B(s)$ accordingly, usually not linearly. This leads to automatically modifying the values of the qubits (spin up or down in the z direction) towards a result that corresponds to the solution of the submitted problem. This annealing process is a magnetic equivalent of classical thermal annealing.

From the mathematical standpoint, the system Hamiltonians \mathcal{H}_p , \mathcal{H}_s and \mathcal{H}_n described in Figure 281 are square matrix operators of dimension 2^N , N being the number of used qubits. The σ_j^z notation in the Ising and annealing Hamiltonian are somewhat confusing.

⁸⁸⁶ See [4-clique network minor embedding for quantum annealers](#) by Elijah Pelofske, January 2023 (15 pages).

⁸⁸⁷ See [Advanced unembedding techniques for quantum annealers](#) by Elijah Pelofske, Georg Hahn and Hristo Djidjev, September 2020-December 2022 (11 pages).

⁸⁸⁸ See [Divide-and-conquer embedding for QUBO quantum annealing](#) by Minjae Jo et al, November 2022 (12 pages).

⁸⁸⁹ See [ATOM: An Efficient Topology Adaptive Algorithm for Minor Embedding in Quantum Computing](#) by Hoang M. Ngo et al, University of Florida, July 2023 (6 pages).

It is the tensor product of the identity operator for all qubits non equal to j and the Pauli z operator for the given qubit j , as follows. A Pauli operator is a 2×2 matrix equivalent to the X, Y and Z single-qubit gates from gate-based quantum computing.

Thus, σ_j^z is a simplified notation of the whole tensor product of dimension 2^N , the full version being the following, I_k being identity matrices of dimension 2×2 for all k between 1 and N at the exception of j :

$$\sigma_j^z = I_1 \otimes \cdots \otimes I_{j-1} \otimes \sigma_j^z \otimes I_{j+1} \otimes \cdots \otimes I_N$$

The same can be said of the product $\sigma_i^z \sigma_j^z$ which is also a tensor product of dimension 2^N using the following equation with I_k for all k between 1 and N at the exception of i and j :

$$\sigma_i^z \sigma_j^z = I_1 \otimes \cdots \otimes I_{i-1} \otimes \sigma_i^z \otimes I_{i+1} \otimes \cdots \otimes I_{j-1} \otimes \sigma_j^z \otimes I_{j+1} \otimes \cdots \otimes I_N$$

System Hamiltonian matrix eigenvalues are the possible energy levels of the system. The annealing process has the effect of maintaining the system in its minimum energy level. It doesn't compute these eigenvalues but finds the qubit spin values (σ_i^z) that are minimizing the Hamiltonian. Another notation of the effect of quantum annealing is to find the combination of N spins noted $\hat{\sigma}$ that minimizes the Hamiltonian. The searched space is Ω_N that contains all N combinations of -1 and $+1$: $\{-1, +1\}^N$.

$$\hat{\sigma} = \arg \min_{\sigma \in \Omega_N} \left(\sum_{i=0}^N h_i \sigma_i^z + \sum_{i < j}^N J_{ij} \sigma_i^z \sigma_j^z \right)$$

At the end of the annealing, the qubits state is read and generates a $+1$ or a -1 for each of them depending on the direction of the magnetic flux of the superconducting loop. By the way, we do not care about it not being a QND – aka quantum non demolition - measurement. As a result, the solved problem search space is discrete and finite. The process is however iterative with several annealing passes and results being averaged. Like with gate-based quantum computing, the process is also probabilistic, and not just because noise gets involved with an unknown time-evolving Hamiltonian $\mathcal{H}_n(t)$.

There are variations in this model's implementation regarding the qubits coupling mechanism. It can be made on one degree (z for D-Wave) or two and three degrees of freedom (x , y and z , in a so-called Heisenberg model) like what **Qilimanjaro** (Spain) is planning to implement.

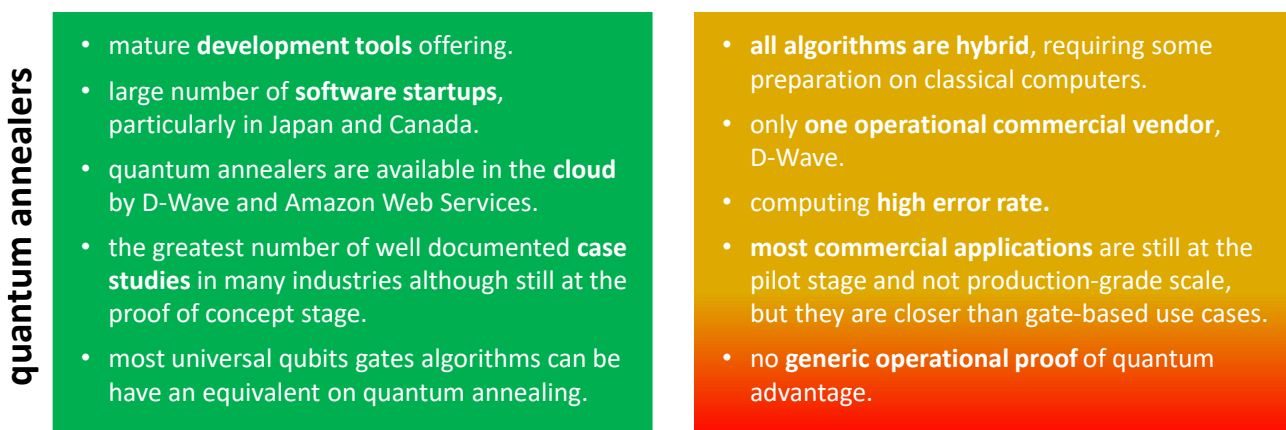


Figure 282: quantum annealers pros and cons. (cc) Olivier Ezratty, 2021-2023.

Qubit operations

Using a quantum annealer works as described in Figure 283. Algorithms are prepared classically with converting the given problem into a QUBO problem that is then translated in an Ising model with setting up the links between qubits in the initialization process and the qubits “weights”.

The annealing process then takes place with controlled evolutions of $A(s)$ and $B(s)$ as described in the previous chart, with tuning the magnetic transverse field affecting the qubits chip. When $s=1$, the system proceeds with reading the qubits values +1 or -1.

D-Wave qubits are niobium-based rf-SQUID exploiting superconducting current loops interrupted by two Josephson effect barriers that are controlled by variable magnetic fluxes (Figure 284).

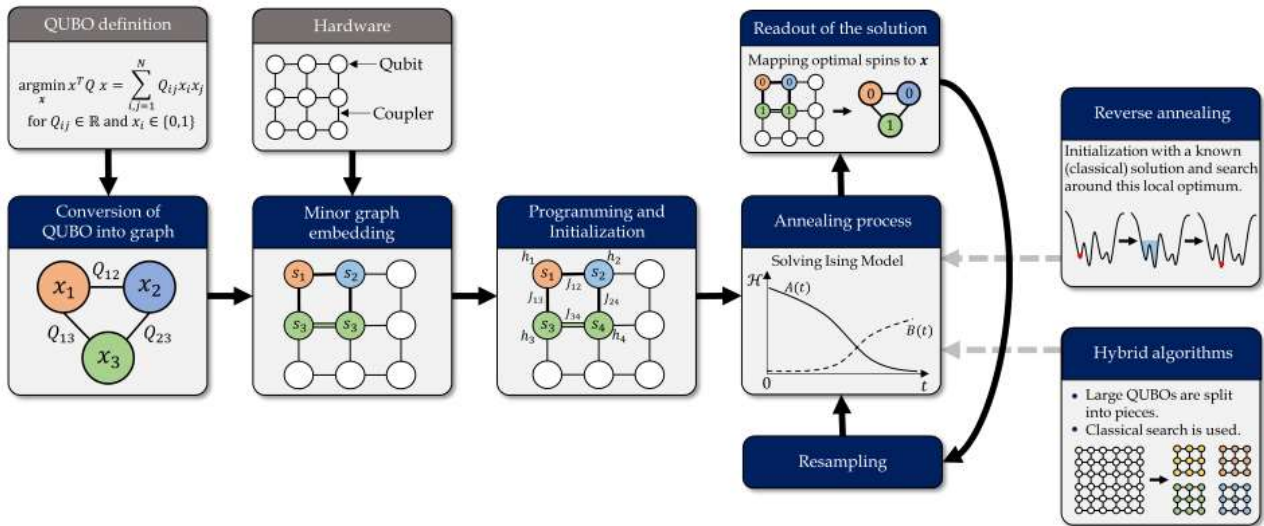


Figure 283: a quantum annealing computing workflow. Source: [Quantum Annealing for Industry Applications: Introduction and Review](#) by Sheir Yarkoni et al, Leiden University and Honda Research, December 2021 (43 pages).

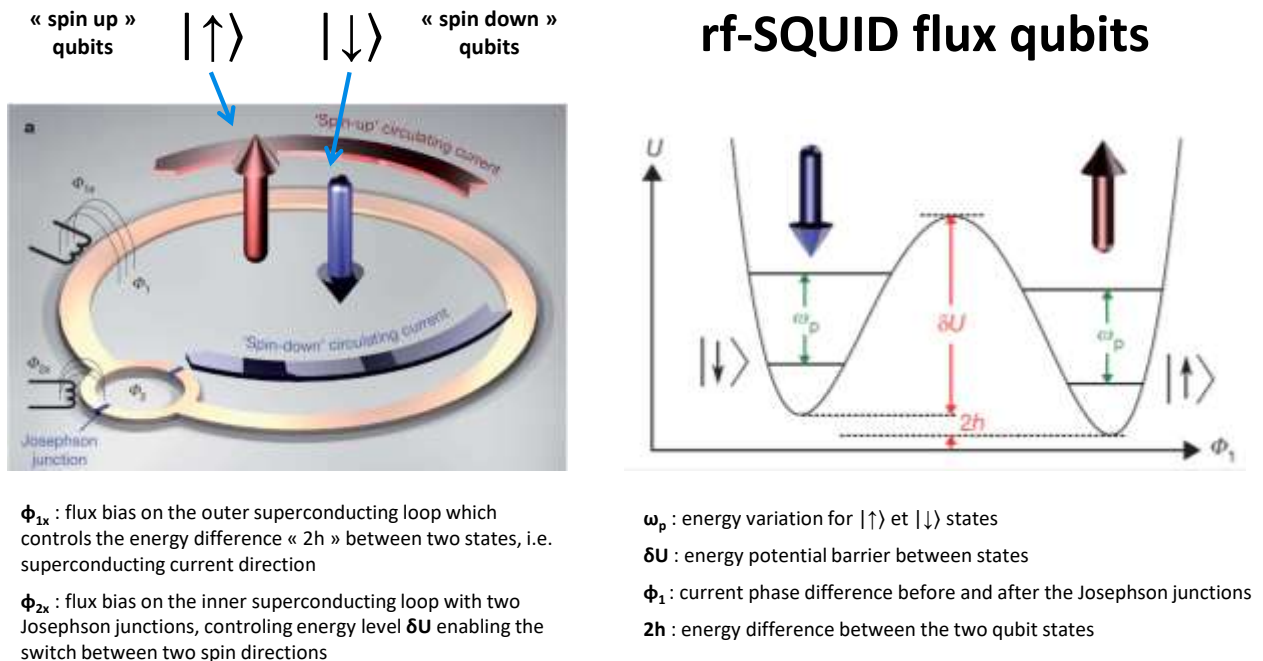


Figure 284: rf-SQUIDs used in a D-Wave quantum annealer. Source: D-Wave.

Taking always the example of D-Wave annealers, we can dig into how the qubits are controlled to prepare and handle an annealing process⁸⁹⁰. The process needs to control several parameters:

⁸⁹⁰ The electronics architecture of superconducting qubits control is described in [A scalable control system for a superconducting adiabatic quantum optimization processor](#) by M. W. Johnson et al, 2009 (14 pages) and [Architectural considerations in the design of a superconducting quantum annealing processor](#) by P. I. Bunyk et al, 2014 (9 pages).

J_{ij} the coupling between vertices V_i and V_j is controlled by DACs (digital to analog converters). These couplers are set with a static DC flux current applied to their compound-junction.

h_i the energy between two states of qubits i is also controlled via a DAC. But other DACs are there to correct the drift created by the annealing process.

$A(s)$ is a transverse magnetic field applied to all qubits and controlled in the chip by analog lines via the CCJJ DACs.

$B(s)$ increases over time during annealing, also controlled by CCJJ analog lines in the chip.

These are optimization problems where the variables J_{ij} can only take two values (-1 or +1 for solving an Ising model or 0 and 1 for solving a QUBO problem) and where they are linked together by different fixed parameters which are defined as floating numbers (FP32) with the boundary constraints $-1 \leq J_{ij} \leq 1$ and $-2 \leq h_i \leq 2$. However, the related DACs introduce significant sampling noise due to their sampling rate with a couple hundred different steps (Figure 285). In the end, the precision of the data of the problem to be solved is much lower, probably below one single byte. We're far from high-precision floating point scientific computation. It should be mentioned that D-Wave systems require frequent recalibration, that can be optimized⁸⁹¹.

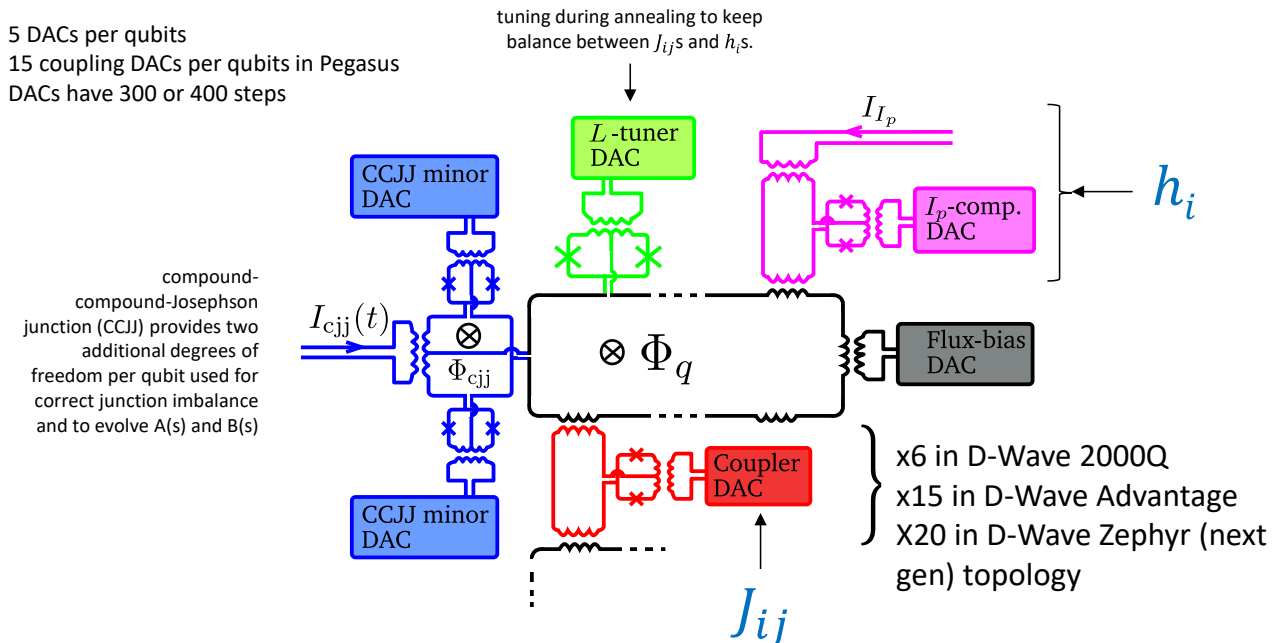


Figure 285: source: how D-Wave qubits are controlled at the physical level. Source: [A scalable control system for a superconducting adiabatic quantum optimization processor](#) by M. W. Johnson et al, 2009.

The initialization of a D-Wave 2000Q takes 25 ms, the annealing itself usually lasts 20 μ s but can be extended to 2 ms, and readout time is 260 μ s. If we repeat the annealing process a thousand times, we end up running the whole thing in less than a second. Between each run, some time was required to enable heat dissipation, with the chip temperature rising to 500 mK with early generations of D-Wave annealers.

The initialization signals of the Hamiltonian are multiplexed and sent in digital format from the outside to the chip. A chip requires an order of magnitude of $O(\sqrt[3]{N})$ external control lines for N qubits, using signals multiplexing.

⁸⁹¹ See [Tutorial: Calibration refinement in quantum annealing](#) by Kevin Chern et al, D-Wave, April 2023 (22 pages).

This greatly simplifies the cabling of the cryogenic enclosure of the computer compared to the superconducting IBM and Google computers, as shown in Figure 286 of a 2000Q. Most of what can be seen in the intermediate stages in the cryostat corresponds to the dilution cryogenics system.

Annealers don't need to send microwave pulses to qubits and thus, avoid the related coaxial cables used in gate-based superconducting qubits.

Some of the magic comes from the integrated DC ramp pulses generation circuits that are built-in in the quantum chip.



Figure 286: Inside a D-Wave system, with the cryostat open. Source: D-Wave.

These circuits use SFQ components implementing DACs, basically superconducting transistors using Josephson junctions close to those of the qubits. Still, these components are noisy and may contribute to the noise affecting the qubits in this architecture⁸⁹².

Research

Let's mention some research work beyond what D-Wave is doing.

Quantum annealing was explored in 2016 by the IARPA agency in its **Quantum-Enhanced Optimization** (QEO) project, which aimed to create an adiabatic computer void of some of the limitations from D-Wave, particularly in terms of connectivity and quality of qubits. Appropriately, in view of IARPA's mission, the goal was to accelerate the production of quantum computers capable of executing Shor's integer factoring algorithm to break the public keys coming from intercepted communications. This project was folded into DARPA's **QAFS** project (Quantum Annealing Feasibility Study) in February 2020 which produced a 25 coherent annealer system.

Stanford University is also working on quantum annealing. In 2016, they created a prototype photonic based annealer with 100 qubits having an all-to-all connectivity (so... 10,000 connections)⁸⁹³. This connectivity is what makes such a system "coherent". This research was still going on in 2021 and involves **NTT** in Japan. A team at Cornell University led by Peter McMahon is proposing a superconducting qubit quantum annealer physical architecture enabling all to all qubit connections, using Josephson parametric oscillators (JPOs), with frequencies modulated by a flux line, are a coupling by a microwave bus resonator⁸⁹⁴.

At last, the H2020 European project **AVaQus** (Annealing-based VARIational QUantum processorS) launched in October 2020 brings together five research laboratories (Institut de Física d'Altes Energies of Barcelona, Karlsruhe Institut für Technologie (KIT) of Karlsruhe, CNRS Institut Néel in France, the University of Glasgow and the Consejo Superior de Investigaciones Científicas in Madrid), associated with three startups **Delft Circuits** (The Netherlands), **Qilimanjaro** (Spain) and **HQS** (Germany). The project is scheduled to end in 2023 and got a funding of €3M, independently of the Quantum Flagship program.

⁸⁹² See [Analog errors in quantum annealing: doom and hope](#) by Adam Pearson, 2019 (9 pages).

⁸⁹³ See [A fully-programmable 100-spin coherent Ising machine with all-to-all connections](#) by Peter L. McMahon, Yoshihisa Yamamoto et al, 2016 (9 pages).

⁸⁹⁴ See [A quantum annealer with fully programmable all-to-all coupling via Floquet engineering](#) by Tatsuhiro Onodera, Edwin Ng and Peter L. McMahon, Cornell University, npj Quantum Information, 2020 (10 pages).

Vendors

We'll of course start with D-Wave and will follow-on with Qilimanjaro and NEC.



Located in Vancouver, **D-Wave** (1999, Canada, \$724M+IPO) was for a very long time the only supplier of commercial quantum processors (Figure 287).

Company. D-Wave was created by Geordie Rose (their first CTO and for some time also their CEO⁸⁹⁵), Haig Farris, Bob Wiens and Alexandre Zagoskin, formerly in charge of research. Geordie Rose received his PhD in Materials Physics in the mid-1990s from the University of British Columbia. The creation of D-Wave is a direct result of this work. He met Haig Farris during his studies while the latter was teaching economics. D-Wave's management team has changed a lot since then. Only one of the co-founders is still part of it, Eric Ladizinsky, who is their Chief Scientist. Their CTO Alan Baratz joined the company in 2017 and became CEO in 2020.

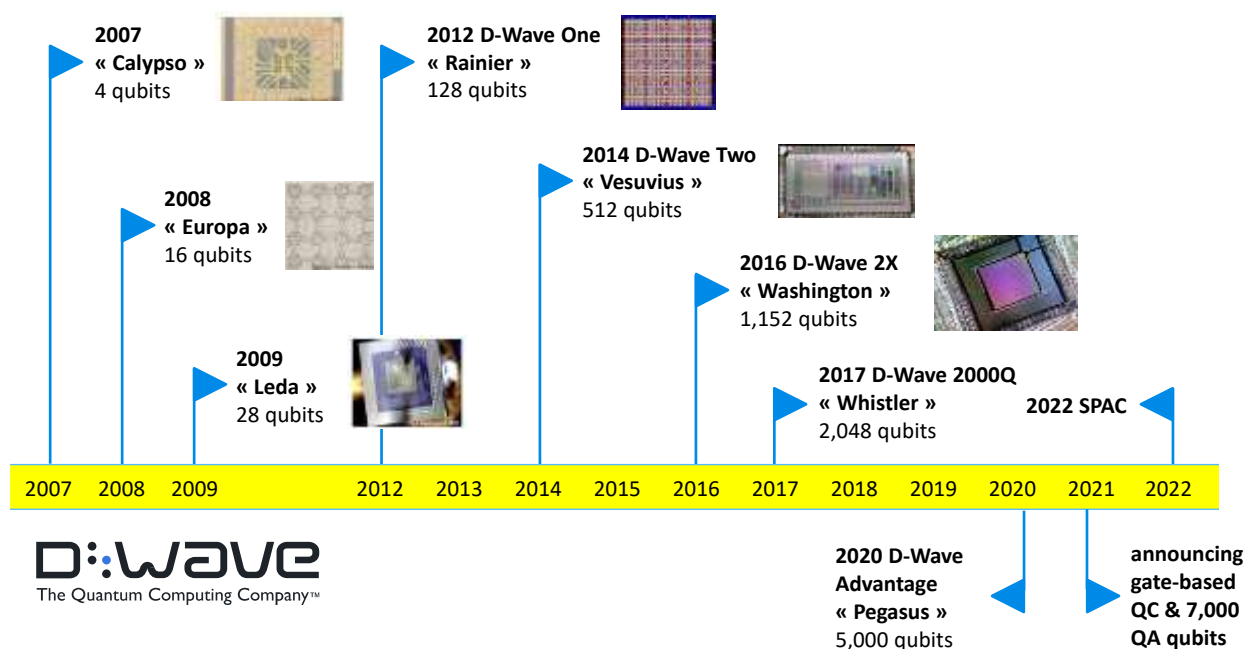


Figure 287: timeline of D-Wave's history. (cc) Olivier Ezratty, 2022-2023.

It took D-Wave eight years to prototype its first chip containing four qubits and a total of 13 years to sell their first quantum computer, the D-Wave One. During these years, they raised \$31M, then \$1.2M in 2012 from InQTel, the CIA's investment fund. In 2011, D-Wave signed a partnership with Lockheed Martin, which does some work for the NSA. All in all, the startup went through 13 rounds of funding, ending with a SPAC finalized in 2022.

In February 2022, D-Wave announced its own SPACification via the dedicated investment fund **DPCM Capital** created by Eric Schmidt (former Google, now Sandbox AQ chairman), Peter Diamandis (Singularity University) and Shervin Pishenar (Hyperloop One founder)⁸⁹⁶. They were to raise \$340M, including \$40M coming from a Canadian pension fund, PSP Investments. Were also involved Goldman Sachs and NEC Corporation. This valued the company at \$1.6B which was IPOed in August 2022. They have another funding source with a line of credit of \$150M from Lincoln Park Capital in exchange of stock issuance.

⁸⁹⁵ Co-founder Geordie Rose then created **Kindred.ai**, a startup that aims to integrate General Intelligence (GIA) into robots. He left Kindred.ai in 2018 to create **Sanctuary**, a spin-off of Kindred, dedicated to AGI, the quest for the Holy Grail of general artificial intelligence.

⁸⁹⁶ See their [February 2022 investor presentation](#) (25 slides).

The company expected a fast growth starting in 2025, generating a \$551M turnover in 2026. As of early 2022, they had a staff of 180 including 36 PhDs and a 200 patents portfolio. In February 2023, D-Wave faced a cash problem and a drop of its stock value, risking a humiliating Nasdaq delisting. Starting in June 2023, the company stock navigating between \$1.4 and \$2.9, above the \$1 threshold⁸⁹⁷. As of April 2023, they had 67 paying customers. They had a revenue of \$7.1M in 2022, \$6.3M in 2021 and \$5.1M in 2020 with net losses of respectively \$51.5M, \$31.5M and \$10M⁸⁹⁸. As of June 2023, their market capitalization was \$265M.

Technology. D-Wave has developed its end-to-end quantum annealing computer solution. It is the first full-featured quantum computer in history with a design that allows it to be easily integrated into a clean room. Their roadmap progressed steadily with the first three generations of prototypes created between 2007 and 2009 and then, starting from 2012, five generations of commercial computers.

It started with the D-Wave One in 2012 with 128 qubits. The D-Wave 2000Q followed in 2017 with 2048 qubits and 128,000 Josephson junctions on a (5.5 mm)² chip and a list price of \$15M. The last commercial iteration is the D-Wave Advantage with the Pegasus chip launched in September 2020 with 5,640 qubits and one million Josephson junctions, each qubit being coupled to 15 other qubits compared to 6 in the 2000Q.

It allows more complex problems to be solved with an equivalent number of qubits^{899 900}. It is a performance given gate-based superconducting qubits have a 1 to 3 (IBM) to 1 to 4 (Google) connectivity at best. The Pegasus chip is larger, being a square of 8.5 mm. It is manufactured in the USA in Skywater's cleanrooms (formerly a Cypress Semiconductor fab) located in Bloomington, Minnesota. The embedding graph or qubits connectivity is branded a chimera their D-Wave 2000Q annealers and a Pegasus graph for their D-Wave Advantage annealers⁹⁰¹ (Figure 288).

In October 2021, D-Wave announced their Clarity roadmap with an upcoming Advantage 2 generation codename Zephyr with 7,000 qubits to be released by 2024, with a first intermediate 500-qubit prototype which was delivered in June 2022. The Zephyr has a 20-way qubits connectivity in a new graph architecture⁹⁰².

They also announced the future release of a gate-based QPU was to be implemented in a separate (fluxonium-based) multi-layer superconducting processor architecture, starting with 60 and then 1,000 qubits to implement error correction. They plan to use surface code QECs and to use some combination of RSFQ and other cryo-electronics to control these qubits.

⁸⁹⁷ See [Globe and Mail Reports D-Wave May Be Facing Cash Crunch](#) by Matt Swayne, The Quantum Insider, February 2023.

⁸⁹⁸ See [D-Wave Reports Fourth Quarter and Year-End 2022 Results](#), D-Wave, April 2023.

⁸⁹⁹ The chimera uses cells with 8 qubits with internal and external couplings. It has 4 internal couplings within cells and 2 external couplings in pre-Pegasus chipsets and 12 internal and 3 external couplings in Pegasus chipsets.

⁹⁰⁰ See [Quantum annealing with manufactured spins](#) by Mark Johnson et al, 2011 (6 pages) which outlines the D-Wave process. As well as [Technical Description of the D-Wave Quantum Processing Unit](#) by D-Wave, 2020 (56 pages) and related [supplemental information](#) (19 pages). The Pegasus architecture from the D-Wave advantage is described in [Next Generation Quantum Annealing System](#) by Mark Johnson, March 2019 (27 slides) and in [Next-Generation Topology of D-Wave Quantum Processors](#) by Kelly Boothby et al, 2019 (24 pages). See [D-Wave Announces General Availability of First Quantum Computer Built for Business](#) by D-Wave, September 2020.

⁹⁰¹ D-Wave's chimera matrix requires a conversion process of its qubit mesh problem. This process is so far mostly exploited for problems that fit well with this qubit organization. For an arbitrary optimization problem, the conversion gives a result that is not convincing in terms of efficiency and acceleration. This is what emerges from the work of Daniel Vert, then PhD student at CEA LIST, in [On the limitations of the chimera graph topology in using analog quantum computers](#) by Daniel Vert, Renaud Sidney and Stéphane Louise, CEA LIST, 2019 (5 pages) and in [Revisiting old combinatorial beasts in the quantum age: quantum annealing versus maximal matching](#) by the same authors, October 2019 (36 pages). D-Wave's chimera structure limits the way a QUBO or other optimization problem can be converted into an Ising problem solvable with D-Wave's chimera structure.

⁹⁰² See [Zephyr Topology of D-Wave Quantum Processors](#) by Kelly Boothby, Andrew D. King and Jack Raymond, D-Wave, September 2021 (18 pages).

They could be highly differentiated for that respect and only challenged by other superconducting qubit vendors partnering with SEEQC. As of mid-2023, they had tested 1- and 2-qubit fluxonium qubit circuits validated a new scalable readout method for gate model architecture. They reduced by a factor of 4 the noise of these qubits. D-Wave published a white paper on its fluxonium qubit development progress in September 2023, with a T_1 of $120 \mu\text{s}$ ⁹⁰³.

They also added a gate model simulator in the Ocean software suite.

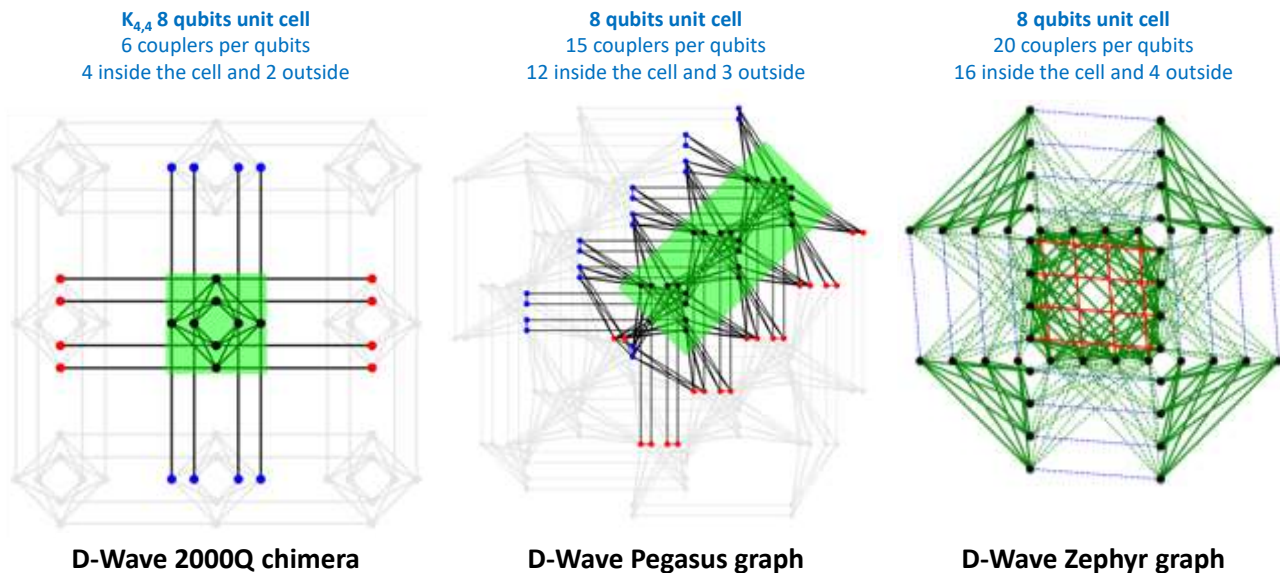


Figure 288: evolution of D-Wave's qubit connectivity. Source: D-wave. 2023.

How about error rates in annealing mode? They are not computed the same way as gate-based single and two qubit gate fidelities. The error rate is measured as a precision with the Ising model parameters, which is about 2% given the DACs precision^{904 905}. The high-error rate of D-Wave annealing systems can be mitigated with some quantum error correction technique, created in 2019⁹⁰⁶ and more recently in 2022 for post-processing error correction⁹⁰⁷ and machine learning aided error correction⁹⁰⁸.

Other researchers found that the thermal noise involved in the annealing process could be used as a resource to enable faster and more reliable computations, involving the curious process or reverse annealing⁹⁰⁹. It could help finding a better solution than an existing solution already computed with a regular annealing process.

The qubits operate at 10 to 15 mK like all gate-based superconducting qubits. The cryostat is thus the same, using a dry dilution system. Cryogeny consumes about 16kW out of a total of 25kW. The remaining 9kW is related to traditional computer control systems that are outside the cryostat. The cryogenic part includes an enclosure with five layers of magnetic isolation.

⁹⁰³ See [High-coherence fluxonium as a probe of D-Wave's QPU environment](#), D-Wave (4 pages).

⁹⁰⁴ The question remains open as to whether this architecture is scalable and provides a real quantum advantage. This is questioned in [Fundamental Limitations to the Scalability of Quantum Annealing Optimizers](#) by Tameen Albash et al, 2019. The reasons: issues of noise and thermodynamics.

⁹⁰⁵ See [Noise Dynamics of Quantum Annealers: Estimating the Effective Noise Using Idle Qubits](#) by Elijah Pelofske et al, September 2022-February 2023 (19 pages).

⁹⁰⁶ See [Analog errors in quantum annealing: doom and hope](#) by Adam Pearson et al, 2019 (16 pages).

⁹⁰⁷ See [Post-Error Correction for Quantum Annealing Processor using Reinforcement Learning](#) by Tomasz Śmierzchalski et al, March 2022 (14 pages).

⁹⁰⁸ See [Boosting the Performance of Quantum Annealers using Machine Learning](#) by Jure Brence et al, March 2022 (14 pages).

⁹⁰⁹ See [Thermodynamic study of D-Wave processor could lead to better quantum calculations](#) by Hamish Johnston, June 2020.

The control electronics are much simpler than with superconducting qubits. A D-Wave annealer doesn't contain a maze of cables in its cryostat since qubit control is done within the chip itself and makes use of DC current pulses.

Quantumness. So, what is quantum in D-Wave? Beyond the many Josephson junctions used in their chip, it comes from the tunnelling effect that allows the system to quickly search for a global energy minimum of an N-body system⁹¹⁰. It is coupled with superposition of the qubit states. According to D-Wave, the system also uses entanglement, which is poor and probably circumvented to nearest neighbor qubits⁹¹¹. This has been questioned by some scientists⁹¹².

Algorithms designed for classical gate-based quantum computers can theoretically be converted into algorithms executable on D-Wave and vice versa at a maximum polynomial time overhead cost, which can be substantial⁹¹³. However, a similar problem will require many more qubits with D-Wave than with a universal quantum computer. On a D-Wave, the number of qubits would need to be up to 32 times the number of quantum gates of an equivalent classical quantum algorithm, but it depends on the problem⁹¹⁴. According to D-Wave, their annealers can solve NP-complete problems, a category of combinatorial problems theoretically solved in polynomial time on D-Wave but which are solved in exponential time on a classical computer⁹¹⁵, like routing problems, the traveling salesperson (TSP) problem and the likes. The caveat is that this can't be proven yet on large scale problems and empirical evidence is not positive⁹¹⁶. D-Wave annealers can also be used to solve statistical problems⁹¹⁷.

In 2017, **John Preskill** estimated that there is no convincing theoretical basis for the advantage of quantum annealing, which is one form of adiabatic quantum computing⁹¹⁸. He thinks this architecture is not theoretically as scalable as a general-purpose quantum computer.

The arguments about D-Wave's annealers non quantumness revolve around the low-scale coherence between qubits which may prevent an efficient implementation of quantum annealing⁹¹⁹. It is also related to the limited connectivity between qubits⁹²⁰.

⁹¹⁰ See the review paper [Quantum Annealing: An Overview](#) by Atanu Rajak et al, India, July 2022 (36 pages).

⁹¹¹ See [Measurement of the energy relaxation time of quantum states in quantum annealing with a D-Wave machine](#) by Takashi Imoto et al, AIST and Denso, February 2023 (7 pages).

⁹¹² Jonathan Dowling thought in the previous reference that the only quantum effects of D-Waves were tunneling and superposition, but without quantum entanglement.

⁹¹³ This is documented in [Adiabatic quantum computation is equivalent to standard quantum computation](#), 2005 (30 pages) and in [How Powerful is Adiabatic Computation?](#) by Wim van Dam, Michele Mosca and Umesh Vazirani, 2001 (12 pages).

⁹¹⁴ From "Automatically Translating Quantum Programs from a Subset of Common Gates to an Adiabatic Representation" by Malcolm Regan et al, seen in [Reversible Computation](#), conference proceedings, 11th International Conference, RC 2019, Lausanne, Switzerland, June 2019 (246 pages).

⁹¹⁵ See [Practical Annealing-Based Quantum Computing](#) by Catherine McGeoch et al of D-Wave, June 2019 (16 pages) which makes an inventory of the benefits of quantum annealing computing, especially in terms of the size of the problems to be solved, which should be neither too small because they are trivial, nor too large because they must then be broken down into sub-problems that are manageable with the capacity of current D-Wave processors. It seems that the problems to be solved must have global minimums and local minimums, the first being difficult to find with classical methods.

⁹¹⁶ See [Performance of Commercial Quantum Annealing Solvers for the Capacitated Vehicle Routing Problem](#) by Salvatore Sinno et al, September 2023 (7 pages).

⁹¹⁷ See [Applications of Quantum Annealing in Statistics](#) by Robert C. Foster, 2019 (30 pages).

⁹¹⁸ In [Quantum Computing for Business](#), 2017 (41 slides).

⁹¹⁹ See [How "Quantum" is the D-Wave Machine?](#) by Seung Woo Shin, Umesh Vazirani et al, 2014 (8 pages).

⁹²⁰ See the example of [Phase-coded radar waveform AI-based augmented engineering and optimal design by Quantum Annealing](#) by Timothé Presles et al, Thales, August 2021 (9 pages). In this use case, no quantum advantage can be seen with D-Wave due to limited qubits connectivity.

Daniel Lidar from the University of Southern California is investigating variations of quantum annealing algorithms that could solve intractable problems on classical computers⁹²¹.

Others think that D-Wave systems can generate at best some quadratic acceleration and not an exponential one, compared to traditional computing⁹²². In 2023, many preprints did showcase various limitations of quantum annealing.

In the good news realm, quantum annealing performed better than gate based QAOA running on IBM's 127 noisy qubits with error suppression techniques⁹²³. Another study found similarly that quantum annealing is closer to be able to solve real-world use cases than gate based QPU. It was based on an ambulance dispatch optimization problem.

Still, a classical Tabu search solution is faring better than quantum annealing⁹²⁴. At last, a French study seems to prove that a Max-Cut can be solved efficiently on a quantum annealer⁹²⁵ and a Bulgarian researcher did the same on the generic Set Cover Problem⁹²⁶.

In the bad news, one benchmark done in Japan on a D-Wave 2000Q, against several state-of-the-art classical optimization algorithms designed for continuous-variable problems found that the D-Wave 2000Q matches classical algorithms only in a limited domain of computation time. It was tested on the more recent D-Wave Advantage but its results were worse than with the 2000Q⁹²⁷. A first test of the Zephyr Advantage 2 prototype chip was done and didn't detect a quantum advantage with optimization problems⁹²⁸. Other studies done in the Netherlands and in the USA found that there can't be any generic advantage for combinatorial optimizations, even not some quadratic speedup^{929 930}.

Software tools. D-Wave's software development environment is Ocean, a suite of open source Python tools and libraries accessible via the Ocean SDK on both the D-Wave GitHub repository and in their Leap quantum cloud service (that is also accessible on Amazon Braket). It contains a large set of libraries to solve various optimization and constraint satisfaction problems. We cover it with more details starting 982. It also contains a problem visualizer, formerly 'problem inspector' to visualize how a problem is encoded in graphs through the minor embedding process.

In October 2021, D-Wave released its Constrained Quadratic Model solver (CQM), that is working with both discrete and continuous variables. It expanded the optimization problems D-Wave's annealers can solve, with up to 100,000 variable constraints⁹³¹ on top of the binary quadratic model (BQM)

⁹²¹ See his [Adiabatic quantum computing](#) page on USC Quantum Computation and Open Quantum Systems web site.

⁹²² This was the opinion of Jonathan P. Dowling in [Schrödinger's Killer App - Race to Build the World's First Quantum Computer](#) by Jonathan P. Dowling, 2013 (445 pages), pages 208 to 216.

⁹²³ See [Quantum Annealing vs. QAOA: 127 Qubit Higher-Order Ising Problems on NISQ Computers](#) by Elijah Pelofske et al, January 2023 (13 pages).

⁹²⁴ See [Using a quantum computer to solve a real-world problem -- what can be achieved today?](#) by R. Cumming and R. Thomas, November 2022 (62 pages).

⁹²⁵ See [Anti-crossings occurrence as exponentially closing gaps in Quantum Annealing](#) by Arthur Braida Simon Martiel and Ioan Todinca, Atos and LIFO Orléans, April 2023 (22 pages).

⁹²⁶ See [Quantum annealing with inequality constraints: the set cover problem](#) by Hristo N. Djidjev, February 2023 (22 pages).

⁹²⁷ See [Quantum annealing for continuous-variable optimization: How is it effective?](#) by Shunta Arai et al, RIKEN and Tokyo University, May 2023 (24 pages).

⁹²⁸ See [Comparing Three Generations of D-Wave Quantum Annealers for Minor Embedded Combinatorial Optimization Problems](#) by Elijah Pelofske, Los Alamos National Laboratory, January-April 2023 (21 pages).

⁹²⁹ See [Why adiabatic quantum annealing is unlikely to yield speed-up](#) by Aarón Villanueva et al, Radboud University, December 2022 (23 pages).

⁹³⁰ See [On the Emerging Potential of Quantum Annealing Hardware for Combinatorial Optimization](#) by Byron Tasseff et al, October 2022 (25 pages).

⁹³¹ See [Hybrid Solver for Constrained Quadratic Models](#), 2021 (8 pages).

solver problems defined with binary values (0,1) and the discrete quadratic model (DQM) solver for problems on nonbinary (multiple choices) values. But quantum annealing can also potentially solve continuous-variable optimization problems⁹³².

Case studies. One of the oldest and famous D-Wave publicized case study came from Google and NASA in 2015. They were using a 2012 D-Wave annealer to solve an optimization and combinatorial problem in a graph whose algorithm was designed in 1994. Google announced that, on that particular case study, D-Wave’s annealer was 100 million times faster than a Intel Xeon server processor core⁹³³. Like many such claims, they were questionable since based on a single optimized algorithm, here, a Quantum Monte Carlo simulating quantum tunneling on a classical computer. Critics abounded about this performance⁹³⁴. It was a first ‘hype’ moment for quantum computing (Figure 289).

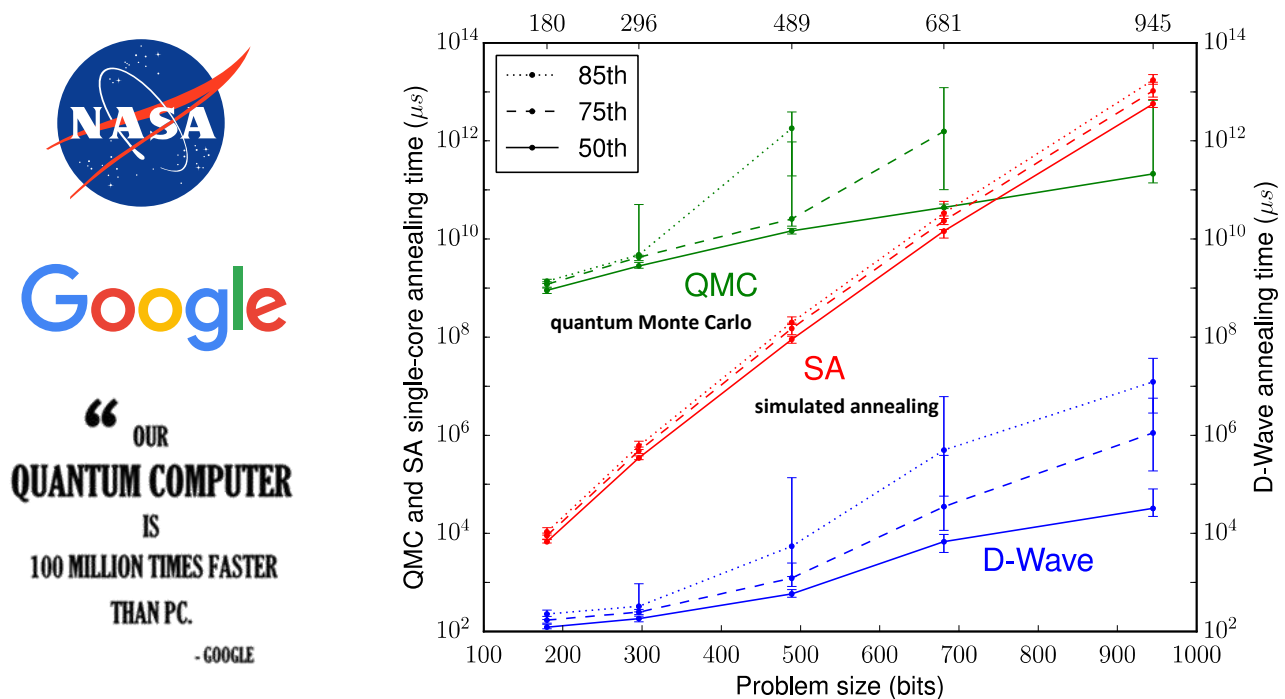


Figure 289: how Google and NASA communicated in 2015 about the performance of a D-Wave annealer. Source: [What is the Computational Value of Finite Range Tunneling](#) by Vasil S. Denchev, John Martinis, Hartmut Neven et al, January 2016 (17 pages).

D-Wave communicates on many other of its pilot references⁹³⁵. A while ago, its web site referenced over 250 case studies, the largest number of any quantum computing vendor⁹³⁶. Although quantum annealers have technical limitations compared to general-purpose quantum computers, they have the advantage of being available and are surrounded by a strong software ecosystem.

⁹³² See [Effectiveness of quantum annealing for continuous-variable optimization](#) by Shunta Arai, Hiroki Oshiyama, and Hidetoshi Nishimori, RIKEN, Tokyo Institute of Technology and Tohoku University, PRA, October 2023 (21 pages).

⁹³³ See [Google's D-Wave 2X Quantum Computer 100 Million Times Faster Than Regular Computer Chip](#) by Alyssa Navarro in Tech Times, November 2015 and documented in [What is the Computational Value of Finite Range Tunneling](#) by Vasil S. Denchev, Sergio Boixo, Sergei V. Isakov, Nan Ding, Ryan Babbush, Vadim Smelyanskiy, John Martinis and Hartmut Neven, January 2016 (17 pages).

⁹³⁴ Including [Temperature scaling law for quantum annealing optimizers](#), 2017 (13 pages), which points out the limitations of quantum annealing.

⁹³⁵ I found this inventory in [Quantum Applications](#) by D-Wave, May 2019 (96 slides).

⁹³⁶ See [Quantum Annealing for Industry Applications: Introduction and Review](#) by Sheir Yarkoni et al, Leiden University and Honda Research, December 2021 (43 pages) which provides an overview of how D-Wave annealers are “programmed” and what kinds of problems it can solve.

However, most of the many case studies published by D-Wave and their customers and partners seem to be proofs of concept. None are production-grade and deployed solutions, or at least providing a proven quantum advantage over classical computing. Here are a couple ones in various domains.

With optimizations, mostly in transportation:

- **Denso**, a Japanese car equipment manufacturer presented at CES 2017 in Las Vegas a system for optimizing a fleet of Toyota delivery vehicles.
- **Toyota** and **Denso** crafted a solution to find the optimal location of electrical components and conductor paths in electric circuit systems⁹³⁷.
- **Volkswagen** simulated the operations of a 418-cab fleet in Beijing with a QUBO based hybrid classical/annealing algorithm using a training data set coming from 10,357 cabs⁹³⁸. The solution was then used in November 2019 to optimize bus shuttles route at Lisbon's WebSummit, in partnership with Here and Volkswagen's Data:Lab in Munich, with 185 trips and 9 buses over 4 days⁹³⁹. None of these solutions were in the quantum advantage regime.
- **Volkswagen** also experimented quantum annealing to optimize its car paint-shop processing in order to minimize color switching, but with no clear quantum advantage⁹⁴⁰, and also a solution to develop new batteries⁹⁴¹.
- Researchers in Poland, Hungary, Brazil and the USA found a way to use D-Wave annealers to **optimize trains dispatching** on single-railways lines⁹⁴².
- **GE Research** experimented a hybrid maintenance resource allocation optimization application. The company has a team of over 80 people working on quantum technologies.
- **Ocado**, a British retailer, prototyped some optimization solution for its robots-based warehouse operations.
- **KAIST** and **LG U+** in Korea optimized some data-transfer routing for a fleet of low-earth orbit telecommunications satellites using a QUBO algorithm, with the help of **Qunova Computing**, a South-Korean quantum software startup⁹⁴³.
- **Lockheed-Martin** produced in 2014 some validation procedures for its embedded software in 6 weeks instead of 8 months with a D-Wave and its QVTRace tool⁹⁴⁴.
- **Mastercard** is working on customer loyalty and rewards allocation, cross-border settlement, and fraud management. The partnership with D-Wave started in 2022.
- **Pattison Food Group** is working on grocery operations optimization.
- **SavantX** developed a port operations optimization prototype in Los Angeles.

⁹³⁷ See [Design Optimization of Noise Filter using Quantum Annealer](#) by Akihisa Okada et al, Toyota and Denso, January 2023 (6 pages). It is about optimizing circuit design with using quantum annealers.

⁹³⁸ See [Traffic flow optimization using a quantum annealer](#) by Florian Neukart et al, Volkswagen and D-Wave, August 2017 (12 pages).

⁹³⁹ See [Quantum Shuttle: Traffic Navigation with Quantum Computing](#) by Sheir Yarkoni et al, D-Wave and Volkswagen, June 2020 (9 pages).

⁹⁴⁰ See [Multi-car paint shop optimization with quantum annealing](#) by Sheir Yarkoni et al, September 2021 (7 pages).

⁹⁴¹ See [Forget quantum supremacy: This quantum-computing milestone could be just as important](#) by Steve Ranger, December 2019.

⁹⁴² See [Quantum annealing in the NISQ era: railway conflict management](#) by Krzysztof Domino et al, December 2021 (23 pages).

⁹⁴³ See [KAIST & LG U+ Team Up for Quantum Computing Solution for Ultra-Space 6G Satellite Networking](#), KAIST press office, June 2022.

⁹⁴⁴ See [Quantum Computing Approach to V&V of Complex Systems Overview](#), 2014 (31 slides) and [Experimental Evaluation of an Adiabatic Quantum System for Combinatorial Optimization](#), 2013 (11 pages).

- **BASF** compared the performance of classical the Gurobi algorithm with quantum annealing (D-Wave) and digital annealing (Fujitsu) versions to solve a transport robot scheduling problem⁹⁴⁵. At this point, Gurobi fares better, particularly with large data sets.
- With various potential use cases in **emergency management**⁹⁴⁶. **Tohoku University** (Japan) developed a quantum-hybrid application to facilitate planning related to tsunami response⁹⁴⁷. With NEC Australia, the Australian Army explored how quantum-hybrid applications can improve last-mile resupply in emergencies with some demonstrated advantage vs classical algorithms⁹⁴⁸. At last, again in Japan, Osaka University developed an application to solve the nurse scheduling problem (NSP) but not to a point to deliver some quantum advantage at large real-life scale in the tested D-2000Q annealer⁹⁴⁹.

In drug design and healthcare:

- **Biogen, 1Qbit** and **Accenture** did prototype in 2012 a screening solution to identify molecules for drug retargeting, with a problem of map staining⁹⁵⁰. It is difficult to say what this has generated in practice. Their partner **Menten AI** performs protein analysis.
- In April 2020, D-Wave opened free access to its cloud computers to researchers looking for **solutions to the covid pandemic19**⁹⁵¹. The solutions developed included solving optimization problems such as optimizing patient routing to hospitals in Japan, modeling the spread of the virus, managing nurses' schedules in hospitals, assessing the rate of virus mutation and screening molecules. It remains to be proven that D-Wave provides a real quantum advantage in solving these different problems.
- In 2022, a study showcased some potential benefits in molecular docking⁹⁵².
- Another one published in 2023 in South-Korea was about X-ray image segmentation⁹⁵³.

In data science:

- **Los Alamos National Laboratory** with **Stanford University** prototyped the detection of the formation of terrorist networks in Syria with analyzing imbalances in social networks⁹⁵⁴.

In marketing:

- **Recruit Group** uses D-Wave's quantum hybrid solver constrained quadratic model (CQM) in production to determine when these TV commercials ads run to optimize their yield⁹⁵⁵,

⁹⁴⁵ See [An Optimization Case Study for solving a Transport Robot Scheduling Problem on Quantum-Hybrid and Quantum-Inspired Hardware](#) by Dominik Leib et al, BASF, September-October 2023 (30 pages).

⁹⁴⁶ See [Emergency management today: Quantum computing is a 21st century solution for 21st century problems](#) by Alan Baratz, D-Wave, Federal News Network, July 2023.

⁹⁴⁷ See [Quantum Technology Innovation hub: Tohoku University](#), February 2023 (31 mn at minute 20).

⁹⁴⁸ See [NEC Australia: Solving the Last Mile Resupply Problem](#), 2021.

⁹⁴⁹ See [Application of Quantum Annealing to Nurse Scheduling Problem](#) by Kazuki Ikeda, Yuma Nakamura and Travis S. Humble, Osaka University and Oak Ridge National Laboratory, Nature Scientific Reports, September 2019 (10 pages).

⁹⁵⁰ Described in [Programming with D-Wave Map Coloring Problem](#), 2013 (12 pages).

⁹⁵¹ See [Can Quantum Computers Help Us Respond to the Coronavirus?](#) by Mark Anderson, April 2020.

⁹⁵² See [Multibody molecular docking on a quantum annealer](#) by Mohit Pandey et al, Menten AI, University of Victoria and Flatiron Institute, October 2022 (20 pages). It would still require larger annealers than available today, to handle sizeable molecules docking.

⁹⁵³ See [Quantum optimization algorithms for CT image segmentation from X-ray data](#) by Kyungtaek Jun, June 2023 (7 pages).

⁹⁵⁴ See [Using the D-Wave 2X Quantum Computer to Explore the Formation of Global Terrorist Networks](#) by John Ambrosiano et al, 2017 (14 pages).

⁹⁵⁵ See [Quantum in Production: Maximizing TV Commercial Reach](#), D-Wave case study (2 pages).

- **Interpublic Group** develops optimization tools for marketing campaigns.

In scientific research:

- **NASA** experimented D-Wave annealers in its joint QUAIL lab with Google in various fields, including the detection of exoplanets by analysis of telescopic observations using the transit method, as well as for various optimization and planning problems⁹⁵⁶.
- In February 2021, D-Wave and Google published a study showcasing a computational advantage of annealing with the **D-Wave Advantage** for simulating some condensed matter physics, 3 million times faster than with classical methods. It didn't exactly describe the classical hardware that is being used as a reference, but it looked like a traditional Intel-based server⁹⁵⁷. These comparisons with a single narrow algorithm are insufficient to draw any conclusions. Another similar work was published in 2022 with using 2,000 qubits for accurate simulations of coherent quantum dynamics at large scales⁹⁵⁸. This paper did show that there was indeed large scale coherence happening in D-Wave annealers, a key feature to solve complex problems.
- Several spin glass simulations have been conducted on D-Wave annealers with a potential quantum advantage^{959 960}.
- A transverse field Ising model magnetization dynamics was implemented in parallel on a D-Wave annealer, reproducing the IBM 2022 kicked Ising model experiment (using 127 superconducting qubits)⁹⁶¹.
- Polymer simulations were also achieved by a team of researchers in Italy with a seemingly quantum advantage⁹⁶².

We can also mention some recent quantum annealing algorithms:

- **Sorting lists** and building search trees or heaps, which can be modeled as QUBO problems⁹⁶³.
- **Neural network training** with using binary encoding the neural network free parameters, polynomial approximation of the activation function and reduction of binary higher-order polynomials into quadratic ones⁹⁶⁴.
- **Physical simulations** of topological matter and phase change⁹⁶⁵.

⁹⁵⁶ See [Quantum Computing at NASA: Current Status](#) by Rupak Biswas, 2017 (21 slides) as well as [Adiabatic Quantum Computers: Testing and Selecting Applications](#) by Mark A. Novotny, 2016 (48 slides).

⁹⁵⁷ See [Scaling advantage over path-integral Monte Carlo in quantum simulation of geometrically frustrated magnets](#), February 2021 (6 pages).

⁹⁵⁸ See [Coherent quantum annealing in a programmable 2000-qubit Ising chain](#) by Andrew D. King et al, Nature, February-September 2022 (24 pages).

⁹⁵⁹ See [Quantum critical dynamics in a 5,000-qubit programmable spin glass](#) by Andrew D. King et al, Nature, April 2023 (45 pages).

⁹⁶⁰ See [Accelerating equilibrium spin-glass simulations using quantum annealers via generative deep learning](#) by Giuseppe Scriva et al, October 2022 (14 pages) and the related presentation [Accelerating spin-glass simulations using quantum annealers through deep learning](#) by Sebastiano Pilati, 2021 (12 slides).

⁹⁶¹ See [Simulating Heavy-Hex Transverse Field Ising Model Magnetization Dynamics Using Programmable Quantum Annealers](#) by Elijah Pelofske et al, Los Alamos National Laboratory, November 2023 (24 pages).

⁹⁶² See [Quantum-inspired encoding enhances stochastic sampling of soft matter systems](#) by Francesco Slongo et al, Science Advances, October 2023 (9 pages) compared a quantum-inspired algorithm and its equivalent running on D-Wave.

⁹⁶³ See [QUBOs for Sorting Lists and Building Trees](#) by Christian Bauckhage et al, March 2022 (6 pages).

⁹⁶⁴ See [Completely Quantum Neural Networks](#) by Steve Abel et al, February 2022 (12 pages).

⁹⁶⁵ See [Observation of topological phenomena in a programmable lattice of 1,800 qubits](#), August 2018 (37 slides).

- **Parallelizing annealing** on several quantum annealers with decomposing a problem graph into several graphs with the DBK algorithm, used for the Maximum Clique problem with 120 nodes and 6,395 edges⁹⁶⁶ ⁹⁶⁷. These smaller disjointed graphs are executed in a D-Wave Advantage. More generic distributed quantum annealing architectures are also investigated⁹⁶⁸.

As of 2022, D-Wave had installed fewer than 10 quantum annealers at customer sites⁹⁶⁹ and operates about 30 of them in its own facilities, with more than half of them dedicated to their cloud access offering, some of them being available through the Amazon Braket cloud offering.

One D-Wave Advantage was ordered by the DoE Los Alamos National Laboratory in September 2019 and deployed since then⁹⁷⁰. In January 2022, the first D-Wave (Advantage) system was deployed in Europe, at the Forschungszentrum Jülich Supercomputing Center near Köln. It was also the first D-Wave coupled with a supercomputer as part of the Jülich UNified Infrastructure for Quantum computing (JUNIQU). The Jülich team and other researchers in Germany have published several benchmarks of various algorithms since then⁹⁷¹.

In summary, quantum annealing may be a technique contested by many specialists, but it has the merit of existing and being testable in many use cases⁹⁷².



Qilimanjaro (2019, Spain) is a startup based in Barcelona created by three physicists coming from different Spanish institutions (Barcelona Supercomputing Center, IFAE, University of Barcelona).

The founding team assembles Jose Ignacio Latorre (Chief Science Officer, also now the Director of CQT in Singapore and Chief Research of CRO Quantum at TII in Abu Dhabi, went through MIT, CERN and Niels Bohr Institute), Pol Forn-Díaz (Chief Hardware Architect, TU Delft, MIT, Caltech and IQC Waterloo), Artur Garcia Sáez (Chief Software Architect, ICFO, Stony Brook), plus Víctor Canivell (Chief Business Officer) and Jordi Blasco (Chief Financial & Legal Officer).

They develop their own quantum annealer based on coherent flux qubits. Their differentiation lies with a better qubit coherence, qubits coupling designs and qubits connectivity.

These qubits will be first controlled by classical electronics working at room temperature. In a later stage, they plan to create cryogenic controls on a separate chip. They rely on two fabs for their qubits designs, the one from IFAE and the one from the Institute of Microelectronics of Barcelona (IMB-CNM, which has similarities with the C2N in Palaiseau, France).

⁹⁶⁶ See [Solving Larger Optimization Problems Using Parallel Quantum Annealing](#) by Elijah Pelofske et al, May 2022 (16 pages).

⁹⁶⁷ See [Parallel Quantum Annealing](#) by Elijah Pelofske, Georg Hahn and Hristo N. Djidjev, November 2021-November 2022 (13 pages).

⁹⁶⁸ See [A path towards distributed quantum annealing](#) by Raúl Santos, Lorenzo Buffoni and Yasser Omar, PQI, December 2022 (11 pages).

⁹⁶⁹ Identified customers are the joint Google/NASA Quail research center, USRA (Universities Space Research Association), Lockheed Martin and the University of Southern California sharing one system, and Jülich Supercomputing Centre in Germany (since 2021). Other customers like in pharmaceutical companies are using D-Wave annealers through their Leap cloud offering.

⁹⁷⁰ See [Nuclear weapons lab buys D-Wave's next-gen quantum computer](#) by Stephen Shankland, September 2019 and [On the Emerging Potential of Quantum Annealing Hardware for Combinatorial Optimization](#) by Byron Tassef et al, October 2022 (25 pages).

⁹⁷¹ Like [Improved variational quantum eigensolver via quasi-dynamical evolution](#) by Manpreet Singh Jattana, Kristel Michielsen et al, February 2022 (19 pages) and [Quantum annealing for hard 2-SAT problems : Distribution and scaling of minimum energy gap and success probability](#) by Vrinda Mehta, Fengping Jin, Hans De Raedt and Kristel Michielsen, February 2022 (17 pages).

⁹⁷² To learn more about D-Wave, here are their [explanations about the structure of their hardware](#), a [video](#) explaining the structure of D-Wave chipsets, a [video from Linus](#), a blogger who gets into the bowels of a D-Wave 2000Q in quite a detailed way, the [video of Colin Williams's](#) presentation at USI in June 2018 in Paris (33 minutes) as well as [Near-Term Applications of Quantum Annealing](#), 2016, an interesting Lockheed Martin presentation on the uses of a D-Wave computer (34 slides). And testimonials from their customers in [Qubits 2017](#). See also [Brief description on the state of the art of some local optimization methods: Quantum annealing](#) by Alfonso de la Fuente Ruiz, 2014 (21 pages).

In a full-stack approach, they are also developing **QIBO**, a quantum software platform in the cloud. It is the cloud operating service to run software batches on the future Qilimanjaro quantum annealer, classical quantum emulators and gate-based quantum computers with a design pattern to create classical/quantum hybrid algorithms.

They extended it in 2023 with **Qibolab**, a software platform to drive qubit control electronics⁹⁷³.

They initially wanted to launch an ICO (initial coin offering) to fund the company when it was trendy but abandoned it. On top of benefiting from public grants, the company started to work for an unnamed French international company involved in logistics to develop quantum inspired optimization algorithms. They then established a partnership with Abu-Dhabi to help the Emirate create its Quantum Research Centre at the Technology Innovation Institute (QRC-TII). They provide Abu Dhabi with their know-how to build the QCR research lab and team, provide access to their technology with the goal of selling them a multi-qubit quantum processor before 2023, and let them then become self-sufficient. Jose-Ignacio Latorre became their TII's Chief Scientist after the deal was made. In 2020, he also became the director of CQT in Singapore after having been a visiting professor since 2013. CQT may play a role first in Qilimanjaro's software development efforts.

Qilimanjaro also benefits from European funding through the project **AVAQUS** already mentioned. This project coordinator is Pol Forn-Díaz, head of the IFAE Quantum Computing Technologies group on top of his role in Qilimanjaro. It involves the superconducting team from Nicolas Roch at Institut Néel in Grenoble who designs the microwave amplifiers used in flux qubits readouts.

NEC At last, let's mention that **NEC** (Japan) is also developing coherent quantum annealers using parametric oscillators and qubits as couplers.

They ambition to have an available system by 2023 with an "all-to-all" qubits connectivity (which is actually a nearest-neighbor one)⁹⁷⁴. They seem to reuse some research work done on superconducting qubits initially aimed at gate-based quantum computing. Meanwhile, they also work on some simulated annealing software running on their classical supercomputer, the SX-Aurora Tsubasa.

In June 2023, NEC announced a partnership with Tohoku University on an 8-qubit quantum annealing QPU that was developed using superconducting technology in association with the ParityQC LHZ counter-diabatic architecture. It is not sure it fares very well with regards to scalability and reaching any quantum advantage.

Superconducting qubits

After describing superconducting-based quantum annealing, let's move on to gate-based superconducting qubits quantum computers. From a physical point of view, D-Wave's accelerators and superconducting qubits ones have in common to be based on Josephson junctions but their qubit physics, overall architectures, control signals and programming models are way different.

Superconducting qubits seem to be the kings in quantum computing town, being exploited or chosen by IBM, Google, Rigetti, Amazon, Alibaba, as well as many startups such as IQM (Finland) and OQC (UK). It is the currently best scalable architecture in the gate-based model with a record of 433 operational qubits for with IBM and 176 in China as of mid-2023 (Figure 290), but with much poorer fidelities than can be demonstrated with trapped-ions (with 32 qubits).

Like all existing gate-based quantum systems, superconducting qubits computers are in the pre-NISQ or NISQ realm, *aka* noisy intermediate-scale computers, with such a low qubit gates and readout fidelity that they are impractical for most industry use cases.

⁹⁷³ See [Qibolab: an open-source hybrid quantum operating system](#) by Stavros Efthymiou et al, August 2023 (18 pages).

⁹⁷⁴ See [Quantum Computing Initiatives](#), NEC.

It is observable with the discrepancy between the number of available physical qubits (72, 80 and 433 with Google, Rigetti and IBM) and the number of qubits that are actually exploited with most useful algorithms, that does not exceed 20 at this point in time.

IBM's quantum volume is currently capped at 9 useful qubits with their best 27 qubits system using their Falcon R10 chip. We will discuss in this part the IBM quantum utility using 127 qubits that was published in June 2023 and the response from the classical computing community.

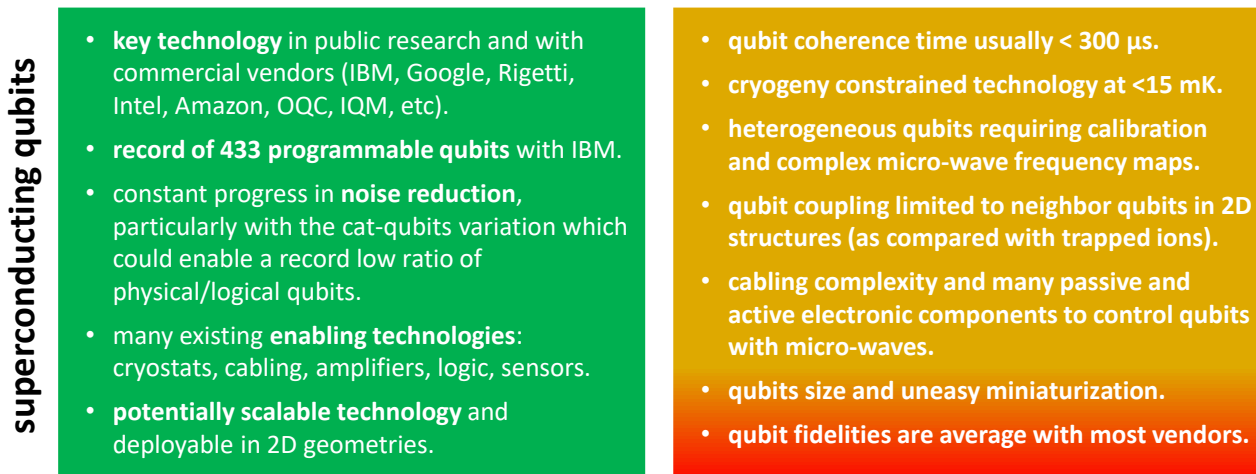


Figure 290: superconducting qubits pros and cons. (cc) Olivier Ezratty, 2021-2023.

The short term workaround of low fidelity is a mix of quantum error mitigation techniques in association with adapted quantum algorithms. Longer term workarounds are quantum error correction and qubits number scalability. It creates problems that are not yet solved with regards to fidelity stabilization with a growing number of qubits, solving the qubits cabling maze with cryogenic electronics or signals multiplexing and scaling cryostats cooling power.

Google and IBM's current approaches to scale their systems are way too optimistic as we'll see later but you can still bet on them solving both fundamental and engineering problems⁹⁷⁵.

The Josephson junction used in these qubits is a thin nanometric insulating barrier between two superconducting metals, creating a tunnel junction. It creates a quantum electrical component with a single degree of freedom, the superconducting phase difference between its electrodes, conjugated to the number of Cooper pairs passed through the junction. The supercurrent through the junction (direct current Josephson effect) is driven by the phase difference. From the electrical point of view, a Josephson junction behaves as a non-dissipative and non-linear inductance whose value depends on the phase, and thus on the current. Superconducting qubits have the particularity of being the only mainstream ones that are macroscopic, in the sense that they are not linked to the control of a single particles such as individual atoms, electrons or photons, as in most other qubit technologies.

At superconducting temperature well below the superconductivity critical temperature, Josephson junctions embedded in an electrical circuit behave as an artificial atom, with gate and/or flux controlled quantum levels and about 10^{11} electrons (100 billion) of electron Cooper pairs. They form an artificial atom with precisely controllable energy levels according to their parameters comprising a Josephson barrier, some capacitances and inductances connected in series and/or in parallel and some readout circuits using a nearby resonator⁹⁷⁶. This artificial atom property was first demonstrated in 1985.

⁹⁷⁵ See for example the review paper [A practical guide for building superconducting quantum devices](#) by Yvonne Y. Gao et al, September 2021 (49 pages).

⁹⁷⁶ This artificial atom property was demonstrated in 1985. See [Energy-Level Quantization in the Zero-Voltage State of a Current-Biased Josephson Junction](#) by John Martinis, Michel Devoret and John Clarke, 1985 (2 pages).

Superconducting qubits use non dissipative elements: capacitors, inductors and the Josephson junction which act as a nonlinear non-dissipative inductor. Capacitors store energy in the electric field while inductors store energy in the magnetic field.

But at any non-zero frequency, superconductors still dissipate some power, through two channels: the transport by the Cooper pairs and by normal charge carriers (quasiparticles), that is proportional to the quasiparticle density, which diminishes exponentially at low temperatures.

History

The history of superconducting qubits started in the mid-1980s but you need to fly back to 1957 with the elaboration of the **BCS theory** that explained (partially) how pairs of opposite spin electrons - *aka* Cooper pairs - behave at low temperatures, generating the superconducting effect. Then, 1962 marks the Josephson effect discovery by **Brian Josephson**, completed by its experimental proof in 1963 by **John M. Rowell** from the Bell Labs.

In 1980, **Anthony Leggett** modeled the collective degrees of freedom of superconducting circuits. A bit like a Bose-Einstein condensate of cold neutral atoms, Cooper-pairs of electrons in a superconducting material behave like a single quantum object with its own quantum wave⁹⁷⁷. Antony Leggett understood that the quantum behavior of a Josephson junction, if any, can be inferred from its classical behavior.

In 1985, **John Clarke**, **Michel Devoret** (his post-doc) and **John Martinis** (his PhD student), demonstrated the phenomenon of Macroscopic Quantum Tunneling of a current-biased Josephson junction out of its zero-voltage state⁹⁷⁸. Soon after, they demonstrated quantum levels for the phase. This was the first artificial electrical atom. Back then, the JJ (the little nickname for Josephson junctions) was implemented with Nb-NbO_x-PbIn (niobium, lead, indium) and cooled with a He₄-based cryostat.

In 1998, **Vincent Bouchiat**, then a PhD in **Michel Devoret**, **Daniel Esteve** and **Cristian Urbina**'s Quantronics group at CEA-Saclay in France, implemented the first Cooper Pairs Box (CPB) and characterized its ground state. Practically speaking, a Cooper pair box is a JJ connected to a voltage source by a capacitor on one side, and a Josephson junction on the other side.

The first demonstration of quantum coherent superposition with the first excited state was achieved in 1999 by **Yasunobu Nakamura** with **Yuri Pashkin** and **Jaw-Shen Tsai** at NEC Labs in Tsukuba, Japan⁹⁷⁹. It was the first "charge qubit" per se, with a tiny coherence time of 2 ns. They extended it in 2001, implementing the first measurement of Rabi oscillations associated with the transition between two Josephson levels in the Cooper pair box, using the configuration developed by Vincent Bouchiat and Michel Devoret in 1998. A first functional qubit version of the Cooper pair box, the quantronium, was demonstrated by the CEA-Saclay Quantronics team in 2002⁹⁸⁰. It took about 12 years to CEA's team to reach 4 qubits (Figure 291).

The modern version of the CPB circuit, the transmon, was developed at Yale University in 2006 (Figure 293). The Yale University research teams led by **Rob Schoelkopf**, **Michel Devoret** and **Steve**

⁹⁷⁷ See [A Brief History of Superconducting Quantum Computing](#) by Steven Girvin, August 2021 (39 mn). In a Josephson junction, the Cooper pair density difference n and the Josephson phase θ are conjugate variables with $[n, \theta]=i$.

⁹⁷⁸ See [Energy-Level Quantization in the Zero-Voltage State of a Current-Biased Josephson Junction](#) by John M. Martinis, Michel H. Devoret and John Clarke, PRL, 1985 (4 pages).

⁹⁷⁹ See [Coherent control of macroscopic quantum states in a single-Cooper-pair box](#) by Yasunobu Nakamura, Yuri Pashkin and Jaw-Shen Tsai, Nature, 1999 (4 pages).

⁹⁸⁰ See [Superconducting quantum bits](#) by Hans Mooij, Physics World, December 2004 that provides more technical insights of what was achieved in Japan and France between 1999 and 2022. It took about 12 years to CEA's team to reach 4 qubits as described in the interesting thesis [Design, fabrication and test of a four superconducting quantum-bit processor](#) by Vivien Schmidt, 2015 (191 pages). Back then, IBM and Google teams were also at a similar stage.

Girvin welcomed many talented theoreticians and experimentalists who were key contributors to the progress of transmon qubits.



Figure 291: Daniel Esteve (CEA Quantronics) showing to the author the first operational two-transmon processor in his laboratory, June 2018.

Alexandre Blais and **Andreas Wallraff** developed around 2003-2004 the key principles of circuit QED (cQED) as shown in Figure 292⁹⁸¹. It allowed quantum non-demolition readout of qubit state in the dispersive regime. A QND readout happens after measurement collapses the wave function onto $|0\rangle$ or $|1\rangle$ and a subsequent readout will yield the same $|0\rangle$ or $|1\rangle$ ⁹⁸².

Then, **David Schuster** and **Jay Gambetta** created between 2007 and 2011 2D and 3D cavity resonators designs⁹⁸³.

Jens Koch created Cooper pair boxes with a large shunting capacitance which created a modest reduction in anharmonicity and enabled strong coupling with microwave photons⁹⁸⁴.

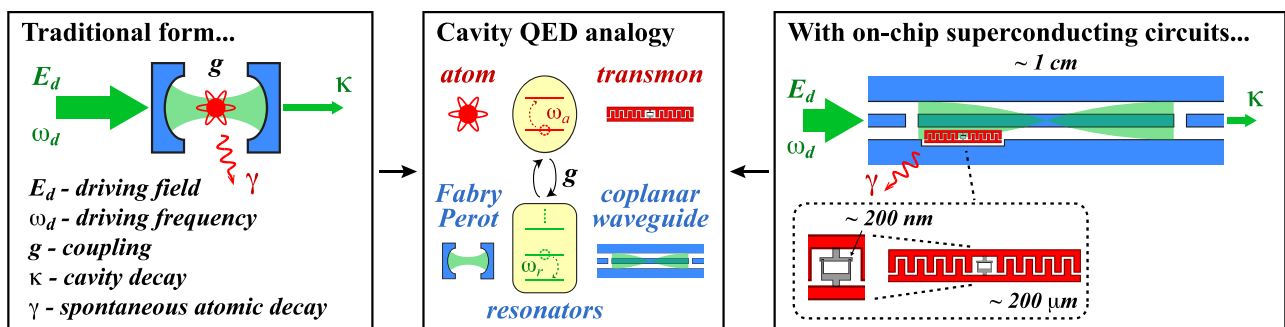


Figure 292: principles of circuit QED.

Source: [Circuit QED - Lecture Notes](#) by Nathan K. Langford, 2013 (79 pages).

⁹⁸¹ cQED was defined in [Cavity quantum electrodynamics for superconducting electrical circuits: An architecture for quantum computation](#) by Alexandre Blais, Ren-Shou Huang, Andreas Wallraff, Steve Girvin and Rob. Schoelkopf, PRA, 2004 (14 pages) and [Strong coupling of a single photon to a superconducting qubit using circuit quantum electrodynamics](#) by Andreas Wallraff, David Schuster, Alexandre Blais, Steve Girvin, Rob Schoelkopf et al, Nature, 2004 (7 pages). See also [Superconducting Qubits: A Short Review](#) by Michel H. Devoret, Andreas Wallraff and John M. Martinis, 2004 (41 pages) and [Circuit QED and engineering charge based superconducting qubits](#) by Steve Girvin, Michel Devoret and Rob Schoelkopf, 2009 (27 pages).

⁹⁸² QND was created by Vladimir Braginsky (1931-2016) in Russia in the early 1980s.

⁹⁸³ See [Circuit Quantum Electrodynamics](#) by David Schuster, 2007 (255 pages), [3D microwave cavity with magnetic flux control and enhanced quality factor](#) by Yarema Reshitnyk et al, 2016 (6 pages) and the foundational paper [Observation of high coherence in Josephson junction qubits measured in a three-dimensional circuit QED architecture](#) by Hanhee Paik, Michel Devoret et al, 2011 (5 pages).

⁹⁸⁴ See [Charge insensitive qubit design derived from the Cooper pair box](#) by Jens Koch, Terri M. Yu, Jay Gambetta, Andrew. Houck, David Schuster, J. Majer, Alexandre Blais, Michel Devoret, Steve Girvin and Rob Schoelkopf, 2007 (21 pages). That's quite a hall of fame for a paper!

superconducting qubits timeline

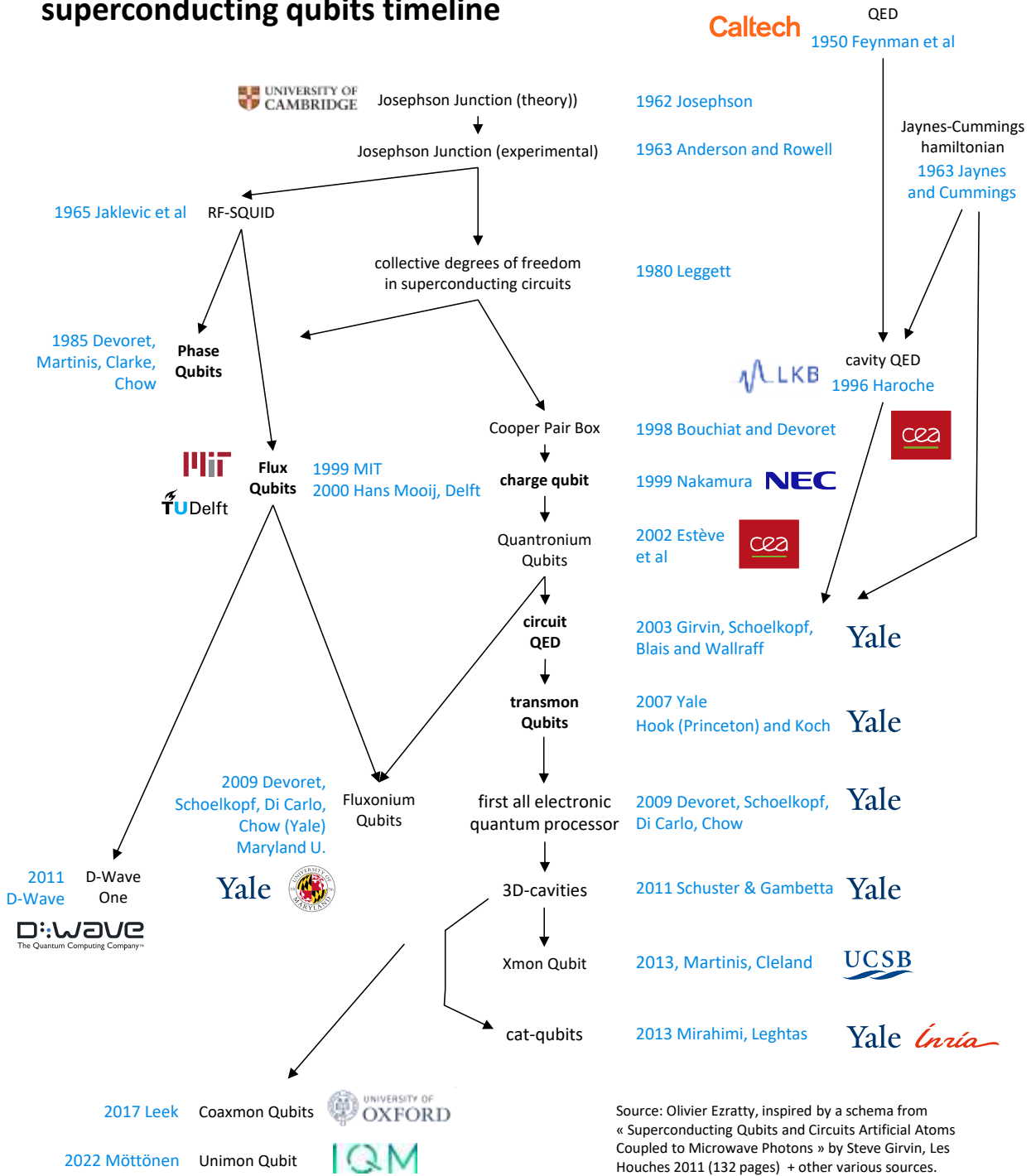


Figure 293: a historical timeline of superconducting qubits. The contribution of scientists at Yale University seems dominant here, thus the nickname of the "Yale gang". (cc) Olivier Ezratty, 2022-2023.

Jerry Chow was also a key contributor between 2005 and 2010 and has since then been at IBM, now leading their quantum hardware system developments in Jay Gambetta's team. In 2009, Devoret, Schoelkopf, **Leonardo Di Carlo** (now at TU Delft), **Jerry Chow** et al created the first programmable two-qubit processor and implemented a small Grover search on it. The first functional two-qubit processor fully fitted with a universal set of gates and individual single-shot qubit readout was then in 2012 demonstrated with Grover's search algorithm by A. Dewes et al at CEA Saclay.

Blake Robert Johnson proposed in 2011 to use a Purcell filter to protect a qubit from spontaneous emission coming from the Purcell effect that is a relaxation through the readout resonator. It is a mix of low-pass and high-pass microwave filter⁹⁸⁵. The spontaneous emission rate (SER) is one key contributor that affects a superconducting qubit coherence time T_1 .

In another domain, **Matt Reagor** and **Hanhee Paik** improved in 2013 the stability of microwaves and qubit coherence (T_1/T_2) with transmons embedded in 3D cavities⁹⁸⁶. These high Q-factor cavities enable long T_1 and are still investigated⁹⁸⁷.

Other contributions worth mentioning are **Hans Mooij** (TU Delft) who created a flux-qubit with three Josephson junctions in 1999 with experiments done in 2000. **Andrew Hook** (Princeton) contributed to the development of the transmon qubit. In 2010, **Andrew Cleland**, **John Martinis** and their PhD **Arron O'Connell** were able to entangle three flux superconducting qubits and to control it with a mechanical resonator⁹⁸⁸. It led to the creation of the Xmon tunable qubit in 2013⁹⁸⁹, which was later used by John Martinis at Google after 2014. **Andrew Cleland** now runs his own lab at the University of Chicago.

In 2017, **Peter Leek** then at Oxford created the coaxmon superconducting qubit, where the qubit and resonator are on opposing sides of a single chip, with control and readout wiring being provided by coaxial wiring running perpendicular to the chip plane⁹⁹⁰. It led the same year to the creation of OQC.

In 2022, **Mikko Möttönen** from IQM created the Unimon superconducting qubit with a simpler setting, better nonlinearity and fidelities⁹⁹¹. However, both these qubits have not yet showcased improved figures of merit vs the state of the art.

Then, cat-qubits were created in 2013 by **Mazyar Mirrahimi** at Yale with Michel Devoret, with later contributions by **Zaki Leghtas** and many advances since then.

Let's now circle back to the different types of superconducting qubits that differ in the way they encode quantum information in two distinct states⁹⁹² (Figure 294):

Phase Qubits use larger Josephson junctions than in charge qubits. Their state corresponds to two levels of current energy in a Josephson junction. This approach was tested by NIST in the USA among other places but no commercial vendor seems to use this type of superconducting qubit. John Martinis tested such qubits back in 2012 at UCSB in a 5-qubit system used to factorize the number 15⁹⁹³. A German (Jülich, University of Munster) and Russian (Kotelnikov Institute) team proposed in early 2020 to use $\text{YBa}_2\text{Cu}_3\text{O}_{7-x}$ nanotubes (also called YBCO, for yttrium, barium, copper and oxide,

⁹⁸⁵ See [Controlling Photons in Superconducting Electrical Circuits](#) by Blake Robert Johnson, a thesis under the direction of Rob Schoelkopf, 2011 (190 pages) which proposed the Purcell filter. See also [Controlling the Spontaneous Emission of a Superconducting Transmon Qubit](#) by Andrew Houck, Jay Gambetta, Michel Devoret, Rob Schoelkopf et al, 2008 (4 pages) and [Quantum theory of a bandpass Purcell filter for qubit readout](#) by Eyob A. Sete et al, 2015 (15 pages). The spontaneous emission rate (SER) is one key contributor that affects a superconducting qubit coherence time T_1 .

⁹⁸⁶ See [Reaching 10 ms single photon lifetimes for superconducting aluminum cavities](#) by Matt Reagor, Hanhee Paik et al, 2013 (4 pages).

⁹⁸⁷ See the review paper [Advancements in Superconducting Microwave Cavities and Qubits for Quantum Information Systems](#) by Alex Krasnok et al, April 2023 (57 pages).

⁹⁸⁸ See [Quantum ground state and single-phonon control of a mechanical resonator](#) by Aaron O'Connell, John Martinis, Andrew Cleland et al, Nature, 2010 (7 pages).

⁹⁸⁹ See [Coherent Josephson qubit suitable for scalable quantum integrated circuits](#) by R. Barends, John Martinis and Andrew Cleland, April 2013 (10 pages).

⁹⁹⁰ See [Double-sided coaxial circuit QED with out-of-plane wiring by J. Rahamim](#), Peter Leek et al, 2017 (4 pages).

⁹⁹¹ See [Unimon qubit](#) by Eric Hyppä, Mikko Möttönen et al, March 2022 (37 pages).

⁹⁹² This is well explained in [Practical realization of Quantum Computation](#), (36 slides).

⁹⁹³ See [Computing prime factors with a Josephson phase qubit quantum processor](#) by Erik Lucero, John Martinis et al, 2012 (5 pages).

which is superconducting at 92K) to create phase qubits controllable by a single microwave photon⁹⁹⁴. Overall, the phase qubit seems to be dead-end.

Flux Qubits: their states correspond to the direction of flow of the superconducting current in its loop. It couples a capacitor, from one to three Josephson junctions and a superinductor and has high coherence and large anharmonicity which also enable the handling of qutrits instead of qubits like what Rigetti is experimenting. Measuring the state of such a qubit uses a SQUID (superconducting quantum interference device) with two Josephson junctions connected in parallel, a magnetometer that measures the current direction in the qubit, thus its basis state 0 or 1. This type of superconducting qubit is adopted by Rigetti, Alibaba^{995 996 997}, Bleximo and Atlantic Quantum in the industry vendor space. It is studied in research labs at the MIT Lincoln Lab and within Atlantic Quantum⁹⁹⁸, the Lawrence Berkeley National Laboratory (Irfan Siddiqi^{999 1000}), the University of Berkeley and Yale University (Shruti Puri), the University of Maryland (Vladimir Manucharyan with a T_2 exceeding 1.35 ms and single-qubit gate fidelity over 99.99%^{1001 1002} and flip-chip packaging with an SFQ electronics chip¹⁰⁰³), Princeton University¹⁰⁰⁴, Stanford University¹⁰⁰⁵, NBI in Denmark¹⁰⁰⁶, in Russia (with two qubits CZ gates fidelities of 99.23%^{1007 1008}) and in Israel at Bar Ilan University (with improved fabrication techniques^{1009 1010}). In recent works, fluxonium qubits generated the best T_1/T_2 with T_1 exceeding 1 ms. They use control frequencies usually below 3 GHz which lowers down dielectric loss effects and leads to long relaxation time T_1 .

⁹⁹⁴ See [Energy quantization in superconducting nanowires](#), February 2020, referring to [Energy-level quantization and single-photon control of phase slips in YBa2Cu3O7-x nanowires](#) by M. Lyatti, February 2020.

⁹⁹⁵ See [Fluxonium qubits for ultra-high-fidelity and scalable quantum processors](#) by Chunqing Deng, (49 minutes).

⁹⁹⁶ See [Fluxonium: An Alternative Qubit Platform for High-Fidelity Operations](#) by Feng Bao et al, 2022 (19 pages).

⁹⁹⁷ See [Characterization of loss mechanisms in a fluxonium qubit](#) by Hantao Sun et al, Alibaba, February 2023 (17 pages).

⁹⁹⁸ See [High-Fidelity, Frequency-Flexible Two-Qubit Fluxonium Gates with a Transmon Coupler](#) by Leon Ding, William D. Oliver et al, MIT and Atlantic Quantum, PRX, April-September 2023 (23 pages).

⁹⁹⁹ See [Scalable High-Performance Fluxonium Quantum Processor](#) by Long B. Nguyen, Irfan Siddiqi Singh et al, January 2022 (29 pages).

¹⁰⁰⁰ See [Blueprint for a High-Performance Fluxonium Quantum Processor](#) by Long B. Nguyen, Shruti Puri, Irfan Siddiqi et al, Berkeley, Yale and Bleximo, PRX Quantum, August 2022 (38 pages) which details very well the design challenges with fluxonium qubits.

¹⁰⁰¹ See [Millisecond coherence in a superconducting qubit](#) by Aaron Somoroff, Vladimir Manucharyan et al, University of Maryland, PRL, March 2021-June 2023 (14 pages). Not only do they have a T_2 exceeding 1.35 ms but their single-qubit gate fidelity also exceeds 99.99% (with a few qubits, though).

¹⁰⁰² See [The high-coherence fluxonium qubit](#) by Long B. Nguyen, Vladimir Manucharyan et al, October 2018 (12 pages).

¹⁰⁰³ See [Fluxonium Qubits in a Flip-Chip Package](#) by Aaron Somoroff, Oleg Mukhanov, Vladimir Manucharyan et al, March-December 2023 (13 pages) which describes flip-chip bonding between a fluxonium qubit chip and a SFQ qubit drive chip.

¹⁰⁰⁴ See [DEC-QED: A flux-based 3D electrodynamic modeling approach to superconducting circuits and materials](#) by Dzung N. Pham et al, Princeton, December 2022 (21 pages).

¹⁰⁰⁵ See [Strong dispersive coupling between a mechanical resonator and a fluxonium superconducting qubit](#) by Nathan R. A. Lee et al, Stanford University, April 2023 (22 pages).

¹⁰⁰⁶ See [Fast universal control of a flux qubit via exponentially tunable wave-function overlap](#) by Svend Krøjer et al, NBI, March 2023 (11 pages).

¹⁰⁰⁷ See [High fidelity two-qubit gates on fluxoniums using a tunable coupler](#) by Ilya N. Moskalenko, Ilya S. Besedin et al, Russian Quantum Center, March 2022 (18 pages).

¹⁰⁰⁸ See [High fidelity two-qubit gates on fluxoniums using a tunable coupler](#) by Ilya N. Moskalenko, Ilya S. Besedin et al, npj Quantum Information, November 2022 (10 pages).

¹⁰⁰⁹ See [Reproducibility and Gap Control of Superconducting Flux Qubits](#) by T. Chang, Michael Stern et al, Bar-Ilan University and University of Melbourne, PRA, December 2022 (20 pages).

¹⁰¹⁰ See [Tunable Superconducting Flux Qubits with Long Coherence Times](#) by T. Chang, T. Cohen, I. Holzman, G. Catelani, and Michael Stern, PRA, February 2023 (12 pages).

Single-qubit gates can have good speed in the range of 10 ns and errors levels around 10^{-4} . In this architecture, both readout and control crosstalk are expected to be small^{1011 1012}. The main shortcomings of flux qubits are their bad protection from both relaxation (T_1) and dephasing (T_2) and circuit complexity for gates and readout.

The **heavy fluxonium** variant uses a different geometry with a 3D transmon shunted by a large linear inductance of a Josephson array¹⁰¹³. Qubit gates can be driven by simple DC and RF flux, removing the need for complex microwave waveforming with AWG (arbitrary waveform generators). It reached two-qubit gate fidelities of 99.9%, although with only two qubits.

In the quantum annealing domain, D-Wave uses flux controlled SQUIDs that are coupled magnetically to implement a quantum annealing process. The company has plans to implement flux qubits in a gate-based mode, with completely different chip designs.

Charge Qubits: their states correspond to current flow thresholds in the Josephson junction of the superconducting loop. Small Josephson junctions delimit a superconducting island with a well-defined electrical charge. The basis states of such charge qubits are the states of charge of the island in Cooper pairs. The most common variant is the **transmon**, for “transmission line shunted plasma oscillation qubit”, which reduces the effect of charge noise but with a weaker anharmonicity¹⁰¹⁴. With transmons, the Cooper pairs box is operated in the phase regime.

The nonlinear Josephson junction inductance makes the LC resonator slightly anharmonic, and its two lowest energy levels are the basis states of the qubit. Transmons are used by IBM, Google, IQM and others. To date, these are the qubits generating the lowest error rate in superconducting qubits but their low anharmonicity creates a toll on gate and readout speeds.

They are divided into at least two categories: qubits with a single Josephson junction (single junction transmon, used by IBM) or with two Josephson junctions connected in parallel (split transmon, used by Google)¹⁰¹⁵.

Then, you have many variations with the **coaxmon** (OQC) and **unimon** (IQM), the **mergemon** or merged element transmon where the Josephson junction is engineered to act as its own parallel shunt capacitor, reducing the size of the qubit¹⁰¹⁶. Here, the split junction is based on a SQUID geometry, equivalent of a tunable Josephson junction. It is very convenient, but sensitive to flux noise. There are other variations like the **Blochnium**¹⁰¹⁷ and the **quartic Blochnium**¹⁰¹⁸, with large inductances made of many Josephson junctions, enabling better anharmonicity, and the **Kinemon** developed in Russia, with inductively shunts transmons to improve the two-level system anharmonicity¹⁰¹⁹.

¹⁰¹¹ See [Transmon and Fluxonium Qubits](#) by Emanuel Hubenschmid, June 2020 (106 slides).

¹⁰¹² See [Characterizing crosstalk of superconducting transmon processors](#) by Andreas Ketterer et al, March 2023 (9 pages).

¹⁰¹³ See [Tunable inductive coupler for high fidelity gates between fluxonium qubits](#) by Helin Zhang, Jens Koch, David I. Schuster et al, University of Chicago, Stanford, Princeton, September 2023 (17 pages).

¹⁰¹⁴ See [Charge insensitive qubit design derived from the Cooper pair box](#) by Jens Koch, Jay Gambetta, Alexandre Blais, Michel Devoret, Rob Schoelkopf et al, 2007 (21 pages).

¹⁰¹⁵ Transmon is a diminutive of "Transmission line shunted plasmon oscillation circuit" created by Rob Schoelkopf, in other words, an oscillator circuit based on shunted Josephson junction. The shunt has become a capacitance that filters low frequencies. A plasmon is the collective behavior of free electrons of metals, here in the form of superconducting Cooper pairs.

¹⁰¹⁶ See [Merged-element transmon](#) by R. Zhao et al, December 2020 (8 pages) and [Merged-Element Transmons: Design and Qubit Performance](#) by H. J. Mamin et al, IBM Research, August 2021 (8 pages).

¹⁰¹⁷ See [The superconducting quasicharge qubit](#) by Ivan V. Pechenezhskiy, Vladimir E. Manucharyan et al, University of Maryland, July 2019-March 2021 (6 pages).

¹⁰¹⁸ See [The quartic Blochnium: an anharmonic quasicharge superconducting qubit](#) by Luca Chirolli, Matteo Carrega, and Francesco Giazotto, April 2023 (9 pages).

¹⁰¹⁹ See [Kinemon: inductively shunted transmon artificial atom](#) by Daria Kalacheva et al, June 2023 (10 pages).

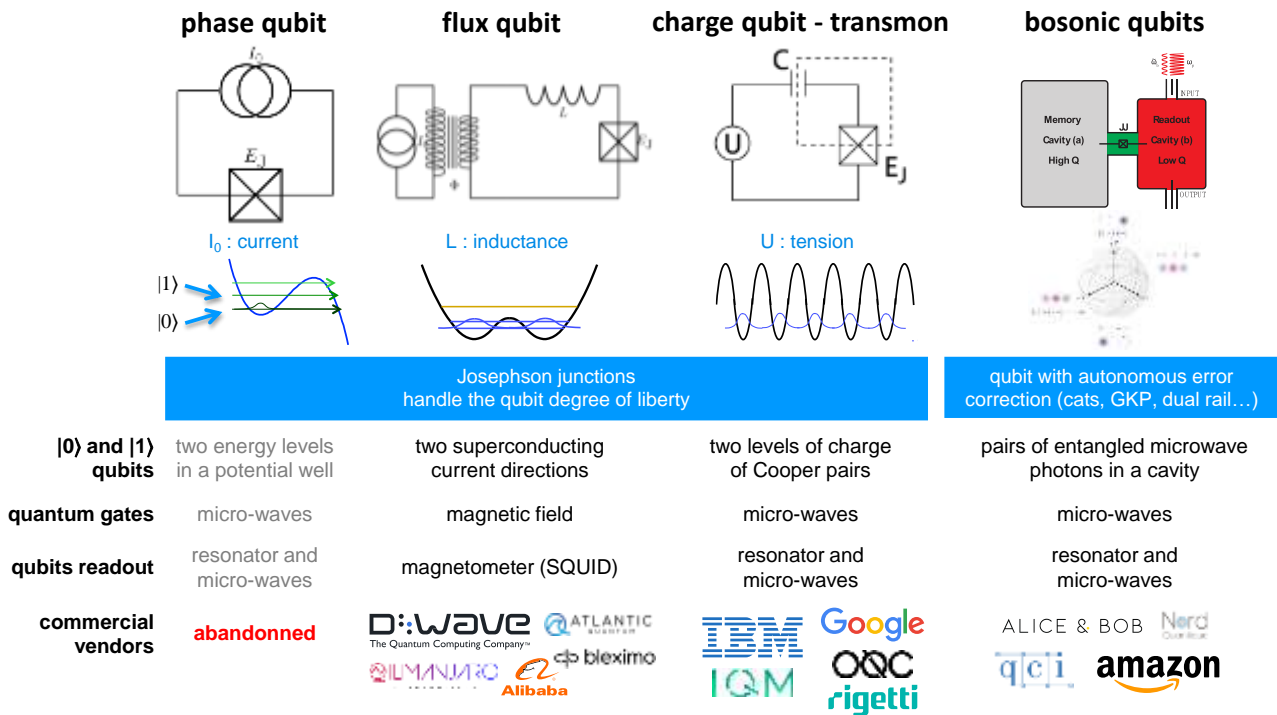


Figure 294: the different types of superconducting qubits and the related industry vendors. inspired from [Implementing Qubits with Superconducting Integrated Circuits](#) by Michel Devoret, 2004 (41 pages) and [Flux Noise in Superconducting Qubits](#), 2015 (44 slides). Updated in 2023.

Andreev Spin Qubits (ASQ) is a research-level qubit that relies on a localized microscopic excitation of the BCS condensate that natively has only two levels and is based on a nanowire. It is not a collective excitation of the superconducting loop circuit. This qubit type was proposed at and is studied at Chalmers in Sweden¹⁰²⁰ (funded as a H2020 program from 2019 to 2023¹⁰²¹), Yale, at CEA Saclay in France¹⁰²², NBI in Denmark and also QuTech in The Netherlands, among other places. Since it manipulates electron spins in relation to a superconducting resonator and makes use of circuit electrodynamics (cQED), it sits in between the categories of superconducting and silicon spin qubits¹⁰²³¹⁰²⁴.

Bosonic qubits correspond to a broad category of qubits that are resilient to noise or generating less noise and make it possible to assemble logical qubits with much fewer physical qubits, in the 10-100 range instead of 1,000-10,000 range¹⁰²⁵.

¹⁰²⁰ See the initial proposal in [Andreev Level Qubit](#) by A. Zazunov et al, PRL, 2003 (4 pages), [Dynamics and phonon-induced decoherence of Andreev level qubit](#) by A. Zazunov et al, PRB, 2005 (22 pages) and the thesis [Coherent manipulation of Andreev Bound States in an atomic contact](#) by Camille Janvier, CEA Quantronics, 2016 (268 pages). And recent research in [Coherent manipulation of an Andreev spin qubit](#) by M. Hays, Michel Devoret et al, Science, 2021 (17 pages) and [Direct manipulation of a superconducting spin qubit strongly coupled to a transmon qubit](#) by Marta Pita-Vidal et al, August 2022 (24 pages).

¹⁰²¹ See [Andreev qubits for scalable quantum computation](#) with an EU contribution of 3.5M€.

¹⁰²² See [Circuit-QED with phase-biased Josephson weak links](#) by C. Metzger, Christian Urbina, Hugues Pothier et al, January 2021 (22 pages).

¹⁰²³ See [Spectroscopy of spin-split Andreev levels in a quantum dot with superconducting leads](#) by Arno Bargerbos, August-September 2022 (27 pages).

¹⁰²⁴ See [Direct manipulation of a superconducting spin qubit strongly coupled to a transmon qubit](#) by Marta Pita-Vidal et al, Nature Physics, May 2023 (24 pages).

¹⁰²⁵ See [Quantum information processing with bosonic qubits in circuit QED](#) by Atharv Joshi et al, 2021 (24 pages).

It contains cat-qubits and **GKP codes**^{1026 1027 1028 1029}. Other protected qubits include the **zero- π qubits** of Peter Brooks, Alexei Kitaev and John Preskill which use two Josephson junctions, the **bifluxon**¹⁰³⁰, **cos(2 θ) qubits**¹⁰³¹, the **Kerr-cat**¹⁰³², **dual-rail** encoding qubits studied at Yale and Oxford University¹⁰³³ and other variants^{1034 1035 1036}. These qubits implement so-called autonomous error correction with engineered dissipation since removing error has the effect to generate some spare energy that must be dissipated¹⁰³⁷. The cat-qubits approach is chosen by **Alice&Bob** (France), and **QCI** (USA) while **Nord Quantique** (Canada) and **AWS** (USA) are using GKP codes. Cat-qubits are also investigated in many other research labs like **RIKEN** in Japan¹⁰³⁸ on top of regular transmon qubits with a record prototype chip of 100 qubits^{1039 1040}.

cat-qubits are cavity-based qubits connected to a transmon qubit used only for their preparation, readout and/or correction depending on the implementation. The cat-qubit technique was devised by Mazyar Mirrahimi and Zaki Leghtas around 2013, particularly during their work at Yale University with Michel Devoret. It was then adopted by Rob Schoelkopf's team at Yale. It is the technology being developed by Alice&Bob^{1041 1042} and AWS although they are also investigating GKP qubits.

The **QuCoS** QuantERA collaborative three-year European project is focused on demonstrating the scalability of cat-qubits. It combines the University of Innsbruck (Gerhard Kirchmair), ENS Lyon (Benjamin Huard), Mines ParisTech and ENS Paris (Zaki Leghtas), KIT (Ioan Pop), Inria (Mazyar Mirrahimi), the Romanian National Institute for Research and Development of Isotopic and Molecular Technologies (Luiza Buimaga-Iarinca) and Quantum Machines (Israel).

¹⁰²⁶ See [Advances in Bosonic Quantum Error Correction with Gottesman-Kitaev-Preskill Codes: Theory, Engineering and Applications](#) by Anthony J. Brady et al, August 2023 (86 pages).

¹⁰²⁷ See [Stability and decoherence rates of a GKP qubit protected by dissipation](#) by Lev-Arcady Sellem, Rémi Robin, Philippe Campagne-Ibarcq and Pierre Rouchon, April 2023 (16 pages) which presents a GKP code correcting both flip and phase errors.

¹⁰²⁸ See [Real-time quantum error correction beyond break-even](#) by V. V. Sivak, Steve M. Girvin, Rob J. Schoelkopf and Michel H. Devoret, Nature, March 2023 (42 pages).

¹⁰²⁹ See [A GKP qubit protected by dissipation in a high-impedance superconducting circuit driven by a microwave frequency comb](#) by Lev-Arcady Sellem, Alain Sarlette, Zaki Leghtas, Mazyar Mirrahimi, Pierre Rouchon, Philippe Campagne-Ibarcq, April 2023 (61 pages).

¹⁰³⁰ See [Moving beyond the transmon: Noise-protected superconducting quantum circuits](#) by András Gyenis, Alexandre Blais, Andrew A. Hook, David I. Schuster et al, June 2021 (14 pages).

¹⁰³¹ See [Cat-qubit-inspired gate on cos\(2 \$\theta\$ \) qubits](#) by Catherine Leroux and Alexandre Blais, April 2023 (12 pages).

¹⁰³² See [Control of the ZZ coupling between Kerr-cat qubits via transmon couplers](#) by Takaaki Aoki et al, March 2023 (8 pages).

¹⁰³³ See [Dual-rail encoding with superconducting cavities](#) by James D. Teoh, Robert J. Schoelkopf et al, PNAS, October 2023 (26 pages).

¹⁰³⁴ See [Superconducting circuit protected by two-Cooper-pair tunneling](#) by W. C. Smith, A. Kou, X. Xiao, U. Vool and M. H. Devoret, 2020 (9 pages) which uses pairs of Cooper pairs to create a qubit that is insensitive to multiple relaxation and dephasing mechanisms.

¹⁰³⁵ See [Encoding qubits in multimode grid states](#) by Baptiste Royer, Shraddha Sing and Steven M. Girvin, January 2022 (38 pages).

¹⁰³⁶ See [Coherent control of a multi-qubit dark state in waveguide quantum electrodynamics](#) by Maximilian Zanner et al, Nature Physics, March 2022 (8 pages).

¹⁰³⁷ See [Hardware efficient autonomous error correction with linear couplers in superconducting circuits](#) by Ziqian Li et al, University of Chicago, March 2023 (8 pages).

¹⁰³⁸ See [Fault-Tolerant Multi-Qubit Geometric Entangling Gates Using Photonic Cat Qubits](#) by Ye-Hong Chen et al, RIKEN, 2021 (12 pages). About a realization of Mølmer-Sørensen multi-qubit cat-qubits gates.

¹⁰³⁹ RIKEN also launched a home-made 64-qubit transmon superconducting QPU in March 2023 that is available in the cloud.

¹⁰⁴⁰ See [RIKEN Center for Quantum Computing Activity Report](#), May 2023 (58 pages).

¹⁰⁴¹ See [High-performance repetition cat code using fast noisy operations](#) by Francois-Marie Le Régent, Camille Berdou, Zaki Leghtas, Jérémie Guillaud, Mazyar Mirrahimi, December 2022 (15 pages).

¹⁰⁴² See [Designing High-Fidelity Gates for Dissipative Cat Qubits](#) by Ronan Gautier, Mazyar Mirrahimi and Alain Sarlette, March 2023 (22 pages).

How about using superconducting qubits for implementing quantum simulations? It is not a common practice. One of the reasons is the lack of generic long-range connectivity that could enable some direct entanglement between all qubits. It would require a different physical arrangement of the qubits and to create specific long-range connections between the qubits. This is possible by using cross-resonance gates that create interactions between qubits with their respective resonance frequencies.

Science

For what follows, we will focus on transmon qubits that are the most common and exploited by IBM, Google and IQM. They are anharmonic and therefore nonlinear oscillators. Their nonlinearity comes from the Josephson junction which allows to better separate two energy states of the superconducting loop (on the right in Figure 295). In a quantum harmonic oscillator (QHO), the energy levels are spaced equally and are multiples of the first energy level ($\hbar\omega_r$ in the diagram). The capacitance has an electrical energy (kinetic) and the inductance has a magnetic energy (potential).

With a transmon qubit, the Josephson tunnel junction has a nonlinear inductance which creates its anharmonicity. In both cases, the flowing current is quantized with discrete energy levels corresponding to the horizontal bars in the graph in Figure 295, with corresponding different current phases corresponding to the intersection between these bars and the parabolic (QHO) and cosinusoidal (JJ) curves.

These energy states are usually controlled by microwave pulses in the 5 GHz regime. These interactions between superconducting qubits and microwave photons are part of a branch of quantum physics called **circuit quantum electrodynamics**, or cQED¹⁰⁴³.

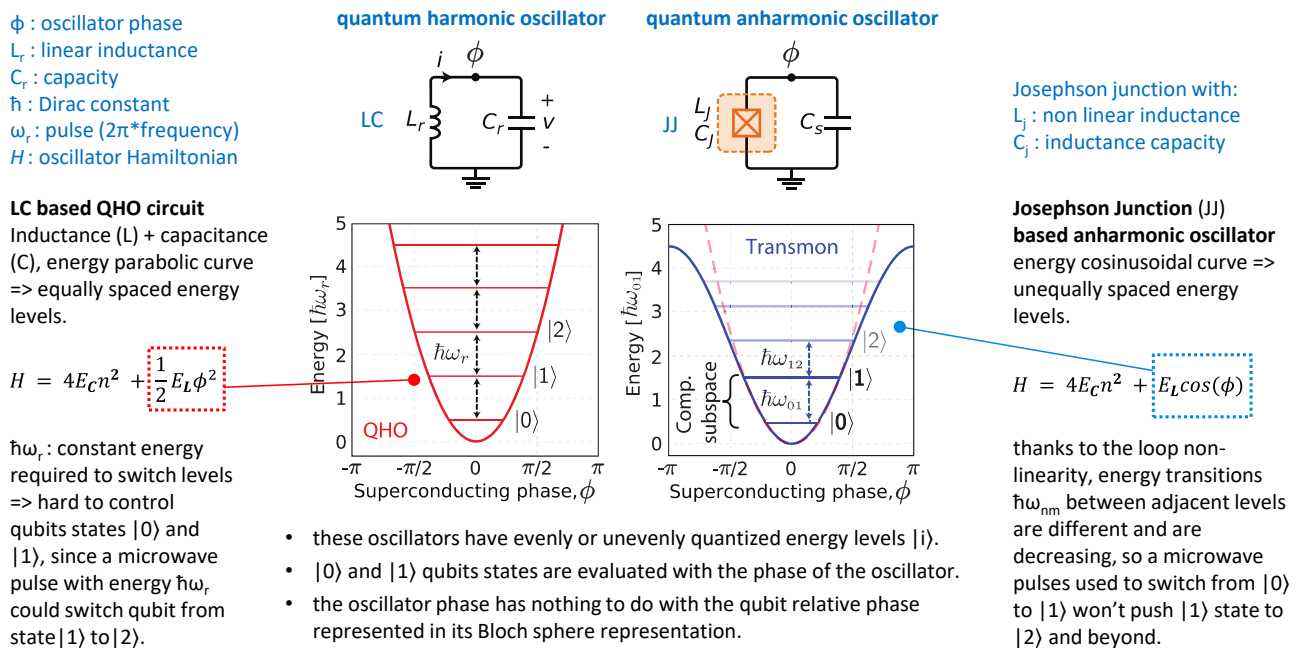


Figure 295: why superconducting qubits use an anharmonic oscillator. (cc) Olivier Ezratty, 2022-2023, with schema from "A Quantum Engineer's Guide to Superconducting Qubits" by Philip Krantz et al, 2019-2021 (67 pages).

¹⁰⁴³ See [Circuit-QED with phase-biased Josephson weak links](#) by C. Metzger, Christian Urbina, Hugues Pothier et al, January 2021 (22 pages). Serge Haroche was awarded the Nobel prize in physics in 2012 for his work on the interaction between cold atoms and superconducting cavities. See on this subject the excellent [Circuit Quantum Electrodynamics](#) by Alexandre Blais, Andreas Wallraff et al, May 2020 (82 pages).

Qubits use a linear superposition of the first two energy levels which have a different wave function relating the phase and current probabilities across the Josephson junction. The superposed states in the Bloch sphere equator like $(|0\rangle + |1\rangle)/\sqrt{2}$ and $(|0\rangle - |1\rangle)/\sqrt{2}$ correspond to an oscillating current that is dampened over time, as Rabi oscillations, in the 10 MHz range, shown in Figure 296.

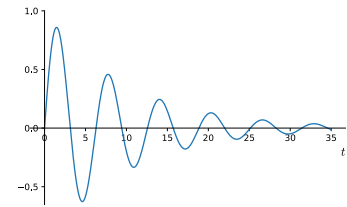


Figure 296: The Rabi oscillation of the superconducting current representing superposed qubit states, at a frequency in the 10 MHz range.

The $\hbar\omega_{01}$ energy level between the basis states $|0\rangle$ and $|1\rangle$ correspond to microwave frequencies in the 4 to 15 GHz band.

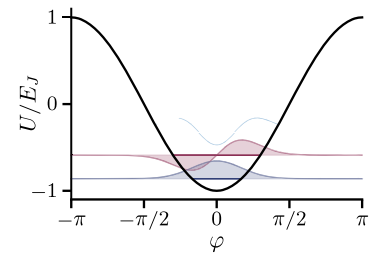


Figure 297: $|0\rangle$ and $|1\rangle$ wave function giving the probability of phase φ in blue and green. Source: [Superconducting circuit protected by two-Cooper-pair tunneling](#) by W. C. Smith et al, 2020 (9 pages).

These frequencies must be well separable from the following ones. This separation is made possible because the (microwave photon) energy sent to move from one level to the other is different from one of these levels to other higher levels (Figure 297). Since the upper levels are less spaced, their related transition energy is lower. As the qubits are activated by microwaves, they are no longer likely to switch to a higher energy level. The anharmonic oscillator in the Josephson loop is provided by a nonlinear inductance L_j . The energy level between $|0\rangle$ and $|1\rangle$ of $\hbar\omega_{01}$ is higher than the energy levels needed to go to the upper levels $\hbar\omega_{12}$ and $\hbar\omega_{23}$. It is also compatible with the cooling temperature of the processor and the ambient noise.

Those of the superconducting qubits control around 5 GHz have an energy level equivalent to a temperature of about 250 mK, much higher than the 15 mK temperature commonly used¹⁰⁴⁴. There are many rationales explaining the microwaves frequencies being used with superconducting qubits. Above 8 GHz, electronics are too expensive and below 4 GHz, the ambient thermal in the cryostat noise is too important. Also, the used microwaves correspond to the lowest frequency modes for which one can reach the ground state with a dilution refrigerator (Figure 298). But quasiparticles in the qubit are not mainly broken by the microwaves brought in, but by higher frequencies and infrared light passing through all microwave lines or entering the cryostat, thus the need for filters, attenuators and various shielding around the qubit chip.

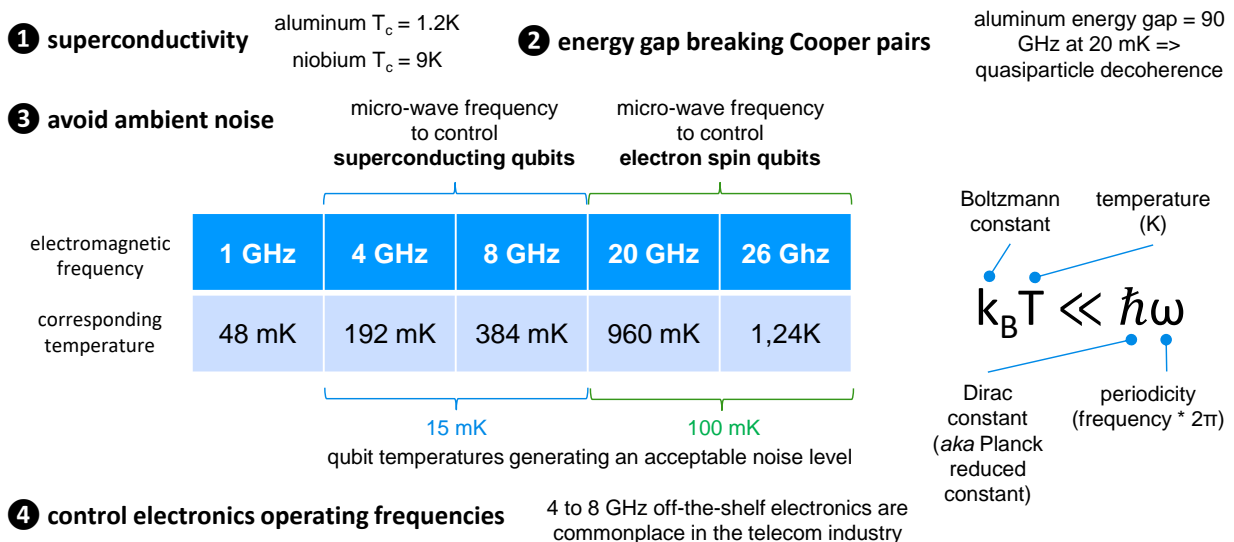


Figure 298: the rationale behind the 15 mK operating temperature of superconducting qubits. Many reasons explain why these qubits are operated at this low temperature. It is not just about materials superconductivity limits. (cc) Olivier Ezratty, 2021-2024.

¹⁰⁴⁴ See [Why 4-8 GHz? The rationale behind common qubit frequencies](#), The Observer, January 2022.

The microwaves for silicon qubit control are located between 8 and 26 GHz and enable qubit temperatures of 100 mK while some can even reach 1.5K.

There is another reason for running the qubit at around 15 mK. It takes a certain amount of energy, known as the energy gap, to break up the Cooper pairs running in a superconducting qubit. In aluminum, that is the typical material used to create the Josephson junction and its surroundings, the energy gap corresponds to 90 GHz at 20 mK, creating quasiparticle decoherence. It is an order of magnitude greater than the energy difference between the two levels in a qubit. It means that the qubit can be driven with lower energies (in the 4-8 GHz range) without breaking up the superconducting current Cooper pairs and altering the quantum coherence of the qubit¹⁰⁴⁵.

What differentiates phase, charge (transmon) and flux qubits are the relative values of the charge energy (E_C , aka Coulomb charge energy), the Josephson coupling energy (E_J) and the qubit inductance energy (E_L)¹⁰⁴⁶ (Figure 299).

		$E_L/(E_J - E_C)$			
		0	$\ll 1$	~ 1	$\gg 1$
E_J/E_C	$\ll 1$	cooper-pair box			
	~ 1	quantronium	fluxonium		
	$\gg 1$	transmon			flux qubit
	$\gg \gg 1$			phase qubit	

Figure 299: periodic table of superconducting circuits. Source: [Introduction to Quantum Electromagnetic Circuits](#) by Uri Vool and Michel Devoret, 2017 (56 pages).

Then, just with transmon qubits, you find other variations with:

- Fixed (IBM, MIT¹⁰⁴⁷) or tunable (Google) qubit frequencies.
- Tunable couplers (Google).
- Architectures mixing digital and analog superconducting computing¹⁰⁴⁸.
- Controlled-phase gates with variable amplitude and frequency which could significantly reduce the depth of quantum circuits particularly for implementing a quantum Fourier transform required in many algorithms like Shor, HHL and QML (C-R₀)¹⁰⁴⁹.
- New techniques to implement faster qubit readout¹⁰⁵⁰.
- And techniques using qutrits instead of qubits, with Rigetti and others¹⁰⁵¹).
- Trying to operate superconducting qubits at higher temperatures with replacing aluminum by niobium¹⁰⁵².

Of course, many researchers are looking for ways to improve qubits fidelities with better materials and designs¹⁰⁵³.

¹⁰⁴⁵ Source: [Superconducting quantum bits](#) by Hans Mooij, Physics World, December 2004.

¹⁰⁴⁶ This is explained in [Experiments on superconducting qubits coupled to resonators](#) by Marcus Jerger aus Bühl, 2013 (140 pages).

¹⁰⁴⁷ See [Cancelling microwave crosstalk with fixed-frequency qubits](#) by Wuerkaixi Nuerbolati et al, April 2022 (5 pages).

¹⁰⁴⁸ See [Superconducting Circuit Architecture for Digital-Analog Quantum Computing](#) by J. Yu, Enrique Solano et al, March 2021 / May 2022 (23 pages).

¹⁰⁴⁹ See [Extensible circuit-QED architecture via amplitude- and frequency-variable microwaves](#) by Agustin Di Paolo, Alexandre Blais, William D. Oliver et al, MIT, April 2022 (29 pages).

¹⁰⁵⁰ See [Fast readout and reset of a superconducting qubit coupled to a resonator with an intrinsic Purcell filter](#) by Yoshiaki Sunada, Yasunobu Nakamura et al, February 2022 (12 pages) and [Realization of fast all-microwave CZ gates with a tunable coupler](#) by Shaowei Li, Jian-Wei Pan et al, February 2022 (12 pages).

¹⁰⁵¹ See [High-fidelity qutrit entangling gates for superconducting circuits](#) by Noah Goss, Irfan Siddiqi et al, Nature Communications, November 2022 (6 pages).

¹⁰⁵² See [Superconducting Qubits Above 20 GHz Operating over 200 mK](#) by Alexander Anferov, Shannon P. Harvey, Fanghui Wan, Jonathan Simon, and David I. Schuster, University of Chicago, Stanford University and SLAC NL, arXiv, February 2024 (17 pages).

¹⁰⁵³ Like with [Engineering superconducting qubits to reduce quasiparticles and charge noise](#) by Xianchuang Pan et al, February 2022 (23 pages) which reduces quasiparticles generation coming from broken Cooper pairs.

In some cases, researchers invent useless things like with trying to entangle superconducting qubits with tardigrades¹⁰⁵⁴. But the physics of a superconducting qubit is much more complicated than that for the neophyte. The qubit itself is coupled to a cavity containing a resonator usually implemented as a **coplanar waveguide** (CPW) resonator on a superconducting circuit. Its length usually corresponds to a quarter-wavelength or the resonator drive frequency. With a 6 GHz drive frequency, it turns into a 1.25 cm resonator that is usually squeezed in a serpentine layout.

The energy of the ensemble is modeled by a **Jaynes-Cummings Hamiltonian** as shown in Figure 300¹⁰⁵⁵. This involves many notions like a Jaynes-Cummings spectrum, a resonant regime (the cavity-qubit are interoperating oscillators), dressed states (the different energy levels of the qubits) and a dispersive regime (enabling qubits readout with the resonator)^{1056 1057}.

Many parameters define a superconducting qubit's characteristics, like its **Q factor**, the ratio between the energy stored in an oscillator and the energy dissipated per oscillation cycle times 2π . It characterizes the stability of a superconducting qubit and determines its T_1 or relaxation time. The greater the Q factor is, the longer T_1 will be¹⁰⁵⁸ but it can be detrimental to noise sensitivity.

$$H = \hbar\omega_r \left(a^\dagger a + \frac{1}{2} \right) + \frac{\hbar\omega_q}{2} \sigma^z + \hbar g (a^\dagger \sigma^- + \sigma^+ a) + \hat{H}_\kappa + \hat{H}_\gamma$$

angular oscillation frequency of the relevant cavity mode
 energy difference of the two qubit levels
 strength of interaction between cavity and qubit
 mediate relaxation and dephasing through coupling to an external bath

total energy of qubit + cavity
 cavity harmonic oscillator energy
 qubit energy
 coherent exchange of excitations between the qubit and cavity
 coupling between cavity and qubit
 cavity qubit
 coupling to environment

resonator photons
 a : annihilation operator
 a^\dagger : creation operator
 σ^z : qubit amplitude
 $\sigma^- = \frac{1}{2}(\sigma^x - \sigma^y) = |-\rangle$ superposed state
 $\sigma^+ = \frac{1}{2}(\sigma^x + \sigma^y) = |+\rangle$ superposed state
 $\omega_{rq} = \omega_q - \omega_r$: detuning of qubit from the cavity

(cc) Olivier Ezratty, 2022

Figure 300: Jaynes-Cumming cQED Hamiltonian, (cc) Olivier Ezratty, 2022.

¹⁰⁵⁴ See [Entanglement between superconducting qubits and a tardigrade](#) by K. S. Lee et al, December (19 pages) and the pushback it generated in [Peers dispute claim that tardigrades were entangled with qubits](#) by Bob Yirka , Phys.org, December 2021, [Schrödinger's Tardigrade Claim Incites Pushback At issue: Quantum-entangled water bears?!](#) by Philippe Ross, IEEE Journal, December 2021 and [Frequency Shifts Do Not Imply Quantum Entanglement](#) by Ben Brubaker, January 2022. The arXiv paper was later published in the [New Journal of Physics](#) from IOP Science.

¹⁰⁵⁵ See [The Jaynes-Cummings model and its descendants](#) by Jonas Larson and Th. K. Mavrogordatos, February 2022 (237 pages).

¹⁰⁵⁶ Some sources to learn cQED: the review paper [Microwave photonics with superconducting quantum circuits](#) by Xiu Gu et al, 2017 (170 pages) that describes well how superconducting qubits interact with microwaves. [Superconducting Qubits and Circuits Artificial Atoms Coupled to Microwave Photons](#) by Steve Girvin, Les Houches 2011 (132 pages), the review [Practical Guide for Building Superconducting Quantum Devices](#) by Yvonne Y. Gao, Adriaan Rol, Steven Touzard and Chen Wang, November 2021 (48 pages) and [Superconducting qubit in a resonator test of the Leggett-Garg inequality and single-shot readout](#) by Agustin Palacios-Laloy, 2010 (253 pages).

¹⁰⁵⁷ See the circuit analysis of superconducting qubits tutorial [The superconducting circuit companion -- an introduction with worked examples](#) by S. E. Rasmussen et al, Aarhus University, March 2021-November 2023 (56 pages).

¹⁰⁵⁸ See [Decoherence benchmarking of superconducting qubits](#) by Jonathan J. Burnett et al, Nature, 2019 (8 pages) and [Extending Coherence in Superconducting Qubits: from microseconds to milliseconds](#) by Adam Patrick Sears, a thesis under the supervision of Rob Schoelkopf, 2013 (178 pages).

The sources of noise in superconducting qubits are multiple and the research literature is still sparse with regards to consolidating quantitative estimations of all sources of noise^{1059 1060}, besides the ones coming from cosmic radiation that we already covered earlier when discussing quantum error correction.

Noise affecting superconducting coherence times come from many sources¹⁰⁶¹ including the influence of external circuits connected to the qubit (resonators, filters, ...), the charge noise coming from motion of charges in the qubit dielectrics and oxides, the critical current noise coming from the motion of charges in the Josephson junction, the **1/f flux noise** corresponding to the motion of trapped vortices in superconductor circuits¹⁰⁶², the fluctuating of paramagnetic spins in the superconducting loop insulator interface, and other spin and current artifacts at the Josephson junction of in the circuit substrate^{1063 1064}, quasiparticle poisoning coming from the tunneling of single quasiparticles in and out of the superconducting island, cosmic rays influence and even perturbations coming from the low-frequencies generated by the compressors and pulse tubes that are cooling the cryostat at 4K¹⁰⁶⁵.

Analog simulations. Superconducting qubits QPUs can also be used to run quantum simulations at the native level, thanks to low level analog control of inter-qubit connections. Various experiments are testing this model^{1066 1067}.

Qubit operations

The general principle of superconducting qubits operations is as follows:

- **Qubit quantum state** in the generic case of a transmon is a two-level charge of Cooper pairs that correspond to a nonlinear oscillator containing at least a Josephson junction and a capacitance laid out in a current loop. A flux bias (direct current pulse) can be used to individually control each qubit resonant frequency if it is frequency tunable. It can help reduce control frequency crosstalk between qubits but at the cost of a lower lifetime (T_1). It is better to have fixed and different qubit frequencies. Qubit initialization must be as fast as possible, and some research is going on to optimize it^{1068 1069 1070 1071}.

¹⁰⁵⁹ See [Modeling low- and high-frequency noise in transmon qubits with resource-efficient measurement](#) by Vinay Tripathi et al, February 2023 (17 pages).

¹⁰⁶⁰ See [Fundamental limits of superconducting quantum computers](#) by Michele Vischi et al, January 2022 (17 pages).

¹⁰⁶¹ See [Physical mechanisms of low frequency noises in superconducting qubits](#) by Lara Faoro, LPTHE, 2008 (36 slides).

¹⁰⁶² The 1/f noise is a low-frequency magnetic-flux noise showing up in the qubit that has a 1/f power spectral density.

¹⁰⁶³ See [Evolution of 1/f Flux Noise in Superconducting Qubits with Weak Magnetic Fields](#) by David A. Rower, William D. Oliver et al, January 2023 (13 pages).

¹⁰⁶⁴ See [Flux Noise in Superconducting Qubits](#) by Clare Yu, Robert McDermott, David Pappas et al, 2016 (44 slides).

¹⁰⁶⁵ See [Mitigation of frequency collisions in superconducting quantum processors](#) by Amr Osman, [Submitted on 8 Mar 2023].

¹⁰⁶⁶ See [Mapping a topology-disorder phase diagram with a quantum simulator](#) by Xue-Gang Li et al, January 2023 (46).

¹⁰⁶⁷ See [Analogue Quantum Simulation with Fixed-Frequency Transmon Qubits](#) by Sean Greenaway et al, November 2022 (12 pages).

¹⁰⁶⁸ See [Active Initialization Experiment of Superconducting Qubit Using Quantum-circuit Refrigerator](#) by Teruaki Yoshioka et al, University of Tokyo, RIKEN and AIST, June 2023 (12 pages).

¹⁰⁶⁹ See [Quantum-circuit refrigeration of a superconducting microwave resonator well below a single quantum](#) by Arto Viitanen, Mikko Möttönen et al, August 2023 (7 pages).

¹⁰⁷⁰ See [Fast Reset Protocol for Superconducting Transmon Qubits](#) by Wei-Ping Yuan et al, November 2022 (8 pages).

¹⁰⁷¹ See [Optimizing resetting of superconducting qubits](#) by Ciro Micheletti Diniz et al, April 2023 (7 pages).

- **Single-qubit quantum gates** are generated by microwave pulses sent via coaxial cables on the qubits. Their frequency is adjusted to the energy level $\hbar\omega_{01}$ mentioned above. This frequency is calibrated to be different on adjacent qubits to avoid crosstalk effects¹⁰⁷². The microwave pulse amplitude controls the rotation angle and its phase adjusts the axis of the gate rotation operation. This makes it possible to create T, S and R gates with a phase other than a quarter or half turn in the Bloch sphere¹⁰⁷³. In practice, two arbitrary waveform generators create a wave form for “in-phase” and “quadrature” (I and Q) signals which are two microwave pulses that have the same (local-oscillator originated) frequency and are 90° out of phase, as shown in Figure 301.

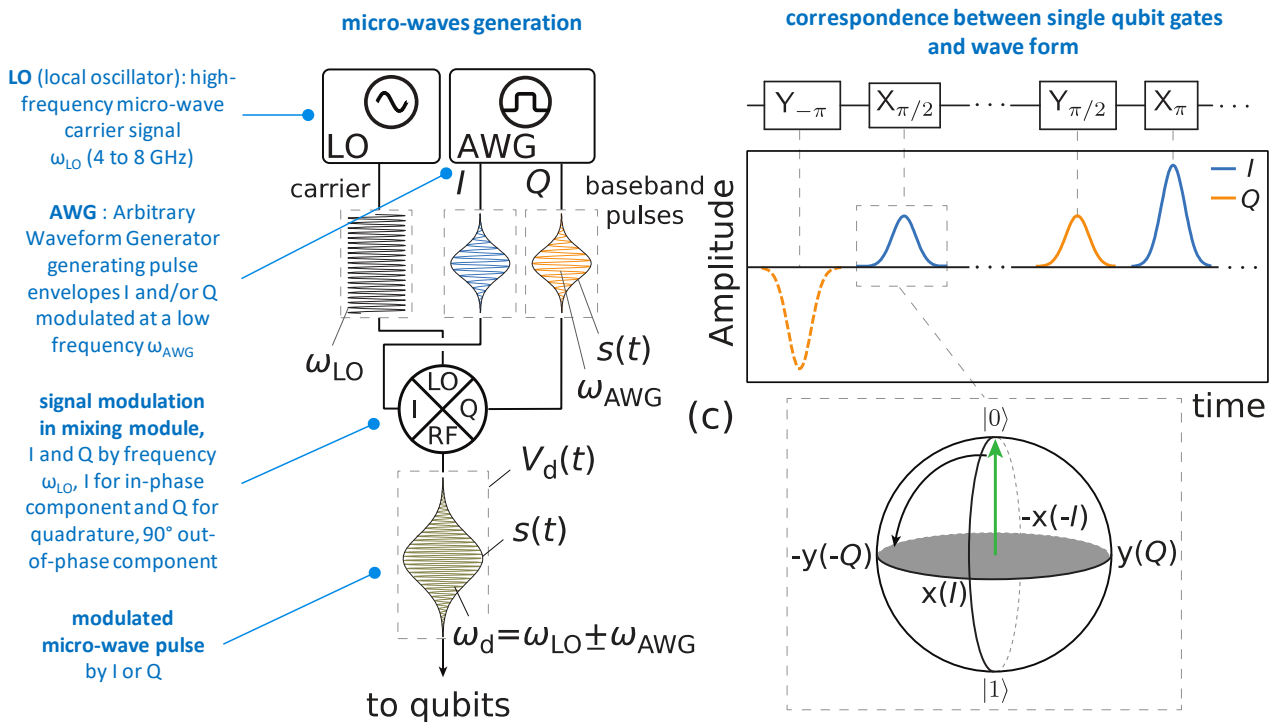


Figure 301: qubit drive microwaves generation. Source: [A Quantum Engineer's Guide to Superconducting Qubits](#), by Philip Krantz et al, 2019 (67 pages).

The I signal is a cosine waveform and the Q signal is a sine waveform. They add-up in the mixer to create a pulse signal with an arbitrary phase depending on the relative amplitudes of the I and Q waveform signals¹⁰⁷⁴. The mixer then adds the local oscillator signal to the resulting signal¹⁰⁷⁵.

¹⁰⁷² A precise calibration of these frequencies is also necessary because of the variability of the behavior of Josephson loops, which are different from one another due to imprecise manufacturing techniques. This variability does not exist for qubits based on single particles such as trapped ions or cold atoms. See [Control and mitigation of microwave crosstalk with frequency-tunable qubits](#) by Ruixia Wang et al, Beijing Academy of Quantum Information Sciences, July 2022 (5 pages) which proposes a quantum error mitigation technique limiting the impact of crosstalk. Static ZZ crosstalk is the one many researchers are working to suppress like in [Frequency adjustable Resonator as a Tunable Coupler for Xmon Qubits](#) by Hui Wang et al, China, August 2022 (12 pages). ZZ crosstalk errors can be described as the amplitude of one qubit influencing the amplitude of other qubits. ZX or ZY errors are linked to the amplitude of a qubit influencing the phase of other qubits.

¹⁰⁷³ These gates can be optimized by modulating the pulsation in an optimal way. See [Implementing optimal control pulse shaping for improved single-qubit gates](#) by J. M. Chow et al., May 2020 (4 pages) which anticipates the capacity to generate single-qubit gates in 1 ns, against a current minimum of around 20 ns.

¹⁰⁷⁴ See [Radio frequency mixing modules for superconducting qubit room temperature control systems](#) by Yilun Xu, Irfan Siddiqi et al, Lawrence Berkeley National Laboratory, July 2021 (7 pages) that describes the role of a signal mixer.

¹⁰⁷⁵ Another option consists in mixing the LO signal separately with the I and Q signals and then merge the resulting signal, removing unwanted spurious frequency components. See [Frequency Up-Conversion Schemes for Controlling Superconducting Qubits](#) by Johannes Herrmann, Andreas Wallraff et al, October 2022 (9 pages).

At 5 GHz, an LO pulse lasts 0.2 ns. Most single qubit gate last at least 10 to 20 ns. It means in that case that a generated microwave packet contains about 50 to a hundred 5 GHz photonic pulses shaped by their wave form. Microwave pulses generated at ambient temperature are progressively attenuated and filtered at every stage of the cryostat so that only a couple hundred microwave photons reach the qubit. The attenuators eliminate photons proportionally to the cooling budget available at each cold plate stage.

Qubit designers must manage complicated trade-offs with regards to single qubit gate times as *“increasing the fidelity of single-qubit gates requires a combination of faster pulses and increased qubit coherence. However, with resonant qubit drive via a capacitively coupled port, these two objectives are mutually contradictory, as higher qubit quality factor requires a weaker coupling, necessitating longer pulses for the same applied power”*^{1076 1077}. But the slowest gates are the two-qubit gates which are about 10 times slower than single-qubit gates in many designs.

- **Two-qubit quantum gates** are realized with a coupling circuit positioned between the two qubits, which can be a simple capacitor or a dynamically controllable system. As we will see later, this coupling is managed with an intermediate qubit in Google's Sycamore processor and their equivalents in China. IBM is not yet using couplers but instead cross-resonance gates but has planned to adopt couplers in future chip designs.
- **Qubits readout** depends on its type. With transmon qubits, a resonator is coupled to the qubit. It transmits a microwave pulse in a resonator that is coupled with the qubit using microwave reflectometry. The qubit state slightly affects the resonator frequency and phase. These readout microwaves are usually amplified in several stages. The method is called “dispersive readout” where for a fixed microwave drive frequency, the resonance frequency of the waveguide resonator shifts depending on the qubit measured state¹⁰⁷⁸ (Figure 302). This measurement technique protects the qubit from all radiation except the readout microwave pulse at ω_r . It amplifies the outgoing signal with the lowest added noise (near the quantum limit). The readout also creates a differentiated phase in the reflected microwave that is analyzed after demixing which generates the in-phase and quadrature signals (I/Q). Measuring the phase of the reflected microwave determines the state of the qubit after measurement without destroying it. It is a QND (quantum non demolition) readout as already explained.

One first stage can use a low-noise superconducting Josephson Parametric Amplifier (JPA) or Traveling Wave Parametric Amplifier (TWPA) operating at the quantum limit, then with a high electron mobility transistor (HEMT) amplifier running at the 4K stage and, at last, with a Low Noise Amplifier (LNA) running at room temperature.

At last, the amplified microwave is converted in digital format with an ADC (analog to digital converter) and analyzed by a FPGA circuit to identify the qubit basis states $|0\rangle$ or $|1\rangle$ with a microwave phase analysis. The result is then exploited by some classical computer that will run some error correction code and drive other qubit operations afterwards. Frequency-based multiplexed readout can be achieved to simplify the wiring exiting the qubit chip. The readout microwave is modulated with a higher frequency than the quantum gates frequency, above 6 GHz¹⁰⁷⁹.

¹⁰⁷⁶ See [Fast superconducting qubit control with sub-harmonic drives](#) by Mingkang Xia et al, Virginia Tech, June 2023 (20 pages).

¹⁰⁷⁷ See [A practical approach to determine minimal quantum gate durations using amplitude-bounded quantum controls](#) by Stefanie Günther et al, Lawrence Livermore National Laboratory, July 2023 (11 pages).

¹⁰⁷⁸ See [Dispersive Readout, Rabi- and Ramsey-Measurements for Superconducting Qubits](#) by Can Knaut, 2018 (25 slides).

¹⁰⁷⁹ Other techniques for measuring the state of superconducting qubits are being considered, such as the activation of qubit fluorescence. It is done by jumping from the $|0\rangle$ to $|2\rangle$ state of the qubit, the transition to the $|1\rangle$ state not being possible with the fluorescence excitation photon. See the thesis [Energy and Information in Fluorescence with Superconducting Circuits](#) by Nathanaël Cottet, 2018 (227 pages).

Qubit readout generates its own noise and errors. Many techniques could help reduce this noise, which can be particularly detrimental to mid-circuit measurements that are used in quantum error correction codes. One, developed at ETH Zurich and Institut Quantique at Sherbrooke University consists in dynamically reducing the qubit-resonator detuning and increase the dispersive shift by bringing the qubit frequency closer to the readout resonator's frequency using a flux pulse. It increases the signal to-noise ratio (SNR) and assignment fidelity, reducing readout errors at 0.25%¹⁰⁸⁰. Another one, from Google AI, associates predictive and heuristics data models¹⁰⁸¹.

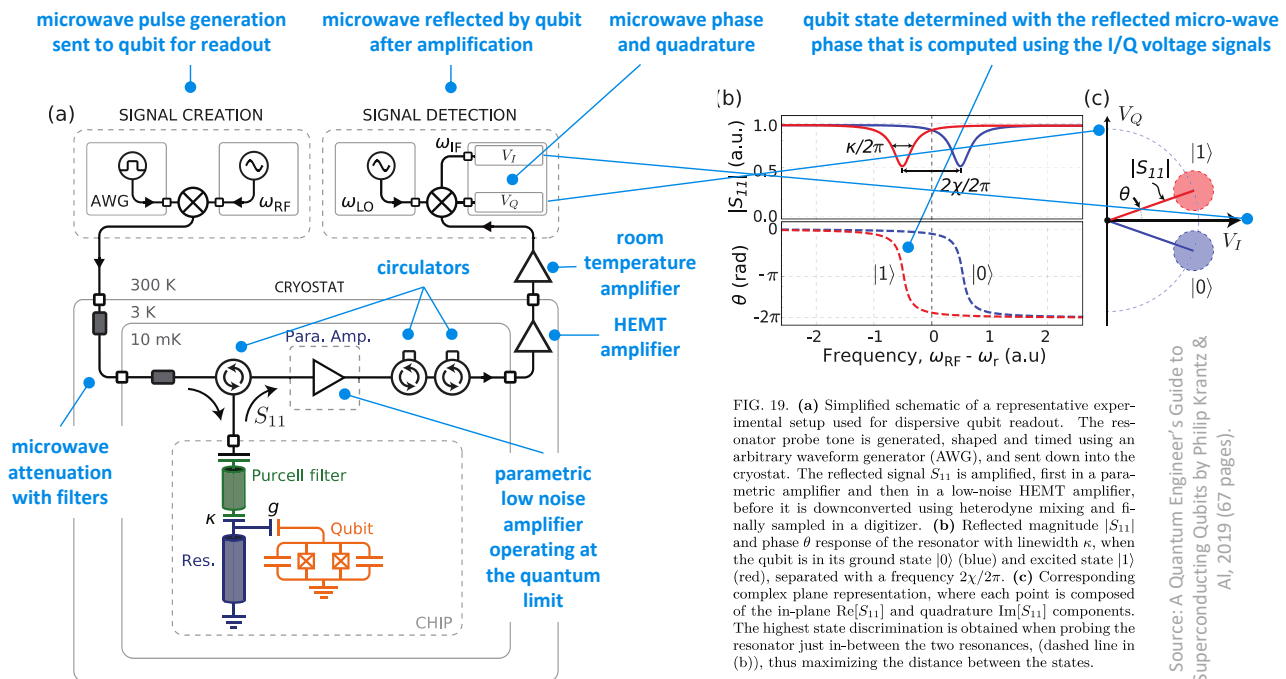


FIG. 19. (a) Simplified schematic of a representative experimental setup used for dispersive qubit readout. The resonator probe tone is generated, shaped and timed using an arbitrary waveform generator (AWG), and sent down into the cryostat. The reflected signal S_{11} is amplified, first in a parametric amplifier and then in a low-noise HEMT amplifier, before it is downconverted using heterodyne mixing and finally sampled in a digitizer. (b) Reflected magnitude $|S_{11}|$ and phase θ response of the resonator with linewidth κ , when the qubit is in its ground state $|0\rangle$ (blue) and excited state $|1\rangle$ (red), separated with a frequency $2\chi/2\pi$. (c) Corresponding complex plane representation, where each point is composed of the in-plane $\text{Re}[S_{11}]$ and quadrature $\text{Im}[S_{11}]$ components. The highest state discrimination is obtained when probing the resonator just in-between the two resonances, (dashed line in (b)), thus maximizing the distance between the states.

Source: A Quantum Engineer's Guide to Superconducting Qubits by Philip Krantz & Al, 2019 (67 pages).

Figure 302: superconducting qubit readout process. Source: [A Quantum Engineer's Guide to Superconducting Qubits](#), by Philip Krantz et al, 2019 (67 pages).

The current superconducting qubit readout technique is quite complicated with its digital-to-analog and analog-to-digital conversion processes, and their significant classical overhead, that becomes problematic when several hundred or thousand physical qubits are needed to build just a single logical qubit.

Thus, the interest of other tested approaches which would generate a 0/1 output in a simpler manner. One technique being considered is the activation of qubit fluorescence. It is done by jumping from the $|0\rangle$ to $|2\rangle$ state of the qubit, the transition to the $|1\rangle$ state not being possible with the fluorescence excitation photon. Also, single microwave photon detectors are also tested¹⁰⁸² ¹⁰⁸³ as well as cryogenic detectors using some microwave to photon conversion¹⁰⁸⁴. These techniques have a much lower overhead but have yet insufficient readout fidelities to be considered in commercial QPUs.

¹⁰⁸⁰ See [Enhancing Dispersive Readout of Superconducting Qubits Through Dynamic Control of the Dispersive Shift: Experiment and Theory](#) by François Swiadek, Alexandre Blais, Andreas Wallraff et al, ETH Zurich and Institut Quantique at Sherbrooke University, July 2023 (14 pages).

¹⁰⁸¹ See [Model-based Optimization of Superconducting Qubit Readout](#) by Andreas Bengtsson et al, Google AI, August 2023 (13 pages).

¹⁰⁸² See [Practical Single Microwave Photon Counter with \$10^{-22}/\sqrt{\text{Hz}}\$ sensitivity](#) by Léo Balembois, Jaime Travesedo, Louis Pallegoix, Alexandre May, Eric Billaud, Marius Villiers, Daniel Estève, Denis Vion, Patrice Bertet and Emmanuel Flurin, July 2023 (8 pages).

¹⁰⁸³ See [Microwave photon detection at parametric criticality](#) by Kirill Petrovnin et al, Aalto University, August 2023 (42 pages).

¹⁰⁸⁴ See [All-optical single-shot readout of a superconducting qubit](#) by Georg Arnold, Johannes M. Fink et al, October 2023 (15 pages).

- **Connectivity** is an important feature of a quantum processor. The more qubits are connected with each other, the fewer SWAP gates must be run to logically entangle them. It can also contribute to make error correction codes more efficient and use a lower overhead of physical qubits, like with the LDPC codes. With 2D structures, one of the problems to be solved lies in the internal connections in the chip. 3D architectures are used with one layer for qubit readout and another for qubit operations, but the qubits topology connectivity is at best with 4 nearest neighbors like with Google’s Sycamore. IBM is using a “heavy hex lattice” connectivity since 2021. Using hexagonal unit cells of 12 qubits with 1-to-2 and 1-to-3 connectivity, it generates better qubit gate fidelities and enables error correction codes implementation.

A new approach consists in using multiple metal layers connectivity chips that are connected to the qubit chip with through-silicon vias (TSVs) vertical connectors¹⁰⁸⁵. The most recent designs from IBM and the MIT Lincoln Labs have between 3 and 7 metal layers. Another design is tested at IMEC using a special arrangement of resonators¹⁰⁸⁶.

- **Digital simulations.** Some software solutions are available to simulate the physical behavior of superconducting qubits at a low level. Among these, **CircuiQ** is a proposal from the MIT, ParityQC and the University of Innsbruck with the participation of Benoît Vermersch (LPMCM, Grenoble)¹⁰⁸⁷. It is a Python open source toolbox that can be used for analyzing superconducting circuits at the physical level, using their Hamiltonian. It can help estimate the qubits T_1 under various noise mechanisms. There are other similar software packages like **scqubits**, developed by researchers from Northwestern University and **SQcircuit** from Stanford¹⁰⁸⁸.

Setups

In the current state of the art, the cryostats housing these qubits are filled with many cables and microwave attenuators driving the qubits and with first stages amplifiers used in the qubits state readout¹⁰⁸⁹ (Figure 305). Implementing quantum error correction will require 1,000 or 10,000 physical qubits per logical qubit, a number that depends on several parameters like the physical qubit fidelities, their connectivity, and the logical qubit target fidelities which can range between 10^{-6} to 10^{-19} depending on the algorithms. Quantum chemical simulation algorithms are particularly demanding here.¹⁰⁹⁰ It will create significant challenges for scaling up the architecture at least, with the existing cabling and external microwave generation and readout systems. Thus, the need for cryogenic electronics and miniaturized microwaves coaxial cabling that we will investigate in the quantum enabling technologies section of this book.

With usual error correction codes like surface codes that implement fault-tolerance corrections, the key determinant of physical qubit overhead is also the number of T gates in the algorithm since these gates are the most expensive to correct. It will create significant challenges for scaling up the architecture at least, with the existing cabling and external microwave generation and readout systems.

¹⁰⁸⁵ See [Qubit-compatible substrates with superconducting through-silicon vias](#) by K. Grigoras et al, January-November 2022 (11 pages).

¹⁰⁸⁶ See [A superconducting quantum information processor with high qubit connectivity](#) by Gürkan Kartal et al, IMEC, July 2023 (8 pages).

¹⁰⁸⁷ See [CircuitQ: An open source toolbox for superconducting circuits](#) by Philipp Aumann, William D. Olivier et al, March 2022 (14 pages).

¹⁰⁸⁸ See [Computer-aided quantization and numerical analysis of superconducting circuits](#) by Sai Pavan Chitta, Jen Koch et al, Northwestern University, June 2022 (12 pages) and [Analysis of arbitrary superconducting quantum circuits accompanied by a Python package: SQcircuit](#) by Taha Rajabzadeh1, Zhaoyou Wang, Nathan Lee, Takuma Makihara, Yudan Guo, and Amir H. Safavi-Naeini, June 2022 (23 pages).

¹⁰⁸⁹ This is well explained in [Superconducting Circuits Balancing Art and Architecture](#) by Irfan Siddiqi of Berkeley Lab, 2019 (34 slides).

¹⁰⁹⁰ Source: [Surface codes: Towards practical large-scale quantum computation](#) by Austin G. Fowler et al, 2012 (54 pages).

Digital-to-analog converters, aka DACs and Analog-to-Digital converters convert microwaves at room temperature and handle a very large volume of outbound or inbound data of 8 to 14 Gbits/s as shown in the diagram in Figure 303 corresponding to Google's Sycamore.

This data is managed in real time. It does not, however, seem necessary to store them. It is not a big-data system!

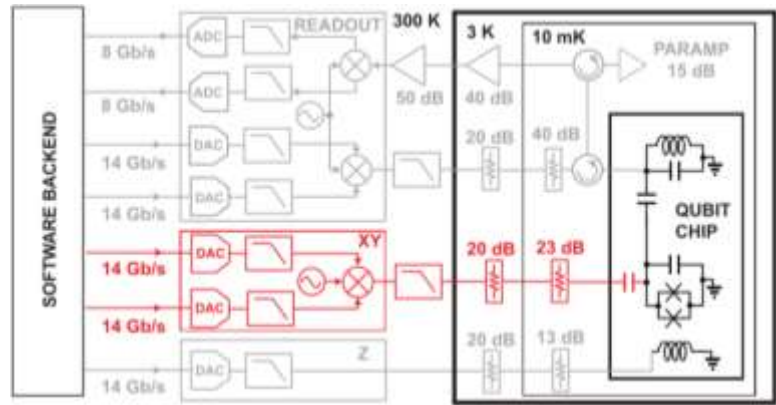


Figure 303: Sycamore's qubit control and readout architecture. Source: Google.

The electronics used in research laboratory equipment is illustrated with the example in Figure 304 of a configuration used to test a 5-qubit superconducting chip in 2015.

It uses classical off-the-shelf equipment from **Rohde & Schwarz** or **Tektronix**. These external generators are appreciated for the quality of the microwave pulses they produce. For a larger number of qubits, multiple microwave generators are used from vendors like **Zurich Instruments**, **Qblox** and **Quantum Motion** that we cover starting 590. Others, like **SEEQC**, are attempting to miniaturize all or part of these components with superconducting electronics which have a much lower power drain and can work within the cryostat.

5 superconducting qubits lab configuration

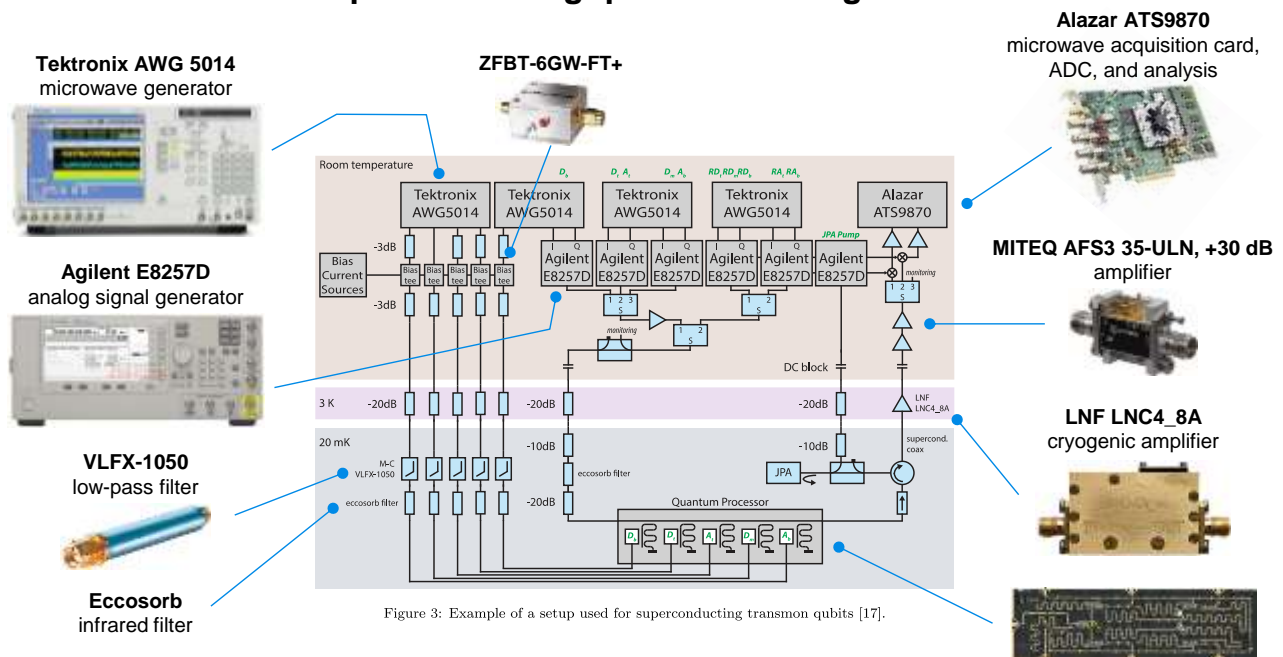


Figure 3: Example of a setup used for superconducting transmon qubits [17].

Figure 304: a superconducting qubits lab configuration. Source: [The electronic interface for quantum processors](#) by J.P.G. van Dijk et al, March 2019 (15 pages). I have added visuals of the electronic components used in the configuration.

Superconducting qubits fidelities are not best-in-class compared to trapped ions. It also decreases with the number of qubits. There is some progress being made to reduce qubit noise. It has several origins such as charge fluctuations, random electrons and materials impurities. Fidelity is currently not high enough to implement error correction codes. Some methods are proposed to improve readout fidelity.

A team of Canadian and American researchers is proposing a miniaturizable optical measurement¹⁰⁹¹. A variant was proposed in 2018 by Robert McDermott of the University of Wisconsin-Madison, with the objective of improving measurement fidelity to 99%¹⁰⁹².

The size of superconducting qubits is in the micron range, making it difficult to create large chips with millions of qubits. Miniaturization always seems possible, but it is difficult to manage because the quality of the superconducting qubits seems to decrease with a smaller size¹⁰⁹³. Therefore, most vendors like IBM, plan to create chips up to about 133 qubits and then connect several of these chips with microwave guides and/or entangled photonic links able to convert qubit quantum states to photonic quantum states. These various quantum processor interconnect currently have a very low TRL (technology readiness level).

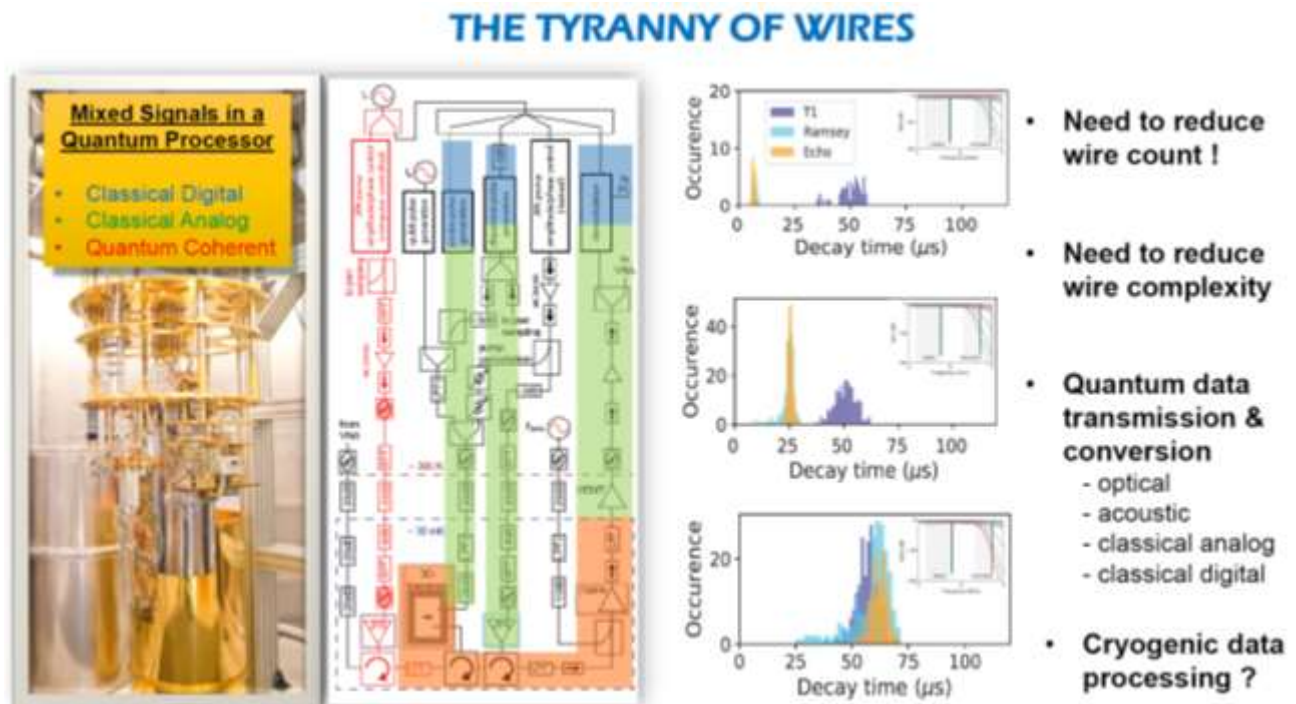


Figure 305: the tyranny of wires in superconducting qubits. Source: [Superconducting Circuits Balancing Art and Architecture](#) by Irfan Siddiqi of Berkeley Lab, 2019 (34 slides).

Manufacturing

Superconducting qubits are electronic circuits built with techniques that are not that far from how classical analog circuits are being produced like in the radar and electronics markets, with some similarities with digital electronics, *aka* CMOS chips.

We'll describe later the specifics of the manufacturing of superconducting qubits. Most thesis coming out of superconducting labs contain a description of the manufacturing techniques being used although it changes over time¹⁰⁹⁴.

Materials used for manufacturing superconducting qubits are different from CMOS chips.

¹⁰⁹¹ See [Heisenberg-limited qubit readout with two-mode squeezed light](#), 2015 (12 pages).

¹⁰⁹² In [Measurement of a Superconducting Qubit with a Microwave Photon Counter](#), March 2018 (11 pages).

¹⁰⁹³ See [Investigating surface loss effects in superconducting transmon qubits](#) by Jay Gambetta et al, 2016 (5 pages) and [On-chip integrable planar NbN nano SQUID with broad temperature and magnetic-field operation range](#) by Itamar Holzman and Yachin Ivry, Technion, April 2019 (7 pages) who prototyped miniaturized 45 nm x 165 nm SQUIDs.

¹⁰⁹⁴ See for example [Design, fabrication and test of a four superconducting quantum-bit processor](#) by Vivien Schmitt, 2015 (192 pages).

It includes aluminum (for the Josephson junction, at least for the dielectric), niobium (for capacitors and resonators and sometimes the Josephson junction¹⁰⁹⁵) and indium (for the chip connectors), bore (in boron-nitride in Josephson junction dielectric¹⁰⁹⁶), titanium nitride (for capacitors, with a better quality factor) and occasionally selenium (associated with niobium and bore in capacitors), silicon or sapphire (for the wafer substrate) and tantalum^{1097 1098} (Figure 306). 3D chips are now commonplace, with at least a qubit chip on top of an interposer, and a resonator and interconnect chip¹⁰⁹⁹.

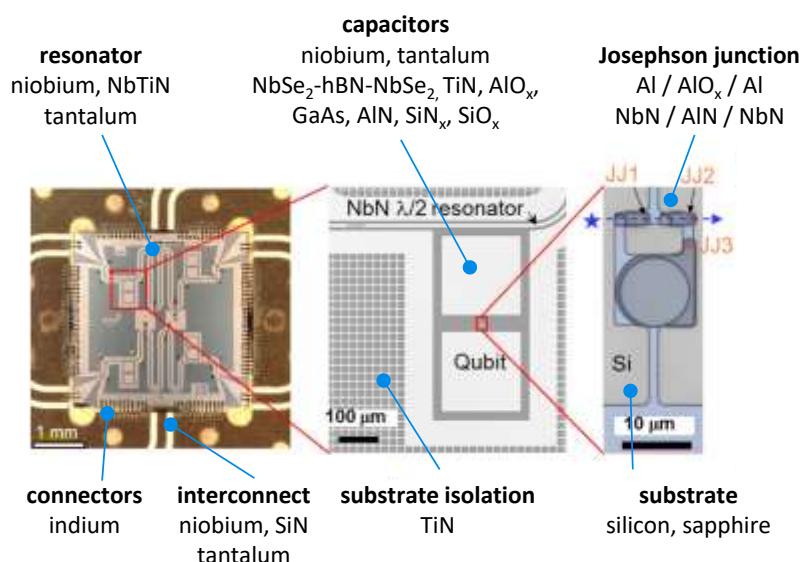


Figure 306: the various components and materials used in a superconducting qubit. Source: [Enhanced coherence of all-nitride superconducting qubits epitaxially grown on silicon substrate](#) by Sunmi Kim et al, September 2021. (cc) Olivier Ezratty, 2022-2023.

Future designs will interconnect several chips next to the other using a chiplet architecture¹¹⁰⁰. As presented at the APS March meeting in Las Vegas in March 2023, the MIT Lincoln Labs also works on modified Dolan Josephson junction process flows. It is testing aluminum on silicon as well as connection using 7 stacked niobium routing layers using an interposer chip with TSV. It also showed good results with hydrofluoric acid treatments of the Josephson junction for cleaning surfaces, using aluminum on silicon substrates. These various advances still have to be embedded in industry vendor processors.

While most deposition techniques generate polycrystalline structures¹¹⁰¹, some are starting to investigate epitaxial deposition to create monocrystalline structures. IMEC already tests such processes avoiding lift-off and angled evaporation, all done with photolithography. They are part of the related EU project **MATQu** with CEA-Leti and others to build superconducting qubits on 300 mm wafers using existing CMOS fabs. IMEC is also testing the manufacturing of tantalum based resonators deposited on silicon¹¹⁰².

¹⁰⁹⁵ See [Improved Coherence in Optically-Defined Niobium Trilayer Junction Qubits](#) by Alexander Anferov, David I. Schuster et al, June 2023 (16 pages).

¹⁰⁹⁶ See [Hexagonal boron nitride as a low-loss dielectric for superconducting quantum circuits and qubits](#) by Joel I-J. Wang, William D. Oliver et al, MIT, Nature Materials, January 2022 (30 pages) and [Enhanced coherence of all-nitride superconducting qubits epitaxially grown on silicon substrate](#) by Sunmi Kim et al, September 2021 (7 pages).

¹⁰⁹⁷ See [Towards practical quantum computers: transmon qubit with a lifetime approaching 0.5 milliseconds](#) by Chenlu Wang et al, NPJ, January 2022 (6 pages).

¹⁰⁹⁸ See [Surpassing millisecond coherence times in on-chip superconducting quantum memories by optimizing materials, processes, and circuit design](#) by Suhas Ganjam, Robert J. Schoelkopf et al, Yale, August 2023 (43 pages).

¹⁰⁹⁹ See [3D integrated superconducting qubits](#) by D. Rosenberg, William D. Olivier et al, June 2017 (6 pages).

¹¹⁰⁰ See [Scaling Superconducting Quantum Computers with Chiplet Architectures](#) by Kaitlin N. Smith et al, University of Chicago, October 2022 (18 pages).

¹¹⁰¹ See [Microscopic relaxation channels in materials for superconducting qubits](#) by Anjali Premkumar, Andrew A. Houck et al, Nature Communications, July 2021 (9 pages).

¹¹⁰² See [Manufacturing high-Q superconducting \$\alpha\$ -tantalum resonators on silicon wafers](#) by D. P. Lozano, et al, IMEC, November 2022 (20 pages).

Superconducting qubits miniaturization is an interesting area of research given they are currently quite large, mainly due to the size of their resonators with a length of $\lambda/4$, λ corresponding to their control wavelength. It can exceed a size of 1 mm^2 . Resonators could be as small as 0.04 mm^2 using special fabrication techniques¹¹⁰³. Similar efforts are undertaken to miniaturize capacitors with van der Waals materials (NbSe_2 -hBN- NbSe_2)¹¹⁰⁴ or with using TSV (vertical “through silicon vias” traversing the chip)¹¹⁰⁵. Another option would be to have remote resonators and an X-Y addressing scheme like with classical RAM, but with the inconvenience of serializing gate operations, and slowing down computing¹¹⁰⁶.

Research

A significant number of research laboratories are working on superconducting qubits all over the world. In the USA, at **Yale University** and **MIT**¹¹⁰⁷, in Europe and in Germany, in Sweden at the **WACQT** of Chalmers University, in France at the **CEA**, in Switzerland at **ETH Zurich**¹¹⁰⁸, in Finland¹¹⁰⁹ and in **Japan**.

Other works aim at lengthening the coherence time of superconducting qubits, notably at Princeton in Andrew A. Houck’s team¹¹¹⁰. Indeed, this coherence time of the order of one hundred microseconds (μs) is still quite limiting. It generates a constraint on the number of quantum gates that can be executed in quantum software, even if the accumulated errors become prohibitive before this limit threshold. New records were broken in 2021 with $1.6 \text{ ms } T_1$ at Princeton and Sherbrooke with a $0-\pi$ circuit (but with a $25 \mu\text{s}$ dephasing time, aka T_2) and $210 \mu\text{s}$ with transmon qubits at Yale¹¹¹¹. In May 2021, a China team obtained a $300 \mu\text{s } T_1$ with a transmon qubit¹¹¹². IBM reached the $1 \text{ ms } T_1$ barrier with one experimental planar transmon qubit in May 2021 as well (but the related paper is still pending).

¹¹⁰³ See [Compact superconducting microwave resonators based on Al-AlOx-Al capacitor](#) by Julia Zotova et al, March 2022 (10 pages) and See [Tiny materials lead to a big advance in quantum computing](#) by Adam Zewe, MIT News Office, January 2022. For a 5 GHz pulse, the wavelength is about 6 cm. A quarter wavelength is then 1.5 cm.

¹¹⁰⁴ See [Miniaturizing transmon qubits using van der Waals materials](#) by Abhinandan Antony et al, Columbia University and Raytheon BBN. September 2021 (6 pages).

¹¹⁰⁵ See [Characterization of superconducting through-silicon vias as capacitive elements in quantum circuits](#) by Thomas M. Hazard, William D. Oliver, Mollie E. Schwartz et al, MIT Lincoln Labs, August 2023 (5 pages).

¹¹⁰⁶ An X-Y addressing scheme would route signals to the qubit resonators from the edge of the chipset, X and Y corresponding to two orthogonal edges. You would then polynomially reduce the number of resonators from N to \sqrt{N} with N being the number of qubits of a square matrix layout chipset.

¹¹⁰⁷ See [Quantum Computing @ MIT: The Past, Present, and Future of the Second Revolution in Computing](#) by Francisca Vasconcelos, MIT, February 2020 (19 pages). They have developed a 16-qubit superconducting chipset, manufactured by Lincoln Labs at MIT.

¹¹⁰⁸ With Andreas Wallraff’s QuSurf team working on superconducting qubits and their error correction codes. This project is funded by the American IARPA agency. In 2019, they were at 7 experimental qubits. It is also supported by the ScaleQIT project (Scalable Superconducting Processors for Entangled Quantum Information Technology) funded by the European Union and by the OpenSuperQ project of the European flagship.

¹¹⁰⁹ VTT’s goal is to manage 50 to 100 superconducting qubits. VTT has its own circuit manufacturing unit with a 2600 m^2 clean room of a similar size to CNRS C2V clean room in Palaiseau, France. See [Engineering cryogenic setups for 100-qubit scale superconducting circuit systems](#) by S. Krinner et al, 2019 (29 pages).

¹¹¹⁰ See [New material platform for superconducting transmon qubits with coherence times exceeding 0.3 milliseconds](#) by Alex P. M. Place, Andrew A. Houck et al, February 2020 (37 pages). Qubits are using tantalum instead of niobium and on a sapphire substrate. The paper describes starting page 8 the manufacturing process of these qubits.

¹¹¹¹ See [Experimental Realization of a Protected Superconducting Circuit Derived from the \$0-\pi\$ Qubit](#) by András Gyenis, Alexandre Blais et al, Sherbrooke, Princeton, U. Chicago and Northwestern University, March 2021 (31 pages) and [Direct Dispersive Monitoring of Charge Parity in Offset-Charge-Sensitive Transmons](#) by K Serniak, R Schoelkopf, Michel Devoret et al, Yale University, March 2019 (11 pages) with transmons at a T_1 of $210 \mu\text{s}$.

¹¹¹² See [Transmon qubit with relaxation time exceeding 0.5 milliseconds](#) by Chenlu Wang et al, May 2021 (15 pages).

The best lab-level record was with a 1.48 ms T_2 coherence time on flux qubits at the University of Maryland in Vladimir Manucharyan's team¹¹¹³ (Figure 308). These records are, however, not necessarily obtained with a great number of functional qubits... when more than 2 are used!

Superconducting qubits lifetime record is still way above this, with 3D SRF cavities (for superconducting radio frequency cavities). These are developed by the DoE Fermilab and have a very high Q-factor.

In 2020, they reached qubit lifetimes of about 2s with special materials design reducing the 2-level system losses. Fermilab researchers plan to implement qubits with these SRFs, packing between 63 and 128 effective qubits into 9 SRF cavities hosting qubits. These cavities are bulky, the size of the device being about one meter long in Figure 307¹¹¹⁴.



Figure 307: the huge SRF superconducting qubits from the DoE Fermilab. Source: [Superconducting Quantum Materials and Systems Center](#) by Anna Grassellino, SQMS Center Director, Fermilab, June 2021 (40 slides),

Other researchers look at implementing superconducting qubits with various means with three or four levels, but, so far, with poor results, particularly with regards to gate fidelities^{1115 1116 1117 1118 1119}.

Other researchers work on using various qubits materials like titanium nitride and tantalum on sapphire substrates, at Princeton, ENS Lyon and Alice&Bob among other locations. These are used in complement to the Al/AlO/Al Josephson junctions, for various other parts of the qubit circuits (isolators, capacitances, resonators)¹¹²⁰.

The Qnantronics team at CEA-Saclay uses transmons for its quantum circuits, but now explores another route based on high coherence impurity spins in insulators for making qubits, with superconducting quantum circuits for controlling them. The rationale is that the electro-nuclear spin levels of such systems may indeed provide more robust qubits for which quantum error correction could be more easily manageable than for transmon qubits.

Other research conducted at the CEA consists in associating superconducting qubits with NV centers, linked by microwaves, to be used as quantum memory as well as a means of more precise readout of superconducting qubits. NV centers spins can serve as quantum memory thanks to a spin coherence time that is 1,000 times longer than that of superconducting qubits (100 milliseconds vs. 100 microseconds). Another field of research is the coupling of superconducting qubits with nuclear spins (instead of electron spins, on phosphorus or bismuth nuclei) via electron spins.

¹¹¹³ See [Millisecond coherence in a superconducting qubit](#) by Aaron Somoroff, Vladimir E. Manucharyan et al, University of Maryland, 2021 (14 pages),

¹¹¹⁴ See [Superconducting Quantum Materials and Systems Center](#) by Anna Grassellino, SQMS Center Director, Fermilab, June 2021 (40 slides), [Materials and devices for fundamental quantum science and quantum technologies](#) by Marco Polini et al, January 2022 (19 pages) and [Three-Dimensional Superconducting Resonators at \$T < 20\$ mK with Photon Lifetimes up to \$\tau = 2\$ s](#) by A. Romanenko, R. Pilipenko, S. Zorzetti, D. Frolov, M. Awida, S. Belomestnykh, S. Posen, and A. Grassellino, March 2020 (5 pages).

¹¹¹⁵ See [Dancing the Quantum Waltz: Compiling Three-Qubit Gates on Four Level Architectures](#) by Andrew Litteken et al, March 2023 (14 pages).

¹¹¹⁶ See [High-fidelity qutrit entangling gates for superconducting circuits](#) by Noah Goss, Irfan Siddiqi et al, Nature Communications, Berkeley University & DoE lab, December 2022 (6 pages). With error rates ranging from 2.7% to 4.8% with CZ gates.

¹¹¹⁷ See [Realization of two-qutrit quantum algorithms on a programmable superconducting processor](#) by Tanay Roy et al, University of Chicago, November 2022 (14 pages).

¹¹¹⁸ See [The 2T-qutrit, a two-mode bosonic qutrit](#) by Aurélie Denys and Anthony Leverrier, October 2022 (20 pages).

^{1119 1119}

¹¹²⁰ See [Chemical profiles of the oxides on tantalum in state of the art superconducting circuits](#) by Russell A. McLellan et al, January 2023 (34 pages).

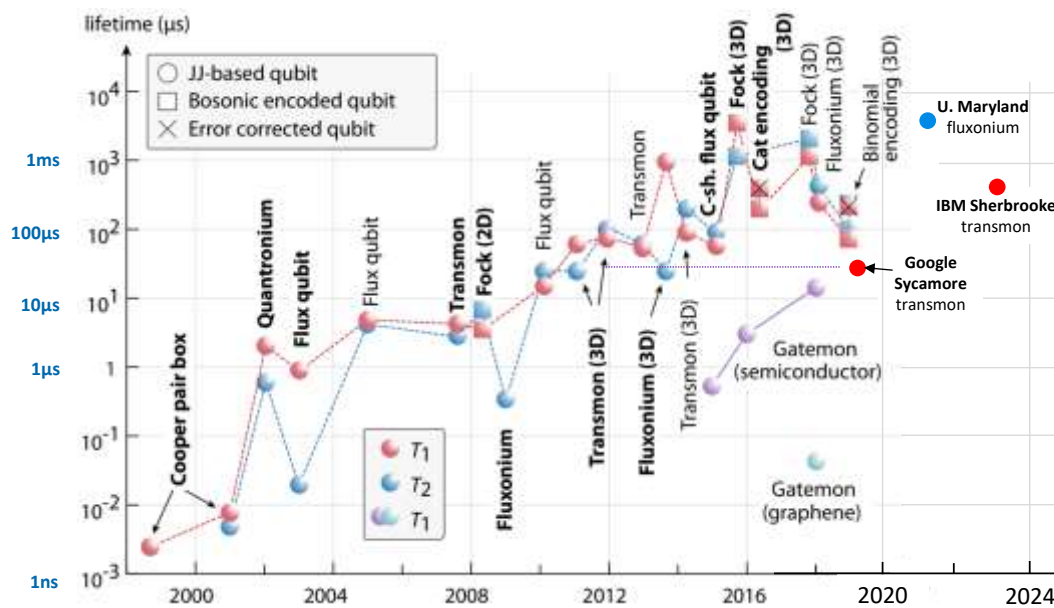


Figure 308: logarithmic evolution of superconducting lifetime over time. Source: [Superconducting Qubits Current State of Play](#) by Morten Kjaergaard et al, 2020 (30 pages). Updated in 2023.

As with many solid-state qubits, one of the key research goals is to transform these microwave photons into photons in the visible/infrared band to allow their long-distance transport, in particular via fiber optic-based telecommunication, which would become the basis of distributed quantum computing¹¹²¹.

There is another interesting field of research aimed at simplifying qubit readout that may avoid the burden of parametric microwave amplification and circulators at the 15 mK stage. One of these consists in using microwave photons counting and Josephson photomultipliers (JPM) that are embedded directly in the qubit chip¹¹²². It has however some shortcomings to overcome like crosstalk and loss of qubit fidelity over time.

In 2021, a **China** research team led by Jian-Wei Pan created a 66 superconducting qubits system and claimed having reached another quantum advantage. In this **Zuchongzhi 2.1** system, they reproduced the Google supremacy experiment with a 2D array of qubits with 13 additional qubits, using the same coupling technology, with 110 couplers¹¹²³. Their fidelities were not best-in-class with 99.86% for single qubit gates, 99.24% for two-qubit gates and 95.23% for qubits readout, on top of a rather low T_1 of 30.6 μ s. In their experiment, though, they did use only 56 of their 66 qubits, showing that qubits fidelities are probably not that good when all qubits are activated¹¹²⁴.

In September 2021, they used 60 qubits on 24 cycles with an improved readout fidelity of 97.74%¹¹²⁵.

¹¹²¹ See for example [Microwave-to-optical conversion via four-wave mixing in a cold ytterbium together](#) by Jacob P. Covey et al, July 2019 which discusses this conversion.

¹¹²² See [High-Fidelity Measurement of a Superconducting Qubit Using an On-Chip Microwave Photon Counter](#) by A. Opremcak, Roger McDermott et al, PRX, February 2021 (15 pages) and the associated thesis [Qubit State Measurement Using a Microwave Photon Counter](#) by Alexander M. Opremcak, 2020 (159 pages).

¹¹²³ See [Strong quantum computational advantage using a superconducting quantum processor](#) by Yulin Wu, Jian-Wei Pan et al, June 2021 (22 pages).

¹¹²⁴ See [Experimental quantum computational chemistry with optimised unitary coupled cluster ansatz](#) by Shaojun Guo, Jian-Wei Pan et al, December 2022-February 2023 (37 pages) that provides some indications on Zuchongzhi 2.0 processor quality.

¹¹²⁵ See [Quantum Computational Advantage via 60-Qubit 24-Cycle Random Circuit Sampling](#) by Qingling Zhu, Jian-Wei Pan et al, September 2021 (15 pages).

China researchers implemented some quantum neuronal sensing application of quantum many-body states in this QPU¹¹²⁶.

In June 2023, Zuchongzhi-2 was upgraded to a 176 qubit version (Figure 309). It is said to be the initial 66 qubit system with the addition of 110 coupled qubits. We can wonder how this upgrade was implemented and if it enables the handling of a 2^{176} Hilbert space. The QPU is supposed to be openly available in the cloud. In November 2022, China research teams from Hangzhou, Beijing and Hefei launched two superconducting qubits QPUs with 121 and 36 qubits (11x11 et 6x6).



Figure 309: a rare glimpse of a China QPU. Source: [New Platform Offers Access to China's Zuchongzhi Quantum Computing System](#) by Qian Tongxin, YiCai Global, June 2023.

The physical qubits worked with subsets of 68 qubits and 20 qubits with $T_1=109.8 \mu\text{s}$ and $T_2=17.9 \mu\text{s}$ (68 qubits) and $T_1=137.5 \mu\text{s}$ and $T_2=16.4 \mu\text{s}$ (20 qubits). Their single-qubit gates fidelities are respectively 99.87% and 99.91%, and two-qubit fidelities are 99.4% (see charts in Figure 310). These qubits were used to create topological logical qubits using toric quantum error correction codes. using non-abelian anyons.

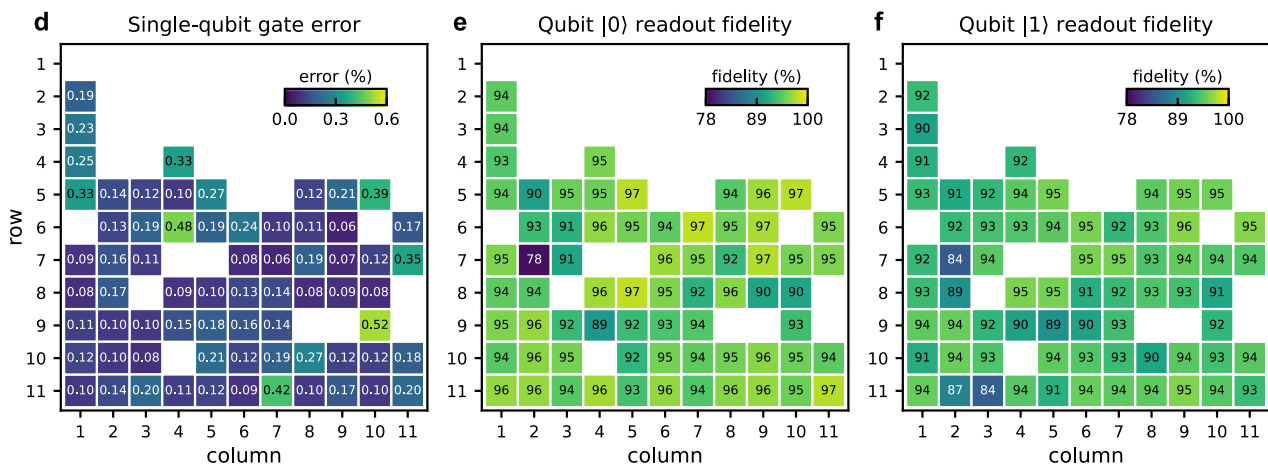


Figure 310: China's 68 qubit fidelities. Source: [Digital simulation of non-Abelian anyons with 68 programmable superconducting qubits](#) by Shibo Xu et al, November 2022 (27 pages). 2023 edition.

These teams are working on large scale and long range tunable couplers using capacitively connecting pads and a flip chip process. It implements CZ coupling gates with 96.2% fidelities. This coupling can be capacitive or inductive¹¹²⁷. In China, another team is working on improving single qubit gates errors to a 10^{-4} record¹¹²⁸ and to also reduce crosstalk errors¹¹²⁹.

¹¹²⁶ See [Quantum Neuronal Sensing of Quantum Many-Body States on a 61-Qubit Programmable Superconducting Processor](#) by Ming Gong et al, January 2022 (14 pages).

¹¹²⁷ See [Tunable Coupling Architectures with Capacitively Connecting Pads for Large-Scale Superconducting Multi-Qubit Processors](#) by Gui-Han Liang, Peng Zhao et al, June 2023 (15 pages).

¹¹²⁸ See [Error per single-qubit gate below \$10^{-4}\$ in a superconducting qubit](#) by Zhiyuan Li et al, February 2023 (7 pages).

¹¹²⁹ See [Mitigating crosstalk and residual coupling errors in superconducting quantum processors using many-body localization](#) by Peng Qian, Hong-Ze Xu, Peng Zhao, Xiao Li and Dong E. Liu, October 2023 (8 pages).

Vendors



IBM is one of the few major players in the IT world that has been investing in fundamental research for a very long time in quantum computing¹¹³⁰. It is the most advanced in quantum computing research, having focused on superconducting qubits for a while.

IBM started to develop quantum computers a while ago. In 2001, they could factor the integer 15 using Shor's algorithm (and a couple tricks) with using a prototype liquid state nuclear magnetic resonance (NMR) 7-qubit chip¹¹³¹. In 2012, IBM also presented a 3-qubit superconducting chip¹¹³². Its commercial inroads in the quantum computing world started to take shape in 2016 with the launch of its Q Experience offering in the cloud (now Quantum Experience).

IBM's quantum activity is driven by Jay Gambetta with researchers in their Yorktown, Poughkeepsie, San Jose, Ehningen (Germany), Tokyo, and Zurich labs, partnering with various American and other countries universities including ETH Zurich and EPFL in Switzerland and the University of Tokyo in Japan. IBM has both the most significant full-stack physics, hardware, software tools and cloud R&D investment and strong market presence. It has at least 623 researchers working in the domain, on top of field operations (sales, marketing, support, services)¹¹³³. Their in-house manufacturing capacity enables them to prototype and produce most of the components needed to build their machines, particularly for their qubit chips and control electronics. Their most visible outside vendor is Bluefors.

Their 2022 roadmap update added a scale-out strategy with their QPUs on top of their scale-in roadmap announced in 2020¹¹³⁴.

They are also very open and reliable, publishing roadmaps and roadmap updates, respecting their planned milestones and with a steady stream of open research publications showcasing their contribution to the complicated quantum computing field even though it sometimes looks like a hard to reassemble puzzle.

IBM's technology is the fixed frequencies transmon superconducting qubits. It is using cross-resonance two-qubit gates which consists in applying a microwave drive to one qubit (the control) at the frequency of another qubit (the target), generating a ZX interaction that is mediated by a bus¹¹³⁵. In the Heron system, they also use CZ gates based on tunable couplers.

Its number of qubits increased steadily from 5 in 2016 to 433 in May 2023. IBM's quantum systems have been running in the cloud since 2016 (Figure 311). These are already used by thousands of researchers, students, startups, and corporations around the world. After creating laboratory computers, IBM ventured into creating packaged ones when announcing the Q System One in January 2019 at the Las Vegas CES, initially a 20-qubit system¹¹³⁶.

¹¹³⁰ Who does fundamental research? Mainly IBM, Microsoft, Google and large telecom companies. The Bell Labs coming from the dismantling of AT&T in 1982 are now part of Nokia after gone through Lucent and Alcatel-Lucent.

¹¹³¹ See [It's been 20 years since "15" was factored on quantum hardware](#) by Robert Davis, IBM, January 2022.

¹¹³² See [IBM edges closer to quantum computing](#) by Daniel Terdiman, CNET, February 2012 presenting a 3 qubit IBM chipset.

¹¹³³ See [Evidence for the utility of quantum computing before fault tolerance](#) by Youngseok Kim et al, Nature, June 2023 (8 pages).

¹¹³⁴ See [The Future of Quantum Computing with Superconducting Qubits](#) by Sergey Bravyi, Oliver Dial, Jay M. Gambetta, Dario Gil and Zaira Nazario, IBM Quantum, September-November 2022 (20 pages), a well-crafted paper detailing their scientific roadmap including quantum error correction trade-off choices, chipset manufacturing and scale-in/scale-out architecture.

¹¹³⁵ See [First-principles analysis of cross-resonance gate operation](#) by Moein Malekakhlagh et al, IBM Research, May 2020 (30 pages) and [Mitigating off-resonant error in the cross-resonance gate](#) by Moein Malekakhlagh et al, August 2021 (20 pages).

¹¹³⁶ Its design was created with the design studios Map Project Office and **Universal Design Studio** (UK) and **Goppion** (Italy), a manufacturer of high-end exhibition devices for museums, which notably designed the protective device for the Mona Lisa in the Louvre Museum and the Queen's jewels in the Tower of London.

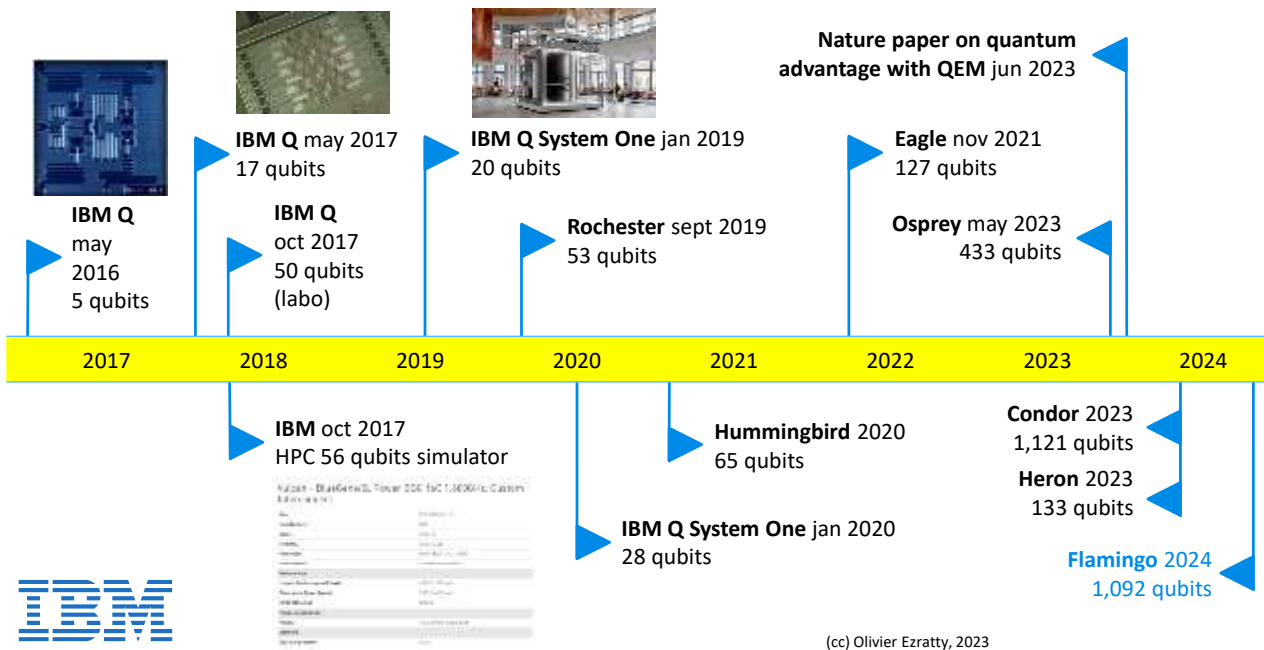


Figure 311: IBM quantum computing timeline. (cc) Olivier Ezratty, 2019-2023.

The Quantum System One is 2.75 m wide, about the size of a D-Wave quantum annealer. In Figure 312, ci-dessous on the right, you can see the Quantum System assembly workshop. IBM is implementing a pre-industrial approach to the production of its quantum computers, despite their very limited capacities and low volume economics. The casing front contains the suspended cryostat while the back contains all the computing, electronics and cryostat compressor and pumps. The Quantum Systems are also self-calibrating.

Most of these units are sitting in IBM's own data center in Poughkeepsie (Figure 317), with some extra systems installed in IBM sites in Germany (operated with the Fraunhofer Institute), Tokyo in Japan, in Korea at Yonsei University, in Canada in Bromont, near Sherbrooke¹¹³⁷ and since 2023 at Cleveland Clinic in the USA¹¹³⁸, and soon in San Sebastian in Spain¹¹³⁹.



Figure 312: IBM System Q without packaging (left) and with packaging (right), as installed since 2023 at Cleveland Clinic in the USA. Source: IBM. 2023.

¹¹³⁷ See [IBM Research launches the first Discovery Accelerator in Canada](#), IBM, February 2022. This deployment represents an investment of CAN \$65M by IBM matched by the Government of Québec. IBM will team up there with Alexandre Blais' team at Institut Quantique in Sherbrooke. The ibm-quebec 127 qubit system was launched in September 2023.

¹¹³⁸ See [Cleveland Clinic Gets Its Own IBM Quantum Processor For Advanced Biomedical Research](#) by Steven Leibson and Tiras Research, Forbes, March 2023. In October 2023, Cleveland Clinic was selected to run some quantum chemistry projects by Wellcome Leap (a kind of NGO funding healthcare research projects following DARPA's methods) and Algorithmiq.

¹¹³⁹ See [IBM and Fundación Ikerbasque Partner to Launch Groundbreaking Quantum Computational Center](#), March 2023.

The non-packaged System One is installed in locations with white-room control of temperature and humidity. Elsewhere, the packaged version is deployed, like it will be at the Rensselaer Polytechnic Institute in New York¹¹⁴⁰.

In October 2022, Joe Biden visited the Poughkeepsie facility¹¹⁴¹ and was presented the Osprey 433 qubit processor that was unveiled later in November 2022¹¹⁴². As of October 2022, IBM had already retired 26 quantum computers with 1, 5, 7, 15, 20, 27, 28, 53 and 65 qubits¹¹⁴³. Many of these systems had been retired as of early 2024.

In September 2020, IBM announced their plan to “scale-in” the number of qubits of their quantum computers¹¹⁴⁴ with a 127 qubits version ("Eagle") introduced in November 2021¹¹⁴⁵, 433 qubits announced in November 2022 and online since May 2023 ("Osprey") and 1,121 qubits in 2023 ("Condor"). This roadmap was updated in May 2022 with the addition of new processors implementing a scale-out approach¹¹⁴⁶ (Figure 314). Chips will be assembled in three-steps: first, Heron (133 qubits, 2023) will be assembled in QPU with many units running the same algorithm in parallel, accelerating the thousands of runs that are necessary with NISQ systems algorithms.

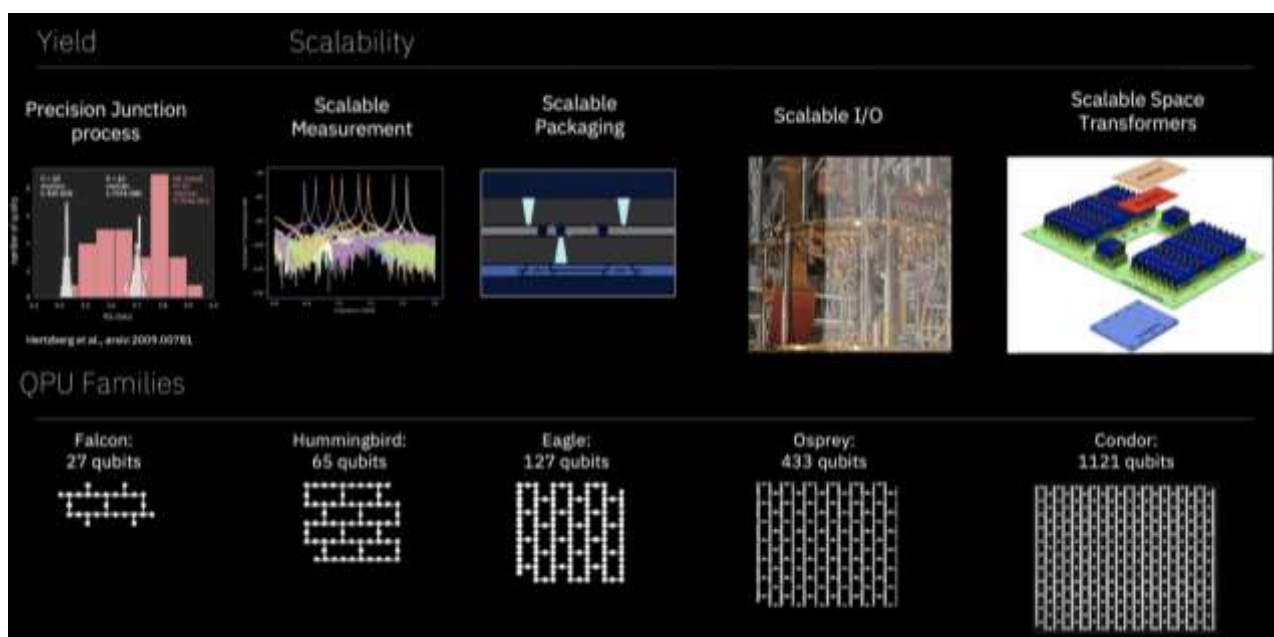


Figure 313: IBM's new superconducting processors from 2020 to 2023. Source: IBM. All these processors implement the heavy-hex qubits topology which explains the number of qubits in these chips. And not the fact that 127 and 433 are prime numbers.

¹¹⁴⁰ See [Rensselaer Polytechnic Institute Plans to Deploy First IBM Quantum System One on a University Campus](#), IBM, June 2023.

¹¹⁴¹ See [U.S. President Biden visits IBM's quantum data center — home of the world's largest fleet of quantum computers](#), IBM, October 2022.

¹¹⁴² See the details of Osprey's November 2022 announcement in [Assessing IBM Osprey 433-qubit quantum computer](#), Olivier Ezratty, November 2022.

¹¹⁴³ See [Retired systems](#), IBM. Extracted on October 24th, 2022.

¹¹⁴⁴ See [IBM's Roadmap For Scaling Quantum Technology](#) by Jay Gambetta, September 2020, completed by [IBM publishes its quantum roadmap, says it will have a 1,000-qubit machine in 2023](#) by Frederic Lardinois in TechCrunch. See also [IBM Envisions the Road to Quantum Computing Like an Apollo Mission](#) by Dexter Johnson, September 2020.

¹¹⁴⁵ See [Eagle's quantum performance progress](#) by Oliver Dial, IBM, March 2022.

¹¹⁴⁶ See [Expanding the IBM Quantum roadmap to anticipate the future of quantum-centric supercomputing](#) by Jay Gambetta, May 2022.

Second, Crossbill will assemble three chips similar to Heron and accumulate 408 qubits in 2024 ($3 \times 133 = 399$, we can presume that the remaining 9 qubits are explained by some connectivity constraints). These chips will be tightly connected with chip-to-chip coupler qubit gates. Then, Flamingo will follow in 2024 with 1,092 qubits (7×156) with three chips blocks interconnected through some short-range microwave-photonic link (less than one meter). Then, Kookaburra will assemble several blocks of three chips associating chip-to-chip micro-wave coupler gates and longer range photonic-based interconnectivity. At last, much later, multiple such units will be connected via photonic links.

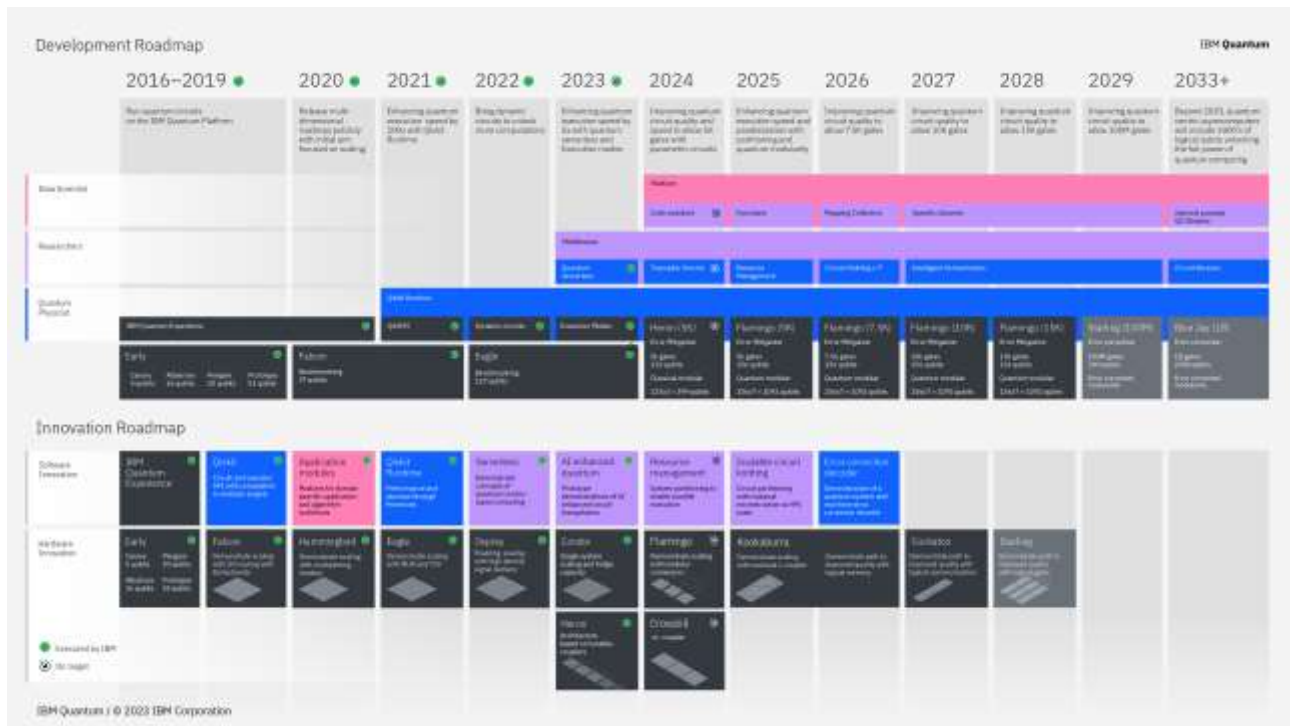


Figure 314: IBM's scale-in and scale-out roadmap. Source: IBM. December 2023.

We will now look at the various technology improvements IBM is implementing or planning to implement in its various superconducting qubits systems¹¹⁴⁷.

Heavy-Hexagon layout. In July 2021, IBM announced a generalization of their hexagon qubits topology. This heavy-hex lattice is the 4th version of IBM Quantum systems qubits topology and has been used upwards of its Falcon processor (27 qubits) as shown in Figure 313 and Figure 315, where useful computing qubits are in yellow, black qubits in the red zones, the phase (Z) errors correction qubits and the white qubits in blue zones, the flip (X) errors corrections qubits¹¹⁴⁸. It uses a hexagonal arrangement with an intermediate qubit on each side of hexagons. The topology is optimized for future implementations of quantum errors correction code, using custom hybrid surface and Bacon-Shor subsystem codes. This topology is different from the square lattice chosen by Google in its Sycamore processors, which, however, uses coupling qubits, a solution that IBM was not relying on until it was announced in May 2022 that they would later implement it. IBM was using fixed frequency qubits when Google uses tunable frequency ones. The hex lattice reduces the effect of frequency collision between qubits.

¹¹⁴⁷ See also this [impressive list](#) of over 800 papers from IBM research and its research partners published on arXiv (as of August 2022).

¹¹⁴⁸ See [The IBM Quantum heavy hex lattice](#) by Paul Nation et al, IBM Research, July 2021 and [Topological and subsystem codes on low-degree graphs with flag qubits](#) by Christopher Chamberland et al, IBM Research, December 2019 (20 pages). Heavy hex requires some tuning with algorithms like QAOA. See [Scaling of the quantum approximate optimization algorithm on superconducting qubit based hardware](#) by Johannes Weidenfeller et al, IBM, February 2022 (20 pages).

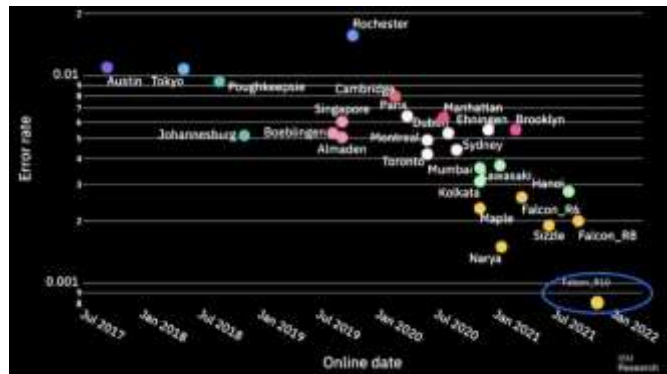
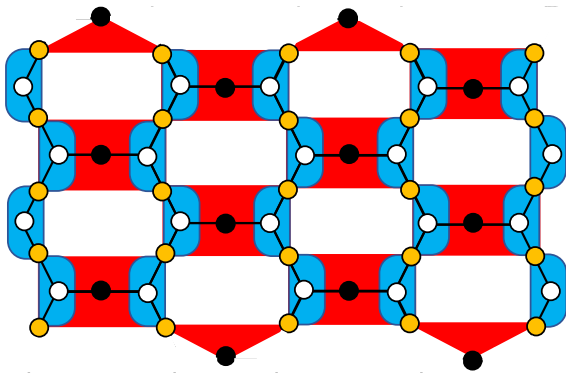


Figure 315: Heavy-Hexagon layout (left) and evolution of IBM's superconducting qubits fidelities over time (right).

IBM now plans to use LDPC correction codes that will require long range connectivity between the qubits, to be implemented with 7-layers connectivity chips. In August 2023, IBM published an important related preprint paper showing that for a logical qubit error rate of 10^{-12} , twelve logical qubits would require 288 physical qubits instead of 4,000 physical qubits with a surface code, assuming a physical qubit error rate of 0.1% (which remains to be seen at such scales)¹¹⁴⁹.

Qubit quality. With improving qubit readouts fidelity using low noise amplifiers (QLA for quantum-limited amplifiers)¹¹⁵⁰. They reached record fidelities in November 2022 with the 33-qubit Egret QPU, with two-qubit ECR gates fidelities of 99.66%. Meanwhile, the larger Osprey has two-qubit gate fidelities in the 98% range for two-qubit gates.

They also improve coherence times on a regular basis within a class of systems processors (like Falcon for 27 qubits)¹¹⁵¹.

Their record is a T_1 of 348 μ s with their Geneva Falcon 27-qubit R8 processor and 1 ms in research ([source](#)). They also continuously improve qubit physical properties¹¹⁵². Like with using laser annealing in their production¹¹⁵³, with new materials design improving their purity and avoiding contaminations and computer aided design¹¹⁵⁴, and with improving chip vacuum isolation during its assembly¹¹⁵⁵. Metallic superconducting nanowires could also be controlled by applying a moderate voltage to a nearby gate electrode. Switches using this effect would require very little power and could mitigate the well-known negative impact of phonons on the coherence of superconducting qubits¹¹⁵⁶.

IBM researchers are also quite prolific in finding ways to improve gates fidelities. Like with enabling efficient SWAP gates implementation with low crosstalk, using dispersively coupled fixed-frequency

¹¹⁴⁹ See [High-threshold and low-overhead fault-tolerant quantum memory](#) by Sergey Bravyi, Andrew W. Cross, Jay M. Gambetta, Dmitri Maslov, Patrick Rall and Theodore J. Yoder, IBM, August 2023 (38 pages). This is however limited to some Clifford gates.

¹¹⁵⁰ See [Rising above the noise: quantum-limited amplifiers empower the readout of IBM Quantum systems](#) by Baleegh Abdo, January 2020.

¹¹⁵¹ T_1 and T_2 reached about 260 μ s in September 2021 with their [Peekskill](#) 27 qubit system. It was a 3-times improvement vs previous systems.

¹¹⁵² See [Materials challenges and opportunities for quantum computing hardware](#) by Nathalie P. de Leon et al, Science, April 2021 (x pages).

¹¹⁵³ See [High-fidelity superconducting quantum processors via laser-annealing of transmon qubits](#) by Eric J. Zhang et al, December 2020 (9 pages) and [Laser-annealing Josephson junctions for yielding scaled-up superconducting quantum processors](#) by Jared B. Hertzberg et al, August 2021 (8 pages).

¹¹⁵⁴ See [What if We Had a Computer-Aided Design Program for Quantum Computers?](#), IBM, October 2020 and [Qiskit Metal: IBM Community Building a Computer-Aided Program for Quantum Device Design](#) by Matt Swayne, October 2020.

¹¹⁵⁵ See [Ultrahigh Vacuum Packaging and Surface Cleaning for Quantum Devices](#) by M. Mergenthaler et al, 2020 (6 pages).

¹¹⁵⁶ See [Vibrations could flip the switch on future superconducting devices](#) by Markus F. Ritter, Andreas Fuhrer and Fabrizio Nichele, March 2022, pointing to [Out-of-equilibrium phonons in gated superconducting switches](#) by Markus F. Ritter et al, Nature Electronics, March 2022 (7 pages).

transmon qubits and simultaneous driving of the coupled qubits at the frequency of another qubit, with a fast two-qubit interaction equivalent to $ZX + XZ$ entangling gates, implemented without strongly driving the qubits¹¹⁵⁷.

3D circuits. It started with stacked pairs of chips separating qubits from microwave controls, using TSV (through-silicon vias) with their 127 qubit systems in 2021¹¹⁵⁸.

This 3D chip layout introduced with Eagle (127 qubits) adds multi-level wiring (MLW) on the backside of the interposer (Figure 316). Control and readout signals are routed as strip lines in the MLW and are well isolated from the interposer and qubit metal levels. Connections between the qubits and this MLW are implemented with superconducting TSVs (through-silicon vias). It reduces crosstalk when pairing qubits. They also improved readout multiplexing with using 9 lines instead of 5 in Eagle. However, this degrades their CNOT gates fidelity due to collisions between qubit readout frequencies.

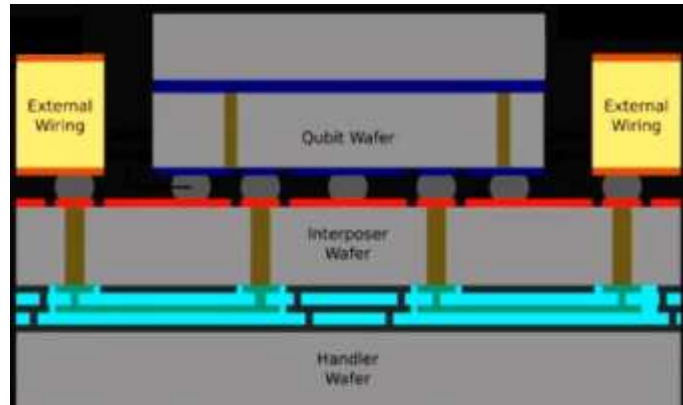


Figure 316: the three stacked die chip architecture used in Eagle's 127 qubit processor. Source: IBM.

The connectivity chip will have 5 layers in Condor (1,121 qubits) and 7 layers in future versions. This will enable the long-range connectivity that is required for implementing LDPC error correction codes.

Scalability. With microwaves signals multiplexing and intelligent filtering for qubit states readouts, starting with Hummingbird 65 qubits system in 2020. They are also using microwave flexible cables to reduce the space used by microwave cabling in cryostats. They are also implementing tunable couplers to control qubits entanglement¹¹⁵⁹.

With Osprey (433 qubits), wires density improved using 24-lines flexible cables and with control electronics of “generation 3”, using custom-made FPGAs (Figure 318).



Figure 317: IBM's quantum data center in Poughkeepsie, New York State. Source: IBM.

Scalability will also come from qubits miniaturization coming from various paths like a simplification of the readout electronics replacing the usual circulator with a “microwave-controlled qubit readout multichip module” (QRMCM)¹¹⁶⁰.

¹¹⁵⁷ See [Cross-Cross Resonance Gate](#) by Kentaro Heya and Naoki Kanazawa, IBM Research Japan, PRX, November 2021 (15 pages).

¹¹⁵⁸ See [Merged-Element Transmons: Design and Qubit Performance](#) by H. J. Mamin et al, March 2021 (7 pages).

¹¹⁵⁹ See [Tunable Coupling Architecture for Fixed-frequency Transmons](#) by J. Stehlik et al, IBM Research, February 2021 (7 pages) and [With fault tolerance the ultimate goal, error mitigation is the path that gets quantum computing to usefulness](#) by Kristan Temme, Ewout van den Berg, Abhinav Kandala and Jay Gambetta, July 2022.

¹¹⁶⁰ See [High-Fidelity Qubit Readout Using Interferometric Directional Josephson Devices](#) by Baleegh Abdo et al, December 2021 (34 pages). Avoiding the magnet-based based circulator for qubit readout using a microwave-controlled qubit readout multichip module (QRMCM) that “integrates interferometric directional Josephson devices consisting of an isolator and a reconfigurable isolator or amplifier device, and an off-chip low-pass filter”. Also, see [Merged-Element Transmons: Design and Qubit Performance](#) by H.J. Mamin et al, PRA, August 2021 (7 pages).

They are also developing CryoCMOS control electronics to be deployed in future systems. Cabling optimization is also on the way. The Osprey system is using 24-lines flexible cables with a goal to reach 100 cables. Condor was tested with a similar setup but quickly dismantled as of early 2024.

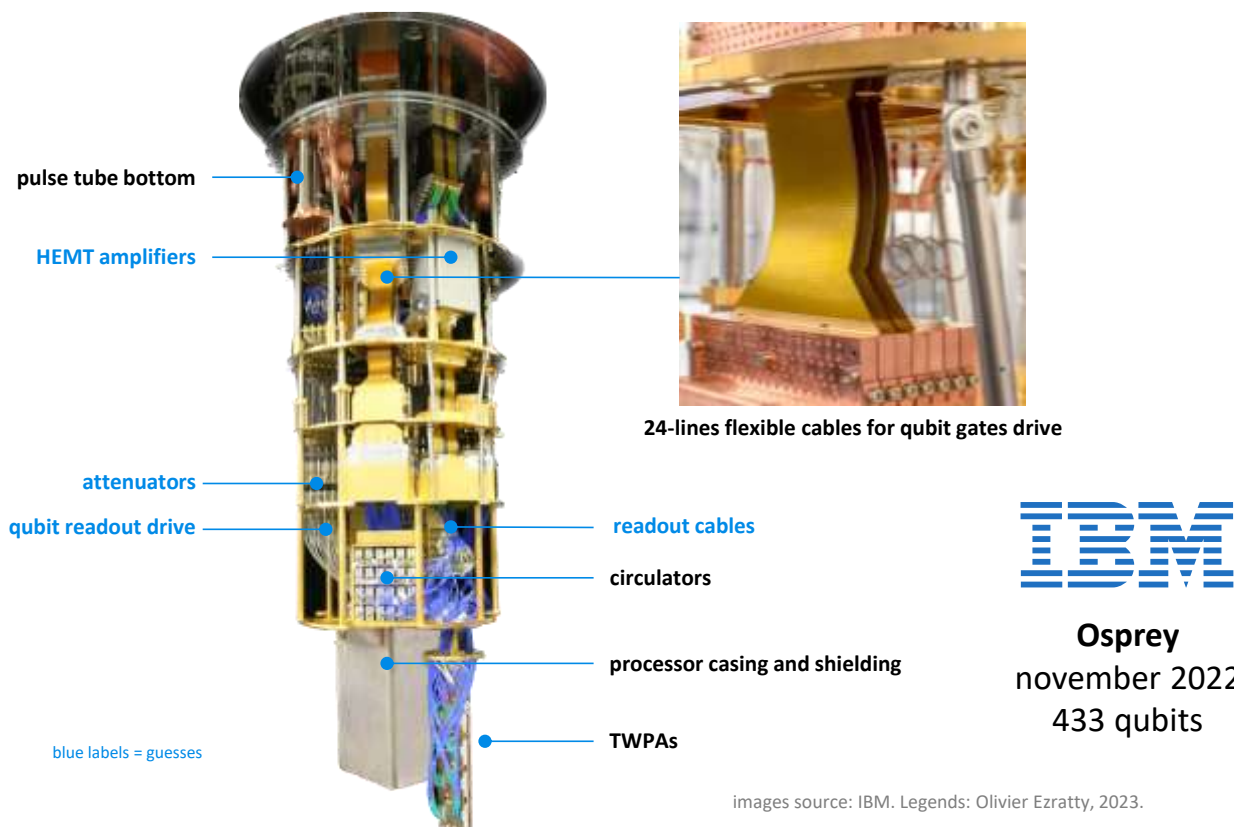


Figure 318: IBM Osprey system showing its flexible cabling and various other parts. Source: IBM and Olivier Ezratty, 2023.

Error Mitigation. Before fault tolerant QPUs are developed, IBM is betting on using quantum error mitigation and error suppression techniques¹¹⁶¹ (Figure 319).

Quantum utility. In June 2023, IBM announced having reached some quantum utility with a 100 breadth x 60 depth circuit running on a Kyiv 127 qubit QPU implementing a kicked Ising model problem solving algorithm, thanks to using quantum error mitigation (ZNE). The performance is documented in a rather small paper in Nature¹¹⁶² and in an IBM blog post¹¹⁶³ and with additional information found in Forbes¹¹⁶⁴. The authors cautiously stated that they “*fully expect that the classical computing community will develop methods that verify the results we presented*”. They didn’t provide insights on the types of problems that could be solved with some encoding into an Ising model although it would be surprisingly close to what D-Wave quantum annealers are achieving since they are directly implementing a Ising model solving scheme¹¹⁶⁵.

¹¹⁶¹ See [With fault tolerance the ultimate goal, error mitigation is the path that gets quantum computing to usefulness](#) by Kristan Temme, Ewout van den Berg, Abhinav Kandala and Jay Gambetta, July 2022.

¹¹⁶² See [Evidence for the utility of quantum computing before fault tolerance](#) by Youngseok Kim, Kristan Temme, Abhinav Kandala et al, IBM Research, RIKEN iTHEMS, University of Berkeley and the Lawrence Berkeley National Laboratory, Nature, June 2023 (8 pages).

¹¹⁶³ See [New paper from IBM and UC Berkeley shows path toward useful quantum computing](#) by Ryan Mandelbaum, IBM, June 2023.

¹¹⁶⁴ See [IBM’s Latest Research Paper Signals A New Era Of Quantum Computing Is Here](#) by Paul Smith-Goodson, Moor Insights and Strategy, Forbes, June 2023.

¹¹⁶⁵ We can suspect it is like with D-Wave systems, enabling solving QUBO problems which in turn are adapted to both solving combinatorial problems or quantum chemistry problems, although with significant overhead. For example, it won’t make VQE easier to implement with these systems.

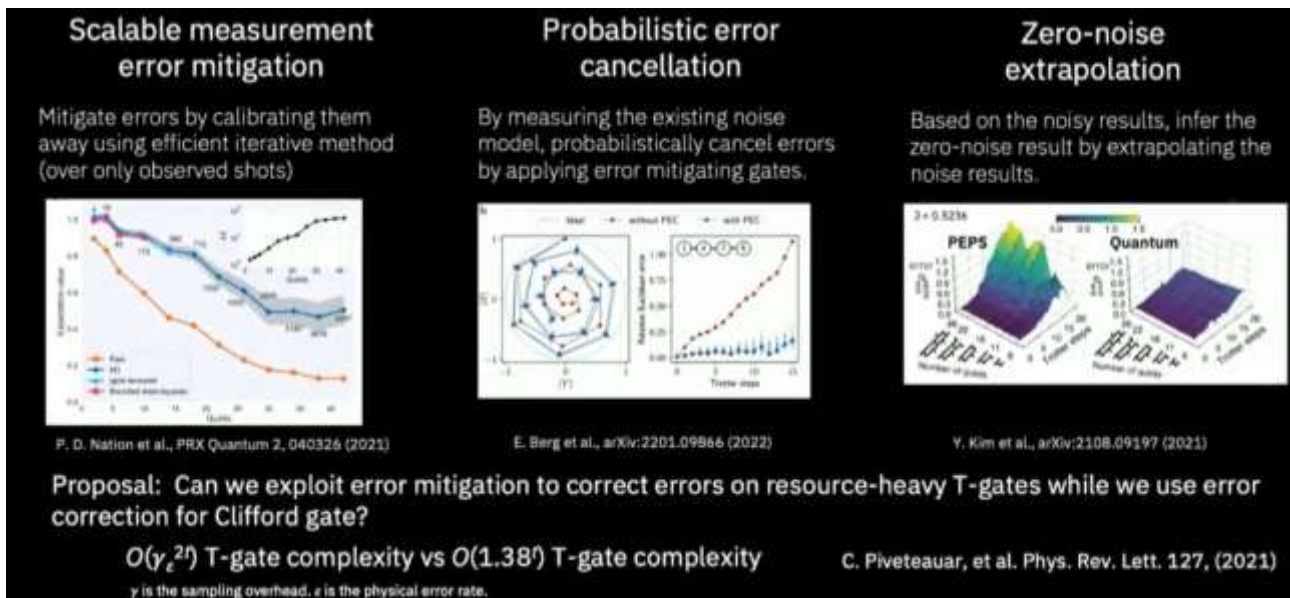


Figure 319: the various quantum error mitigation techniques IBM is working on. Source: IBM.

It did not take long before efficient tensor based classical simulations of the Ising model were developed. A couple weeks later, Miles Stoudenmire et al from the Flatiron Institute did publish a preprint showing a classical solution yielding an accuracy of $\sim 10^{-14}$ running faster than IBM's QPU, in less than 2 minutes. It could even run it with a better accuracy in less than 7 minutes to run on a single Intel Skylake CPU using 0.3 GB of memory¹¹⁶⁶. A couple days later, a Caltech team did a similar experiment and could implement in emulation mode IBM's experiment on a simple laptop¹¹⁶⁷ and a team from Google did the same in one second with using a single GPU¹¹⁶⁸. A research team in China arrived at a similar conclusion in August 2023¹¹⁶⁹. Then, an IBM team benchmarked these various classical solutions and found discrepancies in their results, of about 20%¹¹⁷⁰. A team from Bar-Ilan University in Israel explained why IBM's performance could be achieved with such a noisy QPU¹¹⁷¹, another international team created yet another efficient classical simulation of the IBM kicked Ising model¹¹⁷² and a team led by Multiverse extended this to 433 and 1,121 qubits using another tensor networks variation¹¹⁷³. This quantum/classical computing battle has not ended yet!

Various algorithms optimizations. IBM research teams are finding many ways, more or less efficient, to optimize algorithms run-time.

¹¹⁶⁶ See [Efficient tensor network simulation of IBM's Eagle kicked Ising experiment](#) by Joseph Tindall, Matt Fishman, Miles Stoudenmire and Dries Sels, PRX Quantum, June 2023-January 2024 (16 pages).

¹¹⁶⁷ See [Fast classical simulation of evidence for the utility of quantum computing before fault tolerance](#) by Tomislav Begušić and Garnet Kin-Lic Chan, Caltech, June 2023 (4 pages) which was updated in [Fast and converged classical simulations of evidence for the utility of quantum computing before fault tolerance](#) by Tomislav Begušić et al, Caltech, August 2023 (17 pages).

¹¹⁶⁸ See [Effective quantum volume, fidelity and computational cost of noisy quantum processing experiments](#) by K. Kechedzhi et al, Google AI, NASA, June 2023 (15 pages).

¹¹⁶⁹ See [Simulation of IBM's kicked Ising experiment with Projected Entangled Pair Operator](#) by Hai-Jun Liao et al, China, August 2023 (8 pages).

¹¹⁷⁰ See [Classical benchmarking of zero noise extrapolation beyond the exactly-verifiable regime](#) by Sajant Anand, Kristan Temme et al, UC Berkeley, LBNL and IBM, June 2023 (11 pages).

¹¹⁷¹ See [Dissipative mean-field theory of IBM utility experiment](#) by Emanuele G. Dalla Torre and Mor M. Roses, Bar-Ilan University, August 2023 (4 pages).

¹¹⁷² See [Classical surrogate simulation of quantum systems with LOWESA](#) by Manuel S. Rudolph et al, EPFL, University of Strathclyde, Quantinuum, NPL and JPMorgan Chase, August 2023 (13 pages).

¹¹⁷³ See [Efficient tensor network simulation of IBM's largest quantum processors](#) by Siddhartha Patra et al, September 2023 (6 pages).

For example, they are allowing more computations with the Bernstein-Vazirani algorithm run on 12 qubits, where SWAP gates are replaced with resets, improving fidelity from 0.0007 to 0.80.

They also propose to use “circuit knitting”, i.e., combining smaller circuits to simulate larger problems using entanglement forging¹¹⁷⁴ (Figure 320). However, this technique has a strong tendency to strongly attenuate algorithms quantum advantage and parallelism.

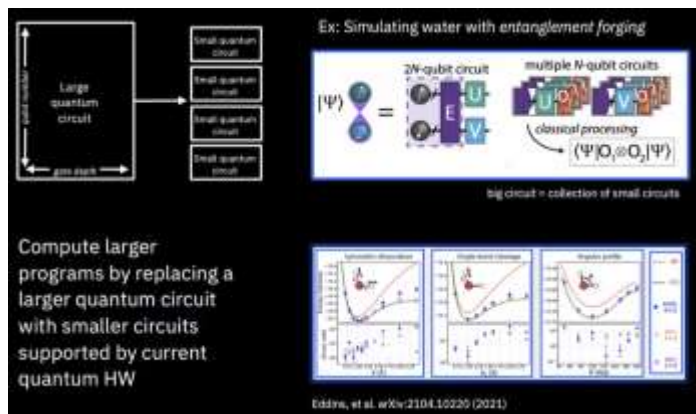


Figure 320: entanglement forging technique. Source: IBM.

Cryogeny. IBM announced in 2020 that it was working on a giant home-made cryostat nicknamed Goldeneye, to host from a thousand to a million physical qubits¹¹⁷⁵, shown in Figure 321. It was due for 2023 after some tests were conducted in 2022 at 25 mK. It has about 12 pulse tubes and 6 dry dilutions with half of the dilution to be inverted at the bottom. The project was however put on hold while IBM’s team was integrating Bluefors KIDE dilution fridges in its System Two.



Figure 321: IBM's giant Goldeneye dilution refrigerator, which is currently put on hold. Source: IBM.

QPU interconnect. Beyond 2023, scale-out will involve various types of couplers. At short to mid-range, these will be microwave couplers. Beyond, interconnecting quantum processing unit will rely on microwave-optical transduction and optical fiber to connect QPUs, with optomechanical coupling or electro-optic coupling. One option is to use optical channels with SiGe/Si optical resonators¹¹⁷⁶. These quantum units will be cooled with a new generation of cryostats, designed by Bluefors as part of their KIDE range using a hexagonal form factor, announced in November 2021.

¹¹⁷⁴ See [Doubling the size of quantum simulators by entanglement forging](#) by Andrew Eddins, Sergey Bravy, Sarah Sheldon et al, April 2021 (17 pages), [Entanglement forging The 2x Gambit: IBM Tech Doubles Qubit Effectiveness](#) by Charles Q. Cho, February 2022, [Simulating Large Quantum Circuits on a Small Quantum Computer](#) by Tianyi Peng, Aram Harrow et al, October 2020, PRL (20 pages), [Quantum Divide and Conquer: Exploring The Effect of Different Noise Sources](#) by Thomas Ayril and F.M Le Régent (Atos) with Zain Saleem, Yuri Alexeev, Martin Suchara (DoE Argonne National Laboratory, February 2021 (21 pages) and [Constructing a virtual two-qubit gate by sampling single-qubit operations](#) by Kosuke Mitarai and Keisuke Fujii, Osaka University, JST PRESTO and RIKEN, January 2021 (13 pages).

¹¹⁷⁵ See [IBM scientists cool down world's largest quantum-ready cryogenic concept system](#) by Pat Gumann and Jerry Chow, September 2022. The device is 3m high and 2m wide with 1.7 m³ of experimental volume and 10 internal plates. Its cooling power is of 10 mW at 100 mK and 24W at 4K.

¹¹⁷⁶ See [Engineering electro-optics in SiGe/Si waveguides for quantum transduction](#) by Jason Orcutt et al, Quantum Science Technology, 2020 and [Ultra-high-Q on-chip silicon-germanium microresonators](#) by Ryan Schilling, Hanhee Paik et al, Optica, 2022 (4 pages).

Serverless. As part of their May 2022 announcements, IBM explained it had adopted a “serverless” architecture, another name for a cloud service driving both classical and quantum computers with a pay-as-you-go pricing¹¹⁷⁷. It involves three techniques: circuit knitting that leverages classical resources cut a quantum problem in smaller problems and circuits to run on NISQ QPUs, and also use classical processing. This is interesting but reduces the quantum acceleration generated by the QPUs who will run quantum algorithms of smaller Hilbert space. Then, entanglement forging is a way to simplify knitting specific to solving chemistry problems. They then use “quantum embedding” to re-frame a problem and split it between pieces running classically and others quantumly “*for only the classically difficult parts of the problem*”. Finally, error mitigation is based on classical post-processing to reduce the impact of some classes of quantum errors.

Benchmarking. IBM now uses three key metrics to benchmark its quantum systems. The first one is simply their number of qubits which define the **scale** of their system. The second is the quantum volume that was introduced in 2019 and described in details page 1007.

It defines their computing **quality**. IBM announced it would double every year. In April 2022, they obtained a record quantum volume of 256, meaning 8 operational qubits and 8 depths of computing, which increased to 512 in May 2022¹¹⁷⁸. Due to limited qubit fidelities, IBMs QPUs quantum volumes have not made progress since 2022 (Figure 322).

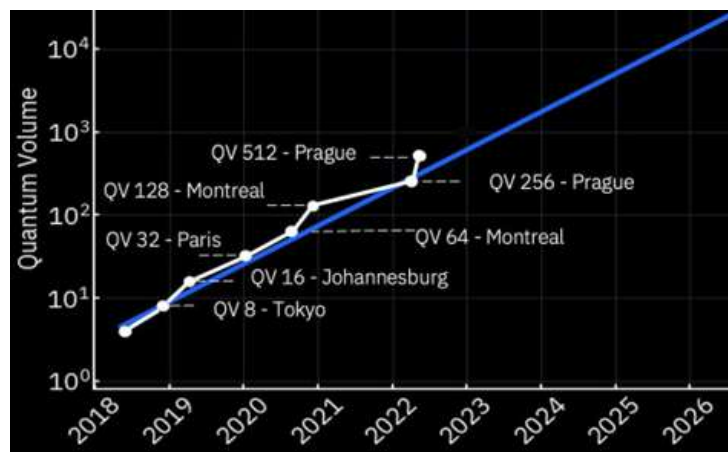


Figure 322: IBM's quantum volume evolution over time. Source: IBM.

In November 2021, IBM introduced CLOPS, or circuit layers operations per second, which defines the **speed** of their QPUs, also labelled in Hz.

It currently sits between 800 and 3,800 CLOPS with a record of 15K obtained on a prototype Falcon chip¹¹⁷⁹ ¹¹⁸⁰. The discrepancy between this speed and quantum gates durations (between 20 ns and 300 ns) comes from the CLOPS metrics accounting for all the classical preprocessing happening before running your quantum code. IBM is caring about the level of large entanglements generated in these systems, *aka* genuine multipartite entanglement (GME). It was done in 2021 by a team of Australian researchers with fidelities of 54% for 27 qubits with using some quantum readout-error mitigation (QREM)¹¹⁸¹. It was also implemented by IBM Research with a 65-qubit QPU¹¹⁸². The schema in Figure 323 shows the history of experimentally prepared quantum states exhibiting N-qubit GME, where $N \geq 3$, with at least 95% confidence in gate-based quantum systems. It illustrates the challenges to create large high-fidelity entangled states.

¹¹⁷⁷ See [Introducing Quantum Serverless, a new programming model for leveraging quantum and classical resources](#) by Blake Johnson, Ismael Faro, Michael Behrendt and Jay Gambetta, May 2022

¹¹⁷⁸ See [Pushing quantum performance forward with our highest Quantum Volume yet](#) by Petar Jurcevic et al, IBM, April 2022.

¹¹⁷⁹ See [Quality, Speed, and Scale: three key attributes to measure the performance of near-term quantum computers](#) by Andrew Wack, Hanhee Paik, Jay Gambetta et al, 2021 (8 pages).

¹¹⁸⁰ See [Quantum-centric supercomputing: The next wave of computing](#) by Jay Gambetta, IBM, November 2022.

¹¹⁸¹ See [Generation and verification of 27-qubit Greenberger-Horne-Zellinger states in a superconducting quantum computer](#) by Gary J. Mooney et al, August 2021 (16 pages).

¹¹⁸² See [Whole-device entanglement in a 65-qubit superconducting quantum computer](#) by Gary J. Mooney et al, October 2021 (15 pages).

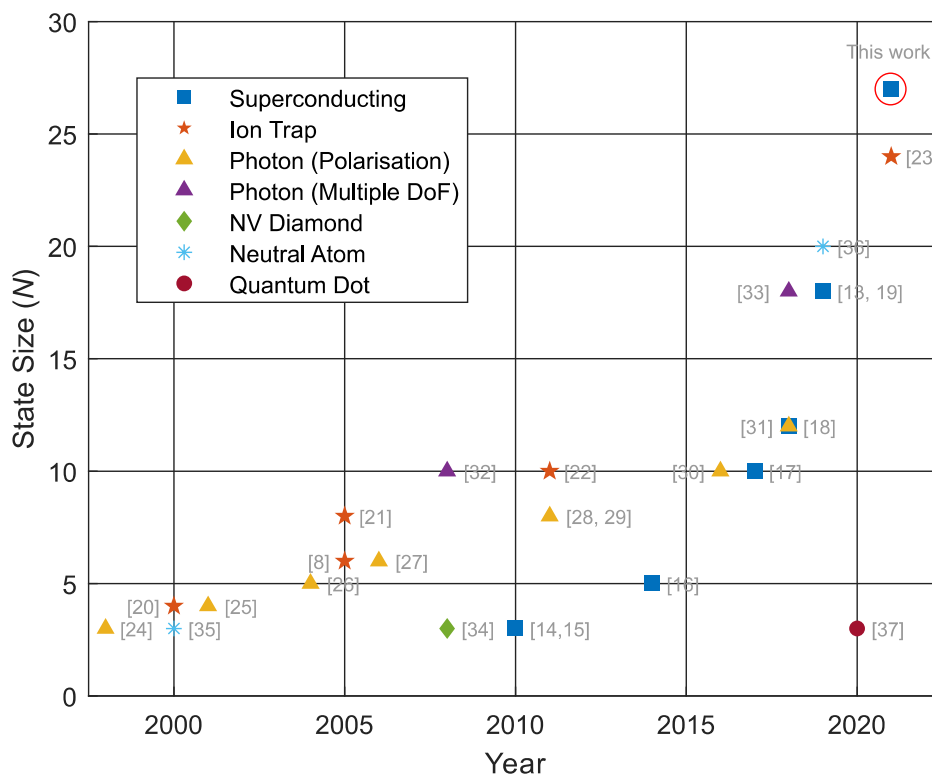


Figure 323: largest multipartite entangled state over time although a bit dated. Source: [Generation and verification of 27-qubit Greenberger-Horne-Zeilinger states in a superconducting quantum computer](#) by Gary J. Mooney et al, August 2021 (16 pages).

Deployments and customer evangelism. IBM has been investing steadily since 2016 to build a worldwide community of developers and users. They launched the IBM Quantum network in 2017. It brings together major Fortune 500 companies, research laboratories and startups interested in developing quantum solutions. This network offered access free access to quantum systems with 5 and 7 qubits. Commercial systems had respectively 16, 27, 33, 65, 127 and 433 qubits. At last, a quantum emulator (branded a simulator) supported 32 qubits, but was discontinued in May 2024. As of June 2022, they had 24 quantum systems online. In September 2023, free access was expanded to 127-qubit systems, with the retirement of many QPUs using a lower number of qubits. A couple 27 qubits QPUs are left online.

IBM also launched a customer Quantum Computation Center in Poughkeepsie, New York, a quantum center in Montpellier, France, in 2018, and then a partnership in Germany with a Fraunhofer Institute in 2019 plus other quantum centers in Japan, Korea and Canada. Their task is to evangelize developers and researchers to encourage them to develop software on their Qiskit platform and their quantum systems sitting in the cloud.

In April 2021, IBM finalized the deployment of a 27-qubit Quantum System in its own site in Ehningen, near Stuttgart, Germany, in relationship with Fraunhofer as an intermediate to reach out the developer community¹¹⁸³. It was even inaugurated remotely by Chancellor Angela Merkel on June 15th, 2021. The access price for the 27-qubit System One is €11,621 and €9,770 per month for the industry and for R&D¹¹⁸⁴. The center is even becoming a “quantum data center” to be opened in 2024, for running hybrid classical and quantum software under the umbrella of the GDPR privacy regulations¹¹⁸⁵.

¹¹⁸³ See [Fraunhofer launches quantum computing research platform in Germany](#), April 2021.

¹¹⁸⁴ See [How do I use the quantum computer?](#), Fraunhofer.

¹¹⁸⁵ See [IBM’s first quantum data center in Europe](#) by Ismael Faro, June 2023.

IBM also announced a partnership of 10 years with Cleveland Clinic in the USA, including the delivery of their 1,121 qubits system around 2024. Meanwhile, the customer will rely on the existing cloud-based Quantum Experience systems¹¹⁸⁶. Then, in June 2021, IBM announced a five year \$300M artificial intelligence and quantum computing research partnership with the UK. They plan to hire 60 scientists as part of the new Hartree National Centre for Digital Innovation (HNCDI)¹¹⁸⁷. IBM has however not put all its eggs in the superconducting qubits basket. Their Zurich research center is also investigating electron spins and Majorana fermions qubits at a fundamental research level, working on this with ETH Zurich and EPFL. Also, in February 2022, IBM invested \$25M in Quantinuum¹¹⁸⁸.

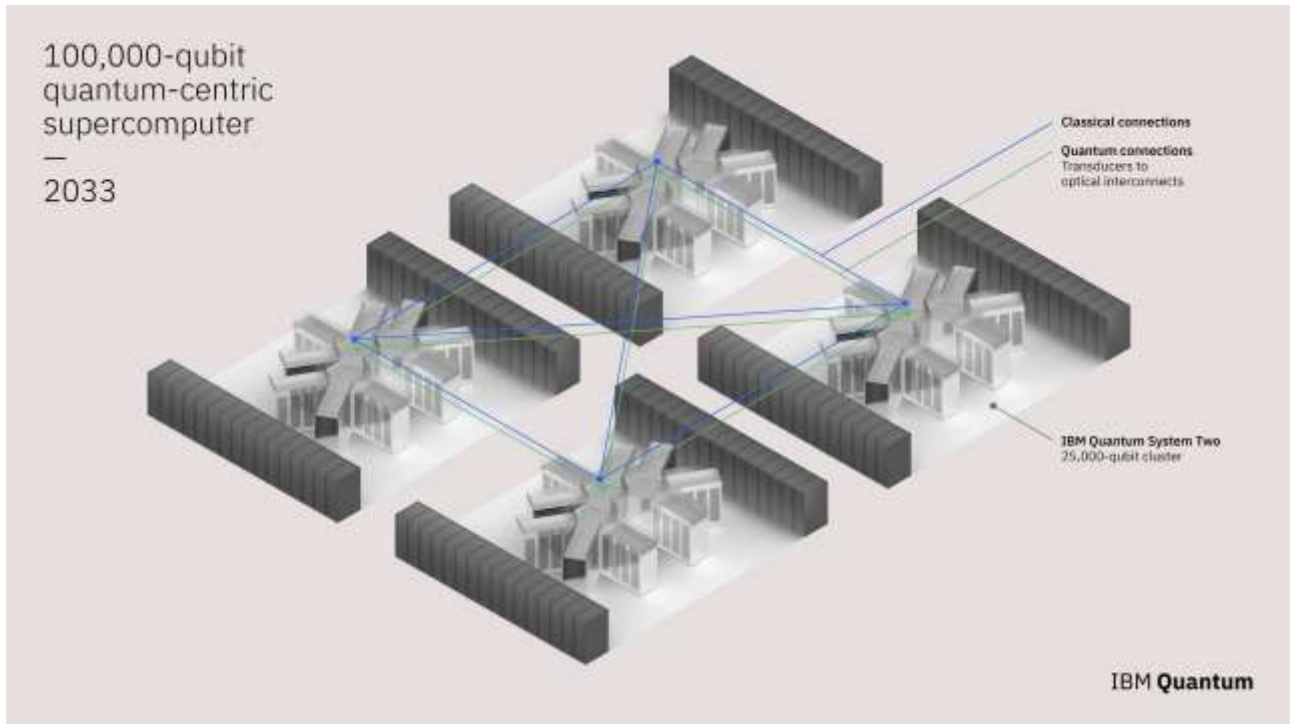


Figure 324: IBM System 2 with 100,000 qubits in total. Source: IBM, 2023.

The IBM System 2 roadmap that was announced in May 2023 will lead to a 100,000 qubit System 2 in 2023. It was introduced jointly with an USA-Japan \$100M partnership over 10 years¹¹⁸⁹ ¹¹⁹⁰. The 100,000-qubit system will be built out of four 25,000 qubits clusters interconnected by photonic links (Figure 324). Each of these clusters will use three high-power dilution fridges connected through long range microwave interconnections. The announced partnership involves the University of Tokyo and the University of Chicago. There may be some connection with IBM Japan Research team working on control electronics, which plays an important role to slowly scale the energy consumption of these QPUs¹¹⁹¹. The University of Chicago is working on error correction codes and photonic interconnection solutions. The \$100M partnership is spread over 10 years across the USA and Japan, meaning the University of Tokyo probably receives less than \$5M a year.

¹¹⁸⁶ See [Cleveland Clinic, IBM launch 10-year quantum computing partnership](#) by Mike Miliard, March 2021.

¹¹⁸⁷ See [UK STFC Hartree Centre and IBM Begin Five-Year, £210 Million Partnership to Accelerate Discovery and Innovation with AI and Quantum Computing](#), June 2021.

¹¹⁸⁸ See [IBM invests in Quantinuum, and other quantum news updates](#) by Dan O'Shea, Fierce Electronics, February 2022.

¹¹⁸⁹ See [Charting the course to 100,000 qubits](#) by Jay Gambetta and Matthias Steffen, May 2023.

¹¹⁹⁰ See [IBM Launches \\$100 Million Partnership with Global Universities to Develop Novel Technologies Towards a 100,000-Qubit Quantum-Centric Supercomputer](#), IBM, May 2023.

¹¹⁹¹ See [IBM wants to build a 100,000-qubit quantum computer](#) by Michael Brooks, MIT Technology Review, May 2023.



Google started to invest in quantum computing in the mid-2010s. In 2014/2015, it tested some algorithms on a **D-Wave** quantum annealing system installed in the joint QUAIL laboratory established with NASA and located at the Ames Research Center in Mountain View.

Google initially wanted to create its own quantum annealer *ala* D-Wave but quickly switched gears towards gate-based superconducting qubits quantum computing, under the direction of **Hartmut Neven** since 2006, who manages quantum hardware and software. In 2019, he put forward an empirical law called Dowling-Neven according to which the power of computers doubles exponentially. This was exaggerated when you look at their evaluation method¹¹⁹²!

Hardware was developed by **John Martinis** et al between 2014 and 2020¹¹⁹³ (Figure 327). All this was done in connection with the University of Santa Barbara in California (UCSB), where he came from with part of his team.

In 2017, Google stated its ambition to obtain some quantum supremacy as defined by John Preskill in 2011¹¹⁹⁴. In April 2017 came a 9 qubits chip followed in 2018 by their Foxtail 22 qubits chip. In March 2018, Google announced a 72 qubits chip named Bristlecone, promising a two-qubits gates fidelity of 99.56%. It seemed however a dead-end and was abandoned. Then came the famous October 2019 so-called quantum supremacy with their Sycamore processor using 53 qubits interconnected with couplers and a random algorithm similar to the boson sampling algorithm imagined by Scott Aaronson in 2012¹¹⁹⁵. NASA and Google science papers were mistakenly posted on the Internet in September 2019 and then officially published in the journal Nature in October 2019¹¹⁹⁶, filing 70 pages with a level of detail never seen before¹¹⁹⁷. Google compared their qubits with the most powerful supercomputer of the time, the IBM Summit installed at the Department of Energy's Oak Ridge

¹¹⁹² The reasoning is as follows: the number of qubits would so far increase exponentially, and the power doubles with each addition of a single qubit. All this, every six months. Unfortunately, the available data on the actual power of today's quantum computers does not comply with this law. There is no doubling of the number of operational qubits every six months! There is even regression! Google announced 72 qubits in March 2018 and then 53 qubits in October 2019. At IBM, we are in the total confusion between the Q System One which went from 20 to 28 qubits between January 2019 and January 2020, which does not look like a doubling every six months. On the other hand, this doubling could eventually be achieved with other technologies such as Honeywell's trapped ions or Pasqal's cold atoms. In his presentation at Q2B in December 2019, John Preskill highlighted another exponential doubling: gate fidelity rates are steadily improving, which would increase quantum volume exponentially. At the same time, the cost of emulating quantum computing on conventional computers increases exponentially with quantum volume. Hence a doubly exponential evolution of computing power. The bug? Nothing says that the fidelity of quantum gates will continue to improve steadily. See [A New Law to Describe Quantum Computing's Rise?](#), June 2019.

¹¹⁹³ John Martinis resigned from Google in April 2020 after being demoted to a scientific advisory role mid-2019. He explained this in an exit interview for Forbes: [Google's Top Quantum Scientist Explains In Detail Why He Resigned](#) by Paul Smith-Goodson, 2020. See also [Google's Head of Quantum Computing Hardware Resigns](#) by Tom Simonite, April 2020.

¹¹⁹⁴ See [Google says it is on track to definitively prove it has a quantum computer in a few months' time](#) by Tom Simonite, April 2017. See also [The Question of Quantum Supremacy](#), May 2018 which references two related papers : [Characterizing Quantum Supremacy in Near-Term Devices](#), 2016 (23 pages) and [A blueprint for demonstrating quantum supremacy with superconducting qubits](#), 2017 (22 pages).

¹¹⁹⁵ See [Quantum Supremacy Using a Programmable Superconducting Processor](#) by John Martinis, October 2019. The most detailed presentation on Google's hardware engineering with Sycamore is available on [Google's quantum computer and pursuit of quantum supremacy](#) by Ping Yeh, September 2019 (63 slides). See also [Quantum Computer Datasheet](#), Google AI, May 2021 (6 pages) which provides detailed indications of Sycamore's qubit fidelities with the Weber version of the processor.

¹¹⁹⁶ See [Hello quantum world! Google publishes landmark quantum supremacy claim](#) by Elizabeth Gibney, October 2019.

¹¹⁹⁷ See [Quantum supremacy using a programmable superconducting processor](#) by Frank Arute, John Martinis et al, October 2019 (12 pages) and [Supplementary information for "Quantum supremacy using a programmable superconducting processor"](#) by Frank Arute, John Martinis et al, October 2019 (58 pages). See also [Quantum supremacy using a programmable superconducting processor](#), a lecture by John Martinis at Caltech, November 2019 (one hour). And [another version](#), played at QC Ware's Q2B conference in December 2019 (19 slides and 32-minute [video](#)). At last, here is this video promoting Google's supremacy: [Demonstrating Quantum Supremacy](#), October 2019 (4'42").

National Laboratory in Tennessee¹¹⁹⁸. Computing for 200 seconds on Sycamore would take 10,000 years once emulated on the IBM Summit. This comparison didn't make much sense as we discuss quantum supremacy and advantages in another part of this book, page 1017.

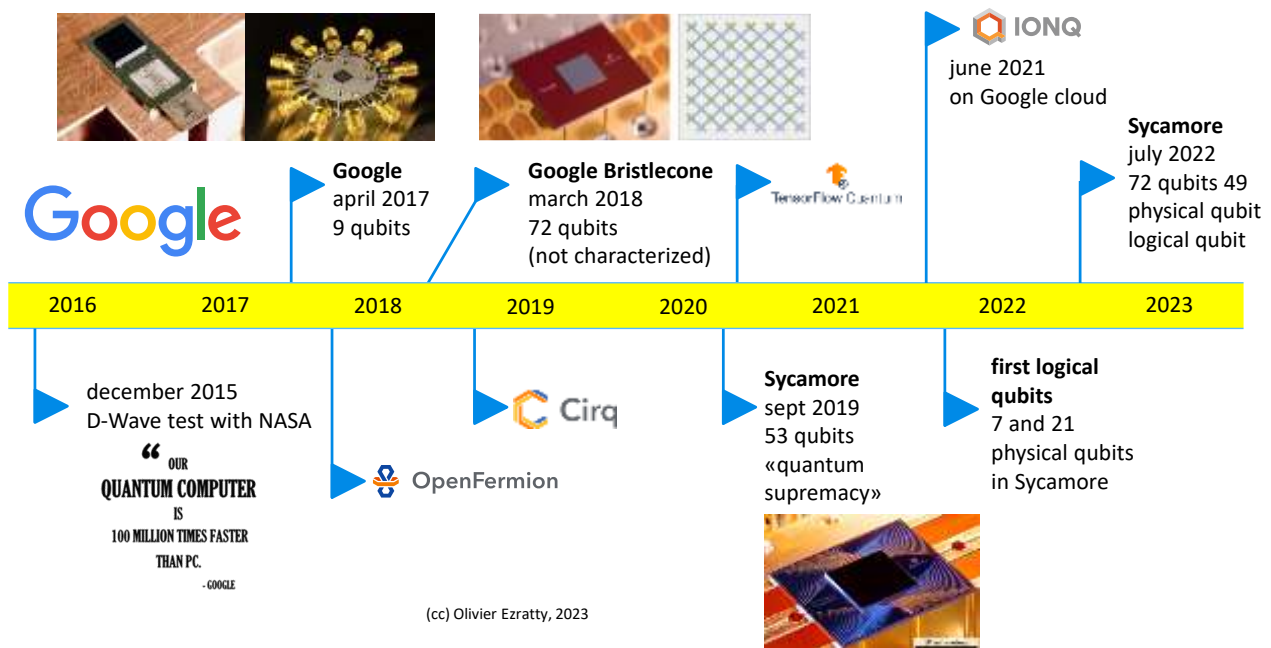


Figure 325: Google's quantum computing timeline. (cc) Olivier Ezratty, 2022-2023.

Let's have a look at Sycamore's engineering and its related supremacy benchmark and its updates over time (Figure 325, Figure 328):

Cross-Entropy Benchmarking (XEB). The benchmark algorithm combined a set of random quantum gates with a homogeneous distribution. This last part scans all the possible values (2^{53}) of qubits superpositions¹¹⁹⁹. In the supremacy regime, the so-called computation has a 0.14% chance to produce the right results. It is executed 3 million times to generate an average measurement mitigating this low fidelity¹²⁰⁰!

It uses superposition on all the qubits (53), allowing maximum performance. Usually, ancilla qubits are necessary to make some calculations. Ancilla qubits are used as buffer values. As a result, the exponential advantage decreases accordingly. Typical algorithms don't benefit from the superposition of 2^{53} states but, for example, a lesser 2^{30} or 2^{40} states. Any quantum advantage would then vanish. This explains why in most vendors roadmap, the end-goal is to create systems with 100 logical qubits and not just between 50 and 55 qubits. The XEB benchmark use a small 20 quantum gates computing depth. Namely, the algorithm tested at full load only chains 20 sequences of quantum gates executed simultaneously. This is related to the noise generated in the qubits which limits this depth.

On October 21, 2019, IBM researchers published an article in which they questioned Google's performance, stating that they could run their algorithm in 2.5 days instead of 10,000 years on the IBM

¹¹⁹⁸ See [Google researchers have reportedly achieved "quantum supremacy"](#) by Martin Giles, in the MIT Technology Review, September 2019 and the [source](#) of the paper on the Internet, with illustrations. They use a type of algorithm that is of little use, but which clearly favors quantum computing and requires a limited number of quantum gates, which is good for noise-generating quantum processors. See also [Why I Coined the Term 'Quantum Supremacy'](#) by John Preskill, October 2019.

¹¹⁹⁹ The following explanation can be found in Kevin Harnett's [Quantum Supremacy Is Coming: Here's What You Should Know](#) in Quanta Magazine, July 2019.

¹²⁰⁰ See [The Google Quantum Supremacy Demo and the Jerusalem HQCA debate](#) by Gil Kalai, December 2019, where he questions the results of Google's quantum supremacy, particularly its evaluation of qubit noise at large scale.

Summit supercomputer¹²⁰¹. This would require adding 64 PB of SSD to the supercomputer, which they had not tested. That's about 7 racks full of SSDs at 2019 capacity. IBM wanted to contradict Google's claim of quantum supremacy, which they turned into some sort of quantum advantage¹²⁰².

Then, as we'll see in the software section of this book, several tensor based emulations of Google's noisy qubits could replicate their 2019 supremacy experiment from 2020 to 2022.

It pushed Google to upgrade its experiment with a new one using 70 of their latest Sycamore 72 qubit chip¹²⁰³. In their related paper, they inadvertently did show that their 2019 supremacy was short-lived, now that it is possible to emulate it classically in just 6.18 seconds, instead of the 2.5 minutes of the quantum experiment (Figure 326).

Exp.	1 amp.	1 million noisy samples		
	FLOPs	FLOPs	XEB fid.	Time
SYC-53 [9]	$6.44 \cdot 10^{17}$	$2.60 \cdot 10^{17}$	$2.24 \cdot 10^{-3}$	6.18 s
ZCZ-56 [10]	$6.24 \cdot 10^{19}$	$6.40 \cdot 10^{19}$	$6.62 \cdot 10^{-4}$	25.3 min
ZCZ-60 [11]	$1.32 \cdot 10^{21}$	$1.41 \cdot 10^{23}$	$3.66 \cdot 10^{-4}$	38.7 days
This work	$4.74 \cdot 10^{23}$	$6.27 \cdot 10^{25}$	$1.68 \cdot 10^{-3}$	47.2 yr

Figure 326: Google's 2019 supremacy can now be classically simulated in 6.18s instead of the initial announced 10,000 years. But 6 seconds on the DoE Frontier supercomputer. With 70 qubits, the classical bar is now at 47 years. Source: [Phase transition in Random Circuit Sampling](#) by A. Morvan et al, Google AI, April 2023 (39 pages).

On top of that, randomized benchmarking used in Google's experiment is an approach that is not unanimously accepted to establish the superiority of quantum computing over classical computing¹²⁰⁴
1205 1206

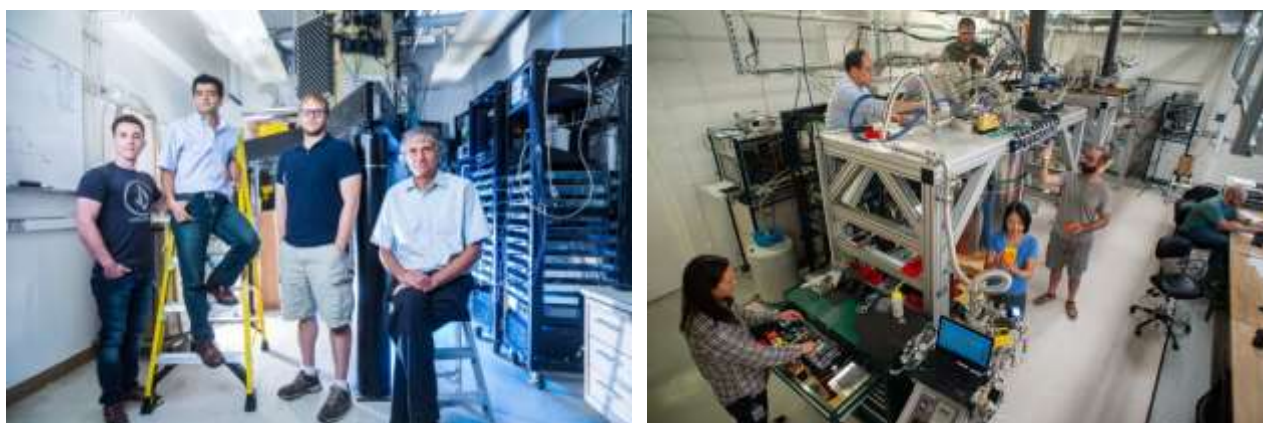


Figure 327: John Martinis and his team when he was at Google and Google's Sycamore's assembly in their lab. Sources: Google.

¹²⁰¹ See [On "Quantum Supremacy" | IBM Research Blog](#) by Edwin Pednault, October 2019 and [Leveraging Secondary Storage to Simulate Deep 54-qubit Sycamore Circuits](#) by Edwin Pednault et al, October 2019 (30 pages).

¹²⁰² Google's quantum supremacy quibbles have gone a long way, including IBM's response. And then [Has Google Finally Achieved Quantum Supremacy?](#), October 2019, which is quite well documented. Then [Quantum supremacy: the gloves are off](#) by Scott Aaronson, October 2019 where he discusses the fact that this case is the equivalent of Kasparov vs. Deep Blue, with IBM playing the role of Kasparov. Not to mention the debate on supremacy terminology that has once again generated a lot of fuss, as reported in [Academics derided for claiming 'quantum supremacy' is a racist and colonialist term](#) by Sarah Knapton, December 2019.

¹²⁰³ See [Phase transition in Random Circuit Sampling](#) by A. Morvan et al, Google AI, April 2023 (39 pages).

¹²⁰⁴ See [Lecture 3: Boson sampling](#) by Fabio Sciarrino (63 slides) and [An introduction to boson-sampling](#) by Bryan Gard, Jonathan P. Dowling et al, 2014 (13 pages).

¹²⁰⁵ See the review [Quantum computers: amazing progress \(Google & IBM\), and extraordinary but probably false supremacy claims \(Google\)](#) by Gil Kalai, September 2019.

¹²⁰⁶ See [The Quest for Quantum Computational Supremacy](#) by Scott Aaronson, September 2019 (16 pages) which was published three weeks before Google's announcement but was still valid.

Qubits couplers. Sycamore uses controllable qubit couplers, a technique pioneered by William D. Oliver’s research team at the MIT Lincoln Labs¹²⁰⁷. There are 86 of them in all, connecting the 53 qubits of the chip. This makes a total of 139 qubits. These couplers are in fact qubits whose frequency is controlled by a direct current line (DC). It allows the implementation of fast two qubits quantum gates, acting in an average 12 ns.

	Metric	Value	Unit	Comments
	Number of qubits	53	qubits	Computing qubits
	Couplers	86	couplers	Qubits used for coupling computing qubits
	Single qubits gates	1,113	gates	Number of single qubit gates executed in benchmark
	Single qubits gates duration	25	nano-seconds	Duration of a single qubit gate
	Single qubit error	0,16%	percent	
	Two qubits gates	430	gates	Number of two qubits gates executed in benchmark
	Two qubits gates duration	12	nano-seconds	Duration of a two qubit gate
	Two qubits gates error	0,93%	percent	
	Readout error	3,80%	percent	
	Gates depth	20	cycles	Number of series of quantum gates executed.
	Gates per cycle	55,65	gates/cycle	Number of quantum gates executed per cycle
	Measured fidelity	0,20%	percent	Total fidelity of system in supremacy regime
	Number of iterations	3,000,000	iterations	Number of full algorithm executions
	Computing time	6,000	seconds	Total computing time
	Quantum computing time	30	seconds	Total quantum computing time
	Readout analog to digital convertors	277	number	Generating 8 bits at 1 GB/s

Figure 328: all the figures of merit of Sycamore processor in 2019. Sources: [Quantum supremacy using a programmable superconducting processor](#) by Frank Arute, John Martinis et al, October 2019 (12 pages) and [Supplementary information for "Quantum supremacy using a programmable superconducting processor"](#) by Frank Arute, John Martinis et al, October 2019 (58 pages).

They implement CZ and CPHASE two-qubit gates. Sycamore’s processor has qubit readout error ranging from 3% to 7% and two-qubit gates have an error rate ranging from 0.5% to 1.5% while single-qubit gates have error between 0.05% and 0.5%.

Machine Learning based calibration. These qubits and couplers are controlled with microwaves carried by coaxial cables, at frequencies between 5 and 7 GHz, adjusted by a DC flux line. Google developed a deep learning-based qubit calibration code, which has made it possible to refine the qubit microwaves activation frequencies to avoid crosstalk between neighboring qubits (Figure 329, right). Scaling this calibration will be a challenge for larger QPUs and Google is working on it¹²⁰⁸.

Isolation. The qubit chip is protected by some Mu-metal shielding, another one in aluminum and a black coating to absorb infrared photons. The processor is made of aluminum and indium on silicon and includes two dies stacked on top of each other or next to the other (Figure 330).

Microwave generation. Figure 330 shows the control electronics inside and outside the cryostat. The system uses 54 external microwave signal generators for the single-qubit gates (X and Y), 54 for qubit frequency control and 86 for qubit control. This is completed by 9 readout microwave control signals, meaning they are frequency domain multiplexing readout by chunks of 6 qubits thanks to their use of a wideband parametric amplifier at the 15 mK stage, what they call an IMPA. The control electronics package includes 277 digital-to-analog converters that occupy 14 6U rack-mount cases. There is a similar number of coaxial cables ending in the cryostat.

¹²⁰⁷ See [Tunable Coupling Scheme for Implementing High-Fidelity Two-Qubit Gates](#) by Fei Yan, William D. Oliver et al, MIT Lincoln Labs, PRX, 2018 (10 pages).

¹²⁰⁸ See [Optimizing quantum gates towards the scale of logical qubits](#) by Paul V. Klimov, Hartmut Neven et al, Google AI and University of California, August 2023 (34 pages).

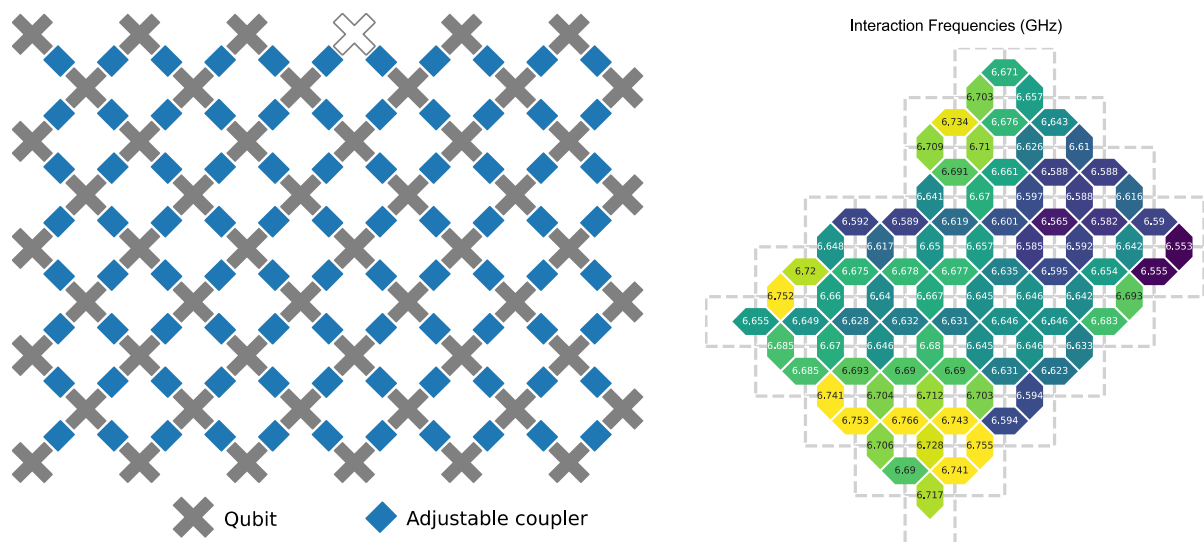


Figure 329: Google's Sycamore qubits layout, with their data qubits and coupler qubits (in blue). On the right, the interaction frequencies with each qubit were calibrated and optimized using a machine learning solution. Source: Sycamore's papers.

Z gates: DC flux lines are also used to create Z gates, or phase gates. They are controlled with microwaves in IBM's superconducting qubits. Using DC flux lines reduces the phase error observed with these gates.

Qubit readouts is done with only a few microwave photons sent to the qubits. The result is amplified by 100 dB in several steps, one at the 15 mK processor stage and another at the 3K stage. The resulting amplified microwaves are converted digitally by an ADC (analog-to-digital converter) and analyzed by a FPGA to detect their phase. The system multiplexes in the frequency domain the readout microwaves of 6 qubits groups conveyed by a single cable, between 5 and 7 GHz. This was a fairly classical setting for superconducting qubits.

Qubits improvements. They implement high fidelity qubits reset, allowing a reuse of qubits in quantum computations. They also worked on addressing cosmic radiation originated noise in circuits¹²⁰⁹. Their fidelity record is with their 72-qubit Sycamore chip with 99.4% two-qubit fidelity.

Error correction codes. Google's plans with quantum error correction is to use surface codes. Their mid-term goal is to create a "logical qubit" prototype with 100 physical qubits, then extend it to 1,000 physical qubits¹²¹⁰. The end goal is to build logical qubits with error rates around 10^{-12} , a level that is required to execute many useful gate-based algorithms (Figure 331, Figure 334, Figure 335).

With surface codes, these logical qubits are organized in squared arrays of about d^2 physical qubits (in blue, green ones are the qubit couplers) where d is the so-called code distance (5 in the example below).

How Google came out with the 1,000 physical qubit per logical qubit number? It comes from the way logical gates error are evaluated, per the formula $1/\Lambda$, Λ being the ratio between the threshold (theorem) error level and the physical gate error level. Λ must be at 10 to reach a 10^{-12} error rate with 1,000 physical qubits per logical qubits (above, right). They implemented their first surface codes with $d=3$ and $d=5$ ¹²¹¹.

¹²⁰⁹ See [Resolving catastrophic error bursts from cosmic rays in large arrays of superconducting qubits](#) by Matt McEwen et al, April 2021 (13 pages).

¹²¹⁰ See [APS March Meeting: Google, Intel and Others Highlight Quantum Progress Points](#) by John Russell, HPCwire, March 2022.

¹²¹¹ See also [Progressing superconducting quantum computing at Google](#) by Kevin Satzinger, April 2022 (47 mn).

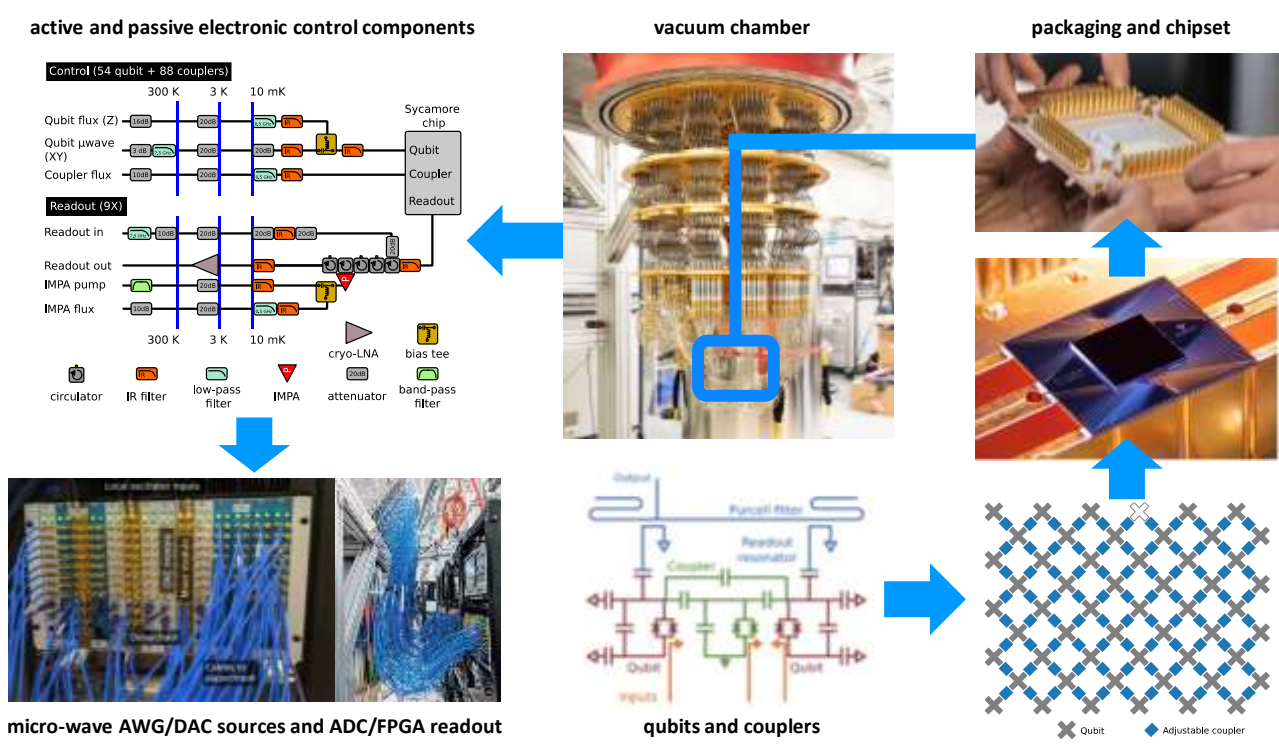


Figure 330: a Russian doll description of Sycamore starting with the qubits and coupler, then with the chip layout, its size, its packaging and connectors, where it is placed in the cryostat and the surrounding control electronics. Source: Google. Compilation (cc) Olivier Ezratty, 2020-2022 with sources from Google.

In 2021, Google experimented two repetition code layouts on a 53-qubit Sycamore chip with 21 qubits in a 1D chain correcting flip or phase errors and a distance-2 surface code of 7 qubits correcting both flip and phase errors as shown in Figure 332. It did show that flip and phase errors could be exponentially suppressed with adding more physical qubits¹²¹². They could assess the impact of a good Λ value. They also propose to use “pulse sequence” to correct unwanted crosstalk and dephasing that are disturbing surface codes¹²¹³.

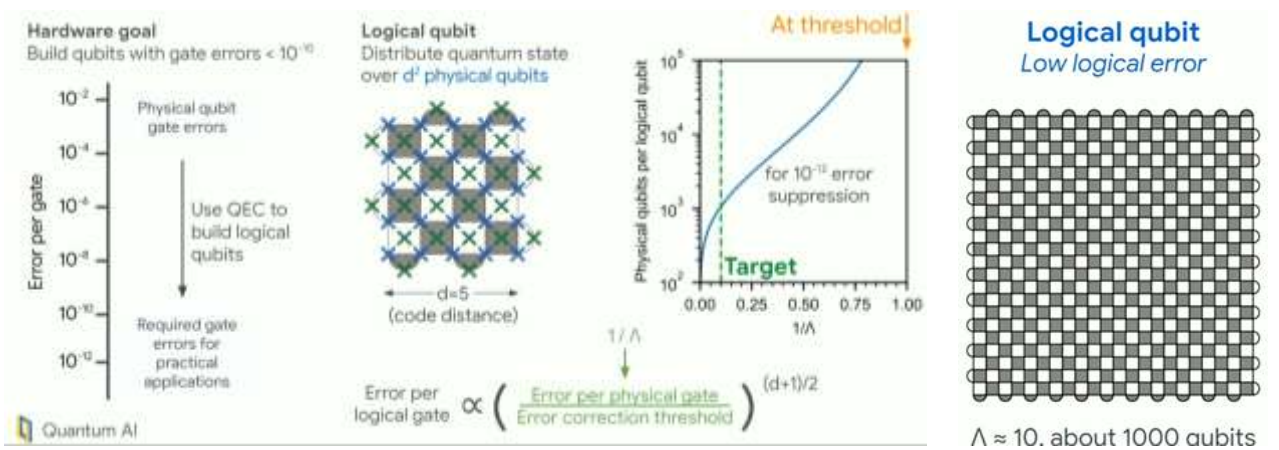


Figure 331: how Google plans to reach an error rate of 10^{-12} with its logical qubits. Source: APS March Meeting: Google, Intel and Others Highlight Quantum Progress Points by John Russell, HPCwire, March 2022.

¹²¹² See [Demonstrating the Fundamentals of Quantum Error Correction](#) by Jimmy Chen et al, August 2021 and [Exponential suppression of bit or phase flip errors with repetitive error correction](#) by Zijun Chen et al, Nature, July 2021 (32 pages). [Removing leakage-induced correlated errors in superconducting quantum error correction](#) by M. McEwen et al, March 2021, Nature Communications (12 pages) deals with another error reduction technique named “multi-level reset” that consists in “pumping” the excess energy from superconducting qubits that leak to their higher energy levels $|2\rangle$ or $|3\rangle$.

¹²¹³ See [Pulse sequence design for crosstalk mitigation](#) by Murphy Yuezhen Niu.

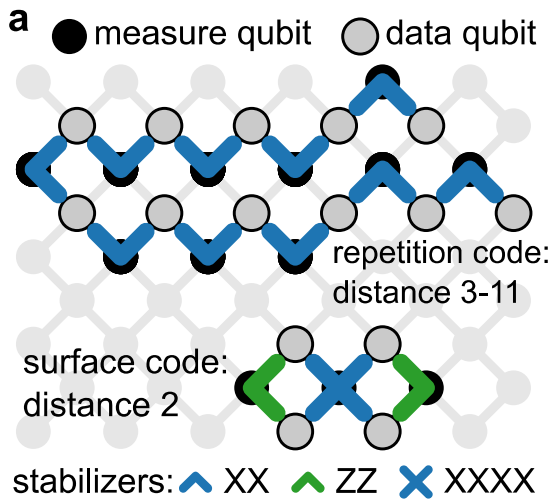


Figure 332: the first logical qubits created on Sycamore in 2021. Source: [Exponential suppression of bit or phase flip errors with repetitive error correction](#) by Zijun Chen et al, Nature, Google AI, July 2021 (32 pages).

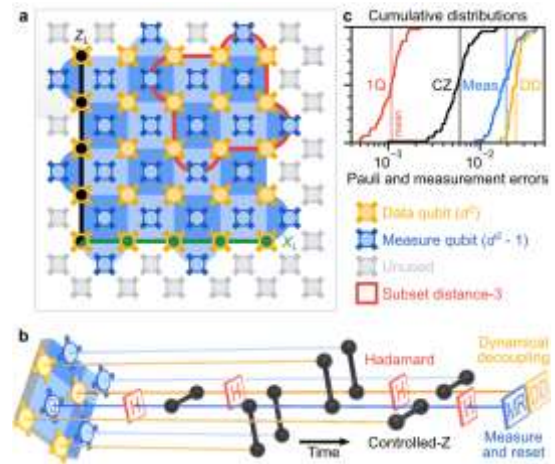


Figure 333: Sycamore's 72 qubit version that implements a distance-5 surface code error correction for a single logical qubit, that is still insufficient to improve qubit fidelities. Source: [Suppressing quantum errors by scaling a surface code logical qubit](#) by Rajeev Acharya et al, Google AI, Nature, July 2022-February 2023 (44 pages).

In March 2023, their July 2022 preprint published in Nature used a 72-qubit Sycamore version implementing a distance-5 surface code for a single logical qubit of 49 physical qubits, as shown in Figure 333. It was still insufficient to create a logical qubit with a better fidelity than the underlying physical qubits¹²¹⁴. The next step is a 105 qubits QPU to implement a distance-7 surface code logical qubit that will be the first to improve fidelities compared to its physical qubits. As of mid-2023, it was tested internally at Google.

In September 2023, Google AI published a paper proposing some new optimizations in surface code implementation with replacing CNOT gates by iSWAP gates¹²¹⁵.

Google's plan are to scale up to a hundred logical qubits¹²¹⁶. In a July 2020 conference, Hartmut Neven announced his 10-year plan to achieve this result, showing impressive mockups of a giant quantum computer containing 100 modules with 10,000 physical qubits each.

It would be a giant installation, as shown on the impressive artist's rendering in Figure 334.

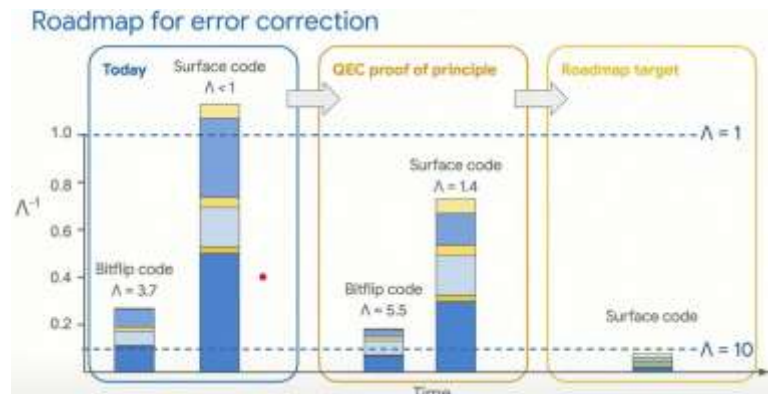


Figure 334: Google's roadmap for error corrections. Source: Hartmut Neven, July 2020.

¹²¹⁴ See [Suppressing quantum errors by scaling a surface code logical qubit](#) by Rajeev Acharya et al, Google AI, Nature, July 2022-February 2023 (44 pages).

¹²¹⁵ See [Relaxing Hardware Requirements for Surface Code Circuits using Time-dynamics](#) by Matt McEwen, Craig Gidney et al, February-September 2023 (55 pages).

¹²¹⁶ Source of the illustrations shown in Figure 334 and Figure 335: [Day 1 opening keynote by Hartmut Neven \(Quantum Summer Symposium 2020\)](#), July 2020 (30 mn) and the [whole symposium](#).

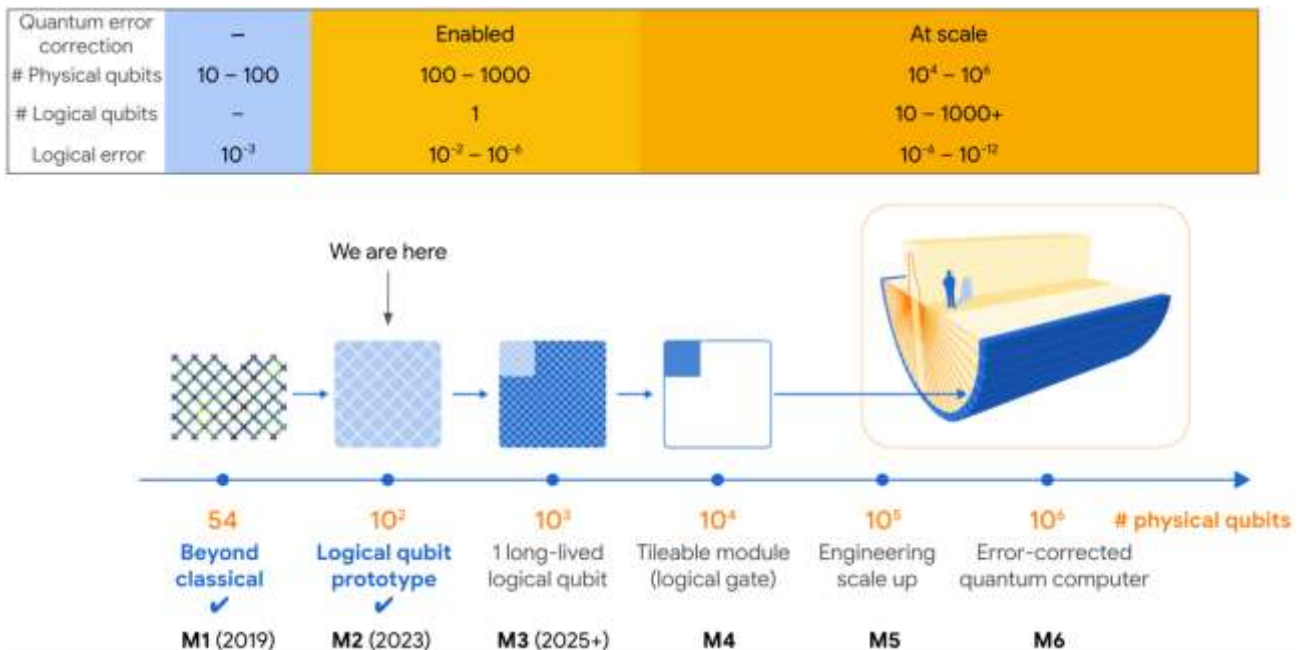
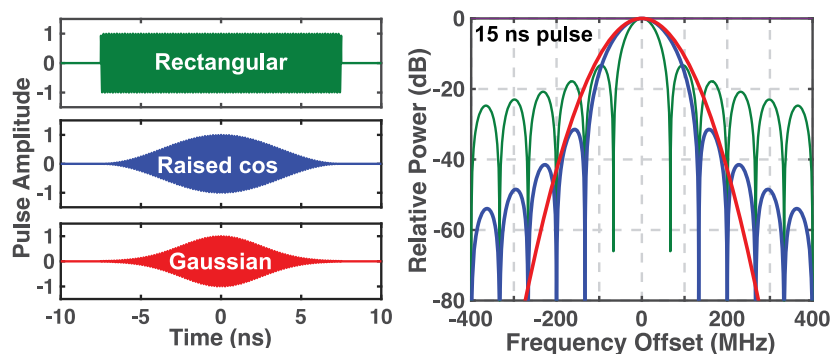


Figure 335: Google's scalability roadmap with logical qubits made of 1,000 physical qubits. And a giant system, as envisioned in 2020. One can wonder how these chips will be connected. At least, it will involve microwave connections and at best, some longer range photonic connections. Source: Hartmut Neven, July 2020 and Google data, updated in 2023.

Cryo-CMOS. To scale up micro-waves generation and put it inside the cryostat, Google published some work on a cryo-CMOS chip operating at 3K, using simple waveform generators consuming a minimum of energy to create only single qubit gates¹²¹⁷.

It has however not yet been deployed. It relies on cosinusoidal shape microwaves with the interest of creating spectral "holes" corresponding to the qubits frequencies harmonics of the state |1⟩ to the state |2⟩ transition, that must be avoided (Figure 336). It corresponds to the wavelength known as ω_{12} as seen in the illustration from page 359.



Raised cosine: good compromise between sidelobes and pulse duration

Figure 336: qubit control signals optimization with spectral holes matching qubit frequencies harmonics. Source: [XY Controls of Transmon Qubits](#) by Joseph Bardin, June 2019 (36 slides).

Sycamore at work. Starting in 2020, Google tried to make some good use of Sycamore to test various algorithms. It covered typical use cases with chemical simulations¹²¹⁸ (Figure 337) and optimization

¹²¹⁷ See [Control of transmon qubits using a cryogenic CMOS integrated circuit](#) by Joseph Bardin, March 2020 (35 minutes) and [28nm Bulk-CMOS 4-to-8GHz <2mW Cryogenic Pulse Modulator for Scalable Quantum Computing](#) by Joseph Bardin, Craig Gidney, Charles Neil, Hartmut Neven, John Martinis et al, February 2019 (13 pages).

¹²¹⁸ See [Hartree-Fock on a superconducting qubit quantum computer](#) by Google AI Quantum and Collaborators, April 2020 (27 pages) with a diimide (NH)₂ molecular simulation algorithm.

tasks¹²¹⁹ down to fundamental research activities like simulating time crystals, blackholes¹²²⁰ and even topological error codes^{1221 1222 1223}.

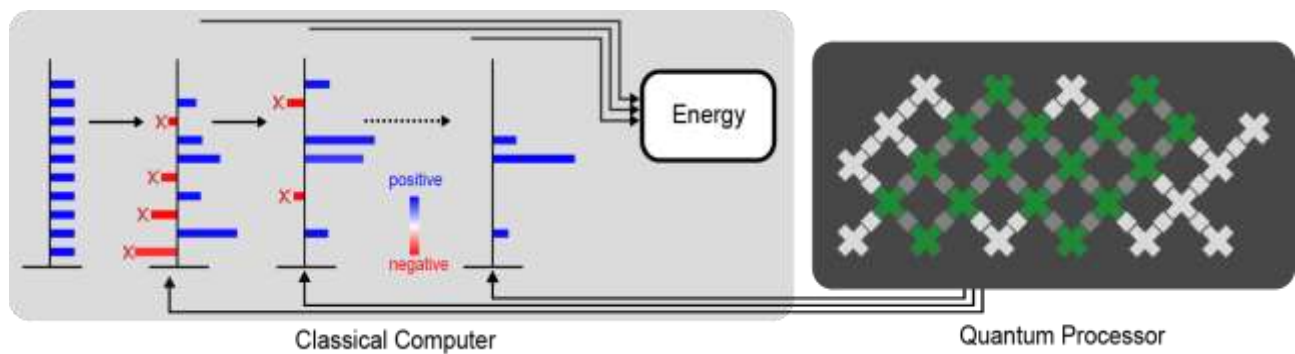


Figure 337: simple schematic of a chemical simulation classical/quantum hybrid algorithm using a Monte Carlo method. Source: [Hybrid Quantum Algorithms for Quantum Monte Carlo](#) by William J. Huggins, March 2022.

There was no more supremacy since most of these experiments didn't use more than 20 qubits. In 2021¹²²⁴, together with researchers from Columbia University, Google's teams created a chemical simulation classical/quantum hybrid algorithm using a Monte Carlo method¹²²⁵.

It was used to compute the ground state of two carbon atoms in a diamond crystal, using 16 qubits. The method was, however, not more efficient than a full classical algorithm.

In November 2022, Google simulated the traversal of a wormhole with 9 qubits and 164 two-qubit gates, creating an obvious debate on its validity^{1226 1227 1228 1229 1230 1231 1232 1233}.

¹²¹⁹ See [Quantum Approximate Optimization of Non-Planar Graph Problems on a Planar Superconducting Processor](#) by Google AI Quantum and Collaborators, April 2020 (17 pages) which deals with three families of combinatorial problems with the QAOA algorithm.

¹²²⁰ See this theoretical paper on the use of quantum computing, not necessarily with Google qubits, to study black holes. See [Google Scientists Are Using Computers to Study Wormholes](#) by Ryan F. Mandelbaum, November 2019 which refers to [Quantum Gravity in the Lab: Teleportation by Size and Traversable Wormholes](#) by Adam R. Brown et al, November 2019 (20 pages).

¹²²¹ See [An important step towards improved quantum computers](#), Google AI, May 2023.

¹²²² See [Non-Abelian braiding of graph vertices in a superconducting processor](#), Google Quantum AI and Collaborators, Nature, May 2023 (17 pages).

¹²²³ See [Noise-resilient Edge Modes on a Chain of Superconducting Qubits](#) by Xiao Mi et al, Google AI, April-December 2022 (29 pages).

¹²²⁴ See [2021 Year in Review: Google Quantum AI](#) by Emily Mount, December 2021.

¹²²⁵ See [Hybrid Quantum Algorithms for Quantum Monte Carlo](#) by William J. Huggins, March 2022 and [Unbiasing Fermionic Quantum Monte Carlo with a Quantum Computer](#) by William J. Huggins, Ryan Babbush, Joonho Lee et al, Nature, July 2021 (28 pages).

¹²²⁶ See [Traversable wormhole dynamics on a quantum processor](#) by Daniel Jafferis, Hartmut Neven, Maria Spiropulu et al, Nature, November 2022 (22 pages).

¹²²⁷ See [Physicists Create a Holographic Wormhole Using a Quantum Computer](#) by Natalie Wolchover, Quanta Magazine, November 2022.

¹²²⁸ See [Making a Dual of a Traversable Wormhole with a Quantum Computer](#) by Alexander Zlokapa and Hartmut Neven, Quantum AI Team, November 2022.

¹²²⁹ See [Traversable wormhole dynamics on a quantum processor](#), Caltech, with a FAQ.

¹²³⁰ See [Comment on "Traversable wormhole dynamics on a quantum processor"](#) by Bryce Kobrin et al, February 2023 (9 pages).

¹²³¹ See [The Neverending Story of the Eternal Wormhole and the Noisy Sycamore](#) by Galina Weinstein, January-May 2023 (23 pages).

¹²³² See [From counterportation to local wormholes](#) by Hatim Salih, March 2023 (17 pages).

¹²³³ See [Google's Sycamore chip: no wormholes, no superfast classical simulation either](#) by Scott Aaronson, November 2022.

In 2022, another simulation of some molecules and materials as published, first with the iron-sulfur clusters of nitrogenase, including the FeMo-cofactor (aka FeMoCo), a component of the natural nitrogen cycle and second with the electronic structure of α -RuCl₃, a candidate material for realizing spin liquid physics¹²³⁴. The experiments were using 5 to 11 qubits, far from any quantum advantage territory.

In 2021, Google also teamed up with **Caltech** to show some quantum superiority when quantum computers directly exploit quantum data coming from quantum sensors. Fewer experiments are required than if the communication between sensors and the quantum processor was classical. The experiment was done with 40 qubits and 1,300 quantum operations¹²³⁵.

Other research. Google AI researchers frequently publish interesting work on various topics. On an optimized way to prepare entangled states¹²³⁶, on NISQ-era many-body physics simulations using time-space symmetries¹²³⁷, on dispersion based qubit readout and qubit leakage with multiple photon number¹²³⁸ and on the creation of solid state circulators using arrays of Josephson junctions¹²³⁹.

Energetics: Sycamore showcases some energy consumption advantage, with a ratio of about one to a million. Its power consumption is about 25 kW and the ORNL IBM Summit is at 12 MW at full charge, and the computing time ratio is 2.5 minutes vs. 2.5 days (1/1440) in the most favorable IBM Summit case. But we are probably comparing apples and oranges given the supremacy doesn't relate to solving some useful problem with input data and parameters.

Google software tools. Several Google teams are working on quantum software, including those working on Cirq, on TensorFlow Quantum and another Google X team working on applications, under the leadership of Jack Hidary¹²⁴⁰. They also released a **Fermionic Quantum Simulator** for quantum chemistry applications in collaboration with **QSimulate** (2018, USA, \$4M) aka qsim. It can simulate noisy quantum circuits with Nvidia GPUs on Google Cloud. Since 2022, it seems branded as the Quantum Virtual Machine. Google also published stim, an open source tool providing a 10,000x speedup when simulating error correction circuits.

Quantum cloud. At last, it has a quantum cloud offering for quantum algorithm simulation and hosts an IonQ trapped ion system and, surprisingly, none of its Sycamore systems which are only accessible to a handful of academic partners, an outreach strategy that is very different from the broadscale one IBM adopted. Google and IBM have very different commercial approaches with quantum computing. For Google, it is a research playing ground while for IBM, it is a way to lock-in large account customers as early as possible.



Rigetti (2013, USA, \$656M) is another commercial superconductor vendor. With D-Wave, IonQ and PsiQuantum, it is the fourth best funded startup in the industry.

¹²³⁴ See [Simulating challenging correlated molecules and materials on the Sycamore quantum processor](#) by Ruslan N. Tazhigulov et al, March 2022 (22 pages).

¹²³⁵ See [Quantum advantage in learning from experiments](#) by Hsin-Yuan Huang et al, December 2021 (52 pages).

¹²³⁶ See [Stable Quantum-Correlated Many Body States via Engineered Dissipation](#) by X. Mi et al, Google AI, April 2023 (25 pages).

¹²³⁷ See [Quantum information phases in space-time: measurement-induced entanglement and teleportation on a noisy quantum processor](#) by Jesse C. Hoke et al, Google AI, March 2023 (26 pages).

¹²³⁸ See [Measurement-Induced State Transitions in a Superconducting Qubit: Within the Rotating Wave Approximation](#) by Mostafa Khezri et al, Google AI, December 2022 (12 pages).

¹²³⁹ See [Josephson parametric circulator with same-frequency signal ports, 200 MHz bandwidth, and high dynamic range](#) by Randy Kwende et al, March 2023 (5 pages).

¹²⁴⁰ See [Alphabet Has a Second, Secretive Quantum Computing Team](#) by Tom Simonite, January 2020. No secret anymore buddy!

It was launched by Chad Rigetti, who got a PhD and did a post-doc at Yale University on microwave driven two-superconducting qubit gates in 2009¹²⁴¹, and then worked as a researcher at IBM between 2010 and 2013.



Figure 338: evolution of Rigetti actual chips over time. Source: Rigetti investor presentation.

Over about 8 years, their QPUs went from 3 to 80 qubits (Figure 338). They had a tendency to oversell their roadmap, having prematurely announced a 128 qubits test version in August 2018 that never saw the light. They started to deploy their system on Amazon Braket with its Aspen-9 processor of 31 qubits in 2020. Their Aspen-M 80 qubits chip announced in December 2021 was commercially available in February 2022 on Rigetti Quantum Cloud Services and Amazon Braket, and subsequently on Azure Quantum, Strangeworks QC and Zapata Computing’s Orquestra platform¹²⁴². It seems they have not sold any QPU on premise to any public customer.

Their fidelities are not as good as with IBM and Google but it is continuously improving, even as they increase the number of qubits.

In 2022, they demonstrated improved two-qubit gates fidelities of 99.5% but with a 9 qubits prototype¹²⁴³ (Figure 339).

Sideways, they are also experimenting the usage of qutrits with three level anharmonic oscillators in their superconducting loops. It was tested on a 5-transmon chip with two qutrits entanglement¹²⁴⁴.

metric	Aspen-9	Aspen-11	Aspen-M-1
number of physical qubits	31	40	80
median T ₁	27 μs	25.7 μs	30.7 μs
median T ₂	19 μs	14.9 μs	23.0 μs
median simultaneous 1Q fidelity	99.80%	99.50%	99.70%
median 2Q XY fidelity	95.40 %	93.70%	95.30%
median 2Q CZ fidelity	95.80 %	90.20%	93.10%
median RO fidelity		97.10%	98.20%
median active reset fidelity		99.20%	99.80%

Figure 339: Rigetti qubits figures of merit for their last generation chip. These number are now fairly well detailed, but they show that it doesn’t compete well with IBM at least on two qubit gates. Data source: Rigetti.

So, what is special with Rigetti? Let’s look at a couple aspects of their qubits and systems engineering.

Coupling qubits. Their qubits were entangled by fixed configurable couplers. They plan to adopt tunable couplers in Ankaa-1 and Ankaa-2 84 qubits chips, bringing more flexibility for managing two qubit gates¹²⁴⁵. These are adjustable transmon qubits using asymmetric SQUIDs (magnetometers).

¹²⁴¹ See [Quantum Gates for Superconducting Qubits](#), 2009 (248 pages).

¹²⁴² See [Rigetti Announces Commercial Availability of their 80 Qubit Aspen-M and a Teaming with NASDAQ to Explore Financial Applications of QC](#), February 2022.

¹²⁴³ See [Rigetti Computing Reports Fidelities as High as 99.5% on Next-Generation Chip Architecture](#), February 2022. The \$900K Novra final product launched in December 2023 with 9 qubits has a 2-qubit gate fidelity of 98.5% with an iSWAP gate.

¹²⁴⁴ See [Beyond Qubits: Unlocking the Third State in Quantum Processors](#) by Alex Hill, Rigetti, December 2021 and [Quantum Information Scrambling on a Superconducting Qutrit Processor](#) by M. S. Blok et al, April 2021 (21 pages).

¹²⁴⁵ This is explained in [Demonstration of Universal Parametric Entangling Gates on a Multi-Qubit Lattice](#) by M. Reagor et al, 2018 (17 pages). The Ankaa-2 chipset was delivered in January 2024, with 2-qubit gate fidelities of 98%.

Electronics optimization. Rigetti made efforts to optimize the physical and electrical components of its accelerators. First, by integrating the control and measurement wiring of the qubits in compact sheets that they patented¹²⁴⁶. They developed their own microwave generation electronics. They also found a way to limit crosstalk between qubits¹²⁴⁷. They also work on merging microwave and DC flux lines into the same wires used for respectively XY and Z single qubit gates, between the 10 mK cold plate and the qubit chip¹²⁴⁸. As a result, they tout performance improvements expressed in CLOPS (circuit layer operations per second) for their 40-qubit Aspen-11 and 80-qubit Aspen-M systems. The first had 844 CLOPS while the second reached 892. It can be compared to IBM's 1,500 CLOPS on their 65 qubits system and 850 with 127 qubits (as of April 2022)¹²⁴⁹. Their Ankaa generation should have two-qubit gates three times faster than with Aspen-M-3.

Modular chips. Rigetti is splitting qubits in multiple semiconductors dies connected with each other with indium-based flip-chip bonded on a single larger carrier die (Figure 340). This reduces qubits crosstalk between modules, at the expense of a smaller fidelity. They first tried this with 4 chips containing each 4 aluminum and niobium-based SQUIDS qubits and 4 static couplers, their fidelities are $99.1 \pm 0.5\%$ and $98.3 \pm 0.3\%$ for iSWAP and CZ gates¹²⁵⁰. They then expanded this to two 40 qubits dies in their Aspen M1 chip released in December 2021. Other improvements include vertical signaling enabling higher qubit density and using tunable couplers¹²⁵¹.

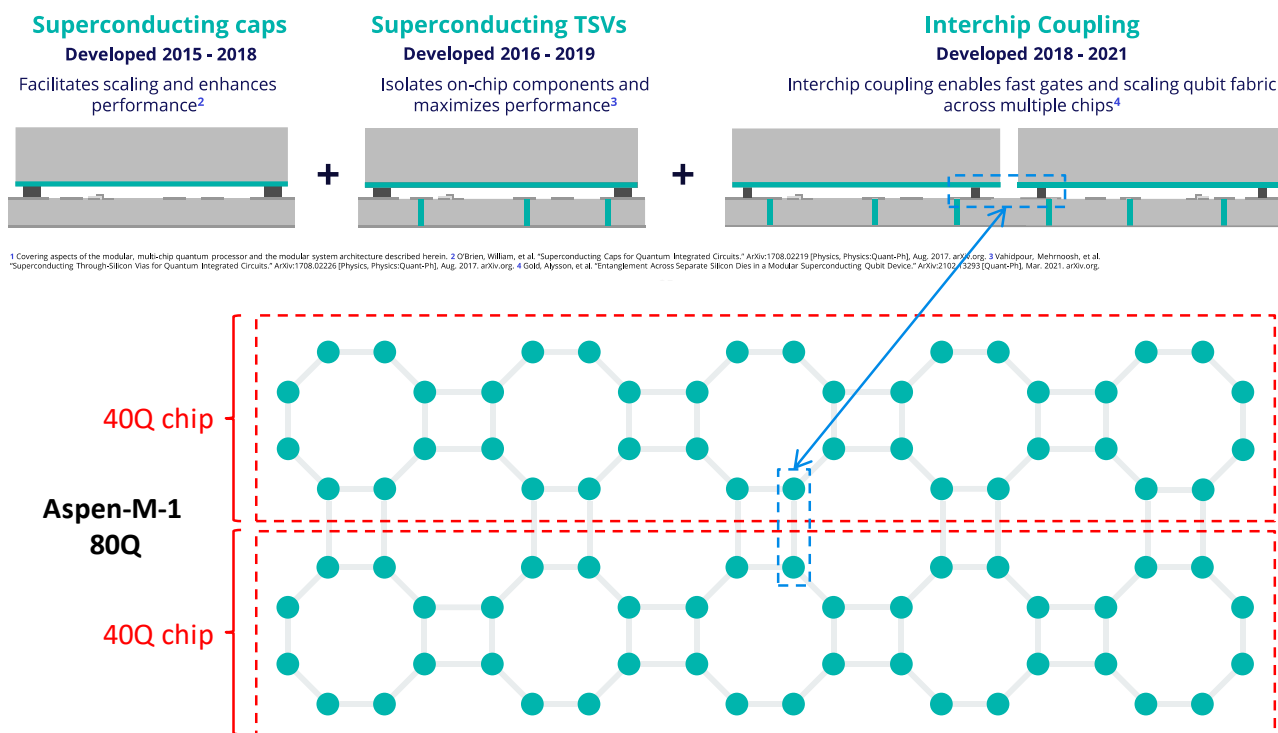


Figure 340: interchip coupling implemented with their Aspen-M-1 80-qubit processor, assembling two dies of 40 qubits.
Source: Rigetti.

¹²⁴⁶ See Connecting Electrical Circuitry in a Quantum Computing System, [USPTO 20190027800](https://www.uspto.gov/patents/applications/pdf/20190027800/20190027800.pdf).

¹²⁴⁷ See [Methods for Measuring Magnetic Flux Crosstalk Between Tunable Transmons](#) by Deanna M. Abrams et al, August 2019 (12 pages).

¹²⁴⁸ See [Full control of superconducting qubits with combined on-chip microwave and flux lines](#) by Riccardo Manenti et al, July 2021 (8 pages).

¹²⁴⁹ See [Optimizing full-stack throughput and fidelity with Rigetti's Aspen-M generation of quantum processors](#), Rigetti, February 2022.

¹²⁵⁰ See [Entanglement Across Separate Silicon Dies in a Modular Superconducting Qubit Device](#) by Alysson Gold, 2021 (9 pages).

¹²⁵¹ See [Modular Superconducting Qubit Architecture with a Multi-chip Tunable Coupler](#) by Mark Field et al, August 2023 (9 pages).

Cleanroom. Rigetti have their own small manufacturing unit producing their semiconducting chips, named Fab-1 (Figure 341). This enables them to create new chips with a 5-15 month cycle. The required and initial investment of about \$10M, which is reasonable even for a startup. The creation of superconducting qubit circuits is done with a very low-level of integration. We are far from the \$20B 5 nm fabs from TSMC. In the case of silicon qubits, on the other hand, it is necessary to have an equipment of at least \$1B¹²⁵²! Still, it is a challenge to use such fabs at full capacity. It explains their five-year contract with the Air Force Research Lab announced in September 2023. It will cover various needs like quantum circuits, quantum-limited amplifiers and cryogenic microwave components.



Figure 341: Rigetti's superconducting cleanroom fab line in Fremont, California. Source: Rigetti.

This multi-dies QPU approach is the main driving technology for them to scale their QPUs. The short term roadmap contains the 84-qubit Ankaa for 2023 and the 336-qubit Lyra for late 2023 (not delivered yet). They have however not yet explained how they will interconnect these multi-dies chips¹²⁵³.

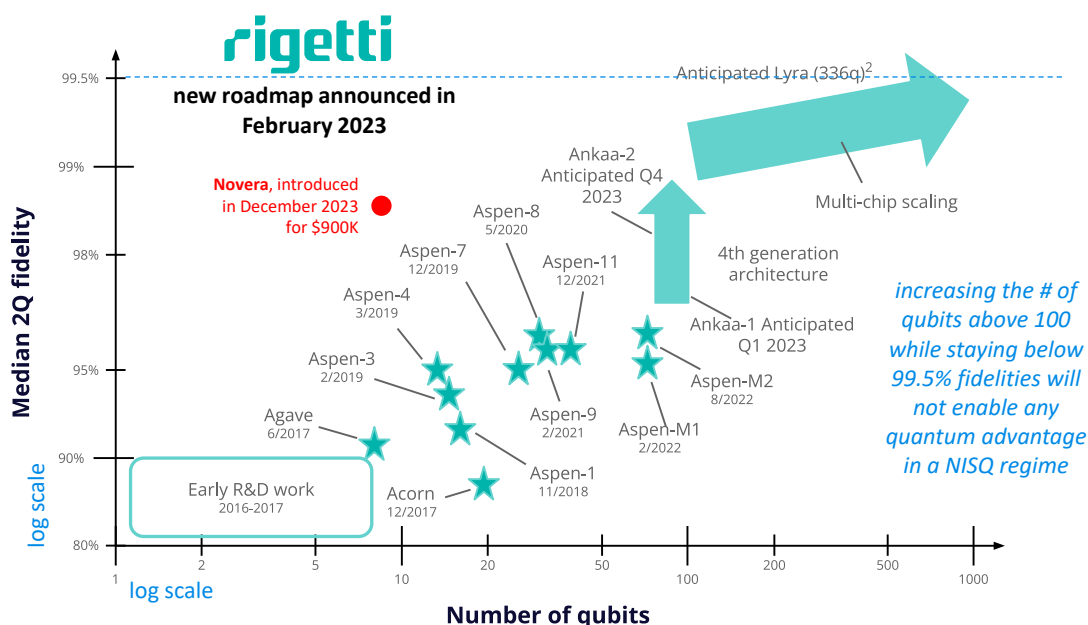


Figure 342: Rigetti's scalability roadmap update from 2023. They removed the 1,000 and 4,000 qubits QPUs that were announced in 2022, to focus on "shorter term" revenue opportunities. They expected to release 84 and 336 qubit chips in 2023. Not done as of January 2024! Unfortunately, given their target fidelities, these chips will seemingly not enable any quantum advantage in the NISQ regime. This seems a dead-end strategy. The 9-qubit Novera system introduced in December 2023 has only 98.5% fidelities with 2-qubit iSWAP gates. A CNOT gate constructed with it would have a much lower fidelity. Source: [Rigetti investor presentation](#), May 2023.

¹²⁵² See [Quantum Cloud Computing Rigetti](#) by Johannes Otterbach, 2018 (105 slides) and the [corresponding video](#), and [Manufacturing low dissipation superconducting quantum processors](#) by Ani Nersisyan et al, Rigetti, 2019 (9 pages).

¹²⁵³ Source: [Rigetti Investor Presentation](#), October 2021 (56 slides).

Full-stack software development. It includes pyQuil for scripting and Quil for quantum gate management. These are both open source and published on Github. Quil allows to synchronize tasks between quantum and classical computing¹²⁵⁴. In 2018, they demonstrated the use of their quantum computer for a machine learning algorithm that does not require a hybrid algorithm¹²⁵⁵.

Summary forecasted financial data (\$M)

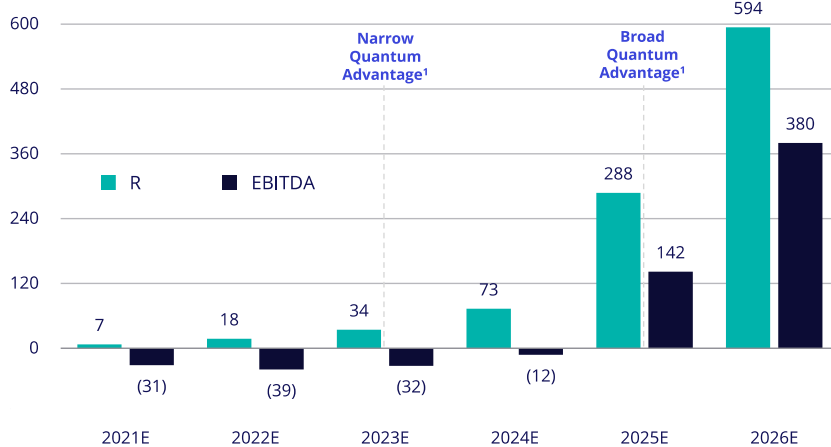


Figure 343: Rigetti's revenue and EBITDA forecasts until 2026. In the first quarter of 2022, they made \$2.1M. It seems their 2022 forecast was optimistic.
Source: [Q1 2022 quarterly report](#).

SPAC. After having raised about \$200M through classical VCs, they went into the stock market after being acquired by a SPAC company in March 2022, Supernova Partners Acquisition Company II. It brought on the table \$345M of funding for a valuation of \$1.152B. As of December 2021, the company had 140 people in the United States, UK and Australia. At their SPAC time, they were forecasting a revenue of \$594M by 2026, based on the release of their 1,000 qubits system in 2024 (Figure 343).

In May 2022, they announced a one-year delay on their roadmap¹²⁵⁶. 2023 was then a bad year for Rigetti. Its bad quarterly results drove its stock below \$1, exposing the company to a Nasdaq delisting by July 2023. It then announced the layoff of 28% of its workforce and the departure of its CEO and founder, Chad Rigetti¹²⁵⁷. It updated its roadmap with basically removing long term goals and focusing on 84 and 323 qubits NISQ platforms. They have however a rather low bar in terms of qubit fidelities (99.5%) which is not enough to make use of that many qubits, as shown in Figure 342. In 2023, 2023 was supposed to be the year of a “narrow quantum advantage”. We’re not there yet.

Cloud. Rigetti offers access to its quantum computers via the cloud, like IBM and D-Wave do with their Quantum Cloud Services. It started running in beta in January 2019. Since early 2020, they are also distributed in the cloud by Amazon in its Braket service.

Acquisition. Rigetti acquired QxBranch in July 2019 to complete its software offering. It was established in the USA, UK and especially in Australia. In September 2020, their UK-based subsidiary announced the launch of a collaborative project to accelerate the commercialization of quantum computers, funded with £10M private/public money. To do so, they will use a latest-generation Proteox cryostat from Oxford Instruments.

Patents. They have a portfolio of 100 patents and applications in interchip coupling and multi-die chips, cabling, processor design, cloud quantum computing and quantum software tools.

Partnerships. On top of Amazon, Microsoft, Zapata Computing and Strangeworks for cloud deployments, they announced in 2022 a new partnership with Ampere Computing (USA) to create hybrid quantum-classical computers designed to run machine learning applications, with Keysight for control electronics and Bluefors for cryogeny. Ampere is a fabless company designing 128-core

¹²⁵⁴ See [A Practical Quantum Instruction Set Architecture](#) by Robert S. Smith, Michael J. Curtis and William J. Zeng, Rigetti Computing, 2017 (15 pages).

¹²⁵⁵ In [Quantum Kitchen Sinks: An algorithm for machine learning on near-term quantum computers](#), July 2018 (8 pages).

¹²⁵⁶ See [Rigetti Pushes Back Roadmap on Development of 1,000-Qubit, 4,000 Qubit Models](#) by Matt Swayne, The Quantum Insider, May 2022.

¹²⁵⁷ In June 2023, Chad Rigetti joined the Dutch investment fund QDNL Participations as a venture partner.

arm chips for servers¹²⁵⁸. They have also various business and academic partnerships running in the UK, which led to the deployment in the UK of a 32-qubit Aspen system in June 2022 (why not the more recent 40 or 80 qubit Aspen?). With **Zapata**, they are building hybrid quantum-classical compilation tools with the support of the 80Q Aspen-M QPU and Rigetti cloud services. At last, they announced a partnership with **Riverlane** (UK) in June 2022 to work on error correction.

Rigetti is working with **DARPA**, having been selected to provide hardware, software and benchmarks for phase two of the DARPA ONISQ program (Optimization with Noisy Intermediate-Scale Quantum). The aim is to create quantum computers able to solve complex optimization problems. This work is jointly done with Universities Space Research Association (USRA) and NASA's Quantum Artificial Intelligence Laboratory (QuAIL). Rigetti has also a strong R&D partnership with the DoE **Fermilab**, which conducts testing and material designs in its Superconducting Quantum Materials and Systems Center (SQMS) led by Anna Grassellino¹²⁵⁹. They are working on using Nb/Si combinations and specific surface treatments, generating 450 μs T_1 . At last, they are also working with **NASA** on variational algorithms optimization techniques¹²⁶⁰.

Customer wise, they have a couple early adopters like **Nasdaq** who plans to use their systems to detect fraud, optimize order matching and handle risk management.



IQM (2018, Finland, 167M€) is a spin-off from the Quantum Computing and Devices group of the Aalto University and from the VTT research center. Its funding is a mix of dilutive capital investment and debt financing through the European Investment Bank (EIB).

In June 2020, IQM received 15M€ capital funding from the European Commission's EIC Accelerator, supplemented by a 2.5M€ grant. A new funding round of 128M€ was announced in July 2022. All-in-all, IQM got a total of 167M€ in funding.

IQM develops superconducting qubits QPUs after having initially created an on-chip cooling technology for superconducting and silicon chips based on electron transfer using an electron tunnel-effect¹²⁶¹. The company states that their qubits are operable with a faster clock speed than competing superconducting qubits thanks to optimizations applied to qubits reset, gates and readout. They use tunable couplers for qubits entanglement. They also developed a fast graphene-based bolometer for qubit readout able to detect a single microwave photon. Its benefits is some power saving compared to parametric amplifiers¹²⁶².

On the R&D stage, IQM participates to a research consortium including Aalto University and VTT which proposed in 2021 a qubit on-chip circuit to create microwaves pulses that could be used to drive superconducting qubits and working at 10 mK¹²⁶³. Its size is one mm and would remove the need to use cables to feed the processor with microwave pulses. So far, it only creates a sinus wave at 1 GHz, still far from what is needed to drive a superconducting qubit, i.e., a short duration pulse with a precise waveform added to some carrier frequency at around 5 GHz.

¹²⁵⁸ See [Ampere Goes Quantum: Get Your Qubits in the Cloud](#) by Ian Cutress, AnandTech, February 2022.

¹²⁵⁹ See [Superconducting Quantum Materials and Systems Center](#) by Anna Grassellino, June 2021 (40 slides).

¹²⁶⁰ See [Design and execution of quantum circuits using tens of superconducting qubits and thousands of gates for dense Ising optimization problems](#) by Filip B. Maciejewski et al, QUAIL, USRA (University Space Research Association) and Rigetti, August 2023 (19 pages).

¹²⁶¹ See [Quantum-circuit refrigerator](#) by Kuan Yen Tan et al, 2017 (8 pages) and [video](#).

¹²⁶² See [Bolometer operating at the threshold for circuit quantum electrodynamics](#) by R. Kokkonen, Mikko Möttönen et al, Nature, September 2020 (19 pages).

¹²⁶³ See [A low-noise on-chip coherent microwave source](#) by Chengyu Yan et al, Nature Electronics, December 2021 (14 pages) and [A new super-cooled microwave source boosts the scale-up of quantum computers](#), December 2021 that is clearly overselling this technology development. It also requires pulse shaping with other techniques (AWG, DAC).

It is closer to a local oscillator source! IQM also uses a TWPA from VTT in the first stage amplification of qubit readout microwaves¹²⁶⁴. This enables 5 to 10 qubits readout multiplexing with using different frequencies for qubits readouts with resonators of different lengths.

In March 2022, IQM introduced a new superconducting-qubit type nicknamed the unimon which has better fidelities, of about 99.9% with single-qubit gates¹²⁶⁵. It uses a single Josephson junction in a resonator, combining high anharmonicity in the superconducting loop, different anharmonicities for each qubit, better insensitivity to low frequency charge noise and insensitivity to magnetic flux noise (Figure 344). As of 2023, they had tested three unimon qubits given they use tunable couplers to create two-qubit gates.

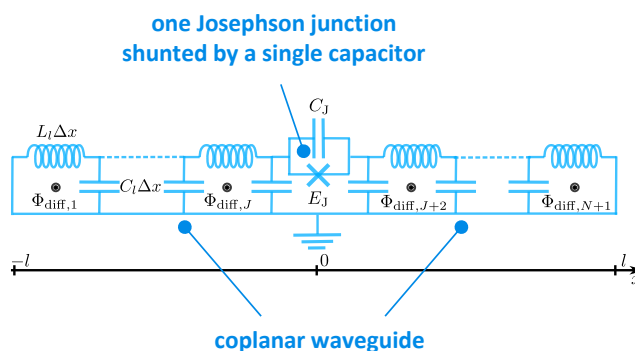


Figure 344: IQM's unimon circuit layout. Source: [Unimon qubit](#) by Eric Hyppä, Mikko Möttönen et al, IQM and VTT, April 2022 (72 pages).

They obtained two-qubit CPHASE gates fidelity above 99% and fidelities of 99.9% for X and Y gates. All with fast 13 ns gate (good), readout probe pulses of 100 ns (fine) and a T_1 of 8.6 μ s (not good). It must be tested with a large number of qubits and with two qubit gates¹²⁶⁶. In August 2022, they also published an arXiv preprint explaining how they will implement long-distance reliable two-qubit CZ gates, based on a custom ETH Zurich transmon design¹²⁶⁷. It can reach fidelities of 99.8%. They are also experimenting qubit readout mechanism using a bolometer, which so far has a low fidelity of 61.8% due to the readout duration of 13.9 μ s that is constrained by a T_1 of 28 μ s¹²⁶⁸.

After relying on VTT Micronova 2,600 m² clean-room fab, they inaugurated their own Espoo 560 m² and 20M€ fab in November 2021 to manufacture their chips, a self-sufficiency strategy also seen with Rigetti. In 2020, the Finland government granted VTT with a 20.7M€ funding to acquire an IQM system. It should reach 54-qubit by 2024 and 150 by 2025. They had 5 qubits as of November 2021 and 20 as of October 2023, with a Q8 Q-Score performance. IQM started to work in December 2022 with Keysight to develop scalable control electronics. In August 2023, the company announced its commercial launch of its Spark system with 5 qubits for the academic market priced at around 1M€.

The company had over 190 people as of September 2022. They opened a research lab in Munich, Germany in March 2020, one office in Spain in 2021, and one in Paris and Singapore in 2022.

IQM's business model is based on selling quantum computing systems to research and supercomputing centers as well as proposing customized hybrid analog/digital "Co-Design QC" quantum processors. The latter could be classified as "quantum ASICs", based on superconducting qubits¹²⁶⁹. These systems are adapted to the execution of hybrid algorithms such as VQE (Variational Quantum Eigensolvers) and QAOA (Quantum Approximate Optimization Algorithm).

¹²⁶⁴ See [Broadband continuous variable entanglement generation using Kerr-free Josephson metamaterial](#) by Michael Perelshtein, Pertti Hakonen et al, March 2022 (15 pages).

¹²⁶⁵ See [Unimon: A new qubit to boost quantum computers for useful applications](#), IQM, November 2022.

¹²⁶⁶ See [Unimon qubit](#) by Eric Hyppä, Mikko Möttönen et al, IQM and VTT, April 2022 (72 pages) which provides a good scientific and technical documentation of unimon qubits.

¹²⁶⁷ See [Long-distance transmon coupler with CZ gate fidelity above 99.8%](#) by Fabian Marxer, Mikko Möttönen, Johannes Heinsoo et al, IQM, QCD Lab and VTT, August-December 2022 (24 pages).

¹²⁶⁸ See [Single-Shot Readout of a Superconducting Qubit Using a Thermal Detector](#) by András M. Gunyhó, Mikko Möttönen et al, IQM, Aalto University and VTT, March 2023 (14 pages).

¹²⁶⁹ Their method is described in [Approximating the Quantum Approximate Optimization Algorithm](#) by David Headley et al, February 2020 (14 pages) and [Improving the Performance of Deep Quantum Optimization Algorithms with Continuous Gate Sets](#) by Nathan Lacroix, Alexandre Blais, Andreas Wallraff et al, May 2020 (14 pages).

IQM will also implement a digital-analog quantum processor together with other partners like Infineon at the LRZ supercomputing center in Garching, near Munich in Germany¹²⁷⁰.

Their co-design offering is based on **KQCcircuits**, an open-source software tool based on KLayout for qubit design, using the OASIS format for masks that is lighter. It enables a graphic-based creation of circuits elements and contains a library with SQUIDs, complex waveguides, coplanar capacitors, qubits, flipchip connectors, indium bumps and other templates.

They are partnering since August 2022 with **Multiverse Computing** for the software implementation of these co-designed QPUs, relying on Multiverse's Singularity SDK. They also announced a partnership with **Eviden**/Atos together with the Finnish supercomputing center **CSC** which bought a classical QLM emulator for their services. This machine is used both to simulate the operation of IQM's quantum accelerator qubits and to drive it¹²⁷¹. CSC will provide scientific quantum computing resources to the country's researchers, much like GENCI+CEA/TGCC do in France and FZJ/JSC in Germany. Atos has also announced its interest to distribute an IQM quantum accelerator, among other market solutions, including the Pasqal simulator.

In December 2022, IQM announced a partnership with **Tech Mahindra** (India) covering quantum computing, cryptography and communication technologies for the development of customer software solutions.



Oxford Quantum Circuits (2017, UK, <\$145M) was launched by Peter Leek from Clarendon Laboratory Oxford. The startup is run by Ilana Wisby and had a team of 60 people as of mid-2022. The company wants to remove the identified barriers that prevent superconducting qubits from scaling.

OQC's technology is based on their "coaxmon" superconducting qubits that are composed of highly coherent planar qubits¹²⁷² and using a 3D structure connecting the qubit chip with an interposer and using a layer for controlling the qubits on top of the chip and another one below for qubit readouts¹²⁷³ (Figure 345). It is based on various works from MIT and the University of Oxford, on an idea from Peter Leek¹²⁷⁴.

They are partnering with Cambridge Quantum Computing (CQC) which is developing a quantum compiler dedicated to their qubits. They also work with Classiq since December 2023. In April 2020, OQC obtained collaborative project funding from the British government of £7M. As part of this project, they are associated with SEEQC UK, Oxford Instruments, Kelvin Nanotechnology, the University of Glasgow and the Royal Holloway University of London.

In July 2021, OQC announced that they were making their first system available only as a QCaaS solution, in private beta (quantum cloud as a service) without even saying how many qubits were deployed. They then announced in December 2021 that an 8-qubit version of their processor nicknamed Lucy would be made available on Amazon Braket and revealed that their July 2021 system had a mere 4 qubits. The OQC system became live on AWS Braket in February 2022.

¹²⁷⁰ See [New EU Consortium shaping the future of Quantum Computing](#), IQM, February 2021. In November 2021, IQM was officially selected to provide its quantum computer to LRZ (Leibniz Supercomputing Centre) in association with an HPC to set-up an hybrid computing system as part of the Q-Exa project. It's part of a €45.3M consortium project funded by BMBF (German Federal Ministry of Education and Research) with €40.1M. Although it was not detailed in the announcement, we can suspect that the provided QPU will have 50 qubits as planned by IQM in 2025.

¹²⁷¹ See [Atos, CSC and IQM join forces to accelerate the commercialization of European quantum technologies](#), June 2020.

¹²⁷² See [Surface acoustic wave resonators in the quantum regime](#), 2016 (40 slides).

¹²⁷³ The 3D layering and TSV structure is inspired from [Solid-state qubits integrated with superconducting through-silicon vias](#) by D. R. W. Yost et al, MIT, September 2020 (9 pages). This project was funded by IARPA.

¹²⁷⁴ See [Double-sided coaxial circuit QED with out-of-plane wiring](#) by J. Rahamim, Peter Leek et al, 2017 (4 pages), [Calibration of a Cross-Resonance Two-Qubit Gate Between Directly Coupled Transmons](#) by A.D. Patterson, Peter Leek et al, 2019 (8 pages) and [Superconducting microwave circuits for quantum computing](#) by Peter Leek, 2018 (42 slides).

Late 2022 during the Q2B and thanks to various third party benchmarks, it became possible to access OQC's qubit fidelities data. The fidelity of the OQC Lucy 8 qubit QPU goes from 89.9% to 96.8% depending on the qubit couples in the chip. The single gate fidelities are above 99.72%. T1 is between 22 μ s and 58.1 μ s¹²⁷⁵. The next iteration of OQC QPUs will have 32 qubits and better fidelities. In March 2023, OQC and Equinix also announced that their systems will be deployed by Equinix to provide cloud access to worldwide customers¹²⁷⁶. It was delivered to Equinix in November 2023, touting "colocation" capabilities in HPC datacenters.

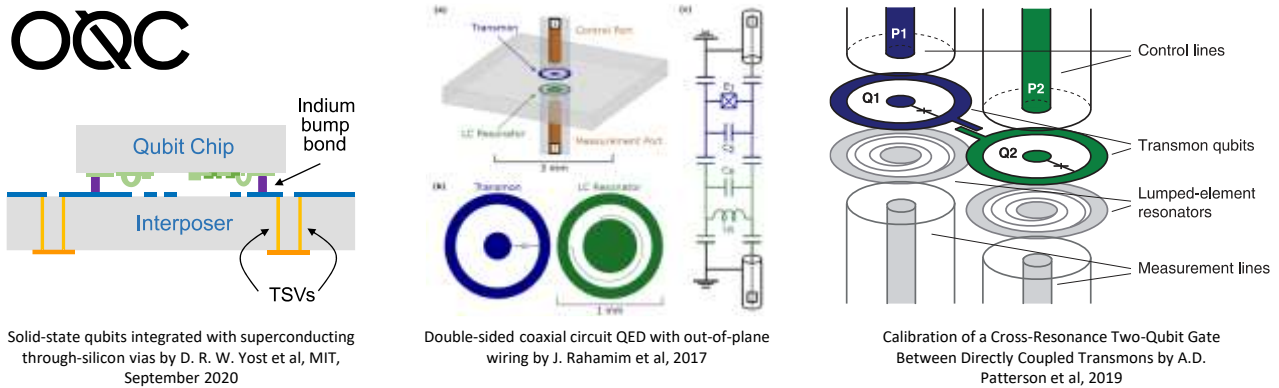
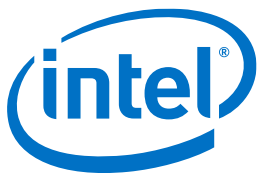


Figure 345: OQC coaxmon schematics showing how microwave controls are distributed vertically onto the qubits and their resonator. Source: OQC.

In April 2023, OQC announced the sale of their future 32 qubit QPU to CESGA in Spain and the creation of a knowledge center in Galicia in September 2023. This will be complemented by Fujitsu's 34 qubit quantum computer simulator running on the FX 700, the FUJITSU Server PRIMERGY HPC.



Intel is another player in the superconducting qubits field. With no commercial solution so far as it is only a research field at this stage, completed by to the more natural avenue of electron spin silicon qubits they are also pursuing. At CES 2018, Intel's CEO proudly showcased a 49-qubit superconducting chip during his keynote, stuck between a passenger drone demonstration and a broad talk on artificial intelligence.

Named Tangle Lake, the chip was tested at **Qutech** in the Netherlands. They were at 7 qubits at the end of 2016, 17 qubits at the end of 2017 and 49 (uncharacterized) qubits in January 2017. Since then, no news. It seems that Intel is now entirely focused on electron spin qubits, along with their partner Qutech in The Netherlands, where they invested \$50M back in 2015.



Anyon Systems (2014, Canada) was created by Alireza Najafi-Yazdi. Their physics team is managed by Gabriel Éthier-Majcher and the startup had about 20 employees as of mid-2023.

They started with creating their Quantum Device Simulator (QDS), a software tool used in quantum computer design and simulation that can run on supercomputers. It was used by John Martinis' Google team in 2017 for the design of their superconducting 6 and 20-qubit processors¹²⁷⁷. Their software was mainly used to predict the level of adjacent qubits crosstalk. It is part of Snowflake, an open source library for creating quantum circuits running both on quantum emulators and quantum computers. Their main goal then became to create superconducting qubits quantum computers.

¹²⁷⁵ The data was presented at the Q2B in Santa Clara in December 2022. See also [Benchmarking simulated and physical quantum processing units using quantum and hybrid algorithms](#) by Mohammad Kordzanganeh et al, TerraQuantum, November 2022 (17 pages).

¹²⁷⁶ See [Oxford Quantum Circuits Installing Quantum Computer in Equinix IBX Data Center With Plans To Open Access to Businesses Globally](#), Equinix, March 2023.

¹²⁷⁷ See [Google's 'supreme' 20-qubit quantum computer](#) by Tushna Commissariat, 2017.

The CEO and cofounder adopted a full stack approach, creating custom control electronics, dilution cryogenics and nearly custom anything.




Figure 346: Anyon Systems superconducting chip and setup for its upcoming 12 qubit Monarq QPU to be delivered to Calcul Québec.
Source: [Quebec enters the era of quantum computing](#) by Matthew Lapierre, CBC, August 2023.

Their first 6-qubit system was deployed internally in 2021. They published related qubit fidelities data in March 2022 with 99.7% for single qubit gates and 95.6% for two qubit gates¹²⁷⁸. Their T_1 is 10 μs and T_2 is 8 μs , which is quite low, but is compensated by fast gates of about 20 ns. Their chip is manufactured at the Quantum-Nano Fabrication and Characterization Facility (QNFCF) from the University of Waterloo in Canada (Figure 346, *left*).

They plan to deploy a 12-qubit system named Monarq in 2023 for Calcul Québec, a regional hybrid HPC-quantum computing research facility whose HPC hosts 1,500 Nvidia GPU. Software wise, they plan to support Cirq and Qiskit frameworks.

I had the opportunity to visit their headquarters and integration laboratory in May 2023 in Montréal, Québec. The machines are real! Their Monarq system has a rather large cryostat with very large low-level cold plates of about 60 cm wide (Figure 346, *right*). It is supposed to support up to 56 qubits, which may mean that their dilution yield is rather bad given the size of the cryostat chamber. You can't easily beat Bluefors and the likes in your own garage! Otherwise, the company does not show any roadmap toward reaching some viable NISQ regime or has any publicized thoughts on FTQC.

 **bleximo** Bleximo (2017, USA, \$1.5M) was founded by Alexei Marchenkov and Richard Maydra, two former Rigetti employees.

It develops superconducting qubits processors tailored for specific needs and adapted to different markets including biotech and financial services¹²⁷⁹. They focus on improving the classical control electronics driving their qubits and are partnering with Q-CTRL which develops error correction codes quantum software. They created a 8-qubit processor, the Vortex 8TQ with qubit lifetime sitting around 100 μs ¹²⁸⁰, a qubit electronics control device, Tabor Electronics Proteus P9484M, with up to 4 AWG channels, some shielding packaging for qubit chips, and even its own EDA software for superconducting circuits design. They are also developing photonic interconnect solutions.

They also develop quantum software solutions (aka “QCO”) for typical use cases like optimization, physics simulation and machine learning.

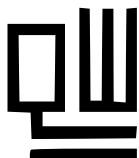
¹²⁷⁸ See [Update on Performance Metrics](#), Anyon Systems, March 2022.

¹²⁷⁹ See [Application-Specific Quantum Hardware is the Most Promising Approach for Early Practical Applications](#) by Fabio Sanches, Chiara Pelletti, and Alexei Marchenkov, February 2022.

¹²⁸⁰ See [Superconducting Quantum Processor Design at Bleximo](#) by Chiara Pelletti and Fabio Sanches, March 2022 and [Bleximo builds its competitive advantage with an application-specific approach](#), PhysicsWorld, June 2022.

In their team, Anastasia Marchenkova is a researcher producing a lot of [educational video content](#).

Their customer base seems made of US research labs (Berkeley University, DoE Berkeley Lab¹²⁸¹, Syracuse University, John Hopkins Applied Physics Laboratory). So, we're not far from a contract research company. This is exemplified by their willingness to create application-specific hardware, which doesn't make much sense from an economical and even practical standpoint¹²⁸².



QuantWare (2021, The Netherlands, \$14.7M) is a designer and manufacturer of superconducting qubits processors created by Matthijs Rijlaarsdam and Alessandro Bruno¹²⁸³. They offer their 25 qubits Contralto processor and a customizable connectivity that could for example help prototype specific quantum error corrections codes.

The chips have AirBridges and a proprietary TSV configuration (through-silicon via). It seems to be classical transmon superconducting qubits. They propose custom processors and a product design-to-delivery cycle of 30 days, leveraging the Van Leeuwenhoek Lab cleanroom at TU Delft.

They don't build full-fledged quantum computers. Their first 5-qubit Soprano QPU had a modest T_1 of 10 μs and a single-qubit gate fidelity of 99.99%. Contralto's 25-qubit processor (shown in Figure 347) could reach a T_1 of 60 μs .

They don't provide data on the most important figures of merit: dual-qubits gates and readout fidelity. Who could use these QPUs? Seemingly, various research labs¹²⁸⁴ and enabling technologies vendors, like their colleagues from Qblox and Delft Circuits and also SEEQC which used it to build a full-fledge 5-qubit QPU in 2023 in Italy using some of their SFQ superconducting control electronics.

They plan to double the number of qubits in their QPUs each and every year. In 2023, they announced a 64-qubit version, Tenor-64¹²⁸⁵. QuantWare has various partnerships in place, including with SEEQC (USA), with QuantrolOx (UK) and QphoX (The Netherlands).

As we'll see later in the cryoelectronics section around page 614, QuantWare also designs Crescendo, a TWPA (qubits readout traveling waves parametric amplifiers). In September 2022, the company got a subsidy funding of 1.1M€ from Quantum Delta NL, the foundation running the Dutch quantum national plan, to develop superconducting qubits based on undefined novel materials.

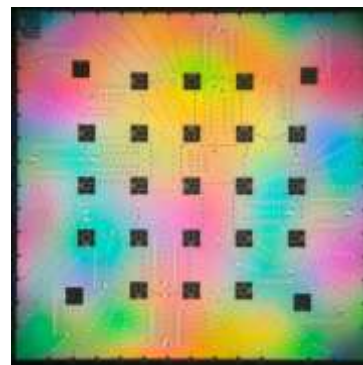


Figure 347: QuantWare's 25 qubit processor. Source: Quantware.

¹²⁸¹ See [Raising the Bar in Error Characterization for Outrit-Based Quantum Computing](#), Monica Hernandez, Lawrence Berkely National Laboratory in HPCwire, September 2021.

¹²⁸² See [Application-Specific Quantum Hardware is the Most Promising Approach for Early Practical Applications](#) by Fabio Sanches, Bleximo, February 2022.

¹²⁸³ Among their scientific advisors are Charlie Marcus, formerly running the Microsoft Quantum Lab in Copenhagen, Denmark. He left Microsoft in November 2021.

¹²⁸⁴ See [Multi-time quantum process tomography of a superconducting qubit](#) by Christina Giarmatzi et al, Macquarie University, Nor-dita, Stockholm University and KTH Royal Institute of Technology, August 2023 (9 pages) which does a multi-time quantum process tomography of a superconducting qubit comparing a Quantware Soprano chipset and an IBM 7 qubit QPU in the cloud, showing a clear advantage to IBM although the experiment is quite tough to interpret, using two different breeds of qubits with flux-tunable and fixed frequencies transmons.

¹²⁸⁵ See [Quantware launches technology that makes superconducting quantum computers massively scalable](#), February 2023.



Atlantic Quantum (2022, USA/Sweden, \$9M) is a startup cofounded by Jonas Bylander from Chalmers University in Sweden, along with Bharath Kannan (CEO), Simon Gustavsson, Youngkyu Sung, William D. Oliver, Shereen Shermak and Tim Menke, from the MIT.

The startup develops scalable fluxonium superconducting qubits-based quantum computers with experts covering all aspects of the quantum computing stack, from chip design and device fabrication to gate calibration and quantum algorithms (Figure 348). The cofounder's research group develops superconducting quantum electronic devices for quantum computing and simulation. Jonas Bylander recently published a paper on an efficient qubit readout solution using two microwave pulses and getting rid of the parametric amplifier, but it does not tell if it is in Atlantic Quantum's roadmap¹²⁸⁶.

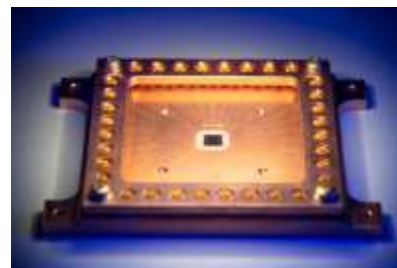


Figure 348: Atlantic Quantum fluxonium superconducting chip. Which is insufficient to have an idea of its qubit fidelities, that is not yet published. Source: Atlantic Quantum.

In September 2023, Atlantic Quantum was awarded a \$1.25M contract by the Air Force Research Lab to develop its prototype fluxonium based quantum processor.



Origin Quantum Computing (2017, China, \$163.4M) aka “Yuanyuan Quantum” is a startup created in Hefei by Guang-Can Guo and Guo Guoping out of the CAS quantum lab in Hefei, with Zhang Hui being their CEO.

It closed a record \$148M Series B funding round in July 2022 for a China quantum startup, making it a unicorn. Initially, it worked mainly on developing quantum algorithms and quantum emulation software. They were behind one of the records for 64-qubit quantum algorithm emulation on a supercomputer¹²⁸⁷. They also created cloud-based emulation appliances supporting 32 and 64 qubits.

The company works on a full-stack quantum offering including a 24 superconducting qubits system, on qubits control electronics (Quantum AIO), cryogenic equipment, on quantum software with an operating system (Origin Pilot), a programming framework (QPanda), the EmuWare virtual machine, a quantum machine learning framework (VQNet), a quantum programming language (QRunes), an integrated development environment (Qurator), and some applications frameworks for quantum chemistry (ChemiQ), fluid dynamics (OriginQ QCFD) and financial optimization. The company also create its NDPT-100, a non-destructive probe electrical measurement platform in December 2022, and the MLLAS-100 laser annealer that is useful for improving quantum chips quality in January 2023¹²⁸⁸.

They started to create their own quantum chips, including superconducting qubits chips with 6 qubits (KF C6-130) and 100 qubits (XW B2-100), using tunable couplers. They expected to reach 1,024 qubits by 2025 with intermediate steps of 64 qubits in 2021 and 144 qubits in 2022. As of January 2024, they 72-qubit Wukong QPU, using 126 tunable couplers, was made available on the cloud. The company is growing fast thanks to selling their QPUs to China's universities investing in quantum computing education.

SpinQ (China) is known for its NMR educational computers. It is working on a “Shoawei” 20-qubit superconducting qubits with an EDA software named Tianyi¹²⁸⁹ and delivered 2 qubits in 2023.

¹²⁸⁶ See [Transmon qubit readout fidelity at the threshold for quantum error correction without a quantum-limited amplifier](#) by Liangyu Chen, Jonas Bylander, Giovanna Tancredi et al, August 2022 (8 pages).

¹²⁸⁷ See [Researchers successfully simulate a 64-qubit circuit](#), June 2018.

¹²⁸⁸ See [China develops MLLAS-100 laser annealer, useful for improving quantum chips quality](#) by Global Times, January 2023.

¹²⁸⁹ See [SpinQ Releases 20-qubit Superconducting System and Chip EDA](#) by Huixuan (Viana) Ma, April 2023.



Alibaba is active in using the resources of its datacenters to simulate quantum algorithms exceeding 50 qubits. China's leading e-commerce company is also partnering with the **University of Science and Technology of China (USTC)** of the Chinese Academy of Sciences (CAS) to create superconducting quantum computers with superconducting qubits.

Their quantum research effort is embedded in its DAMO Academy, established in 2017.

They started with providing cloud access to 11 qubits as of early 2018, on a technology platform developed with USTC. They announced in 2018 that they were creating a subsidiary, **Ping-Tou-Ge**, which develops NPUs (neuromorphic processors for AI) and, eventually, superconducting quantum chips¹²⁹⁰. They have been working on fluxonium superconducting qubits, announcing qubit lifetimes T_1 and T_2 over 100 μs and a 99.5% iSWAP gate fidelity. In August 2023, they implemented a CZ two-qubit gate with a similar fidelity, of 99.53% and fast gate time of 20 ns¹²⁹¹.

However, in November 2023, Alibaba surprisingly seems to have dismantled its whole quantum lab and laid off its 30 employees.



Baidu announced in August 2022 its Qian Shi QPU with 10 superconducting qubits, to be later expanded to 36 qubits using couplers to run two-qubit gates, reusing a concept first pioneered by Google in 2019.

These qubits numbers where: $T_1 = 31 \mu\text{s}$, $T_2 = 8.7 \mu\text{s}$, single qubit gate at 99.8% and two-qubit gates at 96.4% (CX) and 96.8% (CZ). It was less than stellar. In January 2024, Baidu announced it was killing its quantum computing investments and donating its equipment to BAQIS in Beijing.



In April 2021, **RIKEN** and **Fujitsu** created the 20 researchers RIKEN RQC-Fujitsu Collaboration Center in Wako City, Japan, to do joint research and create a transmon based superconducting qubit computer, with a goal of reaching 1,000 physical qubits in 2026 and to develop an associated software platform.

It leverages RIKEN's existing work on superconducting qubits and Fujitsu's computing know-how. The research plan is quite classical: improving qubit manufacturing, reducing the size and noise of driving electronics components and wiring and improving error correcting codes. Some roadmaps were uncovered in August 2022. Fujitsu planned to release a first 64 qubits QPU by spring 2023 and delivered it in October 2023 (with no public qubit fidelities¹²⁹²), combining it with Fujitsu's classical 40-qubit emulator and NTT qubit control software. Fujitsu also delivered #Qmio, a 32 qubits QPU to CESGA in Spain the same month.



Toshiba has been conducting fundamental research in quantum computing since at least 2008, in quantum photonics and with superconducting qubits in its Frontier Research Laboratory.

Here, Hayato Goto is a prolific scientist working in many disciplines. In 2022, he created a double-transmon coupler that turns on/off coupling between two superconducting qubits in an efficient manner, enabling fast computing and two-qubit gate fidelities of 99.99% and time of 24 ns¹²⁹³.

Now, on to cat-qubit and other bosonic qubits vendors...

¹²⁹⁰ See [Alibaba Launches Chip Company "Ping-Tou-Ge"; Pledges Quantum Chip](#), September 2018.

¹²⁹¹ See [Native approach to controlled-Z gates in inductively coupled fluxonium qubits](#) by Xizheng Ma et al, Alibaba, August 2023 (19 pages).

¹²⁹² We only know that RIKEN has reached between 96% and 99.1% two-qubit gate fidelities according to [RIKEN](#) and [Subspace variational quantum simulator](#) by Kentaro Heya et al, PRR, May 2023 (12 pages).

¹²⁹³ See [Double-Transmon Coupler: Fast Two-Qubit Gate with No Residual Coupling for Highly Detuned Superconducting Qubits](#) by Hayato Goto, PRA, March-September 2022 (10 pages).



ALICE & BOB

Alice&Bob (2020, France, \$33M) was created by Théau Peronin (ENS Lyon) and Raphaël Lescanne (ENS Paris). They are designing a fault-tolerant gate-based quantum computer associating superconducting technology and stabilized photon-based (in the microwave regime) cat-qubits. Their technology main benefit is its capability to implement a complete universal fault-tolerant quantum computer with a much lower ratio of physical per logical qubits than traditional transmon based superconducting qubits. It saves at least one order of magnitude, moving from 1,000 to 1 down to 90 to 1 (for a 10^{-8} error rate).

Alice&Bob's technology is based on the PhD thesis from the startup founders and the associated work of the **Mazyar Mirrahimi's** Quantic team from Inria where Raphaël Lescanne was a doctoral student and where **Zaki Leghtas** as well as **Jérémie Guillaud** also work or worked¹²⁹⁴, the CNRS and ENS Lyon and ENS Paris. **Pierre Rouchon** from MinesParistech is also a key contributor¹²⁹⁵.

Their chipsets are manufactured by CEA SPEC in Saclay. You can have a look at the manufacturing process in Figure 351 and at the qubit layout in Figure 350.

Cat-qubits encode the state of a qubit with superposing opposite quantum states in micro-wave photon cavities, precisely, in the two-dimensional Hilbert space spanned by two coherent states of micro-waves of same amplitude and opposite phase¹²⁹⁶. These cat-qubits have a very low bit-flip error rate given it decreases exponentially with the average number of microwave photons used in the cat qubit cavity¹²⁹⁷. It helps them beat a record T_1 of 10 seconds in 2023¹²⁹⁸. Phase-flip errors can be corrected with repetition error codes having a rather low overhead¹²⁹⁹.

Cat-qubits can support a native implementation of 3-qubits Toffoli gates which, combined with Clifford gates, form a universal set of quantum gates. The implementation of such a universal gate set is a prerequisite to run quantum algorithms with a proven exponential speed-up. The Toffoli gate is an alternative to the usual (non-Clifford) T gate used in QFT-based algorithms. This gate can be corrected efficiently with avoiding magic state distillation, enabling fault-tolerance, and limiting error propagation between ancilla qubits¹³⁰⁰.

These qubits are more complex to design and operate but it would only take about 90 of them to create a well-corrected logical qubit with about 10^{-8} error rate, which would make it possible to create a better scalable architecture whereas with the current technologies of IBM, Google and Rigetti, about 1,000 to 10,000 physical qubits are required to create a functional logical qubit given their expected fidelities.

¹²⁹⁴ Mazyar Mirrahimi did work in Michel Devoret's team at Yale University around 2012. See [Dynamically protected cat-qubits: a new paradigm for universal quantum computation](#) by Mazyar Mirrahimi, Zaki Leghtas and Michel Devoret, 2013 (28 pages). Jérémie Guillaud is now Chief of Theory at Alice&Bob.

¹²⁹⁵ See [Quantum computation with cat qubits](#) by Jérémie Guillaud, Joachim Cohen and Mazyar Mirrahimi, March 2022 (75 pages).

¹²⁹⁶ See [Exponential suppression of bit-flips in a qubit encoded in an oscillator](#) by Raphaël Lescanne et al, July 2019 (18 pages) and [Repetition Cat Qubits for Fault-Tolerant Quantum Computation](#) by Jérémie Guillaud and Mazyar Mirrahimi, July 2019 (23 pages).

¹²⁹⁷ See [One hundred second bit-flip time in a two-photon dissipative oscillator](#) by C. Berdou, Zaki Leghtas, Mazyar Mirrahimi, Pierre Rouchon, Raphaël Lescanne, Théau Peronin, Taki Kontos et al, April 2022 (20 pages).

¹²⁹⁸ See [Quantum control of a cat-qubit with bit-flip times exceeding ten seconds](#) by Ulysse Réglade, Pierre Rouchon, Alain Sarlette, Mazyar Mirrahimi, Philippe Campagne-Ibarcq, Raphaël Lescanne, Zaki Leghtas et al, July 2023 (17 pages).

¹²⁹⁹ See [Error Rates and Resource Overheads of Repetition Cat Qubits](#) by Jérémie Guillaud and Mazyar Mirrahimi, March 2021 (17 pages). Based on numerical simulation, it estimates that a fault-tolerant cat-qubits computer with a logical error probability of 10^{-10} can be realized using 140 physical cat-qubits for Clifford gates and an average number of 15 photons per mode. A Toffoli gate could be implemented with only 180 physical cat-qubits including all required ancilla qubits.

¹³⁰⁰ They propose a 'pieceable fault-tolerant' implementation of the Toffoli gate, following the method introduced in [Universal Fault-Tolerant Gates on Concatenated Stabilizer Codes](#) by Theodore J. Yoder, Ryuji Takagi and Isaac L. Chuang, September 2016 (23 pages). This is a substitute to the transversal gates technique.

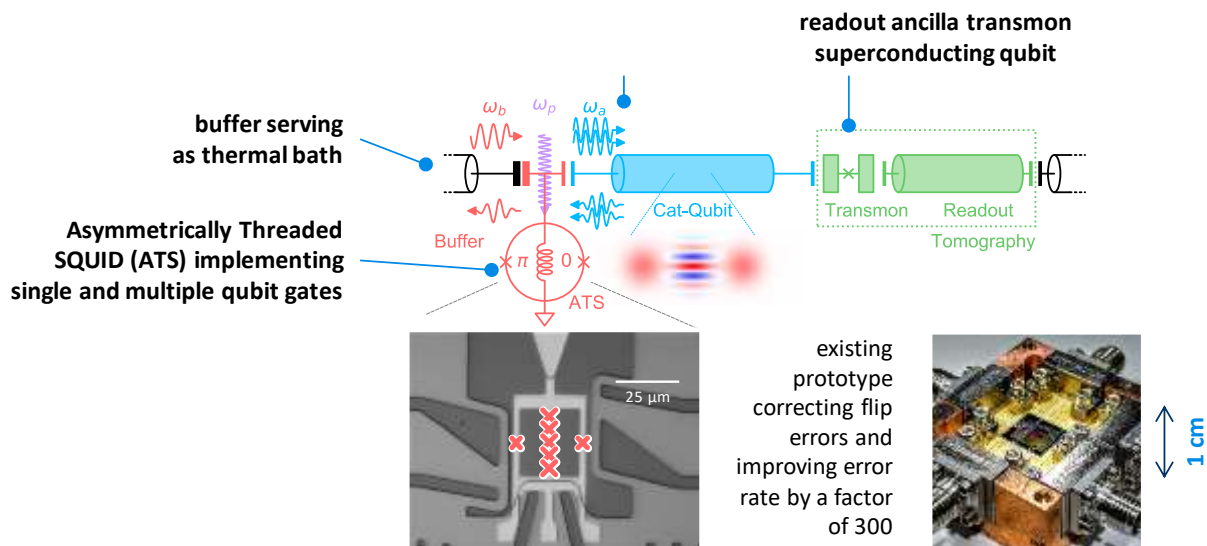


Figure 349: Alice&Bob cat-qubit cavity and its coupling to a transmon qubit and the ATS (asymmetrically threaded SQUID) that implements single and multiple qubit gates. Source: Alice&Bob.

These corrected qubits could also play the role of associative quantum memory. Moreover, their system avoids microwave radiations leaks between adjacent qubits.

The gates they implement on top of a Toffoli gate are a CNOT and a Hadamard gate. SWAP gates are built with three CNOTs in a classical fashion. These are heavily used to circumvent the absence of many to many qubits' connectivity in most 2D qubits layouts. All this will require a specific compiler, to be created later in the startup product lifecycle.

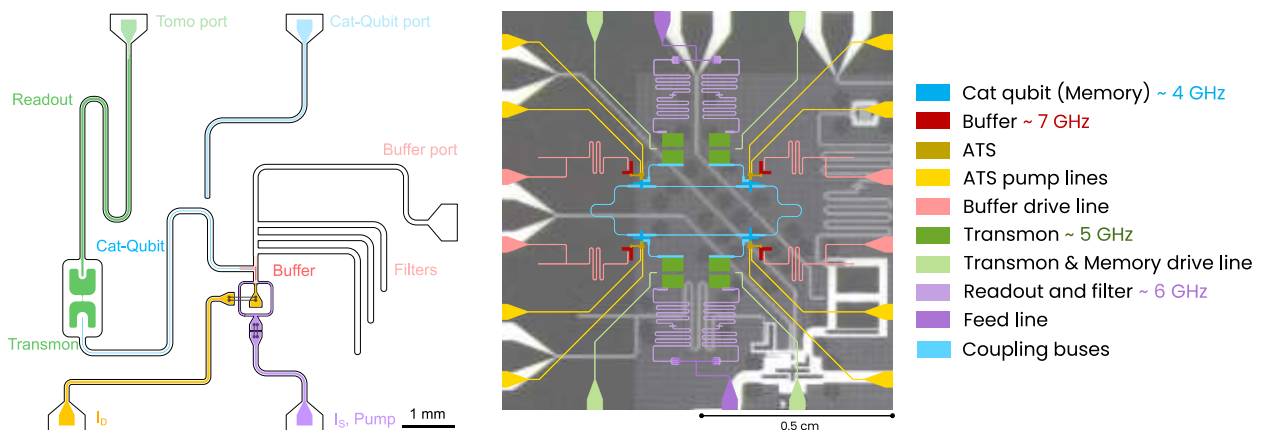


Figure 350: Alice&Bob experimental cat-qubit chip as of mid-2023, with logical layout (left) and physical layout (right). Source: [Cat qubits, a shortcut toward fault-tolerant quantum computer](#), by Antoine Gras, Alice&Bob, CEA Leti Innovation Days – Quantum Computing, June 28th, 2023.

On a practical way, these cat-qubits drives require some more corrections than regular transmon qubits. A continuous pulse tone drives the cat-qubit photons buffer. The qubit error corrections make use of an ATS (Asymmetrically Threaded SQUID), a nonlinear element that is flux biased with an AC current in the 4-8 GHz range (Figure 349). A single qubit gate requires two pulses (cat drive and dissipation phase). A cat-qubit readout uses two pulses on the coupling transmon and a readout pulse. Qubit readout uses 3 inbound pulses and one reflected pulse. And in total, cat-qubits require about 6 control lines¹³⁰¹.

¹³⁰¹ More details on how cat-qubits are physically implemented and controlled can be found in [Autoparametric resonance extending the bit-flip time of a cat qubit up to 0.3 s](#) by Antoine Marquet, Antoine Essig, Nathanaël Cottet, Audrey Bienfait, Théau Peronnin, Sébastien Jezouin, Raphaël Lescanne, Benjamin Huard et al, Alice&Bob and ENS Lyon, July 2023 (26 pages). It includes all the system wiring and lines driving the proposed qubit.

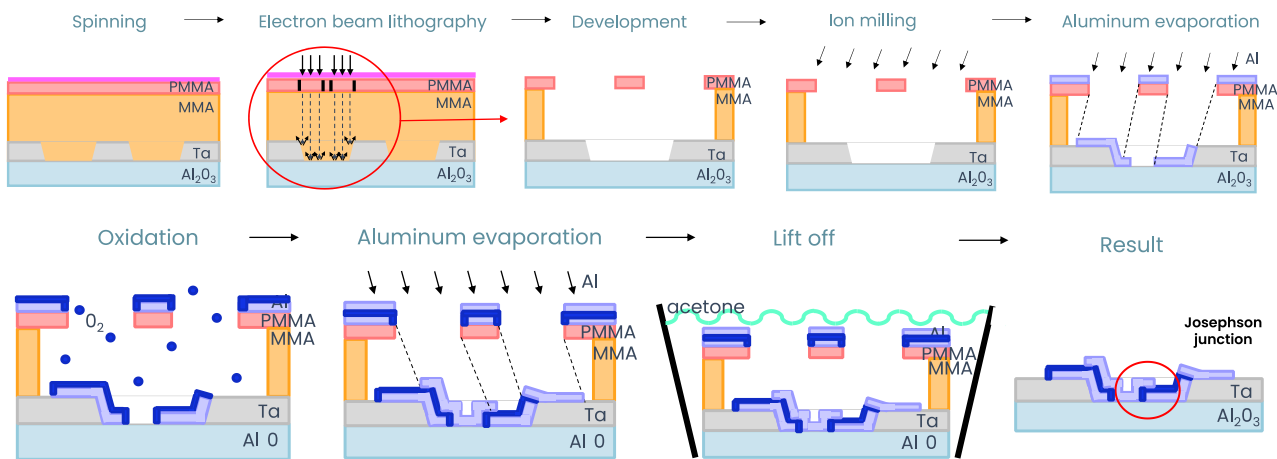


Figure 351: Alice&Bob chips manufacturing steps, in line with typical superconducting qubits manufacturing techniques. Source: [Cat qubits, a shortcut toward fault-tolerant quantum computer](#) by Antoine Gras, Alice&Bob, CEA Leti Innovation Days - Quantum Computing, June 28th, 2023.

Sideways, Alice&Bob launched in July 2023 “The Box” a consulting unit, to help customers with building applications (in the future). They also opened a branch in Boston in October 2023 and announced a partnership with Equinix in November 2023 to serve large account customers using Equinix hosting facilities.



Amazon (USA) started first to announce late 2019 its Amazon Braket cloud offering, based on using third-party quantum computers from D-Wave, Rigetti and IonQ, covered in the cloud section of this book, page 994.

In December 2020, they went out of the woods with announcing their detailed plan to build their own quantum computers, using cat-qubits, in a thorough 118 pages paper¹³⁰².

This work is getting the help from Caltech, including John Preskill, in connection with Yale University where some Caltech students did their PhDs in the teams of Rob Schoelkopf and Michel Devoret. The Amazon effort is led by **Simone Severini** (Director of Quantum Computing at AWS¹³⁰³), **Oskar Painter** (Head of Quantum Hardware at AWS), **Fernando G.S.L. Brandão** (Head of Quantum Algorithms at AWS and also researcher at Caltech) and **Richard Moulds** (GM Amazon Braket).

The bulk of Amazon’s quantum team are based in the new 21,000-sq-ft AWS Center for Quantum Computing building next to Caltech in Pasadena, North of Los Angeles. It was inaugurated in October 2021.

The Amazon initially proposed architecture is largely inspired by what the French teams at Inria have investigated since 2013 with Mazyar Mirrahimi et al, including the founders of Alice&Bob¹³⁰⁴. They wanted to create a FTQC.

As of 2020, Amazon was planning to use an electro-acoustic resonator to host the cat qubits while the circuit element, the Asymmetrically Threaded SQUID (ATS) invented by Raphaël Lescanne and Zaki Leghtas, used by Alice&Bob to stabilize the cat-qubit is superconducting. While Alice&Bob QEC is based on dissipating excess qubit energy to maintain it in low-energy states with encoding it in a

¹³⁰² See [Building a fault-tolerant quantum computer using concatenated cat codes](#) by Christopher Chamberland, John Preskill, Oskar Painter, Fernando G.S.L. Brandão et al, 2020 (118 pages). It is summarized in [Designing a fault-tolerant quantum computer based on Schrödinger-cat qubits](#) by Patricio Arrangoiz-Arriola and Earl Campbell, April 2021. See also [Fault-tolerant quantum computing with biased-noise hardware](#) by Earl Campbell, November 2020 (40 mn). Christopher Chamberland worked at IBM before AWS. He left AWS in 2023 to launch an AI startup that was stealth as of October 2023.

¹³⁰³ See [Decode Quantum with Simone Severini from AWS](#), Fanny Bouton and Olivier Ezratty, May 2023 (1h20mn podcast).

¹³⁰⁴ On top of France’s founding work on cat-qubits, Amazon is also relying on many US Universities research like Caltech, Stanford, Chicago University and Yale University.

linear oscillator driven by 10 GHz microwaves, Amazon chose a variant that uses linear harmonic oscillators-based cat-qubits using very compact piezoelectric nanostructures and phonons. Like with Alice&Bob, these cat-qubits self-corrects flip errors at the hardware level while phase errors are being handled by some QEC requiring, supposedly about 20 physical qubits.

Cat-qubits encode information with microwaves put in coherent states with opposite phases, $|+\rangle$ and $|-\rangle$. The qubit computational basis states are defined as even and odds coherent states cats, meaning using positive and negative sign superpositions for these two cat-states. Like Alice&Bob, they will implement a universal gate set comprising X, Z, CNOT and Toffoli gates. They use two new ideas for implementing fault-tolerant Toffoli gates: an extremely small chip layout (“bottom-up Toffoli”) and a technique to lower the bit-flip error rate (“top-down Toffoli”). They also avoid crosstalk between cat-qubits with using four cat-qubits connected to a single dissipating reservoir. This compact layout is compatible with a scalable architecture but may generate significant crosstalk errors, which could be mitigated with a well-chosen filter design cutting the frequencies to remove crosstalk errors.

They first plan to implement a 9-qubit QEC to obtain a logical error rate of 2.7×10^{-8} . As a result, they expect to use 2000 superconducting qubits to create a 100 logical qubits system. If this works, as with Alice&Bob, it will make a significant difference with IBM and Google who plan to obtain the same number of logical qubits with one million physical qubits. The scalability constraints are much different in both cases, whether it deals with cryogenics, microwave generations and readouts, or cabling. AWS is also working on some interconnect technologies involving piezoelectric based conversion of qubit state from the microwave to the optical domain, to enable long range interconnect between QPUs¹³⁰⁵.

In April 2021, University of Sydney science undergraduate Pablo Bonilla Ataidés published in Nature Communications a paper on its ZXXZ surface code that would reduce the number of required physical qubits to create a logical qubit thanks to a lower error threshold. It brought the attention of Amazon researchers¹³⁰⁶. This surface code could be used by Amazon who made a choice to use a relatively low number of photons per cat qubit (8 to 10, compared to about 15 for Alice&Bob, but the optimum number of photons is still to be determined experimentally), still requiring some first level bit-flip error correction on top of phase-flip correction. That’s where a ZXXZ surface code QEC could come into play. ZXXZ QEC codes are indeed mentioned as an option QEC technique in Amazon’s technical paper from December 2020.

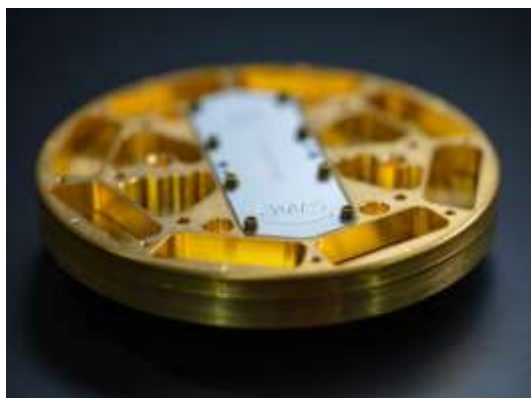
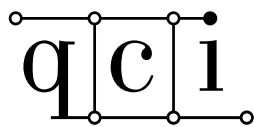


Figure 352: the first prototype Amazon cat-qubit chip of undisclosed characteristics, and their lab in Caltech opened in October 2021. Source: AWS.

¹³⁰⁵ See [Design of an ultra-low mode volume piezo-optomechanical quantum transducer](#) by Piero Chiappina, Oskar Painter et al, AWS, Caltech and Kavli Institute, March 2023 (14 pages).

¹³⁰⁶ See [Student's physics homework picked up by Amazon quantum researchers](#) by Marcus Strom, University of Sydney, April 2021, [Sydney student helps solve quantum computing problem with simple modification](#) by James Carmody April 2021 and [The XZZX surface code](#) by J. Pablo Bonilla Ataidés et al, April 2021, Nature Communications (12 pages).

The AWS Center for Quantum Computing opened at Caltech in October 2021 and houses all Amazon teams working on quantum computing¹³⁰⁷. They even then showcased a picture of a prototype quantum processor, maybe the one with 9 qubits (Figure 352). In 2023, it seemed that AWS was exploring other types of bosonic qubits on top of cat-qubits, like GKP and dual rail bosonic qubits¹³⁰⁸. The AWS research team is also exploring other qubit avenues including photon qubits. In December 2023, it announced having created its first logical qubit, but with no technical details.



QCI (2015, USA, \$18M) or Quantum Circuits Inc is a spin-off from Yale University co-founded by Rob Schoelkopf, Luigi Frunzio and Michel Devoret. Michel Devoret left the company in 2019, preferring to be a full-time researcher at Yale University.

Their technology is also based on bosonic qubits that solve noise and coherence problems, using Rob Schoelkopf's team research at Yale. They have a long track-record in that space although they are not very talkative. They announced in 2019 that their system should be available some day on Microsoft Azure Quantum cloud. But so far, they have apparently not delivered any functional QPU.

Technically, their planned qubits are stabilized by discrete parity measurement using a transmon and a so-called dual rail model^{1309 1310} and their two qubit gates are implemented using SNAP gates (Selective Number-dependent Arbitrary Phase (SNAP) using the same transmon¹³¹¹. They also planned to use micromachined 3D cavities with a good Q factor¹³¹². They plan to obtain a linear gain in qubit lifetime with the number of physical qubits. It will still require some surface codes to fully correct flip-errors (on top of phase errors). They are also at the origin of the **qbsolv** framework that is part of their **Mukai** middleware and development platform launched in January 2020¹³¹³. It supports D-Wave computers, Fujitsu digital-annealed computers and Rigetti superconducting qubits.



Nord Quantique (2019, Canada, \$7.6M) is a startup from the Institut Quantique from the University of Sherbrooke that is working on creating a superconducting quantum computer using more efficient error correction, using GKP codes, another variation of bosonic codes, and 3D cavities created at Yale.

The company was created by Julien Camirand Lemyre and Philippe St-Jean with the scientific support from Alexandre Blais and their investors are BDC Capital (USA), Quantonation (France) and Real Ventures (Canada). The company had a team of 20 as of May 2023, hosted at Institut Quantique in Sherbrooke. They have tested one qubit so far. Their chips were manufactured in Sherbrooke University's nanofab and will soon be manufactured in Bromont with some components also manufactured by RIKEN Center for Quantum Computing¹³¹⁴.

¹³⁰⁷ See [Announcing the opening of the AWS Center for Quantum Computing](#) by Nadia Carlsten, October 2021.

¹³⁰⁸ See [Demonstrating a long-coherence dual-rail erasure qubit using tunable transmons](#) by Harry Levine, Oskar Painter et al, AWS, Caltech, Hebrew University of Jerusalem, July 2023 (20 pages).

¹³⁰⁹ See [Demonstrating Quantum Error Correction that Extends the Lifetime of Quantum Information](#) by Nissim Ofek, Zaki Leghtas, Steve Girvin, Liang Jiang, Mazhar Mirrahimi, Michel Devoret, Rob Schoelkopf et al, February 2016 (44 pages).

¹³¹⁰ See [Demonstrating a superconducting dual-rail cavity qubit with erasure-detected logical measurements](#) by Kevin S. Chou, Shruti Puri, Steven M. Girvin, Robert J. Schoelkopf et al, July 2023 (37 pages).

¹³¹¹ See [Cavity State Manipulation Using Photon-Number Selective Phase Gates](#) by Reinier W. Heeres, Eric Holland (who now works at Keysight), Liang Jiang, Robert Schoelkopf et al, March 2015 (9 pages).

¹³¹² See [Multilayer microwave integrated quantum circuits for scalable quantum computing](#) by Teresa Brecht, Michel Devoret, Rob Schoelkopf et al, Nature, 2015 (5 pages) and the related thesis [Micromachined Quantum Circuits](#) by Teresa Brecht, 2017 (271 pages).

¹³¹³ See [QCI Qbsolv Delivers Strong Classical Performance for Quantum-Ready Formulation](#) by Michael Booth et al, May 2020 (7 pages).

¹³¹⁴ See [Autonomous quantum error correction of Gottesman-Kitaev-Preskill states](#) by Dany Lachance-Quirion, Philippe St-Jean et al, Nord Quantique, October 2023 (32 pages) which describes how autonomous error correction operates in their QKP qubits and their first experimental results.

Quantum dots spins qubits

Electron spins qubits are a new promising qubit technology with a lot of variations (Figure 354). Related research started later than superconducting qubits. Its potential benefits are miniaturization and scalability. It could leverage existing manufacturing processes for standard CMOS semiconductors¹³¹⁵.

History

Electron spin qubits quantum state is generally the spin orientation of an electron trapped in a potential well or of an electron hole, i.e. a missing electron and its virtual inverse impact on structural spin.

It is usually considered that Daniel Loss with David DiVincenzo and Bruce Kane are the first to have devised ideas to use electron spins to create a quantum computer, a couple years after Peter Shor created his famous integer factoring eponymous algorithm.

Daniel Loss (University of Basel) and **David DiVincenzo** (then at IBM Research) published a similar paper in 1996-1997 where they proposed the concept of quantum dots to create qubits with controlling the spin of electrons in a potential well¹³¹⁶. Their design used a two-qubit gate (SWAP) using an electric control of the tunneling barrier between neighboring quantum dots. A low gating voltage creates a coupling – *aka* Heisenberg coupling - between the neighbor qubits. The design also implemented single qubit gates. The Loss-Vincenzo concept was later extended with using pairs of quantum dots electron spins, one being the qubit itself, and the other, capacitively coupled with the first one and being used for qubit readout with a spin-to-charge conversion using conductance measurement, usually with some radio-frequency reflectometry using a microwave pulse, a bit like with superconducting qubit readout.

The first electron spin qubit was created in 2005 by a USA and Brazil team using GaAs on Si substrates¹³¹⁷. But GaAs qubits suffer from a major limitation, a strong hyperfine coupling together with a nonzero nuclear spin that leads to dephasing. So, physicists looked at Si and SiGe alternatives, which showcase lower hyperfine coupling. They could even provide a quasi-noiseless environment for spins thanks to their nuclear-free isotopes ²⁸Si and ⁷²Ge isotopes. But they are much more challenging in terms of manufacturing, regardless of the supply of isotopically purified materials.

The first demonstration of silicon spin qubit was made in 2012 by UNSW teams. In 2016, silicon qubits were demonstrated using industry-grade manufacturing processes by a French team from CEA-Leti and IRIG in Grenoble¹³¹⁸.

This belongs to the Si-MOS category, the most generic and easier to manufacture. Qubits are derived from planar MOS bulk or FDSOI technologies as well as with Fin-FET that are inspired from the latest CMOS manufacturing technologies.

These spin qubits have a size of about 100x100 nm, leading to potential high densities when it will scale¹³¹⁹.

¹³¹⁵ CMOS ("Complementary Metal Oxide Semiconductor") is the dominant technology used to produce microprocessors, for CPUs (Intel, AMD), GPUs (Nvidia, AMD), chipsets for smartphones (Qualcomm, Samsung, MediaTek, HiSilicon, etc.) and in a whole host of specialized sectors (microcontrollers, radio components, etc.).

¹³¹⁶ See [Quantum computation with quantum dots](#) by Daniel Loss and David DiVincenzo, 1997 (20 pages).

¹³¹⁷ See [Coherent Manipulation of Coupled Electron Spins in Semiconductor Quantum Dots](#) by Jason Petta et al, Science, 2005 ([5 pages](#)).

¹³¹⁸ See [A CMOS silicon spin qubit](#) by Romain Maurand, Maud Vinet, Marc Sanquer, Silvano De Franceschi et al, 2016 (12 pages).

¹³¹⁹ See [The path to scalable quantum computing with silicon spin qubits](#) by Maud Vinet, Nature Nanotechnology, December 2021 and [Scaling silicon-based quantum computing using CMOS technology: State-of-the-art, Challenges and Perspectives](#) by M. F. Gonzalez-Zalba, Silvano de Franceschi, Tristan Meunier, Maud Vinet, Andrew S. Dzurak et al, Nature Electronics, November 2020-April 2023 (21 pages).

Bruce Kane (UNSW) presented in 1998 another spin-based quantum computer concept based on placing individual phosphorous atoms (^{31}P) in a pure silicon lattice structure¹³²⁰. This approach is labelled “donors spin”. It is a hybrid scheme using quantum dots and single atom nuclear magnetic resonance (NMR) since qubits associate phosphorus atoms nuclear spin and silicon donors electron spins. The qubits are controlled by electrical and magnetic fields¹³²¹ (Figure 353). The main benefit is the long coherence of nuclear spins, which can theoretically extend to several seconds¹³²².

The challenges lie with the way to precisely position the phosphorus atoms in the silicon lattice and how to handle qubits entanglement and readout.

This is the path chosen by Michelle Simmons at UNSW and in her startup SQC. The individual atoms are positioned in the silicon structure with lithography using a scanning tunneling microscope (STM).

The first processor fully implementing this architecture was announced by SQC in 2022 (we cover it later). Similar options are pursued like the use of antimony nucleus embedded in silicon lattice structures and controlled by microwaves by Andrea Morello from UNSW¹³²³.

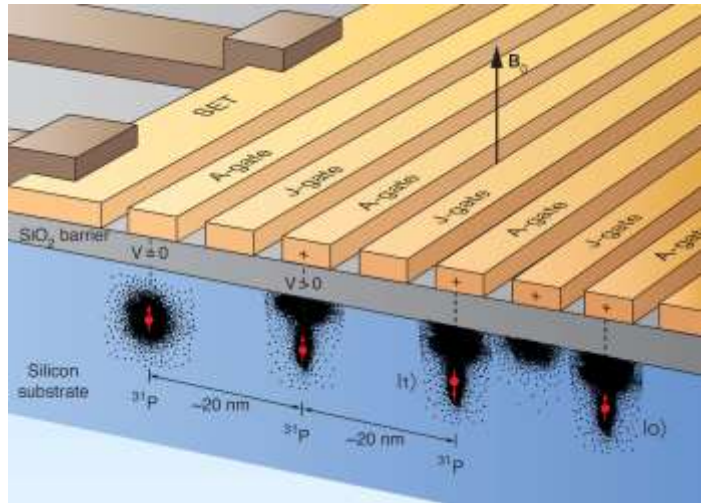


Figure 353: the donor spin architecture with phosphorous atom implanted in a silicon substrate under a SiO_2 isolation layer. Source: [Toward a Silicon-Based Nuclear-Spin Quantum Computer](#) by Robert G. Clark, P. Chris Hammel, Andrew S. Dzurak, Alexander Hamilton, Lloyd Hollenberg, David Jamieson, and Christopher Pakes, Los Alamos Science, 2022 (18 pages).

Later, Andrea Morello and Patrice Bertet designed another hybrid approach, coupling transmon superconducting qubits (for computing) and phosphorus in silicon nuclear spins with a donor electron (for creating a quantum memory)¹³²⁴.

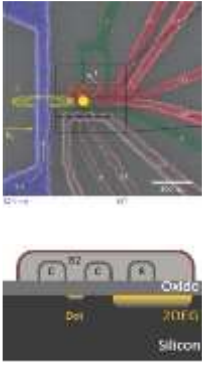
¹³²⁰ See [A silicon-based nuclear spin quantum computer](#) by Bruce Kane, Nature, 1998 and [Silicon-based Quantum Computation](#) by Bruce E. Kane, 2000 (14 pages).

¹³²¹ See [The Race To Make Better Qubits](#) by Katherine Derbyshire, Semiconductor Engineering, November 2021.

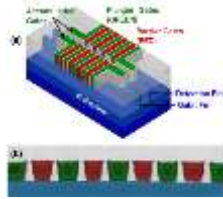
¹³²² The Bruce Kane concept is well described in [Toward a Silicon-Based Nuclear-Spin Quantum Computer](#) by Robert G. Clark, P. Chris Hammel, Andrew S. Dzurak, Alexander Hamilton, Lloyd Hollenberg, David Jamieson, and Christopher Pakes, Los Alamos Science, 2022 (18 pages). It shows linear array of phosphorous donor atoms buried into a pure silicon wafer, operating in the presence of a large magnetic field and at sub-K temperatures. The donor atoms nuclear spins are be aligned either parallel or antiparallel with the magnetic field, corresponding to $|0\rangle$ and $|1\rangle$ qubit basis states. The metal gates are above an insulating barrier of SiO_2 . The A-gates above the ^{31}P atoms enable single qubits gates while the J-gates in between the donors regulate an electron-mediated coupling between adjacent nuclear spins, for two-qubit operations. At last, qubit readout is done with either a single electron transistor (SET) or with a magnetic-resonance force microscope (MRFM, not shown).

¹³²³ See [Coherent electrical control of a single high-spin nucleus in silicon](#) by Serwan Asaad, Andrea Morello, Kohei M. Itoh, Andrew S. Dzurak et al, 2019 (56 pages).

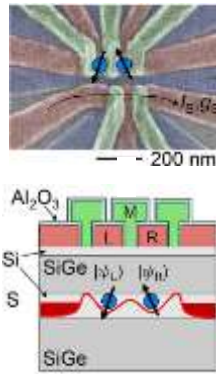
¹³²⁴ See [Donor Spins in Silicon for Quantum Technologies](#) by Andrea Morello, Patrice Bertet and Jarryd Pla, 2020 (17 pages).

Si-MOS, CMOS

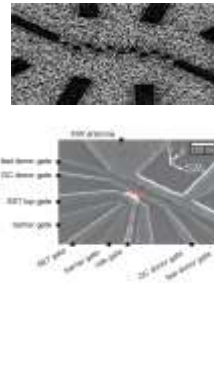
UNSW, Sandia
Labs, CEA-Leti,
Quoblv

Fin-FET

Intel, TU Delft,
IBM, U. Basel

Si/SiGe

Princeton, RIKEN,
HRL, TU Delft,
CEA IRIG. ARQUE

donors

UNSW,
SQC

**carbon
nanotubes/spheres**

C12 Quantum
Electronics,
Archer Materials

**spin on
helium**

EeroQ

Figure 354: various silicon spin qubits. (cc) Olivier Ezratty, 2022-2023.

On top of the above two mainstream paths (Si-MOS/CMOS and donors), several other avenues are investigated in the quantum dots based spin qubit realm:

- **Silicon/silicon germanium (Si/SiGe)** heterostructures qubits (Qutech, CEA IRIG) where germanium is used for the stability of its spin holes^{1325 1326}, large band gaps, higher electron mobility, stronger spin-orbit coupling, its insensitiveness to exchange coupling oscillations and long coherence times. It is however more difficult to manufacture and scale, with gates that are far from the qubits¹³²⁷. Various sources of noise must be mitigated^{1328 1329}. A record breaking 4 entangled qubits was announced late 2020 by TU Delft, based on germanium. Germanium allows the creation of very fast quantum gates ranging from 0.5 to 5 ns¹³³⁰. Spin hole germanium qubits use quantum dots with a Ge layer in between two GeSi layers, and spin germanium use an Si layer between to SiGe layers.
- **Gallium-arsenide (GaAs)**, first tested in 2005, but with very short coherence times due to spin interferences from gallium and arsenic atoms nuclei.
- **Electron spin trapped in carbon nanotubes** (C12 Quantum Electronics) or **carbon nanospheres** (Archer Materials). These structures better protect the spin of a trapped electron, at the expense of more complicated interfaces and controls^{1331 1332 1333}.

¹³²⁵ See the review paper [Recent advances in hole-spin qubits](#) by Yinan Fang et al, October 2022 (46 pages).

¹³²⁶ See [Coherent control of a high-orbital hole in a semiconductor quantum dot with near-unity fidelity](#) by Junyong Yan et al, December 2022 (27 pages).

¹³²⁷ See this excellent germanium review paper: [The germanium quantum information route](#) by Giordano Scappucci, Silvano De Franceschi et al, 2020 (18 pages).

¹³²⁸ See [Simulation of 1/f charge noise affecting a quantum dot in a Si/SiGe structure](#) by Marcin Kępa et al, March 2023 (7 pages).

¹³²⁹ See [Spatial noise correlations beyond nearest-neighbor in ²⁸Si/SiGe spin qubits](#) by Juan S. Rojas-Arias, Daniel Loss et al, February 2023 (11 pages).

¹³³⁰ See also [Quantum control and process tomography of a semiconductor quantum dot hybrid qubit](#), 2014 (12 pages).

¹³³¹ See the review paper [Carbon Nanotube Devices for Quantum Technology](#) by Andrey Baydin et al, MDPI, February 2022 (26 pages).

¹³³² See [Universal quantum computer based on Carbon Nanotube Rotators](#) by Motohiko Ezawa et al, University of Tokyo, November 2022 (7 pages).

¹³³³ See [Long-lived electronic spin qubits in single-walled carbon nanotubes](#) by Jia-Shiang Chen et al, Nature communications, February 2023 (8 pages).

- **Electrons trapped** on solid (inert) neon¹³³⁴ or on superfluid helium¹³³⁵. This last technique is explored in various labs like RIKEN in Japan and also by EeroQ in the USA.

	specs	pros	cons
Si-MOS	silicon quantum dot	mastered fabrication technique and scalability potential	qubit decoherence, poor entanglement, disordered potential in materials
FinFET	silicon quantum dot	mastered fabrication technique and scalability potential	disordered potential in materials
SiGe	holes or spin in Si Ge heterostructures (SiGe-Ge-SiGe or SiGe-Si-SiGe)	longer coherence time, entanglement, relatively high temperature (>1K), clean epitaxial barrier	valley degeneracy making it difficult to differentiate qubit states
GaAs	first Si- GaAs qubits in 2005	stable dopants, single conduction band valley, easy to manufacture, test platform for many characteristics with knowledge transferable to Si-MOS/FinFET/SiGe qubits	nuclear spins effect and very small coherence time (T_2)
atom donors	phosphorus atom spin donor	long coherence time	complicated to manufacture, impact of impurities
electrons on neon or helium	trapped electrons on superfluid helium.	long coherence, high connectivity, fast gates	not very vocal company (EeroQ) on progress made
carbon nanotubes and nanospheres	electron spin trapped in carbon nanotubes or nanospheres	long coherence time, reuse components from other qubit types for qubit control	more complex wiring and control, entanglement

Figure 355: specificities with pros and cons of each silicon spin qubit variety. (cc) Olivier Ezratty, 2022-2023.

These qubits small dimensions and the possibility to integrate control electronics in or around the qubit chip make it an interesting candidate for large-scale quantum computing¹³³⁶. There are however many challenges to overcome, particularly with materials design¹³³⁷ (Figure 355).

While in most cases, silicon qubits are planned to be used in the gate-based paradigm, it can also implement quantum simulations in analog mode¹³³⁸.

Science

Spin qubits may allow the integration of a large number of qubits in a circuit, with potentially up to billions of qubits on a single chip. It seems to be the only technology that can achieve this level of integration. These qubits would have a rather long coherence time and an error rate at least as low as with superconducting qubits¹³³⁹.

¹³³⁴ See [Single electrons on solid neon as a solid-state qubit platform](#) by Xianjing Zhou, Kater W. Murch, David I. Schuster et al, Nature, May 2022 (16 pages). The trapped electrons are coupled to a superconducting resonator on top of solid neon at 10 mK. It should bring better coherence but their current T_2 is at 200 ns.

¹³³⁵ See [Blueprint for quantum computing using electrons on helium](#) by Erika Kawakami et al, RIKEN, QunaSys, OIST, and DLR, March 2023-September 2023 (28 pages).

¹³³⁶ A good up-to-date overview of silicon qubits can be found in [Scaling silicon-based quantum computing using CMOS technology: State-of-the-art, Challenges and Perspectives](#) by M. F. Gonzalez-Zalba, Silvano de Franceschi, Tristan Meunier, Maud Vinet, Andrew S. Dzurak et al, November 2020-April 2023 (21 pages).

¹³³⁷ See [Democratizing Spin Qubits](#) by Charles Tahan, November 2021 (19 pages) which describes the many challenges with quantum dots spin qubits and [Quantum Technologies for Engineering: the materials challenge](#) by Kuan Eng Johnson Goh, Leonid A Krivitsky and Dennis L Polla, IOP Publishing, March 2022 (14 pages).

¹³³⁸ See [Quantum simulation of an exotic quantum critical point in a two-site charge Kondo circuit](#) by Winston Pouse et al, Nature Physics, January 2023 (26 pages).

¹³³⁹ A record silicon qubit coherence time was broken in 2020 by a team from the University of Chicago, reaching 22 ms (T_2). This is 10,000 times longer than the usual coherence times around 100 μ s found in superconducting qubits. These qubits use double gaps in silicon carbide structures. See [Universal coherence protection in a solid-state spin qubit](#) by Kevin C. Miao, David D. Awschalom et al, August 2020 (12 pages). University of Chicago.

The control microwaves used have a higher energy level which explains why silicon qubits can theoretically operate around 1K instead of 15 mK for superconducting qubits¹³⁴⁰. This level corresponds to microwaves with a frequency higher than 20 GHz, compared to the 4 to 8 GHz control microwaves of superconducting qubits.

This higher temperature makes it possible to place denser control electronics around the qubits without heating up the circuit too much. The reference data are as follows: only one milliwatt of energy can be consumed at 100 mK¹³⁴¹.

This limits the control electronics to about 10,000 transistors in CMOS technology¹³⁴². Once developed, silicon qubits will require the use of massive error correction codes, such as surface codes or color codes.

At the state-of-the-art level, the Australians, researchers from QuTech¹³⁴³ and Jason Petta at Princeton have demonstrated two-qubit gates in different geometries. To get to the next step, the challenge is to control the electrostatic potential between the quantum wells where the electrons are stored - and thus their spin - with a number of grids that allow the qubits to be arranged not too far apart, typically on the order of a few tens of nanometers.

Also, a lot must be done in materials design and process manufacturing¹³⁴⁴, particularly to fight charge noise affecting the spins¹³⁴⁵ ¹³⁴⁶. Other issues to address relate to the drift in control frequencies due to gate operations originated system heating¹³⁴⁷ (see also Figure 362).

Note that these qubits can be associated with photonics for long range connectivity. The states of these qubits can be transmitted via photons, which would enable distributed quantum computing architectures¹³⁴⁸.

Qubit operations

The general principle of quantum dots spin qubits consists in confining a spin carrier (an electron or an electron hole) in an electrostatically defined quantum well that is surrounded by tunnel barriers. A static magnetic field enables the creation of a 2-level system with spin up and down. Single gate rotations are handled by submitting the spins/holes to a radio frequency magnetic field. The spin being affected only by this field protects it against electrical noise and other undesirable interactions like phonons (atomic vibrations). Two-qubit gates are created with lowering the tunnel barrier between adjacent dots. Spin state measurement is implemented with a spin-to-charge conversion.

¹³⁴⁰ See [Hotter is easier: unexpected temperature dependence of spin qubit frequencies](#) by Brennan Undseth, Lieven M. K. Vandersypen et al, April 2023 (17 pages).

¹³⁴¹ A milli-Watt of cooling power can be achieved with a double pulsed tube cryostat such as the BlueFors XLD1000 or the Oxford Instruments TritonXL.

¹³⁴² This is explained in [28nm Fully-Depleted SOI Technology Cryogenic Control Electronics for Quantum Computing](#), 2018 (2 pages), from CEA-Leti and STMicroelectronics. It discusses the good performance of CMOS components manufactured in FD-SOI technology and operating at 4K, where the available cooling budget is even higher than at 100 mK. At 4K, the cooling power is in the order of a quarter of a Watt to a Watt.

¹³⁴³ See [A Crossbar Network for Silicon Quantum Dot Qubits](#) by R Li et al, 2017 (24 pages).

¹³⁴⁴ See the review paper [Materials for Silicon Quantum Dots and their Impact on Electron Spin Qubits](#) by Andre Saraiva, Wee Han Lim, Chih Hwan Yang, Christopher C. Escott, Arne Laucht and Andrew S. Dzurak, December 2021 (22 pages).

¹³⁴⁵ See [Effects of Temperature Fluctuations on Charge Noise in Quantum Dot Qubits](#) by Dan Mickelsen et al, May 2023 (8 pages).

¹³⁴⁶ See [Low charge noise quantum dots with industrial CMOS manufacturing](#) by Asser Elsayed et al, IMEC, December 2022 (22 pages).

¹³⁴⁷ See [Interacting Random-field Dipole Defect Model for Heating in Semiconductor-based Qubit Devices](#) by Yujun Choi et al, University of Wisconsin-Madison, July 2023 (9 pages).

¹³⁴⁸ See [Coherent shuttle of electron-spin states](#) by Lieven Vandersypen et al, 2017 (21 pages).

Let's now look at the details¹³⁴⁹:

- **Qubit quantum state** is generally the spin of a trapped individual electron in a potential well. The electrons are confined in a two-dimensional layer semiconductor structure, such as at the interface between two different semiconductors as in GaAs/AlGaAs, in a small quantum well as in Si/SiGe, or between an insulator and semiconductor (MOS), with the two-dimensional conducting layer known as a two-dimensional electron gas (2DEG)¹³⁵⁰. In normal temperature, the energy levels of valence electrons with different spin is the same, or “degenerate”. This spin degeneracy is lifted by using cryogeny at very low temperature (below a couple K) and with exposing the material under a magnetic field.
- **Single-qubit quantum gates** use the principle of electron spin resonance (ESR). As with superconducting qubits, these gates rely on the irradiation of the qubit by microwaves pulses, either using electromagnetic cavities, or with radio-frequency lines in which an alternating current creates a magnetic field, or finally, using micro-magnets. The related microwaves use frequencies between 8 and 20 GHz. These gates are usually R_x and R_y gates with the microwave pulse phase driving the gate rotation around axis X or Y and their amplitude and duration driving the rotation angle.
- **Two-qubit quantum gates** are created by controlling a tunneling interaction between two neighboring qubits with a significant number of electrodes. These interact with each other by modifying the potential barrier that separates the two qubits.

The manipulations, as in single-qubit gates, are performed by applying square pulse currents to qubit barrier and plunger gates (Figure 356).

Common low-level gates of this type are the square root of a SWAP gate and a phase controlled gate.

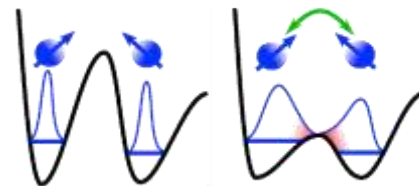


Figure 356: how a two-qubit gate is implemented with reducing the tunnel barrier between two spins. Source: Maud Vinet.

- **Qubit readout** frequently uses the conversion of the electron spin into electrical charge ("spin to charge") which is then exploitable by traditional electronics. It can exploit a second electron-spin positioned next to every computing qubit and using the Pauli spin blockage technique which forces the second electron spin to be the opposite of the measured electron spin¹³⁵¹. The measurement then is based on a microwave pulse sent on the qubit and a reflected signal phase/amplitude analysis, *aka* gate reflectometry¹³⁵². Some other measurement techniques are proposed that avoid collapsing the electron spin to its basis states¹³⁵³ or using resonant tunneling controlled by a conventional transistor as tested by RIKEN¹³⁵⁴.

¹³⁴⁹ See [Silicon Qubits](#) by Thaddeus D. Ladd 2018 (19 pages) which describes various methods other than the one discussed here.

¹³⁵⁰ See the review paper [Quantum Dots / Spin Qubits](#) by Shannon Harvey, April 2022 (20 pages).

¹³⁵¹ See [Rapid single-shot parity spin readout in a silicon double quantum dot with fidelity exceeding 99 %](#) by Kenta Takeda et al, RIKEN, September 2023 (14 pages).

¹³⁵² See an implementation with [Gate-reflectometry dispersive readout and coherent control of a spin qubit in silicon](#) by Alessandro Crippa, Silvano De Franceschi, Maud Vinet, Tristan Meunier et al, July 2019 (6 pages).

¹³⁵³ See [Quantum non-demolition measurement of an electron spin qubit through its low-energy many-body spin environment](#) by Harry E. Dyte et al, University of Sheffield, July 2023 (37 pages) which describes a non-destructive single-shot readout of GaAs qubits with high fidelity $\approx 99.85\%$ without any “wavefunction collapse” and with using off-resonant coupling with thousands of redundant nuclear spin ancillas using RF pulses. It is related to the concept of Quantum Darwinism promoted by W. Zurek in [Quantum theory of the classical: quantum jumps, Born's Rule and objective classical reality via quantum Darwinism](#) by Wojciech Hubert Zurek, 2018 (26 pages).

¹³⁵⁴ See [Readout using Resonant Tunneling in Silicon Spin Qubits](#) by Tetsufumi Tanamoto and Keiji Ono, RIKEN and Teikyo University, August 2023 (11 pages).

In typical circuits, qubit drive is usually implemented with several wirings: L (lead, providing the electron for the quantum dot), P (plunger, control the electron population), T (for tunnel coupling between quantum dots), S (source) and D (drain).

Research

Here are now the main research laboratories that are exploring the silicon spin path, very often in multi-laboratory and multi-country partnership ventures. We'll focus first on the Netherlands, Australia, France and the USA, and will then cover other countries.



In **The Netherlands**, TU Delft and QuTech are among the most active research organizations in Europe around quantum dots based qubits. This activity is centered in Lieven M. K. Vandersypen's lab at QuTech.

Two main technology paths are explored there with Si-MOS quantum dots in partnership with Intel since 2015, and on silicon-germanium qubits under the leadership of Menno Veldhorst and Giordano Scappucci. On top of his main role at Forschungszentrum Jülich in Germany, David DiVincenzo is also a professor at the EEMCS Department at the TU Delft and a contributing scientist at QuTech. TU Delft collaborates on germanium qubits with Purdue University in Indiana and Wisconsin-Madison University.

In 2020, Menno Veldhorst's team demonstrated the feasibility of germanium qubits with two entangled qubits with fidelities of respectively 99.9% and 98% for one and two qubit gates, using germanium electron holes and with two-qubit gate time of 75 ns over a coherence time of about $1\mu\text{s}$ ¹³⁵⁵. These qubits are built on a SOI substrate¹³⁵⁶.

Also in 2020, they implemented the same types of qubits in a 2x2 qubit array with a coherence time of 0.5 ms with 10 ns single qubit gate time¹³⁵⁷ (the qubits are labelled P₁ to P₄ in Figure 357).

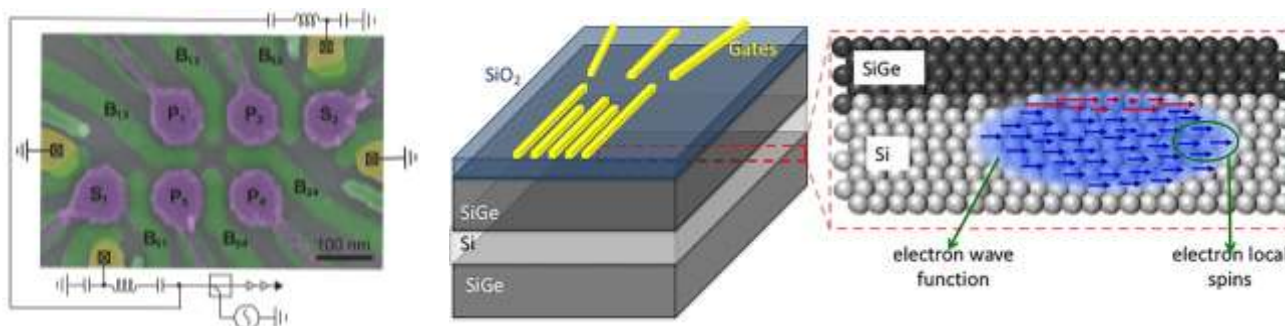


Figure 357: silicon-germanium prototype qubits. Source: [A two-dimensional array of single-hole quantum dots](#) by F. van Riggelen, Giordano Scappucci, Menno Veldhorst et al, August 2020 (7 pages) and [Silicon provides means to control quantum bits for faster algorithms](#) by Kayla Wiles, Purdue University, June 2018.

In 2022, they prototyped a Si-Ge spin qubits phase error correction proof of concept using the same 4 SiGe qubits¹³⁵⁸. They then extended the number of qubits to 6 while preserving good fidelities of 99.77% for single-qubit gates and reaching 71% to 84% for two-qubit gates, with a T₂ coherence time

¹³⁵⁵ See [Fast two-qubit logic with holes in germanium](#) by N.W. Hendrickx, Menno Veldhorst, Giordano Scappucci et al, January 2020 in Nature et on arXiv in April 2019 (6 pages) also described in [Reliable and extremely fast quantum calculations with germanium transistors](#), Qutech, January 2020.

¹³⁵⁶ The SOI for "silicon on insulator" is a technology from the French CEA-Leti and SOITEC. It adds a layer of silicon oxide insulator (SiO₂ or "BOX" for "buried oxide") over the silicon wafers and on which are then etched transistors and other circuits conductors.

¹³⁵⁷ See [A two-dimensional array of single-hole quantum dots](#) by F. van Riggelen, Giordano Scappucci, Menno Veldhorst et al, August 2020 (7 pages) and [A four-qubit germanium quantum processor](#) by N.W. Hendrickx et al, September 2020 (8 pages).

¹³⁵⁸ See [Phase flip code with semiconductor spin qubits](#) by F. van Riggelen, M. Veldhorst et al, QuTech, February 2022 (8 pages).

of several μs ¹³⁵⁹. They also achieved interesting results based on two SiGe qubits, with two-qubit gate fidelities exceeding 99%, paving the road for fault-tolerance (although surface codes QEC would probably require much better fidelities in the 99.99% range and with way above 2 qubits)¹³⁶⁰.

Sideways, the QuTech team in collaboration with research teams from ICREA and IC2N in Spain also made interesting inroads with interfacing their SiGe qubits with a germanosilicide superconducting material.

It could be useful in topological qubits design, to create gate-tunable superconducting qubits (**gate-mons**), to create long-range coupling between spin qubits using superconductivity and microwave guides^{1361 1362}.

At last, they demonstrated also in 2022 a 36×36 gate electrode crossbar supporting 648 narrow-channel field effect transistors (FET) to drive SiGe qubits¹³⁶³, and later developed a compiling solution to target this layout in the SpinQ project¹³⁶⁴.

Qutech is also the testing arm of Intel with its HorseRidge system and Si-MOS double quantum dots qubits. In 2020, QuTech and Intel announced having developed "hot" silicon qubits operating at around 1K, more precisely at 1.1K¹³⁶⁵. At about the same time, UNSW researchers were testing similar qubits at 1.5K¹³⁶⁶.



UNSW
SYDNEY

Australians are among the most active around silicon qubits, whether in the CQC2T teams at UNSW (University of New South Wales) or in other laboratories. Australian Universities are also teaming up with Microsoft Research¹³⁶⁷.

UNSW's CQC2T (Center for Quantum Computing & Communication Technology) laboratory is led by Michelle Simmons. She also cofounded and runs SQC, a silicon qubit startup that spun-out of UNSW. Their specialty is donors spin qubits using phosphorous atoms implanted in silicon wafers, along the Bruce Kane model created in 1998 at UNSW and already described in the history part starting page 414. This is a home run! In 2020, a team from the University of Melbourne showed how machine learning could help calibrate the placement of phosphorus atoms in a 2D structure of qubits

¹³⁵⁹ See [Universal control of a six-qubit quantum processor in silicon](#) by Stephan G.J. Philips, Menno Veldhorst, Lieven M.K. Vandersypen et al, February QuTech and TNO, 2022 (38 pages).

¹³⁶⁰ See [Quantum logic with spin qubits crossing the surface code threshold](#) by Xiao Xue, Lieven M. K. Vandersypen et al, Nature, January 2022 (17 pages).

¹³⁶¹ See [Hard superconducting gap in a high-mobility semiconductor](#) by Alberto Tosato, Francesco Borsoi, Menno Veldhorst, Giordano Scappucci et al, June 2022 (20 pages).

¹³⁶² See [Superconducting-Semiconducting Voltage-Tunable Qubits in the Third Dimension](#) by T.M. Hazard, Charles Tahan et al, PRA, September 2023 (7 pages).

¹³⁶³ See [A quantum dot crossbar with sublinear scaling of interconnects at cryogenic temperature](#) by P. L. Bavdaz, James Clarke, Menno Veldhorst, G. Scappucci et al, Nature, 2022 (6 pages) and [Shared control of a 16 semiconductor quantum dot crossbar array](#) by Francesco Borsoi, Giordano Scappucci, Menno Veldhorst et al, September 2022 (33 pages).

¹³⁶⁴ See [SpinQ: Compilation strategies for scalable spin-qubit architectures](#) by Nikiforos Paraskevopoulos et al, QuTech, January 2023 (18 pages). Not the China NMR QPU company.

¹³⁶⁵ See [Hot, dense and coherent: scalable quantum bits operate under practical conditions](#) by QuTech, April 2020 which refers to [Universal quantum logic in hot silicon qubits](#) by L. Petit, Menno Veldhorst et al, April 2020 in Nature and October 2019 in pre-print (10 pages).

¹³⁶⁶ See [Hot qubits made in Sydney break one of the biggest constraints to practical quantum computers](#) by UNSW, April 2020 referring to [Silicon quantum processor unit cell operation above one Kelvin](#) by C. H. Yang, Andrea Morello, Andrew S. Dzurak et al, February 2019 (15 pages).

¹³⁶⁷ UNSW also received in 2018 a funding of \$53M from the telecom operator Telstra, the Commonwealth Bank and the governments of Australia and the New South Wales region.

on a silicon substrate¹³⁶⁸. We'll cover these phosphorus-based qubits in the part dedicated to SQC a bit later in the vendor's part starting page 427.

Two other key scientists at UNSW are Andrew S. Dzurak and Andrea Morello. Andrea Morello's team working with DoE's Sandia Labs published in 2022 results with a single-qubit gate fidelity of 99.95%, a C-Z two-qubit gate fidelity of 99.37% and 98.95% readout fidelity with two phosphorus nuclear spins coupled with a single silicon spin donor electron. They even produced a three-qubit entangled state (GHZ) with a fidelity of 92.5%. This was interesting but was not a "scalable" demonstration¹³⁶⁹.

Still, Andrea Morello and Andrew S. Dzurak usually work on more classical silicon quantum dots qubits. In 2018, they proved the feasibility of creating silicon qubits and developed protocols for reading the state of the spins of these qubits without the need for averaging via a process called "Pauli spin blockade", paving the way for error correction codes implementation and the creation of large-scale quantum computers¹³⁷⁰. They also obtained in 2019 a 2% error rate for two-qubit quantum gates and a 99.96% fidelity for one-qubit gates¹³⁷¹.

Andrew S. Dzurak found in 2021 a way to improve the scalability of spin qubits with removing some the microwave circuits within the qubit chip and providing these microwaves to the qubits quantum dots with a dielectric microwave resonator (DR) made in potassium tantalate and activated by a discrete loop coupler, made of a simple wire¹³⁷². It drives the ESR (Electron Spin Resonance) magnetic field that enables spin rotations and single qubit gates as well as spin state readout. All this saves at least two microwave circuits in the quantum dots chip, reducing heating and simplifying the chip design and, potentially, qubits topology.

The global magnetic field generated by this system comes from a dielectric microwave resonator of 0.7*0.55*0.3mm and the discrete loop coupler is even larger, while quantum spin qubits can scale down as low as 100 nm x100 nm (Figure 358). The team communicated on this technology as one that could enable scaling quantum dots to million qubits. So how are individual qubits controlled? Individual spin control and readout is activated by some classical direct current tension sent to each quantum dot in the qubit chip, replacing the usual microwave signals sent and reflected in the chip. The next step is to implement the qubit circuit on isotopically purified ²⁸Si and check qubits coherence. While the solution simplifies the qubit chip wiring for some of the microwave lines, the prototype is based on using external microwave generators and readout systems, which doesn't scale at all. It circles back to a cryo-CMOS component that was developed by another Australian team and with Microsoft, which we describe in the cryo-CMOS section, page 597.

Andrea Morello's team is also studying the remote coupling of electron spins via photons in the visible or in radio waves spectrum. His team created silicon qubits exploiting the control of electron spin of intermediate layers of silicon atoms, increasing stability and reducing flip (or charge) errors¹³⁷³.

¹³⁶⁸ See [Machine learning to scale up the quantum computer](#) by Muhammad Usman and Lloyd Hollenberg, University of Melbourne, March 2020. Also seen in [To Tune Up Your Quantum Computer, Better Call an AI Mechanic](#) by NIST associated with UNSW, March 2020.

¹³⁶⁹ See [Precision tomography of a three-qubit donor quantum processor in silicon](#) by Mateusz Madzik, Andrea Morello et al, January 2022 (51 pages).

¹³⁷⁰ See [Tests show integrated quantum chip operations possible](#), October 2018 and [Integrated silicon qubit platform with single-spin addressability, exchange control and single-shot singlet-triplet readout](#) by M. A. Fogarty, Andrea Morello, Andrew S. Dzurak et al, Nature Communications, October 2018 (7 pages).

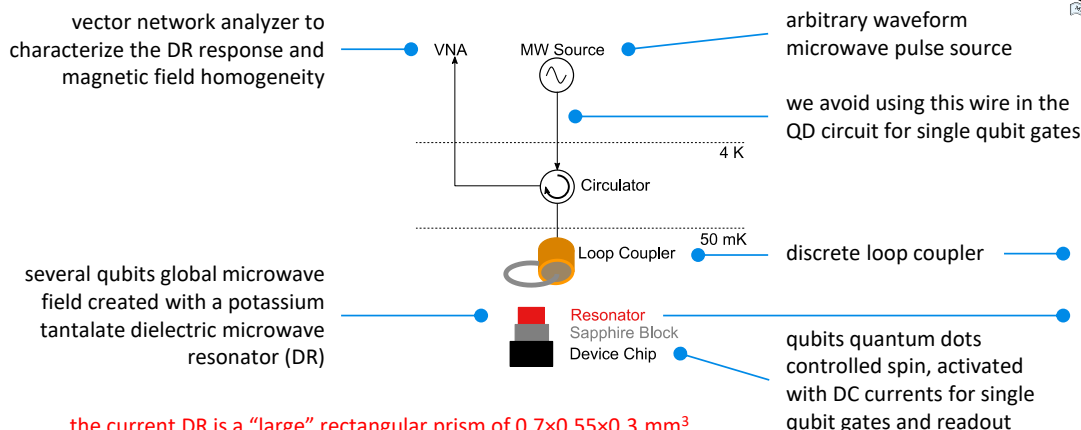
¹³⁷¹ See [Quantum World-First: Researchers Reveal Accuracy Of Two-Qubit Calculations In Silicon](#), May 2019.

¹³⁷² See [Single-electron spin resonance in a nanoelectronic device using a global field](#) by Ensar Vahapoglu, Andrew S. Dzurak et al, Science Advances, August 2021 (7 pages) and [Supplemental Materials](#) (12 pages).

¹³⁷³ See [UNSW use flat electron shells from artificial atoms as qubits](#) by Chris Duckett, February 2020 and [Engineers Just Built an Impressively Stable Quantum Silicon Chip From Artificial Atoms](#) by Michelle Starr, February 2020 which refers to [Coherent spin control of s-, p-, d- and f-electrons in a silicon quantum dot](#) by Andrea Morello et al, 2020 (7 pages).

It also managed, by chance, to control the spin of antimony atomic nuclei with an oscillating electric field¹³⁷⁴.

single-electron spin resonance (ESR) in a global field



the current DR is a “large” rectangular prism of 0.7×0.55×0.3 mm³, it is designed to feed several silicon qubits which are 100 nm x 100 nm squares

Figure 358: a proposal to improve the scalability of spin qubits with removing some the microwave circuits within the qubit chip and providing these microwaves to the qubit quantum dots with a dielectric microwave resonator. Source: [Single-electron spin resonance in a nanoelectronic device using a global field](#) by Ensar Vahapoglu, Andrew S. Dzurak et al, August 2021 (7 pages).



In France, the silicon qubit effort is driven out of a group of research labs in Grenoble with CEA-Leti, CEA-LIST, CEA-IRIG, CNRS Institut Néel and UGA (Université Grenoble Alpes).

In October 2018, the Grenoble-based team of Silvano De Franceschi (INAC, CEA), Tristan Meunier (Institut Néel, CNRS) and Maud Vinet (CEA-Leti) obtained a €14M **ERC Synergy Grant** for their QuQube project, spread over 6 years to produce a 100-qubit electron spin CMOS quantum processor¹³⁷⁵. Since March 2020, the Grenoble team is also coordinating the 4-year European Quantum Flagship project **QLSI** which was formally launched in February 2021¹³⁷⁶.

It consolidates fundamental research in silicon qubits and brings together CEA, CNRS Institut Néel, Atos, SOITEC and STMicroelectronics for France, IMEC (Belgium), Quantum Motion and UCL (UK), Infineon, IHP, U Konstanz, Fraunhofer and RWTH Aachen (Germany), UCPH (Denmark), TU Delft, U Twente and TNO (The Netherlands) and U Basel (Switzerland). With a budget of 15M€ to be shared between all these entities, the objective is to enable the manufacture and testing of 16 silicon qubits with gate fidelity of over 99%, and the preparation of a roadmap to be able to scale beyond a thousand qubits.

The Grenoble silicon qubit project was led until 2022 by **Maud Vinet** (CEA-Leti) and **Tristan Meunier** (CNRS) until they launched **Quobly** in November 2022 (as Siquance).

¹³⁷⁴ See [Engineers crack 58-year-old puzzle on way to quantum breakthrough](#) by UNSW, March 2020 and [Chance discovery brings quantum computing using standard microchips a step closer](#) by Adrian Cho, March 2020.

¹³⁷⁵ See [An ERC Synergy Grant for Grenoble research on quantum technologies](#), October 2018 (6 pages). A European Research Council Synergy Grand funds "moonshots" in European research involving at least two research laboratories. 14M€ is the maximum funding for such projects. 10M€ of core funding and 4M€ which can fund heavy investments or access to large infrastructures.

¹³⁷⁶ See [New EU Quantum Flagship consortium launches a project on silicon spin qubits as a platform for large-scale quantum computing](#), February 2021. QLSI was a follow-up project from the European collaborative project **Mos-quito**, a 3-year project from 2016 to 2019 with 4M€ funding for studying the performance of different types of individual silicon spin qubits to provide recommendations for their large-scale implementation.

This story started about 10 years earlier when CEA-Leti got interested in silicon qubits as a way to extend a then flailing Moore's law. CEA-Leti implemented their first silicon quantum dots qubits in 2016¹³⁷⁷.

Here are some of the specifics of this endeavor.

Different techniques. The Grenoble team mainly bets on Si-MOS silicon spin qubits. But they are still investigating SiGe qubits (CEA-IRIG), well as GaAs (for testing and calibration purpose) as well as silicon spin holes qubits, which are easier to control with a tension on the quantum dot transistor gate¹³⁷⁸.

Manufacturing capacity is a key asset from CEA-Leti, being one of the few public laboratories in the world with a CMOS component test production platform (IMEC is their counterpart in Europe, in Belgium). It includes all the tools required to produce 200 mm and 300 mm wafers.

It allows the production of all kinds of components in silicon, germanium and III-V materials (photonics, gallium arsenide, gallium nitride, etc.).

The CEA-Leti clean rooms are spread over several buildings, with the main one being 185 m long on 8,000 m²¹³⁷⁹ (Figure 359). Here, CMOS qubits manufacturing process uses 300 mm SOI wafers on with an additional thin layer of 99.992% purified 28-isotope silicon¹³⁸⁰. Validated production is to be later transferred to volume production in commercial fabs such like those from STMicroelectronics in Crolles, France, or GlobalFoundries in the USA or Germany.



Figure 359: the CEA-Leti's pre-industrial 200/300 fabs in Grenoble. As of 2018.

In its early stages, the size of the quantum computer market will be modest. In a conventional batch of 25 wafers alone, you can produce several thousand quantum chips in a single run, enough to power a large base of quantum supercomputers. But industry-grade clean rooms ensure quality processes that are not necessarily found in pre-production clean rooms.

Staging progress with the Grenoble team expecting to progress in stages over a six-year period starting in 2019: demonstration of a two-qubit silicon-based gate, demonstration of quantum simulation in a 4x4 array based on III-V material, demonstration six qubits in silicon, development of error correction codes and adapted algorithms, and fabrication of 100 2D array qubits in silicon at the end of this journey.

¹³⁷⁷ See [A CMOS silicon spin qubit](#) by Romain Maurand, Maud Vinet, Marc Sanquer, Silvano De Franceschi et al, 2016 (12 pages) that was already mentioned.

¹³⁷⁸ See [Dispersively probed microwave spectroscopy of a silicon hole double quantum dot](#) by Rami Ezzouch, Maud Vinet, Matias Urdampilleta, Tristan Meunier, Marc Sanquer, Silvano De Franceschi, Romain Maurand et al, 2020 (13 pages) and [A single hole spin with enhanced coherence in natural silicon](#) by Nicolas Piot, Boris Brun, Vivien Schmitt, Maud Vinet, Matias Urdampilleta, Tristan Meunier, Yann-Michel Niquet, Silvano De Franceschi et al, Nature, September 2022 (15 pages).

¹³⁷⁹ Other research clean rooms exist in France: the C2N clean room in Palaiseau, the IEF in Orsay, the Thales TRT clean room in Palaiseau, the IEMN clean room in Lille, Femto-ST clean room in Besançon and the Laas clean room in Toulouse. In production are mainly the fab 200 and 300 at STMicroelectronics in Crolles, near Grenoble. Some of these laboratories are associated in the National Network of Large Technology Plants (Renatech). They make their platforms available to companies in project and contract mode.

¹³⁸⁰ The first test of spin control with isotopically purified silicon was achieved in 2011. See [Electron spin coherence exceeding seconds in purified silicon](#) by Alexei Tyryshkin, Kohei Itoh, John Morton et al, 2011 (18 pages).

Control electronics with the Grenoble team creating control electronics operating at cryogenic temperature. The 2D architecture of Leti's CMOS chip contains several layers with silicon qubits and then the integrated electronics for control and qubit readout wiring. The qubits are distributed in 2D, but the integration of the components is also vertical within the components (Figure 360).

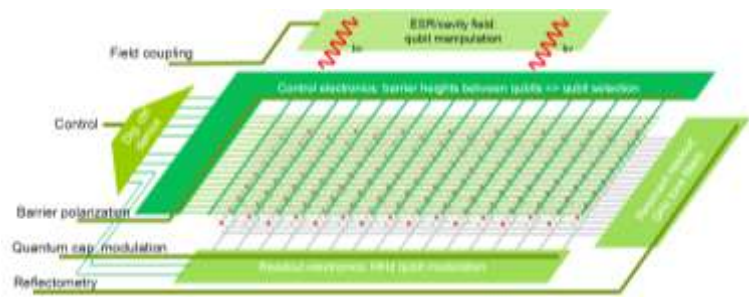


Figure 360: 2D wiring to access spin qubits with scalable wiring.
Source: [Silicon Based Quantum Computing](#), Maud Vinet 2018 (28 slides).

The measurement layer is located below the qubits while the layer for activating the qubits with quantum gates is above. For N^2 qubits, they would need $2N$ control lines (horizontal, vertical) instead of $2N^2$, which would generate an appreciable gain in connectivity. The technique would work to generate one- and two-qubit quantum gates¹³⁸¹.

The great challenge of these architectures is their variability, i.e., the differences in behavior from one qubit to another and from one circuit to another. This leads to a need for precise calibration, qubit by qubit, of the microwaves controlling and reading the state of the qubits. As for superconducting qubits, this calibration can be done using dedicated machine learning software. They use superconducting materials for the metal layer of these circuits, based on titanium nitride. This provides low resistance and reduces the noise of qubit state measurement.

3D stacking is used to arrange chips components in 3D¹³⁸², which can help solve various scalability problems. CEA-Leti is using its CoolCube technology. The reference publications of these teams on CMOS qubits are numerous¹³⁸³.

Spin-photon coupling could be used to create a communication link between remote qubits. At the Néel Institute, the aim is to move electron spins over long-distances ("Long-distance coherent spin shuttling"). Here, a long-distance means 5 μm ! But it makes enough to link qubits together, so it's worth it¹³⁸⁴.



In the USA, on top of Intel, several research labs are working on electron spin qubits. Let's factor in the already mentioned **DoE Sandia Labs** with sites in New Mexico and California (Figure 361), and **Purdue** and **Wisconsin-Madison Universities**.

They work on the physics of silicon qubits and their error correction codes. They are targeting an operating temperature of 100 mK. **Princeton University** and Jason Petta's team created in 2017 a two-qubit silicon CNOT gate with a very high level of reliability and low operating time, respectively 200ns and 99%¹³⁸⁵.

¹³⁸¹ The technique is described in [Towards scalable silicon quantum computing](#) by Matias Urdampilleta, Maud Vinet, Tristan Meunier, Yvain Thonnart et al, 2020 (4 pages) as well as in the presentation [Silicon Based Quantum Computing](#), Maud Vinet, 2018 (28 slides).

¹³⁸² See [CoolCube: A True 3DVLSI Alternative to Scaling Resource Library, Technologies Features](#) by Jean-Eric Michallet, 2015.

¹³⁸³ These include [A CMOS silicon spin qubit](#) by Romain Maurand, Maud Vinet, Marc Sanquer, Silvano De Franceschi et al, 2016 (12 pages) which defines the basis of double quantum dot CMOS qubit, [SOI technology for quantum information processing](#), 2016 which completes this description as well as [Conditional Dispersive Readout of a CMOS Single-Electron Memory Cell](#) by Simon Schaal et al, 2019 (9 pages) which describes, in the framework of a partnership with the University of London, the work on reading the state of a CMOS quantum dot. And then [Towards scalable silicon quantum computing](#) by Maud Vinet et al, 2018 (4 pages).

¹³⁸⁴ See [Coherent long-distance displacement of individual electron spins](#), 2017 (27 pages) and [Quantum Silicon Grenoble, the project on which the Forteza report relies for a quantum computer made in France](#) by Manuel Moragues, January 2020.

¹³⁸⁵ Seen in [Quantum CNOT Gate for Spins in Silicon](#), 2017 (27 pages).

These are also double quantum dots qubits using silicon and germanium. In October 2018, this Princeton team had succeeded in monitoring the state of its CMOS qubits with light and exploiting a microwave field to exchange a quantum between an electron and a photon¹³⁸⁶.

UCLA and Virginia Commonwealth University are working on nanomagnets to drive silicon qubits¹³⁸⁷.

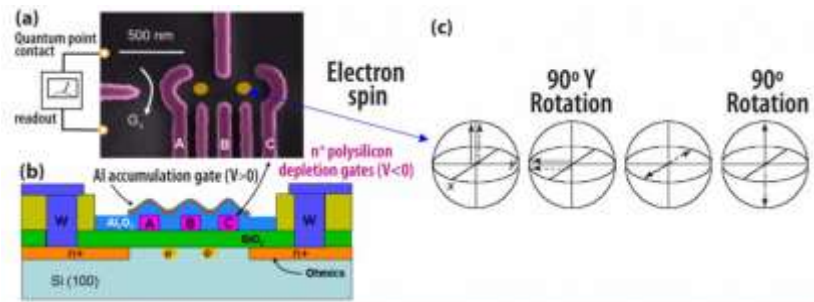


Figure 1: (a) scanning electron microscope image of Sandia's dual quantum dot structure fabricated in silicon (the dots suggest the approximate location of the electron positions); (b) schematic cross section of the quantum dot structure showing the position of the single electron locations; and (c) schematic representation of spin manipulation using rotation and precession of two different spins.

Figure 361: a typical double quantum dots spin qubit. Source: [Toward realization of a silicon-based qubit system for quantum computing](#) by Malcolm Carroll, Sandia Labs, 2016.

Finally, **HRL Malibu**, a joint research subsidiary of Boeing and General Motors located in California is working on both GaAs and Si / SiGe spin qubits. In 2022, they achieved a CNOT gate fidelity of $96.3 \pm 0.7\%$, SWAP fidelity of $99.3 \pm 0.5\%$ with 6 silicon qubits arranged in a 1D array¹³⁸⁸. They also work on triple-dot qubits with long lifetimes and better self-error correction¹³⁸⁹.

Let's finish this list with a couple other countries:

Switzerland: the Swiss National Science Foundation launched **SPIN** (Spin Qubits in Silicon), an electron spin qubits project in December 2019 with a funding of \$18M. The end goal is to create a scalable universal quantum computer with more than a thousand logical qubits. The project led by the University of Basel also gathers researchers from ETH Zurich, EPFL and IBM Research Zurich. It looks like a "Plan B" for IBM who is so far focused commercially on superconducting qubits¹³⁹⁰¹³⁹¹. We've also seen the key role of Daniel Loss in silicon qubits. He still works in Switzerland¹³⁹²! Another key researcher is EPFL's Andrea Ruffino, who is working with the Hitachi Cambridge Laboratory in the design of a mixed silicon qubit and cryo-CMOS readout control circuit¹³⁹³.

UK: is another active country on silicon qubits, particularly in **Oxford University**, **Cambridge University** and **UCL**, and with their startup **Quantum Motion**.

Germany: at the **University of Aachen**, researchers created double quantum dots of silicon with graphene¹³⁹⁴. Also involved are Infineon, Leibnitz Institute IHP Microelectronics, Universität Konstanz and Fraunhofer IPMS with its own cleanroom.

¹³⁸⁶ See [How old-school silicon could bring quantum computers to the masses](#), October 2018 and [In leap for quantum computing, silicon quantum bits establish a long-distance relationship](#) by University of Princeton, December 2019.

¹³⁸⁷ See [Quantum Control of Spin Qubits Using Nanomagnets](#) by Mohamad Niknam et al, March 2022 (11 pages).

¹³⁸⁸ See [Universal logic with encoded spin qubits in silicon](#) by Aaron J. Weinstein et al, HRL, Nature, February 2023 (12 pages).

¹³⁸⁹ See [Full-permutation dynamical decoupling in triple-quantum-dot spin qubits](#) by Bo Sun et al, HRL, August 2022 (12 pages).

¹³⁹⁰ See for example [A spin qubit in a fin field-effect transistor](#) by Leon C. Camenzind et al, March 2021 (14 pages) which describes a FinFET hole spin qubit potentially operating at 4K.

¹³⁹¹ See [Two-qubit logic with anisotropic exchange in a fin field-effect transistor](#) by Simon Geyer et al, IBM Research Zurich and University of Basel, December 2022 (35 pages) showcasing CTRL-R gates of 24 ns duration.

¹³⁹² See [Fully tunable longitudinal spin-photon interactions in Si and Ge quantum dots](#) by Stefano Bosco, Daniel Loss et al, EPFL, March 2022 (18 pages) and [A hot hole spin qubit in a silicon FinFET](#), IBM, March 2021.

¹³⁹³ See [A cryo-CMOS chip that integrates silicon quantum dots and multiplexed dispersive readout electronics](#) by Andrea Ruffino, Edoardo Charbon et al, Nature Electronics, December 2021 (14 pages). The circuit was implemented for three qubits.

¹³⁹⁴ See [Bilayer graphene double quantum dots tune in for single-electron control](#) by Anna Demming, March 2020.

quantum dots spins qubits

- good scalability potential to reach millions of qubits, thanks to their size of 100x100 nm.
 - works at around 100 mK - 1K => larger cooling budget for control electronics vs superconducting qubits.
 - relatively good qubits fidelity reaching 99.6% for two qubits gates in labs for a small number of qubits.
 - adapted to 2D architectures usable with surface codes or color codes QEC.
 - can leverage existing semiconductor fabs.
 - good quantum gates speed.
- active research in the field started later than with other qubit technologies and spread over several technologies (full Si, SiGe, atom spin donors).
 - less funded startup scene.
 - qubits variability to confirm.
 - high fabs costs and long test cycles (18 months average).
 - so far, only 4 to 15 entangled qubits (QuTech, UNSW, Princeton, University of Tokyo).
 - scalability remains to be demonstrated.

Figure 362: quantum dots spin qubits pros and cons. (cc) Olivier Ezratty, 2021-2023.

Denmark: Niels Bohr Institute and CEA-Leti collaborated to build a silicon qubit 2x2 matrix using single electrons quantum dots. These were fabricated on a classical 300 mm SOI wafer coming out of the CEA-Leti fab in Grenoble. While not being operational qubits, these quantum dots electrons were controllable with voltage pulses bases gates. They also implemented electron swaps, that could be useful in optimizing SWAP gates in future systems¹³⁹⁵. In another work with Purdue University in the USA, NBI researchers implemented four GaAs qubits in a 2x2 array¹³⁹⁶.

China also explores silicon qubits. They now publish more papers on this type of qubits¹³⁹⁷ ¹³⁹⁸ ¹³⁹⁹.

Japan silicon qubits are investigated at RIKEN. Their Semiconductor Quantum Information Device Theory Research Team is led by... Daniel Loss, yes, the same one. They were able in 2020 to measure the state of silicon qubits without altering it. This non-destructive measurement uses an Ising interaction model based on ferromagnetism that evaluates the spin of atoms neighboring the atom containing the qubit spin electron¹⁴⁰⁰. Teaming up with Qutech, they also work on shuttling electrons to connect distant silicon QPUs¹⁴⁰¹ ¹⁴⁰², on SiGe high fidelity qubits¹⁴⁰³ and on quantum error correction¹⁴⁰⁴. In 2023, the same team characterized the inter-qubit correlated noise in dense spin qubits¹⁴⁰⁵.

¹³⁹⁵ See [Single-electron operations in a foundry-fabricated array of quantum dots](#) by Fabio Ansaloni, Benoit Bertrand, Louis Hutin, Maud Vinet et al, December 2020 (7 pages).

¹³⁹⁶ See [Simultaneous Operations in a Two-Dimensional Array of Singlet-Triplet Qubits](#) by Federico Fedele et al, October 2021 (12 pages) and [Roadmap for gallium arsenide spin qubits](#) by Ferdinand Kuemmeth and Hendrik Bluhm, 2020 (4 pages).

¹³⁹⁷ See [Semiconductor quantum computation](#) by Xin Zhang Hai-Ou Li et al, December 2018 (23 pages). The document provides an overview of CMOS quantum technology but does not specify the specific contribution of Chinese research laboratories.

¹³⁹⁸ See [Single spin qubit geometric gate in a silicon quantum dot](#) by Rong-Long Ma et al, October 2023 (10 pages).

¹³⁹⁹ See [A SWAP Gate for Spin Qubits in Silicon](#) by Ming Ni et al, October 2023 (25 pages).

¹⁴⁰⁰ See [Scientists succeed in measuring electron spin qubit without demolishing it](#), RIKEN, March 2020, mentioning [Quantum non-demolition readout of an electron spin in silicon](#) by J. Yoneda et al, 2020 (7 pages).

¹⁴⁰¹ See [A shuttling-based two-qubit logic gate for linking distant silicon quantum processors](#) by Akito Noiri et al, February 2022 (25 pages).

¹⁴⁰² See [Conveyor-mode single-electron shuttling in Si/SiGe for a scalable quantum computing architecture](#) by Inga Seidler et al, npj Quantum Information, November 2022 (7 pages).

¹⁴⁰³ See [Fast universal quantum control above the fault-tolerance threshold in silicon](#) by Akito Noiri, Giordano Scappucci et al, 2022 (27 pages).

¹⁴⁰⁴ See [Quantum error correction with silicon spin qubits](#) by Kenta Takeda, Giordano Scappucci et al, RIKEN, Nature, January-August 2022 (23 pages).

¹⁴⁰⁵ See [Noise-correlation spectrum for a pair of spin qubits in silicon](#) by J. Yoneda, Daniel Loss et al, Nature Physics, October 2023 (20 pages).

Vendors

Key silicon based qubits industry vendors and startups are **Intel** (USA), **SQC** (Australia), **Diraq** (Australia), **Quantum Motion** (UK), **Quobly** (France), **ARQUE** (Germany), **SemiQon** (Finland), **C12 Quantum Electronics** (France), **Equal1.labs** (Ireland/USA) and **Archer Materials** (Australia).



Silicon Quantum Computing or **SQC** (2017, Australia, \$133.4M) is a spin-off from UNSW and CQC2T launched by Michelle Simmons. In 2017, their goal was to reach 10 qubits by 2022¹⁴⁰⁶ and they expect to reach 100 qubits by 2028.

SQC uses the spin donor technique, trapping phosphorus atoms on a silicon substrate. Their qubit is made by controlling the association of the phosphorus atom nucleus spin and a silicon donor electron spin. They create two-qubit gates with two phosphorus atoms that are a few nanometers apart, using quantum tunneling. They showcased single-gates fidelity of about 99.99% and two-qubit gates speed of less than one nanosecond¹⁴⁰⁷.

In 2022, they touted having produced the “*first ever quantum circuit*”¹⁴⁰⁸. It was a way to fulfill their 2017 goal and showcase a 10-qubit processor, implemented in a 1D lattice. It was presented in an article published in Nature, implementing a particular physics simulation, the many-body Su–Schrieffer–Heeger (SSH) model (Figure 363). Of course, with just 10 qubits, it can’t showcase any quantum advantage. Unfortunately, the paper doesn’t provide qubit fidelities data¹⁴⁰⁹. The paper was published as SQC announced it was starting a new financial round with a goal to obtain \$130M¹⁴¹⁰. In July 2023, they ended up raising only AUS \$50.4M.

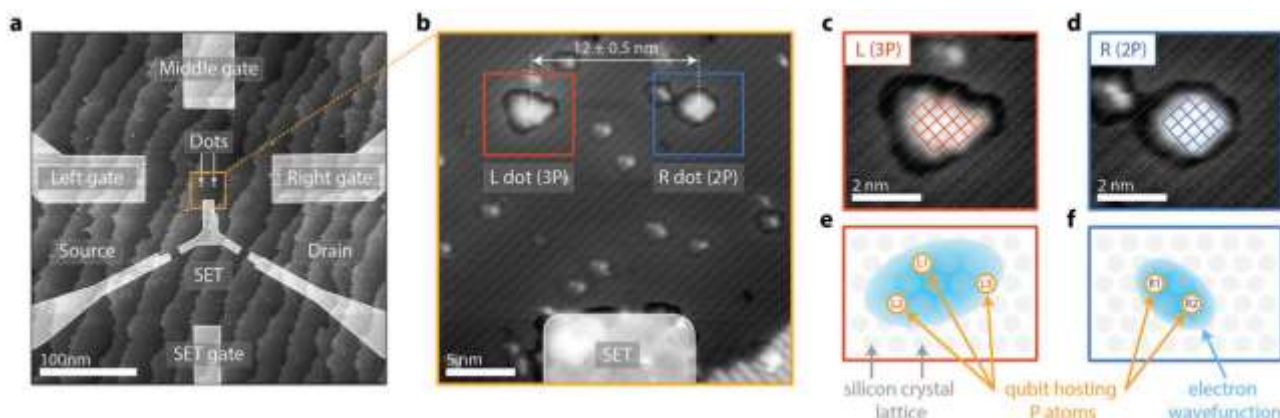


Figure 363: the atomic dots in SQC chips are precisely positioned. They contain several atoms. Source: [The Use of Exchange Coupled Atom Qubits as Atomic-Scale Magnetic Field Sensors](#) by Ludwik Kranz, et al, *Advanced Materials*, October 2022 (9 pages). Added in 2023.

Mid-2021, Andrea Morello and Andrew S. Dzurak quit SQC where they were involved since the beginning. They preferred to focus on SiMOS qubit instead of phosphorus and donor qubits. It led to the creation of their startup Diraq, which we’ll discuss later.

¹⁴⁰⁶ This is documented in [Silicon quantum processor with robust long-distance qubit couplings](#) by Guilherme Tosi, Andrea Morello et al, 2017 (17 pages).

¹⁴⁰⁷ See [Exploiting a Single-Crystal Environment to Minimize the Charge Noise on Qubits in Silicon](#) by Ludwik Kranz, Michelle Simmons et al, 2020 and [A two-qubit gate between phosphorus donor electrons in silicon](#) by Y. He, Michelle Simmons et al, 2019.

¹⁴⁰⁸ See how the media buy in such outrageous claim in [A Huge Step Forward in Quantum Computing Was Just Announced: The First-Ever Quantum Circuit](#) by Felicity Nelson, Science Alert, June 2022. Hopefully, The Quantum Insider is not parroting the fancy claim and titled [Silicon Quantum Computing Announces its First Quantum Integrated Circuit](#) by James Dargan, June 2022.

¹⁴⁰⁹ See [Engineering topological states in atom-based semiconductor quantum dots](#) by M. Kiczynski, Michelle Simmons et al, Nature, June 2022 (11 pages).

¹⁴¹⁰ See [Quantum star kicks off crucial \\$130m funding push](#) by Paul Smith, Financial Review, June 2022.

As a result, SQC sold in May 2022 its patent portfolio and special equipment related to SiMOS to SiMOS Newco, a company created in December 2021, and related to Diraq, that was created a month later¹⁴¹¹.

In 2022, they demonstrated the ability to have readout fidelities of 99%¹⁴¹². In 2023, they created a digital simulation of their qubits which showed that they could reach 99.98% fidelities with two-qubit CNOT gates¹⁴¹³. They also improved their manufacturing capabilities with precisely positioned phosphorus atoms dots in silicon¹⁴¹⁴.



QUANTUM
MOTION

Quantum Motion Technologies (2017, UK, \$63M) is an Oxford University spin-off that wants to create high-density silicon quantum computers.

The startup co-founded by John Morton (UCL) and Simon Benjamin (Oxford University) wants to industrialize a process created by Joe O'Gorman's team at Oxford University, which consists of clearly separating silicon qubits and their measurement. Measurement was supposed to be carried out with a magnetic probe mechanically moved on the surface and making "square" movements, guided by a MEMS (micro-electro-mechanical device). This probe system was designed to avoid the use of control electronics and allow a better separation between the qubits¹⁴¹⁵. A data rate separation process with intermediate mediation rates was limiting leakage effects¹⁴¹⁶. It seems that this technology is not the one they will implement!

In January 2021, Quantum Motion presented with Hitachi Cambridge, University of Cambridge and EPFL a 50 mK cryo-CMOS including quantum dots qubit arrays, row-column control electronics lines and analog LC resonators for multiplexed readout, using 6-8 GHz microwave resonators. This was a first step to implement time- and frequency-domain multiplexing scalable qubits readout¹⁴¹⁷.

In March 2021, Quantum Motion announced a record of stability of 9 seconds for an isolated silicon qubit. The chips were manufactured by CEA-Leti in Grenoble¹⁴¹⁸. Quantum Motion and UCL are part of the Quantum Flagship QLSI on silicon qubit that is led by Maud Vinet¹⁴¹⁹.

Their roadmap consists of producing 5 qubit "small cells" by 2022 in a structure that could then be reproduced in matrix patterns. They believe they can create a quantum computer with 100 logical qubits by 2029, a typical milestone for most quantum computer vendors.

¹⁴¹¹ See [UNSW Sydney spin-out buys quantum computing hardware technology](#) by Lauren Croft, Lawyers Weekly, May 2022.

¹⁴¹² See [Ramped measurement technique for robust high-fidelity spin qubit readout](#) by Daniel Keith, Michelle Simmons et al, September 2022 (7 pages).

¹⁴¹³ See [High-Fidelity CNOT Gate for Donor Electron Spin Qubits in Silicon](#) by Ludwik Kranz, Stephen Roche, Samuel K. Gorman, Joris. G. Keizer, and Michelle Y. Simmons, PRA, February 2023 (12 pages).

¹⁴¹⁴ See [The Use of Exchange Coupled Atom Qubits as Atomic-Scale Magnetic Field Sensors](#) by Ludwik Kranz, Samuel K. Gorman, Brandur Thorgrimsson, Serajum Monir, Yu He, Daniel Keith, Keshavi Charde, Joris G. Keizer, Rajib Rahman, and Michelle Y. Simmons, Advanced Materials, October 2022 (9 pages).

¹⁴¹⁵ See [A silicon-based surface code quantum computer](#) by Joe O'Gorman et al, 2015 (14 pages). The paper is co-authored by John Motin and Simon Benjamin who are two co-founders of the startup Quantum Motion Technologies. Their Si-MOS qubits are mixing planar and 3D SOI components and are laid out to enable surface code error correction.

¹⁴¹⁶ See [A Silicon Surface Code Architecture Resilient Against Leakage Errors](#) by Zhenyu Cai (Quantum Motion Technologies) et al, April 2018 (19 pages).

¹⁴¹⁷ See [Integrated multiplexed microwave readout of silicon quantum dots in a cryogenic CMOS chip](#) by A. Ruffino, January 2021 (14 pages).

¹⁴¹⁸ See [Spin Readout of a CMOS Quantum Dot by Gate Reflectometry and Spin-Dependent Tunneling](#), by Virginia N. Ciriano-Tejel, Maud Vinet, John Morton et al, 2021 (18 pages).

¹⁴¹⁹ See [Remote capacitive sensing in two-dimensional quantum-dot arrays](#) by Jingyu Duan, Michael A. Fogarty, James Williams, Louis Hutin, Maud Vinet and John J. L. Morton, 2020 (31 pages) which described the coupling technique using silicon nanowires (SiNW) to measure qubits spins with remote capacitive charge sensing

They provided an update on their architecture in an arXiv preprint in August 2022¹⁴²⁰. They then showcased in October 2022 the Bloomsbury 3x3mm² chip manufactured at Global Foundries containing 1,024 quantum dots and a year later, how they were efficiently characterizing the chip¹⁴²¹.

In June 2023, they published a preprint describing an original pipelining architecture designed to facilitate the run of several similar shots serially on a single chip. Instead of using a grid with $\sqrt{N} \times \sqrt{N}$ qubits, they create an array with $N \times D$, D being the number of time a given shot must be executed. It can be useful for example for NISQ VQE algorithms where the same (Paul string related) shot must be executed up to a million times. The N qubits are actually shuttling from left to right in the circuit layout as shown in Figure 364 and are subject to series of rotation and coupling gates that are mandated in variational circuits using a QAOA gates ansatz. This supposes that electron shuttling works at this scale. At this point in time, it seems to be a blueprint.

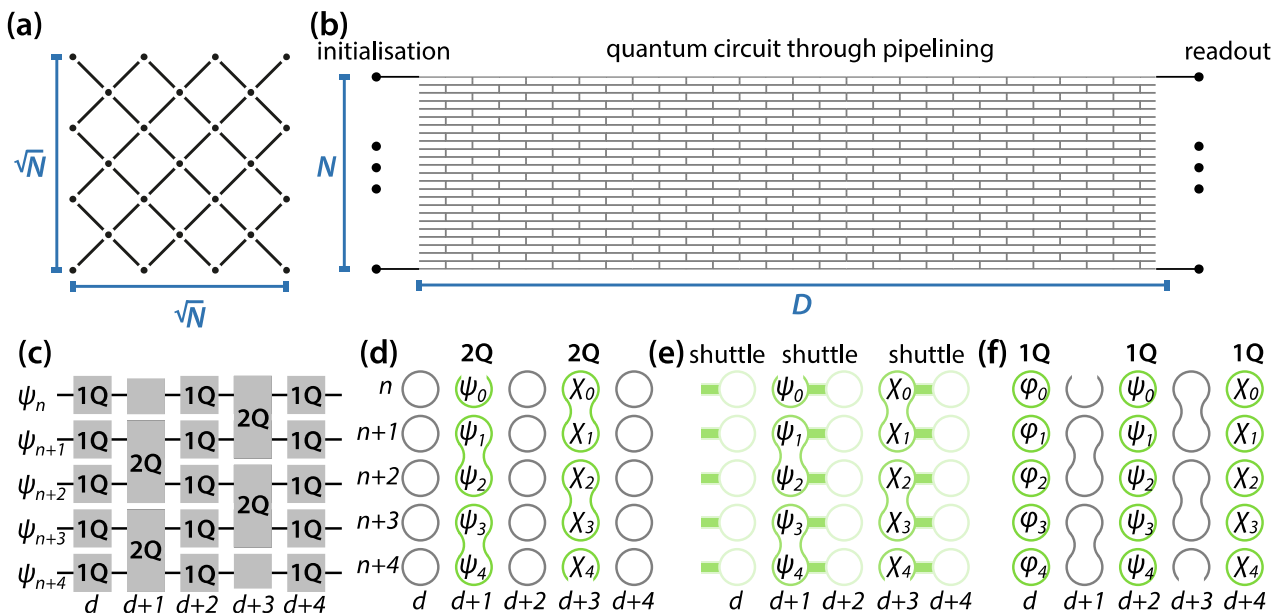
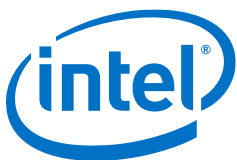


Figure 364: the Quantum Motion proposed pipeline architecture which is adapted to running many shots of the same algorithm in a NISQ fashion. N spin qubits are physically travelling horizontally (shuttling) from left to right in a 2D circuit are subject to series of rotation and entangled gates as they move. This enables the execution of up to D serialized similar shots. Source: [Pipeline quantum processor architecture for silicon spin qubits](#) by S. M. Patomäki, Simon Benjamin et al, June 2023 (21 pages).

In the software area, Quantum Motion developed QuEST, an open source, hybrid multithreaded and distributed, GPU accelerated simulator of quantum circuits. It works both on any laptop or on supercomputers. It supports pure (computational state vector) and mixed states (density matrices) to reproduce the effects of noise and decoherence^{1422 1423}.



Intel is a key contender in the race for silicon qubits (Figure 367). They started working on superconducting qubits, but it seems it was a secondary route for them. They started with producing a wafer with 26 qubit chips in 2017 and made some progress since they, although it is rather hard to evaluate.

¹⁴²⁰ See [Silicon edge-dot architecture for quantum computing with global control and integrated trimming](#) by Michael A. Fogarty, August 2022 (13 pages).

¹⁴²¹ See [Rapid cryogenic characterisation of 1024 integrated silicon quantum dots](#) by Edward J. Thomas et al, Quantum Motion and UCL, October 2023 (22 pages).

¹⁴²² See [QuEST and High Performance Simulation of Quantum Computers](#) by Tyson Jones et al, December 2018 (8 pages).

¹⁴²³ See [Distributed Simulation of Statevectors and Density Matrices](#) by Tyson Jones, Bálint Koczor and Simon C. Benjamin, Quantum Motion and University of Oxford, November 2023 (56 pages) which describes various distributed computing emulation techniques.

Intel's quantum work is managed under the direction of **Anne Matsuura**¹⁴²⁴ and **James Clarke** for hardware. In June 2018, Intel made another announcement with a highly integrated chip using SiMOS qubits, with 1,500 qubits, fabricated in the D1D fab located in Portland, Oregon, with an etch density of 50 nm, six times greater than the early 2018 generation.

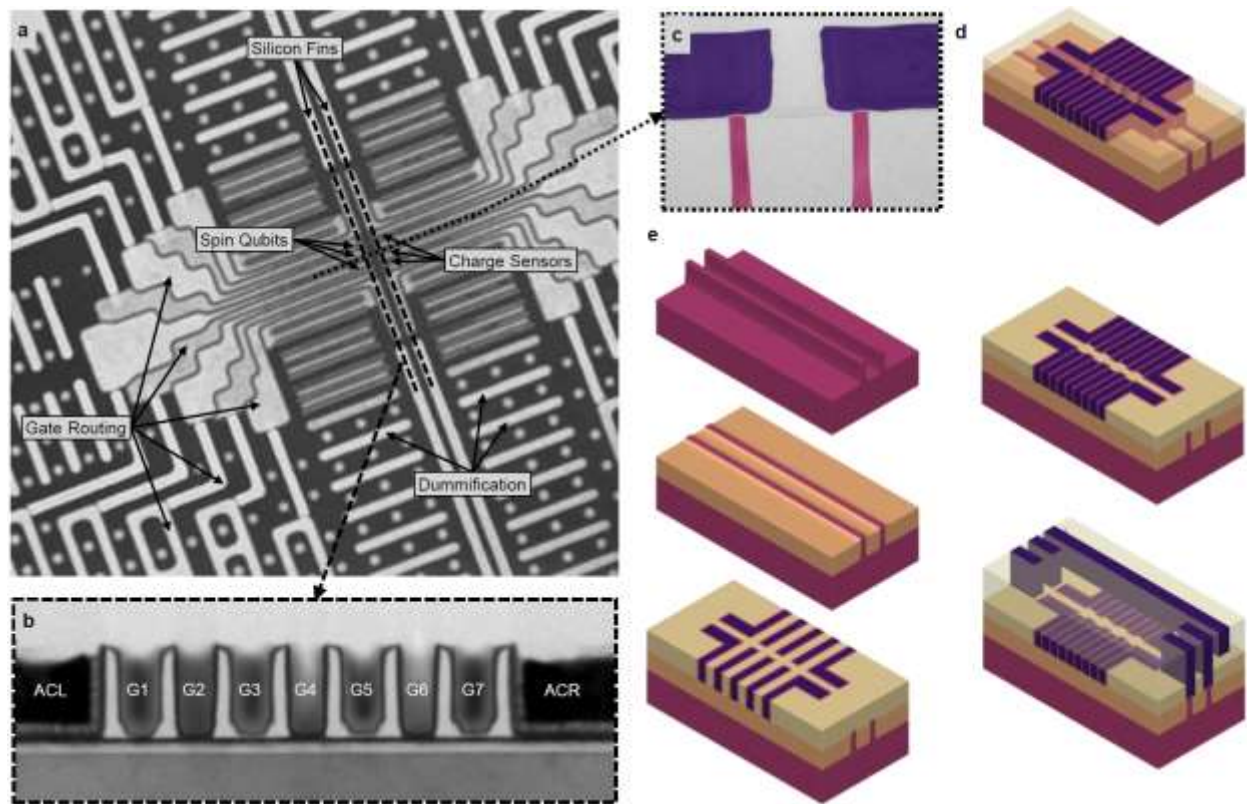


Figure 365: Intel SiGe quantum dots circuit implementation and process quality. Source: [Qubits made by advanced semiconductor manufacturing](#) by A.M.J. Zwerver, Menno Veldhorst, L.M.K. Vandersypen, James Clarke et al, 2021 (23 pages).

But this chip, like many that did follow, was produced to test their manufacturing capacity and their material designs. They were not functional particularly with regards to two-qubit gates. In 2022, Intel did show again some interesting data related to their qubits manufacturing capacity, producing chips with 3 to 55 quantum dots on 300 mm wafers and a >95% production yield, using 193 nm Deep UV immersion photolithography instead of electron beam lithography¹⁴²⁵.

These SiGe qubits have a relaxation time of >1s (T_1), coherence times of >3 ms (T_2) and single qubit gates of >99% (and no published data for two-qubit gates...). These qubits had to be characterized by the DoE Argonne lab in Chicago in its Q-NEXT research center¹⁴²⁶ (Figure 365).

As part of their efforts in manufacturing, they are now using, like CEA-Leti, a cryo-wafer prober provided by Afore and Bluefors, that enables testing entire wafers at 1.6K, significantly accelerating the testing and characterization process (Figure 366, left)¹⁴²⁷.

¹⁴²⁴ See [Intel's quantum efforts tied to next-gen materials applications](#), January 2019 and [Intel's spin on qubits and quantum manufacturability](#), both from Nicole Hemsoth, November 2018 and [Leading the evolution of compute](#), Anne Matsuura, June 2018 (26 slides).

¹⁴²⁵ See [Qubits made by advanced semiconductor manufacturing](#) by A.M.J. Zwerver, Menno Veldhorst, L.M.K. Vandersypen, James Clarke et al, 2021 (23 pages).

¹⁴²⁶ See [Intel to install quantum computing test bed for Q-NEXT](#), April 2022.

¹⁴²⁷ See [Probing single electrons across 300 mm spin qubit wafers](#) by Samuel Neyens, James S. Clarke et al, Intel, July 2023 (15 pages).



Figure 366: how Intel is saving time with a Bluefors/a-Fore cryo-prober. Source: Intel.

QuTech and Intel work well together on these qubits. QuTech got a \$50M investment from Intel in 2015 to explore it. Intel announced in 2018 that it had succeeded in controlling a two-qubit SiMOS processor with single and two quantum gates running Deutsch-Jozsa and Grover algorithms on a very small scale. These silicon-germanium qubits manufactured by Intel were tested by the Vandersypen Laboratory at the University of Delft, part of QuTech¹⁴²⁸. Since 2018, Intel has kept a rather low profile on its silicon qubit advances¹⁴²⁹.

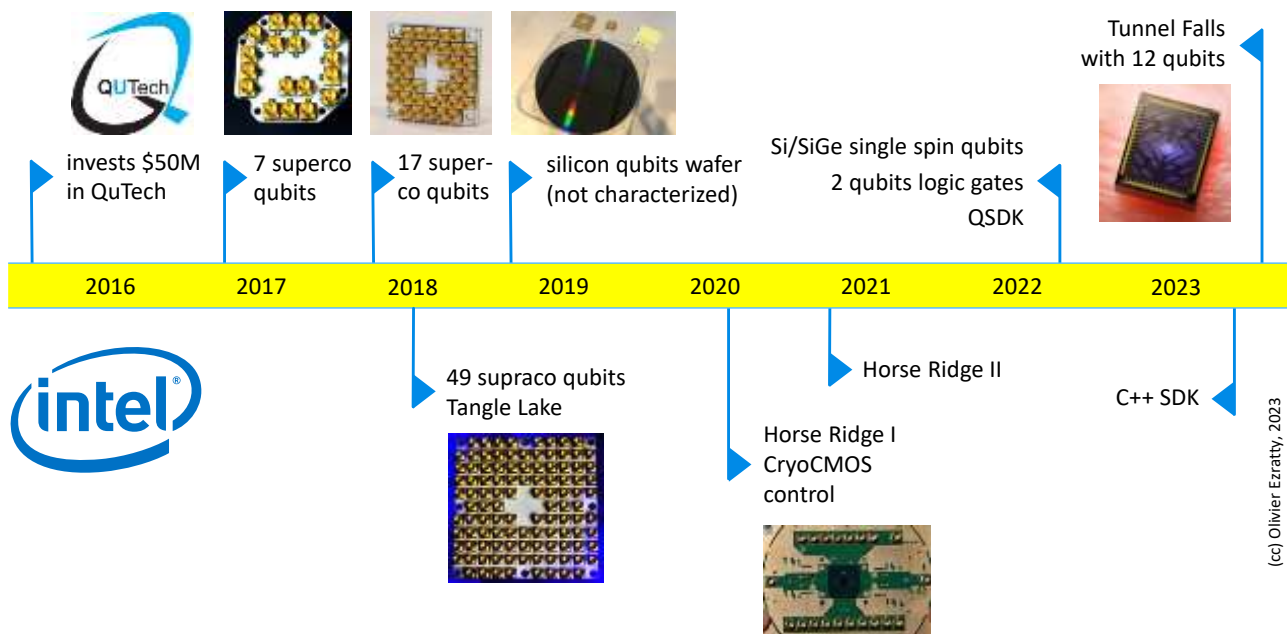


Figure 367: Intel quantum computing timeline. (cc) Olivier Ezratty, 2022-2023.

At the beginning of 2020, Intel announced that it had developed with QuTech the **HorseRidge** cryo-component. It is a CMOS component operating at 4K that is used to generate the microwaves used to drive both superconducting and silicon qubits. A second version was announced in 2021. We cover it in the section dedicated to cryo-CMOS electronics.

In May 2023, Intel and RIKEN announced a research partnership covering classical supercomputing and silicon qubit quantum computing. But it is not clear what they will do respectively in this partnership.

¹⁴²⁸ See [A programmable two-qubit quantum processor in silicon](#) by T F Watson et al, TU Delft, May 2018 (22 pages).

¹⁴²⁹ See [What Intel Is Planning for The Future of Quantum Computing: Hot Qubits, Cold Control Chips, and Rapid Testing](#) by Samuel Moore, August 2020, which provides a rather pedagogical overview of Intel's approach to silicon qubits.

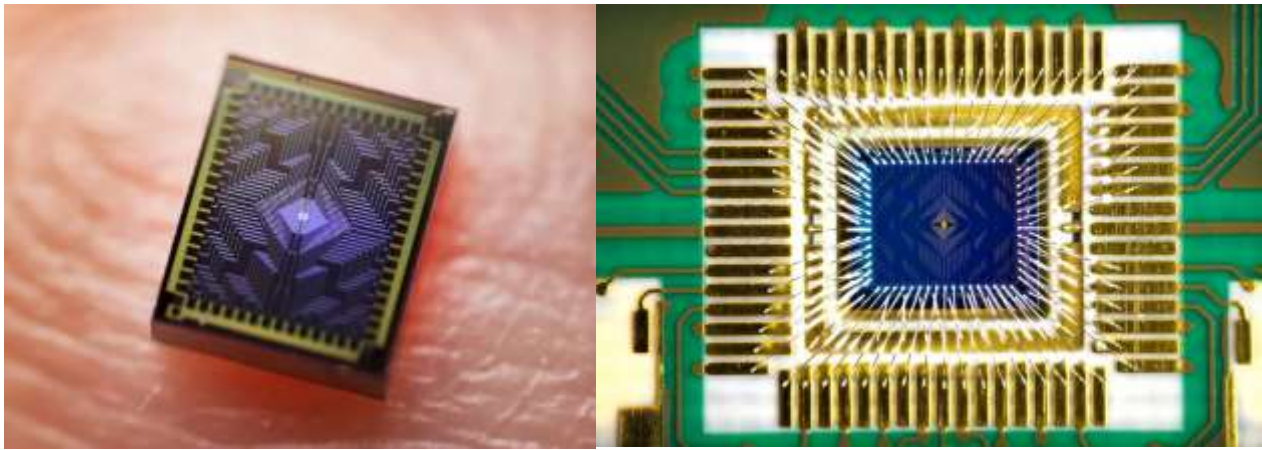


Figure 368: Intel Tunnel Falls 12-qubit chip. Source: Intel. 2023.

In June 2023, Intel presented a 12-qubit prototype chip named Tunnel Falls to be provided to academic partners for testing including the University of Maryland LPS, the DoE Sandia National Laboratories, the University of Rochester and the University of Wisconsin-Madison. It was manufactured on 300 mm wafers at the D1 fab in Hillsboro, Oregon, using EUV lithography from ASML, and with a 95% yield rate. The chip has a size of 50 nm x 50 nm and has 62 control pins (Figure 368).

equal1.labs

equal1.labs (2017, Ireland/USA, 10M€) is creating a charge electron spin qubits chip manufactured in 22 nm FD-SOI technology at GlobalFoundries in Dresden, Germany.

They announced in 2021 a 422 qubits test chip embedded in a full-rack system with its cryogeny, Alice mk1. At this stage, they are just able to inject single electrons in their quantum dots and simulate numerically some one- and two-qubit quantum gates, but not much more¹⁴³⁰.

Their next generation Aquarius is to fit into a desktop packaging, planned for 2022, and is to house one million qubits. They position their systems to run quantum neural networks for imaging applications.

In May 2021, equal1 uncovered a prototype chip operating at 3.7K and including 10 million transistors handling qubits controls and readout with arbitrary waves generation (AWGs), all coupled to an external FPGA, as well as some classical cryogenic memory. There's a caveat with their coherence time being only 150 ns. Equal1 also designs its own cryogenic system.

The company was created by Dirk Leipold, Mike Asker and Bogdan Staszewski from the University of Dublin. Elena Blokhina is their CTO. They expected to raise \$50M by 2022 which has seemingly not happened yet as of this writing in 2023.

diraq

Diraq (2022, Australia, \$3M) is a startup spun out of UNSW created by Andrew S. Dzurak that develops quantum dots electron spin qubits. The company set a goal to build a one billion qubits computer, the largest so far with commercial vendors.

Their first planned steps are to reach 9 and then 256 qubits. The team is already set up with a bunch of scientists and engineers like Arne Laucht, Henry Yang. Andrea Morello from UNSW is also a scientific advisor for the venture. Morello and Dzurak were previously working with Michelle Simmons in her company SQC and they parted away in 2021.

¹⁴³⁰ See [A Single-Electron Injection Device for CMOS Charge Qubits Implemented in 22-nm FD-SOI](#) by Imran Bashir, Elena Blokhina et al, 2020 (4 pages).

The founding team has a good track record in the advancement of quantum dots based qubits with many “firsts” achieved since 2014, including many patented processes (SiMOS - Silicon-Metal-Oxide-Semiconductor qubits, resonators and qubit electrical control, etc).

After the creation of Diraq, some scientific announcements were made through various collaborative research publications, on their qubit initialization fidelities¹⁴³¹, qubit gates fidelities variability¹⁴³², benchmarking¹⁴³³, qubit control^{1434 1435 1436}, direct spin readout with a microwave parametric amplifier^{1437 1438} and error suppression techniques¹⁴³⁹.

In December 2022, Diraq announced some figures of merit for their prototype qubits with 99.96% single qubit gate fidelities and 99% two-qubit gate fidelities, tagged “highest” which may mean many things. Also, with 3 ns one qubit gate speed and 40 ns two qubit gate speed, all operating at 1.5K¹⁴⁴⁰.

Diraq was awarded an AUS \$3M grant from the NSW Quantum Computing Commercialisation Fund (QCCF).



Quobly (2022, France, 19M€), formerly Siquance, is the silicon qubit startup launched in November 2022 by Maud Vinet, Tristan Meunier and François Perruchot out of CEA-Leti and CNRS Institut Néel. Their ambition is to release a 100 physical qubit system by 2026 with some intermediate in between. They seem to work with spin silicon qubits but are also interested in silicon hole spins¹⁴⁴¹.

Their focus is manyfold, with tuning manufacturing processes to ensure the best qubit quality and with an end-to-end system approach, looking at ways to optimize cryogenics and control electronics, including CryoCMOS qubit control chips.

On top of a first round of funding of 19M€ announced in July 2023, they got an EIC Transition grant of 2.5M€ to develop their FD-SOI quantum processor demonstrator using a 4x4 multicore architecture targeting the needs of NISQ applications. With 16 cores sitting on the same chip, they plan to accelerate the execution of variational NISQ algorithms which require running identical circuits a large number of times.

¹⁴³¹ See [Beating the Thermal Limit of Qubit Initialization with a Bayesian Maxwell's Demon](#) by Mark A. I. Johnson, Kohei M. Itoh, Andrew S. Dzurak, Andrea Morello et al, PRX, October 2022 (15 pages).

¹⁴³² See [Bounds to electron spin qubit variability for scalable CMOS architectures](#) by Jesús D. Cifuentes, Andrew S. Dzurak et al, March 2023 (20 pages).

¹⁴³³ See [Stability of high-fidelity two-qubit operations in silicon](#) by Tuomo Tantt, Kohei M. Itoh, Robin Blume-Kohout, Andrea Morello, Andrew S. Dzurak, March 2023 (13 pages).

¹⁴³⁴ See [On-demand electrical control of spin qubits](#) by Will Gilbert, Kohei M. Itoh, Andrea Morello, Andrew S. Dzurak et al, Nature Nanotechnology, January 2023 (21 pages).

¹⁴³⁵ See [Implementation of an advanced dressing protocol for global qubit control in silicon](#) by I. Hansen, Kohei M. Itoh, Andrew S. Dzurak et al, Applied Physics Reviews, September 2022 (9 pages).

¹⁴³⁶ See [Implementation of the SMART protocol for global qubit control in silicon](#) by Ingvild Hansen, Andrew S. Dzurak et al, August-September 2021 (9 pages).

¹⁴³⁷ See [Direct detection of spin resonance with a microwave parametric amplifier](#) by Wyatt Vine, Andrea Morello et al, November 2022 (28 pages).

¹⁴³⁸ See [Gate-based spin readout of hole quantum dots with site-dependent g-factors](#) by Angus Russell, Andrew S. Dzurak, Alessandro Rossi et al, June 2022-April 2023 (16 pages).

¹⁴³⁹ See [Real-time feedback protocols for optimizing fault-tolerant two-qubit gate fidelities in a silicon spin system](#) by Nard Dumoulin Stuyck, Andrew S. Dzurak et al, September 2023 (6 pages).

¹⁴⁴⁰ See [High-fidelity operation and algorithmic initialisation of spin qubits above one kelvin](#) by Jonathan Y. Huang, Natalia Ares, Andrea Morello Andrew S. Dzurak et al, August 2023 (29 pages).

¹⁴⁴¹ See [Strong coupling between a photon and a hole spin in silicon](#) by Cécile X. Yu, Maud Vinet et al, June 2022-May 2023 (26 pages).



SemiQon (2023, Finland, 2.5M€) is a newcomer in the silicon qubit arena that spun out of VTT with Himadri Majumdar (CEO), Mika Prunnila (Chief Research Officer), Janne Lehtinen (CSO) and Markku Kainlauri (Fabrication lead).

The company is based at the Micronova research facility for nano- and microtechnology located in Espoo Finland. They are shooting for a million qubits with ultra-low charge noise quantum dots operating at 1K and driven by house made cryo-CMOS control electronic circuits built on the same chip as the quantum dots. Their first prototype wafer presented in April 2023 contains 32 QPUs with 48 qubits and its CMOS embedded multiplexers and amplifiers control electronics (Figure 369). In July 2023, the company got a 2.5M€ funding from the EIC as part of the SCALLOP project which deals like the company with creating quantum dots qubits integrated by cryo-CMOS for their control. This funding is shared with Qblox as part of this project.

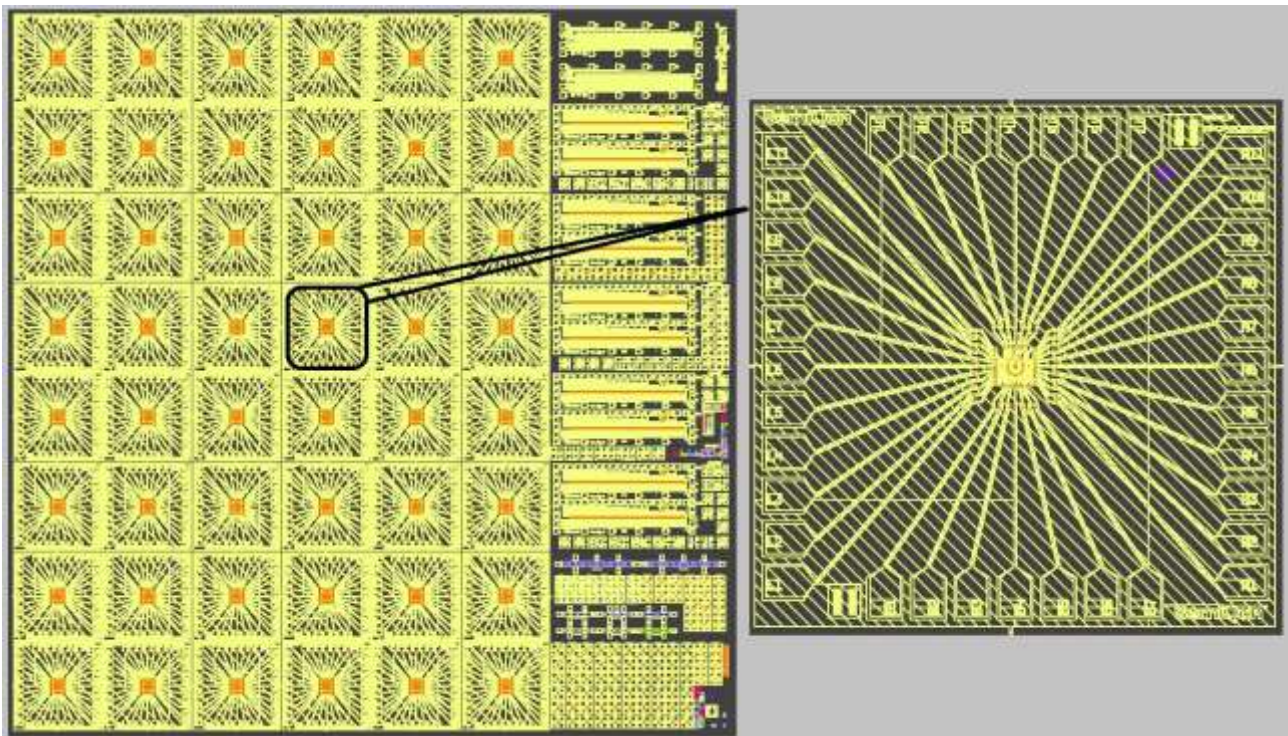


Figure 369: SemiQ first chip prototype sampled in April 2023. Each square is a quantum dot qubit. The circuits on the right are the cryo-CMOS control signals multiplexer and amplifiers. Source: SemiQon web site. 2023.



EeroQ Quantum Hardware (2016, USA, \$7.5M) develops an exotic quantum processor using trapped (and more or less flying/moving) electrons on superfluid helium (“eHe”)¹⁴⁴².

The startup was launched by Johannes Pollanen from the University of Michigan (CSO), Dave Ferguson, Nick Farina (CEO) and Faye Wattleton (EVP)¹⁴⁴³. In May 2021, Steve Lyon, a Princeton University Professor, joined them as their CTO. The company got some undisclosed NSF and private funding from VCapital in 2022.

¹⁴⁴² See the well-crafted [Electron-on-helium qubit](#) page on Wikipedia.

¹⁴⁴³ See [Helium surface fluctuations investigated with superconducting coplanar waveguide resonator](#) by N.R. Beysengulov, Johannes. Pollanen et al, 2022 (10 pages). It deals with a superconducting resonator and not with a qubit.

The idea of using electron floating in vacuum over superfluid helium came out in 1999 at the Michigan State University and Bell Labs^{1444 1445}. It consisted in creating an analog quantum simulator using collective sets of electrons excited at Rydberg energy levels. Johannes Pollanen's conducted research in superconducting and two-dimensional qubits (silicon, graphene) in that same university¹⁴⁴⁶. The 1999 idea was then extended by Steve Lyon between 2003 and 2006 to use the spins of individual electron with quantum coherence exceeding 10 seconds, and with circuit designs resembling ion traps and using shuttling electrons to implement two-qubit gates¹⁴⁴⁷.

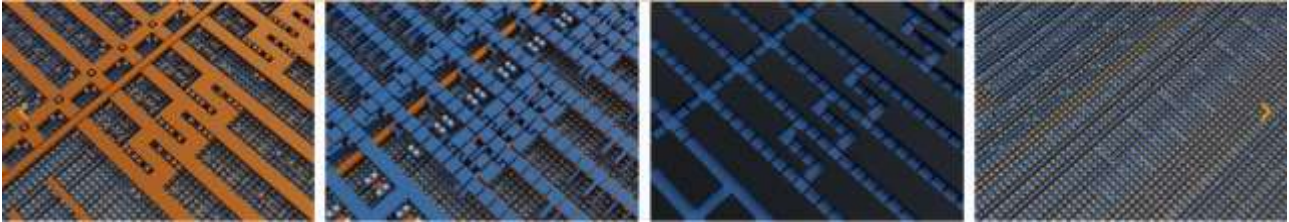


Figure 370: different zoom level on the EeroQ chip showing the CMOS electrodes design to control the placement, spin and individual of individual shuttling electrons. Source: [Building a quantum computer in reverse](#) by Nick Farina, July 2023.

In July 2023, EeroQ announced the “*tape-out*” of its new Wonder Lake chip at a US semiconductor foundry¹⁴⁴⁸. It is probably Global Foundries, which is nearly the only commercial company in the USA able to manufacture such custom CMOS components.

Tape out means the chip was sent for fabrication and production, with probably a couple months of wait as is custom in CMOS manufacturing. This chip contains 2,432 qubits, requiring only around 30 control lines (Figure 370). In that chip, electrons will hover at approximately 10 nm above the helium superfluid surface, being trapped by control voltages from electrodes located beneath the helium on the CMOS circuit. When available, EeroQ will test two-qubit gates, using magnetic dipole-dipole interaction¹⁴⁴⁹. Their plans are to reach >10s qubit coherence times (T_1), have high qubit connectivity, use electrons mobility on the helium surface and obtain 99.9% two-qubit gate fidelities. They plan to scale up to 10,000 qubits using a monolithic chip.

¹⁴⁴⁴ See [Quantum Computing with Electrons Floating on Liquid Helium](#) by P. M. Platzman and M. I. Dykman, Science, June 1999 (3 pages).

¹⁴⁴⁵ See [Quantum computing using floating electrons on cryogenic substrates: Potential And Challenges](#) by Ash Jennings et al, RIKEN, October 2023 (25 pages).

¹⁴⁴⁶ See [Integrating superfluids with superconducting qubit systems](#) by Johannes Pollanen, Kater Murch et al, Michigan State University, Washington University in Saint Louis, 2019 (11 pages).

¹⁴⁴⁷ See [Spin-based quantum computing using electrons on liquid helium](#) by Steve Lyon, PRA, 2003- 2006 (12 pages).

¹⁴⁴⁸ See [Building a quantum computer in reverse](#) by Nick Farina, July 2023.

¹⁴⁴⁹ See [Coulomb interaction-driven entanglement of electrons on helium](#) by Niyaz R. Beysengulov, Johannes Pollanen et al, October 2023 (19 pages).

While EeroQ is the only commercial venture in the spin on helium qubit realm, academic laboratories are investigating the path like Michigan State University (where EeroQ's ideas were born), DoE Argonne National Laboratory, University of Notre Dame, Princeton University (Steve Lyon's origin lab)¹⁴⁵⁰ and RIKEN et al¹⁴⁵¹. Others like the University of Chicago, the DoE Lawrence Berkeley National Laboratory, the MIT and Stanford are investigating electron based qubits on solid neon using niobium on silicon circuitry at 10 mK as shown in Figure 371, with a record 100 μ s coherence time.

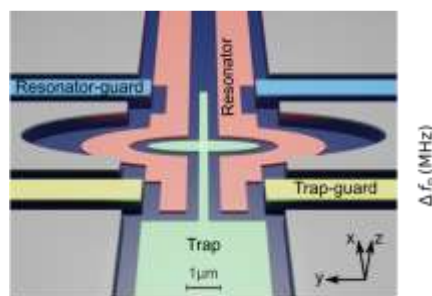


Figure 371: electrons on neon. Source: [Electron charge qubits on solid neon with 0.1 millisecond coherence time](#) by Xianjing Zhou, David Schuster et al, Nature, October 2022-October 2023 (9 pages).

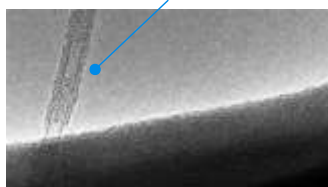
C12

C12 Quantum Electronics (2020, France, \$10M) was launched by Matthieu Desjardins and his twin brother Pierre. It is a project originating from the LPENS at ENS Paris and 15 years of research from Takis Kontos in this lab, with contributions from Jérémie Vienot at Institut Néel Grenoble.

french startup created by Matthieu and Pierre Desjardins

with the help from Taki Kontos (LPENS)
electron spins qubits trapped in carbon nanotubes
expecting 99.9% two-qubit gate fidelities.

qubits are based on a **single electron spin** isolated in a 2 nm diameter carbon nanotube



multiple spins can be coupled for **2-qubit gate** to the same resonator enabling all-to-all connectivity between qubit

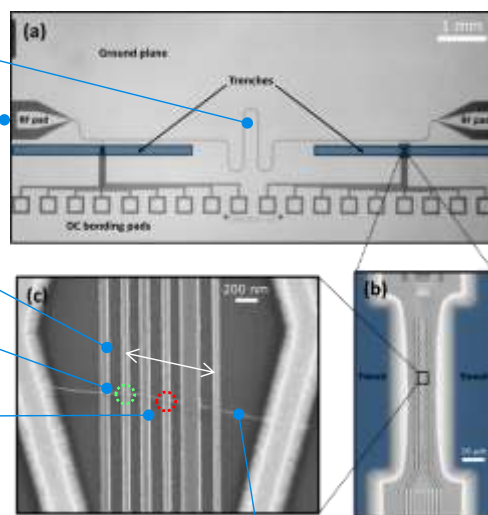
spin qubit manipulated and read-out with a **7 GHz microwave** superconducting resonator

electrons move in **one direction** it can be trapped in a **quantum dot** by defining an electrostatic potential with underneath control electrodes.

coupling to the resonator can be switched on and off by freezing the motion of electron in one of the two quantum dots.



quantum emulator and qubit simulators announced on OVHcloud in 2023



decoherence is limited with using **zero spin isotope C₁₂** in nanotubes, suspending the tube above the substrate and removing the oxide

Figure 372: C12 Quantum Electronics carbon nanotubes and how it is controlled. Source: C12. 2023.

Their goal is to use carbon nanotubes to trap electrons used in electron spin qubits and build the surrounding control circuitry on silicon substrate (Figure 372).

This technology can improve qubits isolation and coherence time by a factor of 100, up to one second, while keeping a strong coupling for fast qubit manipulation. The qubits are controlled by spin-photon coupling in the microwave regime, using frequency multiplexing to avoid crosstalk.

Qubit readout uses spin to charge coupling with a single charge coupling with 8 qubits¹⁴⁵². The challenges sit in materials, design, control electronics, connectivity, topology and error correction codes.

¹⁴⁵⁰ See [Spin dynamics in quantum dots on liquid helium](#) by M. I. Dykman et al, December 2022 (11 pages).

¹⁴⁵¹ See [Hybrid Rydberg-spin qubit of electrons on helium](#) by Erika Kawakami et al, RIKEN, DLR, QunaSys and OIST, March 2023 (27 pages).

¹⁴⁵² A related technique is described in [Charge Detection in an Array of CMOS Quantum Dots](#) by Emmanuel Chanrion, Pierre-André Mortemousque, Louis Hutin, Silvano de Franceschi, Franck Balestro, Maud Vinet, Tristan Meunier, Matias Urdampilleta et al, Grenoble CEA-Leti, CNRS Institut Néel and UGA, August 2020 (8 pages).

The nanotubes are mechanically integrated into the circuit at the end of the manufacturing process¹⁴⁵³. The carbon nanotubes are grown by C12 using a CVD process (chemical vapor deposition). The connection between two qubits is based on microwave cavities, exploiting CQED (Cavity Quantum Electrodynamics). Of course, there are still many challenges to develop this kind of qubit but it is worth exploring. It could even have some use cases beyond computing, in quantum sensing. In March 2022, C12 announced it was starting a manufacturing partnership with CEA-Leti. These will provide their quantum chips on silicon on 200 mm wafers.

These will contain the superconducting electronics controlling the state of their carbon nanotubes that will be positioned on the chips. In October 2023, the company opened its new headquarter in Paris with a small fab handling most processes from building, characterizing and post-selecting nanotubes with the right chirality, and their underlying silicon handling chip, plus two cryostats for testing (Figure 373).



Figure 373: C12's new testing room with two cryostats, a typical setup for many quantum computing startup nowadays. They have two other floors for their carbon nanotube and related circuits manufacturing tooling. (cc) Photo: Olivier Ezratty, 2023.

On the software engineering side, Eviden works with C12 to develop its quantum compiler, to create digital simulation models of its qubits and for co-designing quantum gates. It was announced as Calisto on OVHcloud in June 2023.

ARCHER

Archer Materials (2017, Australia) develops quantum computing and sensing technologies based on carbon nanospheres that operate at room temperature¹⁴⁵⁴.

The company was cofounded by Mohammad Choucair who invented their ¹²CQ chip design and by Martin Fuechsle who contributed to the development of the single electron transistor and worked at UNSW with Michelle Simmons¹⁴⁵⁵. 12 is not a number of qubits but the isotopic weight of the zero spin carbon atoms used in these nanospheres trapping some electron and its spin. Electrons are delocalized around the nanosphere and not setting inside it, contrarily to the C12 Quantum Electronics electrons that are stored inside nanotubes.

They built their first three-nanospheres chip in 2019, in red, in Figure 374, the 50 nm nanospheres being surrounded by driving electrodes, but without any visible coupling between these qubits. In February 2021, Archer announced that they had achieved “electronic transport” in a single qubit at room temperature in its ¹²CQ quantum computing qubit processor chip.

¹⁴⁵³ It is described in [Nanoassembly technique of carbon nanotubes for hybrid circuit-QED](#) by Tino Cubaynes, Matthieu Desjardin, Audrey Cottet, Taki Kontos et al, September 2021 (6 pages).

¹⁴⁵⁴ See [Archer Materials granted trading halt ahead of quantum computing chip agreement](#) by Quantum Analyst, 2020 and [Room temperature manipulation of long lifetime spins in metallic-like carbon nanospheres](#) by Bálint Náfrádi, Mohammad Choucair et al, 2016 (32 pages) which describes in detail this technique of electron spin trapping in a 35 nm wide carbon nanosphere. In April 2021, Archer Materials announced it would sell off all its mineral traditional business to iTech Minerals, to focus on quantum technologies.

¹⁴⁵⁵ Their ¹²CQ processor is patented in the USA, Japan and Europe (since February 2022). See [WO2017091870 - A QUANTUM ELECTRONIC DEVICE](#) (55 pages). The patent dates from 2017 and is very sketchy with regards to single and multiple qubit gates operations. We can still learn they use SiO₂ isolation layers of 200 to 400 nm between control electrodes and nanospheres. Conductors can use unspecified graphene structures. The spin stability in their device is amazingly small, at around 115 ns, not sufficient to run several quantum gates.

It however does not mean that it is a fully functional qubit that can be operated with quantum gates¹⁴⁵⁶. In July 2021, they announced that they were embedding some parts of their qubits control electronics in the qubit chip, that records the Continuous Wave Electron Spin Resonance (cwESR) signals generated by a superconducting on-chip resonator (Figure 374, Figure 375).

In February 2022, through a collaboration with EPFL, they demonstrated the use of a single-chip integrated electron spin resonance (ESR, seemingly at 9.4 GHz according to their patent) detector based on high electron mobility transistor (HEMT) to detect and characterize their qubit at room temperature¹⁴⁵⁷.



Figure 374: Archer qubits.
Source: Archer.

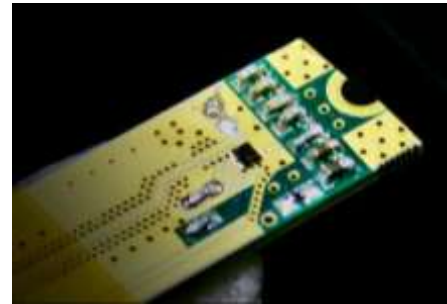


Figure 375: Archer-EPFL spin-resonance circuit. Source: Archer.

The resonator was manufactured by OMMIC (France), a fab company specialized in III-V wafer processes. This technology is as mature as superconducting qubits were in the mid 1990's when it became possible to create the first qubits.

What would be needed are some tomographies for their qubit state, showing real superposition, and a full cycle of reset, flip and phase single qubit quantum gates and qubit readout, then implement this with a couple entangled qubits. One can wonder how they will drive their qubits with microwave pulses at room temperature given the ambient thermal noise will be larger than the pulse themselves. The road ahead is still quite long for them. Based on this 2022 milestone, the company CEO forecasted “*mobile quantum computing*” use-cases. That is quite an oversold proposal. It deserves scrutiny, if not strong skepticism.

In December 2020, Archer launched a partnership with **Max Kelsen**, another Australian company, specialized in QML software development. Max Kelsen and Archer will develop QML algorithms based on Qiskit, eyeing a future execution on Archer's processor. They also announce that GlobalFoundries would become the manufacturer of their 12Q qubit chip. The company is also developing graphene-based biosensor chip aka “lab on chip”. This is a more short-term and credible product proposal than their room temperature spin qubits.

In June 2023, the company announced that their chip was operating not only at room temperature but also in the air, without requiring vacuum conditions.

So, we have nanotubes and nanospheres. How about nanoribbons of carbon? It is investigated at the research stage but there's no startup in the radar¹⁴⁵⁸!



Qpi (2019, India) is a QML software and hardware development company, providing the QpiAI library. They are working on creating the ASGP (AI System Generating Processor), a hybrid classical-quantum compute chip.

Practically speaking, they planned first to introduce a qubit control chip in September 2021 operating at 4K and produced in a 22 nm TSMC CMOS process¹⁴⁵⁹.

¹⁴⁵⁶ Their electron spin T1/T2 is very low, at 175 ns at 27°C. They also said they tested microwave pulses from 4 GHz to 420 GHz. Seen in their video [Archer's Quantum Computing Q&A Webinar](#), April 2020.

¹⁴⁵⁷ See [Quantum information detected using mobile compatible chip technology](#), Archer Materials, February 2022.

¹⁴⁵⁸ See [Ultra-Fast All-Electrical Universal Nano-Qubits](#) by David T. S. Perkins and Aires Ferreira, University of York, July 2023 (16 pages).

¹⁴⁵⁹ Source: [QpiAI in Partnership With IISc Launches Joint Certification for AI and Quantum Computing to Upskill Enterprises, Schools and Colleges](#), March 2021.

This chip was to control the microwaves sent to both superconducting and electron spin qubits processors. They later announced a room temperature control chip named QpiAISense. They are now developing a full-stack classical and silicon qubit solution in a single package. It is supposed to contain a classical chip for optimization (ASGP for “AI System Generating Processor”), their microwaves cryogenic control chip and a silicon spin-qubit based QPU (quantum processing unit).

They signed a partnership with QuantrolOx in April 2022 to develop their QPU and set-up a lab in Finland for that purpose, where part of QuantrolOx team is installed. Their goal is to start with releasing a functional 25 qubits system. They plan later to create a one million electron spin quantum dots qubits processor. Overselling seems not to be an issue for them. QpiAI Tech is a subsidiary selling software services for quantum computing and AI to transportation, materials, manufacturing, finance, and pharmaceutical business.

ARQUE

ARQUE (Germany) is a spin-off of JARA-Institute for Quantum Information of RWTH Aachen University and Research Center Jülich created by Markus Beckers (CEO), Hendrik Bluhm (CSO), Jan Klos (CTO) et al. Their claim is typical, about creating scalable quantum computers.

Their roadmap includes 2-4, 50, 200, 10,000 then 1 million qubits. They plan to use electron shuttling to connect SiGe spin qubits and to have 99.9% gate fidelities¹⁴⁶⁰.

In August 2023, ARQUE announced that it was relying on Infineon to manufacture its qubit chips. It makes sense since they are both German. The other option would have been to rely on GlobalFoundries which also has some manufacturing capabilities in Germany.

NV centers qubits

This qubit technology is based on the control of electron spins trapped in artificial defects of crystalline carbon structures in which one carbon atom is replaced by one nitrogen atom and another carbon atom is replaced by a void, gap or cavity. Practically speaking, it is a bit more complex since the qubits themselves are stored in nuclear spins of surrounding carbon and nitrogen atoms¹⁴⁶¹.

History

Defects in diamonds have been studied since 1930 with the examination of infrared absorption. This made it possible to distinguish two categories of diamonds: type I with an absorption band of 8 μm in the infrared and type II without this band. The defects explain the color of diamond gems.

It was not until 1959 that these impurities were found to be related to the presence of nitrogen, at 7.8 μm and that nitrogen atoms were well isolated in the diamond crystal. In 1975, it was discovered that some heat treatment could control the diffusion of nitrogen atoms in the diamond. These nitrogen centers explain the diamond color. It has four types: one nitrogen atom isolated in a gap, two nitrogen atoms, three nitrogen atoms surrounding a gap and four nitrogen atoms.

It is the first type that is interesting for both quantum computing and quantum sensing. We can visualize these defects with a confocal microscope (having a very shallow depth of field) by illuminating them with a green laser beam that will generate some red light.

These NV centers diamonds are slightly pink. These properties make it possible to generate single-photon sources thanks to the isolation of a NV center. Nitrogen-rich artificial diamonds are used to manufacture these NV centers. Gaps are generated with irradiation.

¹⁴⁶⁰ See [The SpinBus Architecture: Scaling Spin Qubits with Electron Shuttling](#) by Matthias Künne et al, JARA and ARQUE, June 2023 (15 pages).

¹⁴⁶¹ See the review paper [Diamond Integrated Quantum Photonics: A Review](#) by Prasoona K. Shandilya et al, July 2022 (31 pages) which provides a good 360° overview of NV centers, and not only for quantum computing.

Vacuum annealing at about 800°C-900°C moves the vacancies next to the nitrogen atoms in the crystal structure¹⁴⁶² (Figure 376). This is explained by nitrogen atoms being as large as carbon atoms. The gap creates a small bar of electrons that serve as a virtual magnet via their spin.

Diamonds can also be produced at NV centers with vacuum deposition of hydrogen and methane (CVD, for Chemical Vapor Deposition) to create a perfect diamond crystal structure and then with ion implantation with nitrogen ion beams¹⁴⁶³ (Figure 377).

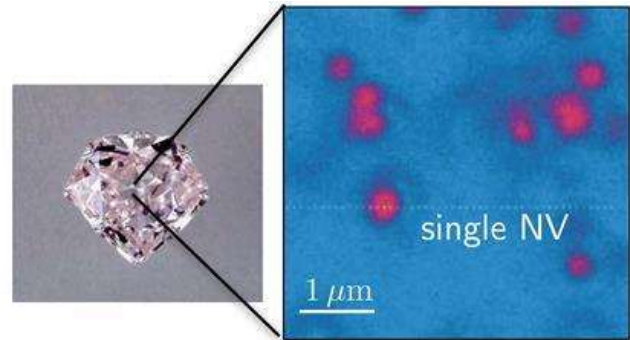


Figure 376: how NV center cavities look in real diamonds. Source: TBD.

The carbon structure surrounding a NV center protects the cavity area well. The state of the gap is unstable and quantum. It is controlled by lasers and microwaves. The qubit state readout is performed using a laser excitation to measure fluorescent brightness.

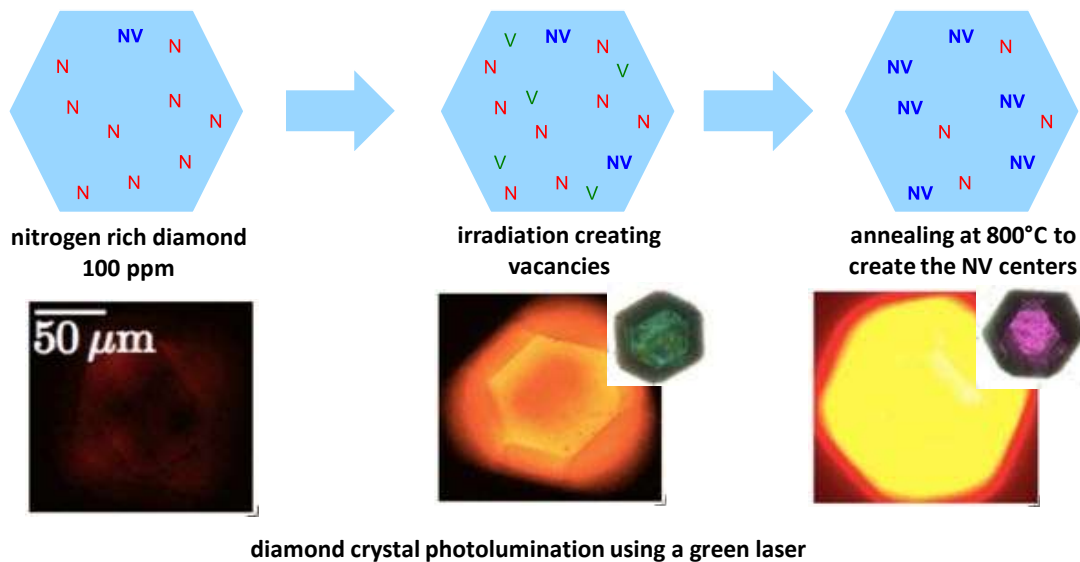


Figure 377: how are nitrogen vacancies created.

Source: [NV Diamond Centers from Material to Applications](#) by Jean-François Roch, 2015 (52 slides).

Science

The free electron from the cavity is coupled to another one from the nitrogen atom near the cavity, as shown in Figure 378. The cavity includes two other pairs of electrons from the nitrogen atom in the cavity, with a total zero spin. The process involves controlling the collective spin of these two free electrons as well as the spin of the nitrogen nucleus of the cavity and possibly of neighboring ¹³C carbon atoms nuclei¹⁴⁶⁴.

¹⁴⁶² See [NV Diamond Centers from Material to Applications](#) by Jean-François Roch, 2015 (52 slides) for an historical view of NV centers and a thesis that describes the different techniques of NV centers creation in [Engineering of NV color centers in diamond for their applications in quantum information and magnetometry](#), Margarita Lesik, 2015 (139 pages).

¹⁴⁶³ See a description of this manufacturing process in [CVD diamond single crystals with NV centres: a review of material synthesis and technology for quantum sensing applications](#) by Jocelyn Achard, Vincent Jacques and Alexandre Tallaire, 2019 (41 pages).

¹⁴⁶⁴ Approximately 1.1% of the carbon atoms in diamond are of the ¹³C isotope. The most common isotope is ¹²C. ¹⁴C is present in trace amounts and is used to date carbonaceous objects due to its half-life of 5,730 years. See [Coherent control of an NV- center with one adjacent ¹³C](#) by Burkhard Scharfenberger et al, 2014 (24 pages).

The cumulative spin of the two electrons of the cavity is 0, 1 or -1 because it adds the spins of two electrons that are either $\frac{1}{2}$ or $-\frac{1}{2}$. These electron spins are controlled by a combination of microwave and magnetic field.

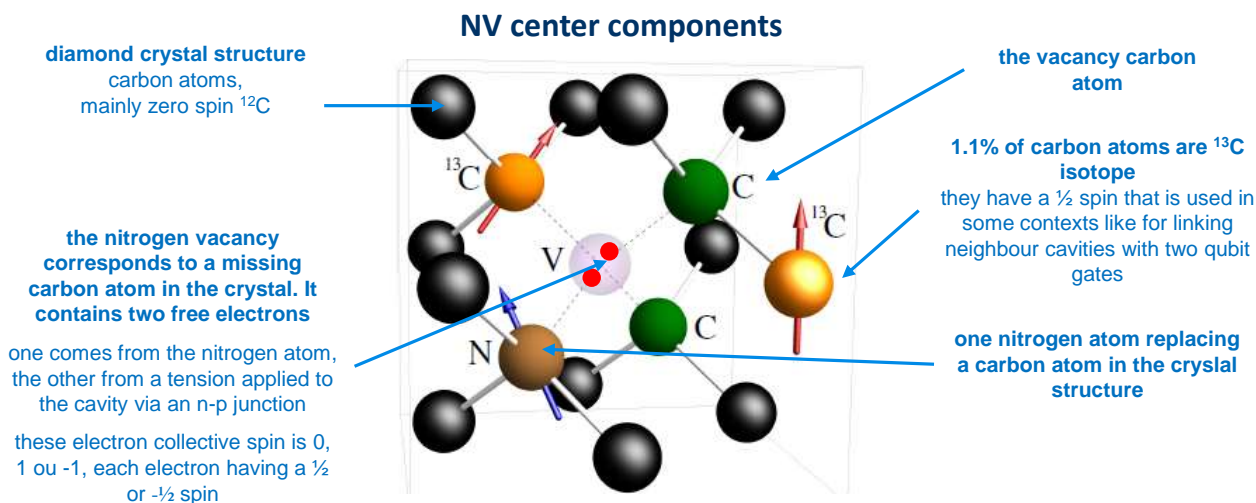


Figure 378: the nitrogen vacancy contains two free electrons with similar or opposite spin which store one qubit of information. The nuclear spins from surrounding ^{13}C are also used to store each one qubit of information, in relation with the cavity spins qubit.
(cc) Olivier Ezratty, 2021. Image source: [The nitrogen-vacancy colour centre in diamond](#) by Marcus W. Doherty, Jörg Wrachtrup et al, February 2013 (101 pages).

Commonly used NV centers are called NV^- because of the addition of an external electron into the cavity. The cavity has 6 electrons, three from the surrounding carbons, two from the nitrogen valence shell and one captured from the bulk. There are other variations like vacancies without this captured electron (NV^0), which are less optically active than the NV^- or positively charges NV^{+1} and NV^{+2} that are optically inactive. For these reasons, they are not commonly used.

Figure 379 contains a diagram that describes what a NV center can look like in practice considering that there are many different implementations, knowing that NV centers are used not only for computing but, in a dominant manner, in quantum sensing as well as for the creation of individual photon sources used in quantum communications and cryptography. NV centers can be integrated in circuits fabricated on an SOI silicon wafer with a layer of SiO_2 insulator. It is then covered with a matrix Fresnel lens, used to focus a control and readout laser¹⁴⁶⁵. It is frequently associated with other photonics components when the NV center spins are used to generate photons for quantum communications¹⁴⁶⁶.

Figure 380 shows a diagram explaining how these rather complex qubits operate with the various energy levels and transitions of the cavity and its free electrons using microwaves and green photons. The vertical arrows represent useful energy transitions¹⁴⁶⁷. This is applicable to the NV^- species. The vacancy qubit state is controlled with 2.87 GHz microwaves that change the spin state of the vacancy electrons and switches the vacancy state between $|0\rangle$ and $|1\rangle$.

The degeneracy of the spins 1 and -1 at the ^3A level (meaning: same energy level for different quantum states) can be lifted by exposing the qubit to a static magnetic field. Other techniques are used to change the qubit state of the surrounding ^{13}C and ^{14}N nucleus spins.

¹⁴⁶⁵ See [Spin Readout Techniques of the Nitrogen-Vacancy Center in Diamond](#) by David Hoper et al, 2018 (30 pages).

¹⁴⁶⁶ See [Hybrid Quantum Nanophotonics: Interfacing Color Center in Nanodiamonds with Si3N4-Photonics](#) by Alexander Kubanek et al, July 2022 (55 pages) that describes such hybrid nanophotonic circuits.

¹⁴⁶⁷ See the excellent review paper [Quantum computer based on color centers in diamond](#) by Sebastien Pezzagna and Jan Meijer, May 2020 (17 pages).

NV center implementation and controls

microlens focusing a laser beam for qubits control and readout in the cavity

the lens base contains light guide that are one fourth micron large

images source: Spin Readout Techniques of the Nitrogen-Vacancy Center in Diamond par David Hoper & Al, 2018 (30 pages).

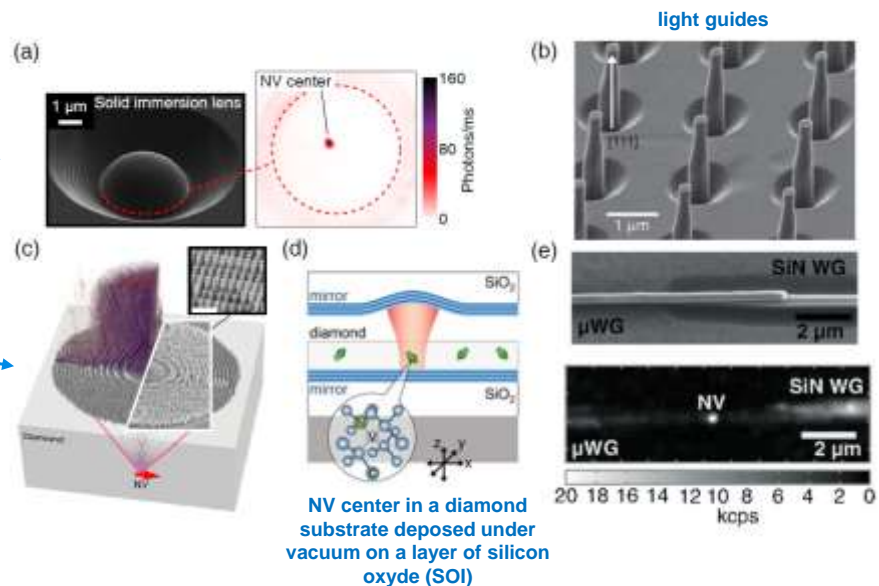


Figure 379: examples of NV centers implementation and controls to guide laser light on the cavities.
Source: [Spin Readout Techniques of the Nitrogen-Vacancy Center in Diamond](#) by David Hoper et al, 2018 (30 pages).

The vacancy qubit readout uses an incoming green photon, usually at 532 nm. It results in an excitation to a state with energy higher than the triplet excited state 3E . Then, the electron relaxes to the 3E state by transmitting part of its energy to atomic vibrations also known as phonons. Subsequently, the relaxation might follow two different paths:

- Back directly to the 3A state by emitting a 637 nm photon (red light).
- Through a channel involving a non-radiative transition from the 3E state to the 1E state assisted by phonons, a radiative transition from the singlet state 1E to the singlet state 1A , which emit an infrared 1042 nm photon and a relaxation back to the 3A state. When following this relaxation path, the final spin state is always zero, regardless of the initial value of the spin.

The probability to follow one or the other relaxation path depends on the spin state. For zero spin state, the first relaxation channel has the highest probability, whereas for ± 1 spin state, the second relaxation channel has the highest probability. As the probability of following one of the two paths is never zero regardless to the spin state, this results in an error in the assignment of the spin state, and therefore generates some spin state readout noise.

As shown in Figure 380, the $|0\rangle$ and $|1\rangle$ qubit states can correspond to null/non null spin cavities at the levels 3A or 3E . The single qubit gates are then generated with microwave pulses at either 2.87 GHz or 1.42 GHz, generating Rabi oscillations in the NV center cavity. Using 3A levels favors long coherence times which is useful to build quantum memories and quantum sensors while using 3E levels enables fast readouts thanks to a better fluorescence differentiation. It is favored in some quantum sensing setups.

NV centers qubits operate theoretically at room temperature¹⁴⁶⁸. Recent experiments have reached a $400 \mu\text{s } T_1$ at ambient temperature¹⁴⁶⁹.

¹⁴⁶⁸ See [A programmable two-qubit solid-state quantum processor under ambient conditions](#) by Yang Wu of Hefei's USTC in China, 2018 (5 pages). He describes an NV center managing two qubits at ambient temperature exploiting the cavity electron spin and the associated nitrogen atom nucleus spin. See also the review paper [Quantum information processing with nitrogen-vacancy centers in diamond](#) by Gang-Qin Liu et al, 2018 (15 pages).

¹⁴⁶⁹ See [Success in mass production technology for ultra-high-purity 2-inch diamond wafer; expected to spur realization of quantum computing](#), August 2022 and [Long spin coherence times of nitrogen vacancy centers in milled nanodiamonds](#) by B. D. Wood et al, PRB, May 2022 (11 pages).

But it seems however that good conditions of operations for managing various transitions, including driving two-qubit gates, are requiring temperatures of about 1K to 4K¹⁴⁷⁰.

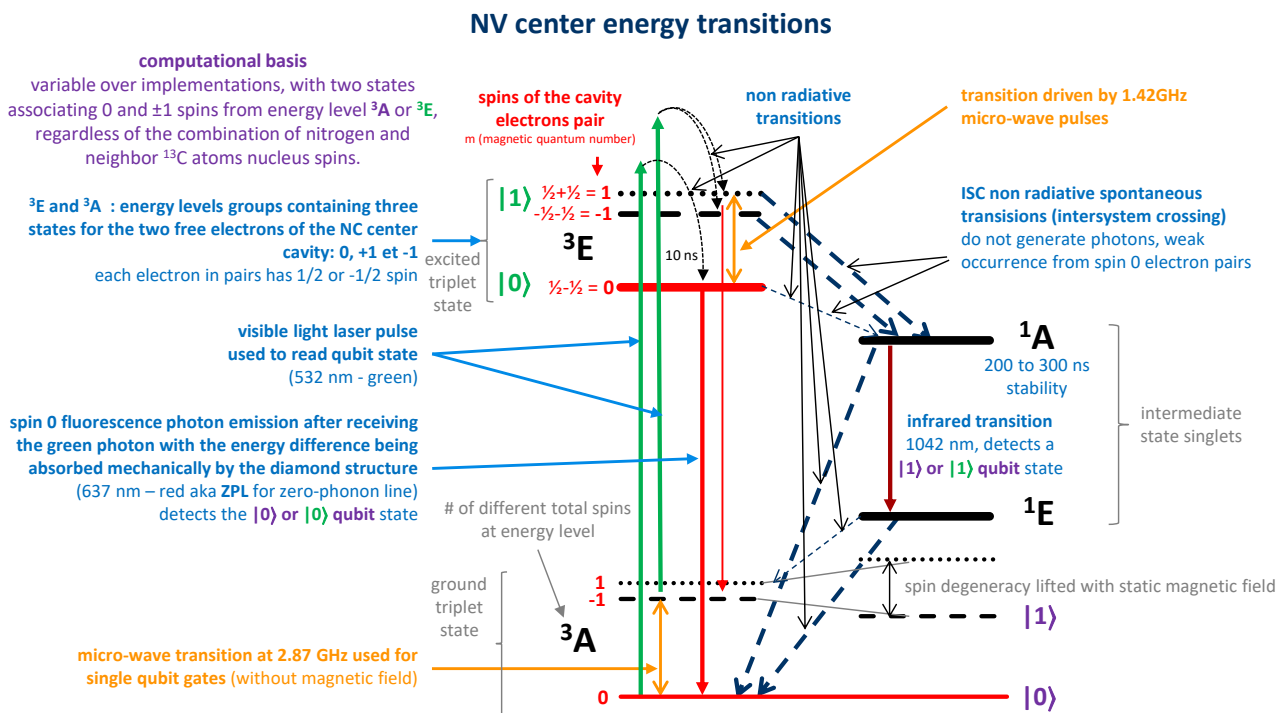


Figure 380: energy transitions in an NV center. (cc) compilation by Olivier Ezratty, 2022-2023.

NV centers have a relatively low DWF of 3%. This Debye-Waller factor which is measured by the ratio between the ZPL (zero-phonon lines) red emission and the total ZPL plus the phonon sideband emission (PSB). The ZPL is the sharp zero-phonon lines of luminescence of NV center in the visible spectrum that is of interest (Figure 381). The phonon sideband is a thermal effect that is problematic¹⁴⁷¹. Also, the DWF gets improved with low operating temperatures. This reduces qubit readout errors and explains why, on practice, a temperature of 4K is mandated¹⁴⁷²! Another reason is that at low temperature, the spectral lines of the different energy states of the cavity are different, better spaced and easier to distinguish¹⁴⁷³.

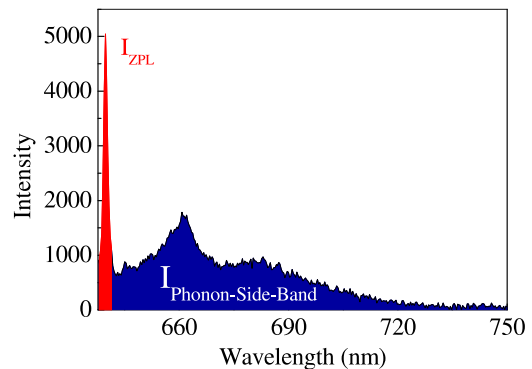


Figure 381: visualizing a ZPL and phonon-side-band. Source: [Suppression of fluorescence phonon sideband from nitrogen vacancy centers in diamond nanocrystals by substrate effect](#) by Hong-Quan Zhao et al, Hokkaido and Osaka Universities, Japan, Optics Express, 2012 (8 pages).

¹⁴⁷⁰ See some architecture aspects of NV center qubits in [Blueprinting quantum computing systems](#) by Simon J. Devitt, July 2023 (35 pages).

¹⁴⁷¹ See [Suppression of fluorescence phonon sideband from nitrogen vacancy centers in diamond nanocrystals by substrate effect](#) by Hong-Quan Zhao et al, Hokkaido and Osaka Universities, Japan, Optics Express, 2012 (8 pages).

¹⁴⁷² The technique is documented in [Quantum information processing with nitrogen vacancy centers in diamond](#) by Gang-Qin Liu and Xin-Yu Pan, 2018 (15 pages) and in [Diamond NV centers for quantum computing and quantum networks](#) by Lilian Childress and Ronald Hanson, 2017 (5 pages).

¹⁴⁷³ This interdependence between hyperfine spectral lines and temperature is not unique to diamond cavities. They are common in crystalline structures because temperature modifies many parameters such as the relative arrangement of the atoms in the crystals which leads to changes in electrical and magnetic gradients and therefore spins, etc.

A joint QuTech-Fujitsu-Element Six team demonstrated in 2022 a fault-tolerant operation of a NV centers based QPU with logical qubits made of 5 physical spin qubits and two additional measurement qubits in a 29-qubit QPU running at 10K¹⁴⁷⁴.

As shown in Figure 382 in page 445, the configuration was using different qubits: the NV center cavity was used as an auxiliary qubit with its two electrons, then the nuclear spin of the nearby nitrogen and five nuclear spins of ¹³C were used for one flag and five data qubits.

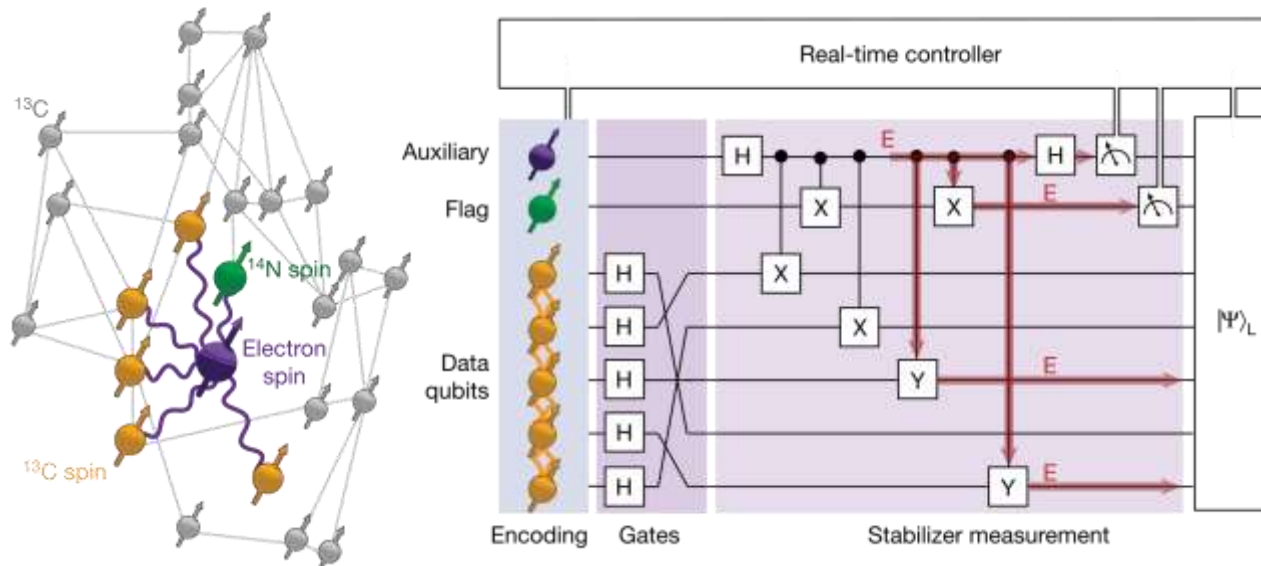


Figure 382: an error correction code implemented with NV centers qubits. Source: [Fault-tolerant operation of a logical qubit in a diamond quantum processor](#) by M. H. Abobeih et al, May 2022 (11 pages).

Another team, in Japan, implemented a similar error correction code with a Shor-3 codes using 6 qubits¹⁴⁷⁵.

Qubit operations

The general principle of operation for these NV center qubits is as follows¹⁴⁷⁶:

- **Qubit quantum state** is based on a two-state computational basis, with $|0\rangle$ corresponding to the ³A energy zero spin base level and $|1\rangle$ to the same level but with a non-zero spin. The computational basis is sometimes $|+1\rangle$ and $|-1\rangle$ corresponding to the two non-zero spin levels of the ³A basis. Most techniques use the neighboring ¹³C and ¹⁴N atoms nuclear spins as qubits and are arranged in clusters. The NV center electrons spin is used as a mediator to control the neighbor atomic spins.
- **Single-qubit quantum gates** are microwave-activated and exploit spin-state energy transitions at a frequency of 2.87 GHz¹⁴⁷⁷.

¹⁴⁷⁴ See [QuTech and Fujitsu realise the fault-tolerant operation of a qubit](#) by Qutech, May 2022 and [Fault-tolerant operation of a logical qubit in a diamond quantum processor](#) by M. H. Abobeih et al, May 2022 (11 pages).

¹⁴⁷⁵ See [Quantum error correction of spin quantum memories in diamond under a zero magnetic field](#) by Takaya Nakazato et al, Nature Communications Physics, April 2022 (7 pages).

¹⁴⁷⁶ I was initially inspired by a diagram from [lecture 3](#) of H el ene Perrin's course, February 2020. Then I integrated other sources of information. See in particular [The nitrogen-vacancy color center in diamond](#) by Marcus Doherty, Joerg Wrachtrup et al, 2013 (101 pages) which describes in particular the energy levels variations of NV centers as a function of their temperature.

¹⁴⁷⁷ As we have seen about trapped ions, hyperfine transitions are energetic transitions of low energy electrons, here in the microwave regime, which are generally related to the interaction between the magnetic polarities of the nucleus of the atoms with the magnetic field generated by the electrons. Knowing that here we are talking about electrons that do not rotate around the nucleus of an atom but in a cavity.

- **Two-qubit quantum gates** use different methods: coupling NV centers with entangled photons which doesn't work well, magnetic coupling, or with coupling the NV center with the nucleus spin of neighboring ^{13}C and ^{14}N atoms with microwaves¹⁴⁷⁸. There are many variations of two-qubit gates like a CNOT¹⁴⁷⁹, a CZ or even a weird $\exp(i\pi S_z \otimes I_z)$ ¹⁴⁸⁰.

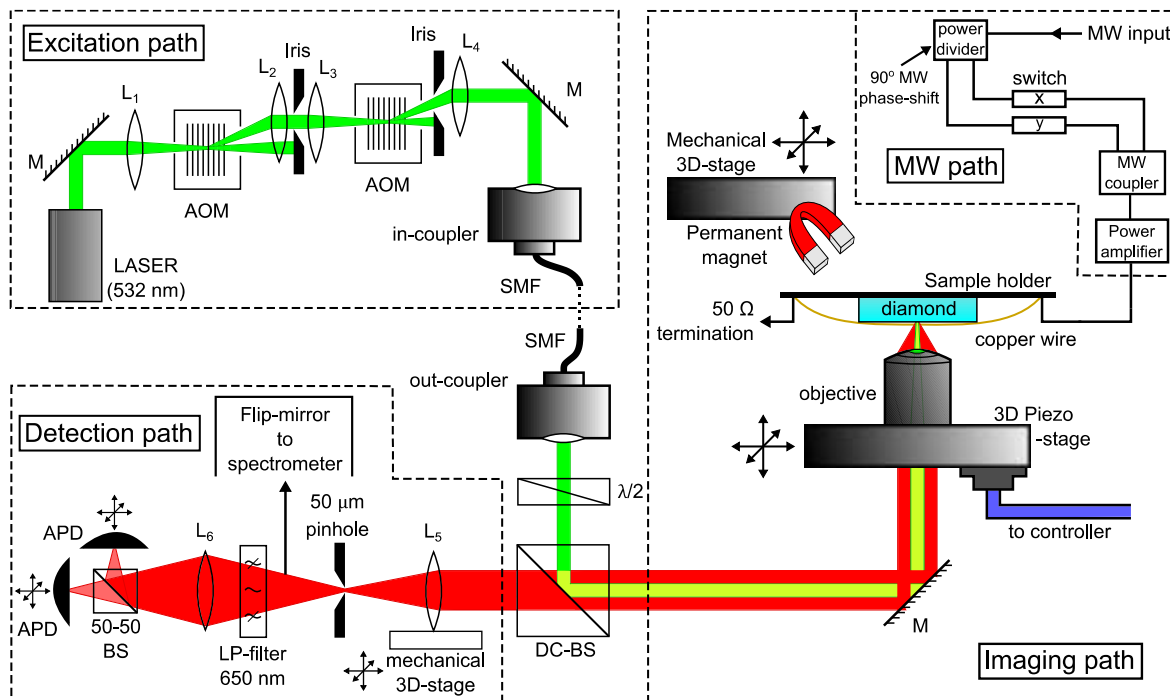


Figure A.1.: Schematic representation of the utilized setup for the characterization of NV centers. Experimental setup utilized for optical characterization and coherent spin manipulation of NV centers, comprising of a home-built confocal microscope, a scanning-stage for the imaging of diamond, and external magnet and microwave apparatus. The excitation wavelength is 532 nm. In the figure, mirrors are represented by M, lenses by L_i , single-mode optical fiber by SMF, beam-splitters by BS, and avalanche photo-diodes by APD.

Figure 383: characterization of NV centers setup. Source: [Forefront engineering of nitrogen-vacancy centers in diamond for quantum technologies](#) by Felipe Favaro de Oliveira, 2017 (235 pages).

- **Qubits readout** uses the capture of the fluorescence of the cavity activated by a laser and with an APD (avalanche photodiode) or a CCD sensor, like what is done with trapped ions and cold atoms. It consists in illuminating the cavity with a green (546 nm) laser. This excites level 3A in 3E but without changing the spin¹⁴⁸¹. The non-zero spin state 3E will generate a non-radiative transition passing through the 1A state. The null spin state 3E will generate the emission of a red photon (689 nm) which will be detected by the CCD sensor. This optical readout of single isolated qubits works only at low temperatures to avoid the creation of perturbation affecting neighbor qubits.

¹⁴⁷⁸ See some explanations in [Entanglement in NV centers](#) by Alexander Okupnik, Andrei Militaru and Ramon Gao, ETH Zurich, 2017 (34 slides).

¹⁴⁷⁹ See some detailed explanations in [Colour centers in diamond](#) by Joerg Wrachtrup, 2017 (36 slides).

¹⁴⁸⁰ See [A programmable two-qubit solid-state quantum processor under ambient conditions](#) by Yang Wu et al, NPI, 2019 (5 pages).

¹⁴⁸¹ This technique is labelled ODMR for optically detected magnetic resonance.

The measurement of the cavity electron spin can exploit other techniques, each with their advantages and disadvantages: SCC (spin to charge conversion¹⁴⁸²), NMR (readout is assisted by the nucleus spin of neighboring atoms) and only by photonics means, knowing that lasers are used in all cases, and spin fluorescence detection, with a microwave photon counter operating at cryogenic temperatures¹⁴⁸³. Only nuclear spin readouts can be nondestructive (QND)¹⁴⁸⁴.

The technology is not easy to industrialize on a large scale, whether it is the chip itself or the control lasers (Figure 384). Figure 383 shows a schematic diagram of the control mechanism for these qubits¹⁴⁸⁵.

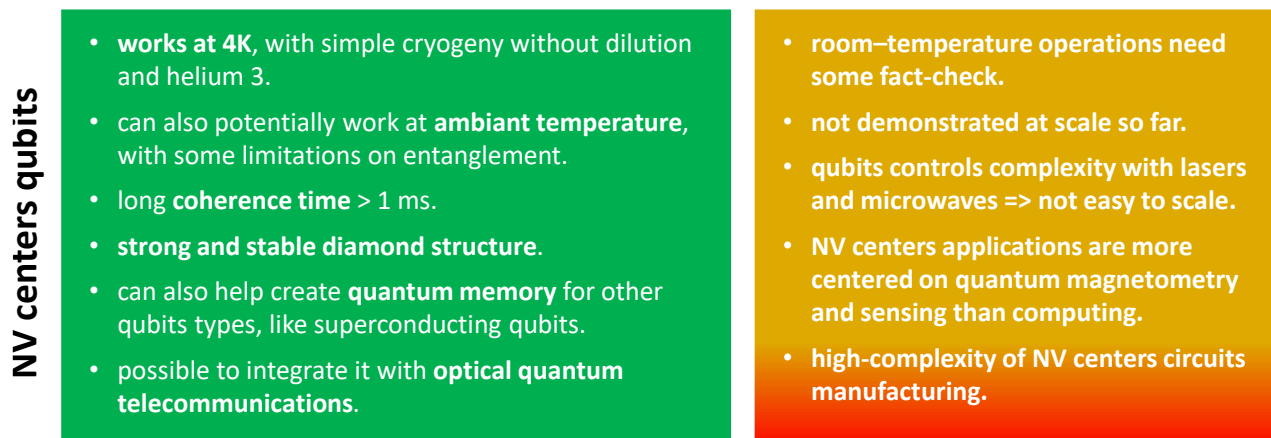


Figure 384: pros and cons of NV centers qubits. (cc) Olivier Ezratty, 2022-2023.

Research

The main countries involved are China, the Netherlands (TU Delft and Qutech¹⁴⁸⁶), Australia (University of Melbourne, Quantum Brilliance), Germany (University of Ulm), Japan (NII and NTT, Fujitsu along with QuTech), some laboratories in France (such as CEA SPEC) and of course in different labs in the USA (Harvard, MIT, ...) and in China.

NV Centers based quantum computers have been very low key for a few years. It seemed that NV centers have more promising uses in quantum sensing for the creation of precision magnetometers or for quantum memories interoperable with qubits realized with other technologies such as superconducting qubits in hybrid systems. This is a path recently explored by the University of Delft¹⁴⁸⁷, in Japan¹⁴⁸⁸ and by CEA-SPEC with Patrice Bertet as shown in Figure 385, with a superconducting qubit linked to a NV center memory qubit.

¹⁴⁸² Explained in detail in [Spin readout via spin-to-charge conversion in bulk diamond nitrogen-vacancy sets](#) by Harishankar Jayakumar, September 2018 (5 pages).

¹⁴⁸³ See [Single electron-spin-resonance detection by microwave photon counting](#) by Zhiren Wang, Léo Balembois, Marianne Le Dantec, Philippe Goldner, Thierry Chanelière, Daniel Estève, Denis Vion, Patrice Bertet, Emmanuel Flurin et al, January 2023 (16 pages).

¹⁴⁸⁴ See [Color Centers in Diamond](#) by Andreas Wallraff, ETH Zurich, 2017 (34 slides).

¹⁴⁸⁵ Seen in [Forefront engineering of nitrogen-vacancy centers in diamond for quantum technologies](#) by Felipe Favaro de Oliveira, 2017 (235 pages).

¹⁴⁸⁶ Qutech demonstrated a 10-qubit prototype with a coherence time of one minute and working at 3.7K in 2019. See [Fully controllable and highly stable 10-qubit chip paves way for larger quantum processor](#), Qutech, 2019.

¹⁴⁸⁷ See [Diamond-based 10-qubit register with coherence more than one minute](#), November 2019.

¹⁴⁸⁸ See [Coherent Coupling between a Superconducting Qubit and a Spin Ensemble](#) by Shiro Saito et al, 2012 (7 pages).

There are also variants of NV center techniques with defects introduced in phosphorus-doped silicon carbide. It would have the advantage of creating qubits whose readout is more accurate since being based on the emission of a narrow frequency fluorescence¹⁴⁸⁹.

In a similar fashion, MIT prototyped in 2020 a NV centers chip replacing nitrogen with silicon and germanium. They assembled 128 qubits but these were not operational¹⁴⁹⁰. China researchers are also experimenting NV center qubits but so far, their prototype has only 3 qubits¹⁴⁹¹. They said could reach 99.92% CNOT fidelities in 2022, to no avail¹⁴⁹². In another work, Australian researchers were able to implement single Clifford group qubit gates with NV⁻ centers with a fidelity of 99.3%¹⁴⁹³. Harvard researchers are working on creating entanglement gates using nanomechanical resonators with programmable connectivity via mechanical transport of qubits in nanopillars. It is weird but interesting¹⁴⁹⁴.

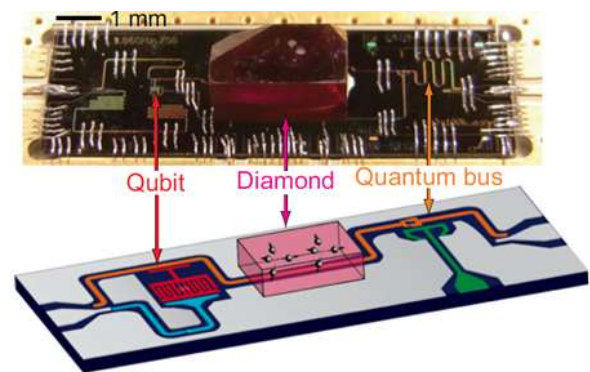


Figure 385: NV center used as a quantum memory for a superconducting qubit, which could lead to create heterogeneous qubits. Source [Quantum technologies with hybrid systems](#), Patrice Bertet et al, 2015 (8 pages).

Manufacturing

Artificial diamonds are produced either with high-pressure high-temperature processes (HPHT) or with chemical vapor deposition (CVD)¹⁴⁹⁵. The latter is used for quantum use cases.

One of the challenges to create functional NV centers quantum processors is the precise implantation of vacancies and nitrogen atoms in diamonds. NV centers are manufactured using various methods. NV vacancies are usually produced by electrons, neutrons, protons or ions irradiation to create the vacancies followed by thermal annealing at temperatures above 650 °C to move the vacancies close to the defect atoms (here, nitrogen). A tiny share of nitrogen atoms impurities are deposited during the CVD (chemical vapor deposition) production of artificial diamond.

One technique makes use of targeted ion depositions of ion beams with masking and ebeam lithography nanopatterning, as shown in Figure 386¹⁴⁹⁶.

¹⁴⁸⁹ See [Study Takes Step Toward Mass-Produced Quantum Computers](#), 2017.

¹⁴⁹⁰ See [Large-scale integration of artificial atoms in hybrid photonic circuits](#) by Noel H. Wan, Dirk Englund et al, MIT, UC Berkeley, Sandia Labs, Nature, 2020 (11 pages).

¹⁴⁹¹ See [Quantum anomaly detection of audio samples with a spin processor in diamond](#) by Zihua Chai et al, January 2022 (8 pages).

¹⁴⁹² See [99.92%-Fidelity CNOT Gates in Solids by Filtering Time-dependent and Quantum Noises](#) by Tianyu Xie et al, December 2022 (46 pages).

¹⁴⁹³ See [High Fidelity Control of a Nitrogen-Vacancy Spin Qubit at Room Temperature using the SMART Protocol](#) by Hyma H. Valabhapurapu et al, UNSW, August 2022 (7 pages). Clifford group gates are the simplest to implement and are not sufficient to create a universal gate set. It misses either a 3-qubit Toffoli gate or a T gate.

¹⁴⁹⁴ See [Programmable Quantum Processors based on Spin Qubits with Mechanically-Mediated Interactions and Transport](#) by F. Fung, M. D. Lukin et al, Harvard University, July 2023 (7 pages).

¹⁴⁹⁵ See the thesis [Engineering of NV color centers in diamond for their applications in quantum information and magnetometry](#) by Margarita Lesik, 2015 (138 pages) and the review paper [Chemical vapour deposition diamond single crystals with nitrogen-vacancy centres: a review of material synthesis and technology for quantum sensing applications](#) by Jocelyn Achard, Vincent Jacques and Alexandre Tallaire, 2020 (30 pages).

¹⁴⁹⁶ See [Scalable fabrication of coupled NV center – photonic crystal cavity systems by self-aligned N ion implantation](#) by T. Schroder and A. Stein, May 2017 (13 pages).

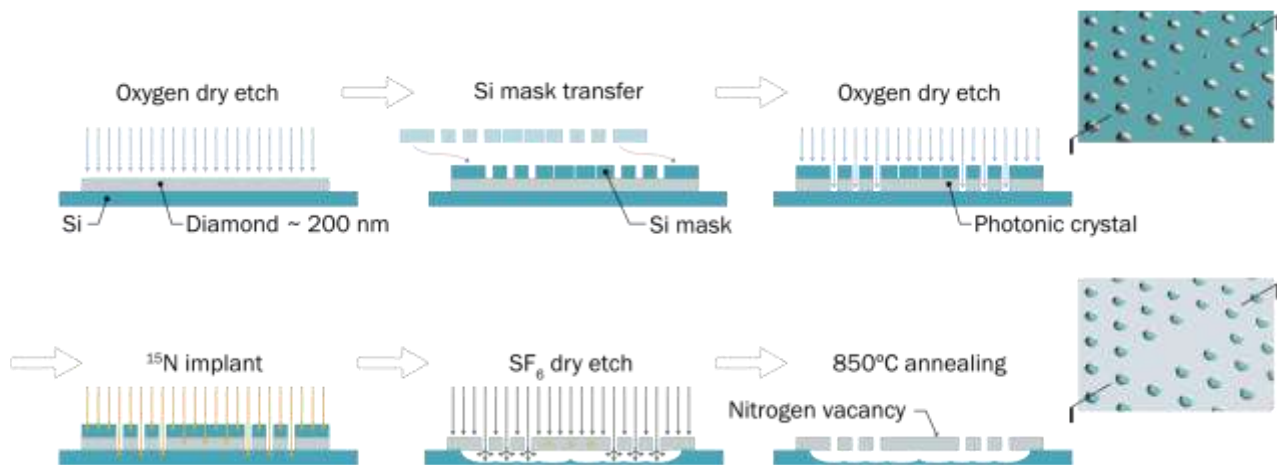


Figure 386: example of NV center implantation technique using a mask. Source: [Scalable fabrication of coupled NV center – photonic crystal cavity systems by self-aligned N ion implantation](#) by T. Schroder and A. Stein, May 2017 (13 pages).

The University of Bristol created a variation of this process with positioning nanodiamonds on a silicon-nitride wafer and using an array of optical fibers to control it¹⁴⁹⁷. Another promising technique created by Berkeley Labs is based on gold ions implantation that could scale to thousands of qubits¹⁴⁹⁸.

Vendors

Quantum Brilliance (2019, Australia), **Turing Inc** (2016, USA), **XeedQ** (2021, Germany) and **Sax-onQ** (2021, Germany) are the startups dedicated to creating NV center-based quantum computers.



Quantum Brilliance (2019, Australia/Germany, \$29.4M) develops a NV centers QPU operating at room temperature, created by ANU (Australian National University) researchers, Andrew Horsley (CEO) and Marcus Doherty (CSO). The company also has offices in Singapore and the UK.

They estimate that their solution will be size/weight/performance/cost/power competitive and bring some quantum advantage earlier than competing systems from Google and IBM that they brand « quantum mainframes ». They want to create “quantum desktops”¹⁴⁹⁹.

They introduced in March 2021 a 5 qubit prototype fitting into a 2U classical 19-inch server form factor¹⁵⁰⁰. They expect to reach 50 top 100 qubits by 2028 and to then scale up this architecture with connecting several units together¹⁵⁰¹. One future step is to fit their whole system in a large PCI board as shown in Figure 387. To learn more about these systems, you need to look at the scientific papers coauthored by Marcus Doherty¹⁵⁰².

¹⁴⁹⁷ See [Heterogeneous integration of solid state quantum systems with a foundry photonics platform](#) by Hao-Cheng Weng et al, University of Bristol, April 2023 (8 pages). The technique seems more adapted to quantum communication than quantum computing.

¹⁴⁹⁸ See [Ion-Trap Advance: Berkeley Lab Pioneers Way That Could Increase Scalability to Over 10,000 Qubits for Quantum Sensing, Quantum Computing](#) by Matt Swayne, May which refers to [Direct formation of nitrogen-vacancy centers in nitrogen doped diamond along the trajectories of swift heavy ions](#) by Russell E. Lake et al, March 2021 (5 pages).

¹⁴⁹⁹ See [Breakthrough: Quantum computers will soon fit in your phone](#) by Maija Palme, Sifted, August 2021.

¹⁵⁰⁰ In some sources, the number of available qubits is two and not five! I found out in a December 2022 preprint that their current commercial GPU has only two qubits fitting in a 6U rack. See [Software for Massively Parallel Quantum Computing](#) by Thien Nguyen et al, November-December 2022 (21 pages).

¹⁵⁰¹ See [Diamond-Based Quantum Accelerator Puts Qubits in a Server Rack](#) by Charles Q. Choi, March 2021. The illustrative picture comes from Quantum Brilliance. See also some technical details in [Quantum accelerators: a new trajectory of quantum computers](#) by Marcus Doherty, Quantum Brilliance, March 2021.

¹⁵⁰² See [Optimisation of diamond quantum processors](#) by YunHeng Chen, Marcus W. Doherty, et al, September 2020 (42 pages), [Spin-to-Charge conversion with electrode confinement in diamond](#) by Liam Hanlon, Marcus W. Doherty et al, August 2021 (16 pages) and [Optical activation and detection of charge transport between individual color centers in room-temperature diamond](#) by Artur Lozovoi, Marcus W. Doherty et al, October 2021 (15 pages).

You find that they have an error rate of 10^{-5} for single qubit gates, which is fine, and expect to have a similar level for two-qubit gates. But what is documented is a 99.2% two-qubit gate fidelity, which is not stellar nor sufficient to implement fault-tolerant quantum computing.

In April 2021, Quantum Brilliance also announced a partnership with **Quantum-South** (Uruguay) and to develop proof of concepts optimization quantum applications for air and maritime cargo companies. This is a bit early given their existing 5-qubits but why not exploring the path.

In January 2022, Quantum Brilliance announced DE-Brill, a joint research project with the Fraunhofer Institute for Applied Solid State Physics IAF and the University of Ulm funded by the German government quantum plan.

The partnership is focused on the development of manufacturing (Fraunhofer) and control (Ulm) techniques of NV center qubits.



Figure 387: Quantum Brilliance PCI board. Source: Quantum Brilliance.

The total investment of this 5-year project starting in December 2021 is €19.9M with 78.4% funded by BMBF, the German ministry of research. In April 2022, the company launched a joint R&D hub with La Trobe University and RMIT University around material design and manufacturing. This and other German universities working on NV centers¹⁵⁰³ create a critical mass of skills in NV centers aimed at quantum computing. Germany's involvement deals with manufacturing these NV center based chips with high precision.

At home in Australia, the **Pawsey Supercomputing Research Centre** announced in June 2022 the installation of a Gen1 Quantum Brilliance quantum accelerator with two qubits. In their current QPU, ^{13}C nucleus spins are controlled with radiofrequencies, microwaves for the cavity electron spins and optical channels for fluorescence readout, with the electron getting its spin from surrounding ^{13}C nucleus, implementing a QND (non-demolition measurement). At this point, the system does not require any cooling but qubit fidelities and other figures of merit may require cooling at some point. All control electronics fit in a 6U 19 inch chassis. Supported qubit gates are RX, RY and CZ. It uses a typical star model with several ^{13}C atoms surrounding one nitrogen vacancy.

In 2023, Quantum Brilliance release its Qristal software suite that contains the Qristal Emulator, supporting C++ and Nvidia CUDA APIs, Nvidia QODA programming environment and MPI (Message Passing Interface, an open library standard for distributed memory parallelization used in large-scale parallel computing¹⁵⁰⁴).

TURING **Turing Inc** (2016, USA, \$15.5M) is a startup willing to create quantum computing hardware and software, based on NV centers qubits and operating at 4K¹⁵⁰⁵.

They also develop error correction systems that they market to other industry specialists. A way to avoid putting all your eggs in the same basket! At last, they seem to work on some form of quantum memories that could be useful in entanglement based QKD deployments.

¹⁵⁰³ See [Optically coherent nitrogen-vacancy defect centers in diamond nanostructures](#) by Laura Orphal-Kobin et al, Humboldt-Universität and Ferdinand-Braun-Institut both in Berlin, 2022 (26 pages).

¹⁵⁰⁴ See [Software for Massively Parallel Quantum Computing](#) by Thien Nguyen et al, November-December 2022 (21 pages).

¹⁵⁰⁵ See [Turing Inc: Large Scale Universal Machines](#), 2017, which details this a little bit.



XeedQ (2021, Germany) is developing XQ1, an NV-center-based multi-qubit mobile quantum processor running at room-temperature. It fits in a desktop format with 4 qubits and consuming only 150 W. Two-qubit gate fidelity is >90% and single qubit gate >95% which is quite average.

The company created by Gopalakrishnan Balasubramanian, formerly at the Max Planck Institute for Biophysical Chemistry in Göttingen and is based in Leipzig. He published a wealth of [papers](#) on the physics of NV centers but not on NV-centers-based quantum computers nor how do you entangle such qubits at room temperatures. They plan to release a version with 256 qubits by 2026 and to deliver their first QPU “Baby Diamond” to Goethe University as of early 2024. It is weird to read on their web site that “*quantum systems offer encryption standards that are virtually impossible to breach. Welcome to future-proof quantum secure communications on a mobile footprint*”. Someone should tell them that PQC doesn’t need a quantum computer to run.

SaxonQ (2021, Germany) wants to create some NV center based mobile quantum computer. The system is mobile, on wheels and has a size of about half a rack.

However, not very surprisingly, it looks like being available on their website but with no characteristics at all (number of qubits, fidelities). The company based in Leipzig was cofounded by Marius Grundmann (CEO), Dominique Bouwes (COO) and Jan Meijer (CTO).

Other spin cavities variants

Besides NV centers, another similar technique is investigated at the research stage that uses various vacancies in silicon carbide crystal structures (SiC), silicon in diamond vacancies (SiV¹⁵⁰⁶ ¹⁵⁰⁷) and even tin vacancies SnV¹⁵⁰⁸. Vacancies can be missing nearby couples of carbon and silicon atoms, called divacancies (V_{Si}V_C⁰) or just a missing silicon atom (V_{Si}⁻)¹⁵⁰⁹.

Others use transition metal defects with chromium, vanadium, molybdenum, tungsten, erbium¹⁵¹⁰ and hexagonal boron nitride (h-BN)¹⁵¹¹. In 2022, a research team from the DoE Argonne National Lab created a prediction model of the coherence time of vacancies depending on their characteristics, which can help investigate new materials¹⁵¹².

SiC qubits could theoretically work at ambient temperature¹⁵¹³.

¹⁵⁰⁶ See [Neutral silicon vacancy centers in undoped diamond via surface control](#) by Zi-Huai Zhang et al, Princeton University, Northwestern University and Element Six, June 2022 (16 pages).

¹⁵⁰⁷ See [Deterministic Creation of Strained Color Centers in Nanostructures via High-Stress Thin Films](#) by Daniel R. Assumpcao et al, Harvard, September 2023 (8 pages) which could operate at about 1.5K.

¹⁵⁰⁸ See [Heterogeneous integration of spin-photon interfaces with a scalable CMOS platform](#) by Linsen Li, Dirk Englund et al, MIT, QuTech, August 2023 (23 pages).

¹⁵⁰⁹ See [Single artificial atoms in silicon emitting at telecom wavelengths](#) by W. Redjem et al, 2020 (4 pages).

¹⁵¹⁰ See [Roadmap for Rare-earth Quantum Computing](#) by Adam Kinos, Alexandre Tallaire et al, March 2021 (47 pages).

¹⁵¹¹ See [First-principles theory of extending the spin qubit coherence time in hexagonal boron nitride](#) by Jaewook Lee, Huijin Park and Hosung Seo, npj, September 2022 (9 pages).

¹⁵¹² See [A mathematical shortcut for determining quantum information lifetimes](#) by Leah Hesla, Argonne National Lab, April 2022 and [Generalized scaling of spin qubit coherence in over 12,000 host materials](#) by Shun Kanai, David D. Awschalom et al, PNAS, April 2022 (8 pages). It shows that the coherence time T₂ of vacancies is dependent on the cavity spin density (n_i) of nucleus i, the crystalline structure, the nuclear spin-factor (g_i), and the nuclear spin quantum number (I_i) according to the formula $T_{2,i} = 1.5 \times 10^{18} |g_i|^{-1.6} I_i^{-1.1} n_i^{-1.0}$ (s).

¹⁵¹³ The DoE Argonne National Laboratory together with researchers from Hungary, Sweden and Russia published in 2019 a work on SiC qubits operating at room temperature. See [Scientists Find Yet Another Way to Get Qubits Working at Room Temperature](#) by David Nield, March 2020 and [Novel Qubit Design Could Lead to Quantum Computers That Work at Room Temperature](#) by Matt Swayne, March 2020 which references [Quantum well stabilized point defect spin qubits](#) by Viktor Ivády et al, May 2019 (20 pages).

While these vacancies could be used to create qubits and quantum processors like with NV centers, they are currently aimed mostly at quantum photonics applications.

One of the reasons is that some SiC vacancies have fluorescence wavelengths corresponding to fiber optics telecom wavelengths in the near infrared band around 1.5 μm , in the so-called 4H-SiC hexagonal lattice version¹⁵¹⁴ (Figure 388).

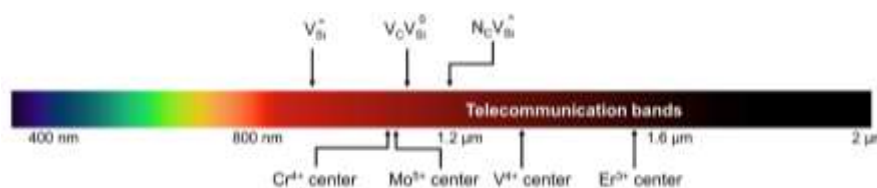


Figure 388: other cavities are interesting due to their transition frequencies that sit in the telecommunication wavelengths. Source: [Quantum Information Processing With Integrated Silicon Carbide Photonics](#) by Sridhar Majety et al, March 2022 (50 pages).

SiC vacancies can indeed be used as interesting sources of single or entangled photons in quantum communications and cryptography. SiC photon sources are implanted on nanophotonic devices¹⁵¹⁵. It could also be used in quantum repeaters thanks to relatively long spin coherence times above 50 ms. Also, SiC vacancies can show a much better DWF (Debye-Waller factor) than diamond NV centers. However, their readout contrast must be improved¹⁵¹⁶.

In quantum information processing, SiC vacancies are investigated in various areas such as with quantum simulation and measurement-based quantum computing. There are some specific technology paths like using SiC spin qubits that are coupled by photons¹⁵¹⁷.

SiC vacancies have very long coherence times in the seconds range¹⁵¹⁸. It leads to theoretically long computing time, although, it would work with solving many other problems like large entanglement capacities and high two-qubit gate fidelities. Thus, when you read in the media that SiC could achieve a hundred million operations, you may get skeptic and right to be so¹⁵¹⁹. Indeed, the related paper simply computes this number of operations by dividing SiC qubit coherence time of 5 seconds by a single-qubit gate time. They have not implemented it yet, particularly given it is useless to do that on a single qubit. It would be nice to have a tomography of a 2-qubit gate...! Then, you have to deal with the specifics of the readout of ²⁹Si and ¹³C nuclear spins readouts used in such devices¹⁵²⁰.

At last, oxygen vacancies (aka ST1) implantation in diamond are studied in China¹⁵²¹ and in Hungary¹⁵²².

¹⁵¹⁴ See the excellent review paper [Quantum Information Processing With Integrated Silicon Carbide Photonics](#) by Sridhar Majety et al, March 2022 (50 pages).

¹⁵¹⁵ See [Integrated quantum photonics with silicon carbide: challenges and prospects](#) by Daniil M. Lukin, Melissa A. Guidry and Jelena Vuckovic, October 2020 (20 pages) and [Fabrication and nanophotonic waveguide integration of silicon carbide colour centres with preserved spin-optical coherence](#) by Charles Babin, Florian Kaiser et al, November 2021 (18 pages).

¹⁵¹⁶ See [Room temperature coherent manipulation of single-spin qubits in silicon carbide with a high readout contrast](#), by Qiang Li et al, July 2021 (10 pages).

¹⁵¹⁷ See [Silicon photonic quantum computing with spin qubits](#) by Xiruo Yan et al, 2021 (28 pages).

¹⁵¹⁸ See [Five-second coherence of a single spin with single-shot readout in silicon carbide](#) by Christopher P. Anderson, David D. Awschalom et al, 2021 (9 pages).

¹⁵¹⁹ See [Quantum Computing: Researchers Achieve 100 Million Quantum Operations](#) by Francisco Pires, Tom's Hardware, February 2022.

¹⁵²⁰ See [Measuring nuclear spin qubits by qudit-enhanced spectroscopy in Silicon Carbide](#) by Erik Hesselmeier, Jörg Wrachtrup et al, October 2023 (9 pages).

¹⁵²¹ See [A neutral oxygen-vacancy center in diamond: A plausible qubit candidate and its spintronic and electronic properties](#) by Y. G. Zhang et al, Applied Physics Letter, August 2014. Not open access.

¹⁵²² See [Investigation of oxygen-vacancy complexes in diamond by means of ab initio calculations](#) by Nima Ghafari Cherati et al, February 2023 (9 pages).



Photonic (2019, Canada, \$140M) is a spin-off from the Silicon Development Lab at Simon Fraser University in Vancouver with Stephanie Simmons as their Chief Quantum Officer, Paul Terry as CEO and 120 employees as of November 2023. Microsoft is one of their investors in their 2023 round of \$100M.

Their technology is based on “T” defects in silicon, *aka* “T centres”, using similar techniques as with SiC and NV vacancies^{1523 1524}. At the physical level, processing and memory qubits are handled with nuclear spins of hydrogen and ¹³C atoms in a ²⁸Si substrate. Silicon vacancy electron spins are used for the indirect non-demolition measurement of these nuclear spin qubits and to create spin-photon interactions in the telecom wavelength band O (around 1,326 nm). The whole nuclear and electron spin ensemble form these T centres and are placed in optical cavities connected in a many-to-many fashion through a web of optical fibers and (not detailed) routing. This helps create short and long-distance entanglement sharing between qubits (but heralded, so in a probabilistic manner), enabling gate teleportation (two-qubit gates). As a result, high-connectivity demanding QLDPC quantum error correction can be implemented. They expect to create chipsets handling up to 1,000 T centres and 4,000 optical fibers, all this being driven by global and local electric and magnetic fields. The way they plan to manufacture these chipsets is not clear yet, particularly with regards to the precise positioning of the T centres in the ²⁸Si substrate. The system operates at about 1K to 2K.



Quantum Transistor (2022, Israel) is a stealth company building a vacancy-based quantum processor that was cofounded by Shmuel Bachinsky (CEO) and Moshe Tordjman (CTO), who was previously a researcher from Technion and MIT.

Topological qubits

In this category of qubits and quantum computing, we must create a distinction between the notion of "topological" which defines a type of qubit based on anyons and the "Majorana fermions" or “Majorana Zero Mode” (MZM) which are a variant of anyons to create topological qubits. Of all the types of qubits, they are the most mysterious and complex to understand¹⁵²⁵ (Figure 394).

History

Ettore Majorana predicted in 1937 the existence of a new class of particles that are its own anti-particles. It was labelled “Majorana fermions”.

The notion of anyon "quasiparticle", i.e. particle representation models that describe the state of electron clouds around atoms, in the superconducting regime and in 2D, was first proposed by Jon Magne Leinaas and Jan Myrheim from the University of Oslo in 1976 and then elaborated by Frank Wilczek in 1982¹⁵²⁶.

Majorana fermions are a specific type of these quasiparticles organized along a small superconducting wire in 1D structures.

¹⁵²³ See [Silicon-Integrated Telecommunications Photon-Spin Interface](#) by L. Bergeron et al, 2020 (15 pages).

¹⁵²⁴ See the blueprint [Scalable Fault-Tolerant Quantum Technologies with Silicon Colour Centres](#) by Stephanie Simmons, Photonic, October 2023 (16 pages) which documents well their architecture.

¹⁵²⁵ See [Topological Quantum Computing](#) by Torri Yearwood, January 2020 and [A Short Introduction to Topological Quantum Computing](#) by Ville Lahtinen and Jiannis K. Pachos, May 2017 (44 pages).

¹⁵²⁶ See [On the theory of identical particles](#) by Jon Magne Leinaas and Jan Myrheim, 1976 (23 pages) and See [Quantum Mechanics of Fractional-Spin Particles](#) by Frank Wilczek, PRL, 1982. See also the essay [Quanta of the Third Kind](#) by Frank Wilczek, November 2021 that provides an excellent simplified view of what are anyons, braiding and quasiparticles. The author explains three specifics of quasiparticles: fractionalization (where quasiparticles have properties that are subparts of usual whole-number multiples like spins or unit of electron electric charge or angular momentum), flux tubes (fractional angular momentum made possible by particles orbiting around tubes of magnetic flux like in type II superconductors) and dimensional reduction (with point-like structures).

They have collective electron behaviors in crystalline networks at very low temperature¹⁵²⁷.

Alexei Kitaev then had the idea in 1997 to use anyons for quantum calculations when he was a researcher at Microsoft. He published two foundational papers in 2000 describing the category of fermionic quantum computers and a model of spinless fermions in a 1D superconducting nanowire, *aka* a Kitaev chain¹⁵²⁸. There are several various variations of fermionic quantum computing being investigated, including analog quantum computing with cold atoms¹⁵²⁹ or with specific superconducting settings like Cooper pair splitters¹⁵³⁰.

In 2008, Liang Fu and C.L. Kane from the University of Pennsylvania predicted that Majorana bound states can appear at the interface between topological insulators and superconductors¹⁵³¹.

In 2012, Leo Kouwenhoven then at TU Delft announced the detection of Majorana Zero Modes quasiparticles at TU Delft and later on in 2018 when he was at Microsoft Research in Delft.

Some other advances came out in 2016 from the MIT and in 2018, from a group of three American universities UC Irvine, UCLA and Stanford, who said they discovered real Majorana fermions. In May/June 2019, German and Austrian researchers said they succeeded in creating two-dimensional topological phenomena like Majorana zero modes¹⁵³².

Princeton researchers also published in June 2019 the results of their work that led them to control the state of a quasiparticle¹⁵³³ (Figure 389).

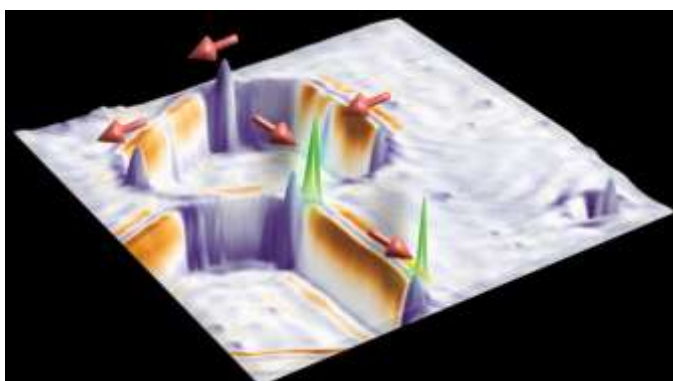


Figure 389: a Majorana Zero mode discovered at Princeton in 2019. Source: [Mysterious Majorana Quasiparticle Is Now Closer To Being Controlled For Quantum Computing](#), June 2019.

2021 marked the beginning of a crisis winter for Majorana fermion. It started with an expression of concern and a withdrawal of Leo Kouwenhoven's 2018 Nature paper¹⁵³⁴.

¹⁵²⁷ This is the thesis of Hugo de Garis in [Topological Quantum Computing The TQC Shock Wave and its Impact on University Computer Science Teaching](#), 2011 (29 pages).

¹⁵²⁸ See [Fermionic quantum computation](#) by Serguei B. Bravyi and Alexei Y. Kitaev, 2000 (18 pages) and [Unpaired Majorana fermions in quantum wires](#) by Alexei Kitaev, 2000 (16 pages).

¹⁵²⁹ See [The Power of Noisy Fermionic Quantum Computation](#) by Fernando de Melo et al, April 2013 (21 pages) and [Quantum register of fermion pairs](#) by Thomas Hartke et al, MIT, March 2021 (10 pages). Fermionic atoms are isotopes with an odd number of neutrons so that its total nucleus and electron spin is half-integer. Fermionic quantum computing was defined by Serguei B. Bravyi and Alexei Y. Kitaev in [Fermionic quantum computation](#), 2000 (18 pages) around the notion of local fermionic modes.

¹⁵³⁰ See [Fermionic quantum computation with Cooper pair splitters](#) by Kostas Vilkelis et al, QuTech and Kavli Institute, September 2023 (15 pages).

¹⁵³¹ See [Superconducting proximity effect and Majorana fermions at the surface of a topological insulator](#) by Liang Fu and C.L. Kane, 2008 (4 pages) and [Josephson Current and Noise at a Superconductor-Quantum Spin Hall Insulator-Superconductor Junction](#) by Liang Fu and C.L. Kane, 2008 (4 pages).

¹⁵³² See [Computing Faster With Quasi-Particles](#), May 2019 referring to [Topological superconductivity in a phase-controlled Josephson junction](#) by Hechen Ren et al, Nature, April 2019.

¹⁵³³ See [Mysterious Majorana Quasiparticle Is Now Closer To Being Controlled For Quantum Computing](#), June 2019 mentioning [Observation of a Majorana zero mode in a topologically protected edge channel](#) by Ali Yazdani et al, Science, June 2019 (12 pages).

¹⁵³⁴ See [Quantized Majorana conductance](#) by Leo Kouwenhoven et al, 2017 (26 pages) which was followed by an "[expression of concern](#)" from the authors warning readers about the veracity of the published results, which were not reproducible due to a problem with the calibration of measuring instruments. The coverage on the paper withdrawal in 2021 was dense, starting with [Data manipulation and omission in 'Quantized Majorana conductance'](#), Zhang et al, Nature 2018 by Frolov et al, March 2021 (31 slides) which spurred [Microsoft's Big Win in Quantum Computing Was an 'Error' After All](#), by Tom Simonite, Wired, February 2021. Another of their paper was later retracted. See [Retraction Note: Epitaxy of advanced nanowire quantum devices](#) by Sasa Gazibegovic, Leo Kouwenhoven et al, Nature, April 2022.

In a [March 2022 Twitter thread](#) Sergey Frolov made an impressive inventory on many other unreliable Majorana research papers with other retracted papers¹⁵³⁵ or that should be retracted. He used to work at TU Delft with Leo Kouwenhoven on Majorana fermions and moved in 2012 to the University of Pittsburgh¹⁵³⁶. The withdrawal came after Sergey Frolov and his fellow Pittsburgh researcher Vincent Mourik unsuccessfully tried to reproduce Kouwenhoven's experiment¹⁵³⁷. Early in 2022, Leo Kouwenhoven left Microsoft in March 2022¹⁵³⁸. Charlie Marcus from Microsoft Research in Denmark also quit Microsoft late 2021 to return to academic research at the Niels Bohr Institute¹⁵³⁹.

Sergei Frolov is himself making discoveries on Majorana bound states using the 4π Majorana-Josephson effect using a fluxonium superconducting qubit, the ensemble being branded a braidonium¹⁵⁴⁰.

He also reported in 2022 that looking at research experimental data from 2012 did show the presence of Majorana modes in nanowire devices¹⁵⁴¹. Other researchers in Germany succeeded in integrating a topological insulator into a superconducting qubit in 2022, following on a 2013 proposal from researchers from Caltech and Harvard¹⁵⁴². Another 2020 proposal is to couple a Majorana qubit playing the role of a well-protected quantum memory and a superconducting qubit for computation and to implement a SWAP gate between these¹⁵⁴³.

In August 2019, NIST physicists led by Nick Butch announced the discovery by chance of interesting properties of uranium ditelluride (UTe₂). It would be superconducting at 1.7K with the ability to do so via Cooper pairs with identical spins in addition to opposite spins, allowing three types of pairs. This would give it a rare ability to get a magnetic flux resistant superconductivity. This material would thus have topological properties in this framework allowing to create topological qubits that are more stable and less subject to decoherence¹⁵⁴⁴. Related work was published by researchers from John Hopkins University in 2018 with superconducting topological qubits made of a bismuth-palladium alloy¹⁵⁴⁵. And the story goes on and on around Majorana fermions that are discovered, believed to be discovered or rediscovered depending on the case. Most of the time, the discoveries deal with very weak experimental signals that are confused with ambient noise.

¹⁵³⁵ See [Chiral Majorana fermion modes in a quantum anomalous Hall insulator–superconductor structure](#), Science, 2017 (7 pages) was the subject of an [expression of concern](#) in December 2021 and was [retracted](#) in November 2022 by Science with the following comment: “Readers who failed to reproduce the findings requested raw data files from the authors, which they provided. Subsequently, the provenance of the raw data came into question; additionally, an analysis of the raw and published data revealed serious irregularities and discrepancies”.

¹⁵³⁶ See [Signatures of Majorana fermions in hybrid superconductor-semiconductor nanowire devices](#), Kavli Institute of Nanoscience, Delft University of Technology, 2012.

¹⁵³⁷ The story is well told in [Major Quantum Computing Strategy Suffers Serious Setbacks](#) by Philip Ball, Quanta Magazine, September 2021. The same Philip Ball that was mentioned in the part of this book related to [quantum matter taxonomy](#), page 116.

¹⁵³⁸ See [Kouwenhoven departs, Microsoft presents Majoranas](#), Delta GTU Delft, March 2022.

¹⁵³⁹ As shown in his LinkedIn profile: <https://www.linkedin.com/in/charles-marcus-02984597>.

¹⁵⁴⁰ See [Braiding quantum circuit based on the \$4\pi\$ Josephson effect](#) by John P. T. Stenger, Michael Hatridge, Sergey M. Frolov and David Pekker, University of Pittsburgh, Physical Review B, 2019 (10 pages).

¹⁵⁴¹ See [We cannot believe we overlooked these Majorana discoveries](#) by Sergey Frolov and Vincent Mourik, University of Pittsburgh and FZ Jülich, March 2022 (9 pages).

¹⁵⁴² See [Integration of Topological Insulator Josephson Junctions in Superconducting Qubit Circuits](#) by Tobias W. Schmitt et al, FZ Jülich, March 2022 (14 pages). And [Proposal for Coherent Coupling of Majorana Zero Modes and Superconducting Qubits Using the \$4\pi\$ Josephson Effect](#) by David Pekker, Chang-Yu Hou, Vladimir E. Manucharyan and Eugene Demler, PRL, 2013 (8 pages).

¹⁵⁴³ See [SWAP gate between a Majorana qubit and a parity-protected superconducting qubit](#) by Luca Chiroli et al, Berkeley, May 2022 (7 pages).

¹⁵⁴⁴ See [Newfound Superconductor Material Could Be the 'Silicon of Quantum Computers' Possible "topological superconductor" could overcome industry's problem of quantum decoherence](#), August 2019, mentioning [Nearly ferromagnetic spin-triplet superconductivity](#) by Sheng Ran et al, 2019.

¹⁵⁴⁵ See [Observation of half-quantum flux in the unconventional superconductor \$\beta\$ -Bi₂Pd](#) by Yufan Li & Al, October 2018 (12 pages).

Majorana fermions are searched on gold¹⁵⁴⁶, on the surface of superconducting nanowires¹⁵⁴⁷, in crystals¹⁵⁴⁸, in 2D graphene¹⁵⁴⁹, not to mention other publications that are not obvious to analyze¹⁵⁵⁰.

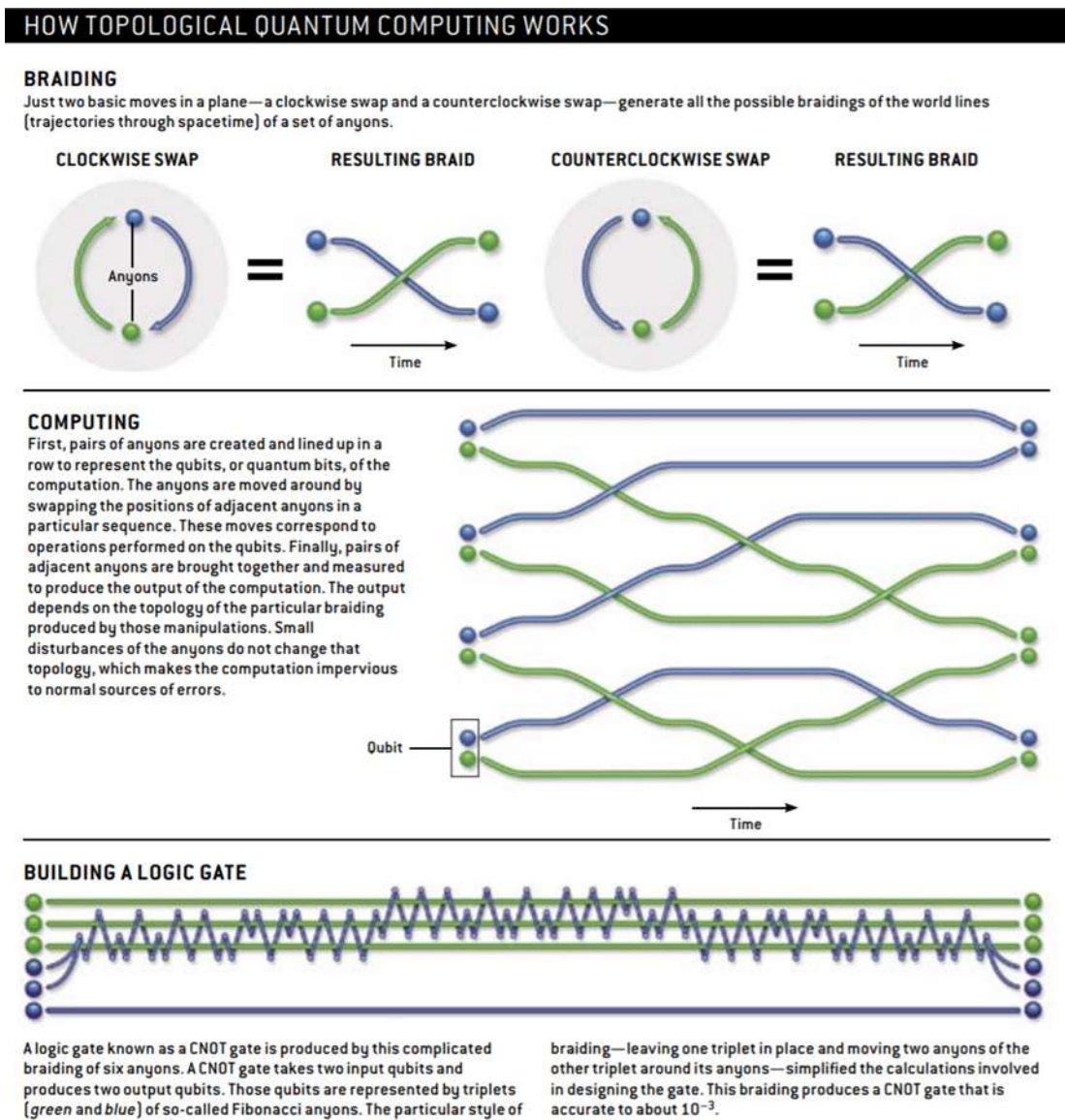


Figure 390: how topological quantum computing is supposed to work.
Source: [Computing with Quantum Knots](#) by Graham Collins, *Scientific American*, 2006 (8 pages).

¹⁵⁴⁶ See [Quantum Computing Breakthrough: First Sighting of Mysterious Majorana Fermion on Gold](#) by Jennifer Chu, MIT, Indian Institute of Technology, University of California & Hong Kong University, 2020. And [Signature of a pair of Majorana zero modes in superconducting gold surface states](#) by Sujit Manna et al, MIT, 2019 (35 pages).

¹⁵⁴⁷ See [Alternative route to topological superconductivity](#) Hub, April 2020. University of Copenhagen in collaboration with Microsoft. Refers to [Flux-induced topological superconductivity in full-shell nanowires](#) by S. Vaitiekėnas et al, March 2020 (38 pages).

¹⁵⁴⁸ See [Building block for quantum computers more common than previously believed](#) by Chanapa Tantibanchachai, Johns Hopkins University, April 2020.

¹⁵⁴⁹ See [Observation of Yu-Shiba-Rusinov states in superconducting graphene](#) by E. Cortés-del Río, Pierre Mallet et al, 2020 (22 pages) and published in *Advanced Materials* in April 2021.

¹⁵⁵⁰ See [The observation of photon-assisted tunneling signatures in Majorana wires](#) par Ingrid Fadelli, May 2020, [Quantum computers do the \(instantaneous\) twist](#) by Chris Cesare, August 2020 on a topological error correction system and [Fractional statistics of anyons in a two-dimensional conductor](#), C2N, April 2020.

Science

The principle of topological quantum computing is based on the notion of anyon which are "quasiparticles" integrated in two-dimensional systems, given that there are Abelian and non-Abelian anyons! Anyons are asymmetrical and two-dimensional physical structures whose symmetry can be modified. This makes it possible to apply some topology principles with sets of successive permutations applied to pairs of anyons that are in proximity in circuits (Figure 391).

The related algorithms are based on the concepts of topological braid or node organizations ("braids"). Their representation explains this, with a temporal evolution of the permutations of temporal anyons going from bottom to top, knowing that in other representations, it may go from top to bottom¹⁵⁵¹.

The diagram in Figure 390 clarifies this a little. Topological quantum gates require a long sequence of anionic permutations as with the CNOT gate shown at the bottom of the diagram. They are a sort of quantum error correction code.

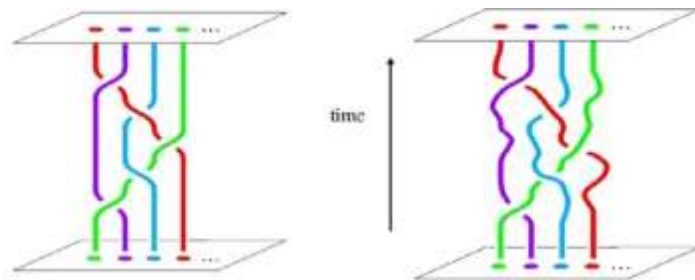


Figure 391: anyon braiding explained topologically.

You need two Majorana fermions to create a single two-level quantum system, *aka* a qubit. With Majorana modes, you implement XX, YY and ZZ two-qubit measurements which are well protected and a CNOT is built with two consecutive such measurements. But a T gate is not natively protected making it hard to implement FTQC. Some researchers in China still found a workaround to create non-Clifford single-qubit phase gates¹⁵⁵².

By the way, let's clarify a little bit the weird vocabulary from this field. Majorana fermions are non-Abelian excitations. They are also called Majorana Zero Modes (MZM) or Majorana bound states or even Majorinos. You have also Majorana Edge Modes (MEM) and Majorana Pi Modes (MPM)¹⁵⁵³. Others non-Abelian anyons exist like Ising anyons, Fibonacci anyons¹⁵⁵⁴ and Jones-Kauffman anyons.

Qubit operations

Let's give a try to explaining how Majorana qubits work on a practical basis, given there are many variations of these.

- **Qubit quantum state** involves a Majorana code also called a Majorana box qubit or Majorana qubit. Correction is partially built in with a Majorana stabilizer code forming the even-fermion-parity ground-state subspace of two parallel Kitaev Majorana chains in their fermionic topological phase. An extension using three Kitaev chains and housing two logical qubits of the same parity is called the "hexon" Majorana code. The proposed circuit in Figure 392 shows superconducting islands containing six MZMs ("hexons") connected together with superconducting topological nanowires, given Microsoft seems to be planning to use four MZMs ("tetrons")¹⁵⁵⁵.

¹⁵⁵¹ Topological qubits could also be realized in photonics-based architecture. See [New photonic chip promises more robust quantum computers](#), September 2018, involving researchers in Australia, Italy and Switzerland.

¹⁵⁵² See [Universal topological quantum computation with strongly correlated Majorana edge modes](#) by Ye-Min Zhan et al, March 2022 (18 pages) which is about creating non-Clifford $\pi/10$ gates.

¹⁵⁵³ To sort things out, see the excellent thesis [Quantum Field Theories, Topological Materials, and Topological Quantum Computing](#) by Muhammad Ilyas, August 2022 (204 pages).

¹⁵⁵⁴ See [A short introduction to Fibonacci anyon models](#) by Simon Trebst, Matthias Troyer et al, 2009 (24 pages).

¹⁵⁵⁵ See [Scalable Designs for Quasiparticle-Poisoning-Protected Topological Quantum Computation with Majorana Zero Modes](#) by Torsten Karzig, June 2017 (34 pages).

- **Single-qubit quantum gates** operations can be driven between the MZMs and semiconducting quantum dots as with the example shown in Figure 392. An H gate can be implemented with an X measurement following by a Z rotation conditioned by the result of the X measurement. In a way, it looks like a form of measurement based quantum computing (MBQC).

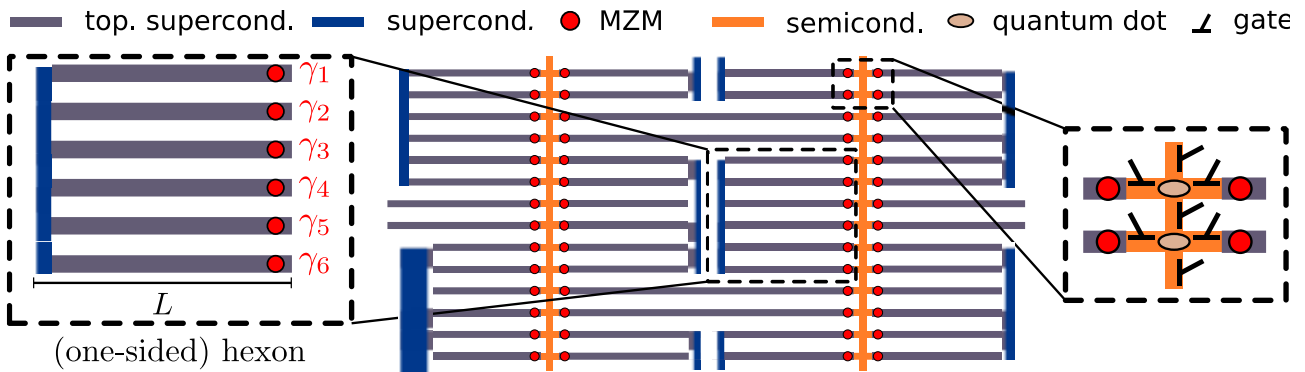


Figure 392: an example of Majorana fermion encoded with 6 MZM connected to topological superconductor nanowires, aka "hexons". Source: [Scalable Designs for Quasiparticle-Poisoning-Protected Topological Quantum Computation with Majorana Zero Modes](#) by Torsten Karzig, June 2017 (34 pages). Added in 2023.

- **Two-qubit quantum gates** like a regular CNOT are created with combinations of single Pauli X and Z measurement with XX and ZZ joint measurement between qubits as shown in Figure 393¹⁵⁵⁶. A T or Toffoli gate in the non-Clifford gates group must be created to achieve universality.

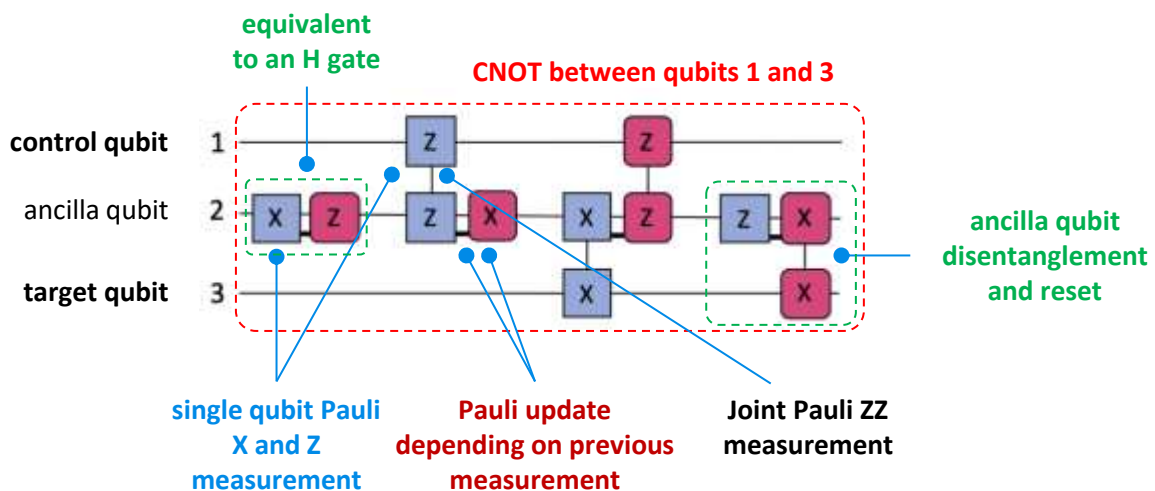


Figure 393: an explanation of the complicated way to implement a CNOT entanglement gate with Majorana fermions. Source: [Optimization of the surface code design for Majorana-based qubits](#) by Rui Chao, Michael E. Beverland, Nicolas Delfosse and Jeongwan Haah, Microsoft and USC, October 2020 (19 pages). Added in 2023.

- **Qubit readout** can use projective measurement using charge sensing¹⁵⁵⁷. It can use cryoCMOS chip operating a low temperature (3K) as tested by Microsoft in Australia with the capability to support up to 1,000 qubits. You can measure only half the qubits at a given time.

¹⁵⁵⁶ Microsoft patented such a CNOT gate, in [Quantum computing methods and devices for majorana tetron qubits](#), USPTO patent US 2018 / 0052806 A1 filed on August 31, 2016 by Microsoft Technology Licensing (14 pages).

¹⁵⁵⁷ See [Readout of Majorana Qubits](#) by Jacob F. Steiner and Felix von Oppen, Freie Universität Berlin April 2020 (28 pages).

- **Error correction.** Majorana have embedded error correction enabling them to potentially reach gate fidelities in the 10^{-6} error zone according to Microsoft. Still, some error correction codes are required to create logical qubits with smaller error rates, in the FTQC regime, but also to implement non-Clifford quantum gates which are not native with Majorana fermions. The planned quantum error correction codes are Floquet codes, a variant of surface codes, and then, LDPC codes. All of this being implemented in a fault-tolerant manner, which adds its own overhead. Particularly with the magic state distillation required to correct T gates.

Research

On top of the above-mentioned labs, different physics laboratories are working on topological qubits, notably in the USA, China, Germany¹⁵⁵⁸, the UK, the Netherlands, Denmark, Australia¹⁵⁵⁹, Japan¹⁵⁶⁰, Finland¹⁵⁶² and also in France.

Maryland¹⁵⁶³, **Caltech**¹⁵⁶⁴, **Wisconsin Madison**¹⁵⁶⁵ and **Purdue**¹⁵⁶⁶ Universities also have teams working on topological quantum computing and/or Majorana fermions, the two later working with Microsoft Research. It is also the case of the Quantum Science Center (QSC) from the DoE **ORNL** as well as the **Sandia Labs**¹⁵⁶⁷ ¹⁵⁶⁸. The KouBit Lab from the **University of Illinois** and led by Angela Kou also investigate topologically protected superconducting qubits as well as a team led by Javad Shabani at the **New York University**. Researchers from **Cambridge University** are proposing to create NISQ QPUs with topological qubits¹⁵⁶⁹.

Even IBM is working on Majorana fermions. In 2022, an **IBM Research** team published a paper showing how they could simulate Majorana Zero Modes (MZM), Majorana Pi Modes (MPM) and

¹⁵⁵⁸ See [Majorana Zero Modes in Fermionic Wires coupled by Aharonov-Bohm Cages](#) by Niklas Tausendpfund et al, University of Cologne, August-September 2022 (16 pages). Theory without experiment.

¹⁵⁵⁹ See [Many-body Majorana braiding without an exponential Hilbert space](#) by Eric Mascot et al, University of Melbourne and University of Illinois, March 2023 (7 pages). Simulation.

¹⁵⁶⁰ See the tutorial [Majorana nanowires for topological quantum computation](#) by Pasquale Marra, University of Tokyo, June 2022-December 2022 (58 pages).

¹⁵⁶¹ See [Topological quantum gates and topological entangled states by braiding Majorana fermions](#) by Motohiko Ezawa, University of Tokyo, April 2023 (15 pages).

¹⁵⁶² See [Ultra-thin designer materials unlock quantum phenomena](#), Aalto University, December 2020 and [Topological superconductivity in a van der Waals heterostructure](#) by Shawulienu Kezilebieke et al, March 2021 (27 pages).

¹⁵⁶³ See [On-demand large conductance in trivial zero-bias tunneling peaks in Majorana nanowires](#) by Haining Pan and Sankar Das Sarma, University of Maryland, March 2022 (8 pages) and [Euler-obstructed Cooper pairing: Nodal superconductivity and hinge Majorana zero modes](#) by Jiabin Yu, Yu-An Chen and Sankar Das Sarma, University of Maryland, Physical Review B, March 2022 (47 pages).

¹⁵⁶⁴ See [Dephasing and leakage dynamics of noisy Majorana-based qubits: Topological versus Andreev](#) by Ryan V. Mishmash, Bela Bauer, Felix von Oppen and Jason Alicea, November 2019 (22 pages).

¹⁵⁶⁵ See [Realizing Majorana zero modes in magnetic field-free InAs-Al nanowires with fewer growth constraints](#) by Benjamin D Woods and Mark Friesen, University of Wisconsin-Madison, April 2023 (13 pages).

¹⁵⁶⁶ See [Ternary Logic Design in Topological Quantum Computing](#) by Muhammad Ilyas et al, Purdue and Portland Universities, April 2022 (53 pages).

¹⁵⁶⁷ See [Logical Majorana fermions for fault-tolerant quantum simulation](#) by Andrew J. Landahl et al, Sandia Labs and University of New Mexico, October 2021-February 2023 (23 pages).

¹⁵⁶⁸ See [Ultra-High-Precision Detection of Single Microwave Photons based on a Hybrid System between Majorana Zero Mode and a Quantum Dot](#) by Eric Chatterjee et al, DoE Sandia Labs, January 2023 (19 pages) which is about the use of MZM to detect single photons.

¹⁵⁶⁹ See [A proposal to demonstrate non-abelian anyons on a NISQ device](#) by Jovan Jovanović et al, University of Cambridge, June-July 2023 (43 pages).

Majorana braiding on 27-qubits quantum computers¹⁵⁷⁰. A large **Google AI** team did a similar experiment with 47 qubits from its Sycamore processor and simulating Majorana Edge Modes¹⁵⁷¹. A team led by the **Flatiron Institute** emulated MZM on ten trapped ions of ytterbium¹⁵⁷².

Teams in **Finland** and **Russia** also work on topological qubits¹⁵⁷³.

Research on topological qubits still goes on at **TU Delft** with some recent work on the way to stabilize entanglement of topological qubits¹⁵⁷⁴.

In **France**, a team at the CEA-IRIG in Grenoble (Julia Meyer, Moïra Hocevar, Edith Bellet-Amalric), Pierre Mallet of CNRS Institut Néel in Grenoble, Hugues Pothier at the CEA in Saclay and Pascal Simon at the LPS in Orsay¹⁵⁷⁵ do work on Majorana fermions and on various topological matter, particularly on Andreev's states, the linked states and the physics of weak links, different areas that remain to be explored in these lines. Some of these researchers are conducting joint projects with TU Delft. Marko J. Rančić from TotalEnergies is also exploring the field with generating MZM out of noisy qubits¹⁵⁷⁶.

Majorana fermions qubits

- **theoretically very stable qubits** with low level of required error correction.
- **long coherence time and gates speed** enabling processing complex and deep algorithms.
- **potential qubits scalability**, built with technologies close to electron spin qubits.
- some researches in the topological matter field could be fruitful with no Majorana fermions.

- **topological qubits programming is different and requires an additional software layer.**
- **rather few laboratories involved in this path.**
- **no startup was launched in this field. Microsoft is the only potential vendor. IBM is investigating the field in Zurich.**
- **works at low cryogenic temperatures like superconducting qubits < 20mK.**
- **no Majorana fermion qubit demonstrated yet.**

Figure 394: pros and cons of Majorana fermions and topological qubits. (cc) Olivier Ezratty, 2022-2023.

Majorana zero modes (MZMs) were also found by researchers in **China** in 2022 with iron-based superconductors showcasing topological vertices^{1577 1578 1579}. In February 2020, **John Preskill** (father of the notions of quantum supremacy and NISQ) predicted that by 2030, we will be able to

¹⁵⁷⁰ See [Observing and braiding topological Majorana modes on programmable quantum simulators](#) by Nikhil Harle et al, Yale University, MIT & IBM Research, March 2022 (14 pages). Tested with 27-qubit superconducting systems.

¹⁵⁷¹ See [Noise-resilient Majorana Edge Modes on a Chain of Superconducting Qubits](#) by Xiao Mi et many al, Google AI, April 2022 (24 pages).

¹⁵⁷² See [Dynamical topological phase realized in a trapped-ion quantum simulator](#) by Philipp T. Dumitrescu et al, Nature, Flatiron Institute, July 2021-July 2022 (18 pages).

¹⁵⁷³ See [Half-quantum vortices and walls bounded by strings in the polar-distorted phases of topological superfluid ³He](#) by J.T. Mäkinen, G.E. Volovik et al, 2018 (17 pages).

¹⁵⁷⁴ See [Topological Entanglement Stabilization in Superconducting Quantum Circuits](#) by Guliuxin Jin and Eliska Greplova, TU Delft, May 2022 (10 pages).

¹⁵⁷⁵ See Pascal Simon's presentation [Majorana zero modes around skyrmionics textures](#), 2021 (75 slides).

¹⁵⁷⁶ See [Exactly solving the Kitaev chain and generating Majorana-zero-modes out of noisy qubits](#) by Marko J. Rančić, TotalEnergies, August-November 2022 (16 pages).

¹⁵⁷⁷ See [Ordered and tunable Majorana-zero-mode lattice in naturally strained LiFeAs](#) by Meng Li et al, Nature, May 2022 (38 pages).

¹⁵⁷⁸ See also [Topologically protected quantum entanglement emitters](#) by Jianwei Wang et al, February 2022 (10 pages) which deals with topologically protected matter although not formally a Majorana fermion

¹⁵⁷⁹ See [Dynamics simulation of braiding two Majorana-zero-modes via a quantum dot](#) by Luting Xu et al, Tianjin University, China, April 2023 (6 pages).

demonstrate two entangled topological qubits, against **Jonathan Dowling** (a photonicist) who did not believe it could be created! The object of this symbolic bet? A good beer and a pizza! Jonathan Dowling died in Summer 2020 and will therefore not be able to see if he won or lost his bet in 2030.

By the way, we cover in this part only the physical topological qubits like Majorana fermions not the topological error correction codes implemented with other types of qubits like superconducting qubits.

Vendors



Microsoft Microsoft Research has investigating topological quantum computing and Majorana fermions for quite a few years but has not shown any prototype.

The company is making a bet there, up to saying that “*if they fail, everybody will also fail in quantum computing*”. While being a little arrogant and a very risky bet, it would bring lots of strategic advantages if it worked! Indeed, Majorana qubits would be much more reliable and generate fewer errors, with the implication that we could avoid using some of the classical quantum error correction codes that are implemented with other types of qubits¹⁵⁸⁰.

A Fields Medal in 1986 for his work on the Poincaré conjecture, Fields Medal winner **Michael Freedman** joined Microsoft in 1997, coming from the University of Santa Barbara. He demonstrated with Alexei Kitaev the possibility of implementing quantum computing with a hypothetical particle, the Majorana fermion, conceptualized in 1937 by Ettore Majorana¹⁵⁸¹. This fermion is a strange particle, whose charge and energy are zero and which is its own antiparticle. Freedman and Kitaev were hired by Microsoft Research. Created by Michael Freedman, Microsoft Quantum Santa Barbara (Station Q) is located on the campus of the UCSB (University of California Santa Barbara). They were complemented by **Leo Kouwenhoven**'s team based in Microsoft's Delft Lab in the Netherlands and with **Charles Marcus** from the Niels Bohr Institute who also joined Microsoft Research. They both left Microsoft in 2022 and 2021. Microsoft also collaborates with **Purdue University** in Indiana, where its dedicated research team **Microsoft Quantum Purdue** works on III-V superconductors.

Majorana fermions are strange behaviors of electrons and their spin that are found at both ends of superconducting wires. They operate at very low temperatures, as for superconducting and silicon-based qubits, at about 15-20 mK¹⁵⁸².

Seen up close, these qubits are sophisticated variants of superconducting qubits (Figure 395). These "topological" mesh associations provide protection against qubit decoherence because the shape of the braids does not matter as long as their topology is stable (Figure 396).

Microsoft announced at the Build conference in May 2018 that they would release their first fermion-based quantum computer from Majorana in 2023¹⁵⁸³. After Leo Kouwenhoven's 2017 paper withdrawal in 2021, this planning seems somewhat challenging¹⁵⁸⁴. But let's not count Microsoft out of the game too rapidly. All discoveries have their ups and downs.

¹⁵⁸⁰ Here are a few examples on how Microsoft communicated on Majorana fermions when they started being vocal about it: [Microsoft Ready to Build a Quantum Computer](#) by Juliette Raynal, 2016, [A Software Design Architecture and Domain-Specific Language for Quantum Computing](#), 2014 (14 pages), [Quantum Computing at Microsoft](#) (56 slides) and [Quantum Computing Research at Microsoft](#) (59 slides) by Dave Wecker and [A short introduction to topological quantum computation](#) by Ville Lahtinen and Jiannis Pachos, 2017, (43 pages). And some videos: [keynote of November 2017](#) with Leo Kouwenhoven (43 mn), [Build conference of May 2018](#) on Q# (1h15mn) and [Majorana qubits](#) by Xiao Hu, in May 2017 (22 mn).

¹⁵⁸¹ See [Topological Quantum Computation](#) by Michael H. Freedman, Alexei Kitaev, Michael J. Larsen and Zhenghan Wang, 2002-2009 (12 pages).

¹⁵⁸² See [Majorana Qubits](#) by Fabian Hassler, 2014 (21 pages).

¹⁵⁸³ See this video ad: [Introducing Quantum Impact \(Ep. 0\)](#), February 2020 (4 minutes).

¹⁵⁸⁴ See [Topological quantum computing for beginners](#), by John Preskill (55 slides).

If a failure meant *stop all research*, Thomas Edison would not have discovered the light bulb and many vaccines and cancer treatments wouldn't see the light of day!

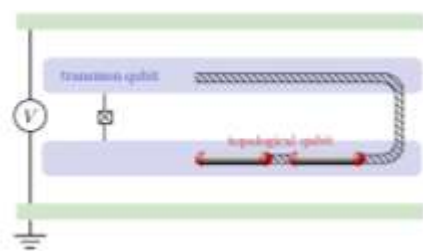


Fig. 6: Read out of a parity qubit in a Cooper pair box. Two superconducting islands (blue), connected by a split Josephson junction (crosses) form the Cooper pair box. The topological Majorana qubit is formed by four Majorana fermions (red spheres), at the end points of two unsplit segments of a semiconductor nanowire (striped ribbon indicates the depleted region). A magnetic flux Φ enclosed by the Josephson junction controls the charge sensitivity of the Cooper pair box. To read out the topological qubit, two of the four Majorana fermions that encode the logical qubit are moved from one island to the other. Depending on the quasiparticle parity, the resonant frequency in a superconducting transmission line enclosing the Cooper pair box (green) is shifted upwards or downwards by the amount which is exponentially small in E_J/E_C .

Figure 395: typical combination of a topological and a superconducting qubit. Source: [Majorana Qubits](#) by Fabian Hassler, 2014 (21 pages).

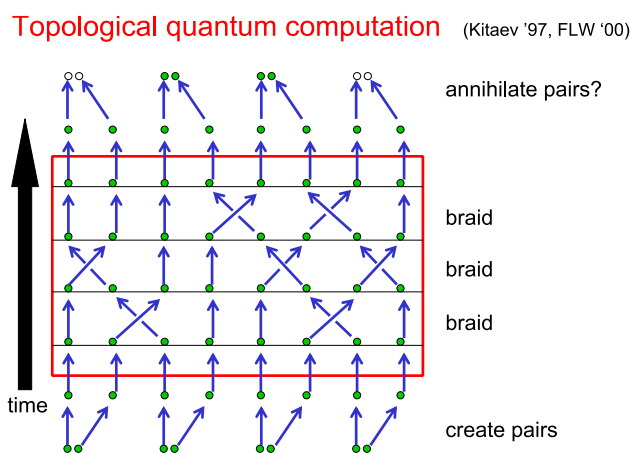


Figure 396: how braiding is sequenced during topological computing. Source: [Topological quantum computing for beginners](#), by John Preskill (55 slides).

In 2022, as Kouwenhoven was leaving Microsoft, the company published some new results related to Majorana fermions and scalable quantum computing. It dealt with the observation of a 30 μeV topological gap in indium arsenide-aluminum heterostructures. But it seemed that this topological qubit was only digitally simulated and not implemented practically¹⁵⁸⁵. Just before, in February 2022, another Microsoft team published a paper related to a quantum error correction code (planar Floquet code) that was suitable for topological qubits and with a very high threshold exceeding 1% (meaning, qubits with 1% error rates are sufficient to implement error correction which seems a very high error-rate compared to what would be needed with superconducting qubits and surface codes, that require errors way below 0.1%)¹⁵⁸⁶.

Between November 2022 and June 2023, Microsoft upped again the ante with publishing a paper on the discovery of Majorana zero modes (MZM), discussing a lot about the TGP protocol used to detect a topological phase^{1587 1588 1589 1590} (Figure 397). But again and again, the results were contested. This paper was actually first submitted to PRX Quantum and rejected by their referees. The paper was then submitted it to PRA with different referees who accepted it although, with some reserves on the lack of experimental data^{1591 1592}. It smells fishy at first glance!

¹⁵⁸⁵ See [In a historic milestone, Azure Quantum demonstrates formerly elusive physics needed to build scalable topological qubits](#) by Jennifer Langston, March 2022, [Microsoft has demonstrated the underlying physics required to create a new kind of qubit](#) by Chetan Nayak, March 2022, based on [Protocol to identify a topological superconducting phase in a three-terminal device](#) by Dmitry Pikulin et al, March 2021 (28 pages).

¹⁵⁸⁶ See [Performance of planar Floquet codes with Majorana-based qubits](#) by Adam Paetznick, Nicolas Delfosse et al, February 2022 (20 pages).

¹⁵⁸⁷ See [InAs-Al Hybrid Devices Passing the Topological Gap Protocol](#) by Morteza Aghaee et al, PRB, July 2022-June 2023 (54 pages).

¹⁵⁸⁸ See [Microsoft's quantum machine: New data available today](#) by Chetan Nayak, Microsoft, November 2022.

¹⁵⁸⁹ See the webinar [Why and what is the future of the topological qubit?](#) by Chetan Nayak, Microsoft, November 2022. Microsoft announced that its Majorana Zero Mode qubits could have fidelities in the 6-nines range, meaning errors around 10^{-6} .

¹⁵⁹⁰ See [Microsoft says its weird new particle could improve quantum computers](#) by Karmela Padavic-Callaghan, New Scientist, June 2023.

¹⁵⁹¹ See [Editorial: Transparency in Physical Review Articles](#), Randall D. Kamien et al, June 2023.

¹⁵⁹² Sergei Frolov [tweet](#) explaining that "Physical review editors are lying. They manipulated peer review to go around our comments. 1 year ago PRX reached out to @VincentMourik and got a full run down on this paper. It got Rejected. Then PRB took it... But it is the same editors!".

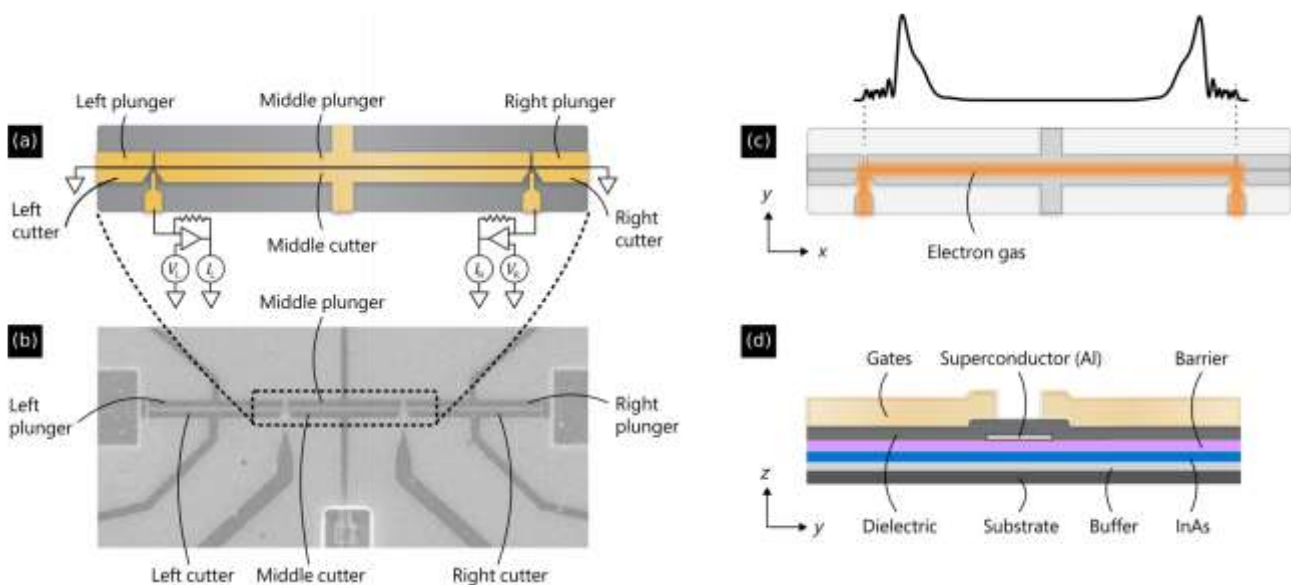


Figure 397: Microsoft's latest iteration of a MZM, published in 2023. Source: [InAs-Al Hybrid Devices Passing the Topological Gap Protocol](#) by Morteza Aghaee et al, PRB, July 2022-June 2023 (54 pages).

Overall, these Microsoft's research results have a very low TRLs have not been successful so far. We have for example no idea about the number of physical or logical qubits that they could implement, and how these are driven from the control and readout standpoint.

Microsoft obviously also invested on software development, first with its Liquid platform, then with F# for scripting and with the Q# language used for quantum programming, launched at the end of 2017. One of the contributors to these efforts is researcher **Krysta Svore** from Columbia University. In 2018, Microsoft recruited a certain **Helmut Katzgraber**, one of the apostles of D-Wave quantum annealing and MBQC (measurement-based quantum computers)¹⁵⁹³.



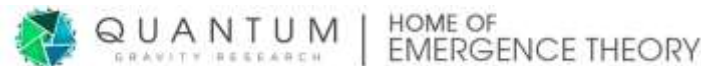
Q-Logo (2021, USA, 6.2M) wants to create a portable quantum computer using topological insulators, and operating at room temperature.

Their CTO is David Carroll, a quantum materials physicist and the Director of the Center for Nanotechnology and Molecular Materials at Wake Forest University in North Carolina. The startup which is based in Alabama has not released any public roadmap.



Nokia's Bell Labs in the USA, located in Murray Hill, New Jersey, work *or worked* on topological qubits¹⁵⁹⁴.

Nokia also supports Oxford University's [Quopal](#) initiative on the use of quantum in machine learning. Nokia likes to remind us that Grover and Shor's algorithms were discovered by their creators when they worked at the Bell Labs. Nokia is also working on quantum cryptography, at least at the level of its transport on optical fibers, as demonstrated by this [partnership](#) with SK Telecom of 2017.



There is even a private research company, **Quantum Gravity Research** (2009, USA) with an overarching goal to create a unified physics theory encompassing gravity and quantum physics that also undertakes research in topological computing¹⁵⁹⁵.

¹⁵⁹³ See [Quantum Driven Classical Optimizations](#), August 2018 (28 min video).

¹⁵⁹⁴ See [Quantum computing using novel topological qubits at Nokia Bell Labs](#) published in 2017, which describes their approach with topological qubits.

¹⁵⁹⁵ See [Exploiting Anyonic Behavior of Quasicrystals for Topological Quantum Computing](#) by Marcelo Amaral et al, Quantum Gravity Research, July 2022 (20 pages).

The organization created by Klee Irwin employs about 20 researchers like Fang Fang, Raymond Aschheim, Marcelo Amaral, Dugan Hammock, Richard Clawson and Michel Planat. They envision “a specific substructure of spacetime at the smallest scale, so that in this view physical reality is like a mosaic tiling language of Planck scale, 3-dimensional, tetrahedron-shaped pixels”. Let’s say it is quite difficult to fact-check these sorts of claims and their practicality!

Trapped ions qubits

Trapped ions are positively ionized atoms that are trapped by electrodes and sometimes also magnetically in a confined space and placed next to each other. The atoms are generally alkaline metals from the second column of Mendeleev's table (called "Group IIA" in Mendeleev's notation or group 2 in the modern notation, with beryllium, magnesium, calcium, strontium, barium), then as ytterbium which is a rare earth in the lanthanide family, and finally, quite rarely, metals of group IIB or 12 (zinc, cadmium, mercury)¹⁵⁹⁶.

History

Before the very notion of a qubit even existed, scientists tried to control ions in space. **Wolfgang Paul** created in 1953 a way to control ions with a mass spectrometer avoiding the use of a magnetic field, named the “Paul trap”. He got the Nobel prize in Physics in 1989. Later, in 1959, **Frans Penning** and **Hans Dehmelt** were able to control individual electrons with a magnetron trap that was later named the “Penning trap”. Penning traps are still being studied, particularly in their 2D variant.

In the USA, **David Wineland** from NIST created the laser cooling technique starting in 1979, using Doppler effect with magnesium ions. He got the Nobel prize in physics in 2012 along with Serge Haroche. In 1989, he used the technique to cool ions at their zero-point energy of motion with the sideband cooling technique that goes farther than Doppler cooling¹⁵⁹⁷.

Juan Ignacio Cirac and **Peter Zoller** from the University of Innsbruck in Austria proposed in 1995 a blueprint to create a gate-based quantum processor with a linear trap of ions controlled by laser beams¹⁵⁹⁸. They initiated a long-lasting experience in the field at Innsbruck, which led to the creation of the startup **AQT** in 2017.

Science

Here are some specifics of trapped ions qubits... (Figure 398).

Why ions? The interest of exploiting ions is to allow to trap them magnetically or with electrodes. It is also possible to couple them at long distance, of the order of several tens of microns. It can also be hybridized with several ion types mixed together, like calcium and strontium, to get their related benefit such as fast gates for calcium and stability for strontium¹⁵⁹⁹. The used elements have several common characteristics related to their electron layer configuration such as excitation levels from the ground state that are of short duration and allow their use for atoms cooling with laser and the Doppler effect. The energy state corresponding to the $|0\rangle$ and the excited energy level corresponding to $|1\rangle$ state are both stable over time, which facilitates the implementation of quantum gate operations.

¹⁵⁹⁶ See this interesting perspective on trapped ions qubits in [Introduction to Trapped Ion Quantum Computing](#) by Gabriel Mintzer from MIT, February 2020.

¹⁵⁹⁷ It is too complex to describe the Doppler cooling limit and how sideband cooling works. See [Laser cooling of trapped ions](#) by Jürgen Eschner, Giovanna Morigi, Ferdinand Schmidt-Kaler and Rainer Blatt, 2003 (13 pages) which describes various ions cooling techniques.

¹⁵⁹⁸ See [Trapped Ion Quantum Computing: Progress and Challenges](#) by Colin Bruzewicz et al from MIT, April 2019 (56 pages). This is a very well-documented state-of-the-art review of trapped ion technology. And the founding article [Quantum Computations with Cold Trapped Ions](#) by Juan Ignacio Cirac and Peter Zoller, 1995 (4 pages).

¹⁵⁹⁹ See [Benchmarking a high-fidelity mixed-species entangling gate](#) by A. C. Hughes et al, Oxford University, August 2020 (7 pages).

Long coherence time. Trapped ions usually have a rather long coherence time of up to several tens of seconds. Although gate times are long, the ratio between coherence time and gate time is currently quite good at up to 10^6 , while it is at 10^3 for superconducting qubits and about 200 for cold atoms qubits.

trapped ions qubits

- **identical ions** => no calibration required like with superconducting/electron spin qubits.
- **good qubits stability.**
- **excellent qubit gate fidelities** and high ratio between coherence time and gate time => supports deep algorithms in number of gate cycles.
- **entanglement** possible between all qubits on 1D architecture which speeds up computing, avoiding SWAP gates.
- requires some cryogeny at **4K to 10K** => simpler.
- **easy to entangle ions with photons** for long distance communications.

- **unproven scalability options beyond 50 qubits** (ions shuttling, 2D architectures, photon interconnect, micro-Penning traps).
- **two-qubit gate times increasing with ion distance** in 1D and 2D settings.
- **relatively slow computing due to long quantum gate times which may be problematic for deep algorithms.**

Figure 398: pros and cons of trapped ions qubits. (cc) Olivier Ezratty, 2022-2023.

Qubit fidelities. Trapped ions show a low error rate with up to single-qubit 99.99987% and two-qubit gates 99.94% fidelity (Figure 399). The table below illustrates these fidelities depending on the quantum gate implementation and used ions. This and long coherence time make it possible to theoretically execute "deep algorithms" with a large number of quantum gates and to obtain a good quantum volume, to use IBM's terminology. However, this error rate seems to increase with the number of qubits, at least in 1D architectures like the one from IonQ.

There's a tendency with trapped ions vendors like IonQ and Quantinuum to measure qubit fidelities with the SPAM method which encompasses the whole process from state preparation to measurement. In March 2022, IonQ tested its new barium ions and improved fidelities with a record 99.96% SPAM fidelity. Quantinuum reached simultaneously a SPAM fidelity of 99.9904% also with barium ions¹⁶⁰⁰, which is clearly best-in-class in the qubit world.

Type	Method	Fidelity	Time (μ s)	Species	Ref.
1-qubit	Optical	0.99995	5	$^{40}\text{Ca}^+$	Bermudez 2017
	Raman	0.99993	7.5	$^{43}\text{Ca}^+$	Ballance 2016
	Raman	0.99996	2	$^9\text{Be}^+$	NIST 2016
	Raman	0.99	0.00005	$^{171}\text{Yb}^+$	Campbell 2010
	Raman	0.999	8	$^{88}\text{Sr}^+$	Keselman 2011
	μ wave	0.999999	12	$^{43}\text{Ca}^+$	Harty 2014
	μ wave		0.0186	$^{25}\text{Mg}^+$	Ospelkaus 2011

Type	Method	Fidelity	Time (μ s)	Species	Ref.
2-qubit (1 sp.)	Optical	0.996	–	$^{40}\text{Ca}^+$	Erhard 2019
	Optical	0.993	50	$^{40}\text{Ca}^+$	Benhelm 2008
	Raman	0.9991(6)	30	$^9\text{Be}^+$	NIST 2016
	Raman	0.999	100	$^{43}\text{Ca}^+$	Ballance 2016
	Raman	0.998	1.6	$^{43}\text{Ca}^+$	Schafer 2018
	Raman	0.60	0.5	$^{43}\text{Ca}^+$	Schafer 2018
	μ wave	0.997	3250	$^{43}\text{Ca}^+$	Harty 2016
	μ wave	0.985	2700	$^{171}\text{Yb}^+$	Weidt 2017
	Ram./Ram.	0.998(6)	27.4	$^{40}\text{Ca}^+ / ^{43}\text{Ca}^+$	Ballance 2015
	Ram./Ram.	0.979(1)	35	$^9\text{Be}^+ / ^{25}\text{Mg}^+$	Tan 2015

Adapted from Bruzewicz et al.

Figure 399: some trapped ions fidelities obtained with different atoms. Data is a little old but since it is coming from research labs, it is not far from what is obtained in 2023 by commercial vendors like IonQ and Quantinuum.

Source: [lecture 1](#) on trapped ions, H  l  ne Perrin, February 2020 (77 slides).

¹⁶⁰⁰ See [High fidelity state preparation and measurement of ion hyperfine qubits with I>1/2](#) by Fangzhao Alex An et al, March 2022 (5 pages).

Connectivity. Trapped ions qubits can all be entangled with each other with using phonons, but it depends on how they are distributed in space¹⁶⁰¹. This simplifies the implementation of many algorithms, avoiding the usage of costly SWAP gates to connect distant qubits. The shortcoming is that it doesn't scale well. The larger the number of qubits, the slower the two-qubit gates will be and the lesser quality they will have. One alternative is to use Rydberg states for two-qubit gates at the expense of a nearest neighbor connectivity instead of one-to-many connectivity. Ion shuttling is another option to scale the number of qubits, at the expense of circuit execution times.

Calibration. Since these qubits are atoms, they are identical and do not require (much) calibration adjustments like with superconducting qubits whose physical properties vary from one qubit to another depending on their materials and manufacturing. Still, qubit transition frequency can vary across the device, for example due to radiofrequency magnetic fields.

Ion variations. There are five main variations of trapped ions being used, depending on the energy transitions applied to manage the two states of a qubit¹⁶⁰². Each of these modes correspond to different transition frequencies:

- **Zeeman qubits** use electromagnetic waves of a few MHz with magnetic field control. They are very sensitive to it but allow to have qubits with a very low error rate once this field is well controlled¹⁶⁰³. Raman based control of these types of qubits is possible¹⁶⁰⁴.
- **Hyperfine structure qubits** use microwaves of a few GHz and laser-based Raman transitions¹⁶⁰⁵. This works with ions having a non-zero spin nucleus. The other cases concern ions with zero spin nuclei, i.e., those whose proton and neutron numbers are both even. This explains why some elements such as calcium are sometimes used in several of these categories, with different isotopes such as ⁴⁰Ca+ in optical qubits and ⁴³Ca+ in qubits of hyperfine structure. The number of neutrons in these ions changes the spin of the nucleus of atoms and its hyperfine energy states. In this category, IonQ and Quantinuum are using hyperfine structure qubits driven by lasers and Oxford Ionics is using microwave gates.
- **Fine structure qubits** use submillimeter waves of a few THz. These are exotic qubits not used in the commercial world.
- **Optical qubits** use photons of a few hundred THz. AQT is using this type of qubits.
- **Rydberg qubits** use so-called Rydberg energy states controlled by VUV ultraviolet rays (vacuum ultraviolet, not transmitted in air, needs vacuum), with wavelengths under 122 nm¹⁶⁰⁶ or at about 243 nm which propagates well in air. It is used by the new startup Crystal Quantum Computing (France), the leading scheme coming from the group of Markus Hennrich from Stockholm University¹⁶⁰⁷.

¹⁶⁰¹ See [Benchmarking an 11-qubit quantum computer](#) by Christopher Monroe et al, March 2019 (8 pages).

¹⁶⁰² See [Ion traps you never knew existed](#) by M. Malinowski, February 2022 which makes an interesting inventory of trapped ions settings.

¹⁶⁰³ See [Comparing Zeeman qubits to hyperfine qubits in the context of the surface code: ¹⁷⁴Yb⁺ and ¹⁷¹Yb⁺](#) by Natalie Brown, April 2018 (7 pages).

¹⁶⁰⁴ See [Fault-Tolerant Parity Readout on a Shuttling-Based Trapped-Ion Quantum Computer](#) by J. Hilder, et al, PRX, February 2022 (16 pages).

¹⁶⁰⁵ See [Controlling Qubits With Microwave Pulses Reduces Quantum Computer Error Rates, Increases Efficiency](#) by Matt Swayne, 2020, which references [Robust and resource-efficient microwave near-field entangling ⁹Be⁺ gate](#) by G. Zarantonello, November 2019 (6 pages). See glossary for Raman transition.

¹⁶⁰⁶ See for example [Speeding-up quantum computing using giant atomic ions](#) by Stockholm University, April 2020.

¹⁶⁰⁷ See [Sub-microsecond entangling gate between trapped ions via Rydberg interaction](#) by Chi Zhang, Markus Hennrich et al, Stockholm University, August 2019 (23 pages).

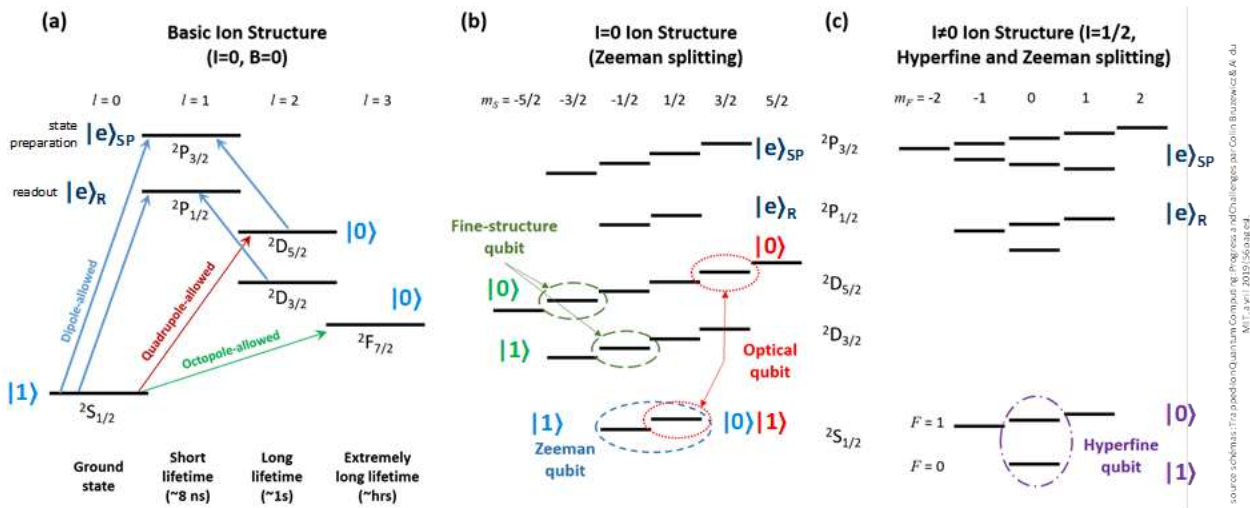


Figure 400: various types of trapped ions and their respective energy transitions.
 Source: [Trapped Ion Quantum Computing: Progress and Challenges](#) by Colin Bruzewicz et al from MIT, April 2019 (56 pages).

Figure 400 contains a description of these variants based on ion energy levels and transitions. On the left, a generic structure of ion energy levels with the transitions allowing the change of qubit state and those used to prepare the qubit state or to read it. These charts showing atoms electronics energy transitions including fine and hyperfine transitions are called Grotrian diagrams. In the middle and on the right, the different energy transitions used to define the $|0\rangle$ and $|1\rangle$ of the qubit. The height between the two levels characterizes the energy level that separates these two states. The higher it is, the higher the frequency used to modify the qubit state, going from radio waves of a few MHz to extreme ultraviolet in the case of Rydberg qubits.

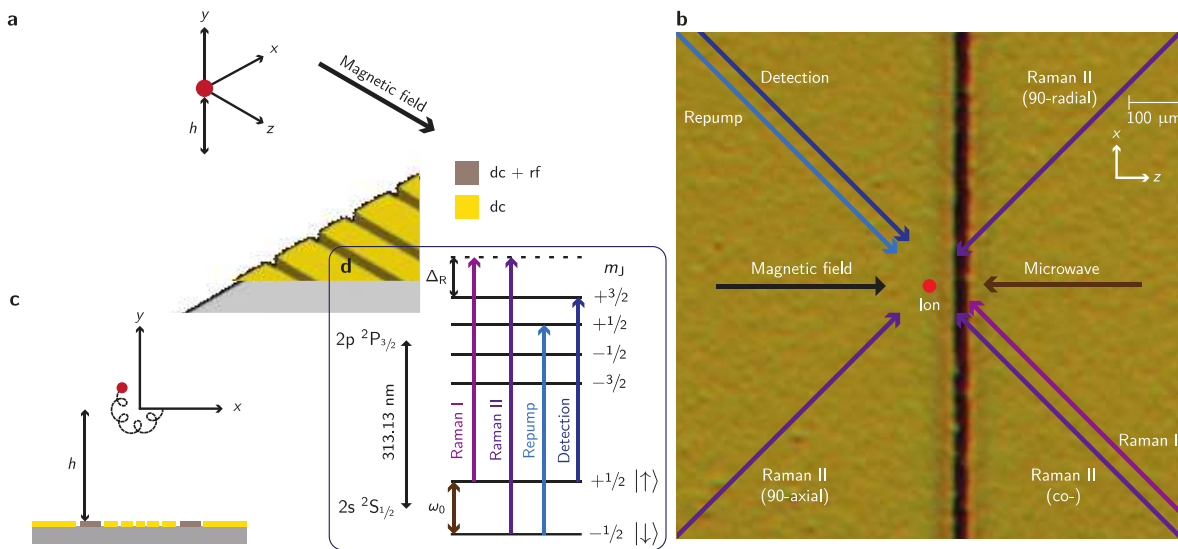


Figure 401: proposal for an array of trapped ions.
 Source: [Unit cell of a Penning micro-trap quantum processor](#) by Shreyans Jain, Jonathan P. Home et al, August 2023 (10 pages).

The spatial stabilization of trapped ions is achieved in two main ways with ion traps that allow individual control of their position¹⁶⁰⁸:

¹⁶⁰⁸ See many details in [Multi-wafer ion traps for scalable quantum information processing](#) by Chiara Decaroli, 2021 (248 pages).

- With a **magnetic field** and an **electric quadrupole**: these are the Penning traps, invented in 1959. Among other places, they have been tested at the ETH Zurich in Jonathan P. Home's team and in a 2D version which has the advantage of being theoretically scalable^{1609 1610} (Figure 401).
- With a **variable electric field**: these are the Paul traps named after Wolfgang Paul. These traps are either linear in 1D structure (in Figure 402 in (f)) or flattened to create 2D structures¹⁶¹¹. They are the most often used. The flat version is used by Quantinuum and IonQ.

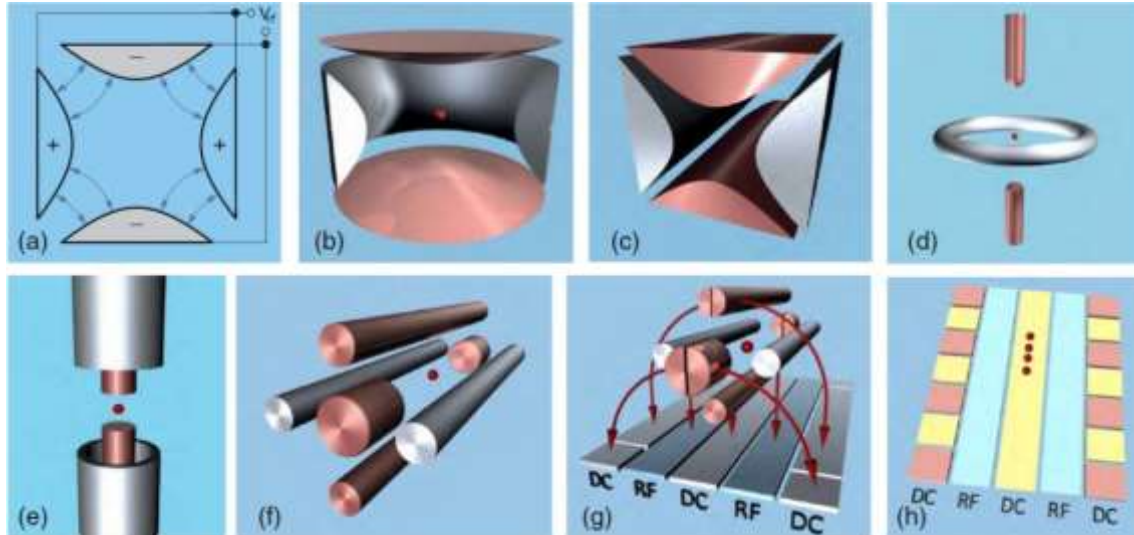


Figure 402: the various ways to trap ions. RF Paul trap geometries with (a) RF trapping basic concept with quadrupolar fields oscillating at an RF frequency produced by parabolic electrodes. (b) The simplest cylindrically symmetric version of the basic RF trap. (c) The simplest translationally symmetric version of the basic RF trap. (d,e) Topologically equivalent deformations of the geometry shown in (b). (f) Topologically equivalent deformations of the geometry shown in (c) with additional endcap electrodes added to form a four-rod, linear trap. (g) The four-rod trap in (f) may be deformed such that all electrodes reside in a single plane, forming a linear "surface-electrode trap." (h) A subset of the electrodes in a linear trap [a surface-electrode trap is depicted here, but segmentation may be applied to other linear trap geometries, such as that shown in (f)] may be segmented to allow trapping in multiple zones, along the axial direction.

Source: [Trapped Ion Quantum Computing: Progress and Challenges](#) by Colin Bruzewicz et al from MIT, April 2019 (56 pages).

These various traps are implemented with integrated circuits using variations of direct current (static) and radio-frequency electrodes to provide ion trapping fields. Then, lasers play several roles to cool the ions with the Doppler effect and by sideband cooling to slow down phonons (these are inter-ions vibrations, kind of shock waves)¹⁶¹², to initialize the energy state of the qubits to its ground $|0\rangle$ state, to create quantum gates and finally, and for qubits state readout¹⁶¹³. Laser beams can be conveyed using wave guides. The ions are usually aligned in rows and separated by about 2 to 5 μm as shown in Figure 403 but other settings are proposed in 2D fashion, like what is planned by Quantinuum, beyond their racetrack 2023 configuration.

Temperature. Trapped ions are supposed to operate at room temperature. In practice, they generate an annoying heating effect, which is not fully explained at the moment. This may require some cooling between 4K and 10K¹⁶¹⁴.

¹⁶⁰⁹ See [Scalable arrays of micro-Penning traps for quantum computing and simulation](#) by S. Jain, Jonathan P. Home et al, April 2020 (21 pages).

¹⁶¹⁰ See [Unit cell of a Penning micro-trap quantum processor](#) by Shreyans Jain, Jonathan P. Home et al, August 2023 (10 pages).

¹⁶¹¹ See [Controlling Two-Dimensional Coulomb Crystals of More Than 100 Ions in a Monolithic Radio-Frequency Trap](#) by Dominik Kiesenhofer, Christian F. Roos et al, April 2023 (16 pages).

¹⁶¹² Ions are controlled in the Lamb-Dicke regime, when ions motion is much smaller than the wavelength of the laser light that is used to control it. This allows the manipulation of the ion's quantum states.

¹⁶¹³ See [Quantum information processing with trapped ions](#) by Christian Roos, 2012 (53 slides) on how trapped ion qubits are driven.

¹⁶¹⁴ See [Closed-cycle, low-vibration 4 K cryostat for ion traps and other applications](#) by P. Micke et al, May 2019 (15 pages) which describes a cryostat for ion trapped processors using a pulsed head.

The interest of such cooling is also to improve the quality of the ultra-high vacuum chamber with cryo-pumping, like with cold atoms settings. It also avoids the potential side effects of thermal photons. Lasers and ions readout imagers may also need some cooling at reasonable temperatures, from 10K to -35°C depending on the case (Figure 404). Scientific cameras are also thermoelectrically cooled at moderate negative temperatures, but not always. Lasers are nowadays usually only passively air cooled and their controllers and supplies use fans.

At last, some ion chips now include integrated detectors like SNSPDs (superconducting nanowire single-photon detectors) which are cooled at 4K. Researchers from the University of Innsbruck and from ETH Zurich are thinking about making the trapped ion technology "portable", using compact cryogenics and requiring more compact lasers¹⁶¹⁵.

They are part of the EU-funded **PIEDMONS** project (E2020). It also involves Infineon Austria¹⁶¹⁶.

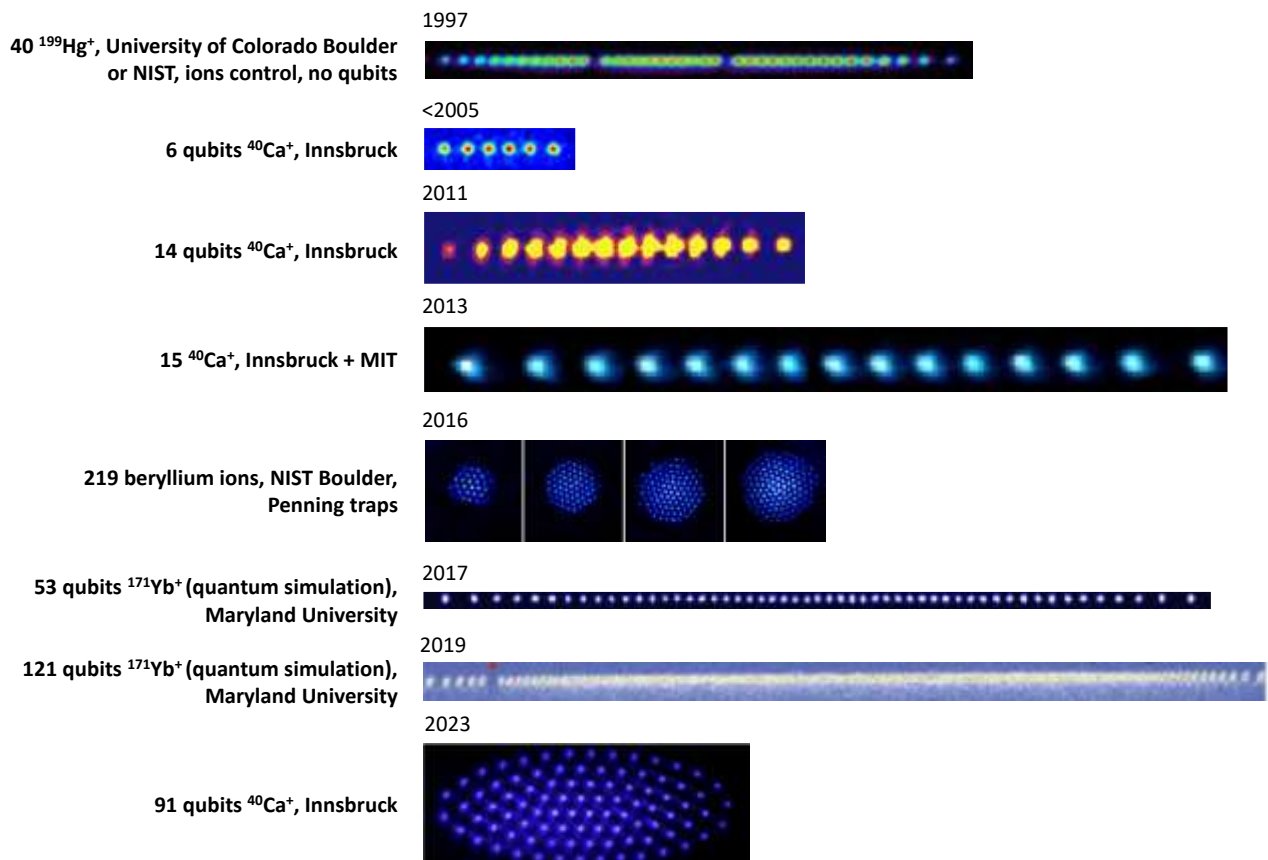


Figure 403: different lines of trapped ions over time. Compilation: Olivier Ezratty. 2020-2023.

Trapped ions or ion traps? These two namings are used but let's separate them. Trapped ions are two-level quantum objects, aka qubits. Ion traps are the circuits on which these ions are controlled electromagnetically. Thus, when referring to a qubit type, I prefer to use the trapped ions naming.

Use cases. Trapped ions have at least two other use cases: quantum memories, and their integration in quantum repeaters for secure quantum telecommunications, including quantum keys distribution¹⁶¹⁷. This involves interactions between trapped ions and photons, using cavities.

Scale-in. The current record of well controlled trapped ions is around 32. What currently limits scalability is the ions heating rate related to the decoherence on the motional "quantum bus" connecting

¹⁶¹⁵ See [Quantum computers to become portable](#), August 2019.

¹⁶¹⁶ See [2D Linear Trap Array for Quantum Information Processing](#) by Philip C. Holz, Rainer Blatt et al, September 2020 (20 pages).

¹⁶¹⁷ See [Single-qubit quantum memory exceeding 10-minute coherence time](#) by Ye Wang (Chine), 2017 (6 pages).

the qubits together. It grows with the surface and is still not fully understood. One solution are micro Penning trap arrays developed by Jonathan Home at ETH Zurich, which gets rid of the RF fields confining the ions. Penning traps can control over 100 ions but are not really “useful”.

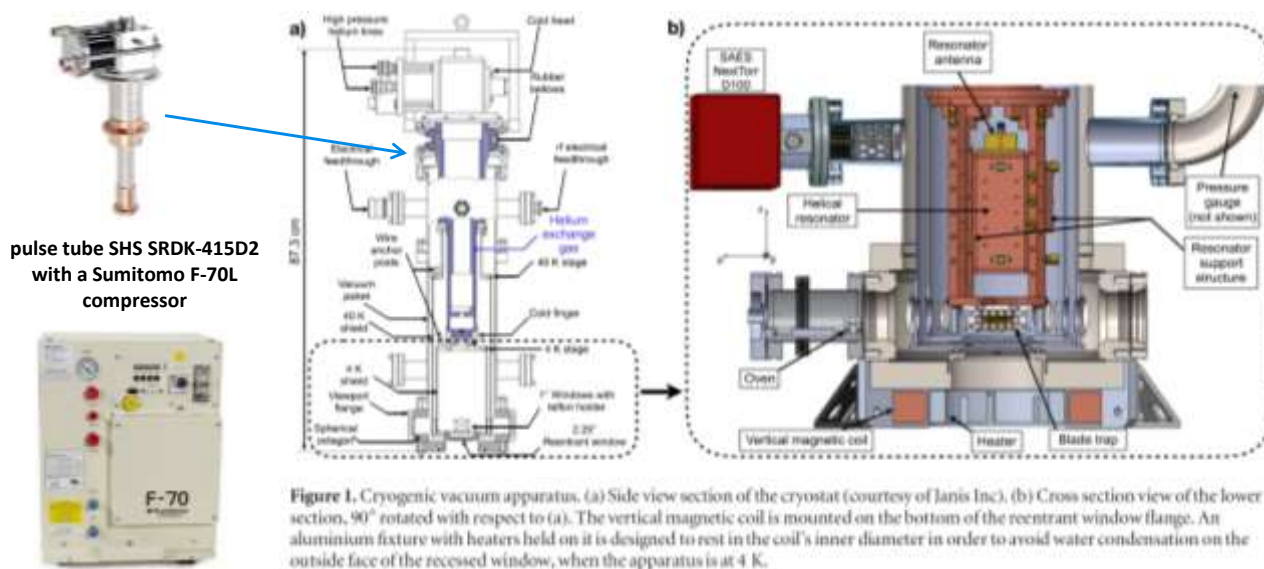


Figure 404: the 4K cryostat used a while ago by Christopher Monroe's team at the University of Maryland to trap more than a hundred ytterbium ions. It operated a 4.2K SHS pulse tube and a Sumitomo compressor¹⁶¹⁸. Source: [Cryogenic trapped ion system for large scale quantum simulation](#) by Christopher Monroe et al, 2018 (17 pages).

Another avenue is using shuttling ions within various zones in a chip¹⁶¹⁹ ¹⁶²⁰. This is the basis of rather old research and is still pursued practically by Quantinuum in their future 2D architecture. It seems to be a credible approach although being plagued by speed constraints.

Scale-out. The most common solution consists in connecting ion qubits with entangled photons in potentially long distances. This would enable the creation of distributed quantum computing architectures, a plan devised among others by IonQ to circumvent the scalability limitations of their qubits¹⁶²¹. Links of over 400 m were tested by a team of researchers led by Tracy Northup and Ben Lanyon from the University of Innsbruck with two calcium ions separated by 230 meters using a 520 m long optical fiber, to be later expanded to 50 km¹⁶²² ¹⁶²³. There is still a long way to go before it enables distributed quantum computing.

¹⁶¹⁸ See the thesis [Towards Cryogenic Scalable Quantum Computing with Trapped Ions](#) by Matthias Brandl, 2016 (138 pages) which documents very well the overall engineering of a quantum computer based on trapped ions.

¹⁶¹⁹ See [Building a prototype for the world's first large-scale quantum computer](#), 2022, related to [Blueprint for a microwave trapped ion quantum computer](#) by Bjoern Lekitsch et al, ScienceAdvances, February 2017 (11 pages). It deals with microwave gates using a static magnetic field with high fidelities and low crosstalk, a technique proposed by Mintert and Wunderlich in 2001. It adds ions transport between trapped ions modules. Laser-based gate control doesn't scale well due to the way phonons work and also due to the complexity of laser beams alignment. They plan to use silicon circuits and X-junction plus on-chip control electronics. Trapping ions would require an area of 103.5×103.5 m² and 23x23 connected vacuum chambers corresponding to the guestimate in 2017 of what was needed to factorize an RSA key of 2048 bits. Now, it's 100 times fewer qubits. It still makes 10.3x10.3 m² with a power dissipation of 300W per module, so, with 4 modules now. It is surprisingly low and deserves some recalculation. See also [A Shuttle-Efficient Qubit Mapper for Trapped Ion Quantum Computers](#) by Suryansh Upadhyay et al, April 2022 (7 pages) which is also pursuing an ion shuttling approach.

¹⁶²⁰ See [High-Fidelity Transport of Trapped-Ion Qubits in a Multi-Layer Array](#) by Deviprasath Palani, Tobias Schaetz et al, University of Freiburg, May 2023 (8 pages).

¹⁶²¹ See [Large Scale Modular Quantum Computer Architecture with Atomic Memory and Photonic Interconnects](#) by Christopher Monroe et al, 2014 (16 pages).

¹⁶²² See [Entanglement of Trapped-Ion Qubits Separated by 230 Meters](#) by V. Krutyanskiy, Maria Galli, Nicolas Sangouard, Tracy Northup et al, PRL, February 2023 (22 pages).

¹⁶²³ See [Atom-photon coupling with trapped ions](#) by Tracy Northup, 2022 (40 slides).

The current showstopper seems to be the very low success rate of these photonic entangled Bell pairs of about 2.18×10^{-4} ^{1624 1625}.

Qudits. One other escape route to scalability is to create qudits using ions and several energy levels extending the Hilbert computing space. The most recent record is with 13 energy levels obtained with $^{137}\text{Ba}^+$ ions controlled by four different lasers¹⁶²⁶. It was evaluated using SPAM benchmarking (state preparation and measurement) with $91.7\% \pm 0.3\%$ fidelities. Some work in Russia deals with code compilation for qudits¹⁶²⁷.

Instead of qudits, there is also a possibility to encode multiple qubits per ions¹⁶²⁸.

Quantum simulations can also be done with trapped ions, so far, with up to 51 qubits¹⁶²⁹. It has also been proposed for the simulation of linear vibronic coupling models (LVCMs)¹⁶³⁰. But this is not available in the commercial domain like with neutral atoms quantum simulations.

Qubit operations

The general principle of trapped ion qubits is as follows:

- **Preparation** with neutral atoms being first heated in a small heating oven and then ionized and cooled by laser beams. Ions are then confined in vacuum in different ways by a magnetic and/or electric fields with variants of Paul and Penning traps as seen earlier. Qubits initialization is relying on electric dipole or quadrupole transitions driven by lasers to set them up at the right energy level corresponding to the $|0\rangle$ ground state. All this happens in an ultra-vacuum chamber.
- **Qubit quantum state** corresponds to two relatively stable energy levels of the trapped ions that are controllable by optical or microwave transitions.
- **Single-qubit quantum gates** are activated by microwave, laser or magnetic dipole electric fields. These gates are very slow compared to superconducting qubit gates, at around $1 \mu\text{s}$. Gates could be as fast as 10 ns with hyperfine qubits but with lower fidelities.
- **Two-qubit quantum gates** often use lasers beams and exploit the phonon phenomenon that links atoms together by vibrations that propagate from one atom to another, which is valid for qubits aligned in linear Paul traps¹⁶³¹. It however doesn't scale well beyond a couple dozen ions. Gates are quite slow, at around $15 \mu\text{s}$ to 1 ms ¹⁶³².

¹⁶²⁴ See [High-Rate, High-Fidelity Entanglement of Qubits Across an Elementary Quantum Network](#) by L. J. Stephenson et al, University of Oxford, PRL, 2020 (6 pages).

¹⁶²⁵ See [Ion Trap with In-Vacuum High Numerical Aperture Imaging for a Dual-Species Modular Quantum Computer](#) by Allison L. Carter, Christopher Monroe et al, UMD, October 2023 (8 pages).

¹⁶²⁶ See [Control and Readout of a 13-level Trapped Ion Qudit](#) by Pei Jiang Low et al, University of Waterloo, June 2023 (23 pages).

¹⁶²⁷ See [Compiling quantum circuits with qubits embedded in trapped-ion qudits](#) by Anastasiia S. Nikolaeva et al, February 2023 (7 pages).

¹⁶²⁸ See [Polyqubit quantum processing](#) by Wesley C. Campbell and Eric R. Hudson, UCLA, October 2022 (9 pages).

¹⁶²⁹ See [Exploring Large-Scale Entanglement in Quantum Simulation](#) by Manoj K. Joshi, Rainer Blatt, Peter Zoller et al, Nature, May-November 2023 (14 pages).

¹⁶³⁰ See [Trapped-ion quantum simulations for condensed-phase chemical dynamics: seeking a quantum advantage](#) by Mingyu Kang et al, Duke University, May 2023 (23 pages).

¹⁶³¹ Photon mediated entanglement was invented in 2004 by Christopher Monroe et al. See [Scalable Trapped Ion Quantum Computation with a Probabilistic Ion-Photon Mapping](#) by L.-M. Duan, B. B. Blinov, D. L. Moehring and Christopher Monroe, University of Michigan, 2004 (6 pages).

¹⁶³² See [Real-time hybrid quantum-classical computations for trapped-ions with Python control-flow](#) by Tobias Schmale et al, March 2023 (8 pages).

And the two-qubit gate error rate scales polynomially with the number of qubits, as $\sim(T/T_2)N^\alpha$, with the gate time T , single-qubit decoherence time T_2 and $1 \leq \alpha \leq 2$, generating the need for faster gates and low α coefficient, depending on many implementation parameters^{1633 1634 1635}. More scalable variants use microwave fields distributed through the ions supporting circuit¹⁶³⁶ or efficiently distribute laser beams on nanophotonic circuits^{1637 1638} or even piezo-optomechanical photonic integrated circuits¹⁶³⁹.

- **Qubits readout** uses the detection of the ion fluorescence with either superconducting photon detectors (SNSPDs)¹⁶⁴⁰ or CCD image sensors after ions are excited by a laser¹⁶⁴¹ (Figure 405). The excited ions corresponding to the $|1\rangle$ state are visible while the unexcited ions corresponding to the $|0\rangle$ state are not.



Figure 405: examples of image sensors for trapped ions qubits readout with an **Oxford Instrument Andor iXon Ultra 888 UVB** (left) and a **Hamamatsu H10682-210 PMT** (right).

Qubit readout could also use NbTiN superconducting nanowire single-photon detectors (SNSPDs) employing grounded aluminum mirrors as electrical shielding that are integrated into linear surface-electrode RF ion traps instead of fluorescence-based camera devices¹⁶⁴².

Setup

The typical trapped ions setup contains an ultra-vacuum chamber containing a chip where the ions are “floating on”. The ions are prepared in a heater with neutral atoms, with ablation loading using a laser pulse on a target or with a MOT (magneto-optical trap) like cold atoms. The chamber is cooled at reasonable temperatures of about 4K.

¹⁶³³ See [Assessing the Progress of Trapped-Ion Processors Towards Fault-Tolerant Quantum Computation](#), PRX, 2017 (41 pages).

¹⁶³⁴ See [Fast design and scaling of multi-qubit gates in large-scale trapped-ion quantum computers](#) by Yotam Shapira et al, Weizmann Institute, July 2023 (13 pages).

¹⁶³⁵ See [Theory of robust multiqubit nonadiabatic gates for trapped ions](#) by Yotam Shapira, Roei Ozeri, Ady Stern et al, PRA, March 2020 (15 pages).

¹⁶³⁶ Trapped ions single and two qubit gates can be generated with only microwave magnetic fields and radiofrequency magnetic field gradients and no lasers. See [High-fidelity laser-free universal control of two trapped ion qubits](#) by R. Srinivas et al, February 2021 (40 pages).

¹⁶³⁷ See [Integrated optical addressing of an ion qubit](#) by Karan K. Mehta et al, Nature Nanotechnology, 2016 (8 pages).

¹⁶³⁸ See [Integrated optical multi-ion quantum logic](#) by Karan K. Mehta, Jonathan P. Home et al, ETH Zurich, Nature, October 2020 (12 pages).

¹⁶³⁹ See [High-fidelity trapped-ion qubit operations with scalable photonic modulators](#) by C. W. Hogle et al, Sandia Lab, MITRE and MIT, npj Quantum Information, July 2023 (6 pages).

¹⁶⁴⁰ See [State Readout of a Trapped Ion Qubit Using a Trap-Integrated Superconducting Photon Detector](#) by S. L. Todaro, David Wine-land et al, NIST, University of Colorado Boulder, University of Oregon, PRL, 2020 (7 pages).

¹⁶⁴¹ See [Real-time capable CCD-based individual trapped ion qubit measurement](#) by S. Halama et al, April 2022 (16 pages) which compares a fast CCD camera with PMT (photomultiplier tubes) and superconducting nanowire single-photon detectors (SNSPDs). It is an Andor iXon Ultra 888 UVB from Oxford Instruments of 1024x1024 pixels and operating at -35°C and 200 frames per seconds with reasonable noise. It works in UV light. The reference PMT comparison example is a Hamamatsu H10682-210.

¹⁶⁴² See [Trap-Integrated Superconducting Nanowire Single-Photon Detectors with Improved RF Tolerance for Trapped-Ion Qubit State Readout](#) by Benedikt Hampel et al, NIST, February 2023 (6 pages).

Ions are positioned and controlled by DC currents, microwave and laser pulses, thus the associated control electronics. Like with cold atoms, an image sensor is involved in the qubit readout using a laser-driven fluorescence. All of this can fit into about two standard data-center racks like with AQT (Austria)¹⁶⁴³ (Figure 406).

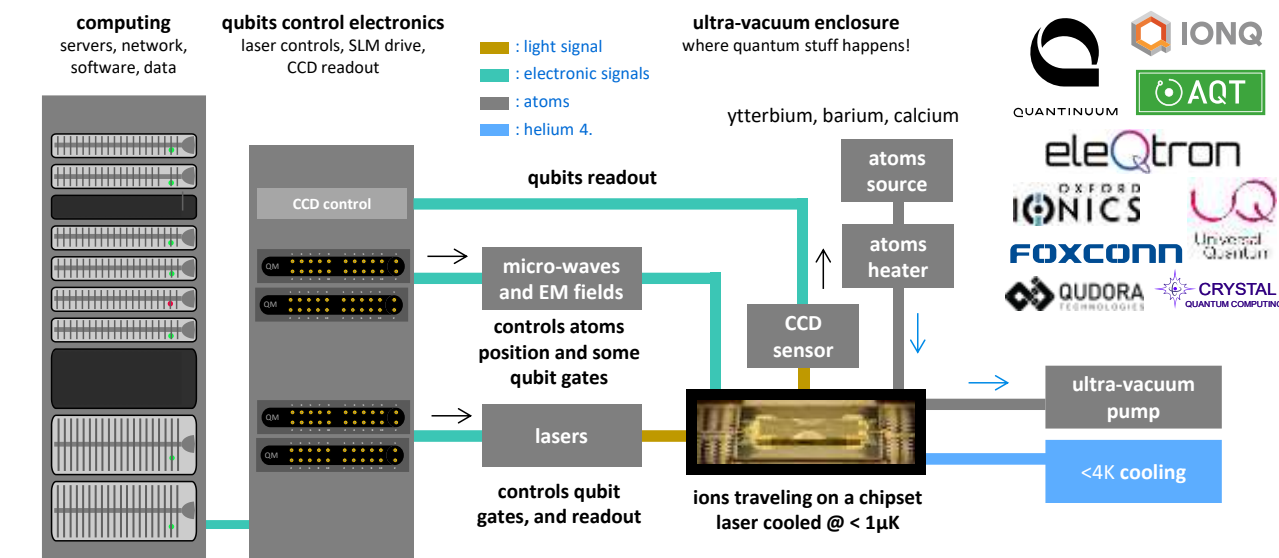


Figure 406: generic architecture of a trapped ion quantum computer which fits into a 2-rack system. (cc) Olivier Ezratty, 2022-2023.

Research

About a hundred research teams around the world are working on trapped ion qubits in almost every country working on quantum technologies (Australia, Austria, Canada, China, Denmark, Finland, France, Germany, India, Israel, Japan, the Netherlands, Singapore, Switzerland, UK, USA)¹⁶⁴⁴.

Rainer Blatt from the University of Innsbruck is one of the pioneers in this field. He created a register of 14 addressable qubits in 2011 and increased it to 20 addressable and individually controllable qubits in 2018, using calcium ions. Rainer Blatt then cofounded **Alpine Quantum Technologies** (2017, Austria) where he [characterized](#) up to 10 high quality trapped ions qubits. In 2021, his team also demonstrated the use of trapped ions to create qudits with 3, 5 and 7 levels, potentially opening the path for more powerful trapped ion based quantum computing¹⁶⁴⁵.

Quantum simulation using trapped ions, and an Ising model as with the D-Wave, is also investigated by some laboratories such as at **ETH Zurich** in Jonathan P. Home's Trapped Ions Quantum Information Group (TIQG), the **University of Maryland**, elsewhere in the USA¹⁶⁴⁶ and also in China¹⁶⁴⁷.

¹⁶⁴³ See some architecture aspects of trapped ions qubits in [Blueprinting quantum computing systems](#) by Simon J. Devitt, July 2023 (35 pages).

¹⁶⁴⁴ There were 98 research laboratories in the world working on trapped ions in 2020. See this table listing them all in [List of Ion Trapping Groups](#), February 2020.

¹⁶⁴⁵ See [A universal qudit quantum processor with trapped ions](#) by Martin Ringbauer et al, September 2021 (14 pages). 8 levels for a calcium-based trapped ion qubit.

¹⁶⁴⁶ See [Digital Quantum Simulation with Trapped Ions](#) by Kenny Choo and Tan Li Bing, 2016 (29 slides) and [Programmable Quantum Simulations of Spin Systems with Trapped Ions](#) by Christopher Monroe et al, 2019 (42 pages) and a follow-up with [Programmable quantum simulations of bosonic systems with trapped ions](#) by Or Katz and Christopher Monroe, July 2022 (7 pages).

¹⁶⁴⁷ See [Probing critical behavior of long-range transverse-field Ising model through quantum Kibble-Zurek mechanism](#) by B.-W. Li et al, August 2022 (10 pages).

In May 2020, Wesley Campbell's **UCLA** team associated with UNSW announced that they had stabilized barium ions ($^{133}\text{Ba}^+$) to build quality qubits in a linear trap¹⁶⁴⁸. The quality of these barium ions is compared to that of 2,014 qubits with a 10-fold improvement. This quality is evaluated only with the SPAM indicator which measures a fidelity on a qubit after preparation, some initialization single qubit gates and measurement (SPAM = "state preparation and measurement").

Let's also mention the **IQQI** (Austria, see Rainer Blatt, one of their laboratories, Figure 407) and the **IQST** (Germany), and their calcium based 20 qubits prototype¹⁶⁴⁹ as well as the Ion Quantum Technology Group from the **University of Sussex** (UK) that is run by Winfried Hensinger and its 10 qubits prototype, proposing an architecture design to scale up to 1,000 qubits through a cluster of quantum processors¹⁶⁵⁰. The group led to the creation of the startup **Universal Quantum** (2019, UK).

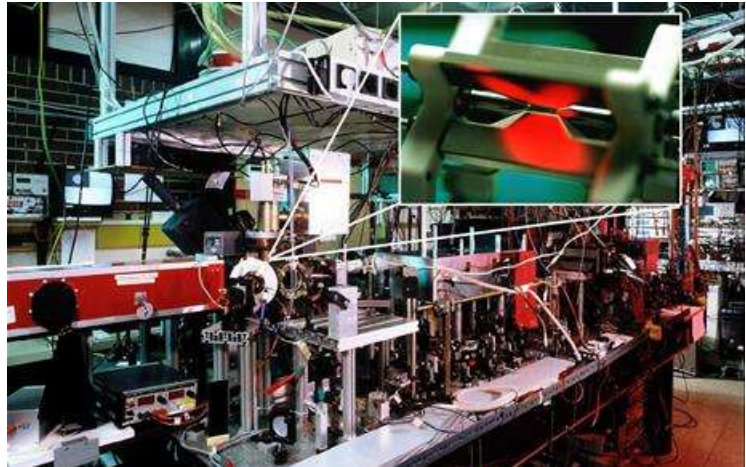


Figure 407: Rainer Blatt's lab in Innsbruck.

In March 2021, the DoE **Sandia Labs** launched the QSCOUT (Quantum Scientific Computing Open User Testbed), a cloud quantum computing resource available to selected researchers from universities and other government research agencies¹⁶⁵¹. It is a ^{171}Yt based trapped ions system of 3 qubits used for benchmarking and for algorithms development, particularly in computational chemistry. It will later be expanded to a 10 and then 32 bits system, by 2023, on par with 2021's IonQ's capacity, which is using Sandia Labs' ion traps. At a low-level, this system is programmed with the in-house assembly language Jaqal ("Just Another Quantum Assembly Language"). In August 2023, Sandia Labs introduced an ion trap capable of controlling up to 200 ions¹⁶⁵².

The **MIT Lincoln Labs** works on integrated silicon photonics for the manipulation of ions¹⁶⁵³.

Also, in the USA, a team from **Georgia Tech** led by Creston Herold and including NIST and DoE Oak Ridge's quantum lab and funded by DARPA is working on rare-earth trapped ion systems using the less used Penning traps, that controls the position of the trapped ions with magnetic and electric fields, using permanent magnets made of neodymium and samarium cobalt¹⁶⁵⁴. At this point, they control 10 trapped ions.

¹⁶⁴⁸ See [Physicists develop world's best quantum bits](#) by Stuart Wolpert of UCLA, May 2020 which refers to [High-fidelity manipulation of a qubit enabled by a manufactured nucleus](#) by Justin Christensen et al, May 2020 (5 pages). First precaution of use: identify the author of the article. It happens to be a certain Stuart Wolpert from UCLA, in charge of media relations at the University where the published work comes from. So he does the PR for the laboratory and publishes his article on a site where it is possible (Physorg).

¹⁶⁴⁹ They coauthored [Observation of Entangled States of a Fully Controlled 20-Qubit System](#), April 2018 (20 pages).

¹⁶⁵⁰ See [Blueprint for a microwave trapped ion quantum computer](#) by Winfried Hensinger et al, 2017 (12 pages) and their review paper [Quantum control methods for robust entanglement of trapped ions](#) by C H Valahu, Winfried Hensinger et al, Journal of Physics B: Atomic, Molecular and Optical Physics, 2022 (27 pages).

¹⁶⁵¹ See [Rare open-access quantum computer now operational](#), Sandia Labs, March 2021.

¹⁶⁵² See [Bigger and better quantum computers possible with new ion trap, dubbed the Enchilada - Sandia Labs produces its first devices capable of supporting 200 trapped ion qubits](#), Sandia Labs, August 2023.

¹⁶⁵³ See [Integrated multi-wavelength control of an ion qubit](#) by Robert J. Niffenegger et al, January 2020-January 2021 (25 pages).

¹⁶⁵⁴ See [DARPA Probing Quantum Computing Capabilities](#) by Meredith Roaten, June 2022 and [Universal Control of Ion Qubits in a Scalable Microfabricated Planar Trap](#) by Creston D. Herold et al, February 2016 (17 pages). Back in 2016, their single qubit gate fidelity was 97% which is far from being stellar for trapped ions.

The European Flagship includes the **AQTION** project, which is led by the University of Innsbruck and has a budget of €9.57M. The objective is to reach 50 operational qubits to prepare the next phase, beyond 100 qubits, by adopting a distributed architecture with photonic links. Alpine Quantum Technologies (AQT), the University of Oxford, ETH Zurich, Fraunhofer IOF and Atos are participating. Atos works on the solution software stacks and applications.

In **Israel**, a team of researchers from the Weissman Institute announced in 2022 the creation of the first local quantum computer using 5 strontium ions¹⁶⁵⁵. It is less than stellar at this point. They plan to reach 64 qubits someday.

In **Russia**, the Russian Quantum Center, the P.N. Lebedev Physics Institute of the Russian Academy of Sciences and Rosatom presented in 2021 a prototype of a trapped ions computer, starting with 4 qubits. Looks like they are late in the catch-up game behind the USA, UK and Austria!

In **China**, various teams are working on gates improvements^{1656 1657} and error mitigation¹⁶⁵⁸.

Vendors



IonQ (2016, USA, \$736M¹⁶⁵⁹) is a spin-off from the University of Maryland specialized in the design of universal quantum computers based on ytterbium trapped ions, and later, barium ions¹⁶⁶⁰.

Co-founded by Christopher Monroe, professor at the university who was their Chief Scientist until October 2023 when he left the company, the company CEO is Peter Chapman, a former e-commerce executive at Amazon. IonQ's cap table includes Google Ventures, Amazon, Samsung Ventures, Microsoft, Lockheed Martin, Bosch and HPE. In June 2020, they created an advisory board including David Wineland, Umesh Vazirani, Margaret Williams (ex-Cray) and Kenneth Brown (Duke University). In March 2021, IonQ announced a new round of funding with a merger agreement through the Special Purpose Acquisition Company (SPAC) mechanism, with the fund dMY Technology Group III. The funding was made of \$350M coming from investors including Hyundai, Kia Corporation¹⁶⁶¹ and Breakthrough Energy Ventures. The remaining \$300M came from dMY and an IPO that was finalized in October 2021¹⁶⁶². As of September 2023, the company had a staff of about 300 people.

Technology. IonQ currently uses 1D arrays of ions of variable length. They are controlled by lasers for both cooling, quantum gates and readout and with a small circuit fitting in a tiny vacuum chamber (Figure 408). Trapped ions enable all-to-all connectivity between ions, making it easier to run algorithms and avoiding the usage of costly SWAP gates. This enables very good optimization of quantum algorithms to minimize the number of gates to be executed as shown in the example in Figure 409.

¹⁶⁵⁵ See [Trapped Ion Quantum Computer with Robust Entangling Gates and Quantum Coherent Feedback](#) by Tom Manovitz, Yotam Shapira, Lior Gazit, Nitzan Akerman and Roece Ozeri, March 2022 (12 pages).

¹⁶⁵⁶ See [A low-crosstalk double-side addressing system using acousto-optic deflectors for atomic ion qubits](#) by Rui-Rui Li et al, June 2023 (6 pages).

¹⁶⁵⁷ See [Entangling gates for trapped-ion quantum computation and quantum simulation](#) by Zhengyang Cai et al, February 2023 (19 pages).

¹⁶⁵⁸ See [Error-Mitigated Quantum Simulation of Interacting Fermions with Trapped Ions](#) by Wentao Chen et al, February 2023 (15 pages).

¹⁶⁵⁹ This amount includes \$84M from VCs and the 2021 SPAC. It excludes the total \$165M grants the company and Christopher Monroe's lab in Maryland University got from the US government, per their 2021 investor presentation.

¹⁶⁶⁰ See [A Reconfigurable Quantum Computer](#) by David Moehring, 2017 (20 slides).

¹⁶⁶¹ They seem to have closed links with South Korea. These investors add up with a partnership with Q Center. See [IonQ and South Korea's Q Center Announce Three-Year Quantum Alliance](#), January 2021. To provide to the Q Center students to the IonQ computer online.

¹⁶⁶² See [QC ethics and hype: the call is coming from inside the house](#) by Scott Aaronson, October 2020, who found this IPO to be pushing the envelope of bullshit a bit too far.

But, as with all trapped ions qubits QPUs, this is achieved at the expense of relatively slow gates in comparison with superconducting and silicon qubits QPUs. The scalability of trapped ions is being questioned and it shows up well in the history of the company. At the beginning of 2018, they announced a record of 53 coherent and entangled qubits, but these were used for quantum simulation and not with gate-based computing.



Figure 408: IonQ trapped ion drive system, the small vacuum enclosure where the ions are located, and the chip controlling the ions position coming from the DoE's Sandia Labs. Sources: IonQ and [Ground-state energy estimation of the water molecule on a trapped ion quantum](#) by Yunseong Nam, Christopher Monroe et al, March 2019 (14 pages).

At the end of 2018, they said they had reached 79 qubits associated with 160 storage qubits but with no fidelity numbers¹⁶⁶³. It never became a product. In 2019, they had 11 characterized qubits¹⁶⁶⁴. In October 2020, IonQ announced that it had created the world's most powerful quantum computer with 32 qubits and a quantum volume of 4,000,000 but it took over a year and a half for this system to become live and tested¹⁶⁶⁵ and made available on Amazon Braket, Microsoft Azure Quantum and Google cloud. They claimed to handle error correction codes with 13 (and sometimes, 16) physical qubits per logical qubits. They also announced the creation of a Quantum Data Center sized to host 10 of their quantum computers.

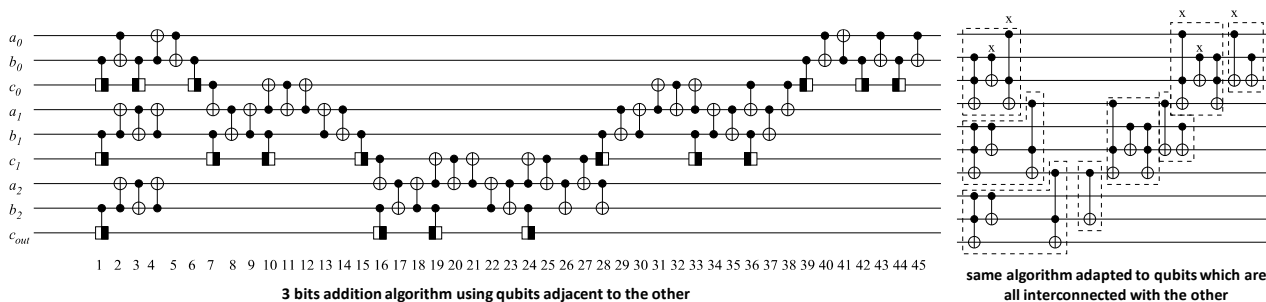


Figure 409: how the good connectivity with trapped ions enables a good compression of the code. Source: [Fast Quantum Modular Exponentiation](#) by Rodney Van Meter and Kohei Itoh, 2005 (12 pages).

Roadmap. In December 2020, IonQ unveiled its 5 years roadmap with plans to use rack-mounted modular quantum computers small enough to be networked together in a datacenter by 2023. IonQ adopted a new benchmark metric of their own: algorithmic qubits, using \log_2 of IBM's quantum volume and a different computing mode that we cover in the benchmarking section of this book, using a set of QED-C benchmarks (page 1011). Their 32 qubits reached 22 algorithmic qubits with plans to reach 29 algorithm qubits by 2023, 64 by 2025 with the Tempo system with using a 16:1 error-correction encoding (meaning: 16 physical qubits per logical qubits¹⁶⁶⁶) and gate-times of 300 μ s.

¹⁶⁶³ See [IonQ Has the Most Powerful Quantum Computers With 79 Trapped Ion Qubits and 160 Stored Qubits](#) by Brian Wang, December 2018.

¹⁶⁶⁴ See [Benchmarking an 11-qubit quantum computer](#) by K. Wright et al, November 2019.

¹⁶⁶⁵ See [IonQ Unveils World's Most Powerful Quantum Computer](#), IonQ, October 2020.

¹⁶⁶⁶ See [Fault-Tolerant Operation of a Quantum Error-Correction Code](#) by Laird Egan et al, IonQ, September 2020-January 2021 (23 pages).

Later, they will rely on a 32:1 ratio. The 29 algorithmic qubits milestone was achieved in 2023 with their 32 qubit Forte system¹⁶⁶⁷, which will expand to 35 algorithmic qubits in 2024 with Forte Enterprise (and 0.4% announced two-qubit error rates). They also reached 29 algorithmic qubits with a prototype 29 qubit system using barium instead of ytterbium in October 2023.

Then, they expected to scale beyond 64 and reach a broad quantum advantage with 256 then 1,024 algorithmic qubits by 2026 and 2028 (Figure 410). The caveat is that this can be achieved only with scaling-out their quantum processors, assembling several units of 64 qubits through photonic links in a distributed computing manner. Something that has not been tested yet beyond one-to-one qubit connectivity¹⁶⁶⁸.

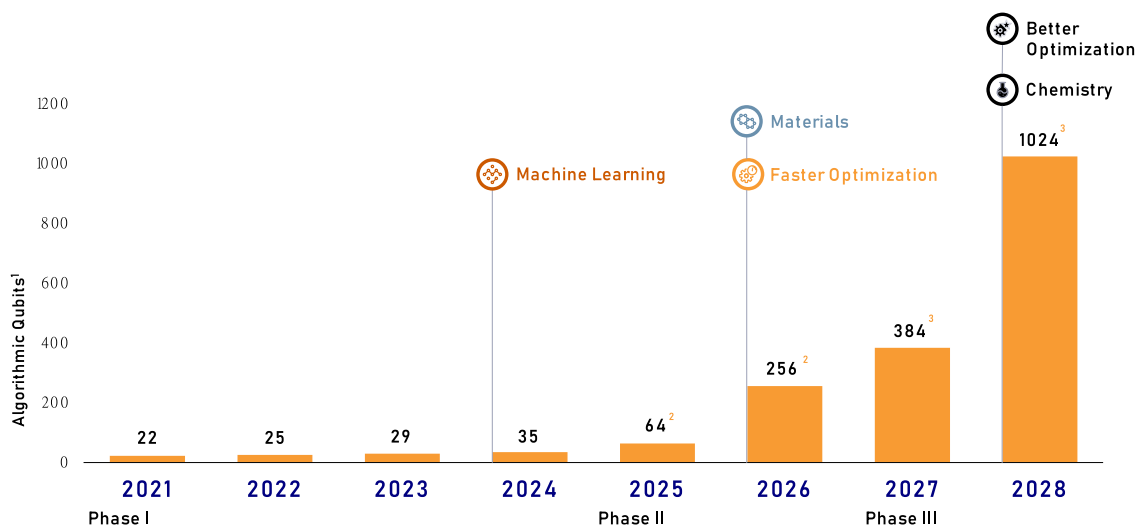


Figure 410: IonQ's qubits roadmap as published in March 2021. They have indeed reached 29 algorithmic qubits in 2023. Source: IonQ.

IonQ announced in August 2021 their Reconfigurable Multicore Quantum Architecture (RMQA) detailing how they would create 64 ions chips (video). It would assemble 4 chains or lines of 16 ions, 12 being usable as qubits and the 4 remaining for cooling, in a single chip manufactured on a glass support (Evaporated Glass Traps) replacing their previous silicon-based platform built by Sandia Labs and Honeywell. These chunks of 16 ions can be moved around, paired and entangled, to create dynamic 32 ions units. IonQ stated that this architecture could scale-up and support even more blocks of 16 ions. Well, if that actually works in practice, why not! They are also working to stabilize two-qubit gates control, using some randomized benchmarking technique¹⁶⁶⁹.

A team associating IonQ, Duke University in Durham and ColdQuanta (now Infleqtion) published an interesting paper describing the architecture of a trapped ions systems cryostat from Montana Instruments that is optimized to minimize the vibrations coming from the pulse tube.

This seems to be one of the figures of merit to ensure the stability of the trapped ions qubits and their control devices likes lasers¹⁶⁷⁰.

¹⁶⁶⁷ See [Benchmarking a trapped-ion quantum computer with 29 algorithmic qubits](#) by Jwo-Sy Chen et al, IonQ, August 2023 (12 pages).

¹⁶⁶⁸ The associated concepts were laid out in [Scaling the ion trap quantum processor](#) by Christopher Monroe and J. Kim, Science, 2013 (7 pages). It consists in associating one qubit of two ions QPUs with probabilistic entangled photons. See also [Large-scale modular quantum-computer architecture with atomic memory and photonic interconnects](#) by Christopher Monroe, Robert Raussendorf et al, PRA, 2013 (16 pages).

¹⁶⁶⁹ See [Extremum seeking control of quantum gates](#) by Erfan Abbasgholnejad et al, September 2023 (5 pages).

¹⁶⁷⁰ See [High stability cryogenic system for quantum computing with compact packaged ion traps](#) by Robert F. Spivey et al, August 2021 (12 pages). ColdQuanta seems involved here given a cold atoms system can reuse some of the experimental setting crafted for trapped ions. Interestingly, in its 2021 investor presentation, IonQ pretended that their system was operating at room temperature!

The qubits are cooled at 5K while laser-based cooling using the Doppler effect cool it at an even lower temperature.

In December 2021, after they had finalized their SPAC and IPO, IonQ announced they were switching from ytterbium to barium ions (precisely $^{133}\text{Ba}^{+1671}$). The reasons were well explained: it provides better gates and readout fidelities, and the ions are primarily controlled with visible light rather than ultraviolet light, using standard silicon photonics technology, which can better enable QPU photonics interconnect¹⁶⁷². They also secured the provisioning of these atoms with a partnership with DoE's PNNL (Pacific Northwest National Laboratory) in February 2022.

In February 2022, IonQ and Duke University presented a new way to create 3-qubit gates including a Toffoli gate using state squeezing¹⁶⁷³. This sort of gate is interesting since it can be the basis for a universal gate-set enabling fault-tolerance. It can help speed up many algorithms including Grover and variational quantum eigensolvers (VQEs). In November 2022, they announced a new generation trapped ions control chip, with multilayered glass trap and better routing of driving signals.

Crisis. On May 3rd, 2022, IonQ was literally attacked by a short-seller financial company, **Scorpion Capital**, which published a scathing report on their business, presented as a scam¹⁶⁷⁴. This 193-page report was very long, apparently detailed and based on many interviews. But it was misplaced (Figure 411).

IONQ (NYSE: IONQ)

The “World’s Most Powerful Quantum Computer” Is A Hoax With Staged Nikola-Style Photos – An Absurd VC Pump With A Recent Lock-Up Expiration Takes SPAC Abuses To New Extremes

- A part-time side-hustle run by two academics who barely show up, dressed up as a “company”
- A useless toy that can't even add 1+1, as revealed by experiments we hired experts to run
- Fictitious “revenue” via sham transactions and related-party round-tripping
- A scam built on phony statements about nearly all key aspects of the technology and business
- CEO appears to be making up his MIT educational credentials

\$1.6B market cap | \$8/share | ADV 6.4MM shares | Short interest 7mm shares ^{5/2/22 per Capital IQ}

Figure 411: Scorpion Capital review cover page with extreme and misleading statements.

It did criticize IonQ wrongly on many points like when explaining that quantum computers couldn't even do a 1+1 calculation. They pinpointed exaggerations that can be found in IonQ investor March 2021 presentation. They even said that their 32-qubit system was non-existent (which is not true at all). They also highlighted that their ions control chip was produced by Sandia Labs, a DoE lab operated by Honeywell, but it was not a secret. The same with **Hyundai** being both one of their investors and also a customer, on far-fetched use-case plans related to battery designs and 3D image recognition. They could have been harsh on their aggressive roadmap, their scalability goals and their related QPU interconnect plans but seemingly lacked the scientific background to do so¹⁶⁷⁵.

All of this was border line defamation as was shown later. IonQ was then defended by preeminent quantum computing analysts¹⁶⁷⁶. A couple days later, IonQ announced the “select” availability of their 31 bits Forte system a couple months after having released its 23-qubits Aria system supporting 20

¹⁶⁷¹ See [Ba-133: the Goldilocks qubit?](#) by UCLA Hudson Lab.

¹⁶⁷² See [IonQ Announces New Barium Qubit Technology, Laying Foundation for Advanced Quantum Computing Architectures](#), IonQ, December 2021.

¹⁶⁷³ See [SNS-body interactions between trapped ion qubits via spin-dependent squeezing](#) by Or Katz, Marko Cetina and Christopher Monroe, February 2022 (7 pages).

¹⁶⁷⁴ See [The “World’s Most Powerful Quantum Computer” Is A Hoax With Staged Nikola-Style Photos – An Absurd VC Pump With A Recent Lock-Up Expiration Takes SPAC Abuses To New Extremes](#) by Scorpion Capital, May 2022 (183 slides).

¹⁶⁷⁵ I mention this in the paper [Mitigating the quantum hype](#), January 2022 (26 pages) that is quoted in Scorpion's presentation on slide 14. They may have just read its title!

¹⁶⁷⁶ See [A short report has placed a spotlight on IonQ, a quantum computing champion. This should not deflect long term interest in this or other quantum technologies](#) by David Shaw, Doug Finke and André M. König, May 2022.

algorithmic qubits (as of August 2022¹⁶⁷⁷). The system featured an Acousto-Optic Deflector (AOD) which dynamically directs laser beams towards individual ions to drive qubit gates and supports up to 40 ions. Like many quantum computing traded companies, their investor presentations are also border line, particularly when representing the competition state of the art¹⁶⁷⁸.

Use cases. IonQ works with a couple customers like **Goldman Sachs** on financial services on top of the above-mentioned Hyundai. They also partner with **Accenture** to develop customer applications. They also published various use cases which are far from reaching any quantum advantage given the number of involved qubits. One involved some oversold fancy human cognition modeling using a mere 11 qubits^{1679 1680}, a Monte Carlo simulation done with 20 qubits with FCAT, a service subsidiary of **Fidelity**, a financial services company^{1681 1682} and some quantum learning testbed implemented with 4 to 8 qubits¹⁶⁸³ which are therefore far from being “business ready”. They also work with **Airbus** on various use cases including QAOA-based cargo plane loading optimizations (details around page 1068). Their CEO said emphatically in 2023 that reaching 64 qubits in 2024 would be a ChatGPT moment. This is highly questionable given the narrow scope of applications that could bring some sort of quantum advantage at this threshold (“quantum machine learning” in IonQ’s plans).

Partnerships. In November 2019, **Microsoft** announced the integration of IonQ's quantum accelerator support into its Azure Quantum cloud offering and its Q#, QDK and Visual Studio development tools. All this was made available to developers from late spring 2020. IonQ is also proposed by **Google** in its own cloud offering, on top of **Amazon AWS Braket**. IonQ became in 2021 the only quantum computer vendor available on Amazon, Google and Microsoft clouds (with 11 qubits, being extended to 32 qubits). In May 2023, IonQ Aria went online on Amazon Braket with 25 algorithmic qubits. In September 2021, IonQ announced the creation of a joint laboratory with the University of Maryland (UMD), the **Q-Lab**, with \$20M funding. Among other things, the lab is tasked with training UMD students on quantum computing. In 2022, they also established business development subsidiaries in Germany and Israel. In January 2023, IonQ announced the opening of an R&D, production and data center site in Bothell, Washington state, near Seattle. 5,785 m². They announced some new partnership with **Dell** in November 2022, with **TII** in Abu Dhabi in 2023 as well as with **Bearing Point**, and finally with **QuantumBasel**, which is to deploy two generations of IonQ systems with 35 and then 64 algorithmic qubits capabilities in their quantum “datacenter” (which is not really an appropriate naming for quantum computing)¹⁶⁸⁴. In September 2023, IonQ got an order from **AFRL** in the USA to deliver two unspecified barium based QPUs for \$25.5M, probably Tempo’s 64 qubit system. It fits a pattern in many countries where defense or civil agencies order pre-quantum advantage QPUs to fund in a non-dilutive way the R&D of the related companies.

In January 2023, IonQ made the acquisition of the assets from **Entangled Networks** (Toronto) which develops a QPU interconnect hardware and software solution.

¹⁶⁷⁷ See [IonQ Aria: Past and Future \(Part Two\)](#) by IonQ, August 2022.

¹⁶⁷⁸ See [IonQ Investor Updates](#), May 2023 (19 slides). Look at the QEC overhead comparison in slide 8 and modular architecture comparison in slide 9, with an image of an ion trap (scaling to a maximum 48 qubits) compared with a full system with a million qubit projected by Google in 2030.

¹⁶⁷⁹ See [IonQ Demonstrates How Human Cognition Models Could Run on Quantum Computers](#) by Matt Swayne, June 2023.

¹⁶⁸⁰ See [Quantum Circuit Components for Cognitive Decision-Making](#) by Dominic Widdows et al, University of California, Berkeley and the University of London and IonQ, Entropy, March 2023 (22 pages).

¹⁶⁸¹ See [IonQ and Fidelity Center for Applied Technology Announce Development of Scalable Quantum State Preparation for Monte Carlo Algorithms](#), May 2023

¹⁶⁸² See [Quantum State Preparation of Normal Distributions using Matrix Product States](#) by Jason Iaconis et al, March 2023 (15 pages).

¹⁶⁸³ See [Generative quantum learning of joint probability distribution functions](#) by Elton Yechao Zhu et al, November 2022 (17 pages).

¹⁶⁸⁴ See [IonQ and QuantumBasel Partner to Achieve Future Quantum Advantages With Deployment of Two Generations of IonQ Quantum Systems in Europe](#), IonQ, June 2023.



Quantinuum (USA/UK) is the result of the merger in June 2021 of Honeywell Quantum Systems (USA, a branch of Honeywell) and the software company Cambridge Quantum Computing (UK), with an investment of \$300M for a stake of 55% for Honeywell in the resulting company¹⁶⁸⁵, with an additional \$300M equity announcement done in January 2024. The Quantinuum renaming occurred in December 2021.

Quantinuum's CEO is Rajeeb (Raj) Hazra since February 2023, formerly from Micron and Intel. He replaced Ilyas Khan who was previously the founder and CEO of CQC who merged with HQS to become Quantinuum. The company has more than 600 people overall. Honeywell started working in quantum computing in 2016 in "stealth" mode. Their team came in particular from the NIST Boulder lab and the University of Colorado with some alumni from the University of Maryland and Christopher Monroe's team (IonQ). In March 2020, they announced the development of a quantum computer that was bound to become be "*the most powerful in the world*", doubling the power of the previous record that was then held by IBM¹⁶⁸⁶. The initial announcement dealt with a four-qubit trapped ions-based quantum processor¹⁶⁸⁷, its power being evaluated using IBM's quantum volume benchmark.

Trapped ion QCCD is the trapped ions technique they are using (for "quantum charge-coupled device"). It uses ytterbium-based ions coupled with barium ions for cooling. This technique was developed in 2002 by Christopher Monroe, David Wineland and Dave Kielpinski¹⁶⁸⁸. They are reusing many other works from various research laboratories spread out between 2008 and 2012.

Ions are generated from a jet of collimated atoms obtained by heating a solid ytterbium target. They are then "hit" by a laser, which removes an electron from the valence layer of the atom (the last one). Only one electron remains in this layer, giving rise to an ion with a positive charge, Yb+. The laser cooling of these ions is well-controlled thanks to their favorable energy level pattern. Thanks to their electrical charge, it is possible to trap and move these atoms using electrostatic and radiofrequency potentials. The ions quantum states correspond to two "hyperfine" energy states related to the interaction between the magnetic moment of the nucleus and that of the electrons of the ion. These hyperfine levels are also used in cesium atomic clocks.



Figure 412: Quantinuum scalability roadmap. In 2023, they delivered the H2 system with a 1D race-track arrangement of qubits. Their key milestone will be to create 2D arrangement with shuttling ions, enabling larger scale quantum computing. Source: Quantinuum. 2023.

¹⁶⁸⁵ See [Honeywell Quantum Solutions And Cambridge Quantum Computing Merge With Go-Public In Mind](#) by Paul Smith-Goodson, June 2021.

¹⁶⁸⁶ See [Honeywell Achieves Breakthrough That Will Enable The World's Most Powerful Quantum Computer](#) and [How Honeywell Made the Leap into Quantum Computing](#) by Honeywell, March 2020. In Honeywell [has it created the world's most powerful quantum computer](#), March 2020, I analyze the ad in detail, with the text embedded in the book as a compacted version.

¹⁶⁸⁷ The performance is described in detail in: [Demonstration of the QCCD trapped ion quantum computer architecture](#) by J. M. Pino et al, 2020 (8 pages). This can be complemented by the presentation [Shaping the future of quantum computing](#) by Tony Uttley, the head of Honeywell's quantum team at the Q2B conference at QC Ware in California in December 2019 ([slides](#)).

¹⁶⁸⁸ It is described in [Architecture for a large-scale ion-trap](#), 2002 (4 pages).

The transition frequency between the two hyperfine levels of ytterbium is 12.6 GHz¹⁶⁸⁹. The hyperfine states of the ytterbium ion are well suited for quantum computation because they are very stable, which allows them to have a long coherence time.

Shuttling ions is a technique used to handle their connectivity. This idea was proposed in 2002 by Dave Wineland and co. This was the first working shuttling ions setup. Usually, qubits based on electrons, cold atoms or superconducting circuits do not move (too much) where they sit. Their system prepares ytterbium atoms, ionizes them and sends them into a hole that feeds the chip. It then uses about ions storage and sorting areas (in orange, yellow and blue in Figure 413).

The ytterbium ions are confined above a rail of three rows of electrodes whose variable voltage allows to control their position and to move them laterally. It enables logical operations between several qubits while moving them at will between storage areas and interaction areas during operations.

Their initial system was using 198 direct current (DC) electrodes for controlling the displacement and positioning of ytterbium ions coupled with barium ions used for cooling. The chip used cryogenic surface traps dynamically rearranging the position of the ytterbium/barium ion pairs and implementing quantum gates running in parallel on several areas of the circuit. Ions circulate above the green band, allowing arbitrary movements of the ions along the band. Once positioned, they are transferred to the middle band to get submitted to a single qubit quantum gate, or in the side bands for two-qubits quantum gates, as explained in Figure 413. One of these operations is a SWAP gate that allows the ions to be physically interchanged. This process is significantly different from the 1D ions arrangements used by IonQ. One challenge is to mitigate dephasing and leakage errors generated by ion shuttling.

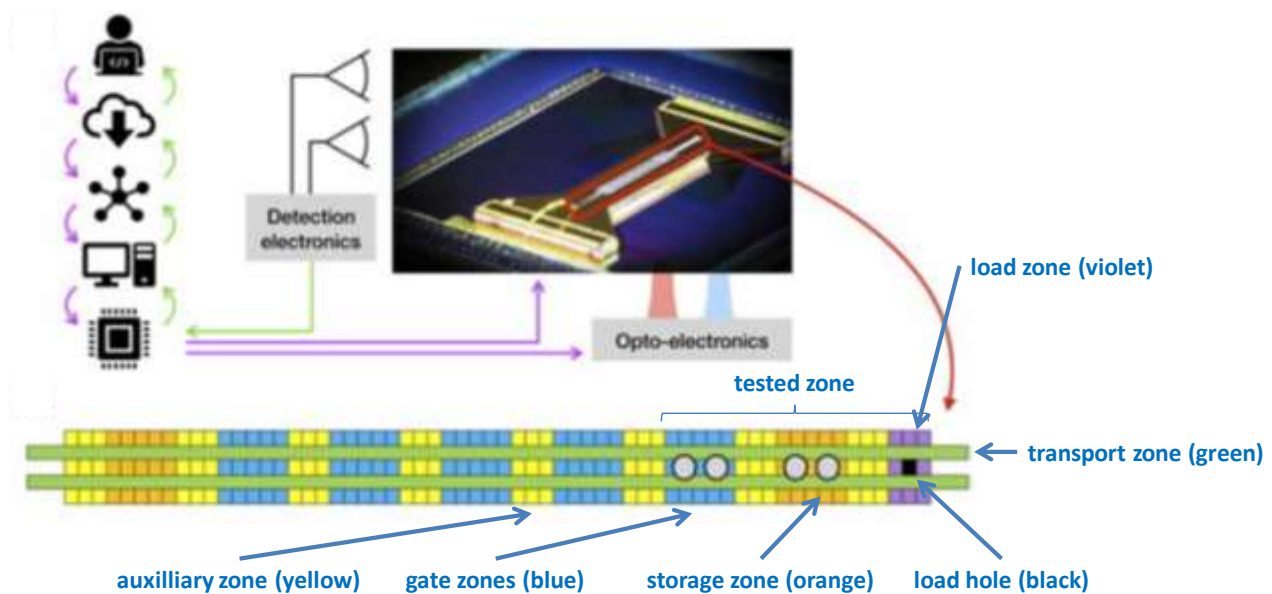


Figure 413: overall control architecture in 1D versions of Quantinuum's trapped ions, as presented in 2020.

Slow gates. The disadvantage of the technique is its slow quantum gates. The time required to configure the ions to create a quantum gate is 3 to 5 ms, which is not negligible, especially for algorithms that require a large number of quantum gates. This is a showstopper with regards to both NISQ and FTQC algorithms that require a very large number of quantum gates, in the range of 10^8 to 10^{15} . This limitation doesn't show up when testing these systems with a rather small number of qubits, below 30 and shallow algorithms.

¹⁶⁸⁹ See [Laser-cooled ytterbium ion microwave frequency standard](#) by S. Mulholland et al, 2019 (16 pages).

Cooling. Their initial system operated at 12.6K and with a temperature stability of 2mK which avoids disturbing the ions and their superposed and entangled quantum states. Helium cooling is complemented by a so-called "sympathetic cooling" technique which combines the use of Doppler effect and Raman cooling on the barium ions next-door to the ytterbium ions. The Coulomb interaction between the barium ions cools the ytterbium ions next to the barium ions. A barium ion cooling operation takes place before each two-qubit gate execution. Ion laser cooling has been operating at room temperature for more than 30 years. Trapped ions cooling at 12.6K also minimizes the abnormal ions heating effect, which is not fully understood. This abnormal heating is greatly reduced when the trap is cooled.

Qubit gates. The system is built around four-qubit chunks and uses one- and two-qubit quantum gates that are activated by lasers, via the Raman effect that requires a pair of beams. The single-qubit gates are activated by a pair of 370.3 nm Raman beams in circular polarization. The system allows the generation of X, Y and Z gates for which quarter and half turns are performed around the three axes of the Bloch sphere. These rotations are done with very high precision according to Honeywell. This ensures a minimum error rate for single-qubit quantum gates.

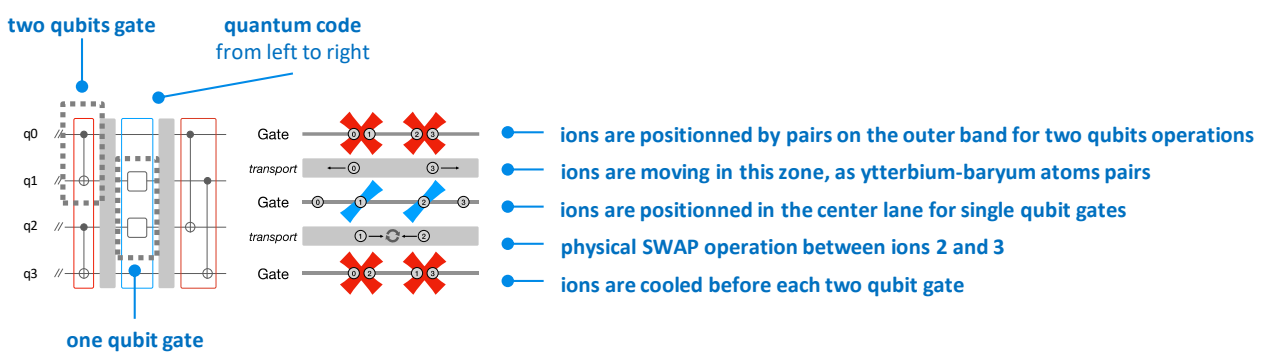


Figure 414: how single and two-qubit gates are implemented in Quantinuum trapped ions systems. Source: Honeywell, 2020.

Two-qubit gates use two additional pairs of laser beams that act on pairs of ytterbium atoms that have been brought closer together by the circuit's positioning control electrodes. Two ions are thus moved by the electrodes into the same potential well before being coupled by laser. The qubits can then be separated and moved elsewhere to interact with other qubits.

Qubits readout is performed with a classical imager that detects the energetic state of the ions via their laser-activated fluorescence. This imager is a PMT array, i.e. a linear array of photomultipliers (Photo-Multiplier Tubes). Their architecture allows a qubit readout during processing, without disturbing the neighboring qubits. This would allow the implementation of conditional logic, with IF THEN ELSE like with classical programming. They are also using the mid-circuit measurement and qubit reuse technique (MCMR) which can be used to optimize the length of quantum algorithms. The system includes an FPGA programmable electronic circuit for qubits controls, sitting outside the cryogenic enclosure.

Qubit fidelities are very good. They launched their 6-qubit H0 system in June 2020, then their 10-qubits H1 system in October 2020 with an initial quantum volume of 128 (7 qubits x 7 gates depth). Their quantum volume reached 512 in March 2021 (9x9 qubits with 10 qubits). Single-qubit gate fidelity were above 99.991% and two-qubit gate fidelity above 99.76% while readout fidelity is at 99,75% with a measurement crosstalk at 0.2%, characterized as the decay of a qubit coherence in an equal superposition state, while repeatedly measuring the nearest qubit¹⁶⁹⁰ (Figure 415).

As of April 2022, they had 12 running qubits reaching a quantum volume of 2^{12} with their System Model H1-2. It is a rare quantum processor with a quantum volume reached with all available qubits. Their related fidelities were 99.994% for single-qubit gates, 99.81% for two-qubit gates and 99.72%

¹⁶⁹⁰ See [Get to Know Honeywell's Latest Quantum Computer System Model H1](#) by Honeywell, October 2020.

for qubits readout¹⁶⁹¹. Meanwhile, their H1-1 system launched in June 2022 has 20 qubits (despite a lower “version” number), which enabled them in September 2022 to reach a QV of 8,192 (2^{13})¹⁶⁹² (Figure 416).

This system adds arbitrary angle two-qubit gates which helps shorten the length of many algorithms, particularly those relying on a QFT (quantum Fourier transform). As of June 2023, their record quantum volume was 2^{19} with a H1-1 system using 20 qubits¹⁶⁹³.

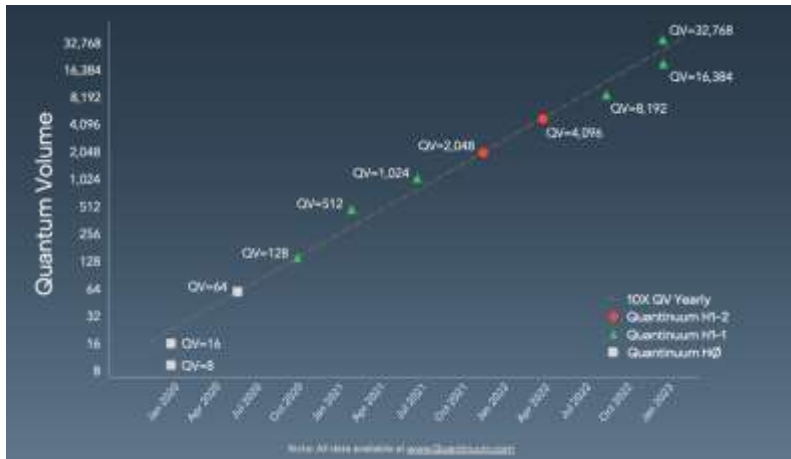


Figure 415: evolution of Quantinuum systems quantum volume. Source: [Quantum Volume reaches 5 digits for the first time: 5 perspectives on what it means for quantum computing](#), Quantinuum, February 2023.

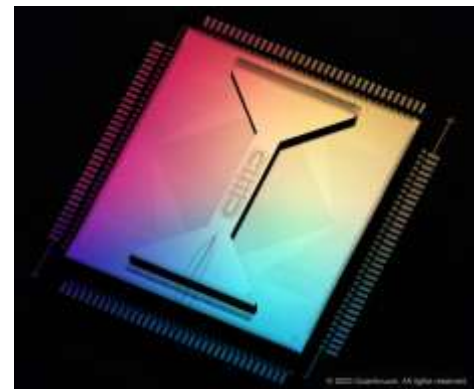


Figure 416: the “race track” processor released in 2023. Source: [A Race Track Trapped-Ion Quantum Processor](#) by S. A. Moses et al, May 2023 (24 pages).

Logical qubits. In July 2021, HQS announced the creation of the first logical qubits using color codes with their 10 trapped ions qubits¹⁶⁹⁴. Their work on correction error went on with creating a QEC toric code implemented thanks to mid-circuit measurement in Quantinuum’s processor¹⁶⁹⁵ and with trials of topological code with 27 qubits¹⁶⁹⁶. As part of this latter work, Quantinuum researchers created a GHZ entangled state of 32 qubits with a fidelity of 82%. This is a state superposing two computational basis states where all the qubits are either with values $|0\rangle$ or $|1\rangle$. Then, late 2022, they created 8 corrected logical qubits encoding in 10 physical qubits using their in-house Iceberg stabilizer code on a 12-qubit H1-2 QPU¹⁶⁹⁷. Fidelities were not documented, but the system had a quantum volume of only 2^8 . They also work with Microsoft to build compilers¹⁶⁹⁸.

From 1D to 2D. Quantinuum started with using a 1D trapped ion bar. They planned to adopt a 2D bar layout that would allow them to move the ions in two directions and accumulate more of them and connect them with their neighbors in two dimensions¹⁶⁹⁹ (Figure 412).

¹⁶⁹¹ See [Quantinuum Announces Quantum Volume 4096 Achievement](#) by Kortny Rolston-Duce, Quantinuum, April 2022.

¹⁶⁹² See [Quantinuum System Model H1 Product Data Sheet Version 5.00](#), June 14, 2022 (9 pages).

¹⁶⁹³ See [Quantinuum H-Series quantum computer accelerates through 3 more performance records for quantum volume: 2¹⁷, 2¹⁸, and 2¹⁹](#), Quantinuum, June 2023.

¹⁶⁹⁴ See [Realization of real-time fault-tolerant quantum error correction](#) by C. Ryan-Anderson et al, HQS, July 2021 (22 pages).

¹⁶⁹⁵ See [Topological Order from Measurements and Feed-Forward on a Trapped Ion Quantum Computer](#) by Mohsin Iqbal et al, Quantinuum, February 2023 (13 pages).

¹⁶⁹⁶ See [Creation of Non-Abelian Topological Order and Anyons on a Trapped-Ion Processor](#) by Mohsin Iqbal et al, May 2023 (26 pages).

¹⁶⁹⁷ See [Protecting Expressive Circuits with a Quantum Error Detection Code](#) by Chris N. Self et al, November 2022 (15 pages).

¹⁶⁹⁸ See [Advances in compilation for quantum hardware -- A demonstration of magic state distillation and repeat-until-success protocols](#) by Natalie C. Brown et al, Quantinuum and Microsoft, October 2023 (35 pages).

¹⁶⁹⁹ See [Transport of multispecies ion crystals through a junction in an RF Paul trap](#) by William Cody Burton et al, June 2022 (6 pages) where they describe how they can transport ytterbium and barium in 2D structures.

In 2023, they launched a “racetrack” 1D close circuit layout with their H2-1 QPU as shown in Figure 416 and described in detail in Figure 417. It adds a lot of nuts and bolts compared with their initial architecture described in Figure 414 with a Magneto Optical Trap (MOT) that replaces the oven used in system H1. It reduces the startup time by cooling the atoms before sending them in the trap.

They also implement more efficient RF electronic signals routing with additional metal layers beneath the trap top metal layer and voltage broadcasting which ties external signals sources to multiple DC electrodes in the trap and relies on conveyor belt regions on each side of the trap where ions are stored. Thanks to the use of only three voltage signals for 20 ion wells on each side of the trap, it greatly improves electrode control efficiency¹⁷⁰⁰.

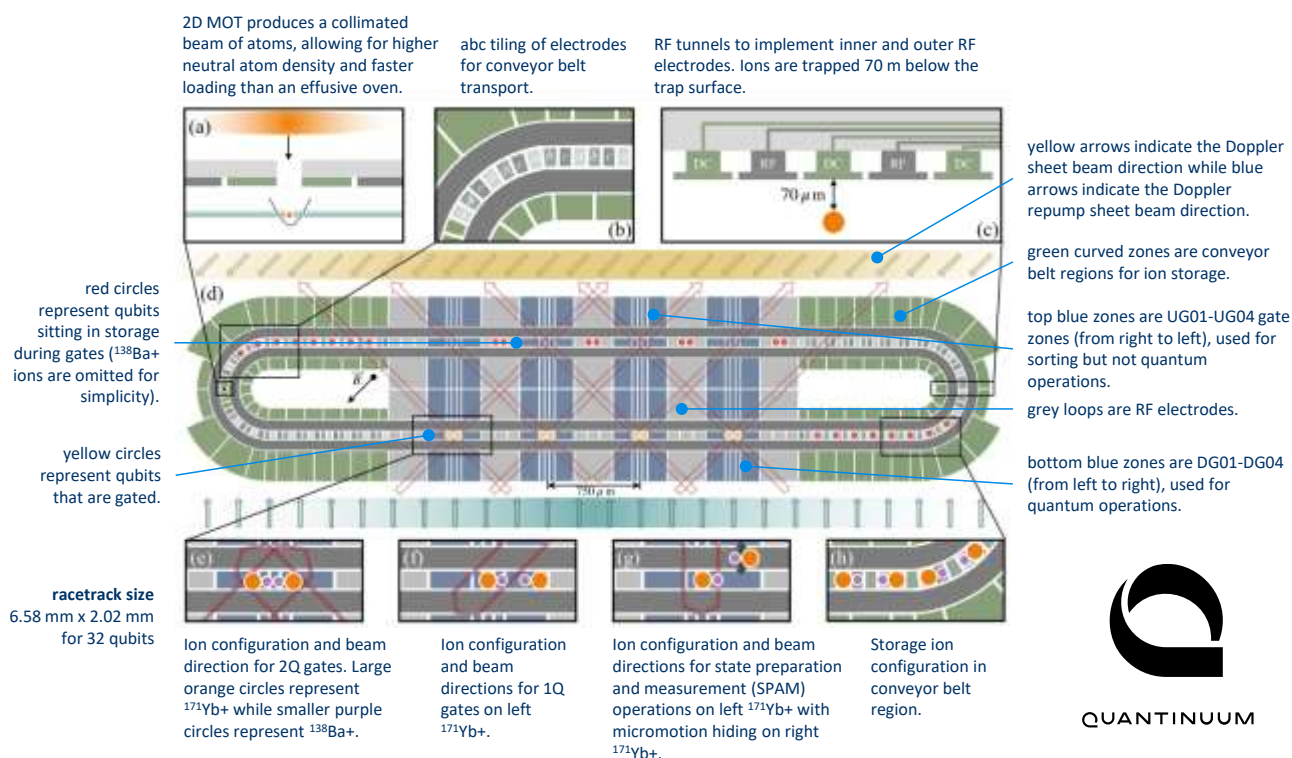


Figure 417: the layout of the “race track” processor released in 2023. Image and legends source: [A Race Track Trapped-Ion Quantum Processor](#) by S. A. Moses et al, May 2023 (24 pages).

Software tools. In May 2022, Quantinuum launched InQuanto, a quantum computational chemistry software platform that was developed with the support of **BMW**, Honeywell, JSR, **Mitsui & Co**, **Nippon Steel Corporation** and **TotalEnergies**. The platform makes it possible to associate various quantum algorithms coupled with chemistry-specific noise-mitigation techniques running on NISQ systems. It also breaks down larger problems into smaller subproblems that fits existing NISQ machines. InQuanto is based on Quantinuum’s open source toolkit **TKET**, which had been downloaded 500,000 times as of September 2022. You can wonder whether there are that many quantum developers in the world!

Quantinuum is investing a lot in QNLP (quantum natural language). They released lambeq in March 2022, a Python library that “converts any natural language sentence into a quantum circuit” that contains Bobcat, a neural-based Combinatory Categorical Grammar (**CCG**) parser, Bobcat. It is used to pre-process natural language training data to be subsequently used for various NLP applications (classification, summaries, etc).

¹⁷⁰⁰ See [A Race Track Trapped-Ion Quantum Processor](#) by S. A. Moses et al, May 2023 (24 pages) which describes in details the race track architecture of system H2.

Case studies. In July 2022, a team assembling researchers from **JP Morgan Chase Bank** and the **University of Maryland** published an amazing paper saying that a (Quantinuum) quantum computer may be better at summarizing long documents¹⁷⁰¹. That was not exactly true. First, it was a hybrid algorithm with a lot of classical data preparation. The classical part analyzed a dataset of 300,000 news articles from CNN and the Daily Mail and precomputed it with a BERT NLP classical deep learning model that handles sentences extraction and converts them into vectors. Second, the experiment worked to summarize text from respectively 20 to 8 and 14 to 8 sentences, corresponding exactly to the number of used qubits in Quantinuum QPUs versions H1-1 and H1-2. On the H1-1, the quantum computing part executed at most 765 two-qubit gates with a computing depth of 159 and 2000 shots. The experiment was based on using three quantum optimization algorithms working under constraints: QAOA, L-VQE¹⁷⁰² and XY-QAOA and the comparison was made vs a classical random guess, with XY-QAOA being the best. This was to date the best optimization under constraint problem ever solved by a quantum computer. But its capacity is obviously limited to simple and short texts. It could not summarize a 300 sentences document given there are not enough physical qubits available, and fidelities allowing very long depth computing accordingly. It could not of course summarize the scientific paper for you since it contains several hundred sentences that are way more complicated than short news from CNN and The Daily Mail. In the end, we always must find out if the thing scales well or not, and under which circumstances, which was not addressed in the paper. In September 2023, they released an interesting paper showcasing a use case involving superconductivity physics simulation, using 32 qubits, which is quite rare nowadays¹⁷⁰³. They also sold a QPU to RIKEN in Japan in October 2023.

Partnerships. Quantinuum initially touted several partnerships: with **Microsoft**, for the integration of its systems in Azure Quantum which became operational in July 2020 and for the support of the QIR (quantum intermediate representation), an investment in **Cambridge Quantum Computing** (2014, UK, which they later merged with) and **Zapata Computing** (2017, USA, \$64M). In February 2022, **IBM** invested about \$25M in Quantinuum, probably more interested by its software branch (CQC) with which they had been partnering for a while. Their first customers include **DHL**, **Merck**, **Accenture** and **Samsung**, who works on new batteries designs and **JPMorgan Chase** to create quantum algorithms in the financial sector. All of this for pilot projects. 12 or 20 qubits are way too few to enable production grade applications. They also work with **JSR Corporation** (Japan) to improve semiconductor design and research with organic and inorganic materials. In May 2023, Quantinuum announced a partnership with **HSBC**. They will first use Quantinuum Quantum Origin QRNG solution based on using their qubits in their cybersecurity deployments, on top of some PQC. They will also investigate future QML use cases, including NLP cases in the likes of the previous reference¹⁷⁰⁴. They also partner with **KPMG** to translate an existing algorithm made for Quantinuum QPUs into Q#¹⁷⁰⁵.



Alpine Quantum Technologies or **AQT** (2017, Austria, \$34.8M) is a spin-off from the University of Innsbruck created by Rainer Blatt. Peter Zoller and Thomas Monz. Ignacio Cirac (MPI) and Jonathan Home (ETH Zurich) are among their scientific advisors.

¹⁷⁰¹ See [Long Story Short: Researchers Say Quantum Computers May be Better at Summarizing Long Documents](#) by Matt Swayne, The Quantum Insider, June 2022, referring to [Constrained Quantum Optimization for Extractive Summarization on a Trapped ion Quantum Computer](#) by Pradeep Niroula et al, June 2022 (16 pages).

¹⁷⁰² See [Layer VQE: A Variational Approach for Combinatorial Optimization on Noisy Quantum Computers](#) by Xiaoyuan Liu et al, May 2022 (22 pages). So, we deal with a very recent algorithm!

¹⁷⁰³ See [Measuring the Loschmidt amplitude for finite-energy properties of the Fermi-Hubbard model on an ion-trap quantum computer](#) by Kevin Hémerly et al, Quantinuum, NIST and the University of Maryland, September 2023 (18 pages).

¹⁷⁰⁴ See [HSBC and Quantinuum Explore Real World Use Cases of Quantum Computing in Financial Services](#), May 2023.

¹⁷⁰⁵ See [KPMG and Microsoft join Quantinuum in simplifying quantum algorithm development via the cloud](#), March 2023

AQT drives its microwave trapped ions without the use of lasers, which simplifies the device. They use only one laser for photoionizing their calcium ions, which creates the ions at start-up, and another for measuring the qubit state by fluorescence after calculations. The fidelity of their qubits is 99.6% for two qubits and drops to 86% for 10 qubits¹⁷⁰⁶.

AQT has 20 working qubits working out of two 19-inches datacenter rack¹⁷⁰⁷. The associated research team had already entangled 14 ions back in 2011¹⁷⁰⁸! It reached 24 qubits in 2023. Their PINE system uses a linear Paul trap that supports up to 50 ions, including from multiple species. It can be used beyond quantum computing for quantum clocks or spectroscopy experiments.

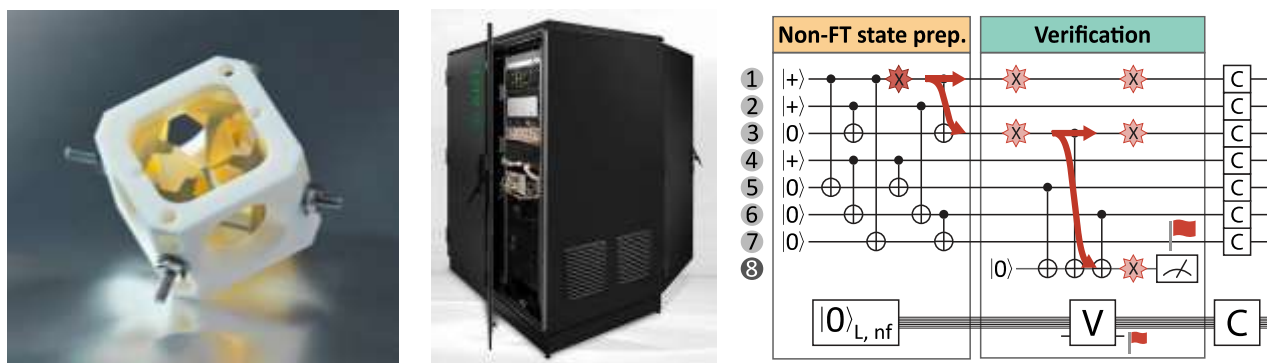


Figure 418: AQT's pane system to trap their calcium ions, the 2-rack system, and how they implemented a fault-tolerant T gate with magic state preparation. Source: [Demonstration of fault-tolerant universal quantum gate operations](#) by Lukas Postler, Rainer Blatt, Thomas Monz et al, Nature, November 2021 and May 2022 (14 pages).

AQT is also experimenting using qudits of dimension 5 with its ions¹⁷⁰⁹. In May 2022, Thomas Monz's team announced the first realization of a fault-tolerant CNOT gate across two logical qubits made with 16 physical qubits and using 7-qubits color codes quantum error correction plus one measurement qubit (above, in Figure 418, right, so $16=2 \times (7+1)$). They also separately implemented a fault-tolerant T gate using magic state preparation with flag qubits, fully using their 16 qubits¹⁷¹⁰. In 2023, they published a blueprint to implement an FTQC architecture although they still have a hard time to scale their number of qubits¹⁷¹¹. The company is also studying the implementation of qudits to scale the computing mathematical space. They experimented the entanglement of two qudits, encoded in five states of calcium ions¹⁷¹².

Their PINE system supports Qiskit, Cirq, PennyLane and Pytket (Figure 419). They team up with NTT on developing financial applications¹⁷¹³.

¹⁷⁰⁶ See [Characterizing large-scale quantum computers via cycle benchmarking](#) by Alexander Erhard et al, 2019 (13 pages).

¹⁷⁰⁷ In [EU Team Make Progress Toward European-Only Compact Quantum Computer That Could Run on Solar Power](#) by Matt Swayne, The Quantum Insider, October 2021, we see them touting an energetic performance: a 24 qubits experimental system consumes only 1,500 W, like a kettle. Unfortunately, with 24 qubits can be emulated on a laptop that consumes less than 30W!

¹⁷⁰⁸ See [14-Qubit Entanglement: Creation and Coherence](#) by Thomas Monz et al, 2011 (4 pages).

¹⁷⁰⁹ See [Native qudit entanglement in a trapped ion quantum processor](#) by Pavel Hrmo, Rainer Blatt, Tomas Monz et al, June 2022 (9 pages).

¹⁷¹⁰ See [Demonstration of fault-tolerant universal quantum gate operations](#) by Lukas Postler, Rainer Blatt, Thomas Monz et al, Nature, November 2021 and May 2022 (14 pages).

¹⁷¹¹ See [Strategies for practical advantage of fault-tolerant circuit design in noisy trapped-ion quantum computers](#) by Sascha Heußen et al, January 2023 (36 pages).

¹⁷¹² See [Native qudit entanglement in a trapped ion quantum processor](#) by Pavel Hrmo, Marcus Huber, Rainer Blatt, Philipp Schindler, Thomas Monz and Martin Ringbauer, Nature Communications, April 2023 (6 pages).

¹⁷¹³ See [Quantum computing in finance - Quantum readiness for commercial deployment and applications](#), NTT, February 2022 (17 pages).

In 2023, they obtained a quantum volume of 128 (7 qubits) with this PINE QPU, which is behind the state of the art in trapped ions as we've seen with IonQ and Quantinuum results¹⁷¹⁴.

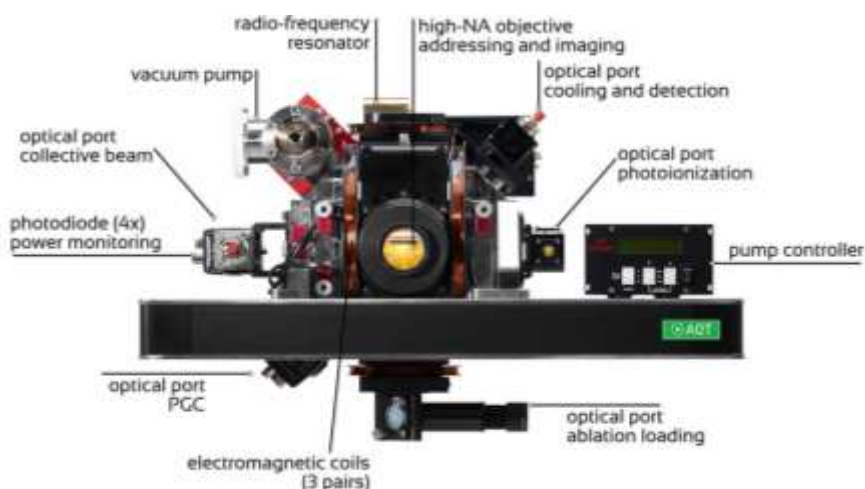


Figure 419: AQT PINE QPU setup.

Source: [Out-of-the-box integration of a fully functional, table-top size quantum processor into your system](#), AQT.

oxford ionics

Oxford Ionics (2019, UK, \$47M) is a spin-off from the Department of Physics at Oxford University created by Chris Ballance and Tom Harty which is developing a trapped ions QPU with low-noise control electronics.

They were originally called Nqie Limited. The company was founded by Thomas Harty and Christopher Ballance and includes Jochen Wolf, all from Oxford University. They announced in July 2022 that they are teaming up with Infineon for the manufacturing of their trapped ions chips but they also work with EPFL. Infineon formally opened its quantum lab near Munich in October 2023, to develop and test ion trap circuits with about 20 researchers. In 2023, Oxford Ionics published a paper describing WISE (Wiring using Integrated Switching Electronics), a proposal to wire an ion-traps chip supporting up to 1,000 ions qubits in a 2D qubit array layout¹⁷¹⁵. They use switches instead of DACs with the benefit of lower power dissipation, plus analog mux and demux components and a 3D chip internal layout.



Universal Quantum (2018, UK, \$14.6M) is a spin-off from the Ion Quantum Technology Group at the University of Sussex in the UK led by Winfried Hensinger. They are developing a trapped ion system that uses microwaves transmitted by electrical circuits, and magnetic fields to control them instead of lasers. They won a \$67M deal with DLR in Germany in November 2022.



Figure 420: Universal Quantum's shuttling ion architecture in their Penning traps. Source: Universal Quantum.

¹⁷¹⁴ See [State of quantum computing in Europe: AQT pushing performance with a quantum volume of 128](#), AQT, February 2023.

¹⁷¹⁵ See [How to wire a 1000-qubit trapped ion quantum computer](#) by M. Malinowski et al, Oxford Ionics, PRX Quantum, May-October 2023 (21 pages).

They use Penning traps which are well known. The company presentation [video](#) gives the impression that they use a 2D process similar to Quantinuum's¹⁷¹⁶ (Figure 420). The cooling required is around 70K, which is done with liquid nitrogen. They still need to use lasers at least for the Doppler based ions cooling during their preparation, then for the qubit state readout combining the usual laser excitation and fluorescence readout with a CMOS or CCD sensor¹⁷¹⁷. They use electrodes to drive qubit gates. In 2022, they announced their plan to reach one million qubits, some day, with using a modular approach¹⁷¹⁸. They plan to use electric fields to connect several modules on their silicon based wafer.



Aquabits (2021, Canada) is developing a trapped ions qubit processor using 'aquaporins', that trap ions inside artificial water channels. It is supposed to avoid using lasers and micro-nano fabrication techniques, making these qubits highly scalable. There's no public way to find out how all these qubits are controlled, entangled and measured.



eleQtron GmbH (2020, Germany, 15.35M€) develops a NISQ trapped ions quantum computer. They use their Magnetic Gradient Induced Coupling (MAGIC) technology to control the qubits which was introduced in 2012.

The project involves the University of Siegen and Infineon. They are partnering with ParityQC (Austria) for software development within the ATIQ consortium with a total funding of 44.5M€ including 37M€ from the German government through DLR, of which eleQtron got 9.1M€. They initially planned to release a 10-qubit processor in 2023.



Qudora Technologies (Germany) is a spin-off from PTB and the University of Leibniz Hannover launched by Amado Bautista (CEO), Henning Hahn (also CEO), Christian Ospelkaus, Piet O. Schmidt and Andreas Waag who have a strong experience in semiconductor circuits design.

They develop a trapped-ion QPU with the goal to assemble 50 qubits. They use a mix of lasers and oscillating magnetic fields embedded inside the processor to control their ions.



Hon Hai / Foxconn (Taiwan) announced in December 2021 it is starting the development of a trapped ions quantum computer in its quantum computing research center, part of its Research Institute¹⁷¹⁹.

The quantum lab is directed by Min-Hsiu Hsieh who was previously an associate professor at the Centre for Quantum Software and Information from the University of Technology Sydney. He's more specialized in quantum information sciences than in trapped ions computing. The lab focuses on hardware development with trapped ion qubits, enabling technologies development and algorithms and software tools development for Foxconn's internal usage. In April 2023, the company announced it would deliver a 5-10 ions QPU within 5 years. The trapped-ion research team is led by Guin-Dar Lin. Their new trapped-ions lab opens at the end of 2023 in the Baokao Science and Intellectual Park Xindian in New Taipei City.



Crystal Quantum Computing (2021, France) was a stealth startup until 2022, created by Quentin Bodart (with a long-lasting experience with neutral atoms, including quantum microgravimeters) and Luca Guidon (from the CNRS MPQ laboratory in Paris).

¹⁷¹⁶ The ion routing process is described in [Efficient Qubit Routing for a Globally Connected Trapped Ion Quantum Computer](#) by Winfried Hensinger et al, February 2020 (13 pages). This is the origin of the illustration used in these lines.

¹⁷¹⁷ The ion control process with Penning Traps used by Universal Quantum seems to be described in [Microfabricated Ion Traps](#) by Winfried Hensinger et al, 2011 (28 pages).

¹⁷¹⁸ See [How Universal Quantum is rising to the million-qubit challenge](#), Universal Quantum, February 2022.

¹⁷¹⁹ See [Hon Hai to develop trapped ion quantum computers](#), Taipei Times, December 2021.

Its goal is to create a trapped ion quantum computer using strontium 88 ions energized at Rydberg levels. Their ions would be easier to control than classical trapped ions, using UV lasers at 243 nm (generated with IR lasers and double frequency doubling) and THz microwave directive antennas, all being handled in a Penning trap on a chip running at 30K.



neQxt (2023, Germany) is a startup cofounded by Sebastian Deuser (CEO), Christian Zimmermann (COO), Björn Lekitsch (CTO), Janine Hilder (CSO), and Ferdinand Schmidt-Kaler (scientific advisor). It spun out of Universität Mainz.

The only thing they communicate on is saying they use a shuttling ions-based architecture and laser driven qubit gates, which are both commonplace¹⁷²⁰.



Quantum Art

Quantum Art (2022, Israel, \$24M) is a trapped-ions startup based in Tel Aviv that was created by Tal David, the former coordinator of the defense minister and then for the whole government quantum strategy for 10 years, with Roe Ozeri from the Weizmann Institute and Amit Ben Kish from Raphael. Their roadmap is to reach 64 qubits based on the 5 trapped-ions experimental system built by Roe Ozeri¹⁷²¹.

Neutral atoms qubits

Neutral atoms, *aka* cold atoms, are another atomic form of qubits in addition to trapped ions¹⁷²². They are both trapped, but not exactly in the same way. Since these atoms are not used in ionized form, they are not trapped with electrodes but with lasers. The atoms preparation is done in multiple steps. An atom cloud is first trapped and cooled in a MOT (magneto-optical-trap)¹⁷²³. Then other lasers using the method of "optical tweezing" or "optical traps" will precisely control the position of the atoms and arrange them in patterns like 2D matrices¹⁷²⁴.

Neutral atoms can be used to create qubits with their two states corresponding to different atomic energy levels, where transitions are controlled by a variable mix of laser beams and microwaves. These atoms have controllable high-energy so-called Rydberg states which can be used as the $|1\rangle$ qubit state and/or for coupling qubits with two-qubit gates or for setting-up a Hamiltonian for a quantum simulation run.

Indeed, neutral atoms qubits can be used in two ways: with gate-based computing using one and two-qubit gates and for quantum simulations, using a prepared state of interconnected qubits that are converging to a minimum energy level, helping to find a solution to chemical simulation and optimization problems. Quantum simulation also simulate the "Hubbard model" (*aka* Fermi-Hubbard model) which modelizes strongly correlated electronic materials like condensed matter and high-temperature superconducting materials¹⁷²⁵.

¹⁷²⁰ See [Quantum Circuit Compiler for a Shuttling-Based Trapped-Ion Quantum Computer](#) by Fabian Kreppel et al, July 2022-November 2023 (35 pages).

¹⁷²¹ See [Scalable architecture for trapped-ion quantum computing using RF traps and dynamic optical potentials](#) by David Schwerdt, Roe Ozeri et al, Quantum Art and Weizmann Institute of Science, November 2023 (19 pages).

¹⁷²² See this excellent review paper: [Quantum simulation and computing with Rydberg-interacting qubits](#) by Manuel Agustin Morgado and Shannon Whitlock, Laboratory of Exotic Quantum Matter, University of Strasbourg, December 2020 (28 pages).

¹⁷²³ It creates a variable magnetic field and associate three pairs of lasers to cool down the atoms below the Doppler limit, using the Zeeman variable shift effect. The frequency of the lasers used for atoms cooling would have to be changed as they are cooled. A workaround is to progressively change their resonance frequency with a varying magnetic field so that it's aligned with the cooling laser frequency.

¹⁷²⁴ See [Quantum information processing with individual neutral atoms in optical tweezers](#) by Philippe Grangier, (47 slides).

¹⁷²⁵ See [Quantum simulation of the Hubbard model with ultracold fermions in optical lattices](#) by Leticia Tarruell (ICFO, Spain) and Laurent Sanchez-Palencia (CPHT, France), January 2019 (38 pages).

Neutral atoms are very versatile and have various other use cases on top of quantum computing and simulation, including quantum sensing, with applications in microgravity detection, electromagnetic spectrum analysis and atomic clocks and also quantum memories and repeaters¹⁷²⁶. We cover these various use cases in other parts of this book.

History

Neutral atom-based computing history starts a long time ago with fundamental physics research before quantum computing was even conceptualized. High energy atom states were formalized by Johannes Rydberg in Sweden in 1887 based on Johann Balmer's series. It was later explained by Niels Bohr in 1913 with his semiclassical model of the hydrogen atom with discrete energy levels. An extended understanding of the observed hydrogen spectrum was done by Wolfgang Pauli in 1926¹⁷²⁷.

In parallel with the many research on Bose-Einstein Condensate, which are not relevant for neutral atoms computing, mechanisms were developed in the 1980s to control individual atoms in vacuum using lasers¹⁷²⁸. It was first demonstrated in 1985 at the Bell Laboratories by Steven Chu, creating what they called "optical molasses" due to the viscosity of the confined sodium atoms used in their experiment.

In 1985, Claude Cohen-Tannoudji, Alain Aspect and Jean Dalibard started to work on laser-based atoms cooling using Doppler effect. In 1987, David Wineland and Wayne Itano improved laser cooling, which led the way for various applications including ultrahigh resolution spectroscopy and atomic clocks. In 1988, scientists led by Claude Cohen-Tannoudji at ENS Paris and others from Stanford University developed new atoms cooling mechanisms based on laser optical pumping, light shifts and laser polarization gradients¹⁷²⁹. They invented "Sisyphus cooling" in 1989, a cold atom cooling, *aka* polarization gradient cooling technique, reaching temperatures below the Doppler cooling limit. This led Claude Cohen-Tannoudji to be awarded the Nobel prize in physics in 1997, together with Steven Chu.

Laser cooling of atoms then reached very low temperatures, in the nK range. It contributed in 1995 to the discovery in the USA, of gaseous Bose-Einstein condensates that was devised in the mid-1920s by Bose and Einstein.

Ultra-cold atoms were used to create more precise atomic clocks than the cesium-based ones running at room temperature starting in 1998 in France.

In the 1980s, Serge Haroche, started to work with Rydberg atoms and their integration in superconducting cavities, pioneering cavity electrodynamics (CQED), light-atoms interactions, cold atoms control and the understanding of quantum decoherence.

So, how about neutral atoms and quantum computing? First, we have the raw idea of a quantum simulator by Richard Feynman in 1981. In 1996, Seth Lloyd demonstrated that it "was possible" to implement such scheme, noticeably with controlled atoms¹⁷³⁰.

While quantum simulation can be theoretically implemented with trapped ions and superconducting qubits, the cold atom way is the only one that is seriously investigated and which has reached the commercial stage.

¹⁷²⁶ See [Highly-efficient quantum memory for polarization qubits in a spatially-multiplexed cold atomic ensemble](#) by Julien Laurat et al, 2018 (6 pages) and [Experimental realization of 105-qubit random access quantum memory](#) by N. Jiang et al, 2019 (6 pages).

¹⁷²⁷ See [Rydberg Physics](#) by Nikola Šibalić and Charles S Adams, 2018 (28 pages).

¹⁷²⁸ See [New Mechanisms for Laser Cooling](#) by Claude Cohen-Tannoudji and William D. Phillips, 1990 (8 pages).

¹⁷²⁹ See [Laser cooling and trapping of neutral atoms](#) by Jean Dalibard and Claude Cohen-Tannoudji (20 pages).

¹⁷³⁰ See [Universal Quantum Simulators](#) by Seth Lloyd, 1996 (7 pages).

Then things started to get serious with two-qubit gates proposals from Dieter Jaksch, J. Ignacio Cirac and Peter Zoller¹⁷³¹ and from Gavin K. Brennen et al in 1998¹⁷³², with improvements from Jaksch, Zoller and Mikhail Lukin in 2000¹⁷³³. In 2012, J. Ignacio Cirac and Peter Zoller proposed a set of criteria for quantum simulators similar to those from David DiVincenzo’s 2000 for gate-based quantum computing (in Figure 421)¹⁷³⁴.

The first two-qubits gates with pairs of Rydberg atoms were implemented in 2009 by Mark Saffman from the University of Wisconsin (with “gg-qubits”, which we cover later) and at the Institut d’Optique in France (“gr-qubits”).

Many progresses were made in the 2010’s which encouraged many scientists to create their own companies. It started with the creation of ColdQuanta (2007), Muquans (2011), both using cold atoms for quantum sensing in micro-gravimetry, BraneCell (2015), Atom Computing (2018), Pasqal (2019) and QuEra (2020). Besides Muquans (now in France’s Exail), all the others are positioned in the quantum computing market although Exail is also a technology provider for Pasqal for lasers.

TABLE I. Criteria for quantum simulators and quantum computers

Criteria	Quantum computers	Quantum simulators
Quantum system	A scalable physical system with well characterized qubits	A system of quantum particles (bosons, fermions, pseudo-spins) confined in space and collectively possessing a large number of degrees of freedom
Initialization	The ability to initialize the state of the qubits to a simple fiducial state, such as $ 000\dots\rangle$	The ability to prepare (approximately) a known quantum state (typically a pure state)
Coherence	Long relevant decoherence times, much longer than the gate operation time	
Interactions	A “universal” set of quantum gates	An adjustable set of interactions used to engineer Hamiltonians/quantum master equations including some that cannot be efficiently simulated classically
Measurement	A qubit-specific measurement capability	The ability to perform measurements on the system; either individual particles or collective properties
Verification		A way to verify the results of the simulation are correct

Figure 421: comparisons of gate-based quantum computing (left) and quantum simulation (right). Source: [Quantum simulation and computing with Rydberg-interacting qubits](#) by Manuel Agustin Morgado and Shannon Whitlock, December 2020 (28 pages).

Science

Neutral atoms are non-ionized atoms with an equivalent number of protons and electrons. Neutral atoms used in cold atoms computing belong to the first column in the table of elements, having a single electron in the valence layer, such as hydrogen, sodium, lithium, cesium, potassium, or rubidium, the last one being the most commonly used. This alkaline metal has interesting energy transitions that correspond to common lasers wavelengths as well as easily generated microwaves between 3 and 10 GHz. It is possible to manage with them so-called closed transitions which allow, with lasers, to make atoms transit between several states in a cyclic and controlled manner. But ytterbium and strontium with two electrons in their valence shell are also used, but with the qubit state stored in the atom nucleus spin and separated with a magnetic field instead of hyperfine electronic states¹⁷³⁵. On top of that, states are stable long enough to perform computations, i.e. about a hundred microseconds. Other elements are investigated like dysprosium and praseodymium who are lanthanide elements.

¹⁷³¹ See [Entanglement of atoms via cold controlled collisions](#) by Dieter Jaksch, H.-J. Briegel, J. Ignacio Cirac, C. W. Gardiner and Peter Zoller, 1998 (4 pages).

¹⁷³² See [Quantum Logic Gates in Optical Lattices](#) by Gavin K. Brennen, Carlton M. Caves, Poul S. Jessen, and Ivan H. Deutsch, PRL, 1998 (7 pages).

¹⁷³³ See [Fast Quantum Gates for Neutral Atoms](#) by D. Jaksch, J. Ignacio Cirac, Peter Zoller, Mikhail D. Lukin et al, PRL, 2000 (4 pages).

¹⁷³⁴ See [Goals and opportunities in quantum simulation](#) by J. Ignacio Cirac and Peter Zoller, Nature Physics, 2012 (3 pages).

¹⁷³⁵ See [Repetitive Readout and Real-Time Control of Nuclear Spin Qubits in ¹⁷¹Yb Atoms](#) by William Huie et al, September 2023 (28 pages).

Cold atoms can be used in Rydberg states, which correspond to a very high level of energetic excitation, between 50 and 100 electron quantum number (layer position in atom against Bohr's model, labelled n or N). This creates very large electron orbits, scaling by N^2 . These high energy states are used to create entanglement between atoms and thus to operate multi-qubit quantum gates or large Hamiltonians in quantum simulation modes. These excited states have a fairly good stability level of about 100 μs .

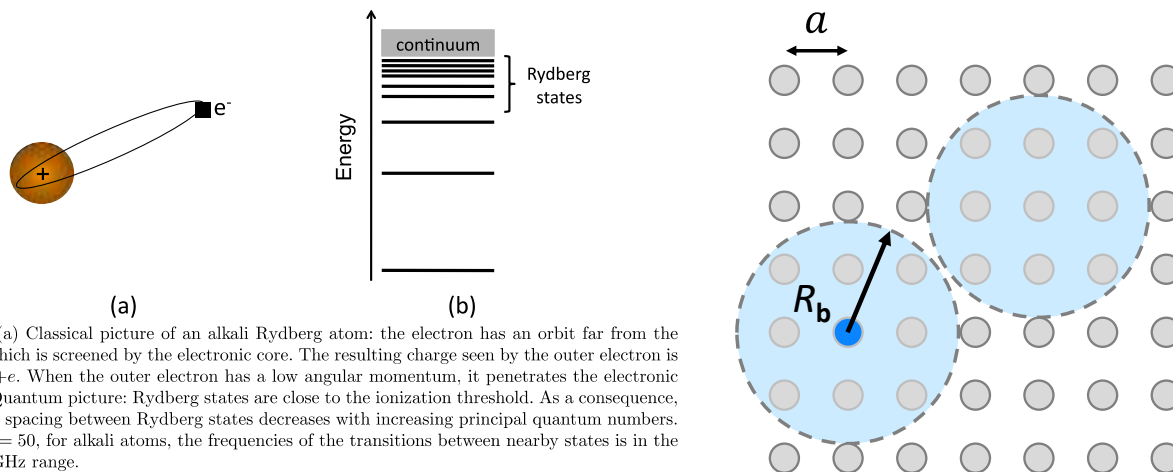


Figure 1: (a) Classical picture of an alkali Rydberg atom: the electron has an orbit far from the nucleus, which is screened by the electronic core. The resulting charge seen by the outer electron is therefore $+e$. When the outer electron has a low angular momentum, it penetrates the electronic core. (b) Quantum picture: Rydberg states are close to the ionization threshold. As a consequence, the energy spacing between Rydberg states decreases with increasing principal quantum numbers. Around $n = 50$, for alkali atoms, the frequencies of the transitions between nearby states is in the 10 – 100 GHz range.

Figure 422: Rydberg state are high-energy level of excited atoms that create a dipole in the atom. It enables entanglement with neighbor atoms. Source: [Interacting Cold Rydberg Atoms: a Toy Many-Body System](#) by Antoine Browaeys and Thierry Lahaye, 2013 (20 pages).

It is several orders of magnitude longer than the classical excited states (hyperfine, which are used for cold atoms qubit states). This stability is somehow equivalent to the coherence time of superconducting qubits.

Cold atoms computing also exploits the Rydberg blockade effect, where a Rydberg atom excited with a high energy level (with $n > 50-70$) prevents neighboring atoms from reaching that level. When excited, these atoms behave like accentuated dipoles, the orbit of the electrons of the valence layer being very inclined as shown in Figure 422. They also have a disproportionate size of up to one micron (μm) in diameter for $n=100$ with ^{87}Rb . This is close to being in an ionized state¹⁷³⁶. Their electromagnetic characteristics make the atoms react with their neighbors whose excitation they block within a perimeter of up to 20 μm , which is huge at the atomic scale. Activated Rydberg atom can also be excited by lasers to generate well-isolated single photons that can be used in nonlinear optics¹⁷³⁷. This provides yet another source of single photons, in addition to quantum dots. The Rydberg blockade phenomenon could also be implemented in quantum telecommunications, in spectroscopy and in atomic clocks¹⁷³⁸.

But as usual with all qubit types, there are many variations of cold atoms qubits (Figure 423). First, you have three breeds of qubits whose manifold is based on classical energy levels. With ground-Rydberg qubits which are controlled by UV, visible and infrared lasers, Rydberg-Rydberg qubits controlled by microwaves and lasers, ground-ground qubits controlled by microwaves and optical lasers, and at last, nuclear spin atoms controlled by optical lasers using Raman transitions.

Some vendors like Pasqal and QuEra are investigating the first three types of qubits, seemingly favoring gr-qubits and rr-qubits for quantum simulation and gg-qubits for gate-based computing.

¹⁷³⁶ This [presentation of 52 slides](#) from 2014 describes well the history and geometry of the Rydberg atoms.

¹⁷³⁷ See [Observation of coherent many-body Rabi oscillations](#) by Yaroslav Dudin and Alex Kuzmich, GeorgiaTech, 2012 (5 pages) and [Nonlinear quantum optics mediated by Rydberg interactions](#) by Sebastian Hofferberth et al, 2016 (26 pages).

¹⁷³⁸ See [Photon-Mediated Quantum Information Processing with Neutral Atoms in an Optical Cavity](#) by Stephan Welte, 2019 (124 pages).

Topological states allowing to create more reliable qubit-based computing systems are also studied¹⁷³⁹.

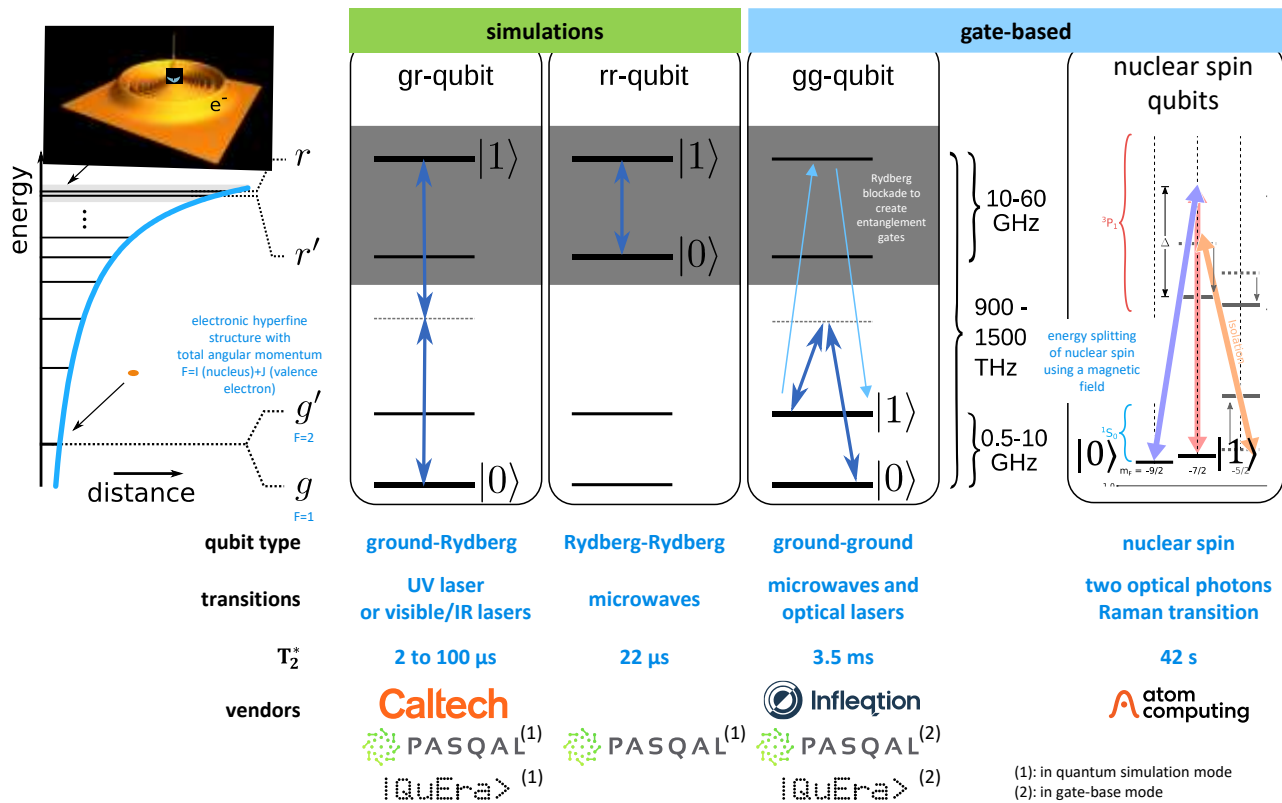


Figure 423: the various ways to control cold atoms. Source: [Quantum simulation and computing with Rydberg-interacting qubits](#) by Manuel Agustin Morgado and Shannon Whitlock, December 2020 (28 pages) and additions by Olivier Ezratty, 2022-2024.

Cold atoms qubits are the most common ones that can be used in both gate-based quantum computing and in quantum simulation computing mode (*aka* analog quantum simulation). In the first case, qubits are individually controlled over time with single and two-qubit gates, to read qubit state at the end of processing¹⁷⁴⁰. With quantum simulation¹⁷⁴¹, a so-called Hamiltonian is prepared with specific atoms geometry and connectivity, usually using Rydberg states, which then converges itself into an energy minimum leading to qubits measurement. Individual qubits are controlled only at the initialization stage and for readout. In that case, there is no sequential programming, but variational algorithms based on a classical cost function minimization can be used.

Most neutral atoms systems and qubit types can be used in both paradigms, but it seems that the gate-based model is the most demanding and complicated to handle¹⁷⁴².

¹⁷³⁹ See [Topologically protected edge states in small Rydberg systems](#) by Antoine Browaeys et al, 2018 (6 pages) and [Observation of a symmetry protected topological phase of interacting bosons with Rydberg atoms](#) by Antoine Browaeys, Thierry Lahaye et al, 2019 (20 pages). Quantum simulation using cold atoms is also a tool to simulate topological matter. See [Scientists unveil first quantum simulation of 3-D topological matter with ultracold atoms](#) by Hong Kong University of Science and Technology, July 2019.

¹⁷⁴⁰ See [Versatile neutral atoms take on quantum circuits](#) by Hannah J Williams, Nature, 2022 (2 pages) which describes two such methods, implemented by QuEra and ColdQuanta and mentioned later.

¹⁷⁴¹ See [Toward quantum simulation with Rydberg atoms](#) by Thanh Long Nguyen, 2016 (182 pages), [Quantum simulations with ultracold atoms in optical lattices](#) by Christian Gross and Immanuel Bloch, 2017 (8 pages), [Tunable two-dimensional arrays of single Rydberg atoms for realizing quantum Ising models](#) by Thierry Lahaye and Antoine Browaeys, 2017 (13 pages), [Quantum read-out for cold atomic quantum simulators](#), par J. Eisert et al, 2018 (20 pages), [Quantum critical behaviour at the many-body localization transition](#) by Markus Greiner et al, 2018 (10 pages), [Quantum Kibble-Zurek mechanism and critical dynamics on a programmable Rydberg simulator](#) by Alexander Keesling et al, 2019 (16 pages) and [Many-body physics with individually controlled Rydberg atoms](#) by Antoine Browaeys and Thierry Lahaye, 2020 (14 pages).

¹⁷⁴² It also requires specific compilation tools, as described in [Computational Capabilities and Compiler Development for Neutral Atom Quantum Processors: Connecting Tool Developers and Hardware Experts](#) by Ludwig Schmid et al, September 2023 (32 pages).

Thus, three situations in the market can be observed: startups like Pasqal and QuEra are explicitly saying that they start first with the quantum simulation paradigm – sometimes labelled “programmable Hamiltonian - with plans to later also support gate-based models, others like Inflektion tout their positioning on gate-based quantum computing but actually start with quantum simulation and at last, others like Atom Computing start readily with a gate-based approach. The landscape suddenly changed in December 2023 when Harvard and MIT announced having created 48 logical qubits and fault-tolerance with 280 cold atoms. Although they modestly improved the physical qubits performance, with using post-selection, it was considered as being a breakthrough¹⁷⁴³.

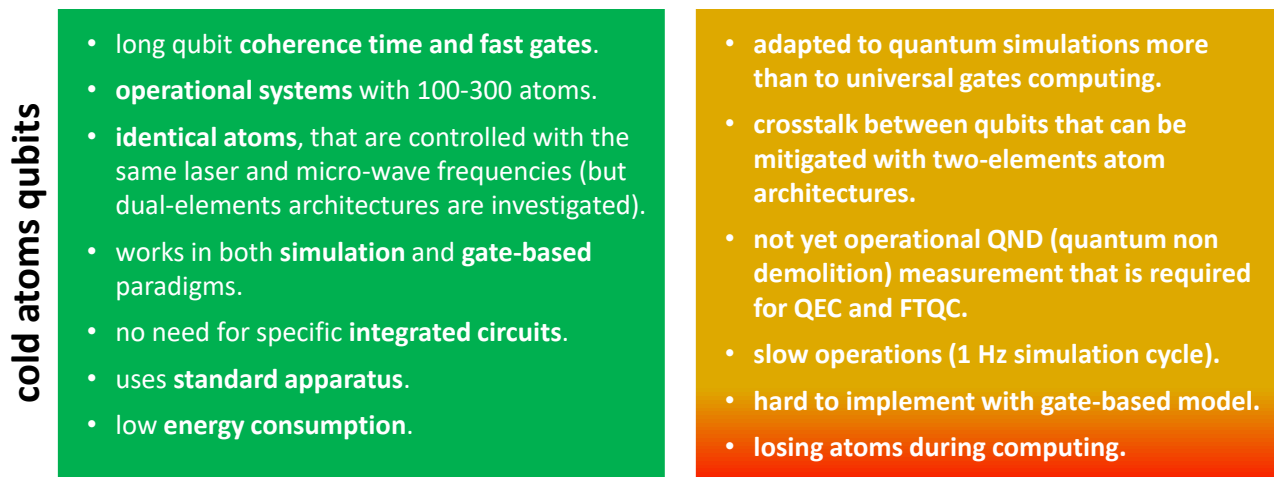


Figure 424: pros and cons of cold atoms quantum computers and simulators. (cc) Olivier Ezratty, 2022-2023.

One concern being addressed is the speed of operations. One single shot can last about half a second, explained by the time it takes to prepare the atoms. Actual computing is quite fast (about 5 μ s) with additional time for the disposal of the used atoms after each shot (about 20 ms). Shot times could potentially be accelerated by one to two orders of magnitude by improving the way atoms are prepared and arranged in the vacuum chamber. Other concerns relate to how these systems can scale with regards to atoms placement and control, particularly given tweezer-based placement control must be deactivated during computing (Figure 424).

Qubit operations

We’ll look here at the way qubits lifecycle works, from initialization to readout, with quantum gates in-between (for gate-based systems)¹⁷⁴⁴. The general principle is as follows:

- **Quantum state** for the $|0\rangle$ and $|1\rangle$ qubit basis corresponds to a ground and excited state, which depends on the qubit type as seen previously with ground-Rydberg, Rydberg-Rydberg, ground-ground and nuclear spin atoms qubits. The most commonplace for gate-based computing seems to be the ground-ground case. The qubit $|0\rangle$ state is usually prepared with laser pumping or with some microwave pulse. Contrarily to superconducting and quantum dots spin qubits who are static in nature in their electronic circuits, atoms must be first arranged in space before any computing can start. The qubits can be arranged in 1D, 2D¹⁷⁴⁵ or 3D matrices¹⁷⁴⁶ (Figure 425).

¹⁷⁴³ See [Logical quantum processor based on reconfigurable atom arrays](#) by Dolev Bluvstein, Mikhail D. Lukin et al, Nature, December 2023 (42 pages) and the corresponding [arXiv](#).

¹⁷⁴⁴ See [Neutral Atom Quantum Computing Hardware: Performance and End-User Perspective](#) by Karen Wintersperger et al, April-May 2023 (27 pages) that contains a good description of neutral atoms computers operations.

¹⁷⁴⁵ See the thesis [Rydberg interactions in a defect-free array of single-atom quantum systems](#) by Daniel Ohl de Mello, 2020 (147 pages) which describes the way to fill a 2D matrix of a hundred heavy atoms.

¹⁷⁴⁶ See [Three-Dimensional Trapping of Individual Rydberg Atoms in Ponderomotive Bottle Beam Traps](#) by Antoine Browaeys, Thierry Lahaye et al, 2019 (8 pages).

They are cooled, controlled, and positioned by several lasers organized in precision optical tweezers¹⁷⁴⁷. A qubit can be based on a single atom or on a group of atoms depending on the methods used. The atoms are prepared with a hot or cold source (some μK) which then feeds an ultra-vacuum chamber where a MOT is cooling them with laser lasers.

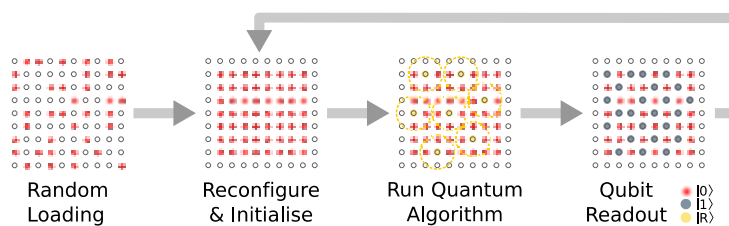


Figure 2. Schematic of a Rydberg array quantum computer. Atoms are initially loaded stochastically, followed by rearrangement to achieve a defect free qubit register. Coherent excitation to Rydberg states allows implementation of quantum algorithms exploiting long-range interactions to couple neighbouring qubits, followed by state-selective readout which is repeated many times to tomographically reconstruct the output state.

Figure 425: how an array of cold atoms is being prepared. Source: [Rydberg atom quantum technologies](#) by James Shaffer, 2019 (24 pages).

- **Single-qubit quantum gates** are activated by a mix of microwaves (a few GHz, compatible with hyperfine states in the case of Rydberg-Rydberg or ground-ground qubits) and laser pumping to change the energy state of the cold atom between its ground and excited state. These gates can also use Raman transitions driven by lasers on two frequencies or by a combination of the Stark effect of spectral line shifting under the effect of an electric field and microwaves. In most cases, cold atoms single qubit gates are $R_z(\theta)$ (arbitrary phase rotation). The best single-qubit gate fidelities were 99.9% as of 2022¹⁷⁴⁸.
- **Two-qubit quantum gates** also use a variable mix of microwaves and lasers most of the time, using Rydberg state, the related Rydberg blockage phenomenon, and dipole-dipole interactions¹⁷⁴⁹. They are applied to atoms in their ground or excited state, which projects its valence layer electrons into a high orbit. For rubidium, there is only one electron to manage in this layer. These quantum gates can in practice involve more than two qubits, which is useful to set up a Hamiltonian in quantum simulation mode. The fidelity of two qubit gates was quite low in 2016 with a maximum of 75% with rubidium and 81% in 2016 with cesium. It increased to a better level of 99.5% with 60 operating qubits in 2023¹⁷⁵⁰ and even 99.85% in 2022¹⁷⁵¹, both with CZ gates. The decoherence of cold atoms qubits has different origins: photoionization, spontaneous emission of photons, transitions induced by black body radiation, stability of control lasers and laser pulse timing and precision control of atoms in space¹⁷⁵². The two-qubit gate set is variable. It can for example contain a CPHASE, CZ (ColdQuanta/Infleqtion, QuEra) and XY gate. These gates usually work in the nearest neighborhood fashion. With cold-atoms, two-qubit gates are usually faster to operate than single qubit gates¹⁷⁵³.

¹⁷⁴⁷ See the review paper [Roadmap for optical tweezers](#) by Giovanni Volpe et al, Journal of Physics Photonics, April 2023 (136 pages). Up to several thousands atom can be positioned and controlled by tweezers using a mix of SLMs and AODs.

¹⁷⁴⁸ See [Multi-qubit entanglement and algorithms on a neutral-atom quantum computer](#) by T. M. Graham et al, ColdQuanta, Nature, April 2022 (25 pages).

¹⁷⁴⁹ In 2019, American researchers were able to create multi-qubit quantum gates with 95% fidelity based on cold atoms, in [Parallel implementation of high-fidelity multi-qubit gates with neutral atoms](#) by H. Levine et al, August 2019 (16 pages). Two-qubit gate bases in [Direct Measurement of the van der Waals Interaction between Two Rydberg Atoms](#) by Lucas Béguin, Antoine Browaeys et al, 2013 (5 pages). And [Quantum information processing with individual neutral atoms optical tweezers](#) by Philippe Grangier (47 slides).

¹⁷⁵⁰ See [Compiling Quantum Circuits for Dynamically Field-Programmable Neutral Atoms Array Processors](#) by Daniel Bochen Tan, Mikhail D. Lukin et al, June 2023 (18 pages).

¹⁷⁵¹ See [Two-qubit gate in neutral atoms using transitionless quantum driving](#) by Archismita Dalal et al, University of Calgary, Jun 2022 (22 pages).

¹⁷⁵² Source: [Quantum Computing with Neutral Atoms](#), 2013 (42 slides).

¹⁷⁵³ It could even reach the nanosecond scale as experimented in [Ultrafast energy exchange between two single Rydberg atoms on a nanosecond timescale](#) by Y. Chew et al, Nature Photonics, 2022 (7 pages).

- **Qubit readout** uses a CCD or CMOS camera detecting the atoms fluorescence with a method like the one used with trapped ions and NV centers. Figure 426 shows a simplified description a cold atom qubits system with laser and microwave-based control tools and qubit measurement using fluorescence and a camera. This method is destructive of the qubit state. It is not yet a QND measurement.

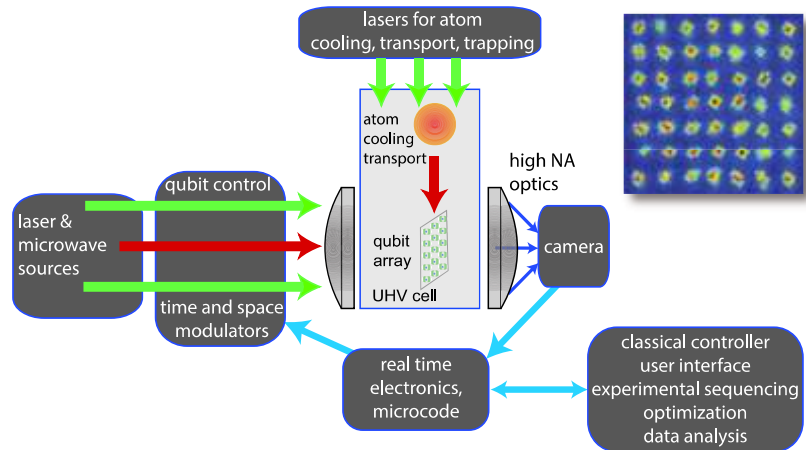


Figure 426: typical devices arrangement to control cold atoms. Source: [Quantum computing with atomic qubits and Rydberg interactions: Progress and challenges](#) by Mark Saffman, 2016 (28 pages).

Cold atoms are not the easiest candidate to implement measurement-based quantum error correction for creating FTQC systems. There are however various investigated solutions to create non demolition measurement like with moving atoms to a readout zone, using a second atomic element as ancilla qubits, shelving data qubits in auxiliary atomic levels, using optical cavities or even ancillary atomic ensembles¹⁷⁵⁴ to implement fault-tolerant error correction without the need for qubit readout¹⁷⁵⁵. Readout fidelities are still to be improved and are currently in the 95% range¹⁷⁵⁶.

Cold atoms quantum computing can also be based with other programming paradigms, like fermionic computing. One proposal from the MIT associates pairs of cold atoms in 2D optical lattices in which the quantum information is encoded in the vibrational state of the atom pairs¹⁷⁵⁷.

Other hybrid paradigms are also investigated involving a mix of gate-based and analog circuits¹⁷⁵⁸.

Setup

In general, cold atom-based systems operate at room temperatures but atoms are cooled at below 1 mK and in ultra-high vacuum. In practice, it is the ultra-high vacuum pumps and the atoms laser cooling that ensures this thermalization, but for a large number of atoms, a 4K cryostat is to be used to cool the inside of the atoms chamber and the vacuum pump. Preparing and controlling the qubits is based on a set of lasers, light structuring devices (SLM and AODs), polarizing beam splitters and microwaves devices (Figure 427). Microwaves are sent in a “one to many” mode and usually coupled with targeted photons to control individual gates. Cold atom qubits vendors often argue that their QPUs work at ambient temperature and do not require any refrigerant based cooling system.

While they do not use cryostats like those that cool superconducting and silicon qubits, they still cool their qubits, using different methods combining ultra-vacuum pumps, magnetic traps and lasers. And now, some are even using a 4K cryostat to cool their ultra-vacuum pump and chamber to avoid the pollution of their tweezer-assembled 2D grid by spare atoms, at least, beyond 200 atoms.

¹⁷⁵⁴ This inventory comes from [High-fidelity parallel entangling gates on a neutral atom quantum computer](#) by Simon J. Evered, Mikhail D. Lukin et al, Nature, April-October 2023 (21 pages) which contains a good related bibliography.

¹⁷⁵⁵ See [Measurement-free fault-tolerant quantum error correction in near-term devices](#) by Sascha Heußen et al, Aachen University and Forschungszentrum Jülich, July 2023 (24 pages).

¹⁷⁵⁶ See [Fast Preparation and Detection of a Rydberg Qubit Using Atomic Ensembles](#) by Wenchao X et al, PRL, July 2021 (6 pages).

¹⁷⁵⁷ See [Quantum register of fermion pairs](#) by Thomas Hartke, Botond Oreg, Ningyuan Jia and Martin Zwierlein, MIT, 2021 (10 pages).

¹⁷⁵⁸ See [Quantum simulation of fermionic systems using hybrid digital-analog quantum computing approach](#) by Nikita Guseynov and Walter Pogosov, December 2021-May 2022 (20 pages).

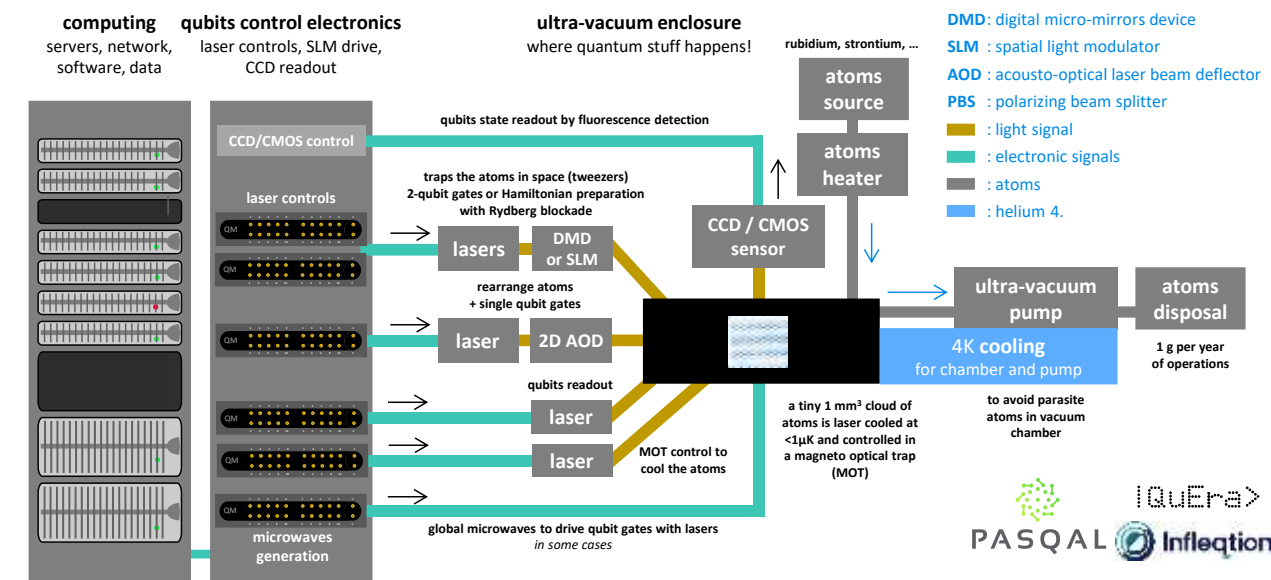


Figure 427: overall architecture of a cold atoms based computer. (cc) Olivier Ezratty, 2022-2023.

Here are some explanations on the mentioned devices¹⁷⁵⁹:

MOT (magneto-optical trap) uses laser cooling and a spatially-varying magnetic field to create a trap for our cold atoms where they are cooled with lasers, Doppler and Sisyphus effects. The MOT contains a weak quadrupolar spatially varying magnetic field generated by a coil of about 8 cm diameter and four to six glass doors letting through circularly polarized red lasers beams which are slowing down the movement of the atoms at the center of the MOT. It enables the atoms to reach very low temperatures of under 1 mK. Figure 428 shows the chamber used by Pasqal, which contains a MOT. It is quite heavy, weighing more than 25 kg. The chamber is pumped to be under ultra-vacuum.



Figure 428: a vacuum chamber from Pasqal, which contains a MOT.

SLM (spatial light modulator) are LCD systems modulating light. The SLMs breeds used in cold atom tweezers modulate the laser light phase using nematic liquid crystal layers instead of just its intensity like in regular LCD chips and create sort of a hologram. Phase SLMs are usually based on LCOS chips thanks to their controllable birefringence, with vendors like Hamamatsu, Holoeye and Thorlabs. SLMs are used to create optical tweezers that precisely control atoms position in vacuum and at the nanometer scale^{1760 1761}. Tweezers are used to create custom 2D layout arrangements, or graphs, of atoms with a precise positioning corresponding to the problem to solve in quantum simulation mode. It is the quantum equivalent of a programmable FPGA circuit¹⁷⁶². The atoms must be separated by about 5 μm in their 2D grid, a distance slightly larger than the Rydberg blockage radius and which also corresponds to the SLM-based holography resolution.

AOM (acoustic-optical modulators) aka **AOD** (acousto-optic deflectors) uses an acousto-optic effect to diffract and shift the frequency of light using sound waves at radio frequencies. It contains a piezoelectric transducer that is attached to a material such as glass.

¹⁷⁵⁹ See [Roadmap on Atomtronics: State of the art and perspective](#) by L. Amico, August 2020-June 2021 (113 pages).

¹⁷⁶⁰ See [High-Precision Laser Beam Shaping and Image Projection](#) by Jinyang Liang, 2012 (126 pages).

¹⁷⁶¹ See [Spatial light modulators](#), MPD, 2020 (6 pages).

¹⁷⁶² See [Field-Programmable Qubit Arrays: The Quantum Analog of FPGAs](#) by Yuval Boger, EETimes, February 2023.

An oscillating electric signal creates transducer vibrations, producing sound waves within the material, changing the refraction index¹⁷⁶³.

Image sensors. They are used as described above for qubit readout but also in combination with tweezers while positioning the atoms¹⁷⁶⁴. They are either CCD or CMOS imagers.

Research

The most active research laboratories with cold atom-based qubits are in the USA (Harvard with **Mikhail Lukin**, University of Wisconsin with **Mark Saffman**¹⁷⁶⁵, **Adam Kaufman** from JILA in Colorado¹⁷⁶⁶, Caltech with **Vladan Vuletic** and **Manuel Endres**, Princeton with **Jeff D. Thompson**, who investigates nuclear spin neutral atoms and circular Rydberg atoms^{1767 1768 1769}, Caltech with **Manuel Endres**¹⁷⁷⁰, GeorgiaTech and the Quantum Systems Accelerator (QSA) from the DoE Lawrence Berkeley National Laboratory), in the UK at the University of Cambridge and the University of Strathclyde in the group of **Jonathan Pritchard**¹⁷⁷¹, in Austria at the University of Innsbruck¹⁷⁷² and the University of Vienna, Germany (Max Planck Institute, Free University of Berlin, University of Stuttgart, University of Darmstadt¹⁷⁷³), The Netherlands (Eindhoven University of Technology¹⁷⁷⁴) and Taiwan¹⁷⁷⁵.

In France we have Institute d'Optique Graduate School with **Antoine Browaeys** and **Thierry Lahaye** who cofounded **Pasqal**, and the **Unistra** laboratory in Strasbourg run by **Shannon Whitlock**, who is behind the project **aQCess** and the European Flagship **EuRyQa** (with Pasqal).¹⁷⁷⁶

Another European H2020 project, **AtomQT**, covers research with cold atoms, both qubits and sensing. In France, it involves the Bordeaux Optics Institute and the LPMC in Grenoble with **Benoît Vermersch**.

¹⁷⁶³ See alternative and more scalable approaches as proposed in [An integrated photonic engine for programmable atomic control](#) by Ian Christen et al, MIT and CSEM, August 2022 (16 pages).

¹⁷⁶⁴ See [High-fidelity detection of large-scale atom arrays in an optical lattice](#) by Renhao Tao, Immanuel Bloch et al, September 2023 (9 pages).

¹⁷⁶⁵ See [Quantum computing with atomic qubits and Rydberg interactions: Progress and challenges](#) by Mark Saffman, 2016 (28 pages).

¹⁷⁶⁶ See [Ytterbium nuclear-spin qubits in an optical tweezer array](#) by Alec Jenkins, Adam M. Kaufman et al December 2021-May 2023 (21 pages).

¹⁷⁶⁷ See [High-fidelity gates with mid-circuit erasure conversion in a metastable neutral atom qubit](#) by Shuo Ma, Guido Pupillo, Shruti Puri, Jeff D. Thompson et al, Nature, May-October 2023 (17 pages).

¹⁷⁶⁸ See [Universal Gate Operations on Nuclear Spin Qubits in an Optical Tweezer Array of ¹⁷¹Yb Atoms](#) by Shuo Ma, Jeff D. Thompson et al, PRX, Princeton University, 2022 (12 pages).

¹⁷⁶⁹ See [Optimizing Rydberg Gates for Logical Qubit Performance](#) by Sven Jandura, Jeff D. Thompson and Guido Pupillo, October 2022 (15 pages).

¹⁷⁷⁰ See [Erasure conversion in a high-fidelity Rydberg quantum simulator](#) by Pascal Scholl, Manuel Endres et al, Caltech and Stanford University, Nature, May-October 2023 (17 pages).

¹⁷⁷¹ See [Randomized Benchmarking using Non-Destructive Readout in a 2D Atom Array](#) by B. Nikolov et al, University of Strathclyde, January 2023 (9 pages).

¹⁷⁷² See [Universal Quantum Computation in Globally Driven Rydberg Atom Arrays](#) by Francesco Cesa and Hannes Pichler, University of Innsbruck and University of Trieste, May 2023 (6 pages).

¹⁷⁷³ See [Defect-free assembly of 2D clusters of more than 100 single-atom quantum systems](#) by Daniel Ohl de Mello et al, February 2019-May 2023 (5 pages).

¹⁷⁷⁴ See [Robust control and optimal Rydberg states for neutral atom two-qubit gates](#) by Madhav Mohan et al, December 2022 (14 pages).

¹⁷⁷⁵ See [High-fidelity Rydberg control-Z gates with time-optimal pulses](#) by T. H. Chang et al, Taiwan, March 2023 (8 pages).

¹⁷⁷⁶ See [Time-Optimal Two- and Three-Qubit Gates for Rydberg Atoms](#) by Sven Jandura and Guido Pupillo, February 2022 (24 pages).

In Germany, **Johannes Zeiher** from the Max Planck Institute of Quantum Optics created SNACQ in 2022, a research group on cold atoms (“Scalable Neutral Atom Quantum Computing”). Its ambition is to create the first error-corrected logical qubit¹⁷⁷⁷. It complements **Immanuel Bloch**’s team (Quantum Many-body Systems), **Gerhard Rempe**’s group (Quantum Dynamics) and **Arno Rauschenbeutel**’s team at Humboldt-Universität in Berlin.

In 2017, Mikhail Lukin's team from **Harvard** University and a team from **MIT** assembled 51 rubidium atoms¹⁷⁷⁸. It went up to 256 qubits in July 2021¹⁷⁷⁹. In 2023, it was handling two-qubit CZ gates with 60 atoms with 99.5% fidelities. Antoine Browaeys’s team at **Institut d’Optique** reached 72 cold atoms in a 3D structure in 2018, 196 in 2020¹⁷⁸⁰, and 500 in 2021. Several startups are positioned in the cold atoms computing market, including **Inflection** (formerly ColdQuanta, 2007, USA, working initially on quantum sensing), **Atom Computing** (2018, USA), **Pasqal** (2019, France), **QuEra Computing** (2020, USA, linked to Mikhael Lukin and Harvard) and **Planqc** (2022, Germany).

neutral atoms gate-based quantum computing scalability challenges

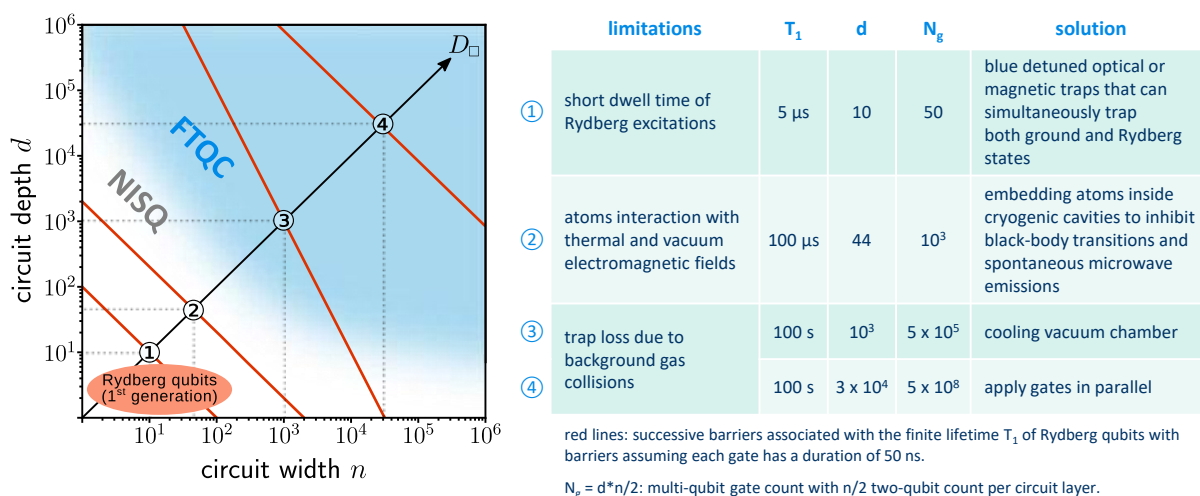


Figure 429: sorting out the cold atoms computing challenges per generation. Source: [Quantum simulation and computing with Rydberg-interacting qubits](#) by Manuel Agustin Morgado and Shannon Whitlock, December 2020 (28 pages) and text formatting by Olivier Ezratty, 2022.

You may obviously wonder whether China is also working on cold atom. You bet they are, like in all quantum fields. It includes the Key Laboratory of Quantum Optics in Shanghai, the Center for Cold Atom Physics in Wuhan, both from the **China Academy of Science**¹⁷⁸¹ and **Xidian University**¹⁷⁸²¹⁷⁸³ ¹⁷⁸⁴. Some of these labs are focused on building cold atom based quantum sensors and repeaters.

¹⁷⁷⁷ See [Johannes Zeiher launches new research group](#), February 2022.

¹⁷⁷⁸ See [Quantum simulator with 51 qubits is largest ever](#) by Matt Reynolds, 2017 which refers to [Probing many-body dynamics on a 51-atom quantum simulator](#) by Hannes Bernien, Mikhail Lukin et al, 2017 (24 pages).

¹⁷⁷⁹ See [Harvard-led physicists take big step in race to quantum computing](#), Harvard, July 2021. Their work is like Pasqal/IOGS based on the same technique with rubidium atoms and SLM tweezers.

¹⁷⁸⁰ See [Synthetic three-dimensional atomic structures assembled atom by atom](#) by Daniel Barredo, Antoine Browaeys et al, 2018 (4 pages).

¹⁷⁸¹ See [Two-qubit controlled-PHASE Rydberg blockade gate protocol for neutral atoms via off-resonant modulated driving within a single pulse](#) by Yuan Sun et al, October 2019 (16 pages) which deals with the improvement of CPHASE two-qubit gates on gg-qubits, with gate time at $1 \mu\text{s}$.

¹⁷⁸² See [Quantum gates with weak van der Waals interactions of neutral Rydberg atoms](#) by Xiao-Feng Shi et al, Xidian University, December 2022 (7 pages).

¹⁷⁸³ See [Hyperentanglement of divalent neutral atoms by Rydberg blockade](#) by Xiao-Feng Shi et al, December 2022 (17 pages).

¹⁷⁸⁴ See [Quantum logic and entanglement by neutral Rydberg atoms: methods and fidelity](#) by Xiao-Feng Shi, Xidian University, December 2022 (57 pages).

They also investigate cold atoms quantum computing¹⁷⁸⁵ with interesting recent achievements in the implementation of gate-based models¹⁷⁸⁶. The many challenges to overcome are, like with all other qubit types, about scalability and, about implementing non-destructive qubit measurement to enable QEC/FTQC.

Scalability can be improved mostly with increasing the lifetime of atom interactions as described in the above chart in Figure 429. It also requires the continuous improvement of single and two-qubit gate fidelities, one goal being to reach three nines (99.9% for two-qubit gates)¹⁷⁸⁷ ¹⁷⁸⁸. One approach, also tested with trapped ions, consists in mixing two species of neutral atoms. It is evaluated in a configuration prototyped at the **University of Chicago**. Shown in Figure 430, it packs 512 atoms in an array using an equivalent proportion of cesium and rubidium atoms in alternating patterns. These atom species have a different laser wavelength for gate drive, which results in a reduction of qubit crosstalk¹⁷⁸⁹.

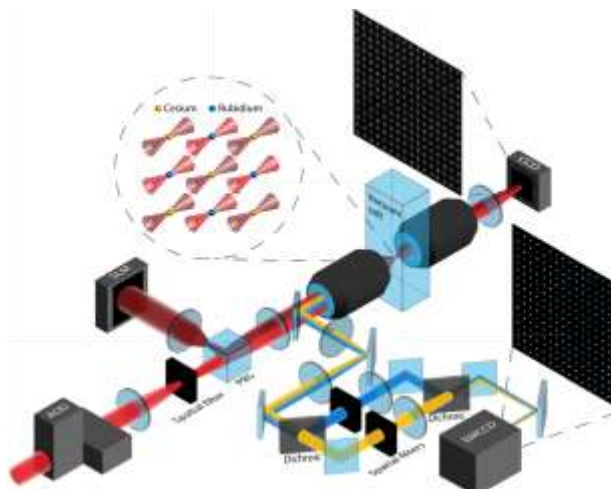


Figure 430: mixing two types of atoms, cesium and rubidium. Source: [Dual-Element, Two-Dimensional Atom Array with Continuous-Mode Operation](#) by Kevin Singh et al, University of Chicago, February 2022 (11 pages).

Many research works are being done to improve quantum simulations capabilities and scaling, with estimating the fidelity of neutral atom based quantum simulators¹⁷⁹⁰, measuring high-dimensional entanglement¹⁷⁹¹, understanding the effect of noise and building resilience to errors¹⁷⁹² ¹⁷⁹³ and on creating measurement techniques beyond the standard basis¹⁷⁹⁴. Other work investigates the capability of organizing the atoms in 3D¹⁷⁹⁵, with up to 30,000 atoms¹⁷⁹⁶.

¹⁷⁸⁵ See [Proposal for practical Rydberg quantum gates using a native two-photon excitation](#) by Rui Li et al, March 2023 (16 pages).

¹⁷⁸⁶ See [Scalable Multipartite Entanglement Created by Spin Exchange in an Optical Lattice](#) by Wei-Yong Zhang, Jian-Wei Pan et al, PRL, August 2023 (19 pages).

¹⁷⁸⁷ See [Two-qubit gate in neutral atoms using transitionless quantum driving](#) by Archismita Dalal and Barry C. Sanders, University of Calgary, June 2022 (22 pages). These researchers could improve CZ two-qubit gate with cesium with fidelities of 99,85%.

¹⁷⁸⁸ See [Demonstration of a Quantum Gate Using Electromagnetically Induced Transparency](#) by K. McDonnell, L. F. Keary, and J. D. Pritchard, PRL, November 2022 (7 pages).

¹⁷⁸⁹ See [Dual-Element, Two-Dimensional Atom Array with Continuous-Mode Operation](#) by Kevin Singh et al, University of Chicago, February 2022 (11 pages).

¹⁷⁹⁰ See [Preparing random states and benchmarking with many-body quantum chaos](#) by Joonhee Choi and Manuel Endres, Caltech, MIT, Harvard, Berkeley, University of Illinois at Urbana-Champaign, University of Innsbruck, Nature, January 2023 (25 pages).

¹⁷⁹¹ See [Detecting high-dimensional entanglement in cold-atom quantum simulators](#) by Niklas Euler and Martin Gärtner, Universität Heidelberg, May 2023 (26 pages).

¹⁷⁹² See [Quantum advantage and stability to errors in analogue quantum simulators](#) by Rahul Trivedi, Adrian Franco Rubio and J. Ignacio Cirac, December 2022 (23 pages).

¹⁷⁹³ See [Optimization of Algorithmic Errors in Analog Quantum Simulations](#) by Nikita A. Zemlevskiy et al, August 2023 (18 pages).

¹⁷⁹⁴ See [Measuring Arbitrary Physical Properties in Analog Quantum Simulation](#) by Minh C. Tran, MIT, Harvard, Stanford and National University of Singapore, December 2022 (34 pages). It deals with implementing neutral atoms measurement in various basis using ancilla atoms.

¹⁷⁹⁵ See [Scalable multilayer architecture of assembled single-atom qubit arrays in a three-dimensional Talbot tweezer lattice](#) by Malte Schlosser, February 2019-March 2023 (13 pages).

¹⁷⁹⁶ See [Picosecond-Scale Ultrafast Many-Body Dynamics in an Ultracold Rydberg-Excited Atomic Mott Insulator](#) by V. Bharti et al, PRL, September 2023 (7 pages). The atoms are not individually controlled. The experiment just validated large scale entanglement.

Other advancements deal with long range entanglement with atom shuttling, reminiscent of what is being done with trapped ions in so-called fermionic quantum processors¹⁷⁹⁷. And with using Circular Rydberg Atoms (CRA) with a maximal orbital momentum number which have longer lifetimes, above 30 ms. They can use $n=48$ and 50 and optical transitions between these levels. These could be used for both quantum simulations¹⁷⁹⁸ and gate-based modes¹⁷⁹⁹. Low angular momentum Rydberg atoms have large elliptical orbitals, creating a dipole. Their lifetime is limited to a couple milliseconds and one atom out of 100 is lost in that timeframe.

Other researchers are using ytterbium instead of rubidium, which is more stable, has more precisely defined energy transitions, reduced sensitivity to environmental factors like magnetic and electric fields, greater scalability, and longer lifetimes. Strontium is also considered due to its longer stability times¹⁸⁰⁰.

Vendors

Let's cover them by order of creation¹⁸⁰¹.



Infleqtion (2007, USA, \$182.6M, formerly ColdQuanta) is a company created by Dana Anderson, now his CTO, which develops laser-based solutions for cooling cold atoms and designs cold atoms-based computers.

It is located in Boulder, Colorado, not far from the NIST Quantum Laboratory. Mark Saffman from the University of Wisconsin is their Chief Scientist for Quantum Information while Fred Chong from the University of Chicago is their Chief Scientist for Quantum Software (he also works for QCI).

Their initial core technology was the Quantum Core (*left* in Figure 431), a light guide that converges laser beams to control cold atoms that are usually cooled to less than $50 \mu\text{K}$. It is integrated in QuCAL, a complete Bose-Einstein condensate generator, and in the Physics Station, a complete optical device for the control of cold atoms that can be used for various purposes. Atom chips are chips that can be integrated in these systems including miniaturized cold atom control optics. The startup uses these generic technologies to create a wide variety of systems, and above all for quantum sensing, especially for geopositioning instead of GPS, microgravimetry or cesium quantum clocks. They also offer ultra-high vacuum pumps for the control of cold atoms, called RuBECi as well as a cryogenic trapped ions package and magneto-optical traps, magnetic coils and cold atoms sources.

Their approach to the market is truly diverse. They have equipped the ISS space station with measuring instruments for NASA and JPL.

Their overarching goal was to create and sell cold atoms-based quantum computers¹⁸⁰². They obtained some funding from DARPA in April 2020 under the ONISQ program with a \$7.4M collaborative project involving numerous universities and Raytheon BBN. DARPA asked them to develop a scalable ($>1,000$ qubits) system that can demonstrate quantum advantage on real-world problems.

¹⁷⁹⁷ See [Fermionic quantum processing with programmable neutral atom arrays](#) by Daniel González-Cuadra, Mikhael D. Lukin, Benoit Vermersch, Jun Ye, Peter Zoller et al, University of Innsbruck, Harvard, JILA, NIST, University of Colorado, UGA, March 2023 (13 pages).

¹⁷⁹⁸ See [Array of Individual Circular Rydberg Atoms Trapped in Optical Tweezers](#) by Brice Ravon, Jean-Michel Raimond, Michel Brune, Clément Sayrin et al, April 2023 (9 pages).

¹⁷⁹⁹ See [Quantum Computing with Circular Rydberg Atoms](#) by Sam R. Cohen and Jeff D. Thompson, Princeton, PRX Quantum, March-August 2021 (26 pages).

¹⁸⁰⁰ See [Cavity-enhanced optical lattices for scaling neutral atom quantum technologies to higher qubit numbers](#) by A. J. Park et al, November 2022 (18 pages).

¹⁸⁰¹ See [Quantum Computing with Neutral Atoms](#) by Russ Fein, January 2023, provides also a good overview of the largest industry vendors in that field.

¹⁸⁰² See [ColdQuanta - Life in Quantum's Slow \(and Cold\) Lane Heats Up](#) by John Russell, April 2020 and the webinar [Powering the Quantum Information Age](#) with Bo Ewald, April 2020 (53 minutes).



Figure 431: ColdQuanta Quantum Core (left), Physics Station (middle) and the atoms control chip (right). Source: ColdQuanta.

The company is focused on creating gate-based systems with 100 qubits¹⁸⁰³ (setup shown in Figure 432). Their first 2021 100-qubit “Hilbert” cloud-based quantum system was supposed to work in July 2021 but was said to be commercially available only by May 2022. It was to use cesium atoms. It seems the DARPA project didn’t get through.

During the summer of 2022, they released some interesting numbers on their gate-based system with fidelities of 99,4% for single qubit gates (lasting between 0.2 and 5 μ s) and 96.5% for two qubit gates (CZ, lasting 0.75 μ s), a measurement time of 1.5 ms, a T_2 of 1 second, all of this with 121 qubits.

In May 2021, Inflektion joined a couple other quantum computers vendors like Pasqal with supporting IBM’s Qiskit, formally joining the “IBM Quantum Network”. The startup had about 170 people onboard as of mid-2022. As a result, it seems it became possible to control neutral atom QPUs with Qiskit back in 2022¹⁸⁰⁴.

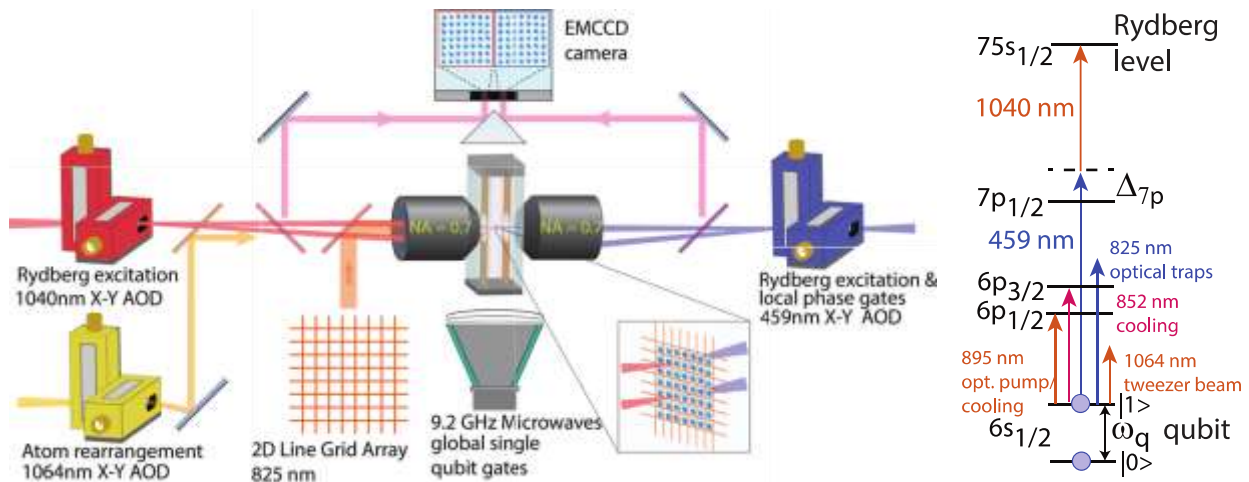


Figure 432: Inflektion/ColdQuanta's gate-based system architecture. Source: [Demonstration of multi-qubit entanglement and algorithms on a programmable neutral atom quantum computer](#) by T. M. Graham, M. Saffman et al, ColdQuanta, February 2022 (25 pages).

In May 2022, they acquired **Super.tech**, a software company providing pulse-level optimization, optimized transpilation and error mitigation techniques (SuperstaQ, which entered as an open beta in

¹⁸⁰³ See [Demonstration of multi-qubit entanglement and algorithms on a programmable neutral atom quantum computer](#) by T. M. Graham, M. Saffman et al, ColdQuanta, February 2022 (25 pages) and published as [Multi-qubit entanglement and algorithms on a neutral-atom quantum computer](#) in Nature in April 2022. It describes their state of the art: a preparation of entangled Greenberger-Horne-Zeilinger (GHZ) states with up to 6 qubits, implementation of quantum phase estimation for a chemistry problem, and Quantum Approximate Optimization Algorithm (QAOA) for the Max-Cut graph problem. Their gates set is made of local R_z phase gates and two-qubit CZ gates, run on a 7×7 grid spaced by $3 \mu\text{m}$. The system is using cesium atoms. See the related See [ColdQuanta, Riverlane and University of Wisconsin–Madison Demonstrate Algorithms on a Programmable Neutral Atom Quantum Computer](#), April 2022.

¹⁸⁰⁴ See [You Can Use Qiskit to Control Cold Atom Systems](#) by Laurin Fischer, Rohit Prasad Bhatt, Fred Jendrzejewski and Daniel J. Egger, May 2022.

September 2023¹⁸⁰⁵) and benchmarking tools (SupermarQ). In September 2022, the company was awarded a contract to build some AI/quantum machine learning solution for the UK Ministry of Defense as part of the project Q-CALC, which will use SuperstaQ. They are also teaming up with **Classiq** to handle code compilation¹⁸⁰⁶ and with **ParityQC** (Austria) for the development of quantum software targeting optimization problems.

In November 2022, the company raised an additional \$111M, but seemingly to help them focus on developing and selling quantum sensors which are generating short and mid-term revenues. They also changed their name to Infleqtion. They introduced SupercheQ in December 2022 at the Q2B in Santa Clara, a quantum algorithm tool that checks if two files are identical. Since their rebranding, Infleqtion has been quite silent about neutral atoms computing but research is going on with gate-based mode control of neutral atoms with the work of Mark Saffman^{1807 1808}. In February 2024, they announced that they reached 1,600 qubits with an 40x40 array of cesium atoms.



Atom Computing (2018, USA, \$81M) aims to create a gate-based quantum computer based on optically controlled neutral atoms with qubit states using atoms nuclear spins, initially with cesium, and later with strontium 87¹⁸⁰⁹.

The company was created by Ben Bloom (CTO, coming from Rigetti) and Jonathan King (Chief Scientist, directly coming from Berkeley), joined in 2021 by Bob Hays (CEO). The company based in Berkeley, California, established an R&D facility in Boulder, Colorado in 2022. They demonstrated in October 2021 their strontium 87-based 100-qubit Phoenix system with a 40 second qubits coherence time (Figure 433). They control their qubits in gate-based mode with individual microwave drives. The qubit manifold states are in the atom electronic ground state, avoiding spontaneous decay and have a record coherence time of 42 seconds. They can run simultaneous gates on individual atoms using two photon Raman transitions¹⁸¹⁰. As pictured in Figure 433, it was demonstrated on 21-qubit arrays of 3x7 qubits. They use the same apparatus as other vendors with SLMs for ytterbium atoms trapping and rearrangement tweezers drive, AOD (acousto-optic deflector), EOM (electronic optical modulator) and a CMOS image sensor for qubits fluorescence readout. In October 2023, they reached a record of 1,180 controlled atoms, although without publishing any qubit fidelities data.

They plan to implement some form of QEC. In May 2023, they published a paper describing how they would implement mid-circuit projective measurement, a technique enabling QND measurement (quantum non-demolition) and quantum error correction^{1811 1812}. The challenge is to avoid losing the atom in its traps while measuring it with non-destructive fluorescence imaging.

In January 2023, the company got the endorsement of DARPA as part of their inclusion in a five-year program to develop FTQC as part of the Underexplored Systems for Utility-Scale Quantum

¹⁸⁰⁵ See [Superstaq: Deep Optimization of Quantum Programs](#) by Colin Campbell et al, Infleqtion, UC Berkeley, DoE Berkeley Labs, September 2023 (13 pages).

¹⁸⁰⁶ See [Classiq and ColdQuanta partner to provide a complete solution to creating and executing 100-qubit quantum circuits and beyond](#), January 2022.

¹⁸⁰⁷ See [Multi-qubit entanglement and algorithms on a neutral-atom quantum computer](#) by T.M. Gragam, Mark Saffman et al, Nature, April 2022 (25 pages).

¹⁸⁰⁸ See [Mid-circuit measurements on a neutral atom quantum processor](#) by T. M. Graham, Mark Saffman et al, University of Wisconsin-Madison, University of Colorado and Infleqtion, March 2023 (18 pages).

¹⁸⁰⁹ See [Quantum computing with neutral atoms](#) by David Weiss 2017 (7 pages).

¹⁸¹⁰ See [Assembly and coherent control of a register of nuclear spin qubits](#) by Katrina Barnes, Michael Yarwood et al, Atom Computing, August 2021 (11 pages).

¹⁸¹¹ See [Mid-circuit qubit measurement and rearrangement in a ¹⁷¹Yb atomic array](#) by M. A. Norcia et al, May-June 2023 (9 pages).

¹⁸¹² See [Mid-circuit operations using the omg-architecture in neutral atom arrays](#) by Joanna W. Lis et al, JILA and University of Bonn, May 2023 ().

Computing (US2QC) program, that also welcomed Microsoft and PsiQuantum¹⁸¹³. They also announced a software partnership with Entropica Labs in June 2023 and with the National Renewable Energy Laboratory (NREL, USA) to work on electric grid optimization use cases.

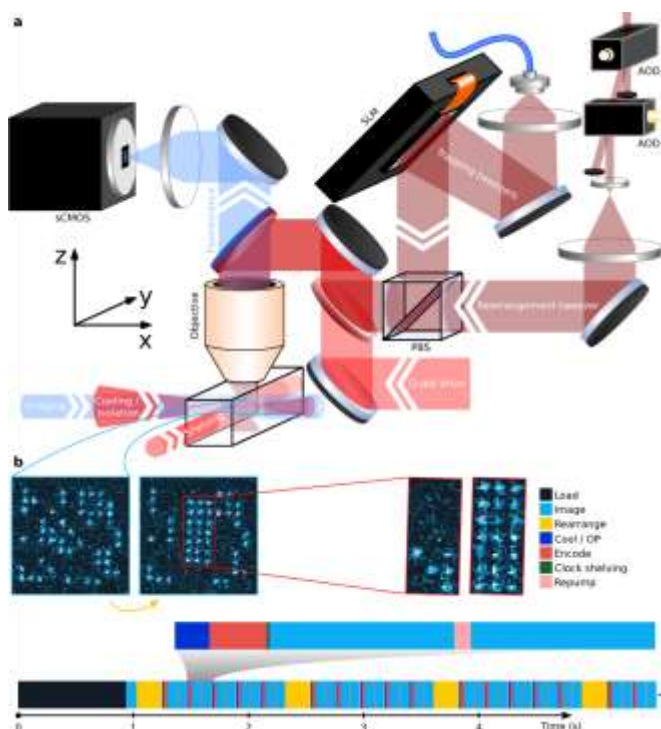
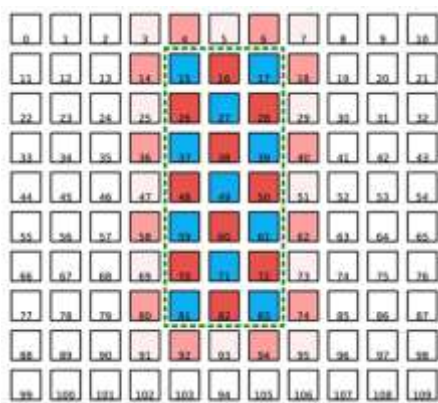


Figure 433: Atom Computing architecture for over 100-qubit gate-based computing.

Source: [Assembly and coherent control of a register of nuclear spin qubits](#) by Katrina Barnes et al, August 2021 (10 pages).



Pasqal (2019, France, 140M€) is a company cofounded by George-Olivier Reymond (CEO) and Antoine Browaeys (CSO), with the help of Alain Aspect (who was awarded the Nobel prize in Physics in 2022) who was one of their first business angels and is a scientific advisor for the company.

Technology. Their current offer as of August 2023 was the Fresnel QPU, an analog quantum simulator with a maximum of 100 controllable atoms (about 50-60 in practice). It is completed by many developer tools stacks including Pulser. They currently use rubidium atoms first cooled in a MOT (magneto-optical trap) using the Doppler laser to reach mK-level temperature and with a variant of the atomic Sisyphus cooling to reach $30 \mu\text{K}$ ¹⁸¹⁴. The atoms are trapped in 2D arrays with a spacing of a few microns thanks to the use of tweezers driven by a laser and an SLM chip controlling the phase of the laser photons reaching the atoms. Qubit states are managed with various modes depending on the use case: ground-Rydberg levels (for Ising quantum simulation models¹⁸¹⁵), two levels of Rydberg-level energy (for XY quantum simulation model using resonant dipole-dipole interactions), and with ground-ground states (for gate-based model, in future versions).

¹⁸¹³ See [DARPA Collaborates with Commercial Partners to Accelerate Quantum Computing](#), DARPA, January 2023

¹⁸¹⁴ This method also uses lasers emitting orthogonally polarized photons. The method was invented by Claude Cohen-Tannoudji who was awarded the Nobel prize in physics in 1997.

¹⁸¹⁵ See [Efficient protocol for solving combinatorial graph problems on neutral-atom quantum processors](#) by Wesley da Silva Coelho, Mauro D'Arcangelo and Louis-Paul Henry, Pasqal, July 2022 (16 pages) that describes how they use a variational analog quantum computing and machine learning to solve graph problems. In that case, the atoms are arranged in a graph with specific distances between atoms that match the problem to be solved. It is not a simple regular 2D array.

The various XX, XY and XYZ models are adapted to different physics simulations, Ising models being fit for ferromagnetism and XY models for organic compounds and atoms in lattices simulations. XYZ models can be created with using the so-called [Floquet engineering](#) in XY mode^{1816 1817}.

Ising model (XX),
similar to D-
Wave annealing.

$$\hat{H} = \sum_{i < j}^N J_{ij} \hat{\sigma}_i^x \hat{\sigma}_j^x$$

XY model with more
degrees of freedom and
dipole-dipole interactions.

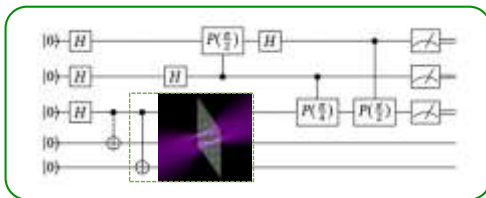
$$\hat{H} = \sum_{i < j}^N J_{ij} (\hat{\sigma}_i^x \hat{\sigma}_j^x + \hat{\sigma}_i^y \hat{\sigma}_j^y)$$

Quantum gates are laser-activated to control the atom energy state. In that case, qubit entanglement comes from atoms excitement in a Rydberg state which allows them to interact with other at long distance¹⁸¹⁸. Pasqal first implemented quantum simulators *aka* PQS (Programmable Quantum Simulator, or analog quantum computers) in their current 100-atom Fresnel QPU. They will scale it to about a thousand atoms.

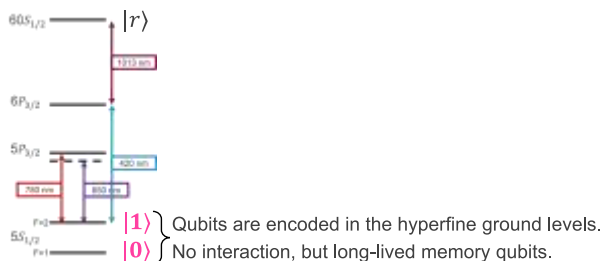
They plan to later move to NISQ gate-based quantum computing¹⁸¹⁹, with some hybrid analog/digital approach¹⁸²⁰ (Figure 434). The whole quantum processing unit fits into a 4-unit wide double-depth data center rack (Figure 435, *right*). It is based on rather standard components and does not require the creation of specific chips as is the case for all other types of qubits.

Digital mode

Programming a logic circuit = **quantum gates**

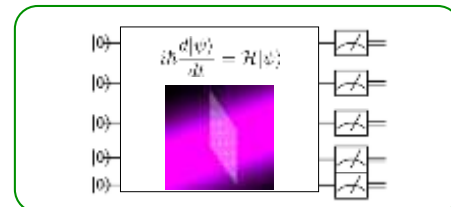


Elementary operations on individual qubits, or on several qubits at the same time → **universal** but very **sensitive to noise**



Analog mode

Programming a **sequence of Hamiltonian** evolutions



The Hamiltonian faithfully describes the dynamics of the physical system → **not universal** but offers **better performances with NISQ processors**.

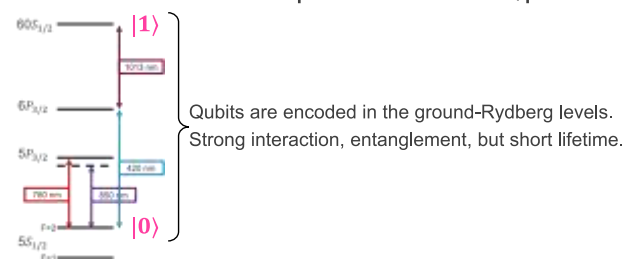


Figure 434: a clear explanation of the difference between a digital gate-based mode and an analog, quantum simulation mode.

Source: Pasqal. 2023.

¹⁸¹⁶ See [Floquet Hamiltonian Engineering of an Isolated Many-Body Spin System](#) by Sebastian Geier et al, May 2021 (12 pages).

¹⁸¹⁷ See [Magnetism and spin squeezing with arrays of Rydberg atoms](#) by Antoine Browaeys, IOGS, SFP Congress, July 2023 (97 slides).

¹⁸¹⁸ See [Quantum Computing with Arrays of Atoms](#) by Lucas Béguin and Adrien Signoles from Pasqal, April 2020, which details the functioning of the startup's quantum processors. And their white paper [Quantum Computing with Neutral Atoms](#), June 2020 (41 pages).

¹⁸¹⁹ See [Why analog neutral atoms quantum computing is the most promising direction for early quantum advantage](#) by Jean-Charles Cabelguen, June 2022.

¹⁸²⁰ See [Microwave Engineering of Programmable XXZ Hamiltonians in Arrays of Rydberg Atoms](#) by P. Scholl, Loic Henriët, Thierry Lahaye, Antoine Browaeys et al, PRX, April 2022 (10 pages) which presents an hybrid analog-digital architecture based on Hamiltonian evolutions and one-qubit gates. Qubits encoding will be different according to the use case. For gate-based computing, qubits are encoded with two hyperfine ground states. For Ising-like Hamiltonian, qubits use a ground state and a Rydberg state and for XY exchange Hamiltonian, they use two Rydberg states.

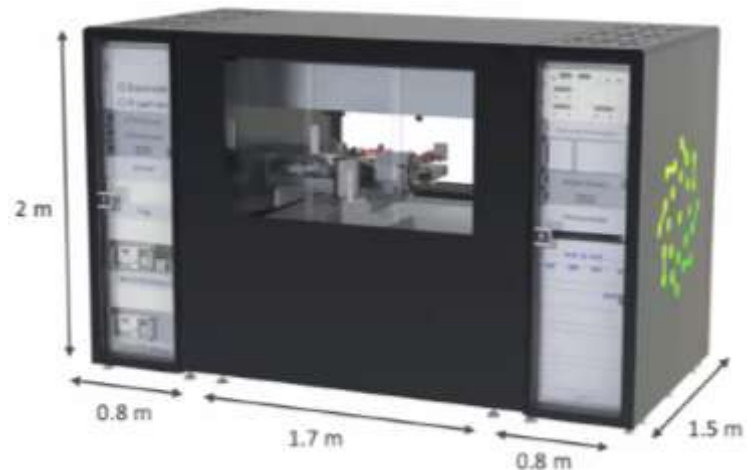
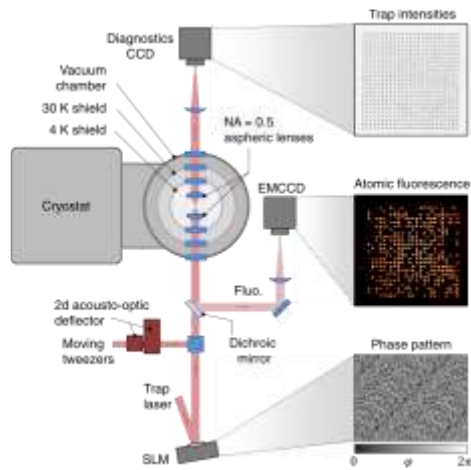


Figure 435: Pasqal's cold atom-based qubit control system includes a spatial light modulator (Spatial Light Modulator, SLM, based on LCoS liquid crystals¹⁸²¹) that controls the phase of the transmitted light in a focal plane with optical micro-traps. Laser tweezers rearranging the atoms and preparing the Hamiltonian problem to solve are controlled by an AOD (Acousto-Optic laser beam Deflector) and added to the beam from the SLM by a PBS (Polarizing Separator Filter). The fluorescent light emitted by the atoms during qubit readout is filtered by a dichroic mirror and analyzed by an EMCCD camera (electron multiplying CCD). The controlled atoms are confined in a small space of 1 mm^3 . The 4K cryostat and pulse tube that cools both the ultra-vacuum pump and the vacuum chamber hosting the atoms will belong to next generation's Pasqal QPU to support above 100 atoms. On the right, Pasqal 100-atom Fresnel QPU current form factor. Added in 2023.

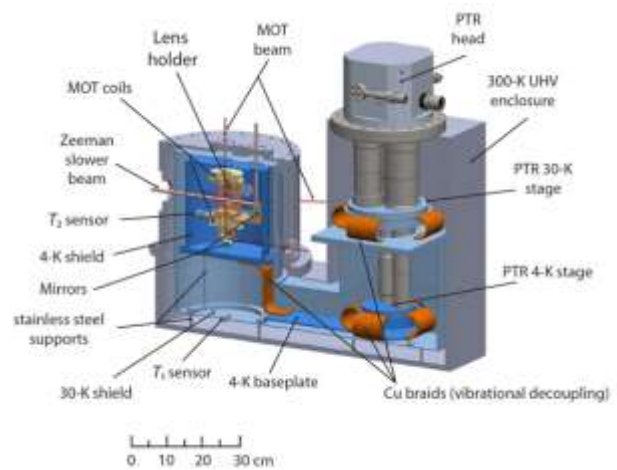
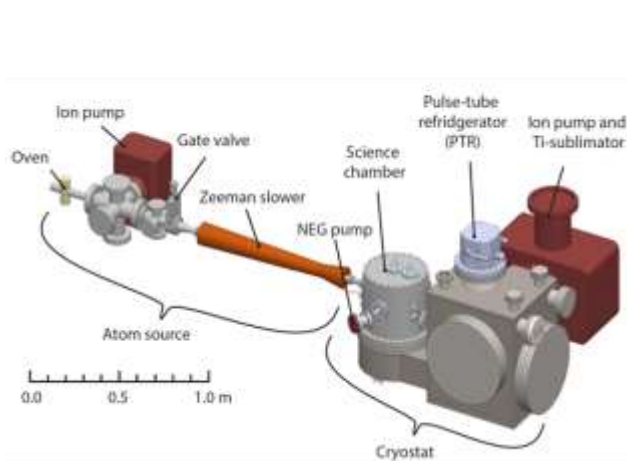


Figure 436: a detailed setup of Pasqal's future system supporting above 100 atoms showing the role of the 4K cryostat to cool both the ion pump and Ti-sublimator and the science chamber containing the cold atoms and its MOT. Source: [Scaling-up the Tweezer Platform - Trapping Arrays of Single Atoms in a Cryogenic Environment](#) by Kai-Niklas Schymik, April 2022 (197 pages). Added in 2023.

Some scientific milestones led by Pasqal and by the research team at IOGS behind Pasqal's cold atom-based system include a 2D matrix of 196 qubits^{1822 1823}, parallel gates execution¹⁸²⁴ and the control of 324 cold atoms in a 2D array, with using a 4K cryostat cooling the ultra-vacuum pump,

¹⁸²¹ See a description of an SLM in [Spatial Light Modulators](#) by Aurélie Jullien, 2020 (6 pages).

¹⁸²² See [Enhanced atom-by-atom assembly of arbitrary tweezers arrays](#) by Kai-Niklas Schymik, Antoine Browaeys, Thierry Lahaye et al, November 2020 (10 pages).

¹⁸²³ The atoms are assembled using optical tweezers and an optimized arrangement technique using fewer than 200 steps. These SLMs enable phase grading and controlling phases spatial pattern. This atoms-positioning system will be extended to 3D arrays.

¹⁸²⁴ See [Pulse-level Scheduling of Quantum Circuits for Neutral-Atom Devices](#) by Richard Bing-Shiun Tsai, Loïc Henriët et al, Pasqal, June 2022 (8 pages) and [Pulsar: An open source package for the design of pulse sequences in programmable neutral-atom arrays](#) by Henrique Silvério, Nathan Shammah, Louis-Paul Henry, Loïc Henriët et al, January 2022 (21 pages).

which helps create a better vacuum and extend the atom qubit lifetime, and also the vacuum chamber, to avoid the effect of electromagnetic radiations^{1825 1826} (Figure 436).

Software tools. Pasqal created its own low-level programming environment that interfaces with high-level programming tools, including support for development platforms such as Google's **Cirq** that is supported in emulation mode, in digital gate-based programming mode¹⁸²⁷, **TensorFlow Quantum** and IBM's **Qiskit**. In April 2023, the company launched Quantum Discovery to provide access to its emulators and 100-atoms QPU through the cloud. The platform contains three modules: a first one for onboarding with video tutorials, demos, and a VR Tour of the QPU hardware, a second to interact with the QPU with running and tuning pre-coded algorithm templates on the QPU or its emulator in Jupyter notebooks and a third one to identify and prioritize use cases through a questionnaire¹⁸²⁸.

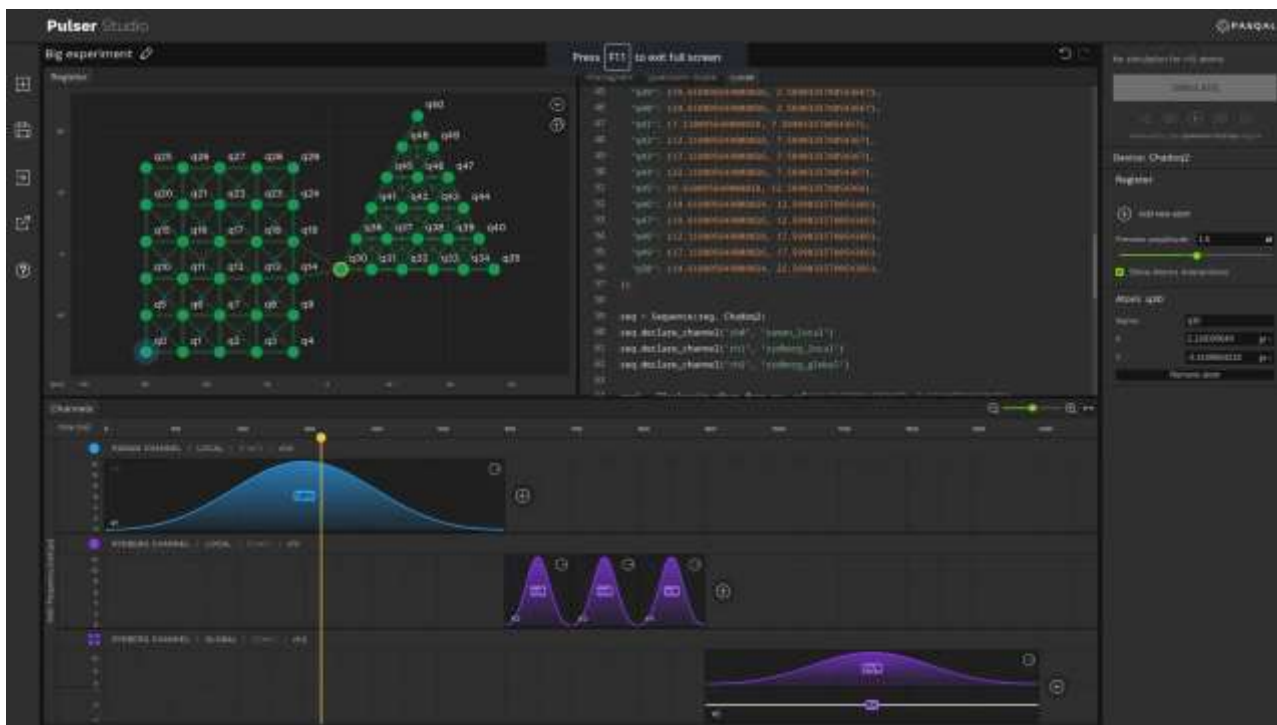


Figure 437: PASQAL Pulser studio user interface showing atoms 2D arrangement and pulse controls. Source: Pasqal. 2023.

In January 2023, PASQAL launched Pulser Studio, a no-code development environment that enables users to graphically build quantum registers and design pulse sequences without coding knowledge (Figure 437). The software platform is open and free to corporate and academic users. It still requires some knowledge on how to run a quantum simulation on PASQAL hardware!

Case studies. Applications wise, Pasqal published many papers with several research partners and customers, many of them being implemented in classical emulation mode. At this point, as of November 2023, these case studies didn't yet demonstrate any quantum advantage although near-term future generation of Pasqal quantum simulators could potentially change the picture.

¹⁸²⁵ See [Single Atoms with 6000-Second Trapping Lifetimes in Optical-Tweezer Arrays at Cryogenic Temperatures](#) by Kai-Niklas Schymik, Sara Pancaldi, Florence Nogrette, Daniel Barredo, Julien Paris, Antoine Browaeys, and Thierry Lahaye, IOGS, PRA, September 2021 (8 pages).

¹⁸²⁶ See [In situ equalization of single-atom loading in large-scale optical tweezer arrays](#) by Kai-Niklas Schymik, Adrien Signoles, Florence Nogrette, Daniel Barredo, Antoine Browaeys, and Thierry Lahaye, PRA, August 2022 (6 pages).

¹⁸²⁷ See [Quantum circuits on Pasqal devices](#).

¹⁸²⁸ See [PASQAL Launches First Neutral Atoms Quantum Computing Exploration Platform](#) by Alexandra De Castro, Pasqal, March 2023.

Some generic cases are about solving Minimum Vertex Coloring problems¹⁸²⁹, nonlinear differential equations¹⁸³⁰ and various quantum machine learning tasks^{1831 1832 1833}.

Then, we have a graph machine learning problem to predict products toxicity^{1834 1835} and a multi-agent reinforcement learning (MARL) task using PASQAL QEK to optimize semiconductor manufacturing processes¹⁸³⁶, solving graph classification problems also using QEK in toxicity screening of chemical compounds and in the identification of optimal chemical reaction pathways, on solving an Ising model simulating ferromagnetism with a 196 cold atoms setup¹⁸³⁷, on the optimization of electrical vehicles smart charging co-developed with EDF, using a QAOA hybrid algorithm and classical emulators of Pasqal systems and the Eviden/Atos QLM emulator¹⁸³⁸, to enable robot navigation with Laplace harmonic equations with LG^{1839 1840}, to determine the ground state of the usual suspects H₂, LiH and BeH₂ molecules, using an “analog VQE” method and single qubit gates for ansatz initialization and Pauli string readouts with 2 to 6 qubits and 36,500 shots lasting 3.5 hours using a digital simulation¹⁸⁴¹, a differentiable quantum circuit algorithm (DQC) to simulate a parallel-plate capacitor in a grounded box, calculating the potential and the electric field in the box for different distances separating the plates and using the vacuum as the insulator between them¹⁸⁴², and for sampling equilibrium water solvent molecules configurations within proteins¹⁸⁴³.

The most interesting case was a fallen angel classification task with CA-CIB and Multiverse in France which was not far from providing a quantum advantage with real-world customer data and which is detailed page 1080.

¹⁸²⁹ See [A quantum pricing-based column generation framework for hard combinatorial problems](#) by Wesley da Silva Coelho, Loïc Henriet et Louis-Paul Henry, January 2023 (15 pages).

¹⁸³⁰ See [Solving nonlinear differential equations with differentiable quantum circuits](#) by Oleksandr Kyriienko, Annie E. Paine, and Vincent E. Elfving, PRA, May 2021 (23 pages).

¹⁸³¹ See [Quantum evolution kernel: Machine learning on graphs with programmable arrays of qubits](#) by Louis-Paul Henry, Slimane Thabet, Constantin Dalyac and Loïc Henriet, PRA, September 2021 (19 pages) that is better explained in [Machine Learning – Pasqal’s Quantum Computers can be used on concrete industrial problems](#), Pasqal, October 2021.

¹⁸³² See [Quantum Extremal Learning](#) by Savvas Varsamopoulos, Vincent E. Elfving et al, May 2022 (21 pages).

¹⁸³³ See [Enhancing Graph Neural Networks with Quantum Computed Encodings](#) by Slimane Thabet, Louis-Paul Henry, Loïc Henriet et al, October 2023 (33 pages).

¹⁸³⁴ See [Predicting toxicity with qubits](#) by Alexandra de Castro, PASQAL, November 2022.

¹⁸³⁵ See [Quantum Feature Maps for Graph Machine Learning on a Neutral Atom Quantum Processor](#) by Boris Albrecht, Loic Henriet et al, November 2022 (19 pages).

¹⁸³⁶ See [Idle vehicle rebalancing in semiconductor fabrication using factorized graph neural network reinforcement learning](#), Kyuree Ahn and Jinkyoo Park, Korea Advanced Institute of Science and Technology, IEEE, 2019

¹⁸³⁷ See [Programmable quantum simulation of 2D antiferromagnets with hundreds of Rydberg atoms](#) by Pascal Scholl, Thierry Lahaye, Antoine Browaeys et al, December 2020 (16 pages). Also published in [Nature](#) in July 2021. This was a result of a research funded through the European Flagship PASQunS project in partnership with labs from Spain, Germany and Austria

¹⁸³⁸ See [Qualifying quantum approaches for hard industrial optimization problems. A case study in the field of smart-charging of electric vehicles](#) by Constantin Dalyac, Loïc Henriet, Emmanuel Jeandel, Wolfgang Lechner, Simon Perdrix, Marc Porcheron and Margarita Veshchezerova, 2021 (29 pages).

¹⁸³⁹ See [How quantum computing can navigate robots through crowded places](#) by Alexandra de Castro, PASQAL, December 2022.

¹⁸⁴⁰ See [Harmonic \(Quantum\) Neural Networks](#) by Atiyo Ghosh et al, Pasqal and LG, December 2022 (29 pages).

¹⁸⁴¹ See [A blueprint for a Digital-Analog Variational Quantum Eigensolver using Rydberg atom arrays](#) by Antoine Michel, Loic Henriet, Antoine Browaeys et al, Pasqal and EDF, January-April 2023 (13 pages).

¹⁸⁴² See [Accelerating and braking made efficient with quantum computing](#) by Alexandra de Castro, PASQAL, November 2022.

¹⁸⁴³ See [Leveraging Analog Quantum Computing with Neutral Atoms for Solvent Configuration Prediction in Drug Discovery](#) by Mauro D’Arcangelo, Louis-Paul Henry, Loïc Henriet, Jean-Philip Piquemal et al, PASQAL and Qubit Pharmaceuticals, September 2023 (19 pages).

As part of the PASQuanS European flagship project, Eviden/Atos researchers evaluated the specifications of a cold atom simulator needed to reach some quantum advantage to solve an optimization task, the UD-MIS problem (Unit-Disk Maximum Independent Set problem)¹⁸⁴⁴. They found out that over 1,000 qubits were required with a time budget of 0.2 seconds, if and when the system coherence could be improved by a factor ten¹⁸⁴⁵. At last, in October 2023, Pasqal announced a partnership with the Quantum Transformation Project (QX-PJ) in Japan to develop "Quantum Sky", a 3D aerial traffic management system able to handle hundreds of drones and other low-altitude flying objects.

Partners. In July 2020, **Cambridge Quantum Computing** (CQC) announced their support of Pasqal's qubits with their development tool t|ket). Pasqal added a partnership with **ParityQC** with a 3-year collaboration to advance quantum optimization and parallelization¹⁸⁴⁶ and released the open source library **Pulser**, co-developed with the **Unitary Fund** enabling the control of their processor at the level of laser pulses¹⁸⁴⁷. They also announced a partnership with **Atos** in November 2020 to integrate a Pasqal accelerator with Atos supercomputers. They also work with **Rahko** as well as with **Multiverse Computing**, in association with Cr dit Agricole CIB. They started a two-year R&D partnership with **Kipu Quantum** in June 2023 to optimize quantum algorithmic and use Kipu's algorithmic compression technology that reduces the length of quantum algorithms.

In January 2021, the Italian HPC consortium **CINECA** announced that they will use Pasqal's Fresnel 100-qubits processor¹⁸⁴⁸. The startup was also selected as part of the project EuroHPC HPC-QS to provide two of their systems to HPC public datacenters, one in Germany (J lich Supercomputing Centre at FZ J lich *aka* J lich Research Centre) and one in France (CEA TGCC with GENCI). Both Pasqal systems will be connected to an Atos QLM for emulation and quantum system drive.

They have various partnerships in place with **EDF**, **Thales**, **GENCI**, **Aramco** (for implementing QML algorithms in the energy business), **Siemens** (for computer-aided-design and engineering, simulation and testing), **BASF** (fluid dynamic problem solving algorithm), **BMW** (material science and material deformation algorithms) and the first sales of two 100-qubit quantum processor to **GENCI** and **FZJ** as part of the HPCQS EU consortium. They opened an office in Boston (USA) and in Sherbrooke (Canada) in June 2022. And their first 100-qubit quantum simulator went online with **OVH-cloud** in May 2022 (in private beta) and will be online later with **Microsoft Azure Quantum**.

Company. Pasqal funding came through an initial round of 2.5M  led by Quantonation and Christophe Jurczak who is their chairman, then a 4.5M  grant from the European Union EIC Accelerator¹⁸⁴⁹, and finally a second round of funding of 25M  announced in April 2021. In January 2022, Pasqal and Qu&Co (The Netherlands) merged, creating an integrated hardware/software company. As of December 2022, they had a staff of >100 people. In January 2023, Pasqal raised an additional 100M . In 2023, they inaugurated an assembly line for their QPU based in the newly built "Espace Quantique 1" established in Sherbrooke, Qu bec, Canada, with a \$90M 5-year investment plan.

¹⁸⁴⁴ A MIS problem consists in determining the size of the largest possible independent set in a graph and returning an example of such a set. The Unit-Disk MIS (UD-MIS) problem is the MIS problem restricted to unit-disk graphs. A graph is a unit-disk graph if one can associate a position in the 2D plane to every vertex such that two vertices share an edge if and only if their distance is smaller than unity.

¹⁸⁴⁵ See [Solving optimization problems with Rydberg analog quantum computers: Realistic requirements for quantum advantage using noisy simulation and classical benchmarks](#) by Michel Fabrice Serret, Bertrand Marchand and Thomas Ayr l, November 2020 (25 pages).

¹⁸⁴⁶ See [ParityQC and Pasqal partner to build the first fully parallelizable quantum computer](#), Pasqal, October 2020. With other researchers in Austria, ParityQC is proposing a way to encode QAOA generic optimization problems into gate-based cold atoms computers using a specific 4-qubit gate as seen in [Quantum computing on neutral atoms: the novel four-body Rydberg gate](#), ParityQC, 2022, referring to: [Quantum Optimization via Four-Body Rydberg Gates](#) by Clemens D laska, Kilian Ender, Glen Bigan Mbeng, Andreas Kruckenhauser, Wolfgang Lechner, and Rick van Bijnen, PRL, March 2022 (11 pages).

¹⁸⁴⁷ See [Pulser: a control software at the pulse-level for Pasqal quantum processors](#) by Pasqal, January 2021.

¹⁸⁴⁸ See [CINECA-Pasqal agreement on quantum computing](#), January 2021.

¹⁸⁴⁹ See [Europe is betting on quantum computing with neutral atoms](#), Pasqal, December 2020.



QuEra Computing (USA, 2018, \$17M) develops cold atom quantum computer, their first generation being named Aquila¹⁸⁵⁰.

Company. It was created by researchers from Harvard University and MIT with Nathan Gemelke, Alexei Bylinskii, Shengtao Wang and Mikhail D. Lukin, who is one of their scientific advisors and works on gate-based cold-atom computing¹⁸⁵¹ (Figure 438). They had a staff of over 50 people as of January 2024.

Technology. They published a research paper on a 2D array 256 programmable cold atom system in 2021 and announced in November 2021 it would become a commercial product¹⁸⁵². It is available on Amazon Braket since November 2022. What they brand “programmable quantum computers” are not gate-based systems and are still quantum simulators where they encode graph problems into a layout of cold atoms^{1853 1854}. A graph problem is expressed as a “maximum weight independent set” (MWIS) problem that is then turned into several unit-disk graph sets (UDG) which are assemblies of nearby neutral atoms using the Rydberg effect for local entanglement. These sets are connected to each other with entangled neutral atoms at their edge. Various problems like QUBO, Ising models and even integer factorization can be mapped onto MWIS problems.

They are however aggressively looking at ways to implement a gate-based programming model on their system. They proposed in 2022 a way to transport qubits to handle two-qubit gates using atoms shuttling with tweezers. They implemented it with a Steane-7 quantum error correction code graph (but not with a full QEC), topological surface code and toric code states using mobile ancilla and with hybrid analog-digital quantum circuits using dynamically reconfigurable array and CZ gates¹⁸⁵⁵. They propose dynamically programmable arrays of atoms (FPQA) that can be changed during computation¹⁸⁵⁶. They are also working on making non-demolition qubit measurement, a key feature to implement full QEC (quantum error correction) and FTQC (fault-tolerant quantum computing). This would be based on moving selected atoms “into a readout zone where their qubit state can be rapidly detected via fast, resonant photon scattering on a cycling transition”. They could also use arrays with two atoms species such as two isotopes of the same element or two different atom elements, with the data atoms being encoded in one atomic species and ancilla atoms encoded in another species that can be easily measured¹⁸⁵⁷.

¹⁸⁵⁰ See [Aquila: QuEra's 256-qubit neutral-atom quantum computer](#) by Jonathan Wurtz, Alexander Keesling et al, June 2023 (39 pages) which documents Aquila very well and is a “best practice” of scientific communication for a quantum computing startup..

¹⁸⁵¹ See [Parallel Implementation of High-Fidelity Multiqubit Gates with Neutral Atoms](#) by Harry Levine, Mikail D. Lukin et al, August 2019 (16 pages).

¹⁸⁵² See [Quantum Phases of Matter on a 256-Atom Programmable Quantum Simulator](#) by Sepehr Ebadi, Mikhail D. Lukin et al, 2020 (20 pages).

¹⁸⁵³ See [This new startup has built a record-breaking 256-qubit quantum computer](#) by Siobhan Roberts, MIT Technology Review, November 2021 and the real stuff in [Quantum Optimization of Maximum Independent Set using Rydberg Atom Arrays](#) by Sepehr Ebadi, Mikhail Lukin et al, February 2022 (10 pages).

¹⁸⁵⁴ See [Quantum optimization with arbitrary connectivity using Rydberg atom arrays](#) by Minh-Thi Nguyen, Jin-Guo Liu, Jonathan Wurtz, Mikhail D. Lukin, Sheng-Tao Wang, and Hannes Pichler, PRX, February 2023 (19 pages).

¹⁸⁵⁵ See [A quantum processor based on coherent transport of entangled atom arrays](#) by Dolev Bluvstein, Mikhail D. Lukin et al, Nature, April 2022 (21 pages).

¹⁸⁵⁶ See [Compiling Quantum Circuits for Dynamically Field-Programmable Neutral Atoms Array Processors](#) by Daniel Bochen Tan, Mikhail D. Lukin et al, June 2023 (18 pages).

¹⁸⁵⁷ See [Hardware-Efficient, Fault-Tolerant Quantum Computation with Rydberg Atoms](#) by Iris Cong, Mikhail Lukin et al, May 2022 (31 pages) making references to [A dual-element, two-dimensional atom array with continuous-mode operation](#) by Kevin Singh et al, October 2021 (11 pages) on reduced cross-talk and QND with two mixed atom elements (cesium and rubidium), [Fast Preparation and Detection of a Rydberg Qubit using Atomic Ensembles](#) by Wenchao Xu et al, May 2021 (11 pages) and [Interaction enhanced imaging of individual atoms embedded in dense atomic gases](#) by G. Günter, Shannon Whitlock et al, June 2011 (6 pages) which also describes a QND measurement of cold atoms state.

In 2023, they implemented a gate-based model with reaching two-qubit CZ gate fidelities of 99.5% with 60 atoms¹⁸⁵⁸, and in December, announced having created 48 logical qubits with 280 atoms and planned to reach 100 logical qubits by 2027 with using over 10,000 physical qubits.

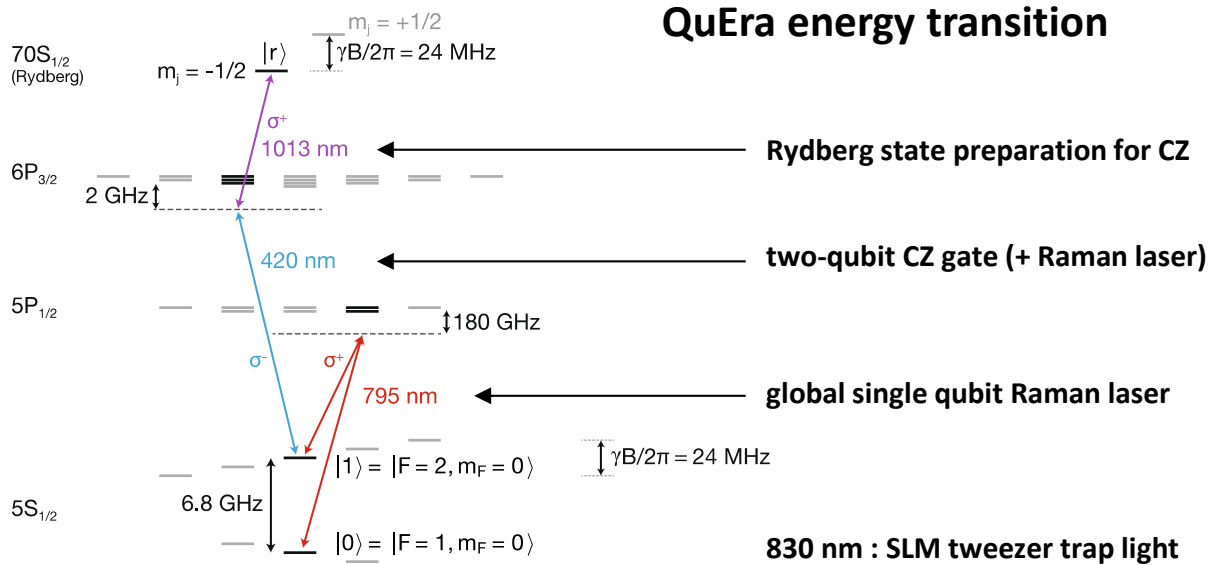


Figure 438: QuEra atomic energy transitions used to control qubits and qubit gates. Source: [A quantum processor based on coherent transport of entangled atom arrays](#) by Dolev Bluvstein, Mikhail D. Lukin et al, Nature, April 2022 (21 pages).

As of August 2023, QuEra’s Aquila-class 256 qubits quantum simulator was available in three forms: through AWS (48 hours per week), directly through QuEra’s Premium Access and leased on-premises.

Software tools. QuEra quantum emulation Bloqade software package is available on Github as a Julia package from July 2022. It emulates on classical computers atom-based quantum simulations. This is akin to Pulser from Pasqal. They got help for this from AWS and the Perimeter Institute.

Partners. In September, QuEra announced a partnership with KAIST and the the Sejong Special Autonomous City in South Korea. It is mostly about putting in place an educational program, international academic exchanges, and work on government projects. QuEra also partners with Wolfram Research to integrate their QPU into the Mathematica software environment. In October 2023, QuEra was awarded with two grants from DARPA as part of the IMPAQT (Imagining Practical Applications for a Quantum Tomorrow) program for “Quantum Reservoir Learning using Neutral Atoms and its Applications” (using MNIST handwritten digit data sets) and “Error-Corrected Quantum Architectures Based on Transversal Logical Gates” (improving QEC overhead with surface code in a FTQC regime). They are partnering here with Moody’s, BlueQubit, Polaris Quantum Biotech and the University of Padova.



Planqc (2022, Germany, 4.6M€) is a startup created in Garching near Munich by Alexander Glätzle (CEO, a researcher at the University of Oxford in the UK), Sebastian Blatt (CTO) who was a researcher at Ludwig-Maximilians-University Munich (and is a son of Rainer Blatt) and Johannes Zeiher (a researcher at MPQ).

Immanuel Bloch and Jose Ignacio Cirac from MPQ and Dieter Jaksch, Professor of Physics at the University of Oxford and the University of Hamburg are their scientific advisors. It is a neutral atom based qubits company that plans to scale its system to thousands of qubits. They are still semi-stealth and do not provide any details on their technology choices and roadmap.

¹⁸⁵⁸ See [High-fidelity parallel entangling gates on a neutral atom quantum computer](#) by Simon J. Evered, Mikhail D. Lukin et al, Nature, April-October 2023 (21 pages).

Looking at the research work from the founders, you may infer that they plan to implement MBQC on large cluster states of entangled cold atoms¹⁸⁵⁹. In May 2023, DLR (Germany) ordered a 100 qubits gate-based quantum computer from Planq as part of a 29 M€ contract that also involves ParityQC and Menlo Systems (EDA software)¹⁸⁶⁰. In November 2023, it was completed by another contract along with d-fine and MQS to develop simulation of water molecules in the QuantiCoM H2Q project.



QUANTier (2022, Hong Kong) is a spin-off from HKUST (Hong Kong University of Science and Technology) which develops a neutral atoms qubits based quantum computer. They got some undisclosed funding from ParticleX, an accelerator and investment fund from Hong Kong.

They are relatively stealth at this point with no indication on the TRL of their technology and differentiation with other neutral atom players like Pasqal and QuEra, neither if they are targeting analog or gate-based quantum computing.



GDQLABS (2022, India) is building a neutral atom-based quantum computer using 2D array. They are based out of IISER Pune and incubated by I-Hub QTF. They also build cold atom based atomic clocks and gravimeters!



NanoQT (2022, Japan, \$10M) aka Nanofiber Quantum Technologies is a quantum computing startup launched out of Waseda University by Takao Aoki (CSO), Masaru Hirose (CEO) and Akihisa Goban (CTO)¹⁸⁶¹.

Their technology is based on the Nanofiber QED resonator invented by Takao Aoki. These are neutral atom-based qubits that are connected with each other through photons and nanofibers. It enables n-to-n two-qubit gates full-connectivity between these qubits. They currently support only a few qubits and say it could scale to 10,000 qubits¹⁸⁶².

Atom Quantum Labs (2021, Slovenia) is also developing an atom based quantum simulator with the goal to support thousand qubits.

At last, **M Squared** (2006, UK, \$56M) who was historically working on neutral atoms sensors entered the neutral atoms quantum computers market in November 2022¹⁸⁶³.

NMR qubits

History and science

Nuclear magnetic resonance was an early technique investigated to create quantum computers. Qubit states are the spin of nuclei within large ensembles of up to 10^{15} molecules. The qubit states are readout using nuclear magnetic resonances, implementing a variant of nuclear magnetic resonance spectroscopy. The NMR phenomenon was discovered in 1945 by **Edward Mills Purcell** (1912-1997, American) for which he was awarded the Nobel prize in physics in 1952, shared with Felix Bloch.

¹⁸⁵⁹ See [Realizing distance-selective interactions in a Rydberg-dressed atom array](#) by Simon Hollerith, Immanuel Bloch, Johannes Zeiher et al, October 2021 (5 pages), See [Quantum Information Processing in Optical Lattices and Magnetic Microtraps](#) by Philipp Treutlein, Immanuel Bloch et al, Max Planck Institute, June 2006 (15 pages). This is a variation of cold atoms qubits adapted to cluster states and MBQC. See also [Quantum simulations with ultracold atoms in optical lattices](#) by Christian Gross and Immanuel Bloch, 2017 (8 pages).

¹⁸⁶⁰ See [DLR OCI awards contract worth 29 million euros for the development of a quantum computer based on neutral atoms](#), DLR, May 2023.

¹⁸⁶¹ See [Waseda University Ventures Invests in Japanese Quantum Computer Hardware Startup](#) by Matt Swayne, The Quantum Insider, February 2023.

¹⁸⁶² See [Photon transport enhancement through a coupled-cavity QED system with dynamic modulation](#) by Shinya Kato and Takao Aoki, Optics Express, 2022 (10 pages).

¹⁸⁶³ See [M Squared reveals state of the art quantum computing system](#), M Squared, November 2022.

Using nuclear spins for quantum computing was first proposed in 1993 by **Seth Lloyd** from the MIT¹⁸⁶⁴ and refined in 1994 by **David DiVincenzo**, then at IBM Research, for the implementation of perfluorobutadienyl two-qubit gates¹⁸⁶⁵.

It was perfected by various proposals coming from the MIT, UCSB and Stanford researchers in 1997 with a computing method using liquid state NMR (molecules in a liquid) and enabling the measurement of the expectation value of quantum observables, ensuring an exponential computing speedup¹⁸⁶⁶. An expectation value of an observable is the average value of the observable and not a random value obtained by a projective measurement, the type of qubit readout measurement usually implemented with other techniques. Using another explanation, this measures a statistical mixture of pure states.

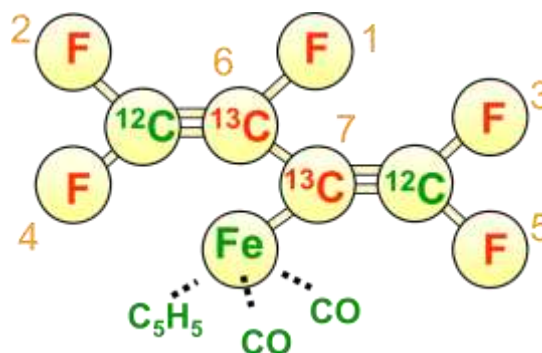


Figure 439: NMR can rely on complex molecule like perfluorobutadienyl. Source: IBM.

In 2001, **IBM** researchers even implemented Shor's algorithm with the number 15 on a 7-qubit NMR quantum processor using a perfluorobutadienyl iron complex where the spins come from the nuclear spins of fluor and carbon atoms (in red in Figure 439)¹⁸⁶⁷. It is still the record to date! In these systems, qubit states where the ensemble nuclear spins $\frac{1}{2}$ in a magnetic field, quantum gates were operated by radiofrequency pulses and qubit readout was done with detecting spin states with a radiofrequency coil¹⁸⁶⁸.

Afterwards, there were some developments with “Solid state NMR” (SSNMR) using nitrogen vacancies and interactions between carbon atomic spins and vacancies electron spins or nuclear spins of ²⁹Si in silicon structures¹⁸⁶⁹. NMR was quite fashionable in quantum computing about 20 years ago. IBM was even planning for the existence of NMR-based tabletop quantum computers¹⁸⁷⁰. 22 years ahead, their (superconducting qubits) quantum computers are 3-meter wide cubes consuming in excess of 25 kW.



Still, research is still ongoing on NMR quantum computing. It goes on in Europe in the Europe 2020 project **FATMOLS** run by a research consortium led by Spain¹⁸⁷¹. Its ambition is to create a molecular spin quantum processor using artificial magnetic molecules implementing spin qubits controlled, read-out and linked with some superconducting circuits.

¹⁸⁶⁴ See [A potentially realizable quantum computer](#) by Seth Lloyd, Science, 1993 (4 pages).

¹⁸⁶⁵ See [Two-Bit Gates are Universal for Quantum Computation](#) by David DiVincenzo, July 1994 (21 pages) and [Bulk Spin-Resonance Quantum Computation](#) by Neil A. Gershenfeld and Isaac L. Chuang, 1997 (7 pages).

¹⁸⁶⁶ See [Ensemble quantum computing by NMR spectroscopy](#) by David G. Cory, Amr F. Fahmy and Timothy F. Havel, MIT, 1997 (6 pages).

¹⁸⁶⁷ See [Experimental realization of Shor's quantum factoring algorithm using nuclear magnetic resonance](#) by Lieven M.K. Vandersypen, Isaac L. Chuang et al, December 2001 (18 pages).

¹⁸⁶⁸ See [NMR Quantum Computing](#), 2012 (43 slides) and [NMR Quantum Computation NMR Quantum Computation](#) by Thaddeus Ladd, Stanford, 2003 (39 slides).

¹⁸⁶⁹ See [Solid-State Silicon NMR Quantum Computer](#) by E. Abe, K. M. Itoh, Y. Yamamoto et al, 2003 (5 pages).

¹⁸⁷⁰ See [Toward a table-top quantum computer](#) by Y. Maguire, E. Boyden and N. Gershenfeld, IBM, 2000 (17 pages).

¹⁸⁷¹ With CSIC, Aragón Materials Science Institute (ICMA), The Centre of Astrobiology (CAB), University of Barcelona, Universidad de Valencia / Instituto de Ciencia Molecular (UVEG), the Keysight team in Barcelona, and outside Spain: University of Manchester Molecular Magnetism Group, University of Oxford Department of Condensed Matter Physics, University of Parma and the Department of Chemistry at the University of Florence, Universität Stuttgart / Institute for Functional Matter and Quantum Technologies, Wolfgang Pauli Institut, Technische Universität Wien and IBM Zurich (Ivano Tavernelli).

Quantum features are implemented with nuclear spins, electronic spins and circuits. Programming models range from quantum simulations to gate-based FTQC. The FATMOLS project's goal is to create a proof-of-concept of one of the repetition unit cells of this platform with at least two molecules with multiple and fully addressable levels and related algorithms.

The end-goal is to reach 100 to 1,000 physical qubits¹⁸⁷². The project runs from March 2020 to August 2023 with a total cost of 3.2M€, entirely funded by the EU.

Research

Various NMR variants are still investigated like the use of large molecular spins¹⁸⁷³, europium molecules with nuclear spins that can interact with luminescent photons carrying the nuclear spin information¹⁸⁷⁴, with molecular ensembles¹⁸⁷⁵ and optically addressable molecular spins¹⁸⁷⁶.

DQC1 (Deterministic Quantum Computation with 1 quantum bit) is a curious quantum computing model created in 1998 by Emanuel Knill and Raymond Laflamme (Figure 440).

It was designed for NMR qubits which we were commonly developed in the late 1990s and were very noisy. It is described as a deterministic quantum computation using one qubit and a classical computer¹⁸⁷⁷.

It computes deterministic functions on one bit and a classical computer is performing probabilistic computing. But there's more than one qubit in the story: the input is indeed constrained to a single qubit in a pure state, but a set of n other qubits is prepared in an identity state and subject to a random unitary transformation U_n and in a completely mixed state. These systems use noise as a resource which is formalized with **quantum discord** mathematical tools¹⁸⁷⁸.

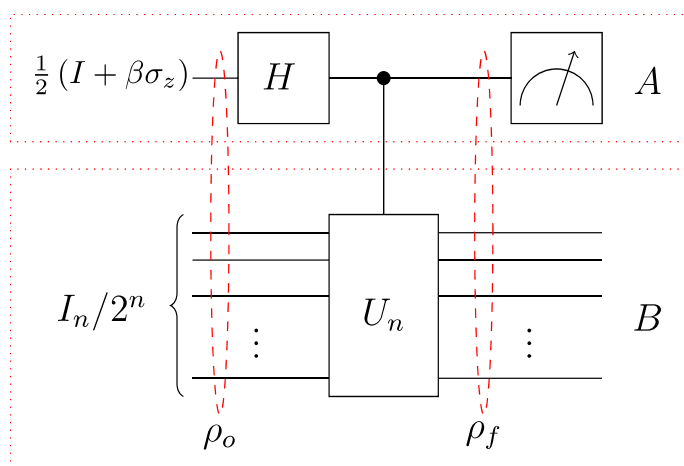


Figure 440: description of the DQC1 model. A qubit at the top is the only input. It is prepared then subject to an Hadamard gate and the result controls the application of the U_n unitary transformation to n other qubits. At the end of this processing, the first qubit is the only one measured, with the process being repeated several times. The output yields a trace of the unitary U_n . Source: [Measurement-Based Quantum Correlations for Quantum Information Processing](#) by Uman Khalid, Junaid ur Rehman and Hyundong Shin, *Nature Research Scientific Reports*, 2020 (9 pages).

¹⁸⁷² See [A perspective on scaling up quantum computation with molecular spins](#) by S. Carretta et al, *Applied Physics Letters*, May 2021 (13 pages).

¹⁸⁷³ See [Optically addressable molecular spins for quantum information processing](#) by S. L. Bayliss et al, April 2020 (9 pages) as well as [Chemical tuning of spin clock transitions in molecular monomers based on nuclear spin-free Ni\(ii\)](#) by Marcos Rubin-Osanz et al, 2021 (11 pages). It involves one lab in Spain and three in France (ICMM Orsay, LCPQ Toulouse and LNCMI Grenoble).

¹⁸⁷⁴ See [Ultra-narrow optical linewidths in rare-earth molecular crystals](#) by Diana Serrano, Senthil Kumar Kuppasamy, Benoît Heinrich, Olaf Fuhr, David Hunger, Mario Ruben and Philippe Goldner, KIT, CNRS, University of Strasbourg and Chimie ParisTech, *Nature*, May 2021-March 2022 (19 pages).

¹⁸⁷⁵ See [A New Approach to Quantum Computing Using Magnetic Resonance Imaging](#) by Zang-Hee Cho et al, June 2022 (9 pages).

¹⁸⁷⁶ See [Enhancing Spin Coherence in Optically Addressable Molecular Qubits through Host-Matrix Control](#) by S. L. Bayliss, David Awschalom et al, April 2022 (13 pages).

¹⁸⁷⁷ See [On the Power of One Bit of Quantum Information](#) by Emanuel Knill and Raymond Laflamme, 1998 (5 pages).

¹⁸⁷⁸ See [Measuring geometric quantum discord using one bit of quantum information](#) by G. Passante, O. Moussa and Raymond Laflamme, 2021 (5 pages), [Introducing Quantum Discord](#) by Harold Ollivier, October 2001 (5 pages) and [Quantum Discord: A Measure of the Quantumness of Correlations](#) by Harold Ollivier and Wojciech H. Zurek, *PRL*, December 2001 (5 pages).

At the end of computing, a measurement takes place on the first qubit. It is not a universal quantum computing model, doesn't use massive entanglement and has a narrow set of use cases although it is supposed to bring some exponential speedups in some circumstances¹⁸⁷⁹.

Vendors

NMR quantum computers don't scale well due to noise affecting qubits and poor entanglement. It didn't prevent one company from China to manufacture and sell an NMR-based quantum computer. And fulfilling IBM's 2000 dream, it is a desktop product.



SpinQ Technology (2018, China, \$14.4M) started with announcing in January 2021 their Gemini \$5K 2-qubit desktop quantum computer and their cloud quantum computing platform Taurus¹⁸⁸⁰.

It followed an initial version launched in 2020 and sold at \$55K. The quantum computer weighs 55 kg and works at ambient temperature. They plan to increase the number of qubits of this device in upcoming versions, up to a maximum of 15 qubits. It would be nice since 2 qubits are totally useless even for quantum programming learning tasks. Meanwhile, you can test for free 7 real superconducting qubits on IBM Quantum Experience cloud systems. The SpinQ computers use liquid dimethyl-phosphite molecules with two OCH₃ groups associated to a phosphorus atom plus one oxygen and one hydrogen atom.

These molecules are controlled with permanent magnets and an RF pulse generation system. They followed-on with the Gemini mini version (also with two qubits) and the Triangulum (with a hefty three qubits). The computer is used for educational purposes¹⁸⁸¹.

Bei Zeng from the USTC in Hong Kong is the chief scientific advisor to the company which is based in Shanghai.



Photon qubits

Contrarily to all the previous qubits, photons have no mass and move at about the speed of light, modulo the optical refractive index of the physical media they pass through. While photons were used everywhere in solid qubits in control and readout features with microwaves or laser beams, they can be used to create qubits exploiting polarization or other physical characteristics such as frequency, amplitude, phase, mode, path or photon number. This is the vast field of linear and nonlinear optics¹⁸⁸². It is found in both the generation of qubits for quantum computation or simulation and with their application in telecommunications and quantum cryptography which we study in another part of this document, starting page 727.

¹⁸⁷⁹ See [Power of Quantum Computation with Few Clean Qubits](#) by Keisuke Fujii et al, 2015 (45 pages).

¹⁸⁸⁰ See [SpinQ Gemini: a desktop quantum computer for education and research](#) by Shi-Yao Hou et al, 2021 (14 pages). It was updated with 3 qubits in September 2021 with their Triangulum version.

¹⁸⁸¹ See [Quantum computing: principles and applications](#) by Guanru Feng et al, October 2023 (76 pages) which is mostly dedicated to describing how NMR works and how SpinQ's software environment can be used to lead quantum computing.

¹⁸⁸² Nonlinear optics is well described in [Nonlinear Optics](#) by Franz X. Kärtner and Oliver D. Mücke, University of Hamburg, December 2016 (255 pages). See also the reference book [Nonlinear Optics](#) by Robert W. Boyd, 2007 (620 pages).

Photonics is both an interesting solution for creating qubits as well as a transversal technology that is indispensable to other types of qubits because it is the only one that allows long-distance communications between quantum sensors, quantum networks and quantum computers. Photons are also used directly in quantum sensing, particularly for precision time measurement and even for pressure measurement.

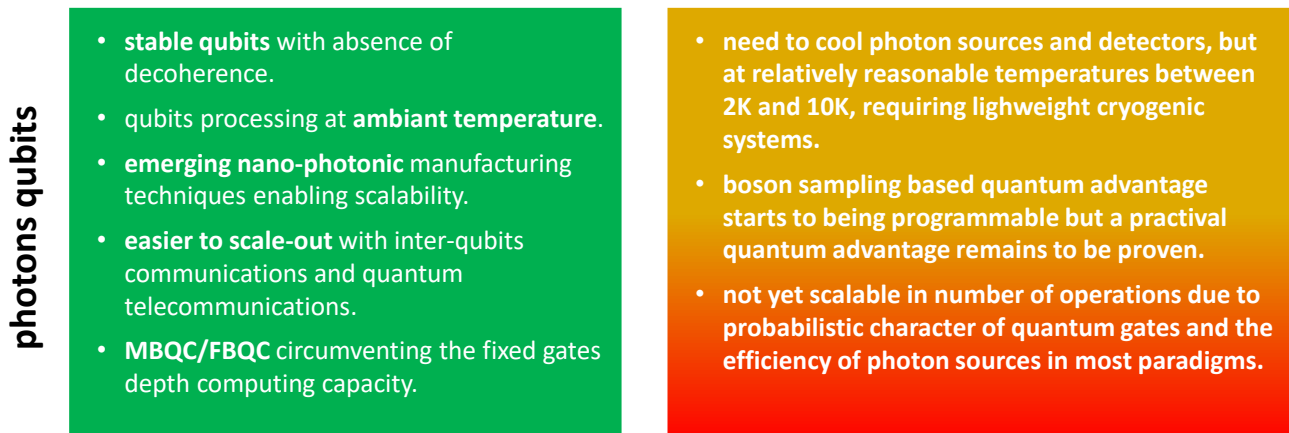


Figure 441: pros and cons of photon qubits. (cc) Olivier Ezratty, 2022-2023.

The advantages of photonics are that it allows to manage quite stable qubits with a very low error rate at the quantum gate level thanks to their weak coupling with the environment. The main source of decoherence is related to the optical losses happening with photons propagation. Photons also operate at any temperature¹⁸⁸³, do not require expensive nanoscopic manufacturing techniques and can be based on nanophotonic CMOS manufacturing processes¹⁸⁸⁴. Their disadvantage lies in the fact that photons are even more probabilistic beasts than any of the other qubits. Scalability issues make it difficult to assemble more than a few dozens of qubits, at least for the moment. Photon sources must be more powerful to accommodate a larger number of entangled qubits (Figure 441).

Current technology developments are based on progresses made with more efficient single photon sources, better photon detectors, nonlinear optics, advanced quantum states preparation (multimode, spatial or spectral multiplexing, non-Gaussian states) with a larger computing space than traditional two-states qubits, using cluster-states measurement-based techniques (MBQC) to avoid the pitfalls of a physically limited quantum gates depth and quantum error corrections.

History

The roots of quantum photonics date back from 1963 with the introduction of Glauber states by Roy J. Glauber which created the notion of coherent states of light explained by the quantization of the electromagnetic field. This corresponded to the beginnings of the laser era which led, among many things, to its broad industry impact, including fiber optics in the telecom realm.

While the first physical qubits were experimented in the mid-1990 (trapped ions, NMR) and early 2000s (superconducting), photon qubits used for computation saw the light much later. Starting in the mid-1980s, quantum photonics were envisioned for implementing quantum key distribution protocols. 2001 was a foundational year with the creation of the KLM theory by Emanuel Knill and Raymond

¹⁸⁸³ In general, solid-state light source must be cooled to 10K and the photon detectors output to about 2K to 4K. At least, one avoids going below 1K, which allows the use of cryogenic systems that are satisfied with helium 4 and do not require helium 3. These cryogenic systems are miniaturizable and require much less energy than the dilution systems used for superconducting and silicon qubits.

¹⁸⁸⁴ See [Photonic quantum information processing: A concise review](#) by Sergei Slussarenko and Geoff Pryde of the Centre for Quantum Dynamics and the Centre for Quantum Computation and Communication Technology at Griffith University in Brisbane, Australia (20 pages) which describes the state of the art of photon qubits. This is the source of the diagram. See also the older [Why I am optimistic about the silicon-photon route to quantum computing](#) by Terry Rudolph, a cofounder of PsiQuantum, published in 2016 (14 pages).

LaFlamme (then at the Los Alamos National Lab) and Gerald Milburn (University of Queensland, Australia)¹⁸⁸⁵.

This model could theoretically implement quantum computing without relying on some sort of nonlinearity for creating entangling quantum gates¹⁸⁸⁶. Implementing for example a CNOT gate with photons is not easy since photons do not easily interact with each other. The KLM model was a breakthrough, making it possible to implement two qubit gates with using photon sources, beam splitters and photon detectors, using a dual rail encoding, represented by the presence of a single photon in one of two spatial optical modes¹⁸⁸⁷ (Figure 442).

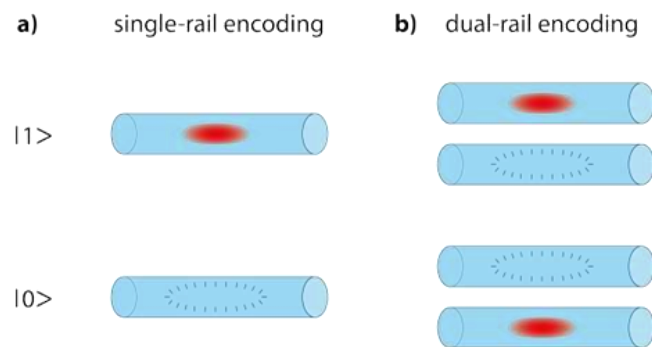


Figure 442: how dual rail encoding works. Source: [No-go theorem for passive single-rail linear optical quantum computing](#) by Lian-Ao Wu et al, Nature, 2013 (7 pages).

It circumvents the need for nonlinear interactions between photons with the use of post-selection with using ancilla photons, many executions and iterations being required. It creates significant overhead which makes the model impractical and not scaling well¹⁸⁸⁸.

There were then many “firsts” with the first universal optical quantum computer in 2015 using a chip handling 6 photons with 15 Mach-Zehnder interferometers and 30 thermo-optic phase shifters and a 12-single-photon detector system¹⁸⁸⁹, a programmable photonic quantum computer created by Xanadu in 2021 with 8 photons¹⁸⁹⁰ and a first quantum computational advantage using gaussian boson sampling in China¹⁸⁹¹. Boson sampling was based on an idea from Scott Aaronson elaborated in 2011¹⁸⁹². It led in 2022 to a similar experiment achieved by Xanadu with a programmable gaussian boson sampler.

Many fundamental research advances were also achieved:

- The MBQC model was created in 2000 by Robert Raussendorf and Hans Briegel. It circumvented some limitations of photon qubits beyond the nonlinearity already discussed, like the finite number of gates that could be executed, the photons being “flying qubits”. We’ll describe this later. The key figure of merit of this architecture is the ability to create large cluster states of entangled photons.
- Quality photon sources, like single and deterministic photon sources, and better, entangled photon sources. Two entangled photons can be created with a photon source and a polarizing crystal.

¹⁸⁸⁵ See [A scheme for efficient quantum computation with linear optics](#) by Emanuel Knill, Raymond Laflamme and Gerard Milburn, 2001 (7 pages).

¹⁸⁸⁶ See the review paper [The Category of Linear Optical Quantum Computing](#) by Paul McCloud, March 2022 (34 pages).

¹⁸⁸⁷ See [No-go theorem for passive single-rail linear optical quantum computing](#) by Lian-Ao Wu et al, Nature, 2013 (7 pages).

¹⁸⁸⁸ This part is inspired from [Twenty Years at Light Speed: The Future of Photonic Quantum Computing](#) by David D. Nolte, December 2021. See also [Photonic quantum technologies](#) by Jeremy L. O’Brien, Akira Furusawa and Jelena Vučković, Nature Photonics, 2009 (11 pages).

¹⁸⁸⁹ See [Universal linear optics](#) by Jacques Carolan, Jeremy O’Brien, Anthony Laing et al, Science, 2015 (6 pages).

¹⁸⁹⁰ See [Quantum circuits with many photons on a programmable nanophotonic chip](#) by J. M. Arrazola et al, Nature, March 2021 (21 pages).

¹⁸⁹¹ See [Quantum computational advantage using photons](#) by Han-Sen Zhong et al, December 2020 (23 pages).

¹⁸⁹² See [The computational Complexity of Linear Optics](#) by Alex Arkhipov and Scott Aaronson, 2010 (94 pages).

More entangled photons can be created with a single deterministic indistinguishable photon sources and delay lines.

- Silicon-based or III-V Quantum Photonic Integrated Circuits (QPICs) that implement quantum gates with waveguides and electronically controllable optical elements like beam splitters and polarizing filters as well as photon sources and photons detectors. They enable miniaturization of these components. Their figures of merit are miniaturization and low photon losses¹⁸⁹³.

Then, since about 2017, a wealth of startups have been created that are all pursuing the goal of creating photon qubits quantum computers, first in the NISQ and then the FTQC realms: **PsiQuantum**, **Xanadu**, **Quandela**, **Orca Computing**, **QuiX**, etc. They all adopt very diverse technological choices as we will see in the vendor section.

Science

To understand photons in quantum information systems, one needs to get a bit deeper in quantum optics and statistical optics. This section constitutes a very rudimentary primer, enabling you to understand some of the vocabulary used by quantum information photonicians. It can also help us segment the various kinds of photonic qubits like discrete variables and continuous variables qubits.

So far, we've mainly mentioned photons as wave-particles interacting with matter, with the photoelectric effect and atoms energy transitions. But exactly, what are photons? How do we define and classify it?

A photon is a moving perturbation of the electromagnetic field with orthogonal magnetic and electric field variations themselves orthogonal to the photon propagation direction.

Photons are described with their quantum numbers which are:

- **Mass and electric charge** equal to zero.
- **Wavelength** λ or frequency ν which define the photon energy and momentum. Several photons with same or different frequencies can be coherently superposed and create a “photon number” or a “wave packet”. Wave packets are usually generated by femto-lasers pulses, mostly in the visible and infrared ranges, or by digital-to-analog microwave generators like those used to drive superconducting and electron spin qubits.
- **Spin angular momentum** (SAM), which corresponds to their angular momentum having quantized values $+\hbar$ or $-\hbar$ (spin = +1 or -1 since spins are expressed in \hbar units) corresponding to circular right or left polarization. Any single monochromatic photon is a linear superposition of these two circular polarizations, including linearly horizontally or vertically polarized photons.
- **Orbital angular momentum** (OAM) where the electromagnetic field is rotating helically along its propagation axis or vector¹⁸⁹⁴. Equals $\ell\hbar$ with ℓ being any integer.

Photons interact with other particles, mainly electrons either tied to atom nucleus, for photons absorption and/or emission, or free electrons like with the Compton effect.

They can be created, destroyed and modified by many of these interactions. Pairs of photons can also be generated by the collision between particles and their antiparticles. Their behavior is mainly described with Maxwell's equations and its derivatives.

¹⁸⁹³ See the review paper [Silicon photonic devices for scalable quantum information applications](#) by Lantian Feng et al, August 2022 (20 pages).

¹⁸⁹⁴ See [Quantum advantage using high-dimensional twisted photons as quantum finite automata](#) by Stephen Z. D. Plachta et al, February 2022 (20 pages) which proposes to use qubits encoded in orbital angular momentum to implement a Quantum finite automata (QFA) to solve binary optimization problems.

Photon directionality. Is a photon directional? Textbooks usually make a distinction between spontaneous emission with photons going in any direction, from a lightbulb or the Sun, and stimulated emission, with directional light, coming from lasers. Radio-frequency antennas can also create spherical radiation going in many directions.

But whatever its source and wavelength, a single photon is mostly always directional and moving in space as a planar wave. A photon electromagnetic wave is represented by orthogonal electric and magnetic fields variations travelling along a vector orthogonal to them. A photon direction can change when it traverses various materials having different refraction indices.

Can we have non-planar photons? “Any direction” photons can come from a statistical view of random multidirectional photons emissions or from a coherent superposition of photons emitted in several directions. With light bulbs, many photons are emitted in various directions by random thermal processes, with various photon wavelengths. Laser coherent light is made of photons with the same wavelength, phase and direction. The distinction between a wave and a point-like particle is as blurred with photons as it is with electrons as far as their exact physical nature and dimensional scope is concerned (Figure 443).

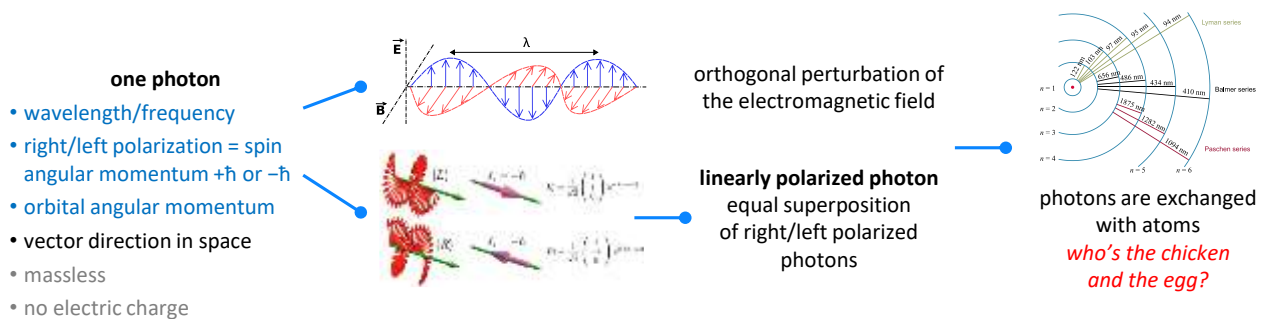


Figure 443: photon characteristics, polarization.

Photon length and size are thus notions that are rarely mentioned. According to the Hunter-Wadlinger electromagnetic theory of the photon established in 1985 and verified experimentally for some wavelengths, an optical photon has a shape similar to an elongated ellipsoid of length λ and diameter λ/π , λ being the photon’s wavelength.

What this means is the usual graphic representation in Figure 444 in green is not realistic! According to other literature, the longitudinal length of a single photon is half of its wavelength ($\lambda/2$)¹⁸⁹⁵.

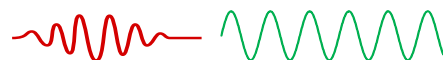


Figure 444: a photon wave packet or pulse, and a single frequency photon... of undetermined length. The first has many harmonic frequencies shaped like a Gaussian curve in their Fourier transform while the single frequency photon Fourier transform is a single point.

This length’s range is quite broad, with 1 nm for X-rays and several orders of magnitude smaller for gamma rays, to over one millimeter and up to several kilometers for radio waves. A classical representation in the above illustration with an EM field of 1.5 wavelengths doesn’t correspond to a single photon according to this interpretation, but to three or 1.5 consecutive single photons.

Nothing says that this can represent reality. On top of that, with a photon having half a wavelength, its Fourier transform won’t be decomposed with a single frequency, but with some harmonic frequencies. We’re safe since this can be explained with Heisenberg’s indeterminacy, related here to two complementary properties, the photon length, and its wavelength. In other words, if you try to describe with precision the length of the photon wave (time/space domain), you end up losing precision with its wavelength (energy domain).

¹⁸⁹⁵ See [Electromagnetic fields, size, and copy of a single photon](#) by Shan-Liang Liu, 2018 (4 pages) and [The Size and Shape of a Single Photon](#) by Zhenglong Xu, 2021 (22 pages).

And vice versa¹⁸⁹⁶!

Photon modes are not that easy to define, and their simplified descriptions are diverse. These are defined by coherence and orthogonality properties of the EM field. These are orthogonal solutions of the EM wave equations. Different photon modes do not interfere. The energy of a linear superposition of modes equals the sum of the energy of the individual modes. Only photons with the same mode can be coherent and interfere.

There are two types of photon modes: spatial modes that are transverse to their direction of propagation and temporal modes in the direction of propagation (time and frequency)¹⁸⁹⁷.

We find these multimode photons in various quantum optics setups like with boson sampling experiment that we will describe a bit later, as well as in quantum key distribution settings¹⁸⁹⁸.

Photon number is a way to describe groups of similar photons. Several photons with the same wavelength and polarization can be at the same place and at the same time. They also share the same direction vector. These photons are indistinguishable. This is a property of bosons which are elementary or composite particles with the same quantum characteristics which can get together, following Bose-Einstein statistics, while fermions with the same quantum characteristics can't be together, following the Fermi-Dirac statistic.

A group of similar photons form an electromagnetic wave whose energy $E = h\nu N = \hbar\omega N$, i.e. the energy of each photon multiplied by the number of added photons having that wavelength¹⁸⁹⁹.

A photon number is this number of “clustered” photons forming a higher energy EM field than a single photon¹⁹⁰⁰. You can even create superpositions of multi-photons (or single-mode Fock state as we'll see later) with 0, 1, 2 and 3 photons. This can be used to create photon-number Bell states, namely entangled states of superposed photon numbers¹⁹⁰¹, leading to the teleportation of Fock states¹⁹⁰². This is mind blowing and quite hard to visualize!

Quantum optics is heavily based on the model of the **quantum harmonic oscillator**, the quantum-mechanical analog of the classical harmonic oscillator, with quantized energy.

The energy of a quantum oscillator can be described with a simple equation, N being the photon number. When $N=0$, the oscillator energy corresponds to the vacuum state energy.

$$\text{energy } E \text{ and photon number } N: \quad E = \hbar\omega \left(N + \frac{1}{2} \right) \quad \text{photon wavenumber } k = \frac{2\pi}{\lambda}.$$

Photon wavenumber is the spatial frequency of a wave, measured in radians per unit distance. It is defined as k with the above right formula using the photon wavelength.

¹⁸⁹⁶ See [Limits for realizing single photons](#) by Jan Gulla, Kai Ryen and Johannes Skaar, September 2021-November 2023 (22 pages) which describes the real structure of photons generated by single photon sources.

¹⁸⁹⁷ See [The concept of modes in optics and photonics](#) by René Dändliker, 1999 (6 pages).

¹⁸⁹⁸ See the review paper [Roadmap on multimode photonics](#) by Ilaria Cristiani et al, 2022 (39 pages) which also covers classical use cases of multimode photonics.

¹⁸⁹⁹ Here, ν is the photon frequency, h in Planck's constant, \hbar is Planck's reduced constant or Dirac's constant and ω is the photon angular frequency with $\omega = 2\pi\nu$, in radians per second, 2π radians corresponding to a 1 Hz frequency.

¹⁹⁰⁰ A powerful radio of digital TV emitter is creating these kinds of photons, in the radiowave range! Same for a radar.

¹⁹⁰¹ See [Generation of non-classical light in a photon-number superposition](#) by J. C. Lored, Pascale Senellart et al, November 2018 (13 pages), [Generating superposition of up-to three photons for continuous variable quantum information processing](#) by Mitsuyoshi Yukawa et al, 2013 (7 pages), and [Generation of light in a photon-number quantum superposition](#), August 2019. And the entangled photon numbers in [Photon-number entanglement generated by sequential excitation of a two-level atom](#) by S. C. Wein, Pascale Senellart et al, June 2021 and in Nature Photonics, April 2022 (18 pages).

¹⁹⁰² See [Quantum teleportation of a genuine vacuum-one-photon qubit generated via a quantum dot source](#) by Beatrice Polacchi, Fabio Sciarrino et al, October 2023 (20 pages).

Creation and annihilation operators or ladder operators are mathematical operators used with quantum harmonic oscillators and many-particles systems. An annihilation operator \hat{a} reduces the number of particles in a given state by one and a creation operator \hat{a}^\dagger increases this number by one. It is the adjoint operator of the annihilation operator. These operators act on states of various types of particles, and with photons, adding or removing a quantum of energy to an oscillator system.

The use of these operators instead of wavefunctions is part of the second quantization formalism. It explains why the canonical quantum physics postulates that we described in an earlier part page 100 are not entirely applicable to quantum optics, particularly the time evolution postulate related to Schrödinger's wave equation that is applicable only to non-relativistic massive particles and even the structure of the quantum state ψ .

Mathematically, a photon occupation number operator is a Hermitian operator $\hat{N} = \hat{a}^\dagger \hat{a}$. And a photon number of n superposed photons created by the operator \hat{a}^\dagger applied n times to the vacuum state $|0\rangle$ creates the state $|n\rangle = \frac{1}{\sqrt{n!}} (\hat{a}^\dagger)^n |0\rangle$.

Second quantization is the broad field of quantum physics that deals with many-body quantum systems. It was introduced by **Paul Dirac** in 1927 and developed afterwards by **Vladimir Fock** and **Pascual Jordan**. While the first quantization dealt with individual quantum objects and their description by the Schrödinger wave equation, the second quantization describes many-body systems which are represented mathematically by Fock states and Fock spaces.

Its formalism introduces creation and annihilation operators to construct and handle the Fock states, providing the mathematical tools to the study quantum many-body systems.

Instead of describing such a system as a tensor product of all its constituent quantum objects, it is simplified with chaining $|n_{k_i}\rangle$ describing the n_i quantum objects that are in the same quantum state k_i as described in the above equation related to the creation operator.

A many-body system is described as the tensor product of the Fock states $|n_{k_i}\rangle$ corresponding to each individual quantum states in the system: $|n_{k_0}\rangle \otimes \dots \otimes |n_{k_n}\rangle$, given that the photon number n_i for the Fock state $|n_{k_i}\rangle$ can be 0 or 1 for fermions and any positive number for a boson. When all occupation numbers are equal to zero, the Fock state corresponds to the vacuum state.

A Fock state with only one non-zero occupation number is a single-mode Fock state. Contrarily, a multi-mode Fock state has several non-zero occupation numbers.

Quantum optics. This field of quantum physics started quite late. In 1956, the Hanbury-Brown-Twiss (HBT) experiment was about observing the intensity correlations of the radiation of a mercury lamp and from some bright stars. After traversing a beamsplitter (with a mercury lamp) or at two spatially separated points (for stars), the intensities measured by two detectors were fluctuating, and these fluctuations were correlated.

It was then explained by the emission of photon bunches coming from thermal sources. But it could be explained without using photons and quantum physics.

Quantum optics really started when it became possible to create non classical light sources like pairs of photons and single photons, respectively in 1967 and 1977. Photon pairs were first created with using cascaded atom decay and parametric down conversion¹⁹⁰³.

Semi-classical light. It describes interactions between quantized matter such as atoms and electrons with classical light fields. Continuous laser light belongs to this category.

¹⁹⁰³ Source: [Lecture 1. Basic concepts of statistical optics](#) (7 pages).

Non-classical light. Light and photons are always quantum, just because it comes from quantized energy exchanges with matter. Still, light is considered to show non-classical and quantum effects when the electromagnetic field is quantized and photons are handled individually. This happens in a couple situations: creation of entangled Bell states, antibunching, photon noise and negative probabilities with the Wigner function. We'll look at each of these phenomena.

Bell states where single photons behave probabilistically and in the general case have no *a priori* properties like polarization, wavelength, wavevector before being measured. These properties are revealed while being measured and show correlations between entangled photons whose measured properties will be random.

Anti-bunching corresponds to a light field where photons are equally spaced in time, much better than with a coherent laser field. It is detected with a HBT (Hanbury Brown & Twiss) intensity autocorrelator... with no correlations. It refers to sub-Poissonian photon statistics, that is a narrow photon number distribution (Figure 445 and Figure 446).

It can be generated by single photon sources as well as from pulse mode lasers. A coherent state from a laser has Poissonian statistics generating random photon spacing and a thermal source light field has super-Poissonian statistics and yields bunched photon spacing. All these aspects belong to the field of statistical optics.

The quality of single photons source is measured with data from two experiments. The first uses a variant of a **Hanbury Brown and Twiss (HBT)** intensity autocorrelator that checks the photons are emitted in a very regular way, like a metronome.

From a starting click on one of the two photon detectors, it analyzes the time distribution of the appearance of the following photons. This produces the plots in Figure 446. The ideal model would be that of a high peak on either side of the center. The low peaks represent the system noise. This experiment, originally created to detect the size of stars, also enabled the validation of the corpuscular nature of photons. The experiment can be easily interpreted in an intuitive way: photons pass through a one-way mirror, whether or not it crosses randomly. Behind this mirror are two photon counters, here with SPADs (avalanche diodes).

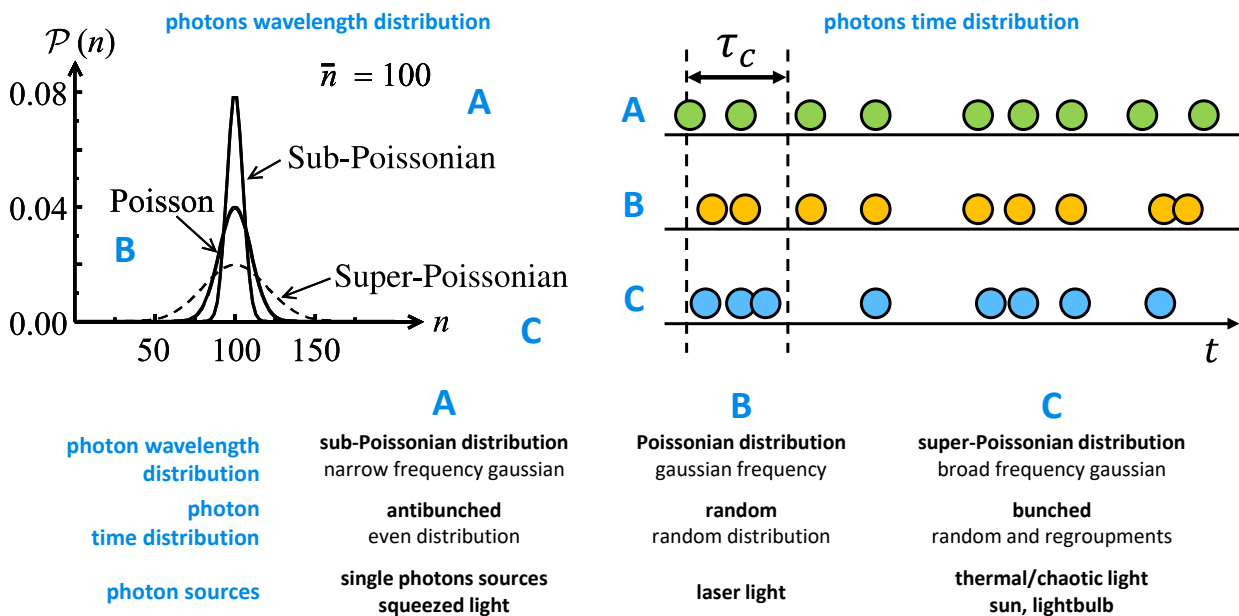


Figure 445: poissonian, sub-Poissonian and super-Poissonian photons wavelength distribution and photons time distribution. Compilation: Olivier Ezratty, 2021.

The system detects when a photon is detected at the same time by both sensors. If the photons take the same way to reach both detectors, there will be no coincidence since the emitted photons are sent in well-ordered trains and can only be on one side or the other. By adding a delay line between the mirror and one of the sensors that is proportional to the period of emission of the photons, it creates many occurrences with photons arriving simultaneously in both sensors.

This is what we see in the two curves, one of them being with a linear scale of coincidences (measured over a period of time sufficient to capture hundreds of them) and another logarithmic which allows to better characterize the noise of the system.

The second experiment called H.O.M. for **Hong-Ou & Mandel** and created in 1987 uses a Mach-Zehnder interferometer to validate the fact that the emitted photons are indeed identical and impossible to distinguish¹⁹⁰⁴.

Quadratures representation is a way to describe the electromagnetic field and its related uncertainty. An EM wave is positioned in two axis X and Y or X_1 and X_2 corresponding to the rotation of the electric field in the EM field, thus the equations describing X_1 and X_2 below, with the cosine and sine of ωt (angular frequency \times time). Said otherwise, a quadrature describes the real and imaginary parts of a complex amplitude. This EM field complex amplitude is rotating so what's interesting is not the grey circle position in the chart but its shape and size which represents the photon measurement uncertainty.

It is represented by the variation of the length of the vector which is the photon number and of the width of the circle, orthogonally to the vector, which corresponds to the phase uncertainty. For unsqueezed coherent light, this uncertainty is the same as the vacuum state.

antibunching measurement

$g^2(0) = 0.019$
 time correlation of second order or of intensity between pairs of photons with a zero delay. the closer to zero, the better. describes the level of noise in the system.

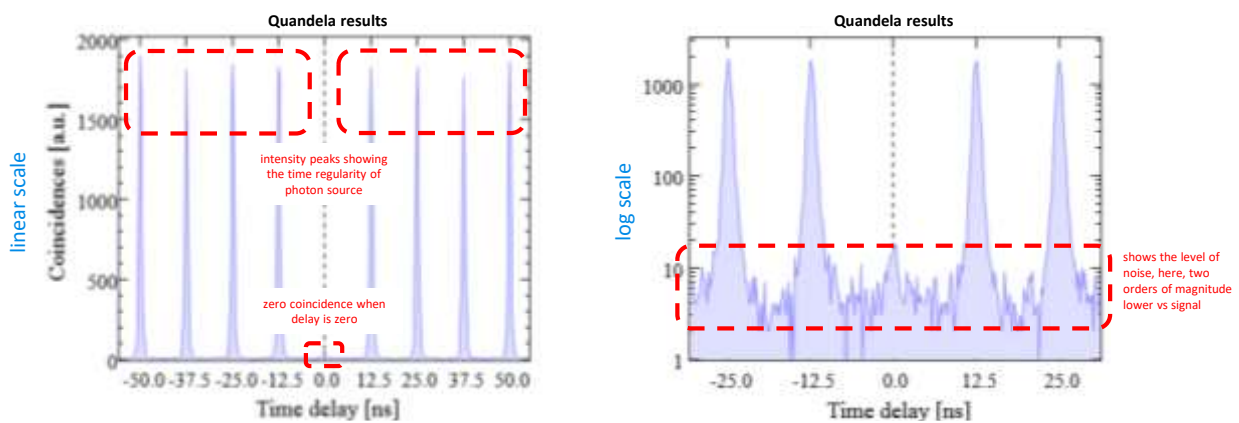
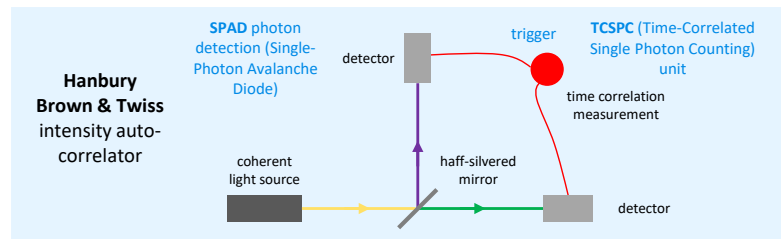


Figure 446: how antibunching is measured. Sources: various.

Photon noise aka shot noise is found in the detection of light and corresponds to quantum fluctuations in the electromagnetic field. This noise or imprecision can be squeezed in one dimension.

¹⁹⁰⁴ See [High-performance semiconductor quantum-dot single-photon sources](#) by Pascale Senellart, Glenn Solomon and Andrew G. White, 2017 (14 pages) which describes the various ways to characterize the quality of single photons sources.

Squeezed light corresponds, in a quadrature or phasor diagram representation, to wave functions which have an uncertainty in one of the quadrature amplitudes (phase or photon number) smaller than for the ground-state corresponding to the vacuum state. It can be generated by different means like a parametric down conversion¹⁹⁰⁵. Balanced homodyne detectors are used to detect squeezed light.

Wigner function is yet another representation of a quantum state, richer than the phase diagram above which is used to measure the level of quantumness of a light pulse. It is not far from a probability distribution of the electric field in the (Q, P) plane that can take negative values in some conditions, for so-called non-Gaussian states¹⁹⁰⁶. With coherent states, W(Q, P) is a symmetric Gaussian function peaking at the average values of the sine and cosine components of the electric field with the peak width corresponding to the vacuum noise like in the quadrature representation. The Wigner function equation looks like this in Figure 447 with ψ being the quantum object wave function, Q and P the position and momentum and y, the variable used in the integral.

$$W(Q, P) = \frac{1}{\pi\hbar} \int_{-\infty}^{+\infty} \psi^*(Q + y)\psi(Q - y)e^{2iPy/\hbar} dy$$

Figure 447: Wigner function which helps measure the quantumness of light.

It returns a real value that can be positive or negative. Q and P could be replaced by the sine and cosine components of the quantized electric field like in the phasor diagram (see also Figure 448).

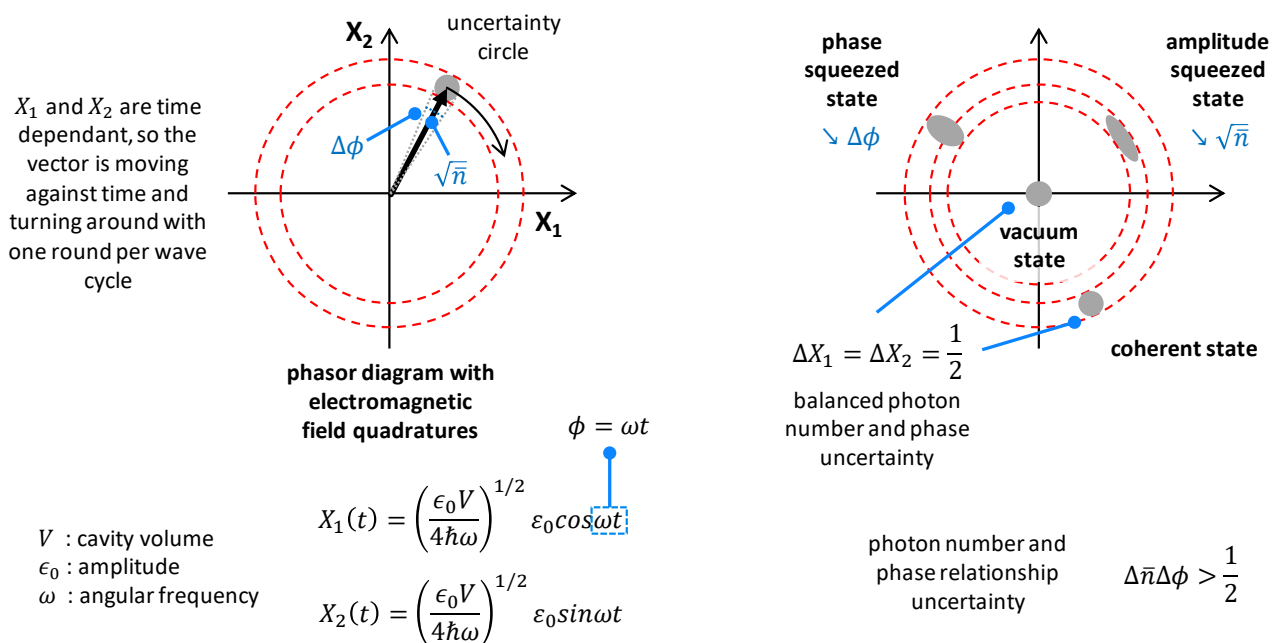


Figure 448: what squeezed light looks like when using quadratures representation. (cc) Olivier Ezratty, 2023.

In Figure 449 are presented a set of Wigner functions, ranging from the most classical to the most quantum fields. A is a coherent state¹⁹⁰⁷, B, a squeezed state, C a single-photon state and D a Schrödinger's-cat state.

¹⁹⁰⁵ See [Generation of squeezed states by parametric down conversion](#) by Ling-An Wu et al, University of Texas, Physical Review Letter, 1986 (4 pages).

¹⁹⁰⁶ See [Conversion of Gaussian states to non-Gaussian states using photon number-resolving detectors](#) by Daiqin Su et al, Xanadu, April 2019 (37 pages), the tutorial paper [Non-Gaussian Quantum States and Where to Find Them](#) by Mattia Walschaers, LKB - Collège de France, April 2021 (55 pages) and the review paper [Production and applications of non-Gaussian quantum states of light](#) by A. I. Lvovsky, Philippe Grangier et al, June 2020 (50 pages).

¹⁹⁰⁷ The vacuum state has a similar Wigner function, but centered around P=0 and Q=0.

The projections or shadows of the Wigner function are the probability distributions of the quantum continuous variables Q or P . The Wigner function is a Gaussian function for A and B but takes negative values for the non-Gaussian strongly quantum states C and D¹⁹⁰⁸. These negative values vanish very quickly with decoherence.

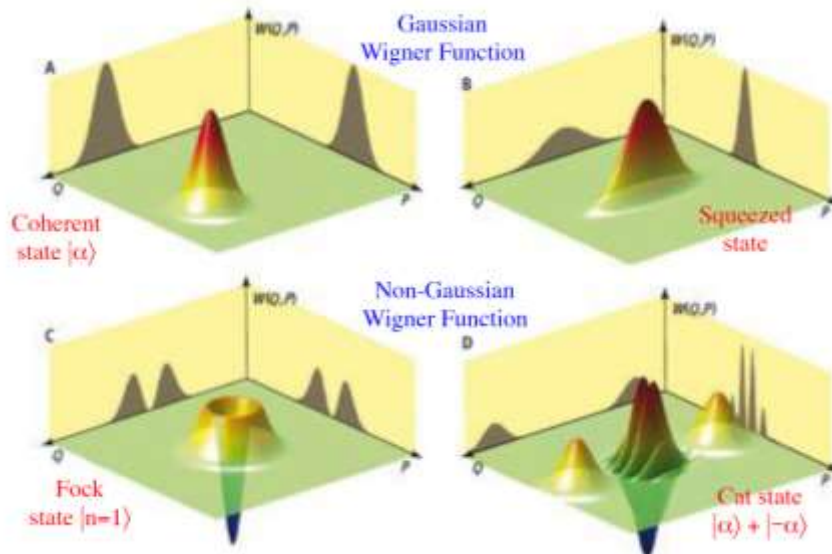


Figure 449: various 3D representations of the Wigner function, for Gaussian and non-Gaussian light.
Source: [Make it quantum and continuous](#) by Philippe Grangier, Science, 2011.

Parametric down-conversion is a nonlinear optical process converting one photon of high energy into a pair of photons of lower energy. It is used to generate pairs of entangled photons.

Photons zoo. Figure 450 shows some various photon states as a summary of this section. Random photons in spontaneous light coming from the Sun or light bulb and “photon number” waves assembling several similar photons belong to classical light.

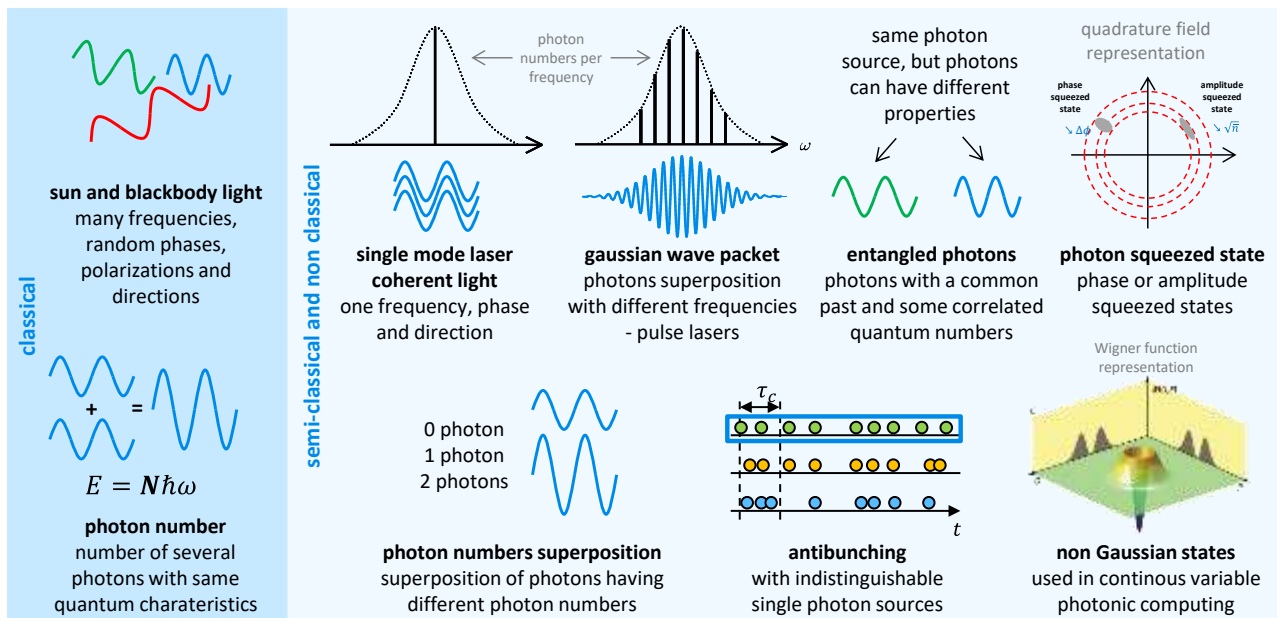


Figure 450: a zoo of photons. (cc) Olivier Ezratty, 2021-2023.

¹⁹⁰⁸ See [Recent advances in Wigner function approaches](#) by J. Weinbub and D. K. Ferry, 2018 (25 pages) which shows the various use cases of the Wigner function.

Other forms of light described here are semi-classical or non-classical: photon number superposition, squeezed states where the precision is improved in photon number, amplitude or phase at the expense of the others, single-mode coherent laser light, wave packets created by pulse lasers or microwave coming from waveform generators used with superconducting and electron spin qubits, entangled photons used in QKD and photon qubits, and non-gaussian states which are weird beasts too complicated to describe in a couple of words that are used to implement non-Clifford quantum gates with photon qubits.

Qubit operations

Photons are "flying qubits". They are the only ones having this characteristic with flying electrons, which are investigated at the fundamental research level. There are two main classes of photon qubits: discrete variable and continuous variable qubits¹⁹⁰⁹ (Figure 451).

Discrete Variable qubits use single photons and use a two-dimensional space like orthogonal polarizations or the absence and presence of single photons (Figure 458). DV systems can even be based on qudits using more than one degree of liberty^{1910 1911}. DV qubits rely on highly efficient, deterministic and indistinguishable single photon sources. They are using the "particle" side of photons. Their indistinguishability must exceed 95%, meaning this percentage of photons must be indistinguishable. The photon sources must also be efficiently connected to dynamically controllable photonic computing chips. Efforts are also undertaken to create cluster states of entangled photons used in MBQC and to create deterministic multi-qubit gates using spin-photon interactions like in NV centers or other silicon spin defects¹⁹¹².

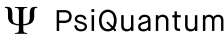






	discrete variables	continous variables	boson sampling
quantum information	discrete degree of freedom of a photon Fock states: $ 0\rangle, 1\rangle, 2\rangle \dots$ single or many photon properties	quadrature of a light field coherent states, qumodes, spectral and time modes	multimode photons
photon sources	single indistinguishable photon sources	entangled photons sources squeezed states, ...	unique photons source
representation	density matrix	Wigner function	permanent
gates	KLM model, MZI (Mach-Zehnder Interferometer) gates	determinist gates modes measurement gaussian and non gaussian gates	MZI and interferometer
photon detectors	photon counters /detectors APD, SNSPD, VLPC, TES	homodyne and heterodyne detectors	single photons detectors
players	 PsiQuantum  ORCA Computing  QUANDELA  DUALITY QUANTUM PHOTONICS	 XANADU	 

Figure 451: comparison of the main models of photon-based quantum computing. (cc) Olivier Ezratty, 2021.

¹⁹⁰⁹ See this good review paper: [Integrated photonic quantum technologies](#) by Jianwei Wang et al, May 2020 (16 pages) and [Hybrid entanglement of light for remote state preparation and quantum steering](#) by Adrien Cavaillès et al, LKB (41 slides) which positions well the difference between DV and CV computing.

¹⁹¹⁰ See [Efficient qudit based scheme for photonic quantum computing](#) by Márton Karácsony, László Oroszlány and Zoltán Zimborás, February 2023 (19 pages).

¹⁹¹¹ See [Deterministic generation of qudit photonic graph states from quantum emitters](#) by Zahra Raissi, Edwin Barnes and Sophia Economou, Virginia Tech, November 2022 (14 pages).

¹⁹¹² See [Multidimensional cluster states using a single spin-photon interface coupled strongly to an intrinsic nuclear register](#) by Cathryn P. Michaels et al, University of Cambridge, April 2021 (11 pages).

Continuous Variable qubits encode information in the fluctuations of the electromagnetic field, in their quadrature components, in qubits that are sometimes baptized qumodes¹⁹¹³. We are playing here with the wave nature of photons.

Photons readout can be done with a Gaussian measurement comprising homodyne detection for one of the two quadrature components and heterodyne detection on one of these¹⁹¹⁴, and a non-Gaussian measurement implementing photon counting returning an integer. There, you hear about Wigner function amplitude, phase encoding, Gaussian states¹⁹¹⁵, including squeezed states generated with nonlinear media and non-Gaussian gates to execute non-Clifford group gates bringing a real exponential speedup for quantum computing. Quantum gates can be deterministic, homodyne detectors are cheaper than single photons detectors, and quantum states are more robust. CV qubits are implementing larger cluster states for MBQC, using a large number of photon modes (in the thousands)¹⁹¹⁶.

In the CV qubit domain, **PhotoQ** (Denmark) is a collaborative project implementing this architecture with using surface codes for fault-tolerance¹⁹¹⁷. The project is built around research from DTU with participating organizations being AMCS Group, Aarhus University, Kvantify and NKT Photonics (lasers) with a public funding of 3M€ from Innovation Fund Denmark. They are (wonder why) focused on solving logistics and pharmaceutical industries problems. The **PANDA consortium** is another European CV photonic quantum computing project, funded by the EIC Pathfinder-2023 challenge grant. The project led by Sorbonne Université (Nicolas Treps and Valentina Parigi, LKB) also gathers Pixel Photonics (photonic detectors), ICFO (Spain), IOGS (Paris) and Pasqal (France).

There you will also find cat-qubits and GKP states¹⁹¹⁸. Hybrid DV/CV qubits approaches are also investigated¹⁹¹⁹. CV computing can be used with universal gates quantum computing as well as with quantum simulations.

Quantum Walks based simulation is another computing technique using photons. Similarly to the CV/DV computing segmentation, you have two classes of photon-based quantum walk systems: discrete-time quantum walks with discrete steps evolutions¹⁹²⁰ and continuous-time quantum walks with a continuous evolution of a Hamiltonian coupling different sites¹⁹²¹. A research team in China created a CV-quantum walk system handling a Hilbert space of dimension 400 as shown in Figure 452.

¹⁹¹³ For an explanation of the difference between qumodes and qubits, see [Introduction to quantum photonics](#) from Xanadu.

¹⁹¹⁴ On the measurement of CV qubits, see [Optical hybrid architectures for quantum information processing](#) by Kun Huang, LKB, 2017 (215 pages). This is not the same Kun Huang as the discoverer of phonon-polaritons in 1951.

¹⁹¹⁵ Understanding how Gaussian states work is already quite a challenge. See [Gaussian Quantum Information](#) by Christian Weedbrook, Seth Lloyd et al, 2011 (51 pages).

¹⁹¹⁶ See [A fault-tolerant continuous-variable measurement-based quantum computation architecture](#) by Mikkel V. Larsen, January 2021 (16 pages).

¹⁹¹⁷ See [A fault-tolerant continuous-variable measurement-based quantum computation architecture](#) by Mikkel V. Larsen et al, August 2021 (19 pages) and [Deterministic multi-mode gates on a scalable photonic quantum computing platform](#) by Larsen, Mikkel V. et al, Nature Physics, August 2021 (32 pages).

¹⁹¹⁸ These light states require specific preparation techniques. See for example [Robust Preparation of Wigner-Negative States with Optimized SNAP-Displacement Sequences](#) by Marina Kudra, Jonas Bylander, Simone Gasparinetti et al, Chalmers University, PRX Quantum, September 2022 (12 pages) with interesting cavity-based preparation of various quantum light states usable in CV photon qubit systems.

¹⁹¹⁹ See [Hybrid Quantum Information Processing](#) by Ulrik L. Andersen et al, 2014 (13 pages) and [Hybrid discrete and continuous-variable quantum information](#) by Ulrik L. Andersen et al, 2015 (11 pages), [Visualization of correlations in hybrid discrete—continuous variable quantum systems](#) by R P Rundle et al, February 2020 (15 pages) and [Remote creation of hybrid entanglement between particle-like and wave-like optical qubits](#) by Olivier Morin, Claude Fabre, Julien Laurat, LKB France, 2013 (7 pages).

¹⁹²⁰ See for example [Quantum walks of two correlated photons in a 2D synthetic lattice](#) by Chiara Esposito, Fabio Sciarrino et al, April 2022 (18 pages).

¹⁹²¹ See [Purdue University Scientists Say 'Quantum Rainbow' May Allow Room-Temperature Quantum Computing](#) par Matt Swayne, 2021 referring to [Probing quantum walks through coherent control of high-dimensionally entangled photons](#) by Poolad Imany et al, July 2020 (9 pages).

It even takes the form of a seemingly packaged and designed product despite coming out of a public research lab and not a startup. There are even hybrid fermion/bosons approaches that are proposed but that are very theoretical and with very few hardware implementation details¹⁹²².



Figure 452: the continuous-variable quantum walk system YH QUANTA QW2020 from China. Source: [Large-scale full-programmable quantum walk and its applications](#) by Yizhi Wang et al, August 2022 (73 pages).

Boson sampling is a separate technique we will cover later in a dedicated section, page 538. It is a research field that has not yet brought to life programmable computing.

Coherent Ising Machines is another technique based on using optical neural networks that can solve combinatorial optimization problems with mapping them onto NP-hard Ising problems¹⁹²³.

Practically speaking, Ising models can solve many problems: planning and scheduling, financial portfolio optimizations, graph problems and even material and molecular design. These problems are defined by couplings between a set of spins. The solution is the spin orientation that minimizes the energy function of the system. CIM systems use single-mode photon squeezing, oscillation at degenerate frequency, Optical Parametric Amplifiers in a Cavity (OPO) and a measurement feedback technique (Figure 453). Leveraging delay lines, time division multiplexing and measurement feedback, CIM can implement many-to-many connectivity. The largest CIM system was built in Japan in 2021 with 100,000-spins¹⁹²⁴. It competed with quantum annealing (from D-Wave) and also classical CMOS-based annealing (from Fujitsu).

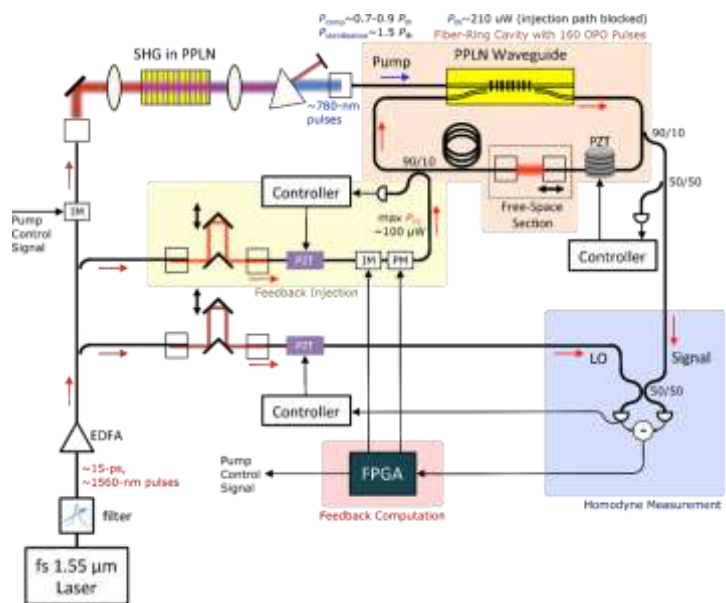


Figure 453: example of realization of a coherent Ising Machine. Source: [Coherent Ising Machines: non-von Neumann computing using networks of optical parametric oscillators](#) by Peter McMahon, Cornell University, October 2020 (100 slides).

¹⁹²² See [Two-level Quantum Walkers on Directed Graphs I: Universal Quantum Computing](#) by Ryo Asaka et al, December 2021 (20 pages) and [Two-level Quantum Walkers on Directed Graphs II: An Application to qRAM](#) by Ryo Asaka et al, April 2022 (23 pages).

¹⁹²³ CIM is described in the presentation [Coherent Ising Machines: non-von Neumann computing using networks of optical parametric oscillators](#) by Peter McMahon, Cornell University, October 2020 (100 slides). It reminds us that HPE and Ray Beausoleil worked on a CIM before abandoning all quantum computing endeavors altogether. The source of the illustration was found on slide 55.

¹⁹²⁴ See [100,000-spin coherent Ising machine](#) by Toshimori Honjo et al, September 2021 (8 pages).

A bit like the difference we discovered between (D-Wave) quantum annealing solving Ising “Z” problems¹⁹²⁵ and quantum simulation models implementing XY qubits connectivity, there are also photonic based coherent XY models that compete with CIM¹⁹²⁶.

Hybrid atoms-photons qubits. Stanford University researchers devised a new hybrid quantum photonic approach using a single atom that modifies photons states via quantum teleportation and implement quantum gates and qubit readout¹⁹²⁷.

It reduces the need for multiple photon emitters and greatly simplifies the hardware setting that makes use of a photons storage ring made of a fiber loop, optical switches in the loop, a beam splitter, a phase shifter, a photon scattering unit and a cavity containing a single atom controlled by a laser, the atom getting entangled with the photon (Figure 454).

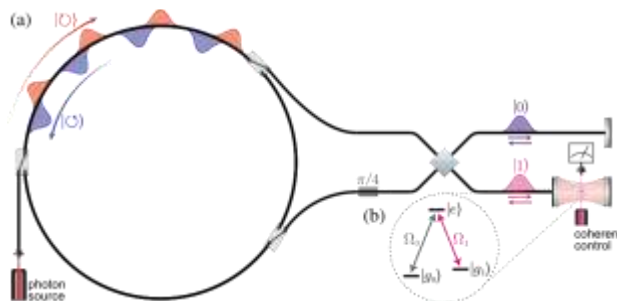


Figure 454: an example of hybrid atoms-photons system. Source: [Deterministic photonic quantum computation in a synthetic time dimension](#) by Ben Bartlett, Avik Dutt and Shanhui Fan, *Optica*, November 2021 (9 pages).

The photon source is a single photon train source. But this is not a perfect solution. It has some requirements on the cavity quality, on low fiber attenuation, on very low insertion losses optical switches and can’t implement quantum gates in parallel.

The general principle of quantum computing systems using photon qubits is as follows:

- **Photon sources** are lasers, often associated with single and indistinguishable photon generators¹⁹²⁸. They are critical to generate simultaneously a large number of indistinguishable photons that will feed in parallel several qubits, thanks to delay lines. These are well time-isolated unique and indistinguishable photons generated in well-spaced in time series. These single photons are individually detectable at the end of processing with single or multiple photon detectors (when computing Fock states with additions of single identical photons). The key metrics of these photon sources are the system efficiency (probability that at least one photon is created per pulse), purity (probability of getting a maximum of one photon per pulse) and coherence (how generated photons are quantum mechanically identical or indistinguishable). The purity and high probability to get a photon per clock cycle are the enabler of quantum interferences based multiple qubit gates with discrete variable qubits. High-efficiency sources are qualified as “on-demand” or “deterministic” with the alternatives of heralded sources, where photon emission time can be accurately evaluated.

¹⁹²⁵ CIM is supposed to work better than D-Wave that also implement Ising models according to [Practical Application-Specific Advantage through Hybrid Quantum Computing](#) by Michael Perelshtein et al, 2021 (14 pages) that is described in [A poor man’s coherent Ising machine based on opto-electronic feedback systems for solving optimization problems](#) by Fabian Böhm et al, *Nature Communications*, 2019 (9 pages). See also [Experimental investigation of performance differences between coherent Ising machines and a quantum annealer](#) by R. Hamerly et al, *Sci. Adv.*, 2019 (26 pages) for the comparison with D-Wave 2000Q. The compared CIM machine is from NTT and Stanford. The Stanford CIM is described in [A fully programmable 100-spin coherent Ising machine with all-to-all connections](#) by Peter L. McMahon et al, *Science*, 2016 (9 pages). The NTT CIM is described in [A coherent Ising machine for 2000-node optimization problems](#) by T. Inagaki et al, *Science*, 2016 (6 pages). See also [Training Multi-layer Neural Networks on Ising Machine](#) by Xujie Song et al, November 2023 (22 pages) on using an Ising machine for some neural network training task.

¹⁹²⁶ Coherent Ising machines models and challenges are described in [Coherent Ising machines - optical neural networks operating at the quantum limit](#) by Y. Yamamoto et al, *npj Quantum*, December 2017 (16 pages).

¹⁹²⁷ See [Deterministic photonic quantum computation in a synthetic time dimension](#) by Ben Bartlett, Avik Dutt and Shanhui Fan, *Optica*, November 2021 (9 pages) also described in [Researchers propose a simpler design for quantum computers](#) by McKenzie Prillaman, Stanford University, *Physorg*, November 2021.

¹⁹²⁸ See [Near-ideal spontaneous sources in silicon quantum photonics](#) by S. Paesani et al, 2020 (6 pages) which describes a single photon source based on a photonics component. It is an Anglo-Italian research project.

There are two main types of single photons sources (SPSs)¹⁹²⁹:

Quantum dot single-photon source are the best-in-class devices, able to generate photons with a 99.7% single-photon purity, and over 65% extraction efficiency, which could potentially reach 80% (meaning, 4 photons generated out of 5 clock cycles). See below in Figure 455 how these efficiencies are improved. These sources also have an over 99% photon indistinguishability. In the second quantization formalism, they create a single Fock state with a photon number equal to one.

The leaders in this market are **Quandela**¹⁹³⁰ and **Sparrow Quantum**¹⁹³¹. And many research labs are working on other varieties of quantum dots¹⁹³². These photon sources must be cooled at about 3K to 4K. In their Prometheus indistinguishable photon source, Quandela directly couples the quantum dot to a fiber, avoiding the use of cumbersome confocal microscopes and significantly increasing the photon generation yield. It creates a path to reaching a combined source–detector efficiency closer to the 2/3 threshold that is mandatory for scalable discrete variable optical quantum computing. Others are trying to operate these quantum dots at hotter or even ambient temperature. That’s the case with the quantum dots single photon emitters developed at EPFL, with a mix of gallium nitride and aluminum nitride (GaN/AlN) on silicon substrate, or with solid-state emitters operating at 28.8K instead of 4K that are studies in the UK¹⁹³³.

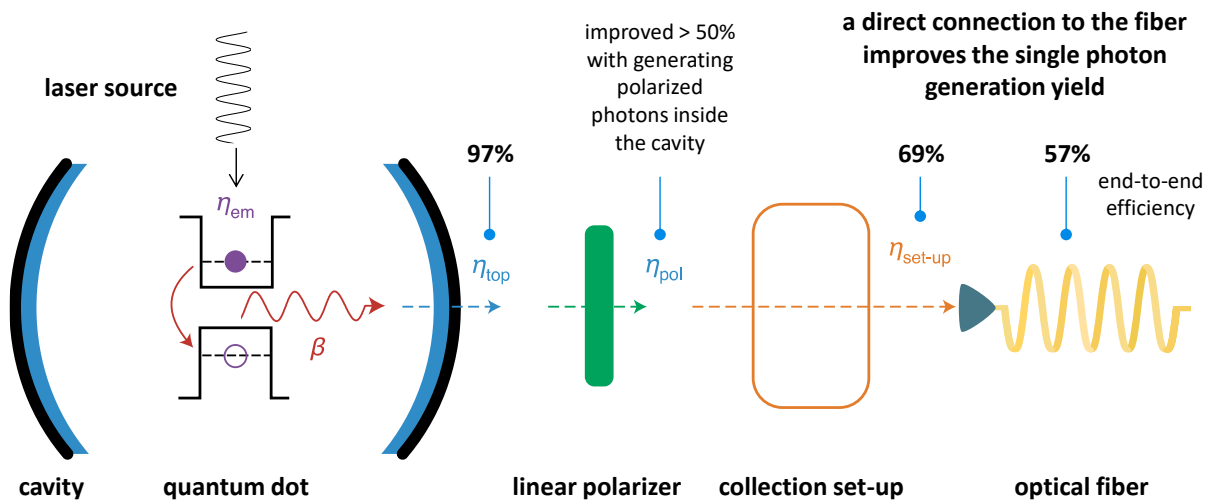


Figure 455: what characterizes the efficiency of a quantum dots photon generator. Source: [The race for the ideal single-photon source is on](#) by Sarah Thomas and Pascale Senellart, *Nature Nanotechnology*, January 2021 (2 pages) and comments by Olivier Ezratty, 2021.

These are showcasing a single-photon purity of 95% at cryogenic temperatures (below 50K) and a purity of 83% at room temperature.

¹⁹²⁹ See [Integrated photonic quantum technologies](#) by Jianwei Wang et al, May 2020 (16 pages).

¹⁹³⁰ See [The race for the ideal single-photon source is on](#) by Sarah Thomas and Pascale Senellart, *Nature Nanotechnology*, January 2021 (2 pages) which describes the various ways to improve the yields of single photon sources, [Sequential generation of linear cluster states from a single photon emitter](#) by D. Istrati, Niccolo Somaschi, Hélène Ollivier, Pascale Senellart et al, October 2020 and [Reproducibility of high-performance quantum dot single-photon sources](#) by Hélène Ollivier, Niccolo Somaschi, Pascale Senellart et al, October 2019 (10 pages) on benchmarking single photon sources.

¹⁹³¹ See [Scalable integrated single-photon source](#) by Ravitej Uppu et al, December 2020 (7 pages) which describes the latest advancements of their technology.

¹⁹³² See [Planarized spatially-regular arrays of spectrally uniform single quantum dots as on-chip single photon sources for quantum optical circuits](#) by Jiefei Zhang et al, University of Southern California and IBM, November 2020 (8 pages) describes an array with 32 quantum dots and a simultaneous purity of single-photon emission over 99.5%.

¹⁹³³ See [Towards Generating Indistinguishable Photons from Solid-State Quantum Emitters at Elevated Temperatures](#) by Alistair J. Brash et al, University of Sheffield, University of Manchester, May 2023 (18 pages).

The photon emission rates reach 1 MHz with a single-photon purity exceeding 50%¹⁹³⁴.

Parametric photon-pair sources are laser pumping nonlinear optical waveguides or cavities that create photon-pairs. It can be integrated in nanophotonic circuits. They are using either spontaneous four-wave mixing (SFWM) or spontaneous parametric down-conversion (SPDC¹⁹³⁵) processes in nonlinear crystals.

The efficiency is lower than with quantum dots, reaching about 50% with a 95% photon indistinguishability from separated SPSs. Photons are created non-deterministically with a rather low 5% to 10% probability, which can be increased to above 60% with time and spatial domains multiplexing.

Such solutions are embedded in hybrid nanophotonic chips like with PsiQuantum and others who consolidate photon sources, waveguides and circuits and then photon detectors¹⁹³⁶.

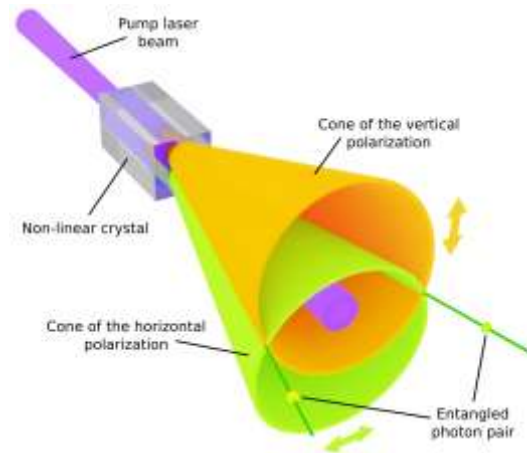


Figure 456: how entangled photons are generated with SPDC method. Source: [Wikipedia](#).

SPDC sources work at room temperature but for efficient multiplexing (>95%), it is necessary to use SNSPD detectors running at low temperature.

Progress is being made with nanophotonic-based single photons generation, although their performance still lags quantum-dots sources¹⁹³⁷. Figure 456 shows a SPDC method to create pairs of entangled photons. The conversion creates pairs of orthogonally polarized photons in two light cones with entangled photons at their intersection.

- **Rydberg single-photon sources** with excitation blockade creating efficient preparation of single atomic excitation, which are converted into high-quality single photons with high indistinguishability¹⁹³⁸.

One key challenge with implementing MBQC, one dominant photonic quantum computing architecture that we'll cover later, is the ability to create large cluster-states of entangled photons. There are many options to implement it. Quantum dots source can be tailored for this need. Good indistinguishable and deterministic photon sources can be coupled with delay lines and mixers to create these cluster states.

¹⁹³⁴ See [Toward Bright and Pure Single Photon Emitters at 300 K Based on GaN Quantum Dots on Silicon](#) by Sebastian Tamariz, Nicolas Grandjean et al, January 2020 (19 pages).

¹⁹³⁵ See [Spectrally multimode squeezed states generation at telecom wavelengths](#) by Víctor Roman-Rodríguez, Nicolas Treps, Eleni Diamanti, Valentina Parigi et al, June 2023 (11 pages).

¹⁹³⁶ See [All optical operation of a superconducting photonic interface](#) by Frederik Thiele et al, February 2023 (9 pages).

¹⁹³⁷ See [High-efficiency single-photon generation via large-scale active time multiplexing](#) by F. Kaneda et al, October 2019 (7 pages), [Researchers create entangled photons 100 times more efficiently than previously possible](#) pointing to [Ultra-bright Quantum Photon Sources on Chip](#) by Zhaohui Ma et al, October 2020 (5 pages) and [A bright and fast source of coherent single photons](#) by Natasha Tomm et al, University of Basel and Ruhr-Universität Bochum, July 2020 (14 pages).

¹⁹³⁸ See [High-fidelity photonic quantum logic gate based on near-optimal Rydberg single-photon source](#) by Shuai Shi et al, Nature Communications, 2022 (6 pages). It says that to achieve a linear-optical quantum logic gate with an error rate below 1%, a single-photon source must have a $g^{(2)}(0) < 7 \times 10^{-3}$ and an indistinguishability greater than 99%. In the paper, they perform a KLM CNOT gate with an entangling gate fidelity of 99.69(4)%.

There are even solutions to create hundreds of pairs of entangled photons, as investigated by the University of Virginia, using frequency combs. Here, the photon source is a continuous laser emitting a single continuous wave, a small 3 mm Kerr microcavity creates a frequency comb generating pairs of entangled photons around the pump frequency as described below. This could lead to massive multimode photonic quantum computing¹⁹³⁹ (Figure 457).

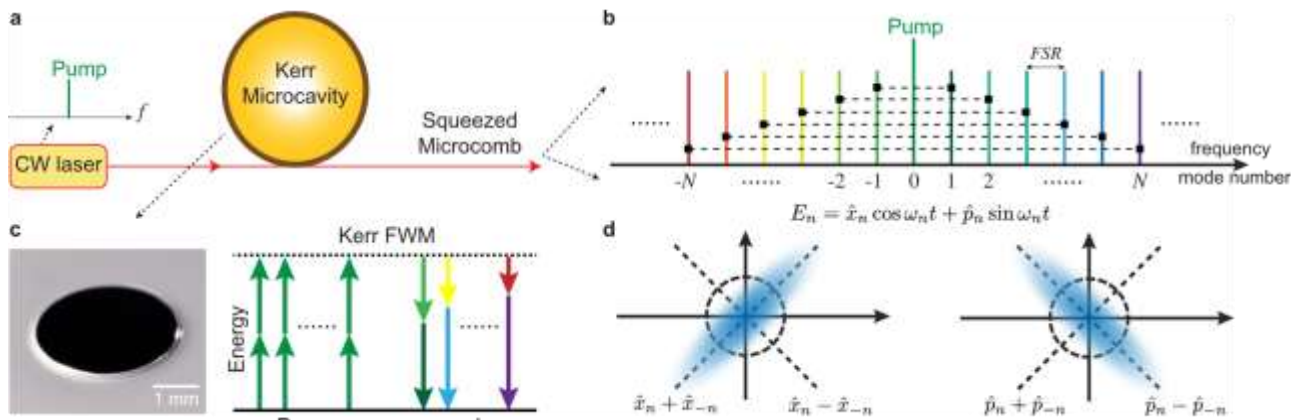


Figure 457: a frequency comb method to generate a large cluster state of entangled photons. Source: [A squeezed quantum microcomb on a chip](#) by Zijiao Yang et al, Nature Communications, August 2021 (8 pages).

Other photon sources are explored like Rydberg atoms in cavities which can create photon couples that are dephased by π , enabling two photon quantum gates^{1940 1941}.

- **Quantum state** is based on a single or several properties of the photons. The most common is their polarization with a computational basis based on horizontal and vertical polarization. Other parameters of photons are also explored to create qubits. It can be their phase, amplitude, frequency¹⁹⁴², path, photon number (*aka* Fock states) and spin orbital momentum. It can even be their orbital angular momentum^{1943 1944}.

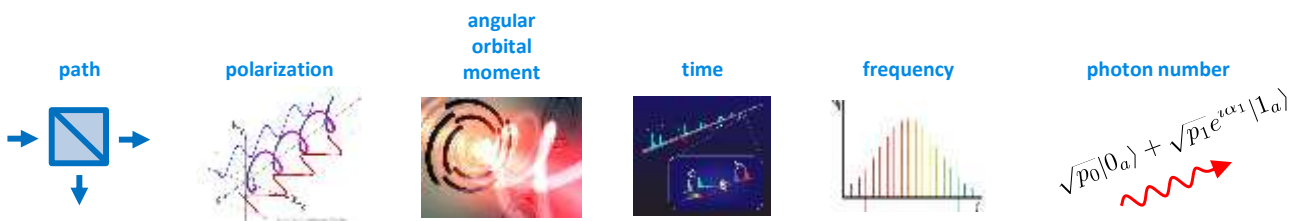


Figure 458: the various properties or observables of photons that can be used to create a qubit. You have many more solutions than the old-fashioned polarization! Compilation (cc) Olivier Ezratty, 2021.

¹⁹³⁹ See [A squeezed quantum microcomb on a chip](#) by Zijiao Yang et al, Nature Communications, August 2021 (8 pages) covered in [Researchers open a path toward quantum computing in real-world conditions](#) by Karen Walker, University of Virginia, August 2021.

¹⁹⁴⁰ See [An Intracavity Rydberg Superatom for Optical Quantum Engineering: Coherent Control, Single-Shot Detection and Optical \$\pi\$ Phase Shift](#) by Julien Vaneecloo, Sébastien Garcia and Alexei Ourjoumteev, PSL University, November 2021 (9 pages).

¹⁹⁴¹ See [Deterministic Free-Propagating Photonic Qubits with Negative Wigner Functions](#) by Valentin Magro, Julien Vaneecloo, Sébastien Garcia and Alexei Ourjoumteev, PSL University, September 2022 (10 pages).

¹⁹⁴² See [Characterization of Quantum Frequency Processors](#) by Hsuan-Hao Lu et al, DoE Oak Ridge lab, Purdue University, Arizona State University, February 2023 (14 pages).

¹⁹⁴³ This multiplicity of parameters also makes it possible to encode not only qubits but also qudits, with a greater number of states. But it is quite complex to manage and, if only to manage two-qubit quantum gates, we are happy with qubits instead of using qudits. See also [Forget qubits -scientists just built a quantum gate with qudits](#) by Kristin Houser, July 2019, which refers to [High-dimensional optical quantum logic in large operational spaces](#) by Poolad Imany et al, 2019 (10 pages). See the definition of orbital angular momentum in the glossary. It was discovered in 1992.

¹⁹⁴⁴ See [Orbital angular momentum of light and the transformation of Laguerre-Gaussian laser modes](#) by Les Allen et al, 1992 (5 pages).

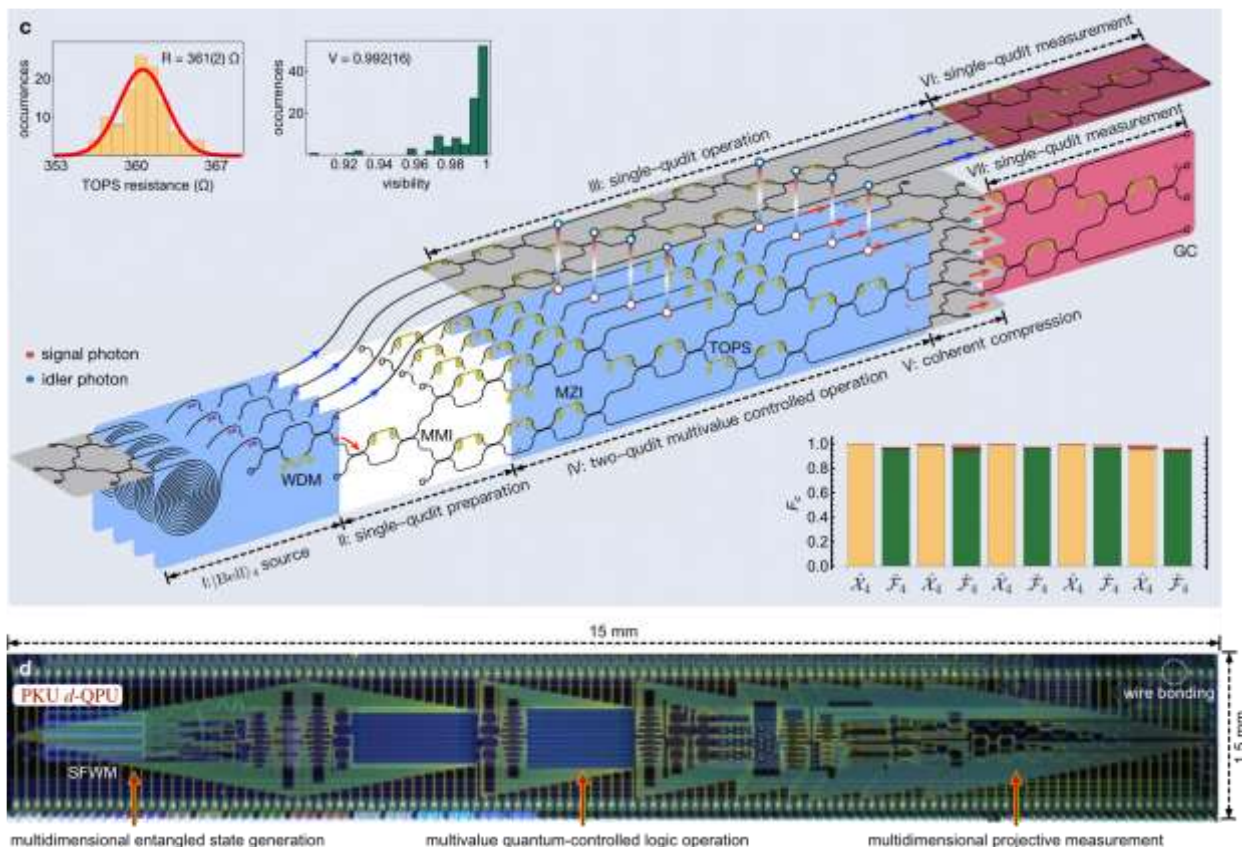


Figure 459: a ququart photons processor created in China.

Source: [A programmable qudit-based quantum processor](#) by Yulin Chi, Jeremy O'Brien et al, Nature, March 2022 (10 pages).

This potentially allows the creation of qutrits or qudits managing more than two exclusive values. Photons are "flying qubits" because they move in space and are not static or quasi-static at the macroscopic scale unlike most other types of qubits¹⁹⁴⁵.

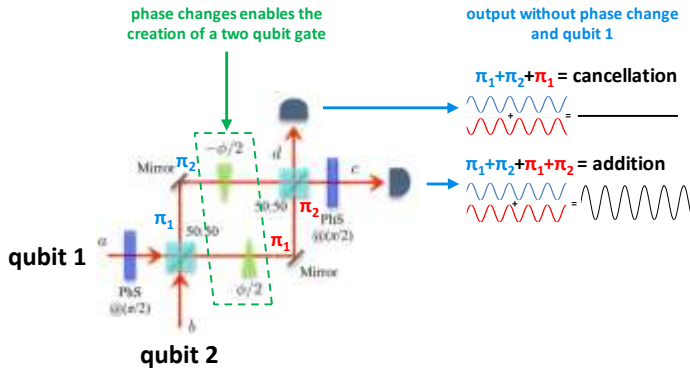
One such implementation was achieved in 2022 by a China-international team using ququarts states, which are quantum objects with four dimensions instead of the two dimensions of qubits¹⁹⁴⁶ (Figure 459). The experiment shown above in Figure 459 was implemented in a programmable silicon CMOS photonic integrated chip of 15 x 1.5 mm implementing linear optics and enhancing parallelism. It was tested with a QFT, Deutsch-Jozsa and Bernstein-Vazirani, quaternary phase estimation and factorization algorithms. The system creates four-level entangled state in an array of four integrated identical SFWM (spontaneous four-wave mixing) sources.

The photons then traverse wavelength-division multiplexing filters (WDM), Mach-Zehnder interferometers (MZI), thermal-optic phase shifters (TOPSs), multimode interferometer beamsplitters (MMI) and qudit states measurement.

¹⁹⁴⁵ The other qubits are "non-flying": spin-controlled electrons trapped in a cavity, cold atoms (which are stabilized in space) and trapped ions (which can move, but in a limited space), NV centers (cavities do not move) and superconducting circuits (which are fixed in space even if they use pairs of circulating Cooper electrons).

¹⁹⁴⁶ See [A programmable qudit-based quantum processor](#) by Yulin Chi, Jeremy O'Brien et al, Nature, March 2022 (10 pages) covered in [Scientists Make Advances in Programmable Qudit-based Quantum Processor](#) by Matt Swayne, The Quantum Insider, March 2022.

- **Single-qubit quantum gates** use simple optical circuitry, including beamsplitters, waveplates, mirrors and semi-reflective mirrors, and phase shifters¹⁹⁴⁷. For example, a Hadamard gate (H) uses a beamsplitter or waveplate, a Pauli X gate (bit flip) combines a beamsplitter and a Hadamard gate, and a Pauli Z gate (phase flip) uses a phase shifter causing a 180° phase change (π) (Figure 460).



Mach-Zehnder interferometer (MZI)
creates an interference between two photons with introducing a dephasing linked to the number of mirrors reflections (the π s) and phase changers

The implementation of various quantum logic gates using optical MZI is tabulated in Table. 3.

Quantum Logic Gate	Unitary Matrix	Relation for MZI implementation	Elements
Beam Splitter(B(θ))	$\begin{bmatrix} \cos\theta & -\sin\theta \\ \sin\theta & \cos\theta \end{bmatrix}$		
50-50 Beam Splitter(B)	$\frac{1}{\sqrt{2}} \begin{bmatrix} 1 & -1 \\ 1 & 1 \end{bmatrix}$		
Hadamard(H)	$\frac{1}{\sqrt{2}} \begin{bmatrix} 1 & 1 \\ 1 & -1 \end{bmatrix}$	H=BZ	50-50 Beam splitter
Phase flip gate (Z)	$\begin{bmatrix} 1 & 0 \\ 0 & -1 \end{bmatrix}$	Z=HB	π Phase shifter
Bit Flip gate (X)	$\begin{bmatrix} 0 & 1 \\ 1 & 0 \end{bmatrix}$	X=BH	Beam Splitter, Hadamard
T gate	$\begin{bmatrix} 1 & 0 \\ 0 & \exp(i\pi/4) \end{bmatrix}$		$\pi/4$ phase shifter
S gate	$\begin{bmatrix} 1 & 0 \\ 0 & i \end{bmatrix}$		Quarter wave plate
Pauli Y gate	$\begin{bmatrix} 0 & -i \\ i & 0 \end{bmatrix}$		
CNOT gate	$\begin{bmatrix} 1 & 0 & 0 & 0 \\ 0 & 1 & 0 & 0 \\ 0 & 0 & 1 & 0 \\ 0 & 0 & 0 & 1 \end{bmatrix}$	$(I \otimes H) \times K \times (I \otimes H)$	Kerr Media(K) Hadamard(H) Identity(I)

MZI based quantum gates

a one qubit gate can be created with introducing some dephasing in one or two of the circuits, and two qubit gate with using two entries and some dephasing. The table shows the correspondence between quantum gates and the used filters elements.

Figure 460: how a Mach-Zehnder Interferometer works. Source: [Quantum Logic Processor: A Mach Zehnder Interferometer based Approach](#) by Angik Sarkar and Ajay Patwardhan 2006 (19 pages).

- **Two-qubit quantum gates** are difficult to realize because it is not easy to have photons interact with each other, particularly when they are not perfectly indistinguishable. They use optical circuits based on beamsplitters or Mach-Zehnder interferometers with two inputs integrating phase changes on the optical paths, based on the KLM method already quoted in footnote. This does not work well when the photons are uneven, such as those coming from lasers. Namely, in only a few % of the cases. With indistinguishable photons, gates are more than 95% efficient since photons can interfere with each other. It facilitates Mach-Zehnder interferometry operations. These sources have the additional advantage of being very bright, which allows them to multiply the incoming photons and then to pass through many quantum gates. There are also solutions based on cavities. Research is also active on the creation of nonlinearities to improve the reliability of these quantum gates¹⁹⁴⁸. Ideally, nonlinear separating cubes should be used¹⁹⁴⁹.

But loop-based setting using only linear optics are also proposed^{1950 1951}.

¹⁹⁴⁷ This is based on the KLM scheme proposed in [A scheme for efficient quantum computation with linear optics](#) by Emanuel Knill, Raymond Laflamme and Gerard Milburn, 2001 (7 pages).

¹⁹⁴⁸ See [Quantum Computing With Graphene Plasmons](#), May 2019 which refers to [Quantum computing with graphene plasmons](#) by Alonso Calafell et al, 2019. This is the creation of two-qubit quantum gates with graphene-based nonlinear structures. It comes from the University of Vienna in Austria and from Spanish and Serbian laboratories. As well as [Researchers see path to quantum computing at room temperature](#) by Army Research Laboratory, May 2020 which refers to [Controlled-Phase Gate Using Dynamically Coupled Cavities and Optical Nonlinearities](#) by Mikkel Heuck, Kurt Jacobs and Dirk Englund, 2020 (5 pages).

¹⁹⁴⁹ It is a function that can be realized with Quandel's single photon generation component, diverted from its original use. See also [Researchers see path to quantum computing at room temperature](#), May 2020 which refers to [Controlled-phase Gate using Dynamically Coupled Cavities and Optical Nonlinearities](#) by Mikkel Heuck, September 2019 (5 pages) and discusses a nonlinear cavity optical quantum gate technique.

¹⁹⁵⁰ See [Universal multi-mode linear optical quantum operation in the time domain](#) by Kazuma Yonezu et al, University of Tokyo, October 2022 (11 pages).

¹⁹⁵¹ See [Deterministic entangling gates with nonlinear quantum photonic interferometers](#) by Francesco Scala et al, June 2023 (22 pages).

How about photonic gates execution times? It must be fast since photons traverse optical devices at nearly the speed of light in vacuum. Traversing a one meter long series of optical instruments would last only 3 ns. If the circuit is nanophotonic based, we'll get into the cm realm and reach tens of pico-seconds. But that's not the right way to evaluate the speed of quantum computing here, particularly when dealing with non-deterministic photon sources where computing has to be repeated many times. Then, you may need to take into account the speed of the electronics that define the various quantum gates along the photon route and we may end-up adding milliseconds.

- **Qubit readout** uses single photon detectors that also capture their quantum state. This detection is still imperfect. Several single-photon detection technologies are competing: SPAD (avalanche photodiodes, which detect photon occurrences but not photon number)¹⁹⁵², transition edge sensor (TES, which can detect photon numbers) and Superconducting Nanowire SPDs (SNSPDs, which also detect photon numbers, and can be arranged in arrays¹⁹⁵³). Fully integrated SNSPDs are based on GaAs, Si and Si₃N₄ waveguides. In order to limit the dark count phenomenon coming from thermal effects, these SNSPDs are usually cooled between 800 mK and 3K which requires a dilution refrigeration system^{1954 1955}.

NbTiN-based SNSPDs could work with higher-temperature cooling, between 2.5K to 7K¹⁹⁵⁶ with some records reaching 25K¹⁹⁵⁷. One goal is to integrate these photon detectors directly in photonic computing circuits. Other detectors are specialized for analyzing continuous variables qubits, like homodyne and heterodyne detectors. There are even concepts of single photon detectors that can also detect their frequency with high precision¹⁹⁵⁸. In the continuous variable types of qubits, qubit readout uses homodyne detectors to detect the photon quadrature such as optical parametric amplifier (OPA)¹⁹⁵⁹. Some SNSPDs can still support homodyne measurement to support continuous variable photon qubits¹⁹⁶⁰.

Others are experimenting photon detectors operating at a relatively hot temperature of 20K, using cuprates who are known for their relatively high superconducting temperature¹⁹⁶¹.

¹⁹⁵² See recent progress with SPADs in [Low-noise photon counting above 100 × 106 counts per second with a high-efficiency reach-through single-photon avalanche diode system](#) by Michael A. Wayne et al, NIST, December 2020 (6 pages).

¹⁹⁵³ See [GHz detection rates and dynamic photon-number resolution with superconducting nanowire arrays](#) by Giovanni V. Resta et al, ID Quantique, March 2023 (26 pages).

¹⁹⁵⁴ See [The potential and challenges of time resolved single-photon detection based on current-carrying superconducting nanowires](#) by Hengbin Zhang et al, October 2019 (19 pages) and [Superconducting nanowire single-photon detectors for quantum information](#) by Lixing You, June 2020 (20 pages). Dark counts are detected photons coming from the environment due to thermal or tunneling effects.

¹⁹⁵⁵ See [Optimal Amplitude Multiplexing of a Series of Superconducting Nanowire Single Photon Detectors](#) by Fabio Chiarello et al, March 2023 (6 pages).

¹⁹⁵⁶ See [Superconducting nanowire single photon detectors operating at temperature from 4 to 7 K](#) by Ronan Gourgues et al, Optics Express, 2019 (9 pages).

¹⁹⁵⁷ See [Superconducting single-photon detectors get hot](#) by Jin Chang and Iman Esmail Zadeh, Nature Nanotechnology, March 2023

¹⁹⁵⁸ See [Nanoscale Architecture for Frequency-Resolving Single-Photon Detectors](#) by Steve M. Young et al, Sandia Labs, May 2022 (20 pages).

¹⁹⁵⁹ See [Towards a multi-core ultra-fast optical quantum processor: 43-GHz bandwidth real-time amplitude measurement of 5-dB squeezed light using modularized optical parametric amplifier with 5G technology](#) by Asuka Inoue et al, May 2022 (18 pages).

¹⁹⁶⁰ See [Low-noise Balanced Homodyne Detection with Superconducting Nanowire Single-Photon Detectors](#) by Maximilian Protte et al, Paderborn University, July 2023 (5 pages).

¹⁹⁶¹ See [Two-dimensional cuprate nanodetector with single photon sensitivity at T = 20 K](#) by Rafael Luque Merino, Dmitri K. Efetov et al, August 2022 (27 pages). I also found out [Graphene-based Josephson junction single photon detector](#) by Evan D. Walsh, Thomas A. Ohki, Dirk Englund et al, September 2017 (12 pages) but it seems not applicable for photonic qubit readout. It works at 25 mK.

There are also variants of SNSPD named SWSPD (Superconducting Wide-Strip Photon Detectors) with higher efficiency and operating in the convenient 1,550 nm telecom wavelength range¹⁹⁶².

From a physical point of view, these items are classical photonic components: single and identical photon sources, light guides, optical delay lines (optical fibers or voltage-controlled Pockels cells), Mach-Zehnder interferometers, beam splitters (splitters, which divide an optical beam into two beams, generally identical), birefringent filters (which have two different refractive indices), phase shifters and single photon detectors¹⁹⁶³ (Figure 461).

To conduct experiments, these discrete and very affordable components are installed on carefully calibrated optical tables of a few square meters with lots of instruments and photons that circulate largely in the free space of a darkened room. Fortunately, these optical components are miniaturizable on semiconductor integrated circuits. This is part of the vast field of nanophotonics. Nanophotonics components are etched with densities between 220 nm and 3 μm^{1964 1965}.

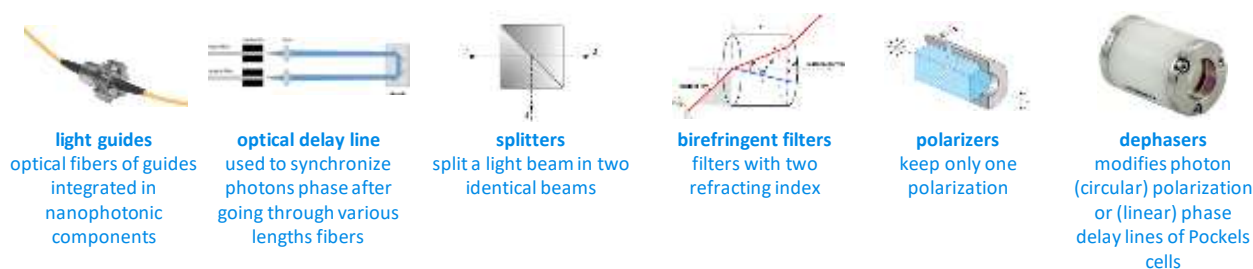


Figure 461: the various optical tools to control light in a quantum processor. These are made for experiments and can be miniaturized in nanophotonic circuits. Compilation (cc) Olivier Ezratty, 2021.

In nanophotonics, quantum gates are dynamically programmed by the conditional routing of photons in optical circuits and/or with their modification (phase, polarization, frequency, ...).

These circuits are often etched on CMOS (silicon) or III/V (germanium and also GaAs) components. These components could be assembled in a modular way as shown in the functional diagrams in Figure 462. Many semiconductor fabs in the world are helping photonicians design and prototype nanophotonic circuits to support photon qubits. We'll mention here only a few of them. Many fab technologies are investigated with classical silicon-based CMOS, hybrid CMOS with silicon nitride (SiN) and lithium niobate (LiNbO₃)¹⁹⁶⁶, III/V materials (GaAs¹⁹⁶⁷, InP, ...), etc¹⁹⁶⁸.

¹⁹⁶² See [Superconducting wide strip photon detector with high critical current bank structure](#) by Masahiro Yabuno et al, NIST, Optica Quantum, October 2023 (9 pages).

¹⁹⁶³ This is well explained in [Silicon photonic quantum computing](#) by Syrus Ziai, PsiQuantum, 2018 (72 slides) as well as in [Large-scale quantum photonic circuits in silicon](#), by Nicholas C. Harris, Dirk Englund et al, Nanophotonics, 2016 (13 pages).

¹⁹⁶⁴ See for example the work of InPhyNi discussed in [High-quality photonic entanglement based on a silicon chip](#) by Dorian Oser, Sébastien Tanzilli et al, 2020 (9 pages).

¹⁹⁶⁵ See the review [The potential and global outlook of integrated photonics for quantum technologies](#) by Emanuele Pelucchi, Dirk Englund, Jian-Wei Pan, Fabio Sciarrino, Christine Silberhorn et al, Nature Review Physics, December 2021 (no open access).

¹⁹⁶⁶ See [High-speed thin-film lithium niobate quantum processor driven by a solid-state quantum emitter](#) by Patrick I. Sund et al, NBI, CeNTech, Science Advances, May 2023 (9 pages).

¹⁹⁶⁷ See [Expanding the Quantum Photonic Toolbox in AlGaAsOI](#) by Joshua E. Castro et al, May 2022 (9 pages). They implement non linear elements, edge couplers, waveguide crossings, couplers, and MZIs in Aluminum gallium arsenide-on-insulator (AlGaAsOI).

¹⁹⁶⁸ See the review paper [Roadmap on integrated quantum photonics](#) by Galan Moody, Jacqueline Romero, Eleni Diamanti et al, August 2021 (108 pages).

In France, **CEA-Leti** is also building an integrated silicon photonic qubits platform including single photons source, phase shifters and superconducting nanowire single-photon detectors (SNSPD) or CdHgTe avalanche photodiodes (APD), working at 2.5-4K that is compatible with single photon detectors. They are initially targeting secured QKD based telecommunications.

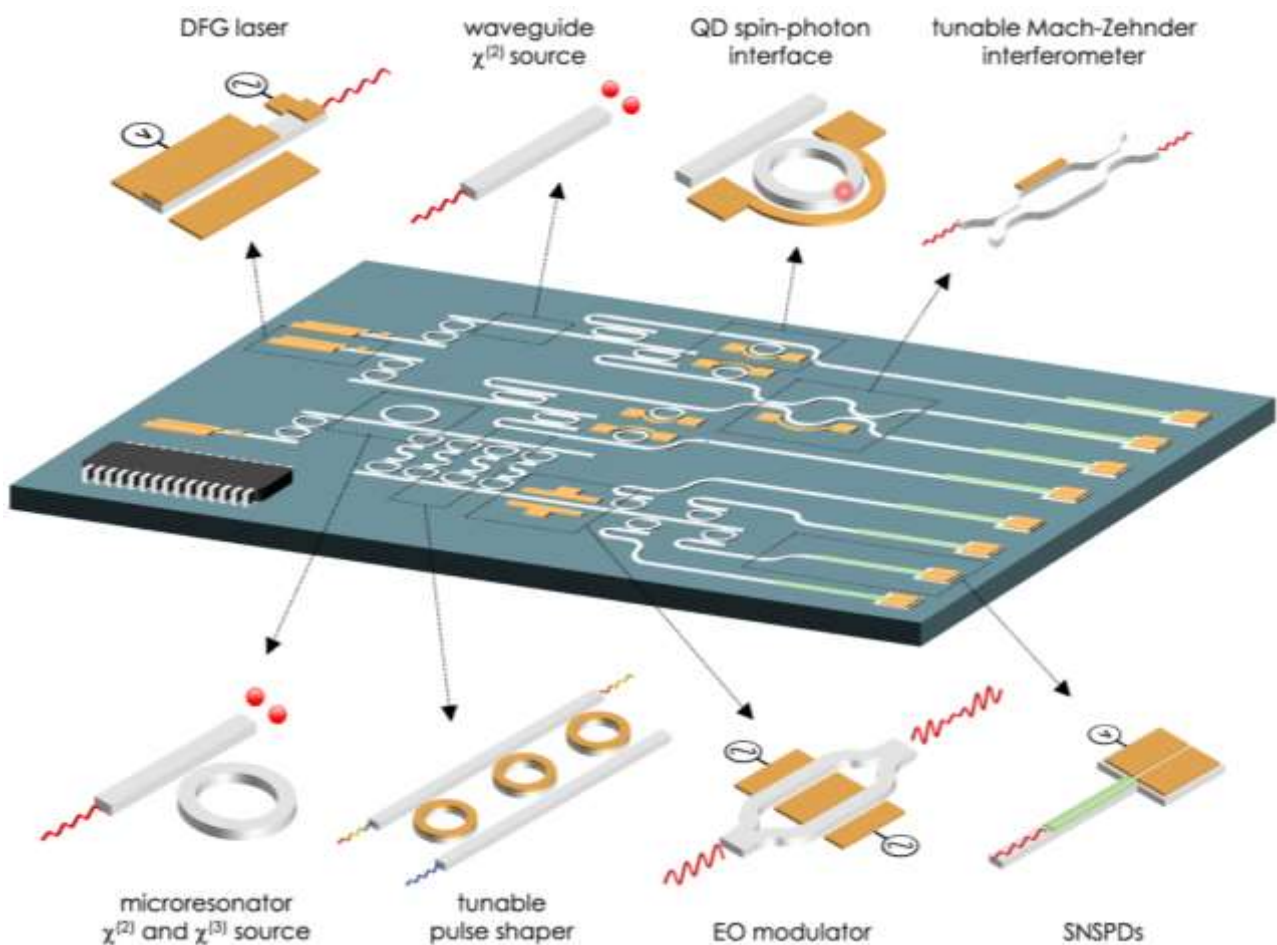


Figure 462: an examples of photonic functions embedded in a nanophotonic circuit, here in GaAs. Source: [Nonlinear integrated quantum photonics with AlGaAs](#) by F. Baboux, G. Moody and Sara Ducci, *Optica*, November 2022-July 2023 (15 pages).

Ultimately, a photon qubits quantum computer would consolidate three key components as shown in Figure 463 and Figure 464: a single photon generator, integrated photonic circuits and single photon detectors. The first and last ones are integrated with a cryogenic system operating at about 10K and 2K-4K respectively. But it seems also possible to integrate photon sources and detectors in a single photonic chip^{1969 1970}.

The most active countries in the field seem to be China, the UK (particularly at the Universities of Oxford, Bristol, Cambridge and Southampton)¹⁹⁷¹, France (C2N, LKB, ...), Italy¹⁹⁷², Germany (Universities of Stuttgart and Paderborn), Austria, Australia, Japan and of course the USA.

¹⁹⁶⁹ See [Integrated nanophotonics for the development of fully functional quantum circuits based on on-demand single-photon emitters](#) by S. Rodt and S. Reitzenstein, *APL Photonics*, December 2020 (14 pages).

¹⁹⁷⁰ See [4 ways to put lasers on silicon](#) by Roel Baets, Joris, Van Campenhout, Bernardette Kunert and Gunther Roelkens, *IEEE Spectrum*, April 2023.

¹⁹⁷¹ According to [Quantum Age technological opportunities](#) from the UK Government Office of Science in 2016 (64 pages).

¹⁹⁷² Fabio Sciarrino of La Sapienza University in Rome, carried out in 2013 a sampling of bosons with a chip with 13 input ports and 13 output ports, with three photons. See [Efficient experimental validation of photonic boson sampling against the uniform distribution](#), 2013 (7 pages).

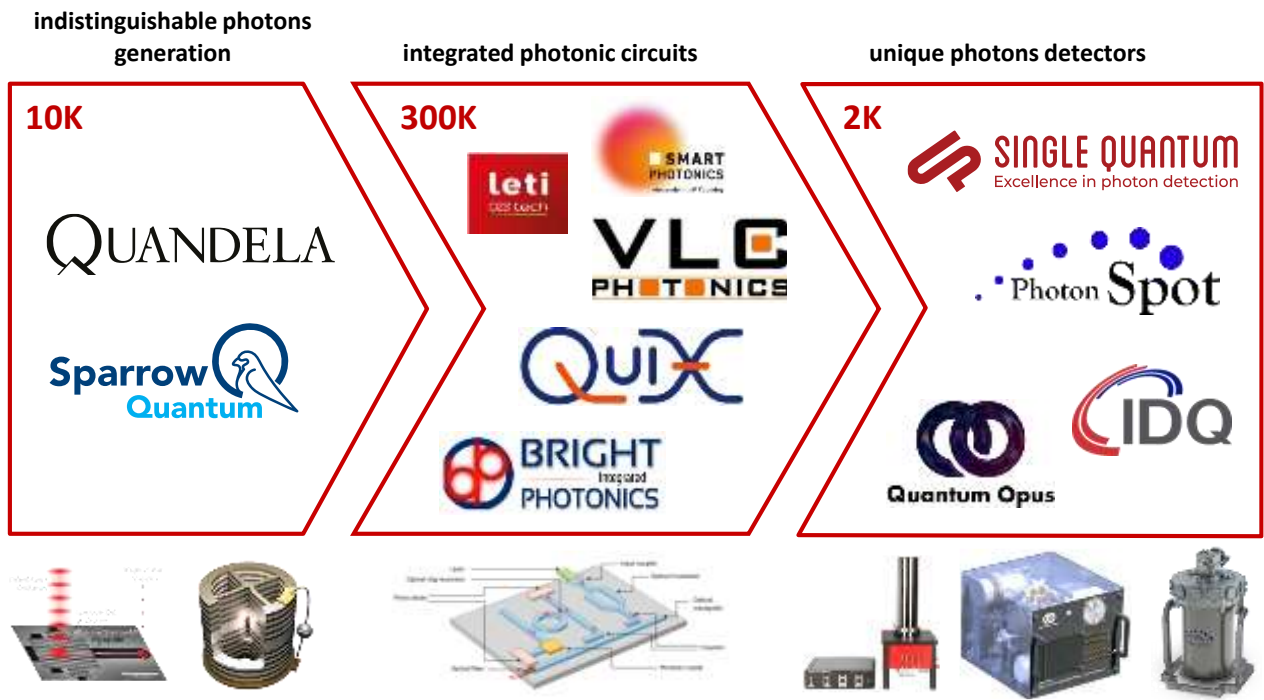


Figure 463: the key components of a photonic quantum computer: quality photon sources, preferably deterministic, nanophotonic circuits for processing, and photon detectors for readout. Source: adapted from *Photonic quantum bits* by Pascale Senellart, June 2019 (31 slides) in slide 11. (cc) Olivier Ezratty, 2023.

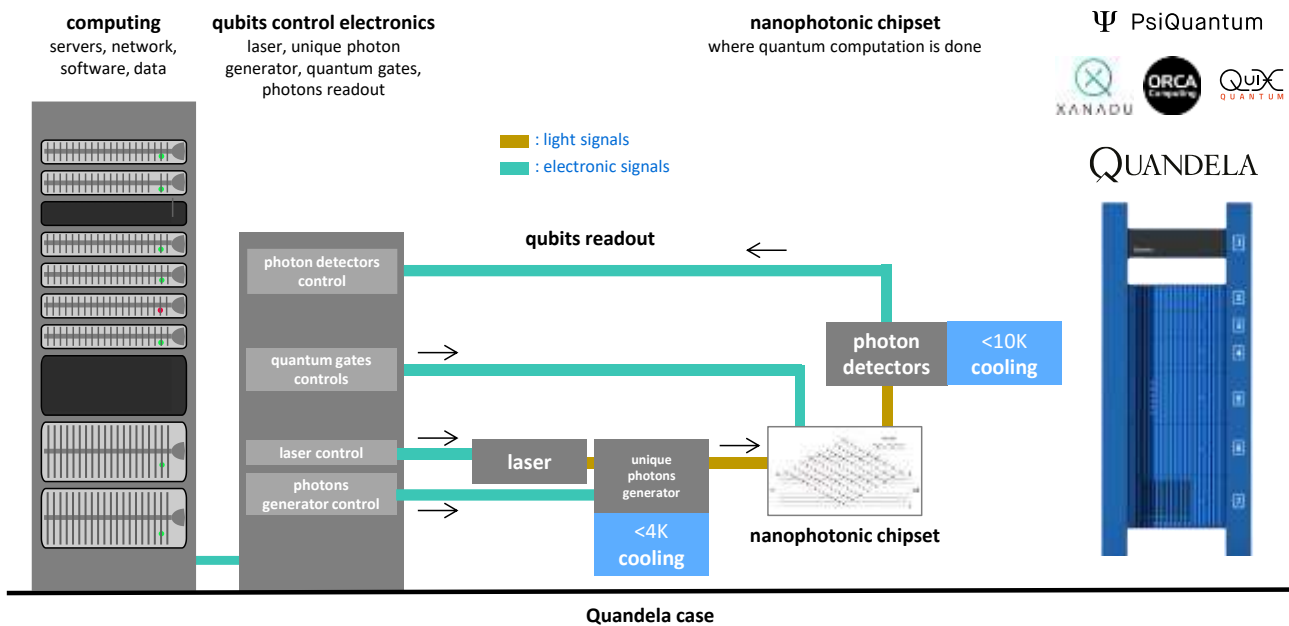


Figure 464: typical architecture of a photon qubits quantum computer. (cc) Olivier Ezratty, 2022-2023.

Photon qubits are the specialty of some startups like **PsiQuantum**, **Orca Computing**, **Tundra Systems Global**, **QuiX**, **Quandela**, **Nu Quantum**, and **Xanadu**.

Boson sampling

The idea of boson sampling came from **Scott Aaronson** and **Alex Arkhipov** from the MIT in a seminal paper published in 2010¹⁹⁷³. They devised a linear optics-based experiment that would be impossible to easily emulate on a classical supercomputer¹⁹⁷⁴.

Boson sampling is about solving a problem of sampling the probability distributions of identical and indistinguishable photons being mixed in an interferometer and reaching photon detectors. This physical process is impossible to emulate above a certain threshold, which generates yet another so-called "quantum supremacy" or "advantage". It becomes an "advantage" only if the system is able to solve a particular problem with some input data and useful output data.

A classical emulation of a boson sampling experiment requires extremely heavy matrix computing: the evaluation of square matrix permanents even more complicated computing¹⁹⁷⁵.

This sits in the "#P difficult" problem class of the complexity theories zoo¹⁹⁷⁶. The verification of the obtained result can't even be carried out by a classical computer¹⁹⁷⁷.

Boson sampling is the quantum and photonic analogue of the famous **Galton** plate experiment where balls cross rows of nails in a random way and end up in columns, with a Gaussian distribution (Figure 465). This experiment is based on various probability concepts: convergence of a binomial distribution law towards a normal or Gaussian distribution, Moivre-Laplace theorem, etc. In the photon-based experiment, photons are injected into a series of interferometers combining them with their neighbor in a random way. On the other hand, the distribution at the end does not follow a Gaussian curve. It depends on the photons being sent upstream.

The appropriateness of the boson sampling style exercise is questionable. It implements a physical phenomenon with photons that is difficult to emulate in a classical way¹⁹⁷⁸. However, it is not strictly a form of calculation with some problem input data. There is not even a real notion of qubits, quantum gates and programming, except in the choice of the photons we send into the system.

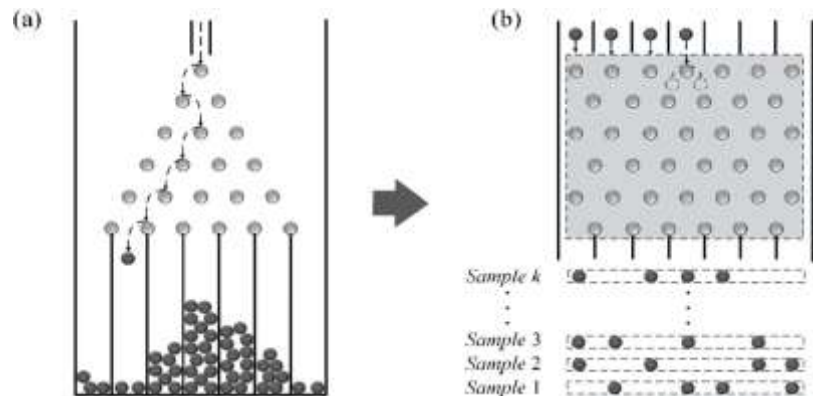


Figure 465: the typical Galton plate experiment that inspires Boson sampling. Source: [Quantum Boson-Sampling Machine](#) by Yong Liu et al, 2015.

¹⁹⁷³ See [The computational Complexity of Linear Optics](#) by Alex Arkhipov and Scott Aaronson, 2010 (94 pages).

¹⁹⁷⁴ In quantum computing, we rely on only one type of boson: the photon. The other bosons are elementary particles such as gluons or Higgs bosons that can only be observed in particle accelerators. There are also composite particles such as the Cooper pairs (double electron) which are at the origin of superconducting currents. But when we talk about boson sampling, we always mean "photon".

¹⁹⁷⁵ If you want to explore the question, see for example [Lecture 3: Boson sampling](#) by Fabio Sciarrino, University of Rome, (63 slides) and [Experimental boson sampling with integrated photonics](#) (33 slides) by the same author who describes laser-based techniques for etching integrated photonic components. As well as [Permanents and boson sampling](#) by Stefan Scheel, University of Rostock, 2018 (21 slides). As for the definition of the notion of permanent in [Wikipedia](#), it uses notions and notations of linear algebra that are not even explained. The permanent of a matrix is a variant of its determinant. If the classical resolution of sampling requires the computation of matrix permanents, its resolution by linear optics system does not allow the computation of matrix permanents.

¹⁹⁷⁶ #P is the class of function problems that counts the number of solutions of NP problems.

¹⁹⁷⁷ In 2018, a Chinese team carried out a numerical simulation of 50 photon boson sampling using 320,000 processors from the Tianhe-2 supercomputer. See [A Benchmark Test of Boson Sampling on Tianhe-2 Supercomputer](#), 2018 (24 pages). With the 20 photons and 60 modes of the Chinese experiment published in October 2019, a supercomputer is no longer able to follow.

¹⁹⁷⁸ But this is a valid reality for the simulation of many complex physical phenomena, such as the folding of a protein or the functioning of a living cell, except that these remain in the realm of the living and are not simulated in a machine.

In the first boson sampling experiments, the used optical components were all passive and static, except for the photon generators and detectors¹⁹⁷⁹. The experiment generates additive and subtractive photon interferences and superpositions of quantum states¹⁹⁸⁰.

Chinese researchers are particularly active in the field¹⁹⁸¹, but they are not alone. Xanadu (Canada), and Fabio Sciarrino in Italy, Australian and French teams have also been conducting interesting boson sampling experiments for a while, using Fock states boson sampling settings¹⁹⁸².

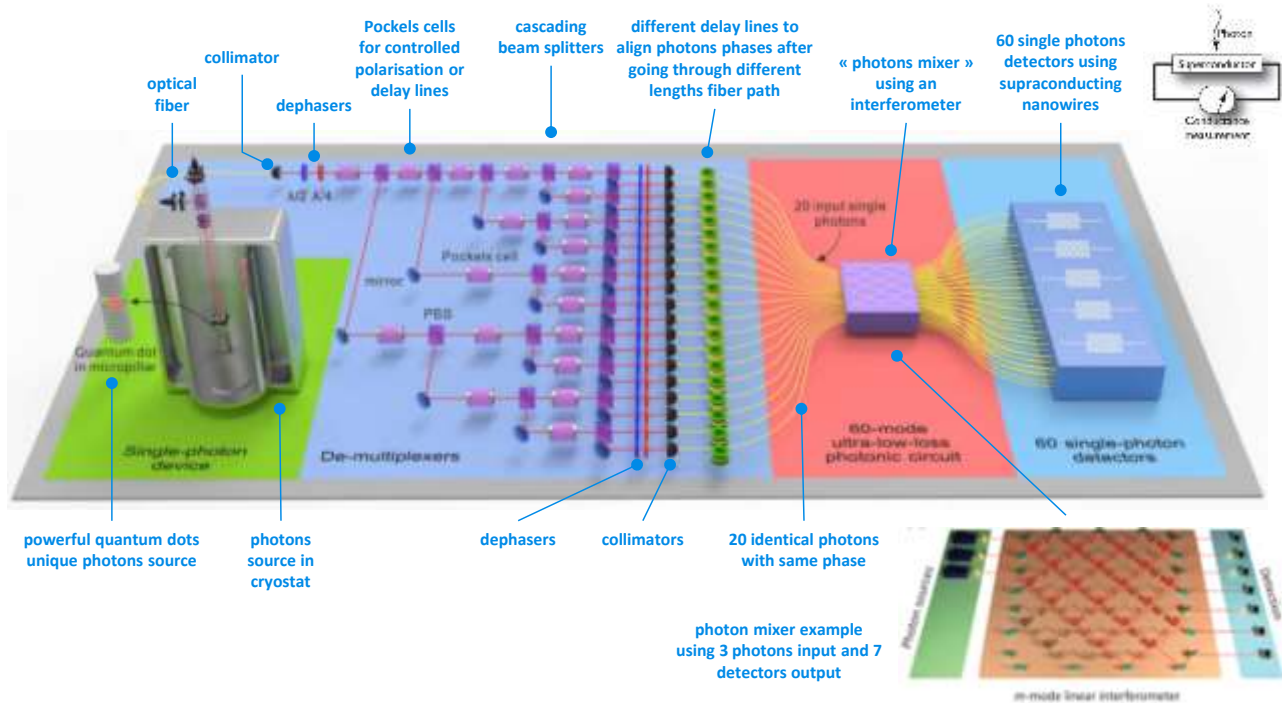


Figure 466: one of the first Boson sampling experiment made in China, in 2019, with 20 photon modes. Source: [Boson sampling with 20 input photons in 60-mode interferometers at \$10^{14}\$ state spaces](#) by Hui Wang et al, October 2019 (23 pages).

In June 2019, the **Hefei** laboratory created a boson sampling using six photons with three degrees of freedom, their traveled path, polarization and orbital angular momentum¹⁹⁸³. It had a high gate error rate of 29%. In October 2019, they upgraded the feat to 20 photons with an experiment presented as reaching quantum supremacy, at the time of Google Sycamore supremacy announcement¹⁹⁸⁴. In this experiment described in Figure 466, 20 indistinguishable photons were sent in a series of splitters and ended up in 60 photon detectors. The output Hilbert space was limited to 14 detectors, with a size of $3.7 \cdot 10^{14}$ or 2^{48} . With the 60 activated detectors, this space was to reach a size of 60^{20} or 2^{118} .

¹⁹⁷⁹ See [An introduction to boson-sampling](#) by Jonathan Dowling et al, 2014 (13 pages) which describes well the issues involved in conducting boson sampling.

¹⁹⁸⁰ See the animation [Boson Sampling with Integrated Photonics](#), 2015 (3mn) which describes the path of photons in a boson sampling experiment as well as [Photonic implementation of boson sampling: a review](#) by Fabio Sciarrino, 2019 (14 pages) which describes in detail this kind of experiment.

¹⁹⁸¹ See [Chinese researchers on the road to the 'ultimate' quantum processor?](#) by Bruno Cormier, September 2018 which points to [Building Quantum Computers With Photons Silicon chip creates two-qubit processor](#) by Neil Savage, September 2018 which discusses the creation of a two-qubit quantum processor. The original article is [Large-scale silicon quantum photonics implementing arbitrary two-qubit processing](#), September 2018 (23 pages). The researchers involved were Chinese, English and Australian.

¹⁹⁸² See [Boson Sampling with single-photon Fock states from a bright solid-state source](#) by J. C. Loredo, M. A. Broome, Paul Hilaire, O. Gazzano, I. Sagnes, Aristide Lemaitre, M. P. Almeida, Pascale Senellart, and Andrew G. White, 2017 (11 pages), on Fock-state boson sampling.

¹⁹⁸³ See [18-Qubit Entanglement with Six Photons Three Degrees of Freedom](#) by Xi-Lin Wang et al, June 2019 (14 pages).

¹⁹⁸⁴ See [Boson sampling with 20 input photons in 60-mode interferometers at \$10^{14}\$ state spaces](#) by Hui Wang et al, October 2019 (23 pages).

The size of Hilbert's space of such a device is evaluated with the size of the Fock space of M modes occupied by N photons. This would give a binomial space $\binom{M+N-1}{M}$ so $\binom{79}{60}$ which is equal in size to $\frac{79!}{60! \cdot 19!}$ ¹⁹⁸⁵.

The researchers in China indicated that they could use several hundred detectors in output and use some photons double encoding using polarization and spatial encoding to multiply the power of their system and thus make it able to create a NISQ (noisy intermediate scale quantum computer) system.

This represents the number of incoming photon detectors at the power of the incoming photon number. The previous record was 5 photons over 16 modes and the sampling was verifiable on a classical computer whereas with these 20 photons and 60 modes, it was no longer possible. The photon generator was realized with quantum dots in gallium and indium arsenide, placed in a 4K¹⁹⁸⁶ cryostat. The photon mixer used 396 beam splitters and 108 mirrors (Figure 467). For the experiment to work, one photon must arrive at the same time in all the inputs of the photon mixer.

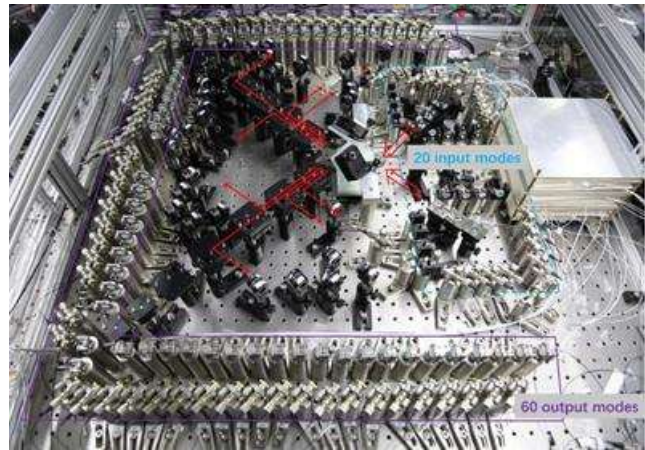


Figure 467: optics table of the 20 photons/60 modes China experiment.

The corresponding probability is very low. They used active demultiplexers with Pockels cells to demultiplex and direct the photons.

While the first boson sampling experiments did not show any usefulness, this has changed progressively. It was initially thought that boson sampling could eventually lead to applications in homomorphic encryption and blind computing¹⁹⁸⁷. Some algorithms also exist for the simulation of molecular vibration spectra¹⁹⁸⁸. In 2020, a team in China conducted an experiment similar to boson sampling to play a variant of the Go game¹⁹⁸⁹.

In 2020, another China team used an optical quantum calculator to solve a useful problem, the subset-sum problem, which is complete NP. The system shown in Figure 468 uses a nanophotonic chip. The problem was to determine, apart from a set of signed integers, whether it is possible to add a subset of them together to obtain a given integer¹⁹⁹⁰. The system used a laser as a source of photons. The benchmark was realized with $N=4$ integers. With some extrapolation, their system was to beat all other known methods of solving this kind of problem.

¹⁹⁸⁵ Source: [Binomial coefficient](#), Wikipedia.

¹⁹⁸⁶ The photon source would come from a German laboratory located in Würzburg, Bavaria. It is largely inspired by the reference work in the field of Pascale Senellart's team from the CNRS C2N.

¹⁹⁸⁷ Seen in [Introduction to boson-sampling](#) by Peter Rohde, 2014 (34 minutes) which refers to [A scheme for efficient quantum computation with linear optics](#) by Emanuel Knill, Raymond Laflamme and Gerard Milburn, 2001 (7 pages) which theorized that quantum computation based on linear optics was plausible. We owe them the KLM scheme or protocol (their initials), a linear optics quantum computing (LOQC) programming model that has the disadvantage of being very heavy in terms of the number of hardware devices.

¹⁹⁸⁸ See [Boson sampling for molecular vibronic spectra](#) by Joonsuk Huh, Alán Aspuru-Guzik et al, 2014 (7 pages) and [Vibronic Boson Sampling: Generalized Gaussian Boson Sampling for Molecular Vibronic Spectra at Finite Temperature](#) by Joonsuk Huh et al, 2017 (10 pages).

¹⁹⁸⁹ See [Quantum Go Machine](#) by Lu-Feng Qiao et al, July 2020 (16 pages).

¹⁹⁹⁰ See [Photonic computer solves the subset sum problem](#), February 2020 which points to [A scalable photonic computer solving the subset sum problem](#) by Xiao-Yun Xu et al, January 2020 (8 pages). See also [Supplementary Materials for A scalable photonic computer solving the subset sum problem](#) (7 pages).

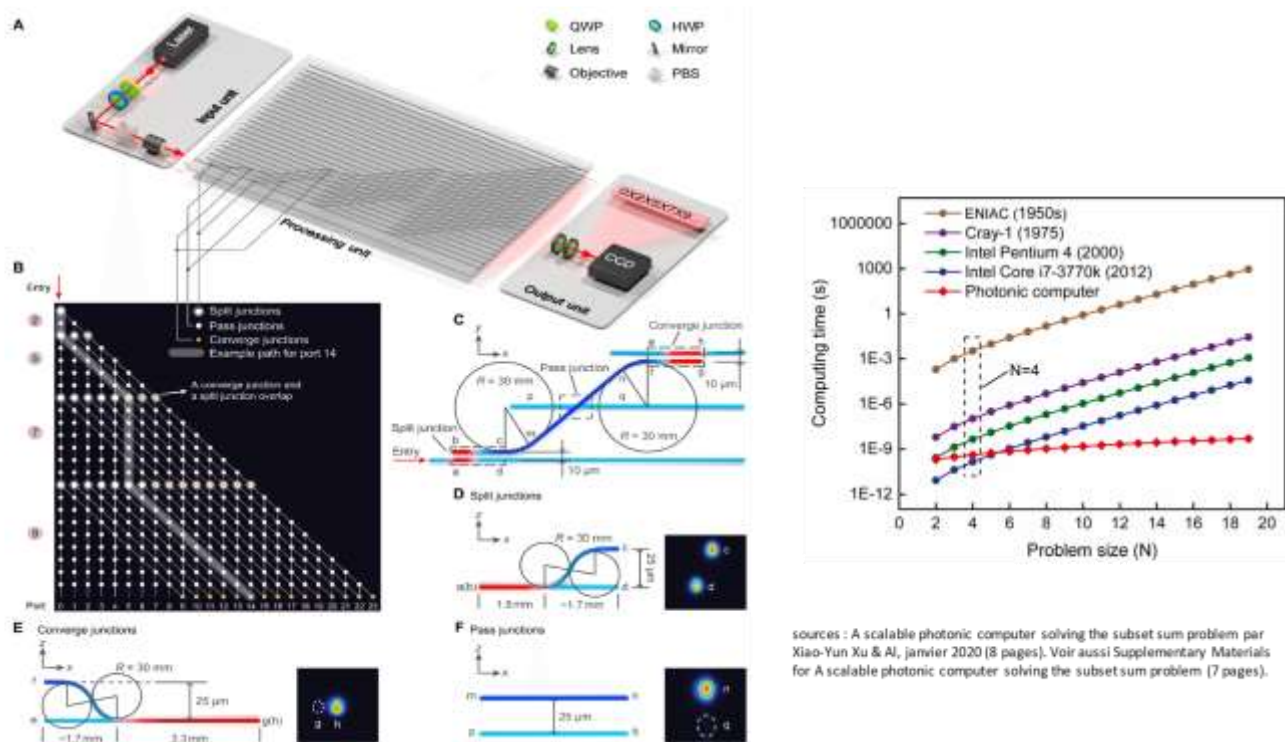


Figure 468: a first optical calculator to solve a useful problem created in 2020.

Source: [A scalable photonic computer solving the subset sum problem](#) by Xiao-Yun Xu et al, January 2020 (8 pages).

Jiuzhang 1.0 was a **gaussian boson sampler** (GBS) setup implemented in December 2020 with 70 photons modes¹⁹⁹¹. The experiment was even more impressive than the previous ones and the publicized quantum advantage reached new heights. The system, shown in Figure 469, was not more programmable than the previous ones. So, any computing advantage claim was still dubious.

Late 2020, a competing Chinese team implemented another form of boson sampling using “membosonsampling” for which an emulation requires even more complicated Haar-random unitary matrix¹⁹⁹². But it was not programmable.

Jiuzhang 2.0 came in June 2021 and was a somewhat programmable GBS, ramping it up to 113 detection events extracted from 144 photon modes circuit shown in Figure 470. The input squeezed photons are phase programmable before they enter the fixed part of the system in the interferometer that implements random unitary transformations. The experimenter still worked on some real-world algorithms and benchmarks to demonstrate some sort of quantum computing advantage¹⁹⁹³. It was finally presented in 2023, with using a 50 single mode squeezed states input to solve two graph problems, the Max-Haf problem and the dense k-subgraph problem¹⁹⁹⁴. However, the research team wrote that it was still unsure whether the GBS could yield a real quantum advantage compared to improved classical and quantum inspired algorithms. Also, like in many such advantage claims, the GBS advantage depends on the properties of the input graphs.

¹⁹⁹¹ See [Chinese Scientists Begin Climb Toward Universal Quantum Computer](#) by Matt Swayne, December 2020, [Chinese scientists say they’ve achieved a quantum computing breakthrough](#) by Shiyin Chen et al, December 2020 and [Quantum computational advantage using photons](#) by Han-Sen Zhong et al, December 2020 (23 pages) and the [supplemental materials](#) (64 pages). See [Benchmarking 50-Photon Gaussian Boson Sampling on the Sunway TaihuLight](#) by Yuxuan Li et al, 2020 (12 pages) for the classical emulation on classical supercomputers.

¹⁹⁹² See [Quantum Advantage with Timestamp Membosonsampling](#) by Jun Gao, December 2020 (30 pages).

¹⁹⁹³ See [Phase-Programmable Gaussian Boson Sampling Using Stimulated Squeezed Light](#) by Han-Sen Zhong, Chao-Yang Lu, Jian-Wei Pan et al, June 2021 (9 pages).

¹⁹⁹⁴ See [Solving Graph Problems Using Gaussian Boson Sampling](#) by Yu-Hao Deng et al, February 2023 (7 pages).

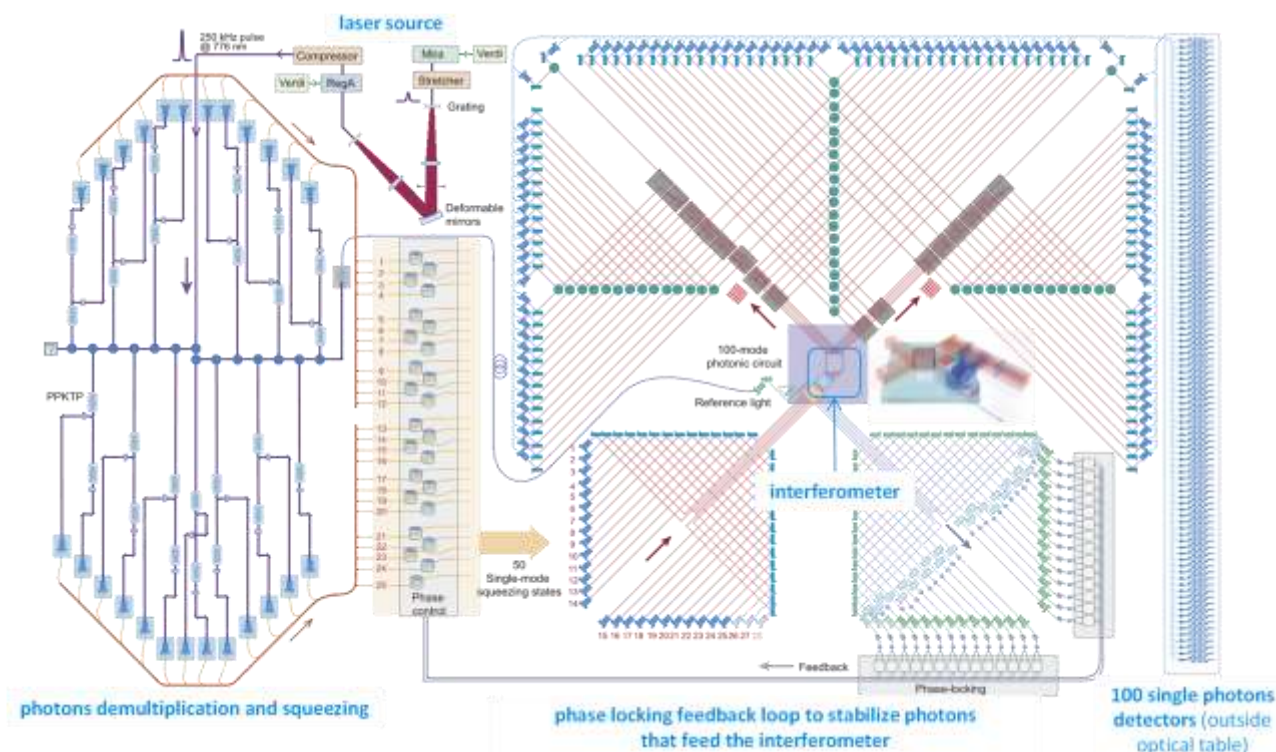


Figure 469: a 2020 generation China boson sampling experiment with up to 70 simultaneous photon modes. Source: [A scalable photonic computer solving the subset sum problem](#) by Xiao-Yun Xu et al, January 2020 (8 pages).

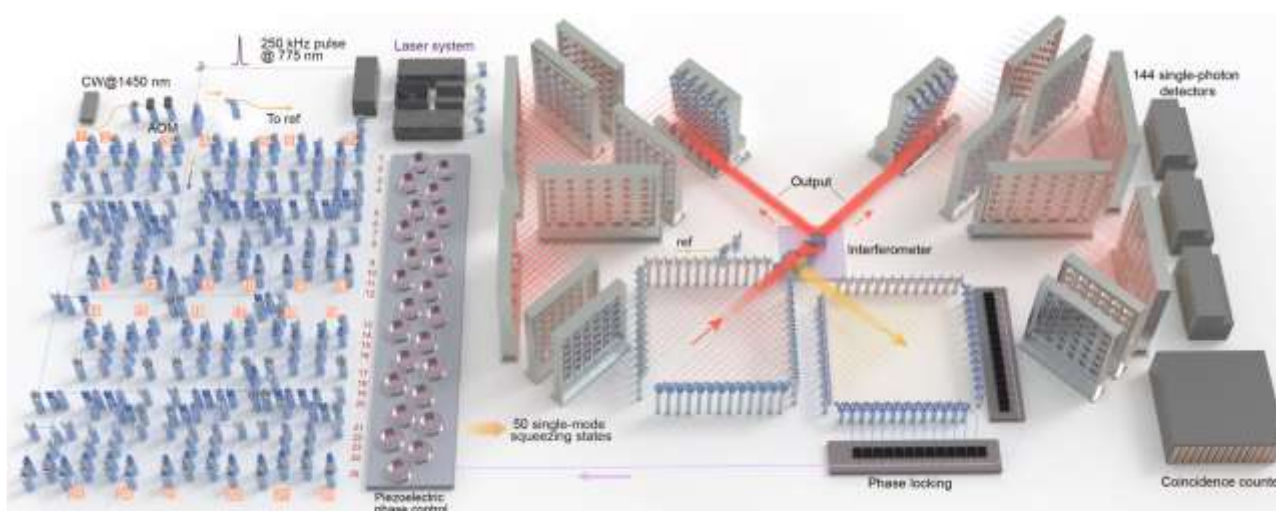


Figure 470: the latest Boson sampling experiment achieved in China in 2021 with 144 photon modes. Source: [Phase-Programmable Gaussian Boson Sampling Using Stimulated Squeezed Light](#) by Han-Sen Zhong, Chao-Yang Lu, Jian-Wei Pan et al, June 2021 (9 pages).

Jiuzhang 3.0 was introduced in 2023 and could detect photon numbers at the output with up to 255 click events and provide better performance¹⁹⁹⁵. The team said that an Aurora Frontier supercomputer would take about 600 years compared to 1.27 μ s to produce a sample, with an extreme 3.1×10^{10} years to generate the hardest sample from the experiment which used temporal spatial demultiplexing ala Xanadu. It was however not linked to some practical use case and the interferometer didn't seem to be anymore programmable than the one in Jiuzhang 2.0. Future experiments with some input data and a programmable interferometer may change that.

¹⁹⁹⁵ See [Gaussian Boson Sampling with Pseudo-Photon-Number Resolving Detectors and Quantum Computational Advantage](#) by Yu-Hao Deng et al, China, PRL, April-October 2023 (6 pages).

In 2022, **Fabio Sciarrino** in Italy also demonstrated that it was possible to create a programmable interferometer in a boson sampler^{1996 1997}.

In 2022, **Xanadu** did create a programmable GBS using some simpler time-bin multiplexing. It was even made available in the cloud but with caveats we'll describe in the photonic qubits vendor section. It could be used to solve dense subgraph identification problems¹⁹⁹⁸.

In 2023, a South-Korea and US research team proposed a shallow-depth linear optics architecture implementing both Fock-state and Gaussian boson sampling with the capability to bring some computing advantage¹⁹⁹⁹.

A last note here: boson sampling experiments can also be implemented with cold atoms²⁰⁰⁰.

Measurement Based Quantum Computing

MBQC is a very particular approach to quantum computing. It consists in exploiting the initialization of entangled qubits and then performing step-by-step measurements on certain qubits to obtain a result on the last measured qubits at the end of the run. There are several variants, the *one-way quantum computing* (1WQC²⁰⁰¹) which uses two-dimensional qubits matrices to create cluster states and the *measurement-only QC* which only measures qubits, without prior entanglement. We will focus here on the first method which seems to be the most commonplace.

MBQC allows the execution of classical quantum algorithms with universal gates. Where is it relevant? It is particularly interesting in qubit-based quantum systems where it is difficult to create multi-qubit quantum gates exploiting entanglement and where the number of chained gates is limited for physical reasons. The model was initially created for cold atoms qubits and even trapped ions²⁰⁰² but it later made more sense with photon qubits for which deterministic two-qubit gates are impossible to create.

Photons are also indicated because they allow to easily manage rotation angles in the Bloch sphere that are used in the single-qubit quantum gates of the process, via a phase control of the photon qubits. It can also be implemented with other types of qubits like silicon carbide defects²⁰⁰³.

¹⁹⁹⁶ See [Reconfigurable continuously-coupled 3D photonic circuit for Boson Sampling experiments](#) by Francesco Hoch, Fabio Sciarrino et al, npj quantum information, May 2022 (7 pages).

¹⁹⁹⁷ See [Large-scale error-tolerant programmable interferometer fabricated by femtosecond laser writing](#) by Ilya V. Kondratyev et al, Russia, August 2023 (14 pages).

¹⁹⁹⁸ See [Using Gaussian Boson Sampling to Find Dense Subgraphs](#) by Juan Miguel Arrazola and Thomas R. Bromley, March-July 2018 (6 pages).

¹⁹⁹⁹ See [Exploring Shallow-Depth Boson Sampling: Towards Scalable Quantum Supremacy](#) by Byeongseon Go et al, Seoul National University and the University of Chicago, June 2023 (18 pages).

²⁰⁰⁰ See [Boson Sampling with Ultracold Atoms](#) by Carsten Robens et al, MIT, MQCST, Harvard, August 2022 (16 pages).

²⁰⁰¹ MBQC was designed in 2000 by Robert Raussendorf and Hans Briegel. See [A computationally universal phase of quantum matter](#) by Robert Raussendorf, 2018 (41 slides), [Measurement-based Quantum Computation](#) by Elham Kashefi, University of Edinburgh (50 slides) and the extensive [Introduction to measurement based quantum computation](#) by Tzu-Chieh Wei from Stone Brook University, 2012- (88 slides) and a one pager: [Universal measurement-based quantum computation with Mølmer-Sørensen interactions and just two measurement bases](#). Other information sources include [Blind quantum computation](#) by Charles Herder (10 pages), [Cluster-state quantum computation](#) by Michael Nielsen, 2005 (15 pages), [Fault-tolerant quantum computation with cluster states](#) by Michael Nielsen and Christopher Dawson, 2004 (26 pages), [2D cluster state](#) (50 slides), [Quantum Computing with Cluster States](#) by Gelo Noel Tabia, 2011 (18 pages), [Quantum pictorialism for topological cluster-state Computing](#) by Clare Horsman 2011 (18 pages) and [Cluster State Quantum Computing](#) by Dileep Reddy et al, 2018 (11 pages). See also [Quantum computing with photons: introduction to the circuit model, the one-way quantum computer, and the fundamental principles of photonic experiments](#) by Stephanie Barz, 2015 (26 pages). At last, see the review paper [Realizations of Measurement Based Quantum Computing](#) by Swapnil Nitin Shah, December 2021 (7 pages).

²⁰⁰² See [Measurement-based quantum computation with trapped ions](#) by B. P. Lanyon, Cornelius Hempel, Rainer Blatt et al, August 2013 (18 pages).

²⁰⁰³ In [Quantum Information Processing With Integrated Silicon Carbide Photonics](#) by Sridhar Majety et al, March 2022 (50 pages).

With MBQC, things are done a bit backwards with respect to classical quantum computing: we first apply single-qubit gates and measure them progressively, whereas in gate-based quantum computing, we implement reversible unitaries (single and two-qubit quantum gates) and then make measurements at the end of the circuit. A big warning here: understanding how MBQC works is not easy. You can easily get lost in how things are organized in space and time.

An MBQC calculation is **logically irreversible**, unlike a quantum algorithm based on universal quantum gates. Indeed, the process of measuring qubit states cannot be logically reversed except when the state of the qubits read corresponds exactly to their basis states $|0\rangle$ and $|1\rangle$.

A quantum computation executed with universal gates is the equivalent of applying a unitary transformation embodied by a giant square matrix of dimension 2^N to a set of N qubits initialized in the state $|0\rangle$. This matrix can be inverted by scrolling backwards the quantum gates that were used to create it. With MBQC, this is not possible. This irreversibility of MBQC calculations explains why it is also called 1WQC for One Way Quantum Computing. There is no way of going back.

This model is also **probabilistic**, due to the probabilistic nature of the state measures of qubits at each step of the calculation. The successive measurements provide information on the state of the qubits, which makes it possible to become determinist again in the rest of the computation by applying a kind of error correction on the fly. A bit like using 3-qubit error correction codes.

MBQC is a **hybrid** method since its implementation depends on interactions between quantum computing and the exploitation of qubits readout data by a classical computer controlling the system and in real time. This must happen very fast, at the scale of photon speed in photonic circuits.

Qubits used in the cluster state based MBQC are of four different classes: those that are prepared and measured (the ancilla qubits), those that are only measured during computing, those that are only prepared (but measured at the end of computing) and those that are neither prepared nor measured (and are used for the rest of computing).

The principle is based on the sequencing of so-called NEMC sequences with four steps²⁰⁰⁴:

- Using a set of **ancilla qubits** (step N), those of the first type which are measured with a Z projection.
- Creating **cluster-states of entangled qubits** (step E)²⁰⁰⁵. With photons, there are many ways to generate these cluster states and it is one of the key scientific and technology challenges with MBQC. Theoretically, you could generate these cluster states with regular independent qubits and apply to these photons a series of single and entangling quantum gates (H, CNOT, etc). These entangling gates are difficult to create with photons and MBQC is a method that gets rid of these in the first place. So, scientists are looking for ways to generate these cluster states with other means. There are many figures of merits here: the source must be as deterministic as possible and avoid so-called heralding and post-selection methods that reduce the chance to get a full cluster state at a given moment. There are also 1D and 2D cluster states. PsiQuantum is generating rather small photonic cluster states and connecting them with so-called “fusions”, that implements probabilistic measurements. Another option consists in creating cluster states with photons entangled using multiple properties (polarization, phase, etc.)²⁰⁰⁶.

²⁰⁰⁴ Information sources: [Advanced Quantum Algorithms](#) by Giulia Ferrini et al, 2019 (30 pages) and [An introduction to Quantum Computing](#) by Elham Kashefi, School of Informatics University of Edinburgh, 2020 (119 slides).

²⁰⁰⁵ See the review paper [Physical Realization of Measurement Based Quantum Computation](#) by Muhammad Kashif and Saif Al-Kuwari, Hamad Bin Khalifa University at Qatar Foundation, January 2023 (41 pages) which covers well the creation of cluster states in both CV and DV modes.

²⁰⁰⁶ See [Resource-efficient photonic quantum computation with high-dimensional cluster states](#) by Ohad Lib and Yaron Bromberg, The Hebrew University of Jerusalem, September 2023 (26 pages).

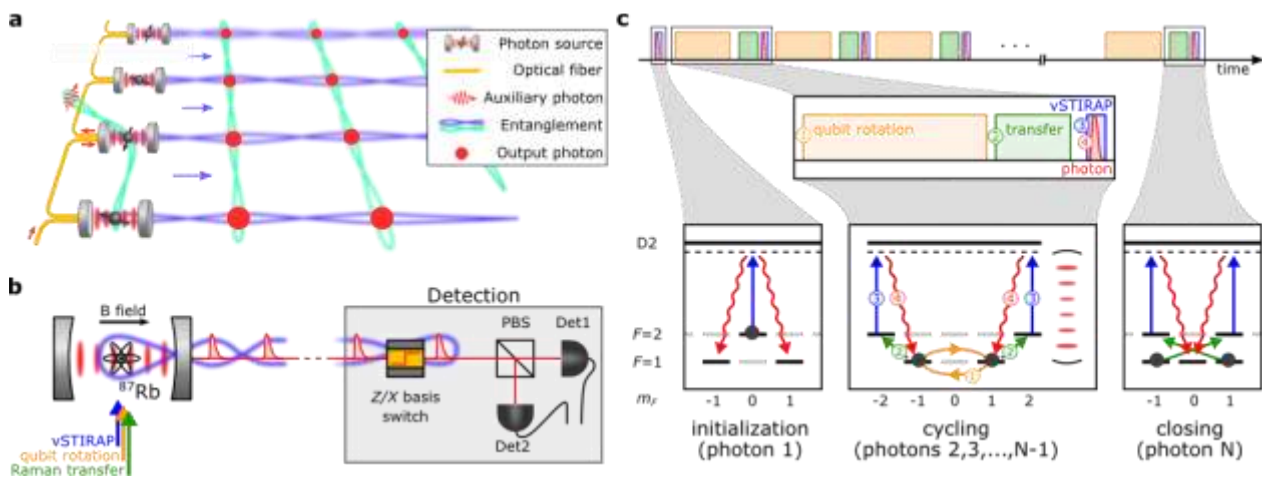


Figure 471: one solution to generate a cluster state of entangled photons for MBQC.

Source: [Efficient generation of entangled multi-photon graph states from a single atom](#) by Philip Thomas, Leonardo Ruscio, Olivier Morin and Gerhard Rempe, MPI, May 2022 (10 pages).

Photonic cluster states can be generated in many ways which have evolved over time with SPDC (spontaneous parametric down-conversion) using powerful laser single photons source heralding with a probabilistic outcome that is detected post-selectively and doesn't scale well beyond a dozen qubits²⁰⁰⁷, atom based **cavity QED** generation²⁰⁰⁸ (Figure 471) that was later extended to **ensemble of Rydberg atoms**^{2009 2010}, with connected **coupled cavity arrays (CCAs)**²⁰¹¹, individual **neutral atoms**, **spin-photon entanglement** to deterministically generate linear cluster states aka the Lindner-Rudolph protocol²⁰¹² with recent improvements²⁰¹³, with **quantum dots**

²⁰⁰⁷ See [12-Photon Entanglement and Scalable Scattershot Boson Sampling with Optimal Entangled-Photon Pairs from Parametric Down-Conversion](#) by Han-Sen Zhong, Jian-Wei Pan et al, PRL, 2018 (17 pages) with a ~97% heralding efficiency and ~96% photons indistinguishability. They generated 12-photon entanglement with a state fidelity of 0.572 ± 0.024 . It was use for early Boson sampling experiments.

²⁰⁰⁸ See [Sequential generation of matrix-product states in cavity QED](#) by C. Schön, K. Hammerer, M. M. Wolf, J. I. Cirac, and E. Solano, 2006 (11 pages) and [Efficient generation of entangled multiphoton graph states from a single atom](#) by Philip Thomas et al, Nature, August 2022 (12 pages) with a generation of 14 qubits GHZ states and linear cluster states of 12 photons.

²⁰⁰⁹ See [Sequential generation of multiphoton entanglement with a Rydberg superatom](#) by Chao-Wei Yang, Jian-Wei Pan et al, December 2021 (11 pages). One disadvantage of this method is its slow emission rate.

²⁰¹⁰ See [Quantum Metasurfaces](#) by Rivka Bekenstein, Mikhail D. Lukin et al, April 2019 (16 pages).

²⁰¹¹ See [Multipartite entanglement generation in coupled microcavity arrays](#) by Marc Bostelmann et al, November 2022 (16 pages).

²⁰¹² See [Proposal for Pulsed On-Demand Sources of Photonic Cluster State Strings](#) by Netanel H. Lindner and Terry Rudolph, PRL, 2009, published initially as [A photonic cluster state machine gun](#) on arXiv (10 pages), a first demonstrations obtained with semiconductor quantum dots spins in [Deterministic generation of a cluster state of entangled photons](#) by I. Schwartz, D. Gershoni et al, Technion and University of Washington, Science, 2016 (28 pages) with series of 5 entangled photons and recent improvements in [Probing the dynamics and coherence of a semiconductor hole spin via acoustic phonon-assisted excitation](#) by Nathan Coste, Niccolo Somaschi, Loic Lanco, Pascale Senellart et al, C2N and Quandela, July 2022 (6 pages).

²⁰¹³ See the first results of high photon indistinguishability in [A deterministic source of indistinguishable photons in a cluster state](#) by Dan Cogan, David Gershoni et al, Technion, October 2021 (17 pages) where quantum dot emits indistinguishable polarization-entangled photons with a Gigahertz rate deterministic generation of >90% indistinguishable photons in a cluster state of over 10 photons and [High-rate entanglement between a semiconductor spin and indistinguishable photons](#) by Nathan Coste, Sophia Economou, Niccolo Somaschi, Alexia Auffèves, Loic Lanco, Pascale Senellart et al, Nature Photonics, July 2022 (17 pages) is about the efficient generation of three qubits cluster state with one semiconductor spin and two indistinguishable photons with 2 and 3 particle entanglement with fidelities of 80 % and 63 % respectively, with photon indistinguishability of 88%. The spin-photon and spin-photon-photon entanglement rates exceed by three and two orders of magnitude respectively the previous state of the art. The photons are entangled in polarization and time multiplexed. Their number depends on the stability of the electron spin in the quantum dot. This stability is rapidly increasing.

molecules²⁰¹⁴, with the **entanglement of several single photon sources**²⁰¹⁵, **time-domain multiplexing** using indistinguishable photon sources which has the advantage to be theoretically unlimited^{2016 2017}, **2D spin-photon cluster states**²⁰¹⁸, creating **large GHZ states** using regular linear optics²⁰¹⁹, etc. You can also add **spectral domain multiplexing** on top of time-domain multiplexing as a complement to SPDC sources²⁰²⁰.

- Measuring **state of intermediate qubits** during computing (M). It is carried out with a variation of projective measurement. It consists in first applying one or more X or Y gates to a qubit to create a rotation in their Bloch sphere and then to measure their state on the computational basis. It is a bit like rotating the Z ($|0\rangle/|1\rangle$) axis in the Bloch sphere to change the reference point.

$$|\pm\rangle = \frac{|0\rangle \pm |1\rangle}{\sqrt{2}}$$

$$|\pm_\alpha\rangle = \frac{|0\rangle \pm e^{i\alpha}|1\rangle}{\sqrt{2}}$$

The projective measurement basis is in the form of states of the type $|\pm_\alpha\rangle$, α being generally a half or quarter turn in Bloch's sphere. A measured qubit is always an intermediate resource and is not an output resource. This helps obtaining some information that can be used to manipulate the qubits afterwards to propagate computation. Projective Z measurements have the effect of removing the measured qubits from the cluster.

- These successive **corrections** make computing deterministic (step C) with X and Z gates. They are applied according to the result of the projective measurements made in (M). No correction gate acts here on a qubit already measured. This model makes it possible to apply any gate to a qubit which is in fact a combination of $Rz(\gamma)Rx(\beta)Rz(\alpha)$, i.e., rotations around the three axis of the Bloch sphere of angles γ , β and α ²⁰²¹.

What has just been described allows to interpret the lower right-hand part of the illustration in Figure 472 which explains how the MBQC equivalents of the CNOT (two-qubit), H or S quantum gate equivalents are realized in MBQC. Each X or Y circle is an X and Y projective measurement that combines an X or Y gate followed by a qubit readout. The result conditions the type of projective measurement performed immediately afterwards in the order indicated (1 to 15 and 1 to 5).

²⁰¹⁴ See [Deterministic generation of entangled photonic cluster states from quantum dot molecules](#) by Arian Vezvaei, Sophia Economou et al, June 2022 (5 pages).

²⁰¹⁵ See [Multi-photon entanglement from distant single photon sources on demand](#) by Almut Beige et al, 2006 (9 pages) and [Protocol for generation of high-dimensional entanglement from an array of non-interacting photon emitters](#) by Thomas J Bell et al, University of Bristol and NBI, New Journal of Physics, January 2022 (9 pages).

²⁰¹⁶ See [Sequential generation of linear cluster states from a single photon emitter](#) by D. Istrati, Pascale Senellart, H.S. Eisenberg et al, 2020 (8 pages), [Deterministic generation of a two-dimensional cluster state](#) by Mikkel Vilsbøll Larsen et al, Science, September 2019 (30 pages), using two OPOs (Optical Parametric Oscillator) and [Generation of time-domain-multiplexed two-dimensional cluster state](#) by Warit Asavanant et al, Science, 2019 (23 pages).

²⁰¹⁷ See [Generation of large-scale continuous-variable cluster states multiplexed both in time and frequency domains](#) by Peilin Du et al, October 2022 (10 pages).

²⁰¹⁸ See [Multidimensional cluster states using a single spin-photon interface coupled strongly to an intrinsic nuclear register](#) by Cathryn P. Michaels et al, University of Cambridge, October 2021 (14 pages) and [Deterministic multi-mode gates on a scalable photonic quantum computing platform](#) by Mikkel V. Larsen et al, DTU, Nature Physics, July 2021 (30 pages) which deals with creating an universal gate set with cluster states, with CV qubits using telecommunication wavelengths (1,550nm).

²⁰¹⁹ See [Preparation of multiphoton high-dimensional GHZ state](#) by Wen-Bo Xing et al, April 2023 (8 pages).

²⁰²⁰ See [Spectrally shaped and pulse-by-pulse multiplexed multimode squeezed states of light](#) by Tiphaine Kouadou, Nicolas Treps, Valentina Parigi et al, September 2022 (9 pages) which is about generating continuous variables entangled field modes which could also be used for Gaussian boson sampling.

²⁰²¹ The decomposition of quantum gates into a computational method that can be used for MBQC has been [patented](#) by Krysta Svore of Microsoft, who leads the QuArC group there.

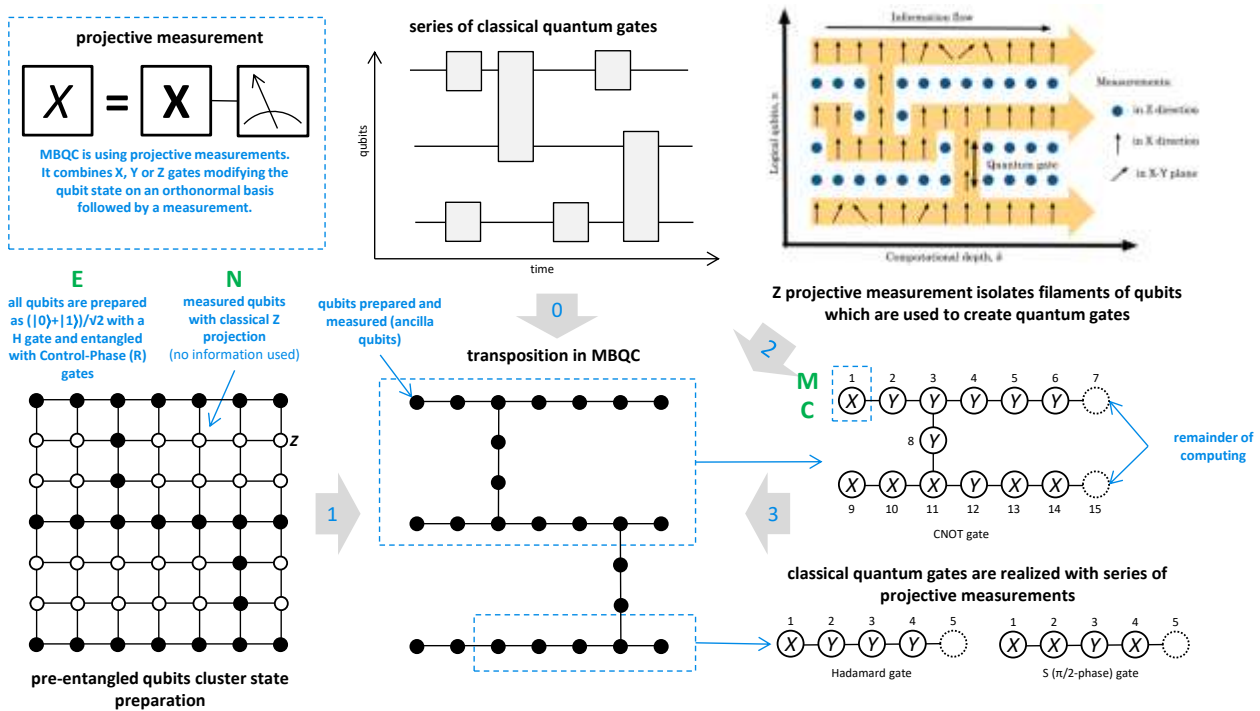


Figure 472: a tentative summary of how MBQC works. Usually, learning it works like a Write Once Read Never (WORN) memory! (cc) Compilation, Olivier Ezratty, 2021, and [Basics of quantum computing and some recent results](#) by Tomoyuki Morimae, 2018 (70 slides).

Two forms of measurements affect the inner working of the qubit matrix: Z measurements separate the qubits by digging sort of grooves in the qubit matrix, a bit like Pacmans, then classical measurements along the "wires" or on the "bridges" between these wires simulate single-qubit gates like Hadamard's and the two-qubit CNOT gates. The sequence of operations depends on the result of each measurement along the wires. The computation result is located in the last qubits whose state is not yet measured and which will be measured last.

This combination of NEMC sequences allows the reproduction of the operation of one- and two-qubit quantum gates. A complete quantum computation is a sequence of multiple NEMCs that ends with the measurement of the state of the remaining qubits!

The consequences of what we have just seen are multiple:

- MBQC requires way **more qubits** than in a conventional circuit-based model. We've seen that a single X or Y gate results from the combination of four X and Y gates and as many measurements. This in turn creates a "pressure" on the classical part of the calculation, linked to the measurement.
- MBQC still requires **error correction codes** such as foliated quantum codes²⁰²². They too will multiply by several orders of magnitude the number of physical qubits necessary for computing any algorithm. It could be facilitated if we could organize the qubits in 3D matrices, the third dimension being used to align the qubits necessary for error correction, especially with surface codes. On the other hand, since MBQC models contains its own error correction mechanisms, it may be less demanding in terms of additional qubits for error correction necessary for the creation of "fault tolerant" quantum computers²⁰²³.
- The **temporal dimension** of computing is modified compared to classical gate-based quantum computing. As we can parallelize operations coupling gates and measurements, MBQC is a bit

²⁰²² See [Foliated Quantum Error-Correcting Codes](#) by A. Bolt et al, University of Queensland and Université de Sherbrooke, PRL, July 2016 (5 pages) and [Decoding Schemes for Foliated Sparse Quantum Error Correcting Codes](#) by A. Bolt et al, 2018 (23 pages).

²⁰²³ See one proposal of correction codes in [Error-protected qubits in a silicon photonic chip](#) by Caterina Vigliar et al, VTT, Nature Physics, September 2021 (31 pages).

like Nutella on the breadcrumbs: we can spread it out! The depth of the available computation is no longer linked to the ability to chain quantum gates in time as in the middle-high diagram in the previous illustration, but to execute a large number of them in parallel over a very large number of qubits (modulo the required error correction). The sequences of measurements labeled 1, 2 ... n will be carried out simultaneously in groups 1, 2 ... n, n being limited to 15. Therefore, the required physical calculation depth if defined by the maximum number of physical gates to execute to create a CNOT. This is an argument in favor of photon qubits. The depth of an algorithm no longer depends on the ability to chain quantum gates with one and two qubits, but on the entanglement capacity of the qubits at startup in the model's cluster states. In short, sequential quantum computing is replaced by massively parallel quantum computing with a very shallow depth. This is the approach chosen by PsiQuantum.

- An MBQC model is easily exploitable to take advantage of teleportation and **distributed quantum computing** algorithms. Cluster states will be able to be linked together via remote optical links. It is also one of the tools of blind computing²⁰²⁴.
- Finally, there is a direct link between the MBQC and the **ZX Calculus**. ZX Calculus is a graph model that help formalizing MBQC, its cluster states and the associated error corrections²⁰²⁵.
- **Algorithms** are specific to this kind of architecture²⁰²⁶. It is not yet experimental because it requires a large number of qubits that are not yet practically available. Still, QAOA could easily be translated into the MBQC formalism²⁰²⁷. There is also a proposal for some variational generative model using MBQC²⁰²⁸.

Vendors

Ψ PsiQuantum **PsiQuantum** (2016, USA/Europe, \$728M) is a startup created by Jeremy O'Brien, a former Stanford and Bristol University researcher, who wants to create a photon-based quantum processor in CMOS silicon technology.

Other cofounders are Pete Shadbolt (co-inventor of the VQE algorithm with Jeremy O'Brien and Alán Aspuru-Guzik), Mark Thompson and Terry Rudolph, who discovered when he finished his physics thesis that he was a grandson of Erwin Schrödinger, which may have helped with fundraising! The company employs over 250 people, most of them in Palo Alto in the USA, but some of them work remotely all over the world, including a couple ones in Europe.

Early in 2021, the company started to be more open on its technology²⁰²⁹. It published a paper describing their qubit architecture, using an **FBQC** system, aka Fusion-based quantum computation, a variant of MBQC that we study page 544. It uses micro-clusters states with groups of 4 qubits connected together and using Resource State Generators (RSGs) (Figure 473).

²⁰²⁴ See [Measurement-based and Universal Blind Quantum Computation](#) by Anne Broadbent, Joseph Fitzsimons and Elham Kashefi, 2016 (41 pages).

²⁰²⁵ Seen in [Universal MBQC with generalised parity-phase interactions and Pauli measurements](#) by Aleks Kissinger and John van de Wetering, 2019 (21 pages).

²⁰²⁶ See for example [Changing the circuit-depth complexity of measurement-based quantum computation with hypergraph states](#), May 2019 (16 pages). The article describes an MBQC method based on the exploitation of Toffoli (CCZ) and Hadamard (H) gates. They allow to simulate topological quantum computation, reducing the error rate of quantum computation.

²⁰²⁷ See [A native measurement-based QAOA algorithm, applied to the MAX K-CUT problem](#) by Massimiliano Proietti et al, PRA, April 2023 (16 pages).

²⁰²⁸ See [Variational measurement-based quantum computation for generative modeling](#) by Arunava Majumder, Hans J. Briegel et al, October 2023 (12 pages).

²⁰²⁹ See [Silicon Photonic Quantum Computing - PsiQuantum at 2021 APS March Meeting](#) by Jeremy O'Brien, April 2021 (25 mn).

It is replacing measurement of entangled states by double measurement of non-connected adjacent qubits to create entanglements between them²⁰³⁰. Qubits are encoded in path, using dual rail encoding with lines for photon states $|0\rangle$ and $|1\rangle$.

Two qubit gates use XX nondeterministic and ZZ deterministic measurements (measuring two photons simultaneously with the same polarization basis), implemented with a beam splitter then combining fusions to create small cluster states.

With that, the qubit computing depth is quite shallow, avoiding the pitfalls of qubits error rates. It is replaced by a large breadth of computing and commutative operations, replacing “depth-computing” by “breadth-computing”²⁰³¹.

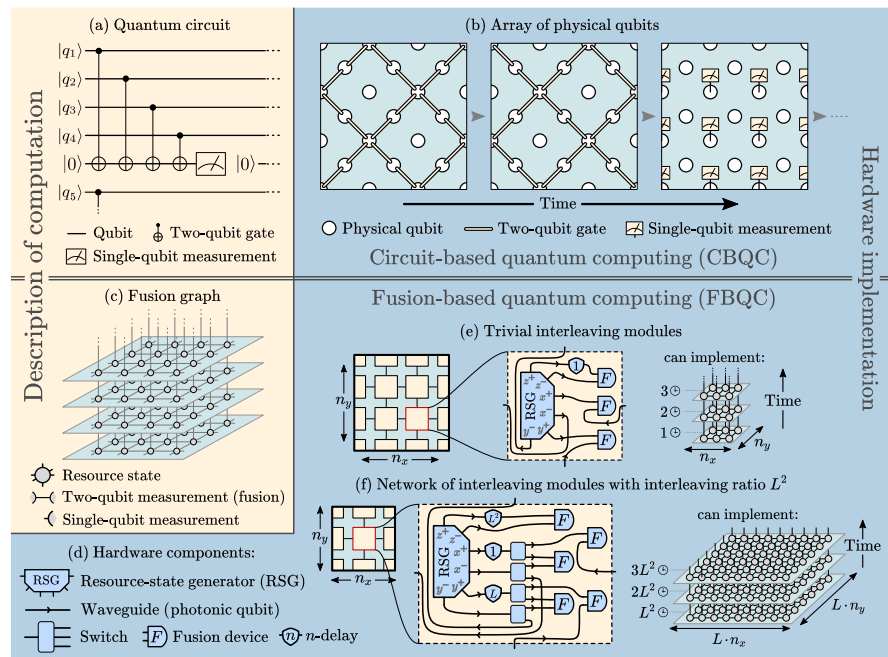


Figure 473: FBQC method description. Source: [Interleaving: modular architecture for fault-tolerant photonic quantum computing](#) by Hector Bombin et al, 2021 (22 pages).

Their ambition is to produce a system with one million physical qubits generating the equivalent of 100 logical qubits. Their photonic chips manufacturing is handled at the 300 mm wafers **Global-Foundries** Luther Forest Technology Campus in upstate New York.

They announced having produced a first q1 chip sample in April 2021 integrating tens of thousands single (non-deterministic “spontaneous parametric down-conversion” aka SPDC) photon sources and detectors²⁰³². Their physical architecture is using sandwiches assembling a 22 nm CMOS electronic chip of 750M transistors using superconducting nanowires bonded with 100K connections to a photonic chip containing thousands of photon sources, detectors and other optical devices. The photonic chip has 200 optical fiber entries and exits that are used to interconnect similar photonic chips together in a distributed architecture manner.

The final PsiQuantum one million physical qubits computer will be made of thousands of computing chips connected together so we can presume each chip is implementing fewer than 1,000 physical qubits. The whole system will run at a temperature of 4K, requiring only a pulse tube refrigeration system, that is much simpler than a dilution system for sub 100mK temperatures and with more cooling power. They are also using fiber delay lines as optical memory thanks to its low loss rate. It is mixed with topological fault tolerance codes. This is supposed to multiply by 5,000x the number of usable qubits²⁰³³.

²⁰³⁰ FBQC is fairly well explained in [Quantum Computing at the Speed of Light](#) by Terry Rudolph, November 2021 (1h13 video).

²⁰³¹ See [Percolation thresholds for photonic quantum computing](#) by Mihir Pant, 2017 (14 pages). The process is also documented in [Towards practical linear optical quantum computing](#) by Mercedes Gimeno-Segovia, 2015 (226 pages). This was the last publication on the PsiQuantum architecture until when they released [Fusion-based quantum computation](#) by Sara Bartolucci et al, January 2021 (25 pages). See also [QIP2021 Tutorial: Architectures for fault tolerant quantum computing](#) by Naomi Nickerson, January 2021 (3h).

²⁰³² See [PsiQuantum partners with GLOBALFOUNDRIES to bring up Q1 quantum system](#) by Mercedes Gimeno-Segovia, PsiQuantum, May 2021.

²⁰³³ See [Interleaving: modular architecture for fault-tolerant photonic quantum computing](#) by Hector Bombin et al, 2021 (22 pages).

To date, PsiQuantum is the best funded startup in the world in quantum computing, even ahead of D-Wave and Rigetti and on par with IonQ and its 2021 SPAC. Originally from the United Kingdom, it moved part of the team to the USA²⁰³⁴. They even have Microsoft as investors as well as Pascal Cagni's investment fund, C4 Ventures. Their last funding round of \$450M in July 2021 cemented this funding lead. In October 2022, PsiQuantum also got a funding from the US Federal Government through an US Air Force Research Laboratory contract of \$22.5M.

It is often said that PsiQuantum is a very secretive company. It is somewhat true for the advancement of their chip design and prototype manufacturing at Global Foundries. But they are still publishing interesting papers around the practical implementation of their FBQC model, like about the ways to reduce its resources requirements²⁰³⁵, to reduce the Shor 2048-bit algorithm circuit size and runtime²⁰³⁶, with the creation of a scalable framework for decoding in real time the streams of classical data in the decoder, used in quantum error correction, using parallelizable real-time decoding²⁰³⁷, and how to deal with probabilistic single photon sources and gates^{2038 2039}.

The company opened a UK R&D facility in March 2023 that is dedicated to the development of large scale cryogenic solutions. It is located at STFC's Daresbury Laboratory in the north-west of England where they access a large liquid-helium cryogenic plant providing about 100W of cooling power at 4K. As part of this, they benefited from UK's government funding in the tune of £9M.



Xanadu Quantum Technologies (2016, Canada, \$235.6M) is a startup created by Christian Weedbrook, a prolific researcher having started at MIT and the University of Toronto, among others.

Hardware. The startup is developing a photon qubit quantum computer targeting FTQC capabilities. In September 2020, they launched a cloud-based testing platform of 8 and 12 qubits. Their qubits are qumodes based on squeezed states using continuous variables encoding. Their work and research is rather well documented with over 100 published papers^{2040 2041 2042 2043}. The 8-qubit silicon-nitride chip is 4mm x 10 mm wide, fed by infrared laser pulses and generating “squeezed states” superposing multiple photons, then flowing through an interferometer made of beam splitters and phase shifters performing quantum gates, and exiting to superconducting photon detectors²⁰⁴⁴. Their photon sources and photon detectors require some cooling. Their currently used superconducting transition edge sensor (TES) photon counting detectors are working 100 mK²⁰⁴⁵.

²⁰³⁴ See the presentation [Measurement-based fault tolerance beyond foliation](#) by Naomi Nickerson of PsiQuantum in September 2019 and [Quantum Computing With Particles Of Light: A \\$215 Million Gamble](#) by Paul Smith-Goodson, April 2020.

²⁰³⁵ See [Increasing error tolerance in quantum computers with dynamic bias arrangement](#) by Hector Bombin et al, PsiQuantum, March 2023 (11 pages).

²⁰³⁶ See [Active volume: An architecture for efficient fault-tolerant quantum computers with limited non-local connections](#) by Daniel Litinski and Naomi Nickerson, PsiQuantum, November 2022 (42 pages).

²⁰³⁷ See [Modular decoding: parallelizable real-time decoding for quantum computers](#) by Héctor Bombín et al, March 2023 (23 pages).

²⁰³⁸ See [Photonic quantum computing with probabilistic single photon sources but without coherent switches](#) by Terry Rudolph, March 2023 (16 pages).

²⁰³⁹ See [What is the logical gate speed of a photonic quantum computer?](#) by Terry Rudolph, June 2023.

²⁰⁴⁰ Their process is documented in [The power of one qumode for quantum computation](#), 2016 (10 pages) with an example of implementation in [Continuous-variable gate decomposition for the Bose-Hubbard model](#), 2018 (9 pages).

²⁰⁴¹ See [Optical hybrid approaches to quantum information](#) by Peter van Loock, 2010 (35 pages).

²⁰⁴² See also [Quantum computing with multidimensional continuous-variable cluster states in a scalable photonic platform](#) by Bo-Han Wu et al, 2020 (22 pages).

²⁰⁴³ See the review paper [Quantum computing overview: discrete vs. continuous variable models](#) by Sophie Choe, June 2022 (12 pages)

²⁰⁴⁴ See [In the Race to Hundreds of Qubits, Photons May Have "Quantum Advantage"](#) by Charles Q. Choi, March 2021.

²⁰⁴⁵ See [Noise-free high-efficiency photon-number-resolving detectors](#) by Danna Rosenberg, Adriana E. Lita, Aaron J. Miller and Sae Woo Nam, 2005 (4 pages).

They plan to later use room-temperature detectors using SPADs (single photon avalanche diodes) and QFC (quantum frequency conversion)²⁰⁴⁶.

In 2021, a team of Xanadu and Canadian researchers published a blueprint with more details on the Xanadu FTQC architecture. It is based on MBQC and three-dimensional resource states comprising both GKP bosonic qubits and squeezed states of light. This hybridization would enable the implementation of both Clifford and non-Clifford gates, all of this running on 2D photonic chips²⁰⁴⁷. In August 2021, Xanadu announced that their FTQC silicon-nitride chips would be manufactured by IMEC in Belgium but in March 2022, they switched gear and announced a partnership with GlobalFoundries for the manufacturing of their chip on 300 mm silicon wafers, like PsiQuantum. They expect to scale up to 1,000 logical qubits, which would require about 10,000 racks.

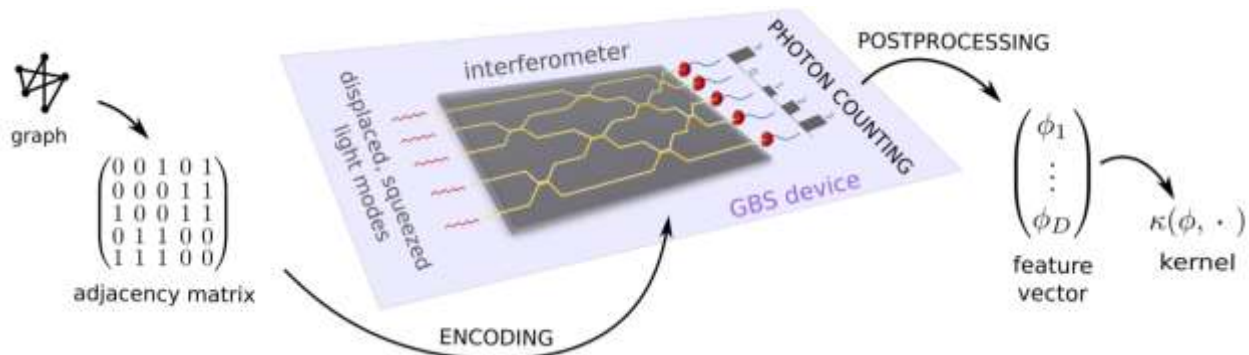


Figure 474: Xanadu's architecture for their 2022 GBS. Source: Xanadu.

In June 2022, Xanadu announced their own quantum advantage with their own gaussian boson sampling architecture (GBS). Their Borealis QPU reached a record of 216 photon modes to using frequency multiplexing and delay lines implementing time-bin multiplexing (Figure 474). Their system was programmable with parametrizable photon phases and it was put online on the cloud on Amazon Bracket. However, Xanadu was cautious in saying that it didn't yet find use case with some useful quantum advantage²⁰⁴⁸. Since then, it seems that Xanadu decided not to pursue the path of parametrizable GBS in its photonic computer roadmap.

Xanadu is also working on linear optical quantum circuits with photon number resolving (PNR) detectors are used for both Gaussian Boson Sampling (GBS) and for the preparation of non-Gaussian states such as Gottesman-Kitaev-Preskill (GKP), cat states and NOON states which combine N quantum objects in the $|0\rangle$ state and as many in the $|1\rangle$ state²⁰⁴⁹.

Software. Xanadu develops the open source software platform **Strawberry Fields** and **PennyLane** in Python²⁰⁵⁰. It includes the Blackbird language and targets chemistry use cases, graph theory problems and quantum machine learning. Their main application is the analysis of similarities between graphs to identify those that are similar and/or separate them into several classes of similarity. Classical methods for solving this kind of problem are similar to finding a matrix determinant²⁰⁵¹.

²⁰⁴⁶ See [On the Road to Room Temperature Quantum Computation](#), Xanadu, June 2020.

²⁰⁴⁷ See [Programmable optical quantum computer arrives late, steals the show](#) by Chris Lee, March 2021 referring to [Blueprint for a Scalable Photonic Fault-Tolerant Quantum Computer](#) by J. Eli Bourassa et al, February 2021 (38 pages).

²⁰⁴⁸ See [Quantum computational advantage with a programmable photonic processor](#) by Lars S. Madsen et al, Xanadu, June 2022 (11 pages) and the earlier and more detailed [Quantum Computational Advantage via High-Dimensional Gaussian Boson Sampling](#) by Abhinav Deshpande et al, February 2021 and January 2022 (24 pages).

²⁰⁴⁹ See [A quadratic speedup in the optimization of noisy quantum optical circuits](#) by Robbe De Prins et al, Ghent University, Telecom Paris, University of Chicago and Xanadu, March 2023 (16 pages).

²⁰⁵⁰ This is documented in [Strawberry Fields: A Software Platform for Photonic Quantum Computing](#), 2018 (25 pages).

²⁰⁵¹ See [Measuring the similarity of graphs with a Gaussian Boson Sampler](#) by Maria Schuld et al, 2019 (11 pages).

Case studies. On the customer side, Xanadu is like most vendors in a hurry to display some practical use cases for their systems. They are partnering with **BMW** on machine learning use cases, with prototypes using only 4 qubits, billion miles from any quantum advantage^{2052 2053} and with **Volkswagen** and IQbit to simulate lithium-ion batteries $\text{Li}_2\text{FeSiO}_4$ oxides, which would require 2,375 to 6,652 logical qubits that are about 10 years away in Xanadu's roadmap²⁰⁵⁴.

Partnerships. In January 2023, Xanadu announced a partnership with **KAIST** (Korea Advanced Institute of Science and Technology) in South-Korea with the aim to create quantum algorithms for designing next-generation lithium-ion batteries, a rather long-term goal given it indeed sits in the FTQC realm²⁰⁵⁵. In September 2023, this partnership was extended “*to train and educate South Korea's future quantum workforce*”.

Also, the Canadian federal government invested about 27M€ in Xanadu in January 2023²⁰⁵⁶.

QUANDELA

Quandela (2017, France, 67.5M€) decided in 2020 to expand its historical single photon source activity to create photon qubits computers as part of their project ROQC (Reconfigurable Optical Quantum Computer).

Hardware. Their first quantum computer is MosaiQ, which handles from 2 to 12 photon modes and consumes 1kW. It was first deployed online in November 2022. Their first target use cases are certified QRNGs using Bell states with the Entropy solution using 2 qubits, hybrid quantum machine learning algorithms²⁰⁵⁷ and chemical simulations. Their initial plans are to use a KLM probabilistic model using Fock states as shown in Figure 477²⁰⁵⁸ and then, later, a MBQC cluster-states based model. Quandela is always teaming up with Pascale Senellart's C2N research lab. They are making sustained progress in generating cluster states of entangled photons²⁰⁵⁹ and the generated photons polarization being determined by an electron in the quantum dot with a spin controlled by a surrounding magnetic field²⁰⁶⁰. With Fabio Sciarrino's team from Sapienza University in Rome, Italy, they qualified the ability of Quandela's photon source to create entangled states that are used in MBQC computation. They developed an interferometer to assess the indistinguishability of 4 entangled photons generated by their quantum dots source, as shown in Figure 476²⁰⁶¹.

They announced in October 2022 that some future photonic chips will be designed and manufactured by CEA-Leti in Grenoble using SiN and embedding photon detectors in the circuit in a future version as shown in Figure 475.

²⁰⁵² See [Tensor-network quantum circuits](#) by Diego Guala, Esther Cruz-Rico, Juan Miguel Arrazola and Shaoming Zhang, March-June 2022.

²⁰⁵³ See [Towards quantum machine learning with tensor networks](#) by William Huggins, E Miles Stoudenmire et al, UC Berkeley and Flatiron Institute, 2019 (12 pages).

²⁰⁵⁴ See [Simulating key properties of lithium-ion batteries with a fault-tolerant quantum computer](#) by Alain Delgado et al, Xanadu, Volkswagen, April 2022-February 2023 (31 pages).

²⁰⁵⁵ See [Xanadu and Korea Institute of Science and Technology partner to expand industrial use cases of quantum computing](#), Xanadu, January 2023.

²⁰⁵⁶ See [Supporting Canada's leadership in quantum computing to grow the economy and create jobs](#), Xanadu, January 2023

²⁰⁵⁷ See [Photonics: The fast lane towards useful Quantum Machine Learning?](#) by Quandela, November 2022.

²⁰⁵⁸ See their blueprint [A general-purpose single-photon-based quantum computing platform](#) by Nicolas Maring, Pierre-Emmanuel Emeriau, Nadia Belabas, Shane Mansfield, Pascale Senellart, Jean Senellart, Niccolo Somaschi et al, June 2023 (27 pages).

²⁰⁵⁹ See [High-rate entanglement between a semiconductor spin and indistinguishable photons](#) by Nathan Coste, Sophia Economou, Niccolo Somaschi, Alexia Auffèves, Loic Lanco, Pascale Senellart et al, Nature Photonics, July 2022 (17 pages).

²⁰⁶⁰ See [Controlling photon polarisation with a single quantum dot spin](#) by Elham Mehdi, Pascale Senellart, Loic Lanco et al, December 2022 (9 pages).

²⁰⁶¹ See [Quantifying n-photon indistinguishability with a cyclic integrated interferometer](#) by Mathias Pont, Fabio Sciarrino, Pascale Senellart, Andrea Crespi et al, PRX, January-September 2022 (21 pages).

Processing/manipulation of photonic qubits

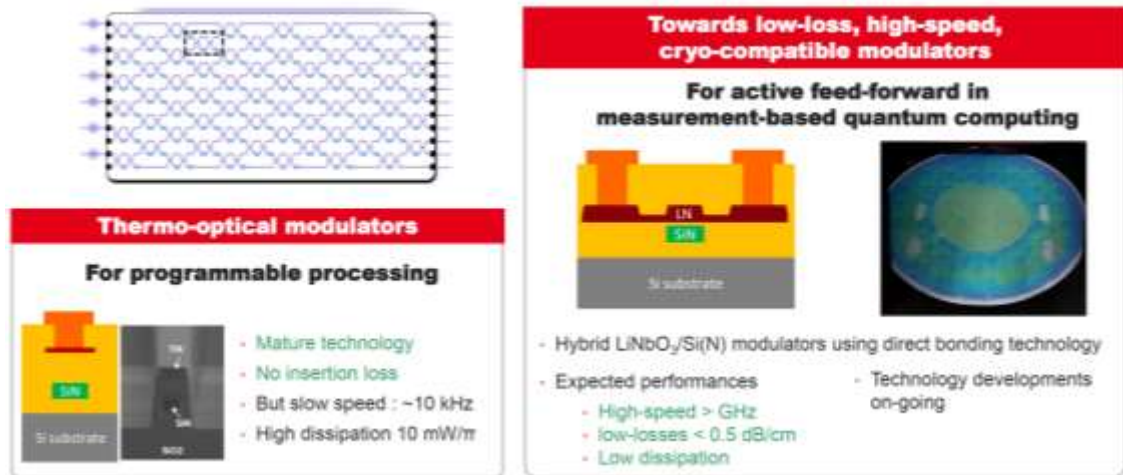


Figure 475: two generations of programmable photonic modulators to implement MZI (Mach-Zehnder Interferometers) in path encoding photonic computing. The first is using thermo-optical modulators (left) and the second will be based on hybrid $\text{LiNbO}_3/\text{Si(N)}$ modulators using direct bonding. Source: [Building an integrated technology platform for photon-based quantum computing](#) by Ségolène Olivier, CEA Leti, CEA Leti Innovation Days – Quantum Computing, June 28th, 2023.

In February 2022, Rawad Mezher and Shane Mansfield from Quandela proposed a single-number benchmark metric, the **Photonic Quality Factor (PQF)**, defined as the largest number of input photons for which the output statistics pass all tests. It covers photons quantum computing using single photon sources, multi-mode linear optics and photon detectors, including boson sampling experiments²⁰⁶².

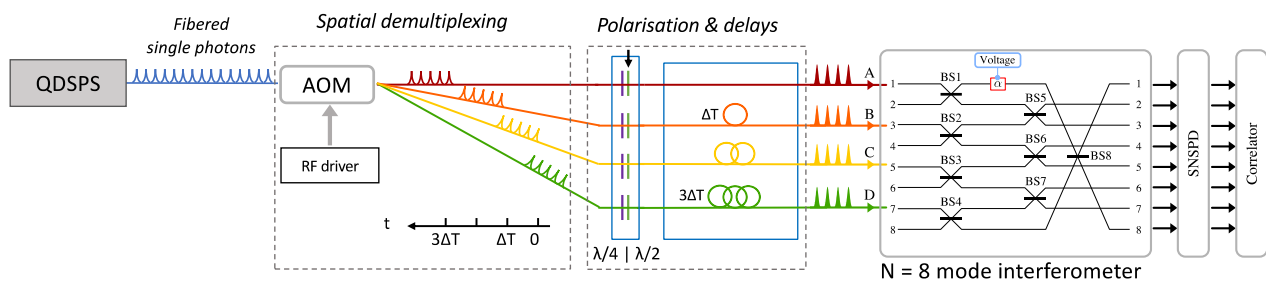


Figure 476: an interferometer used to validate the indistinguishability of a set of generated photons paving the way for the creation of cluster states of entangled photons. Source: [Quantifying n-photon indistinguishability with a cyclic integrated interferometer](#) by Mathias Pont, Fabio Sciarrino, Pascale Senellart, Andrea Crespi et al, PRX, January-September 2022 (21 pages).

In November 2023, Quandela released a blueprint of an original spin-optical quantum computing (SPOQC) QLDPC based FTQC architecture using quantum dots as computing qubits and photons as ancilla qubits, probabilistic two-qubit “repeat until success” (RUS) CZ gates and photon routing to connect all these quantum-dots based qubits²⁰⁶³.

Software. In April 2022, Quandela released **Perceval**, their photon qubits physical classical simulation software. It enables the simulation at low level of photonic linear circuits (PBS, ...), help understand how photon qubits work and create adapted algorithms like Grover, Shor, GBS, VQE and QML²⁰⁶⁴.

²⁰⁶² See [Assessing the quality of near-term photonic quantum devices](#) by Rawad Mezher and Shane Mansfield, Quandela, February 2022 (30 pages).

²⁰⁶³ See [A Spin-Optical Quantum Computing Architecture](#) by Grégoire de Gliniasty, Paul Hilaire, Pierre-Emmanuel Emeriau, Stephen C. Wein, Alexia Salavrakos, Shane Mansfield, Quandela and LIP6, November 2023 (20 pages).

²⁰⁶⁴ See [Perceval: A Software Platform for Discrete Variable Photonic Quantum Computing](#) by Nicolas Heurtel et al, April 2022 (31 pages).

These efforts benefit from a research collaboration with Inria teams^{2065 2066}. They later announced that Perceval was proposed in the cloud in partnership with **OVHcloud** and connector with popular programming frameworks like Qiskit.

Quandela developed a certified device independent QRNG solution with their two-photons MosaiQ QPU, based on Bell state pair generations and their Entropy patented protocol²⁰⁶⁷. It led to OVHcloud ordering a two-photons Quandela QPU, to generate random numbers in their cloud offering for security data encryption²⁰⁶⁸. The QPU was installed in OVHcloud data centers in October 2023. Also, Quandela announced a partnership with PQC vendor CryptoNext Security for the same reason²⁰⁶⁹.

Ascella is their 6-photons and 12-mode QPU that is publicly available online. In June 2023, Quandela inaugurated its assembly, integration and testing production line in Palaiseau, France.

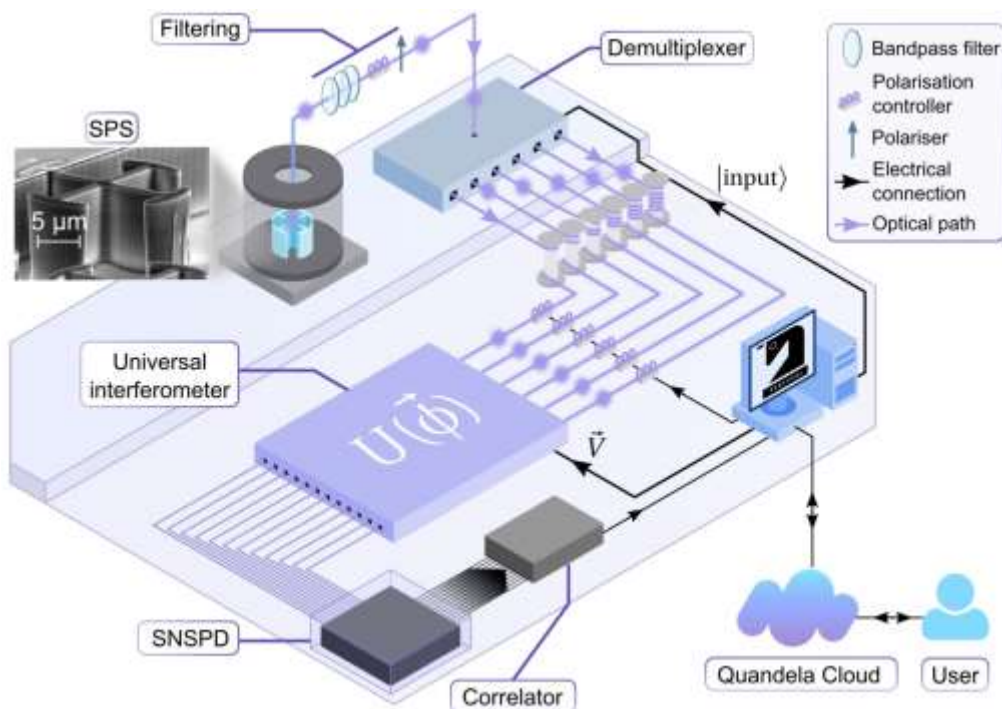


Figure 477: a typical Quandela QPU first generation setup using photon path encoding with the quantum dot source, a time-bin demultiplexer with output delay lines, a universal programmable interferometer with 6 photons input, and 12 SNSPD photon detectors at the exit. The Quandela photonic architecture enables several computing modes: one using quantum gates, another one labelled “photon native” used for some quantum machine learning task and a boson sampling mode using a randomized 12x12 matrix. Source: [A general-purpose single-photon-based quantum computing platform](#) by Nicolas Maring, Pierre-Emmanuel Emeriau, Nadia Belabas, Shane Mansfield, Pascale Senellart, Jean Senellart, Niccolo Somaschi et al, Quandela. June 2023 (27 pages).

Case studies. Application wise, Quandela started to work with EDF work on solving [partial differential equations](#) and MBDA to calculate the behavior of polymer materials.

²⁰⁶⁵ See [Strong Simulation of Linear Optical Processes](#) by Nicolas Heurtel, Shane Mansfield, Jean Senellart and Benoît Valiron, June 2022 (23 pages).

²⁰⁶⁶ See [QuaCS and Quandela: highlighting the potential of quantum algorithms](#), Inria, December 2022.

²⁰⁶⁷ See [Certified randomness in tight space](#) by Andreas Fyrillas, Boris Bourdoncle, Aristide Lemaitre, Isabelle Sagnes, Niccolo Somaschi, Nadia Belabas, Shane Mansfield et al, Quandela, C2N and University of Bristol, January 2023 (23 pages).

²⁰⁶⁸ See [OVHcloud purchases its first Quandela quantum computer to spur innovation in the Quantum ecosystem](#), OVHcloud, March 2023.

²⁰⁶⁹ See [CryptoNext Security and Quandela announce business partnership to offer an integrated security solution](#), March 2023.

It partners with **Data Reply** (Italy, France) to develop quantum solutions. They also published a paper on solving graph problems computing a permanent using their Ascella system²⁰⁷⁰.



ORCA Computing (2019, UK, \$18.7M including some UK public funding) is developing a quantum computing platform based on qumodes photons and a proprietary photonic memory using delay lines plus programmable beam splitters²⁰⁷¹ (Figure 478). They use photon frequency multiplexing (PT-series) and plan to later add time and space multiplexing (PA-Series) using a boson sampling mode. Their first chip was manufactured by **Ligentec** in Switzerland.

The startup was cofounded by Richard Murray (CEO, former head of the UK quantum program), Josh Nunn (CTO, former Oxford University, and also working with VeriQloud) and Cristina Escoda (COO), an entrepreneur with a background in finance and deep tech²⁰⁷². Quantonation is among their investors.

The startup leverages research done by Ian Walmsley's Ultra-fast and Nonlinear Quantum Optics Group from the University of Oxford. They work on the efficient preparation of cluster states using dual-rail photonic qubits and fusion measurement reminiscent of the PsiQuantum FBQC model^{2073 2074}.

They also developed machine learning and QUBO algorithms with their Python software library²⁰⁷⁵.

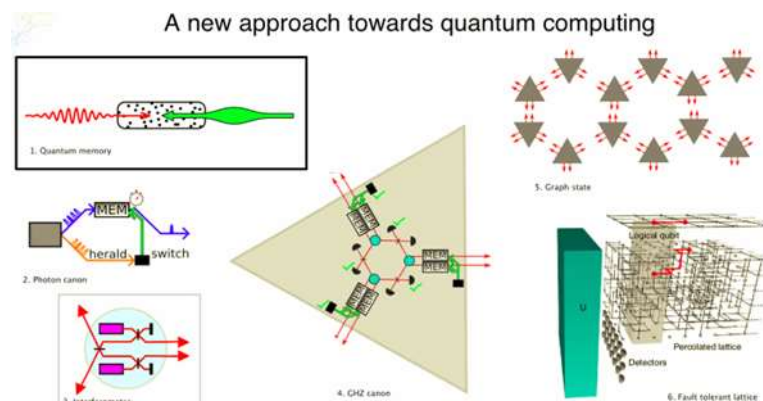


Figure 478: Orca's view of quantum computing. Source: Orca Computing.

In June 2022, the UK Minister of Defense announced the procurement of Orca's PT-1 quantum computer, which fits into a single rack and manages 8 qumodes. They plan to support 128 qumodes by 2024. Orca also sold a PT-1 QPU to Israel's Quantum Computing Centre managed by Quantum Machines in July 2022 and two PT-1 to Poznań Supercomputing and Networking Center in Poland.



TundraSystems (2014, UK) is developing a linear optics quantum processor operating supposedly at room temperature. They seem to create a photonic microprocessor and not necessarily, a quantum computer with qubits using linear optics.

Their Advisory Board includes two Chinese scientists, Xinliang Zhang and Pochi Yeh who are specialized in optronics ([site](#)).

²⁰⁷⁰ See [Solving graph problems with single-photons and linear optics](#) by Rawad Mezher, Ana Filipa Carvalho and Shane Mansfield, Quandela, PRA, January-August 2023 (6 pages) also documented in [Exploring Graph Problems with Single Photons and Linear Optics](#), Quandela Team, January 2023.

²⁰⁷¹ See [One-Way Quantum Computing in the Optical Frequency Comb](#) by Nicolas C. Menicucci, Steven T. Flammia and Olivier Pfister, April 2018 (4 pages) and [High-speed noise-free optical quantum memory](#) by K. T. Kaczmarek et al, April 2018 (12 pages).

²⁰⁷² See some details on their approach in [Photonic quantum processors](#), Orca Computing, April 2020 (27 slides).

²⁰⁷³ See [High photon-loss threshold quantum computing using GHZ-state measurements](#) by Brendan Pankovich et al, Orca Computing, August 2023 (15 pages).

²⁰⁷⁴ See [Flexible entangled state generation in linear optics](#) by Brendan Pankovich et al, Orca Computing, October 2023 (20 pages).

²⁰⁷⁵ See [Certain properties and applications of shallow bosonic circuits](#) by Kamil Bradler and Hugo Wallner, December 2021 (34 pages).

In September 2022, the company signed a 14M€ contract with **DLR**, the German Aerospace Center, to build a 64-qubit quantum computer and as a result opened an office in Germany. The company plans to build a 10K qumodes system after 2030.

In May 2023, **Qware** (a Terra Quantum company) and QuiX announced the creation of a hybrid quantum-classical platform with combining photonic and classical computing in a collocated data-center at Enschede in the Netherlands. It was to become operational in August 2023 for commercial applications deployments, promising tenfold speed improvement for unspecified use cases.

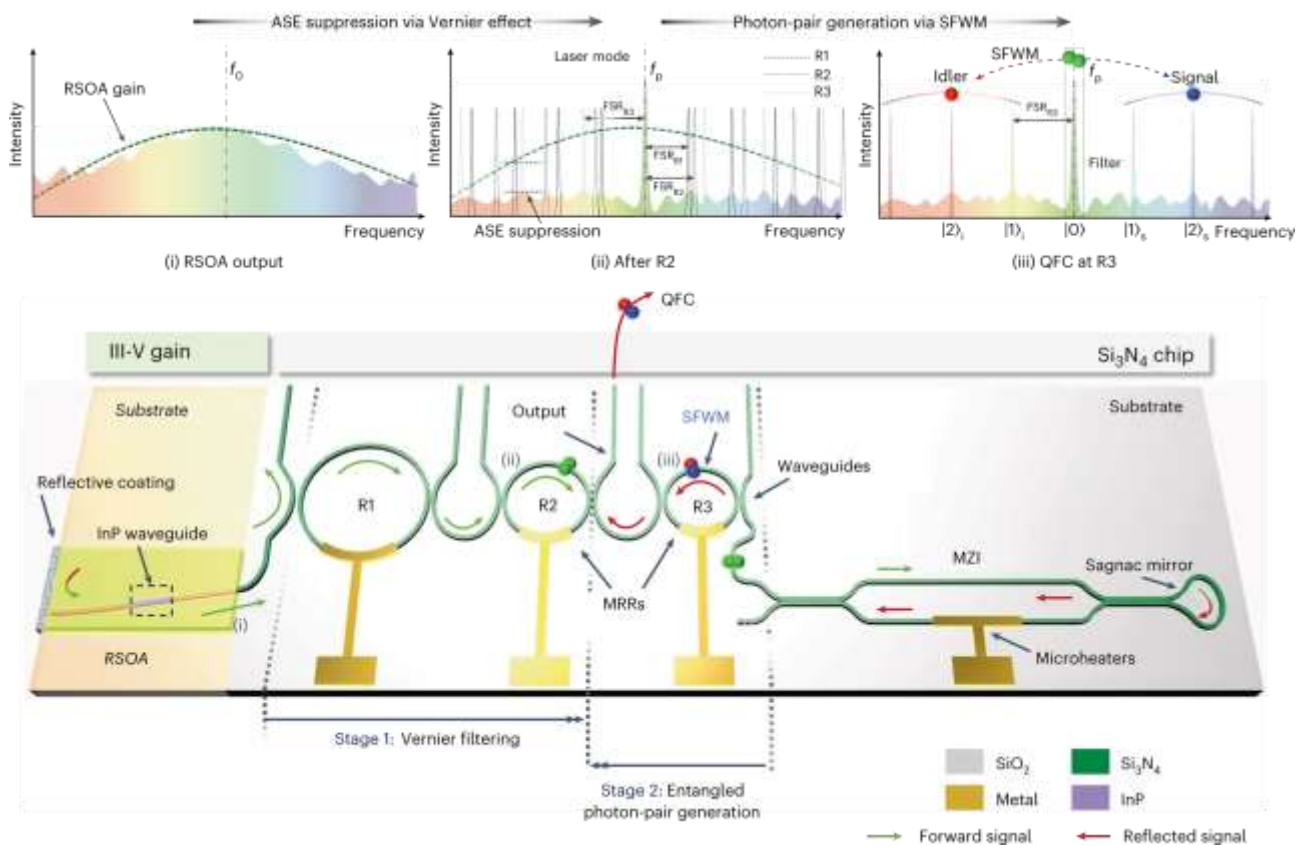


Figure 480: the chip based QuiX entangled photonic source showing how entangled photons are created with different frequencies (i), (ii) and (iii). Source: [Fully on-chip photonic turnkey quantum source for entangled qubit/qudit state generation](#) by Hatam Mahmudlu et al, *Nature Photonics*, June 2022-April 2023 (11 pages).



QBoson (2020, China, \$3M) aka “Bose Quantum” was founded by Wen Kai in Chaoyang (200 km North-East of Beijing), who studied at Tsinghua University and later got a PhD from Stanford in quantum computing.

He also worked at Google AI in the USA. The company is creating photon-based quantum computers with, in sight, a hybrid AI applications approach.

They claim to have completed the construction of a laboratory and of a 1,000 photon-based qubit quantum computer with a plan to reach 1 million-qubits in 3 to 4 years. The first part is probably a little oversold even if the second part is not far from PsiQuantum promises²⁰⁸⁰. Another promise is that this computer works at ambient temperature, which is a highly dubious claim since you generally need some form of cooling for your light sources and photon detectors. I finally found out in August

²⁰⁸⁰ Wen Kais thesis is [Experimental study of tune-out wavelengths for spin-dependent optical lattice](#) in ⁸⁷Rb Bose-Einstein condensation by Kai Wen et al, September 2021 (9 pages). It relates to cold atoms qubits, not photons. But QBoson’s communication is about photonic qubits controlled by lasers ([source](#)). All in all, one thing is sure: these guys don’t want you to know what they are doing exactly.

2022 that they are working on some sort of coherent Ising machines using spiking neurons in an arXiv paper²⁰⁸¹.



Duality Quantum Photonics (2020, UK) is a Bristol-based startup created in February 2020. Its founder is Anthony Laing, from the Department of Physics at the University of Bristol where he developed a quantum simulator based on lithium niobate generated photons.

He targets drugs design for the pharmaceutical industry. They were supposed to create a prototype in 2021.



TuringQ (2021, China, \$79M) creates lithium niobate on insulator (LNOI) optical quantum computer chips and femtosecond lasers. Not to be confused with Turing Quantum (USA) who is specialized in NV centers computing and Turing (USA) who develops quantum software. The company was created in Shanghai by Xianmin Jin, a student from Jian-Wei Pan.



Quantum Computing Inc. (aka QCI), also covered in the software vendors section, announced in February 2022 a “*business partnership and exclusive marketing agreement with QPhoton, Inc*”.

In the current newspeak, it simply means an [acquisition](#)! QPhoton (USA) was a stealth quantum photonics computing and sensing company based in New Jersey. They hold a portfolio of patents on quantum hardware, authentication protocols, simulators, photonic Lidar, imaging and covert communications. They were mostly a contract research company working for DARPA, DoD, NASA and other US federal agencies who spent \$30M on these projects. The company was created and headed by Yuping Huang, a professor from Northwestern University (Evanston, Illinois) and the Stevens Institute of Technology (Hoboken, New Jersey).



Figure 481: QCI photonic quantum computer package.
Source: QCI.

How about their Quantum Photonic System (QPS)? It is a nonlinear system. That’s all you need to know from them at this point (Figure 481)!

QCI announced in July 2022 having solved a combinatorial problem with 3,854 variables with its “Entropy Quantum Computing” (EQC) hardware that was running 70x faster than QCI’s 2021 hybrid DWave implementation²⁰⁸². We can suspect it is based on some form of photonic coherent Ising model and on QPhoton QPS architecture. In September 2022, its Dirac 1 Entropy Quantum Computer (EQC) was launched as a cloud-based subscription. In December 2022, the company announced that it was working with **Rabobank**, using the Dirac 1 EQC, to improve fraudulent card transactions detection. We’ll wait for a documented case study.


The company made the acquisition in May 2023 of **millionways** (2017, USA, \$10M) which develops an emotional AI platform that combines analysis and matchmaking algorithms using user-generated text or audio-to-text data with at least 500 words that is based on the Personality Systems Interactive (PSI) theory²⁰⁸³.

²⁰⁸¹ See [Combinatorial optimization solving by coherent Ising machines based on spiking neural networks](#) by Bo Lu et al, August 2022 (6 pages).


²⁰⁸² See [QCI Solves 3,854-Variable Problem in Six Minutes in BMW Group, AWS Quantum Computing Challenge](#) by Matt Swayne, The Quantum Insider, July 2022.

²⁰⁸³ See [Quantum Computing Inc. Signs Letter of Intent to Acquire Privately Held Artificial Intelligence Platform millionways](#), QCI, May 2023.


In February 2023, QCI spined out a subsidiary named **QI Solutions Inc** (QIE) to work with the U.S. Government and the DoD, working on entropy quantum computing, quantum communications and sensing.

 **QCDESIGN** (2021, Germany) was initially named It's Q and a photonic qubits startup created by Christine Silberhorn from the Institute for Photonic Quantum Systems (PhoQS) of the University of Paderborn.


The company was based on her research on frequency multiplexed qubits (“field-orthogonal temporal modes”), including the related pulsed photon pairs sources, and MBQC as well as quantum walks²⁰⁸⁴, using LiNbO₃ on silicon oxide insulator circuits (lithium niobate). Christine Silberhorn is also investigating GBS (gaussian boson sampling) avenues as part of the German project PhoQuant led by Q.ANT. Quantonation was one of It's Q seed investors. In 2023, the company abandoned the photonic qubit route and Christine Silberhorn left the venture which was renamed into QCDESIGN. It presented its plans at the Q2B in Paris in May 2023. The company provides FTQC architectural designs and blueprints to third parties. Their IP assets seem to revolve around the way to implement surface codes. They developed Plaque, their own FTQC simulator. The company CEO is Ish Dhand, a quantum computing researcher and former architecture team lead at Xanadu.

 **Quantum Source Labs** (2022, Israel, \$27M) is a photonic computer startup created by Oded Melamed (CEO), Gil Semo (R&D VP), Dan Charash (Chairman) and Barak Dayan (Chief Scientist, Associate Professor at the Weizmann Institute of Science, head of the Weizmann Quantum Optics group).

In May 2023, they added former prime minister Naftali Bennet to their board. They seem to run some contract research programs and among others, work with PsiQuantum. Given their founders background, you can infer that they have skills in designing photon guides in nanophotonic circuits, qubit conversions, nanofibers, MBQC and photon detection. They actually work on the generation of photonic qubits and clusters of photonic entangled states, based on single atoms trapped on a high-quality photonic integrated circuit. They look to fit one million photonic qubit source in a simple server rack²⁰⁸⁵.

 **PhotonicsQ** (2021, Israel) is a startup developing a photonics QPU chipset implementing some routing architecture to enable direct interactions between any qubits, independently of their physical proximity or quantity.

It is reusing concepts coming from classical CMOS and optical chip technology like pipeline processing through the use of photonic registers for intermediate result storage and tristate photonic buses to facilitate data-path structures. The company was cofounded by Moti Kintzlinger (CEO), Ron Folman (CSO and President, a professor of Quantum Physics at Ben Gurion University) and Itay Harel (COO).

 **Quanfluence** (2021, India) is a stealth company building some photonics-based quantum computer. The company was cofounded by Aditi Vaidya and Sujoy Chakravarty.



Rotonium (2022, Italy) is creating a photonic quantum computer using photon orbital angular momentum to encode quantum information. The company was created by Roberto Siagri (CEO) and Fabrizio T. (CTO).

²⁰⁸⁴ See for example [Fabrication limits of waveguides in nonlinear crystals and their impact on quantum optics applications](#) by Matteo Santandrea, Michael Stefszky, Vahid Ansari and Christine Silberhorn, March 2019 (16 pages).

²⁰⁸⁵ See [Investing in Quantum Source: best in class team & technology](#) by Omri Green, April 2023.

HP conducted research in quantum computing at its Bristol laboratory, UK, covering quantum computing, cryptography and quantum communications. They invested in "The Machine", conceptually far from a universal quantum computer and uses an optical bus to link the different components of a super-computer.

In partnership with HP, American and Japanese scientists proposed in 2008 the creation of an HPQC, High Performance Quantum Computer, with 3D qubit arrays realized in linear optics containing 7.5 billion physical qubits allowing to accumulate 2.5 million logical qubits²⁰⁸⁶. This project was left aside. HPE abandoned quantum computing entirely and explained it in 2019. They said they preferred to focus on neuromorphic processors and memristors²⁰⁸⁷. Their photonics specialist is **Ray Beausoleil**, based in Silicon Valley. He specialized in photonics and NV centers and abandoned this track, becoming a quantum computing skeptic. Somewhat along the lines of Gil Kalai, he believes that errors would increase faster than the growth in the number of qubits. Still, HPE invested in **IonQ** in October 2019 to show that it didn't entirely leave the quantum stage.

Quantum computing hardware key takeaways

- Superconducting qubits are the most common nowadays, implemented by IBM, Google, Rigetti, IQM and Origin Quantum among others. But they are noisy and do not scale well. One solution may be bosonic qubits like the GKP and cat-qubits which combine trapped microwave photons in cavities and superconducting qubits for their manipulation and readout (Alice&Bob, AWS and Nord Quantique). Also, the fluxonium qubits breed seems to generate some traction with work from Alibaba (China) and Atlantic Quantum (Sweden/USA).
- Quantum dots spin qubits could scale well due to their small size, the reuse of classical CMOS semiconductors manufacturing known-how, their higher working temperature enabling the usage of control cryo-electronics. They have however been demonstrated only at a very low scale at this stage.
- NV centers qubits have the benefit to be stable and to work potentially at ambient temperature. An increasing number of startups are playing in this field, like Quantum Brilliance (Australia and Germany).
- Topological qubits could bring the benefit of being resilient to some quantum errors and to scale better than other solid-state qubits. It doesn't really exist yet, particularly the Majorana fermions species looked after by Microsoft.
- Trapped ions qubits have the best fidelities so far, but they are hard to scale beyond about 40 qubits, at least with their main vendor, IonQ, Quantinuum and AQT.
- Cold atoms qubits are mostly used in quantum simulation where it could scale up to a thousand qubit and it could potentially also be used in gate-based quantum computing although it's not really demonstrated at a large scale. Pasqal (France), QuEra (USA), Atoms Computing (USA) and Planqc (Germany) are the key industry vendors in this field.
- Photon qubits are flying qubits, moving from a source to detectors and traversing optical devices implementing quantum gates. There are many investigated techniques, with the distinction between single/discrete variable photons and continuous variable photons. Scalability is also an issue, particularly with photon sources and the probabilistic nature of photons generation. Their limited quantum gates computing depth requires the implementation of specific computing techniques like MBQC and FBQC, this last one being used by PsiQuantum, the best funded quantum computing startup with IonQ as of 2022. Quandela (France), Xanadu (Canada) and QuiX (The Netherlands) are other key players in that space. One key capability to implement MBQC is the generation of deterministic high volume cluster states of entangled photons. It is still in its infancy.

²⁰⁸⁶ See [High performance quantum computing](#) (7 pages).

²⁰⁸⁷ See [Why HPE abandoned quantum computing research](#) by Nicole Hemsöth, April 2019.

Quantum enabling technologies

Building a quantum computer, and other second quantum revolution related products, requires combining a number of complex technologies, some of which are quantum-specific and others that have more generalist uses. These enabling technologies, which are covered in this section of the book, are critical components, especially in quantum computing, as their characteristics and performances frequently have a direct impact on the performance and scalability. We look here the following enabling technologies and their respective vendors in cryogenics, cabling, classical electronics, lasers, photonics (Figure 482) and also semiconductor manufacturing. The chapter will also address their supply chain, most specifically the provenance, scarcity and transformation of the raw materials.



Figure 482: a market map of key enabling technology vendors. (cc) Olivier Ezratty, 2020-2024.

Cryogenics

Most types of qubits require cryogenic technology, the most demanding being the very low operating temperatures of superconducting qubits, at 15 mK. Other technologies like photon qubits require lightweight cryogenics operating at about 4K for their photon sources and detectors²⁰⁸⁸. Detectors must indeed be cooled to avoid the photon dark count effect, when thermal noise originated photons are detected instead of useful photons.

In the following section, we will focus on the 15mK dry dilution refrigeration systems used by superconducting qubits. Among other reasons, these qubits must be cooled to this low temperature to avoid noise sources from the environment, particularly when compared with the microwave pulses used to control qubits and handle their readout²⁰⁸⁹.

²⁰⁸⁸ By definition, cryogenics operates below 123K or -150°C. Bearing in mind that -153.15°C is the temperature below which permanent gases, i.e. gases in the ambient air, all condense into liquid at ambient pressure.

²⁰⁸⁹ It is governed by the equation $k_B T < \hbar \omega$. The Boltzmann constant multiplied by the temperature must be inferior to the product of the Dirac constant and the microwaves frequency in Hz. This leads us to adopt a temperature of about 15 mK for superconducting qubits.

These cryogenic technologies are central to the operation of many quantum computers, and will need to integrate many innovations to accommodate the growth of quantum computers with large numbers of physical qubits.

Wet and dry dilution refrigeration

Superconducting qubit quantum computers from IBM, Google and others are frequently pictured as gold chandeliers containing wires, various devices and circular plates segmenting the central column into different sections. The systems combine passive and active control electronics that reach the qubits processor and control the low temperature cooling system. The bottom section of the chandelier houses the quantum processor. The chamber must isolate the chip from unwanted perturbances, requiring control over temperature, magnetism, vacuum, and even mechanical vibrations.

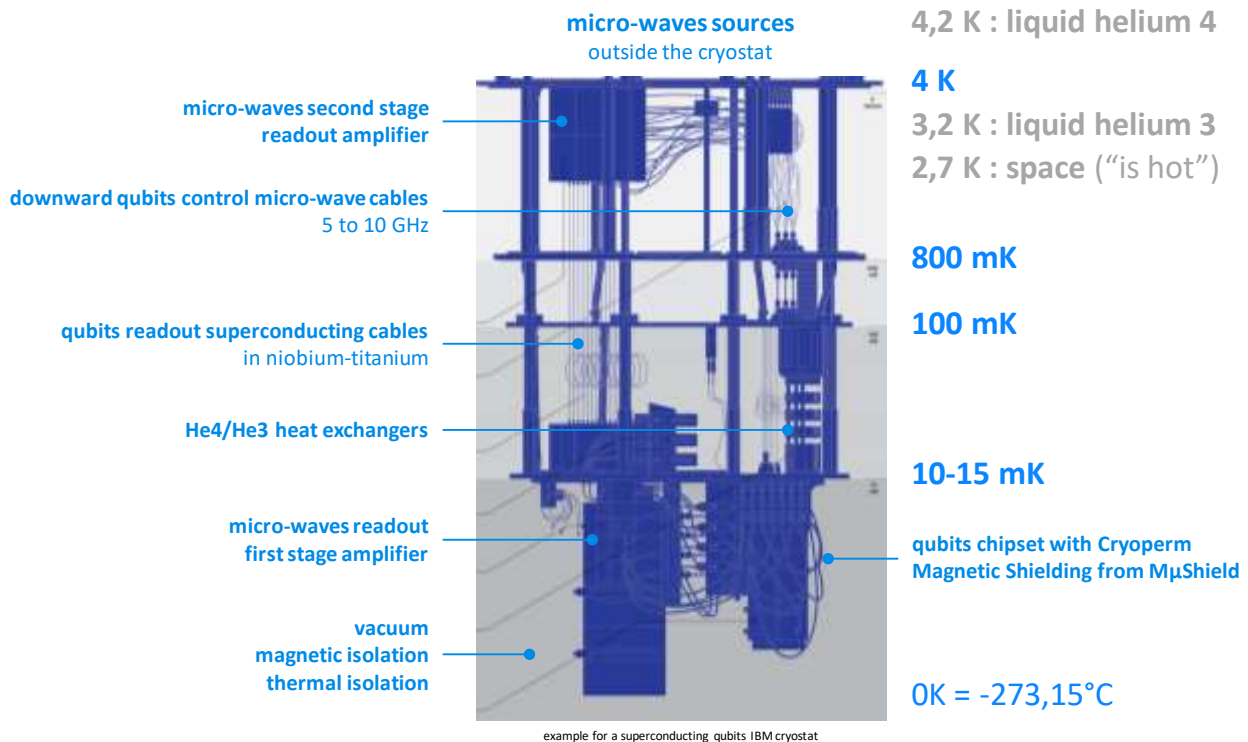


Figure 483: a documented interior of an IBM superconducting qubit cryostat. Image source: [Quantum Computers Strive to Break Out of the Lab](#), 2018. Legends by Olivier Ezratty.

The central column is the refrigerated part of a quantum computer with superconducting or silicon qubits. It is divided into stages, with the warmest sections at the top as shown in Figure 483:

- On the upper level, a plate, usually not represented in diagrams and pictures, is thermalized at 50K. This is where both the electronic cables for controlling and reading the qubits as well as the fluids used for refrigeration arrive in the cryostat.
- One level below, running at 4K, i.e., 4°C above absolute zero (-273.15°C)²⁰⁹⁰, sits the lower part of the pulse tube, which achieves cooling through oscillatory compression and expansion of an ideal gas within a closed volume.

²⁰⁹⁰ The Kelvin scale starts at absolute zero. This temperature where atoms literally no longer move is unreachable. If it were, Heisenberg indeterminacy would be broken! It is approached asymptotically. The lowest temperature record is 38 pK (pico-kelvin), reached in 2021. See [Collective-Mode Enhanced Matter-Wave Optics](#) by Christian Deppner, David Guéry-Odelin, Ernst M. Rasel et al, PRL, August 2021 (7 pages). See how fast these records have been broken over the last decades in [Moore's Law for Low Temperature Physics](#) by Pramodh Senarath Yapa, December 2021.

- The below plate is at around 800 mK. Between these two floors is the lowest temperature in space, which is 2.7 K and also corresponds to the cosmic background radiation.
- Another plate is generally located at a temperature of 100 mK.
- The lowest stage plate is where the quantum processor sits, and is cooled between 10 and 25mK, usually around 15mK. It is also called the "mixing chamber cold plate". A cold plate is a one-stage copper plate and the mixing chamber is the last level at the bottom of the dilution refrigeration system that we will explore later²⁰⁹¹.

We will now study the detailed characteristics of the very low temperature cryogenics used in these superconducting quantum computers²⁰⁹².

It uses a **dilution refrigeration**, which is based on the association of two helium isotopes: helium 4 and helium 3, which have different and complementary physical properties²⁰⁹³. They have respectively a boiling temperature of 4.2K and 3.2K. Helium 4 is superfluid at 2.17K while helium 3 is superfluid at a much lower temperature of 2.5 mK, at ambient pressure. The cryostat exploits the combination of three phases: a gaseous ³He phase and two liquid phases, one with ³He and the other with a mixture of ³He and ⁴He, with evaporation of the ³He in a mixed chamber²⁰⁹⁴. Let's explain first why helium is so important for low temperature cryogenics. Hydrogen becomes liquid at 20.3K²⁰⁹⁵, nitrogen at 77.4K and oxygen at 90.2K. These gases are useless for low temperature cryogenics.

On the other hand, ⁴He liquefies at 4.2K at ambient pressure and a ⁴He cryostat can reach 1K while ³He cryostats can go as low as 300 mK (Figure 484). The mix of ⁴He and ³He is used in so called dilution refrigerators reaching 15 mK²⁰⁹⁶. Note the low density of ⁴He which is 125g/L at 4.2K. There are two types of dilution refrigerators: "dry" and "wet".

In **wet dilution refrigerators**, a first system cools the enclosure to 4K with liquid ⁴He. A second so-called dilution system uses a mixture of liquid ⁴He and ³He with a flow circulating in ducts connecting the metal plates down to less than 15 mK in the bottom stage.

Wet dilutions system was used until the early 2000s (Figure 485). It was then replaced by dry dilution systems that are simpler to operate, especially to create quantum computers that are easy to install at customer sites, thanks to avoiding liquid helium.

²⁰⁹¹ In [Top 5 Trends in Quantum Technologies to Look for in 2020](#) by QuantumXchange, January 2020, we find: "Interestingly, IBM and Google are taking different approaches in the infrastructure of quantum computers. IBM's hardware resembles a chandelier with rings whereas the Google device looks like a chip". Which shows that they did not understand at all that IBM and Google had both a candlestick and a chipset. So they did not explore the hardware architecture of a superconducting quantum computer!

²⁰⁹² See [Cryostats Design ⁴He and ³He cryostats](#) by Guillaume Donnier-Valentin, CNRS Institut Néel, 2011 (91 slides), [Some Fundamentals of Cryogenic and Module Engineering with regard to SRF Technology](#), Bend Petersen, ESY Cryogenic Group MKS (95 slides) and [Development of Helium-3 Compressors and Integration Test of Closed-Cycle Dilution Refrigerator System](#), 2016 (5 pages).

²⁰⁹³ Helium was discovered indirectly in 1868 through the discovery of an unexplained spectral line in the light spectrum of the sun by astronomers Pierre Jules Janssen (1827-1907, France) and Joseph Norman Lockyer (1836-1920, United Kingdom). It was then isolated for the first time in 1895 by the Scottish chemist William Ramsay (1852-1916).

²⁰⁹⁴ See the video [Quantum Cooling to \(Near\) Absolute Zero](#) by Andrea Morello of UNSW which explains very well how dilutions work, 2013 (10 minutes). This illustration is inspired from a schema seen in inspired by [Cryostat design below 1K](#) par Viktor Tsepelin, October 2018. Bcc means body-centered cubic and hcp, hexagonal close-packed. These are two states of solid helium which are of no interest in dilution refrigerators. A phase diagram shows the phase of the element as a function of temperature (in X in logarithmic scale) and pressure conditions (in Y, 1 bar = atmospheric pressure). It shows that in the regime used below 1K, helium 3 is liquid and helium 4 is superfluid. This difference makes it possible to operate refrigeration at these low temperatures.

²⁰⁹⁵ Liquid hydrogen cryogenics uses spin variations of hydrogen, instead of isotopic ones. H₂ molecule exists in two forms, with both hydrogen atoms having the same spin (orthohydrogen) or an opposite spin (parahydrogen). At 300K, the ratio is 75% orthohydrogen and 25% parahydrogen. At low temperature, the ratio is different and the conversion between orthohydrogen and parahydrogen is exothermic, used in the refrigeration process.

²⁰⁹⁶ The first liquefaction of helium was achieved in 1908 in Leyden, the Netherlands, by Kamerlingh Onnes. The dilution cryostat concept was proposed by Heinz London in 1951 and was tested in 1965 at the University of Leiden, when it reached 220 mK. The record temperature went down to 60 mK in 1972 and then to 1.75 mK in 1999.

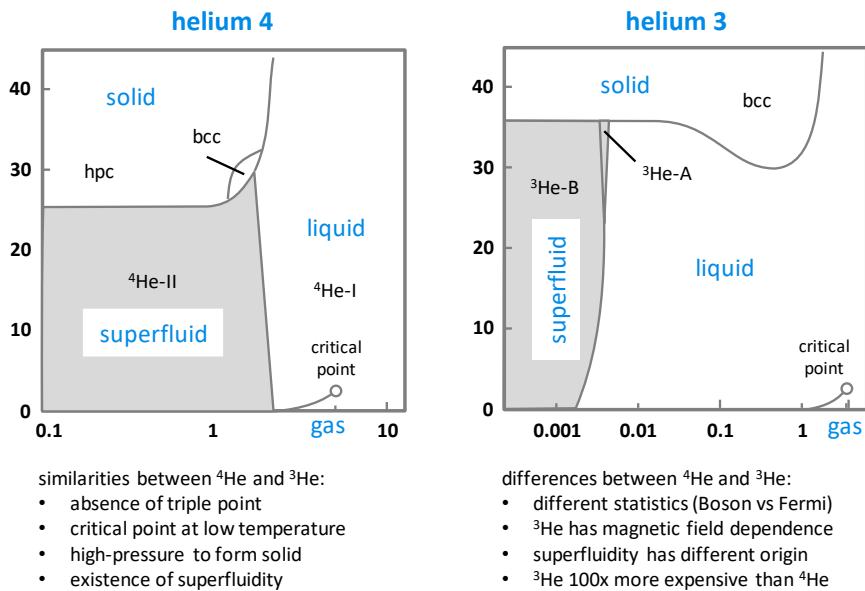


Figure 484: phase differences between helium 3 and helium 4. Source: [Cryostat design below 1K](#) by Viktor Tsepelin, October 2018 (61 slides).

However, wet dilution systems are still used for various physics experiments where the dry system is not appropriate, but usually not for quantum computing.

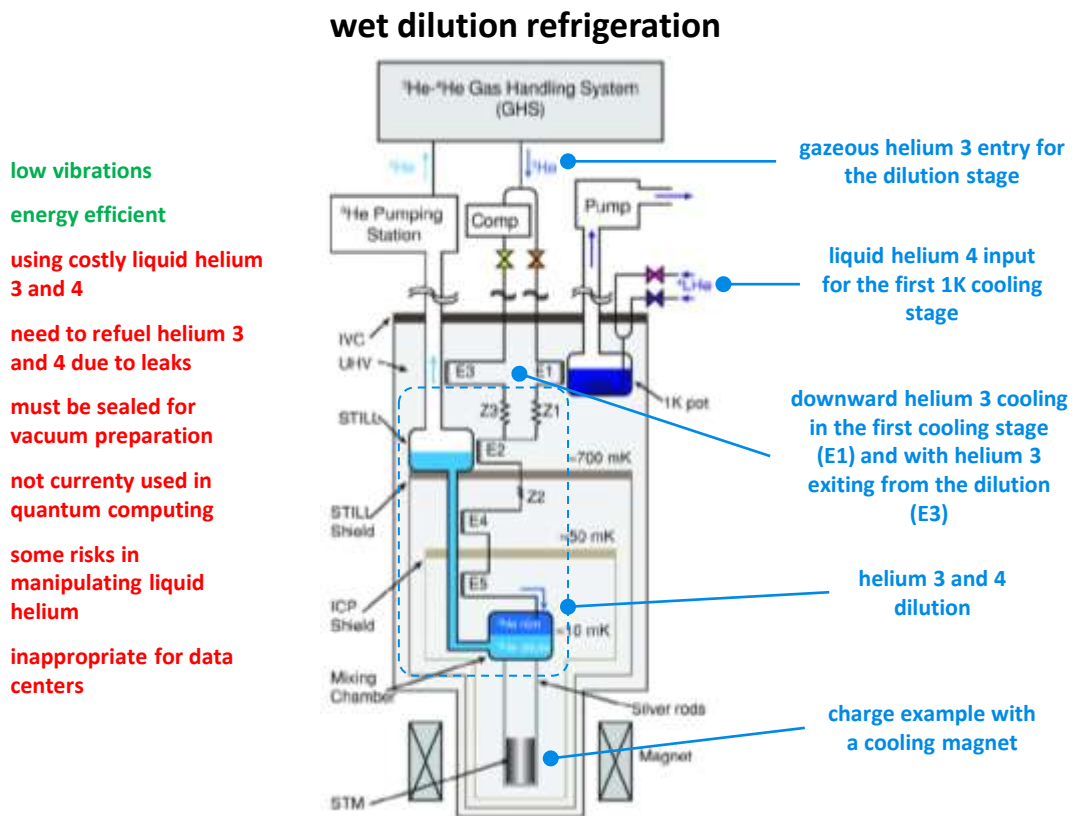


Figure 485: wet dilution refrigerator operations. Schema from Source: [Cryostat design below 1K](#) by Viktor Tsepelin, October 2018 (61 slides) and legends from Olivier Ezratty, 2020.

One interesting breed of wet dilution cryostats are inverted dilution refrigerators (IDR). I saw many of them at CNRS Institut Néel in Grenoble which has a dedicated cryogeny lab crafting custom cryostats for various use cases, including for astronomy. These inverted cryostats enable fast and easy experiment samples loading and fast cooling as well. Figure 486 shows an example IDR from Nicolas Roch's laboratory at Institut Néel.

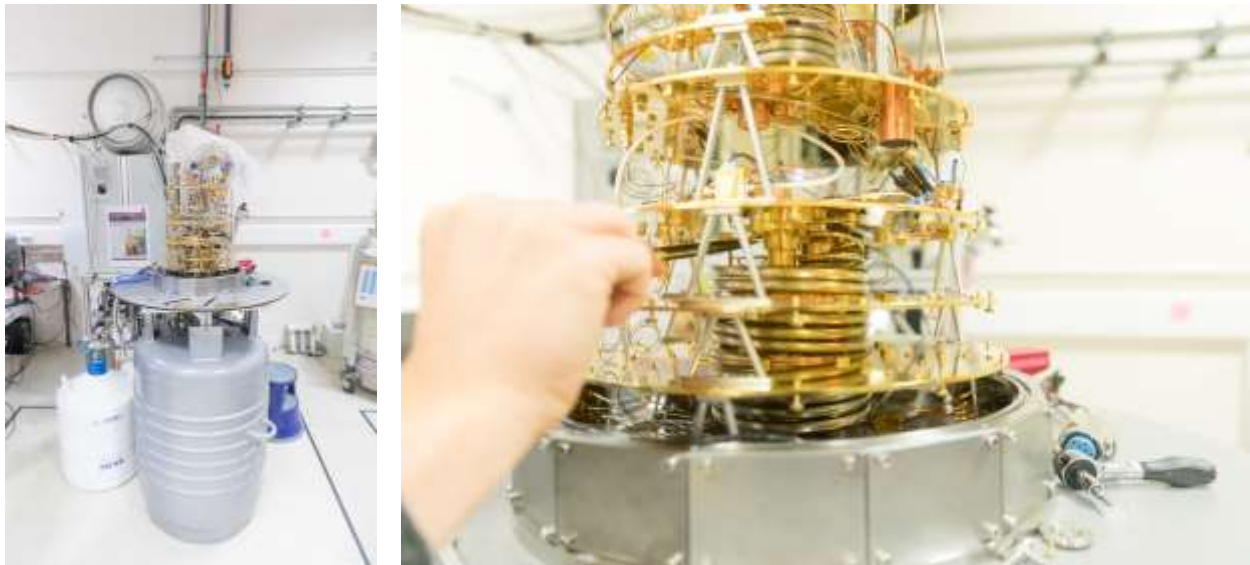


Figure 486: custom made bottom-up cryostats made at CNRS Institut Néel in Grenoble. Pictures source: Olivier Ezratty.

While most cryostats for quantum computers use dry dilutions, Fermilab is currently putting the final touch on an impressive wet dilution system developed to house a 3D supercomputing system, probably co-developed with Rigetti. Its numbers are impressive: it's got 625W of cooling power at 4.5 K. 50W at 2K and, above all, 300 μ W at 20 mK for a load fitting in a 2m wide cylinder. And it is using 2000 liters of liquid helium²⁰⁹⁷. What is interesting here is that 625K cooling power at 4.5K could have another application: superconducting (non-quantum) computing²⁰⁹⁸.

Likewise, PsiQuantum announced in March 2023 a collaboration with STFC's Daresbury Laboratory (UK) to build PsiQuantum's cryogenic for their photonic circuits handling photon generation, processing and detection. The developed cryogenic modules will support 100W of cooling power at about 3K. The project got £9M of funding from the UK government's Department for Science, Innovation and Technology (DSIT).

Dry dilution refrigerators or so-called cryogen-free refrigerators do not use liquid helium. They are using only gaseous helium 3 and 4. Like wet systems, they have two stages: the lower dilution stage is about the same with controlled expansion of helium 3 which is bathed at the bottom in liquid helium 4 in a dilution chamber. This covers cooling to temperatures lower than 1K.

The upper stage relies on the pulsed tube technique that manages cryogenics down to about 2.8K with helium 4 gas and a large external water-cooled compressor. This technique has been mastered for about twenty years and has been progressing incrementally since then. Its arrival coincides with the first experiments with superconducting qubits. Dry dilution refrigerators are generally used for the cryogenics of qubits requiring to go below 1K. Figure 487 explains how it works.

The pulsed tube is associated with a **Stirling** or **Gifford-McMahon** type compression and expansion system. The latter seems to be the most frequently used, particularly at **CryoMech**. It uses a piston. Stirling engines are used to cool infrared devices but not in dilution systems.

It can be seen in the curve on the right of Figure 489 that the available cooling power decreases rapidly with temperature. It is currently around 1W at 4K²⁰⁹⁹.

²⁰⁹⁷ See [A large millikelvin platform at Fermilab for quantum computing applications](#) by Matthew Hollister, Ram Dhuley and Grzegorz Tatkowski, Fermilab, August 2021 (10 pages).

²⁰⁹⁸ See [It's colossal: Creating the world's largest dilution refrigerator](#), Fermilab, December 2022.

²⁰⁹⁹ With larger liquid helium cryogenic installations like Helial SF from Air Liquide, a cooling power of 100W to 1kW can be generated at 4K.

There are no moving mechanical parts inside the cryostat, both in the pulse tube and in the dilution.

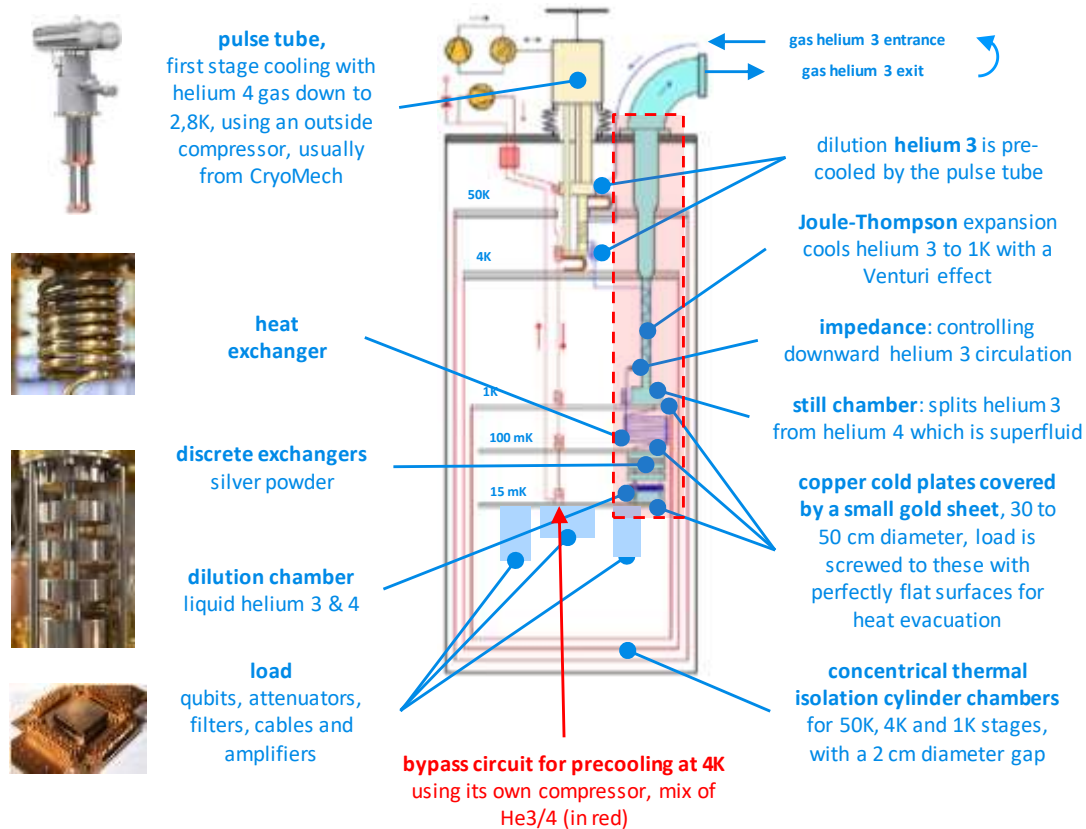


Figure 487: dry dilution schematic inspired from [Cryostat design below 1K](#) by Viktor Tsepelin, October 2018 (61 slides), illustrations from CryoMech documentation, Janis, [Dry dilution refrigerator with 4He-1K-loop](#) by Kurt Uhlig, 2014 (16 pages) and IBM.

This avoids the generation of unwanted vibrations that could disturb the wiring and the qubits which are very sensitive beasts. The flow of gases and liquids produces very little disturbance in the dilution process.

A refrigeration system is often evaluated in % of the Carnot cycle. This cycle describes a perfect thermodynamic cycle using four perfectly reversible thermodynamic processes involving work-heat exchange²¹⁰⁰. The efficiency of a thermal machine is never perfect with 100% of this cycle.

For a pulsed tube, a perfect Carnot efficiency would be about 1.4%, i.e. it would take 70W of energy to extract 1W at 4.2K²¹⁰¹! In practice, it requires about 10 kW, i.e. 152 times more! We thus obtain a **Carnot efficiency** of less than 1%. That's <1% of 1.4%! Indeed, we spend more than 10 kW to get 1W of power at 4.2K. So... at 15 mK to get 10 μ W? We do not evaluate the efficiency of the 15 mK stage of Carnot because it operates isobarically, i.e., at constant pressure, the thermal cycle being linked to a phase variation of helium 3. This stage is powered by heat exchanges between the pulsed tube and the helium 3 gas circuit.

The circuit shown in red in Figure 487 is used to pre-cool the cryostat in the thermalization preparation. This is done in three steps: first, by starting the pulse tube which cools the 50K and 4K stages with helium 4 gas and the external compressor of about 12 kW, in yellow.

²¹⁰⁰ See Cryogenic Systems by Pete Knudsen, 2018 (71 slides) which describes well the Carnot cycle principle.

²¹⁰¹ See [Lecture 5 Refrigeration & Liquefaction \(Part 1\)](#) by J. G. Weisend II (17 slides).

Then by using the pre-cooling circuit which will circulate a helium 3 and 4 mixture to the lower stages, and which will have been cooled by the pulse tube, in the circuit in red in the diagram²¹⁰². Finally, the dilution system takes over from the second one and is launched to be able to go down to 15 mK in the lower cold plate (in light blue).

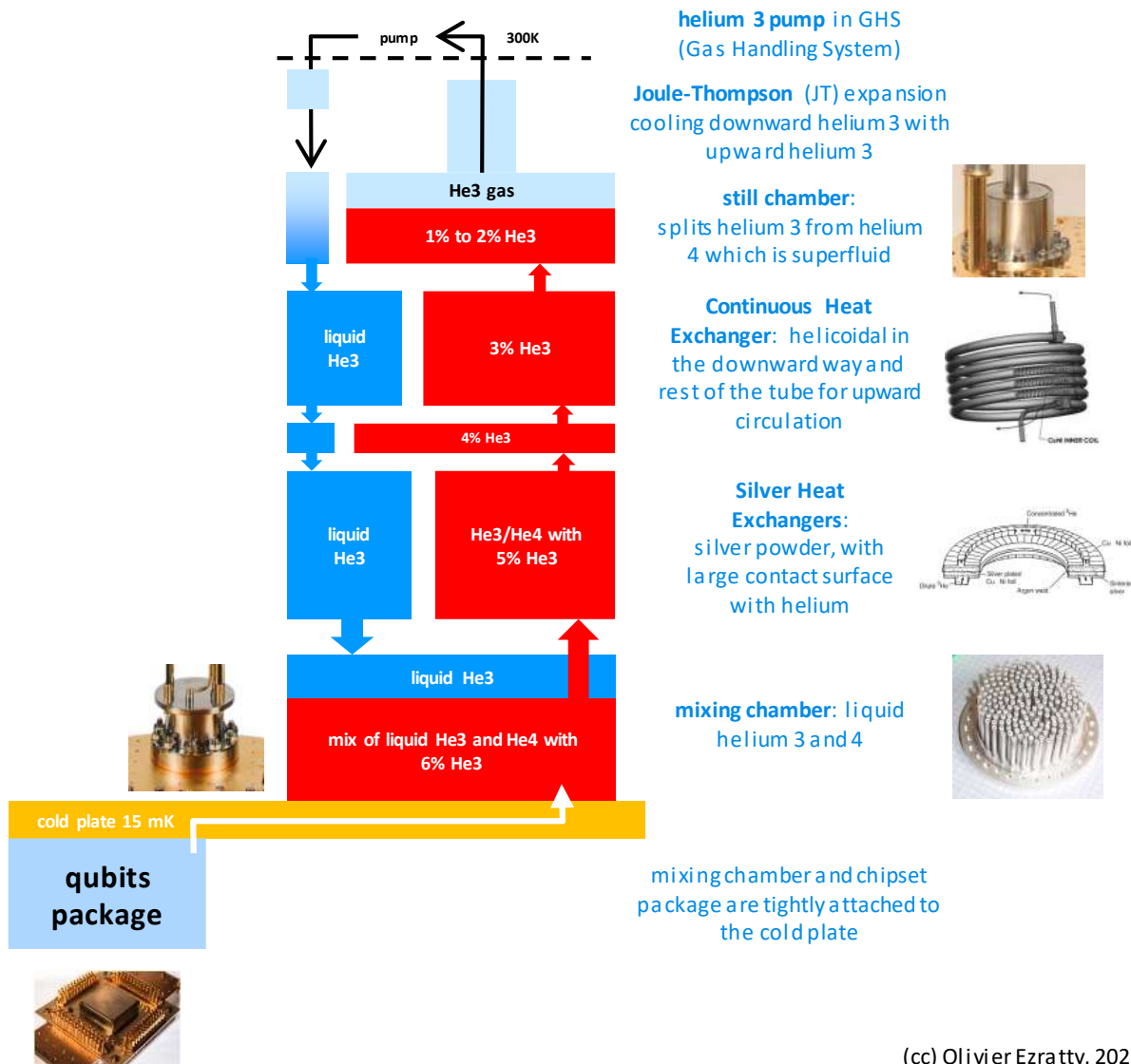


Figure 488: details of the dilution inner working and the phases of helium 3 and 4 that are used. (cc) Olivier Ezratty, 2021.

By adopting a rocket analogy, the pulsed tube and its 7 to 12 kW compressor are the equivalent of the first stage of a Saturn V rocket. The pre-cooling system is the analogue of the rocket second stage and the dilution system is the equivalent of the third stage that sends the lunar module and the LEM to the moon, here, the chip. Extracting the Earth's gravity over a large mass is equivalent to cooling a large metal mass inside the cryostat to 50K and 4K. While the dilution system is responsible for cooling a smaller mass from 4K to 15 mK, the lower cold plate and the payload attached to it.

The pulse tube compressor must itself be cooled, usually with water. Regular water-air based cooling systems add about 2 kW per pulse tube to the energetic bill.

²¹⁰² At CryoMech, the compressors adapted to these dilution systems consume from 7.9 to 12kW; from PT410 to PT420. About 4kW must be added for the GHS (Gas Handling System) which manages the dilution circuits with their pumps and controls as well as for the computer and the assembly dashboard.

Pulse Tube Cryocoolers

- Two general types
 - Stirling type
 - High frequency ~ 60 Hz
 - High efficiency: 25% of Carnot
 - Operation down to 10 K
 - GM type
 - Low frequency ~ 1-2 Hz
 - Split design = very low vibration
 - Ideal for 4 K operation (≤ 1 watt)

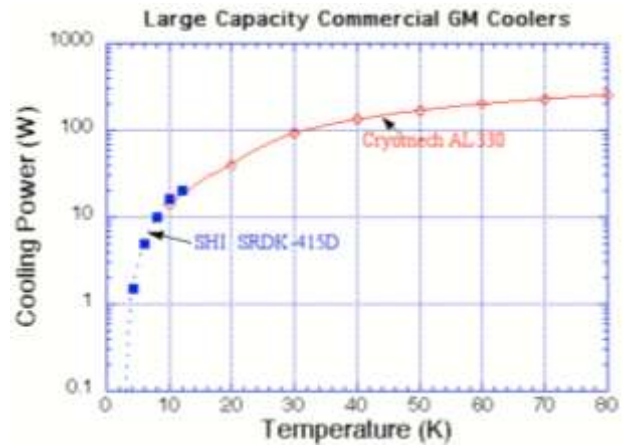
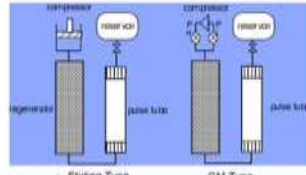


Figure 489: pulse tubes models with Stirling and Gifford-McMahon types. And commercial capacities available. Source: [Lecture 2.2 Cryocoolers](#), University of Wisconsin (25 slides).

These systems require optimization with a large number of parameters. The modeling of a cryostat could one day benefit from quantum computation, especially since the fluids used are in a superfluid quantum state.

A good part of the power is used to lower the temperature to 1K, because the mass to be cooled is the most important. The cylinder that protects the part cooled at 4K receives thermal radiation coming from the 50K stage. This makes a big thermal difference to absorb.

In a 15 mK cryostat of about 16 kW, about 12 kW will correspond to the 4K compressor, then about 1 to 2 kW to the dilution system, which is used to lower the temperature at 15 mK, containing the GHS (Gas Handling System) pumps and its control electronics, and at last, a water/air chiller to cool the water that cools the 4K compressor and can consume about 2 kW.

The dilution system does not use a compressor. The helium 3 circulating outside is just driven by a pump located in the GHS. The reason is that the helium 3 that returns to the cryostat is cooled by the pulse tube. In practice, all the cryostat heat is evacuated by the compressor of the pulse head which is itself cooled by water.

Figure 488 details the operation of the dilution system as well as the phase (liquid or gaseous) and the concentration of helium 3 and 4 in each stage and component. It shows the descending circuit of helium 3 which becomes liquid from the condensation at the boiler.

In the circuit going up from the mixing chamber, a liquid mixture of helium 3 and 4 rises and the concentration of helium 3 goes down as the stages go up. It is only in the boiler that helium 3 becomes gaseous. Helium 4 remains liquid and is evacuated downwards. It has moreover a tendency to rise due to superfluidity. A trick is to cut this rising film and send helium 4 back down.

The helium 3 landing in the dilution chamber at the bottom must end up there at a temperature barely above 1mK of the chamber temperature. It is pre-cooled by the helium 3 that is moving upward. The only way to achieve this is to increase the contact surfaces, which is done in the discrete heat exchangers just below the cold plate at the 100 mK level.

These dry cryostats still use a cryogen, liquid nitrogen at 77K, to filter helium gas and remove impurities²¹⁰³. This filtration is based on zeolite powder, made of microporous aluminosilicate crystals.

²¹⁰³ LN₂ for liquid nitrogen, gaseous nitrogen being a molecule of two nitrogen atoms.

The liquid nitrogen tank used for this pre-cooling is called a "cold trap"²¹⁰⁴. This filtering is completed in the cryostat 4K stage by another filtering system based on activated carbon powder which works better at low temperatures and increases the contact surfaces with the gas to better filter it.

As a general rule, the complete thermalization of a quantum computing cryostat takes about 24 hours. The so-called "1K" stage was actually cooled at about 1.2K in wet cryogenics and is around 800 mK for dry cryogenics. The power consumption is identical between the thermalization phase and the temperature maintenance of the instruments once the thermalization is completed.

Cryogenics at 10-20 mK is specific to quantum computers whose qubits must be cooled at very low temperatures, mainly those based on electrons (superconductors, electron spin, Majorana fermions). Theoretically, silicon qubits should only be cooled down to 1K but for the moment, they are still cooled down to about 15mK. An Australian team created a proof of concept of silicon qubits running even at 1.5K and another one from Intel and Qutech at 1.1K²¹⁰⁵.

To reach **lower temperatures**, below 3 mK, a complementary technique is used, adiabatic nuclear demagnetization (ADR or Adiabatic Demagnetization Refrigeration)²¹⁰⁶. It is not necessary for quantum computing. This type of refrigeration can be added to a wet or dry dilution cryostat. The principle consists in using a paramagnetic salt which is magnetized with a strong enough field, of 6 Tesla or more. This will heat the salt. The heat is evacuated via a 4K liquid helium bath. The suppression of the magnetic field cools the salt by expansion. The process complexity lies in the heating-cooling cycle which can disturb the cooled equipment. It is treated by combining several devices that take turns to smooth the temperature curve of the system. The process has been tried and tested for a long time, but the cooling power available is very low.

Even colder temperatures can be obtained with neutral atom cooling and Bose-Einstein condensates, below the nK threshold²¹⁰⁷. It is based on using laser-based cooling, magneto-optical traps and the likes.

kiutra (2017, Germany) uses this technique to obtain more classical temperatures of a few hundred mK, one of its advantages being that it does not generate vibrations²¹⁰⁸. These temperatures are interesting for cooling silicon qubits.

It is a startup from the TUM (Technical University of Munich) launched by Alexander Regnat. It was seed financed by APEX Ventures and German investors, but the amount is not known. Kiutra had a staff of 40 as of early 2023.

²¹⁰⁴ Liquid nitrogen is also sometimes used to pre-cool the metallic structure of the cryostat during the warm-up. This is unrelated to the helium circuit. This can save up to five hours for the cryostat thermalization. But this process is not commonly used for quantum computer cryostats. It is used for precooling heavier payloads for physics experiments using equipment weighing up to several hundred kilograms, including superconducting magnets. This technique is not used for quantum computing.

²¹⁰⁵ See [Hot qubits made in Sydney break one of the biggest constraints to practical quantum computers](#) by UNSW, April 2020 related to [Operation of a silicon quantum processor unit cell above one kelvin](#) by Andrew S. Dzurak et al, April 2020 (in nature) and in February 2019 on arXiv. The test was performed on 2 qubits with a unit gate reliability rate of 98.6% quite average but in line with what is currently obtained with silicon qubits. See also [Universal quantum logic in hot silicon qubits](#), 2019 (11 pages).

²¹⁰⁶ We owe the creation of the process to William Giaque (1895-1982, USA) in 1927. He was awarded the Nobel prize in physics in 1949.

²¹⁰⁷ See an interesting discussion on the limits of cooling in [Landauer vs. Nernst: What is the True Cost of Cooling a Quantum System?](#) by Philip Taranto, Marcus Huber et al, June 2021-September 2022 (61 pages) which makes a connection between Landauer's bound, the creation of quantum pure states and Nernst's unattainability principle, according to which infinite resources (time, energy) are required to cool a system to absolute zero temperature. They create a new Carnot-Landauer limit that generalizes Landauer's principle

²¹⁰⁸ See also [Cryogenic Fluids](#) by Henri Godfrin (now retired), 2011 (50 slides), from Institut Néel in Grenoble, which includes a leading research team on cryogenics. With a record of 100 μ K obtained with the DN1 cryostat using nuclear demagnetization.

Their cryostat range goes down to 100 mK (in pulsed mode) or 300 mK (in continuous mode), which is insufficient to cool superconducting Josephson effect quantum computers but could possibly be suitable for electron spin silicon chips that can theoretically be satisfied with a temperature of 1K.

Their system uses the magnetocaloric effect which was discovered in stages in 1881, 1917 and demonstrated in 1933 to reach a temperature of 250 mK.

The Kiutra process is based first on this classical effect also called adiabatic demagnetization. It consists in magnetizing a solid material with magnetocaloric properties (Figure 490). This makes it increase its temperature. This entropy is evacuated by a conventional heat transfer fluid, which is not specified. It may be helium 4 if it is a question of going down to a temperature of less than a few Kelvins. Then, the magnetization is stopped which leads the material to cool down (Figure 491).

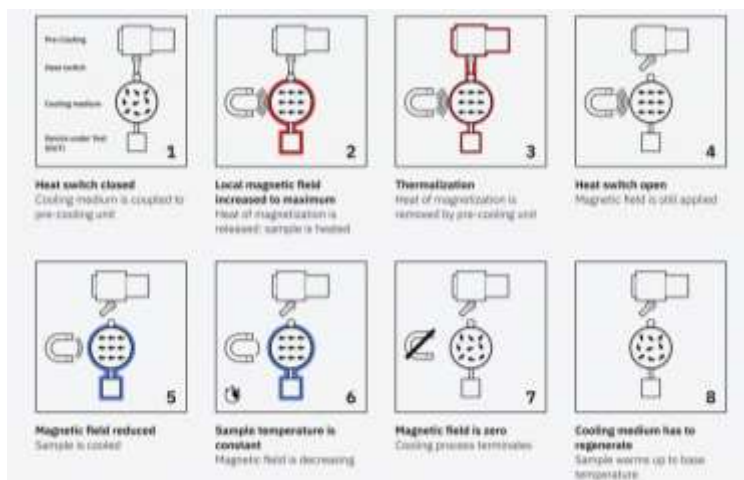


Figure 490: the Kiutra magnetic refrigeration process. Source: Kiutra.

To smooth in time and space this heating/cooling cycle, they combine several cooling units with what they call cADR (continuous Adiabatic Demagnetization Refrigeration)²¹⁰⁹.

The apparatus proposed by Kiutra seems to be mainly designed to cool small samples and does not seem to be yet adapted to the usual architectures of quantum computers with their cooling stages stacked between 4K at the top and 15 mK at the bottom. On the other hand, some dry cryostats can reach temperatures situated between 5 and 10 mK.

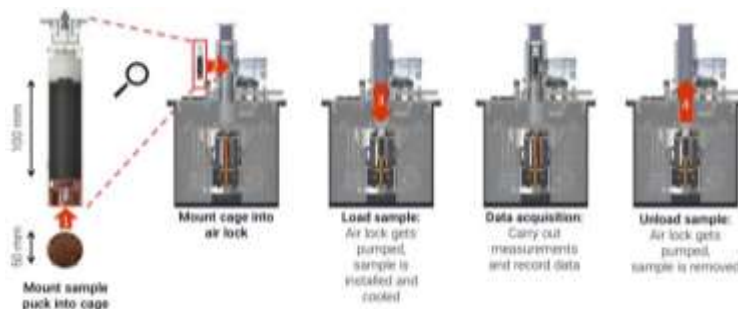


Figure 491: Kiutra cooling process. Source: Kiutra.

They are dedicated to physics experiments unrelated to quantum computing such as the search for dark matter (for the detection of WIMP, Weakly Interacting Massive Particles) and the analysis of cosmic radiation using calorimeters operating between 5 mK and 7 mK²¹¹⁰.

Dry dilution installation

A dry dilution refrigeration system is divided into two large parts with the compressor, pumps, liquid nitrogen and helium gas reservoirs positioned in one room, and the refrigerated enclosure in another room. This is quite logical since the compressor will generate heat that will have to be dissipated, via an incoming and outgoing water pipe²¹¹¹.

²¹⁰⁹ I discovered occasionally that this technique was also being explored at the Institut Polytechnique de Grenoble. See in particular the thesis [Magnetic Refrigeration: Conceptualization, Characterization and Simulation](#) by Morgan Almanza, 2015 (160 pages).

²¹¹⁰ This is the case, for example, of the CUORE (Cryogenic Underground Observatory for Rare Events) bolometer installed in Italy. The cryostat comprises five pulse tubes and cools a 750 kg payload of tellurium dioxide to 10 mK. It was looking for signs of beta decay that could prove the existence of Majorana fermions. In the end, it did not find any.

²¹¹¹ See this well crafted detailed explanation of how a dry dilution cryostat works: [Design and Analysis of a Compact Dilution Refrigerator](#) by Jacob Higgins, 2017 (47 pages) and [Dilution Refrigerators for Quantum Science](#) by Matthew Hollister, 2021 (47 slides).

With dry dilution refrigerators, the safety constraints are quite light compared to wet versions (see a typical setting in Figure 492). Wet dilution uses up to 80 liters of liquid helium which could drive a cryostat explosion if heated too abruptly because the expansion of the gas is important compared to its liquid state, with a ratio of 1 to 700. It was necessary to handle liquid helium canisters and fill tanks with protective equipment against splashes.

The oxygen level in the room could also dangerously decrease due to the accidental evaporation of nitrogen or liquid helium. Contact with cryogenic materials, particularly carbon steel, should also be avoided. Rooms must be large enough and care must be taken of in the higher zones in the room where helium can be concentrated since it is lighter than air.

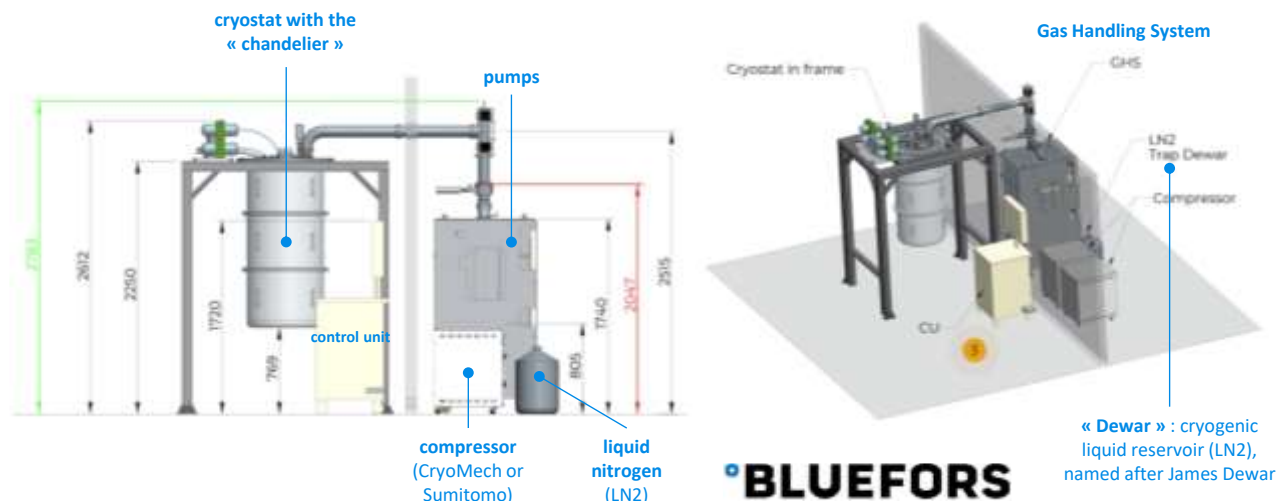


Figure 492: Bluefors recommendations for setting up one of their dilution refrigerators. Source: Bluefors documentation.

The wet dilution installation in Figure 493 is from CEA-IRIG in Grenoble, which deployed in June 2019 two systems from **Bluefors**. I visited it at the end of June 2019. These systems cost about 1M€ each. The CEA teams installed a device that allows the tested sample to be changed in just 7 hours. Thermalization can thus be planned at night, and in the early morning, the experiments can be resumed.

The phenomena of materials **expansion and compression** are significant at very low temperatures. This has an impact on the design of the whole device and the choice of materials. The materials that can be used are special steels with nickel, chromium, aluminum, bronze, copper, composite materials, niobium-titanium for wiring, nickel-copper alloys, indium for joints, kapton and mylar for insulation.

The refrigerated system is usually placed in **vacuum**. The management of high vacuum and ultra-high vacuum (UHV) are industrial specialties. Knowing that cryostats of superconducting and silicon quantum computers only require high vacuum between 5 and 10 mBar. They use commercially available pumps from e.g. **Pfeiffer** (Germany). Pumping only takes place when the system starts up and is deactivated once the system is thermalized at low temperature. Cooling down to 15 mK does not require ultra-vacuum pumping because in practice, at this temperature, all the gases become solid and settle on the walls of the material, generating a very good vacuum.

Using too much pumping to generate ultra-high vacuum could propagate dust from these solidified gases, damaging the qubits or the rest of the equipment in the cryostat. Ultra-high vacuum is used for cold atom-based computers.

Thermal leaks are coming from cables entering and leaving the enclosure or radiation. Numerous layers of thermally insulating materials are integrated in the cryostat. They are cylinders stacked upside down like Russian dolls. It is made of aluminum, copper and steel. Each cylinder and plate acts as a thermal insulator vs the lower cylinder.



Figure 493: Bluefors installation at CEA IRIG in Grenoble. Photos: Olivier Ezratty. 2019.

The quantum chip is **magnetically isolated** from the outside. Magnetic isolation uses several Russian doll enclosures made of various alloys, including **Mu-metal**, an alloy of nickel, iron and molybdenum, aluminum alloys and other superconducting alloys. The quantum processor can also be magnetically shielded. IBM uses a Cryoperm Magnetic Shielding from **M μ Shield**.

Apart from this magnetic isolation, cryostats in research laboratories may be supplemented by **superconducting magnet** systems that occupy the lower part of the cryostat cylinder. They have a cylindrical shape that surrounds a measuring instrument. These magnets are also supplied with liquid helium to guarantee the superconducting effect that is used to generate intense magnetic fields of several Teslas.

These fields are used to set up various experiments, particularly in astronomy or fundamental physics. They are sometimes used in quantum computing, especially with silicon qubits for electrons spin control²¹¹². At D-Wave, the magnetic field is reduced to one nano-Tesla (nT) in the computer enclosure, compared to the Earth's magnetic field, which can reach 65 micro-Teslas, giving us a ratio of 1 to 65,000. D-Wave communicates on a ratio of 1 for 50,000.

The **cold plates** at each stage of the cryostat are generally made of 99.99% pure copper with very low oxygen content to maximize their thermal conductivity²¹¹³ (Figure 494). They are covered with a thin a few microns thick layer of gold which serves as a protection against oxidation and radiation. It also has good thermal conductivity and is soft, which is very useful for solidly anchoring and cooling all the attached components.

On the right, an example of a BlueFors cryostat cold plate. These plates are custom perforated to allow all the cables to pass through, not including the cryostat components. All the holes must be used to avoid thermal leaks between the bottom and top of these cold plates.



Figure 494: cold plate with a gold finish which is used to facilitate the assembly with experimental devices and optimize thermal conductivity. Photo: Bluefors.

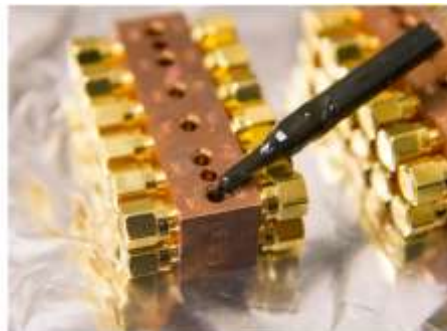
²¹¹² At CryoConcept, 8 or 14 Tesla magnets can be installed on the 4K stage next to the dilution unit.

²¹¹³ It is OFHC for oxygen-free high thermal conductivity. Source of this information: [Flying Qubit Operations in Superconducting Circuits](#) by Anirudh Narla 2018 (219 pages).

Infrared rays must be prevented from passing from one level to another and generating downward heat leakage.

These plates must be optically totally watertight screens so as not to let a single photon pass through! The trend is to increase the size of the cold plates, with a diameter reaching 50 cm. Knowing that their size is slightly decreasing from the top to bottom cold plates because of the concentric cylinder shields surrounding them.

In cryostats for quantum computers, the current standard for the bottom plate is 30 cm to 40 cm for research and 50 cm in production, to accommodate more electronic components. It could soon reach 100 cm. Infrared photons are filtered with an **Eccosorb** resin that surrounds the superconducting cables in the lowest stage of the system. This resin is a mixture of epoxy and metal powder. It is injected into copper filters (OFHC) that surround the cables in the coldest stage of the cryostat as shown in Figure 495²¹¹⁴. The resin is usually supplied by **Laird Performance Materials** (UK).



(A) ECCOSORB injection. Inject slowly and at a flat angle such that the liquid creeps onto the edge of the fill opening and into the cavity. Injecting too fast or steep will cause a planar bubble to form which blocks the opening (see Figure 3.8b).

Figure 495: how the Eccosorb resin is injected in the filters.

To reach ultra-low temperatures of 1 mK, the **Continuous Nuclear Demagnetization Refrigerator** technique can also be used, in complement with dry refrigeration²¹¹⁵. This temperature is required for some physics experiments but not with solid-state based quantum computers (superconducting or electron spin qubits). At such a low temperature, the cooling budget is equally super low, at just 20 nW.

Cryostats vendors

The main suppliers of cryostats for quantum computers are **BlueFors Cryogenics** (Finland), which equips IBM, Rigetti and many others, **Oxford Instruments** (UK), which is used by D-Wave and Microsoft, **Form Factor** (USA), used by Google, **Maybell Quantum** (USA), **Leiden Cryogenics** (the Netherlands)²¹¹⁶, which manufactures the most powerful cryostats on the market, used mainly for physics experiments, and **CryoConcept** (France), a branch of **Air Liquide** since 2020 (Figure 496). The world market for cryogenic systems, all categories combined, was about \$1.8B in 2020²¹¹⁷. Market share wise, BlueFors leads the pack with over 60% and >\$100M revenue, followed by Oxford Instruments and the rest.

Let us recall that the science of low temperatures used in quantum computing has benefited from numerous advances from other fields: space and especially space telescopes where a large part of the instruments needs to be cooled such as infrared sensors or bolometers, particle accelerators with their superconducting magnets and finally, medical imaging, especially MRI, which also needs low temperatures to cool its superconducting magnets.

²¹¹⁴ See some explanations of the Eccosorb resin in [Improving Infrared-Blocking Microwave Filters](#) by Graham Norris, 2017 (114 pages) and [Development of Hardware for Scaling Up Superconducting Qubits and Simulation of Quantum Chaos](#) by Michael Fang, 2015 (56 pages). Eccosorb is a product from Laird, a subsidiary of Dupont. It came from the acquisition of Emerson and Cuming in 2012. Eccosorb is a laminated structure of polyurethane foam generating a controlled conductivity gradient.

²¹¹⁵ See [Development of a sub-mK Continuous Nuclear Demagnetization Refrigerator](#) by David Schmoranzer, Sébastien Triqueneaux et al, Institut Néel, 2020 (7 pages).

²¹¹⁶ See [Leiden Cryogenics BV](#) brochure (28 pages).

²¹¹⁷ See [Cryocooler Market by Type \(GM, PT, JT, Stirling, and Brayton Cryocoolers\), Services \(Technical Support, Repair, Preventive Maintenance\), Heat Exchanger Type \(Recuperative and Regenerative\), Application, and Geography - Global Forecast to 2022](#), December 2019. This market represented \$1.4B in 2018 and is expected to grow 9.3% annually by 2027. But beware, the market for quantum computers cryostats is a rather small share of this market.

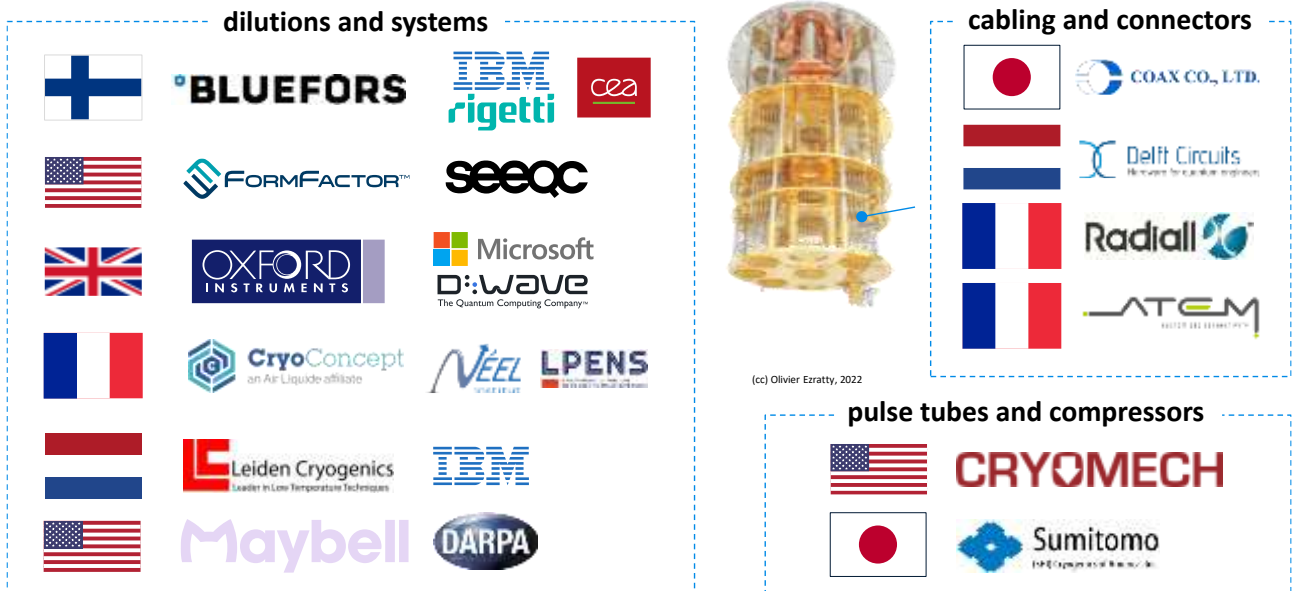


Figure 496: the main vendors for quantum computer low temperature cryostats, their compressor, cabling and connectors. (cc) Olivier Ezratty, 2020-2022.



Bluefors (2007, Finland) is the worldwide leader of low temperature cryogenic systems, using dry dilution with a market share exceeding 70% for dilution refrigerators. It is focused on the quantum computing market.

The spin-off from Aalto University delivered over 700 systems with its 250+ employees. It has a broad range of dry dilution systems, with some cabling (coaxial, ribbon, optical) and filters, QDevil X, codeveloped with **QDevil**. They acquired **Cryomech** (USA) in March 2023, the leader in 4K compressors. Figure 497 presents a typical configuration of their entry level cryostats.

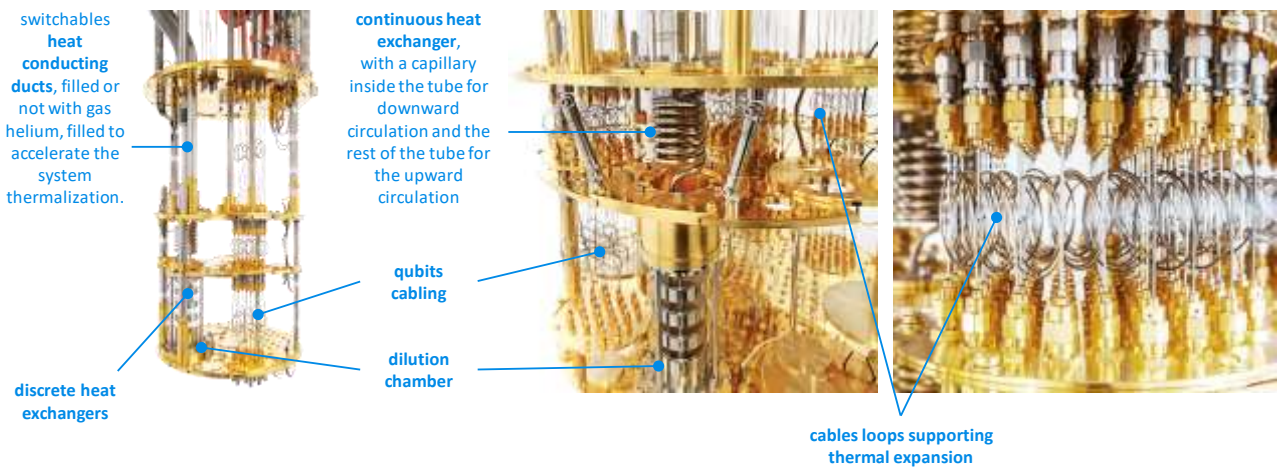


Figure 497: details of a Bluefors cryostat with custom comments. Source: Bluefors.

In March 2021, Bluefors announced a partnership with **Linde** (Germany) to create high-capacity cryogenic systems dedicated to scalable quantum computers. Linde is a gas producer competing with Air Liquide!

They also developed with **Afore** (Finland) a Cryogenic Wafer Prober, a system used for the characterization of 300 mm wafers at 4K (Figure 498). It was acquired by **CEA-Leti** in 2021 to test the quality of their silicon qubits wafers.

Intel acquired a similar tool as well, for their own silicon qubits development efforts in their D1D fab in Hillsboro, Oregon, USA.



Figure 498: the Bluefors/Afore cryoprober used by Intel and CEA-Leti.

In November 2021, Bluefors announced KIDE, its new generation of cryostats, that has a hexagonal shape to make it easier to assemble them next to each other for distributed QPU setups and with 9 pulse tubes and three dilutions each (Figure 499). Its production started in 2023 for IBM and Rigetti. The KIDE seems to have a width of about 1.5 m wide for the vacuum chamber. Its steel and aluminum doors are easy to open for loading stuff. It contains 9 pulse tubes and 3 dilutions.

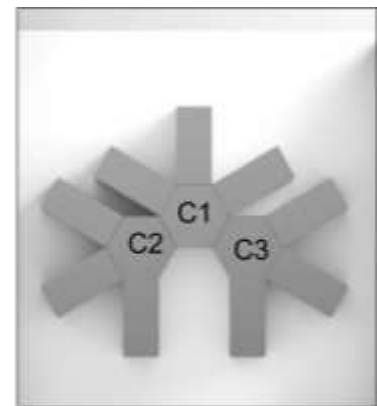
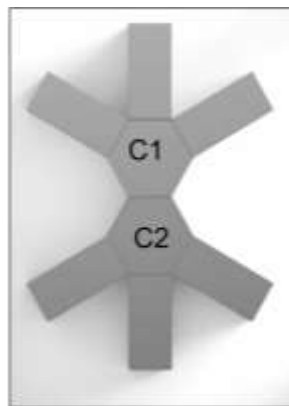


Figure 499: BlueFors KIDE dilution refrigerator (left) and how it could be arranged with 2 or 3 joined units, enabling short-range microwave interconnection between close QPUs. Sources: Bluefors and IBM. 2022.



JanisULT (1961, USA) was initially Janis, a generalist cryostat manufacturer. In 2020, they sold their ‘classical’ laboratory cryostats business to Lake Shore.

They kept their ultra-low temperature cryostat business under the brand Janis ULT. They have an offering of wet and dry dilution refrigerators for various use cases, including quantum computing. Their high-end wet dilution refrigerator is the JDry-500-QPro with a 508 mm cold plate and >450 μ W of cooling power at 100 mK achieved with a single pulse tube, coming from Sumitomo SHI.



FormFactor (1993, USA) is a provider of electronic test and measurement tools for the semiconductor industry with some products dedicated to quantum technologies who is consolidating the dry dilution refrigerators business in the USA.

They acquired in early 2022 the dry-refrigerator business line from Janis ULT. Their offering covers chipsets inspection and metrology, characterization, modeling, reliability, and design debug, to qualification and production test. In 2020, they acquired **High Precision Devices** (1993, USA), which develops cryogenic instruments adapted to superconducting quantum chipsets. Thus, their HPD IQ3000, a cryogenic probe stations for on-wafer and multi-chip measurements (left in Figure 500). It can embed IR-sensor test, radiometric test and configurable DC and RF cabling and custom probe cards. It supports 150 mm, 200 mm and 300 mm wafers at 4 K (while Bluefors’ probe station also supports 300 mm wafers).

The HPD IQ2000 is a chip-scale prober for individual die testing operating at 2K or at 4 K. The tested chipset can be thermalized from 300 K to 4 K in less than an hour (*right* in Figure 500).



Figure 500: FormFactor HPD IQ3000 cryoprober and HPD IQ2000 chip-scale prober. Source: FormFactor. 2023.

They sell dry dilution refrigerators supporting 10 mK and below temperatures that are used for test and measurement (JDRY-250, JDRY-500, and JDRY-600, this last one offering a 630 μ W cooling power at 100 mK and 17 μ W at 20 mK), all coming from Janis ULT.

They also sell one or two-stage ADR (Adiabatic Demagnetization Refrigerators) using a salt crystal to strong magnetic fields, complementing dilution refrigerators. Among others, FormFactor partners with SEEQC and Keysight.



Oxford Instruments (1959, UK) is an established British company, listed on the London Stock Exchange since 1999, specializing in scientific instrumentation including cryogenic systems capable of reaching 5 mK²¹¹⁸.

They also provide CCD cameras to detect the state of trapped ion qubits, electron microscopes, vacuum deposition systems, X-ray sources and cameras, and nuclear magnetic resonance spectrographs. The company had acquired VeriCold Technologies (Germany) in 2007 to gain control of pulsed tubes used in the first stage refrigeration for dry dilution cryostats. Their last product is the Proteox, a high-end and flexible dry dilution system with removable cabling (Figure 501).

In March 2021, they launched the ProteoxLX. It expands the qubits hosting capacity with a larger sample space and coaxial wiring capacity, low vibration and integration of cryo-electronics components. It offers a cooling power of 25 μ W at 20 mK and 850 μ W at 100 mK with twin pulse tubes providing up to 4 W cooling power at 4 K.

They also designed a Q-LAN, a cryogenic link that could be used to connect two dilution fridges. The payload can reach 20 kg at 20 mK and 125 kg at 4K.

²¹¹⁸ See [Principles of dilution refrigeration](#) by Oxford Instrument (20 pages) which also documents well the architecture of a cryostat.

Enabling the future of Quantum Computing scale-up

- Exceptional capacity for signal lines and cold electronics
 - 530 mm diameter mixing chamber plate
 - Two large Secondary Inserts with 117 mm x 252 mm fully customisable space – up to 256 UT85 SMA lines per system
 - 10 KF50 non line of sight ports for DC wiring
- Highest cooling power system
 - 25 μ W at 20 mK
 - Twin pulse tubes at 1.5 W or 2.0 W per Pulse Tube Refrigerator (PTR) provide up to 4.0 W cooling power at 4 K
- Low base temperature < 7 mK



Figure 501: Oxford Instruments ProteoxLX. Source: Oxford Instruments.



CryoConcept (2014²¹¹⁹, France, acquired by Air Liquide in July 2020) stands out with cryostats ensuring a very low-level of vibration via their UltraQuiet technology.

They have deployed more than 120 cryostats in 13 countries for various players such as the CEA in Saclay and the ENS²¹²⁰. Since 2018, CryoConcept has been collaborating with CEA-Leti to deliver two large cryostats to equip the QuCube project for silicon qubits. They sell worldwide including in the USA, Japan and South Korea in a market driven by dark matter research and bolometry. The unique low-level of vibrations of their cryostat is related to the absence of mechanical contact between the pulse tube and the cryostat.

Thanks to this feature, vibrations are reduced in the range from 1Hz to 1kHz. This absence of vibration is useful to preserve qubits coherence as for cryostats installations containing bolometers that are used to perform physics experiments such as in dark matter research. This experience in bolometry enabled CryoConcept to develop highly reliable dilution fridges, with systems running for more than one year without interruption. This reliability is a key attribute sought after to operate future quantum data centers.

Historically, CryoConcept started by manufacturing wet cryostats and kept an expertise in this field even though dry systems are now the most commonly manufactured dilutions. Now associated with Air Liquide, CryoConcept is working on coupling helium liquefiers with dilution refrigerators in order to overcome the current cooling power limitation at 4K, thanks to their refrigeration technology from 300 K down to 20 mK. This will ensure cooling power adapts as the number of qubits in the related quantum processors is growing.

With the acquisition by Air Liquide, CryoConcept has standardized the manufacturing of the dilution core of its system, with a production capacity of about 20 units per year. Those units can each deliver

²¹¹⁹ CryoConcept was in fact created in 2001 by technology transfer from the CEA where Olivier Guia had worked. The company has had several different owners including French company Segula Technologies and American company CryoMagnetics. Olivier Guia took over the company in 2014. They then reintegrated the in-house R&D and in particular recovered the technological mastery that was at the CEA.

²¹²⁰ See the quantum equipment of the ENS (Ecole Normale Supérieure, in France) in their [Labtour](#).

20 μ W of cooling power at 20mK and can be inserted in systems of arbitrary size. One of those large systems is currently being manufactured for the French consortium QRYOlink, and one even larger for a major quantum computing industry player.



Leiden Cryogenics (1992, the Netherlands) was founded by Giorgio Frossati and Alex Kamper. The former had been working on dilution refrigeration since the 1970s. Among other things, he invented silver powder heat exchangers.

He started to work at the Centre de Recherche sur les Très Basses Températures in Grenoble, which became the research center on Condensed Matter and Low Temperatures (MCBT) of the Institut Néel of the CNRS. He then became a professor at the University of Leiden in the Netherlands. He designed there a dilution refrigerator reaching a record temperature of 1.85 mK with a cooling power of 25 μ W at 10 mK. The heat exchanger technologies he developed were licensed to Oxford Instruments. At last, BlueFors was created by Giorgio Frossati's post-docs! What a small world!

Leiden is behind what looks like the largest very low temperature cryostat ever build for a large load as shown in Figure 502. It was achieved between 2016 and 2018 for CUORE (Cryogenic Underground Observatory for Rare Events).

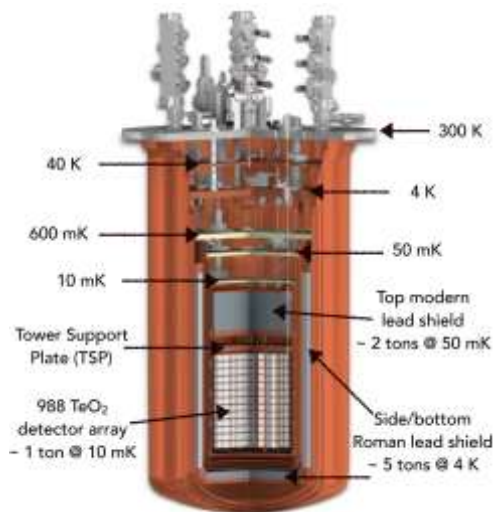


Figure 502: the CUORE mega-cryostat cooling a load of one ton.

It is a bolometric experiment for neutrinoless double-beta decay detection in TeO² (tellurium dioxide) that is installed at the underground facility of Laboratori Nazionali del Gran Sasso (LNGS) in the Alps. The CUORE cryostat is cooling a one ton mass of metal with a one cubic meter size to 7mK. It is using a three stage cooling system with liquid Helium vapors for the first stage at 50K, 5 CryoMech PT415 pulse-tubes and compressors for the 4K stage and only a single Leiden modified dilution for the <10mK stage. Interestingly, the cooling power of the lowest stage is only of 3 μ W at 12 mK, lower than the max cooling power at 15mK of most dilutions analyzed in this section. The difference is it took 26 days to cool down the experiment, including only 4 days for the last stage of one ton after 22 days to reach 3.4K²¹²¹.



ICE (2004, UK) aka ICEoxford was created in 2004 by Chris Busby and Paul Kelly to design and manufacture custom wet and dry Ultra Low Temperature (ULT) cryostats (but not below 300 mK) and High Magnetic Field equipment for research applications.



Maybell Quantum (2022, USA, \$26M) is a new company created in Colorado by Corban Tillemann-Dick (CEO, formerly at the BCG), Kyle Thompson (CTO, from the MIT Lincoln Labs and Janis ULT) and Brian Choo.

The company initial funding came from Colorado's Advanced Industry Accelerator (AIA) venture fund and the US DoD National Security Innovation Capital fund (NSIC) which belongs to the Defense Innovation Unit. The company said it already has some contracts from DARPA. It develops a dilution refrigerator, the Icebox, that is intended to support three times more qubits in 10% of the usual space, all at a temperature below 10 mK. Above all, they announce a capacity of 4,500 cables to drive qubits with microwaves up to 12 GHz (meaning: superconducting qubits and electron spin qubits) thanks to their Flexlines, ultra-high-density RF ribbon cables and Super-Flex NbTi ribbons cables for the lower

²¹²¹ See [The CUORE cryostat](#) by A. D'Addabbo et al, August 2018 (8 pages).

stages of the cryostat. Their Resito-Flex (CuNi-NbTi, BeCu-NbTi, CuNi-CuNi) and Atenu-Flex (SS-NbTi, SS-SS, SS-CuNi) ribbons are adapted to higher-temperature stages. It is optimized for 1,000 qubits QPUs. They also provide classical coaxial cabling and fiber optics connectivity. The whole cryostat fits into two 19” server racks formats with extra space available for 9U of electronics and computing. But it doesn’t contain the compressor and the GHS (gas handling system) that controls the flow of helium in and out of the compressor and requires a space equivalent to their own system. The helium compressor can be cooled with air or water. On top of that, the Maybell Icebox experimental part is supposedly accessible with a simple door (Figure 503, *left*).

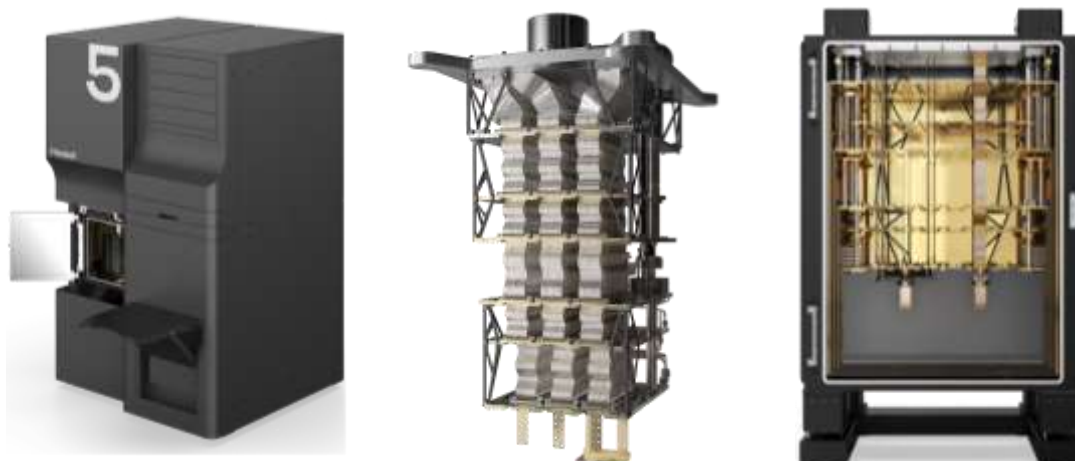


Figure 503: the Maybell Quantum cryostat unveiled at the APS March meeting 2022 in Chicago (*left*) and the Big Fridge announced in 2023 (*right*). In the middle, their dense flexible cables setup. Source: Maybell Quantum.

In 2023, Maybell Quantum launched its Big Fridge, a whole dilution refrigerator solution designed for scale. It has 130L of sample volume and 600L of total internal volume, and over 4,000 cm² of area on the mixing chamber plate (Figure 503, *right*). In September 2023, Maybell Quantum set up a European headquarters and regional R&D center in Copenhagen, Denmark.



Absolut System (2010, France) was created by Alain Ravex, former head of the low temperature department of the CEA in Grenoble in the 1980's and 1990's, then a consultant for Air Liquide. He sold the company to his partners and now consults for them and other players in the cryogeny field.

The company develops custom cryostats running at temperatures higher than 1.8K and targets a wide range of applications in research and in the industry, particularly for the production of liquid nitrogen. Their customers include CEA-Leti, Thales and Air Liquide. They are based near Grenoble.

They developed the ACE-Cube (Advanced Cryogenic Equipment), a cryogen free helium cryostat using a remote cooling technique. It is implemented for specific infrared detectors and semiconductors characterization and above 10K.

They also launched AFCryo (2017), a joint subsidiary in New Zealand, with Fabrum Solutions (2004) also based in New Zealand²¹²².



MyCryoFirm (2013, France) produces dry cryostats, running at 3K with a cold plate of 250 mm diameter with a 300 mW cooling power at 4.2K. They rather target the field of research in quantum optics, quantum physics and quantum sensing.

²¹²² See [Commercial Cryocoolers for use in HTS applications](#) by Christopher Boyle, Hugh Reynolds, Julien Tanchon and Thierry Trollier, 2017 (29 slides).

They propose various experiment decks/plates adapted to creating magnetic fields, spectroscopy applications and the likes. In 2022, they did add a dilution option on their Optidry250 cryostat and made it operate at 50 mK at Météo France. The company was acquired by Pasqal in 2022. Pasqal indeed needs 4K custom cryostats assemblies to cool its QPU ultra-vacuum pump and atom chamber.

CRYOMECH (1963, USA) is a supplier of components for cryostats and in particular dry cooling systems comprising a pulsed tubes and a compressor which are integrated in the cryostats of most market players such as BlueFors and CryoConcept.

These pulse tubes (Figure 505) and compressors (Figure 504) are the first stage of dry dilution refrigeration systems. They use an expansion system of compressed gas outside the cryostat with no rotating parts in the cryostat²¹²³. The compressor is water-cooled, with a flow rate of 5 to 12 liters per minute depending on the incoming temperature. But this water must also be cooled, and it can require up to an additional 10 kW of electric power unless the computer is located in a cool region.

Their pulse tubes range includes the PT415 and PT420 (*right in Figure 505*). Its main competitor is the SHI Cryogenics Group subsidiary of **Sumitomo** (Japan, *left in Figure 505*)²¹²⁴. These compressors are sold combined with their related pulsed tubes. At the APS March meeting in Las Vegas, in March 2023, Cryomech introduced a new high-range compressor (CP3000) and pulse tube (PT450) with a record cooling power of 5.0 W at 4.2 K.

In March 2023, Bluefors announced its acquisition of Cryomech, creating some turmoil in the dilution refrigerator industry, given Cryomech is the de facto standard with many of them.



Figure 504: a Cryomech compressor, that is connected to a pulse tube (on the right). Source: Cryomech.



Figure 505: Cryomech PT420 and Sumitomo pulse tubes, that cool a cryostat down to 4K. It is also used to cool down the helium 3 and 4 mixture circulating in a dilution that is attached to the pulse tube. Source: Cryomech.



Intelline (2018, Canada) produces customized cryogenic refrigeration systems that are expected to be more affordable than those of its competitors. But they seem to target markets other than quantum computer cryogenics, at least at temperatures below 1K.



CryoFab (1971, USA) provides liquid helium containers and related accessories.

²¹²³ These pulsed tubes are used in particular in the semiconductor industry, in vacuum deposition machines (CVD, MOCVD) and plasma deposition machines. They are down to 10K, which is sufficient for semiconductor production.

²¹²⁴ There are other pulse head and compressor manufacturers such as Fabrum Solutions (New Zealand) but the latter only targets temperatures of 77K for liquid nitrogen production.



Cryogenic Limited (1991, UK) provides a various set of cryogenic systems and superconducting magnets. It includes liquid helium systems and ultra-low temperature systems using their own magnet and an off-the-shelf cryostat from Leiden.



Qinu (Germany) is a new company selling mK and 4K cryostats. It was created by a former researcher from Institut Néel in Grenoble, which has its own cryostats design laboratory.



Attocube Systems (2001, Germany) has different line of businesses including cryostats mainly targeting the research community. It sells the attoDry series, closed-cycle dry cryostats (with cooling temperatures ranging from 1.65K to 4K), and the attoLIQUID series (300 mK), liquid helium cryostats.



Montana Instruments (2009, USA) develops cryostats and vacuum pumps, used in trapped ions (including IonQ) and NV centers computers as well as photon-sources (Sparrow Quantum).

One of their added values is to reduce the vibrations coming from the pulse tube. They cover temperatures ranging from 3.2K to 4.9K.



Zero Point Cryogenics (2017, Canada) is a company created by John P. Davis (CTO) from the University of Alberta. It provides compact dilution fridge designs including an inverted dilution (Model I) and a classical dilution (Model L).

Ulvac Cryogenics (Japan) provides various cryogenics solutions including 4K pulse tubes and also 4K cryopumps that can be used in cold atoms and trapped ions QPU settings.

There are many other cryostats and cryogenic devices vendors, but they are less specialized in serving the needs of quantum technologies providers²¹²⁵.

Cooling budgets

The level of cooling power at ultra-low temperature is quite low. This limits the energy that can be released by the qubits themselves and by the microwave attenuation and amplification circuits used to read the state of the qubits. Figure 506 shows a comparison of these cooling power budgets by supplier.

	cryostat	pulse tubes	minimum temperature	20mK stage	100mK stage	MC cold plate
°BLUEFORS	LD250	1	10 mK	12 μW	250 μW	30 à 50 cm
	XLD400	2	8 mK	14 μW	450 μW	30 à 50 cm
	XLD1000	2	8 mK	34 μW	1000 μW	30 à 50 cm
FORMFACTOR™	JDry-500-QPro	1	7 mK	14 μW	500 μW	50 cm
OXFORD INSTRUMENTS	TritonXL	2	5 mK	25 μW	1000 μW	43 cm
	TritonXL-Q	2 ou 4	7 mK	25 μW	850 μW	50 cm
	Proteox	1	10 mK	>25 μW	500 μW	36 cm
CryoConcept	HD200	1	10 mK	11 μW	350 μW	30 à 50 cm
	HD400	1	10 mK	10 μW	400 μW	30 à 50 cm
Leiden Cryogenics	CF2400 Maglev	2	4 mK	? μW	2000 μW	49 cm
	CF1400 Maglev	2	8 mK	? μW	1000 μW	49 cm

Figure 506: cooling power per temperature and cryostat vendor. (cc) Olivier Ezratty, 2020-2022.

The **BlueFors'** refrigeration thermal budget ranges from 12 μW (LD250) to 30 μW (XLD1000) at 20 mK, and from 250 μW (LD250) to 1,000 μW (XLD1000) at 100 mK.

²¹²⁵ See [61 Ice Hot Companies Transforming The Cryogenics & Alternative Cooling Systems Industries](#), January 2021.

Oxford Instruments' TritonXL also has a thermal budget of 1,000 μW at 100 mK but with two pulsed tubes, while the new Proteox reaches 500 μW ... with only one pulsed tube. It is completed by a removable system for qubit control cables supporting up to 140²¹²⁶. The **Janis JDry-500-QPro** has a thermal budget of 14 μW at 20 mK and 450 μW at 100 mK (*above*, in-house compilation).

The current record can be found at **Leiden Cryogenics** with a recent cryostat with a thermal budget of 2000 μW on the 100 mK stage, but the budget at 20 mK is not indicated in their literature. On the 4K stage, the available thermal budget is around 1W. But beware, these extreme performances above 500 μW are often obtained with two pulsed tubes instead of one and thus, double the external compressor and power drain. All this with a double dilution refrigeration system to go below 1K. It is also possible to have systems with a single pulse tube and two dry dilution systems.

The thermal budget of the coldest stage is conditioned by the equation: $Q_m = 84\dot{n}_3 T^2$ where Q_m is the cooling power in W, \dot{n}_3 is the flow velocity in mol/s of helium 3 in the cryostat at this stage and T is the temperature of the stage in Kelvin. This law that can be simply called "Q=84NT²" explains that the thermal budget at 15 mK is very low compared to the cooling budget available at the upper stages (up to 25 μW at 15 mK, 1 mW at 100 mK and 1.5W at 4K).

There is another constraint related to the Kapitsa resistance. It limits heat exchanges between helium 3 and the heat exchanger. These exchanges are proportional to T^4 . If we therefore want to multiply heat exchanges by 10, the exchange surfaces in the lower parts of the dilution system would have to be multiplied by 10,000! This is done using silver powders integrated into the discrete heat exchangers above the dilution chamber. These powders are structured to maximize the heat exchange surface area with the helium gas flowing through them. Their deposition process must maximize the flat contact surface with the small tanks where they are located. It is possible to increase cryostats cooling power by adding more cooling stages, improving their Carnot efficiency and with multiplying the pulse tubes and dilutions.

Other cryogenics

For the other types of qubits, the cooling requirements are different: trapped ion qubits are not theoretically refrigerated, but Honeywell's prototype ion-trap chips announced in early March 2020 are cooled to 12.6K, a temperature that can be obtained with helium 4 based cryostats.

In photon-based quantum processors, the optical components traversed by the photons (mirrors, prisms, interferometers, whether miniaturized in nanophotonics or not) are not refrigerated, but the photon sources and photon detectors are, at temperatures between 1K and 10K. The associated cryogenics are much lighter and consume less energy compared to dilution cryostats.

Other techniques allow very localized cooling. This is the case of the **Doppler effect** which works on cold atoms suspended in a vacuum. Another solution developed by researchers from the VTT Technical Research Centre in Finland would cool silicon components with a phonon-based electronic cooling technique. It seems that this cooling capacity is very low, very localized, and still requires pre-cooling the system to at least 244 mK. It is therefore still necessary to operate a helium 3 and 4 dilution cryostat²¹²⁷.

Thales Cryogenics **Thales Cryogenics** (France, the Netherlands) is a subsidiary of Thales Group which creates various specialized cryocoolers for military and commercial applications.

²¹²⁶ See the very interesting presentation [50 years of dilution refrigeration](#), by Graham Batey of Oxford Instruments, 2015 (26 slides).

²¹²⁷ See [Thermionic junction devices utilizing phonon blocking](#) by Emma Mykkänen et al, 2020 (9 pages). It reads: "*The cooling power for this sample is about 2 pW/ μm^2 at 300 mK.*" "*Our best-performing sample is S2 (subchip with 1-mm diameter and 0.4-mm height). Its maximal absolute and relative temperature reductions are 83 mK (at 244 mK) and 40% (at 170 mK), respectively.*" Therefore, it is already necessary to reach 244 mK before starting, and it is therefore necessary to use a helium 3 and 4 cryostat.

It includes rotary and linear Stirling coolers, mini-coolers, high-pressure gas compressors, miniature DC/AC rotary and linear converters, linear pulse tube cryocoolers etc.

Thales' NV centers-based quantum sensors use miniaturized cooling using liquid nitrogen and occupying only half a cubic decimeter²¹²⁸ (Figure 507). The required temperature is lower, around 70K which is quite hot compared to 15 mK! These cryostats are used for various breeds of quantum sensors.



Figure 507: a small Stirling cooler for embedded systems. Source: [Closed Cycle Refrigerator](#) by John Wilde, 2018 (11 slides).

Qubits control electronics

Most of the time, driving qubits with quantum gates and for their state readout requires sending them some sort of photons (Figure 508). For superconducting qubits and electron spin qubits, these photons are in the microwave spectrum. In a counterintuitive fashion, these microwaves are transmitted in coaxial cables and not over the air like radio waves. Their frequencies range between 1 and 15 GHz for superconducting qubits (but, usually, between 5 and 6 GHz) and between 12 and 26 GHz for electron spin qubits. These are in between higher-frequencies photons that can be transmitted in optical fiber and lower frequencies signals which are transmitted as classical electrical current in wires. These photons are generated as pulses of various shapes and duration (cosine signals shaped with an envelope, base pulses of diverse forms, cosine or other, and direct-current pulses which are the simplest to generate).

We will look here into two sorts of micro-wave generation technologies: those coming from room temperature electronics and those generated within the cryostat at cryogenic temperature, including cryo-CMOS, SFQ superconducting electronics and other discrete electronic components working at these low temperatures like the TWPAs used for qubits microwave readout signals amplification.

Direct current signals are also used to drive qubits, like with Z gates with some superconducting qubits and to drive some amplifiers²¹²⁹. To be complete, we'll then also look at cabling and filtering components and their vendors.

With photons, cold atoms and trapped ions qubits, control techniques involve photons and lasers operating in the infrared and near visible spectrum which we don't cover here. There are probably missing elements in Figure 508 related to photonic and atom based qubits.

We'll try here to answer many questions: how are all these electronics affecting the quality of qubits? How is it scaling as you need to significantly increase the number of physical qubits to accommodate the requirements of fault-tolerant quantum computing? How do you optimize the existing cumbersome wiring? What are the solutions to run all or part of these electronic systems inside the cryostat? What is the power consumption of these various solutions? How can room temperature electronics and cryogenic electronics scale?

Wiring. How many wires are needed to control solid states qubits? It depends but there are usually half a dozen wires needed to control a superconducting or quantum dot spin qubit. One or two microwave wires to drive qubit gates, one or two DC pulses wires to control other gates and then, two

²¹²⁸ These are usually systems using a Stirling engine. Thales Cryogenics produces such miniaturized refrigeration systems. The [RM2](#) cools a payload to 77K for a mass of 275g and a thermal budget of 400 mW at this temperature. It is notably used for cooling infrared cameras in embedded systems. This type of small cryostats can also be found at SunPower (USA), capable of cooling down to 40K and with a larger mass of 1.2 kg. Ricor (1967, USA) is another manufacturer of this kind of mini-cryostats.

²¹²⁹ This excellent review paper [Microwaves in Quantum Computing](#) by Joseph Bardin et al, January 2021 (25 pages) provides an excellent overview of the challenges of microwave based qubit controls for superconducting, electron spin and trapped ion qubits. The table/chart in this page is inspired from this document. Z gates are driven by direct currents with Google's Sycamore qubits while IBM's are driven by microwaves, like the XY gates. See also [Engineering cryogenic setups for 100-qubit scale superconducting circuit systems](#) by S. Krinner et al, 2019 (29 pages) which makes a good inventory of energy consumption sources in the cryostat.

microwave wires for qubit readout (one in and one out of the qubit). One DC bias is sometimes used to change energy spacing for tunable superconducting qubits. When you scale the number of qubits, this creates a massive number of wires.

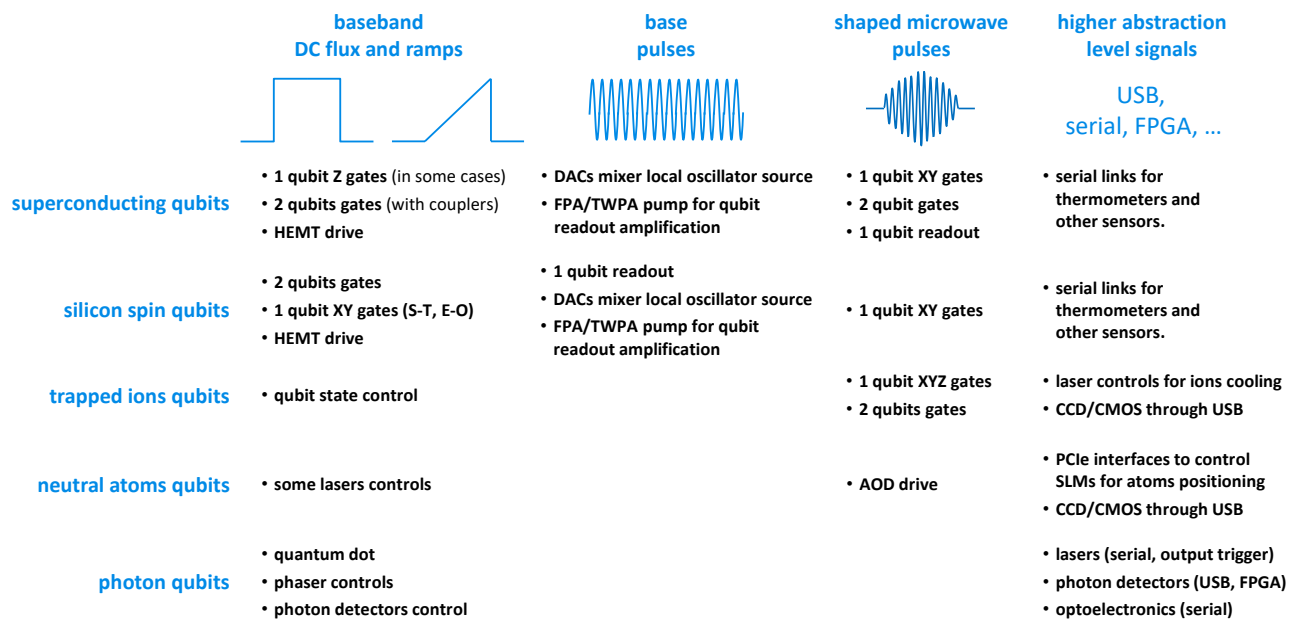


Figure 508: compilation of the various electronic and photonic signals used to drive various types of qubits. This diagram will later be completed with more signals used to drive atoms and photon qubits. (cc) Olivier Ezratty, 2021-2023.

Multiplexing. Work is being done to multiplex these qubit drive signals with different methods. One is frequency domain multiplexing that is already implemented for qubit readout with up to 8 microwave frequencies in a single wire and could also be implemented for qubit drive²¹³⁰. A second would be frequency multiplexing with up and down convert to higher frequencies such as in the optical domain. Nanophotonic circuits sitting very close to qubit chips could be used for microwave up/down frequency conversion from microwave photons to optical photons and their multiplexing²¹³¹. One proposed conversion technique uses VCSEL (Vertical-cavity surface-emitting lasers) that are known to operate at low temperature of 2.6K, which is still high²¹³². A third method consists in using time domain multiplexing which probably has some limitations in scaling, making it impossible to run several gates simultaneously and therefore potentially slowing down computing and quantum error correction²¹³³. To ensure scalability, these solutions must demultiplex the signal as close as possible to the qubit chip and have a very low power drain, compatible with the very low cryostat cooling budget at low cold-plate stages, and if not, at the 4K stage. Some researchers are also proposing to optically multiplex qubit readout signals using piezo-optomechanical transducers²¹³⁴.

²¹³⁰ See [Multiplexed control scheme for scalable quantum information processing with superconducting qubits](#) by Pan Shi et al, December 2023 (8 pages).

²¹³¹ See [Supporting quantum technologies with a micron-scale silicon photonics platform](#) by Matteo Cherchi et al, VTT, 2022 (17 pages) and [Control and readout of a superconducting qubit using a photonic link](#) by F. Lecocq et al, NIST, September 2020 (13 pages).

²¹³² See [Recent Advances in 850 nm VCSELs for High-Speed Interconnects](#) by Hao-Tien Cheng et al, February 2022 (27 pages) and [Microwave-optical quantum frequency conversion](#) by Xu Han et al, Optica, 2021 (15 pages). See also [Scaling up Superconducting Quantum Computers with Cryogenic RF-photonics](#) by Sanskriti Joshi et al, University of Washington, October 2022 (10 pages).

²¹³³ See [Multiplexed superconducting qubit control at millikelvin temperatures with a low-power cryo-CMOS multiplexer](#) by Rohith Acharya et al, IMEC, Nature Electronics, September 2022-September 2023 (22 pages, [arXiv](#)). The “1 to 4” drive multiplexer has a power consumption of around 0.24 μ W of static power and 0.5 μ W of dynamic power, with \sim 0.2 μ W power consumption per qubit channel making it suitable to control 100 qubits and 1,000 qubits with some optimizations, within the constraints of today’s cryostats.

²¹³⁴ See [High-fidelity optical readout of a superconducting qubit using a scalable piezo-optomechanical transducer](#) by T.C. van Thiel, Simon Gröblacher et al, QPhoX, Qblox and Rigetti, October-November 2023 (10 pages).

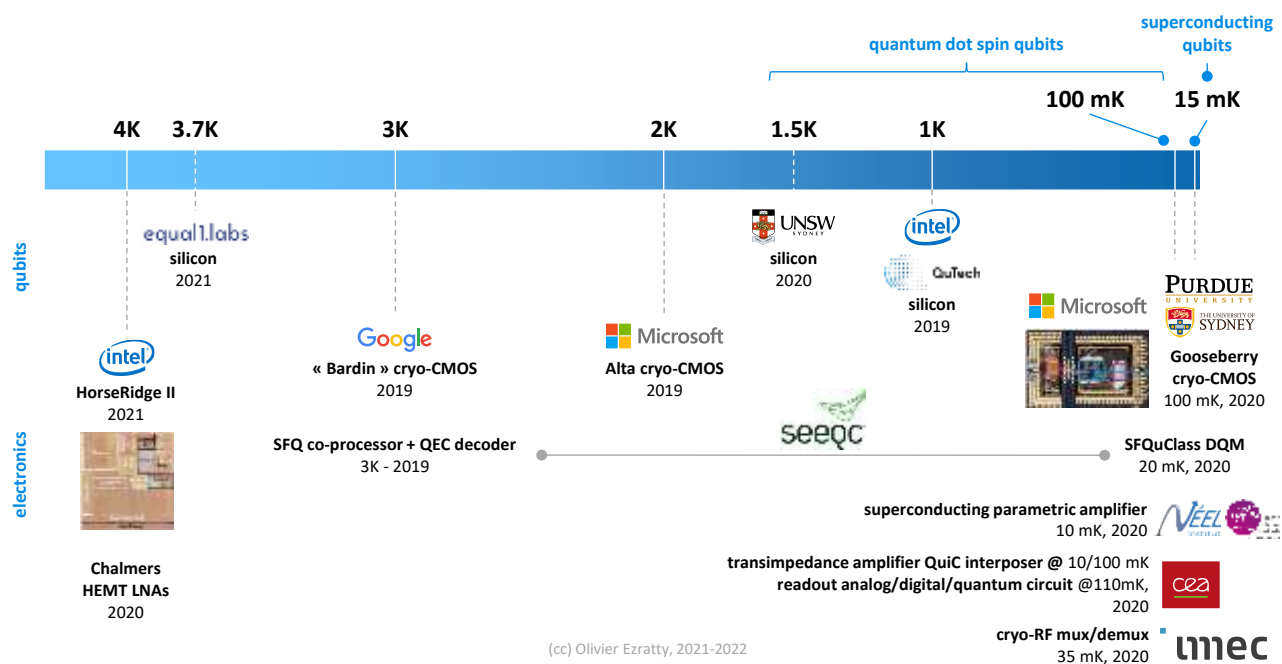


Figure 509: comparison of the temperature and feature of various qubits and cryo-electronic chips. (cc) Olivier Ezratty, 2022.

Cryo-electronics options. Many options exist that we'll cover in this part. Cryo-electronics can operate at the 4K stage (HorseRidge) down to the lower stages (15 mK to 100 mK) as shown in Figure 509. What are their limitations? Also, what are the pros and cons of cryo-CMOS vs SFQ electronics? All these cryo-electronics solutions must be compared with detailed specifications. The generated microwave quality depends on the sampling rates used in their DAC and ADCs, on the number of points used in generating the wave envelope (16,384 points for HorseRidge 2, aka 14-bit sampling), their power consumption per qubit, their frequency range (targeting superconducting and/or electron spin qubits), their clock, their noise level and their real scalability potential with a large number of qubits. These electronic components must also be as isolated as possible from the qubit chips.

Optimization. Cryo-electronics are an interesting solution for many respects: it potentially reduces the wiring burden as seen above, it creates miniaturized electronics that can help constrain the total size and weight of a quantum computer, it has the potential to minimize the control/readout/processing cycle latency and its energy consumption can be much smaller than room temperature electronics.

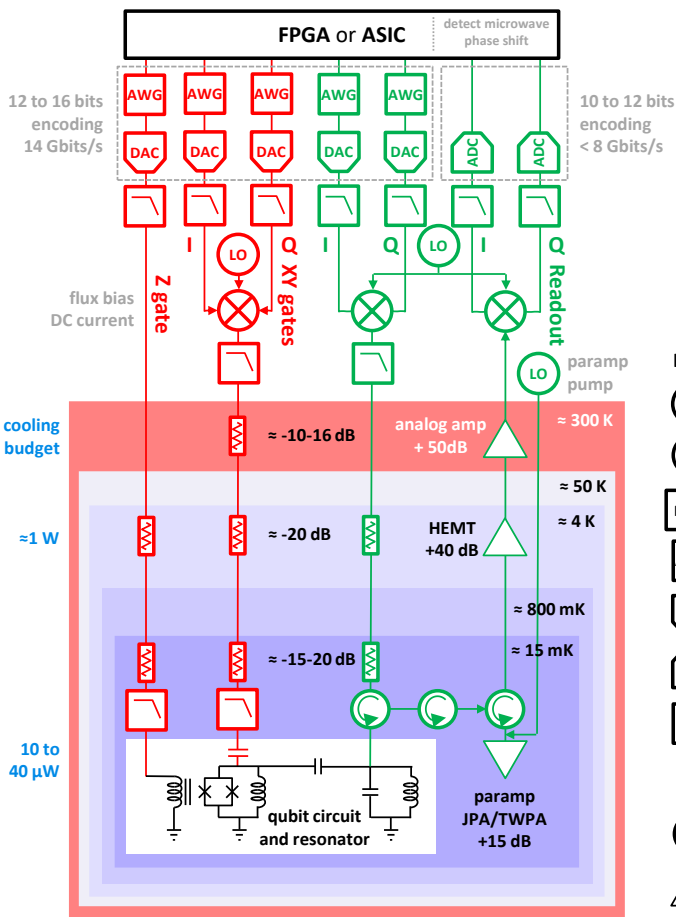
If the cryo-electronics components are not at the same stage as the qubits, you'll still need some (expensive superconducting) wiring. And it has a significant indirect energetic cost. These cryo-electronics components generate heat that must be extracted from the cryostat. As you get in the lower cryostat stages, its cooling power gets drastically reduced proportionally to T^4 , T being the cryostat stage temperature.

The current cooling budget at 15 mK is lower than $40 \mu\text{W}$ and goes up to 1W at the 4K stage. You can still bet on the creation of larger cooling power cryostats but their energetic cost will skyrocket. It explains why some cryo-electronics components are designed to stay at intermediate stages (2K to 4K). This balance depends also on the qubit operating temperature.

For superconducting qubits, the constraint is much bigger than with spin/silicon qubits which could operate at higher temperatures (100 mK to 1K).

Recent modelling did show that for superconducting qubits, the control electronics energetic cost is surprisingly optimized with room temperature electronics²¹³⁵.

²¹³⁵ See [Optimizing resource efficiencies for scalable full-stack quantum computers](#) by Marco Fellous-Asiani, Jing Hao Chai, Yvain Thonnart, Hui Khoon Ng, Robert S. Whitney and Alexia Auffèves, arXiv , September 2022 (39 pages).



typical superconducting qubits control and readout electronics

there are of course variable implementations: Z qubit gates are sometimes managed by microwave pulses and two-qubit gates can be driven by flux-biased qubit couplers (Google Sycamore). Other variations are related to multiplexing several qubit readout frequencies at the room temperature stages, putting the quantum limit amplifier in or near the qubit circuit.

apart from the paramp pump local oscillator, all the described components are needed for each and every qubit

- I / Q in-phase and quadrature signal modulation which, when merged with the local oscillator in the mixer, create a microwave pulse with the right phase
- LO local oscillator, provides carrier microwave signal, 4 to 8 GHz
- Mixer frequency mixer, in our case, it's both an upconverter and an adder of I and Q upconverted waveform signals (way down) and down-converter (way up)
- FPGA fully-programmable gate-array, programmable processor handling feedback loop with qubit, including error correction
- AWG arbitrary waveform generator, create a waveform that will shape the high-frequency coming from the local oscillator
- DAC digital to analog converter, converts the digital waveform coming from the AWG into analog signal, to be mixed with the LO
- ADC analog to digital converter, digitize the waveform readout signal coming from the cryostat
- Filter filter, limit the propagation of high frequencies, heating source
- Attenuator attenuator, reduces the number of transmitted microwave photons, is a heating source in the cryostat
- Circulator circulator, with single-way microwave pulses propagation across successive entries
- paramp : readout microwave parametric amplifier (JPA/TWPA)
HEMT amplifier, room temperature analog amplifier

(cc) Olivier Ezratty, 2022

Figure 510: description of the various electronic tools that control superconducting qubits. (cc) Olivier Ezratty, 2022.

Control electronics and qubit fidelities. The relation between qubit fidelities (one and two qubit gates + idling + qubit readout) and control electronics precision has been widely studied. A paper from Intel and Dutch researchers from 2019 did show this correlation and created a model to reach 99.9% fidelities for all these operations (Figure 511). With solid state qubits, two sorts of control signals are generated: DC pulses and wave formed pulses in the microwave regime. There is a clear link between qubit fidelities and the precision of microwave signal generation regarding their duration, amplitude, frequency and phase. It demonstrated that it was a reachable goal for state of the art classical room temperature electronics²¹³⁶.

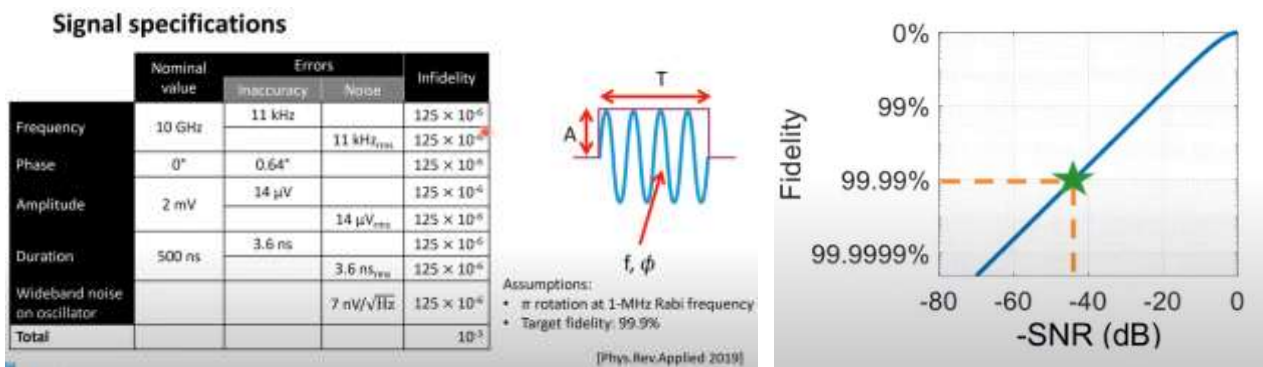


Figure 511: specifications of a qubit control microwave pulse and of the infidelity sources. Data source: [Impact of Classical Control Electronics on Qubit Fidelity](#) by J.P.G. van Dijk, Menno Veldhorst, L.M.K. Vandersypen, E. Charbon, Fabio Sebastiano et al, PRA, 2019 (20 pages).

²¹³⁶ See [Impact of Classical Control Electronics on Qubit Fidelity](#) by J.P.G. van Dijk, Menno Veldhorst, L.M.K. Vandersypen, E. Charbon, Fabio Sebastiano et al, PRA, 2019 (20 pages).

The noise affecting qubits and coming from control electronics comprises many aspects: phase noise coming from source clock jitter feeding the master and local oscillators, AWGs and DACs originated harmonics, leakage signals from mixers, various amplitude signal to noise ratios (SNR) and noise coming from reference voltage sources like the BVGs (bias voltage generators) that are used to generate DC pulses, as shown in Figure 510 for the case of superconducting qubits.

Various improvements are thus sought in qubit control electronics:

LO Phase Noise. The local oscillators used in the AWG (arbitrary waves generators) must have a reasonable phase noise²¹³⁷ (Figure 512). Phase error noise becomes important as qubit fidelities are improved with better control of environmental sources of decoherence. Lab-grade oscillators may already limit the performance of qubits having microsecond scales gate times, like with trapped ions. Thus, the need to use low phase noise high precision local oscillators instead of traditional lab-grades LOs.

Table 2. Time until a qubit physical error rate p is reached solely due to phase fluctuations in the LO

Time to Reach LO-Induced Error Rate p					
p	10^{-3}	10^{-4}	10^{-5}	10^{-6}	10^{-7}
Lab-Grade LO	4.0 μ s	900 ns	200 ns	30 ns	< 10 ns
Precision LO	> 100 ms	> 100 ms	> 100 ms	80 ms	600 μ s

These times may be viewed as an upper bound on the allowable QEC cycle period. Achievable cycle periods will be reduced because of other error sources. Error rates are derived from free-evolution calculations presented in Figure 2b. Driven operation error rates (see Figure 2c) yield similar results.

Figure 512: [The role of master clock stability in quantum information processing](#) by Harrison Ball et al, NPJ Quantum Information, November 2016 (8 pages)

There is a 10^{-4} difference in phase noise errors between lab-grade and precision LOs! Given superconducting gates time span 10 ns to 600 ns, a 10^{-5} error rate only due to LO phase noise could be reached during this time. We're not far from the required threshold for QEC!

Low Latency control/readout cycles. There's also a need to minimize the duration of the qubit control and readout cycle. It minimizes the impact of the errors that can happen during the cycle due to decoherence, enabling a higher quality QEC. The quantum feedback latency must be several orders of magnitude under superconducting qubits coherence times that are in the range of 50 μ s to 100 μ s and could potentially exceed 1 ms. So, we're in for a maximum of a few 100 ns. Some techniques exist to optimize the duration of the readout microwave pulses²¹³⁸. The control system must also be well synchronized across all qubits, which can be achieved with a distributed synchronous clock and trigger architecture²¹³⁹.

Labs also make use of spectrum analyzers. Another feedback loop optimization comes with handling qubits gates AWGs, their DACs and readout data acquisition in the same FPGA²¹⁴⁰.

From FPGA to ASIC. At this point, the most advanced qubit control systems are FPGA based. Their advantage is sound economics for small scale use cases but at an energetic cost. Using CMOS ASICs could bring some energetic advantage on top of further reducing control cycle latency, but it has a significant cost few qubit developers can afford at least in research labs. Also, the ASIC design and manufacturing cycle is much longer than with an off-the-shelf FPGA board.

²¹³⁷ See [The role of master clock stability in quantum information processing](#) by Harrison Ball et al, NPJ Quantum Information, November 2016 (8 pages) and [A 2–20-GHz Ultralow Phase Noise Signal Source Using a Microwave Oscillator Locked to a Mode-Locked Laser](#) by Meysam Bahmanian and J. Christoph Scheytt, 2021 (11 pages).

²¹³⁸ See [Fast quantum gate design with deep reinforcement learning using real-time feedback on readout signals](#) by Emily Wright and Rogerio de Sousa, May 2023 (9 pages).

²¹³⁹ In [FPGA-based electronic system for the control and readout of superconducting quantum processors](#) by Yuchen Yang et al, USTC China and Alibaba, February 2022 (12 pages), a Chinese team describes how it implemented such a system, to control 2 qubits for a starter. It's based on using FPGAs in 3U (3 units heights in electronics racks) PXIe modules, the instrumentation equivalent of the PCIe bus used in microcomputers and created by National Instruments in 1997. As an example, the 3U PXIe-1095 below has 18 slots. The team used a FS725 Rubidium Clock running at 10 MHz with ultralow phase noise, coming from Stanford Research Systems (1980, USA). They are also using the physical layer "Low Voltage Differential Signaling" system (LVDS) which has a low latency.

²¹⁴⁰ See [Hardware for multi-superconducting qubit control and readout](#) by Zhan Wang et al, 2021 (11 pages). In this work, the feedback latency reached 178.4 ns. It's using a 28 nm Xilinx XC7K325T FPGA with 326K logic cells.

Thus, the move from FPGA to ASIC is not just a technological driven choice but also an economical one. At some point, it will be conditioned by the growth in volume of the quantum computers market.

Memristors DC control. A Canadian French team proposed to control spin qubits quantum-dot gate biases with DC sources with a cryogenic solution using Al₂O₃-TiO₂-based tunable memristors with a ±1V range and 100 μV resolution. Memristors are non-volatile systems with tunable resistance. It fits the need to tune these DC pulses due to qubits variability. It was demonstrated at 4.2K²¹⁴¹. It doesn't support the other needed type of electronic controls, microwave pulses, that are needed to drive single qubit gates. This solution simplifies the DC wiring between room temperature control electronics and the 4K stage in the cryostat, but it still requires DC lines between this stage and the qubits chip at below 1K. These memristors are dissipating 1.77 mW. As a result, a current generation cryostat with 1.5W cooling power at 4.2K could accommodate about 800 such memristors. We're still far from the LSQ realm.

Pulse control optimization. At the software level, pulse control can benefit from some optimization techniques, requiring a verticalized approach crossing the usual layers between high-level gate-based code and pulse control. Such cross-layers optimizations are proposed by IBM and Q-CTRL²¹⁴². It is particularly useful in NISQ regimes since it makes use of many arbitrary single qubit rotation gates in variational algorithms. At the pulse waveform level, optimizations can also be made with using some data compression which is important given that with many superconducting qubits, every qubit and couplers are driven by a unique waveform for each supported physical gate, which is tuned in calibration cycles to maximize gate fidelities²¹⁴³.

Topological qubits controls. These qubits, at least those that Microsoft is trying to create, are driven by simpler signals, mostly on/off DC signals and with no microwaves or pulsed microwaves. As a result, these qubit controls have a much smaller required bandwidth and can be implemented with a lower space and energetic footprint in cryo-CMOS chips. Older literature however mentions that topological qubits are driven by waveformed pulses^{2144 2145}.

Consolidated projects. Several qubit control and electronics research and development projects were recently launched in Europe. In Germany alone, you have three related projects:

QuMIC (Qubits Control by Microwave Integrated Circuits, 6.3M€, 2021-2024) which involves four academic and two industry partners (Infineon, Supracon AG) and deals with miniaturization of RF electronics to control superconducting and trapped ions qubits.

qBriqs (2M€, 2021-2024) which also involves four academic and two industry partners (Rosenberger and Stahl Electronics) and deals with compact cryogenic connectors, qubit readouts TWPA and HEMT amplifiers, filters and attenuators, DACs and ADCs and DC flux current generators.

HIQuP (2021-2024, 2.2M€) with, again, four academic and two industry partners (Supracon AG and IQM Germany) which works on superconducting and cryogenic qubit control electronic circuits.

²¹⁴¹ See [Memristor-based cryogenic programmable DC sources for scalable in-situ quantum-dot control](#) by Pierre-Antoine Mouny et al, March 2022 (13 pages).

²¹⁴² See [Summary: Chicago Quantum Exchange \(COE\) Pulse-level Quantum Control Workshop](#) by Kaitlin N. Smith, February 2022 (17 pages).

²¹⁴³ See [COMPAQT: Compressed Waveform Memory Architecture for Scalable Qubit Control](#) by Satvik Maurya and Swamit Tannu, University of Wisconsin-Madison, December 2022 (19 pages).

²¹⁴⁴ See [Flux controlled quantum computation with majorana fermions](#) by T. Hyart et al, PRB, 2013 (17 pages).

²¹⁴⁵ See [Detecting majorana modes in one-dimensional wires by charge sensing](#) by Gilad Ben-Shach et al, Harvard, University of Maryland and Weizman Institute, PRB, 2015 (12 pages).

In France, the **QRYOlink** project combines CEA-Leti and Institut Néel from Grenoble, Radiall, ATEM, Air Liquide, C12 and Alice&Bob to develop a scalable architecture for cryogeny and cabling aimed at supporting solid-state qubits. Other related projects also cover scalable control electronics targeting large scale quantum computing architectures.

Room temperature electronics

Room temperature electronics is the dominant solution used both in research labs and with most commercial vendors (IBM, Google, Rigetti, IQM, etc). The key components are on the way in for each and every qubit:

- **AWGs** (arbitrary waveform generators) which create microwaves pulse forms and usually generate about 2 GigaSamples/s. These are used to create single qubit gates and also readout pulses. Alternative techniques are proposed which generate pulses width modulation (PWM) that would be less costly without jeopardizing qubit fidelities ²¹⁴⁶.
- **DACs** (digital to analog converters) which use a 14-bit to 16-bit amplitude resolution to convert into analog format the output of the AWGs.
- **Mixers** of the waveform and a **LO** (local oscillator) signal in the used microwave range (around 5 GHz for superconducting qubits). The output is called a “heterodyne” signal.
- **Direct current** sources, to drive certain types of qubit gates *aka* bias drives.

Since we mentioned heterodyne measurement, let’s make a pause with describing the three main different techniques used to measure an electromagnetic signal with homodyne measurement (one observable), heterodyne measurement (two orthogonal observables like in-phase and quadrature) and photon measurement or counting. These three techniques are used for optical frequencies photons and radio-frequency photon signals, with, of course, many differences and variations (Figure 513).


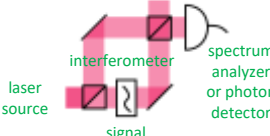

	homodyne measurement	heterodyne measurement	photon counting
			
definition	extracts information encoded as modulation of the phase and/or frequency of an oscillating signal with comparing that signal with a standard oscillation carrying no information.	extracts information along two orthogonal components in phase space like, for RF signals, the in-phase and quadrature signals coming out of an I/Q mixer, use a reference oscillator source (LO).	measure the excitation quanta as degree of freedom in an electromagnetic signal
process			
pros/cons	better precision	more information but less precision	photon losses
output data	signal phase or frequency, signal spectrum	signal quadrature (in-phase and quadrature)	number of superposed photons or the presence of photons
implementation	homodyne interferometry	RF I/Q mixer, heterodyne interferometer, I/Q components analysis with ADC+digital signal processing	photodetection with SPAD, SNMPD, FMCW lasers, ...
use cases	QKD detection with balanced homodyne detection (BHD)	qubit microwave readout processing, CV photon qubits readout	DV photon qubits readout

Figure 513: explanation of the various ways to detect a photon or electronic signal with homodyne and heterodyne measurement and photon counting. (cc) Olivier Ezratty, 2022.

(cc) Olivier Ezratty, 2022

²¹⁴⁶ See [Quantum Optimal Control without Arbitrary Waveform Generators](#) by Qi-Ming Chen et al, Aalto University, Princeton and Tsinghua University, September 2022 (14 pages). The paper however doesn’t provide some indications of the associated power savings.

On the way out of the cryostat, we have:

- A last-stage **analog amplifier**, following the cryogenic amplification stages (TWPA and HEMT).
- **ADCs** (analog to digital converter) of the readout microwave signal, usually with a 1 GigaSamples/s sampling rate and a 8 to 12-bit encoding.
- **SoC** (systems on chip), **FPGA** or **ASIC** circuits used to interpret the output of the ADCs to get the qubit state, and which may manage a closed-loop control of the whole cycle to implement error correction (QEC).

All these components are integrated in one or several boxes, or boxes with interchangeable modules. The FPGAs are programmable, usually with Python and some extension (library or language extension).

This field is well covered by electronics industry vendors addressing research and commercial quantum computing markets. Beforehand, many quantum computing research laboratories were relying on generic micro-wave generator and readout systems coming from vendors like **Rohde & Schwarz**, **Tektronix** and **Keysight**²¹⁴⁷. Over time, some of these vendors have developed specialized offerings for quantum computing, particularly through some acquisitions (for Rohde & Schwarz and Keysight). Specialized quantum computing electronics emerged like **Zurich Instruments**, **Qblox** and **Quantum Machines**. Large shops like **Google** also developed their own electronics.

Some hardware and software open source control systems have also been proposed like the **QICK** (Quantum Instrumentation Control Kit) from Fermilab²¹⁴⁸ and **QubiC** from Lawrence Berkeley National Lab, both from the DoE^{2149 2150}. They are cost efficient when compared to commercial solutions and adapted to the needs of research labs. These kits are all based on Xilinx FPGAs containing their own DACs and ADCs. Researchers from Chalmers and KTH in Sweden created **Presto**, a fully integrated room-temperature system on chip using a Zynq UltraScale+ RFSoc from Xilinx with full control operations for superconducting qubits²¹⁵¹.



Zurich Instruments (2008, Switzerland, \$112K) is a manufacturer of electronic test and measurement equipment, including a range of microwave generation and analysis tools.

The company was acquired by Rohde & Schwarz in July 2021. Their offer is built around their Quantum Computing Control System, which bridges the gap between the quantum computer software control tools and the associated electronic instrumentation.

²¹⁴⁷ Tektronix provides an AWG that can be used to drive qubit signals, the 16-bit AWG5200 supporting up to 32 output channels with 2 Gbits/s sampling (and local oscillator frequency go up to 5 GHz) and the 6 Series Low Profile Digitizer for 4-channel qubits readout (up to 8 GHz).

²¹⁴⁸ See [The QICK \(Quantum Instrumentation Control Kit\): Readout and control for qubits and detectors](#) by Leandro Stefanazzi et al, Fermi Lab, Princeton University, Seconda Università degli Studi di Napoli, GE Healthcare Institute, CNEA - Argentina, and University of Chicago, March 2022 (15 pages). It's based on Xilinx based RFSoc (Radio-Frequency System-on-chip) ZCU111 Evaluation Kit with a Xilinx XCZU28DR FPGA containing 8 14-bit DAC and 8 12-bit ADC. This is an "hybrid FPGA" with a programmable logic part and a more classical SoC part with a quad-core Arm Cortex A53 cores, various I/Os and memory. It supports microwaves output up to 6 GHz. The toolkit is programmed in Python. The QICK power consumption is 50 W and it seems able to drive 4 qubits. It could support up to 100 qubits with frequency domain multiplexing.

²¹⁴⁹ See [QubiC: An Open-Source FPGA-Based Control and Measurement System for Superconducting Quantum Information Processors](#) by Yilun Xu, Irfan Siddiqi et al, Lawrence Berkeley National Laboratory and University of California at Berkeley, September 2021 (11 pages). QubiC uses a Xilinx Virtex-7 FPGA and separate DACs and ADCs from the Abaco Systems FMC120 and its four 16-bit ADC and four 16-bit DACs. The conversion circuits come from Texas Instruments (ADS54J60 ADC and DAC39J84).

²¹⁵⁰ See [QubiC 2.0: An Extensible Open-Source Qubit Control System Capable of Mid-Circuit Measurement and Feed-Forward](#) by Yilun Xu et al, September 2023 (7 pages) which extends QubiC 1.0 with mid-circuit measurement control capabilities.

²¹⁵¹ See [Measurement and control of a superconducting quantum processor with a fully-integrated radio-frequency system on a chip](#) by Mats O. Tholén et al, Chalmers, May-October 2022 (14 pages). This type of chipset has a power drain of at least 70W ([source](#)). It seems it can handle about 8 qubits in total in a 2U 19-inch package.

This system consists of several components. First, the PQSC (Programmable Quantum System Controller, which is used to program and control all the devices. It is equipped with a Xilinx UltraScale+ FPGA that can be driven by the LabOne software using Python, C, MATLAB, LabVIEW and Microsoft's .NET framework.

It controls up to 18 HDAWG (High-Density Arbitrary Waveform Generator) microwave generators and manages up to a hundred qubits. LabOne became LabOne Q in October 2022 with some extensions easing the setting and optimization of Zurich Instruments tools.

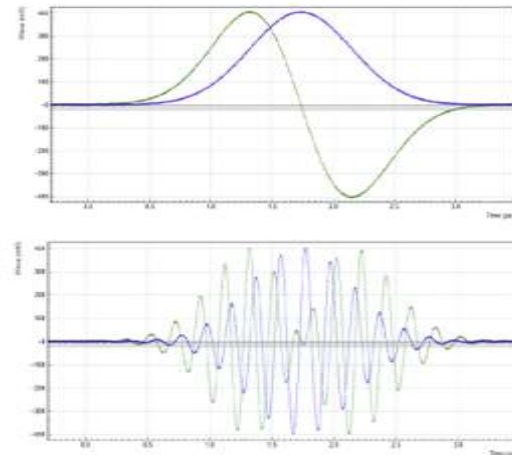


Figure 3.15. Dual-channel signal generated by the AWG and captured by the scope. The top figure shows two envelope waveforms played without modulation, the bottom figure shows the same envelope waveforms played with enabled modulation.

Figure 514: Zurich Instruments QCCS containing a PQSC (program and control), two HDAWG (arbitrary waves generators) and three SHFQC (signals generators and readout) and one SHFPPC (tone pulse for parametric amplifier) for qubit control and readout. On the right, the types of microwave pulse signals generated. Source: Zurich Instrument product documentation. 2023.

These are sold at 23K€. These generators create microwave pulses that combine a waveform (Gaussian or other, in Figure 514 on the right) modulated by a high-frequency signal, usually between 5 and 10 GHz, adapted to superconducting qubits drive and readout. It can control up to 8 channels. These microwaves are sent to the qubits to reset them to zero, activate quantum gates or handle state readout. The single-qubit quantum gates are generated by sending a modulated microwave that modifies the energy level of the qubits and changes its state.

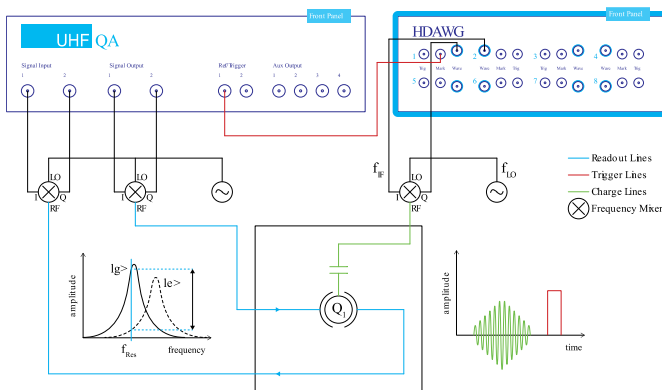


Figure 515: UHFQA and HDAWG cabling. Source: Zurich Instruments.

This is complemented by the UHFQA (Ultra-High Frequency Quantum Analyzer) which can analyze the readout state of 10 qubits. In the diagram, F_{LO} is the frequency of the microwave signal to be modulated and F_{IF} is the modulation waveform (Figure 515).

On the UHFQA side, the system detects the modulation or phase modification of the signal recovered through a resonator associated with the qubits, I_g and I_e respectively for ground states and excited states.

In April 2021, Zurich Instruments launched a new signal generator, the SHFSG with better microwaves signal spectral purity and stability. It can handle up to 144 qubit control channels and is accommodated with 4 or 8 channels, controlling up to 8 qubits. In August 2022, they introduced their SHFPPC (Super High Frequency Parametric Pump Controller), a room temperature tone pulse generator that feeds the parametric amplifiers like the TWPAs sitting at the lowest stage of the cryostat.



Figure 516: an SHFQC can control up to 16 qubits.

It was then completed by the software reconfigurable and programmable SHFQC launched in November 2021 (Figure 516), which bundles 6 signal generator control channels and a readout channel analyzer supporting up to 16 qubits. Several SHFQC can be combined to support up to 100 qubits and “beyond”.

Launched in August 2023, the QHub Quantum System Hub coordinates these various devices assembled in several QCCS (Quantum Computing Control System, shown in Figure 514). It can synchronize up to 448 microwave channels, enabling the control of over 100 superconducting qubits.



Qblox (2018, the Netherlands, \$5M) is a spin-off from QuTech that develops scalable control electronics for superconducting qubits. Their latest generation controls up to 20 qubits with a 4U rackable system and 100 qubit par full rack.

These clusters consume about 1 kW (Figure 517). The device contains both micro-wave generators for qubits gates (QCM module, blue) and qubits readout and electronics for qubit readout (QRM module, white). Each unit relies on small custom FPGAs. In a classical manner, it creates waveforms mixed with a microwave carrier signal after DAC conversion. Readout uses an ADC and a phase detection system.



Figure 517: this Qblox system can control up to 20 qubits.

Their DACs/ADCs have a high sampling rate of 16 bits. A high sampling rate is important to create precise waveformed microwaves. This precision is a way to ensure a good fidelity for qubit gates generated by these generated microwave pulses.

Their architecture could scale up to controlling 1,000 superconducting qubits. Calibration is done with the help from **Orange Quantum Systems** and cabling comes from **Delft Circuits**, two other spin-offs of Qutech in the Netherlands.

They also sell the desktop Pulsar QRM (quantum readout module) that handles a few qubits control in small factor format. As their Cluster modules, these can be coupled and synchronized together with using their homegrown protocols SYNQ (synchronized start within $\ll 1$ ns) and LINQ (distributing measurement outcomes in < 200 ns).

Qblox developed in 2023 their Q-Profile benchmarking tool to benchmark and optimize control electronics. On a small scale QAOA implementation with up to 14 qubits, they used it to optimize the algorithm speed by $\times 3$ ²¹⁵².

As of 2023, the company had a staff of 80 people.



Quantum Machines (2018, Israel, \$100M) provides a qubit control layer for superconducting quantum computers that combines hardware and software²¹⁵³. It is a spin-off from the Braun Center for Submicron Research Laboratory at the Weizmann Institute. The company had a staff of 150 and 250 customers throughout the world as of August 2023.

²¹⁵² See [Q-Profile: Profiling Tool for Quantum Control Stacks applied to the Quantum Approximate Optimization Algorithm](#) by Koen J. Mesman et al, Qblox, March 2023 (8 pages).

²¹⁵³ See [The Story of the First Israeli Quantum Computing Startup](#) by Eliran Rubin, December 2018.

They developed their own classic qubit control processor, an FPGA operating at room temperature, which generates the pulses for controlling qubits and measuring their states either with microwaves and lasers²¹⁵⁴. Packaged as their OPX/OPX+ systems, it supports superconducting, electron spin, NV centers, trapped ions and cold atoms qubits (working with QuEra). In March 2022, they announced the availability of Octave, a compact and rack-mountable all-in-one RF up/down-conversion module which completes their OPX systems. It contains its own built-in Local Oscillator (LO) sources and provides continuous self-calibration features. In August 2023, Quantum Machines announced its OPX1000 3U high-density controller supporting up to 64 output and 16 input analog channels, compared to 10 output and 2 input channels in the OPX+ (Figure 518).

The company was created by Itamar Sivan (CEO, who did a Master's degree at the ENS Paris between 2009 and 2011), Yonathan Cohen (CTO, former Weizmann Institute managing director) and Nissim Ofek (Chief Engineer, who had a post-doc position in Rob Schoelkopf's lab in Yale University where he developed a FPGA based control and QEC code).

They partner with Q-CTRL which develops qubits firmware level control software. Their processor is integrated into their "Quantum Orchestration Platform", which also combines a software layer²¹⁵⁵. In June 2020, they announced the creation of the **QUA** language, positioned as a language for creating hybrid quantum and classical algorithms, such as VQE and QAOA, which need rapid feedback between classical and quantum processors. This programming language works with all types of qubits, superconductors, silicon, cold atoms and trapped ions. The compiler thus takes into account the differences in the implementation of qubits: their connectivity, the homogeneity or heterogeneity of their coupling, the coherence times, the error rates, etc.



Figure 518: OPX1000 is a full-stack solution for qubit control and measurement, enabling closed-loop error correction with 64 output line for qubit control and 16 input lines for qubit readout, spread in 8 modules, and packed in a 3U rack. Source: Quantum Machines. 2023.



Figure 519: QDevil QCage.64 chip packaging for a superconducting qubit chip. Source: QDevil.


In April 2022, Quantum Machines, together with their customers Alice&Bob, Benjamin Huard's team from ENS Lyon and Florian Marquardt of the Max Planck Institute for the Science of Light in Germany, announced the launch of [Artemis](#), a 3-year EU funded project (900K€) as part of QUANTERA to use a real-time neural network to improve the accuracy of quantum controls and quantum error correction. It will lead to the creation of a full-stack QEC universal quantum controller. It will be complemented by an (unspecified) cloud-based quantum processor.

In March 2022, Quantum Machines made the acquisition of QDevil (Denmark) which gives them a foothold in the cryogenic electronics space with filters and a low noise DACs. In February 2023, QDevil introduced QCage.64, a superconducting test chip carrier enabling high-fidelity operations. The qubit chip is enclosed in a microwave cavity to minimize losses and decoherence. It has 64 transmission lines enabling testing of about a dozen qubits (Figure 519).

²¹⁵⁴ See the video [MLQ2021 Session Th2: Quantum Machines](#), March 2021 (46 mn) explaining their process.

²¹⁵⁵ See [Quantum Machines raises \\$17.5M for its Quantum Orchestration Platform](#) by Frederic Lardinois, March 2020, [Israel gets ready to join global quantum computing race](#) by Amitai Ziv, December 2019 and [The quantum computer is about to change the world. Three Israelis are leading the revolution](#) by Oded Carmeli, February 2020.

They also have a partnership with Nvidia to develop low-latency controls using Nvidia DGX servers with classical GPGPUs. In March 2023, they both announced the integration of Quantum Machines OPX+ with the latest Nvidia DGX using the Grace Hopper system through a PCIe bus enabling very low latency in the sub-microsecond scale between GPUs and QPUs²¹⁵⁶.

 **KEYSIGHT** **Keysight Technologies** (USA) is an electronics measurement company spun-out of Agilent in 2014, which itself was coming from Hewlett Packard in 2000.

It then expanded its portfolio through several acquisitions: Signadyne (FPGA-based PXI digitizers and AWGs initially used with trapped ions qubits) in 2016, Ixia (software), Liberty Cal (calibration services) and ScienLab (test solutions in eMobility systems) in 2017, Labber Quantum in 2019 (MIT spun-out specialized in qubits control and software) and Quantum Benchmark in 2021 (quantum error diagnosis and suppression, and benchmarking software). The company has now a broad portfolio of measurement and control electronic systems widely used in the quantum real, in its three markets: computing, sensing and communications, including optical instruments (Figure 520). Most quantum research labs already have some Keysight test and measurement systems. In qubits control electronics, they provide pulse laser controls, basebands pulse controls and pulsed microwaves controls (AWGs like the M3202A PXIe Arbitrary Waveform Generator with 1 GSa/s, 14 bit sampling, DAC) as well as ADCs for qubit readout (like the M3102A 14-bit PXIe Digitizer). Interestingly, they address one source of electronics signals quality variability: the fluctuating room temperature. Thus, a solution to control rack temperature with air flow operating at 35°C.

Their Quantum Control System assembles various software and hardware components to drive single and multi-qubit lab experiments. The hardware part is the Quantum Engineering Toolkit (QET) and contains a PC workstation with a PXIe Interface Module, a PXIe chassis containing an AWG, a DAC, and In-Phase and Quadrature modulator and demodulator, a Vector Signal Generator and other optional electronics (Figure 521). Among other places, this toolkit is used since 2020 at the MIT EQuS (Engineering Quantum Systems Group) testbed.

Keysight is involved in several quantum computing related projects like the Boulder Cryogenic Quantum Testbed launched in 2019, a joint effort of Google, the NIST and the University of Colorado Boulder, housed in the JILA laboratory on the CU Boulder campus. It helps US researchers working on superconducting qubits at the characterization level. The lab is equipped with a 10 mK Janis JDry 250 mini dilution refrigerator. They also participate to MATQu, an EU funded German project which ambitions to produce superconducting qubits on 300 mm silicon-based process flows.

Keysight hardware is also used in quantum sensing (AWGs, ADCs, DACs, analog signal generation, measurement of current-voltage (“I-V”) and capacitance-voltage (“C-V”), oscilloscopes) and CV-QKD signal generation and detection (with waveform/pattern generation, oscilloscopes, lightwave detectors and variable optical attenuators). In the vendors space, they partner with IBM on Qiskit Metal, an open source software solution to design your own superconducting qubits to understand qubits crosstalk effects.

In most of their solutions, Keysight uses Xilinx FPGAs but it also has its own cleanroom facilities to design custom ASICs, like in photonics. They plan to implement control electronics with cryo-CMOS only in the long term, after 2030-2040. Until then, classical electronics will do the job.

Keysight announced in June 2022 its new generation of qubit control electronics, Quantum Control System (QCS), based on a proprietary ASIC integrating microwave signals AWGs, 14-bit DACs and 12-bit readout ADCs with the effect of reducing phase jitter in the generated signals and enabling fast closed-loop quantum error correction (Figure 522).

²¹⁵⁶ See [NVIDIA Announces New System for Accelerated Quantum-Classical Computing](#), Nvidia, March 2023.

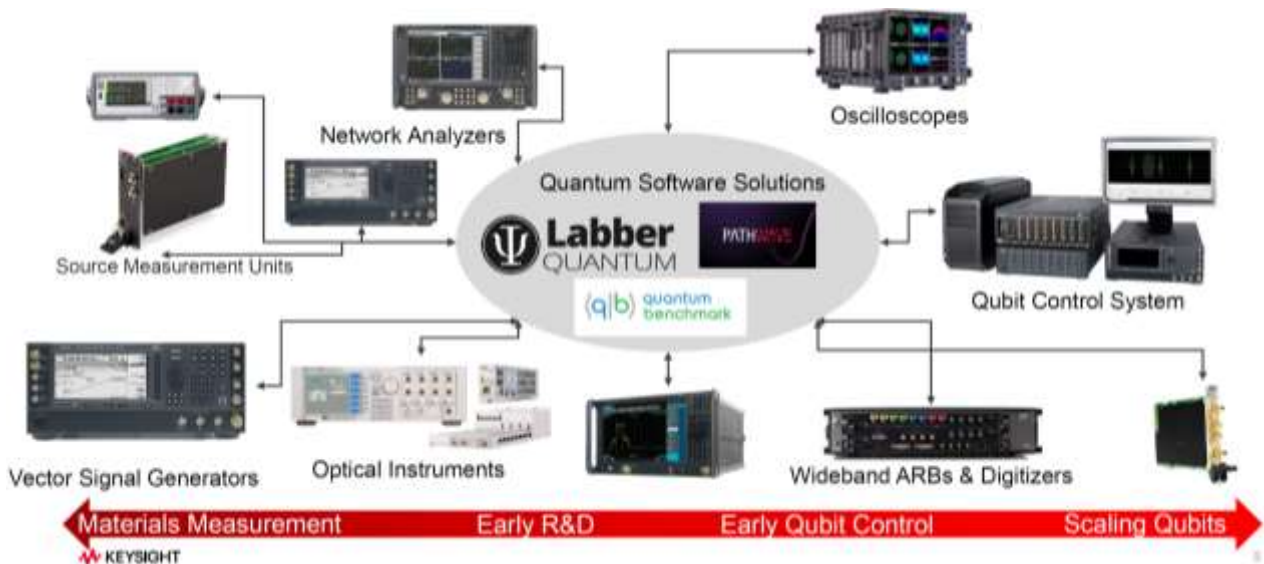


Figure 520: the Keysight control electronics family, mostly used in research laboratories.

It is packaged in PXIe cards format and a 4U box can control 20 qubits. It is completed by a Python API. It seems to be the first offering of this type with some ASIC drive components. The readout lag is only 20 ns, from the reception of the readout microwave to outputting its result. The first announced customers of QCS are Alice&Bob and Rigetti.

In August 2023, Keysight announced QuantumPro, an integrated EDA (electronic design automation) software tool for the design and simulation of superconducting qubits. It embeds five features into the PathWave Advanced Design System (ADS) 2024 platform with schematic design, layout creation, electromagnetic analysis, nonlinear circuit simulation, and quantum parameter extraction.



Figure 521: Keysight PXIe Quantum Control System.

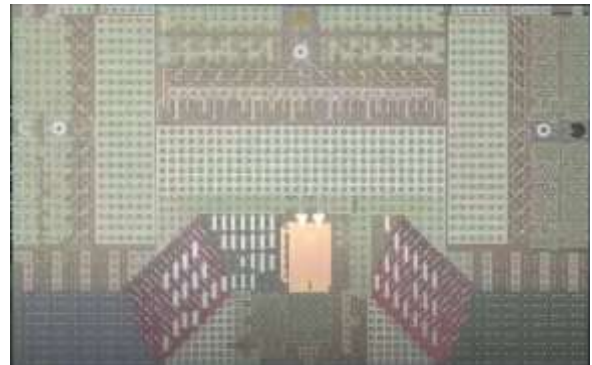


Figure 522: Keysight's first ASIC to control qubits.



QuantrolOx (2021, Finland-UK, \$8M) is an enabling technology company creating a deep learning software solution to optimize the automatic tuning and optimization of qubits settings²¹⁵⁷.

Their solution Quantum Edge that was developed with the help from DeepMind is using small training data sets and works in two steps: one with coarse tuning and a second with fine tuning. It efficiently adjusts the parameters of many qubits and is applicable to all sorts of qubits but particularly with those who express the largest variability like superconducting and electron spins qubits. In August 2023, they integrated their solution with Qblox control electronics for the drive of superconducting qubits.

²¹⁵⁷ See [Machine learning as an enabler of qubit scalability](#) by Natalia Ares, Nature, 2021 (3 pages) and [Learning Quantum Systems](#) by Valentin Gebhart, Natalia Ares et al, July 2022 (26 pages) which provides a broad view on machine learning use-case for various types of qubits quantum error mitigation.

The company has already about a staff of 10 including Vishal Chatrath (CEO, UK), Andrew Briggs (Executive Chair, UK, Professor of Nanomaterials, University of Oxford), Natalia Ares (Chief Scientist, UK, with a strong background on quantum thermodynamics and machine learning, Professor at University of Oxford), Dominic Lennon (Head of Quantum Technologies, UK, also from Oxford University) and Juha Seppä (CTO, Finland). Mostly based in the UK, the startup is positioned as a Finish one, maybe to make it easier to get some EU funding! Their first investors are Nielsen Ventures, Hoxton Ventures, Voima Ventures, Remus Capital, Hermann Hauser (cofounder of Arm) and Laurent Caraffa.

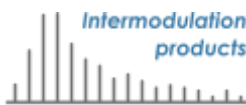
We can also mention a Chinese project, a superconducting microwave generator for the control of superconducting qubits based on a Xilinx FPGA²¹⁵⁸. In other similar and older projects, China's research teams showcased scalability claims that were not really sustained by a real scalable architecture²¹⁵⁹.



Active Technologies (2003, Italy) is a spin-off of University of Ferrara creating AWGs and Pulse/Pattern Generators. It can control experimental solid state qubits as well as electro-optical and electro-acoustic modulators used with cold atoms qubits. Its flagship product is the AWG-5000, a fast 16-bit AWG with 8 output channels.



CIQTEK (2016, China, \$15M) aka Guoyi Quantum develops high-precision pulse generator (ASG) and arbitrary waveform generator (AWG) used in qubits control, electron parametric resonance spectrometers and scanning electron microscopes. They also manufacture NV centers-based magnetometers and <Diamond I>, a 2-qubit computing system for educational purpose. It is based in Hefei and has 500 employees.



Intermodulation Products (2018, Sweden) is a spin-off company of KTH, the Royal Swedish Institute of Technology. They market Vivace, a microwave generator in the 4 GHz band used to drive superconducting qubits.



Quaxys (2020, USA) provides hardware and software solutions for superconducting and spin qubits electronic control, including Quantuware 4840, a compact qubit control and measurement unit.



Teledyne E2V (USA/UK/France) is a designer, manufacturer and provider of DACs and ADCs circuits used for microwave processing with superconducting qubits, noticeably with IBM. These are designed and manufactured near Grenoble, France.



Creotech Instruments (2008, Poland) is a satellite electronics developer which developed Sinara, an electronic system to drive trapped-ion qubits that implements quantum errors mitigation protocols.

It was built as part of the European Flagship AQTION project led by the University of Innsbruck. The system contains ADCs, DACs, digital I/Os, RF amplifiers, clock distribution, AWG and other electronic controls.

Cryo-CMOS

Cryo-electronics sit inside the cryostat, control the qubits and manage their readout in place of the some of the external electronic devices we're just covered, totally or partially depending on the systems generation.

²¹⁵⁸ See [Scalable and customizable arbitrary waveform generator for superconducting quantum computing](#) by Jin Lin, 2019 (9 pages).

²¹⁵⁹ See [High Performance and Scalable AWG for Superconducting Quantum Computer](#) by Jin Lin et al, 2018 (5 pages).

Many research teams and industry vendors are working on this strategic set of technologies which may help to unlock qubit scalability. We have among others the **University of Sidney**, **TU Delft** in the Netherlands²¹⁶⁰, **VTT** in Sweden, **CEA-Leti** and **CNRS Institut Néel** in France, **POSTECH** in South Korea and industry vendors like **Intel** and **IBM**. Cryo-electronics could help save a lot of quite expensive and embarrassing cabling, filters, attenuators, amplifiers, and reduce thermal losses in the cryostat.

It can also contribute to shorten the qubit gate to qubit readout cycle which can fasten the execution of quantum correction codes that will be required when operating large scale quantum processors.

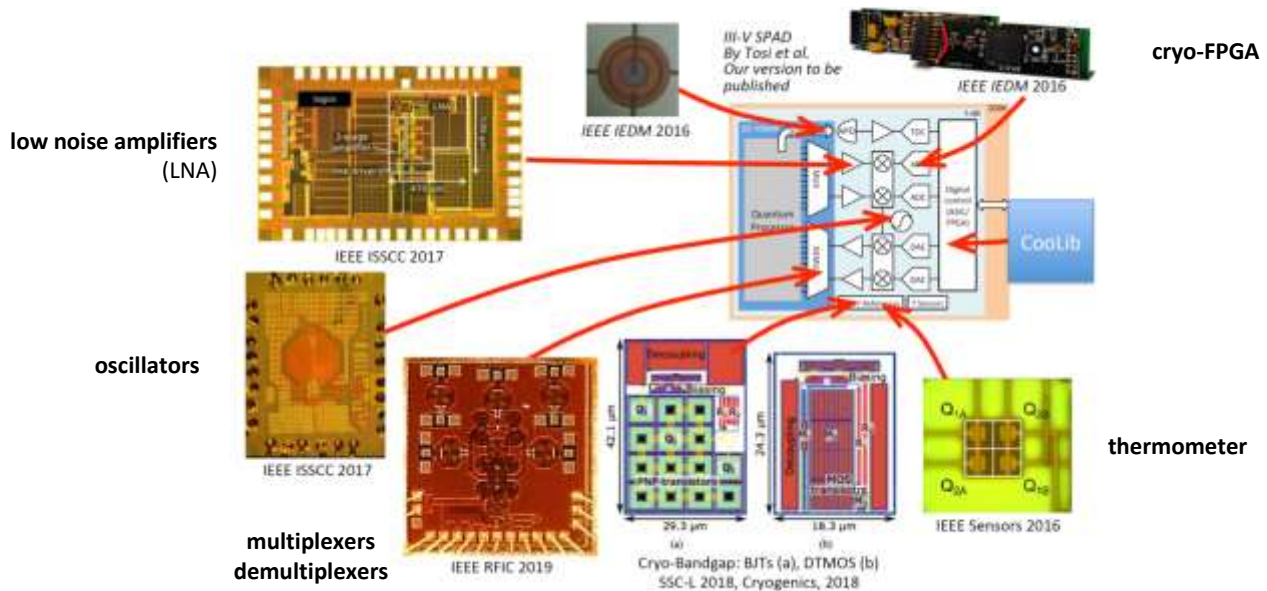


Figure 523: initially, research labs tried to build specific cryogenic component chips for many qubit control functions. Then, players like Intel tried to consolidate these in fewer components. There are still many components around, even with integrated cryo-CMOS for qubit control and readout, like the parametric amplifiers and HEMT. Source: [The Role of Cryo-CMOS in Quantum Computers](#) by Edoardo Charbon, EPFL Lausanne, February 2019 (91 slides).

It must meet rigorous specifications²¹⁶¹. Figure 523 describes the variety of component functions that can be integrated in the 1K-4K stages and even, when possible, at the qubit chip stage at less than 20 mK²¹⁶². These components must be certified to operate at these temperatures. These are data multiplexers and demultiplexers, local oscillators, AWGs, DACs, ADCs, low-noise amplifiers, DC flux bias generators, thermometers and other various sensors. The trend is to put within the cryostat a maximum of these electronic components. However, the heat they released is limited by the dilution refrigeration system cooling power²¹⁶³. It also conditions at which cold plate stage these components can operate. There is a complicated trade-off between the cryostat power overhead and what is saved by reducing cabling and filters between room temperature and the 4K cryostat stage where most of these Cryo-CMOS circuits are installed.

²¹⁶⁰ See [Large-Scale Quantum Computers: The need for Cryo-CMOS](#) by Fabio Sebastianio, TU Delft, April 2021 (57 mn video).

²¹⁶¹ See [Engineering cryogenic setups for 100-qubit scale superconducting circuit systems](#) by S. Krinner et al, 2019 (29 pages) which describes the issues with superconducting qubit control. In 2018, they proposed an optimized approach of wiring and electronics allowing up to 150 superconducting qubits to be embedded in a cryostat.

²¹⁶² Source of the diagram: [The Role of Cryo-CMOS in Quantum Computers](#) by Edoardo Charbon, EPFL Lausanne, February 2019 (91 slides). See also an earlier work from Purdue University and Australian colleagues: [Cryogenic Control Architecture for Large-Scale Quantum Computing](#) by J. M. Hornibrook, 2014 (8 pages) which describes well what should be done where in the cryostat.

²¹⁶³ See [Cryogenic Control Beyond 100 Qubits](#) by Ian Conway Lamb, 2017 (103 pages) which describes the technological challenges of components operating at cryogenic temperature, here for superconducting qubits. And the short version: [Cryogenic Control Architecture for Large-Scale Quantum Computing](#) by Ian Conway Lamb et al, 2017 (8 pages). See also [Semiconductor devices for cryogenic amplification](#) by Damien Prêle, 2013 (30 slides) and [Cryo-CMOS Circuits and Systems for Quantum Computing Applications](#) by Bishnu Patra et al, 2018 (14 pages).

Starting in 2016, separate solid-state electronic components started to be designed and tested at cryogenic temperatures. IMEC (Belgium) developed in 2020 a cryo-CMOS RF MUX multiplexing the in and out microwave signals used in qubit readouts and operating at 32 mK (Figure 524). Working at up to 10 GHz, it is suitable for superconducting qubits readouts and not yet for all electron spin qubits²¹⁶⁴.

It was to greatly simplify cabling between RF control and readout electronics. It runs at 4K. They created a similar solution operating at 15 mK in 2022 that is suitable for time-domain microwaves multiplexing for the drive of superconducting qubits.

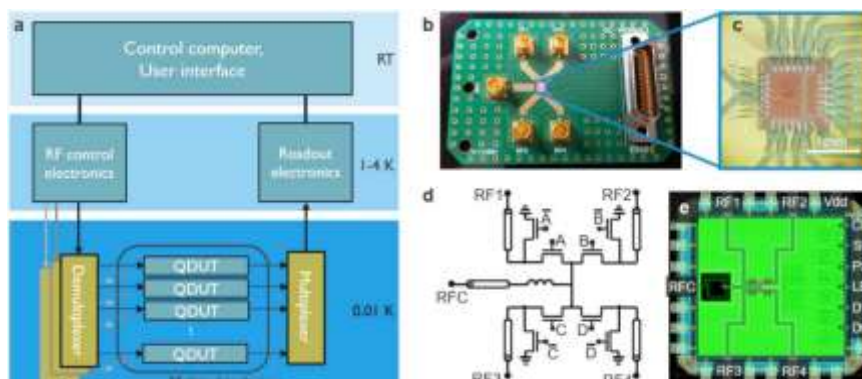


Figure 524: a qubit control multiplexing solution developed by IMEC. Source: [Millikelvin temperature cryo-CMOS multiplexer for scalable quantum device characterisation](#) by Anton Potočnik et al, IMEC, November 2020 (35 pages).

The trend is to integrate all these components in a minimum number of chips, preferably one, and working as close as possible to the qubit chip. The best level of integration so far was reached with **Intel** HorseRidge 2 announced in 2021 and the coldest operation was achieved with the Gooseberry chip from **Microsoft** and the **University of Sidney** as well as with a cryo-CMOS from **CEA-Leti**.

The first approach was to miniaturize these circuits at the 4K stage of the cryostat. It was studied in 2019 at **TU Delft** for silicon qubits state readout with their QuRO, for Quantum Read-Out²¹⁶⁵. The readout was using microwaves photon reflectometry. It sent an unmodulated RF frequency and evaluated the amplitude and phase of the reflected RF photon. The technique allows multiplexing qubits readout before sending the information out of the cryostat. This simplifies the output wiring. The prototype was based on a CMOS low noise amplifier (LNA) supplemented by a SiGe (silicon-germanium) transistor amplifier, followed by an analog-to-digital converter (ADC) implemented in a Xilinx Artix 7 FPGA. This FPGA made it possible to multiplex the readout state of several qubits. They use some copper cooling radiator in the 4K stage of the dilution refrigeration. They relied on standard market off-the-shelf passive and active components operating correctly at 4K. This prototyping did not deal with the waveform generation and DAC circuits driving qubit gates.

The energy saving of this kind of system is related to the quantum error correction load on qubit measurement. Bringing readout electronics closer to qubits speeds up error correcting codes. It is also interesting for simplifying the connectivity and improving quantum computers scalability. A similar approach was initially adopted by **Intel** in collaboration with **QuTech** for its 2020 HorseRidge superconducting and silicon qubits driver component capable of handling the microwave pulses of this frequency driver from 2 to 20 GHz. This component is sitting at the 4K stage of the cryostat²¹⁶⁶. Introduced in 2021, **HorseRidge 2** improved cryo-electronics integration to an unprecedented level (Figure 525).

²¹⁶⁴ See [Millikelvin temperature cryo-CMOS multiplexer for scalable quantum device characterisation](#) by Anton Potočnik et al, IMEC, November 2020 (35 pages).

²¹⁶⁵ See [Cryogenic electronics for the read-out of quantum processors](#) by Harald Homulle, TUDelft, 2019 (185 pages).

²¹⁶⁶ See [Cryo-chip overcomes obstacle to large-scale quantum computers](#) by QuTech, February 2020.

drive: arbitrary waveform microwave pulse generation
=> creates single qubit gates R_x and R_y
pulse phase => rotation axis X or Y
amplitude + duration => rotation angle

spin down
spin up

readout: multitone microwave pulse
reflected signal phase/amplitude analysis => spin up or down readout

gate pulsing: square pulse generation for qubit barrier and plunger gates
=> creates two-qubits gates

microcontroller: manages firmware instruction set
serial communication with outside the cryostat

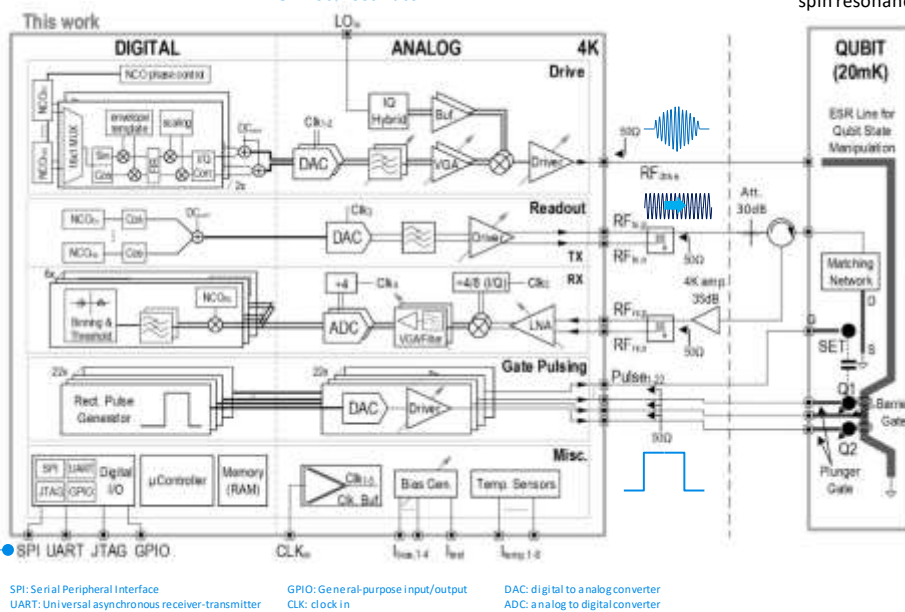


Figure 525: Intel HorseRidge 2 presented in 2021 is probably the most integrated qubit control chip being developed. Source: [A Fully Integrated Cryo-CMOS SoC for Qubit Control in Quantum Computers Capable of State Manipulation, Readout and High-Speed Gate Pulsing of Spin Qubits in Intel 22nm FFL FinFET Technology](#) by J-S. Park et al, February 2021 (3 pages).

It added multigate pulsing making it possible to control several qubits simultaneously, qubit readout and a programmable microcontroller. Gate pulsing creates multi-qubit gates with square DC signals controlling the barrier and plunger gates of the quantum dots while single-qubit gates use modulated RF signals and qubit readout use regular RF signals.

The chip uses frequency multiplexing to reduce the number of RF cables for qubits drive and readout. It drives up to 16 spin qubits with frequency ranges between 11 and 17 GHz. It reads the state of up to 6 qubits simultaneously. The control chip contains 22 DACs to simultaneously control the gate potentials for many qubits.

The chip is manufactured in a 22nm low-power FinFET technology (22FFL), operates at 4K and contains 100 million transistors²¹⁶⁷. In May 2021, Intel and Qutech demonstrated high-fidelity two-qubit control with this HorseRidge 2 control chip.

In 2022, **POSTECH** from South Korea proposed a similar architecture to HorseRidge 2 with a CMOS SoC sitting at 3.5K. It adds local oscillators²¹⁶⁸. It was prototyped in 40 nm TSMC bulk CMOS and consumes about 15 mW per qubit.

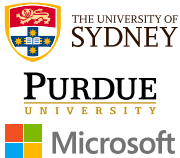
In 2019, an American-Australian team from the **University of Sydney**, **Purdue University** and **Microsoft Research** designed Gooseberry, a CMOS circuit to control superconducting, electron spin or (yet to be seen) Majorana fermion qubits²¹⁶⁹ (Figure 526).

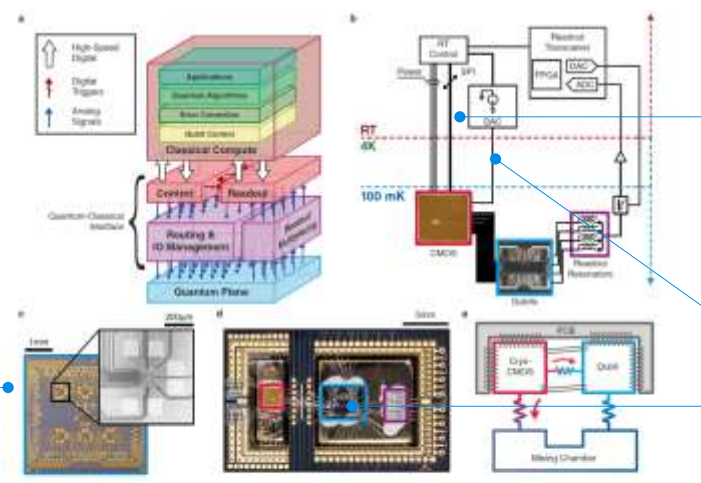
²¹⁶⁷ See [A Fully Integrated Cryo-CMOS SoC for Qubit Control in Quantum Computers Capable of State Manipulation, Readout and High-Speed Gate Pulsing of Spin Qubits in Intel 22nm FFL FinFET Technology](#) by J-S. Park et al, February 2021 (3 pages) and 41 slides (not free access).

²¹⁶⁸ See [A Cryo-CMOS Controller IC for Superconducting Qubits](#) by Kiseo Kang et al, August 2022 (14 pages). Computing the power per qubit was not obvious since the drain per function is not clearly presented in the paper (readout pulses vs readout pulses analysis).

²¹⁶⁹ See [A Cryogenic Interface for Controlling Many Qubits](#) by D.J. Reilly et al, December 2019 (7 pages). It was then published in [Nature](#) in January 2021.

Designed by David Reilly's team from the joint Microsoft Quantum Laboratories at the University of Sydney, it is operating at 100mK, just next to the qubit circuit on the same PCB support but without supposedly disturbing the qubits (in that case, only for silicon qubits since superconducting qubits would sit at the 15 mK cold plate stage). It seems to save power with a low sampling rate in AWG/DAC/DACs (4 bits). The circuit is using a microwave carrier signal source (LO or local oscillator) positioned outside the cryostat. It uses a round-robbing scheme to distribute modulated microwaves to each qubit in a sequential way. Qubit readout is done here with external circuits (ADC and FPGA). It is a bit the opposite of Harald Homulle's solution from TUDelft. The test CMOS is realized in FDSOI in 28nm. The chip greatly simplifies the control circuitry coming from outside.


mixed analog/digital CMOS with low-leakage transistors
28 nm FDSOI CMOS operating at 100 mK
chargelock fast-gate (CLFG) multiplexing command voltage to many variable outputs, with sequential time multiplex qubits activation
 contains master oscillator, wave form memory, configurable ring oscillator



input: digital instructions arriving via a serial peripheral interface (SPI) requiring just four low-bandwidth wires from room temperature

 micro-wave carrier coming from outside the cryostat

 benchmarked on a GaAs silicon spin qubit

FIG. 1. The quantum-classical interface of a quantum computer. a. The generic stack of elements needed for quantum computing. b. Control and readout sub-systems, distributed between room temperature and 100 mK. The brown cryo-CMOS chip addresses the IO bottleneck for control signals. c. Photograph and electron micrograph of our qubit test platform based on 30 GaAs quantum dots (see Supp. Mat. for details). d. Photograph showing the cryo-CMOS chip (red box), qubit test chip (blue box), and readout chip (purple box). Each chip is soldered to a gold-plated copper thermalization pillar, with a separate pillar used for the CMOS chip. e. Schematic thermal conductance model of the setup. The intended use of the partially separate cooling pillars is to increase the thermal conductivity to the mixing chamber (big red arrow) while reducing the direct heat (little red arrow) flowing from the hot CMOS chip to the qubit device.

source: A Cryogenic Interface for Controlling Many Qubits by D.J. Reilly et al, December 2019 and published in Nature in January 2021.

Figure 526: Microsoft prototype another control chip that support fewer functions than HorseRidge but it run next to the qubit chip at lower temperature, suitable for silicon spin qubits. Source: [A Cryogenic Interface for Controlling Many Qubits](#) by D.J. Reilly et al, December 2019 (7 pages).

This low-power chip generates control pulses of 100 mV at 18 nW per cell. The control of the qubits can also use superconducting microwave generation and reading circuits, their interest being a much lower thermal dissipation²¹⁷⁰.

In 2020, CEA-Leti in Grenoble created a mixed analog, digital and quantum cryo-CMOS circuit manufactured in 28 nm FDSOI and operating at 110 mK. It handles all the qubits driving and readout cycle with charge pumping, generating continuous tone GHz microwaves and measuring the induced current with a multiplexed transimpedance amplifier (TIA). At this experimental stage, it drives only a couple qubits but looks promising with regards to the ability to control quantum dots qubits at their operating temperature, at least for silicon qubits working between 100 mK and 1.5 K depending on their type and experimental settings. And the quantum dot qubits were in the circuit itself!

One key technology to master when assembling electronic components at the qubit level is packaging and connectivity. That's where a French team from CEA-Leti, CEA LIST and CNRS-Institut Néel made progress in February 2021 with building a prototype interposer enabling the integration of quantum and control chips fabricated from different materials, processes and sources. Named QuIC (Quantum integrated circuits with cryo-CMOS), the prototype demonstrator controls quantum chips with integrated control electronics and operating at below 1K.

²¹⁷⁰ See [Quantum Computer Control using Novel, Hybrid Semiconductor-Superconductor Electronics](#) by Erik P. DeBenedictis of Zettaflops, 2019 (15 pages), which describes an approach for controlling qubits mixing superconductors (JJ) and adiabatic circuits, Cryogenic Adiabatic Transistor Circuits (CATCs). The paper gives an overview of the energy efficiency of cryo-CMOS components and various known superconductors (RQL, AQFP, ...).

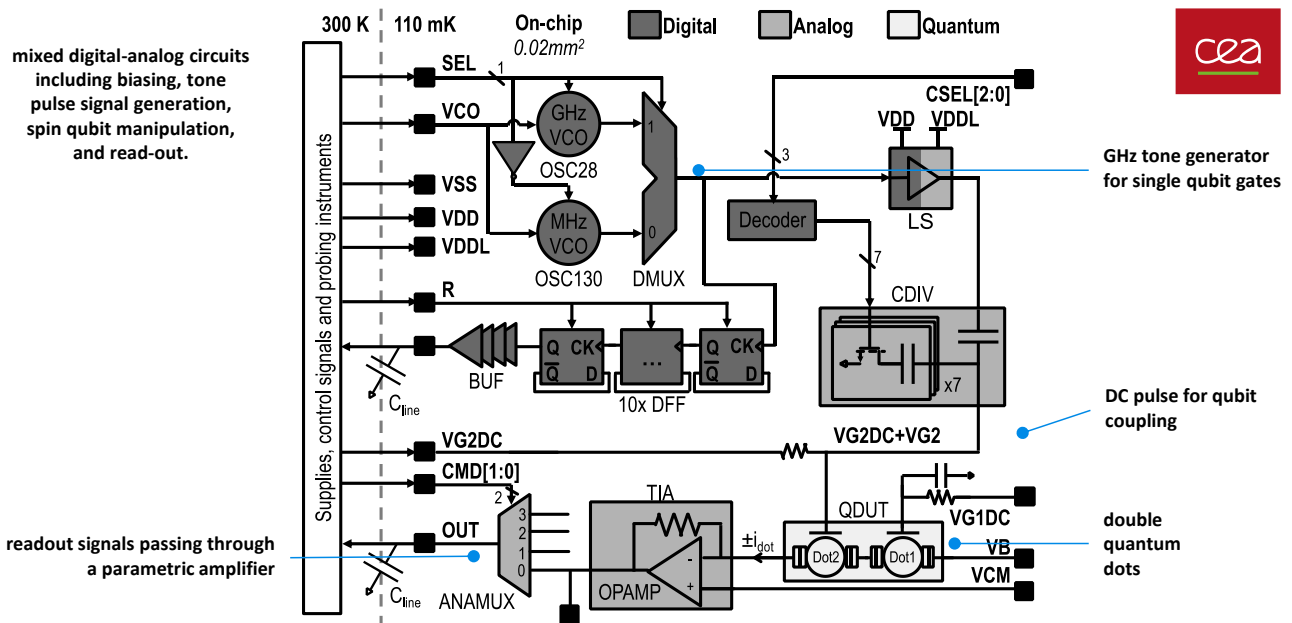


Figure 527: this chip from CEA-LIST runs at the same temperature as Microsoft's chip seen before. It is tailored for silicon spin qubits control. Source: [A 110mK 295μW 28nm FD-SOI CMOS Quantum Integrated Circuit with a 2.8GHz Excitation and nA Current Sensing of an On-chip Double Quantum Dot](#) by Loick Le Guevel, Silvano de Franceschi, Yvain Thonnart, Maud Vinet et al, February 2020, ISSCC (12 pages).

The integration uses a 3D flip-chip process. The control electronics are made on standard FDSOI 28nm by STMicroelectronics. Passive elements and filter devices will be integrated in future versions (Figure 527)²¹⁷¹.

The integrated packaging increases the number of qubits that can be controlled by reducing the number of coaxial cables flowing through the cryostat from the upper stages. It also avoids chip wire bonding since qubits and control electronics are coupled by routing lines on the interposer. The packaging allows thermal decoupling between the quantum chip and the electronics control chip.

They also use a die-to-wafer process from CEA-Leti that are used to build interconnects working at under 1K.

CEA is also replacing indium bumps with other materials that are compatible with existing CMOS manufacturing processes, like SnAg microbumps and directly bonded Cu pads from Cu/SiO₂²¹⁷².

In another work published by an EPFL team in January 2021, a 40 nm CMOS chip operating at 50 mK hosted both 9 silicon quantum dots qubits organized in a 3x3 array and some digital electronics using analog LC resonators implementing time- and frequency-domain multiplexing for qubit readout, all operating at 50 mK²¹⁷³.

IBM is also designing cryo-CMOS components. They prototyped the first one manufactured in a 14 nm process. It supports 4.5-to-5.5GHz RF AWG for pulse control generation and does not rely on TDM or FDM (time or frequency multiplexing)²¹⁷⁴.

²¹⁷¹ See also [A Compact TIA in 22nm FDSOI CMOS for Qubit Readout in Monolithic Quantum Processors](#) by Domenico Zito et al, AGH University of Science and Technology and Aarhus University, October 2023 (4 pages).

²¹⁷² See [Die-to-Wafer 3D Interconnections Operating at Sub-Kelvin Temperatures for Quantum Computation](#), September 2020.

²¹⁷³ See [Integrated multiplexed microwave readout of silicon quantum dots in a cryogenic CMOS chip](#) by A. Ruffino et al, EPFL, January 2021 (14 pages).

²¹⁷⁴ See [A Cryo-CMOS Low-Power Semi-Autonomous Qubit State Controller in 14nm FinFET Technology](#) by David J Frank et al, IBM Research, ISSCC IEEE, February 2022 (no free access).

Another 2023 iteration of the chip added a full implementation of a cross-resonance two-qubit gate drive with the same energy consumption per qubit and²¹⁷⁵. It contains an SRAM based AWG, a technique that IBM also prototyped in 2022 to drive spin qubits²¹⁷⁶. However, it seems that LO (local oscillator) leakage negatively impacts gate fidelities and will need some work. IBM created blueprints to integrate all readout features in such chips in the future²¹⁷⁷.

	DC pulses	LO	AWG	DAC	I/Q mixers	I/Q demod	readout parametric amplification	readout ADC	readout signal analysis	temp	power / qubit
cryo-CMOS	Google - Bardin 2019		for X and Y gates	yes	yes					3K	2 mW
	Microsoft/Sydney /Purdue, FD-SOI 28 nm, 2019	yes	yes	only external signal routing to qubit						100 mK	N/A, low power
	CEA List/Leti FD-SOI 28 nm 2020	Yes	yes				Yes TIA amplification			110 mK	295µW
	QuTech& Intel FinFET 22 nm 2020			Yes, 8-10 bits	Yes	yes					12 mW
	HorseRidge 2 FinFET 22 nm, Intel 2021	yes		yes, 14-bit	yes	Yes	yes	only LNA between paramp and HEMT	yes	4K	27 mW (to check)
	EPFL, CMOS 40 nm 2021						yes	time and frequency domain readout signal multiplexing		50 mK	
	POSTECH Korea CMOS 40 nm 2022		2	yes, 4 bits	yes, 4 bits	yes	yes	LNA	yes	3.5K	15 mW
	IBM, FinFET 14 nm 2022			Yes		Yes				3.5K	23 mW
	IBM, FinFET 14 nm 2023			Yes (adds two-qubit cross resonance gate)		Yes				4K	23 mW
SFQ	SeeQC, SFQ 2019 DigiQ, USC, Chicago, Nvidia 2022 (*)	yes	replaced by series of single amplitude pulses				yes			3K/600 mK (SFQ copro) & 20 mK (DQM)	0,24 mW (*)
	IBM QEC, SFQ 2022								partial surface code QEC	4K	10µW to 500µW per logical qubit
	SeeQC, Maryland University, 2023										passive

(cc) Olivier Ezratty, 2023

Figure 528: compilation of various cryo-chips developed so far. (cc) Olivier Ezratty, 2022. Sources: Google – Bardin: [A 28nm Bulk-CMOS 4-to-8GHz <2mW Cryogenic Pulse Modulator for Scalable Quantum Computing](#), February 2019 (13 pages), Intel HorseRidge 2: [A Fully Integrated Cryo-CMOS SoC for Qubit Control in Quantum Computers Capable of State Manipulation, Readout and High-Speed Gate Pulsing of Spin Qubits in Intel 22nm FFL FinFET Technology](#) by J-S. Park et al, February 2021 (3 pages), Microsoft / Sydney / Purdue: [A Cryogenic Interface for Controlling Many Qubits](#) by D.J. Reilly et al, December 2019 (7 pages), CEA List/Leti: [A 110mK 295µW 28nm FD-SOI CMOS Quantum Integrated Circuit with a 2.8GHz Excitation and nA Current Sensing of an On-chip Double Quantum Dot](#) by Loïck Le Guevel et al, February 2020, ISSCC (12 pages). QuTech: [A Scalable Cryo-CMOS Controller for the Wideband Frequency-Multiplexed Control of Spin Qubits and Transmons](#) by Jeroen Petrus Gerardus Van Dijk, Menno Veldhorst, Lieven M. K. Vandersypen, Edoardo Charbon et al, November 2020 (17 pages). EPFL: [Integrated multiplexed microwave readout of silicon quantum dots in a cryogenic CMOS chip](#) by A. Ruffino et al, EPFL, January 2021 (14 pages), POSTECH: [A Cryo-CMOS Controller IC for Superconducting Qubits](#) by Kiseo Kang et al, August 2022 (14 pages). IBM: [A Cryo-CMOS Low-Power Semi-Autonomous Qubit State Controller in 14nm FinFET Technology](#) by David J Frank et al, IBM Research, ISSCC IEEE, February 2022 (no free access), [Using Cryogenic CMOS Control Electronics To Enable A Two-Qubit Cross-Resonance Gate](#) by Devin L. Underwood et al, IBM Research, February-August 2023 (33 pages), SEEQC: [Hardware-Efficient Qubit Control with Single-Flux-Quantum Pulse Sequences](#) by Robert McDermott et al, 2019 (10 pages), [DigiQ: A Scalable Digital Controller for Quantum Computers Using SFQ Logic](#) by Mohammad Reza Jokar et al, February 2022 (15 pages). IBM QEC: [Have your QEC and Bandwidth too!: A lightweight cryogenic decoder for common / trivial errors, and efficient bandwidth + execution management otherwise](#) by Gokul Subramanian Ravi et al, August 2022 (14 pages). Updated in 2023.

As seen in IBM and Intel designs, cryo-CMOS chips consuming 25 mW at 4 K per qubit would turn into a total 5 W per qubit consumption at room temperature due to the 200× cryostat overhead at 4K.

²¹⁷⁵ See [Using Cryogenic CMOS Control Electronics To Enable A Two-Qubit Cross-Resonance Gate](#) by Devin L. Underwood et al, IBM Research, February-August 2023 (33 pages).

²¹⁷⁶ See [A cryogenic SRAM based arbitrary waveform generator in 14 nm for spin qubit control](#) by Mridula Prathapan et al, IBM Research, November 2022 (4 pages). The chipset consumes 2 to 4 mW for AWG and DAC at 8-bit sampling, to drive spin qubits.

²¹⁷⁷ See [A system design approach toward integrated cryogenic quantum control systems](#) by Mridula Prathapan et al, IBM Research Zurich, November 2022 (4 pages).

One million physical qubits would then require 5 MW of power, and this doesn't take into account many other power drain sources like the classical part of error correction codes and the related data flow. One interesting research avenue to improve the energy-efficiency of cryo-CMOS would be to implement some form of reversible logic in it. This seems theoretically possible outside the DAC and ADC parts²¹⁷⁸.

For a helicopter view, all these cryo-CMOS projects seem to make more sense to drive silicon spin qubits than superconducting qubits. One reason is the available cooling budget is much higher at the operating temperature of spin qubits that sits between 100 mK and 1 K while superconducting qubits operate at about 15 mK.

Figure 528 contains a detailed comparison of the various cryo-chips studied in the section and the next on superconducting logic. It shows a discrepancy of power consumption per qubit which is explained by several factors: the different electronic features supported by the chips, their mutualization across a given number of qubits and the manufacturing node technology.

It is completed by Figure 529 which shows which part in the table corresponds to which function in the pulse management sequences from qubit drive to qubit readout.

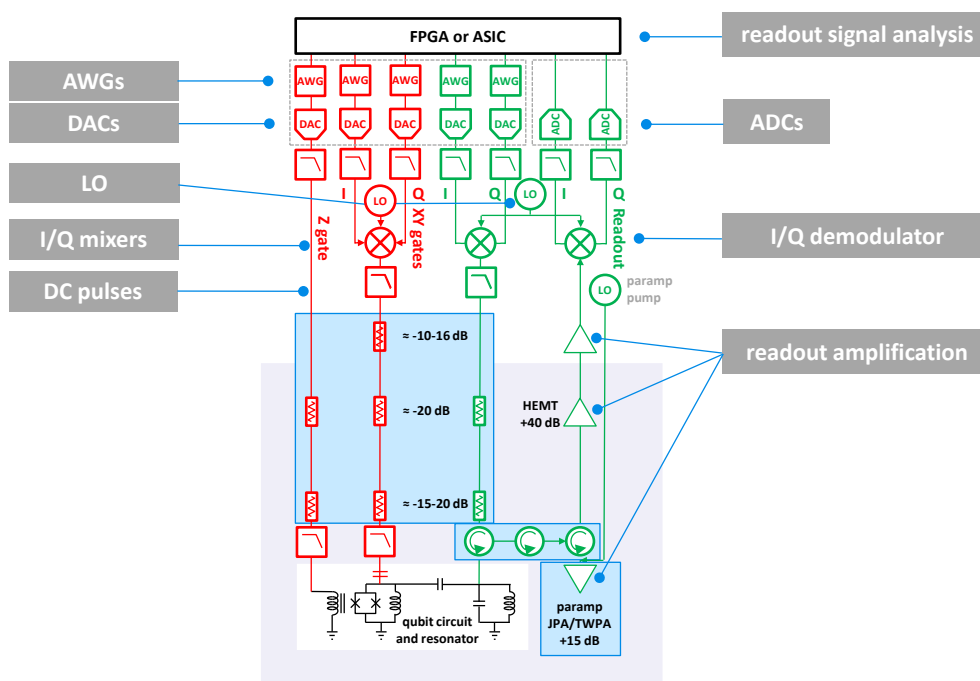


Figure 529: feature list chosen for the table in Figure 528. (cc) Olivier Ezratty, 2022.

Superconducting electronics

The other option for qubit control and readout at low temperature is to rely on superconducting logic based on Josephson junctions²¹⁷⁹. The most common one is SFQ, for “single flux quantum” and then RSFQ for “rapid SFQ”²¹⁸⁰.

²¹⁷⁸ See [Rebooting Quantum Computing](#) by Erik P. DeBenedictis and Elie K. Track, Zettaflops and Hypres, December 2022 (6 pages).

²¹⁷⁹ See [Superconducting electronics at 4 K for control and readout of qubits](#) by Adam Sirois et al, NIST, ASC 2020 (27 slides) and [Flux Quantum Electronics](#) by NIST which cover their broad research in the domain.

²¹⁸⁰ SFQ logic families are divided into two groups: ac-biased and dc-biased. Reciprocal Quantum Logic (RQL) and Adiabatic Quantum Flux Parametron (AQFP) are in the first group, and Rapid Single Flux Quantum (RSFQ), Energy-efficient RSFQ (ERSFQ) and energy-efficient SFQ (eSFQ) are in the second group. The dc-biased logic family with higher operation speed (as high as 770GHz for a T-Flip Flop (TFF)) and less bias supply issues are more popular than ac-biased logic family. Source: [NISQ+: Boosting quantum computing power by approximating quantum error correction](#) by Adam Holmes et al, Intel, University of Chicago and USC, April 2020 (13 pages).

Their potential benefit is a very low power consumption, up to 500 times less than CMOS logic²¹⁸¹, the ability to operate at the same temperatures as superconducting qubits, and their enablement of a much simpler cabling scheme within the cryostat²¹⁸².

The eSFQ variant can even potentially be 10^4 more efficient than cryo-CMOS for some functions²¹⁸³. However, this technology has some shortcomings: it may be a significant source of noise affecting qubits fidelities with so-called quasiparticle poisoning and antenna effect²¹⁸⁴, there are some constraints on high-frequency power sources, classically generated AWG wave formed pulses are replaced by trains of single amplitude SFQ pulses of less than 2 ps duration which drives its own preparation overhead to create qubit gates (Figure 530)²¹⁸⁵, limited Josephson junctions density and some qubit backaction, SFQ logic can't be used to store data. Many cryogenic memory solutions are investigated but are still in the making: cryogenic spintronics, magnetic tunnel junction (MTJ)²¹⁸⁶, RQL (reciprocal quantum logic)²¹⁸⁷, SQUID-based, hybrid Josephson–CMOS, JMRAM and OST-MRAM memories and even classical SRAM²¹⁸⁸. We pass on the whereabouts of these various technologies²¹⁸⁹.

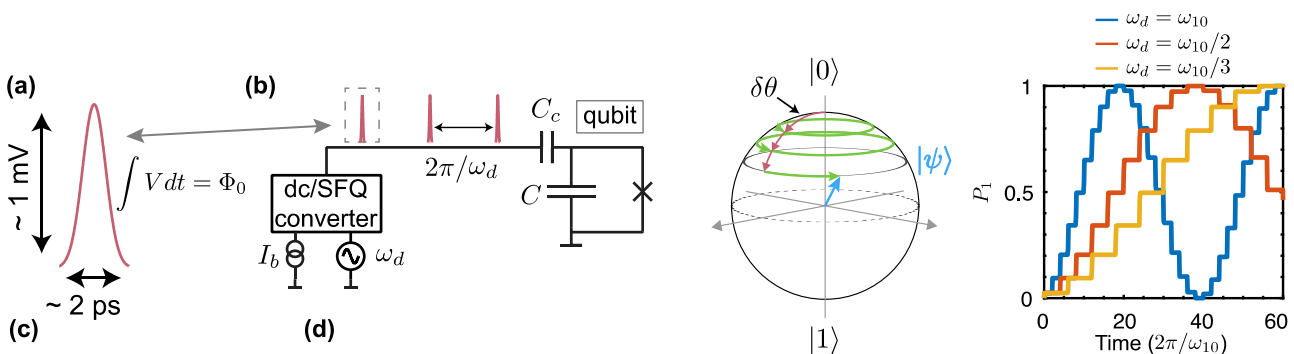


Figure 530: SFQ based wave pulse generation process.

Source: [Digital coherent control of a superconducting qubit](#) by Edward Leonard, Robert McDermott et al, 2018 (13 pages).

There are many interconnected research fields here, and SFQ qubits drive logic is frequently of sub-product of more general research in superconducting electronics.

Since the 1970s, there were many ups and downs with research in using superconducting electronics to override the apparent limitations of Moore's law with classical semiconductors. Also, superconducting electronics have other use cases like with single photon detection, magnetism sensing with SQUIDS and analog amplifiers working at the quantum limits (JPAs, SPMs, TWPAs, that we cover in the part starting page 614).

²¹⁸¹ Source: [Superconducting Microelectronics for Next-Generation Computing](#) by Leonard M. Johnson, February 2018 (27 slides).

²¹⁸² With room temperature classical control electronics on a 1,000 qubit system, you'd need between \$5M and \$10M of niobium-titanium cables for the 4K to 15 mK stages. Each such cable costs in excess of \$2K.

²¹⁸³ See [Quantum-Classical Interface Based on Single Flux Quantum Digital Logic](#) by Roger McDermott, Oleg A. Mukhanov, Thomas A. Ohki et al, October 2017 (16 pages).

²¹⁸⁴ See [Single Flux Quantum-Based Digital Control of Superconducting Qubits in a Multi-Chip Module](#) by Chuan-Hong Liu, R. McDermott et al, PRX Quantum, January-July 2023 (15 pages) that addresses the quasiparticle poisoning problem with separating the SFQ chipset from the qubit chipset.

²¹⁸⁵ At this point, in D-Wave annealers, SFQ circuits create DC signals and ramp currents with DACs (digital-to-analog converters) to configure the system and drive the magnetometers used for qubits readouts.

²¹⁸⁶ See [Cryogenic Memory Architecture Integrating Spin Hall Effect based Magnetic Memory and Superconductive Cryotron Devices](#) by Minh-Hai Nguyen et al, 2020 (11 pages).

²¹⁸⁷ See [Superconducting logic circuits operating with reciprocal magnetic flux quanta](#) by O.T. Oberg, 2011 (337 pages).

²¹⁸⁸ See [Cryogenic In-Memory Computing for Quantum Processors Using Commercial 5-nm FinFETs](#) by Shivendra Singh Parihar et al, IEEE Journal of Circuit and Systems, August 2023 (13 pages).

²¹⁸⁹ See the review paper [Cryogenic Memory Technologies](#) by Shamiul Alam et al, July 2022 (21 pages).

Qubit readout function can also be implemented with SFQ with readout signal generated through a JPM amplifier²¹⁹⁰ and converted with ADCs²¹⁹¹.

Tone signal generation can also be implemented in SFQ logic²¹⁹².

IBM studied classical electronics based on the Josephson junction from the 1960s to 1983, using lead and then lead/niobium. The technology was only supported by IBM and could not compete with CMOS processors, drive by Moore's law and the whole semiconductor industry, particularly with Intel. Japan's MITI had also launched a superconducting computing initiative throughout the 1980s leading to a 4-bit machine using 1 Kbits of RAM. The Bell labs also worked on niobium/aluminum oxide Josephson junctions.

Hypres. Then, the invention of the more efficient and energy efficient RSFQ in USSR in 1985 led to its transfer to the USA via its coinventor Oleg Mukhanov when he joined Hypres in 1991. It led to a short lived superconducting supercomputing project (1997-2001).

Starting in the early 2000s, attention then turned to superconducting qubits with investments throughout the world (USA, France, Japan, ...) leading to major developments from IBM, Google and others. Hypres did use superconducting electronics for non-quantum use cases, particularly in the defense industry and with radars, and quantum sensing using SQUIDs. Interestingly, some of the interest in classical electronics made with SFQ and RSFQ came with quantum computing and the need for energy efficient control electronics.

D-Wave was probably the first to use SFQ electronics in its systems and since its inception. At their beginning, they hired skilled engineers coming from IBM, Stony Brooke University in New York and coming from Stellenbosch University in South Africa having a good experience in superconducting physics and electronics.

D-Wave's quantum annealers contain flux superconducting qubits and superconducting SFQ circuits handling signals control generation, control and qubit state readout, and for up to 5,000 qubits. This is a little-known technological feat from D-Wave. It allows them to greatly simplify the wiring that leads to the quantum processor since all their SFQ electronics sits in the same chip handling the qubits. Figure 531 shows how it looks like.

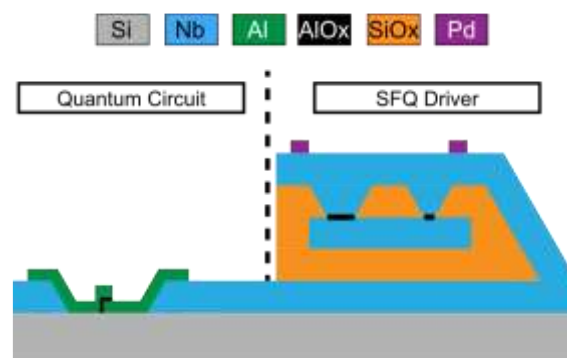


Figure 531: a side-by-side comparison of the stacking of elements in a superconducting qubit (left) and with SFQ logic (right). Source: [Digital coherent control of a superconducting qubit](#) by Edward Leonard, Robert McDermott et al, 2018 (13 pages).

Who else is working with SFQ electronics to control solid state qubits? Let's start with the USA who are the most active here.

- **SEEQC**, a spin-off / split-off from Hypres that we'll detail later and is specialized in superconducting electronics for qubits control.

²¹⁹⁰ See [Interfacing Superconducting Qubits With Cryogenic Logic: Readout](#) by Caleb Howington, Alex Opremcak, Robert McDermott, Alex Kirichenko, Oleg A. Mukhanov and Britton L. T. Plourde, August 2019 (5 pages) with more details in the related thesis [Digital Readout and Control of a Superconducting Qubit](#) by Caleb Jordan Howington, December 2019 (127 pages).

²¹⁹¹ See [History of Superconductor Analog-to-Digital Converters](#) by Oleg Mukhanov, 2011 (19 pages) and [Superconductor Analog-to-Digital Converters](#) by Oleg A. Mukhanov et al, 2010 (21 pages).

²¹⁹² See [A low-noise on-chip coherent microwave source](#) by Chengyu Yan, Mikko Möttönen et al, November 2021 (14 pages) and [Digital Control of a Superconducting Qubit Using a Josephson Pulse Generator at 3 K](#) by L. Howe et al, PRX Quantum, 2022 (11 pages).

- **Raytheon BBN (USA)** is investigating the usage of SFQ systems and a mix of SFQ and spintronics for controlling qubits²¹⁹³. They have a wide-ranging partnership with IBM and some IBM researchers worked with BBN on SFQ back in 2018 but it doesn't tell whether IBM is keen to adopt SFQs to control their superconducting qubits.
- **University of Wisconsin-Madison** has a Department of Physics run by Robert McDermott that investigates SFQ logic. He pioneered qubit control with trains of SFQ pulses²¹⁹⁴. They authored the paper with Raytheon BBN on SFQ qubit control mentioned with Raytheon above.
- **MIT Lincoln Labs** has been working for a while on SFQ logic in the “beyond CMOS” roadmap funded by IARPA as part of the Quantum Enhanced Optimization (QEO) and Logical Qubit (LogiQ) programs^{2195 2196}. In 2017, they developed a 3D Integrated Superconducting Qubit Platform using three layers: the qubit chip, an interposer with through-substrate vias and a supporting chip with a routing layer and a TWPA for qubit readout microwave amplification. They are also leveraging their own superconducting cleanroom. The Lincoln Lab is even providing many labs across the world with their own custom TWPA and for free.
- **University of Chicago** is also involved in the design of SFQ-based qubit control electronics. In 2022, they demonstrated low-error two-qubit operations using SFQ pulses drive working with fluxonium superconducting qubits²¹⁹⁷ (Figure 532). They also led the DigiQ project launched by the NSF.

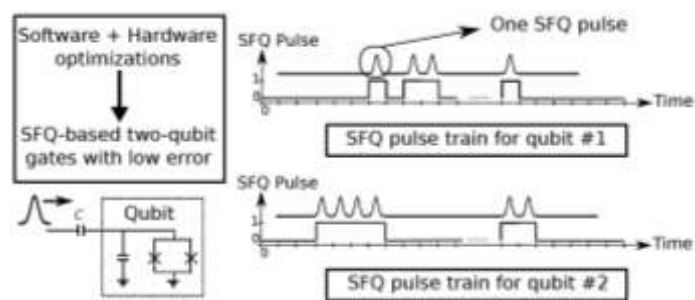


Figure 532: SFQ wave packet optimization. Source: [Practical implications of SFQ-based two-qubit gates](#) by Mohammad Reza Jokar et al, February 2022 (11 pages).

It was funded as part of the Enabling Practical-scale Quantum Computation (EPiQC)²¹⁹⁸.

- **Northrop Grumman** is also working on SFQ for qubit controls and even patented one related solution back in 2008²¹⁹⁹. They also developed RQL techniques.
- **IBM** together with the Universities of Chicago and Southern California, and Super.tech (from ColdQuanta) presented in August 2022 the development of an SFQ-based cryogenic circuit to implement part of the logic of the most common errors in quantum error correction for surface

²¹⁹³ See [Quantum Engineering and Computing Group](#) by Thomas Ohki, March 2021 (39 slides). The team has a staff of 20 and [Digital coherent control of a superconducting qubit](#) by Edward Leonard, Robert McDermott et al, 2018 (13 pages). It identifies a shortcoming of SFQ: quasi-particles poisoning that negatively impacts qubit fidelities. Back in 2018, they said it could be addressed with putting SFQ logic on a separate chip that would be bonded (with indium) to the qubit chipset. Nowadays, this is an available technology.

²¹⁹⁴ See [Accurate Qubit Control with Single Flux Quantum Pulses](#) by Robert McDermott and M.G. Vavilov, 2014 (10 pages), [Quantum-Classical Interface Based on Single Flux Quantum Digital Logic](#) by Robert McDermott et al, 2017 (16 pages) and [Scalable Hardware-Efficient Qubit Control with Single Flux Quantum Pulse Sequences](#) by Kangbo Li, Robert McDermott and Maxim G. Vavilov, 2019 (10 pages).

²¹⁹⁵ See [Superconducting integrated circuits](#), MIT Lincoln Labs.

²¹⁹⁶ See [Superconducting Microelectronics for Next-Generation Computing](#) by Leonard M. Johnson, February 2018 (27 slides).

²¹⁹⁷ See [Practical implications of SFQ-based two-qubit gates](#) by Mohammad Reza Jokar et al, February 2022 (11 pages).

²¹⁹⁸ See [DigiQ: A Scalable Digital Controller for Quantum Computers Using SFQ Logic](#) by Mohammad Reza Jokar et al, February 2022 (15 pages). The project is run with Amazon, Nvidia, Super.tech and USC. The qubits are driven by series of small SFS pulses, not by arbitrary waveform pulses. Theoretically, SFQ logic could still create these waveforms thanks to clock speed exceeding 100 GHz. It could create waveforms with basebands of 4 to 25 GHz. But this would require superconducting DACs and ADCs which happen to need resistances, thus being irreversible and dissipative, creating some thermal constraints.

²¹⁹⁹ See [Method and apparatus for controlling qubits with single flux quantum logic](#) patent.

codes²²⁰⁰. The decoder could support between 2000 and 100,000 logical qubits depending on the code distance.

And in the rest of the world:

- **Japan** has a very active group in SFQ, the group of Nobuyuki Yoshikawa from Yokohama National University. They are working in the field of superconducting electronics, SFQ and adiabatic circuits mostly as “beyond than Moore” solutions²²⁰¹. He participated to the development of AQFP (Adiabatic Quantum-Flux-Parametron), an energy-efficient superconductor logic element²²⁰² and started to publish work on its implementation for qubits control in 2023²²⁰³. RIKEN also has a team working on using SFQs²²⁰⁴.
- **Canada** has a team spread over Sherbrooke, Waterloo and 1Qbit working on improving SFQ qubit drive²²⁰⁵.
- **Germany** has a couple labs and fabs looking at superconducting electronics and their potential usage in qubits control. You can count with Per J. Liebermann and Frank K. Wilhelm from Saarland University who work on improving qubit fidelities with varying the time distance between SFQ pulses in the train using control theory and (classical) genetic algorithms²²⁰⁶. The Leibniz-IPHT in Jena, Thuringia, has a cleanroom that works, among other things, on producing RSFQ circuits and SQUIDs for quantum sensing. Leibniz-IPHT is coordinating the German project HIQuP dealing specifically with superconducting qubit control electronics and partnering with IQM Germany and Supracon AG, itself a spin-out of the Leibniz-IPHT that is specialized in SQUID based magnetometers. The PTB has also investigated SFQ circuits in the past²²⁰⁷. There was also the EU project RSFQubit from 2004 to 2007, involving many German players and coordinated by Chalmers University, Sweden, with a funding of 2.6M€.
- **France** with Pascal Febvre from CNRS Chambéry working on a project funded by ODNI and DARPA²²⁰⁸.
- **Finland** also conducts some research in SFQ logic at VTT under the leadership of Matteo Cherchi²²⁰⁹. Their aCryComm project develops converters and input/outputs for simple SFQ processors²²¹⁰. This work could also lead to some potential collaboration with IQM.

²²⁰⁰ See [Have your QEC and Bandwidth too!: A lightweight cryogenic decoder for common / trivial errors, and efficient bandwidth + execution management otherwise](#) by Gokul Subramanian Ravi et al, August 2022 (14 pages).

²²⁰¹ See a review paper he coauthored in 2004: [Superconducting Digital Electronics](#) by Hisao Kayakawa et al, 2004 (15 pages).

²²⁰² See [Adiabatic Quantum-Flux-Parametron: A Tutorial Review](#) by Naoki Takeuchi, Nobuyuki Yoshikawa et al, January 2022 (14 pages).

²²⁰³ See [Scalable quantum-bit controller using adiabatic superconductor logic](#) by Naoki Takeuchi, Nobuyuki Yoshikawa et al, October 2023 (10 pages).

²²⁰⁴ See [Inter-temperature Bandwidth Reduction in Cryogenic QAOA Machines](#) by Yosuke Ueno et al, RIKEN, October 2023 (4 pages).

²²⁰⁵ See [Compact Pulse Schedules for High-Fidelity Single-Flux Quantum Qubit Control](#) by Ross Shillito et al, September 2023 (10 pages).

²²⁰⁶ See [Optimal Qubit Control Using Single-Flux Quantum Pulses](#) by Per J. Liebermann and Frank K. Wilhelm, Saarland University, 2016 (5 pages).

²²⁰⁷ See [Low-noise RSFQ Circuits for a Josephson Qubit Control](#) by M Khabipov, D Balashov, E Tolkacheva and A B Zorin, PTB, 2008 (7 pages).

²²⁰⁸ See [Superconductor modulation circuits for Qubit control at microwave frequencies](#) by Sasan Razmkhah, Ali Bozbey and Pascal Febvre, November 2022-September 2023 (5 pages). This new work seems to deal with integrating a mixer and a signal modulator in the SFQ control chipset.

²²⁰⁹ See [Superconducting chips to scale up quantum computers and boost supercomputers](#) by Matteo Cherchi, March 2021.

²²¹⁰ See [Supporting quantum technologies with an ultra-low loss silicon photonics platform](#) by Matteo Cherchi et al, VTT, January 2022-February 2023 (24 pages).

- **China** launched a 200M€ project on SFQ electronics. The Shanghai Institute of Microsystem and Information Technology's (SIMIT) Laboratory of Superconducting Electronics is studying SQUIDs (Superconducting quantum interference device used in sensing), SNSPD (superconducting nanowire single-photon detectors) and Superconducting large scale integrated circuits with a 50 persons team. They ambition to create a 64 bits SFQ-based microprocessor. They have their own cleanroom. A side project could well become SFQ-based qubits control chips.
- **Russia** has some researchers working on superconducting electronics and even on SFQ qubit drive electronics, particularly at Lomonosov Moscow State University and Lobachevsky State University of Nizhny Novgorod²²¹¹.



SEEQC (2017, USA, \$34.2M) was created as a subsidiary of Hypres, an American company specialized in the creation of superconducting electronics, by John Levy, Matthew Hutchings and Oleg Mukhanov²²¹².

Its parent company Hypres (1983, USA, \$50K) is a long-time specialist in superconducting electronic circuits. It was created by Sadeg Faris, a Libyan who invented the quiteron at IBM, a superconducting transistor. He created Hypres the same year IBM pulled the plug on superconducting electronics and used IBM patents under license.

They have been the only superconducting electronics company for three decades and lived out of SBIR funding and some defense business, like with radars and spectrum analysis. They are a mix of nationalities with Indians, Russians, and a Lebanese. Hypres split in two in 2020. The RF business did stay at Hypres working mostly for the DoD, and SEEQC specialized in SFQ based qubit drive while keeping Hypres's cleanroom based in Elmsford, New York State. The remained of Hypres then worked with other cleanrooms like with SkyWater and the MIT Lincoln Labs. But SEEQC also manufactures superconducting chips for the DoE, NASA and DoD as well as other commercial and academic teams.

SEEQC stands for "Superconducting Energy Efficient Quantum Computing". It focuses on the creation of superconducting circuits completed with spintronic technology memories²²¹³. The company was initially funded under IARPA's C3 project launched in 2016. Then SEEQC created a lab at Federico II University of Naples, Italy, and the UK, mostly to capture EU/UK public funding. It fared better with the UK than with the EU. They got grants from Innovate UK's Industrial Challenge Strategy Fund as part of four consortiums.

- The first, announced in April 2020, totaling £7M, is led by Oxford Quantum Circuits includes Oxford Instruments, Kelvin Nanotechnology, University of Glasgow (Martin Weides' team) and the Royal Holloway University of London, to create a superconducting qubit computer.
- The second, launched in September 2021, is NISQ.OS, totaling £5.363M, is focused on building an operating system and an hardware abstraction layer is led by Riverlane and includes, Hitachi Europe, Universal Quantum, Duality Quantum Photonics, Oxford Ionics, Oxford Quantum

²²¹¹ See [Beyond Moore's technologies: operation principles of a superconductor alternative](#) by Igor I. Soloviev et al, 2017 (22 pages), [Flux qubit interaction with rapid single-flux quantum logic circuits: Control and readout](#) by N. V. Klenov, Low Temperature Physics, 2017 (11 pages), the excellent review presentation [Superconducting digital electronics](#) by Igor Soloviev, 2021 (115 slides), [Genetic algorithm for searching bipolar Single-Flux-Quantum pulse sequences for qubit control](#) by M.V. Bastrakova et al, September 2022 (9 pages) that deals with the optimization of SFQ pulses to drive qubits, using a genetic machine learning algorithm and [Speeding up qubit control with bipolar single-flux-quantum pulse sequences](#) by Vsevolod Vozhakov, Igor I. Soloviev, October 2023 (17 pages).

²²¹² See [SEEQC Cuts Its Own Path to the Quantum Era With Integrated Circuit Approach](#) by Matt Swayne, The Quantum Daily, September 2020. By setting up offices in Milan and the UK, the startup found a way to secure European funding for its research. Otherwise they collaborate with Robert McDermott's team at the University of Wisconsin and the Syracuse team in upstate New York.

²²¹³ See [Single Flux Quantum Logic for Digital Applications](#) by Oleg Mukhanov of SEEQC/Hypres, August 2019 (33 slides). Oleg Mukhanov also worked on a TWPA, in [Symmetric Traveling Wave Parametric Amplifier](#) by Alessandro Miano and Oleg Mukhanov, April 2019 (6 pages).

Circuits, arm and the UK National Physical Laboratory, another SEEQC partner in the UK. SEEQC and Riverlane announced in June 2021 that they had integrated Riverlane’s operating system Deltaflow.OS with SEEQC’s qubit driving components.

- The third consortium was launched in November 2021 in partnership with Merck who is also an investor in SEEQC as well as with Riverlane, Oxford Instruments, the University of Oxford and Medicines Discovery Catapult, with a total funding of £6.85M grant from Innovate UK’s Industrial Strategy Challenge Fund (ISCF) to build a “commercially scalable application-specific quantum computer designed to tackle prohibitively high costs within pharmaceutical drug development” (aka QuPharma project). A bit like IQM’s strategy, SEEQC is to create “an application-specific quantum computer” to simulate quantum chemistry, an idea that I found a bit questionable. The announcement didn’t mention either a number of qubit or expected fidelities, but the project is due for completion “in 18 months”.
- The fourth consortium is a project led by sureCore, with £6.5M to support the integration of SEEQC’s technology with cryo-CMOS components for qubit controls. SEEQC’s role is to “determine what IP blocks the project will need to create for the Cryo-CMOS chips”. Other partners are Oxford Instruments, SemiWise, Synopsys, Universal Quantum and the University of Glasgow.

In December 2021, SEEQC also announced a partnership with QuantWare (the Netherlands) for the development of a QPU containing QuantWare’s superconducting qubits and SEEQC’s SFQ cryogenic control electronics. It adds another superconducting vendor to SEEQC’s partners, on top of OQC (UK). The difference here is that QuantWare will embed SEEQC’s technology in its QPU in multi-chip modules.

SEEQC’s architecture was initially based on two chips: a classical SFQ control chip and the SFQu-Class DQM, both using Josephson junctions in SFQ superconducting circuits. The first chip runs at 3K or as low as 600 mK and uses an energy efficient ERSFQ or eSFQ variant of RSFQ logic. It removes a lot of wiring clutter thanks to digital control signals multiplexing (Figure 534).

It controls the DQM and handles error corrections without requiring an external classical computer. The SFQuClass DQM (Digital Quantum Management) includes the microwave generators used to drive the qubits (with DACs, digital-to-analog signal converters) and for qubits readouts (with ADCs, analog to digital microwave signal converters) (Figure 533).

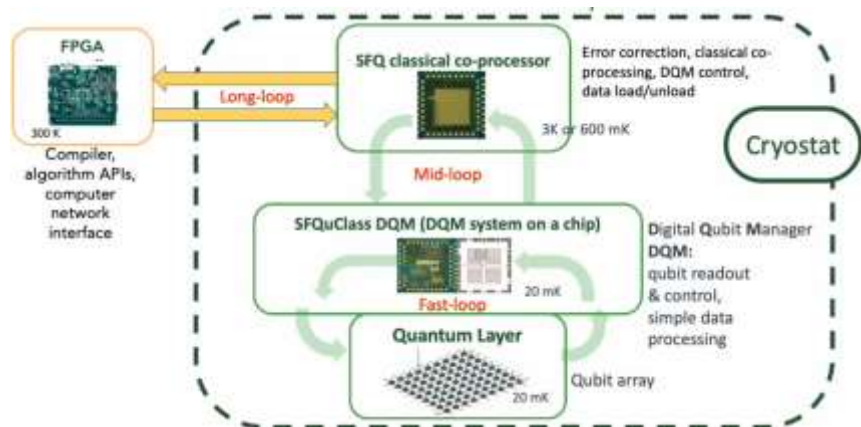


Figure 533: SEEQC overall architecture with a classical coprocessor running at 3K/600mK and the DQM that sits close to the qubit chip at 20 mK. Source: SEEQC.

Its power drain is only 0.0002 mW per qubit when it could reach over 20 mW per qubits with cryo-CMOS but we have to check these kinds of comparison making sure the same electronics functions are implemented or not implemented.

The mid-loop between the SFQ co-processor and the DQM also reduces the latency for qubits controls and is particularly interesting for implementing error correction codes. When we can generate qubit control signals inside the cryostat, it still must be exchanged both ways digitally with the outside of the cryostat. This can be done through signals multiplexed on copper, fiber optics, or even, it is under study, radio waves at very high frequencies (in THz).

It also helps maximize thermal and vacuum insulation with the outside^{2214 2215}.

An optical fiber has the advantage of being made of glass, which does not generate thermal expansion and is a weak heat conductor. Still, SEEQC has scalability plans that will require using a growing number of wires with the number of qubits, with a better “Rent’s rule” than with classical control²²¹⁶.

"Quantum" Rent's Rule			
Qubit Count	Qubit Control Wiring Overhead		Application
	Google	seeQC	
2	4	3	Prototype
10	20	3	Prototype
100	200	31	Prototype
1k	2,000	76	Optimization / chemistry
10k	n/a	330	Optimization / chemistry
100k	n/a	~1,600	Big data / ML
1m	n/a	~6,000	Encryption

Figure 534: how many wires are necessary for controlling qubits comparing Google’s Sycamore system and SEEQC’s solution. Source: SEEQC.

In April 2023, SEEQC demonstrated its first full-stack quantum computer in its laboratory in Naples, Italy, System Red with 5 superconducting qubits, quite fast two-qubit gates at 39 ns, but with a paltry 98.4% fidelity. It assembled QuantWare’s 5 superconducting qubit chip and SEEQC’s SFQ chip for qubit drive as well as digital demultiplexing features. They even say they communicate wirelessly when it may actually use metal layers in another chip underneath both chips in the packaging, with up to 9-layer in niobium²²¹⁷. At this point, they use a single cable to control four RF signals with future version controlling 16 signals. The next system iteration will support SFQ based qubit readout which in the first edition seems implemented classically at room temperature²²¹⁸. They didn’t indicate whether they were using a 4K-level bridge chip.

Circulators

Circulators are used in the qubit readouts chain at the lowest level of a cryostat.

The generic role of a n-way circulator is to send the microwave from input i to input i+1 in a directional *aka* non-reciprocal way. The signal from i+1 can’t be sent or is sent with strong attenuation to input i (Figure 535). It is used to convey the readout microwave from their AWG/DAC source to the qubit resonator and its response microwave to the first amplification stage. The amplified microwave is sent upwards to the next amplification stage, without being sent back to the resonator. There are settings variations based on using between one and four circulators to improve the various components isolation in the readout food chain.

²²¹⁴ See [Quantum-classical interface based on single flux quantum digital logic](#) by Robert McDermott, 2018 (19 pages), [Digital coherent control of a superconducting qubit](#) by Edward Leonard Jr. et al, 2018 (13 pages). The diagram in Figure 533 suggests that microwave generation is always performed outside the cryostat. This is related to the experiment containing a double qubit control: by direct current to drive the microwave generation by the SFQ near the qubits, and in the traditional way outside the cryostat, used to compare the two methods fidelities.

²²¹⁵ See [Digital coherent control of a superconducting qubit](#), by Oleg Mukhanov (CTO and co-founder of SEEQC), Robert McDermott et al, September 2019 (39 slides) and [Hardware-Efficient Qubit Control with Single-Flux-Quantum Pulse Sequences](#) by Robert McDermott et al, 2019 (10 pages).

²²¹⁶ Rent’s rule compute the maths of connections needed to control an electronic system and how it scales with size. See [Microminiature packaging and integrated circuitry: The work of E. F. Rent, with an application to on-chip interconnection requirements](#), 2005 (28 pages) which describes the history of Rent’s rule that dates from 1960 and [Rent’s rule and extensibility in quantum computing](#) by D.P. Franke, James Clarke, L.M.K. Vandersypen and Menno Veldhorst, 2018 (8 pages) that describes how these rules could be applied in quantum computing.

²²¹⁷ See [Flip-Chip Packaging of Fluxonium Qubits](#) by Aaron Somoroff, Oleg Mukhanov et al, March 2023 (14 pages) which describes their flip-chip bonding combining an SFQ and a fluxonium qubit chipset. It still seems to be a different design from System Red.

²²¹⁸ See [Discriminating the Phase of a Coherent Tone with a Flux-Switchable Superconducting Circuit](#) by Luigi Di Palma, Oleg Mukhanov et al, SEEQC, June 2023 (15 pages).

Indeed, the reciprocal protection is not perfect, as measured in decibels and is usually of about 17 to 18 dB. So, chains of circulators enable a protection of about 35 dB, if not over 50 dB. The circulator protection must exceed the first amplifier (or paramp) gain with is currently sitting between 15 and 20 dB.

Circulators protect the qubits from unwanted noise coming from the output measurement chain. It avoids back-action of the amplifier on the qubits. They are key contributors to the qubit readout being “nondestructive” of the resulting quantum state (*aka* QND for quantum non-demolition measurement).

Isolators are similar symmetry breaking devices, but with only two connectors they enable a one-way microwave circulation. Conceptually, these are like “microwave diodes”, letting microwaves be transmitted in only one direction (Figure 537).

Traditional circulators use a ferrite magnet. A microwave entering the circulator through one port is subject to a Faraday rotation in the ferrite, changing its phase²²¹⁹. It creates a constructive microwave interference in one direction of circulation and a destructive interference in the other direction. Such circulators can’t be integrated in or near qubit circuits due to their ambient magnetism. Circulators can still be mutualized for the readout of several qubits with frequency-domain multiplexing used at the AWG/DAC and ADC/FPGA levels in the upper data processing stages²²²⁰.

Nowadays, this multiplexing is not exceeding 8 qubits, but it could theoretically reach 100 qubits, such as with a 10 MHz bandwidth and equivalent 10 MHz spacing, spread in a 2 GHz bandwidth centered at 6.5 GHz, although 20-qubit multiplexing seems more reasonable given the specifications of existing parametric amplifiers (mostly TWPAs).

Also, the shorter the microwave bandwidth, the longer the qubit readout microwave will be, which contradicts the needs of quantum error correction which must be fast.

Existing Faraday circulators used with superconducting qubits are relatively large components, being several centimeters wide (Figure 536). This length is conditioned by the microwave length, which is 5 cm for 6 GHz wavelengths. With cabling, filters and attenuators, circulators are the key components located in the cryostat that limit qubit scaling, thus the need to find alternative and less bulky solutions.

Ideal circulators would fit into the qubit chips and use compatible (superconducting) circuits, have a high protection (in the 20 dB region), a large and controllable bandwidth (between 500 MHz and up to 2 GHz, to enable qubit readout multiplexing) and low power drain if they are active and depending on the cryostat stage where they are operating (15 mK or 4K). They’d also be combined with the first stage quantum-limit low-noise amplifier like a TWPA.

These new types of circulators can be segmented by their underlying physical process. I will simplify this and have, first, classical electronics systems:

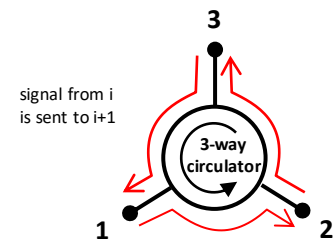


Figure 535: principle of operation of a circulator which circulates microwaves in a one-way fashion.



Figure 536: a typical commercial bulky circulator. QuinStar Technology.

²²¹⁹ This effect was described first in [The Ferromagnetic Faraday Effect at Microwave Frequencies and its Applications](#) by C. L. Hogan, 1952 (31 pages).

²²²⁰ See the interesting presentation [Hall Effect Gyrotors and Circulators](#) by David DiVincenzo, Quantum Technology - Chalmers, 2016 (53 slides).

- **Hall effect circulators** as developed by David DiVincenzo in Germany and whose size is not constrained by the readout microwave wavelength²²²¹.
- **LC based cryo-CMOS circulators** as prototyped at TU Delft²²²².

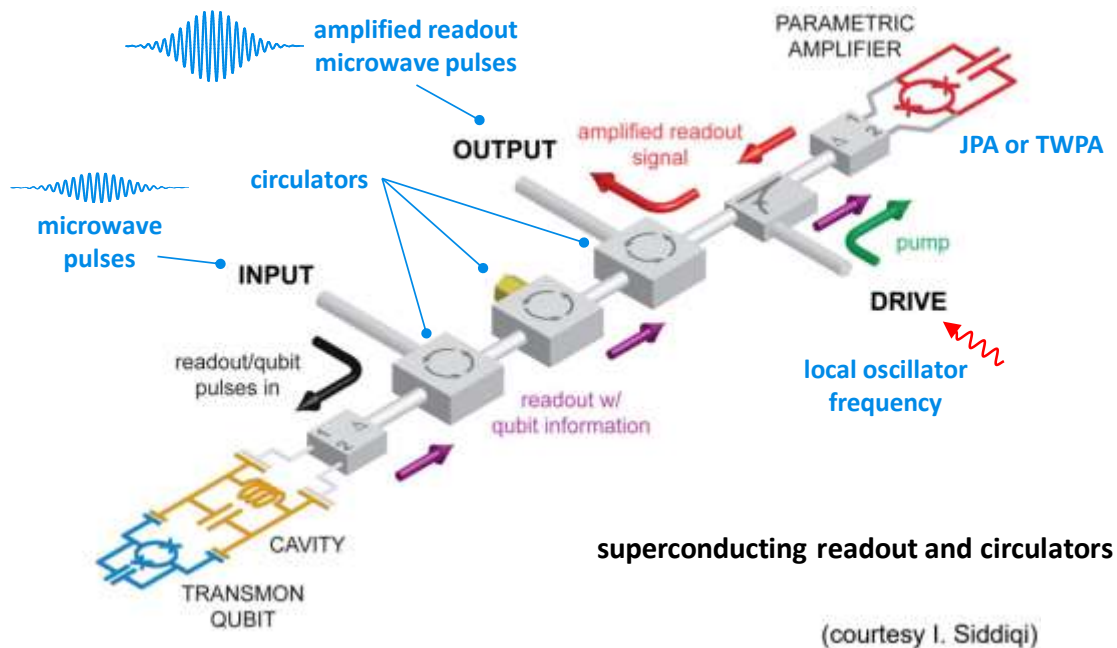


Figure 537: several circulators are actually used for each set of qubits controlled through frequency multiplexing.
Source: Irfan Siddiqi.

And then, various superconducting circuits using Josephson junctions like:

- **Interferometric and parametric Josephson circulators**, developed at IBM^{2223 2224}, RIKEN²²²⁵ and Google AI (as shown in Figure 539)²²²⁶, with the advantage of being very low power hungry.
- **Superconducting quantum tunnelling capacitors**, developed by Clemens Mueller at ETH Zurich and the University of Queensland²²²⁷. These are passive systems or can be controlled with just

²²²¹ See [Hall Effect Gytrators and Circulators](#) by Giovanni Viola and David DiVincenzo, 2014 (18 pages) and [On-Chip Microwave Quantum Hall Circulator](#) by A. C. Mahoney et al, 2017 (9 pages) which is based on III/V GaAs and AlGaAs electronics.

²²²² See [A Wideband Low-Power Cryogenic CMOS Circulator for Quantum Applications](#) by Andrea Ruffino, Fabio Sebastiano and Edoardo Charbon, IEEE & EPFL, 2020 (15 pages). It uses resonant LC circuits level combining inductance (L) and capacitors (C). The circuit provides a 18 dB isolation and consumes a total of 10.5 mW. It runs at 4.2K and not at the lowest 15 mK. It was tested with a 40 nm node with an active area of 0.45 mm² in an experimental 1.5 mm wide square circuit.

²²²³ See [Active protection of a superconducting qubit with an interferometric Josephson isolator](#) by Baleegh Abdo, Jerry M. Chow et al, IBM Research, 2018 (10 pages) and [High-fidelity qubit readout using interferometric directional Josephson devices](#) by Baleegh Abdo et al, IBM Research, 2021 (32 pages).

²²²⁴ See [Wideband Josephson Parametric Isolator](#) by M. A. Beck et al, IBM, December 2022 (10 pages).

²²²⁵ See [Magnetic-Free Traveling-Wave Nonreciprocal Superconducting Microwave Components](#) by Dengke Zhang and Jaw-Shen Tsai, RIKEN, 2021 (18 pages), with a bandwidth of 580 MHz around 6 GHz and an isolation of 20 dB.

²²²⁶ See [Josephson parametric circulator with same-frequency signal ports, 200 MHz bandwidth, and high dynamic range](#) by Randy Kwende et al, Google AI, May 2023 (6 pages).

²²²⁷ See [Breaking time-reversal symmetry with a superconducting flux capacitor](#) by Clemens Müller, Thomas M. Stace et al, 2018 (10 pages). This circulator uses a small superconducting capacitor, using the quantum tunnelling of the magnetic flux around it, allowing a flow of microwave energy in one direction.

some DC (direct current) input, as shown in Figure 538²²²⁸. These could be potentially directly implemented in superconducting qubit chips.

- **On-chip microwave circulators** with a wide tunable frequency, developed in 2017 at the University of Colorado in Boulder²²²⁹, a variation with SQUIDs superconducting components.

Also, Josephson based quantum diodes, also named superconducting diodes, are being developed using similar designs^{2230 2231 2232}.

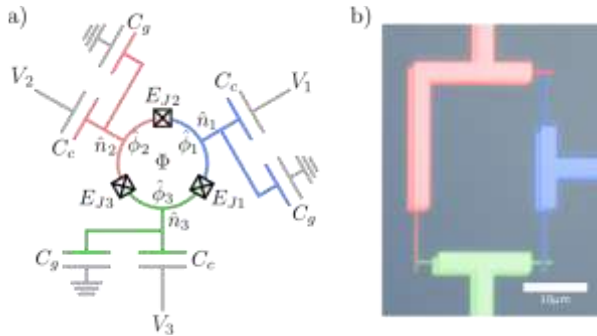


Figure 538: a) prototype passive superconducting circulator that could potentially be integrated in a superconducting qubit chip. Source: [Passive superconducting circulator on a chip](#) by Rohit Navarathna et al, August 2022.

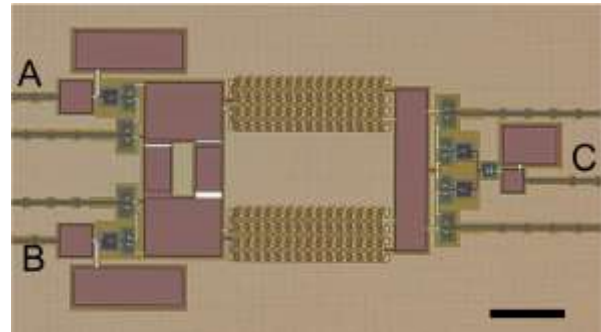


Figure 539: a parametric Josephson junctions based circulator proposed by Google. Source: [Josephson parametric circulator with same-frequency signal ports, 200 MHz bandwidth, and high dynamic range](#) by Randy Kwende et al, Google AI, May 2023.

While there are many such prototype solutions, and we've not covered them all, it seems they have not yet reached the commercial stage at this point, although some have use cases beyond qubits control like in the telecom and radar markets.



Analog Quantum Circuits (2022, Australia, \$2M) is a company created by Tom Stace (CEO) and Arkady Fedorov (CSO) that is developing on-chip circulators for solid state qubits, based on the work of Fedorov. They also have plans to develop other components like TWPAs and attenuators.

Amplifiers

Analog qubit readout microwave signals must be amplified several times before they are converted digitally with an ADC and then analyzed, usually with an FPGA programmable circuit. Superconducting readout microwaves are amplified at least three times: first, at the lowest cryogenic stage (15 mK) with a parametric amplifier (“paramp”) operating at the quantum limit (JPA, TWPA), then at the 4K stage with an HEMT amplifier, then at ambient temperature with a classical RF analog amplifier that may also be an HEMT. The paramp serves as a low-noise signal preamplifier before the noisier HEMT. They all add a gain of respectively about 15 dB, 40 dB and 50 dB to readout microwaves.

²²²⁸ See [Passive superconducting circulator on a chip](#) by Rohit Navarathna, Thomas M. Stace, Arkady Fedorov et al, PRL, August 2022-January 2023 (11 pages). This led to the creation of Analog Quantum Circuits (Australia).

²²²⁹ See [Widely Tunable On-Chip Microwave Circulator for Superconducting Quantum Circuits](#) by Benjamin J. Chapman, Alexandre Blais et al, 2017 (16 pages) and the related thesis [Widely tunable on-chip microwave circulator for superconducting quantum circuits](#) by Benjamin J. Chapman, 2017 (144 pages). See also [Design of an on-chip superconducting microwave circulator with octave bandwidth](#) by Benjamin J. Chapman et al, 2018 (12 pages).

²²³⁰ See [Microwave quantum diode](#) by Rishabh Upadhyay, Jukka P. Pekola et al, April 2023 (13 pages).

²²³¹ See [Gate-tunable superconducting diode effect in a three-terminal Josephson device](#) by Mohit Gupta et al, Nature Communications, May 2023 (8 pages).

²²³² See [The superconducting diode effect](#) by Muhammad Nadeem, Michael S. Fuhrer and Xiaolin Wang, Nature Reviews Physics, January-September 2023 (26 pages, [arXiv](#)).

Paramps. To make things short, two main generations of parametric amplifiers have been used for qubits readout. They are based on exciting and pumping a material with nonlinear polarization using an intense electromagnetic field. A weak microwave signal can then get amplified via the interaction with the medium. The first paramps used with qubit readouts were the JPAs (Josephson Parametric Amplifiers)²²³³. These are simple amplifiers, using one or two Josephson junctions, easy to manufacture, with a good gain of about 15 to 20 dB²²³⁴. Their main shortcoming is their narrow bandwidth which prevents their implementation with frequency-domain qubits readout multiplexing, where a single amplifier processes a readout signal coming from several chained qubits using different resonant frequencies. It is due to JPAs being based on cavities. Some variant using Josephson based FET transistors (JoFET) are frequency tunable but have a low bandwidth as well²²³⁵.

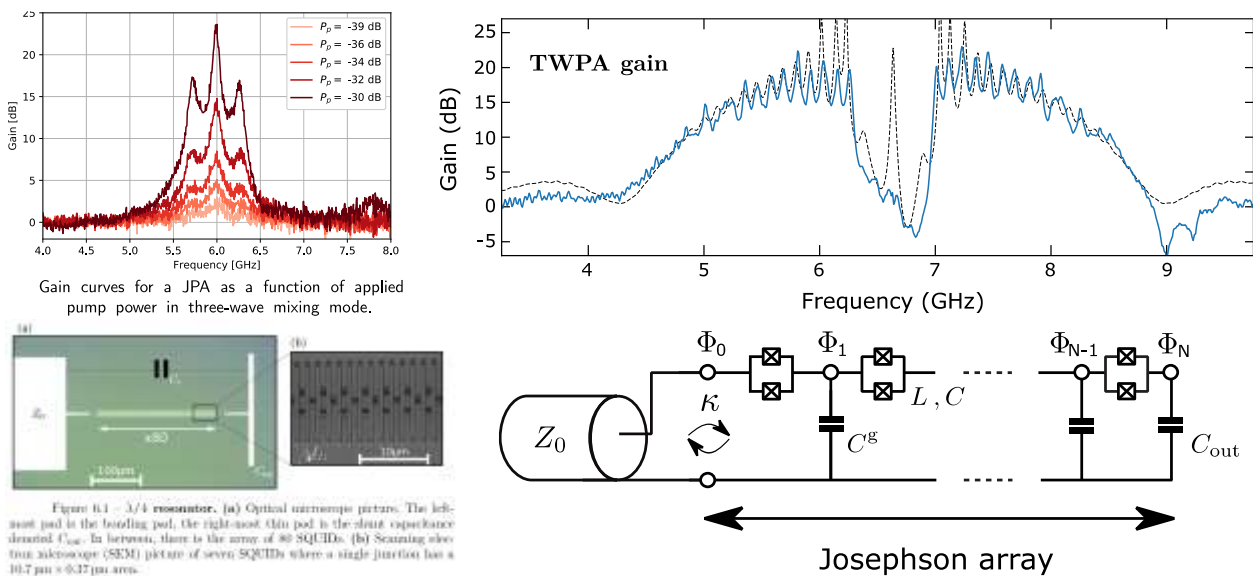


Figure 540: top left, the typical narrow-band response curve of a JPA, and top right, the typical frequency response curve of a TWPA that has over 2 GHz available with a gain superior to 15 dB in two parts, below 6.2 GHz and above 7 GHz. Bottom left is a typical TWPA circuit, with 2000 series of Josephson junction bridges, as described on the right.

Source: [Resonant and traveling-wave parametric amplification near the quantum limit](#) by Luca Planat, June 2020 (237 pages).

TWPA (*aka*, usually, JTWPA) practically emerged in 2015²²³⁶. Recent TWPAs are based on long arrays of about 2000 series of Josephson junctions and as such are considered to be “meta-materials”. They are more complicated to manufacture.

This explains the interest for a relatively new generation of paramps, the TWPAs (travelling waves parametric amplifiers) which were pioneered by Bernard Yurke (USA) in 1996²²³⁷ and successfully implemented in an array of SQUIDs in 2007 by Manuel A. Castellanos-Beltran from JILA (USA)²²³⁸, and then, in 2008, with an intrinsic noise below the standard quantum limit (SQL) and over 20 dB of

²²³³ See [Superconducting Parametric Amplifiers](#) by Jose Aumentado, IEEE Microwave Magazine, August 2020 (15 pages) (*not open access*).

²²³⁴ A Japanese team was able to reach a gain of 40 dB with a JPA in 2022, but with a narrow bandwidth. With a 20 dB gain, they obtain a bandwidth of only 400 kHz. See [A three-dimensional Josephson parametric amplifier](#) by I. Mahboob et al, May 2022 (5 pages).

²²³⁵ See [Gate-tunable, superconductor-semiconductor parametric amplifier](#) by D. Phan et al, IST Austria, June 2022-May 2023 (13 pages).

²²³⁶ See [Traveling wave parametric amplifier with Josephson junctions using minimal resonator phase matching](#) by T.C. White, John Martinis et al, UCSB, 2015 (15 pages) and [A near-quantum-limited Josephson traveling-wave parametric amplifier](#) by C. Macklin, William D. Olivier, Irfan Siddiqi et al, 2015 (3 pages). Despite the first work involving John Martinis in 2015, Google Sycamore was using JPAs and not TWPAs. Google is still investigating, naturally, how to use TWPAs in their systems.

²²³⁷ See [A low-noise series-array Josephson junction parametric amplifier](#) by Bernard Yurke et al, 1996 (4 pages).

²²³⁸ See [Widely tunable parametric amplifier based on a superconducting quantum interference device array resonator](#) by Manuel A. Castellanos-Beltran et al, 2007 (9 pages).

power gain²²³⁹. These amplifiers are used for qubit readout, in high-energy particle physics, radioastronomy and astrophysics²²⁴⁰, like for the detection of dark matter.

Their broader bandwidth could potentially enable up to 10-20 qubits readout multiplexing²²⁴¹. Their other figures of merit are their saturation and dynamic range (linked to minimum and maximum input signal power), and noise level (noise temperature, under 1K). New options arise with Floquet mode TWPAs from MIT, decreasing noise level and across a wide bandwidth of 6 GHz, further increasing qubits readout multiplexing capabilities. And it has a better directionality²²⁴² (Figure 540).

Both JPAs and TWPAs are active components that are driven by a constant microwave pulse acting as a “pump”. JPAs are fed with a pulse of -80 dB while TWPAs use a -70 dB or just a tiny 0.1 nW. This is the power reaching the paramps. It is much larger from the outside local oscillator and must be attenuated on the way down in the cryostat.

With TWPAs, there are variations with three-wave mixing (3WM) using one pump photon yielding one signal photon and one idler residual photon and four-wave mixing (4WM) using two pump photons yielding one signal and one idler photon. The pump microwave usually comes from a local oscillator source outside the cryostat.

Other qubit readout options are investigated, including:

- **Low-noise cryo-CMOS amplifiers**, prototyped in 2020 by CEA-Leti that operates at 10 mK²²⁴³. In another recent work involving the UK and CEA-Leti in France, quantum-dots based readout amplification is studied, and is adapted to silicon spin qubits. With some improvements, it could reach gains of classical JPAs (15 dB) although on a small bandwidth²²⁴⁴.
- **Semiconducting nanowire amplifier** developed in the Netherlands, working at near-quantum-limited performance, with >20 dB gain and a 30 MHz gain-bandwidth, good saturation powers of -120 dBm, magnetic field compatibility up to 500 mT and frequency tunability over a range of 15 MHz²²⁴⁵. However, its bandwidth is limited compared to TWPA, making it difficult to multiplex the readout of several qubits with a single cable and amplifier.
- **Superconducting amplifier running at up to 1.5K**, which may be useful for silicon spin qubits with near quantum limit noise reduction²²⁴⁶.
- **Nanobolometers** operating in the gigahertz regime could also be of some use here, but more for metrology²²⁴⁷.

²²³⁹ See this good TWPA review paper [Perspective on traveling wave microwave parametric amplifiers](#) by Martina Esposito, Arpit Ranadive, Luca Planat and Nicolas Roch, September 2021 (8 pages).

²²⁴⁰ See [Demonstration of a Quantum Noise Limited Traveling-Wave Parametric Amplifier](#) by Nikita Klimovich et al, Caltech and JPL, June 2023 (6 pages).

²²⁴¹ TWPAs however generate undesired mixing processes between the different frequency multiplexed tones as described in [Intermodulation Distortion in a Josephson Traveling Wave Parametric Amplifier](#) by Ants Remm, Andreas Wallraff et al, October 2022 (11 pages).

²²⁴² See [Floquet Mode Traveling-Wave Parametric Amplifiers](#) by Kaidong Peng et al, MIT, PRX Quantum, April 2022 (20 pages). This work from MIT was funded by Amazon AWS Center for Quantum Computing and by NEC.

²²⁴³ See [Low-power transimpedance amplifier for cryogenic integration with quantum devices](#) by L. Le Guevet et al, March 2020 (13 pages).

²²⁴⁴ See [Quantum Dot-Based Parametric Amplifiers](#) by Laurence Cochrane, Fernando Gonzalez-Zalba, Maud Vinet et al, PRL, May 2022 (7 pages).

²²⁴⁵ See [Gate-tunable kinetic inductance parametric amplifier](#) by Lukas Johannes Splitthoff et al, QuTech and Kavli Institute for Nanoscience, Delft University of Technology, August 2023 (12 pages).

²²⁴⁶ See [Radiatively-cooled quantum microwave amplifiers](#) by Mingrui Xu et al, Yale, August 2023 (9 pages).

²²⁴⁷ See [Cryogenic sensor enabling broad-band and traceable power measurements](#) by J.-P. Girard et al, IQM, Aalto University, VTT and Bluefors, Review of Scientific Instruments, May 2023 (11 pages).

- **Microwave photon counters** using Josephson Photo Multiplier (JPM) that can be directly embedded in the qubit chip. It doesn't require low-noise amplification with a JPA or a TWPA and provides a good readout fidelity >98% although it's a bit slow, lasting 500 ns²²⁴⁸. Another microwave photon counter was realized at CEA SPEC in Saclay using a SQUID connected to a coil²²⁴⁹.

Before looking at cryogenic amplification commercial vendors, let's mention the **MIT Lincoln Lab** team from William D. Oliver who has been pioneering TWPAs for a while, and is providing many labs in the world with its own TWPAs since 2015, and for free (pictured in Figure 541). A gift for science development! On the industry vendors side, **IBM** and **Rigetti** developed their own TWPAs. **IQM** uses TWPAs from VTT.

In Finland, **VTT** is also manufacturing TWPAs using 1,600 Josephson junctions. 40 nm CMOS. In Sweden, **Chalmers University** researchers are working on their own optimized 3WM TWPA²²⁵⁰.

In Italy, various labs launched DARTWARS, for designing a TWPA with very large bandwidth covering 5 to 10 GHz with low noise temperature of 600 mK. It will use two techniques with Josephson junctions (JTWPAs) and kinetic inductances (KITWPAs)²²⁵¹. There was also a 4-year EU TWPA project named **ParaWave**, run by German, Italian and British partners from 2018 to 2021²²⁵².

Google is not following the TWPA path but improving JPAs with their home-made SNIMPA or 'snake impedance matched parametric amplifier' which has a high dynamic range, large bandwidth, high saturation and where the active nonlinear element is implemented with an array of rf-SQUIDs²²⁵³.

HEMT. At last, at the 4K cryostat stage sit the second qubit microwaves readout amplifiers named HEMT (High-electron-mobility transistor). They provide a large gain amplification of about 40 dB with high dynamic range and a large-bandwidth >6GHz for the inbound microwave readout signal coming from the paramps from the first cryostat stage, which benefited from a first level 15 to 20 dB low-noise amplification at or near the quantum limit.

Many labs and vendors produce HEMTs for qubit readout, like Chalmers University of Technology in Sweden using indium phosphide (InP) transistors which are very efficient at 4K²²⁵⁴. The main vendor here is **Low Noise Factory** (described later, below) as well as **Cosmic Microwave Technology**, with HEMTs designed at Caltech.

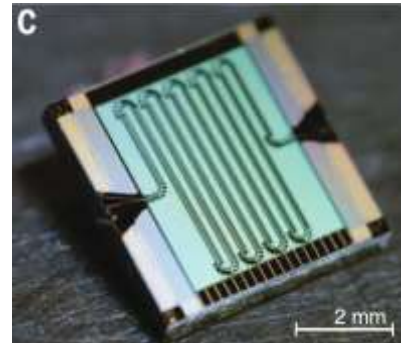


Figure 541: an MIT Lincoln lab TWPA. Source: [A near-quantum-limited Josephson traveling-wave parametric amplifier](#) by C. Macklin, William D. Oliver, Irfan Siddiqi et al, 2015 (3 pages)

²²⁴⁸ See [High-Fidelity Measurement of a Superconducting Qubit Using an On-Chip Microwave Photon Counter](#) by A. Opremcak, Robert McDermott et al, February 2021 (13 pages). On top of give researchers from Wisconsin University, this work involves six researchers from Google and one from Syracuse University in New York.

²²⁴⁹ See [Emission of Photon Multiplets by a dc-Biased Superconducting Circuit](#) by G. C. Ménard, Denis Vion, Daniel Estève et al, PRX, April 2022 (15 pages).

²²⁵⁰ See [Three-wave mixing traveling-wave parametric amplifier with periodic variation of the circuit parameters](#) by Anita Fadavi Roudsari, Per Delsing et al, September 2022 (6 pages).

²²⁵¹ See [Ultra low noise readout with travelling wave parametric amplifiers: the DARTWARS project](#) by A. Rettaroli et al, July 2022 (4 pages).

²²⁵² See [Josephson travelling wave parametric amplifier and its application for metrology](#), 2018 (7 pages).

²²⁵³ See [Readout of a quantum processor with high dynamic range Josephson parametric amplifiers](#) by T.C. White, Charles Neil, Frank Arute, Joseph C. Bardin et many al, September 2022 (9 pages). They tested it on a 54-qubit Sycamore processor.

²²⁵⁴ See [InAs/AlSb HEMTs for cryogenic LNAs at ultra-low power dissipation](#) by Giuseppe Moschetti et al, 2020, Solid State Electronics (7 pages).

Still, commercial HEMT amplifiers dissipate 10 mW of power, which can be a problem when the number of qubits scale, even though the cooling power at the 4K stage is quite larger than at 15 mK, with about 1W to 2W.

One solution would be to use a variety of weakly dissipative TWPAs sitting at the 4K stage, using superconducting materials operating at this temperature like NbTiN and put an HEMT at the 70K cryogenic stage²²⁵⁵. This would reduce the heat generated at 4K.

Then, we have room temperature analog amplifiers adding about 50 dB to the signal coming from the HEMT at 4K. These amplifiers are also usually HEMT-based. They consume about 250 mW, which is shared for the multiplexed readout signals of several qubits, usually between 5 and 10 with the potential to grow to 20 and even 100 qubits, depending on the readout speed. Indeed, the shorter the readout pulse, the broader the pulse frequency spectrum will be, limiting multiplexing over a bandwidth of about 2 GHz. The longer the pulse, the smaller the pulse spectrum will be, but it will be detrimental to the efficiency of error correction. That's another design trade-off to take into account in designing these systems.

Now let's look at the amplification vendors I have identified so far.



Low Noise Factory (2005, Sweden) designs and produces low-noise amplifiers (HEMT) operating at ambient or cryogenic temperatures as well as circulators and JPAs, including double circulators.

They are part of the European **OpenSuperQ** project, led by the University of Saarland in Germany, VTT in Finland and Chalmers in Sweden, to create commercial TWPAs. The consortium demonstrated in 2019 a TWPA with a maximal gain of 10 dB over a 1.4 GHz bandwidth.



SILENT WAVES

Silent Waves (2022, France) is a spun-out startup from CNRS Institut Néel in Grenoble. It was founded by Luca Planat, Nicolas Roch and Baptiste Planat.

Their offering is a very efficient TWPA, based on the research conducted by CNRS-Institut Néel-UGA and the LPMCM in Grenoble²²⁵⁶. Their commercial TWPA added noise is near the quantum limit of noise. It enables high-fidelity single-shot qubit readout on a wide frequency band and with a gain that can exceed 20 dB. Based on a patented fabrication process, Silent Waves' amplifiers are currently being manufactured in the Grenoble CNRS Institut Néel clean room²²⁵⁷ (Figure 542). They address both superconducting and silicon spin qubits readout. As a first stage, they will enable 5 and 10 qubits readout multiplexing.

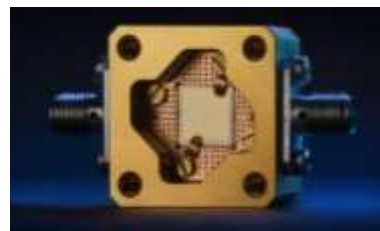


Figure 542: a Silent Waves TWPA in its packaging.
Source: Silent Waves. 2023.



Qubic Technologies (2020, Canada) is developing JPAs and TWPAs, the aim being to produce more correlations and better filtered noise. They also use this technology to improve radars. The company was created by Jérôme Bourassa (CEO), a former researcher from the Institut Quantique at the Université de Sherbrooke. He also collaborates with the Institute for Quantum Computing from the University of Waterloo.

²²⁵⁵ See [Performance of a Kinetic-Inductance Traveling-Wave Parametric Amplifier at 4 Kelvin: Toward an Alternative to Semiconductor Amplifiers](#) by M. Malnou et al, NIST and University of Colorado Boulder, October 2021 (11 pages). Their KI-TWPA dissipates only 1 μ W.

²²⁵⁶ See [A photonic crystal Josephson traveling wave parametric amplifier](#) by Luca Planat et al, October 2019 (17 pages).

²²⁵⁷ TWPAs could have applications beyond superconducting qubits readout, in microwave photonics, quantum sensing and quantum information with continuous variables as described in [Observation of two-mode squeezing in a traveling wave parametric amplifier](#) by Martina Esposito, Olivier Buisson, Nicolas Roch, Luca Planat et al, first published in November 2021 and revised in April 2022 (16 pages).



QuantWare (The Netherlands) is not just providing custom superconducting qubits chips but also their Crescendo TWPA. It provides a gain of >18 dB gain on a bandwidth of over 1.5 GHz.

At last, let's mention again **Cosmic Microwave Technologies** (2016, USA) which produces cryogenic LNAs (low noise amplifiers) used for qubits readouts and is a spin-out of Caltech.

Cabling, connectors and filters

In current quantum systems based on superconducting qubits, copper coaxial cables carry **microwave photon pulses** at frequencies between 5 and 10 GHz that act on the qubits for their reset, for implementing quantum gates and handling qubit readouts.

Microwaves are generated by devices generally located outside the refrigerated enclosure. Frequencies below 5 GHz and above 10 GHz are filtered out²²⁵⁸. These microwaves are also attenuated and filtered at the input on the 4K cold plate. An attenuation of 60db, carried out in three steps of 20 dB which each time divide by 100 the transmitted power. It is used to limit the thermal noise that is conveyed in the cables. It is reduced so as not to represent by more than one thousandth of the photons that end up in the qubits. Each filter absorbs energy that must be dissipated at the stages where they are placed.

The thermal conductivity of a cable Q is calculated as follows, using the product of the cable conductivity k, its cross-section A, the temperature gradient T2-T1 and L the length of the cable.

$$Q = kA \frac{T_2 - T_1}{L}$$

Coaxial superconducting cables - having theoretically zero resistance at low temperature - connect the qubits to their reading system (thus, in the upward direction in the diagrams). They are made of niobium and titanium alloy (NbTi). They include loops to absorb the metal contraction that occurs during cryostat cooling and warm-up²²⁵⁹. With qubit readout, microwave signals are amplified at least twice before leaving the cryostat including once at superconducting temperature, below 1 K.

These cables are used between the 4K and 15-100 mK cold plates in a cryostat. They come from various vendors including **CoaxCo** (Japan). This company seems to be the only one in the world that produces NbTi cables²²⁶⁰. The 2 mm diameter cable consists of a conductive outer jacket and a central conductor, both made of niobium-titanium which are separated by a Teflon (PFTE) or Kapton insulation (Figure 543).

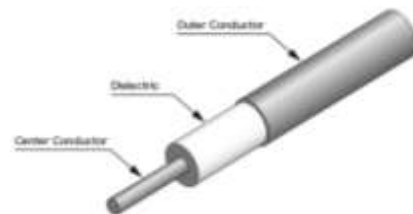


Figure 543: a typical CoaxCo niobium-titanium cable.
Source: [CoaxCo](#).

Other vendors like Delft Circuits are also proposing superconducting cables but they seem to rely on CoaxCo for the base cables they're then integrating in their own solutions. Most vendors are now trying to miniaturize this cumbersome cabling, mostly by using flexible cables.

Other avenues are pursued, at the research level, using optical cables and frequency conversion from 5 GHz to 200 THz and the other way around, using phonon-based mechanical resonators cavity

²²⁵⁸ See [Engineering the microwave to infrared noise photon flux for superconducting quantum systems](#) by S. Danilin et al, 2022 (22 pages).

²²⁵⁹ See [Challenges in Scaling-up the Control Interface of a Quantum Computer](#) by D. J. Reilly of Microsoft, December 2019 (6 pages) which states that superconducting cables have resistance and capacitance when microwaves are passed through them and therefore have a thermal release that must be taken into account.

²²⁶⁰ See [We'd have more quantum computers if it weren't so hard to find the damn cables](#), by Martin Giles, January 2019.

optomechanics, optomechanical crystal resonator²²⁶¹ or coplanar waveguide and optical cavity using the dark state protocol²²⁶². You then must look at the thermal cost of demultiplexing this signal in the cryostat and the quality of the microwave signal after its dual transduction to and from optical wavelengths. This is an option IBM is investigating for scaling its superconducting computer systems²²⁶³. Above 4K, the coax cables are using more regular materials like copper alloys.

Microwave qubit control downlink cables are made of various materials including copper-nickel, copper-beryllium or bronze alloys. After passing through the 4K stage, they are replaced by superconducting versions to limit their heat conduction. Between the two, 20 dB attenuators are inserted. In addition, conventional twisted pair cables carrying direct current are used to power the active electronic components integrated in the cryostat, in particular the qubit state readout amplifiers.

This creates significant **wiring clutter**. Figure 544 contains *on the left* a Google cryostat with its bunch of cables and wires connecting the different cold plates. This is the wiring for only 53 qubits (actually, you need to add the 88 coupling qubits). It seems that it is possible to miniaturize some of this, especially with flat ribbon cables. These various cables cost several thousand dollars per unit. For today's 72-qubit superconducting quantum computer, this cabling costs more than the entire cryostat, more than half a million dollars. **Bluefors** offer their own optimized cabling system, such as their 168-cable High-Density Wiring, which appears to be sized to support 56 qubits (*center*). The same is true with the removable cable system of the **Oxford Instruments** Proteox (*right*).

The most expensive cables are the niobium-titanium coax sitting between the 4K and 15 mK stages, up to \$3K each. A 1,000 qubit QPU could have \$10M of cabling in its bill of materials!



Figure 544: from left to right, Google Sycamore cable clutter, BlueFors optimized cabling system and Oxford Instrument removable cabling system. Sources: Google, Bluefors, Oxford Instruments.

Now, onto the vendors in this space...



QDevil (2016, Denmark, 1M€) sells filters used in cryostats including the QFilter, based on a collaboration between Harvard University and the University of Copenhagen. It is a cryogenic filter reducing electron temperatures below 100 mK.

²²⁶¹ See [Cavity optomechanics](#) by Markus Aspelmeyer, Tobias J. Kippenberg, and Florian Marquardt, Review of Modern Physics, 2014 (65 pages), [Two-dimensional optomechanical crystal cavity with high quantum cooperativity](#) by Hengjiang Ren, Oskar Painter et al, 2020 (21 pages) and the review paper [Mesoscopic physics of nanomechanical systems](#) by Adrian Bachtold et al, February 2022 (87 pages).

²²⁶² See [Proposal for transduction between microwave and optical photons using ¹⁶⁷Er:YSO](#) by Faezeh Kimiaee Asadi et al, University of Calgary, February 2022 (8 pages).

²²⁶³ See [Optomechanics with Gallium Phosphide for Quantum Transduction](#) by Paul Seidler, May 2019.

They also sell the QDAC, a 24-channel low noise DAC, the QBoard, a PCB-based fast-exchange cryogenic chip carrier system, and the QBox, a 24-channel breakout box. They are partnering with Bluefors. The company was acquired by Quantum Machines (Israel) in March 2022.



Delft Circuits (2016, the Netherlands, 6.5M€) was created by Sal Jua Bosman (CEO), Daan Kuitenbrouwer (COO) and Paulianne Brouwer (CFO), the first two coming from TU Delft.

They offer cables and flexible mats used to carry the control microwaves of superconducting qubits such as CF3 (Cri/oFlex) and supporting frequencies ranging from 2 to 40 GHz with 8 embedded cables. Delft Circuit also introduced in March 2022 their Tabbi, an ultra-high density modular flexible microwave interconnect that consolidates the equivalent of 8 SMA cables in about 10 mm and embed its own filters (Figure 545). The startup had 24 people as of early 2022. They manufacture their products out of a 150 m² lab located at the Delft Quantum Campus. The company got financial support from many EU programs (AVaQus, MATQu and SPROUT).



Figure 545: a Delft Circuit Tabbi flat cable and connector.



XMA Corporation (2003, USA) provides the OmniSpectra product line comprising adapters, attenuators, couplers and other passive cryo-electronic components used in quantum computing.



Radiall (France) is an industry company specialized in connectors and cabling, very active in the aerospace vertical. They are now addressing quantum technology needs.

The company creates custom solutions for the quantum industry, including ultra-miniature microwave board-to-board connectors, 3D cabling and cryogenic switches. Radiall is currently expanding its product portfolio with microwave solutions supporting various quantum computing technology that require microwave components meeting strict electromagnetic compatibility/electromagnetic interference (EMC/EMI) constraints, cryogenic, non-magnetic and density specifications.

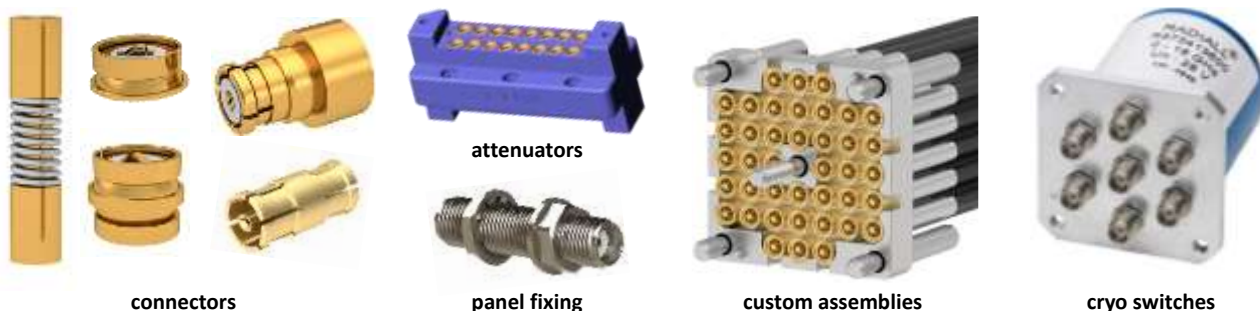


Figure 546: examples of Radiall connectors, attenuators, panel fixing, custom assemblies and cryo switches. Source: Radiall.



CryoCoax (UK/USA) is a division of **Intelliconnect** (UK/USA) that provides RF interconnect assemblies for various markets including quantum computing, based on niobium-titanium, cupro-nickel, beryllium-copper, stainless steel and brass.

They provide high-density multiway connectors using the SMPM interface (created by Carlisle Interconnect Technologies) that supports a 4.75mm pitch instead of a classical 15 mm pitch with SMA connectors. They also distribute the cabling solutions from Delft Circuits and passive components from OmniSpectra.



Atem (1990, France) is a coaxial cables designer and manufacturer. It wants to enter the quantum computers space with its Qryolink project to propose superconducting coaxial cables.

Rosenberger

Rosenberger Group (Germany) is involved in the German qBriqs projects to build connectors, attenuators components, niobium-titanium and stainless cables assembly to be incorporated in 80 channel multiport connectors and flat cables (with a 1 mm pitch) developed by **Supracon AG** and **LPKF**. They plan to produce these flat cables with 3D printers.



VIQTHOR (2022, France) is aiming to create an optical-based fiber multiplexing solution for microwave drive.

At last, let's mention the IARPA funded **SuperCables** US program that aims to develop high-data rate and low-power transport solutions for cryogenic electronics. It started in 2019. Its goal is to optical fiber connectivity between room temperature and cryogenic electronics to limit heating. It works on creating electro-optic modulators converting digital signals into and from optical data. It was a 2-year effort targeting a bandwidth of 50 Gbits/s. Which in itself is insufficient for qubits control! Cabling must also be scaled at a lower dimension, around the qubit chips. As qubit count will grow, the number of control lines reaching the chips will grow. It could scale as $2\sqrt{N}$, N being the number of qubits if cabling was using a classical X-Y addressing mode but it doesn't seem to be applicable since qubit gating is not easy to serialize. Thus, the need to miniaturize the wiring reaching chips. The current lab-grade grid spacing between these wires is 10 μm , as tested by Fraunhofer IZM using indium²²⁶⁴.

Other electronics vendors

Let's now look at other commercial vendors in the cryogenic electronics area, given they don't create any cryo-CMOS at this point.



Atlantic Microwave (1989, USA) produces and markets radiofrequency and microwave components operating at cryogenic temperatures.

They are used to control superconducting and silicon qubits in cryostats. This includes microwave attenuators, filters, microwave amplifiers and bias tees. It is a subsidiary of the British group ETL Systems, founded in 1984.



Raditek (1993, USA) is a designer and provider of RF signals processing systems, including the circulator magnet-based filters used between the first stage microwave amplifier (at 15 mK) and second stage amplifier (at 4K) used usually with superconducting qubits.



QuinStar Technology (1993, USA) is a vendor of cryogenic circulators, coming from the acquisition of **Pamtech** (USA) in 2010.



RF-Lambda (2003, USA) also provides circulators and low-noise amplifiers.



CryoHEMT (2019, France) is a company created by Quan Dong and Yong Jin in Orsay, France. It designs and manufactures low-noise HEMT microwave amplifiers which amplifies microwaves at the 4.2K cryostat stages.

²²⁶⁴ See [Deepfreeze electronics for supercomputers - Fraunhofer technology prepares quantum computing for industrial use](#), February 2023.

Their technology is based on the PhD [thesis](#) from Quan Dong done under the supervising of Yong Jin in France in 2013. It seems not being used in quantum information systems.



Diramics (2016, Switzerland) is a spin-off from ETH Zurich creating ultra-low noise transistors in III-V materials (InP, indium-phosphorus) with a technology named pHEMT (pseudomorphic high-electron-mobility transistor, using junctions with two semiconductors with different band gaps).

It can be used in low temperature electronics. It is currently mostly used in astronomy applications.



Marki Microwave (1991, USA) is a supplier of microwave control components: amplifiers, bias tees, couplers, mixers and filters.



Quantum Microwave (2016, USA) creates microwave components operating at cryogenic temperatures for quantum computers, including JPA amplifiers, attenuators, frequency couplers, multiplexers, bias tees, diplexers, filters, image reject mixers and directional couplers.



One main applied research domain for **Raytheon** is related to superconducting qubits controls. They work on arbitrary pulse sequencers (APS) creating superconducting qubits control microwaves, an FPGA readout system using low noise parametric amplifiers and a custom made three-way mixing mode JPAs with 20 dB gain as show in Figure 547.

They are also exploring SFQ based control logic (Josephson gate-based logic) and spintronics based low-power memories. They are mainly found in superconducting qubits quantum computers (IBM, Google, Rigetti, D-Wave). However, they do not push forward the miniaturization of these components like what SEEQC is doing. In October 2021, they announce a technology partnership with IBM, with not many details²²⁶⁵. On top of that, they also develop Josephson junction based infrared photon detectors²²⁶⁶.

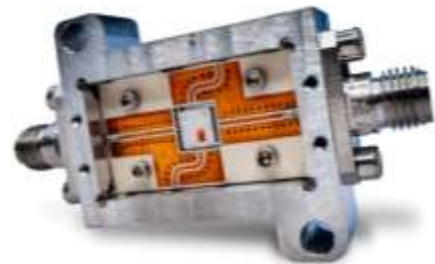


Figure 547: a Raytheon BBN JPA.



Holzworth Instrumentation (2004, USA) is a provider of multi-channel RF sources and AWGs. They also provide phase noise analyzers. The company was acquired by Wireless Telecom in 2019.



apitech (1999, USA) is a provider of cryo-attenuators targeting the quantum computing market and covering signals from DC to 40 GHz, and with SMA, and SMPM connectors.



AnaPico (2005, Switzerland) is a provider of low phase noise RF signals generators, for the local oscillators used in qubits control and readout, running up to 6.1 GHz.



Wenteq Microwave Corp (2006, USA) provides low-noise amplifiers, attenuators, circulators and coaxial connectors, in the RF/microwave range.



Scaling (2022, Sweden) was created by a team coming from Chalmers University who wants to help superconducting quantum computers companies design larger QPUs.

²²⁶⁵ See [Raytheon, IBM partner for quantum in defense, aerospace](#) by Nicole Hemsoth, in TheNextPlatform, October 2021.

²²⁶⁶ See [Josephson junction infrared single-photon detector](#) by Evan D. Walsh et al, April 2021 (12 pages).

It designs a QPU chip sample holder named LINQER, with currently 16, 36 and 80 connectors, and the potential to scale up to 300 connectors. It provides low crosstalk, an innovative magnetic shielding technology, and supports chip sizes up to $20 \times 20 \text{ mm}^2$. The company was created by Zaid Saeed (CEO), Lisa Rooth (VP) and Robert Rehammar (CTO). They announced a partnership with Qblox in September 2023 which makes sense. Indeed, Qblox hardware outputs are connectors for coaxial cables that can land in Scaling's connectors. The company is also partnering with Atlantic Quantum, another Swedish startup.



Ohtama (1964, Japan) is a magnetic shields vendor some of which could be used to protect qubit chips in the cryostat.



QuEL (2021, Japan) is a startup that provides room temperature qubit control electronics that came out of Osaka University.

The QuEL-1 is an all-in-one 3U rackable solution to control qubits from gates to readout. It has 8 16-bit output and 4 12-bit input channels in the 7-11 GHz range.



T0.technology (2021, Canada) develops quantum computing control electronics solutions.

It supports over a thousand independent pulses per I/O, arbitrarily sequenced or combined, low-latency feedback, direct digital synthesis at RF-frequencies and real-time pulse generation, using pre-computed or algorithmically determined pulse-profiles. The company also manufactures superconducting sensors.

Thermometers

It is possible to measure **pressure** (ambient, gas), **temperature** (everywhere) and **flow** (of gas) at cryogenic temperatures. Specific sensors are installed in cryostats, attached to different locations in the “chandelier” (with superconducting qubits). Temperatures are measured with cryogenic thermometers! There are many types of low temperature thermometers as shown in Figure 548.

These are found in particular at **Lake Shore Cryotronics** with its Cernox thermometers which go down to 100 mK and resist well to the ambient magnetic field and its ruthenium oxide thermometers which go down to 10 mK. At less than 20 mK, noise thermometers using Josephson junctions are used (and the loop is closed...). Some thermometers are placed on the plates opposite the heat exchange tubes and the mixing box. Still, progresses need to be done even in this area, noticeably to measure precise temperatures in the 10 mK range and with no delay.

Low Temperature Thermometers

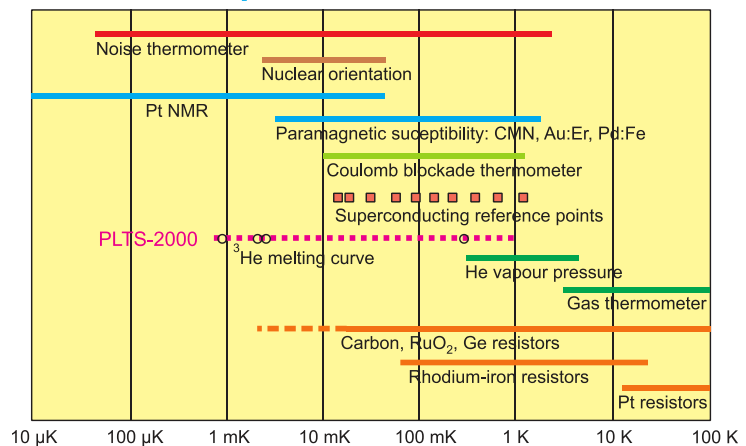


Figure 548: categories of low-temperature thermometers. Source: [Thermometry at low temperature](#) by Alexander Kirste, 2014 (31 slides). We can see that there are about ten types of thermometers that go down to less than 1K. The most commonly used one exploits the Coulomb block based on tunnel junction. The electrical voltage of the junction varies linearly with the cryogenic temperature.

Temperature can even be measured within cryo-CMOS chips operating at 20 mK to a couple K²²⁶⁷.

²²⁶⁷ See [CMOS on-chip thermometry at deep cryogenic temperatures](#) by Grayson M. Noah et al, Quantum Motion, August 2023 (14 pages).

Vacuum

Besides photon qubits, most other qubit types require some form of vacuum to isolate the qubits from their environment. We usually make a distinction between different levels of vacuum. The most stringent ones are used with trapped ions and cold atoms which require ultra-high vacuum (UHV) conditions whereas solid-state qubits like superconducting and electron spins are less demanding. UHV starts at 10^{-9} mbar.

One problem to avoid when creating vacuum is outgassing. It manifests with particles being ejected from the internal enclosure surfaces and materials, including residual water coming from the air. The phenomenon is avoided by carefully selecting the materials.

Cold atoms qubits require a pressure of 10^{-10} mbar while trapped ions goes down to 10^{-12} mbar. In both cases, low pressures and outgassing are obtained with heating the system enclosure above 200°C for several hours while the vacuum pumps are operating. This “bake-out” process removes water and other trace gases sitting on the chamber surface. Heating is done with heater stripes placed around the chamber. The chamber exterior can also be cooled with liquid nitrogen to contain any further gassing.

There are many vacuum and ultra-high-vacuum systems vendors. The most commonly seen in research labs come from **Pfeiffer** (Germany). Some pumps must be cooled at low temperature, like the 4K pump used by Pasqal to cool their atoms.

Finally, measuring pressure in vacuum is also a challenge. Classical mechanical pressure measurement is of no use in the UHV to XUV (extreme ultra-vacuum) ranges covering 1×10^{-6} to 1×10^{-10} Pa. The NIST in the USA is proposing a solution applicable to cold atoms to cover these ranges of pressures²²⁶⁸. A dedicated part on quantum pressure sensors is located page 832.

Lasers

Masers and lasers are applications of three successive discoveries and inventions:

- **Fabry-Pérot resonant cavities**, named after Charles Fabry²²⁶⁹ (1867-1945) and Alfred Pérot (1963-1925). Their system invented in 1898 was originally used to create an interferometer.
- **Stimulated emission**, formalized by Albert Einstein in 1917. It occurs when an excited atom receives a photon of energy equivalent to a transition between two energy levels. It then re-emits two photons identical to the received one and the energy level of the atom is reduced to its ground state.
- **Optical pumping**, invented by Alfred Kastler in 1949 at ENS in France, which earned him the 1966 Nobel prize in Physics.

It generates a population inversion, creating a high proportion of atoms excited at level E_2 in the diagram below compared to level E_1 . Optical pumping often excites atoms to energy levels higher than E_2 in Figure 549, with a non-radiative transition from these levels to the E_2 level and then from the E_1 level to the fundamental level of the E_0 atom.

If pumping was performed only between levels E_1 and E_2 , their proportion would balance, and the laser effect could not be triggered. Three-level pumping is used with pulse lasers and four-level pumping with continuous lasers.

²²⁶⁸ See [Development of a new UHV/XHV pressure standard](#) (Cold Atom Vacuum Standard) by Julia Scherschligt et al, 2018 (15 pages).

²²⁶⁹ We owe to Charles Fabry the creation of the Institut d'Optique, of which he was the first director in 1926 of the engineering school that was originally called SupOptique or Ecole Supérieure d'Optique.

A laser is based on a resonant cavity filled with a gain or amplifier medium. The pumping of this gain medium is optical, electrical or chemical. Once at the high energy level (E_2 in Figure 549), the atom drops to the E_1 energy level either spontaneously or stimulated.

The mechanism can be self-sustained since the spontaneously emitting photons then generate the stimulated emission of identical twin photons in frequency, phase and amplitude.

The stimulated emission is sustained by placing the atoms in a transparent cavity, filled with solid, liquid or gas, and parallel mirrors trapping the photons. One of the mirrors is slightly semi-reflective, allowing some of the amplified light to exit the laser.

This system of mirrors plays the role of a resonator. It reflects off-axis and thus undesirable photons out of the laser and the wanted on-axis photons back into the excited population where they can continue to be amplified thanks to the laser pumping.

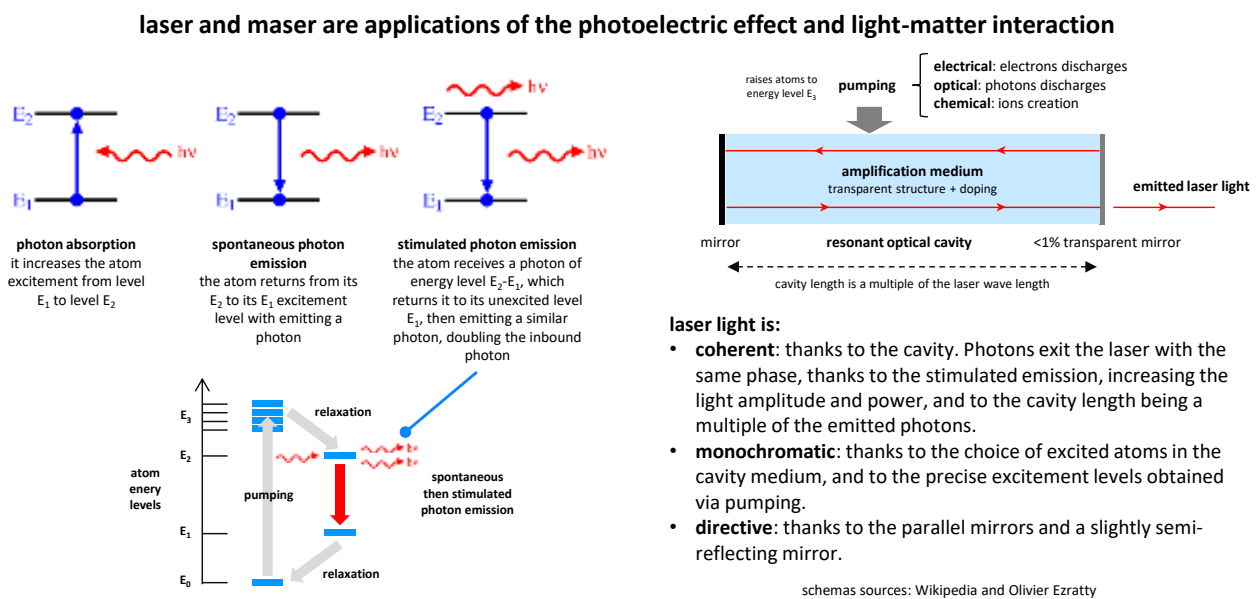


Figure 549: how lasers work. (cc) Olivier Ezratty, 2021.

The light resulting from this process is **directive** (thanks to the resonator and its parallel mirrors), **monochromatic** (thanks to the choice of excited atoms and the fineness of the cavity) and **coherent** (the photons are in phase and with the same wavelength/frequency thanks to the stimulated emission and the length of the cavity being a multiple of the laser wavelength). The laser photons frequency depends on the materials used in the cavity and the optical length of the cavity. As an order of magnitude, a 1mW red laser emits 3×10^{15} photons per second.

Lasers (light amplification by stimulated emission of radiation) appeared conceptually in 1958 in an article by Arthur Leonard Schawlow and Charles Hard Townes. The first **gas laser** was created in 1960 by Theodore Maiman, using helium-neon. **Excimer**-based gas lasers cover ultraviolet.

We then had successively **doped crystal lasers** (also named solid-state lasers, such as ruby which is Al_2O_3 doped with Cr^{3+} , or YAG, Yttrium garnet and Aluminum $\text{Y}^{33}+\text{Al}^{53}+\text{O}_{12}^{2-}$), **chemical lasers** (covering the infrared spectrum), **semiconductor diode lasers** (the most common today, usually based on gallium arsenide, or GaAs), **fiber lasers** (using rare earth elements like neodymium, erbium and thulium, mainly used in optical communications), and finally, **free electron lasers**, which we already briefly covered in relativistic quantum mechanics section (Figure 552).

Lasers operate either in pulses or continuously. The first mode is used to create very high-power levels. It led to the creation of femtolasers and even attolasers with very short pulses of a few hundred attoseconds in the UV range. **Anne L'Huillier** (French, Lund University, Sweden), **Pierre Agostini** (French, Ohio State University) and **Ferenc Krausz** (MPI) were awarded the Nobel prize in physics

in October 2023 for their seminal work on attolasers. This opens the path to explore how electrons behave in atoms. To create very powerful lasers, laser amplifiers are created which consists of chains of lasers with a primer laser that is connected to a series of lasers that successively amplify the light generated by the previous laser.

Lasers applications are quite various: industrial diamond drilling and cutting (1965), barcode readers (1974), laser printing (1981), office scanners, Laserdisc (1978), audio CDs (1982), DVDs (1995), surgery, particularly in ophthalmology (glaucoma, retinal detachment, refractive surgery), cosmetic surgery, in dermatology, for tattoo and hair removal, telecommunications, laser pointers, depth sensors, focus sensors for smartphones, iPhone FaceID sensor, measurement and alignment in construction, all sorts of LiDARs, stereolithography 3D printing, confocal microscopy (very shallow depth images), flow cytometry (cell counting), DNA chips analysis, video projector light sources, velocity measurement, the stripping of certain materials, various weapons, nuclear fusion, telescopes adaptive optics, atoms cooling, quantum telecommunications, quantum cryptography and finally, quantum computing, and on and on and on. In short, lasers are everywhere!

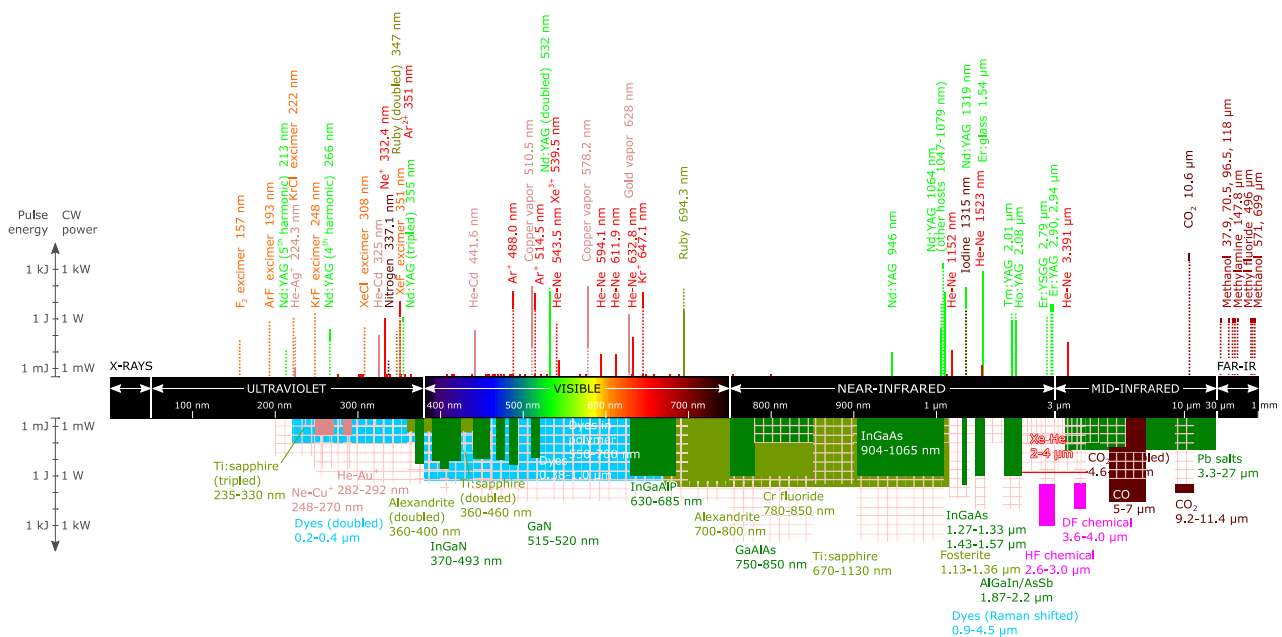


Figure 550: the great variety of lasers covering the electromagnetic spectrum from ultraviolet to mid-infrared waves.

Source: [Wikipedia](https://en.wikipedia.org/wiki/Laser#/media/File:Electromagnetic_spectrum_of_lasers.png).

The frequency ranges covered by lasers range from infrared to ultraviolet (Figure 550). There are even types of lasers with adjustable frequency. Free electron lasers go as far as X-rays. Gamma-rays lasers - or grasers - do not yet exist.

In quantum technologies, the most commonly used laser wavelengths are 775 nm (beginning of the near infrared region next to red) and 1,550 nm (middle of the near infrared region). The first one is used for quantum computing thanks to efficient photon generation and single photon detection (particularly with APD, avalanche photo diodes). The second is used in optical fiber for long distance communications, data transmission and QKD systems (Figure 551).

There are many solutions to up and down-convert photons from/to these two wavelengths. For example, these conversions are mandatory when connecting several photon-based quantum computers through a fiber optic link. Solid-state qubits require another type of conversion, mostly from microwaves to 1,550 nm infrared photons, given the conversion must convert the quantum information in the solid-state qubit to some encoding in the resulting photons, like their polarization.

Another breed worth mentioning are femtosecond lasers, which create short pulses of coherent light in the range from the femtosecond (10^{-15} s) to the picosecond (10^{-12} s).

They are used in micro-machining and various other tasks, including quantum sensing in relation with frequency combs²²⁷⁰.

The **Maser** (1953) or "Microwave Amplification by Stimulated Emission of Radiation" was invented before the laser, in 1953, by Nikolay Basov, Alexander Prokhorov and Charles Hard Townes, who were awarded the Nobel prize in Physics in 1964. It is the equivalent of the laser but emits microwaves instead of visible light. The first masers were using ammonia and generated 24 GHz microwave photons. Hydrogen Masers followed in 1960.

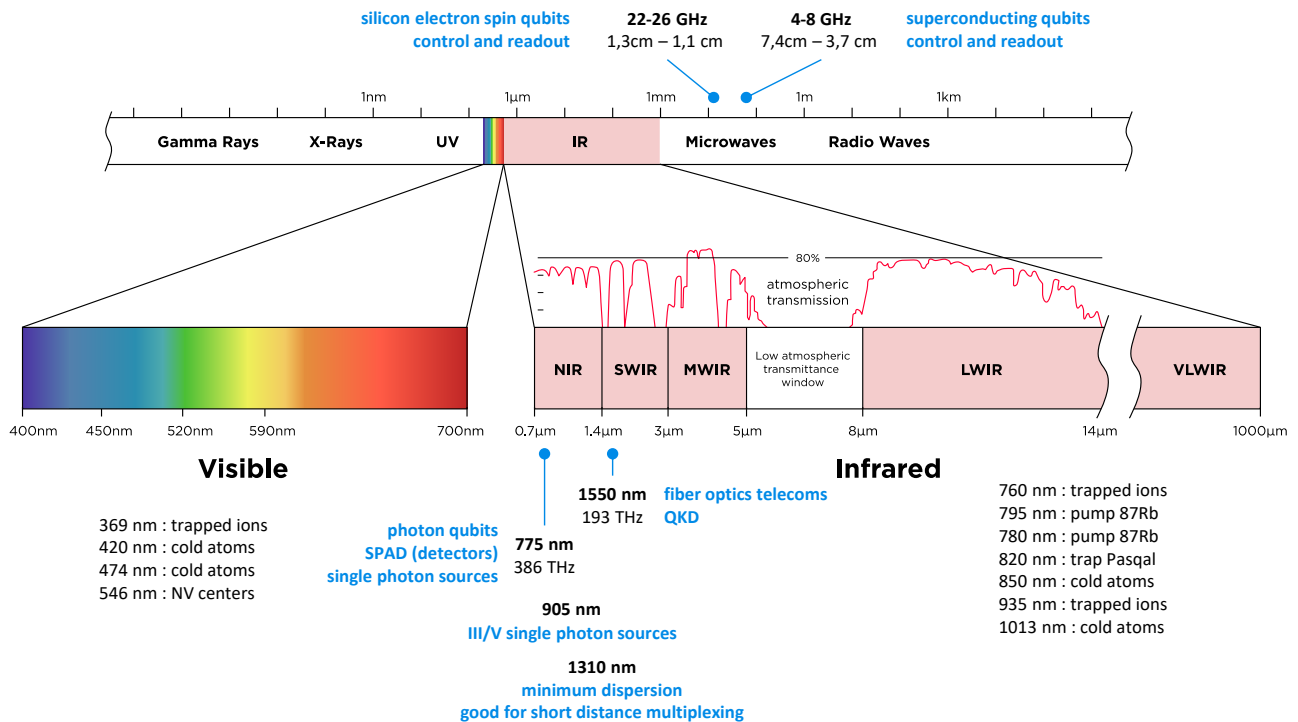


Figure 551: lasers used in the visible and infrared spectrum. Source: <http://www.infinitioptics.com/technology/multi-sensor/>.

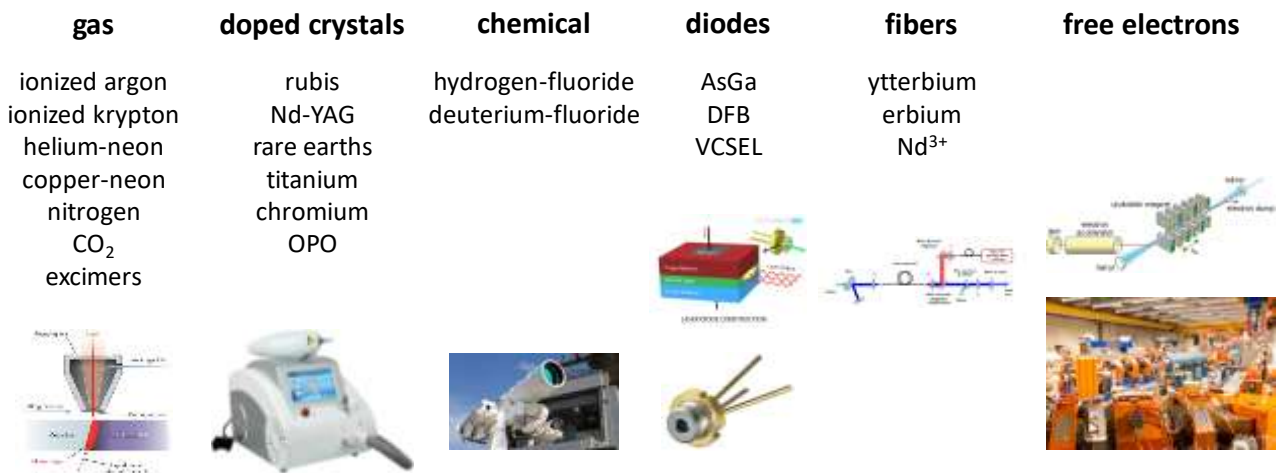


Figure 552: the various types of lasers and their cavity materials. (cc) Olivier Ezratty, 2021.

There are many laser vendors who play a role in the second quantum revolution, both with photon qubits, quantum telecommunications, quantum cryptography and quantum sensing. Lasers are also used to control cold atoms and trapped-ions qubits.

²²⁷⁰ See [20 years of developments in optical frequency comb technology and applications](#) by Tara Fortier and Esther Baumann, NIST, 2019 (16 pages).



Chromacity (2013, UK) is a manufacturer of lasers targeting various industry and research needs, including quantum communications.



DenseLight Semiconductors (2000, Singapore) manufactures various laser products.



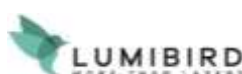
FemTum (2016, Canada) creates mid-infrared lasers which can be used in quantum optics and silicon photonics applications and quantum sensing using optical frequency combs. It is a spin-off from the Center of optics, photonics and laser (COPL) in Quebec City.



FocusLight Technologies (2007, China) produces laser diodes and laser optics components.



Freedom Photonics (2005, USA) manufactures lasers and photodiodes using InP and GaAs semiconductor, SiGe-based photonics and planar lightwave waveguides. It was acquired by **Luminar** in March 2022.



Lumibird (1970, France) is a supplier of lasers. Formerly Quantel and Keopsys, it is a large SME with more than 800 employees and a turnover of 110 M€, 80% of which is exported.



Toptica Photonics (1998, Germany) is a photonics equipment manufacturer developing laser sources covering a wide range of frequencies from 190nm (UV) to Terahertz waves, including laser diodes and frequency combs (Figure 553). Their lasers can be used to control trapped ions and cold atoms.

Their flagship product, the Chromacity OPO, has a tunable optical parametric oscillator that covers near-IR and mid-IR wavelengths. Some of their lasers can create entangled photons. They employed over 320 people in 2022 for a revenue of \$82M.

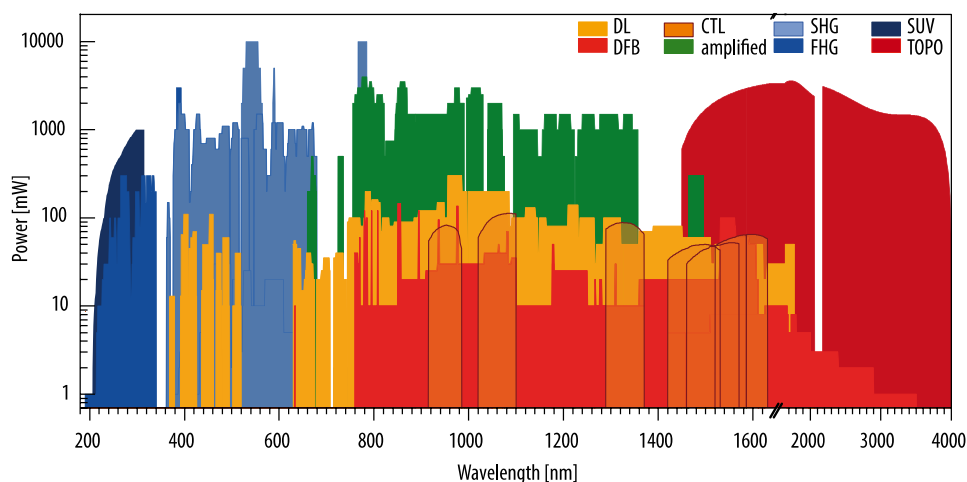


Figure 553: wavelengths coverage of Toptica lasers. Source: [The Control of Quantum States with Lasers in Photonics View, 2019 \(3 pages\)](#).



Stable Laser Systems (2009, USA) offers Fabry-Perot lasers and cavities that can be used for cold atom confinement.

The startup launched by Mark Notcutt is based in Boulder, Colorado, one of the nerve centers of quantum technologies in the USA, near NIST and the University of Colorado. His team also includes Jan Hall, winner of the 2005 Nobel prize in Physics for the discovery of the effect that bears his name.





GLOphotonics (2011, France) sells hollow-core photonic crystal fiber (HC-PCF) and their functionalized form Photonic Microcells (PMC). These lasers use a proprietary fiber technology and gas photonics. They are partnering with CNRS XLIM lab in Limoges.



iPronics (2019, Spain) develops general-purpose integrated programmable photonic systems, where optical hardware complements software to perform multiple functions.



Q.ANT (2018, Germany, 11M€ public funding) has a product line organized in four segments: particle metrology, atomic gyroscope, magnetic sensing and photonic computing.

They develop a green laser optimized for NV centers quantum sensors. It is a subsidiary of the TRUMPF Group. It also manufactures powerful lasers used in ASML lithography machines and light channels on silicon for qubits transport. They are also working on photonic-based quantum computing using lithium-niobate circuits using path encoding, phase modulation, interferometers (MZI), fiber couplers, electro-optical modulators and resonators. They lead a relate German consortium with 50M€ funding including 42M€ public funding from the German government. As of November 2022, the company had 50 employees.



Silentsys (2021, France) created a closed-loop voltage regulation electronic system that complements lasers and their servo controller to reduce the emitted laser noise and improve its frequency precision.



UnikLasers (2013, UK, £4.1M) sells ultra-narrow linewidth, high power lasers at the specific wavelengths related to the exact atomic transitions targeted for quantum sensing applications.

It can transform a MHz linewidth laser into an Hz linewidth laser. It is currently adapted to continuous lasers running in the 1,550 nm and 1,050 nm wavelengths and fits in a 2U rack system. Their OFD system (optical frequency discriminator) delivers a continuous voltage signal driving the laser diodes that is proportional to the frequency fluctuations of the input laser beam. The technology core is optical, using frequency combs. They also propose low power voltage power systems. One of their OFD can drive two lasers.



Vexlum (2017, Finland) produces high-power narrow-linewidth vertical external-cavity surface-emitting lasers (VECSELs) including blue and UV lasers, used among other things, to control trapped beryllium ions.

It is a spinoff from Tampere University of Technology Optoelectronics Research Centre (ORC).

And also: **Spectra Physics** (1961, USA), **Altitun** (1997, Sweden, \$10M), **Calmar Laser** (1996, USA) and **Ampliconyx** (2016, Finland who manufactures short-pulses lasers), **Active Fiber Systems** (2009, Germany) which creates femtoseconds fiber lasers and is a spin-off from Fraunhofer IOF, **InnoLume** (2002, Germany, \$26.8M, which sells laser diodes), **FISBA** (1957, USA) which develops multi-wavelengths lasers, **Intense Photonics** (1994, USA, \$51M, which develops single and multi-mode monolithic laser array products, and high power laser diodes and was acquired by Orix Group), **Lytid** (2015, France) which manufactures terahertz cascade lasers, **Spark Lasers** (2015, France) and their picosecond and femtosecond lasers, **Amplitude Laser Group** (2001, France) and their femtosecond lasers, **neoLASE** (2007, Germany) a supplier of various laser products including laser amplifiers, **Alpes Lasers** (1994, Switzerland) which sell infrared quantum cascade lasers, **Luna Innovations** (1990, USA, \$13.1M), **Vector Photonics** (2020, UK, £1.6M) is a spin-off from the University of Glasgow which develops semiconductor lasers based on PCSELs (Photonic Crystal Surface Emitting Lasers) and **OEwaves** (2000, USA, \$15M) provides lasers, oscillators and optical/RF tests and measurement systems.

Photonics

Let's now look at other photonics equipment manufacturers. They sometimes also manufacture lasers but even more.



Accelink (1976, China) sells optoelectronic components, including fiber optics modulation and demodulation systems, lasers and SiO₂/Si material plane optical waveguides. They probably play a role in the deployment of quantum telecommunication networks.



Aurea Technology (2010, France) is a photonics equipment manufacturer targeting various markets including quantum communications (QKD) and quantum sensing.

It sells twin photon sources (TPS), time correlated single photon detectors (Picoxea), ultra-low-noise NIR single-photon counting detection modules (SPD_A and SPD_OEM_NIR²²⁷¹), time correlators (Chronoxea) and high-resolution fiber sensors (q-OTDR) and picosecond pulse lasers (Pixea). They also developed Fluoxea, a fluorescence lifetime imaging mapping system using time-correlated single photon counting that can be used to characterize semiconductors, qualify quantum dots or measure local magnetic fields (with the help of NV centers). The company has its own assembly plant in Besancon, France. It is a spin-off company from the optics department of FEMTO-ST, a public research lab based as well in Besancon.



Azurlight Systems (2010, France) develops high-power laser amplification systems in the visible and near-infrared spectra (from 488 nm to 1,065 nm) using ytterbium-based fibers with low thermal dissipation. These can be used for atoms cooling and trapping. The company was acquired by **Topptica** (Germany) in 2023.



Cailabs (2013, France, \$46.2M) is a company based in Rennes, France, which is a spin-off from the LKB of ENS Paris and markets photonics equipment and in particular spatial multimode multiplexing systems for optical fibers supporting up to 45 nodes.

This is what makes it possible to multiply the speed of the optical fibers of the telecom operators' networks. In particular, they have KDDI (Japan) as a customer. The startup is managed by Jean-François Morizur (CEO) and Guillaume Labroille (CTO) with Nicolas Treps from LKB being their scientific advisor.



Quandela (2017, France, €35M) is a startup that was initially specialized in the generation of indistinguishable photons with quantum dot fed by a laser (Figure 554). They pivoted in 2020 in the quantum computing market.

Quandela's team is composed of Valérian Giesz (CEO), an engineer from the Institut d'Optique with a PhD in photonics²²⁷², Niccolo Somaschi (CTO), PhD from the University of Southampton and Pascale Senellart (CSO), CNRS research director at C2N from CNRS and Université Paris-Saclay. It had a staff of about 70 people in Summer 2022 and several international customers, mainly in Europe, Russia and Asia. Their team also includes Shane Mansfield, who is their Director of Research (theory, algorithms and software) and Jean Senellart (CPO).

²²⁷¹ The SPD_OEM_NIR is using an InGaAs single photon avalanche diode (SPAD in the 900 to 1700 nm wavelength range with very low dark count rate noise (DCR<700 Hz). It is cooled with the Peltier effect. The supported wavelengths make is suitable to photon counting in telecom wavelengths based QKDs (1,550 nm). It also fits into a standard datacenter rack in a 2U package.

²²⁷² See his thesis in [Cavity-enhanced Photon-Photon Interactions With Bright Quantum Dot Sources](#) by Valérian Giesz, 2016 (228 pages) where he describes his work in Pascale Senellart's team and the various evolutions of their quantum dot photon source that led in 2017 to the creation of Quandela.

With a trapped artificial atom comprised of a couple thousand atoms forced to emit periodically single photons in a given direction by laser-activated cavity quantum electrodynamics, they are able to generate photon streams that are well separated in time and with stable quantum characteristics, with wavelengths from 924 nm to 928 nm in the near infrared, this range being progressively extended²²⁷³. This creates a very bright photon source that can then be time-bin multiplexed to create indistinguishable photons used in photon qubit quantum computers, first with using a KLM probabilistic model²²⁷⁴. The next goal is to create large cluster states of entangled photons, given various techniques are investigated here and there (spin-photon entanglement mechanism²²⁷⁵ ²²⁷⁶, photon number entanglement²²⁷⁷, frequency-bin entanglement, etc.).

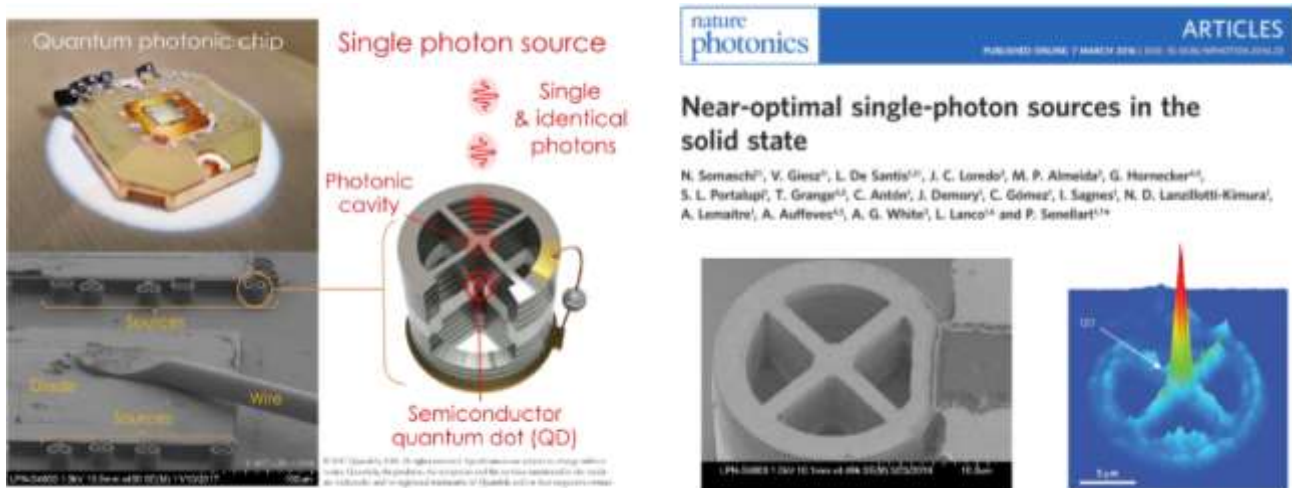


Figure 554: Quandela's quantum dots single photon source. Source: [Near-optimal single-photon sources in the solid-state](#) by Niccolo Somaschi, Valerian Giesz, Pascale Senellart et al, 2015 (23 pages).

They are developing single photon sources running at telecom wavelength as part of the project Paris-RegionQCI, a regional project, led by Orange, with an end goal to deploy a QDK-fibered link between Paris and the Paris-Saclay University.

They also work on the generation of cluster states of entangled photons as part of the European Union FET Open Qcluster project (2019-2023). This project is critical for the implementation of a scalable MBQC model in their QPU.

The photon source must be cooled down to about 4K, which is achievable with compact cryostats costing only a few thousand Euros and using helium 4, such as the attoDRY800 from **Attocube** (Germany). These cryostats use a simple pulsed tube, reminiscent of the first cooling stage of the dry dilution cryostats used with superconducting and quantum dot spin qubits.

²²⁷³ See [Near optimal single-photon sources in the solid state](#), Niccolo Somaschi, Valerian Giesz, Pascale Senellart et al, 2016 (23 pages). The quantum dot is made with InGaAs (indium, gallium, arsenide) and is surrounded by stacked Bragg-reflectors made respectively with GaAs and Al_{0.9}Ga_{0.1}As (aluminum, gallium, arsenide). Pascale Senellart describes in detail how Quandela's photon generators are made in her talk [Quantum optics with artificial atoms](#) in a Rochester Lecture in June 2018 (1h10mn). The prestigious [Rochester Lectures](#) are held once a year in Durham, UK. The 2017 edition welcomed Peter Knight and the 2012 edition Alain Aspect.

²²⁷⁴ The process was improved in Pascale Senellart's laboratory in 2020 to generate even brighter and purer photon sources from a spectral and polarization point of view thanks to quantum dot excitation with phonons. See [Efficient Source of Indistinguishable Single-Photons based on Phonon-Assisted Excitation](#) by S. E. Thomas, Pascale Senellart et al, July 2020 (10 pages).

²²⁷⁵ See [Ideal refocusing of an optically active spin qubit under strong hyperfine interactions](#) by Leon Zaporski et al, Nature Nanotechnology, January 2023 (23 pages).

²²⁷⁶ See [On-chip spin-photon entanglement based on photon-scattering of a quantum dot](#) by Ming Lai Chan et al, May 2023 (7 pages).

²²⁷⁷ See [Photon-number entanglement generated by sequential excitation of a two-level atom](#) by Stephen C. Wein, Maria Maffei, Paul Hilaire, Niccolo Somaschi, Aristide Lemaître, Loïc Lanco, Alexia Auffèves, Pascale Senellart et al, April 2022 (22 pages).

Quandela launched in 2020 a compact and integrated version of its indistinguishable photons generator, fitting into a datacenter rack named Prometheus. The fiber is glued to the photon source, which eliminates the mechanical part of the calibration. The pulsed head of the 4K cryostat is also integrated in the rack, the compressor being outside and water-cooled at first. Eventually, it will be integrated in the rack and cooled by air.

The rack was designed by **Pentagram**, the same British designer that IBM used for the Q System One launched in January 2019. It is 1.75m high and 80 cm wide. The whole thing consumes about 5 to 6 kW, the bulk of it coming from the cryostat.

Quandela and the C2N laboratory collaborate with research labs around the world to create advanced photonics platforms. In 2020, they published with a team from the **Hebrew University of Jerusalem** a paper on the creation of a 4-photon cluster state for quantum computing (Figure 555). The idea is to use single photons and to entangle them with each other via a delay line and inject them into a computing circuit based using cluster states and MBQC (measurement based quantum computing) method.

In Europe, they collaborate mainly with **Fabio Sciarrino's** team in Italy, in Spain with **INL** and other teams in Austria, the United Kingdom, Slovakia and Israel. They are part of the European FET project PHOQUSING for boson sampling led by Fabio Sciarrino's team.

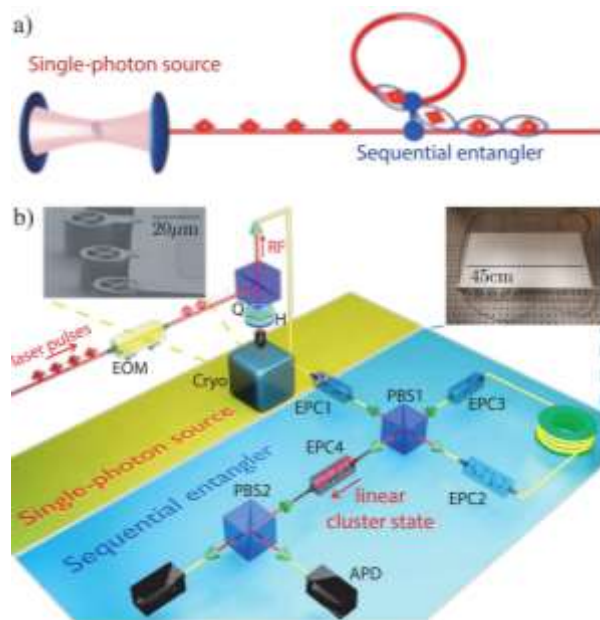


Figure 555: creation of cluster state photons with a serial entangler using a delay line. Source: [Sequential generation of linear cluster states from a single photon emitter](#) by D. Istrati et al, 2020 (14 pages).

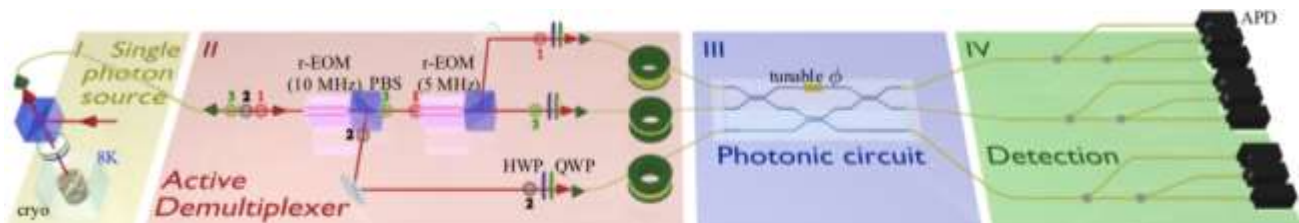


Figure 556: three entangled photon source using Quandela quantum dots. Source: [Interfacing scalable photonic platforms: solid-state based multi-photon interference in a reconfigurable glass chip](#) by Pascale Senellart et al, 2019 (7 pages).

In 2019, they experimented with Quandela's photon source to demultiplex it into three photons which were then injected into a photonic integrated circuit integrating a programmable quantum gate. The photonic circuit was precisely etched with a femtosecond laser (Figure 556).

Since 2020, Quandela has started working on creating a photon-based quantum computer using their own photon source. We cover this core part of their business in the photonic qubits vendor section.



Control Systems (2016, UK) develops photonics components including photonics device status readout modules and backplanes (boards) on which several of these modules can be installed. These modules drive photonics devices via a 12V voltage and read signals with 18-bit accuracy. This is control electronics.



Quantum Opus (2013, USA) develops single photon detectors based on superconducting nanowires, the Opus One. The compact version Opus Two is an 8U data center rack-mount package, including cryostat²²⁷⁸. This company benefited from US federal funding, including \$100K in 2015 and \$1.5M in 2015 from DARPA and \$125K from NASA in 2018. They are a provider of the Chinese team who did run the gaussian boson sampling experiment announced in December 2020.



SCONTEL (2004, Russia) offers single photon detectors in the visible and infrared (SSPD, for Superconducting Single Photon Detecting Systems). These detectors are cooled at 2.2K helium-4 using a Sumitomo SRDK 101 pulse head system with a water-cooled HC-4E compressor.



Single Quantum (2012, the Netherlands) offers Qos single photon detectors integrated in a 2.5K liquid helium cooled cryostat.

Their sensor uses the SNSPD (superconducting nanowire single photon detector) technique, made of a thin film of superconducting nanowires shaped into a flattened serpentine coil. This device captures a single photon from an optical fiber and has a detection efficiency of 85% to 90%, covering wavelengths from 800 nm to 1,550 nm (Figure 557).

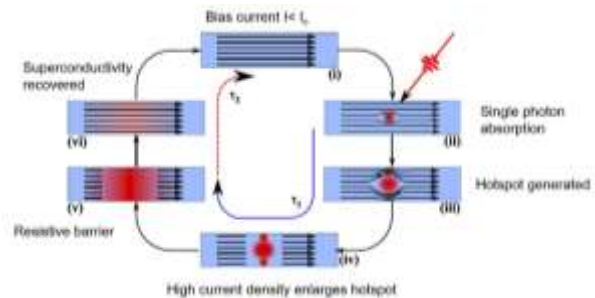
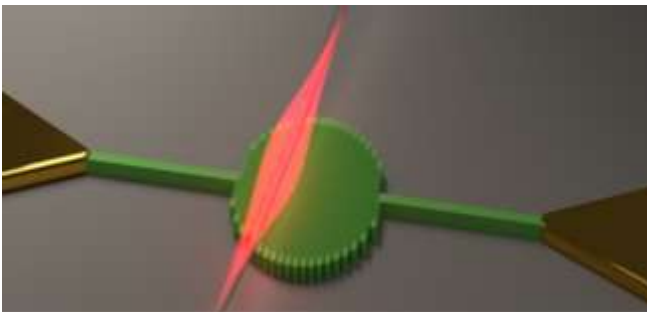


Figure 557: SingleQuantum SNSPD photon source.



Sparrow Quantum (2016, Denmark, \$9.9M) is a spin-off from the Niels Bohr photonics research laboratory. Like Quandela and Qubitekk, they offer single photon sources.

Their solution is based on InAs quantum dots. Their engineering differentiation lies with the quantum dot efficient coupling with a slow-light photonic-crystal waveguide. A laser is illuminating the quantum dots with using a confocal microscope. Their photon coherence indistinguishability is between 95% and 98% with their Sparrow Chip 2021 Resonant. They are generated in the 920-980 nm wave range. The photon generation system is cooled at 6K. It generates streams of 100 single high quality photons at a rate of over 20 million single photons per second in a fiber.



VLC Photonics (2011, Spain) produces photonics equipment and fabless design of photonic integrated circuits. The company is involved in European Flagship projects.

It is a spin-off of the University of Valencia. The company was founded by Iñigo Artundo, Pascual Muñoz, José Capmany and José David Domenech. They also market technical reports at prices ranging from 4K€ to 5.4K€ per piece.

²²⁷⁸ See [Introduction to Quantum Opus and revolutionary superconducting detection systems](#) (14 slides).



Excelitas (2010, USA) sells various photonics devices including Single-Photon Counting Modules (SPCMs).



Pixel Photonics (2020, Germany, 1.45M€) develops single photon detectors (SNSPD) targeting quantum computing, QKD and imaging markets. With HTGF (Germany) and Quantonation (France) as seed investors.



Hamamatsu Photonics (1953, Japan) provides silicon photodiodes, electron multipliers for detecting electrons, ions, and charged particles, photon counters, LCoS based spatial Light Modulators (SLM) used for cold atoms controls, laser cooling systems, quantum imaging and image sensors for the detection of neutral atoms, trapped ions and NV centers fluorescence.



Miraex (2019, Switzerland) has two main quantum technologies in its portfolio: photonic based quantum sensors for vibration, acceleration, acoustic, pressure, electrical field and temperature measurement and a quantum system converting matter qubits into photon qubits and vice versa. It is a spin-off from EPFL.



Micron-Photons-Devices (2004, Italy) aka MPD creates Single Photon Counting Avalanche Diodes, “SPAD”, fabricated using custom silicon, standard CMOS and InGaAs/InP technologies. It also sells photon counting based QRNGs.



Qubitrium (2020, Turkey) develops entangled photon sources, laser current drivers and single photons detectors.



Teem photonics (1998, France) creates lasers and integrated photonics components including erbium doped waveguide amplifiers and arrayed-waveguide gratings. Not the same AWGs than the arbitrary waveform generators used to control solid-state qubits, although these can be used to signals multiplexing/demultiplexing.



Alcyon Photonics (2018, Spain, \$560K) is a spin off from IO (Instituto de Óptica) in Spain. Its expertise is on sub-wavelength grating (SWG) technology. They create complex photonic circuits like high-performance Application Specific Photonic Integrated Circuits (APICs). The company was co-founded by the researcher Aitor Villafranca.



Scintil Photonics (2018, France) develops mixed silicon and III/V photonic components, using their BackSide-on-BOX process, that mixes active and passive optical components.

Their technique bonds InP/III-V dies on the backside of processed Silicon-On-Insulators (SOI) wafers, only where it is needed. Their fabrication process is classical CMOS. Their components integrate lasers (WDM laser arrays and tunable lasers), modulators, waveguides, wavelength filters, surface fiber couplers, semiconductor optical amplifiers (SOA), and photodetectors.



Qlibri (2022, Germany) provides optical micro-cavities used in absorption microscopy and quantum technologies. It is used in quantum computation and single-photon sources. It can be used to sample inhomogeneous nanosystems like quantum dots, NV-centers, or 2D-Materials.

Muquans/Exail (France) is also a provider of laser and intelligent frequency tunable lasers, laser frequency doublers and narrow-linewidth lasers used in various quantum technologies.

Photon Force (2015, UK) creates single-photon cameras of 32x32 pixels. It can be used in various photonic based quantum sensing applications. It enables time-tagging of incoming photons with a time resolution of 55 pico-seconds.

Covesion (2009, UK) develops laser frequency conversions devices that are used in many quantum optics applications. It is a spin-off from the University of Southampton.

ICON Photonics (2018, France) offering is made of optical coupling and packaging solutions for high speed optical communications using 3D wafer-level polymer optical beamshaping. It can be used for the development of quantum communications and quantum computing solutions.

We also have **Ibsen Photonics** (1991, Denmark) which provides spectrometers and various photonic equipment, **Lumiphase** (2020, Switzerland) which develops optical modulators, **Bay Photonics** (2007, UK) which provides photonic circuits assembly and packaging, **MenloSystems** (2001, Germany) and their optical frequency combs, terahertz systems and femtosecond lasers, **Qubig** (2008, Germany) which develops light modulators (amplitude and phase modulators, phase shifters, Pockels cells) that can be used in quantum computing or communications, **Menhir Photonics** (2018, Switzerland) which create femtolasers, **Photek** (1991, UK) with its photon and imaging detectors and **g2-zero** (2020, Spain) which manufactures single photon detectors.

Fabs and manufacturing tools

Many quantum technologies components are nanofabrication based and must be manufactured somewhere. It is the case with superconducting qubits, superconducting electronics, quantum-dots based electron spin qubit circuits, quantum nanophotonic circuits, NV center based qubits and sensors, single-photon generating quantum dots, photon detectors, trapped ions supporting circuits, travelling wave parametric amplifiers and the likes. You could wonder how these circuits are manufactured and where. Like your regular smartphone chip processor, is it coming from a giant \$20B TSMC 5 nm fab in Taiwan? Well, most of the time, no!

Foundries

We are in a very different technology and market realm. Quantum related components have some distinct characteristics compared to mass market semiconductors that you'll find in your TV, smartphone, laptop or tablet. They are very specialized and use sometimes special manufacturing processes and/or materials like III/V semiconductors or niobium/aluminum deposition for superconducting qubits and electronics. They are most of the time experimental with many try/error cycles. They are sometimes manufactured with specialized tools. And finally, they are produced in rather small quantities. Surprisingly, given the experimental nature of many components, the related fabs are usually less impressive in size and cost.

Fabs contain cleanrooms, where the concentration of airborne particles is controlled on top of temperature, humidity and sometimes, other parameters like ambient magnetism and vibrations. Cleanrooms are classified according to the number and size of particles suspended in the atmosphere. Cleanroom ISO classes range from 1 to 9, with an (exponential) increased number and size of particles per volume unit, 1 being the "cleaner". Most specialized quantum technologies fabs have a less stringent cleanroom class requirement than the most expensive and modern semiconductor fabs since they are not creating high-density chips and do not care so much about yield. They are rather class 100 to class 1000 cleanrooms.

We can segment quantum technologies fabs in a couple categories as shown in Figure 558:

Research fabs. These are most of the time fabs from national research organizations labs and universities. These fabs have cleanrooms with sizes ranging from 100 m² to 4,000 m². Their teams and the associated researchers are creating the "recipe" of new semiconductor technologies. These fabs usually produce 200 mm or smaller wafers.

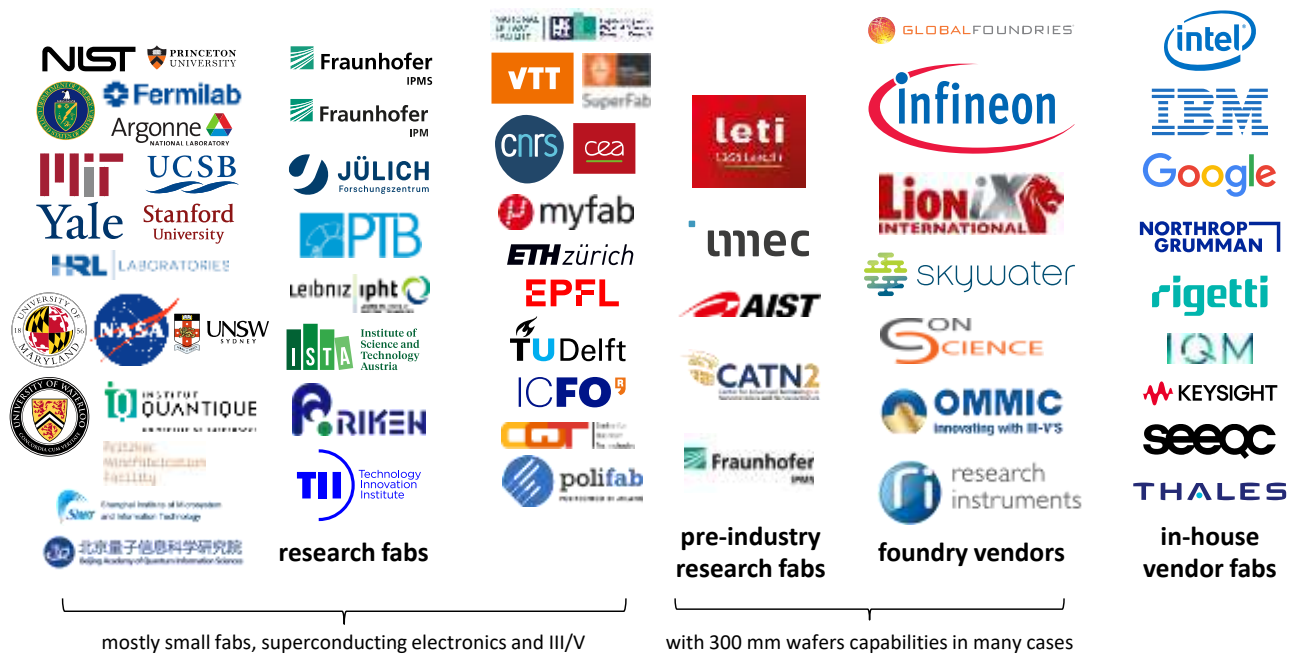


Figure 558: research and industry cleanrooms fabricating semiconductors for quantum use cases. (cc) Olivier Ezratty, 2022-2023.

North-America with the famous MIT Lincoln Labs in the USA (superconducting electronics and qubits, trapped ions chips, with 1,629 m² of clean rooms), Princeton (1,350 m² cleanroom, silicon and III/V, up to 100 mm wafers), HRLabs in California (all sort of things in a 900 m² clean room), UCSB Nanofab (1,170 m², superconducting qubits, MEMS, photonics, imaging sensors), Harvard CNF (966 m²), Yale University (108 m², superconducting qubits), Stanford (180 m², various quantum techs), NIST NanoFab (1,800 m² cleanroom), DoE Argonne Quantum Foundry (500 m²) and Fermilab SQMS Center and the Fermilab Quantum Computing Lab Two, University of Chicago (890 m², Pritzker Nanofabrication facility) and the University of Waterloo Quantum Nano Fabrication and Characterization Facility (600 m²).

Europe with VTT in Finland (2,600 m² cleanroom for 150 and 200 mm wafers, superconducting qubits and electronics, photonics), DTU Nanofab ini Denmark (1,350 m²), the superconducting Royal Holloway cleanroom in the UK (350 m²), CNRS C2N (2,900 m² clean room near Paris, photon quantum dots sources in GaAs, polaritons circuits, etc), CNRS Institut Néel (220 m², near Grenoble, superconducting electronics and qubits, graphene, diamonds growth²²⁷⁹), Van Leeuwenhoek Lab at TU Delft (3,500 m² cleanroom used by Qutech and TNO in The Netherlands), MyFab (Sweden), Fraunhofer IPM (400 m² clean room in Freiburg, various optical quantum sensors), Fraunhofer IPMS near Dresden (200 mm wafers 1,500 m² cleanroom) and also PTB, Leibniz IPHT and Jülich in Germany, PoliFAB from Politecnico di Milano which created an interferometer used by Pascale Senellart’s team to demonstrate the indistinguishability of photon clusters²²⁸⁰, ISTA Nanofabrication Facility in Austria (450 m²), EPFL and ETH Zurich in Switzerland and the UK National Epitaxy Facility.

Asia-Pacific with RIKEN and AIST (superconducting electronics, but also a strong CMOS 300 mm manufacturing capacity) in Japan, UNSW in Australia and the Shanghai Institute of Microsystem And Information Technology (SIMIT) has also its own fab.

²²⁷⁹ See [Fabrication of superconducting qubits](#) by Vladimir Milchakov (IQM), September 2020, who describes the Institut Néel superconducting manufacturing capability and process. This fab also produces the TWPA electronics from Silent Waves, a spin-off startup from Institut Néel created in 2022.

²²⁸⁰ See [Quantifying n-photon indistinguishability with a cyclic integrated interferometer](#) by Mathias Pont, Pascale Senellart, Fabio Sciarrino, Andrea Crespi et al, January 2022 (21 pages).

Pre-industry research fabs. These are the likes of IMEC (Belgium) and CEA-Leti (France) who create new semiconductor components and design new manufacturing processes before they are volume-produced in commercial fabs. These are larger fabs than the aforementioned research fabs. CEA-Leti operates 11,000 m² of cleanroom in Grenoble. IMEC cleanrooms totals 12,000 m² in Leuven, Belgium. CEA-Leti produces silicon qubits wafers for its own usage as well as for vendors like Quantum Motion (UK). These fabs produce wafers up to 300 mm.

Likewise, the Center for Advanced Technology in Nanomaterials and Nanoelectronics (CATN2) from SUNY Polytechnic Institute in New York State has a cleanroom of 12,000 m² producing 200 mm and 300 mm wafers for AI, photonics, CMOS spin qubits, superconducting qubits and digital electronics.

Foundry vendors. These are independent foundries manufacturing semiconductors for third parties. GlobalFoundries manufactures nanophotonic chips for PsiQuantum and Xanadu in Malta, New-York State in their 41,400 m² clean room on top of classical CMOS chips like the IBM Power processors. Infineon's Villach fab in Austria manufactures trapped ions chips in its 23,000 m² cleanroom for Oxford Ionics²²⁸¹. In Germany, Infineon is an industry partner of many other projects with superconducting qubits, silicon qubits, ion traps, qubit control electronics and NV centers qubits and sensing²²⁸². In the USA, SkyWater is the largest foundry for superconducting electronics, working among others for D-Wave, on top of working on various space applications and with DARPA. Formerly Cypress Semiconductor, Control Data and VTC, they consolidate a 7,360 m² clean room in Minnesota and another one of 3,300 m² in Florida and support 90 nm features geometries on 200 mm wafers. Lionix in The Netherlands manufactures nanophotonic circuits for its subsidiary QuiX. Larger foundries are usually needed for high-density chips, particularly with silicon qubits where patterns are relatively small, down to about 10 nm. OMMIC (2000, France) is a small foundry specialized in manufacturing III-V MMIC (monolithic microwave integrated circuit) which could comprise cryogenic amplifiers used in quantum computing. It was acquired in 2023 for 38.5M€ by MACOM Technology Solutions (USA), a company specialized in radio, microwave and millimeter wave semiconductors²²⁸³. At last, let's mention Research Instruments Gmbh which manufactures special components for research and industry applications, including some superconducting components used in quantum computing and ConScience AB (Sweden), a clean room fab service with various capabilities including the manufacturing of superconducting chipsets. It proudly announced in September 2023 to have "*delivered its first quantum technology components to a US based quantum computing company*" without any details. It may be related to Atlantic Quantum and its fluxonium chips.

In-house vendor fabs. These are the fabs from quantum technology vendors who are self-sufficient for this respect. Intel manufactures its own quantum dots spin qubits chips in one of its clean rooms at its Hillsboro facility in Oregon. IBM also has its own manufacturing capacity for superconducting qubits and high-density silicon chips with a cleanroom of 3,600 m² in Yorktown, New York State. Rigetti in the USA and IQM in Finland have their own small \$20M fabs for their superconducting qubits chips. Google has also an in-house fab in Santa Barbara, California. SEEQC has a small 150 mm wafers 200 m² cleanroom dedicated to manufacturing superconducting electronics. Keysight also has its own III/V 1,200 m² cleanroom, the High Frequency Technology Center (HFTC) in Santa Rosa, California²²⁸⁴. Northrop Grumman's fab in Maryland creates 150 mm silicon, SiGe, GaAs, GaN-on-SiC, GaN-on-Si, indium based nitrides and SiC wafers. Qilimanjaro relies on a fab that was put in

²²⁸¹ See [Development of novel micro-fabricated ion traps](#) by Gerald Stocker, November 2018 (96 pages) and [Trapped ion quantum computing](#), Infineon.

²²⁸² See [Infineon Participates in 6 Research Projects, Expands Commitment to Quantum Computing](#) by Matt Swayne, The Quantum Insider, February 2022. It formally opened a quantum lab near Munich in October 2023 with about 20 researchers.

²²⁸³ In July 2023, however, a scandal was revealed involving the former management of OMMIC who sold protected technology to Russia and China. See [Ommic case: How a French company allegedly handed over military secrets to China and Russia](#), July 2023.

²²⁸⁴ Their equipment is well documented in [Keysight High Frequency Tech Center \(HFTC\)](#) (15 pages).

place in 2021 at TII in Abu Dhabi. At last, Thales has an in-house 4,000 m² III/V fab with CEA-Leti as a partner.

Having your own fab makes sense when you need to have a fast turnaround and test repetitively many generations of qubit chips. It is relatively affordable for producing superconducting qubits on small wafers.

The USA, European Union and China all want to increase their share, self-reliance and supply security with semiconductor manufacturing. In February 2022, the European Union launched the European Chips Act to “*foster development of capacities in advanced manufacturing, design and system integration as well as cutting-edge industrial production*”, with a public/private funding of €43B until 2030. It includes international partnerships like when Intel is installing a new fab in Germany. The plan contains a provision for quantum technologies, to “*set up advanced technology and engineering capacities for quantum chips in the form of design libraries for quantum chips, pilot lines, and testing and experimentation facilities*”. This may provide some additional funding for the extension of the many quantum-related fabs mentioned before.

In March 2022, the US Senate voted on the CHIPS Act, with \$52B funding. It was finally signed by POTUS in August 2022. It contains an additional Federal budget of \$152M per year for quantum technologies for the 2023-2027 period, although seemingly not specific to components manufacturing. Chips USA manufacturing market share is in the 12% mark, above EU’s that sits around 9%. The rest is in Asia, mostly Taiwan, South Korea, China and Japan²²⁸⁵.

Generic processes

We’ll describe here the generic processes used to produce chips regardless of their use case, the most commonplace being bipolar, CMOS and BiCMOS chips²²⁸⁶. The story always begins with a wafer, as shown in Figure 559.

Wafers are usually made of monocrystalline silicon sliced with wired diamond saws out of ingots manufactured with the Czochralski crystal growth method. They are sometimes completed with a thin buried layer of SiO₂ (aka SOI, for silicon on insulator) and another thin layer of regular Si, using the SmartCut process invented by CEA-Leti and implemented by SOITEC and its licensing partners²²⁸⁷. SOI wafers have many interesting characteristics like reduced parasitic capacitances and low leakage currents. They are frequently used for nanophotonic circuits (like those from PsiQuantum manufactured by GlobalFoundries) or for silicon qubits chips (CEA-Leti, Qutech, ...). In other cases, wafers are made of III/V semiconducting materials (like GaAs or GaN, for manufacturing some nanophotonic circuits) or even sapphire (for some superconducting qubits and trapped ion circuits). A wafer has a thickness ranging from 40 μm to 700 μm and its diameter ranges from a couple inches (for III/V and other small volume processes) to 300 mm and even 450 mm (for volume CMOS processes).

²²⁸⁵ See [Quantum Technology Manufacturing Roadmap](#), SRI for NIST, October 2023 (69 pages) which makes a broad inventory of the technology challenges of enabling technologies features and manufacturing.

²²⁸⁶ Bipolar transistors have a very high speed and are used in analog devices. CMOS transistors are slower and do not handle such high power as bipolar transistors but are aggressively scaled down in density and require far less power to operate. BiCMOS used both bipolar and CMOS logic that are co-integrated within the same chip, which requires additional process steps and incur higher costs.

²²⁸⁷ The SmartCut process is not using a wire diamond saw like the ones used to slice wafers out of silicon ingots. It first creates a layer of SiO₂ on a Si wafer using Si thermal oxidation in wet atmosphere, PECVD or CVD. Then, an ionic implantation of H or He is made on another Si wafer creating a sort of “glue”. The SiO₂ side of the first wafer is bounded with this “glued” Si wafer and a thin layer of Si of that wafer is deposited on the SiO₂ using a “layer splitting” process created by thermal annealing. The second Si wafer can be reused for another Si deposit cycle. Both the SiO₂ and the overlay Si layers can be as thin as 10 nm. A variant of the SmartCut process is also used to deposit a thin Si layer on sapphire wafers and thermal annealing is created with laser beams in a so-called “LLO” process, for laser lift-off. I found interesting SmartCut process descriptions in [The advanced developments of the SmartCut technology: fabrication of silicon thin wafers & silicon-on-something hetero-structures](#) by Raphaël Meyer, 2018 (252 pages).

The most generic chips production processes then involve several cycles with the following successive steps with a repeat cycle ranging from resist coating to planarization including patterning, removing and adding matter.

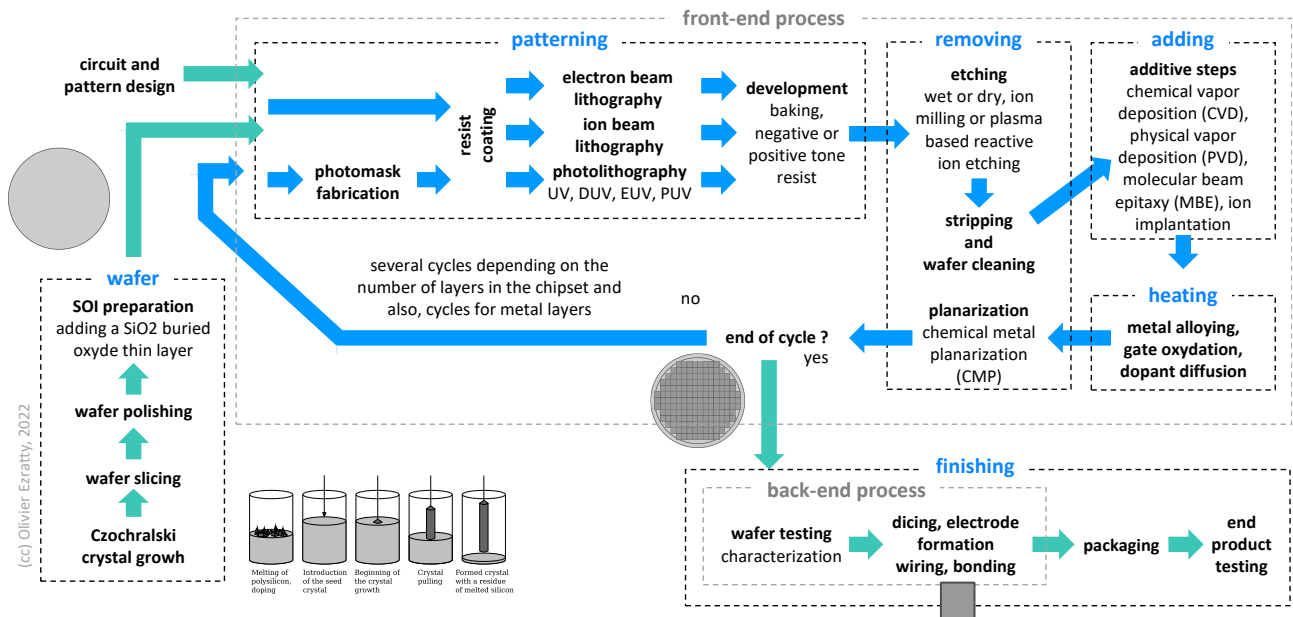


Figure 559: a generic layout of a chip manufacturing process. (cc) Olivier Ezratty, 2022.

When this cycle is over will all chip layers added on top of the other, the process ends with various finishing steps up to a packaged chip ready for integration.

Patterning

These are the process steps that define the places in the wafer where matter has to be removed with etching or added afterwards. It involves several steps that are defined during the design stages exploiting automated electronic design automation (EDA) software tools like those from ANSYS, Cadence, Keysight Technologies, Synopsys, Xilinx and Mentor Graphics (in Siemens group).

Resist coating is applied on the wafer with a photoresist liquid that will be later exposed during the lithography process and selectively removed during development. The coating is mechanically added with a dispenser nozzle positioned above the center of the rotating wafer attached to a chuck and spindle with vacuum pumping²²⁸⁸ (Figure 560).

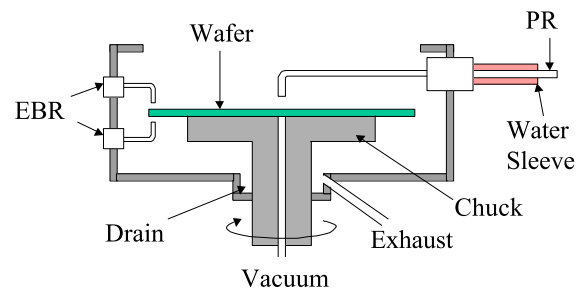


Figure 560: resist spin coating. Source: [Introduction to Semiconductor Manufacturing Technology](#) by Hong Xiao (2148 slides).

EBR (edge bead removal) removes excess coating at the wafer edge with a solvent. Then a N₂ based soft bake evaporates most of the solvent.

Photolithography is used to expose a special coating on selected areas (Figure 561). The photolithography technique makes use of a photomask and ultra-violet rays exposing a photoresist film or coating. It's being used to produce silicon qubits and nanophotonic chips. The usual photolithography process involves a stepper which moves the wafer under the camera to expose the wafer for each and every chip to produce, and with a very high precision (<1 nm).

²²⁸⁸ See the incredibly rich [Introduction to Semiconductor Manufacturing Technology](#) by Hong Xiao (2148 slides) and its eponymous book published in 2012 (524 pages).

It replaces mask aligners that are used when the photolithography process exposes the whole wafer in a single step. The size of the chip is limited by the size of the photolithography reticle, which conditions the mask maximum size. Across time and density improvements, various ranges of ultra-violet wavelengths have been used.

It started with UV, to DUV or deep ultra-violet under 248 nm, then to EUV (extreme ultra-violet) at 13 nm and PUV at 6.5 nm which is border line to soft X Rays. Starting with EUV, there is only one provider of photolithography system, ASML.

Electron beam lithography (EBL) is another lithography technique, that is focusing a beam of electrons on an electron-sensitive resist film to remove matter in specified areas, without requiring a mask like with photolithography. EBL can reach precisions of 1 nm which is excellent and better than photolithography. It is used to create precision nanostructures like with photon-generating quantum dots and also superconducting qubit chips. It is a very slow process compared with photolithography, so adapted to low volume and custom productions. An EBL looks like an electron microscope. Existing electron microscopes can be converted to run EBL tasks.

Other less used varieties of lithography are ion-beam (using helium), laser lithography, the latter being used for resolutions above 500 nm, and STM (Scanning Tunnelling Microscopy) that can reach sub-nm resolutions.

Development which removes the photoresist coating where it was or wasn't exposed during the photolithography or electron beam lithography step. It depends on the photoresist material used which is either a negative (insoluble after exposure) or positive resist material (soluble after exposure).

Positive photoresist enables better lithography resolution but is more expensive than negative photoresist. It uses so-called hard baking above 100°C to polymerize and stabilize the photoresist coating.

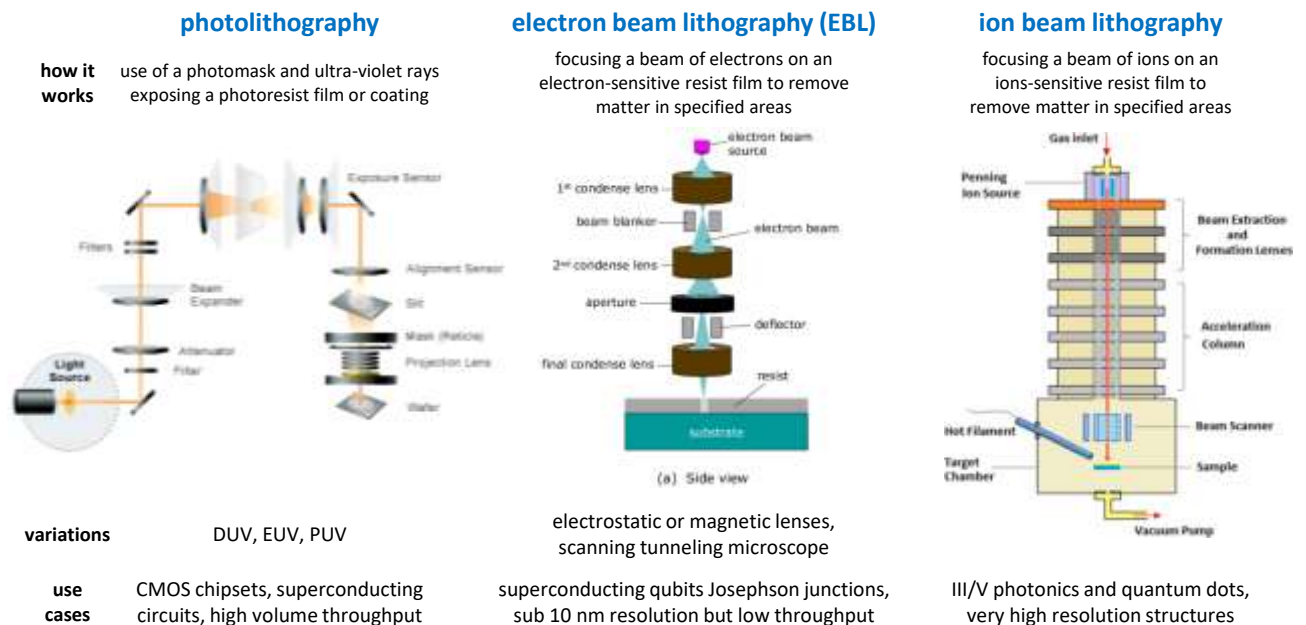


Figure 561: the three main lithography techniques used for semiconductors manufacturing. Compilation (cc) Olivier Ezratty, 2022-2023.

There are many resist coatings depending on the process (photolithography or electron beam lithography) and whether we are using a negative or positive resist. With positive resist, coating can be made of long polymer chains with weak chain bonds. Exposure creates chain scission in the exposed areas. These are dissolved during the chemical development process while the longer chains do not dissolve. Another process consists in using resist creating hydrophilic product when exposed, which are then dissolved by water. Negative coating can be made of monomers that polymerize when exposed to light and become non dissoluble by the solvent used in the development process.



Figure 562: two examples of such cluster tools, on the left with a Kurt Lesker OCTOS Automated Thin Film Deposition Cluster Tool ([source](#)) and on the right an Applied Materials Endura Clover MRAM PVD System ([source](#)).

The photolithography process contains in total about 10 stages (coating, soft-baking, exposure, cleaning, hard-baking, ...). In volume production, these are handled in cluster tool systems, using one or several robotized systems to move the wafer from one tool to the next in a controlled environment. This ensure both productivity and production quality (Figure 562).

Photolithography clusters vendors include Dainippon Screen, who partners with ASML. Cluster tools are also in place for other parts of manufacturing seen later, like etching and additive steps. Multi-axis robots and roof conveyors like those from Kuka and Muratec move wafer cassettes (handling 25 wafers) from one cluster to the other.

Removing matter

These steps correspond to the removal of matter on the wafer based on the zones defined by the lithography process (Figure 563).

	ion milling or sputter etching	ion beam etching (IBE)	plasma based reactive ion etching (RIE)
how it works	the ions of an inert noble gas like argon are accelerated from a wide beam ion source on the target in vacuum to mechanically remove material on the target.	the ions of active molecules like CF_4 , Cl_2 or CHF_3 are accelerated from a wide beam ion source on the target in vacuum to mechanically remove material on the target.	energetic and neutrally charged free radicals reacting at the surface of the wafer, attacking the wafer from all angles, aka, being anisotropic.
variations	reactive ion etching deep reactive ion etching	ion polishing, ion cutting, reactive ion beam etching (RIBE, RIE), chemically assisted ion beam etching (CAIBE).	MEMS, nanophotonics, niobium resonators in superconducting qubits
use cases	superconducting qubits	III/V chipsets, single photon quantum dots shapes, MEMS	

Figure 563: the various ways to remove matter in semiconductor manufacturing. Compilation (cc) Olivier Ezratty, 2022-2023. Illustration sources: Wikipedia, others.

Etching removes matter in the uncovered areas, using wet chemical or dry physical methods, the dry methods being the most commonplace for high-density (VLSI) circuits. Various dry etching techniques include ion milling or sputter etching, and plasma based reactive ion etching. The first uses the projection of inert ionized noble gas while the second uses neutrally charged free radicals that react with the target surface. In general, plasma is an ionized gas with the same proportion of positive and negative charges. There are also variants with anisotropic (orientation independent) or directional etching (orientation dependent).

Stripping and cleaning remove the remainder of the photoresist material. In volume production clean rooms, etching and stripping is handled by cluster tools with robotized handlers moving wafers from the etcher to the stripper tool, with a loading and unloading station extracting wafers from its carrier box (usually, containing 25 wafers in volume production environments).

Planarization of the wafer uses physical polishing. It can be based on CMP (Chemical Metal Planarization). It is generally implemented after additive steps.

Adding matter

Additive steps consist in adding some materials in the visible areas, like silicon or doped silicon in classical CMOS transistors, using boron or indium (for p-doping) and arsenic (As), phosphorus (P), antimony (Sb) or aluminum (Al) (for n-doping). Some of these processes are implementing an epitaxy, creating a perfect crystalline structure with the added material, in the feature layers (doped silicon, gates). Other processes like PVD and sputtering are not epitaxial and are used for the production of superconducting qubits.

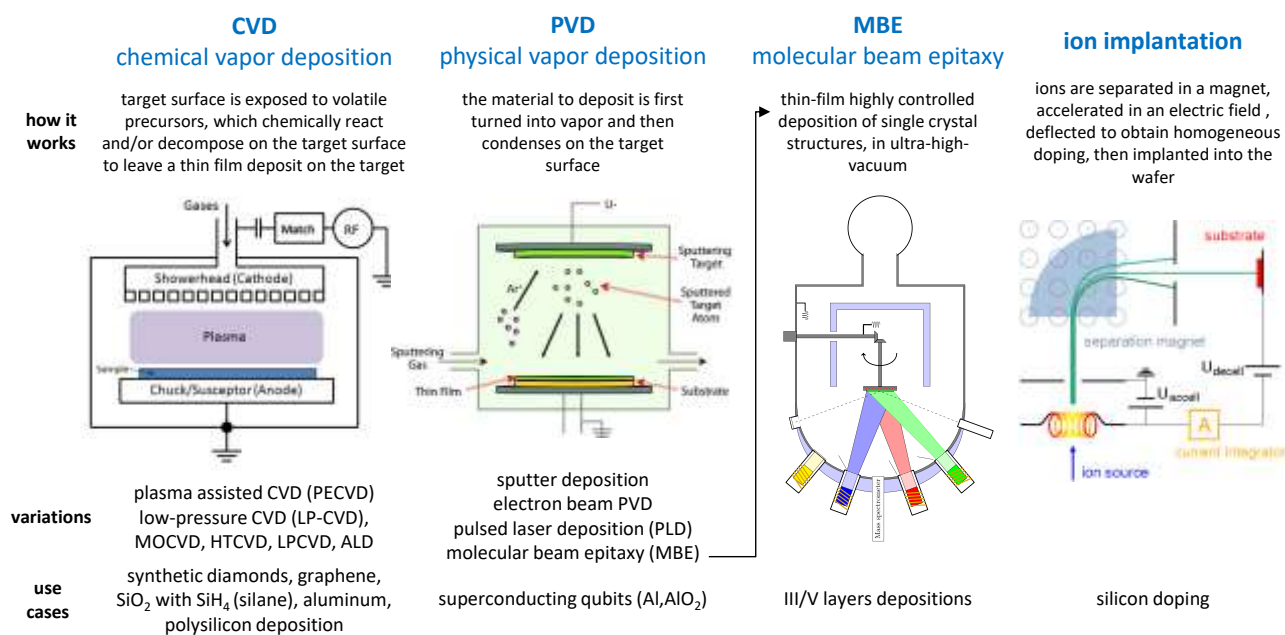


Figure 564: the various ways to add matter in semiconductor manufacturing. Compilation (cc) Olivier Ezratty, 2022-2023.

Additive steps can use various techniques like ion implantation, CVD (chemical vapor deposition, where the target surface is exposed to one or more volatile precursors, which chemically react and/or decompose on the target surface to leave a thin film deposit on the target, e.g. using silane SiH₄ to deposit Si on the wafer, generating 2 H₂ molecules), ALD (atomic layer deposition, a variation of CVD to create highly precise epitaxial atomic layers using repeat cycles), PVD (physical vapor deposition under low pressure, where the material to deposit with evaporation, sputtering or plasma and then condenses on the target surface), sputtering being one type of PVD (using ion projection to pull material from a source and deposit it on the target wafer or ionized gas like argon that, thanks to a high-voltage applied to the target, is projected on the target and creates a plasma with the target atoms

that then condenses on the surface of the chip), e-beam deposition (another variety of PVD using electron beams to evaporate the matter to deposit on the wafer), PLD (pulse laser deposition, using femtoseconds laser pulses to extract matter from a source and then sent to the target), MBE which is a variety of PVD (molecular beam epitaxy, for thin-film deposition of single orderly crystal structures). CVD can be plasma based (Figure 564).

In the last process cycles, these steps are related to the creation of several superposed metal layers connecting the various semiconducting circuits created in the earlier steps. With superconducting qubits, aluminum, and aluminum oxide (or niobium) sputtering is implemented in this step.

Metal layers. When all cycles related to the functional parts of the circuits are finished, some electrodeposition of metal is made to connect the chip to the outside world, usually copper or aluminum (in the case of superconducting qubits and electronics) and copper-aluminum alloys.

Metal layers are created with a mix of lithography-etching and PVD/CVD.

As metal layers are added, their density decreases. Then, some wiring may be added and bonding or bumps plus packaging.

In CMOS designs, the “front-end-of-line” (FEOL) contains the individual active elements (transistors, capacitors, etc.) while the “back end of line” (BEOL) contains the metal layers (Figure 565).

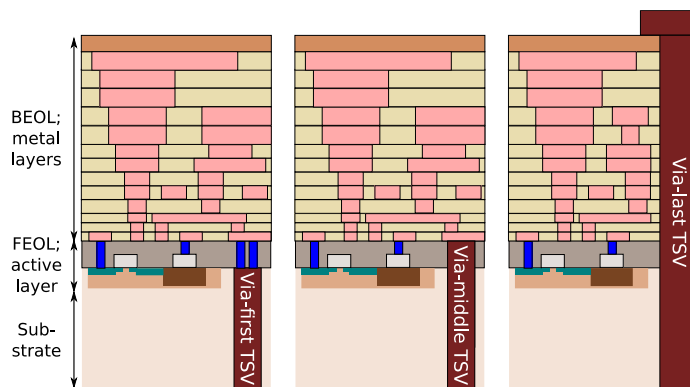


Figure 565: typical metal layers of a semiconductor.

So-called 3D chips like the superconducting qubits chips from IBM, OQC and others result from the assembly and perfect alignment of stacked chips. CEA-Leti (France) is collaborating with Intel in the design of such innovative 3D packaging technologies. 3D stacking makes use of TSV or through silicon vias, which establishes a metal connection from top to bottom of a chip or from the active layer to the front plane through the wafer.

A TSV hole is created with reactive ion etching, copper electrochemical deposition for creating a seed layer and electroplating to fill the hole²²⁸⁹.

Heating

Thermal processes are implemented for various purposes like dopant activation and diffusion, gate oxidation ($\text{Si} + 2\text{O} \rightarrow \text{SiO}_2$), metal reflow which smooths its surface usually in an atmosphere of N_2 or H_2O , metal alloying and chemical vapor deposition. One used technique involves rapid thermal annealing, using a vertical or horizontal furnace.

Finishing

These are the product finishing tasks undertaken when the patterning-removing-adding-heating cycle is completed (the front-end process). The aim here is to turn the chip on its wafer into a functional component with its connectivity. It is also called the back-end process (Figure 566).

Wafer testing. Then, testing and characterization is done to make sure the manufactured components meet the required quality. One inspection tool used is electron microscopes, which can also be used to analyze the patterning quality between each patterning cycle. Wafers containing chips operating at cryotemperatures can be tested by a cryo-prober like the one provided by Bluefors/Afore and being used by Intel in Oregon and CEA-Leti in Grenoble.

²²⁸⁹ See [Tutorial on forming through-silicon vias](#) by Susan L. Burkett et al, January 2020 (16 pages).

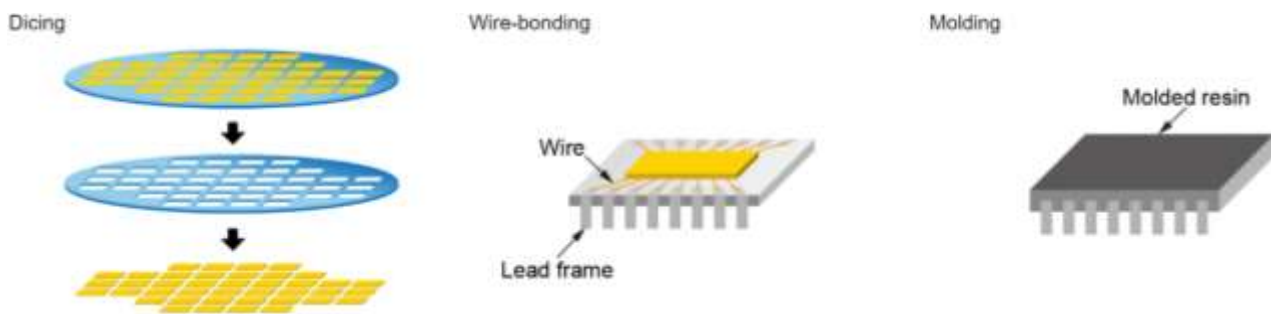


Figure 566: the finishing steps of semiconductor manufacturing with dicing, wire bonding and molding. Compilation (cc) Olivier Ezratty, 2022 and [The semiconductor manufacturing process \(back-end process\)](#), Matsusada, February 2022.

Electrode formation, wiring and bonding. These are more traditional steps to add macro-elements to the circuit that will connect them to the outside world. This is done after the chips are extracted from the wafer with dicing.

Packaging. It is mostly about putting plastic and sometimes metal shielding for specific applications (space, military, quantum) around the chip and its bonds/wires. The component can be then integrated in a system with its surrounding electronics.

End-product testing. The electronic circuit is fully functionally tested here before being used.

The manufacturing yield is the percentage of functional chips at the end of manufacturing. Each intermediate manufacturing step has its own yield, and the end yield is the result of the multiplication of each step yield.

Quantum process specifics

Each and every chip is manufactured with a specific recipe with many steps involving different tooling and dozens of parameters (tool, chemical compounds, temperature, pressure, angles, ...). Putting in place such processes is tedious and require very specialized skills. The whole manufacturing process for a chip can last from a couple hours to a couple months depending on its complexity. All in all, a new chip design, manufacturing and testing can last between a couple weeks to 2.5 years depending on the product and process.

Superconducting qubits

Manufacturing a superconducting qubit chip is both rather specific and simple, at least, compared to classical silicon CMOS chips and their epitaxy processes, creating pure crystalline semiconducting structures. It explains why so many labs in the world have their own cleanroom able to prototype such chips. A superconducting chip wafer can usually be produced in less than a week when it can last months if not over a year for CMOS chips on 300 mm wafers²²⁹⁰. There are of course many variations and as the superconducting chips become more complicated, assembling up to three stack chiplets, and with more lithography steps, the production cycle gets longer.

We'll describe here one of the methods to create a superconducting qubit chip which is derived from the bridge-based Niemeyer-Dolan technique²²⁹¹ (Figure 567). The superconducting qubit core feature is its Josephson junction made of three layers: a conducting metal like aluminum and its oxide

²²⁹⁰ See a couple examples of superconducting qubits manufacturing process descriptions in [Manufacturing low dissipation superconducting quantum processors](#) by Ani Nersisyan et al, Rigetti, January 2019 (9 pages), [Simplified Josephson-junction fabrication process for reproducibly high-performance superconducting qubits](#) by A. Osman et al, Chalmers, November 2020 (7 pages) and the thesis [Micromachined Quantum Circuits](#) by Teresa Brecht, Yale University, December 2017 (271 pages).

²²⁹¹ There are other Josephson junction techniques like the Manhattan bridge. See [Improving Quantum Hardware: Building New Superconducting Qubits and Couplers](#) by Thomas Michael Hazard, Princeton, 2019 (136 pages).

insulator variant in between. It is surrounded by metal structures for creating capacitances and a resonator²²⁹².

- The wafer substrate is made of either **sapphire** or **intrinsic silicon**, meaning monocrystalline and undoped. Silicon is commonplace but has its shortcomings: it must be deoxidized, since SiO₂ is damaging the qubit's quality. Sapphire can't be oxidized but is less commonplace²²⁹³. The wafer may be gold plated on its unpolished side to ensure good electric and thermal contacts between the chip and the chip-carrier.
- Resist deposition is done using the spin-coating technique and with two layers of resist one on top of each other. The bottom one is more sensitive to the e-beam than the one above.
- E-beam lithography exposes some of the resist to an electron beam. This is a rather slow process. It uses a double insolation process with different strengths to attack the two resins layers.
- Development where the resist is removed from the hole exposed by the e-beam and etching which creates an undercut carved in the resist.
- First metal evaporation where a first layer of aluminum is deposited with an angle + θ . It creates the first layer of the Josephson junction.
- An aluminum oxide layer is grown during an oxidation step. This gate is less than 2 nm thick.
- Second angled metal evaporation to create a new layer above the oxidized aluminum from the Josephson junction gate. It is done in the opposite angle - θ to cover a different area in the hole.
- The residual resist may in some situations be removed with a CMP process or more classically dissolved in solvent during the lift off step. For these, no additional layer or isolation layer is added on the Josephson junction.

All this process was just about creating a single Josephson junction that is usually 200 nm wide. A classical superconducting qubit contains at least two other circuits: capacitances (about 100 μm to 600 μm wide), a resonator (*aka* superconducting coplanar waveguide) and a microwave network.

The network and resonator can be created using 193 nm UV lithography or laser lithography and negative resist etching, meaning the metal is first deposited everywhere (except on the Josephson junction) and then, the resist coating is removed where it was not exposed. RIE (reactive ion etching) can also be used, particularly for creating resonators. This process can make use of aluminum, niobium, TiN (titanium nitride) as developed by John Martinis in 2013 and even indium²²⁹⁴.

TiN is appreciated thanks to its ability to avoid oxidation. Titanium nitride (TiN) can be used as an isolation layer on top to a sapphire substrate to avoid dielectric losses between the various qubit's components²²⁹⁵.

Superconducting qubits circuits are usually rather simple and only 2D with no additional metal layers. Still, insulators like tantalum are tested over the parts of the chip outside the Al/AlO_x/Al Josephson

²²⁹² The schema below comes from [Resonant and traveling-wave parametric amplification near the quantum limit](#) by Luca Planat, June 2020 (237 pages). It describes the process for the creation of a Josephson junction in a TWPA and is very similar to a superconducting qubit.

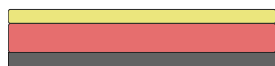
²²⁹³ See [Fabrication of Al/AlO_x/Al junctions with high uniformity and stability on sapphire substrates](#) by Yuzhen Zheng et al, China, May 2023 (10 pages).

²²⁹⁴ See [Sputtered TiN films for superconducting coplanar waveguide resonators](#) by S. Ohya, John Martinis et al, UCSB, 2013 (9 pages).

²²⁹⁵ See [Titanium Nitride Film on Sapphire Substrate with Low Dielectric Loss for Superconducting Qubits](#) by Hao Deng et many als, Alibaba, May 2022 (10 pages). The use of TiN enables qubit lifetimes of up to 300 μs .

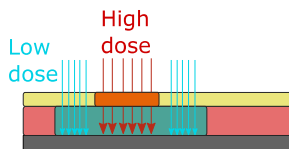
junction, like on the various niobium circuits (resonators, ...) avoiding the formation of Nb_2O_5 oxides. It can improve the qubit stability (T_1)²²⁹⁶.

resist deposition with spin-coating: two layers of resist are spin-coated on each other, the bottom one being more sensitive to the ebeam than the top one. $1A < Q$



Resist deposition

ebeam lithography exposing the resist. It uses a double insolation process with different strength to attack the two resins layers.

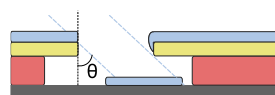


Ebeam writing

development and etching which creates an undercut carved in both resists with different widths.

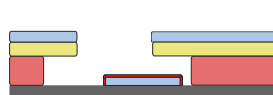


Development



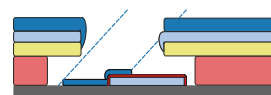
Metal evaporation #1

a first layer of aluminum is deposited via metal evaporation/sputtering with an angle $+\theta$ to create the first layer of the Josephson junctions



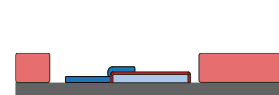
Static O₂ oxidation

the Josephson gate is created with oxidizing the aluminum in the "lift off" stage. The oxide gate is less than 1 nm deep.



Metal evaporation #2

another angled aluminum sputtering with direction $+\theta$ creates a new layer above the oxidized aluminum from the Josephson junction gate



residual resin and metal removal

Figure 567: the process of manufacturing a superconducting qubit or superconducting component like a TWPA. Source: [Resonant and traveling-wave parametric amplification near the quantum limit](#) by Luca Planat, June 2020 (237 pages). Comments added by Olivier Ezratty in 2022.

There's an empty space of a minimum 2 mm height above and below the chip in its (copper) packaging. On the other hand, superconducting electronics dies can superpose up over 10 alternating layers of niobium and dielectric, usually SiO_2 . The surrounding connections are themselves superconducting and the chip edge is connected to gold or aluminum wires and bonds. Some elements on the chip may be connected together with 'airbridges' which consist of wired connections between two distant elements 'flying' over a qubit component, with a small layer of air/vacuum between the circuit and the wire²²⁹⁷.

Andreas Fuhrer Janett from IBM Zurich labs developed a process and apparatus to put the chip in ultra-high vacuum (UHV) during assembly²²⁹⁸. According to IBM, the UHV can contribute to creating less noisy qubits.

The connectivity constraints explain for example the limitations of the chimera structure in D-Wave superconducting qubits layout. The trend is to create 3D structures, assembling several chips, with one being dedicated to electronic signals controlling the qubits, like with Google, IBM and OQC.

The chips are assembled using wafer bonding, connecting metal layers using indium thanks to its ductility, even in low temperatures and at relatively low temperature (156°C). Chips also use TSV (through-silicon vias) to facilitate signals routing between the connectivity chip and the qubit chip²²⁹⁹.

²²⁹⁶ See [Systematic Improvements in Transmon Qubit Coherence Enabled by Niobium Surface Encapsulation](#) by Mustafa Bal, Anna Grassellino et al, FermiLab, NIST, Rigetti, Northwestern University, April Louisiana State University, 2023 (17 pages). The tested qubits were manufactured at the Pritzker Nanofabrication (PNF) facility.

²²⁹⁷ See [How Google \(Probably\) Made the Quantum Supremacy Chip](#) by Russ Renzas, September 2019 which describes, among other things, the various layers in Google original Sycamore circuit and its airbridges.

²²⁹⁸ See [Ultrahigh vacuum packaging and surface cleaning for quantum devices](#) by M. Mergenthaler, Andreas Fuhrer et al, 2021 (6 pages).

²²⁹⁹ See [Fabrication of superconducting through-silicon vias](#) by Justin L. Mallek, William D. Oliver et al, March 2021 (14 pages).

The chip density is not very high as compared with classical CMOS chips. The quality and fidelity of the superconducting qubits depends on several factors including materials purity²³⁰⁰. The manufacturing yield of superconducting chips can however be as low as 1% but is usually above 70%²³⁰¹. One avenue to potentially improve the manufacturing quality of superconducting qubits would be to produce them with 300 mm CMOS fab technologies. That's what IMEC has been experimenting in 2022 with producing qubits of rather good quality (but not stellar), using argon milling²³⁰² and subtractive processes²³⁰³.

We mentioned a lot of aluminum so far. It is not the only superconducting metal used with Josephson junctions, among other reasons due to the stability of the aluminum oxides that creates the thin junction. Niobium, niobium-titanium nitride, and tantalum^{2304 2305} can be used for large structures like resonators. Niobium is also used in superconducting electronics (SFQs, already covered) and SQUIDS sensors with the advantage of being a superconductor at 9K versus 1.2K for aluminum. Niobium is easy to etch but oxides quickly.

Superconducting nanowire single photon detectors

Superconducting nanowire single photon detectors (SNSPDs) can be manufactured with NbTiN sputtering on sapphire²³⁰⁶.

Trapped ions circuits

These circuits implementing Paul or Penning traps are manufactured using a mix of techniques with e-beam metal evaporation-based deposition of titanium and gold, etching process, and femtosecond-laser machining for 3D surfaces shaping using tools like those from **FEMTOprint**²³⁰⁷.

Photon-generating quantum dots

Like the ones from CNRS C2N and Quandela are manufactured with adding about 100 layers alternating GaAs and GaAsAl compounds using molecular beams epitaxy. Adding these many layers can still be implemented in a couple hours. In the middle of the road, special techniques are used to deposit the planar λ cavity made of a couple hundred of InGaAs. The cylinder cut for the quantum dot enclosing is implemented with ion milling²³⁰⁸.

Silicon qubits

Their manufacturing is very close to traditional CMOS manufacturing techniques (Figure 568). It requires UV/EUV photolithography due to the relatively high features density in the chips (which can

²³⁰⁰ See [Material matters in superconducting qubits](#) by Conal E. Murray, IBM Quantum, 2019 (98 pages).

²³⁰¹ It was the yield with IBM's 17 qubits chipsets in 2018 according to [Towards Efficient Superconducting Quantum Processor Architecture Design](#) by Gushu Li et al, 2019 (15 pages).

²³⁰² See [Argon milling induced decoherence mechanisms in superconducting quantum circuits](#) by J. Van Damme et al, IMEC, February 2023 (13 pages) describing how argon milling can negatively affect the quality of niobium resonators.

²³⁰³ See [Path toward manufacturable superconducting qubits with relaxation times exceeding 0.1 ms](#) by J. Verjauw et al, npj, August 2022 (7 pages).

²³⁰⁴ See [New material platform for superconducting transmon qubits with coherence times exceeding 0.3 milliseconds](#) by Alexander P. M. Place, Nathalie P. de Leon, Andrew A. Houck et al, Nature Communications, March 2021 (6 pages).

²³⁰⁵ See [High-quality superconducting \$\alpha\$ -Ta film sputtered on heated silicon substrate](#) by Yanfu Wu et al, May 2023 (12 pages).

²³⁰⁶ See [NbTiN for improved superconducting detectors](#) by Julien Zichi, KTH Sweden, 2019 (86 pages).

²³⁰⁷ See the thesis [Multi-wafer ion traps for scalable quantum information processing](#) by Chiara Decaroli, ETH Zurich, 2021 (248 pages) which provides a lot of insights on trapped ion architectures and circuits manufacturing.

²³⁰⁸ See the details in [Near-optimal single-photon sources in the solid-state](#) by Niccolo Somaschi, Valerian Giesz, Pascale Senellart et al, 2015 (23 pages).

go as low as 10 nm). The etching processes are also rather similar. The materials purity is an important figure of merit to ensure the quality of the manufactured qubits as it is with superconducting qubits.

The silicon wafers used to create spin qubits are covered by a layer of about 100 nm of ^{28}Si using a wafer scale CVD process. All the other functional and isolation layers using silicon are also based on ^{28}Si , mostly through silane (SiH_4). There are many variants with Si/SiGe heterostructures, Al/ AlO_x structures, etc. Indeed, superconducting features must be integrated in these chipsets on top of more regular CMOS ones²³⁰⁹. The chip vertical structure is relatively simple, with only a few metal layers, and some control electronics are usually placed in a separate chip that is bonded to the qubits in a 3D.

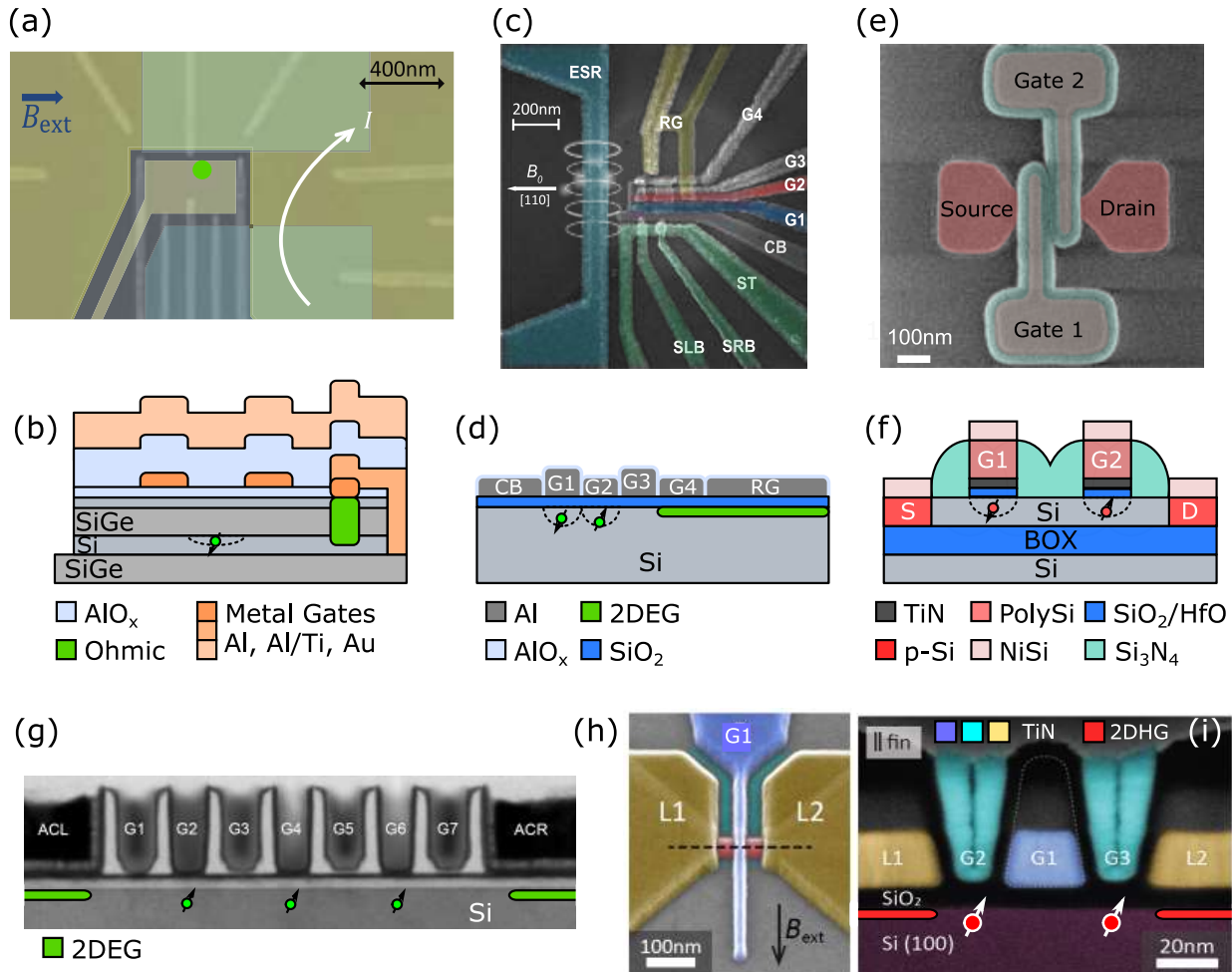


FIG. 1. Silicon QD devices. (a) Scanning electron microscope (SEM) image of an accumulation mode Si/SiGe heterostructure. Two layers of gates, bottom (light grey) and top (dark green) are designed to form two QDs (centre of image) and a single-electron transistor for readout (right). The structure contains a micromagnet in an upper metal layer (light green) to produce a magnetic field gradient. The green dot indicates the position of a QD used in ref. [16]. (b) Cross-sectional schematic of a Si/SiGe QD device. (c) SEM image of a metal-oxide-semiconductor multi QD device with QD gates (G1-4), confinement gate (CB), reservoir gate (RG), an integrated single-electron transistor (green) and microwave antenna for magnetic resonance spin control (blue) used in ref. [17]. (d) Cross-sectional view of the MOS QD device in (b). (e) SEM image of a CMOS p-type double QD on an etched silicon-on-insulator nanowire used in ref. [18] and schematic cross section (f). SEM (g) and TEM image (h) of a hole spin double QD device in a self-aligned double layer gate structure. L1(2) are 2 dimensional hole gas (2DHG) accumulation layers. G2, 3 are qubit control gates and G1 control the tunnel coupling [20].

Figure 568: various implementations of silicon spin qubits. Source: [Scaling silicon-based quantum computing using CMOS technology: State-of-the-art, Challenges and Perspectives](#) by M. F. Gonzalez-Zalba, Silvano de Franceschi, Edoardo Charbon, Maud Vinet, Tristan Meunier and Andrew S. Dzurak, November 2020-April 2023 (21 pages).

²³⁰⁹ See an example with [Strong hole-photon coupling in planar Ge: probing the charge degree and Wigner molecule states](#) by Franco De Palma et al, EPFL, October 2023 (22 pages).

In its various research papers published at APS March meeting in 2022, **Intel** did showcase how manufacturing quality had an impact on the quality of quantum dots spin qubits. In October 2022, they added some information on the quality and yield of their silicon qubits wafers²³¹⁰.

Tools

We'll cover here some specific manufacturing tools that are used for producing quantum technologies semiconductor components. The breadth of tools in semiconductor fabs is much broader with tools from vendors like **ASML** (UV and EUV photolithography) and **Applied Materials** (PVD, CVD, etching and stripping, ...). Their tools are used in high-volume large fabs while many of the quantum-specific production tools are used more for research purposes and for small scale industrial production.



Plassys Bestek (1987, France) develops and manufactures vacuum and ultra-high-vacuum thin film deposition systems with a turnover of about 7M€. Most of their tools are based on physical vapor deposition (PVD) processes (vaporization of metal or compounds for deposition on a substrate, all under vacuum).

Positioned at the end of the 1990s as a key supplier of equipment for the fabrication of superconducting qubits, they have developed a wide range of electron beam deposition systems dedicated to controlled angle evaporation under the name "MEB" which makes Plassys the leader for this technology (Yale University, Rigetti Computing, QCI, NTT, Oxford, CEA Saclay, Qilimanjaro, TU Delft, VTT... rely on their tools). The "MEB" tools used an electron beam to melt and to evaporate materials that allows the deposition of aluminum films for forming the Josephson junctions or for resonators as well as of niobium as underlayer or as resonators. They also provide sputtering tools for depositing various kind of superconducting films (Al, Ti, Nb, Ta, MoSi, MoGe, nitrides...) and other elemental materials or complex compounds. Sputtering tools integrate cathodes on which a bias voltage is applied under a controlled atmosphere of gas mixture including argon for generating a plasma around 10^{-3} – 10^{-2} mbar. Positive ions from the plasma are attracted by the cathodes on which a "target" is made from the material source you want to deposit. The high energy of the ions sputters the target inducing then the generation of a vapor that condensates onto the substrate.

They also supply the SDDR150 chemical vapor deposition (CVD) reactor for the growth of ultra-pure diamonds which is the raw material for the development of NV center based technologies. This CVD process is using hydrogen and methane (CH_4) at a pressure around 100 millibars²³¹¹ with the assistance of a microwave source generating a high density plasma. They also handle diamond doping with nitrogen, boron, phosphorus....



Figure 569: various production machines from Plassys-Bestek. Source: Plassys-Bestek.

²³¹⁰ See [Intel Hits Key Milestone in Quantum Chip Production Research](#), Intel, October 2022.

²³¹¹ The CVD diamond growth process is described in [Diamond growth by chemical vapour deposition](#) by J. J. Gracio et al, 2011 (75 pages).

Their R&D and production machines dedicated to quantum technologies are now grouped under the Qutek Series brand (Figure 569). In addition to the MEB systems, Qutek series includes MP systems (sputtering deposition for superconducting or photonic devices) and thermal evaporation system for indium bumps (used for connecting superconducting qubits).



Angstrom Engineering (1992, Canada) is a manufacturing tool vendor. Their Quantum Series line of physical vapor deposition (PVD) systems is adapted to the creation of Josephson Junctions, from using an electron beam source to deposit aluminum, magnetron sputtering for niobium and ion beam cleaning.



Kelvin Nanotechnology (2020, UK) is an electron beam lithography and nanofabrication tooling company. It manufactures various miniaturized MEMS and photonic components used in quantum technologies.

These include 3D ion traps, various photonic devices, MEMS gravimeters and lasers built on 200 mm wafers in features going as low as 20 nm. They are based at the James Watt Nanofabrication Centre (JWNC) in Glasgow, Scotland.



Orsay Physics (1989, France) is a subsidiary of **Tescan Orsay Holdings** (Czech Republic - France). It provides manufacturing tools for focused ion and electron beam processes.

Out of these, their nitrogen-FIB (i-FIB, for focused ion beam) is being used to create NV centers in nano- and micro-structures with high precision, like in NV center arrays with 2 μm separations between the centers²³¹².



Riber (1987, France) is a manufacturer of MBE reactors, used mostly in III/V and II/VI multi-layers epitaxy processes.

They handle various MBE processes: solid sources MBE, Plasma-Assisted MBE (PAMBE), Metal-Organic MBE (MOMBE), Gas Source MBE (GSMBE) and full gaseous Chemical Beam epitaxy (CBE). A Riber MBE reactor is being used to manufacture the 100+ layers quantum dots based photon sources from Quandela.



Raith (1980, Germany) provides nanofabrication and electron beam lithography instruments. These tools are involved in the manufacturing of all sorts of qubits, trapped ions, superconducting, electron spin, topological qubits, NV centers and nanophotonics.



Picosun Group (2003, Finland, 17.4M€) is a manufacturer of atomic layer deposition (ALD) tooling used in the production of various electronic components (imaging sensors, LEDs and OLEDs, MEMS, etc).

Their technology can be used to create graphene structures among other things. They are one of the Finish industry partners of **QuTI**, a 10M€ collaborative research project on quantum related components manufacturing and testing. They partner with VTT, Bluefors, Afore, IQM, Quantastica, Saab, Vexlum and the Finish offices from Rockley Photonics (USA) and CSC (USA).



Encapsulix (2011, France) develops ultra-short cycle time ALD systems. It is mostly used in the production of OLED in encapsulated quantum dots.



Samco Inc (Japan) is a provider of thin film deposition, microfabrication and surface cleaning, CVD and other treatment machines.

²³¹² See [i-FIB application note](#).

Their tooling includes PECVD systems (plasma-enhanced CVD), SiC CVD systems, ALD (atomic layer deposition) systems, reactive-ion etching (RIE) systems, Inductively Coupled Plasma (ICP) etching systems, Silicon Deep Reactive Ion Etching (DRIE) systems for MEMS device fabrication and TSV (through-silicon-vias) via-hole etching and plasma cleaners. These systems are used to produce various sorts of quantum components like niobium and tantalum based superconducting circuits, from qubits to surface acoustic waves filters^{2313 2314} and GaAs photonic components.



ADNANOTEK (Taiwan, 1999) is a provider of MBE, PLD (pulsed laser deposition which is a variation of PVD) and Laser MBE PLD, various sputtering systems, EBE (electron beam evaporators), Ion Beam Sputter Deposition (IBSD), ALD (atomic layer deposition), Plasma Enhanced Atomic Layer Deposition (PEALD) and various ultra-high vacuum equipment.



CVD Equipment Corporation (USA) is specialized in CVD and dry etching systems that can be used for various semiconductor production, including III/V and nanophotonic chips.



Plasma-Therm (USA) has a broad range of plasma and ion beam etching and deposition used among other things in GaAs components manufacturing.

The company made several acquisitions: Advanced Vacuum Europe of Lomma (1993, Sweden) in 2011, Nanoplas France in 2015, Nano Etch Systems (2009, USA) in 2016, Kobus and Corial (France) in 2018, JLS Designs Ltd (UK) in 2020. The company opened in 2018 its European Head Office in Grenoble, France, and in 2020, one process and technical support office in Singapore.



Izovac Photonics (Lithuania) provides the IZOVAC range of products vacuum coating equipment using vacuum sputtering (magnetron sputtering, Ion Beam Assisted Deposition, Ion beam sputtering, DLC (Diamond-Like Carbon) coating by PECVD (Plasma Enhanced Chemical Vapor Deposition). Their main market are the display and touch screen manufacturing. They also develop customized vacuum deposition equipment.



Evatec (Switzerland) provides a family of evaporation, sputtering and PECVD products covering various needs including in MEMS and photonics applications. They also develop and sell wafer cassette-to-cassette processing tools in their Clusterline family.



Prevac (Poland) has a breadth of semiconductors manufacturing tools including an UHV Magnetron Sputtering System working with 3-inches wafers and PLD systems. They also sell an UHV multichamber cluster tool to automate a process with a thin film layer growth deposition chamber, load-lock chambers and a transferring tunnel.



Seki Diamond Systems (Japan) is a subsidiary of **Cornes Technologies** (USA) that sells CVD diamond reactors producing synthetic diamonds and supporting Microwave Plasma CVD, Hot-Filament CVD and Low Temperature CVD. It covers broad industry use cases.



Polyteknik (2005, Denmark) provides PVD and coating systems, including their Flextura e-beam PVD system.

²³¹³ See [Towards practical quantum computers: transmon qubit with a lifetime approaching 0.5 milliseconds](#) by Chenlu Wang et al, NPJ, January 2022 (6 pages).

²³¹⁴ See [Niobium \(Nb\) Plasma Etching Process \(RIE or ICP-RIE\)](#), Samco.



Besi (1995, the Netherlands) or BE Semiconductor Industries, is the world-wide leader in semiconducting assembly machines (die attach, packaging, plating). One key use case is 3D chiplets assemblies. The company participates in the EU project MATQu to create a manufacturing capacity of superconducting chips on 300 mm silicon wafers.



Onnes Technologies (2018, the Netherlands) is a startup created by Max Kouwenhoven (CEO) that develops the arQtika Linear Cryo-Walker for Quantum Scanning Probe Microscopy (qSPM).

It is a low-dissipation cryogenic nanopositioner, that can be used to study the structure of protein complexes, such as ferritin, a protein in the human brain linked to Alzheimer's disease, with excellent precision and accuracy. It was developed in collaboration with Leiden Cryogenics. Their solution can also be used to characterize various aspects of transmon qubits.



SOITEC (1992, France) is a company producing SOI wafer which contain an isolation layer of SiO₂. These wafers are commonplace in many quantum technologies semiconductor components.

SOITEC acquired EpiGaN (2010, Belgium, 4M€) in 2019. It adds GaN wafers production to their portfolio.

Some other vendors can be mentioned like **RECIF Technologies** (France) with its wafers handling and sorters, **Heidelberg** (Germany) and its mask writer, **Süss MicroTec** (Germany) and its photomask handling and mask aligners, Keysight Technologies (and its NX5402A silicon photonics hybrid wafer testing system), **Oxford Instruments** (UK) and its RIE plasma etchers from the Plasmalab family and ALD systems, **Vistec** (USA) and **STS Elionix** (USA) and their e-beam writers, **Transene Company** (USA) and their etching systems, **Pureon** with its diamond based Chemical Mechanical Planarization tools (CMP)²³¹⁵, **Polygon Physics** (2013, France) which provides ion, electron, plasma and atom sources based on ultracompact and ultralow power electron cyclotron resonance plasma technology (ECR) and Multi Beam Sputtering tools (MBS), **JEOL** (Japan) and **Multibeam** (USA) and their e-beam lithography systems, **Thermo Fisher** (USA) and its e-beam lithography and ion milling systems, **Veeco** (USA) and its lithography, MBE, CVD, PVD, ion beams, ALD and dicing systems, **Aixtron** (1983, Germany) and its CVD systems, **NuFlare** (Japan) and its mask writers and epitaxial growth reactors, **AJA International** (1989, USA) and its thin film deposition systems including magnetron sputtering, e-beam evaporation, thermal evaporation, and ion milling systems and **Denton Vacuum** (1964, USA) and its evaporation, sputtering, PE-CVD and ion beam deposition tools.

EDA

The electronic design automation (EDA) software tools running on classical computers are unsung heroes of semiconductor advances²³¹⁶. They kept pace with the growth of chips complexity and come from Cadence, Synopsys and Siemens (formerly from Mentor Graphics) to name a few vendors, in a market that is being consolidated.

One famous tool to design and even test your 'home-made' superconducting chip is IBM Qiskit Metal, that was announced in 2021²³¹⁷. In February 2023, Amazon AWS introduced Palace (PARallel, LARge-scale Computational Electromagnetics), a finite element open-source code for full-wave electromagnetics simulations capable of simulating a single transmon qubit with its readout resonator coupling

²³¹⁵ In 2020, Microdiamant (Switzerland) acquired Eminess Technologies from Saint Gobain and was rebranded as Pureon.

²³¹⁶ This part comes from [Is there a Moore's law in quantum computing](#), Olivier Ezratty, March 2023 (32 pages). It was updated for this book.

²³¹⁷ See [Qiskit Metal documentation](#), IBM.

and a terminated coplanar waveguide (CPW) transmission line for input/output²³¹⁸. A similar tool, QuantumPro, was launched by Keysight in August 2023.

Cadence tools are used to design spin qubits and control electronics chips like with IQM²³¹⁹. Qubit designers usually assemble their own suite of multiscale EDA tools ranging from the physics of the qubits at low level to the whole behavior of chip circuits and, in between, for designing specific parts of these circuits like Josephson junctions, resonators²³²⁰ or couplers²³²¹ in the case of superconducting qubits, or, for example, of readout lines for quantum dots spin qubits²³²².

Tools frequently mentioned include Sonnet ABS (Adaptive Band Synthesis), Ansys HFSS 3D High Frequency Structure Simulation Software Multipurpose that helps the design and simulation of high-frequency electronics and Ansys RaptorQu which is used for electromagnetic simulations of superconducting qubit circuits.

Drawpy is a Python framework based on HFSS that creates circuits drawings. SPICE is an open-source software used to digitally simulate analog circuits. At a higher level, Synopsis Technology Computer-Aided Design (TCAD) helps design a whole circuit.

One challenge here is to create software suites able to implement digital twins of qubit chips in a full-stack manner, from the lower quantum physics level at the atomic scale up to all the circuitry and including various material defects and noise models. At the atomic scale level, we're up with using quantum physics digital simulations using DFTs and other classical methods, and, in the future, quantum algorithms. At the circuit level, simulations use various methods: Method of Moments (MoM) for planar and stacked planar structures, Finite Element Method (FEM) for 3D structures and Finite Difference Time Domain (FDTD) for handling large problems²³²³. At the highest abstraction level, circuit designers are using MBSE (Model-Based System Engineering) and ESL (Electronic System Design) methods as well as the SysML (System Modeling Language) for the creation of product specifications. Also, Automatic Test Pattern Generation (ATPG) tools are used to model circuit defects.

NANOACADEMIC
TECHNOLOGIES

NanoAcademic Technologies (2008, Canada) is a company created by Hong Guo from McGill University and Yu Zhu and Leil Liu (all coming from China) which sells quantum materials software simulation tools like NanoDCAL. It is used to simulate the physics of quantum chips like superconducting qubits. In 2023, it introduced QTCAD, its spin-qubit modeling tool.



QuantCAD (2021, USA) is a company created by Michael Flatté and based in Iowa that develops and sells CADtronics and qNoise, a suite of simulation software that models noise and current in quantum devices. It is used to design various quantum components, including quantum sensors and optoelectronic devices.

²³¹⁸ See [AWS releases open-source software Palace for cloud-based electromagnetics simulations of quantum computing hardware](#) by Sebastian Grimberg, Hugh Carson, and Andrew Keller, Amazon AWS, February 2023.

²³¹⁹ See [IQM Uses AWR to Make RF/Microwave Chips for Quantum Computers](#), Cadence.

²³²⁰ See [Fast analytic and numerical design of superconducting resonators in flip-chip architectures](#) by Hang-Xi Li, Jonas Bylander et al, VTT, May 2023 (12 pages).

²³²¹ See [Quantum Chip Design Automation in Superconducting Coupler Architecture](#) by Fei-Yu Li et al, Baidu Research, December 2022 (11 pages).

²³²² See [RF simulation platform of qubit control using FDSOI technology for quantum computing](#) by H. Jacquinet, Maud Vinet, Tristan Meunier et al, April 2023 (11 pages).

²³²³ See [Getting Started with EDA Tools for EM Simulation and Analysis](#) by Gary Breed, High Frequency Electronics, 2010 (2 pages).

Other enabling technologies vendors

These companies are developing physical components and enabling technologies that can play a role in building quantum computers.

More often, as this market remains limited to research, these startups are more generalist and target broader markets than quantum computing, covering physics research in general and even various industrial applications.



Aeponyx (2011, Canada, \$11.4M) is a fabless micro-optical switch semiconductor chips designer and manufacturer, specialized in Micro-Electro-Mechanical-Systems (MEMS) and silicon-nitride based silicon photonics.



Alter Technology (2006, Spain/Germany) is a subsidiary of the German group TÜV NORD specialized in micro and optoelectronics engineering for space and harsh environment applications.

It has labs in UK, France, Spain and Italy. They develop several quantum enabling technologies like frequency-stabilized lasers used to control cold atoms, an ion-trap chip carrier, entangled sources of photons for space based QKD, a squeezed light quantum MEMS gravimeter.



AuroraQ (2017, Canada) creates communication systems based on superconducting qubits, including quantum communication repeaters. It is complemented by the QSPICE Design software which allows the design of superconducting quantum circuits. In other words, this is an ultra-niche market²³²⁴.



DiamFab (2019, France) is a spin-off of Institut Néel in Grenoble specialized in the growth of doped diamond layers on a diamond wafer substrate.

Among other markets, they also target NV center use cases in quantum technologies. Diamond is also used as a high-performance semiconductor for power applications for diodes and field-effect transistors.

HiQuTe Diamond (2022, France) is a company created by Riadh Issaoui, Ovidiu Brinza, Fabien Bénédict, Alexandre Tallaire and Jocelyn Achard, who are researchers from LSPM in Paris, France (Laboratoire des sciences des procédés et des matériaux). They produce high quality diamond crystals used in quantum technologies.



Elementsix (1946, Luxembourg) is a subsidiary of De Beers Group, the world's leading diamond producer, which, among other things, manufactures synthetic diamonds for use in NV centers based systems, mostly used in quantum sensing.

They hold many patents in the related processes. In September 2021, they launched DNV-B14, a new chemical vapor deposition (CVD) made quantum-grade diamond with a uniform and x 10 higher density of NV spin centers.



Hummink (2020, France) developed a patented technology combining a nanometric “pen” with an oscillating macro-resonator to perform a capillary deposition of various liquids.

It can print conducting materials with an existing choice of 10 different materials. It can be used to add precision items on devices in 3D.

²³²⁴ See [The Geometry of a Quantum Circuit and its Impact on Electromagnetic Noise](#), 2018 (15 pages). QSPICE is a derivative from the SPICE open source project ("Simulation Program with Integrated Circuit Emphasis") used to digitally simulate analog circuits.



Labber Quantum (2016, USA) develops software solutions for controlling the qubits of experimental quantum computers with Python scripting handling electronics hardware control (AWGs, DACs, ADCs), data storage and visualization. They are used to calibrate qubits. The startup was acquired by **Keysight Technologies** in March 2020.



LakeDiamond (2015, Switzerland, €2M) produced synthetic diamonds used to create NV centers qubits in diamonds or with quantum sensing.

They use vacuum deposition with the CVD method (Chemical Vapor Deposition). The company closed in February 2020 after getting funding from an ICO in 2018 (Initial Coin Offering, using some crypto currency).



Lucigem (2016, Australia) manufactures fluorescent nano-diamonds that can be used in various quantum applications, particularly for medical imaging. The company is the result of work carried out at Macquarie University in Sydney.



Diatope (2021, Germany) creates diamonds with NV centers for quantum sensing and quantum computing applications. It is a spinoff from the Institute for Quantum Optics at Ulm University by Johannes Lang, Christoph Findler and Christian Osterkamp.

They produce NV centers using isotopically purified ^{12}C and do provide NV centers benchmarking services.

Qzabre (2018, Switzerland) creates NV center-based tips and probes to be used in scanning microscopes. They also sell a NV center microscope, the QSM. The startup was created by Christian Degen from ETH Zurich.



Adamas Nano (2010, USA) sells nanodiamond particles for various use cases including NV centers-based sensors. **Bikanta** (2013, USA, \$1.7M), **Cymaris Labs** (2004, USA) and **FND Biotech** (2016, Taiwan) sell fluorescent nanodiamond targeting medical imaging applications. **Diamond Materials** (2017, Germany) is a manufacturer of various variations of diamonds including NV centers. **Quantum Diamant** (Germany) also produces NV centers diamonds, for quantum sensing.

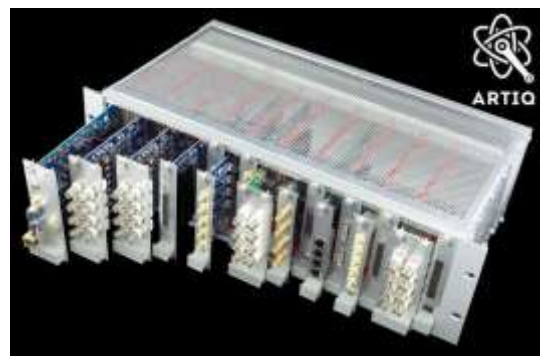
It is a spin-off from TUM (the Technical University of Munich). **Photonanometra** (2011, Russia) is another producer of diamond with NV-center defects.



M-Labs (2007, Hong Kong), formerly known as Milkymist, is working on the ARTIQ (Advanced Real-Time Infrastructure for Quantum physics) project.

This system combines hardware and a real-time operating system to control quantum computer hardware based on trapped ions. It is a bit like the trapped counterpart of startups such as the Israeli Quantum Machines. They have developed their own FPGA circuit for ARTIQ, all programmed in Python. The solution has been developed with the Ion Storage Group team at NIST in the USA, working on trapped ions qubits.

The company was founded by a French engineer, Sébastien Bourdeauducq.





Nano-Meta Technologies (2010, USA) is a spin-off from the University of Perdue that aims to create a quantum information storage system. It is in fact a private contract research laboratory.

It commercializes intellectual property on technologies associating photonics and nanomaterials that could be used in quantum cryptography systems.



ParTec (2001, Germany) is a supercomputer and quantum technologies integrator also involved in software tools development. It participates in the European HPCQS project to deploy and integrate two Pasqal quantum simulators and supercomputers.

It provides solutions to connect classical hardware to QPUs as part of the German project QSolid. It also developed with Quantum Machines QBRIDGE, to integrate HPC workflows and QPUs which will be deployed at the Israeli Quantum Computing Center (QCC) before the end of 2023. At last, the company is investing 5 M€ in the buildup of a production facility for the assembly and testing of cryogenic and non-cryogenic systems.



Photon Spot (2010, USA) develops nanowires based single photon detectors. They have received a DARPA funding of \$100K in 2014 and \$1.5M in 2015.



QBee.eu (2020, Belgium) is a sort of quantum accelerator or incubator created by Koen Bertels, who also leads the Quantum Computer Architectures Lab in TU Delft and also works at Qutech.

They run various research projects like defining a quantum micro-architecture for quantum accelerators using the OpenQL language from TU Delft, a quantum computing emulator, quantum genomics, quantum chemistry²³²⁵, and quantum finance plus some services in education and consulting.



Q-Lion (2019, Spain) develops an error correction code solution for trapped ion qubits. The startup is a spin-off from the Bank of Santander's Explorer incubation program. It was created by Andrea Rodriguez Blanco, who was still working on a thesis in 2020.

QuantTera (2005, USA) is a contract R&D company created by Matt Kim that develops nano-engineered photonic devices targeting photonic telecommunications and wireless applications. It is mainly using silicon-germanium based photonics. It says it targets quantum applications, with no details.



S-Fifteen Instruments (2017, Singapore) is a spin-off from CQT that develops qubit control systems, entangled photon sources, single photons detectors and quantum cryptography solutions covering QKD and QRNGs.



StarCryo Electronics (1999, USA) creates SQUIDs sensors used mostly in quantum sensing and other cryo-electronics products (cables, connectors, ...).

²³²⁵ See "[Toward Metal-Organic Framework Design by Quantum Computing](#)" by Kourosch Sayar Dogahe et al, September 2023 (10 pages).

Vapor Cell
Technologies



Vapor Cell Technologies (2020, USA) provides alkaline atom capsules, mainly rubidium, for use in various miniaturized solutions using cold atoms²³²⁶. The company was founded by Doug Bopp, a former NIST researcher from Boulder, Colorado.

Zyvex Labs (1997, USA) develops atomic precise manufacturing (APM) solutions based on STM (Scanning Tunneling Microscopy) that can be used to produce components for use in quantum computing (such as the deposition of dopants for superconducting qubits and silicon) and quantum metrology.

They were funded by NIST, DARPA and the Department of Energy SBIR research programs. The company was founded by Jim Von Ehr. Zyvex announced in September 2022 a sub-nm version of its STM solution, the ZyvexLitho1.

Raw materials

For any new hardware technology, it is now a common practice to wonder about its environmental friendliness. We've already been dealing with the energetic dimension of quantum computing. Another key aspect to investigate is the raw materials that are used. What are their sources of supply, their global reserves, their economic and environmental cost of extraction, consumable raw materials if any, and finally, the recycling processes of these materials?

In this exclusive content, I propose a first broad inventory of the different raw materials used in and around quantum technologies of all types, particularly in quantum computers. All these elements are positioned in an in-house Mendeleev periodic table of elements, Figure 570²³²⁷.

We mainly have two types of materials to study: those used in qubits and the supplemental materials, particularly for cables and other supporting structures as well as the gases used in cryostats, mostly helium 3 and 4.

The materials used in qubits are sometimes quite rare (strontium, ytterbium, beryllium). Their selection is based on their energy transitions which correspond to laser or microwave wavelengths that can be used practically with market sources.

Other constraints explain their choice such as the stability of some of these energy levels. Some materials are very rare but their needs in quantum technologies remain marginal in proportion to their production and world consumption. This is at least the case if millions of quantum computers using them are not manufactured. We are not yet at the stage where the consumption of certain elements would come mostly from quantum technologies, as may be the case for smartphones concerning certain rare earths and minerals such as the famous coltan²³²⁸.

How about rare earth elements? Out of the 17 elements in that category who mainly sit in the lanthanum row in Mendeleev's elements table, about 6 of them are used in quantum technologies: yttrium, praseodymium, dysprosium, europium, erbium and ytterbium, the two later being commonplace in trapped ions computing.

²³²⁶ See [Chip-scale atomic devices](#) by John Kitching, 2018 (39 pages) which makes a very interesting inventory of measurement components using this technology: magnetometers, gyroscopes, atomic clocks. You will say that this should go in the metrology section and you will be right.

²³²⁷ See also this very nice illustrated poster: [The Periodic Table of the Elements](#), in Pictures.

²³²⁸ The coltan is the contraction of columbite-tantalite. It is used to recover tantalum and niobium. If it is an important source for tantalum, it is in fact secondary for niobium compared to other minerals. See USGS [Mineral Commodity Summaries 2020](#), the equivalent of the French BRGM (204 pages) that helped me create this part.

elements used in quantum technologies

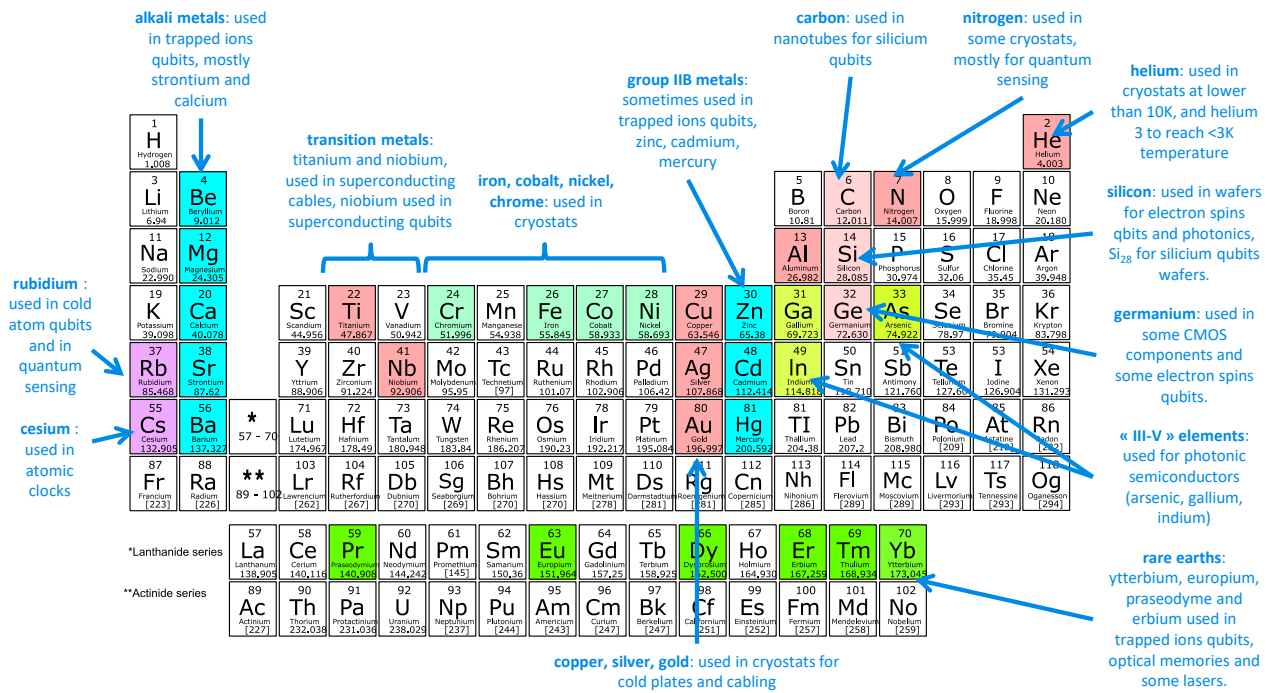


Figure 570: table of elements and those which are used in quantum technologies. (cc) Olivier Ezratty, 2021-2023.

In July 2022, Turkey announced the discovery of large reserves of rare earths minerals potentially exceeding China’s reserves. But the announcement was probably overstated, preprocessed minerals getting out of mines and rare earth oxides produced after separation²³²⁹.

One differentiating aspect of quantum technologies relates to the isotopes used which are sometimes the rarest of their elements. This is the case for helium (3) used in cryogenics below 4K or for cesium (133) for atomic clocks or rubidium (87) in cold atoms. Silicon (28) is used in silicon qubits and, although it is the most abundant isotope, requires costly refining. Carbon (12) is also used in nanotubes like with the startup C12 Quantum Electronics, while Carbon 13 is used in some NV center structures. Some of these isotopes are purified with centrifugal separation, a technique well known in nuclear physics, both civil and military.

I do not mention in this inventory the materials used in the production of semiconductors, such as fluorine and other various solvents. And there are many of these!

We will also not deal with the recycling of quantum computers, an issue that has not yet arisen due to their current very limited number. However, it can be reduced to the more generic issue of recycling various electronic devices.

Helium

Helium is a great paradox in the table of elements. It is the second most abundant element in the Universe after hydrogen. Nuclear fusion does the rest to create all the other elements in first- and second-generation stars. Yet, this element is quite rare on Earth and its reserves are dwindling. It is a noble, inert gas that does not interact chemically with any other element because its electron layer is complete with two electrons. Lighter than air, it tends to leave the atmosphere. As we have seen in detail in the cryostats section, starting page 563, helium is used for cooling superconductors and electron spins qubits systems.

²³²⁹ See [Turkey Discovers 694 million mt of Rare Earth Element Reserves, with Infrastructure Construction Starting This Year](#), July 2022 and [Turkey Probably Hasn’t Found the Rare Earth Metals It Says It Has](#) by Chris Baraniuk, Wired, July 2022.

As soon as one needs to go below 1K, one must use a mixture of two helium isotopes, ^4He which is the most common and stable (with two neutrons) and ^3He which is much rarer (with only one neutron). For cryogenics above 1K, ^4He is sufficient.

For at least a decade, many specialists have been concerned about a shortage of ^4He supply. It is commonly used for cooling superconducting magnets in particle accelerators such as the CERN LHC and in MRI scanners or to inflate balloons. It is also used as a neutral gas for the production of semi-conductors. Fortunately, new sources of natural gas from which ^4He can be extracted have emerged, notably in Tanzania and Qatar²³³⁰.

But a low annual growth in demand of just 1.6% is too high compared to production forecasts. Air Liquide is one of the major players in this global market, operating a large ^4He extraction and production unit in Qatar, linked to their gas operations. It seems however than the shortage is temporarily gone²³³¹.

The ^3He isotope is rather rare, therefore quite expensive! It was historically a by-product of the storage of tritium-based H-bombs. Tritium gradually disintegrated to produce ^3He as shown in Figure 571. It was therefore recovered from H-bomb stockpiles! It could also be produced in some nuclear fusion plants... when it works someday.

With the reductions in nuclear weapons stockpiles, the production of ^3He is now coming from specialized nuclear power plants. Tritium can be produced with irradiating lithium or with tritium-controlled decay in specialized nuclear facilities, such as those controlled by the US Department of Energy. Tritium is an isotope of hydrogen with one proton and two neutrons.

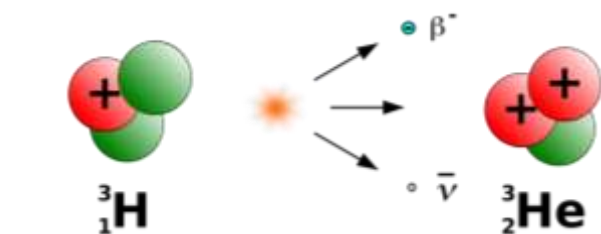


Figure 571: Helium 3 is a by-product of tritium, an isotope of hydrogen with two neutrons.

^3He is produced at the U.S. Department of Energy's Savannah site in South Carolina (Figure 573) and at the Canadian CANDU power plant²³³².



 <p>helium 4 2 protons 2 neutrons relatively abundant</p>	 <p>helium 3 2 protons 1 neutron rare</p>
<p>\$5-\$20 per liter of gas >100L per computer</p>	<p>\$1500 to \$2000 per liter of gas >\$10K helium 3 per computer</p>

Figure 572: price tags for helium 3 and 4... as gas!

The price of ^4He gas is around €20 per liter while the price of ^3He gas is between €2K and €3K per gas liter (Figure 572).

A typical dilution-based cryostat requires 15 to 18 liters of ^3He gas for a little over 100 liters of ^4He gas! The gases are purchased separately and mixed at the right dosage by the manufacturer of the dry cryostat.



Figure 573: Savannah River Site is one of the few places where helium 3 is produced in the world.

At the end, it is therefore necessary to pay at least 30 to 40K€ of ^3He and ^4He per dry cryostat.

The ^4He which feeds the pulsed head and passes through the large compressor must be highly purified.

²³³⁰ See [Helium - Macro View Update](#), Edison Investment Research, February 2019 (21 pages).

²³³¹ See [Helium shortage has ended, at least for now](#), June 2020.

²³³² See [Savannah River Tritium Enterprise](#) (4 pages). Helium-3 is also exploited in various specialized applications: in neutron detectors used in security systems, in oil exploration, in medical imaging and in nuclear fusion research. Also see [CANDU Reactor](#), Wikipedia.

France has some ^3He production capacities located in a CEA nuclear reactor in Grenoble. But it does not necessarily use them for quantum computers because this production is too expensive²³³³.

We can also find ^3He on the surface of the Moon but it is not very practical to extract it and ship it back to Earth even if it is technologically possible²³³⁴! This isotope could be interesting to feed nuclear fusion reactions, pending its complicated technological development.

^3He is therefore a real bottleneck in the production of superconducting and electron spin quantum computers! It cannot even be avoided for the latter, which requires a temperature of about 1K²³³⁵.

Silicon

Silicon is the key element in many semiconductor components used in or around quantum processors. While being the second most abundant element in the Earth's crust after oxygen, the silicon used in semiconductors comes from a few quartz mines. This is because quartz is composed of at least 97% silicon, which is easier to refine. After chemical-based refinement, silicon is turned into large cylindrical ingots which are then sliced into thin wafers. Wafers are then processed in semiconductor fabs with transistors that combine silicon oxide and different doping materials such as hafnium.

Silicon qubits require using ^{28}Si , because the null spin of its nucleus does not interfere with the spin of the trapped electrons used as the qubit observable. The silicon wafers on which the qubits are etched are covered with a thin layer of ^{28}Si . ^{28}Si is the most abundant variant of the element while ^{29}Si represents less than 4%.

^{28}Si made headlines in 2010 when some German researchers created a perfect crystal ball made of ^{28}Si to accurately determine the Avogadro number, which determines the number of elements, here atoms, in a mole²³³⁶. The tests were carried out on a 5 kg sample at a cost of 1M€ In 2014, an American team improved the purity of ^{28}Si to 99.9998% with pumping silicon ions in a magnetic field, allowing it to be separated by mass²³³⁷.

This continued in 2017 with 99.999%²³³⁸ ^{28}Si produced by a team of Russian and German researchers. The interest of ^{28}Si was to allow a precise counting of the number of silicon atoms in the mass considered, because of its perfect crystal structure, dimensioned by X-ray interferometry. The Avogadro number determined by the 2010 experiment was $N_A = 6.022\,140\,84(18) \times 10^{23}$. The ambition of these two projects was to create a new material standard of the kilogram, the 1889 material standard preserved in France that degrades by oxidation.

²³³³ See [Isotope Development & Production for Research and Applications \(IDPRA\). Supply and Demand of Helium-3](#), 2016, [Responding to The U.S. Research Community's Liquid Helium Crisis](#), 2016 (29 pages) and [How helium shortages will impact quantum computer research](#) by James Sanders, April 2019.

²³³⁴ See [There's Helium in Them Thar Craters!](#). China is planning to harvest Helium 3 on the Moon.

²³³⁵ Helium-4 is used to cool superconducting magnets in MRI systems. It is also used to cool the magnets of the LHC at CERN. The constraints are different: it is just a matter of obtaining superconductivity for the magnets that focus the particle beams. The required temperature is between 1.8K and 4.5K, much "hotter" than the 15 mK of electron-based quantum processors (superconductors, silicon, NV Centers, Majorana fermions). On the other hand, the volumes to be cryogenized are much larger. In some cases, however, the required temperature can fall below 1K, particularly for the search for dark matter. In CERN's LHC, 9 Tesla magnets are cooled to 1.8K with 18 kW cryostats that handle 120 tons of helium 4.

²³³⁶ See [An accurate determination of the Avogadro constant by counting the atoms in a \$^{28}\text{Si}\$ crystal](#) by B. Andreas, 2010 (4 pages). Silicon 28 was obtained by centrifuging silicon fluoride (SiF_4) gas, then transformed into SiH_4 which was then used to create the crystal by vacuum deposition of purified silicon. All this was carried out in different laboratories in Russia, in Nizhny-Novgorod and Saint Petersburg. The researchers involved also came from Italy, Australia, Japan, Switzerland and BIPM in France, from their respective weights and measures offices.

²³³⁷ See [Purer-than-pure silicon solves problem for quantum tech](#) by Jonathan Webb, 2014 which refers to [Enriching \$^{28}\text{Si}\$ beyond 99.9998% for semiconductor quantum computing](#) by K J Dwyer et al, 2014 (7 pages).

²³³⁸ See [A new generation of 99.999% enriched \$^{28}\text{Si}\$ single crystals for the determination of Avogadro's constant](#) by N V Abrosimov et al, 2017 (12 pages) which describes very well the process of purification of ^{28}Si , the source of the illustration on this page.

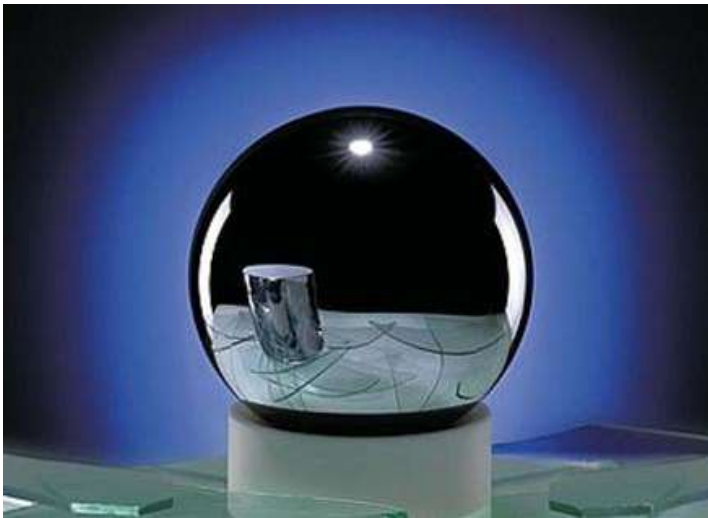


Figure 574: silicon 28 was initially produced to create a replacement for the reference kilogram used in the international metric system, as a way to determine the Avogadro number. Purifying silicon 28 was a figure of merit of this quest that is now reused in the silicon spin realm.

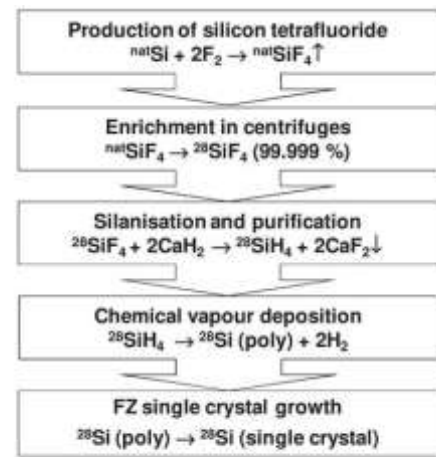


Figure 4. Main technological steps of the ²⁸Si crystal production (^{nat}Si: silicon of natural isotopic composition).

Finally, in 2018, the Avogadro number was redefined in the international measurement system as a slightly different constant of $6.022\,140\,76 \times 10^{23} \text{ mol}^{-1}$. Indirectly, however, these two experiments did advance the know-how of ²⁸Si purification, at a time when its interest in creating silicon qubits was barely in the radar. What a good illustration of serendipity in science!

The silicon purification process is complex. It involves the production of silicon tetrafluoride (SiF₄) of all isotopes. Enrichment in ²⁸Si is carried out in a centrifuge, originally at the Central Design Bureau of Machine Building in St. Petersburg, in fact, a former plutonium enrichment plant reassigned for this use in 2004.

The gas is transformed into silane (²⁸SiH₄) at the **Institute of Chemistry of High-Purity Substances** of the Russian Academy of Sciences in Nizhny-Novgorod. It can then be deposited by vapor deposition (CVD) on silicon, releasing hydrogen. The resulting ingot can then be stretched to create a perfectly crystalline silicon ready to be sliced into wafers. CEA-Leti researchers are also working with Russian teams at Nizhny-Novgorod on the process for vacuum deposition of ²⁸Si on 300 mm wafers²³³⁹. In October 2021, **Orano** announced its ambition to produce ²⁸Si in France, to start in 2023. Likewise, **Silex Systems** (Australia) got an AUS \$5.1M funding from the Australian government in 2023 to also produce ²⁸Si (in the form of silane) using a new laser enrichment technique that could reach a ~99.998% purity.

Air Liquide is also partnering with the Nizhny-Novgorod laboratory for this process of CVD (chemical vapor deposition) of ²⁸Si on a 30 to 60 nm thin film that is 99.992% pure²³⁴⁰ above a conventional silicon wafer. Knowing that Air Liquide also masters the conversion of SiF₄ into silane.

Germanium

Germanium is a semiconductor metalloid that is part of the III-V family. It is used in many fields: in photonics, in SiGe heterojunction bipolar transistors which are used for the amplification of weak microwave signals as well as in electron spin qubits chips.

²³³⁹ See [99.992% 28Si CVD-grown epilayer on 300 mm substrates for large scale integration of silicon spin qubits](#) by V. Mazzocchi of CEA-Leti and colleagues from France and Russia, 2018 (7 pages).

²³⁴⁰ See [Quantum computing: progress toward silicon-28](#), April 2018.

With spin qubits, it must be isotopically purified to generate ^{73}Ge which corresponds to 7.36% of its proportion (in purple in the chart *opposite*). It is a stable, natural and non-radioactive isotope. Germanium is generally extracted from zinc ores and also from zinc-copper ores. In 2019, 130 tons of germanium were produced, with China being the main supplier with 85 tons²³⁴¹. Data on known reserves are variable and are estimated at approximately 9,000 tons, mainly located in China, Canada and the USA. Along with gallium and indium, which are also III-V materials, germanium is considered a critical resource. Isotopic purification of germanium is carried out by the same Russian teams at Nizhnii Novgorod as those producing ^{28}Si , ^{74}Ge being of particular interest (Figure 575).



Figure 575: Germanium natural isotopes distribution.

It uses a germanium tetrafluoride centrifugation process like the one used to produce germanium tetrafluoride and explained in Figure 574²³⁴².

Rubidium

Rubidium is an alkali metal used to create cold atom qubits that are excited into highly energetic Rydberg states.

It is also used in quantum sensing, notably to create atomic clocks and micro-gravimeters. It is an alkaline, soft, silvery metal with a melting temperature of only 39.3°C (in Figure 576). In a neutral atom computer, the metal is used very sparingly. It is supplied in ampoules of a few solid grams.

It is heated in a small box to be sublimated into gas which then feeds the vacuum chamber where the lasers will trap individual atoms. The metal costs about \$85 per gram and about \$1,600 per 100g. It is readily available from chemical companies. Only 5 tons are produced annually worldwide, including China, Canada, Namibia and Zimbabwe²³⁴³. It is a by-product of the extraction of cesium and lithium. The isotope ^{87}Rb is the most used and represents 27.8% of available rubidium. It is radioactive but with a half-life longer than the age of the Universe, so it is very stable. World reserves are estimated at 100,000 tons, which is enough to keep up with the current rate of production and consumption.



Figure 576: rubidium in molten state. , in molten state. Source [Wikipedia](#).

Niobium

Niobium is a transition metal used in superconducting qubits as well as in microwave cables driving superconducting and electron spin qubits. **Coax Co** (Japan) has a monopoly in the manufacturing of these cable, which are very expensive, about \$3K per half a meter segment. And three are needed per superconducting qubits, positioned between the 4K and 15mK cryostat cold plates.

In industry, it is used in the production of high-strength special steels, in superconducting magnets, in particle accelerators, in arc welding, in bone prostheses associated with titanium, in optics, as a catalyst for rubber synthesis, in aircraft engines and in gas turbines.

²³⁴¹ See [Refinery production of germanium worldwide in 2021](#), by country, Statista.

²³⁴² See [Production of germanium stable isotopes single crystals](#) by Mihail Fedorovich Churbanov et al, April 2017 (6 pages).

²³⁴³ Each human weighing 70 kg contains about 0.36g of it. However, we are not going to create a variant of Soylent Green to exploit it. Rubidium mining in Canada is carried out by Tantalum Mining Corporation, which belongs to the Chinese group Sinomine Resources since June 2019.

World production was estimated at 68,000 tons per year in 2018, with Brazil accounting for 88%, followed by Canada for just over 9%, generated by a single mine. It comes from the exploitation of pyrochlore, an ore combining calcium, sodium, oxygen and niobium (Figure 577).

It is not very expensive and is priced at \$45 per kilogram, but in its ferro-niobium form. The reserves are 9 million tons, enough to last 130 years at the current usage rate. But in practice, niobium is considered a "risky" resource because its demand is growing rapidly even though it comes from relatively safe geopolitical places.



Figure 577: niobium is a relatively cheap metal.

Ytterbium

Ytterbium is a rare earth of the lanthanide series, which is used in trapped ions qubits, quantum memories, atomic clocks, doping of certain lasers and, more rarely, in cold atom qubits (Figure 578).

Otherwise, it is used to reinforce certain specialized steels.

The metal is extracted from monazite, a tetrahedral crystalline rock structure of phosphorus oxide associated with various rare earths, which contains only 0.03% of it. Production follows a complex cycle using sulfuric acid and ions exchange. Quantum applications use isotope 171, one of the 7 non-radioactive isotopes of the element. It represents 14% of its proportion in the rocks from which it is extracted. This isotope is probably more expensive than the regular multi-isotope version which is sold between \$500 and \$1K per kilogram.

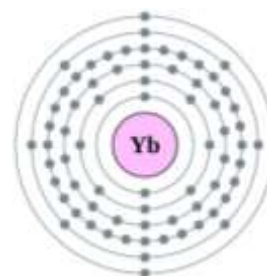


Figure 578: ytterbium atomic structure.

Approximately 50 tons are produced annually, mainly in China, the USA, Brazil, India and Australia, with reserves estimated at one million tons. Creating trapped ions computers require about one gram per quantum processor.

Erbium

This rare earth of the lanthanide family is used in quantum memories, in some fancy cold atom qubits and in certain lasers (Er:YLF type for yttrium lithium fluoride or Er:YAG type for yttrium aluminum oxide). It is found in some optical fibers used in optical amplifiers (Figure 579).

Finally, it can be used to create vanadium alloys found in cryostats thanks to its high thermal mass heat absorption capacity. China is the main producer, followed by the USA. It comes from extracting xenotime (phosphate ore) and euxenite (an ore also containing niobium, titanium and yttrium). The ore is processed with hydrochloric or sulfuric acid and then neutralized with soda ash. After a bunch of chemical treatments, erbium ions are extracted by ion exchange on polymer resins.



Figure 579: erbium.

Erbium is then obtained by heating its oxide with calcium at 1,450°C in a neutral argon atmosphere. All this is a long and expensive chemical process, probably polluting of lot but carried out on small volumes. Erbium is produced at a rate of about 500 tons per year. Its price per gram is about \$20, which is quite affordable to integrate it in memories or cold atoms qubits.

Strontium

Strontium is the most common alkali metal used to create trapped ions qubits, with its isotope 87, representing 7% of its five isotopes. It is used as a red dye in fireworks.

Mexico and Germany are the main producers, with an estimated world production of 220,000 tons per year and reserves of over one billion tons. It is notably used in bones anti-cancer radioactive chemotherapies.

Strontium is considered to be toxic. This is the case of all these rare metals which, being pure, oxidize quickly whatever happens. In particular, it explodes when being in contact with water.

Gold

In quantum technologies, gold is mainly used as a thin layer covering the copper plates of the cold plates in cryostats. It prevents copper oxidation and adds good thermal conductivity. The volume used is quite small in relation to gold production and global reserves. About 3000T of gold are produced every year worldwide.

Titanium

Titanium is mainly used in association with niobium in superconducting microwave cables.

In industry, it is used for its resistance to corrosion, particularly in the aerospace industry. Some submarines have an all-titanium hull. Titanium oxide is used as a painting white pigment. It is found in great quantities on Earth since it is the fifth most abundant metal. But only a few ores contain a high enough concentration of it to make its production profitable. The main producing countries are Australia, South Africa, Canada and Norway at a rate of 4.2 million tons per year. Reserves are in excess of 600 million tons.

Nitrogen

Liquid nitrogen is used in cryostats to clean the gaseous helium that feeds them. It is also found in small quantities in NV Centers crystals. It is not a rare commodity. But its production in liquid form is quite energy consuming.

Other materials

Many other relatively common materials are used in quantum technologies.

Copper is found in cryostat cold plates and with some of the various electrical connectors. It is purified at 99.99% to become free of impurities and oxygen (OFHC for oxygen-free high conductivity), in order to improve its thermal conductivity and electrical conductance. It is also widely used in trapped ions chambers. As far as its depletion is concerned, its consumption in quantum technologies is minor.

Carbon is exploited in a variety of places, including with carbon nanotubes from C12 Quantum Electronics. This carbon must be purified to keep only its isotope ^{12}C is acquired in the form of methane in bottles acquired in the USA for \$10K. It is 99.997% purified. The isotopic separation of ^{12}C uses a chemical process applied to CO_2 . Carbon is also used in NV centers.

Aluminum²³⁴⁴ is used in some superconducting qubits as well as for part of the connector technology in cryostats. It is abundant.

Manganese is used in very small quantities as a dopant in some superconducting qubits and can be used with trapped ions qubits.

Silver is mainly used in powder form in some heat exchangers in dilution refrigeration systems.

Iron is a commodity used in the form of steel in the structure of quantum computers.

²³⁴⁴ The spelling is aluminum in American and Canadian English and aluminium elsewhere. This document is mostly in American English.

Rhenium and **tantalum** are used in some superconducting qubits.

Cesium is mainly used in atomic clocks, in its isotope 133. Reserves are sufficiently abundant in relation to identified needs. They are mainly located in Canada.

In addition to germanium, **gallium** and **indium** play a key role in III-V components used mainly in photonics and **Neodymium** is used in lasers. This is one of the few areas of quantum technologies where there is a strong dependence on China as a source of supply. Finally, **beryllium**, **calcium**, **zinc**, **cadmium** and **mercury** can be used in trapped ion qubits, but the most commonly used are ytterbium, barium and calcium.

Element	Quantum computing	Quantum sensing and others	Main country sources	Rarity	Cleanliness
Helium 3	Cryostats		USA, Canada		
Helium 4	Cryostats	Cryostats	Qatar		
Silicon 28	Silicon Qubits		Russia, France		
Rubidium	Cold Atoms	Cold Atoms	China, Canada, Namibia and Zimbabwe		
Niobium	Cables, supra qubits		Brazil, Canada		
Ytterbium	Trapped ions, memory		China, USA, Brazil, India and Australia		
Europium	Memories	Repeaters	Mongolia, China, Russia		
Erbium	Cold atoms, memory		China		
Barium	Trapped ions		UK, Romania, Russia		
Strontium	Trapped ions		Mexico, Germany		
Neodymium	Lasers	Lasers	China, United States, Brazil, India, Sri Lanka, Australia		
Gold	Cold plates		Peru, Mexico, Indonesia		
Titanium	Cables		Australia, South Africa, Canada, Norway		
Gallium		Photonics	China, Germany, Kazakhstan, Ukraine		
Germanium		Photonics	China, Canada, Finland, Russia, USA		
Indium		Photonics	China, Belgium, Canada, Japan, Peru, South Korea.		
Nitrogen	Cryostats	NV Centers			
Aluminum	Cryostats, supra qubits		China, India, Russia, Canada		
Silver	Cryostats		Mexico, China, Peru, Chile, Poland		
Caesium		Clocks	Canada, Zimbabwe, Namibia		
Carbon	NV Centers, nanotubes	NV Centers			

Figure 580: table with elements used in quantum technologies with their country or origin, rarity and environmental footprint. Consolidation (cc) Olivier Ezratty. 2022.

Figure 580 features a table with a summary of this part with a list of materials, their main usage in quantum technologies, their main countries of production, rarity, and production cleanliness.

Quantum enabling technologies key takeaways

- Quantum enabling technologies covers a broad field with cryogenics, electronics, lasers, photon sources and detectors, semiconductor manufacturing techniques and even specific materials production. They are strategic to enabling future quantum systems, particularly scalable quantum computers. From a business standpoint, they are the equivalent of shovels in the gold rush. Many of these technologies have use cases beyond quantum technologies.
- Cryogeny is a key quantum computing enabling technology particularly for solid-state qubits which work at temperatures between 15 mK and 1K. These systems rely on a mix of helium 3 and 4 in so-called dry-dilution refrigeration systems. Other simpler cooling technologies target the 3K to 10K temperature ranges and are used with photon sources and detectors for photon qubits systems as well as with trapped ions and cold atoms setups.
- Cabling and filters play another key role, particularly with solid-state qubits. Superconducting cables are expensive with 3K€ per meter and come from a single vendor source from Japan. Signals multiplexing may be on the way.
- Microwave generation and readout systems used with superconducting and quantum dots electron spin qubits are other key enabling technologies. The challenge is to miniaturize it and lower their power consumption and, if that makes sense, to put them as close as possible to the qubits, operate them at cryogenic temperatures and simplify system cabling. It is a key to physical qubits scalability, particularly to implement quantum error correction. A lot of different technologies compete here, mostly around cryo-CMOS and superconducting electronics. Other components deserve attention like circulators and parametric amplifiers that we cover in detail in this new edition. Lastly, error correction requires extensive classical processing that is frequently forgotten in the resource estimations of fault-tolerant quantum computing.
- Many lasers and photonics equipment are used with cold atoms, trapped ions, and photon qubits and also quantum telecommunications, cryptography and sensing. It includes single indistinguishable photon sources as well as single photon detectors. The lasers field is also very diverse with products covering different ranges of wavelengths, power, continuous vs pulsed lasers, etc.
- Manufacturing electronic components for quantum technologies is a strategic topic covered extensively in this book with a description of generic fab techniques and some that are specific to quantum technologies like with the fabrication of superconducting qubits and quantum dots.
- Quantum technologies use a lot of various raw materials, some being rare but used in very small quantities. While some materials may have some incurred environmental costs, most of them do not seem to be scarce and they have multiple sources around the planet. The next challenge will be to analyze full product lifecycle costs and reduce the overall environmental footprint of emerging quantum technology, particularly for those who may be used in volume.

Unconventional computing

This part consolidates a set of technologies and companies that propose to significantly increase the power of computing machines while not relying on quantum technologies.

Quantum computing belongs to the broad **unconventional computing** field like digital annealing, reversible and adiabatic classical computing, superconducting computing, analog computing, probabilistic computing, photonics computing and chemical computing²³⁴⁵. The category is quite broad since it also includes nanomagnets (energy efficient, non-volatile, used with neural networks), spintronic and memristors (for neural networks and spiking neurons), magnetic excitations (spin wave, skyrmions), in-memory processing, dynamical systems (Ising machines) and brain inspired computing^{2346 2347}.

Many of these avenues have been explored by major players such as IBM for superconducting computing or by startups and with ups and downs. Some, such as MemComputing and InfinityQ, go so far as to tout exponential computing accelerations versus traditional architectures while being based on classical CMOS components and to the point of asserting a capability to solve exponential (NP) problems in polynomial time.

Unconventional computing paradigms differ in one way or another from Turing's machine-based technologies and Von Neumann's architecture based on control units, computing, registers and memory that are the basis of today's classic computers. A bit like quantum computing, their benefit compared to classical computing could be about bringing some speedup but not only. It can also deal with system energetic footprint or with the ability to solve specific types of problems.

It is particularly true with **natural computing** solutions that use physical elements from nature or are inspired by nature as shown in Figure 581. This includes computers based on biological components like DNA, probabilistic computers, chemical computers, membrane computers, as well as spintronics and neuromorphic processors that are adapted to artificial intelligence processing²³⁴⁸. I won't cover them all since they are not necessarily relevant to bring some computing speedup vs classical computing.

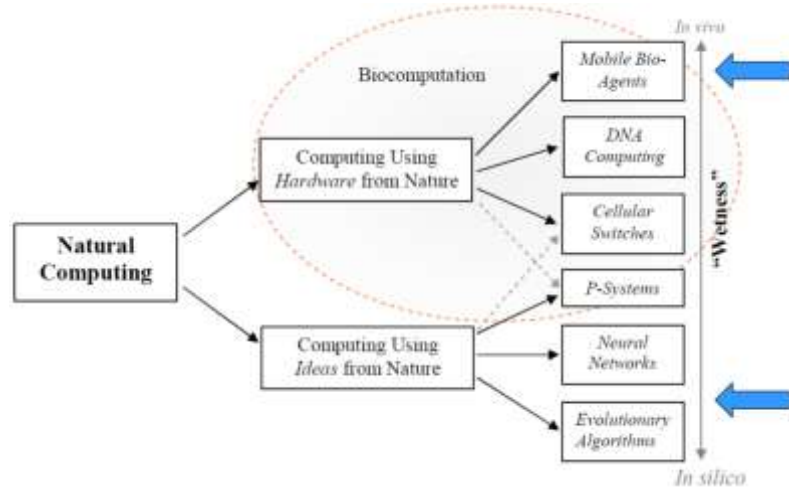


Figure 581: how biomimetics is used in computing. Source: [Unconventional Computing: computation with networks biosimulation, and biological algorithms](#) by Dan Nicolau, McGill University, 2019 (52 slides).

²³⁴⁵ I don't cover analog computing which seems entirely out of fashion. See [Analog Computers](#) by Francis Massen (80 slides).

²³⁴⁶ See [Roadmap for Unconventional Computing with Nanotechnology](#) by Giovanni Finocchio et al, January 2023 (88 pages) which inventories many unconventional computing categories

²³⁴⁷ See [Unconventional Computation Including Quantum Computation](#) by Bruce MacLennan, University of Tennessee, 2022 (308 pages).

²³⁴⁸ See [Unconventional Computation](#) by Bruce MacLennan, University of Tennessee, who is a reference in the field, October 2019 (306 pages) and [Unconventional Computing](#) by Andrew Adamatzky et al, Springer, 2018 (698 pages).

For many of the domains in unconventional computing, you'll find a couple startups and even large established companies trying to create viable products, based on various levels of fundamental research TRL (technology readiness level). But, after nearly 60 consecutive years of CMOS-based Moore's law expanding the scope of classical computing, none of these paths got traction.

What are they missing? It depends. First, it may not work at all. Then, it may operate at small scale but not beyond, when it could exceed to performances of classical computers. Then, it may cover very narrow use cases, making it difficult to find a market. Also, it may have a hard time competing with the progress of classical computing both in the hardware and software realms.

It can also be economical, with not enough funding fueling the domain. At last, these technologies have a very small ecosystem of scientists, vendors and users. It makes it hard to evaluate.

Analog computing was a good example of failure, with some work done between the 1950s and the 1970s. It was abandoned in favor of digital electronic systems due to their better flexibility and absence of noise. It could be revived thanks to bringing some energetic advantage²³⁴⁹. For some respect, quantum computing is a return of the analog computing paradigms.

Superconducting classical computing could be useful to allow quantum computers to "scale". We can therefore also evaluate these different technologies from the point of view of their complementarity, rather than competition, with quantum computing.

Supercomputing and HPCs

The so-called "quantum supremacy" announced by Google in October 2019 systematically referred to power comparisons with supercomputers, in particular with the **IBM Summit** installed at the Oak Ridge laboratory of the US Department of Energy since 2018²³⁵⁰. This kind of supercomputer falls within the field of "High Performance Computing" (HPC), which we will study briefly here to put it into perspective in relation to quantum computing.

Definitions

The notion of HPC has not always been well defined, particularly since it is a moving target. The power of a supercomputer from the 1980s is now available in a simple recent server if not in your smartphone. However, it is possible to describe the category with its application requirements. HPC and supercomputers are essentially used for digital simulation and the analysis of complex data. These tools are provided to both researchers, public services and industry for their most advanced computational needs²³⁵¹.

HPCs are used for weather forecasting²³⁵², organic and inorganic chemistry simulations, aerospace and automotive simulation, nuclear weapon simulation²³⁵³, in financial services, more recently in machine and deep learning and, we tend to forget, also to create advanced computer graphics in movie and TV series productions. The mathematical models used in supercomputers are used in particular to solve partial differential equations and to carry out N-body simulations.

²³⁴⁹ See [The Unbelievable Zombie Comeback of Analog Computing](#) by Charles Platt, Wired, March 2023.

²³⁵⁰ We'll see in a later part that this comparison was non-sense and was mixing apples and oranges in an unfair way towards the IBM Summit and HPC overall. With factoring-in the noise generated by Sycamore, emulating it requires only the power of a simple PC.

²³⁵¹ See this good review paper on HPCs: [Reinventing High Performance Computing: Challenges and Opportunities](#) by Daniel Reed et al, Universities of Tennessee, Utah and ORNL, March 2022 (22 pages).

²³⁵² As for IBM Weather Channel and its GRAPH (Global Hi-Resolution Forecasting System) forecasting model which is accurate to within 3 km. It is based on an HPC, the Dyeus with 76 nodes of 4 V100 GPUs and 2 Power 9 CPUs. See [High Performance Computing for Numerical Weather Prediction at The Weather Company, an IBM Business](#) by Todd Hutchinson and John Wong, 2019 (18 slides).

²³⁵³ This is the role of the supercomputer at CEA-DAM in Bruyères-le-Châtel in the Ile-de-France region, which is fed with data from the Megajoule laser located in Aquitaine.

These systems are demanding in several ways: in computing capacity, often evaluated in floating-point operations per second, if possible, in double precision (FLOPS), in data storage capacity, and above all, in the ability to transfer data rapidly between storage, memory and processing units. It is in these areas that supercomputers are most distinct from commodity servers used in data centers.

These systems however do not belong to the “unconventional computing” domain since they are based on classical computing systems: CPU, GPU, memory and storage. They are just a little extreme in their size and capacity.

History

When the mainframe computers era started in the 1960s, you had general purpose solutions coming for example from IBM with its famous family of 360 systems with a range of power of 1 to 25 depending on the configuration. Then, you had specialized vendors like Control Data who targeted the scientific market with more specialized systems.

The history of supercomputers started with the advent of the **Cray 1** in 1976. Its founder Seymour Cray participated in the creation of one of the first startups in computing, ERA and later cofounded Control Data! Cray supercomputers relied on home-grown vector processors and various proprietary massively parallel systems²³⁵⁴.

These proprietary systems have been wiped away over the last decade by cluster-based architectures using CPU and GPGPUs standard processors like those from Nvidia, starting around 2017. A cluster contains several nodes, each containing several CPUs and/or GPGPUs, themselves multi-core, and fast interconnection between these nodes, between clusters, and fast access to data storage, increasingly based on SSDs, which are much faster than hard disks, and at last fast networking access.

According to Precedence Research, the current size of the HPC market is estimated at around \$44B in 2023, to nearly double by 2032 (Figure 582). Quantum computing market sizes must be compared to this gauge. We can expect that its size will correspond to a share of this pie, in the 10% to 30% range depending on the actual capabilities of quantum computers.

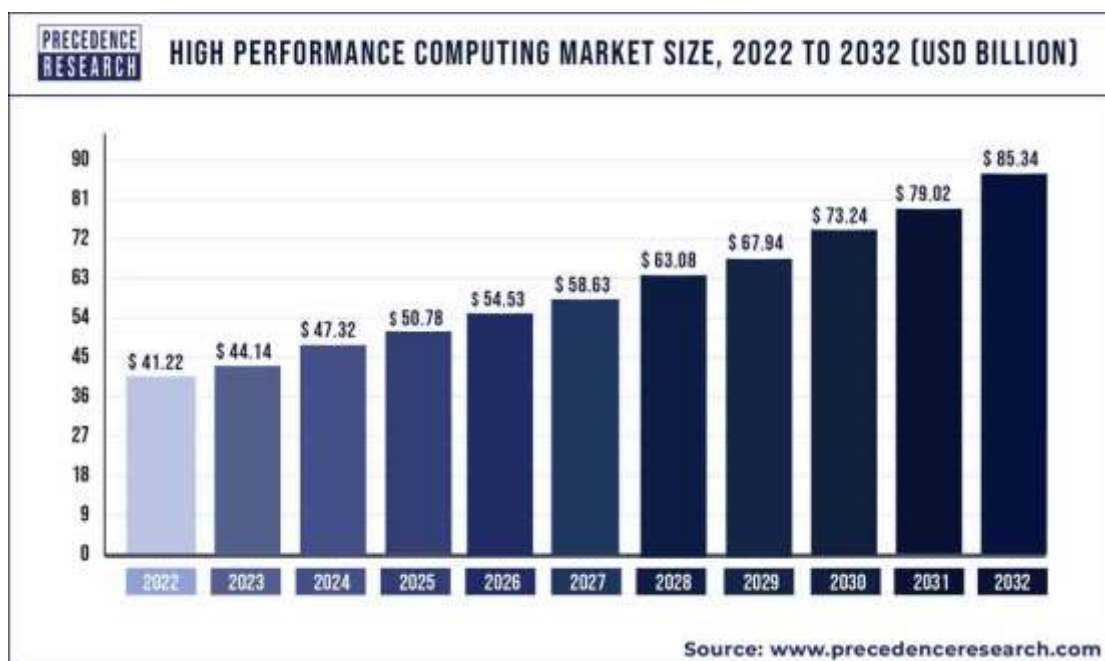


Figure 582 : HPC market size forecast. Source : Precedence Research.

²³⁵⁴ Cray was acquired by HPE in 2019.

HPC architecture

Clusters based on standard microprocessors now account for over 90% of the 500 largest supercomputers in the world²³⁵⁵. The CPUs most often come from Intel (Xeon), AMD (Opteron and then EPYC), IBM (Power9, who withdrew from that market) while Nvidia dominates the market with its GPGPUs (general purpose GPUs), including the famous V100 generation Volta launched in 2017 and its successors A100 Ampere announced in May 2020 and the H100 Hopper in March 2022 with 80 billion transistors and a data transfer speed of 3 TB/s with its associated HBM3 RAM. 60% of the top 25 HPC are now equipped with Nvidia GPGPUs while AMD is providing the CPU for 52% of them and Intel only 28%, showing how market positions can quickly change. This trend accelerated as the OpenMP and OpenACC frameworks were ported to Nvidia GPUs, making these easier to use for a host of existing scientific applications.

This is a form of commoditization of supercomputing, even if these are still heavyweight systems installed in large clean rooms. The technology added value shifted to interconnection, memory and storage architecture as well as, of course, software.

Interconnection in clusters uses technologies such as Nvidia's NVLink, which connects GPUs and CPUs at high speed. Clusters are interconnected by multiple 200 Gbits/s fiber optic links, often from **Mellanox**, Nvidia's subsidiary since 2019. On a larger scale, HPE is promoting the **Gen-Z** architecture optimized for data access in distributed "data-centric" systems.

Operations on supercomputers are programmed with different development tools. One example is **OpenFOAM**, an open source SDK used to simulate fluid mechanics, chemical reactions, heat transfer, solid mechanics, electromagnetism and also in finance. And besides **LS-DYNA** for structural simulation. Finally, the parallel application development library for Fortran, C and C++ **OpenMP** is very commonly used for scientific computing, as is **OpenACC**. Let's not forget also that there are many optimization algorithms based on practically acceptable approximations, such as for traveling salesperson type problems.

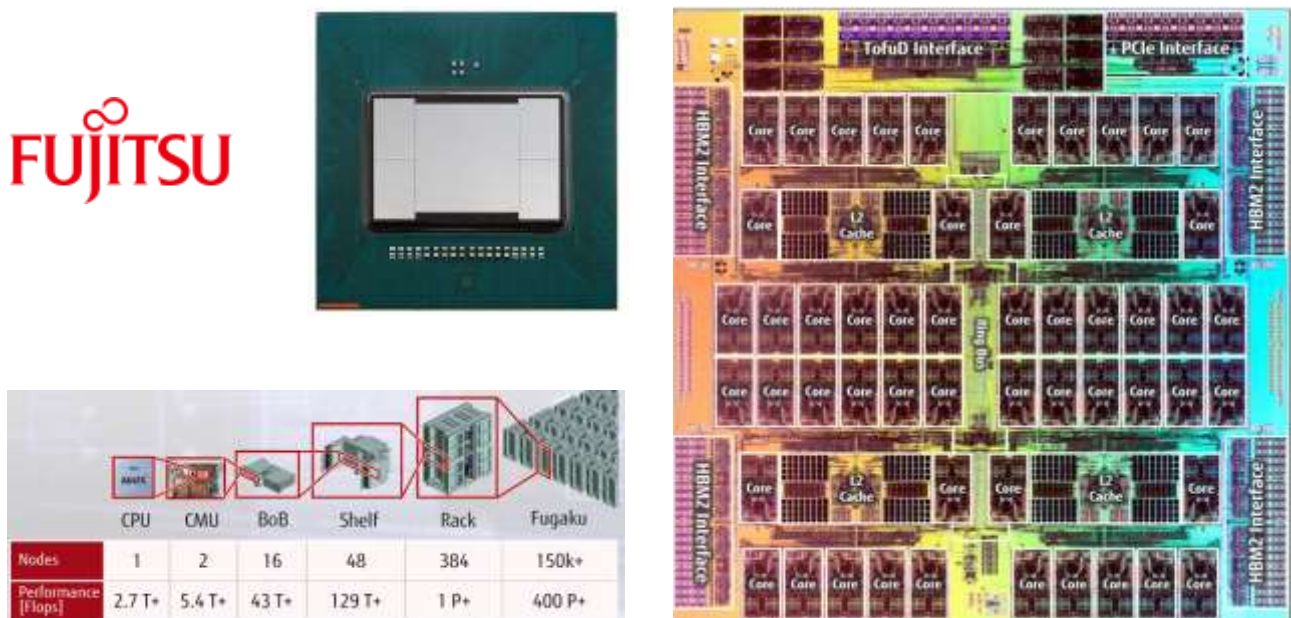


Figure 583: Fujitsu's Fugaku supercomputer is one of the largest in the world. It uses Fujitsu A64FX chips containing each 52 Arm cores and 32GB of HBM2 memory. Source: Fujitsu.

²³⁵⁵ The Top 500 is based on a standardized benchmark, the HPL for High Performance Linpack. It is used to solve a set of linear equations using Gaussian elimination using dense matrices and floating number calculus. See the last published version as of the writing of this book was from June 2023. <https://www.top500.org/lists/top500/2023/06/>.

Vendors from Japan and China are creating their own custom supercomputers microprocessors, in order to limit their dependence on USA companies.

In Japan, the **Fujitsu Fugaku** supercomputer uses Fujitsu A64FX chips comprising 52 Arm cores and 32GB of HBM2 memory delivering a nominal power rating of 2.7 TFLOPS (processor layout *below*). The Fugaku, which is not a poisonous fish, has a total of 415 double precision PFLOPS with 396 racks and 152,064 processors (Figure 583). Its installation was completed in June 2020 and enabled Fujitsu to win first place on the podium of the world's most powerful supercomputers ahead of the USA with the IBM Summit²³⁵⁶.

China's largest supercomputer is the **Sunway TaihuLight** at the National Supercomputing Center in Wuxi. With a capacity of 93 PFLOPS, it uses 40,960 SW26010 256-core 64-bit RISC architecture home-built processors (with a simplified instruction set). As of June 2022, China had deployed 26.8% of the world's Top 500 supercomputers, with the USA accounting for 30%, but China accounted for only 2 of the TOP50 HPCs with 19 in the USA (see Figure 584).

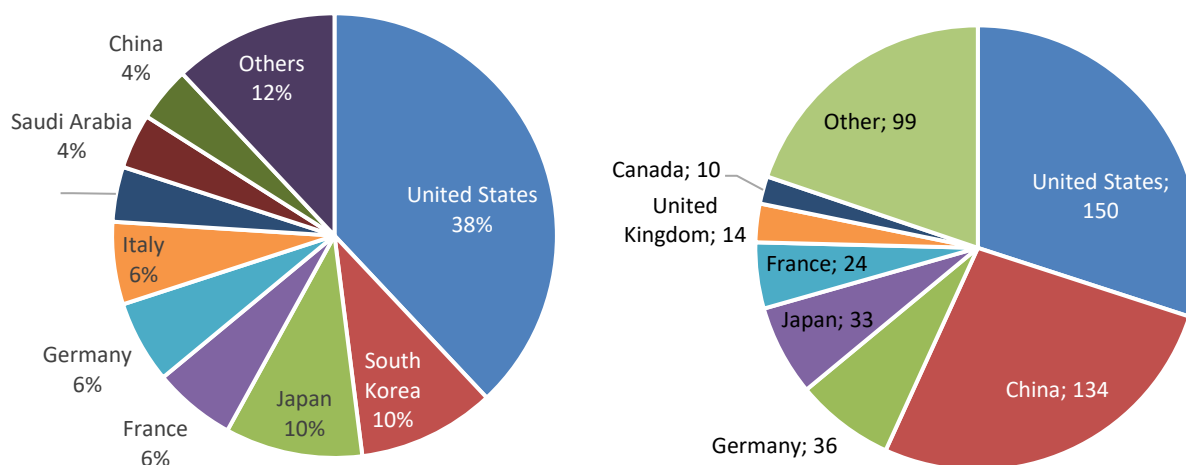


Figure 584: the TOP 50 (left, in percentage) and top 500 (right, in number of systems) HPC worldwide. Data source: <https://www.top500.org/lists/top500/2023/06/>. 2023.

In September 2021, the DoE started the installation of its Frontier new generation supercomputer in its Oak Ridge lab, the Aurora system built by HPE with 9,400+ Cray EX nodes, each equipped with one AMD Epyc CPU and four Radeon Instinct MI250X GPUs. Operational since 2022, it currently provides 1.1 exaflops of HPC and AI computing power and consume only 21 MW, reaching a record of 52 GLOPS/W²³⁵⁷.

In 2018, the European Union launched the **EPI** (European Processor Initiative), a project aiming to bring technology independence with supercomputers multicore microprocessors. It mainly involves German, Spanish, and French players, notably **Eviden**, **CEA** and **SiPearl**.

The productization and commercialisation effort is carried out by the startup **SiPearl**, led by Philippe Notton. It is part of the **EuroHPC** programme to create supercomputers encompassing processors designed in Europe. EuroHPC's first two exascale systems planned in Germany and in France, will use SiPearl technology. EuroHPC R&I projects such as EPI are co-funded evenly between the European Union and EuroHPC participating states.

In France, GENCI invests in a coordinated way in supercomputers for public research, on behalf of the Ministry of Research, together with CNRS, CEA, as well as France Universités and INRIA. GENCI's

²³⁵⁶ See [Fujitsu and RIKEN Take First Place Worldwide in TOP500, HPCG, and HPL-AI with Supercomputer Fugaku](#), June 2020 and [Japanese Supercomputer Development and Hybrid Accelerated Supercomputing](#) by Taisuke Boku, 2019 (59 slides), [Supercomputer Fugaku](#), 2019 (13 slides) and [The first "exascale" supercomputer Fugaku & beyond](#) by Satoshi Matsuoka, August 2019 (80 slides).

²³⁵⁷ See [US Closes in on Exascale: Frontier Installation Is Underway](#) by Tiffany Trader, HPCwire, September 2021.

main systems are deployed and operated in three national supercomputing centres, resp. at CNRS/IDRIS, CINES and CEA/TGCC. Use case for these systems are scientific simulation and machine learning. IDRIS is more specifically specialising in HPC-fueled AI, and TGCC on quantum computing.

The GENCI **Jean Zay** supercomputer is deployed at CNRS/IDRISS. It is equipped with 2,696 Nvidia V100 GPUs and over 3,462 Intel Xeon Cascade Lake CPUs (Figure 585). It is cooled by "hot water", from 30°C to 42°C.

Its GPU AI-oriented extension was deployed in 2021 as part of the French AI plan announced in 2018 with 52 8-GPU nodes.



Figure 585: the Jean Zay supercomputer in France is typical of the new generation of HPCs launched since 2018 with a mix of CPUs and GPGPUs from Nvidia. Source: GENCI.

The GENCI computing center is due to house a quantum accelerator, probably from **Pasqal**, within a few years. It will be integrated into a hybrid computing architecture. Many other European HPC centers have similar plans, in Germany, Italy and the Netherlands, among others.

HPC in the cloud

Since the advent of the cloud, HPC and supercomputing resources are now available on demand. Cloud data centers do not necessarily provide HPC resources. This depends on the servers and clusters deployed architectures and on the packaging of the cloud vendor's offering. This notion can be associated with the notion of hyperscale, which covers the capacity of a cloud infrastructure to adapt to the increasing customer computing needs.

Machine learning and deep learning applications are the most recent applications implemented on supercomputers, particularly since they are using GPGPUs that run tensors enabling efficient matrix operations, which are very common in neural networks. In practice, however, most supercomputers continue to run scientific simulation applications.

The market for microprocessors dedicated to machine learning and deep learning acceleration has been booming for several years. A wide variety of approaches have been adopted by its vendors. It can be represented as in Figure 586 on two axes: in the Y axis, the level of cores specialization, and on the X axis, the number of cores.

Google's TPUs (Tensor Processing Units) are highly specialized for training neural networks, especially convolutional image recognition networks. Nvidia's GPUs contain thousands of classical arithmetic calculation cores as well as hundreds of tensors for matrix computing, which optimizes their versatility.

The most extreme processor is the **Cerebras V2** launched in 2021 with its 850,000 cores. It is a 21 cm square chip containing a hefty 2.6 trillion 7 nm transistors and 40 GB of integrated SRAM ultra-fast cache memory. Their first version launched in 2019 is already deployed in two test servers at the DoE in the USA with one and two of these chips. The first benchmarks published late 2019 did show excellent performance in neural networks training. In 2022, TotalEnergies found 100x speedups vs conventional GPGPU with various material simulations applications²³⁵⁸.

²³⁵⁸ See [Cerebras shows off scale up AI performance for big pharma and big oil](#) by Timothy Prickett Morgan, TheNextPlatform, March 2022.

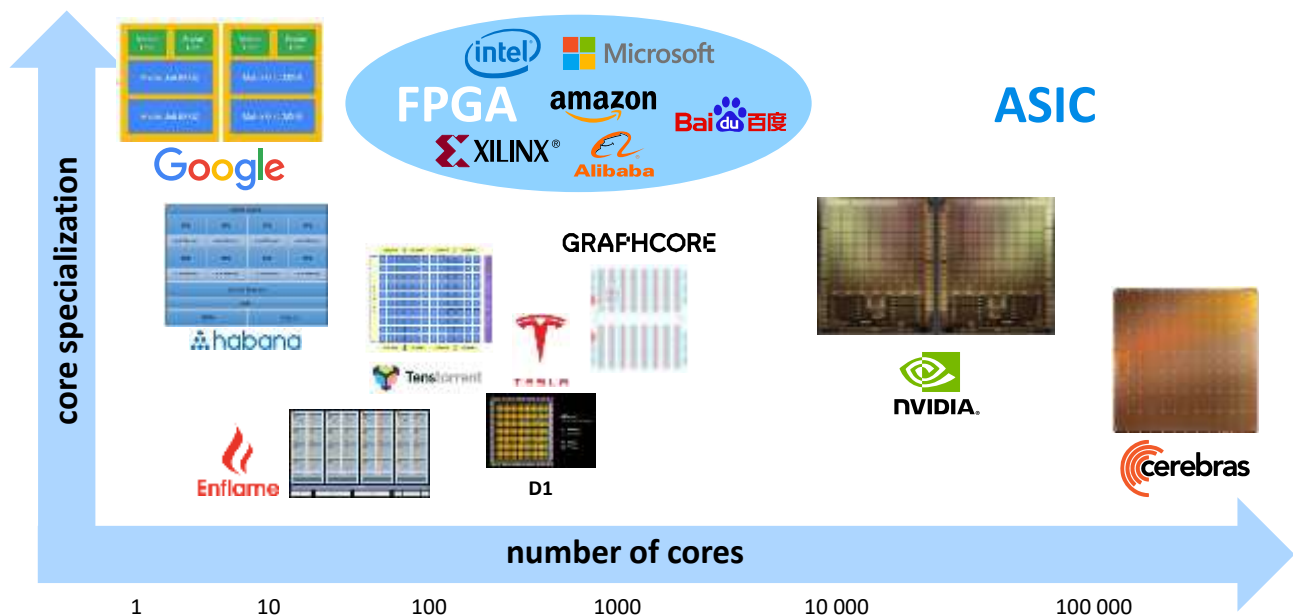


Figure 586: a map of the tensor-based processors with two dimensions: the number of cores and their specialization. The more specialized cores are in Google's TPU with large tensor operations capacity (128x128 values) while Cerebras's wafer scale chip has 845,000 relatively simple cores. (cc) Olivier Ezratty, 2022-2023.

The company raised a total of \$720M, a similar amount to PsiQuantum.

Finally, **FPGAs** are dynamically programmable circuits that allow the creation of custom circuits at rather low cost and high flexibility²³⁵⁹. These are used by some cloud vendors such as Microsoft (with its Brainwave chips) and Chinese cloud companies like **Alibaba** and **Baidu**. The FPGA field is also lively with two trends, one is the integration of DSA (domain specific architecture) modules like arm cores, GPU cores, NPU cores and the like next to programmable arrays. The other is the CGRA (Coarse Grain Reconfigurable Array) which is about using higher level of abstraction modules than implementing just typical lookup tables logic²³⁶⁰.

Some of these cloud players are developing their own supercomputers. **Google** has created its TPU pods over several generations for its data centers. A TPU v3 board contains four TPU chips, each with two cores, with 16 GB of HBM memory for each TPU core. A TPU v3 Pod has up to 2048 TPU cores and 32 TB of memory.

Graphcore (2016, UK, \$692M) is another contender in this crowder market. It is now using 3D chips bonding using a TSMC technology, the main chip containing processing units and the secondary underneath chip containing connectivity between the computing chips cores. Its current processors have 1,472 cores and 900MB on-chip SDRAM memory, which helps them outperform Nvidia chips on some tasks²³⁶¹.

Nvidia integrates its A100 GPUs in SuperPods totaling 140 DGX A100 and 1120 A100 servers and 4 Po of storage, for 700 PFLOPS. These FLOPS are, however, not necessarily the same as those used to evaluate the TOP 500 supercomputers. Vendor communication is sometimes misleading.

²³⁵⁹ The FPGA market is currently dominated by two vendors: Intel, after its acquisition of Altera in 2015, and AMD, after its acquisition of Xilinx in 2020. In 2019, Xilinx had a 52% revenue market share and Intel about 35%.

²³⁶⁰ See [A Survey on Coarse-Grained Reconfigurable Architectures From a Performance Perspective](#) by Artur Podobas, Kentaro Sano and Satoshi Matsuoka, RIKEN, KTH Royal Institute of Technology and Tokyo Institute of Technology, July 2020 (25 pages).

²³⁶¹ See [Graphcore Uses TSMC 3D Chip Tech to Speed AI by 40% Unveils plan for \\$120-million "brain-scale" supercomputers in 2024](#) by Samuel K. Moore, IEEE Spectrum, March 2022.

Both to improve performance and to reduce energy consumption, there are a number of ways to make these calculations more efficient: **Approximate Computing**, which reduces precision in neural network training and/or inferences without affecting the results, **Quantization**, which switches from floating-point calculations to integer computing during or after training, **Binary Neuron Networks**, which is even simpler with 1 bit output neurons taking us back to the Perceptrons era of 1957 and **Sparse Computing**, which allows computations to occur on compressed representation of matrices, this being useful only for sparse matrices, without prior decompression.

The logo for Quantum Silicon Inc (QSi) features the letters 'QSi' in a stylized font. The 'Q' is red, and the 'Si' is black.

Silicon Reinvented

Quantum Silicon Inc (2011, Canada, \$80K) is developing spin qubit chips using the donor spin variety. It is supposed to operate at room temperature. It seems not to be quantum computing per se, with qubits, but nano-classical computing using single-atom silicon quantum dots.

It is non quantum atomic scale computing. The surface of a pure silicon substrate is hydrogenated and the dots correspond to silicon where the bounded hydrogen atom has been removed with atomic probe microscopes. It used the process of hydrogen lithography, also prototyped at IBM. The careful arrangement of atoms and holes enables the implementation of classical Boolean gates like the OR two-bit gate. Two key benefits could come from this: faster operations and 100x less energy consumption. QSi was created by Ken Gordon (CEO), Robert A. Wolkow (CTO), James Chepyha (CFO). Given the company's creation date and funding, it seems the technology may be hard to turn into a real product. They may however pivot in the sensing market.

Whatever happens with quantum computers, supercomputers will always be relevant. Applications using large amounts of data are not suitable for quantum computing, even with zillions of qubits. Indeed, data loading time in qubits is a huge bottleneck because it relies on very long series of quantum gates that are not as fast as classical data processing. Applications adapted to quantum computing should not rely on high-volume data feeds. This is the case with weather forecasts which requires heavy data sets. It will rely on classical supercomputing for a long time despite some exaggerated claims²³⁶².

Power efficiency

Supercomputers are quite power hungry. Their increasingly powerful microprocessors consume several hundreds of Watts. A third of the electrical energy consumed by a data center is spent on cooling. Specialized server racks now easily consume up to 30kW. It has now reached the point where liquid cooling is preferred for removing heat from components, usually with water. This provides greater efficiency.

The table in Figure 587 describes the power consumption gap between computing and memory access, which are becoming increasingly expensive the further away memory is from computing. The ratio goes up to more than 1 to 1,000! It explains the attempts to bring memory closer to computing units like what **UpMem** (France) does with its DRAM memory modules integrating dozens of RISC-V cores to perform in-memory computing and speed-up certain processes by a factor of 10, particularly for big data applications.

HPC power efficiency comes from progress in CPU/GPU designs and architecture but also depends on the efficiency of software tools and libraries which have significantly contributed to the improvement of HPCs energy efficiency²³⁶³ (Figure 588).

²³⁶² See [Forecasting the Weather Using Quantum Computers](#) by IQbit, 2017. The paper references [CES 2019: IBM unveils weather forecasting system, commercial quantum computer](#) by Abrar Al-Heeti, January 2019, which covers two entirely unrelated announcements from IBM, one on weather forecasting using classical computing and another, related to their Q System One, both introduced at CES 2019. See also [Rigetti Enhances Predictive Weather Modeling with Quantum Machine Learning](#), December 2021 who does this with a mere 32 qubits!

²³⁶³ See [Computational Efficiency through Tuned Approximation](#) by David Keyes, November 2022 (62 slides).

Function	Energy in Picojoules
8-bit add	0.03
32-bit add	0.1
FP Multiply 16-bit	1.1
FP Multiply 32-bit	3.7
Register file access*	6
Control (per instruction, superscalar)	20-40
L1 cache access	10
L2 cache access	20
L3 cache access	100
Off-chip DRAM access	1,300-2,600

Figure 587: in classical computing, the biggest energy cost comes with moving the data and not computing. It may be the same with quantum computing, if not worse given data loading in a QPU will be quite slow and energy consuming. Source: [The End of Moore's Law & Faster General Purpose Computing and a Road Forward](#), by John Hennessy 2019 (49 slides).

However, most organizations running the largest supercomputers in the world have created a sort of top limit on the power drain of their systems, around 20 MW. This is one of their motivations to be interested in quantum computers since they may potentially bring some energetic advantage on top of some computing advantage as we're already covered in this book in the engineering section.

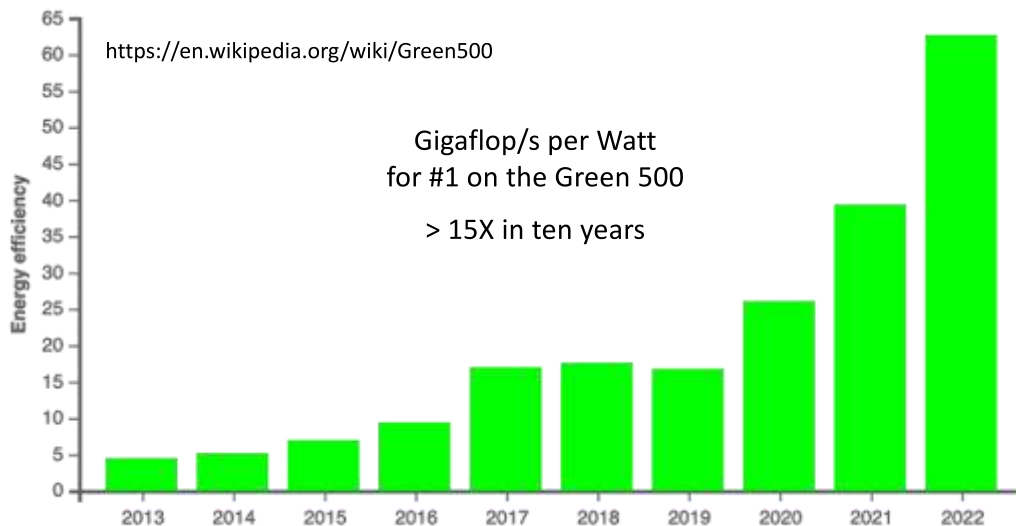


Figure 588: HPC energy efficiency progress over time. Source: [Computational Efficiency through Tuned Approximation](#) by David Keyes, November 2022 (62 slides). Added in 2023.

Quantum computing in HPC centers

Even if and when scalable quantum computer become available with an exponential computing power gain, we will still need classical HPCs as shown in Figure 590. The main reasons are that quantum computers, even in the FTQC regime, won't be able to handle big data efficiently. They will always rely on HPC to process and prepare complex data in order to feed quantum computers with simpler data. Quantum computing is made for solving high-complexity problems with relatively small data while HPCs may be limited in the size of addressable problems but have much better capabilities in data processing. You understand this with the bandwidth of typical classical systems shown in Figure 589.

As a comparison, you can feed a quantum computer very slowly. Let's say you can use 4,000 logical qubits. You will be able to feed one bit for each qubit at each gate cycle. Current gate cycles are 2 kHz with IBM systems, without the burden of quantum error correction. It is even much slower with trapped ion systems. You end up being able to feed roughly 1 MB per second in such a quantum computer! Some architecture ingenuity will be required to accelerate this pace, including using quantum memories and fastening the QPU cycle rate (measured in CLOPS).






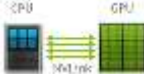


		max bandwidth	capacity
SSD M.2 PCIe storage		3 GB/s	>1 TB
DDR4 CPU external memory		10 GB/s	>16 GB
Infiniband interserver comm	 	25 GBs/s	<i>data bus</i>
GDDR6X GPU external memory		1 TB/s	2 GB – 12 GB
NVLink 2.0 inter-GPU/CPU comm		1.350 TB/s *	<i>data bus</i>
HBM3E / HMC GPGPU external memory		8 TB/s *	192 GB*
cache & registers CPU/GPU internal memory		> 16 TB/ s	50 MB (L2)* 44 GB **

Figure 589: data bandwidth and capacity of typical systems memory, storage and interconnect. (cc) Olivier Ezratty, 2020-2024.

*: in Nvidia B200 GPGPU **: in Cerebras CS-3

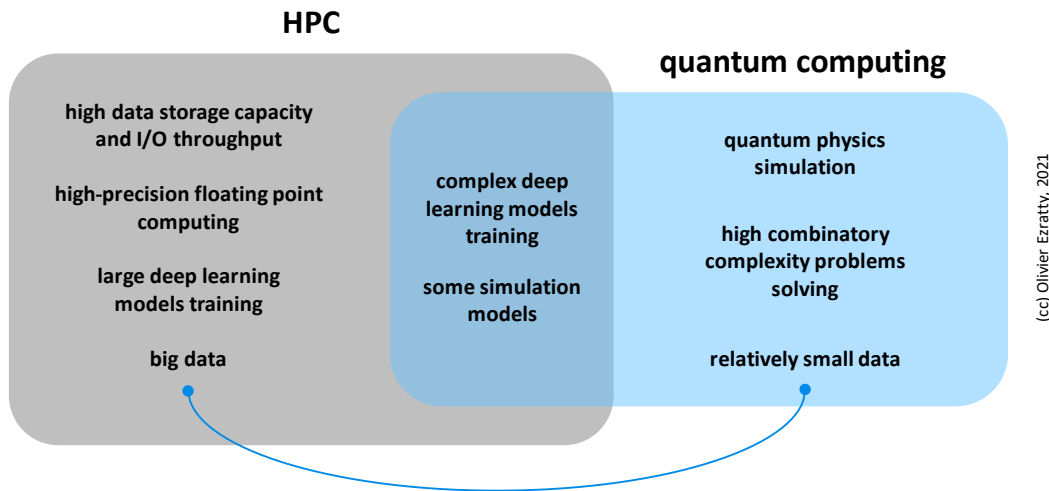


Figure 590: how to position HPCs vs (scalable) quantum computers. HPCs are for big data and high-precision computing. Quantum computing will be adapted to high complexity problems but with relatively reasonable amounts of data. There's some cross-over between both systems and they will work in sync in many cases. (cc) Olivier Ezratty, 2021.

(cc) Olivier Ezratty, 2021

Digital annealing computing

Digital annealing classically implements the adiabatic theorem seen when discussing quantum annealing in the quantum hardware part of this book. It can make use of custom chips designed to improve the efficiency of digital annealing.

Several industry vendors are in this market with **Fujitsu** and **Hitachi**. This part also includes some related solutions coming from **MemComputing** and **InfinityQ**. Research in that area comes for example from the University of Toronto (Canada) and the University of Rochester (USA)²³⁶⁴.



Fujitsu announced in early June 2018 a digital annealing computer operating at room temperature. Fujitsu is one of the world leaders in the supercomputer market with HPE and Eviden/Atos.

²³⁶⁴ See [A CMOS Ising Machines with Coupled Bistable Nodes](#) by Richard Afoakwa et al, University of Rochester, July 2020-November 2022 (25 pages).

It was therefore logical that they explored ways to upscale their HPC offering. It is supposed to scale much better than D-Wave quantum annealers²³⁶⁵.

Their digital annealers use custom CMOS DAU chips developed in partnership with the University of Toronto. It is proposed as a cloud offering and is used to solve optimization problems and to carry out molecule screenings. The dedicated chip contains 1,024 bit update blocks incorporating memory to store their weights with a precision of 16 bits, logic blocks to perform value inversions and the associated control circuits (Figure 591, Figure 592). This is reminiscent of memristor-based neural networks. As with D-Wave, problems are loaded into the system in the form of graphs with biases in the links between elements and the system looks for a minimum energy state to solve the problem. It has some familiarity with the Ising model used in D-Wave. Some case studies are available in optimization tasks²³⁶⁶.



Figure 591: Fujitsu's DAU processor for implementing optimized digital annealing. Source: Fujitsu.

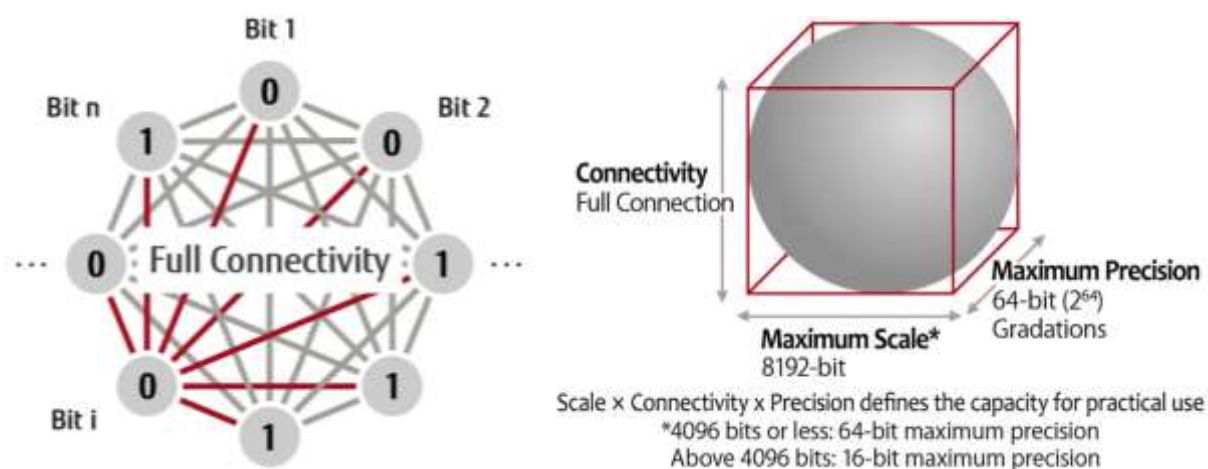


Figure 592: Fujitsu's DAU high-level architecture. Source: Fujitsu.

Its designer, **Hidetoshi Nishimori** of the Tokyo Institute of Technology, believes that Fujitsu will be able to create solutions that outperform D-Wave. In 2019, Fujitsu announced its second generation of chips with 8,192 blocks followed by a third generation with 100K blocks in 2020 and a fourth generation in 2020 with a 10x speed improvement. They have sold only a few of these machines in Japan and one in Taiwan²³⁶⁷. Development tools are provided by **IQBit**, in which Fujitsu has made an investment. Fujitsu has been collaborating since April 2020 with **Quantum Benchmarks (Canada)** on quantum algorithms and error suppression codes, based on an IA Fujitsu algorithm and their experience with their digital annealing²³⁶⁸. Fujitsu is also partnering with **Entanglement (USA)** which developed a Covid vaccine logistics optimization solution with its annealer.

²³⁶⁵ See [Fujitsu's CMOS Digital Annealer Produces Quantum Computer Speeds](#), 2018.

²³⁶⁶ See [Solving Job-Shop Scheduling Problems with QUBO-Based Specialized Hardware](#) by Jiachen Zhang, Giovanni Lo Bianco, J. Christopher Beck, 2022 (9 pages) and [Solving Combinatorial Optimization Problems on Fujitsu Digital Annealer](#) by Yu-Ting Kao et al, National Chengchi University, Taiwan, November 2023 (5 pages)

²³⁶⁷ See [Fujitsu delivers Quantum-Inspired Digital Annealer for research center at Chung Yuan Christian Center in Taiwan](#), Fujitsu, November 2022.

²³⁶⁸ See [Fujitsu Laboratories and Quantum Benchmark Begin Joint Research on Algorithms with Error Suppression for Quantum Computing](#), April 2020 and [Fujitsu Laboratories and Quantum Benchmark Begin Joint Research on Algorithms with Error Suppression for Quantum Computing](#) by Fujitsu, March 2020.

Some advertised case studies involve **Toyota Systems Corporation** for supply chain optimization, stadium seat allocation optimization in Berlin, and peptide drug discovery with **Pepti-Aid Corporation**.

HITACHI Hitachi also launched a related initiative although, contrarily to Fujitsu, it seems it did stay in research lab and didn't reach commercialization.

Their system is implementing a hardware solution to solve Ising models. It is mixing probabilistic and deterministic approaches running in a CMOS component to find some energy minimum of a combinatorial problem expressed as an Ising model²³⁶⁹ (Figure 593). It doesn't find the absolute minimum to the problem but an acceptable solution. The CMOS uses SRAM to store the virtual "spin states" of the Ising model problem. Hitachi stated that it could help solve combinatorial optimization problems such as the travelling salesman problem efficiently. The architecture was first relying on FPGAs which makes sense given it didn't reach volume production.

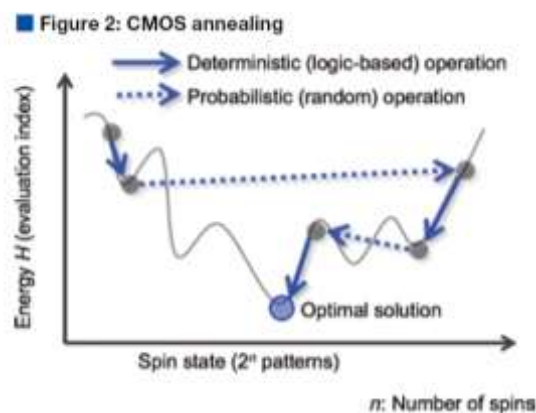


Figure 593: CMOS annealing principle.



The mysterious startup **MemComputing** (2016, USA) was founded by **John Beane**, a serial entrepreneur, with two physics researchers, **Massimiliano Di Ventra** and **Fabio Traversa**, who have done extensive work on memory computing²³⁷⁰.

It can be positioned in a category close to Fujitsu's offer. It is a solution inspired by quantum annealing computation. They use the principle of invertible computing units, able to circulate data both ways, from input to output and output to input.

It also uses oscillating Boolean gates implementing a non-Von-Neumann computing model and some sort of tunnel effect²³⁷¹. Their hardware solution MemCPU Coprocessor is to place memory next to computing units in processing unit²³⁷² (Figure 594). These memristor-like computing cells have symmetrical inputs and outputs interconnected to neighboring cells. It computes exclusively with integer numbers. There is no floating-point computing at all. They would automatically find a complex balance of a parameterized system. This is the principle of SOLGs (Self Organizing Logic Gates) shown in Figure 595²³⁷³.

The company positions its technology as competing with quantum computing with a market ready solution although its real existence and packaging is in question²³⁷⁴. Their architecture is supposed to solve various classes of NP-complete and NP-difficult problems in polynomial time such as 3-SAT

²³⁶⁹ See [CMOS Annealing Machine – developed through multi-disciplinary cooperation](#) by Hitachi, Ltd., November 2018, [Overview of CMOS Annealing Machines](#) by Masanao Yamaoka, January 2019 (4 pages) and [CMOS Annealing Machine: an In-memory Computing Accelerator to Process Combinatorial Optimization Problems](#), April 2019.

²³⁷⁰ See [Universal Memcomputing Machines](#) by Fabio Traversa and Max Di Ventra, 2014 (14 pages) and [Perspective: Memcomputing: Leveraging memory and physics to compute efficiently](#) by Fabio Traversa and Massimilio Di Ventra, 2018 (16 pages).

²³⁷¹ See [Global minimization via classical tunneling assisted by collective force field formation](#) by F. Caravelli, F. C. Sheldon and Fabio L. Traversa, February 2021 (15 pages).

²³⁷² It is described in [Memcomputing: fusion of memory and computing](#) by Yi Li et al, 2017 (3 pages) where this schema comes from.

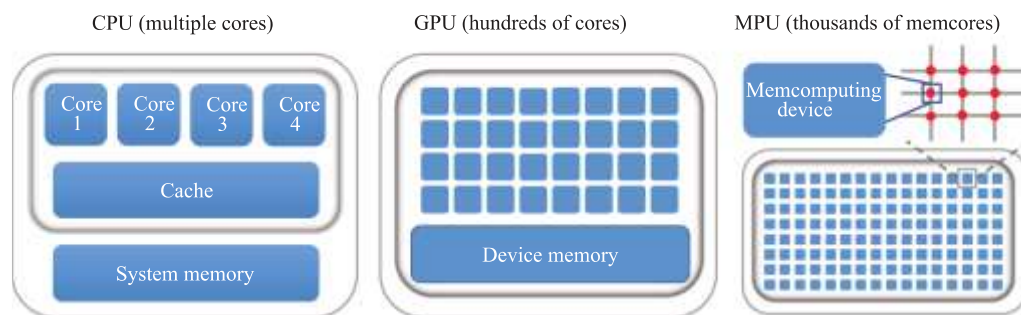
²³⁷³ SOLGs are described in the patent [Self-Organizing Logic Gates and Circuits and Complex Problem Solving With Self-Organizing Circuits](#), March 2018 (37 pages). It is further detailed in [Coupled oscillator networks for von Neumann and non von Neumann computing](#) by Michele Bonnin, Fabio L. Traversa and Fabrizio Bonani, arXiv preprint, December 2020 (29 pages).

²³⁷⁴ See [MemComputing vs Quantum Computing](#) by MemComputing, August 2022.

problems²³⁷⁵. They tout significant performance gains such as four orders of magnitude for machine learning applications, i.e., performance multiplied by 10,000! Their solution is emulated in conventional computers like with the AMD EPYC microprocessor and provided as an SDK operated in the cloud, which they have designed in partnership with **Canvass Labs** (2017, USA). Their electronic architecture was also prototyped at a small scale using **Analog Devices** standard analog multiplier circuits²³⁷⁶.

The application domains include the resolution of planning and optimization problems such as the traveling salesperson problem, combinatorial optimizations and searches²³⁷⁷, bioinformatics, neural network training²³⁷⁸ and even integer factoring²³⁷⁹, each time with the promise of an exponential gain in computing time compared to traditional computing.

They announced that they would need to embed some memristor technology in their component, which could create significant delay in the manufacturing given this technology is not really mature. They handle problems such as MIPLIB (Mixed Integer Programming Library), which are considered intractable with a 60-second response time on a server running Linux and have even beaten a D-Wave. This is used to find a combination of given integers that can generate zero when added together (the "Subset Sum problem").



(Color online) Comparison of CPU, GPU, and MPU.

Figure 594: MemComputing architecture compared with classical computing. It is basically a mix of in-memory processing with bidirectional computing. Source: MemComputing.

The startup manages to obtain a quantum scale advantage by emulating its process on classical computers. This amounts to challenging all current theories of complexity.

In April 2020, MemComputing announced that it would make its XPC (Xtreme Performance Computing) software stack available in the cloud for researchers working on Covid-19²³⁸⁰.

So, is this technology simply revolutionary and could it nullify many efforts in quantum computing, or are there one or more shortcomings? There are plenty of them. How do you initialize the system so that it is close to a global minimum? What is their real capacity to create these SOLGs in current CMOS components?

²³⁷⁵ See [Memcomputing NP-complete problems in polynomial time using polynomial resources and collective states](#) by Fabio Traversa, Massimilio Di Ventra et al, 2014 (10 pages) and [Evidence of an exponential speed-up in the solution of hard optimization problems](#) by Fabio Traversa et al, 2018. Then, See this [Conference](#) from Massimiliano Di Ventra at Berkeley in 2016 (26 minutes).

²³⁷⁶ See [Implementation of digital MemComputing using standard electronic components](#) by Yuan-Hang Zhang and Massimiliano Di Ventra, October 2023 (9 pages).

²³⁷⁷ See [Stress-testing memcomputing on hard combinatorial optimization problems](#) by Fabio Traversa, Massimiliano Di Ventra et al, 2018 (6 pages).

²³⁷⁸ See [Accelerating Deep Learning with Memcomputing](#) by Haik Manukian, Fabio Traversa and Massimiliano Di Ventra, 2018 (8 pages).

²³⁷⁹ See [Polynomial-time solution of prime factorization and NP-hard problems with digital memcomputing machines](#) by Fabio Traversa and Massimiliano Di Ventra, 2017 (22 pages).

²³⁸⁰ See [MemCPUXPC SaaS Platform available free for COVID-19 Research](#), 2020.

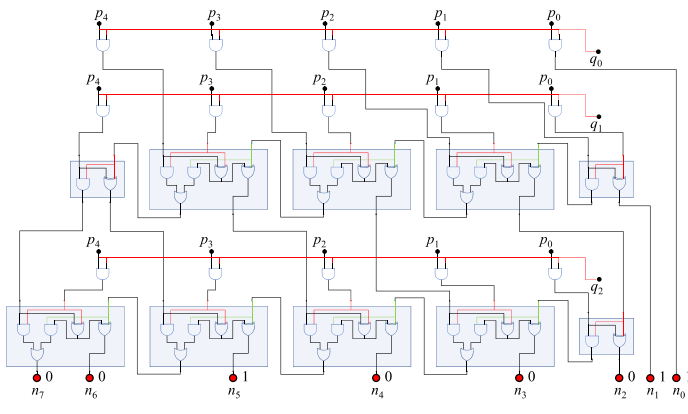


FIG. 2. A possible Boolean circuit that multiplies two integers p and q to give $n = 35 = (10011)_2$ (in the little-endian notation).

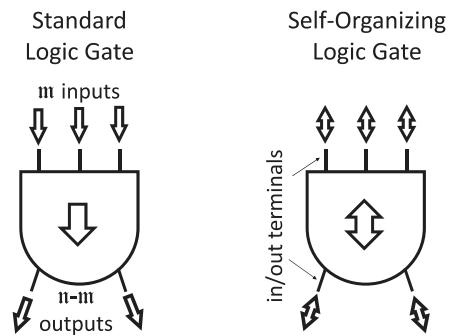


FIG. 3. Left panel: sketch and symbol of a standard \mathcal{N} -terminal logic gate with m inputs and $\mathcal{N} - m$ outputs. Right panel: sketch and symbol of the corresponding self-organizing logic gate.

Figure 595: SOLGs (Self Organizing Logic Gates) from MemComputing. Source: MemComputing.

How is noise managed in their system²³⁸¹? Is the system scaling well? Their approach would not be scalable according to several specialists including Scott Aaronson²³⁸².

In 2022, MemComputing published two papers in partnership with a scientist from the DoE Los Alamos lab on the potential effect of a tunneling effect with memristors to find global minimum, a task commonly used to solve various optimization and machine learning problems²³⁸³. All this remains very theoretical.

In 2023, MemComputing published a pre-print paper on its platform capability to factorize large bi-prime integers²³⁸⁴. Their paper contains a projected estimate of the time it would take to factorize a RSA-2048 key with their platform. It would require about 100 years on a classical emulation of their platform and tens of minutes on its ASIC version... which remains to be seen and tested at such a scale. The research was funded by the US Air Force.



InfinityQ (2019, Canada, \$6M) stated initially that they had built the “*first quantum computing CMOS microchip technology to work at room temperature*”.

The company was launched by Aurelie Hélois (CEO) with Kristina Kapanova (CTO, who later left the company) and John Mullen, former Assistant Director of the CIA.

Their qubit architecture was presented as an analog quantum computer with between 1,000 and 5,000 qubits. and “*based on an artificial atom in a lambda configuration*” which “*exploits superposition and entanglement to achieve quantum computing without the burden of maintaining very fragile quantum objects*”.

It was a cloud native platform and quantum analog-computing technology that could run any coding language, any problem up to 100,000x faster than an average laptop, with the same energy consumption as a lightbulb. Their first-generation machine was supposed to solve complex optimization problems, linear system and FFTs (fast Fourier transforms). Lots of promises!

²³⁸¹ They provide an answer in [Directed percolation and numerical stability of simulations of digital memcomputing machines](#) by Yuan-Hang Zhang and Massimiliano Di Ventra, April 2021 preprint on arXiv (12 pages).

²³⁸² See [A Note on 'Memcomputing NP-complete problems' and \(Strong\) Church's Thesis](#) by Ken Steiglitz, 2015 (2 pages) which quickly demonstrates that this is not possible. The same goes for [Memrefuting](#) by Scott Aaronson in 2017 and for [A review of Mem-computing NP-complete problems in polynomial time using polynomial resources](#) by Igor Markov, 2015 (3 pages).

²³⁸³ See [MemComputing Announces Collaboration with Los Alamos National Lab](#), January 2022, [Global minimization via classical tunneling assisted by collective force field formation](#) by Francesco Caravelli et al, Science Advances, December 2021 (9 pages) and [Projective Embedding of Dynamical Systems: uniform mean field equations](#) by Francesco Caravelli et al, MemComputing and DoE Los Alamos lab, January 2022 (45 pages). PEDS, projective embedding of dynamical systems (PEDS).

²³⁸⁴ See [Scaling up prime factorization with self-organizing gates: A memcomputing approach](#) by Tristan Sharp, Rishabh Khare, Erick Pederson and Fabio Lorenzo Traversa, MemComputing, September 2023 (23 pages).

They created a proof of concept with 10 qubits late 2020 and announced a 100 qubits MVP in 2021 with full commercialization planned after 2025. In April 2021, they mentioned that they had solved a traveling salesperson problem with 128 cities while other “*non-classical machines*” have solved such problems with a maximum of 22 cities, the actual record being 7,515,755,956 steps²³⁸⁵. They also made business claims such as having projects starting with major unnamed UK and Canada banks, with a Swiss pharmaceutical and the Canadian government²³⁸⁶. Their technology could be classified as some sort of reservoir computing running on CMOS doing rabi flops emulation²³⁸⁷. Their quantum, superposition and entanglement claims seemed totally overexaggerated.

In 2022, the company made a pivot, did reset its web site and claimed that its solution was “*A quantum-inspired technology to serve gaming & metaverse's intensive computation demands*”. Really!?! In 2023, they came back with another story, about “the World’s largest Ising machine able to handle 112,000 variables, based on a Restricted Boltzmann Machine (RBM), with methods coming from research done by their new CTO Saavan Patel and Sayeef Salahuddin from UC Berkeley. They can solve QUBO and MaxCut formatted problems. The underlying hardware is using one Nvidia A6000 GPU card using an A100 chip.

Reversible and adiabatic calculation

Since the 1960s, researchers have been considering reducing computer power consumption by several orders of magnitude based on the principle of adiabatic reversible computing²³⁸⁸ (Figure 597). The goal is primarily energy-based. It does not accelerate computing. In most cases, it is even contradictory with Moore’s law, as the main techniques used result in a calculation speed decrease.

All this is due to our understanding, since the 1960s, of the link between computation and thermodynamic processes. **Rolf Landauer** created in 1961 the equation according to which the process of information processing that dissipates energy is related to memory erasure²³⁸⁹. The erased information is turned into heat sent outside the computer, increasing the environment entropy. Rolf Landauer estimated that the dissipated energy was always greater than $kT\ln(2)$ per erased bit, k being Boltzmann's constant (1.38×10^{-23} J/K), T the temperature in Kelvin and $\ln(2)$ the logarithm of 2 (about 0.69315). At room temperature, this gives 0.017 eV.

This is the famous Landauer limit. Landauer's limit was experimentally verified fifty years later, in 2011, by a team from ENS Lyon in Sergio Ciliberto's group²³⁹⁰ (Figure 598).

²³⁸⁵ Source : [World TSP](#).

²³⁸⁶ See a [video of their presentation](#), December 2020 (17 mn).

²³⁸⁷ See [Quantum reservoir computing with a single nonlinear oscillator](#) by L. C. G. Govia et al, Raytheon, January 2021 (9 pages).

²³⁸⁸ To write this part, I used the many references from the excellent presentation [Reversible Adiabatic Classical Computation - an Overview](#) by David Frank, 2014, IBM (46 slides), as well as from [The Future of Computing Depends on Making It Reversible](#) by Michael P. Frank, 2017 and [The Case for Reversible Computing](#) by Michael P. Frank, 2018 (19 pages). See also [Computers That Can Run Backwards](#) by Peter Denning and Ted Lewis, 2017 and [Theory of Reversible Computing](#) by Kenichi Morita, 2017 (463 pages). See also the review paper [Quantum Foundations of Classical Reversible Computing](#) by Michael P. Frank and Karpur Shukla, April 2021 (70 pages).

²³⁸⁹ See [Irreversibility and heat generation in the computing process](#) by Rolf Landauer, in IBM Journal of Research & Development, 1961 (9 pages).

²³⁹⁰ See [Experimental verification of Landauer's principle linking information and thermodynamics](#) by Antoine Béruit et Al, 2011 (4 pages) and [Information and thermodynamics: Experimental verification of Landauer's erasure principle](#) by Antoine Béruit, Artyom Petrosyan and Sergio Ciliberto, ENS Lyon, 2015 (26 pages). Other experiments followed to validate this, with magnetic memories, such as [Experimental test of Landauer's principle in single-bit operations on nanomagnetic memory bits](#) by Jeongmin Hong et al, 2016 (6 pages). The principle consists in lowering the energy barrier of the bit state transition when an operation is required and then to raise it again to preserve the bit state. See also Delft's 2018 experiment in [Quantum Landauer erasure with a molecular nanomagnet](#) by R. Gaudenzi et al, 2018 (7 pages).

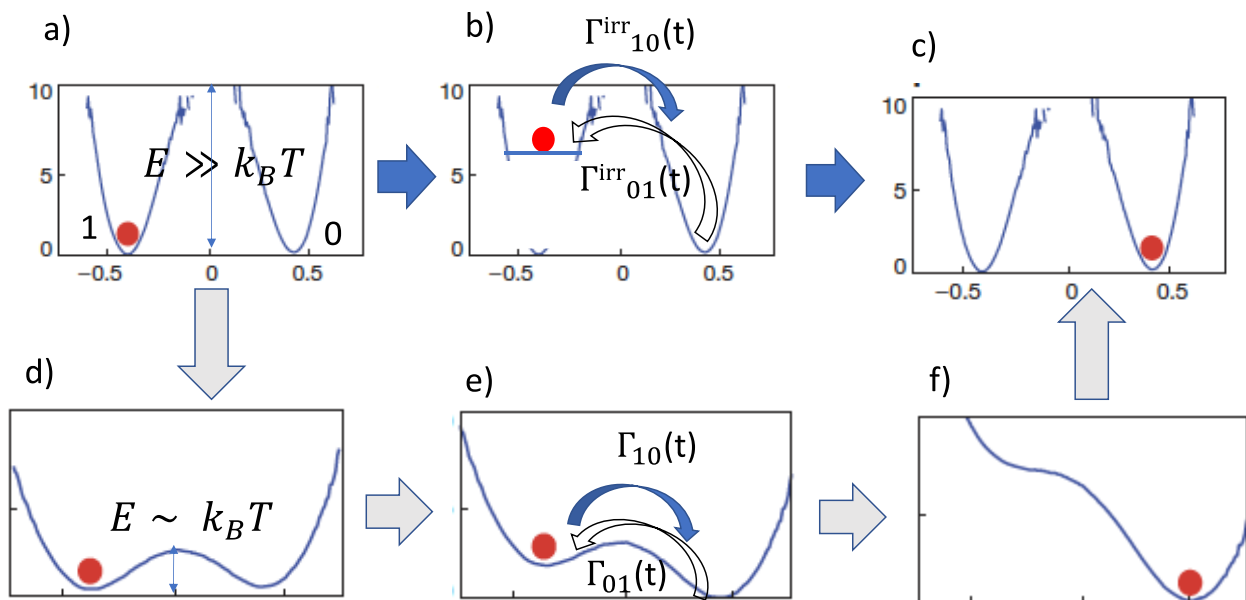


Figure 596: the thermodynamic principle of reversible computing. Source: "Thermodynamics of computing, from classical to quantum" by Alexia Auffèves, May 2020 (11 pages), adapted from [Experimental verification of Landauer's principle linking information and thermodynamics](#) by Antoine Bérut et Al, 2011 (4 pages).

More generally, Landauer's limit illustrates the link between the notions of logical and physical reversibility of computation. The first is linked to the ability to determine the input values of a calculation according to the output values.

The second is that the unfolding of a physical process in reverse may not violate the laws of physics, including the inescapable second law of thermodynamics according to which the entropy of a thermodynamic system always increases unless the process is reversible.

Today, a CMOS component spends 5,000 eV energy to erase one bit, almost 300,000 times more than the Landauer's limit. One could gain an order of magnitude and go down to 500 eV, but that would still be 30,000 times more than the Landauer limit. So, in order to reduce the computing energy consumption, why not avoid erasing information and, in the process, make all computing physically and logically reversible? This would require a review of all current computational logic that relies at low-level on irreversible logic gates that destroy information, such as NAND or XOR gates that generate one bit from two bits.

In 1973, **Charles Bennett**, another IBM researcher and colleague of Rolf Landauer's, imagined a calculation method that would avoid this energy-dissipating erasure of information without requiring an infinite memory²³⁹¹.

He was followed by **Edward Fredkin** and **Tommaso Toffoli** who, in 1978 and 1982, imagined reversible logical gates inspired by a metaphorical physical model based on billiard balls, the BBM for billiard ball model²³⁹². These logic gates have as many outputs as inputs and it is easy to understand why they become reversible. Although their model was not practically feasible with contemporary electronics, it was then applied to the quantum equivalent of these gates that we already covered.

Konstantin Likharev proposed in 1976, then in 1982, to implement this reversible computational logic by manipulating the energy levels of superconducting Josephson junctions, under the name of "parametric qantrons"²³⁹³.

²³⁹¹ See [Logical reversibility of computation](#) by Charles Bennett, IBM Journal of Research and Development, 1973 (8 pages). Charles Bennett is also the creator of BB84 codes with Georges Brassard, which laid the foundations of quantum key distributions.

²³⁹² See [Conservative Logic](#) by Edward Fredkin et Tommaso Toffoli, International Journal of Theoretical Physics, 1982 (35 pages).

²³⁹³ He tells this story in [Josephson Digital Electronics in the Soviet Union](#) by Konstantin Likharev, 2012 (18 slides).

In 1991, this became the "quantron flux parametron" (QFP), capable of operating up to 10 GHz and developed by a Japanese team²³⁹⁴.

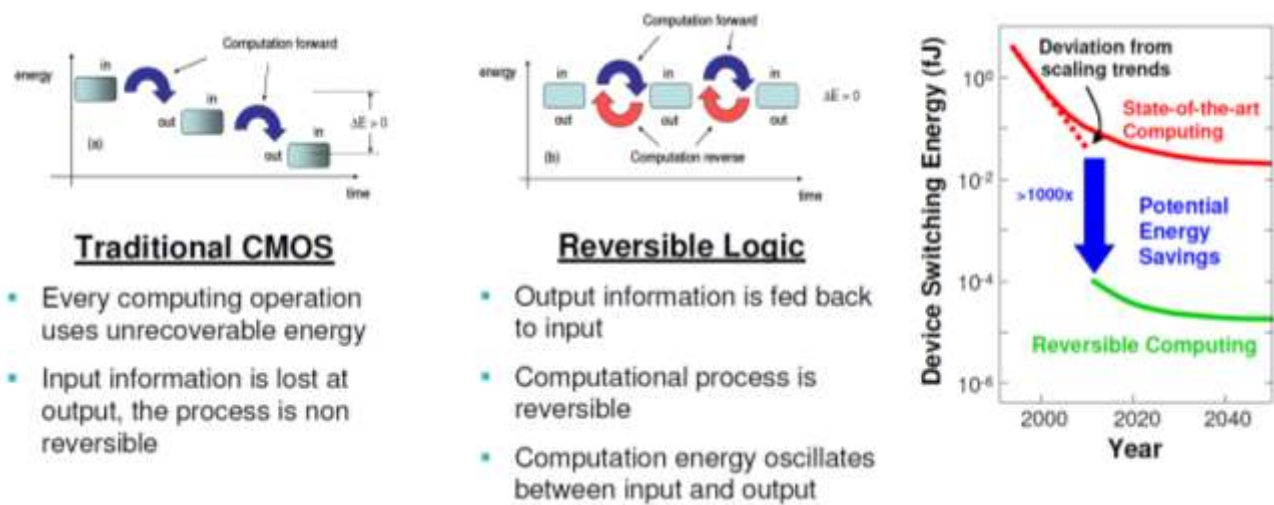


Figure 597: why reversible logic could help save energy. But it won't make it faster. Source: [Reversible Adiabatic Classical Computation - an Overview](#) by David Frank, 2014, IBM (46 slides).

This led then in 2003 to **Vasili Semenov's** idea to use nSQUID circuits to realize these circuits, the n meaning "negative" because of a negative inductance that connects two SQUIDs of the device. As for any Josephson junction, it works under cryogenic temperature²³⁹⁵.

Reversible computing is often associated with adiabatic computing but one could work without the other. The general principle of adiabatic computing is illustrated in Figure 596: in a classical calculation, the energy barrier to switch the state of a system between a) and c) is high. In a quasi-adiabatic calculation, a physical system lowers the state energy transition barrier (in d) to trigger it (in e) and then in f, by raising the level of the barrier to its normal state.

The processing energy cost is thus lowered by approaching Landauer's limit. The high level of the non-calculation barrier guarantees the stability of the information managed outside of this operation. Lowering the barrier and raising it are often managed by trapezoidal voltage control of the transistors instead of looking like a square wave signal.

Between 1985 and 1993, reversible or partially reversible CMOS and CCD computing components were designed.

Craig Lent then proposed in 1997 an adiabatic computation system based on quantum dots and cellular automata (QCA for Quantum dots Cellular Automata) to operate up to 100 GHz²³⁹⁶.

In the same manner, **Krishna Natarajan** suggested in 2004 to use MEMS (electro-micro-mechanical components) to drive the trapezoidal voltage control necessary to create adiabatic CMOS components with a very low energy dissipation of 1 eV²³⁹⁷.

²³⁹⁴ See [Quantum Flux Parametron: A Single Quantum Flux Device for Josephson Supercomputer](#) by Mitsumi Hosoya et al, June 1991.

²³⁹⁵ See an explanation of the process in [Engineering and Measurement of nSQUID Circuits](#) by Jie Ren, 2012 (26 slides). nSQUIDs are double SQUIDs connected by a negative inductance. SQUID = Superconducting Quantum Interference Device, a system used to accurately measure the magnetism of superconducting Josephson effect loops. These nSQUIDs were manufactured by Hypres.

²³⁹⁶ See [A Device Architecture for Computing with Quantum Dots](#) by Craig Lent and Douglas Tougaw, 1997 (17 pages).

²³⁹⁷ See [Driving Fully-Adiabatic Logic Circuits Using Custom High-Q MEMS Resonators](#) by Krishna Natarajan et al, 2004 (7 pages).

The idea was pursued by a team from **CEA-Leti** and **Delft** in the Netherlands in 2017 and **Ralph Merkle** in 2019, with prototype circuits based on this kind of technology²³⁹⁸.

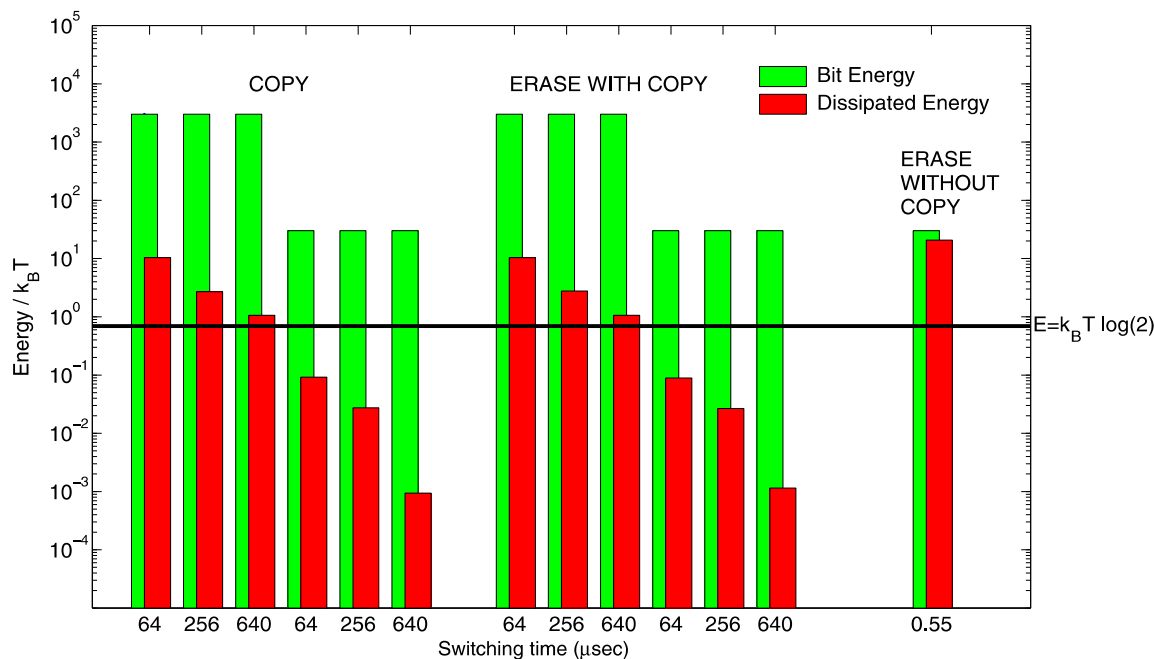


Figure 598: Source: [Experimental Test of Landauer's Principle at the Sub-kBT Level](#) by Alexei Orlov, Craig Lent et al, 2012 (5 pages).

In 2012, **Alexei Orlov** et al. experimentally validated Landauer's limit and, above all, the possibility of overcoming it (from below) with reversible calculation, all with a few discrete classical electronic components, resistors and capacitors²³⁹⁹ (Figure 599). Their experiment showed that a bit copy or erasing with copy could be done with an energy lower than Landauer's limit, at the price of slowing down the operation as shown in Figure 598.

Pure and simple erasing did consume more energy than Landauer's limit. The model was safe! And it all worked at room temperature. In 2019, Alexei Orlov's team from Notre Dame University in Indiana produced the equivalent of an 8-bit microcontroller using a subset of a RISC-type MIPS instruction set with 5,766 transistors, 40% of which are adiabatic²⁴⁰⁰. This seems to be, to date, the most successful realization of a reversible adiabatic processor. It remains, however, experimental and far from industry requirements. Its industrialization could be of interest to create microcontrollers for low power connected objects.

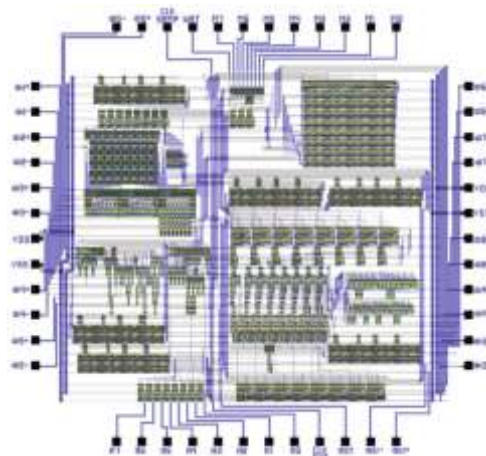


Figure 599: Source: [Experimental Tests of the Landauer Principle in Electron Circuits, and Quasi-Adiabatic Computing Systems](#) by Alexei O. Orlov et al, 2012 (5 pages).

²³⁹⁸ See [Adiabatic capacitive logic: A paradigm for low-power logic](#) by Gaël Pillonnet et al, CEA-Leti, 2017 (5 pages) and [Mechanical Computing Systems Using Only Links and Rotary Joints](#) by Ralph Merkle et al, 2019 (34 pages).

²³⁹⁹ See [Experimental Test of Landauer's Principle at the Sub-kBT Level](#) by Alexei Orlov, Craig Lent et al, 2012 (5 pages).

²⁴⁰⁰ See [Experimental Tests of the Landauer Principle in Electron Circuits, and Quasi-Adiabatic Computing Systems](#) by Alexei O. Orlov et al, 2012 (5 pages) which is integrated in [Energy Limits in Computation](#) by Craig Lent, Alexei Orlov et al, 2019 (245 pages).

However, this adiabatic CMOS technique requires a larger number of transistors. Therefore, emerges a new trade-off between a larger and more expensive to design and manufacture power saving component vs cheaper but more energy hungry conventional counterparts. Still, the environmental cause has recently revived interest in reversible and adiabatic computing. It is promoted by the Computer Community Consortium group of the American **Computing Research Association** with the lead from Michael P. Frank's team at **Sandia National Labs**²⁴⁰¹.

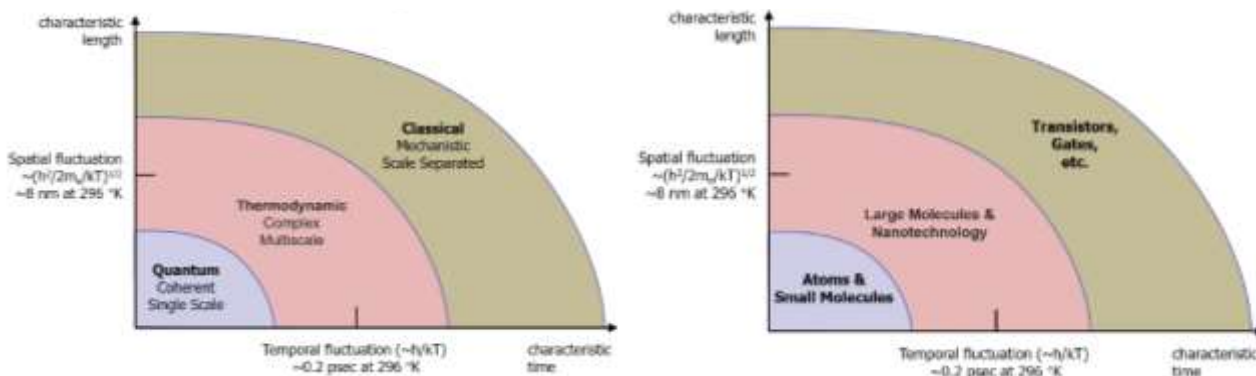


Figure 600: Source: [Thermodynamic Computing](#), Computer Community Consortium of the Computing Research Association, 2019 (36 pages).

They position it as an intermediate architecture between classical and quantum computing, but on quantities that are not necessarily relevant (dimension of components and duration of state fluctuation, see Figure 600)²⁴⁰². The purpose of the manifesto is to obtain US federal credits to finance this research. So, the story is not over!

Superconducting computing

The idea of creating superconducting computers capable of taking advantage of the lack of resistance of low temperature electronic components dates back to the early 1960s. Its history evolves in parallel with reversible and adiabatic computing. It started with the discovery of the Josephson effect in 1962. This effect was later used to create two-states superconducting qubits with research starting in the early 1980s.

The expected benefits of superconducting transistors are an increase in clock frequency and a decrease in power consumption²⁴⁰³! The gain is more significant with the clock frequency than with energy consumption. For example, in a Japanese SFQ component realized in 2019, the clock was 32 GHz while the power drain was 2.5 TOPS per Watt, in the average of most deep learning CMOS chips²⁴⁰⁴ (Figure 601).

²⁴⁰¹ See [Thermodynamic Computing](#), Computer Community Consortium of the Computing Research Association, 2019 (36 pages). It is a manifesto to develop thermodynamically responsible computing inspired by biomimicry. The document is the result of a workshop with about 40 participants, almost all American except one researcher from London and another from Luxembourg, from universities and a few private actors such as Google, Rigetti, HPE, Knowm (which develops memristor-based circuits for AI applications, their kT-RAM technology) and Daptics (ex Protolife, created by Norman Harry Packard (1954) and which develops chemical simulation algorithms).

²⁴⁰² See [Quantum Foundations of Classical Reversible Computing](#) by Michael P. Frank and Karpur Shukla, April 2021 (70 pages) and [The Reversible Computing Scaling Path: Challenges and Opportunities](#) by Michael P. Frank, February 2022 (40 slides).

²⁴⁰³ See this very interesting presentation on superconducting electronics: [Superconducting Microelectronics for Next-Generation Computing](#) by Leonard Johnson, MIT Lincoln Labs, November 2018 (27 slides). The gain in power consumption would be between 10 and 1,000. The integration level is currently low, of the order of 200 nm compared to 7 nm for the densest CMOS processors. But it is steadily increasing. There are even investigations to combine superconducting transistors, optoelectronics and neural networks. See [Superconducting Optoelectronic Loop Neurons](#) by Amir Jafari-Salim, 2018 (48 pages).

²⁴⁰⁴ See [29.3 A 48GHz 5.6mW Gate-Level-Pipelined Multiplier Using Single-Flux Quantum Logic](#) by Ikki Nagaoka et al, 2019.

Appealing Feature of SFQ Circuits

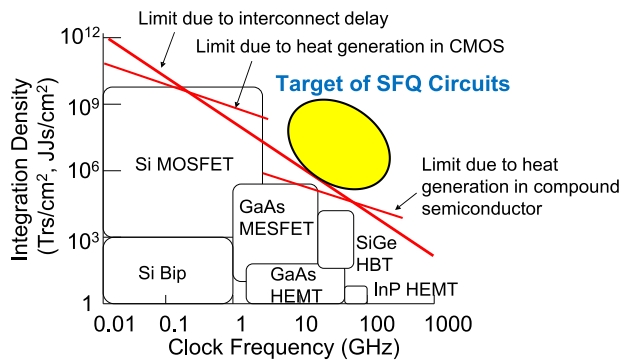


Figure 601: schematic positioning SFQs in terms of clock speed and integration compared to traditional electronic components. Source: [Impact of Recent Advancement in Cryogenic Circuit Technology](#) by Akira Fujimaki and Masamitsu Tanaka, 2017 (37 slides).

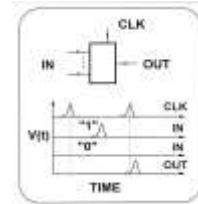
RSFQ - Rapid Single Flux Quantum

Timeline:

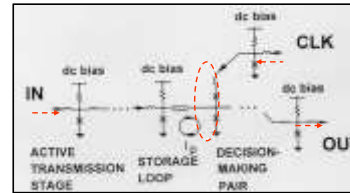
invented in 85-86, generally accepted in 90, adopted in the US in 91, became the main digital superconducting electronics by mid-end of 90s, first product by mid-00s

$$\int V dt = \Phi_0 = h/2e = 2.07 \text{ mV} \cdot \text{ps}$$

$$E_{\text{SFQ}} = 10^{-19} \text{ J}$$



Both Data and Clock are SFQ voltage pulses $V(t)$ with quantized areas



- > 750 GHz digital frequency divider demonstrated
- > internal memory
- > gate-level pipelining
- > high-throughput
- > low switching power
- > dc bias only
- > local timing
- > amendable for synchronous and asynchronous schemes

Several generations of superconducting components have been developed over time²⁴⁰⁵:

- **SFQ** (Single Flux Quantum) was a first-generation circuit, limited to a 1 GHz and 300 Mhz clock frequency. Work started at IBM in the 1960s. They had invested the equivalent of \$100M today in a program that was partly funded by the NSA and which was abandoned in 1983 which are also based on the Josephson effect²⁴⁰⁶. D-Wave's superconducting qubit use SFQ-type components for generating and reading qubit control signals²⁴⁰⁷.
- **RSFQ** (Rapid Single Flux Quantum) was coinvented in Russia in the mid-1980s by Konstantin K. Likharev and his then-PhD student Oleg Mukhanov. Mukhanov then moved to the USA and joined Hypres in 1991 to launch the industry development of RSFQ. The first ones were produced in the mid-2000s²⁴⁰⁸ (Figure 602). They have the advantage of being able to operate up to 750 GHz. They can be used to create ALUs (Arithmetic Logic Units²⁴⁰⁹) running at 20/30 GHz as well as ADCs (analog to digital converters) running up to 40 GHz²⁴¹⁰. In RSFQ logic, binary information is managed in the form of quantum states of the Josephson junction flux, which is transferred as voltage pulses²⁴¹¹. However, the technology does not use state superposition and entanglement as in superconducting qubits. **Hypres** develops radio frequency reception systems using two superconducting components: **SQUID** (Superconducting Quantum Interference Device) based antennas that allow to capture magnetism with precision (invented in 1964) and an RSFQ chip running at 30 GHz with 11K JJ (Josephson junctions)²⁴¹²!

²⁴⁰⁵ See [Single Flux Quantum \(SFQ\) Circuit Fabrication and Design: Status and Outlook](#) by V. Bolkhovskiy et al, Lincoln Laboratory at MIT, 2016 (34 slides) which provides an interesting view on their manufacturing process and metal layers, and IRDS [Cryogenic Electronic and Quantum Information Processing](#), IEEE, 2021 (93 pages) which provides a good overview of the various SFQ technologies around.

²⁴⁰⁶ See [The Long Arm of Moore's Law: Microelectronics and American Science](#) by Cyrus Mody, 2017 (299 pages), page 58.

²⁴⁰⁷ See [Architectural considerations in the design of a superconducting quantum annealing processor](#) by P. I. Bunyk et al from D-Wave, 2014 (9 pages).

²⁴⁰⁸ Source: [Single Flux Quantum Logic for Digital Applications](#) by Oleg Mukhanov of SEEQC/Hypres, August 2019 (33 slides).

²⁴⁰⁹ See for instance [qBSA: Logic Design of a 32-bit Block-Skewed RSFQ Arithmetic Logic Unit](#), 2020 (3 pages).

²⁴¹⁰ This would be very useful to generate the microwaves to drive superconducting and silicon qubits.

²⁴¹¹ Time management in logic programming must take this into account. On this topic, see [A Computational Temporal Logic for Superconducting Accelerators](#) by Georgios Tzimpragos et al, 2020 (14 pages).

²⁴¹² See [Superconducting Quantum Arrays for Wideband Antennas and Low Noise Amplifiers](#) by Oleg Mukhanov et al, 2014 (36 slides).

- **AQFP** (Adiabatic Quantum Flux Parametron) which comprises two superconducting Josephson loops connected together by an inductance, reminiscent of the nSQUID principle²⁴¹³. The process is very energy efficient due to its ability to be reversible. A recent work from Japanese researchers prototypes a AQFP processor using 20,000 Josephson gates operating at 4.2K²⁴¹⁴.
- **RQL** (Reciprocal Quantum Logic)²⁴¹⁵, **eRSFQ** (Energy Efficient RSFQ) and **eSFQ** (Energy Efficient SFQ) are variants of the RSFQ that are more energy efficient due to the absence of bias resistance, replaced by an inductance. This is the variant chosen by Hypres and its subsidiary SEEQC. Their SFQs combine eRSFQs, of which they are the originators, and eSFQs. RQLs are studied to create superconducting memories.

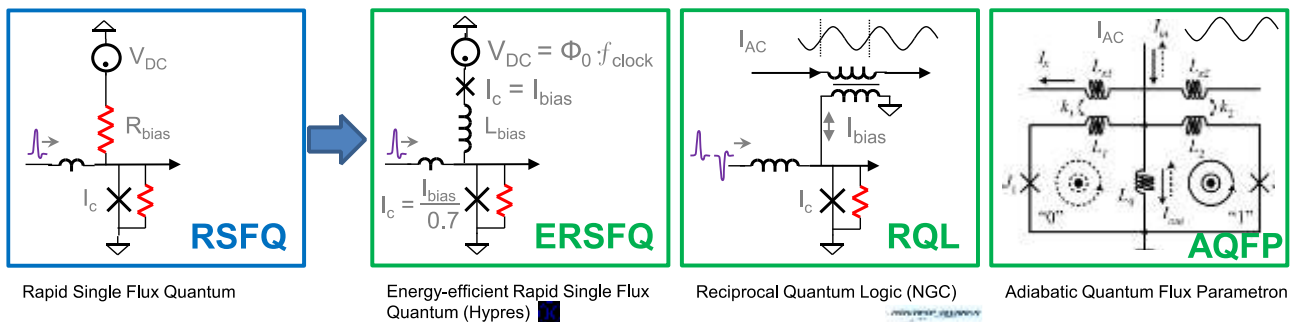


Figure 602: RSFQ and its evolutions, ERSFQ, RQL and AQFP. Source: [Single Flux Quantum Logic for Digital Applications](#) by Oleg Mukhanov of SEEQC/Hypres, August 2019 (33 slides).

- **SFETs** (Superconducting FETs, Field Effect Transistors) which implement a concept similar to adiabatic CMOS, but with a superconducting component. These components have been developed since the 1980s²⁴¹⁶.

There are a few other variants of superconducting components that I will just mention (SSV, SVJJ, STTJJ, S3JJ) because they do not seem to be common, on top of JM RAM that is investigated for implementing superconducting memory. Also, some researchers are looking into the way to create superconducting diodes using the Meissner effect, which could be useful in creating superconducting computing solutions²⁴¹⁷.

To date, the integration record for this type of component is only 144,000 Josephson junctions in a chip, realized in a 248 nm integration²⁴¹⁸ if we don't account for D-Wave's Pegasus chip with its million Josephson junctions including about 10,000 JJs used in their annealer qubits, the rest being used for qubits control logic and digital signals multiplexing/demultiplexing.

²⁴¹³ See [Adiabatic Quantum-Flux Parametron: Towards Building Extremely Energy-Efficient Circuits and Systems](#), by Olivia Chen et al, 2018 (10 pages) and [Design and Implementation of a Bitonic Sorter-Based DNN Using Adiabatic Superconducting Logic](#) also from Olivia Chen et al, 2019 (24 slides).

²⁴¹⁴ See [MANA: A Monolithic Adiabatic iNtegration Architecture Microprocessor Using 1.4-zJ/op Unshunted Superconductor Josephson Junction Devices](#) by Christopher L. Ayala et al, December 2020 (14 pages). They provide some impressive cryogenic needs for using this technology at a supercomputing scale.

²⁴¹⁵ See [Ultra-Low-Power Superconductor Logic](#) by Quentin P. Herr et al, 2011 (7 pages).

²⁴¹⁶ See [Josephson Junction Field-effect Transistors for Boolean Logic Cryogenic Applications](#) by Feng Wen, 2019 (7 pages) and [Superconducting silicon on insulator and silicide-based superconducting MOSFET for quantum technologies](#) by Anaïs Francheteau, 2017 (153 pages).

²⁴¹⁷ See [Ubiquitous Superconducting Diode Effect in Superconductor Thin Films](#) by Yasen Hou et al, MIT, PRL, July 2023 (6 pages).

²⁴¹⁸ See [Advanced Fabrication Processes for Superconducting Very Large Scale Integrated Circuits](#) by Sergey K. Tolpygo, 2015 (43 slides).

Another key component has been developed, superconducting diodes with zero resistance in one direction. They were experimented in 2022 with europium sulfide thin film separating a superconducting aluminum and a normal metal copper layer²⁴¹⁹ and, separately, with niobium bromide placed between layers of niobium diselenide²⁴²⁰.

In the mid-2000s, the NSA invested \$400M in the RSFQ over the 2005-2010 period. Its goal was to create a processor with one million logic gates running at 50 GHz. The NSA document describing the project is surprisingly detailed and highly informative. It reveals the scope of the related technological challenges²⁴²¹ (Figure 604). In particular, for creating cryogenic memories, superconducting or not: CMOS-Josephson junction hybrid, spintronic based²⁴²², SFQ or monolithic RSFQ-MRAM. Then the communication between the cryogenic electronics and room temperature components, with a 25 Gbits/s optical fiber that we would probably now reach 100 or 200 Gbits/s, leaving aside the question of the optical signal modulation and demodulation.

Cryogenics must be sized to support a large number of components. For testing purpose, a simple pulsed tube would be sufficient but more imposing installations are planned as computing power would grow, as in the illustration in Figure 603 on the right.

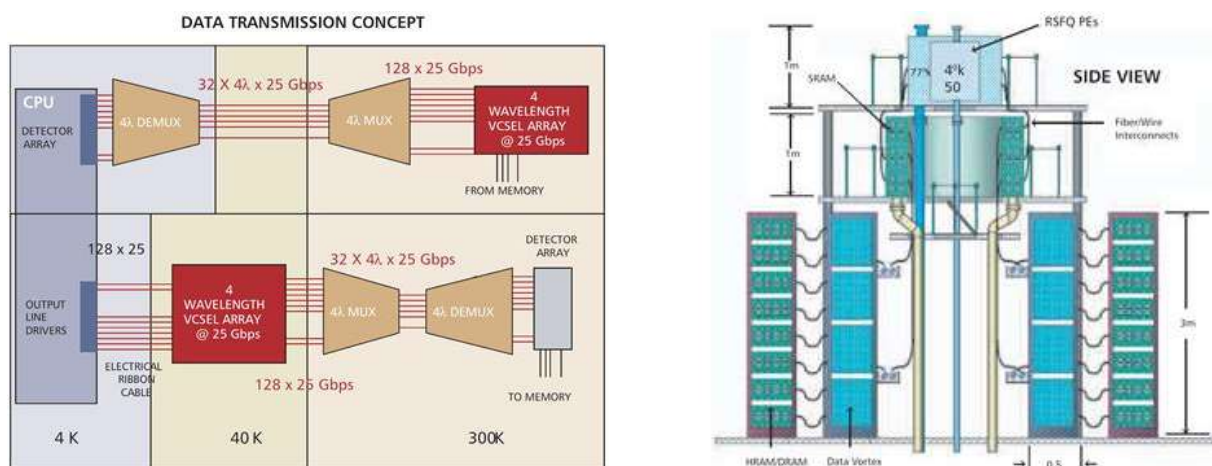


Figure 603: Left: A 64-fiber system for bi-directional transmission totaling 6.4 Tbps between a superconducting processor operating at 4K and high speed mass memory at ambient temperature. Optical connections are shown in red and electrical in black. This technology was to be available by 2010. Right: concept for a large-scale system including cryogenic cooling unit for supercomputers. Source: [NSA Superconducting Technology Assessment, 2005 \(257 pages\), pages 100 and 125.](#)

The project relied mainly on **Hypres**, the only American company entirely dedicated to the creation of superconducting components, who runs its own foundry since 1983, but then divested it to SEEQC and now seems to rely on SkyWater's foundry. They were supplying radio frequency components for military use cases. Out of this, they developed an 8-bit RSFQ processor and 28,000 Josephson junctions.

There is also **Northrop Grumman** with its foundry located in Linthicum, Maryland. Finally, **Chalmers University** in Sweden and various research laboratories in the USA (JPL, Berkeley, Stony Brook) as well as the **NIST** Boulder laboratory were also involved. **IMEC** has a lab in Florida that designs superconducting circuits with densities in the 10 nm to 20 nm range.

²⁴¹⁹ See [Superconducting spintronic tunnel diode](#) by E. Strambini et al, Nature Communications, May 2022 (7 pages).

²⁴²⁰ And [The field-free Josephson diode in a van der Waals heterostructure](#) by Heng Wu et al, Nature, April 2022 (17 pages).

²⁴²¹ See [NSA Superconducting Technology Assessment, 2005 \(257 pages\)](#). The document is quite old but still very well crafted and interesting.

²⁴²² See [Cryogenic Memory Architecture Integrating Spin Hall Effect based Magnetic Memory and Superconductive Cryotron Devices](#) by Minh-Hai Nguyen et al, July 2019 (12 pages) and [Modeling the computer memory based on the ferromagnet/superconductor multilayers](#) by Serhii E. Shafraniuk, Ivan P. Nevirkovets and Oleg A. Mukhanov, July 2019 (27 pages).

TABLE 2-2. SUPERCONDUCTOR RSFQ MICROPROCESSOR DESIGN PROJECTS					
Time Frame	Project	Target Clock	Target CPU Performance (peak)	Architecture	Design Status
1997-1999	SPELL processors for the HTMT petaflops system (US)	50-60 GHz	~250 GFLOPS/CPU (est.)	64-bit RISC with dual-level multithreading (~120 instructions)	Feasibility study with no practical design
2000-2002	8-bit FLUX-1 microprocessor prototype (US)	20 GHz	40 billion 8-bit integer operations per second	Ultrapipelined, multi-ALU, dual-operation synchronous long instruction word with bit-streaming (~25 instructions)	Designed, fabricated; operation not demonstrated
2002-2005	8-bit serial CORE1 microprocessor prototypes (Japan)	16-21 GHz local, 1 GHz system	250 million 8-bit integer operations per second	Non-pipelined, one serial 1-bit ALU, two 8-bit registers, very small memory (7 instructions)	Designed, fabricated, and demonstrated
2005-2015 (est.)	Vector processors for a petaflops system (Japan)	100 GHz	100 GFLOPS/CPU (target)	Traditional vector processor architecture	Proposal

TABLE 3.2-2. STATUS OF LOW-LATENCY CRYO-RAM CANDIDATES					
Type/Lab	Access Time	Cycle Time	Power Dissipation	Density	Status
Hybrid J-CMOS (UC Berkeley)	500 ps for 64 kb	0.1 - 0.5 ns depending on architecture	12.4 mW read 10.7 mW write (Single cell writing)	64 kb in < 3x3 mm ²	All parts simulated and tested at low speed
RSFQ decoder w/ latching drivers (ISTEC/SRL)	?	0.1 ns design goal	107 mW for 16 kb (Estimate)	16 kb in 2.5 cm ² (Estimate*)	256b project completed (Small margins)
RSFQ decoder w/ latching drivers (NG)	?	2 ns	?	16 kb/cm ² *	Partial testing of 1 kb block
SFQ RAM (HYPRES)	400 ps for 16 kb (Estimate)	100 ps for 16 kb (Estimate)	2 mW for 16 kb (Estimate)	16 kb/cm ² *	Components of 4 kb block tested at low speed
SFQ ballistic RAM (Stony Brook University)	?	?	?	Potentially dense Requires refresh	Memory cell and decoder for 1 kb RAM designed
SFQ ballistic RAM (NG)	?	?	?	Potentially dense Requires refresh	SFQ pulse readout simulated
MRAM (40K)	Comparable to hybrid CMOS	Comparable to hybrid CMOS	< 5mW at 20GHz (Estimate)	Comparable to DRAM (Estimate)	Room temperature MRAM in preproduction; Low temperature data sparse

*Densities of 1J memories are given for the technologies in use at the time of the cited work. Greater densities can be expected when a 20 kA/cm² process is used. The symbol ? signifies insufficient data.

Figure 604: various superconducting electronic projects launched about 20 years ago with processors on the left and cryo-RAM on the right, reminding us how long these projects can last or have their ups and downs. These projects became the C3 IARPA project that lasted until 2022. Source: [NSA Superconducting Technology Assessment, 2005 \(257 pages\), pages 28 and 53.](#)

The IARPA agency has taken over with the **Cryogenic Computing Complexity (C3)** project launched in 2014. It involved IBM, Northrop Grumman (Quentin Herr, who works at IMEC in Belgium since May 2021), Raytheon and Hypres and was due to end in 2018²⁴²³ (Figure 606).

It ended in 2022. A total of \$700M was spent in R&D there given the project was considered to be strategic. Some of the showstoppers there were the lack of EDA tools (electronic design automation) adapted to superconducting circuits and of scalable cryogenic cabling (leading to the Supercables project). There are solutions with signals frequency upconvert to optical wavelengths with VCSEL chips, but these are consuming a lot of energy.

This project was part of the **National Strategic Computing Initiative (NSCI)** launched in 2015 by the White House, which focused on the development of supercomputers. It is difficult to find out what this project has achieved (Figure 605).

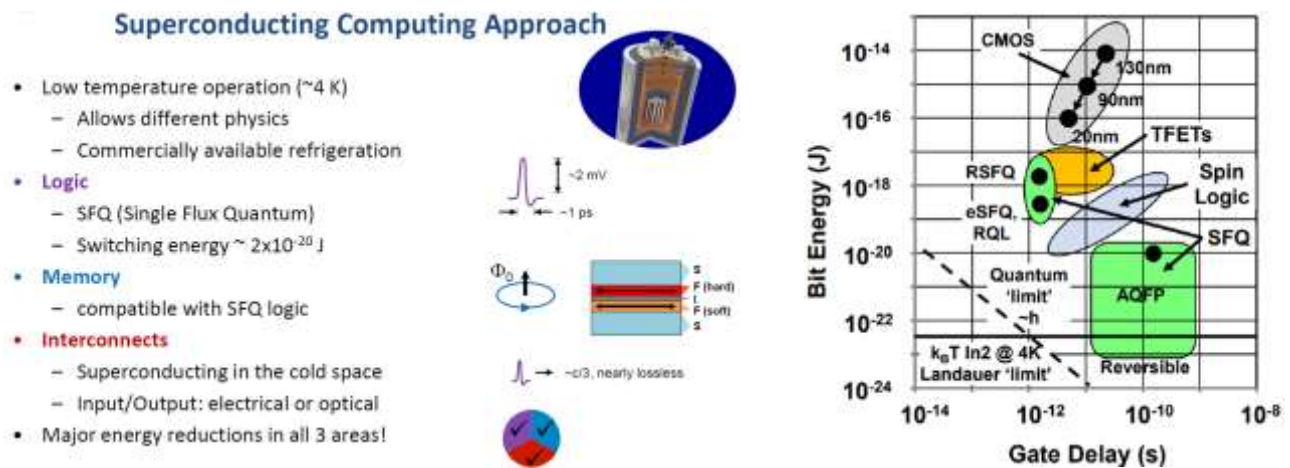


Figure 605: superconducting approach and gate delay. Source: TBD.

²⁴²³ See [Superconducting Computing and the IARPA C3 Program](#) by Scott Holmes, 2016 (57 slides). All the presentations of the C3 conference are [here](#).

In the USA, the **DISCoVER** (Design & Integration of Superconductive Computation for Ventures beyond Exascale Realization) expedition is working on a “SuperSoCC” SFQ-based niobium chip (superconductive system of cryogenic computing cores) operating at 4.2K. The project is led by Masoud Pedram, Timothy Pinkston and Murali Annavaram from USC. They are working on on-chip memory design and interface between room electronics and cryo-electronics. The team touts a potential energy gain of /100 vs classical computing or 10x speed improvement with the same energy consumption. With a relatively modest funding of \$15M coming from the NSF, the project also involves Auburn University, Cornell University, Northeastern University, Northwestern University, University of Rochester and Yokohama National University in Japan.

Outside the USA, the **Japanese Superconducting Computing Program's** ambition in 2004 was to create a processor running at 100 GHz generating 100 GLOPS in SFQ, supplemented by 200 TB of DRAM running at 77K to generate a 1.6 PFLOPS system comprising 16,384 processors (Figure 607).

PROCESS	Current density [kA/cm ²]	minimum area [μm ²]	Maximum integration	Maximum frequency [GHz]
Hypres #03-10-45	0.03 1.0 4.5	~ 3,14	15,000	80 GHz RnIc=1.3mV @ 4.5 kA/cm ² 200 GHz @ 30 kA/cm ²
Hypres #S45/100/200	0.1 1 4.5 10 20 30	~ 0.4	10,000	240 GHz RnIc=2.17 mV @ 50 kA/cm ² 80 GHz
MIT Lincoln Lab SFQx	10 20 50	~ 0.06	~ 800,000	80 GHz
ADP2	10	1.0	1100 JJ/mm ²	30 GHz - 150 GHz
STP2	2.5 - 20	0.25 - 4.0	100 JJ/mm ² - > 2,000 JJ/mm ²	80 GHz
HSTP	10	1.0	70,000	40 GHz RnIc = 0.256 mV
Fluxonics standard	1	12.5	100 JJ/mm ²	300 GHz RnIc = 0.1mV - 0.7mV
INRIM SNIS	up to 100	25	1,000 JJ/mm ²	300 GHz RnIc = 0.1mV - 0.7mV
NIST Nb/Nbx Si1-x/Nb	up to 110	?	70,000	300 GHz
INRIM SNIS 3D FIB	up to 100	0.1	10,000 JJ/mm ²	300 GHz RnIc=0.1mV - 0.7mV

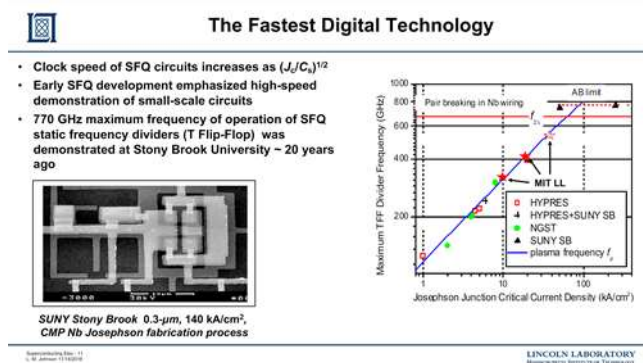


Figure 606: the left table comparing different types of superconducting components comes from [Superconducting Computing](#) by Pascal Febvre, CNRS, 2018 (56 slides). The right slide comes from [Superconducting Computing and the IARPA C3 Program](#) by Scott Holmes, 2016 (57 slides).

All this with a cryostat consuming 12 MW and generating a thermal power of 18 kW at 4.2K. It has not yet seen the light of day about 17 years later²⁴²⁴. Meanwhile, the IBM Summit supercomputer using traditional processors and GPUs generates 200 petaFLOPS consuming 13 MW, so why bother?



Figure 607: the left slide comes from [Superconducting Computing and the IARPA C3 Program](#) by Scott Holmes, 2016 (57 slides) and the right schema comes from [Superconducting Computing](#) by Pascal Febvre, CNRS, 2018 (56 slides).

²⁴²⁴ They managed to create the CORE1 α in 2003 at 4,999 JJ (Josephson junctions) running at 15 GHz, the CORE1 β in 2006 at 10,955 JJ running at 25 GHz, the CORE1 γ with 22,302 JJ also at 25 GHz, the CORE100 in 2015 at 3073 JJ and 100 GHz, the COREe2 in 2017 at 10,655 JJ and 50 GHz with an integrated memory. See [Impact of Recent Advancement in Cryogenic Circuit Technology](#) by Akira Fujimaki and Masamitsu Tanaka, 2017 (37 slides). This continued in 2019 with an 8-bit multiplier containing 20,251 JJ running at 48 GHz and consuming 5.6 mW. Source: [29.3 A 48GHz 5.6mW Gate-Level-Pipelined Multiplier Using Single-Flux Quantum Logic](#) by Ikki Nagaoka et al, 2019.

China announced in 2018 a \$145M plan to build a superconducting computer by 2022. They had then created a chip with 10,000 Josephson junctions. Not sure they are ready for this milestone. **Russia** also has ambitions in this field²⁴²⁵.

In **France**, the laboratory CMNE (Micro Nano Electronic Components) of the IMEP-LaHC (Micro-electronics, Electromagnetism, Photonics, Microwave) of the UGA (Grenoble) was working in this area, under the responsibility of Pascal Febvre who is based in Chambéry.

In **Korea**, researchers from Seoul National University have proposed another path, creating computers with CryoMOSFET chips operating at a relatively hot temperature of 77K, reducing cooling costs. Its benefits are less impressive than superconducting computing with an improvement of only 41% in single thread performance for the same power budget or a power reduction of 38% for the same performance, all of this including of course the cooling power budget²⁴²⁶.

One lone warrior in that space is **Quentin Herr**, a former engineer of Northrop Grumman who now works at IMEC in Florida. He and his wife Anna Herr and his team at IMEC are working on superconducting electronics in many areas. He is expecting superconducting HPCs to reduce power drain by 100 compared to classical HPCs²⁴²⁷. He is working on improving superconducting components density with multilayers chips²⁴²⁸, on creating Josephson based memories^{2429 2430}, on synchronous and asynchronous data communication^{2431 2432} and on amplifiers²⁴³³.

In the end, this branch of the superconducting computer industry is for the moment still immature. It has suffered from the uninterrupted advance of Moore's Law in the last few years and the difficulties of its practical implementation. It is not impossible that synergies will develop between quantum computing and this somewhat neglected branch. They can help each other, as can be seen with superconducting circuits for driving superconducting qubits or silicon. As we know, quantum computing will perhaps indirectly revive this sector²⁴³⁴!

²⁴²⁵ See [The Outlook for Superconducting Computers](#) by R Colin Johnson, 2018.

²⁴²⁶ See [CryoCore: A Fast and Dense Processor Architecture for Cryogenic Computing](#) by Ilkwon Byun et al, 2020 (14 pages).

²⁴²⁷ See [Superconducting Digital Computing: Promise-Progress-Prospects](#) by Quentin Herr and Anna Herr, IMEC, November 2021 (24 slides).

²⁴²⁸ See [Scaling NbTiN-based ac-powered Josephson digital to 400M devices/cm²](#) by Anna Herr, Quentin Herr et al, IMEC, March-April 2023 (7 pages).

²⁴²⁹ See [Superconducting Pulse Conserving Logic and Josephson-SRAM](#) by Quentin Herr, Trent Josephsen and Anna Herr, IMEC, March 2023 (6 pages).

²⁴³⁰ See [Experimental demonstration of a Josephson magnetic memory cell with a programmable \$\pi\$ -junction](#) by I. M. Dayton, Quentin Herr et al, November 2017-February 2018 (5 pages).

²⁴³¹ See [Isochronous Data Link Across a Superconducting Nb Flex Cable with 5 femtojoules per Bit](#) by Haitao Dai, Anna Herr, Quentin Herr et al, September-October 2021 (7 pages).

²⁴³² See [Synchronous Chip-to-Chip Communication with a Multi-Chip Resonator Clock Distribution Network](#) by Jonathan Egan, Quentin Herr, Anna Herr et al, September 2021-July 2022 (8 pages).

²⁴³³ See [True Differential Superconducting On-Chip Output Amplifier](#) by Jonathan Egan, Andrew Brownfield and Quentin Herr, April 2021 (5 pages).

²⁴³⁴ At last, see this good review paper [Beyond Moore's technologies: operation principles of a superconductor alternative](#) by Igor I. Soloviev et al, Russia, 2017 (22 pages). It mentions the potential of a two orders of magnitude gain in energy efficiency with superconducting based supercomputers, cryogenics included. On top of the various variations of SFQ, RQL and SQUID superconducting circuits, the review also covers cryogenic memory. One of the limitations of superconducting circuits is their low potential miniaturization. Josephson junctions density seems limited to 2.5 million junctions per cm². To be compared with billions of CMOS transistors with 5nm/7nm nodes!

Probabilistic computing

Probabilistic processors are another variation of exotic processors. They use probabilistic p-bits that can fluctuate rapidly between 0 and 1 with a low transition energy level. They are supposed to allow the resolution of so-called "quantum" problems without relying on quantum mechanisms. p-bits can be realized with nanomagnets, with regular transistors²⁴³⁵, with photonic devices²⁴³⁶ and with the weird membrane computing field²⁴³⁷.

Various applications are promoted such as the creation of neural networks called BSN (Binary Stochastic Neuron), restricted Boltzmann Machines (RBM)²⁴³⁸ and the resolution of optimization problems like those treated by quantum annealing and gate-based quantum computing. The accelerations obtained are not qualified as exponential. It may be just polynomial, which is still interesting.

Work in this direction is quite recent and comes from the **MIT**, **UCSB**, **Cornell University**, **Purdue University** in Indiana²⁴³⁹ and from **Tohoku University** in Japan²⁴⁴⁰. **HawAI.tech** (France), a Grenoble-based startup, is positioned on the same niche and targets applications in the field of AI in embedded systems using data from various sensors²⁴⁴¹.



Their roadmap should lead to the creation of a complete probabilistic computer by 2024.

One original application of probabilistic computing is the simulation of quantum algorithms with mapping each qubit on 8 probabilistic bits, but it doesn't describe how it is handling entangled states²⁴⁴².

Optical computing

Many research laboratories and startups are working on the creation of analog optical processors that are not based on photon qubits²⁴⁴³. Some are creating classical optical neural networks, others are adapted to convolutional neural networks or spiking neurons, the latter being closest to the way the human brain works^{2444 2445}. Others are even proposing to handle vector/matrix manipulation and solve NP complete problems with Ising models, beyond the coherent Ising model machines I briefly

²⁴³⁵ See an explanation of p-bits in [Waiting for Quantum Computing? Try Probabilistic Computing](#) by Kerem Camsari and Supriyo Datta, IEEE Spectrum, March 2021, then [Integer factorization using stochastic magnetic tunnel junctions](#) by William A. Borders et al, 2019, [p-Bits for Probabilistic Spin Logic](#) by Kerem Y. Camsari, 2019 (11 pages), [Stochastic for Invertible Logic](#) by Brian Sutton et al, 2017 (19 pages) and [Probabilistic computing with p-bits](#) by Jan Kaiser and Supriyo Datta, October 2021 (8 pages).

²⁴³⁶ See [MIT Makes Probability-Based Computing a Bit Brighter The p-bit harnesses photonic randomness to explore a new computing frontier](#) by Margo Andreson, IEEE Spectrum, July 2023, which refers to [Biasing the quantum vacuum to control macroscopic probability distributions](#) by Charles Roques-Carnes et al, MIT and Harvard University, Science, July 2023 (9 pages).

²⁴³⁷ See [A quick introduction to membrane computing](#) by Gheorghe Paun, The Journal of Logic and Algebraic Programming, May 2010 (4 pages).

²⁴³⁸ See [Machine Learning Quantum Systems with Magnetic p-bits](#) by Shuvro Chowdhury et al UCSB, October 2023 (3 pages).

²⁴³⁹ See [From Charge to Spin and Spin to Charge: Stochastic Magnets for Probabilistic Switching](#) by Kerem Y. Camsari et al, February 2020 and [Hardware Design for Autonomous Bayesian Networks](#) by Rafatul Faria et al, 2020 (10 pages).

²⁴⁴⁰ See [Demonstrating the world's fastest spintronics p-bit](#) by Tohoku University, March 2021 and [Waiting for Quantum Computing? Try Probabilistic Computing](#) by Kerem Camsari and Supriyo Datta, 2021.

²⁴⁴¹ See [Bayes from Cell to Chip](#) by Pierre Bessière, 2018 (33 slides).

²⁴⁴² See [Simulation of quantum algorithms using classical probabilistic bits and circuits](#) by D. D. Yavuz and A. Yadav, University of Wisconsin, July 2023 (61 pages).

²⁴⁴³ See the review paper [Analogue Photonics Computing for Information Processing, Inference and Optimisation](#) by Nikita Stroeve and Natalia G. Berloff, Weizmann Institute of Science and University of Cambridge, January 2023 (117 pages).

²⁴⁴⁴ See [Analog optical computing for artificial intelligence](#) by Jiamin Wu et al, Engineering, 2021 (9 pages).

²⁴⁴⁵ See [The role of all-optical neural networks](#) by Matuszewski Michał et al, June 2023 (13 pages).

discussed in the part dedicated to photon qubits. These solutions' potential advantage is computing speed as well as power efficiency.

I will try here to correctly segment this broad field²⁴⁴⁶.

SLMs and Fourier lenses systems which program linear operations and summation by collecting light power encoded signal. They are sending an image generated with a DMD, DLP or SLM chip illuminated by a laser and sent on various structures such as random matrices or various metamaterials. They are often based on the principle of the Optical Fourier Transform which allows to decompose a 2D image into spatial frequencies, itself represented in 2D. This transform is an image that contains key points representing shapes and repetitions in the analyzed images. This can be leveraged to build convolution layers in convolutional neural networks. These serve to detect the presence of shapes in an image, the shapes being represented by filters. The Fourier transform helps to automatically identify these key shapes in the image.

These systems capture the result with a CMOS sensor, usually with a very high resolution, much higher than that of the DLP or DMD chip used upstream. The diffraction thus carries out a projection in a space of larger dimension than the original image. All this is supported by serious mathematics²⁴⁴⁷.

These different solutions are in their infancy. They could accelerate certain calculations for training complex neural networks. These accelerations seem to be rather polynomial and not exponential as quantum computing is supposed to generate. Except that they do not seem to be handicapped by noise issues as qubits are.



Lighton.io (2016, France, \$3.7M) started with selling an optical coprocessor to accelerate neural networks training on large volumes of training data, such as with convolutional networks.

In their first system, a laser emitted a beam that is magnified with some lenses to illuminate a parametrized DLP micro-mirror chip. The generated image then traversed a static random matrix playing the role of a scattering medium with focusing lenses L1 and L2 before and after the filter as illustrated in Figure 608. A monochrome CMOS imaging sensor then analyzed the resulting image²⁴⁴⁸. The sensor captured the interferences generated by the set and some mathematical computing interprets the result. This process enabled a reduction of a complex data set dimensionality.

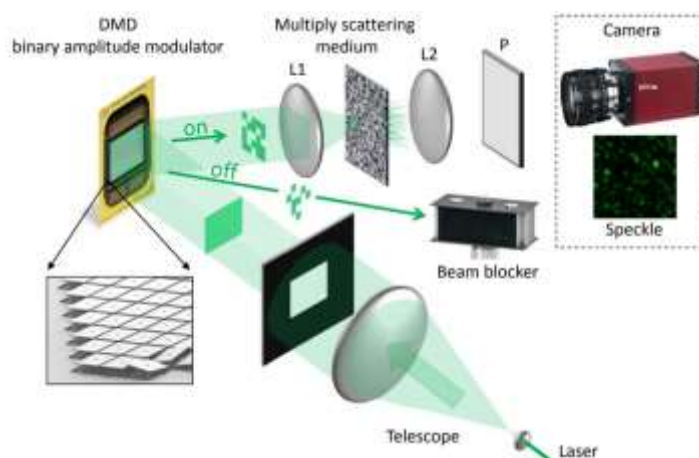


Figure 608: the LightOn optical accelerator architecture. Source: [Random Projections through multiple optical scattering: Approximating kernels at the speed of light, 2015 \(6 pages\)](#).

Everything was driven by Python libraries developed with TensorFlow. The targeted applications are first and foremost genomics and Internet of Things solutions. Since 2020, LightOn also worked on creating a photonic processor named QORE using reconfigurable linear optical networks to

²⁴⁴⁶ See [The physics of optical computing](#) by Peter L. McMahon, Cornell University, July 2023 (31 pages).

²⁴⁴⁷ See [An optical Fourier transform coprocessor with direct phase determination](#) by Alexander Macfaden et al, 2017 (8 pages) and [Performing optical logic operations by a diffractive neural network](#) by Chao Qian et al, 2020 (7 pages).

²⁴⁴⁸ The process is described in [Random Projections through multiple optical scattering: Approximating kernels at the speed of light, 2015 \(6 pages\)](#).

implement optical quantum information processing using multimode fiber with the programmable wavefront shaping of a SLM (spatial light modulator). It can have up to 8 laser inputs and 38 outputs, with fidelities $>93\%$ and losses $<6.5\text{dB}$. The device fits in a standard 19" server rack²⁴⁴⁹. The computing advantage brought by this platform is not obvious. However, its creators indicate that it could create high-dimensional entanglement from few single photon states, so these large photonic cluster states that are the Holy Grail of MBQC. The QORE project was funded as part of the H2020 OPTO-logic project (Figure 609).

In the end, the company pivoted and is now a software company working on classical LLMs (large language models) and all these fancy optical processors were abandoned.

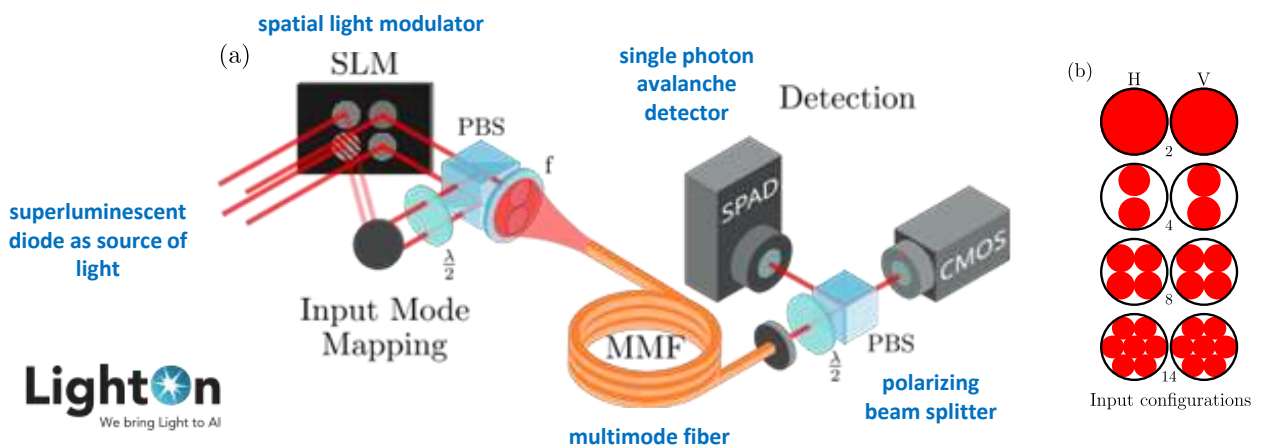


Figure 609: schematic of the Light QORE quantum processor. Source: [A high-fidelity and large-scale reconfigurable photonic processor for NISQ applications](#) by A. Cavaillès, Igor Caron, Sylvain Gigan et al, May 2022 (5 pages) with legends by Olivier Ezratty.



Optalysys (2013, UK, \$5.2M) is a spin-out of the University of Cambridge created by Nick New, Robert Todd and Ananta Palani. Their FT:X 2000 system is structured around the realization of optical fast Fourier transforms based on diffraction²⁴⁵⁰ (Figure 610).

Once input and reference data is converted into symbol representations, the data is addressed into the optical system and matches are identified on a camera sensor:

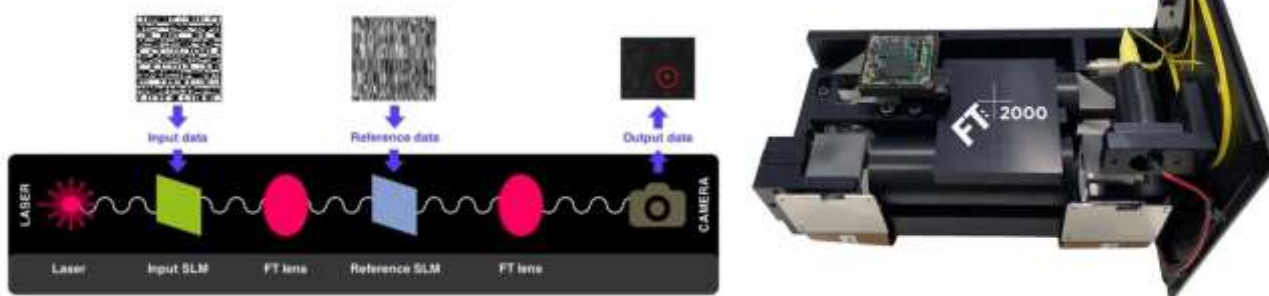


Figure 610: Optalysys process and apparatus. Source: Optalysys.

They were involved in various projects, one in genetics to do genome sequence alignment, GENESYS, carried out with the **Earlham Institute**. The other project dealt with weather forecasting for the European center ECMWF and a third one for plasma and fluid dynamics simulation, for DARPA.

²⁴⁴⁹ See [A high-fidelity and large-scale reconfigurable photonic processor for NISQ applications](#) by A. Cavaillès, Igor Caron, Sylvain Gigan et al, May 2022 (5 pages).

²⁴⁵⁰ See [Optalysys - Revolutionary Optical Processing for HPC](#), September 2017 (23 mn).

They also did run a convolutional network in 2018 on a MNIST base with 60,000 letters for training and 10,000 for testing. Its success rate was only 70%.

On-chip optical circuits can rely on wavelength multiplexing or beamsplitter meshes.

A collaborative effort in photonic chips development is run by the **PhotonDelta Foundation** (the Netherlands, 1.1B€ including 470M€ from the Dutch government), a public and private European Integrated Photonics Ecosystem fund that supports photonic chip ventures, in collaboration with the MIT. They invested in 177 projects. The program launched in 2022 is supposed to last 6 years. IMEC, LioniX and Bright Photonics are among the industry partners of this fund which gathers 26 companies, 11 technology partners and 12 R&D partners.



SaliENCE Labs (2021, UK, \$11.5M) is a startup cofounded by Vaysh Kewada (CEO) and Johannes Feldmann (CTO) and spun out of Oxford and the University of Münster in Germany.

It develops a hybrid photonic-electronic silicon chip dedicated to AI applications. Other research participants are the Universities of Pittsburgh (USA) and Exeter (UK), EPFL and IBM Research Zurich. It implements fast tensor processing running at 100 GHz. It implements sort-of in-memory photonic computing implementing optical frequency combs coupled with a classical SRAM (Static Random Access Memory)²⁴⁵¹. They could also use phase-change materials developed by Oxford University instead of SRAM²⁴⁵².



Lightelligence (2017, USA, \$36M) develops PACE, another photonic processor that is supposed to be 100 times faster than a Nvidia RTX 3080 GPU. It is designed to solve Ising models problems like D-Wave quantum annealers and Fujitsu digital CMOS-based annealers.

Their chip uses 12,000 thermal phase shifters and Mach-Zehnder interferometers (MZI) and runs at 1 GHz²⁴⁵³. It implements parallel photonic recurrent network²⁴⁵⁴. Now, how does it scale is yet to be shown.



The **Copac** project funded as part of a H2020 project is creating an optical processor that could evaluate all the variables of a logical function in parallel.

It is based on a quantum dots-based architecture that can be excited simultaneously on several frequencies by wideband lasers. The results are read by 2D spectroscopy of quantum dots. The machine would operate at room temperature. The process mixes classical computation (for the evaluation of functions) and quantum methods (to do it simultaneously on several sets of variables) (Figure 611).

²⁴⁵¹ It is documented in [Parallel convolution processing using an integrated photonic tensor core](#) by J. Feldmann et al, Nature, January 2021 (35 pages).

²⁴⁵² Oxford University researchers designed a light-based silicon photonic chip with hybridized-active-dielectric (HAD) nanowires enabling light polarization-selective tunability. They demonstrated the use of polarization as a parameter to selectively modulate the conductance of individual nanowires within a Ge₂Sb₂Te₅ (GST for germanium-antimony-tellurium, a phase changing material also used in RW optical discs and phase-change memories) and silicon multi-nanowire system. See [Polarization-selective reconfigurability in hybridized-active-dielectric nanowires](#) by June Sang Lee and al, Science Advances, June 2022 (8 pages).

²⁴⁵³ See [Deep Learning with Coherent Nanophotonic Circuits](#) by Yichen Shen et al, October 2016 (8 pages) and [Accelerating recurrent Ising machines in photonic integrated circuits](#) by Mihika Prabhu et al, Optica, April 2020 (8 pages). It seems the system can parametrize an Ising model only with coupling graph nodes with the equivalent of a longitudinal field, but not with setting longitudinal interactions at the graph node level like with D-Wave quantum annealers.

²⁴⁵⁴ The system implements hybrid photonic/classical computing with the photonic part performing a unitary matrix product of a state-preparation rotation matrix R, the desired unitary (U or U†), and one of two homodyne detection matrices (h1 or h2). Phase-intensity reconstruction, a diagonal matrix multiplication, Gaussian noise addition, and a nonlinear threshold unit are performed classically.

The project is conducted with the Universities of Liège (Françoise Remacle), Hebrew University of Jerusalem (Raphael Levine), University of Padua, the CNR Institute for Physical and Chemical Processes of Bari, the company **KiloLambda** (2001, Israel) which manufactures the quantum dots and **ProBayes** (France), a subsidiary of La Poste which produces the compiler of the solution (Emmanuel Mazer and David Herrera-Marti, who now works at CEA-LIST)²⁴⁵⁵. The great uncertainty in this project, as is often the case, concerns its scalability. It depends on the superposition of optical frequencies. The project documentation does not describe well the application domains of the possible in terms of complexity classes of addressable problems.

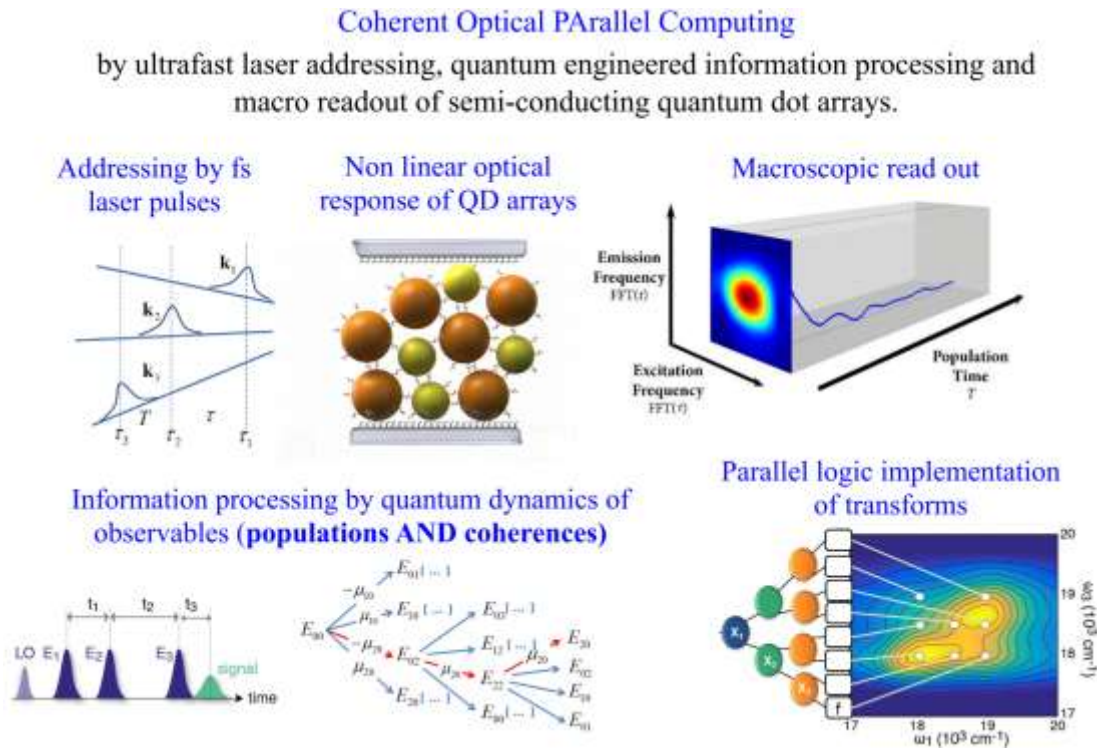


Figure 611: the optical technology behind the European Copac project.

Laser networks are complex lasers (degenerate cavity lasers, multimode fiber amplifiers, large-aperture VCSELs) with many spatial degrees of freedom and controllable nonlinear interactions. These systems can be used for reservoir computing (RC) or for matrices computing.



Luminous Computing (2018, USA, \$115M) aims to create a high-performance optical component that would replace 3000 Google TPUs! It would exploit multicolor lasers and light guides. According to the publications of their CTO, Mitchell Nahmias, it seems that they use optical spike neurons²⁴⁵⁶. They can perform calculations very quickly, including in classical CMOS.



LightSolver (2019, Israel) is a startup founded by Ruti Ben Shlomi (CEO) that develops a quantum-inspired computing solution using optically coupled lasers. It solves Max-2-SAT and 3-Regular 3-XORSAT combinatorial optimization problems.

²⁴⁵⁵ See [Coherent Optical Parallel Computing](#), 2017. The European project is funded until 2021. See more details in [Coherent Optical Parallel Computing Project Summary](#).

²⁴⁵⁶ See [Progress in neuromorphic photonics](#) by Thomas Ferreira de Lima, Mitchell Nahmias et al, 2017 (23 pages).

Neural network optical circuits which implement computing using wave mixers as shown in Figure 612. These optical neural networks can implement inferences as well as backpropagation training tasks depending on their architecture. In the case of large models, it could bring some significant energetic advantage compared to classical CMOS based inferences²⁴⁵⁷.

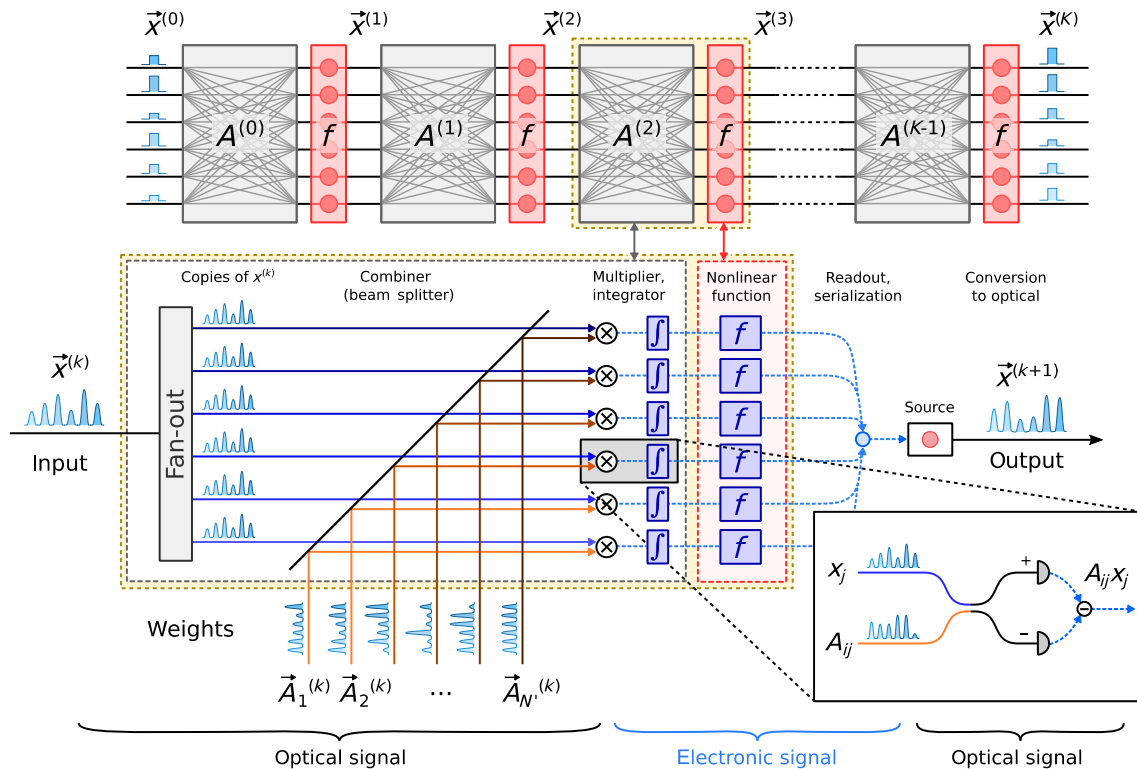


Figure 612: Source: [Large-Scale Optical Neural Networks Based on Photoelectric Multiplication](#) by Ryan Hamerly, Dirk Englund et al, MIT, PRX, 2018 (12 pages). Added in 2023.

Optical parametric oscillators (OPO) can be used to solve Ising models, like with the DOPO-based simulator and coherent Ising machines (CIM) (Figure 613).

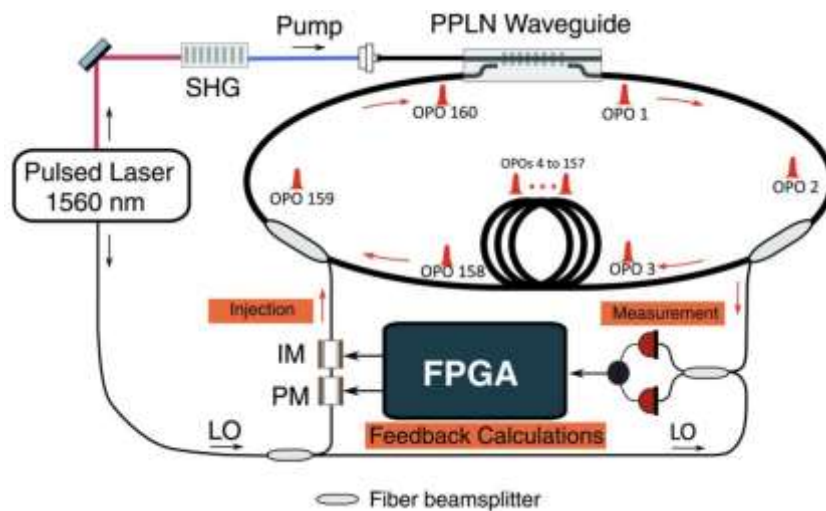


Figure 613: an OPO based optical computing system. Source: [A fully-programmable 100-spin coherent Ising machine with all-to-all connections](#) by Peter L. McMahon et al, Science, 2016 (9 pages). Added in 2023.

²⁴⁵⁷ See [Optical Transformers](#) by Maxwell G. Anderson, Shi-Yuan Ma, Tianyu Wang, Logan G. Wright, Peter L. McMahon, Cornell University, February 2023 (27 pages).

Reservoir computing is a specific category of recurrent neural networks used to process time series (in language processing, finance, energy, robotics)^{2458 2459}. Their particularity is to use neuron weights and links between neurons randomly fixed in the reservoirs, all with nonlinear activation functions for these links. The hundreds of neurons in a reservoir are fed by input data stored in the reservoirs. The activation functions nonlinearity makes this memory evanescent.

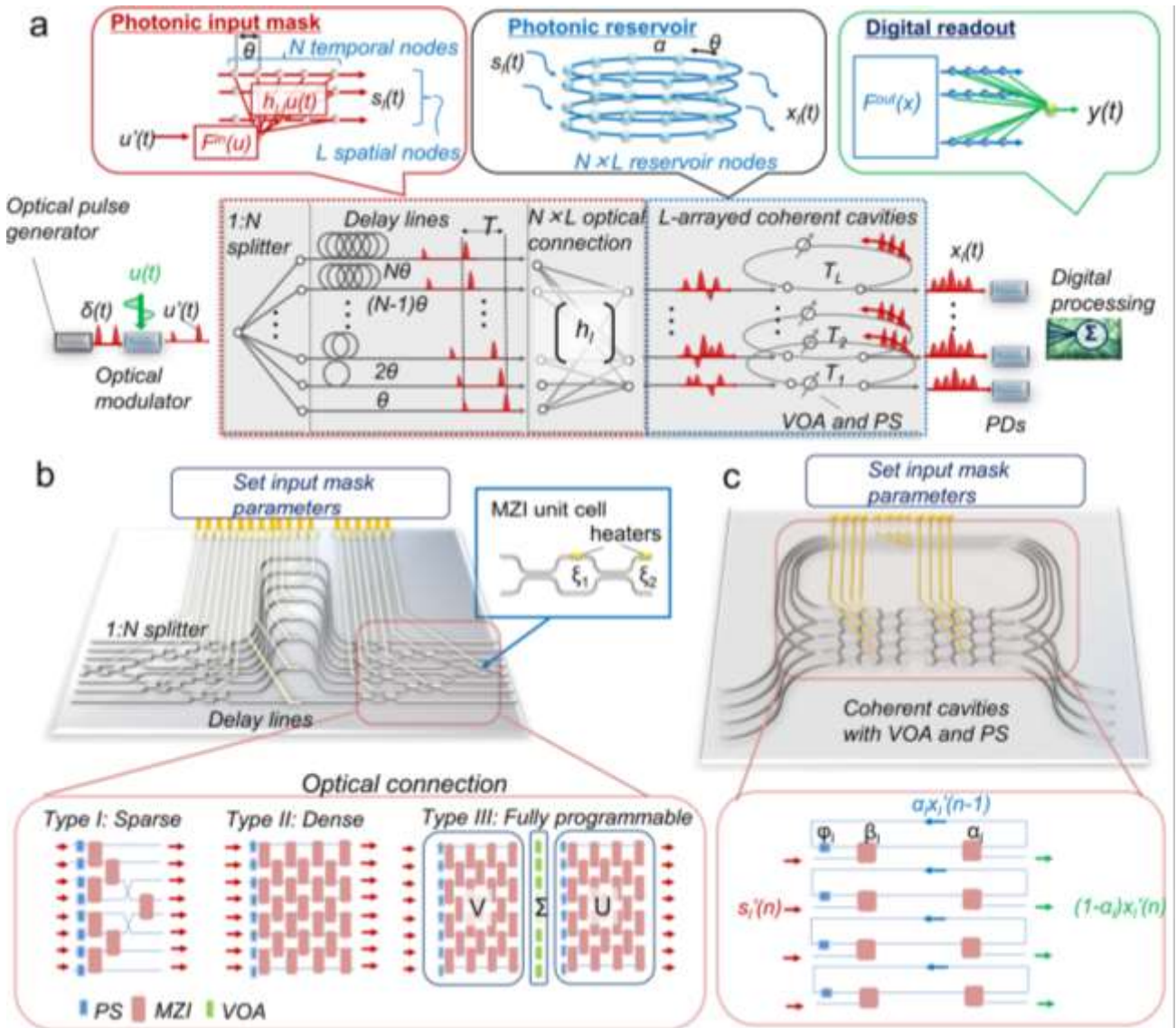


Figure 614: Source: [Scalable reservoir computing on coherent linear photonic processor](#) by Mitsumasa Nakajima, Kenji Tanaka and Toshikazu Hashimoto, *Nature Communications Physics*, February 2021 (12 pages). Added in 2023.

²⁴⁵⁸ The concept of reservoir computing dates back to 2007. See [Toward optical signal processing using Photonic Reservoir Computing](#) by Kristof Vandoorne et al, 2008 (11 pages). It is also described in [Novel frontier of photonics for data processing - Photonic accelerator](#) by Ken-ichi Kitayama, 2019 (25 pages) as well as in this beautiful presentation [Introduction to Reservoir Computing](#) by Helmut Hauser (282 slides). The notion is different from the one of [reservoir engineering](#).

²⁴⁵⁹ See [Advances in photonic reservoir computing](#) by Guy Van der Sande et al, 2017 (16 pages) which provides an excellent focus on optronics based reservoir computing

The training parameters of these networks are located in the weights of the neurons that connect the reservoirs to the output data. Reservoir computing can be implemented with photonics as shown in Figure 614. There are other implementations with memristors²⁴⁶⁰, five types of optical reservoir computing and even quantum versions, for quantum reservoir computing²⁴⁶¹!

Chemical computing

Chemical computing is yet another form of unconventional computing. The underlying physical phenomenon was discovered in 1951 by a Russian chemist, Boris Belousov, with a self-reversible chemical reaction alternating the color of solution mixing salts and acids. It would enable the creation of chemical logic gates. It was thought initially that it broke the second law of thermodynamics (a bit like time crystals...). It was found later that it was not the case and that some form of logic gate could be implemented using this phenomenon and a chemical oscillator that is akin to chemical concentration waves blocking or amplifying each other depending on their setting. One benefit is a low energy consumption²⁴⁶².

Research in the domain started to generate some experimental results in 1989 and onwards, particularly in the UK, at EMPA in Switzerland, Stanford, Harvard and the University of Washington. But the benefits of this architecture are not obvious, noticeably due to its relatively slow speed. The most recent work came in 2020 from the University of Glasgow who used 3D-printed programmable chemical processor with a 5 by 5 array of cells filled with a switchable oscillating chemical and magnetic stirrers to control their oscillations and compute binary logic gates to perform pattern recognition²⁴⁶³. It can control 2.9×10^{17} chemical states.

The array is programmed by setting chemical relations between these chemical cells. It can implement a chemical autoencoder used for pattern recognition. Now, more comparisons have to be made with classical computing to see how it scales²⁴⁶⁴!

²⁴⁶⁰ See [Memristors and Beyond: Recent Advances in Analog Computing](#) by Nick Skuda, 2019 (12 slides).

²⁴⁶¹ See [Universal quantum reservoir computing](#) by Sanjib Ghosh et al, from Singapore, 2020 (23 pages) as well as [Integrated Nanophotonic Structures for Optical Computing](#) by Laurent Larger et al, 2019 (50 slides). See [Experimental photonic quantum memristor](#) by Michele Spagnolo et al, Nature Photonics, March 2022 (7 pages) which describes a way to implement quantum memristors and quantum reservoir computing. As explained in [Quantum memristor: A memory-dependent computational unit](#) [Quantum memristor bridges conflicting quantum requirements in single device](#) by Chris Lee, ArsTechnica, April 2022, a quantum memristor is a memristor that will change its properties based on the qubit traversing it, in the case of photons. And at last, see [Quantum reservoir neural network implementation on a Josephson mixer](#) by Julien Dudas, Erwan Plouet, Alice Mizrahi, Julie Grollier and Danijela Marković, September 2022 (7 pages) which proposes to use a large number of densely connected neurons by using parametrically coupled quantum oscillators instead of physically coupled qubits.

²⁴⁶² See [Chemical Computing, the Future of Artificial Intelligence](#) by Javier Yanes, January 2019.

²⁴⁶³ See [A programmable chemical computer with memory and pattern recognition](#) by Juan Manuel Parrilla-Gutierrez, Lee Cronin et al, Nature Communications, March 2022 (8 pages).

²⁴⁶⁴ See the video [The First Programmable Turing Complete Chemical Computer](#) with Lee Cronin from the University of Glasgow (1h11mn).

Quantum unconventional computing key takeaways

- Various non-conventional computing technologies may compete with classical and quantum computing or even bring some help, like reversible and superconducting technologies that may be useful to create cryogenic electronics enabling the creation of scalable quantum computers. These technologies are so diverse and with different underlying science that they would deserve a lot of time and energy to be properly evaluated and benchmarked by both physicists and computer science specialists. None of these technologies have been proven to solve NP problems efficiently... in a scalable way.
- Digital annealing computing is mostly proposed by Japanese companies like Fujitsu and Hitachi, using classical CMOS chipsets. These solutions are supposed to solve intractable problems faster than classical-classical computers, but their scalability remains questionable.
- Reversible and adiabatic computation has been researched for a long time and has not yet turned into commercial products. It could probably be more interesting to create energy saving solutions more than faster solutions with some potential use case in quantum computing enabling technologies.
- Superconducting computing is an interesting area of research to create more energy efficient supercomputers, despite the cooling cost that, hopefully is not as expensive as with superconducting qubits quantum computers. There are synergies between this research area and superconducting logic electronics that could be used to control superconducting and quantum dots spin qubits at low temperatures.
- Probabilistic and optical computing are interesting research areas. These solutions may be competitive to solve specific problems.
- Optical processors are mainly used in the deep learning space, to accelerate the training and inferences in some layers of convolutional networks. Some variants can solve combinatorial problems.
- Chemical computing is one of the many other areas in unconventional computing that may be interesting but have probably various scaling limitations. Other unconventional computing like DNA computing and other variations are not studied here, particularly since they are not deemed to solve untractable problems.

Quantum telecommunications and cryptography

Quantum telecommunications cover a wide spectrum of use cases including quantum communications between quantum sensors, quantum computers and quantum key distribution used in cryptography (Figure 615). Some but not all of these technologies are based on using photon entanglement and quantum teleportation as resources. The field started to develop experimentally and industrially with quantum cryptography. It is already being deployed experimentally or at large scales like in China, while quantum telecommunications associated with quantum computers is still in its infancy.

Interest in quantum cryptography (using various quantum effects like measurement randomness and/or entanglement as resources to generate identical secured encryption keys between two communication endpoints) as well as in post-quantum cryptography (classical cryptography using techniques that are resilient to attacks by quantum computers) were triggered by the creation of Shor's algorithm in 1994. It theoretically enables integers factoring on a quantum computer in reasonable times, provided large scale quantum computers are available. This algorithm has been destabilizing computer security specialists since the advent of the first programmable quantum processors in the early 2000s and related scale-up promises and forecasts. It would make it possible to break the codes of many public key cryptography systems that are commonly used on the Internet. It is still highly hypothetical because quantum computers capable of executing Shor's algorithms for RSA-2048 keys and requiring millions of high-fidelity qubits are really far in the distant future at best.

Once they are aware of the threat, however, governments, counterintelligence, intelligence and sensitive industries become seriously concerned or at least interested. The threat of quantum computing on cybersecurity even touches critical parts of the Bitcoin and Blockchain signatures and some proof of work protocols. Even though the threat is quite remote, the readiness inertia to counter this potential quantum threat means, for some, that it is necessary to launch it now.

Even before Shor's phantom menace materializes, the cyber security industry started to prepare countermeasures. The markets affected first will be the IT and telecommunications industry in general, which will have to update many software and hardware offerings, financial institutions, the energy sector, healthcare, and government utilities and the military.

In this part, we will describe:

- The basic principles of classical cryptography, in particular **public key cryptography**, with the example of RSA public keys.
- The **nature of the threat** coming from integer factoring and other quantum algorithms and the cryptographic solutions involved.
- **Quantum random number generators** which have become an indispensable complement to classical cryptographic solutions and also quantum cryptography as well.
- **Quantum Key Distribution** based systems that secure the physical part of communications for the safe distribution of random symmetric keys.
- **Post-Quantum Cryptography** that is used to distribute public encryption keys using classical computation that are resilient to codebreaking done by quantum computers.
- **Quantum telecommunications** applications, outside of those related to cryptography, and in particular for the creation of distributed quantum computing systems.

- **Quantum Physical Unclonable Functions** which are sitting in between QRNG, embedded systems and cryptography.
- **Vendors** in these sectors around the world, in a market that already includes many players and in particular many startups.

Encryption and cryptography involve mathematical concepts that are not always obvious. I'll share with you here what I have been able to understand about it and make it as accessible as possible.

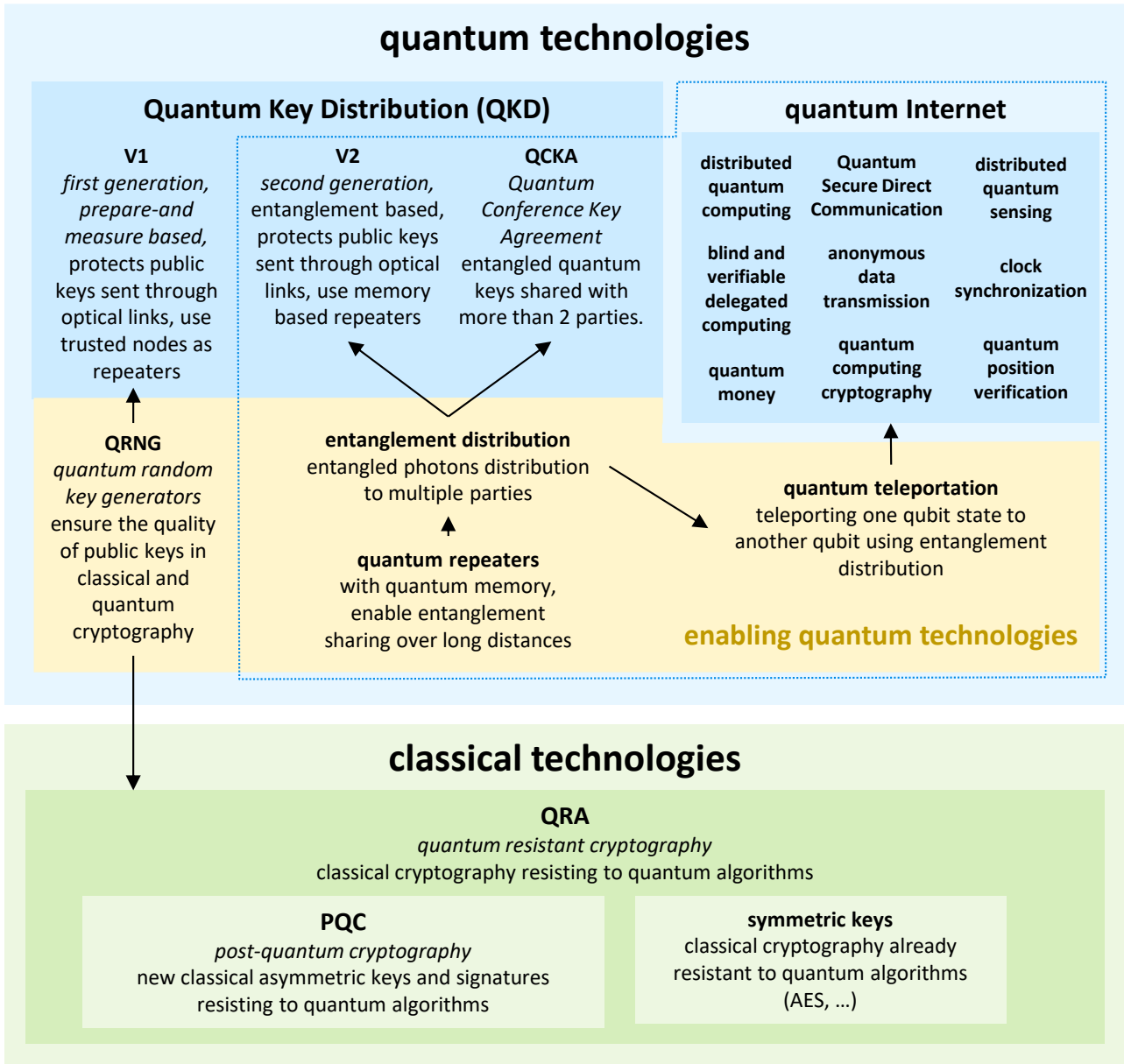


Figure 615: the various types of technologies covered in this part and their relationship. (cc) Olivier Ezratty, 2023. See the review paper [Towards Quantum-Native Communication Systems: New Developments, Trends, and Challenges](#) by Xiaolin Zhou et al, November 2023 (52 pages).

Public key cryptography

Cryptology is the science of secrets. It allows the transmission of sensitive information between a transmitter and a receiver in a secure manner. Cryptology includes cryptography, which secures transmitted and stored information, and cryptanalysis, which seeks to decrypt it by attack, or code breaking.

In the case of asymmetric public-key cryptography, encryption uses only public keys and decryption uses both public and private keys. Code-breaking exploits only the public keys, while trying to deduce the private keys through intensive computing.

Cryptography secures transmitted information in several ways:

- **Confidentiality:** only the recipient can retrieve the unencrypted version of the transmitted information.
- **Integrity:** the information has not been modified during its transmission.
- **Authentication:** the sender and receiver are who they claim to be.
- **Non-repudiation:** the issuer cannot deny having transmitted the encrypted information.
- **Access control:** only persons authorized by the issuer and the recipient can access unencrypted information.

Before computer telecommunications, confidentiality was ensured by the knowledge of a common secret between transmitters and receivers, the encryption and decryption codes, which could be the position of the wheels of a German Enigma machine during the World War II. This worked in closed environments such as for military communications or between embassies and their home countries.

With Internet communications, this modus operandi is inapplicable for consumer applications and for business relationships in general. Hence public key cryptography systems, such as RSA, which enabled most open Internet data exchanges. There are still highly protected systems using private and symmetrical keys, mainly used in government related applications (army, security, intelligence) as well as in various other cases (some file transfers, email encryption, server/client exchanges, in smart cards and associated payment terminals).

Asymmetric (public-key) cryptography is also exploited for pre-establishing common encryption keys between users of private-key systems, for managing the integrity of communications, and for authentication as in the TLS Internet protocol. Sensitive information is then encrypted with these keys and a symmetrical AES-type algorithm. AES is used to encrypt communications in WhatsApp, Messenger and Telegram. These applications often also use asymmetric cryptography for authentication, key exchange, and communication integrity management. Asymmetric cryptography is very flexible while symmetric cryptography is more computationally efficient. In many cases, symmetric cryptography systems coexist with asymmetric (public key) cryptography systems. As a result, when you communicate securely over the Internet, different complimentary security protocols are activated.

With public key systems, different keys are used for encryption and decryption of the information transmitted, so that it is very difficult (if not sometimes impossible) to guess the private decryption key from the public encryption key. The message receiver sends its public key to the sender, who in turn uses it to encrypt the message. The receiver uses the private key that was kept to decrypt the received message. As explained in Figure 616, the private key is never transmitted. This is also called a PKI, for "Public Key Infrastructure".

The **RSA** cryptography system is the most widely used system for protecting public key information transmissions over the Internet. It was created in 1978 by **Ron Rivest** (1947, American), **Adi Shamir** (1952, Israeli) and **Leonard Adleman** (1945, American).

You don't necessarily need to understand the following that explains how keys are constructed. It starts by determining p and q , two large random prime numbers, with a "good" random number generator. We will see later that quantum physics can be used to create real random numbers. We calculate $N = pq$ which is a very large integer. A good RSA key requires to have N stored on at least 2048 bits knowing that the NSA recommends 3,072 bits keys for critical applications.

We then evaluate e , a prime number by exploiting $O(N)$ which equals the number of prime integers between 1 and N relative to N , and which, as p and q are prime, equals $(p-1)(q-1)$. d is a large integer which is co-prime of $O(N)$ and is chosen according to: $e^d = 1 \pmod{O(N)}$. At the end, we get a public key that includes the integers N and e , and a private key that includes d .

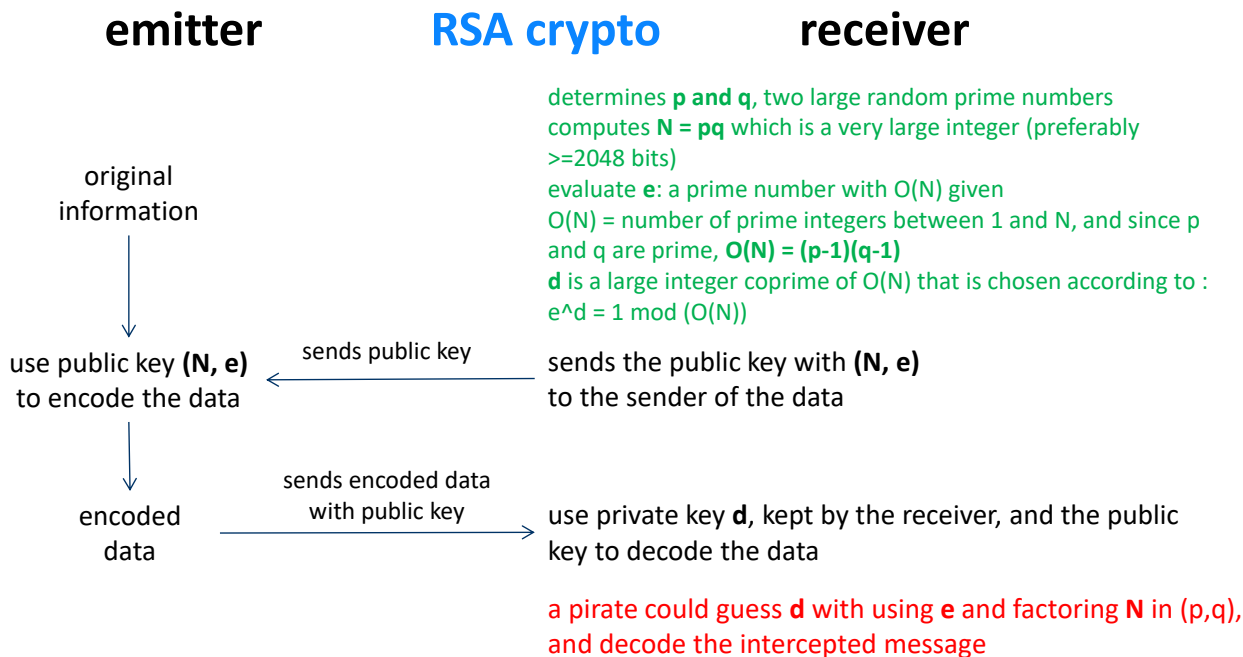


Figure 616: description of the RSA key generation process. (cc) Olivier Ezratty, 2022-2023.

All of this is based on the theory of numbers and uses Fermat's little theorem and Euler's theorem which make it possible to create two distinct keys that are the inverse of each other.

With that, anyone can encrypt a message using the public key and this message is decipherable only by the person who has the private key that splits the public key into primitives.

A hacker could decrypt the information sent by intercepting e (the end of the public key) and factoring N , the other end of the public key, into the integers p and q , and then rebuilding the private key d from it.

In the symmetric key realm, you'll find encryption systems using protocols like AES with usual keys of 256 bits, that have been in use since 2001. These keys are shared by two parties in a channel and time that can be different from the encrypted data transmission.

The best symmetric key system is called the "one time pad" with key size equaling the size of the encrypted data. It means that the key can be very large depending on the data size. But this is the best secure system. It, however, requires the ability to create a random and totally unpredictable key.

Quantum cryptanalysis threats

Assessing cryptanalysis threats for any deployed cryptography solution has always been critical. Classical cryptanalysis is one of the threats on the security of government, public services, businesses and consumers digital assets, on top of viruses, phishing, other social engineering tricks and various physical attacks. The looming threat of quantum computers adds to this already busy mix.

The diagram below in Figure 617 points out the main encryption algorithms vulnerable or not to known quantum algorithms²⁴⁶⁵.

²⁴⁶⁵ Seen in [IDQ: Quantum-Safe Security relevance for Central Banks](#), 2018 (27 slides) and slightly supplemented by some captions.

Broadly speaking, common public key encryption systems are vulnerable. Only post-quantum cryptography systems are supposed to be resilient. But things are moving fast and some SIDH, lattice and multivariate keys are now classically broken!

Name of Cryptographic Algorithm	Type	Purpose	Resilience against Quantum Computer
AES-256	Symmetric Key	Encryption	Ok but larger key sizes needed
SHA-256, SHA-3		Hash function	Ok but larger output needed
Lattice-based (NTRU)	Public Key	Encryption; signature	Believed
Code-based (Mc Eliece)	Public Key	Encryption	Believed
Multivariate polynomials	Public Key	Encryption; signature	Believed
Supersingular elliptic curve isogenies (SIDH)		Encryption; possibly signature	Believed
ECDSA, ECDH (Elliptic Curve Crypto)	Public Key	Signatures, Key exchange	No longer secure
RSA	Public Key	Signatures, Key establishment	No longer secure
DSA (Finite Field Crypto)	Public Key	Signatures	No longer secure

High level of confidence

Under investigation

threatened by quantum algorithms

Figure 617: what key generation services are quantum safe or not. Source: NIST.

One reason to worry is that today's sensitive communications can be stored for a long time by private or state hackers, and exploited much later, when quantum computers are up to the task. This attack is nicknamed **Store Now, Decrypt Later (SNDL)**. Some present day information may have some value later, whether it is financial transactions, private communications, healthcare records, trade secrets, diplomatic, military and various other state secrets. Forward secrecy, a feature used to protect the transport layer like SSL used with HTTPS with separate keys for each session, is not enough against quantum computing-based attacks. Quantum computing is thus a Damocles sword whose fall is difficult to predict and rather distant in time by at least a very long decade. Beyond that time, it is almost impossible to make educated predictions.

Shor's phantom menace

Peter Shor's 1994 integer factoring algorithm sparked interest in quantum computing when there was even no single working qubit around that was controllable by quantum gate. Shor's algorithm enables theoretically to factor integers in a reasonable time that is proportional to their logarithm. It is thus a factorization in a linear time as a function of the number of key bits. This could be detrimental to all public key-based cryptography²⁴⁶⁶.

When and if the needed quantum hardware work, Shor's algorithm applied to large RSA public key breaking could have quite a negative impact on most Internet security since being integrated in the **TLS** and **SSL** protocols that protect websites and file transfers via **HTTPS** and **FTP**, in the **IPSEC** protocol that protects IP V4 in the IKE sub-protocol, in the **SSH** protocol for machines remote access and in the **PGP** protocol that is sometimes used to encrypt emails. RSA and derivatives are also used in many **HSM** (Hardware Security Modules) such as in cars ECUs (Electronic Central Units)²⁴⁶⁷.

²⁴⁶⁶ See this presentation which describes in great detail how Shor's algorithm works: [On Shor's algorithms, the various derivatives, their implementation and their applications](#) by Martin Ekerå, 2019 (135 slides).

²⁴⁶⁷ See [Post-Quantum Secure Architectures for Automotive Hardware Secure Modules](#) by Wen Wang and Marc Stöttinger, 2020 (7 pages).

The threat also deals with software **electronic signatures** and therefore their automatic updates, **VPNs** used for remote access to protect corporate networks, email security with **S/MIME**, various **online payment** systems, as well as **ECDH**, **ECDSA** and **3-DES** elliptic curve cryptography. The **Signal** protocol used in WhatsApp would also be in the spotlight. So, a lot of Internet security is more or less in the line of sight.

ECC (Elliptic Curve Cryptography) is the first algorithm with elliptic curves, created in 1985 by Neal Koblitz and Victor Miller (Figure 618). The most common variants today are **ECDH** (Elliptic-curve Diffie-Hellman) and **ECDSA** (Elliptic Curve Digital Signature Algorithm, launched in 2005).

These variants were deployed from 2005 and more widely only from 2015, so 30 years after the creation of the first ECC! Incidentally, the elliptic curves allowed Andrew Wiles to demonstrate the Fermat's last theorem in 1992, which has nothing to do with cryptography²⁴⁶⁸.

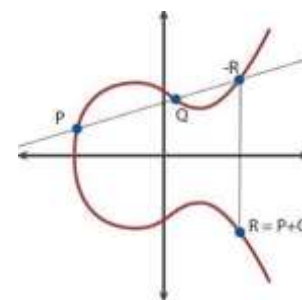


Figure 618: an elliptic curve.

One of the interests of elliptic curve-based codes is to use shorter public keys than with RSA encryption. But these elliptic curves are also theoretically breakable with quantum computing with a reasonable time because of our friend Peter Shor and the resolution of the discrete logarithm problem (DLP)²⁴⁶⁹. Moreover, an ECDSA backdoor was revealed by Edward Snowden in 2013, housed by the NSA in its Dual EC DRBG random number generator and not in the elliptic curve itself. It was then recommended by NIST in 2014 and NSA in 2015 for the transmission of sensitive information²⁴⁷⁰.

Grover, Dlog and Simon threats

Symmetric cryptography systems are not affected by Shor's algorithm. These include the **Data Encryption Standard** (DES) which uses keys of 64 bits or more and is outdated, replaced by the **Advanced Encryption Standard** (AES) which has been a US government standard since 2002, with private keys ranging from 128 to 256 bits.

To date, the best quantum breaking algorithms for symmetric **AES** keys would take more than the age of the Universe (13.8 billion years) to run on 128-bit keys. With AES-256 bits, we are therefore in peace, and it is the recommended key length to be quantum resistant! They are based on mechanisms that are quite different from the mathematical problem-solving of public key ciphers²⁴⁷¹.

Keys are shared upstream of the exchanges and are generally themselves encrypted with the asymmetric **Diffie-Hellman** algorithm. But this Diffie-Hellman encryption is based on elliptic curves, which is breakable by Shor's algorithm. The problem lies then with the vulnerability of the majority of encryption systems using asymmetric keys which are used to share symmetric keys.

A hash function converts data of arbitrary size such as a file to a number of fixed size. This makes it possible to do quick searches to compare files. For example, it can be used to check that a file has not been altered during transmission.

²⁴⁶⁸ As in [Elliptic curves cryptography and factorization](#) (86 slides).

²⁴⁶⁹ As documented in [Shor's discrete logarithm quantum algorithm for elliptic curves](#) by John Proos and Christof Zalka, 2003 (34 pages). The discrete log problem consists in finding an integer k verifying $a^k = b$ modulo p , a , b and p being known integers. This allows to break the elliptic and Diffie-Hellman curve keys.

²⁴⁷⁰ See Ben Schwennesen's [Elliptic Curve Cryptography and Government Backdoors](#), 2016 (20 pages).

²⁴⁷¹ See [Hacking Cryptographic Protocols with Advanced Variational Quantum Attacks](#) by Borja Aizpurua, Roman Orus et al, Multi-verse, November 2023 (12 pages) is an algorithm proposal to break S-AES, a simplified version of AES as well as Blowfish, another symmetric key protocol. But it does not describe the resources needs to break some AES-256 key.

SHA algorithms (Secure Hash Algorithms) are standard hash functions that consist in replacing data of arbitrary size by a unique key size. The **SHA-1** hash algorithm is resistant to Shor's algorithm, but it has been broken by other methods and is therefore considered outdated. It is the **SHA-3** which is the most up-to-date and since 2015. The SHA algorithm could be broken by Grover's search algorithm, but with many logical qubits, at least 6,000 logical qubits for common keys²⁴⁷².

This represents an order of magnitude close to the qubit requirements for breaking RSA keys with Shor's algorithm. For example, a hash key or fingerprint can be used to verify the integrity of content such as software or simply a password. The problem is to resist collisions, i.e., methods to find or create an object whose fingerprint would be the one you have, which is quite different from finding the original object (like an image) from its fingerprint, which is rather difficult.

	SHA-256	SHA3-256	
Grover	T-count	1.27×10^{44}	2.71×10^{44}
	T-depth	3.76×10^{43}	2.31×10^{41}
	Logical qubits	2402	3200
	Surface code distance	43	44
	Physical qubits	1.39×10^7	1.94×10^7
Distilleries	Logical qubits per distillery	3600	3600
	Number of distilleries	1	294
	Surface code distances	{33, 13, 7}	{33, 13, 7}
	Physical qubits	5.54×10^5	1.63×10^8
Total	Logical qubits	$2^{12.6}$	2^{20}
	Surface code cycles	$2^{153.8}$	$2^{146.5}$
	Total cost	$2^{166.4}$	$2^{166.5}$

Table 3. Fault-tolerant resource counts for Grover search of SHA-256 and SHA3-256.

Figure 619: the staggering level of quantum resources required to break SHA-256 symmetric keys with Grover's algorithm. Source: [Estimating the cost of generic quantum pre-image attacks on SHA-2 and SHA-3](#), 2016 (21 pages).

The number of qubits needed to break keys depends on the size of the key. SHA-1 and SHA-2 have small key sizes that can be recovered in a reasonable time with **Grover's** quantum search algorithm, but this is not the case for SHA-3 which exploits larger keys (Figure 619). This is the same logic as for AES.

Shor's Dlog (discrete log) algorithm threatens Digital Signature Algorithms, Diffie-Hellman key exchanges and El-Gamal encryption. And **Simon's** algorithm can also break Even-Mansour ciphers that are used in some disk encryption solutions, although with a lot of caveats, the attacker needing to encrypt a superposition of inputs all with the same keys²⁴⁷³. All in all, Shor is not the only quantum threat to cybersecurity (Figure 620)!

Peter Shor factoring algorithm - 1994

integer factoring

exponential acceleration

$$O(e^{1.9(\log N)^{\frac{1}{3}}(\log \log N)^{\frac{2}{3}}}) \Rightarrow O((\log N)^2 (\log \log N))$$

threatens public key based cybersecurity

RSA, ECDH, ECDSA, SSL/TLS, VPNs (IPSEC), SSH, PGP, S/MIME, Signal (Whatsapp), Bitcoin & Blockchain signatures

Peter Shor dlog algorithm - 1994

exponential acceleration

$$O(e^{(\log N)^{\frac{1}{3}}(\log \log N)^{\frac{2}{3}}}) \Rightarrow O((\log N)^2 (\log \log N))$$

threatens Digital Signature Algorithm, Diffie-Hellman key exchanges and El-Gamal encryption

LoV Grover search algorithm - 1996

brute force to break symmetric codes

polynomial acceleration

$$O(N) \Rightarrow O(\sqrt{N})$$

threatens symmetric keys cybersecurity

improves brute force attack of hash functions (SHA) and block ciphers (AES) used in symmetric encryption

David Simon algorithm - 1996

exponential acceleration

$$O(2^{N/2}) \Rightarrow O(N)$$

threatens Even-Mansour ciphers used in some disk encryptions

Figure 620: Shor's algorithm is not the only quantum algorithm that could threaten existing cybersecurity using symmetric and asymmetric cryptography. (cc) Olivier Ezratty, 2021-2023.

²⁴⁷² Based on [Estimating the cost of generic quantum pre-image attacks on SHA-2 and SHA-3](#), 2016 (21 pages).

²⁴⁷³ See [Breaking Symmetric Cryptosystems Using Quantum Algorithms](#) by Gaëtan Leurent with Marc Kaplan, Anthony Leverrier and María Naya-Plasencia, 2016 (58 slides).

Blockchain and Cryptocurrencies vulnerabilities

What about **Bitcoin**, other crypto-currencies and the **Blockchain**? The answer is summarized in Figure 621 with a good inventory of the cryptosystems used by use as a starting point²⁴⁷⁴.

Otherwise, experts have opposite views on the quantum risk, from let's forget it²⁴⁷⁵, to it will come sooner than expected²⁴⁷⁶.

Basically, the Blockchain is based on a patchwork of cryptographic algorithms including AES, RSA and SHA-3. It uses a hash algorithm to ensure the integrity of the chain of trust, and a digital signature to authenticate new transactions that are incrementally added to the Blockchain. Bitcoin uses a SHA-256 crypto hash, which is quantum resistant, and a signature that exploits ECDSA elliptic curves, which is not. In a similar manner, **Ethereum** uses a quantum resistant SHA-3 hash and a vulnerable ECDSA signature.

Table 3. Main Algorithms Types Used for Cryptography, and Uses For Smart Ledgers¹⁹

Type of Algorithm	General Use	Example Algorithms of This Type	Example Uses for Smart Ledgers
Symmetric	Secret communications	AES, DES, 3DES, RC4	Protection of resources stored on ledger
Public key	Secret communications (including key exchange) or digital signature	RSA, Diffie-Hellman, El Gamal, ECDSA	User authentication; signature of transactions, data or software
Hash	Generating fixed-length digest of arbitrary-length text	SHA-256, SHA-512, SHA-3	Ensuring authenticity of blockchain

Figure 621: algorithms used in cryptos and smart ledgers. Source: [The Quantum Countdown Quantum Computing and The Future of Smart Ledger Encryption](#) by Long Finance, 2018 (60 pages).

However, an Eth2 upgrade to Ethereum published in 2021 has replaced ECDSA based signatures by Lamport Q-R signatures which are quantum safe, with the inconvenience of being very large (over 200 times bigger than an ECDSA signature).

A recent review paper lists Bitcoin, Ethereum, Litecoin, Monero and ZCash as highly vulnerable to Shor's algorithm and all these, except Monero, to be moderately vulnerable to Grover search²⁴⁷⁷.

All in all, quantum computing will not allow to alter the Blockchain, nor the proof of work used by Bitcoin which relies on the repeated use of quantum-resistant hash. The vulnerability of the Blockchain lies in the signature that relies on the ECDSA elliptic curve algorithm which can be broken with Shor's algorithm. This would make it possible to impersonate someone else in a transaction involving a Blockchain or Bitcoins. That's still a whole lot of potential troubles! For example, if a Bitcoin transaction was intercepted to retrieve the sender's ECDSA signature, it could be exploited to transfer Bitcoins from that sender's wallet.

What is the "size" of the quantum computer that would break the ECDSA signature of the Bitcoin? The required number of qubits depends on the desired computing time. It would be 317 million physical qubits to break the key in one hour using a surface code, a code cycle time of 1 μ s (IBM's cycle is right now at about 1 ms) and qubit fidelities 99.9% (IBM reached it with 27 qubits in 2021). In one day, the requirement is lower, at 13 million physical qubits.

²⁴⁷⁴ The answer is well documented in [The Quantum Countdown Quantum Computing and The Future of Smart Ledger Encryption](#) by Long Finance, 2018 (60 pages).

²⁴⁷⁵ See [Here's Why Quantum Computing Will Not Break Cryptocurrencies](#) by Roger Huang, December 2020.

²⁴⁷⁶ See [Q-Day Is Coming Sooner Than We Think](#) by Arthur Herman, Forbes, June 2021. It mentions a crack of a RSA 2048-bit encryption key in 10 seconds with 4,099 stable qubits without mentioning the source of this performance. I have searched it and didn't found the source reference of these 10 seconds mentioned in various places. The only detail is it would require a perfect quantum computer executing one million operations per second.

²⁴⁷⁷ See [Vulnerability of blockchain technologies to quantum attacks](#) by Joseph J.Kearney et al, 2021 (10 pages).

Whatever, as we have seen in studying the scalability of various quantum computing architecture and their enabling technologies, it is clear we are very far from seeing this threat to materialize²⁴⁷⁸. And like some like to assert, it does not matter since the Bitcoin may not outlast the current NISQ era!

Workarounds can obviously be created until a quantum threat to transaction integrity is confirmed. This can be done by encrypting the signatures used by the blockchains with a PQC system, as we will see later²⁴⁷⁹.

It is also possible to encrypt the data circulating in a Blockchain with a quantum computationally resistant algorithm such as AES-256, with the disadvantage that it is symmetrical and therefore requires keys to be exchanged beforehand. However, there are already some workarounds.

A protocol using a longer validation time for Bitcoin transactions would allow to bypass the use of integer factoring to break the Bitcoin electronic signature algorithm, ECDSA²⁴⁸⁰. But this would only amplify a key flaw of Bitcoin as a currency: a lengthening of transaction times that are already far from real time! Bitcoin mining is potentially vulnerable by Grover's algorithm although its real practical speedup on a LSQC (large scale quantum computer) is questionable. Researchers are proposing some changes in the rules (and timing) applied by miners to mitigate this threat²⁴⁸¹.

We can also mention the open source Blockchain project resisting quantum attacks, [Quantum Resistant Ledger](#). It is based on the XMSS (Extended Merkle Signature Scheme) electronic signature protocol²⁴⁸². There is also a risk of attack at the mining level, with Grover's algorithm.

But here again, solutions are available^{2483 2484}. The **Long Finance** document from which this table is extracted summarizes all these risks on Smart Ledgers by separating the transactions that are relatively protected and those that rely on vulnerable electronic signatures that are not vulnerable to hacking of the SSL and TLS protocols^{2485 2486} (Figure 622).

Table 4. Risks to Blockchain Architectures from Quantum Computing

	Transactions	Data on Blockchain	Software on Blockchain
Read historical records without authorization	No (blockchains are intended to allow access to transaction information)	No, unless confidential and secured with vulnerable cryptography	No, unless confidential and secured with vulnerable cryptography
Alter historical records	No	No	May be able to run software without authorisation if signature used
Spoof ongoing records	Yes, possibly	Yes, possibly	Yes, possibly

Figure 622: potential long term quantum threats on cryptos. Source: [The Quantum Countdown Quantum Computing and The Future of Smart Ledger Encryption](#) by Long Finance, 2018 (60 pages).

²⁴⁷⁸ See [The impact of hardware specifications on reaching quantum advantage in the fault tolerant regime](#) by Mark Webber et al, September 2021 (16 pages).

²⁴⁷⁹ See [Blockchained Post-Quantum Signatures](#) by Chalkias Brownly Hearnz, 2018 (8 pages).

²⁴⁸⁰ It is documented in [Committing to Quantum Resistance A Slow Defence for Bitcoin against a Fast Quantum Computing Attack](#), 2018 (18 pages).

²⁴⁸¹ See [On the insecurity of quantum Bitcoin mining](#) by Or Sattath, February 2019 (22 pages).

²⁴⁸² See also [Blockchained Post-Quantum Signatures](#) by Chalkias Brownly Hearnz, 2018 (8 pages).

²⁴⁸³ See [On the insecurity of quantum Bitcoin mining](#) by Or Sattath, February 2019 (22 pages).

²⁴⁸⁴ See the excellent review paper [Navigating the Quantum Computing Threat Landscape for Blockchains: A Comprehensive Survey](#) by Hassan Khodaiemehr, Khadijeh Bagheri and Chen Feng, September 2023 (62 pages).

²⁴⁸⁵ See also [The quantum threat to payment systems](#) by Michele Mosca of the University of Waterloo, 2017 (52 minutes). Mosca is one of the world references in the quantum cryptography field.

²⁴⁸⁶ See also [The Quantum Countdown Quantum Computing And The Future Of Smart Ledger Encryption](#), Long Finance, February 2018 (62 pages)

This section on threats would not be complete without mentioning the disagreements between cybersecurity specialists. Some are rather conservative and consider that one should not touch too much of what works well. They think Shor's threat is exaggerated. Others, such as the NIST and NSA in the US, are more alarmist and believe that the most critical cryptographic systems should be updated as soon as possible²⁴⁸⁷. And we also have arguments between the compared advantages of QKD and PQC, the two systems that can protect cybersecurity from quantum computing long-term threats²⁴⁸⁸.

Threat assessments

Since I have been tracking this field, I have observed that the cybersecurity threat coming from quantum computers has been overestimated.

One past example shown in Figure 623 came from the European standardization organization ETSI²⁴⁸⁹, based on very optimistic predictions on QPUs capabilities to exploit Shor's algorithm. If that prediction was exact, as of 2023, RSA 2048 keys would already be broken by quantum computers!

The orange part of the graph should be shifted into the future by at least 10 to 20 years.

The cyberthreat is usually exaggerated by cybersecurity specialists who are not aware of the various difficulties of creating scalable quantum computers. And they also have stuff to sell, with the myriad of diagnostic tools and services, on top of the new post-quantum cryptography solutions, as they are being standardized by NIST and others.

Many predictions are entirely wrong whether they talk about a “quantum apocalypse²⁴⁹⁰”, an equivalent of a “nuclear threat”²⁴⁹¹ or when some folks predicted in 2020 that the Bitcoin security would be broken by 2022²⁴⁹². They were confusing physical and logical qubits requirements among other mistakes! The same mistake was reiterated a year and a half later with a cybersecurity poll²⁴⁹³. The main issue with these polls is that they are asking a question to cybersecurity specialists and other commentators who have no clue about the scalability challenges of quantum computing²⁴⁹⁴.

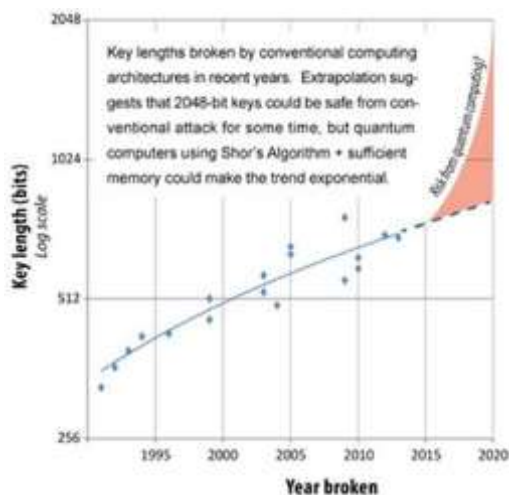


Figure 623: how Shor's risk is usually overestimated with a past example. Source: [Quantum Safe Cryptography and Security](#), 2015 (64 pages).

²⁴⁸⁷ Analysts are amplifying the fear, as in [Executive's Guide to Quantum Computing and Quantum-secure Cybersecurity](#) from Hudson Institute, a US conservative think tank, March 2019 (24 pages), [Preparing Enterprises for the Quantum Computing Cybersecurity Threats](#) by CSA, May 2019 or [Global Risk Report 2020](#) from the World Economic Forum.

²⁴⁸⁸ See [Quantum crypto-economics: Blockchain prediction markets for the evolution of quantum technology](#) by Peter P. Rohde et al, February 2021 (12 pages) that modelize different scenarios depending on the reality of the quantum threat.

²⁴⁸⁹ See [Quantum Safe Cryptography and Security](#), 2015 (64 pages).

²⁴⁹⁰ See [What is the quantum apocalypse and should we be scared?](#) by Frank Gardner, BBC, January 2022.

²⁴⁹¹ See [‘Nuclear Threat to Cybersecurity’ — Post-Quantum Cybersecurity Rapidly Gains Attention of U.S. Congress, Administration](#) by Matt Swayne, The Quantum Insider, July 2022.

²⁴⁹² See [Quantum computers could crack Bitcoin by 2022](#) by Robert Stevens, May 2020.

²⁴⁹³ See [Cybersecurity Experts Say Quantum, Advanced Technology Will Break Standard Encryption Within Two Years](#) by Matt Swayne, The Quantum Insider, December 2021.

²⁴⁹⁴ One good example is this paper [Quantum Computing Threatens to Collapse the Grid](#) by Alexander Boulden, December 2021 that forecasts doomsday for grid management due to quantum computing threat on cybersecurity. The chart from Statistica/CBInsights is both false and outdated, showing three qubit systems that never worked: Intel 49 superconducting qubits, Google's Bristlecone 72 qubits (it ended up being 53 functional qubits with Sycamore in 2019) and Rigetti's 128 qubits that were announced in 2018 and never released. They are up to 80 qubits as of 2022.

And that's true as well for a former NSA director²⁴⁹⁵!

A report produced late 2022 by the X9 Financial Industry Standards organization created the notion of Cryptographically Relevant Quantum Computer (CRQC) and tried to estimate when the threat will materialize²⁴⁹⁶. It mentioned a RSA security risk countdown ending by 2030, established by the [Cloud Security Alliance](#) (CSA). Hopefully, the report is well documented, particularly when describing existing and PQC related cryptographic solutions.

A Financial Times 2023 demonstration of how a quantum computer works and how it could break an RSA key contained lots of visuals and simplifications²⁴⁹⁷. Peter Shor gave his best guess as to when this might happen: “*between 20 and 40 years,*” but he does not rule out the possibility that the physics challenges will prove too hard, and we will never build workable quantum computers.

Only a few analysts think that the quantum threat is overestimated²⁴⁹⁸. It is the result of a mix of an unbalanced knowledge of the actual quantum threat between quantum information and cybersecurity specialists. On top of that, cybersecurity vendors have a natural interest to increase the threat perception, in order to sell PQC-based upgraded security solutions²⁴⁹⁹. There's a nice potential market to address with \$5.5B to \$10B by 2030^{2500 2501}. So, if quantum computers were able to scale to a point to break today's asymmetric cryptography, it would indeed create a quantum apocalypse. The question is whether it is realistic or not. There is a bigger risk to kill all electronic devices with solar flares than asymmetric cryptography with a large scale quantum computer.

The fear is also fueled by governments' paranoia and the global fight between the USA and China for quantum technology dominance. On top of that, a lot of myths abound about the NSA and its capabilities, up to many folks thinking that this organization already owns an RSA-breaker QPU in its datacenters. While you can never efficiently prove that something does not exist, a good understanding of the scalability challenges with quantum computing makes serious people think this thing is just a bad nightmare. But if the cost of getting protected against this potential threat is reasonable, then it makes sense to implement PQC solutions.

Mosca's inequality

Michele Mosca created an inequality that explains the time risk. It is expressed in the form $D+T>G_c$, where D is the length of time during which today's data circulating in encrypted form must be secured, T, the time needed to make my transition from its encryption systems to solutions resistant to quantum computing, and G_c , the time it will take to develop quantum computers capable of breaking the public keys of current encryption systems. You specify D. You can plan for T according to your information systems and available commercial solutions and standards. How about G_c ? You must evaluate it with your gut feeling because current estimates span from 5-10 years to... never! For example, some researchers from the UK and USA tried in 2020 to predict when a FTQC would show up²⁵⁰².

²⁴⁹⁵ See [Podcast with Adm. Mike Rogers - former NDA director](#) by Yuval Boger, March 2022.

²⁴⁹⁶ See [New X9 Report Demystifies Quantum Computing Risks](#), BusinessWire, December 2022 which points to [Quantum Computing Risks to the Financial Services Industry](#), X9, 2022 (122 pages).

²⁴⁹⁷ See [Quantum computing could break the internet. This is how](#), by Sam Learner, John Thornhill, Sam Joiner and Irene de la Torre Arenas, Financial Times, May 2023.

²⁴⁹⁸ See [Quantum Cryptanalysis: Hype and Reality](#) by Chris Jay Hoofnagle and Simson Garfinkel, February 2022 think that the quantum cybersecurity threat is overestimated.

²⁴⁹⁹ See [The race to save the Internet from quantum hackers](#) by Davide Castelvecchi, Nature, February 2022.

²⁵⁰⁰ See [IQT Research Forecasts Revenues from Post Quantum Cryptography to Reach \\$6.7 Billion by 2032](#), July 2023.

²⁵⁰¹ See [The Quantum Insider Report Forecasts Quantum Security Market Worth \\$10 Billion by 2030](#), February 2022.

²⁵⁰² See [Forecasting timelines of quantum computing](#) by Jaime Sevilla and C. Jess Riedel, December 2020 (23 pages).

With a sort of logistic regression, their model predicted that proof-of-concept fault-tolerant quantum computers will be developed between 2026 and 2033 with 90% confidence with the median in early 2030, and that RSA-2048 Shor attacks will become feasible between 2039 and 2058 with a 90% confidence and median in 2050. Making predictions with such a method for a 30-year timeframe seems preposterous.

Michele Mosca and Marco Piani from evolutionQ publish a report every year collecting the opinion of about 40 renowned respondent experts on the potential advent of a quantum threat to public-key cryptography. The 2022 edition showcases similar results as in the previous editions, as shown in Figure 624. My take is that the best prediction one should make is: “*we don’t know!*”! And when you are paranoid, it easily becomes “*who knows?*”.

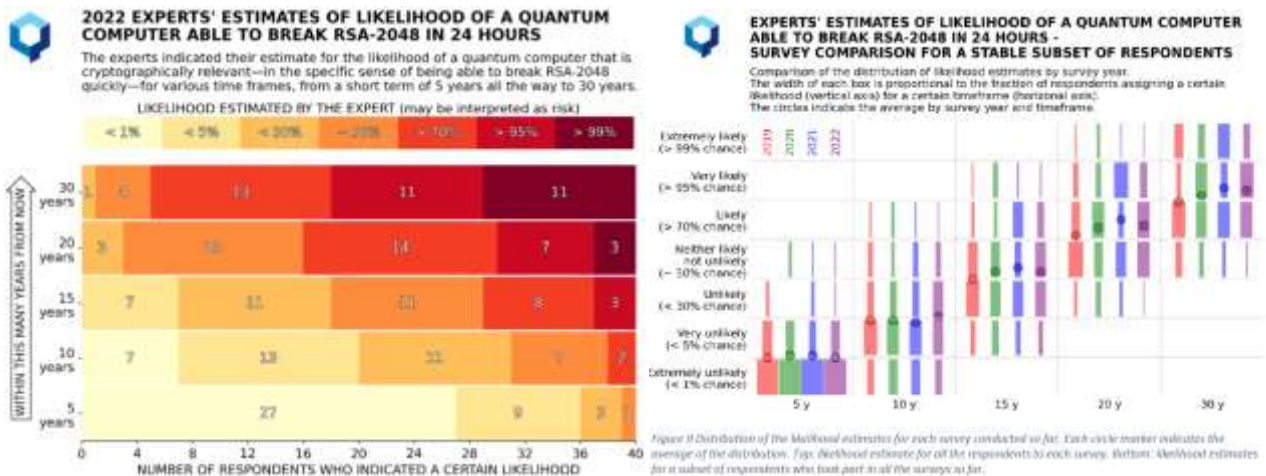


Figure 624: evolutionQ’s yearly report on the quantum cyber risk as estimated by specialists from various disciplines and the way their opinion changed over that last four surveys. Source: [2022 Quantum Threat Timeline Report - Global Risk Institute](#), 2022 (67 pages).

As an illustration, a US report from 2004 prepared with the best scientists of this period planned by the year 2012 to see the implementation of a concatenated quantum error-correcting code and to obtain 50 physical qubits²⁵⁰³. These qubits came by 2019 and we don’t have yet a sufficient number of qubits to implement concatenated codes. In 2012, the surface code was invented that is more efficient and has been experimented only at a very low scale by Google and Quantinuum.

Quantum cryptanalysis resource estimates

Quantum cryptanalysis is about code breaking. The usual landmark quantum break is dealing with an RSA 2048-bit key. Many resource estimates have been done accordingly.

To date, prime number factoring requires a traditional machine power that grows with the square root of the number to be factorized. The official classical RSA key factoring record was 768 bits in 2010, 795 bits in 2019 and 829 bits in February 2020²⁵⁰⁴ (see Figure 625). Even if this doesn’t consider undisclosed NSA records, it provides an idea of the problem scale.

²⁵⁰³ See [A Quantum Information Science and Technology Roadmap Part 1: Quantum Computation](#), 2004 (268 pages).

²⁵⁰⁴ This factorization of an RSA-250 digits (829 bits) and the previous RSA-240 digits (795 bits) was achieved by an international team led by French researchers from Inria: Fabrice Boudot (Université de Limoges), Pierrick Gaudry (CNRS), Aurore Guillevic, Emmanuel Thomé and Paul Zimmermann (Inria) and Nadia Heninger (University of California). Computation used 2,700 core-years, of Intel Xeon Gold 6130 CPUs running at 2.1 GHz. See [The State of the Art in Integer Factoring and Breaking Public-Key Cryptography](#) by Fabrice Boudot, Pierrick Gaudry, Aurore Guillevic, Nadia Heninger, Emmanuel Thomé and Paul Zimmermann, June 2022 (9 pages) and [Factoring RSA-240 and computing discrete logarithms in a 240-digit prime field with the same software and hardware](#) by Fabrice Boudot, Pierrick Gaudry, Aurore Guillevic, Nadia Heninger, Emmanuel Thomé and Paul Zimmermann, Inria, March 2021 (87 slides).

We are far from having a classical computer breaking an RSA 2048-bit code given the problem size is exponential with the size of the RSA key. As of 2023, the largest number ever factored on a gate-based quantum computer with Shor’s algorithm is 35 (7x5), with an IBM QPU²⁵⁰⁵. It followed a 2002 premiere with factoring 15 on an NMR qubit QPU from IBM²⁵⁰⁶. The largest Shor algorithm factoring is actually larger, with 549,755,813,701 = 712,321 × 771,781, but achieved on a Shor emulation done with classical GPUs in 2023²⁵⁰⁷.

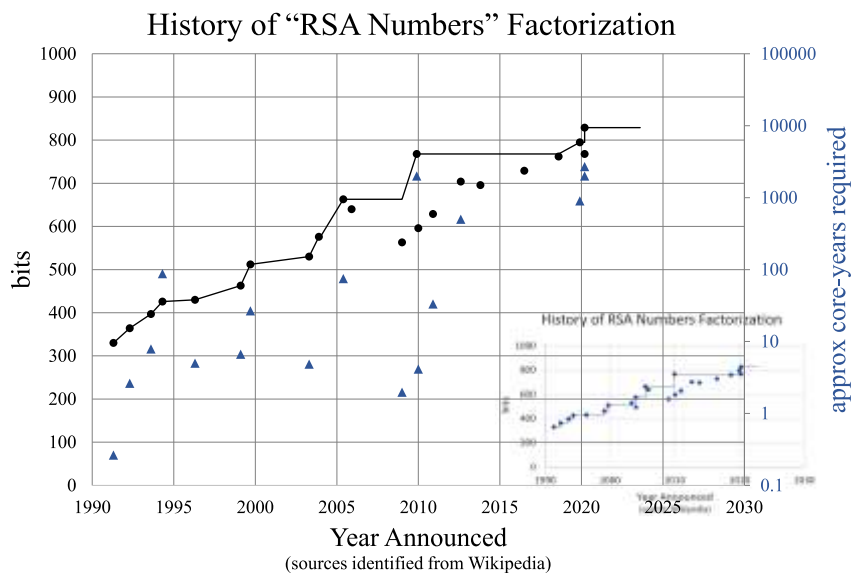


Figure 625: evolution of record classical factorization of RSA keys. Source: Prime Factorization by Tristan Sharp and Fabio Traversa, DISA TEM, August 2023 (35 slides).

Using a hybrid Variational Quantum Factoring algorithm itself based on a QAOA algorithm, **Zapata Computing** factored the number 1,099,551,473,989 (=1,048,589 multiplied by 1,048,601) with 5 IBM superconducting qubits in 2021 (which could be emulated on your smartwatch)²⁵⁰⁸.

Meanwhile, the largest number factored on a D-Wave 2000Q annealer was achieved in 2019 was 376,389 using a block multiplication table method²⁵⁰⁹. Then, in 2023, a South Korea team factorized 102,454,763 and 1,000,070,001,221 on a D-Wave annealer²⁵¹⁰. It however doesn’t seem to scale well. They used only 26 logical qubits while D-Wave Advantage has over 300 of them. A 762-bit RSA key close to the 2010 record would require a D-Wave annealer computer with 5.5 billion qubits, far from the existing 5,000 qubits²⁵¹¹. A D-Wave annealer with 5,893 qubits could do the job if all qubits could be arbitrarily coupled to the other, which is not possible due to the way these 2D chips are currently designed. Also, we should not discount threats coming from quantum machine learning algorithms²⁵¹².

In 2019, **Google’s** Craig Gidney published a reference algorithm and QPU architecture blueprint using surface codes that would break an RSA 2048-bit key in 8 hours with 22 million physical qubits

²⁵⁰⁵ See [An Experimental Study of Shor's Factoring Algorithm on IBM Q](#) by Mirko Amico, Zain H. Saleem and Muir Kumph, 2019 (10 pages).

²⁵⁰⁶ See [Experimental realization of Shor's quantum factoring algorithm using nuclear magnetic resonance](#) by Lieven M. K. Vandersypen et al, Nature, 2002 (18 pages).

²⁵⁰⁷ See [Large-scale simulation of Shor's quantum factoring algorithm](#) by Dennis Willsch, Madita Willsch, Fengping Jin, Hans De Raedt and Kristel Michielsen, August 2023 (31 pages).

²⁵⁰⁸ See [Analyzing the performance of variational quantum factoring on a superconducting quantum processor](#) by Amir H. Karamlou et al, npj, Zapata Computing October 2021 (6 pages).

²⁵⁰⁹ See [Breaking RSA Security With A Low Noise D-Wave 2000Q Quantum Annealer: Computational Times, Limitations And Prospects](#) by Riccardo Mengoni et al, Cineca and ENI, 2019 (8 pages).

²⁵¹⁰ See [HUBO and QUBO models for Prime factorization](#) by Kyungtaek Jun, January 2023 (11 pages).

²⁵¹¹ According to [High-fidelity adiabatic quantum computation using the intrinsic Hamiltonian of a spin system: Application to the experimental factorization of 291311](#) by Nike Dattani, Xinhua Peng and Jiangfeng Du, June 2017 (6 pages).

²⁵¹² See [Capgemini and Fraunhofer IAIS lead study in quantum machine learning for it security commissioned by the German Federal Office for Information Security](#), November 2021.

having an error rate of 0.1%²⁵¹³. Four years later, this blueprint is still a reference. When it was published, it was a key progress compared to the billion qubits that were needed in previous instances of Shor's algorithm.

On paper, breaking a 2048-bit RSA key requires a number of logical qubits that is at least equal to twice the size of the key used +2, so 4098 qubits. Depending on the technologies used, this number should be multiplied by 30 to 10,000s to obtain the related number of physical qubits. This scalability is one of the greatest challenges for building viable quantum computers as we've seen in other parts of this book.

Moreover, as we have seen in the section on Shor's algorithm, the quantum Fourier transform underlying it uses phase-controlled R-quantum gates whose implementation is far from obvious. Indeed, when the phase rotation has an angle of $(1/2,048) \times 2\pi$, the controlled rotation of the phase can be inferior to the error rate of a one or two-qubit quantum gate. We must therefore bet on the ability of error correction codes to handle this. Some researchers argue that may not be possible to run Shor algorithm with noisy qubits to implement these precise rotation gates, even in a FTQC regime²⁵¹⁴.

Various recent resources estimates have refined these numbers. A French team estimated that 349,133 cat qubits could break an RSA 2048 key with Shor's algorithm in 4 days and 126,133 qubits for a 256-bit elliptic curve key²⁵¹⁵. As of 2023, 4 cat-qubits had been assembled and not yet fully characterized by vendors like Alice&Bob. In June 2023, a PsiQuantum engineer estimated that breaking a similar 256-bit elliptic curve key would require about 6 million photonic qubits and 'only' 50 million Toffoli gates²⁵¹⁶.

Late 2022, **Classiq** estimated that 354,562 physical qubits could be enough to factorize an RSA 2048 key²⁵¹⁷. They used the default Azure Resource Estimator settings which assumes qubits have 99.9% error rates for single, two qubit and T gates as well as with readout, which is highly optimistic. It uses a surface code of distance 13 and logical qubit error rate of $5.1 \cdot 10^{-9}$. Still, the result is not far from Alice&Bob's above estimate.

Fujitsu published in 2023 an estimate of its own on the resources needed to factorize an RSA 2048 key using its 39-qubit classical quantum emulator²⁵¹⁸. They ended up with 10,000 logical qubits and 104 days of computing. They used their Fugaku supercomputer to factorize $N = 253$ in 463 seconds instead of 16 hours thanks to some optimization in their emulator. This could be done instantaneously using brute force on any classical computer!

Even better, a 2021 paper by Nicolas Sangouard et Elie Gouzien stated that theoretically, an RSA-2048 key could be broken by only 13,436 physical qubits in 177 days provided it could exploit a 40 million modes quantum memory²⁵¹⁹.

²⁵¹³ See [How to factor 2048 bit RSA integers in 8 hours using 20 million noisy qubits](#) by Craig Gidney and Martin Ekerå, 2019 (25 pages).

²⁵¹⁴ See [Shor's Algorithm Does Not Factor Large Integers in the Presence of Noise](#) by Jin-Yi Cai, University of Wisconsin-Madison, June 2023 (21 pages).

²⁵¹⁵ See [Performance Analysis of a Repetition Cat Code Architecture: Computing 256-bit Elliptic Curve Logarithm in 9 Hours with 126 133 Cat Qubits](#) by Élie Gouzien, Diego Ruiz, Francois-Marie Le Régent, Jérémie Guillaud, and Nicolas Sangouard, PRL, July 2023. And the corresponding arXiv, [Computing 256-bit Elliptic Curve Logarithm in 9 Hours with 126133 Cat Qubits](#), February 2023 (39 pages).

²⁵¹⁶ See [How to compute a 256-bit elliptic curve private key with only 50 million Toffoli gates](#) by Daniel Litinski, PsiQuantum, June 2023 (19 pages).

²⁵¹⁷ See [Making academic quantum algorithms automatically executable](#), Classiq, December 2022.

²⁵¹⁸ See [Fujitsu quantum simulator assesses vulnerability of RSA cryptosystem to potential quantum computer cryptography threat](#), Fujitsu, January 2023.

²⁵¹⁹ See [Factoring 2048-bit RSA Integers in 177 Days with 13436 Qubits and a Multimode Memory](#) by Nicolas Sangouard and Élie Gouzien, September 2021 (20 pages).

This sort of memory would be simpler to build than tens of millions of computing qubits, but it is still a huge challenge to create it.

Other proposals abound beyond FTQC architectures. For example, **ParityQC** (Austria) is proposing to use its reversible parity gates architecture. But breaking an RSA2048 key would require about 14 million qubits, not much less than the 23 million qubits from Craig Gidney's 2019 algorithm²⁵²⁰. Some US researchers are proposing a variational algorithm to factorize integers. It could factorize 143 as 11×13 and 323 as 19×17 but lacks any resource estimations at scale for breaking a 2048-bit RSA key²⁵²¹. So, forget it!

In December 2022, a China team of 25 researchers made the news with a so-called NISQ algorithm that could break an RSA 2048-bit key with only 372 physical qubits, using a hybrid lattice-based scheme based on the classical Schnorr factoring algorithm, accelerated by a QAOA quantum part²⁵²². It was demonstrated factoring a 48-bit key with only 10 superconducting qubits. It looked like the crypto-Armageddon was already there and drove its good share of visibility. Many experts including Peter Shor and Scott Aaronson expressed doubts that it could be achieved practically^{2523 2524}. Reasons abound: the Schnorr algorithm is not necessarily competitive with classical and quantum NFS (Number Field Sieve) approaches to factorize integers^{2525 2526}, the paper didn't provide any indication of the required computing time and it looked it was actually in the million years range, the quantum QAOA algorithm is known to have bad scalability in a NISQ regime, and on top of that, the algorithm needs 1,139 to 1,490 gate cycles, requiring qubit fidelities in the 5-nines range minimum, thus mandating some quantum error correction and significant physical qubit overhead in the thousands, thus invalidating their 372 qubits sizing claim. A Google team proved in July 2023 that the proposed algorithm cannot scale beyond a key of 70 bits, even with perfect qubits, with using a classical quantum emulator²⁵²⁷. An IonQ team found in August 2023 that lattice-based factoring does not scale successfully to larger numbers, whatever the role of a quantum computer in the setup²⁵²⁸. A team in Russia also proved that the classical part of the algorithm does not scale well²⁵²⁹. Another one also expressed doubts on the scalability of another optimized QAOA method²⁵³⁰. Case closed, for the moment!

A team from **Kipu Quantum** (German) upped the ante in January 2023 with proposing a lightly documented variation of the Schnorr/QAOA hybrid algorithm that would be adapted to their DAQC

²⁵²⁰ See [Scalable set of reversible parity gates for integer factorization](#) by Martin Lanthaler, Benjamin E. Niehoff and Wolfgang Lechner, ParityQC, Nature Communications Physics, May 2023 (8 pages).

²⁵²¹ See [Shallow Depth Factoring Based on Quantum Feasibility Labeling and Variational Quantum Search](#) by Imran Khan Tutul et al, Alfred University (USA), May 2023 (9 pages).

²⁵²² See [Factoring integers with sublinear resources on a superconducting quantum processor](#) by Bao Yan et al, December 2022 (32 pages).

²⁵²³ See [Chinese researchers claim success in breaking encryption using quantum computers](#) by Richard Waters, Financial Times, December 2022.

²⁵²⁴ See [Cargo Cult Quantum Factoring](#) by Scott Aaronson, January 2023.

²⁵²⁵ See [A low-resource quantum factoring algorithm](#) by Daniel J. Bernstein, Jean-François Biasse and Michele Mosca, 2017 (17 pages) which requires $O(n^{2/3})$ logical qubits, n being the number of bits in the RSA key to factorize.

²⁵²⁶ See [On speeding up factoring with quantum SAT solvers](#) by Michele Mosca, João Marcos Vensi Basso and Sebastian R. Verschoor, Nature Scientific Reports, September 2020 (11 pages).

²⁵²⁷ See [A comment on "Factoring integers with sublinear resources on a superconducting quantum processor"](#) by Tanuj Khattar and Nour Yosri, Google, July 2023 (6 pages). Schnorr algorithm doesn't scale.

²⁵²⁸ See [Quantum and Classical Combinatorial Optimizations Applied to Lattice-Based Factorization](#) by Willie Aboumrad et al, IonQ, August 2023 (23 pages).

²⁵²⁹ See [Pitfalls of the sublinear QAOA-based factorization algorithm](#) by S.V. Grebnev et al, March-Septembre 2023 (19 pages).

²⁵³⁰ See [Integer Factorization through Func-QAOA](#) by Mostafa Atallah et al, September 2023 (25 pages).

(digital analog quantum computing) architecture. They tested it at a small scale with a 48-bit key with 10 Quantinuum qubits but its potential scale is also in question²⁵³¹.

Another China team proposed in April 2023 to turn Shor's integer factoring algorithm into a hybrid classical/quantum version with distributing its period finding part over several QPUs²⁵³². They would implement non-local quantum gates thanks to some qubit teleportation in parallel for a number of qubits equivalent to the size of the RSA key to factorize which is not yet available, at least, deterministically. In a way, it is about moving the goal post elsewhere. In August 2023, an algorithm proposed by Oded Regev traded a better computing time with some classical parallelization and post-processing and a larger number of logical qubits²⁵³³. It does not increase the quantum computing threat on cybersecurity.

In 2023, a US-India research team was able to factorize tetra and penta prime integers on an IBM QPU²⁵³⁴. Nice! Tetra and penta prime integers are integers with 4 and 5 prime integers factors, which are easier to find than integers with only two prime factors like in RSA keys. On top of that, the performance was achieved with 3 and 4 qubits of a 7-qubit IBM QPU. Which means that there is no quantum advantage at all, since these qubits can be perfectly emulated on a Raspberry Pi, or even a microcomputer from the late 1970s!

At last, let's mention that, in 2021, **Terra Quantum** (Switzerland) announced that AES encryption was threatened by quantum algorithms running on some D-Wave annealer of the future²⁵³⁵. It seemed to be a dubious claim^{2536 2537}.

As usual, this kind of sensational paper generates some FUD (fear, uncertainty, and doubt) and leverages the famous Brandolini's law according to which the resources needed to counter an invalid claim are at least one order of magnitude larger than the ones used to broadcast the claim. With that said, you can probably sleep very well and keep worrying about other cybersecurity vulnerabilities!

Quantum Random Numbers Generators

Quantum, post-quantum and traditional cryptographic systems are all fed by random number generators. They have been around for ages. Random numbers are also used in a large set of applications beyond classical cryptographic protocols.

It includes gaming and casinos to draw lottery winning numbers, playing card shuffling, and various bets-related numbers, statistical analysis like the ones using Monte Carlo simulations in the finance sector, selecting random samples from large data sets like with machine learning, various scientific simulations and testing (like the Wheeler which-way or delay-choice experiment we already described page 114), and smart networks simulations.

In all these use cases, the main concern is to create truly random numbers. Namely sequences of 0s and 1s without repetitions of any sequence and a balanced proportion of 0 and 1, as in the decimals of π .

²⁵³¹ See [Digitized-counterdiabatic quantum factorization](#) by Narendra N. Hegade and Enrique Solano, January 2023 (3 pages).

²⁵³² See [Distributed Quantum-classical Hybrid Shor's Algorithm](#) by Ligang Xiao et al, Sun Yat-sen University and QuDoor Technologies, April 2023 (15 pages).

²⁵³³ See [An Efficient Quantum Factoring Algorithm](#) by Oded Regev, New York University, August 2023 (12 pages).

²⁵³⁴ See [Factorization of large tetra and penta prime numbers on IBM quantum processor](#) by Ritu Dhaulakhandi et al, April 2023 (12 pages).

²⁵³⁵ See [Swiss firm Terra Quantum uncovers vulnerabilities that imperil encryption](#) by Ryan Gallagher, Bloomberg, February 2021.

²⁵³⁶ See [Does Terra Quantum AG break AES and Hash Algorithms?](#), Crypto Stackexchange, 2021.

²⁵³⁷ See [Quantum Security Analysis of AES](#) by Xavier Bonnetain et al, Sorbonne Université and Inria, 2019 (39 pages).

These number generation processes must also be non-deterministic, not reproducible and with no correlations, meaning that series of randomly generated numbers must be statistically independent. We could indeed generate good random numbers but if they were similar in time, it wouldn't be satisfactory at all.

Unfortunately, most used random number generators are pseudo-random and happen to be deterministic. These are branded **PRNGs** (Pseudo-Random Number Generators).

Some mathematical formula deterministically produces a series of numbers, and some randomness is introduced by using as seed parameters some highly variable elements such as time with a millisecond precision, GPS coordinates, thermal noise or other contextual information. It still generates deterministic sequences of numbers with some repeat period, although passing regular randomness tests successfully.

Most PRNG systems now use a randomness extractor merging the output of a random entropy source and a short random seed. Despite these initialization variables and various tricks of the trade, common random number generators still create some periods within their generated numbers²⁵³⁸. Still, it may be useful to use deterministic RNGs in some cases where reproducibility is mandatory. Also, PRNGs have the advantage to be fast²⁵³⁹ (Figure 626). To avoid determinism, we must use a truly random physical process for the generation of numbers, aka **TRNGs** (True Random Number Generators), based on some chaotic physical phenomenon. One common technique consists in measuring the thermal noise of an electronic component or the atmospheric electromagnetic noise²⁵⁴⁰.

Thermal noise TRNGs are implemented in most microprocessors like those from **Intel** since 2013 and from **AMD** since 2015 but with various identified weaknesses²⁵⁴¹. It can for example rely on voltage randomness in resistive materials (Johnson's effect), Zener noise in diodes or, more commonly, on some amplified free-running oscillator.

So here come **QRNGs** (Quantum Random Number Generators), a subclass of TRNGs. They rely on quantum physics laws and one that is particularly important: Born's probability rule, based on Schrödinger's wave equation. It replaces a generic chaotic system by a non-deterministic measurement of a physical property of some quantum objects, usually individual photons. In quantum physics, a quantum object's properties measurement is intrinsically random, at least, as far as we know²⁵⁴².

Quantum is the kingdom of randomness²⁵⁴³! But this randomness is not a guarantee to obtain truly nondeterministic random numbers. There are weaknesses in all these systems, particularly with their classical or semi-classical components like the beam splitters or photon detectors it is using, or with the software part handling the so-called randomness extraction.

²⁵³⁸ However, there are still other solutions for generating non-quantum random numbers that need to be equally random, although this is still questionable. See for example [Scientists Develop 'Absolutely Unbreakable' Encryption Chip Using Chaos Theory](#) by Davey Winder, 2019.

²⁵³⁹ See [Quantum Random-Number Generators: Practical Considerations and Use Cases Report](#) by Marco Piani, Michele Mosca and Brian Neill, evolutionQ, January 2021 (38 pages). This is the best document I found that explains the various subtleties of QRNGs, particularly about the device dependent and device-independent species.

²⁵⁴⁰ Atmospheric noise is used by the service [random.org](#) operated by Randomness and Integrity Services Ltd (1998, Ireland).

²⁵⁴¹ Since 2013, Intel processors have been using the RDRAND function that is part of their 32 and 64 bits instruction set, returning a random number generated by an on-chip thermal noise based entropy source. AMD provides support for this instruction set since June 2015.

²⁵⁴² See the review paper [A Comprehensive Review of Quantum Random Number Generators: Concepts, Classification and the Origin of Randomness](#) by Vaisakh Mannalath et al, March 2022-December 2023 (38 pages) and [Quantum Random Number Generators : Benchmarking and Challenges](#) by David Cirauqui et al, June 2022 (15 pages).

²⁵⁴³ See [Can Free Will Emerge from Determinism in Quantum Theory?](#) by Gilles Brassard and Paul Raymond-Robichaud, 2012 (22 pages). Even this is however arguable. See for example [Quantum randomness is chimeric](#) by Karl Svozil, April 2021 (16 pages) which comes back on the eternal debate of quantum measurement and its related randomness.

Its consequence is an intense competition between QRNG vendors. They all claim to generate “truly” random numbers contrarily to their QRNG competitors.

Many differentiation features are also important: the random numbers generation rate (in bits/seconds, some applications may be very demanding), the time it takes to warm up and stabilize the system (some QRNGs are slow to warm-up and may require hours to stabilize), is it device independent (impacts randomness quality but also RNG rates; but no such commercial systems are available yet), certifiability (some are black-boxes that are really difficult to audit, others are said to be self-certified) and other standard characteristics that may be important depending on the use case (weight, size, price and power drain).

At last, vendor trust is a key criterion, particularly when you discover that some Switzerland cybersecurity products contained backdoors created on behalf of the CIA²⁵⁴⁴. It also explains why, whatever the technology used, western countries may not and probably should not rely on Chinese or Russian TRNG/QRNG vendors. It is now up to you to understand how these systems are benchmarkable and benchmarked to figure out whether such and such QRNG is safe or not. Many different QRNG techniques have been created to date. The most commonplace are those using photons, with components that are now easy to miniaturize, even in a smartphone.

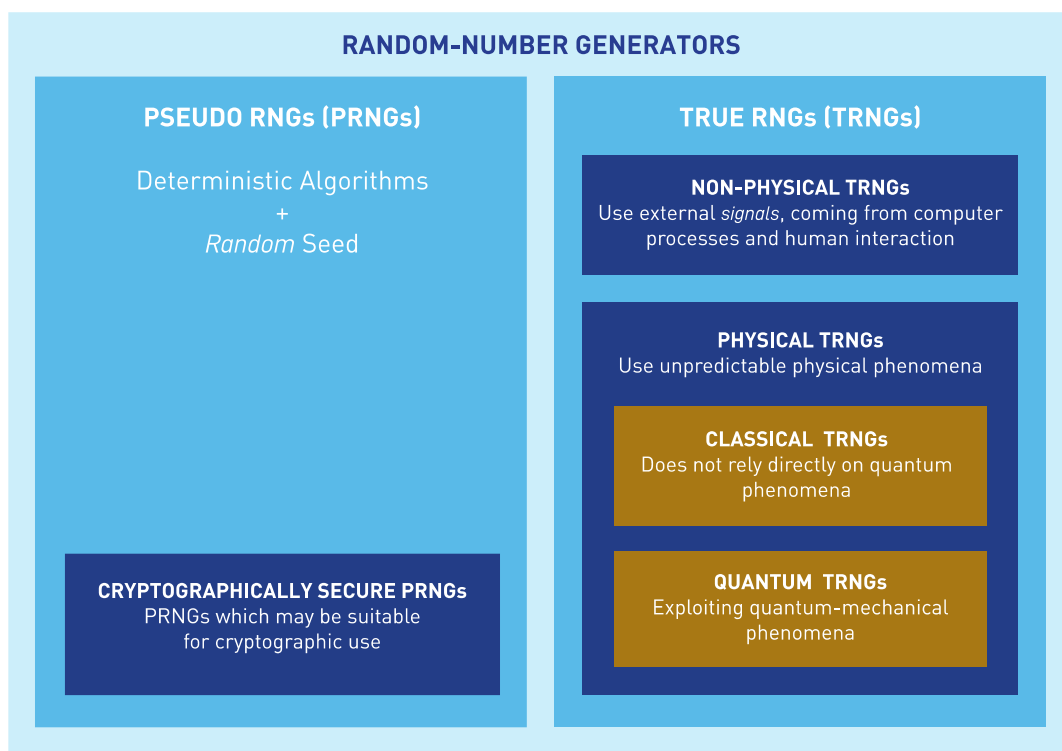


Figure 626: taxonomy of random numbers generators. Source: [Quantum Random-Number Generators: Practical Considerations and Use Cases Report](#) by Marco Piani, Michele Mosca and Brian Neill, evolutionQ, January 2021 (38 pages).

Photons counting aka photon-number resolving is the most common method, based on the measurement of single photons emitted individually in series, passing through a regular balanced beam splitter and analyzed by two detectors²⁵⁴⁵. The series of generated 0s and 1s are theoretically random. Quantum physics mathematical formalism and experiments say so!

²⁵⁴⁴ See [The intelligence coup of the century? - For decades, the CIA read the encrypted communications of allies and adversaries](#) by Greg Miller, Washington Post, February 2020. It deals with the Crypto AG company created in 1952 and dissolved in 2018.

²⁵⁴⁵ See [Quantum Random Number Generators](#) by Miguel Herrero-Collantes, 2016 (54 pages). This setting is frequently referred to as a welcher-weg experiment, or “which way” experiment.

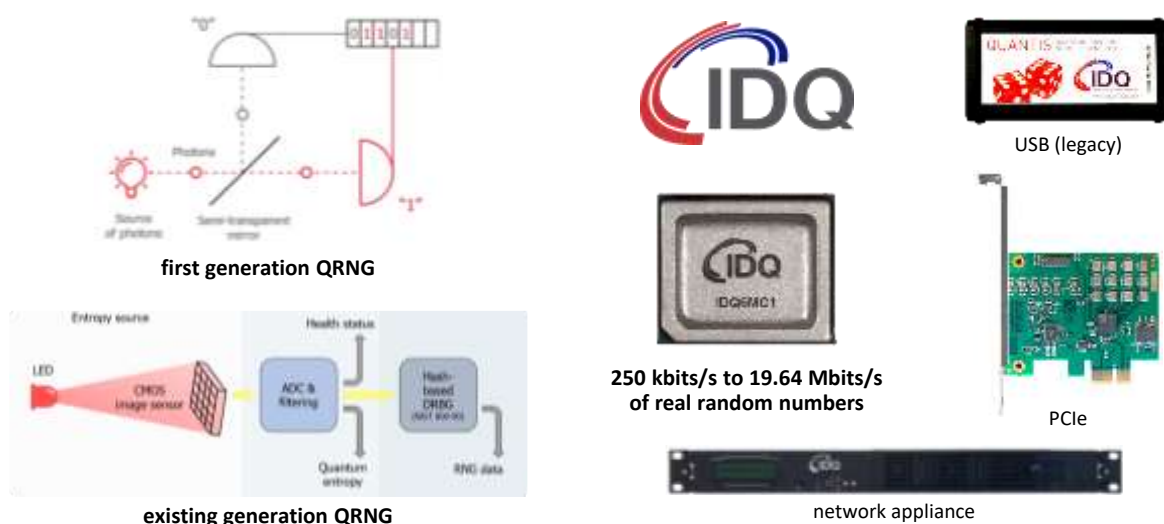


Figure 627: IDQ quantum number generators. Source: IDQ.

Each detected photon creates at most only one bit, but not all photons are detected. The detection speed is limited by the photon detectors bandwidth and their saturation level. This QRNG technique was pioneered by **IDQ** (Switzerland) in 2001 (Figure 627).

One of its shortcomings is the used light source that can't necessarily be certified. In some products, there's also some warm-up time before real random numbers can be generated. Some solutions can certify the numbers generation randomness in such situation, like using a first beam splitter and detector before photons are separated by a polarizing beam splitter²⁵⁴⁶.

Nowadays, photon counting is (seemingly) done without a polarizing beam splitter. The light source is some LED diode, lighting a small CMOS image sensor, and generating “shot noise”. That's what IDQ is now selling with its miniaturized Quantis chip. It is adapted to mass market use cases, in smartphones, laptops and cars. Such QRNG first appeared in a consumer product in 2020 in a version of the **Samsung** Galaxy A71 5G smartphone called Galaxy A Quantum, marketed by **SK Telecom** only in Korea. It probably won't change much in terms of user security, but it can make a lasting impression. In June 2023, the Samsung Galaxy Quantum 4 was released with the latest 2.5mm×2.5mm IDQ QRNG chipset.

In April 2021, Samsung announced a new version of this smartphone, the Galaxy Quantum2, adapted to 5G and with similar QRNG features using an IDQ Quantis chip²⁵⁴⁷. The same chip is found in a Vsmart Aris 5G smartphone, coming from Vietnam! In February 2023, IDQ launched a new revision of its QRNG chip, the IDQ250C3 which, surprisingly, is a little larger than the former IDQ250C2, with a size of 3x3x0.8 mm.

Q→NU, **CryptaLabs** and **Qrypt** are also commercializing such type of QRNGs.

Photon arrival time aka “time bin qubits” is about evaluating the arrival time of successive single photons in a simpler setting coupling a photon source like a LED or a laser and a photon counter to a high-resolution counter, down to a couple nanoseconds²⁵⁴⁸.

²⁵⁴⁶ See [Using the unpredictable nature of quantum mechanics to generate truly random numbers](#) by Bob Yirka, 2021 that refers to [Certified Quantum Random Numbers from Untrusted Light](#) by David Drahi, December 2020 (32 pages). Its RNG output is 8.05 Gb/s.

²⁵⁴⁷ The QRNG chipset is a square of 2.5mm creating random codes by capturing noise from an LED and a CMOS sensor.

²⁵⁴⁸ See [Photon arrival time quantum random number generation](#) by Michael A. Wayne et al, 2009 (7 pages) which describes the principles of this random numbers generation methods.

Practically, randomness comes from evaluating the variation of this arrival time compared with the decaying exponential waiting-time distribution²⁵⁴⁹. The system can also use a photon counting setting with a regular beam splitter and two photon detectors coupled each with a counter²⁵⁵⁰. It has low latency and is quickly up to speed. **Qnu Labs, PicoQuant and QuTools** are providers of such QRNGs. A variation of this technique recently developed uses a LED light illuminating a matrix of SPADs (single photon avalanche detectors) on a CMOS circuit, with a RNG capacity of 400 Mbit/s²⁵⁵¹.

Spontaneous emission uses amplified spontaneous emission, detection and digitization of optically filtered amplified spontaneous emission noise from a light source such as superluminescent diode (SLD)²⁵⁵². It can even support entangled photons generation²⁵⁵³ and device independence²⁵⁵⁴.

Phase noise and phase diffusion (PD-QRNG²⁵⁵⁵) are variations of spontaneous emission QRNGs. It uses a photons counting method variation proposed in 2009²⁵⁵⁶. Implementations can use a VCSEL laser (single mode vertical cavity surface emitting laser) that is associated with a phase noise measurement using a delay self-homodyne method²⁵⁵⁷. The photons from the laser are traversing a beam splitter. Among its benefits are a very high-bit rate, of potentially several tens of Gbits/s of random bits.

The technique is used by vendors like **Quside, Quantum eMotion and Kets**. One way goes to the next beam splitter, and the other traverses a delay line, and is then merged back with the main line. An APD (avalanche photodetector), then counts the exiting photons and its signal is converted from analog to digital with an ADC²⁵⁵⁸ (Figure 628).

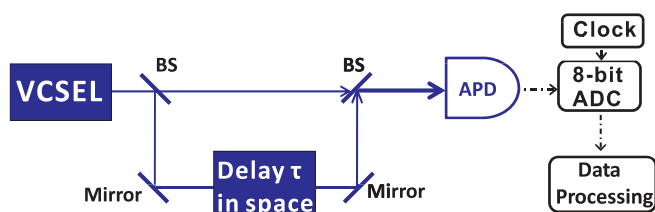


Figure 628: Source: [Truly Random Number Generation Based on Measurement of Phase Noise of Laser](#) by Hong Guo et al, Peking University, January 2010 (4 pages).

²⁵⁴⁹ See [Quantum random number generation using an on-chip nanowire plasmonic waveguide](#) by C. Strydom et al, June 2023 (10 pages).

²⁵⁵⁰ See [First high-speed quantum-safe randomness generation with realistic devices](#), NTT, February 2021, which refers to [A simple low-latency real-time certifiable quantum random number generator](#) by Yanbao Zhang et al, 2021 (8 pages).

²⁵⁵¹ See [A High Speed Integrated Quantum Random Number Generator with on-Chip Real-Time Randomness Extraction](#) by Francesco Regazzoni et al, February 2021 (9 pages).

²⁵⁵² See [Quantum Random Number Generator Based on LED](#) by Mohammadreza Moeini et al, Iran, May 2023 (7 pages).

²⁵⁵³ See [Generation of quantum-certified random numbers using on-chip path-entangled single photons from an LED](#) by Nicolò Leone et al, March 2023 (23 pages).

²⁵⁵⁴ See [Quantum random number generation based on a perovskite light emitting diode](#) by Joakim Argillander et al, December 2022 (9 pages).

²⁵⁵⁵ See [Quantum entropy source on an InP photonic integrated circuit for random number generation](#) by Carlos Abellan et al, Optica, 2016 (7 pages) and [Real-time interferometric quantum random number generation on chip](#) by Thomas Roger et al, Journal of Optical Society, 2019 (7 pages).

²⁵⁵⁶ In [Experimental demonstration of a high speed quantum random number generation scheme based on measuring phase noise of a single mode laser](#) by Bing Qi, Yue-Meng Chi, Hoi-Kwong Lo and Li Qian, 2009 (7 pages).

²⁵⁵⁷ VCSEL. See [Gain-switched vcsel as a quantum entropy source: the problem of quantum and classical noise](#) by Roman Shakhovoy and E.I. Maksimova, January 2023 (5 pages).

²⁵⁵⁸ See [Truly Random Number Generation Based on Measurement of Phase Noise of Laser](#) by Hong Guo et al, Peking University, January 2010 (4 pages).

Quantum vacuum fluctuations uses a balanced homodyne measurement of vacuum fluctuations of the electromagnetic field contained in the radio-frequency sidebands of a single-mode (usually 780 nm) laser diode²⁵⁵⁹ (Figure 629). Two diodes compute the difference of the signals coming from the two exits of a polarizing beam splitter and the resulting signal is amplified and digitized, to be processed by a randomness extractor. Such a QRNG system is implemented in a web site run by ANU (Australian National University) with the qStream QRNG from **Quintessence Labs**, which generates keys at a >3.5Gbps rate²⁵⁶⁰. A record of 100 Gbps rate was obtained by a European team in 2022²⁵⁶¹.

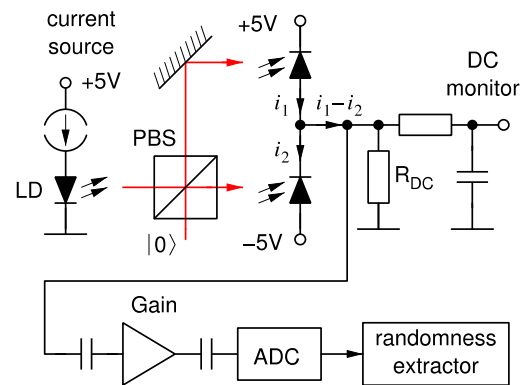


Figure 629: quantum vacuum fluctuation QRNG. Source: [Random numbers from vacuum fluctuations](#) by Yicheng Shi et al, 2016 (5 pages)

Variations have been proposed like device-independent sources²⁵⁶² and controlling “biased” quantum randomness²⁵⁶³.

Radioactive decay was one of the first developed QRNG technologies, based on the random timing of decay of radioactive atoms, detected with a Geiger counter. It has limited bit rates and is not widely used, on top of not being very practical to implement given it is based on radioactive materials. There is however a vendor in that space, **EYL**.

Other various techniques are mentioned but seemingly not widely used: **laser chaos** that creates a time-delayed optical feedback via a reflector, **Raman scattering**, **attenuated pulse** and **Optical Parametric Oscillators (OPO)** and as proposed in 2022, **skyrmions**-based QRNGs²⁵⁶⁴.

Another technique consists in merging in a single platform several QRNG methods. That’s what a Chinese team released in July 2021 on an Alibaba Cloud server, mixing four types of QRNGs: single-photon detection, photon-counting detection, phase-fluctuations, and vacuum-fluctuations²⁵⁶⁵. Three of these QRNG sources were off-the-shelf (Quantis-PCIe-16M from ID Quantique, QRG-100E from QuantumCTek and QRN-16 from MPD).

Device Independence deals with the difference between randomness and privacy. An SDI (source device independent) QRNGs ensures private randomness, where the created random numbers can’t be known by any adversary. With SDI QRNGs, the randomness source is assumed to be untrusted but the measurement devices are trusted. It is more secured than a trusted device or device dependent QRNG where the device is well characterized and trusted. Device independence must also deal with

²⁵⁵⁹ A homodyne measurement consists in extracting information encoded as modulation of the phase and/or frequency of an oscillating signal. In the mentioned case, it’s the phase. See an example in [Random numbers from vacuum fluctuations](#) by Yicheng Shi et al, 2016 (5 pages) and in [A homodyne detector integrated onto a photonic chip for measuring quantum states and generating random numbers](#) by Francesco Raffaelli et al, University of Bristol, Quantum Science and Technology, February 2018 (10 pages).

²⁵⁶⁰ See <https://qrng.anu.edu.au/> and [Real time demonstration of high bitrate quantum random number generation with coherent laser light](#), by T. Symul et al, 2021 (4 pages) and [Maximization of Extractable Randomness in a Quantum Random-Number Generator](#) by J. Y. Haw, 2015 (13 pages). The operations are linked to the offer of QuintessenceLabs.

²⁵⁶¹ See [100-Gbit/s Integrated Quantum Random Number Generator Based on Vacuum Fluctuations](#) by Cédric Bruynsteen et al, Ghent University, DTU, Politecnico & Università di Bari, PRX Quantum, March 2023 (11 pages).

²⁵⁶² See [Realization of a source-device-independent quantum random number generator secured by nonlocal dispersion cancellation](#) by Jining Zhang et al, 2023 (10 pages).

²⁵⁶³ See [Biasing the quantum vacuum to control macroscopic probability distributions](#) by Charles Roques-Carmes et al, MIT, Science, July 2023 (9 pages).

²⁵⁶⁴ See [Single skyrmion true random number generator using local dynamics and interaction between skyrmions](#) by Kang Wang et al, Nature Communications, February 2022 (8 pages).

²⁵⁶⁵ See [Quantum random number cloud platform](#) by Leilei Huang, Hongyi Zhou, Kai Feng and Chongjin Xie, Nature, July 2021.

detector attacks in the QRNG²⁵⁶⁶. These have a high bit rate in the Gbits/s range while SDI QRNGs have a much lower bit rate, in the kbits/s range due to a more complicated setup. SDI QRNG can rely on entanglement and nonlocality or be based on quantum computation (this is a variation of the qubit measurement technique mentioned above). SDI QRNG enables real-time estimate of the output entropy which can quantify and certify the QRNG randomness without possessing a detailed knowledge of the entropy source device. The device independence certification comes with loophole free violation of Bell's inequalities²⁵⁶⁷.

A record rate of 17 GBits/s key generation with a SDI-QRNG was obtained in 2018 in an Italian lab²⁵⁶⁸. It was also experimented in a highly integrated photonic circuits, using a self-tested randomness expansion protocol with multi-dimensional encoding²⁵⁶⁹.

There are also MDI-QRNGs, where the source is trusted, and the measurement device is untrusted. It is for example used with time-bin QRNGs with a testing mode used to create a 4-quantum states ($|0\rangle$, $|1\rangle$, $|+\rangle$ and $|-\rangle$) tomography²⁵⁷⁰.

Qubits measurement is a more generic way of generating quantum randomness than photon counting after traversing a polarizing beam splitter. It uses gates-based quantum processing units applied to one or several qubits and creating superposition. The simplest is a single Hadamard gate, but it is not sufficient to create enough randomness. The common practice is to create entangled states, or Bell states, which is done combining Hadamard and CNOT gates²⁵⁷¹.

The useful states are those where there is some correlation or anticorrelation between the qubits from a Bell pair, showing that they were random. Quantinuum is providing such a solution, named Quantum Origin, running on superconducting qubits in the cloud, in partnership with IBM and also running on Quantinuum trapped ions qubits. And they are not alone supporting IBM QPUs^{2572 2573}. Quandela is also proposing such a solution with its Entropy offering using a 2-photon qubit processor with certified device-independence randomness²⁵⁷⁴.

There are variations of QRNG exploiting computing qubits that are based on quantum walks²⁵⁷⁵, randomized benchmarks²⁵⁷⁶ and even quantum annealers²⁵⁷⁷.

²⁵⁶⁶ See [Source-independent quantum random number generator against detector blinding attacks](#) by Wen-Bo Liu et al, April 2022 (14 pages).

²⁵⁶⁷ See [Experimental Certification of Quantum Transmission via Bell's Theorem](#) by Simon Neves, Damian Markham, Eleni Diamanti et al, April 2023 (34 pages).

²⁵⁶⁸ See [Source-device-independent heterodyne-based quantum random number generator at 17 Gbps](#) by Marco Avesani et al, 2018 (7 pages). It uses a POVM measurement of continuous variable observables.

²⁵⁶⁹ See [Multidimensional quantum entanglement with large-scale integrated optics](#) by J. Wang et al, Science, 2018 (24 pages).

²⁵⁷⁰ See [Experimental measurement-device-independent quantum random number generation](#) by You-Qi Nie et al, China, 2016 (16 pages).

²⁵⁷¹ See [Quantum random number generators with entanglement for public randomness testing](#) by Janusz E. Jacak et al, 2020 (9 pages) and [Reference Standard RS-EITCI-QSG-EQRNG-PROTOCOLS-STD-VER-1.0](#), EITCI, 2019 (21 pages).

²⁵⁷² See [A Programmable True Random Number Generator Using Commercial Quantum Computers](#) by Aviraj Sinha et al, Southern Methodist University, April 2023 (15 pages).

²⁵⁷³ See [Practical Quantum Computing with QuantumPath: 3-qubit random number generator](#), José Luis Hevia and Alonso Martin-Toledano, aQuantum, November 2022.

²⁵⁷⁴ See [Certified randomness in tight space](#) by Andreas Fyrrillas, Boris Bourdoncle, Aristide Lemaître, Isabelle Sagnes, Niccolo Somaschi, Nadia Belabas, Shane Mansfield et al, Quandela, C2N and University of Bristol, January 2023 (23 pages).

²⁵⁷⁵ See [Quantum Walk Random Number Generation: Memory-based Models](#) by Minu J. Bae, University of Connecticut, July 2022 (12 pages).

²⁵⁷⁶ See [Certified Randomness from Quantum Supremacy](#) by Scott Aaronson and Shih-Han Hung, March 2023 (84 pages).

²⁵⁷⁷ See [Analysis of a Programmable Quantum Annealer as a Random Number Generator](#) by Elijah Pelofske, Los Alamos National Laboratory, July-December 2023 (9 pages).

Quality. Quantum random number generators are not equal. The source may be a true RNG but other components may contain weaknesses and be hacked in some circumstances: the photon source²⁵⁷⁸, the photon measurement system which could deviate or be defective, and at last randomness extractor various other weaknesses²⁵⁷⁹. Also, it can be difficult to distinguish classical hardware noise from the quantum randomness coming from the QRNG in evaluation tests.

Evaluation. Random series of numbers must be incompressible. This algorithmic randomness can be tested with Borel normality. An infinite sequence of binary numbers is random if every binary string of length n appearing in the sequence has a frequency of 2^{-n} .

There are various tests of algorithmic randomness like the NIST SP 800-22 1A Test²⁵⁸⁰. It contains 15 tests, but other tests suites exist that complement the NIST set, totaling 40 tests²⁵⁸¹ (Figure 630).

Test	Defect detected	Property
Frequency (monobit)	Too many zeroes or ones	Equally likely (global)
Frequency (block)	Too many zeroes or ones	Equally likely (local)
Runs test	Oscillation of zeroes and ones too fast or too slow	Sequential dependence (locally)
Longest run of ones in a block	Oscillation of zeroes and ones too fast or too slow	Sequential dependence (globally)
Binary matrix rank	Deviation from expected rank distribution	Linear dependence
Discrete fourier transform (spectral)	Repetitive patterns	Periodic dependence
Non-overlapping template matching	Irregular occurrences of a prespecified template	Periodic dependence and equally likely
Overlapping template matching	Irregular occurrences of a prespecified template	Periodic dependence and equally likely
Maurer's universal statistical	Sequence is incompressible	Dependence and equally likely
Linear complexity	Linear feedback shift register (LFSR) too short	Dependence
Serial	Non-uniformity in the joint distribution for m-length sequences	Equally likely
Approximate entropy	Non-uniformity in the joint distribution for m-length sequences	Equally likely
Cumulative sums (cusum)	Too many zeroes or ones at either an early or late stage in the sequence	Sequential dependence
Random excursions	Deviation from the distribution of the number of visits of a random walk to a certain state	Sequential dependence
Random excursions variants	Deviation from the distribution of the number of visits (across many random walks) to a certain state	Sequential dependence

Figure 630: the NIST test suite for QRNG. Source: [Random Number Generators: An Evaluation and Comparison of Random.org and Some Commonly Used Generators](#) by Charmaine Kenny, April 2005 (107 pages).

Recent TRNG/QRNG benchmarking tools use machine learning techniques and a convolutional network to detect patterns in the generated numbers²⁵⁸².

²⁵⁷⁸ See for example [QRNG: Out-of-Band Electromagnetic Injection Attack on a Quantum Random Number Generator](#) by P.R. Smith et al, January 2021 (12 pages).

²⁵⁷⁹ See [Improved Real-time Post-Processing for quantum Random Number Generators](#) by Qian Li et al, CAS, January 2023 (11 pages).

²⁵⁸⁰ See [A Statistical Test Suite for Random and Pseudorandom Number Generators for Cryptographic Applications](#) by Andrew Rukhin et al, NIST, 2010 (131 pages). Then, [Experimentally probing the algorithmic randomness and incomputability of quantum randomness](#) by Alastair Abbott, Cristian Calude and al, UGA/Institut Néel France and University of Auckland, 2018 (17 pages) and [Recommendations and illustrations for the evaluation of photonic random number generators](#) by Joseph D. Hart et al, 2017 (29 pages).

²⁵⁸¹ See [Random Number Generators: An Evaluation and Comparison of Random.org and Some Commonly Used Generators](#) by Charmaine Kenny, April 2005 (107 pages).

²⁵⁸² See [Machine Learning Cryptanalysis of a Quantum Random Number Generator](#) by Nhan Duy Truong et al, 2019 (13 pages) and [Benchmarking a Quantum Random Number Generator with Machine Learning](#), 2020 (26 slides).

However, while these tests may detect weaknesses in QRNG randomness, it won't ensure real non-determinism. Other tests are required, like loophole free Bell tests, already mentioned.

QKD or PQC? We'll describe these two cryptography solutions later on. Which one will make use of QRNGs? Post-quantum cryptography requires large classical random keys, so QRNGs will be very useful, particularly those who have a large throughput. Quantum Key Distribution (QKD) needs randomness to select its active basis choice for each and every detected pair of photons like their polarization angle. So again, a good and fast QRNG will be mandatory. This QRNG functionality can however be embedded in some specific QKD systems with relying on the randomness of the time between photons detection in the SPCMs (Single Photon Counting Modules)²⁵⁸³. But QRNGs have a much broader addressable market: classical cryptography and all the businesses in need of random numbers like casinos, online gaming and lotteries.



Figure 631: a map of QRNG vendors. (cc) Olivier Ezratty, 2022.

Let's now look at the QRNG industry vendor's landscape (Figure 631). As said before, this technique has been mastered for a long time by **ID Quantique (IDQ)**, a company cofounded by Nicolas Gisin, which belongs to SK Telecom since 2018. Other players abound like **CryptoMathic**, **Crypta Labs**, **Quside**, **InfiniQuant**, **Kets**, **PicoQuant** and **Quantropi**²⁵⁸⁴. **Axion Technologies** (2017, Canada) also created a random number generator competing with the Swiss IDQ.



Alea Quantum Technologies (2023, Denmark) provides a simplified vacuum based QRNG solution using an arbitrary transmissivity beam splitter ($\eta < 1$) and replacing one of the photodiodes by a beam dump, allowing a compact implementation. The entropy source uses a VCSEL laser source, a single photodetector and a photodiode.



CryptoMathic (1986, Denmark) develops quantum random key generators and various keys generation systems.



EYL (2015, USA, \$900K) sells radioactive isotopes-based entropy chips of 3mmx3mm and QRNG chips. They form factor is a USB key.

²⁵⁸³ This is described in [Practical random number generation protocol for entanglement-based quantum key distribution](#) by G. B. Xavier et al, 2008 (10 pages).

²⁵⁸⁴ These companies are described in the [quantum telecommunication and cryptography](#) vendors section since they provide some PQC or QKD solution on top of QRNGs.



PicoQuant (1996, Germany) is a Berlin-based SME specialized in photonics and which markets photon counters (SPADs) and diode lasers. But they are here because they also offer a photon arrival time QRNG, the PQRNG 150, with a throughput of 150 Mbits/s. It is much less miniaturized than the random number generator component from IDQ that is integrated in Samsung's Galaxy 5G announced in May 2020²⁵⁸⁵.



Qrypt (2018, USA) develops cryptographic solutions using a high speed QRNG powered by multiple entropy sources exclusively licensed from Oak Ridge National Lab and other labs. It will support NIST PQC standards when selected. Qrypt invested in Quside (Spain), which is developing high quality and high speed QRNGs.



Qnu Labs (2016, India, \$11.5M) sells its Tropos Quantum Random Number Generation, which allows the creation of random numbers of any size and quite quickly, at a rate of up to 1.5 random Mbits/s, or even several tens of Gbits/s. It also sells a QKD solution, Armos and a quantum secure platform for key management, Hodos. They were helped by the Intel startup program.



Quside (2017, Spain, 10.1M€) proposes a QRNG using phase diffusion, with a 400 Mbits/s key generation rate. It is a spin-off of ICFO, the Institute of Photonics of Barcelona with a staff of 30 as of January 2023. Quside QRNGs were used in many of the 2015 loophole-free Bell test experiments thanks to their high key rate. Their latest offering is the miniaturized QN 100 Quantum Entropy Source built with CMOS manufacturing techniques.



Quantum Dice (2019, UK, £2M) is a spin-off from the University of Oxford selling a “true” “self-certified” and fast QRNG device. It uses a patented DISC protocol ensuring that randomness comes only from the quantum process and is protected from external influences.

Their October 2021 £2M investment round was led by French venture capital fund Elaia Partners. They also got a £1M non-dilutive grant from the Quantum Accelerator Group led by IP Group, in partnership with Innovate UK as part of the UK national quantum plan.



Quantropi (2018, Canada) is a company created in Ottawa by James Nguyen (CEO) and Randy Kuang (Chief Scientist).

It was initially created to distribute a software generator of “lightweight ultra-high-entropy” random encryption keys. It then evolved into selling a complicated cybersecurity offering mixing custom-made PQC, a specific scheme for quantum key distribution solution, all that packaged in a gibberish marketing lingua mixing classical and quantum crypto²⁵⁸⁶.

Their QiSpace end-to-end quantum security SaaS platform contains a lot of stuff:

- **MASQ**, their asymmetric encryption offering, with a PQC for key exchange and digital signature containing a MPPK for Multivariate Polynomial Public Key, but they also have a Quantum Permutation Pad aka QPP. These things are supposed to support NIST PQC finalists and Quantropi’s own PQC.

²⁵⁸⁵ They contribute to research projects in QKD infrastructures like in [Ultrafast quantum key distribution using fully parallelized quantum channels](#) by Robin Terhaar et al, July 2022 (13 pages).

²⁵⁸⁶ This leads to some extreme marketing claims as seen on [Startup: Only Quantum Cryptography Can Save The \\$100 Trillion Global Digital Economy](#) by John Koetsier in Forbes, March 2021.

- **QEEP**, their symmetric encryption offering, providing “quantum-secure symmetric encryption that’s up to 18 times faster than AES-256”.
- **SEQUR**, their “quantum entropy as a service” (QEaaS) offering which contains some form of QRNG, branded QiSpace SEQUR NGen pseudo-QRNG (so, it is not a real QRNG) and their SEQUR SynQK, a sort of QKD that is supposed to deliver 5 simultaneous Quantum-key streams over distances ranging from 4,000 to 15,000 km at 130 to 190 megabits per second. What’s quantum in-here? Their “coherent-based Two-Field Quantum Key Distribution (CTF-QKD)”, a signal modulation scheme using coherent optical communications hardware and infrastructure²⁵⁸⁷.



ComScire (1994, USA) is the developer of several random number generators including PureQuantum QRNG, which creates 4 to 128 million bits per second. Is it really quantum? Not really sure!

Its entropy source seems to be coming from CMOS shot noise, using an Altera FPGA²⁵⁸⁸. The company also markets QNGmeter 3.6, a software tool testing the randomness and nondeterministic nature of generated numbers.

Terra Quantum (Switzerland) also provides a photonic based QRNG generated 1.2 Mb/s of random bits.

Quantum Key Distribution

Quantum cryptography is based on "quantum key distribution" which consists in allowing the exchange of symmetrical encryption keys, by optical means (optical fiber, air link or satellite optical link) using a system to protect its transmission against intrusions²⁵⁸⁹.

QKD protocols have the particularity of allowing the detection of any intrusion in the transmission chain and to indicate that someone has tried to read its contents or if, disturbances have occurred, "on the line"²⁵⁹⁰.

QKD principles

One early version was the **BB84** protocol invented by **Charles Bennett** and **Gilles Brassard** in 1979 and published in 1984²⁵⁹¹. They are even the creators in 1982 of the expression "quantum cryptography"²⁵⁹². This protocol is about sending photon-based information with four types of rectilinear/diagonal polarizations, *aka* non-orthogonal states: 0°, 45°, 90° and 135°. Alice and Bob exchange through a classical channel their polarization basis, used for encoding by Alice and for measurement by Bob, after the photons have been sent to make sure Bob keeps only the relevant bits where his random measurement was done in the same as the polarization basis used by Alice.

The qubits read by an intruder would modify the key, by projecting their polarization at 0° or 90°, or 45°/135° depending on the case and randomly. Any reading intrusion would be detected by Alice and

²⁵⁸⁷ It seems documented in [Quantum Public Key Distribution using Randomized Glauber States](#) by Randy Kuang and Nicolas Bettenburg et al, 2020 (7 pages).

²⁵⁸⁸ Its functioning is described in [Entropy Analysis and System Design for Quantum Random Number Generators in CMOS Integrated Circuits](#) by Scott A Wilber, 2013 (28 pages).

²⁵⁸⁹ See the review paper [Quantum Key Distribution Secured Optical Networks: A Survey](#) by Purva Sharma et al, September 2021 (35 pages) which contains a very good description of the various QKD technologies and protocols, their challenges and the way they are addressed and [The Evolution of Quantum Key Distribution Networks: On the Road to the Qinternet](#) by Yuan Cao, IEEE, 2021 (59 pages).

²⁵⁹⁰ See the review paper [Advances in Quantum Cryptography](#) by Stefano Pirandola et al, 2019 (118 pages).

²⁵⁹¹ In [Quantum cryptography : public key distribution and coin tossing](#), 1984 (5 pages).

²⁵⁹² Here is a general overview of QKD and PQC: [The Impact of Quantum Computing on Present Cryptography](#), March 2018 (10 pages).

Bob during their classical communication because of the inevitable disturbances it would cause (Figure 632). This is also named the “monogamy of entanglement”²⁵⁹³. If the protocol detects an intruder, it can take this into account and block the communication of sensitive information because the encoding key has been captured and, maybe, chose another quantum channel. And there are solutions to avoid a denial of service in such a case²⁵⁹⁴. This type of QKD is called a prepare-and-measure QKD.

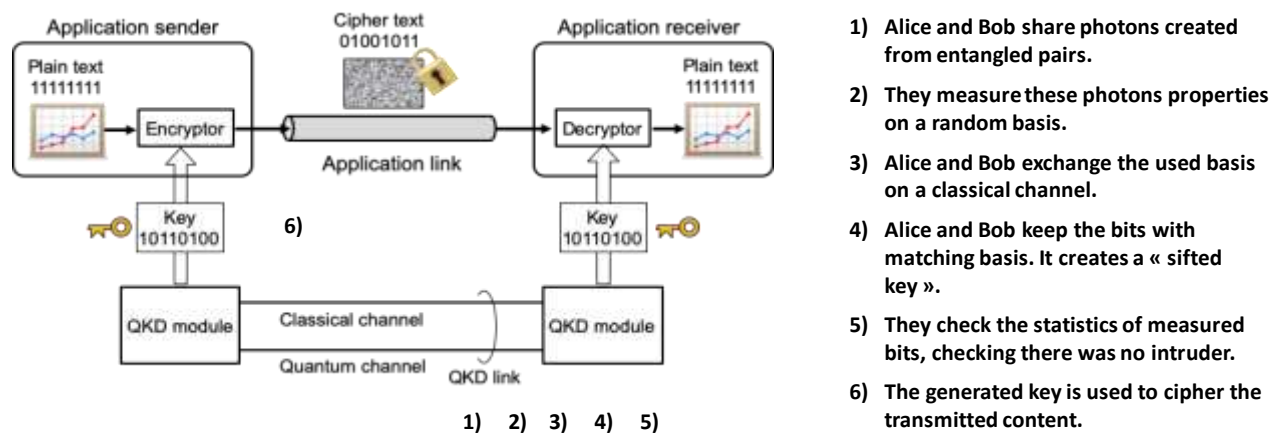


Figure 632: general principle of quantum key distribution. Source: TBD.

Artur Ekert then created the **E91** protocol in 1991 with using quantum entanglement and nonlocality, avoiding the explicit transmission of photon information that is used in BB84 and that could be intercepted by an intruder²⁵⁹⁵.

With E91, Alice and Bob share the photons created from entangled pairs. They can then share a randomly generated key with a sequential measurement of these photons. Like with BB84, this measurement must be done in a random orthogonal polarization basis that has to be shared afterwards between Alice and Bob. They will retain the randomly generated bits when their polarization was synchronized, creating a “sifted key”. If an eavesdropper Eve intercepted the entangled photons, their projections would be different. To make sure there was no eavesdropper, Alice and Bob compute a Bell test statistic which must yield ideally a so-called Bell parameter $|S| = 2\sqrt{2}$, called Tsirelson bound, otherwise, there was an eavesdropper.

One key difference between BB84 and E91 is the origin of randomness in the shared keys. With BB84, it must be generated by Alice with a random number generator, preferably a TRNG (true random numbers generator) and not a PRNG (pseudo-random numbers generator) as described in the earlier section on QRNGs, page 717. With E91, it comes directly from the randomness of the entangled photon pairs readouts. All in all, E91 consolidates a quantum communication protocol and a quantum random number generator.

QKD protocols have since made their way. They are at the origin of the creation of the whole field of quantum cryptography, which has now left the exclusive realm of research and experimentation to enter actual deployments like in China, even though there are still problems remaining to be fixed such as the creation of safe repeaters, to replace the commonplace unsafe trusted nodes (even in

²⁵⁹³ See [Quantum Advantage in Cryptography](#) by Renato Renner and Ramona Wolf, ETH Zurich, June 2022-January 2023 (31 pages).

²⁵⁹⁴ See for example [A quantum key distribution protocol for rapid denial of service detection](#) by Alasdair Price et al, from the University of Bristol, in EPJ Quantum Technology, 2020 (20 pages).

²⁵⁹⁵ And published in the article [Quantum Cryptography Based on Bell's Theorem](#) (3 pages). Artur Ekert has been a member of Atos Scientific Council since 2016, along with Alain Aspect, Daniel Esteve, Serge Haroche, Cédric Villani and David DiVincenzo.

China) where the key bits are turned into classical data at each and every node station, given you need to have one of these about every 80 km.

QKD was expanded with CV-QKD (continuous variable) which modulates both the phase and the amplitude of the transmitted optical signal. It notably allows multiplexing several communications on the same optical fiber and to exploit the existing infrastructures of telecom operators. **Philippe Grangier** was one of its designers, along with **Frédéric Grosshans** from CNRS-LIP6, in 2002²⁵⁹⁶. CV-QKD complements discrete variables QKD (DV-QKD) as are called the previously mentioned QKD protocols, based on the properties of single photons, which require some cooling on the single-photon detector side.

Figure 633 and Figure 634 make a rough comparison between DV-QKD and CV-QKD. Nowadays, CV-QKD seems preferred for telecom fiber deployments²⁵⁹⁷. Figure 636 describes a typical optical architecture for the implementation of a CV-QKD protocol based on BB84, without entanglement given CV-QKD can also be implemented with entanglement-based protocols. It uses a simple photon source in the telecom wavelength band around 1,550 nm followed by amplitude and phase modulators. On the Bob side, a homodyne detector will demodulate the signal.

The integration of a QKD in conventional telecommunication optical fibers is typically done using three methods: by frequency multiplexing (WDM), for instance with a QKD signal on 1,310 nm and data sent on 1,550 nm, by time sharing (TDM) or by using a dedicated fiber embedded in a sheath (SDM)²⁵⁹⁸. China has a very good experience in that domain²⁵⁹⁹ (Figure 635).

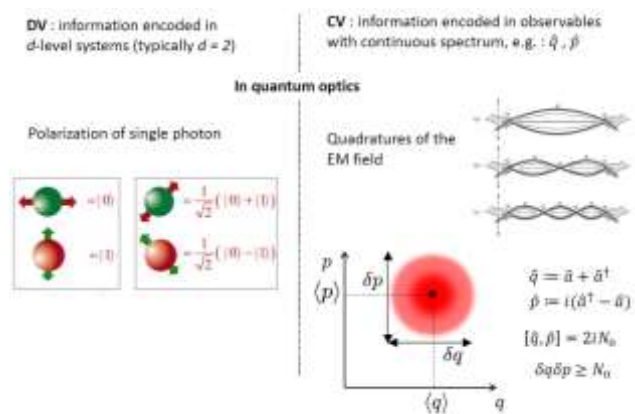
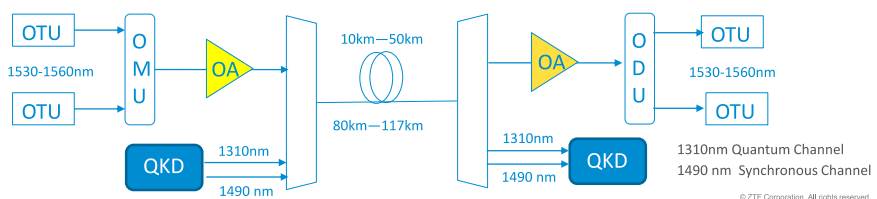


Figure 633: DV and CV in QKD. Source: TBD.

	DV-QKD	CV-QKD
Quantum state	Polarization, phase, or time bin of a single photon	Quadrature components of quantized electromagnetic field
Source	Single-photon source	Coherent-state or squeezed-state source
Detector	Single-photon detector	Homodyne or heterodyne detector
Channel model	Lossy qubit channel	Lossy bosonic channel
Distance limitation	Performance of single-photon detectors	Efficiency of post-processing techniques

Figure 634: comparison between DV-QKD and CV-QKD protocols. Source: [The Evolution of Quantum Key Distribution Networks: On the Road to the Qinternet](#) by Yuan Cao, IEEE, 2021 (59 pages).

Co-Fiber Experiment in China Telecom Laboratory



- Experiment 1
 - High coding rate in co-directional fibers
 - Classical optical power reduce the coding rate, so we need control their power to increase coding rate.
- Experiment 2
 - Huge large Capacity Service Datas 8T (80x100G)
 - Ultra-long transmission distance (80km-117km)
 - High QKD code rate (16kpbs-1kpbs)
 - Smooth upgrade, service can be real-time quantum encryption

Figure 635: co-fiber experiment in China Telecom laboratory distributing quantum keys over telecom fiber lines. Source: [QKD Application: Coexistence QKD Network and Optical Networking the same optical fiber network](#) by JiDong Xu, ZTE, June 2019 (15 slides).

²⁵⁹⁶ Their QKD protocol is baptized accordingly GG02.

²⁵⁹⁷ See a CV-QKD implementation in [Experimental demonstration of Continuous-Variable Quantum Key Distribution with a silicon photonics integrated receiver](#) by Yoann Piétri, Philippe Grangier, Amine Rhouni, Eleni Diamanti et al, November 2023 (11 pages).

²⁵⁹⁸ A sheath is an outer protective layer that surrounds and shields the core and cladding of an optical fiber.

²⁵⁹⁹ See [Quantum Encrypted Signals on Multiuser Optical Fiber Networks Simulation Analysis of Next Generation Services and Technologies](#) by Rameez Asif, 2017 (6 pages) and [Quantum experiments explore power of light for communications, computing](#) by Elizabeth Rosenthal, January 2020.

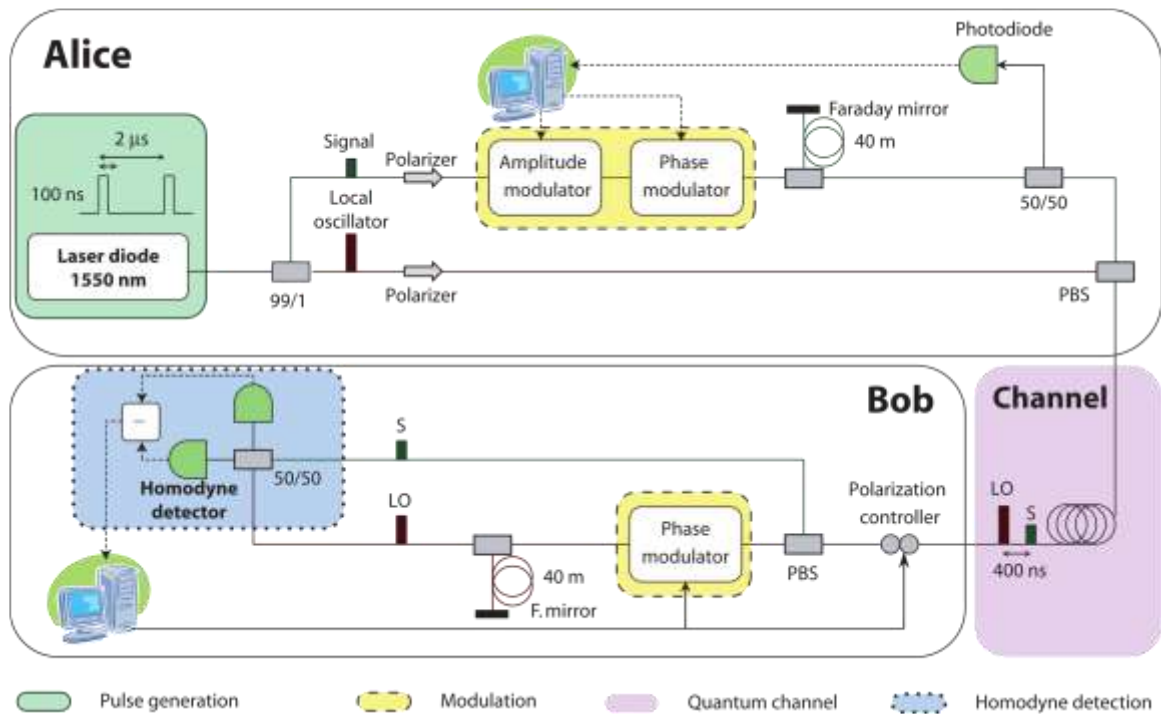


Figure 636: an example of CV-QKD implementation of the BB84 protocol. Source: [The SECOQC quantum key distribution network in Vienna](#) by M. Peev, C. Pacher, Romain Alleaume, C. Barreiro, J. Bouda, W. Boxleitner, Thierry Debuisschert, Eleni Diamanti, et al, 2009 (39 pages).

With entanglement-based CV-QKD protocols, the initial entanglement done before sending the two bits in the qubits avoids violating the Holevo theorem, already mentioned several times, according to which a set of qubits cannot carry more information than its equivalent number of classical bits. On the other hand, the information encrypted with the transmitted key is usually sent over a traditional channel^{2600 2601}. It is still often encrypted using SSL, which protects the relationship between your browser and the websites you visit and supports the secured https protocol.

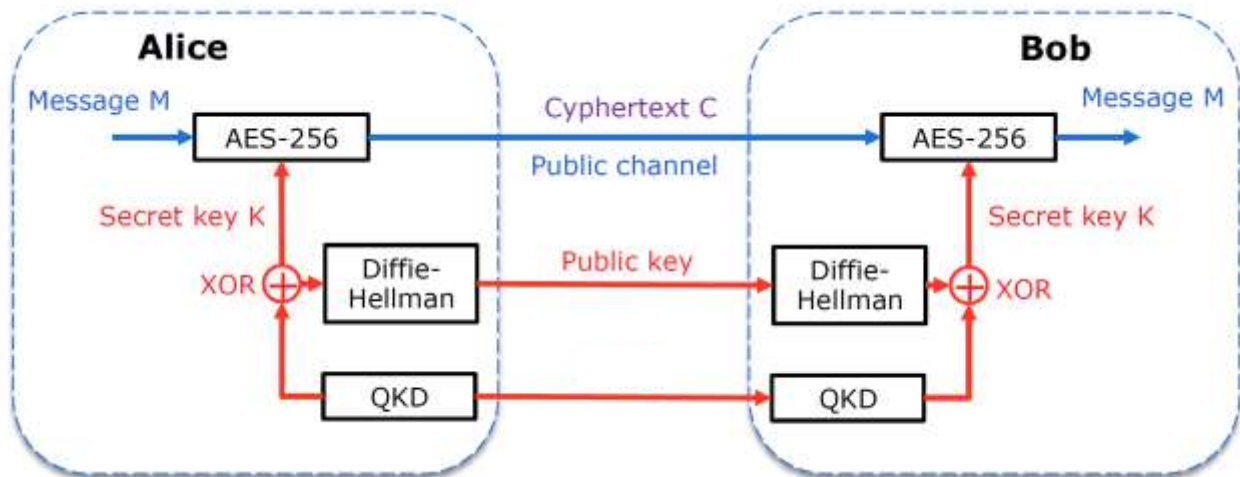


Figure 637: a description of the data and key transmission with QKD applicable to both prepare-and-measure and entanglement based QKD. source: [How to Quantum-Secure Optical Networks?](#) by Helmut Griesser, ADVA Optical Networking SE, 2016 (31 slides).

²⁶⁰⁰ Classical information can take a very different path. For example, a quantum key can be transmitted by satellite and data can be transmitted terrestrially over fiber optics.

²⁶⁰¹ See the review paper [Continuous-variable quantum key distribution system: A review and perspective](#) by Yichen Zhang et al, October 2023 (53 pages).

In practice, keys transmission using a QKD is using a complex system of "key distillation" that manages the communication imperfections with classical error correction codes (which have nothing to do with the quantum error correction codes seen at the qubit level elsewhere in this document, page 240), an amplification of confidentiality and an authentication system using private keys already shared by the correspondents, making it possible to avoid so-called *man-in-the-middle* attacks by hackers pretending to be one of the interlocutors (Figure 638).

Error correction codes and the rest of the protocol generate on-line losses of about 80% of the quantum key communication²⁶⁰². Implementing a QKD combines a quantum random key generator such as those from IDQ, an authenticated classical channel to exchange QKD basis information and a QKD channel to share random keys, which can generally be transported on a dark fiber from a B2B telecom operator.

The useful data is encrypted with the QKD generated key with classical encryption protocols like AES²⁶⁰³ and transmitted over a traditional channel, which may also be a classical optical fiber or other physical communication media, even cellular communications (see Figure 637).

This is well documented by ETSI²⁶⁰⁴. On arrival, a quantum key receiver and the system for decrypting the signal arriving via the traditional channel is used (Figure 639).

The secret keys throughput is an important issue and is currently at its maximum in Mbits/s vs. the Tbits/s of the operators' optical links²⁶⁰⁵. Many optimizations must be implemented to make QKD practical, first with closing the many discovered security loopholes, many being linked to the post-selection of Bell tests²⁶⁰⁶.

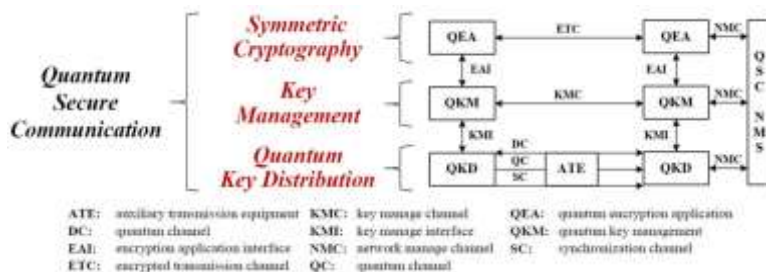


Figure 638: the three components of quantum secure communication with a symmetric cryptography, key management and a QKD. Source: [Development and evaluation of QKD-based secure communication in China](#) by Wen-yu Zhao, June 2019 (15 slides).

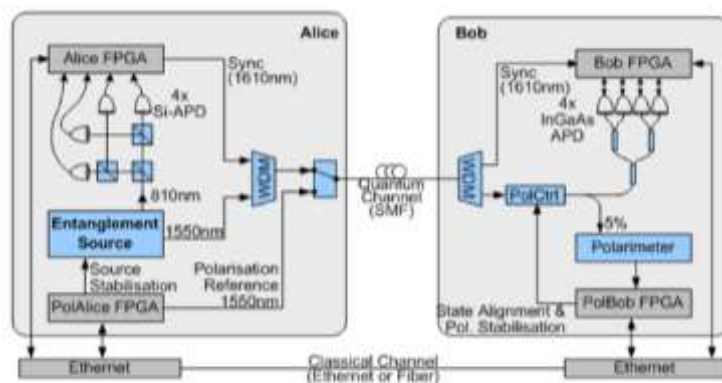


Figure 4.6: Schematic of an entanglement-based QKD system

Figure 639: Source: [Quantum Key Distribution \(QKD\) Components and Internal Interfaces](#) from ETSI, 2018 (47 pages).

²⁶⁰² According to the excellent overview [Quantum Key Distribution Protocols and Applications](#) by Sheila Cobourne, University of London, 2011 (95 pages).

²⁶⁰³ One-time pads encryption techniques can also be used with QKD. It consists in creating a key that is as large as the content to be encrypted. This technique makes the content uncrackable with brute force.

²⁶⁰⁴ In [Quantum Key Distribution \(QKD\) Components and Internal Interfaces](#) from ETSI, 2018 (47 pages) which describes the different QKD techniques available to date. It also describes very well the photon sources used in QKDs as well as the associated quantitative and qualitative parameters.

²⁶⁰⁵ See [Experimental Demonstration of High-Rate Discrete-Modulated Continuous-Variable Quantum Key Distribution System](#) by Yan Pan et al, March 2022 (5 pages) which describes a record of high-speed CV-QKD distribution over distances of 5 to 50 km with keys generations ranging from 288 Mbits/s to 7.6 Mbits/s. A record key rate of 1 Gbits/s with a source of entangled photons in the 1,550 nm telecom wavelengths was obtained in 2022 by an Austrian team but the practical key rate would be much lower in practical use cases due to fiber attenuation over long distances. See [Experimental entanglement generation for quantum key distribution beyond 1 Gbit/s](#) by Sebastian Philipp Neumann et al, September 2022 (11 pages).

²⁶⁰⁶ See ['Frequency-modulated' pulsed Bell setup avoids post-selection](#) by Mónica Agüero, July 2023 (4 pages).

Other improvements can be achieved with implementing clock synchronization without an additional dedicated channel and develop protocols to increase raw key rates²⁶⁰⁷. The quantum keys transfer rate can be much lower than the physical data rate available. There are fundamental bounds on how many secret keys can be generated over a noisy quantum channel. A 2023 record was broken by a team in China, with secret keys generated at 115.8 Mb/s over a 10 km standard optical fiber, and distributed keys over up to 328 km of ultralow-loss fiber for more than 50 hours. The precedent record secret key rate was of 10 Mb/s over 10 km standard optical fiber²⁶⁰⁸.

The QKD quantum channels and classical data can be conveyed on the same fiber. It was experimented in 2023 by Orange and Toshiba Europe over 50 km using a 1,310 nm fiber for the co-propagation of a QKD quantum channel and classical signals using 60-channel WDM (wavelength division multiplexing) at 100 Gb/s²⁶⁰⁹.

There are also other fundamental questions about the overall architecture and topology of QKD networks, most of the time working in “point to point” and relying on so-called trusted nodes, which can be considered as “classical” repeaters²⁶¹⁰. Proposals abound to create large multi-point networks and routing protocols²⁶¹¹ and on entanglement distribution optimization²⁶¹².

There are a few other varieties of QKD protocols beyond the DV-QKD and CV-QKD as shown in Figure 640 with **DIQKD**, a more secure Device-Independent QKD that prevents side-channel attacks on hardware^{2613 2614} and the less safe **MDI-QKD** for “measurement-device-independent” QKD²⁶¹⁵.

Quantum Conference Key Agreement (QCKA) is an extension of QKD protocols to enable the generation of quantum secret keys among several users. The protocol can make use of N-dimension entangled GHZ states share across the parties or work with continuous variable photons²⁶¹⁶. There is even an MDI-QCKA variant using post-selected GHZ states²⁶¹⁷.

²⁶⁰⁷ See for example [Operational real field entangled quantum key distribution over 50 km](#) by Yoann Pelet, Sébastien Tanzilli et al, July 2022 (7 pages).

²⁶⁰⁸ See [High-rate quantum key distribution exceeding 110 Mb/s](#) by Wei Li et al, Nature Photonics, July 2023 (27 pages).

²⁶⁰⁹ See [Co-propagation of 6 Tb/s \(60*100Gb/s\) DWDM & QKD channels with ~17 dBm aggregated WDM power over 50 km standard single mode fiber](#) by P. Gavignet et al, Orange and Toshiba, May 2023 (3 pages).

²⁶¹⁰ See an example of trusted node deployment with [Trusted Node QKD at an Electrical Utility](#) by Philip G. Evans et al, March 2021 (10 pages).

²⁶¹¹ See [A Quantum Internet Architecture](#) by Rodney Van Meter et al, December 2021 (17 pages), [Cost and Routing of Continuous Variable Quantum Networks](#) by Federico Centrone, Frederic Grosshans and Valentina Parigi, April 2022 (20 pages), [A quantum router architecture for high-fidelity entanglement flows in quantum networks](#) by Yuan Lee, Eric Bersin, Axel Dahlberg, Stephanie Wehner and Dirk Englund, npj, June 2022 (8 pages) and [An Efficient Routing Protocol for Quantum Key Distribution Networks](#) by Jia-Meng Yao et al, April 2022 (27 pages).

²⁶¹² See [40-user fully connected entanglement-based quantum key distribution network without trusted node](#) by Xu Liu et al, January 2022 (15 pages) and [Genuinely Multipartite Entanglement via Quantum Communication](#) by Ming-Xing Luo et al, April 2022 (9 pages).

²⁶¹³ See the international review paper [Advances in device-independent quantum key distribution](#) by Víctor Zapatero et al, August 2022 (15 pages).

²⁶¹⁴ See [Experimental quantum key distribution certified by Bell's theorem](#) by D. P. Nadlinger, Nicolas Sangouard et al, Nature, 2022 (6 pages).

²⁶¹⁵ See [Measurement-device-independent quantum key distribution](#) by Hoi-Kwong Lo, Marcos Curty and Bing Qi, 2011 (7 pages) and this good overview of QKD and its technical challenges in [Practical challenges in quantum cryptography](#) by Eleni Diamanti et al, 2016 (25 pages).

²⁶¹⁶ See [Quantum Conference Key Agreement: A Review](#) by Gláucia Murta, Federico Grasselli, Hermann Kampermann and Dagmar Bruß, Heinrich-Heine-Universität Düsseldorf, Advanced Quantum Technologies, September 2020 (13 pages).

²⁶¹⁷ See [Breaking universal limitations on quantum conference key agreement without quantum memory](#) by Chen-Long Li et al, Nature Communications Physics, May 2023 (7 pages).

Protocol	Type	Approach	Year
BB84	DV	Prepare-and-measure	1984
E91	DV	Entanglement-based	1991
BBM92	DV	Entanglement-based	1992
GG02	CV	Prepare-and-measure	2002
DPS	DV	Prepare-and-measure	2002
Decoy-state	DV	Prepare-and-measure	2003–2005
SARG04	DV	Prepare-and-measure	2004
COW	DV	Prepare-and-measure	2005
MDI	DV/CV	Prepare-and-measure	2012
TF	DV	Prepare-and-measure	2018
PM	DV	Prepare-and-measure	2018

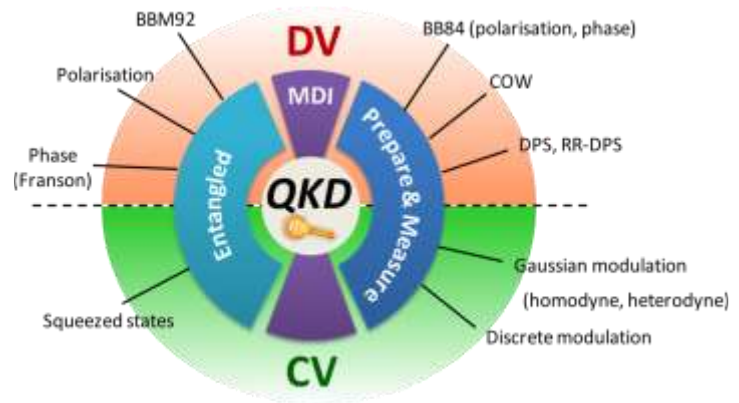


Figure 640: a map of QKD protocols between DV and CV ones. I don't cover them all in this book. Sources: Source: [The Evolution of Quantum Key Distribution Networks: On the Road to the Qinternet](#) by Yuan Cao, IEEE, 2021 (59 pages) and VSCW19-QKD-part1. <https://quantum-uniqorn.eu/wp-content/uploads/2019/06/VSCW19-QKD-part.pdf>.

QKD experiments and deployments

Besides China which has deployed an operational intercity QKD network, QKD deployments in other parts of the world are essentially experimental. Many breakthrough experiments have been conducted both in the open air and with optical fibers, particularly in Europe (Figure 641). These mostly deal with BB84-type QKD, and yet much on entanglement based QKD and quantum communications.

Open-air QKD demonstrations started in 1996 in the USA on a 75 m distance, then on 144 km to connect the islands of La Palma and Tenerife in the **Canary Islands** and conducted by Austrians in 2007 and 2010²⁶¹⁸, in 2019 in urban areas in Italy with a distance of 145 m²⁶¹⁹, in India in 2022 over 300 m²⁶²⁰ and in Austria in 2023 over a distance of 10 km²⁶²¹. While these experiments used optical photons, other approaches are investigated like using mm and THz electromagnetic waves, which would require photon sources and detectors operating at 4K, which is not very practical on a large scale²⁶²². Open air QKD distribution has its own challenges due to various atmospheric perturbations²⁶²³.

An experiment took place in **Vienna** in 2008 as part of the European **SECOQC** (*SE*cure *CO*muni-*CA*tion based on Quantum Cryptography) project launched in 2004, involving some 40 research laboratories and vendors, using a "mesh" architecture and a CV-QKD optical link²⁶²⁴.

This went on in Switzerland with **IDQ** with local banks. In 2007 they also set up an election vote counting system based on a QKD.

²⁶¹⁸ See [Second Generation QKD System over Commercial Fibers](#) by Laszlo Bacsardi et al, 2016 (5 pages) et [Feasibility of 300 km Quantum Key Distribution with Entangled States](#) by Thomas Scheidl et al, 2010 (14 pages).

²⁶¹⁹ See [Full daylight quantum-key-distribution at 1550 nm enabled by integrated silicon photonics](#) by Matteo Schiavon et al, July 2019 (7 pages). QKD key transmission over the 145m air link took place at 1,550 nm in the infrared band that is commonly used in fiber optic transmissions and therefore compatible with many existing telecommunication equipment. They used a silicon chipset doing all the work with an error rate of only 0.5% and a data rate of 30 kbits/s. Their QCosOne ("Quantum Communication for Space-One") used telescopes with 120 and 315 mm optics for transmission and reception. It worked during daytime, but there were still problems in case of turbulence and depending on the time of day and the side effects coming from the sun. Performance was better in the evening. They used triple photon encoding: temporal, spatial and spectral.

²⁶²⁰ See [Indian Scientists Demonstrate Wireless Quantum Key Distribution Over 300 Meters](#) by Matt Swayne, The Quantum Insider, February 2022.

²⁶²¹ See [Distribution of genuine high-dimensional entanglement over 10.2 km of noisy metropolitan atmosphere](#) by Lukas Bulla et al, Austria, January 2023 (6 pages).

²⁶²² See [Millimetre-waves to Terahertz SISO and MIMO Continuous Variable Quantum Key Distribution](#) by Mingqi Zhang et al, January 2023 (9 pages).

²⁶²³ See [A Review on Practical Challenges of Aerial Quantum Communication](#) by Umang Dubey et al, September 2023 (21 pages).

²⁶²⁴ See [The SECOQC quantum key distribution network in Vienna](#) by Romain Alléaume, Eleni Diamanti et al, 2016 (39 pages).

UK deployed in 2018 its UK Quantum Communications hub between Bristol, London, Cambridge and Ipswich²⁶²⁵.

In France, **Orange** announced in May 2019 the launch of tests of a QKD protected communication with the University Côte d'Azur (UCA) which provides the solution via the InPhyNi laboratory. It connects the Valrose and Inria campuses in Sophia Antipolis with an access point on the Plaine du Var IMREDD campus in Nice, using dark fibers provided by the telecom operator²⁶²⁶. The test network was operational in September 2021. Orange is studying the reliability of trusted optical network nodes in such a configuration. The operator is also looking to combine QKD solutions to protect physical links and PQC solutions that could be used as a method of encrypting data transmitted in association with a QKD.

Denmark's DTU launched a CV-QKD trial with Danske Bank in 2022²⁶²⁷ and another one between NBI and DTU²⁶²⁸.

Ireland announced in 2022 the creation of a Quantum Communications Infrastructure network, co-founded by the EU as part of the EuroQCI project, with a total investment of \$10M. The project is run by 6 local universities along with HEAnet and ESB Telecoms.

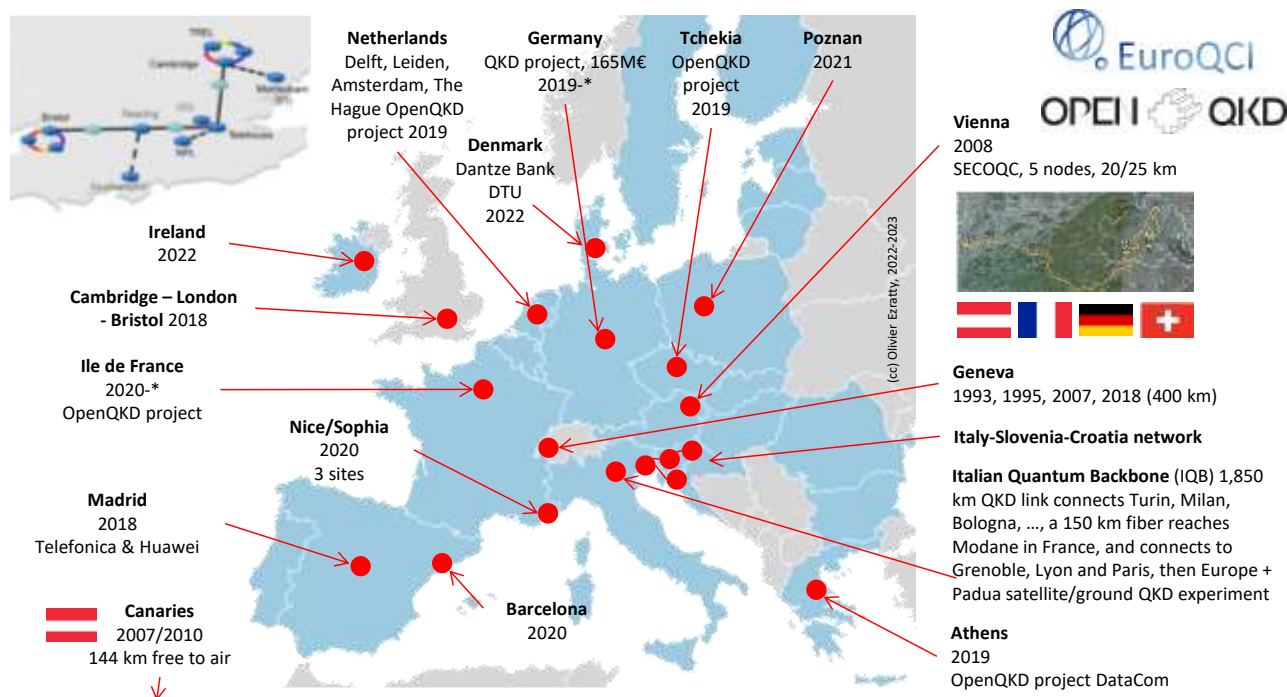


Figure 641: a map of QKD test deployments throughout Europe. (cc) Olivier Ezratty, 2022-2023.

Greece's Space Hellas and the University of Athens launched in 2022 a pilot QKD deployment after having started an OpenQKD project in 2019 with Datacom.

Cyprus announced in 2022 its deployment of a QKD network with a EuroQCI EU funding of 7.5M€ as part of the CYQCI project.

²⁶²⁵ Seen in [IDQ: Quantum-Safe Security relevance for Central Banks](#), 2018 (27 slides). The network was extended in Cambridge in 2019 as seen in [Cambridge quantum network](#) by J. F. Dynes et al, 2019 (8 pages).

²⁶²⁶ See [Experimenting quantum key exchange over the Côte d'Azur](#), Orange, December 2019. And for Orange's QKD projects in general: [Orange and quantum technologies for secure data exchange](#), June 2020.

²⁶²⁷ See [First quantum-safe data transfer in the Nordic region](#) by Anne Kirsten Frederiksen, February 2022.

²⁶²⁸ See [Quantum Key Distribution using Deterministic Single-Photon Sources over a Field-Installed Fibre Link](#) by Mujtaba Zahidy et al, January-April 2023 (9 pages).

Poland launched a QKD network using trusted nodes with 380 km of connections with the help of IDQ²⁶²⁹.



The European consortium **OpenQKD** is experimenting a terrestrial QKD network.

It prepares the ground for the launch of the **EuroQCI** network which would be an operational implementation of a terrestrial and satellite European QKD network²⁶³⁰.

This involves in particular France, Germany, Austria, Italy, Spain, the Netherlands, Greece, Switzerland and Poland and vendors like Thales Alenia Space (satellite communication), Orange and Mellanox (a subsidiary of Nvidia). From a practical point of view, it is about deploying a large interoperable experimental QKD network on a European scale, exploited by applications in various fields (healthcare, energy grids, transportation, finance, government, education, and the likes). The consortium also intends to influence QKD standardization. And as far as possible, it is also about contributing to the development of a European industry offering in QKD and associated technologies. There is at least a deployment of QKD across Italy, Slovenia and Croatia²⁶³¹. In France, the test area will be the Paris region and its major research laboratories with the Institut d'Optique, Telecom Paris, LIP6 in Jussieu and Nokia labs in Villarceau. The project has received €15M in European funding from Horizon 2020, independently of Quantum Flagship. Thales announced in December 2021 that it was participating to the QSAFE consortium with Deutsche Telekom, Telefonica and the AIT (Austrian Institute for Technologies) to create a European quantum telecommunication infrastructure as part of EuroQCI, with both terrestrial and satellite links.

USA's first experiments were conducted in Boston by **DARPA** between 2004 and 2007. A QKD network piloted by **Battelle** was tested in Ohio in 2013²⁶³². Tests were also conducted in 2015 at **MIT**, linking two sites 43 km apart. It became the Boston-Area Quantum Network (BARQNET) linking the MIT Lincoln Laboratory, MIT, and Harvard University²⁶³³. A commercial deployment of QKD on an unused 800 km fiber optic network connecting Boston to Washington DC is also being deployed by **Quantum Xchange** and **Zayo**, to connect Wall Street finance businesses with their back-offices in New Jersey. It uses some trusted node technology²⁶³⁴. An 85 km facility was also deployed in Chicago in 2019²⁶³⁵. In July 2020, the Department of Energy announced the expansion of the QKD network to link all of its research laboratory sites²⁶³⁶. In 2022, it connected the DoE Argonne and Fermi labs and enabled fast network synchronization of quantum and classical signals coexisting on the same optical fiber over a distance of 59 km²⁶³⁷. In 2023, the **Stony Brook University** was awarded a \$6.5M grant from the Long Island Investment Fund to build a Quantum Internet Test Bed.

²⁶²⁹ See [A new 380 km-long intercity QKD infrastructure in Poland](#), IDQ, September 2022.

²⁶³⁰ See [Nine more countries join initiative to explore quantum communication for Europe](#), December 2019 and [Quantum communications infrastructure architecture: theoretical background, network structure and technologies. A review of recent studies from a European public infrastructure perspective](#) by Adam M. Lewis and Petra F. Scudo, January 2022 (40 pages).

²⁶³¹ See [Deploying an inter-European quantum network](#) by Domenico Ribezzo et al, March 2022 (8 pages).

²⁶³² See [Battelle Installs First Commercial Quantum Key Distribution Protected Network in U.S.](#), 2013.

²⁶³³ See [Development of a Boston-area 50-km fiber quantum network testbed](#) by Eric Bersin et al, July 2023 (11 pages).

²⁶³⁴ See [New plans aim to deploy the first US quantum network from Boston to Washington, DC](#), October 2018.

²⁶³⁵ See [Argonne and UChicago scientists take important step in developing national quantum internet](#) by Louise Lerner, February 2020.

²⁶³⁶ See [Department of Energy \(DOE\) Unveils Blueprint for a U.S. Quantum Internet](#) by Doug Finke, July 2020.

²⁶³⁷ See [Quantum Network Between Two National Labs Achieves Record Synch](#) by Matt Swayne, June 2022 and [Picosecond Synchronization of Photon Pairs through a Fiber Link between Fermilab and Argonne National Laboratories](#) by Keshav Kapoor et al, August 2022 (7 pages).

Canada launched in November 2020 its Canada Quantum Network through a partnership between Xanadu, the Creative Destruction Lab and the startups service company MaRS around Toronto. Another similar testbed project was launched in Quebec in October 2023, around Sherbrooke.

India's Defence Research and Development Organisation (DRDO) with IIT Delhi demonstrated a QKD for a distance of 100 km in 2022. The country launched its first operational QKD network in 2023 between two sites in Delhi.

Japan's, Toshiba announced in September 2018 that a QKD solution co-developed with the Tohoku Medical Megabank Organization (ToMMo) at Tohoku University had achieved a QKD throughput of more than 10 Mbps during one month.

Singapore's Quantum Engineering Program (QEP, 2018) from the National University of Singapore (NUS) launched the National Quantum-Safe Network (NQSNet) which is starting classical and quantum network trials supporting both QKD and PQC.

They plan to have 10 fiber nodes. This is done in partnership with Amazon Web Services and Thales. One of the challenges in deploying QKD is the miniaturization of its components. Whereas initially a complete rack of hardware was needed for quantum key transmitting/receiving stations, the goal is to fit everything in a photonics component a few mm long. This is what NTU researchers in Singapore did in 2019 to manage a CV-QKD supporting existing telecom operators' fiber infrastructures²⁶³⁸. But this miniaturization concerns here only the photonics part (Figure 642). These photonic circuits must be completed by classical electronic components.

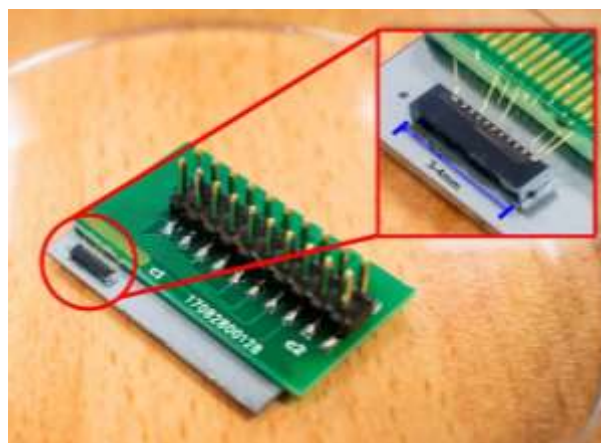


Figure 642: Source: [Researchers create quantum chip 1,000 times smaller than current setups](#), PhysOrg, October 2019

The development of such integrated photonics components will also be supported in the framework of European Horizon Europe projects that follows Europe 2020 projects over the 2021-2027 period.

A point-to-point 3 km QKD testbed was deployed in 2023 with the help of AWS, Horizon Quantum Computing and Fortinet, with a VPN tunnel using both a QKD and AWS Edge Compute hardware²⁶³⁹.

Korea has an ongoing project with 800 km of QKD implementing any to any connection, also with the help of IDQ.

China stands out since 2016 with impressive QKD experiments and deployments. The country invests heavily in QKD with a now classical multi-pronged strategy: to protect its sensitive communications against any attacker and to develop an industry in a promising emerging technology field. A first deployment was carried out in 2012 in the Hefei area to link various Chinese government entities²⁶⁴⁰. It was then expanded with an installation of a QKD-secured fiber optic link between Shanghai and Beijing, covering 2,000 km. The line installed between 2013 and 2016 was deployed by a local startup, **QuantumCTek**. The network relies on 32 transponders with secured physical access²⁶⁴¹. Indeed, the signal attenuation was then too strong beyond about 50 km on one optical fiber.

²⁶³⁸ See [Researchers create quantum chip 1,000 times smaller than current setups](#), PhysOrg, October 2019 which references [An integrated silicon photonic chip platform for continuous-variable quantum key distribution](#) by G. Zhang et al, December 2019 (5 pages).

²⁶³⁹ See [Implementing a quantum-secured network in a metropolitan area](#) by Juan Moreno and Cyrus Proctor, AWS, March 2023.

²⁶⁴⁰ See [Unhackable Chinese Communication Network Launches Soon](#) by Rechelle Ann Fuertes, 2017.

²⁶⁴¹ Source: [Security assessment and key management in a quantum key distribution network](#) by Xiongfeng Ma, June 2019 (21 slides).

The entities using this line are government agencies, including various financial sector regulatory agencies and banks. The country also plans to protect its energy grid infrastructure with this network²⁶⁴².

China then launched in 2017 a deployment of an additional 33,000 km of the **National Quantum Secure Communication Backbone Network**, to be completed by 2025 (Figure 643). It had started with the creation of a Hefei-Wuhan link²⁶⁴³. Hefei is the city where Jian-Wei Pan's main quantum technologies laboratory is located²⁶⁴⁴. It seems this deployment was stalled and turned into several metropolitan QKD networks connected together with QKD satellite links.

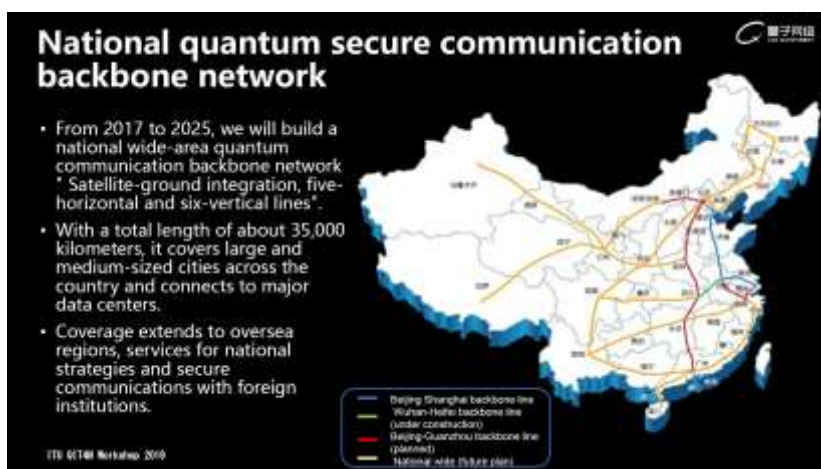


Figure 643: China's QKD 33k km planned backbone as of 2019, which was replaced since then by metropolitan networks connected with satellite links.

Still, as of 2023, 10,000 km of QKD lines had been deployed in total. In September 2023, a team led by Jian-Wei Pan reported the deployment of a three-node entanglement-based QKD setup at a city scale in Hefei using quantum nodes with atomic quantum memories²⁶⁴⁵.

China Telecom announced in 2023 an investment of \$438M in quantum communications research and development²⁶⁴⁶.

In France, the civil cybersecurity agency ANSSI published an information note in May 2020 in which it expressed certain reserves about the QKD²⁶⁴⁷. It highlighted the fact that it does not address a common problem, cannot guarantee perfect inviolability, and requires dedicated optical infrastructures. Instead, it recommends focusing on PQC. This followed a memo of equivalent content from their British NCSC counterparts published in April 2020²⁶⁴⁸. A similar publication from the NSA was released in October 2020²⁶⁴⁹.

It was renewed in 2021 and 2022. Scientists from ETH Zurich published a documented rebuttal to these objections in 2023²⁶⁵⁰, followed by another one from Terra Quantum²⁶⁵¹.

²⁶⁴² See [Application In Power Industry Promotes the Development of Quantum Cryptography Technology](#) by Yonghe Guo, June 2019 (13 slides).

²⁶⁴³ See [Towards large-scale quantum key distribution network and its applications](#) by Hao Qin, 2019 (17 slides).

²⁶⁴⁴ The extended BB84 based QKD network is documented in [Implementation of a 46-node quantum metropolitan area network](#) by Teng-Yun Chen et al, September 2021 (14 pages). It describes the intra-metropolitan network infrastructure deployed in Hefei, with 46 nodes.

²⁶⁴⁵ See [A multinode quantum network over a metropolitan area](#) by Jian-Long Liu, Jian-Wei Pan et al, September 2023 (21 pages).

²⁶⁴⁶ See [China Telecom establishes quantum technology group](#) by Casey Hall, Reuters, May 2023.

²⁶⁴⁷ See [L'avenir des communications sécurisées passe-t-il par la distribution quantique de clés?](#) by ANSSI, May 2020 (6 pages).

²⁶⁴⁸ See [Quantum Security Technologies](#), NCSC, March 2020 (4 pages) and a detailed response in [Quantum safe cryptography - the big picture - Fact Based Insight](#) by David Shaw, 2020.

²⁶⁴⁹ See [NSA Cybersecurity Perspectives on Quantum Key Distribution and Quantum Cryptography](#), NSA, 2020.

²⁶⁵⁰ See [The debate over QKD: A rebuttal to the NSA's objections](#) by Renato Renner and Ramona Wolf, ETH Zurich, July 2023 (14 pages).

²⁶⁵¹ See [Applicability of QKD: TerraQuantum view on the NSA's scepticism](#) by D. Sych et al, Terra Quantum, August 2023 (4 pages).

The bulk of the answers is: “*work in progress*”, particularly as QKD related hardware is being shrunk-wrapped and commoditized. Also, it would make sense to deploy quantum networks implementing entanglement resources, which are the only ones enabling a broad scope of use cases including connecting quantum networks, quantum computers and quantum sensors.

QKD by satellite, UAVs and underwater

Satellite quantum communication is another way to distribute quantum keys that makes sense over long distance. These keys can be created across two locations while the encrypted data may be transported in more classical terrestrial, or satellite means. This would be theoretically simpler than using QKD distribution over large fiber networks full of (so far, non-existent) quantum repeaters.

One advantage is that the photon loss is much lower with satellites than with fibers. Indeed, with satellites, photon losses coming from the atmospheric absorption and scattering occurs only in the lower 10 km of the atmosphere, with about a 3 dB loss on a clear day.

Still, the atmospheric refractive index inhomogeneity modifies the direction of the propagating beam and larger-scale turbulence causes beam deflection, while small-scale turbulence induces beam broadening²⁶⁵². Turbulences have a larger impact for photon emission from Earth, particularly on the quality of entanglement²⁶⁵³ ²⁶⁵⁴ (Figure 644). The rest of the distance is in near vacuum, with nearly no absorption and decoherence and the loss caused by beam diffraction is approximately proportional to the square of distance whereas the losses in fiber are mainly due to the absorption and scattering of the fiber medium, which is proportional to the exponent of the distance. It means that for long communicating distances of several hundred km, satellite-ground channels have an advantage over fiber-based channels in terms of channel losses²⁶⁵⁵.

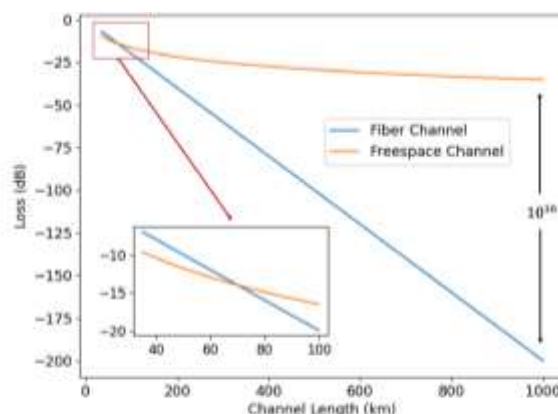


FIG. 10 Typical losses in fiber and free-space channels. The attenuation parameter of fiber is $\sim 0,2 \text{ dB/km}$. The parameters of free-space channel are based on the design of Micius satellite. The free-space channel shows advantage for a distance over $\sim 70 \text{ km}$

Figure 644: how photon losses compare between fiber and freespace channel using satellite. Source: [Micius quantum experiments in space](#) by Chao-Yang Lu, Yuan Cao, Cheng-Zhi Peng and Jian-Wei Pan, August 2022 (53 pages).

However, free to air channels are vulnerable to attacks like various forms of denials of service (DoS) that mandate their own countermeasures²⁶⁵⁶.

China has been a pilot country in satellite QKD distribution, having launched two QKD satellites. **Micius-1** launched in 2016 is also named **Mozi** for a western/Chinese pronunciation (Figure 645). **Jinan-1** was launched in 2022. Micius-1 was used for running several different experiments: a satellite-to-ground decoy-state QKD with kHz keyrates over up to 1,200 km and satellite-replayed

²⁶⁵² See [Satellite-based Quantum Key Distribution over Atmospheric Channels: Reviews and Research Challenges](#) by Hong-fu Chou et al, University of Luxembourg, July 2023 (6 pages).

²⁶⁵³ See [Satellite-based entanglement distribution and quantum teleportation with continuous variables](#) by Tasio Gonzalez-Raya, Stefano Pirandola and Mikel Sanz, March 2023 (16 pages).

²⁶⁵⁴ See [Phase Correction using Deep Learning for Satellite-to-Ground CV-QKD](#) by Nathan K. Long et al, UNSW, May 2023 (6 pages).

²⁶⁵⁵ This paragraph is largely inspired from the excellent and well detailed review paper [Micius quantum experiments in space](#) by Chao-Yang Lu, Yuan Cao, Cheng-Zhi Peng and Jian-Wei Pan, August 2022 (53 pages).

²⁶⁵⁶ See [Quantum Communication Countermeasures](#) by Michal Krelina, Czech Technical University in Prague, October 2023 (24 pages).

intercontinental key exchange, a satellite-based entanglement distribution to two Earth locations separated by 1205 km and a ground-to-satellite qubit teleportation as part of the QUESS project (Quantum Experiments at Space Scale)²⁶⁵⁷. The satellite weighs 640 kg and consumes 560W.

A 2018 experiment was about creating a videoconference between China and Austria using a quantum key sent every minute²⁶⁵⁸. Why with Austria? Because Jian-Wei Pan did his PhD thesis in Austria under the supervision of Anton Zeilinger, who piloted the European part of the experiment.

China is planning to launch a cloud of satellites in low orbit by 2030 dedicated to sending quantum keys by repeating this process²⁶⁵⁹. If they are banking on QKD for symmetric key management, it seems that China is also investing in post-quantum cryptography but in a quieter way.

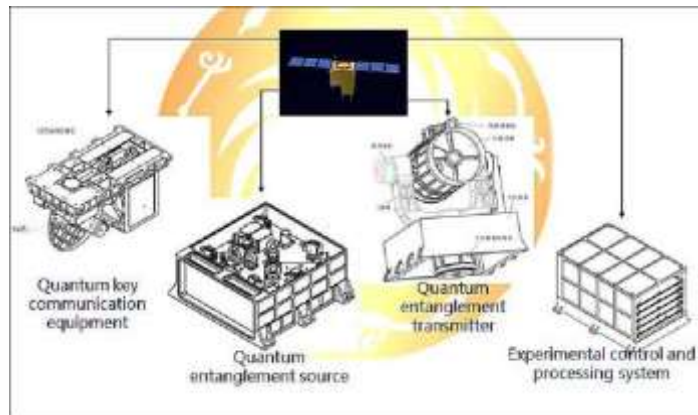


Figure 645: QKD satellite from China.

Micius-1 experiments could handle 5.9 million pairs of entangled photons per second, but due to error corrections, only one useful photon pair was exploitable per second²⁶⁶⁰.

As a result, Chinese scientists are studying scheduling approaches to load balance key distribution over time²⁶⁶¹. Also, it works only at night!

At the beginning of 2020, China announced that it had miniaturized its ground receiving station for quantum key communication with the Micius satellite from 10 tons to 80 kg. The key bitrate was reduced, from 40Kbits/s to 4-10Kbits/s. The experiment took place on the Earth side in Jinan and

²⁶⁵⁷ See respectively [Satellite-to-ground quantum key distribution](#) by Sheng-Kai Liao, Jian-Wei Pan et al, Nature, August 2017 (18 pages), [Satellite-Relayed Intercontinental Quantum Network](#) by Sheng-Kai Liao, Jian-Wei Pan et al, PRL, 2018 (10 pages), [Satellite-to-ground entanglement-based quantum key distribution](#) by Juan Yin, Jian-Wei Pan et al, PRL, 2017 and [Ground-to satellite quantum teleportation](#) by Ji-Gang Ren, Jian-Wei Pan et al, Nature, 2017 (16 pages). The principle was first described in 1993 in [Teleporting an Unknown Quantum State via Dual Classical and EPR Channels](#) by Charles Bennett, Gilles Brassard (from Montreal), Claude Crépeau, Richard Jozsa, Asher Peres and William Wootters. See also [Quantum Communication at 7,600km and Beyond](#) by Chao-Yang Lu and Cheng-Zhi Peng, Jian-Wei Pan, November 2018.

²⁶⁵⁸ See [Real-world intercontinental quantum communications enabled by the Micius satellite](#), USTC, PhysOrg, January 2018. Experiments or equivalent experiences have been launched by European teams. See [Quantum Photonics Technologies for Space](#), October 2018 (22 pages) and [Nanobob CubeSat mission](#), 2018 (31 pages). This is also being done in the UK, where an experimental Cubesat micro-satellite project is planned to cover the country. See [QUARC: Quantum Research Cubesat - A Constellation for Quantum Communication](#) by Luca Mazzarella et al, 2020 (27 pages).

²⁶⁵⁹ See some details on the satellite QKD deployment architecture in [Approaches to scheduling satellite-based quantum key distribution for the quantum network](#) by Xingyu Wang et al, 2021 (11 pages).

²⁶⁶⁰ See [A step closer to secure global communication](#) by Eleni Diamanti, Nature, June 2020, which describes the practical conditions and limitations of these satellite key transmission experiments. And in particular the most recent one described in [Entanglement-based secure quantum cryptography over 1,120 kilometers](#) by Juan Yin et al, Nature, June 2020. The actual key bitrate was 0.12 bits per second!

²⁶⁶¹ See [Approaches to scheduling satellite-based quantum key distribution for the quantum network](#) by Xingyu Wang et al, 2021 (11 pages).

Shanghai, so it seems at sea level²⁶⁶². The Bank of China would already secure transactions by sending keys via the Micius/Mozi Beijing satellite and remote provinces.

In June 2019, Chinese researchers announced that they had demonstrated the use of optical QKD aerial links established within a network of 35 kg octocopter UAVs spaced 200 m apart during a 40-minute flight at an altitude of 100 m²⁶⁶³.

The payload handling quantum communication weighed 11.8 kg. It can still be miniaturized, since the Chinese are aiming to integrate it into mass-market UAVs.

China was also proud to announce in 2021 that they had created the world's first integrated quantum communication network, combining 700 terrestrial optical fibers with two ground-to-satellite links, achieving quantum key distribution over 4,600 km²⁶⁶⁴. China researchers also developed a portable ground satellite QKD station of only 100 kg²⁶⁶⁵.

China announced yet another premiere in August 2022, with transmitting QKD keys from its Tiangong-2 space lab to four ground stations who are also connected to Micius which is positioned in a higher orbit, thanks to using Tiangong-2 as a repeater²⁶⁶⁶.

At last, China launched Jinan-1, a new 100 kg low-earth orbit (LEO) QKD satellite in July 2022.

But China is not alone there.

In **Europe**, there are also satellite QKD plans and architecture proposals²⁶⁶⁷. The EU is planning the launch of a 6B€ satellite program announced in February 2022 with QKD support, to be deployed by 2028. A project run by a 20-company consortium led by SES (Astra) and the European Space Agency with the support of the EU will launch in 2024 its EAGLE-1 QKD low-earth orbit satellite-based system that will last three years to enable BB84 QKD use cases²⁶⁶⁸. It will use a **Tesat** QKD satellite payload. TeQuants is an EU supported research project led by Thales Alenia Space that is about building a quantum network supporting entanglement and its applications, as part of EuroQCI (Figure 646). On the science front, Eleni Diamanti's LIP6 team in France is working on using adaptive optics to improve key sharing with satellite²⁶⁶⁹. Her team is also working with InPhyNi and Thales on satellite QKD architecture designs and simulations^{2670 2671}.

Singapore and its universities and startups are working on CubeSat based tiny QKD distribution satellites²⁶⁷².

²⁶⁶² See [China has developed the world's first mobile quantum satellite station](#) by Donna Lu, January 2020.

²⁶⁶³ See [Drone-based all-weather entanglement distribution](#) by Hua-Ying Liu et al, May 2019 (16 pages) and [World's First "Quantum Drone" for Impenetrable Air-to-Ground Data Links Takes Off](#) by Charles Q. Choi, IEEE Spectrum.

²⁶⁶⁴ See [Chinese Scientists Report World's First Integrated Quantum Communication Network](#) by Matt Swayne, 2021.

²⁶⁶⁵ See [Portable ground stations for space-to-ground quantum key distribution](#) by Ji-Gang Ren, Jian-Wei Pan and al, May 2022 (9 pages).

²⁶⁶⁶ See [Space-ground QKD network based on a compact payload and medium-inclination orbit](#) by Yang Li et al, Optica, August 2022 (6 pages).

²⁶⁶⁷ See [Satellite-based Quantum Information Networks: Use cases, Architecture, and Roadmap](#) by Laurent de Forges de Parny, Eleni Diamanti, Sébastien Tanzilli et al, February 2022 (21 pages).

²⁶⁶⁸ See [EAGLE-1: Advancing Europe's Leadership in Quantum Communications](#), SES, 2022..

²⁶⁶⁹ See [Analysis of satellite-to-ground quantum key distribution with adaptive optics](#) by Valentina Marulanda Acosta, Eleni Diamanti et al, November 2021 (17 pages).

²⁶⁷⁰ See [Satellite-based quantum information networks: use cases, architecture, and roadmap](#) by Laurent de Forges de Parny, Eleni Diamanti, Sébastien Tanzilli, Mathias Van Den Bossche et al, Nature Communications Physics, January 2023 (17 pages).

²⁶⁷¹ See [Connecting Quantum Cities: Simulation of a Satellite-Based Quantum Network](#) by Raja Yehia, Matteo Schiavon, Valentina Marulanda Acosta, Tim Coopmans, Iordanis Kerenidis, David Elkouss and Eleni Diamanti, July 2023 (24 pages).

²⁶⁷² See [A CubeSat platform for space based quantum key distribution](#) by Srihari Sivasankaran et al, April 2022 (6 pages).

Canada launched a plan to build a quantum communication satellite network in 2021, which makes sense with regards to the country size²⁶⁷³. This **QEYSSat** (Quantum Encryption and Science Satellite) project plans a satellite launch in 2025-2026 with a mission of one year extendable for one additional year. It is run by the Institute for Quantum Computing (University of Waterloo) with the industry help from Honeywell. It seems to be about a first generation QKD distribution, with no entanglement being mentioned in the project description.

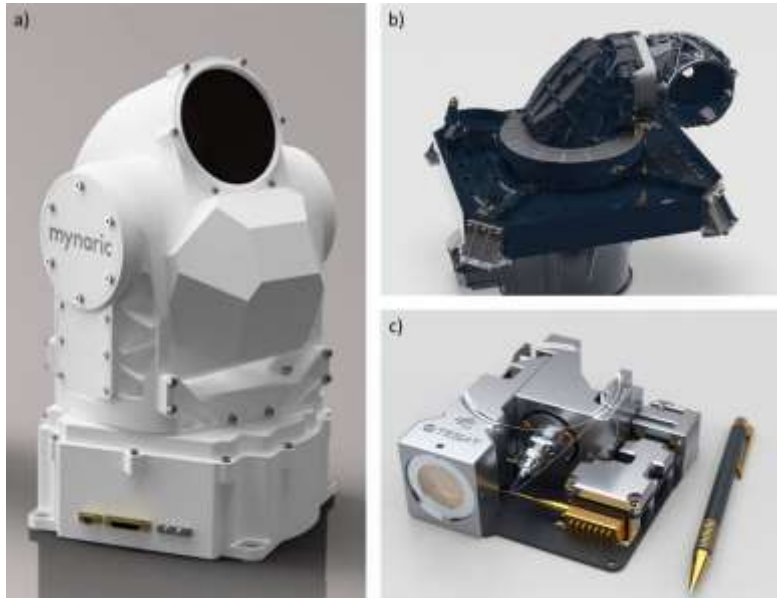


Figure 646: examples of ground station and satellite laser equipment for satellite based quantum communication.
Source: Mynaric, Tesat and Simera Sense. Added in 2023.

UK's Quantum Communications Hub is running its In Orbit Demonstration (IOD) mission to demonstrate QKD from space starting in 2024 with a satellite payload supporting new quantum signal transmission and quantum receivers in its Hub Optical Ground Station (OGS). It will rely on ISISPACE Group (the Netherlands) for satellite systems and services.

NASA's SEAQUE (Space Entanglement and Annealing QUantum Experiment) is a small experiment being launched in the ISS to test photon entanglement distribution in space, particularly to assess self-healing solutions against radiation damages. The project has contributions from the USA, Canada and Singapore. The experiment designed by **AdvR** (2019, USA) is to be docked outside the ISS in the "Bishop airlock" that is by Nanoracks, a private in-space services company²⁶⁷⁴.

QKD distribution was even tested in zero-G flights to see the impact of gravity changes, with positive results²⁶⁷⁵.

After space, how about distributing QKD underwater, I mean "free to water"? It's not a joke. It is being investigated in Turkey and China²⁶⁷⁶! The first simulations deal with 10 to 40 m distances. It is far from being sufficient to enable communications with submarines, particularly of the nuclear breed.

²⁶⁷³ See [QEYSSat 2.0 -- White Paper on Satellite-based Quantum Communication Missions in Canada](#) by Thomas Jennewein et al, University of Waterloo, University of Calgary and Institut National d'Optique, June 2023 (108 pages).

²⁶⁷⁴ See [NASA is launching a new quantum entanglement experiment in space](#) by Charlotte hu, March 2022.

²⁶⁷⁵ See [Photonic entanglement during a zero-g flight](#) by Julius Bittermann et al, March 2023 (19 pages).

²⁶⁷⁶ See [On the Optimization of Underwater Quantum Key Distribution Systems with Time-Gated SPADs](#) by Amir Hossein Fahim Raouf and Murat Uysal, Ozyegin University in Istanbul, June 2022 (6 pages) and [Practical underwater quantum key distribution based on decoy-state BB84 protocol](#), by Shanchuan Dong et al, March 2022 (10 pages).

Another option is to use underwater fibers, which is both more and less practical, as tested in 2023 between Italy and Malta over 100 km²⁶⁷⁷ and between the UK and Ireland over 224 km²⁶⁷⁸.

And beyond Earth, some are even devising how some extraterrestrial civilization could communicate with us with entangled photons. I am just wondering how these photon sources could be detected out of the noise coming from distant stars, even using all the technologies around to detect exoplanets (transit methods, spectrography, etc.)²⁶⁷⁹.

QKD photon sources and detectors

We've already covered photon sources for quantum computing and seen some of their requirements like the creation of deterministic and indistinguishable photons, on top of the even harder challenge to create large clusters of entangled photons.

The stakes with photons generation for QKD are slightly different. What is required are steady streams of individual photons, preferably generated in the telecom wavelengths between 1,200 nm and 1,550 nm. Entanglement based QKD also requires the generation of entangled pairs of photons. Finally, these sources should be lightweight and easy to integrate in telecom infrastructures. Preferably, they shouldn't be power hungry and not require cryogeny, thus a preference for ambient temperature solid-state solutions.

The breath of technologies used or investigated for photon generation is amazing. Let's mention a few of these recent advances:

- **Silicon with carbon atoms defects** creating optical wavelength photons at 1,279 nm²⁶⁸⁰ (Figure 647).
- **Vanadium defects in silicon-carbide** operating between 100mK and 3K with the benefit from a relative long stability²⁶⁸¹.
- **Silicon-nitride MRR** (microring resonator) that can generate 8 pairs of heralded entangled photons directly in the telecom wavelengths around 1,550 nm²⁶⁸². Microring resonators are tiny optical waveguides looped back onto themselves in circle or spiral, usually implemented in silicon semiconductors. They enable interference phenomena, the creation of delay lines, and the likes²⁶⁸³.

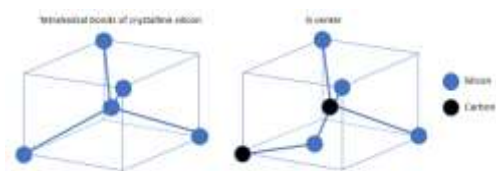


Figure 647: a G center and its two carbon atoms.

²⁶⁷⁷ See [Quantum Key Distribution over 100 km underwater optical fiber assisted by a Fast-Gated Single-Photon Detector](#) by Domenico Ribezzo et al, March 2023 (6 pages).

²⁶⁷⁸ See [Quantum communications feasibility tests over a UK-Ireland 224-km undersea link](#) by Ben Amies-King et al, October 2023 (11 pages).

²⁶⁷⁹ See [Viability of quantum communication across interstellar distances](#) by Arjun Berera and Jaime Calderón-Figueroa, June 2022 (18 pages), a fancy topic that was covered everywhere like in [Mathematical calculations show that quantum communication across interstellar space should be possible](#) by Bob Yirka, Phys.org, July 2022.

²⁶⁸⁰ See [Single G centers in silicon fabricated by co-implantation with carbon and proton](#) by Yoann Baron, Anais Dréau et al, April 2022 (5 pages). The electronically active G center is a complex of two substitutional carbon atoms and an interstitial silicon atom. See also the review paper on silicon defects [A bright future for silicon in quantum technologies](#) by Mario Khoury and Marco Abbarchi, 2022 (12 pages). Another intrinsic silicon defect resulting from irradiation of Si crystals is also studied, aka the W-center. See [Detection of single W-centers in silicon](#) by Yoann Baron, Jean-Michel Gérard, Vincent Jacques, Isabelle Robert-Philip, Anais Dréau et al, April 2022 (10 pages). See also [Wafer-scale nanofabrication of telecom single-photon emitters in silicon](#) by M. Hollenbach et al, April 2022 (20 pages) that covers the controllable fabrication of single G and W centers in silicon wafers using focused ion beams (FIB) with a probability exceeding 50%.

²⁶⁸¹ See [Vanadium in Silicon Carbide: Telecom-ready spin centres with long relaxation lifetimes and hyperfine-resolved optical transitions](#) by T. Astner et al, June 2022 (9 pages).

²⁶⁸² See [High-quality multi-wavelength quantum light sources on silicon nitride micro-ring chip](#) by Yun-Ru Fan et al, September 2022 (13 pages). Works with silicon chipsets and at ambient temperature. Creates 8 pairs of frequency multiplexed heralded entangled photons.

²⁶⁸³ See the review paper [Silicon microring resonators](#) by Wim Bogaerts et al, Laser & Photonics Review, 2012 (27 pages).

- **NV center-based** sources, like the ones studied by AWS and Element Six²⁶⁸⁴.
- **GaAs quantum-dot** single photon sources with high-source brightness ensuring high-speed quantum communication^{2685 2686}. A record of 175 km distance was broken in 2022 using GaAs/In-GaAs quantum dots and a finite key rate of 13 kbps over 100 km²⁶⁸⁷.
- **AlGaAs sources** with spontaneous parametric down-conversion (SPDC) enable the creation of polarization and/or frequency entangled sources of photons at telecom wavelengths^{2688 2689 2690}.
- **InAs** quantum dots embedded in GaAs with a conversion to telecom wavelength at 1,550 nm generating indistinguishable photons^{2691 2692}.
- **Si-based SPDC** to create pairs of entangled photons²⁶⁹³.
- **Rare-earth doped fibers** with potential room temperature operations²⁶⁹⁴.
- **CV-QKD squeezed states** preparation with off-the-shelf telecom equipment²⁶⁹⁵.
- **Photon based qudits** using larger dimension frequency bin entanglement^{2696 2697}. In mid-2019, other Chinese researchers experimented the teleportation of qutrits, allowing a transmission of more information per photons²⁶⁹⁸. This could be used to increase the rate of QKD key transmission.

Then, we have photon detectors and counters. They use various techniques depending on the QKD protocol used (entangled-based or not, etc.). **SPD** (single-photon detectors) are used after the photons traverse a polarization filter with several variants:

²⁶⁸⁴ See [Perfect imperfections: how AWS is innovating on diamond materials for quantum communication with Element Six](#) by Bart Machielse and Daniel Riedel, AWS, April 2023.

²⁶⁸⁵ See [Enhancing quantum cryptography with quantum dot single-photon sources](#) by Mathieu Bozzio et al, April 2022 (37 pages).

²⁶⁸⁶ See [Quantum-dot single-photon sources for the quantum Internet](#) by Chao-Yang Lu and Jian-Wei Pan, December 2021 (7 pages).

²⁶⁸⁷ See [Single-emitter quantum key distribution over 175 km of fiber with optimised finite key rates](#) by Christopher L. Morrison et al, September 2022 (9 pages).

²⁶⁸⁸ See [On-chip generation of hybrid polarization-frequency entangled biphoton states](#) by S. Francesconi, Sara Ducci, Perola Milman et al, MPQ and C2N, July 2022 (10 pages).

²⁶⁸⁹ See [Broadband biphoton generation and polarization splitting in a monolithic AlGaAs chip](#) by Félicien Appas, Sara Ducci et al, August 2022 (16 pages).

²⁶⁹⁰ See [Spectrally multimode squeezed states generation at telecom wavelengths](#) by Victor Roman-Rodriguez, David Fainsin, Guilherme L. Zanin, Nicolas Treps, Eleni Diamanti and Valentina Parigi, June 2023 (11 pages).

²⁶⁹¹ See [A Pure and indistinguishable single-photon source at telecommunication wavelength](#) by Beatrice Da Lio et al, NBI, January 2022 (7 pages).

²⁶⁹² See [On-demand Generation of Indistinguishable Photons in the Telecom C-Band using Quantum Dot Devices](#) by Daniel A. Vajner et al, University of Berlin, DTU and Wrocław University of Science and Technology, June 2023 (5 pages).

²⁶⁹³ See [Near perfect two-photon interference out a down-converter on a silicon photonic chip](#) by Romain Dalidet, Sébastien Tanzilli, Camille-Sophie Brès et al, InPhyNi at Nice in France, EPFL and Ligentec. February 2022 (8 pages).

²⁶⁹⁴ See [Room-temperature addressing of single rare-earth atoms in optical fiber](#) by Mikio Takezawa et al, PRA, October 2023 (12 pages).

²⁶⁹⁵ See [Plug-&-play generation of non-Gaussian states of light at a telecom wavelength](#) by Mohamed Faouzi Melalkia, Sébastien Tanzilli, Virginia D'Auria et al, May 2022 (6 pages).

²⁶⁹⁶ See [A reconfigurable silicon photonics chip for the generation of frequency bin entangled qudits](#) by Massimo Borghi et al, CEA-Leti and Italian labs, January 2023 (15 pages).

²⁶⁹⁷ See [Spin-orbit microlaser emitting in a four-dimensional Hilbert space](#) by Zhifeng Zhang et al, Penn University, Nature, November 2022 (no open access).

²⁶⁹⁸ See [Qutrits experiments are a first in quantum teleportation](#) by Daniel Garisto in Scientific American, August 2019, which refers to [Experimental multi-level quantum teleportation](#) by Xiao-Min Hu et al, April 2019 (12 pages) and [Quantum teleportation in high dimensions](#) by Yi-Han Luo, June 2019 (23 pages).

- **APD**, avalanche photodiodes and **SPAD**, single photon avalanche photodiode which can detect single photons.
- **SNSPD**, superconducting nanowire single-photon detectors, requiring <4K cooling^{2699 2700 2701}.
- **VLPC** (visible light photon counter) which are silicon based.

Researchers and industry vendor are creating integrated solutions fitting in silicon and GaAs photonic circuits with DV or CV photon source, receiver and amplifiers²⁷⁰².

QKD nodes and repeaters

The range of QKD transmission over fiber has improved with only 30 cm in 1989 (IBM with Charles Bennett), 1,100 m at the University of Geneva in 1993, then 23 km in 1995 with the BB84 protocol, all via fiber optics.

China researchers created a 404 km QKD fiber connection without a repeater in 2016²⁷⁰³, then extended this record in 2020 to 509 km of transmission without repeater²⁷⁰⁴ and to 511 km using the TF-QKD protocol (aka twin-field QKD)^{2705 2706}.

The technique was improved in 2020 by a mix of British and American researchers to reach 600 km²⁷⁰⁷.

The record was broken in 2022 with 833 km as shown in Figure 648²⁷⁰⁸. In Austria, an entanglement distribution was achieved over 248 km in 2022²⁷⁰⁹. At these large distances, the error rates are so high that it becomes impractical. The key rates are very low, getting under 10^{-7} for distances larger than 400 km.

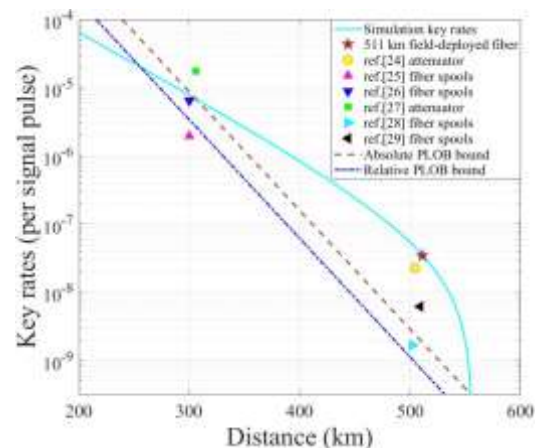


Figure 648: relationship of QKD keyrates and distance without repeaters. Source: See [Twin-Field Quantum Key Distribution over 511 km Optical Fiber Linking two Distant Metropolitans](#) by Jiu-Peng Chen, Jian-Wei Pan et al, January 2021 (32 pages).

²⁶⁹⁹ See an example with [Heterogeneously integrated, superconducting silicon-photonic platform for measurement-device-independent quantum key distribution](#) by Xiaodong Zheng et al, October 2021 (8 pages).

²⁷⁰⁰ See [High-speed detection of 1550 nm single photons with superconducting nanowire detectors](#) by Ioana Craiciu et al, JPL and Caltech, October 2022 (12 pages).

²⁷⁰¹ See [GHz detection rates and dynamic photon-number resolution with superconducting nanowire arrays](#) by Giovanni V. Resta et al, IDQ and University of Geneva, March-June 2023 (28 pages).

²⁷⁰² See [Continuous-Variable Quantum Key Distribution at 10 GBaud using an Integrated Photonic-Electronic Receiver](#) by Adnan A.E. Hajomer et al, May 2023 (7 pages) with a small system board operating at 10 GBaud, generating secret key rates at over 0.7 Gb/s over a distance of 5 km, and 0.3 Gb/s over 10 km.

²⁷⁰³ Documented in [Measurement device independent quantum key distribution over 404 km optical fiber](#), 2016 (15 pages).

²⁷⁰⁴ See [Study achieves a new record fiber QKD transmission distance of over 509 km](#) by Ingrid Fadelli, March 2020.

²⁷⁰⁵ See [Twin-Field Quantum Key Distribution over 511 km Optical Fiber Linking two Distant Metropolitans](#) by Jiu-Peng Chen, Jian-Wei Pan et al, January 2021 (32 pages).

²⁷⁰⁶ See [Twin-field quantum key distribution without phase locking](#) by Wei Li, Jian-Wei Pan et al, December 2022 (31 pages) which improved the experiment without using phase locking, the synchronization of the phase of optical signals between the sender and receiver.

²⁷⁰⁷ See [600-km repeater-like quantum communications with dual-band stabilization](#) by Mirko Pittaluga et al, 2020 (14 pages).

²⁷⁰⁸ See [Twin-field quantum key distribution over 830-km fibre](#) by Shuang Wang et al, Nature, January 2022 with a 140 dB loss!

²⁷⁰⁹ See [Continuous entanglement distribution over a transnational 248 km fibre link](#) by Sebastian Philipp Neumann et al, March 2022 (23 pages).

There is even an upper bound for these key rates, $-\log_2(1-\eta)$ with η being the transmissivity of the lossy quantum channel, whatever the protocol²⁷¹⁰. China again broke this record in 2023 with reaching a distance of 1,002 km also using TF-QKD, with a very low key rate of 0.0034 bps²⁷¹¹. These records are nice, but their key rate is not practically acceptable.

Quantum channels used for QKD are subject to noise and leaks. Transmitting a useful photon requires several trials and its number grows exponentially with distance. And when the photon arrives at its destination, its state fidelity also decreases exponentially with distance. As a result, for large distances, we need nodes and/or repeaters.

They must guarantee a good key rate and fidelity and be tolerant to errors. They are essential for distributing quantum keys over long distances, beyond 80 km²⁷¹². QKD networks also use classical optical switches using frequency multiplexing. It enables the routing of QKD signals from one emitter to different receivers, but once at a time. They also use SDN (software defined network) to dynamically configure the networks and their nodes, particularly trusted nodes.

There are three main kinds of nodes and repeaters:

Trusted node relays where keys must be revealed classically in the intermediate stations, thus the need for it to be in “trusted” locations. These nodes are mostly used with the BB84 protocol but can also work with entanglement based QKDs. They can be implemented to create an arbitrary distance QKD connection. This is the dominant solution. It is used in the 2,000 km Beijing-Shanghai QKD line and in the various EU OpenQKD projects.

Untrusted node relays are safer than trusted node relays work but work only with the family of entanglement-based QKD protocols like MDI-QKD and for relatively short distance. It avoids security loopholes at the measurement side and allows the relay to be controlled by an eavesdropper without endangering the security of the shared keys. Complex networks can contain both trusted and untrusted nodes depending on their location and physical safety.

Quantum repeaters which are safer than trusted node repeaters²⁷¹³. They use entanglement swapping techniques which keep the key sharing link quantum from end-to-end between Alice and Bob. They do not implement any measurement or cloning but, instead, quantum states purification which consists in keeping trusted entangled pairs selected out of many imperfect pairs. They must usually be equipped with some form of quantum memory to propagate the state of the photons to be transmitted through entanglement swapping²⁷¹⁴. These quantum memories are still unproven and a field of fundamental research. These are different kinds of quantum memories than the ones that needed for quantum computing and that we covered in the quantum memory part starting page 278. These quantum memories for quantum repeaters need a single qubit per link.

It can be implemented with many tools, the following list being essentially a topic bibliography:

²⁷¹⁰ See [Fundamental Limits of Repeaterless Quantum Communications](#) by Stefano Pirandola et al, 2017 (61 pages).

²⁷¹¹ See [Experimental Twin-Field Quantum Key Distribution Over 1000 km Fiber Distance](#) by Yang Liu, Jian-Wei Pan et al, PRL, May 2023 (47 pages).

²⁷¹² Knowing that the record distance for quantum telecommunication without repeaters is 509 km as we have already seen. See also [Viewpoint: Record Distance for Quantum Cryptography](#) by Marco Lucamarini, Toshiba & Cambridge, November 2018 and [Recent progress on Measurement-Device-Independent \(MDI\) Quantum Key Distribution \(QKD\)](#) by Marco Lucamarini, 2018 (71 slides).

²⁷¹³ See the review paper [Quantum repeaters: From quantum networks to the quantum internet](#) by Koji Azuma, Sophia E. Economou, Liang Jiang, Paul Hilaire et al, December 2022 (68 pages).

²⁷¹⁴ See [Quantum Nodes for Quantum Repeater](#) by Hugues de Riedmatten, ICFO, January 2021 (60 slides).

- **Rare earth** doped crystals using ytterbium²⁷¹⁵, europium^{2716 2717}, erbium^{2718 2719}, yttrium²⁷²⁰ and praseodymium^{2721 2722 2723}.
- **Cold atoms** single atoms^{2724 2725}, atomic vapors or ensembles^{2726 2727}.
- **SiC** silicon vacancies²⁷²⁸.
- **SiV**^{2729 2730 2731}, **nitrogen**^{2732 2733} vacancies in diamond, which can also be arranged in arrays²⁷³⁴.
- **Optomechanical memories**, as proposed by NBI in Denmark, using optomechanical induced transparency²⁷³⁵.

²⁷¹⁵ See [Remote distribution of non-classical correlations over 1250 modes between a telecom photon and a \$^{171}\text{Yb}^{3+}\text{Y}_2\text{SiO}_5\$ crystal](#) by Moritz Businger et al, Université de Genève, Chimie ParisTech and Sorbonne Université, May 2022 (8 pages) that uses ytterbium and yttrium.

²⁷¹⁶ See [Storage of photonic time-bin qubits for up to 20 ms in a rare-earth doped crystal](#) by Antonio Ortu, Adrian Holzäpfel, Jean Etesse and Mikael Afzelius, npj, March 2022 (7 pages) describes a 20 ms quantum memory using crystals doped with europium, operating near 0K,

²⁷¹⁷ See [On-demand Integrated Quantum Memory for Polarization Qubits](#) by Tian-Xiang Zhu et al, January 2022 (20 pages) with europium and yttrium.

²⁷¹⁸ See [Indistinguishable telecom band photons from a single Er ion in the solid state](#) by Salim Ourari et al, Nature, August 2023 (20 pages) which is using erbium and telecom wavelength.

²⁷¹⁹ See [Quantum storage of entangled photons at telecom wavelengths in a crystal](#) by Ming-Hao Jiang et al, Nature Communications, November 2023 (8 pages).

²⁷²⁰ See [On-demand storage of photonic qubits at telecom wavelengths](#) by Duan-Cheng Liu et al, January 2022 (11 pages) which uses erbium-yttrium crystals.

²⁷²¹ See [Storage and analysis of light-matter entanglement in a fiber-integrated system](#) by Jelena v. Rakonjac et al, Science Advances, July 2022 (6 pages) with praseodymium and yttrium.

²⁷²² See [Multiplexed storage and real-time manipulation based on a multiple-degree-of-freedom quantum memory](#), by Tian-Shu Yang et al, China CAS, 2018 (9 pages) using praseodymium.

²⁷²³ See [Efficient cavity-assisted storage of photonic qubits in a solid-state quantum memory](#) by Stefano Duranti et al, IFCO and ICREA, July 2023 (7 pages).

²⁷²⁴ See [Entangling single atoms over 33 km telecom fibre](#) by Tim van Leent et al, Nature, July 2022 (16 pages).

²⁷²⁵ See [Highly efficient storage of 25-dimensional photonic qudit in a cold-atom-based quantum memory](#) by Ming-Xin Dong et al, January 2023 (14 pages).

²⁷²⁶ See the review paper [Broadband Quantum Memory in Atomic Ensembles](#) by Kai Shinbrough et al, January 2023 (49 pages).

²⁷²⁷ See [Single-Photon Storage in a Ground-State Vapor Cell Quantum Memory](#) by Gianni Buser et al, PRX Quantum, June 2022 (10 pages).

²⁷²⁸ See [Scalable quantum memory nodes using nuclear spins in Silicon Carbide](#) by Shravan Kumar Parthasarathy et al, February 2023 (15 pages).

²⁷²⁹ See [A Quantum Repeater Platform based on Single SiV Centers in Diamond with Cavity-Assisted, All-Optical Spin Access and Fast Coherent Driving](#) by Gregor Bayer et al, October 2022 (8 pages).

²⁷³⁰ See [Telecom networking with a diamond quantum memory](#) by Eric Bersin et al, MIT, Harvard, Stanford University, AWS, July 2023 (17 pages).

²⁷³¹ See [Efficient Photonic Integration of Diamond Color Centers and Thin-Film Lithium Niobate](#) by Daniel Riedel, Jelena Vučković et al, June 2023 (21 pages).

²⁷³² See [Proposal for room-temperature quantum repeaters with nitrogen-vacancy centers and optomechanics](#) by Jia-Wei Ji et al, University of Calgary, March 2022 (20 pages).

²⁷³³ See [A fully packaged multi-channel cryogenic quantum memory module](#) by David J. Starling et al, February 2023 (10 pages) which deals with the cryogenic module of a NV center circuit.

²⁷³⁴ See [Electric-Field Programmable Spin Arrays for Scalable Quantum Repeater](#) by Hanfeng Wang et al, April 2022 (12 pages).

²⁷³⁵ See [A Long-lived and Efficient Optomechanical Memory for Light](#) by Mads Bjerregaard Kristensen et al, NBI, August 2023 (10 pages).

- **Trapped ions** with the benefit of directly using telecom wavelengths^{2736 2737 2738 2739} and sometimes using two sorts of ions²⁷⁴⁰.
- **All-photonic quantum processes (APQR)** using a photonic graph state and Shor error correction code²⁷⁴¹.
- **Fiber optics** delay lines used as memory given the challenge is to limit their losses^{2742 2743}.

These repeaters technologies are still at basic research stage and with some limitations²⁷⁴⁴.

The DLCZ protocol created by Harvard, Austria and China scientists in 2001 made it possible to improve entanglement sharing on lossy communication channels and has been continuously improved since then²⁷⁴⁵. It is based on using clouds of identical atoms instead of individual atoms, beam splitters and single-photon detectors with moderate efficiencies with a communication efficiency that scales polynomially with distance.

In July 2019, Chinese researchers announced that they succeeded using a photonic repeater technology based on 12-photon interferometers without any quantum memory, encoding a qubit in a cluster state and using error correction in repeaters²⁷⁴⁶.

Securing QKD

In 2000, Peter Shor and John Preskill published a theoretical proof that BB84 is a secure protocol²⁷⁴⁷. But QKD is not the solution-that-fixes-all-problems. It can still be subject to jamming, denial of services and various attacks which we cover later. Its safety also depends on the security of both ends of telecommunication like with any other solution.

²⁷³⁶ See the thesis [A memory-based quantum network node with a trapped ion in an optical fibre cavity](#) by Pascal Kobel, 2021 (222 pages). It uses ytterbium ions which have coherence time exceeding the second range and transitions in the microwave band.

²⁷³⁷ See [Telecom-Wavelength Quantum Repeater Node Based on a Trapped-Ion Processor](#) by Victor Krutyanskiy, Marco Canteri, Martin Meraner, James Bate, Vojtech Krčmářsky, Josef Schupp, Nicolas Sangouard and Ben P. Lanyon, PRL, October 2022-May 2023 (32 pages).

²⁷³⁸ See [Robust Quantum Memory in a Trapped-Ion Quantum Network Node](#) by P. Drmota et al, University of Oxford, October 2022 (9 pages).

²⁷³⁹ See [Telecom Quantum Photonic Interface for a ⁴⁰Ca⁺ Single-Ion Quantum Memory](#) by Elena Arenskötter et al, November 2022 (16 pages).

²⁷⁴⁰ See [Robust Quantum Memory in a Trapped-Ion Quantum Network Node](#) by P. Drmota et al, Oxford University, October 2022-April 2023 (10 pages).

²⁷⁴¹ See [Loss-tolerant all-photonic quantum repeater with generalized Shor code](#) by Rui Zhang et al, March 2022 (8 pages).

²⁷⁴² See [A fiber-integrated quantum memory for telecom light](#) by K. A. G. Bonsma-Fisher et al, University of Ottawa, March 2023 (8 pages).

²⁷⁴³ See [Fiber Loop Quantum Buffer for Photonic Qubits](#) by Kim Fook Lee et al, Northwestern University, September 2023 (14 pages).

²⁷⁴⁴ See [Tutorial on quantum repeaters](#) by Rodney Van Meter and Tracy Northup, 2019 (178 slides), [Overcoming the rate-distance limit of quantum key distribution without quantum repeaters](#), 2018 (5 pages), [An Information-Theoretic Framework for Quantum Repeater](#) by Roberto Ferrara, 2018 (144 pages) and [Quantum Internet Protocol Stack: a Comprehensive Survey](#) by Jessica Illiano et al, February 2022 (25 pages) which explains how entanglement is used as a resource in quantum Internet and how it is handled in quantum repeaters. Quantum repeaters, namely, devices implementing the physical process called entanglement swapping and perform a BSM (Bell state measurement). It then covers higher level quantum Internet protocols proposals.

²⁷⁴⁵ See [Long-distance quantum communication with atomic ensembles and linear optics](#) by Lu-Ming Duan, Mikhail Lukin, Juan Ignacio Cirac and Peter Zoller, Nature, May 2001 (11 pages).

²⁷⁴⁶ See [Scientists Firstly Realize All-photonic Quantum Repeater](#), July 2019 and [Experimental quantum repeater without quantum memory](#) by Zheng-Da Li et al, 2019 (12 pages).

²⁷⁴⁷ See [Simple Proof of Security of the BB84 Quantum Key Distribution Protocol](#) by Peter W. Shor, and John Preskill, March-May 2000 (5 pages).

Securing a chain depends on its weakest links and here it is the transmitters and receivers before they even exchange via a QKD. Furthermore, QKDs are not a panacea because they depend on a point-to-point link and not on a routing technique that allows several paths to be used. This could lead to a form of denial of service by blocking the used physical communication, but rerouting techniques are investigated²⁷⁴⁸.

The table in Figure 649 lists a whole bunch of vulnerabilities in the QKD, many of which having since been removed²⁷⁴⁹. Other weaknesses sit in the potential defects of the random number generators used in the QKD protocols to send the measurement basis. However, this can be fixed²⁷⁵⁰. All the side-channel attacks from the table in Figure 649 and others using RF detection on QKD hardware can be typically fixed with various countermeasures^{2751 2752}.

Attack	Target component	Tested system
Distinguishability of decoy states A. Huang <i>et al.</i> , Phys. Rev. A 98 , 012330 (2018)	laser in Alice	3 research systems
Intersymbol interference K. Yoshino <i>et al.</i> , poster at QCrypt (2016)	intensity modulator in Alice	research system
Laser damage V. Makarov <i>et al.</i> , Phys. Rev. A 94 , 030302 (2016); A. Huang <i>et al.</i> , poster at QCrypt (2018)	any	5 commercial & 1 research systems
Spatial efficiency mismatch M. Rau <i>et al.</i> , IEEE J. Sel. Top. Quantum Electron. 21 , 6600905 (2015); S. Sajeed <i>et al.</i> , Phys. Rev. A 91 , 062301 (2015)	receiver optics	2 research systems
Pulse energy calibration S. Sajeed <i>et al.</i> , Phys. Rev. A 91 , 032326 (2015)	classical watchdog detector	ID Quantique
Trojan-horse I. Khan <i>et al.</i> , presentation at QCrypt (2014)	phase modulator in Alice	SeQureNet
Trojan-horse N. Jain <i>et al.</i> , New J. Phys. 16 , 123030 (2014); S. Sajeed <i>et al.</i> , Sci. Rep. 7 , 8403 (2017)	phase modulator in Bob	ID Quantique
Detector saturation H. Qin, R. Kumar, R. Alleaume, Proc. SPIE 88990N (2013)	homodyne detector	SeQureNet
Shot-noise calibration P. Jouguet, S. Kunz-Jacques, E. Diamanti, Phys. Rev. A 87 , 062313 (2013)	classical sync detector	SeQureNet
Wavelength-selected PNS M.-S. Jiang, S.-H. Sun, C.-Y. Li, L.-M. Liang, Phys. Rev. A 86 , 032310 (2012)	intensity modulator	(theory)
Multi-wavelength H.-W. Li <i>et al.</i> , Phys. Rev. A 84 , 062308 (2011)	beamsplitter	research system
Deadtime H. Weier <i>et al.</i> , New J. Phys. 13 , 073024 (2011)	single-photon detector	research system
Channel calibration N. Jain <i>et al.</i> , Phys. Rev. Lett. 107 , 110501 (2011)	single-photon detector	ID Quantique
Faraday-mirror S.-H. Sun, M.-S. Jiang, L.-M. Liang, Phys. Rev. A 83 , 062331 (2011)	Faraday mirror	(theory)
Detector control I. Gerhardt <i>et al.</i> , Nat. Commun. 2 , 349 (2011); L. Lydersen <i>et al.</i> , Nat. Photonics 4 , 686 (2010)	single-photon detector	ID Quantique, MagiQ, research systems

Figure 649: QKD sources of vulnerabilities. The source is quite old and many of these weaknesses have been fixed since then. Also, entanglement based QKD are way more secured with enabling device independence security. Source: [QKD Measurement Devices Independent](#) by Joshua Slater, 2014 (83 slides).

Entanglement based QKD is by design more secure than BB84-based QKD. It brings device independence which means you can trust a system without the need to control all its elements. It is verified with loophole free Bell tests. Work is very active in the area²⁷⁵³.

²⁷⁴⁸ On QKD vulnerabilities and methods to avoid them, see [QKD Measurement Devices Independent](#) by Joshua Slater, 2014 (83 slides).

²⁷⁴⁹ See [Certification of cryptographic tools](#) by Vadim Makarov from Quantum Hacking Lab in Moscow, 2019 (15 slides).

²⁷⁵⁰ See [Randomness determines practical security of BB84 quantum key distribution](#) by Hong-Wei Li et al, Nature Scientific Reports, 2015 (8 pages).

²⁷⁵¹ See [Side-channel-secure quantum key distribution](#) by Cong Jiang et al, May 2023 (10 pages).

²⁷⁵² See [Deep-Learning-Based Radio-Frequency Side-Channel Attack on Quantum Key Distribution](#) by Adomas Baliuka et al, October 2023 (14 pages).

²⁷⁵³ See [Cryptographic Security Concerns on Timestamp Sharing via Public Channel in Quantum Key Distribution Systems](#) by Melis Pahali et al, March 2022 (6 pages) and [Improved Finite-Key Security Analysis of Quantum Key Distribution Against Trojan-Horse Attacks](#) by Alvaro Navarrete and Marcos Curty, February 2022 (18 pages).

Cryptography is fascinating for the speed at which security devices can be broken by researchers before they are deployed en masse. Thus, QKDs would be vulnerable due to an implementation vulnerability associated with Bell's theorem that can be handled with better quality detectors²⁷⁵⁴. It's a never-ending race!

QKD and Blockchain

QKD could be used to secure a Blockchain. This is obviously delicate to deploy end-to-end on a large scale. Indeed, Blockchain users don't have a satellite link in the mountains or a secured fiber on hand, even when they are mobile. But so be it.

This is the proposal of Evgeny Kiktenko of the Russian Quantum Center in Moscow²⁷⁵⁵ and Del Rajan and Matt Visser of Victoria University of Wellington in New Zealand²⁷⁵⁶. Why exactly is not all data transmitted protected in the same way as the QKD? It seems at least to be limited by the low bitrate of existing QKDs.

Still, JPMorgan Chase, Toshiba and Ciena are piloting a QKD network of 100 km mixed fibers (handling both QKD and classical data distribution) to secure “mission critical Blockchain application”²⁷⁵⁷. If it is so critical and requires a proprietary network, why does it need a Blockchain in the first place?

Other theoretical architectures have been proposed in various places like India that would rely on quantum computing to improve Blockchain security^{2758 2759 2760}. There are even proposals for a sort of quantum Bitcoin and smart contracts coming from Israel²⁷⁶¹.

Also, quantum computing could be potentially used to mine Bitcoin with the proof of work method although its resources estimate is not clear²⁷⁶². When you mix a complicated system with a couple others that are as complicated, it doesn't make it simpler to grasp.

QKD over 5G

You may hear about plans to deploy QKD security in 5G networks. Of course, it doesn't deal with the radio portion of 5G and with your smartphone, but only about securing the backbone landline fiber networks of telecom operators²⁷⁶³.

²⁷⁵⁴ It is documented by Jonathan Jogenfors in [Breaking the Unbreakable Exploiting Loopholes in Bell's Theorem to Hack Quantum Cryptography](#), 2017 (254 pages).

²⁷⁵⁵ Documented in [First Quantum-Secured Blockchain Technology Tested in Moscow](#), June 2017.

²⁷⁵⁶ In [Quantum Blockchain using entanglement in time](#), 2018 (5 pages).

²⁷⁵⁷ See [JPMorgan Chase, Toshiba and Ciena Build the First Quantum Key Distribution Network Used to Secure Mission-Critical Blockchain Application](#), February 2022. See also [DV-QKD Coexistence With 1.6 Tbps Classical Channels Over Hollow Core Fibre](#) by Obada Alia et al, March 2022 (7 pages) which documents the coexistence of QKD and classical communication on the same fiber.

²⁷⁵⁸ See [Quantum blockchain using weighted hypergraph states](#) by Shreya Banerjee et al, Physical Review Research, 2020 (7 pages).

²⁷⁵⁹ See [Quantum Blockchain based on Dimensional Lifting Generalized Gram-Schmidt Procedure](#) by Kumar Nilesh and P. K. Panigrahi, January 2022 (16 pages).

²⁷⁶⁰ See [The Next Generation of Blockchain: Quantum Blockchain Networks](#) by Manan Narang from OneQuantum, March 2022, which confuses “quantum computing” and “quantum cryptography” and PQC to secure Blockchains.

²⁷⁶¹ See [Quantum Prudent Contracts with Applications to Bitcoin](#) by Or Sattath, April 2022 (49 pages).

²⁷⁶² See [Quantum advantage on proof of work](#) by Dan A Bard, Joseph J Kearney, and Carlos A Perez-Delgado, 2022. Which casts a quantum mining superiority over classical mining by 2045, using a very simplistic Moore's law applied to quantum computing.

²⁷⁶³ See [Quantum Key Distribution for 5G Networks: A Review, State of Art and Future Directions](#) by Mohd Hirzi Adnan, Zuriati Ahmad Zukarnain and Nur Ziadah Harun, 2022 (28 pages).

Market and standards

What about the size of the QKD market? **Inside Quantum Technology** (a UK analyst company) made an estimate with a first \$1B dollars reached in 2024, then an exponential growth leading to \$7B in 2028²⁷⁶⁴ (Figure 650).

These are simplistic exponential growth curves, as usual. We'll see. One key market driver would be the adoption of QKD by cloud and data center operators²⁷⁶⁵.

China is very active in defining a set of QKD standards²⁷⁶⁶. The ITU is also working on QKD standards²⁷⁶⁷. Europe is represented in the standardization work carried out at ISO, IEEE, ETSI and CENELEC, the European Committee for Standardization in Electronics and Electrotechnology.

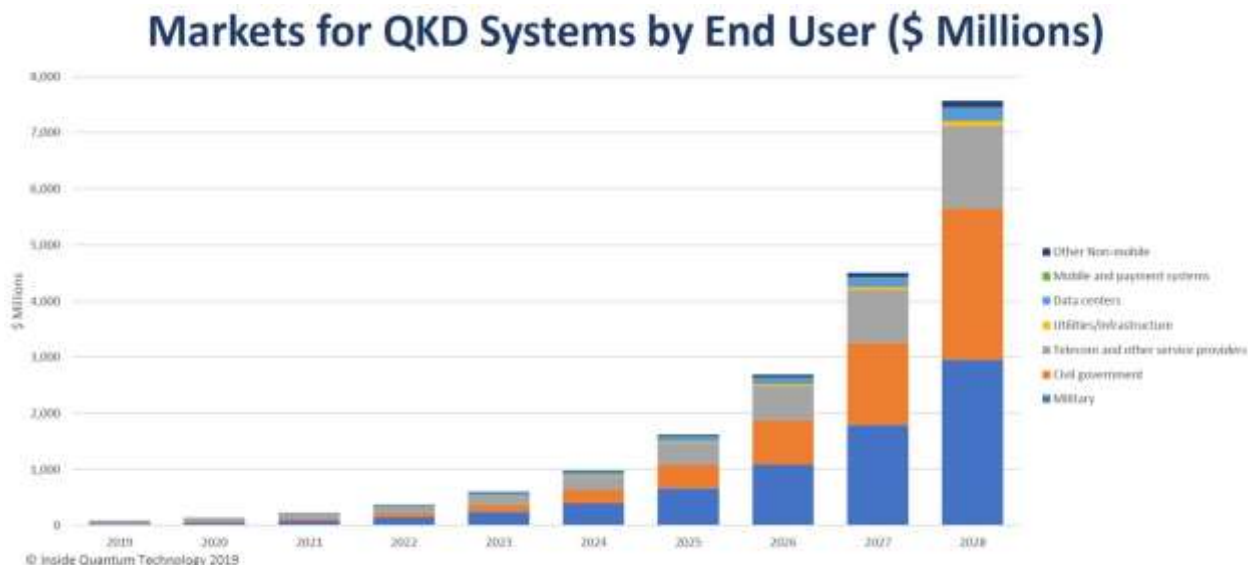


Figure 650: Inside Quantum Technology's QKD market assessment as done in 2019. Source: [The Future of the Quantum Internet A Commercialization Perspective](#) by Lawrence Gasman, June 2019 (11 slides).

Post-quantum cryptography

The physical protection of symmetric key transmission is not easily applicable in a generalized way, if only because it requires some optical link (direct free to air or by optical fiber) between transmitters and receivers. This, for example, does not work with radio links like with smartphones.

So, cybersecurity also requires the creation of cryptography systems capable of resisting the onslaught of quantum computers whether coming from Shor's or Grover's algorithms. Breaking encrypted messages - without private keys - should be an NP-Complete or NP-Hard problem to withstand future quantum assaults.

Post-Quantum Cryptography (PQC) complements Quantum Key Distribution (QKD) for this respect. It is certainly easier to deploy on a large scale because it is independent from the telecommunications infrastructures. It is made to resist to CRQC (Cryptanalytically-Relevant Quantum Computer) attacks.

²⁷⁶⁴ See [The Future of the Quantum Internet A Commercialization Perspective](#) by Lawrence Gasman, Inside Quantum Technology, June 2019 (11 slides) and [The Future of the Quantum Internet A Commercialization Perspective](#) by Lawrence Gasman from Inside Quantum Technology, June 2019 (11 slides). Seen in [ITU Workshop on Quantum Information Technology for Networks](#).

²⁷⁶⁵ See [Quantum key distribution for data center security -- a feasibility study](#) by Nitin Jain et al, DTU and KPMG, July 2023 (23 pages).

²⁷⁶⁶ See [Introduction of Quantum secured Communication Standardization in CCSA](#) by Zhangchao Ma, June 2019 (16 slides) and [An overview of current quantum information technology \(QIT\) standardization](#) by Wei Qi, June 2019 (13 slides).

²⁷⁶⁷ See [ITU-T Focus Group on Quantum Information Technology for Networks \(FG-QIT4N\)](#), 2019.

However, it can be combined by sending PQC public keys over physical QKD links or with using some PQC for authenticating the classical link used for the exchange of the photon measurement basis²⁷⁶⁸. Different PQC systems differ in many parameters and have different trade-offs between signature size, processing speed for encryption and decryption, and public key size (Figure 655).

Let's look at the PQC timeline²⁷⁶⁹:

- **1978**: the first algorithm resistant to quantum computers is created by **Robert McEliece** (details below) even before Richard Feynman even mentioned the idea of creating quantum computers and the creation of both Shor and Grover's algorithms!
- **2003**: the term "post quantum cryptography" (PQC) is created by **Daniel Bernstein**²⁷⁷⁰.
- **2006**: the first international **PQCrypto** workshop is held in Belgium to study ways to circumvent quantum computer attacks at a time when you can barely assemble two qubits. The program consists in finding successors to the quantum-resistant public key cryptography algorithms RSA and ECC²⁷⁷¹. The 12-person program committee includes among others Louis Goubin from the University of Versailles and Phong Nguyen and Christopher Wolf from the ENS. From this first edition, four of the five pillars of the PQC are established with the code-based crypto, lattice codes, hash Lamport signature and multivariate cryptography. The isogenies will arrive later. Two French researchers propose two of these four tracks: Nicolas Sendrier, from Inria, with "Post-quantum code-based cryptography" and Jacques Stern from ENS with "Post-quantum multivariate-quadratic public key schemes"²⁷⁷². These workshops have since been held every one to two years around the world. The [2013 edition took place](#) in Limoges, France.
- **2012**: the **NIST** (National Institute for Standards & Technologies) launches its first projects and a team on PQC.
- **2014**: the **European Union** launches a Horizon 2020 call for projects on PQC. At the same time, ETSI, the European Telecoms Standardization Body, also launches its working group on PQC.
- **2015**: **NIST** organizes its first PQC workshop. ETSI published a reference document on QC²⁷⁷³. The NSA woke up and declared that the transition to PQC would become a priority²⁷⁷⁴. The NSA is playing two roles each time: it wants to protect itself and the sensitive communications of the U.S. government with good encryption systems but at the same time maintain the ability to break the codes of standard commercial communications and those from other countries. This relies on the brute force of giant supercomputers and a highly asymmetrical technical resources. In 2015, the European project PQCrypto coordinated by Tanja Lange is launched²⁷⁷⁵.
- **2016**: NIST publishes [QCP Progress Report](#) (15 pages) and an associated standardization roadmap.

²⁷⁶⁸ See [Experimental authentication of quantum key distribution with post-quantum cryptography](#) by Liu-Jun Wang et al, May 2021 (7 pages).

²⁷⁶⁹ I extracted a piece of it from [Quantum cryptanalysis - the catastrophe we know and don't know](#) by Tanja Lange, a researcher from the Netherlands, 2017 (33 slides).

²⁷⁷⁰ Daniel Bernstein is the author with Johannes Buchmann and Erik Dahmen of the impressive book [Post-Quantum Cryptography](#), 2009 (254 pages) which describes well the challenges of PQC.

²⁷⁷¹ The proceedings are in [PQCrypto 2006 International Workshop on Post-Quantum Cryptography](#), May 2006 (254 pages).

²⁷⁷² Source: [Quantum Computing and Cryptography Today](#) by Travis L. Swaim, University of Maryland University College (22 pages).

²⁷⁷³ See [Quantum Safe Cryptography and Security](#) (64 pages).

²⁷⁷⁴ See [Commercial national security algorithm suite and quantum computing FAQ IAD](#) (11 pages).

²⁷⁷⁵ It is documented in [Post-Quantum Cryptography for Long-Term Security](#) (10 pages).

- **2017:** marks the end of the PQC standardization proposal submissions to NIST. By the end of 2017, 69 applicants are accepted out of 82, mainly with Euclidean networks (lattice codes) and error correction codes (code based PQC). In the same year, the 8th PQCrypto workshop was held in Utrecht, the Netherlands. These candidates had to meet increasing security levels labelled SL1, SL3 and SL5 which corresponds to key size thresholds. These key sizes are between 30 bytes and 5 KB depending on the PKI/signature and the security level.
- **2019:** 26 candidates are selected by NIST in February to move to the second stage, including 17 candidates for public key encryption solutions and 9 for signatures²⁷⁷⁶. These include three projects involving Worldline, which until 2019 was part of the Atos Group. For its part, Inria (France) was involved in 7 of the 26 selected projects (Figure 651).

2019 second round candidates, 2020 finalists and 2020 alternate candidates		
BIKE Classic McEliece CRYSTALS-DILITHIUM CRYSTALS-KYBER FALCON FrodoKEM GeMSS HQC LAC	LEDAcrypt LUOV MQDSS NewHope NTRU NTRU Prime NTS-KEM Picnic qTESLA	Rainbow ROLLO Round5 RQC SABER SIKE SPHINCS+ Three Bears

Figure 651: NIST PQC selection in 2019.

- **2020:** results of the third round of NIST candidate selection in July, which kept 15 out of the 26 candidates from the previous round²⁷⁷⁷. This selection includes 7 teams that were finalists for this stage and 8 teams that propose lower quality solutions that need to be further evaluated (aka “alternate candidates”). See their list in the tables below²⁷⁷⁸. It must be noted that the NIST challenge embedded some constraints on intellectual property. Strictly said, NIST doesn’t object to the contestants having some patents related to their submitted protocols. But they favor royalty-free ones and IP licensing without compensation, under reasonable terms (RAND) and conditions that are demonstrably free of unfair discrimination. While this could certainly accelerate their adoptions, this may indirectly favor large cybersecurity vendors who already have an existing customer base.

In Figure 652 and Figure 653 are the participants countries, research teams and vendor organizations per project. It shows in green the solutions that were later selected in July 2022. In red are the two solutions that were found to be defective in 2022.

- **2022:** in January, the Biden administration published a Memorandum and Executive Order 14028 asking all Federal administration to prepare a PQC deployment plan in 2022²⁷⁷⁹. It even required the deployment of PQC solutions for stored and transiting data.
- **2022:** in July, NIST published a first final list of 4 validated PQC standards, 1 for a PKI and 3 for a digital signature²⁷⁸⁰. These are in green in the tables in Figure 652 and Figure 653. In the PQC standardized signatures, Falcon is recommended for those applications requiring smaller signatures than the ones generated by CRYSTALS-Dilithium. SPHINCS+ signatures are based on a different scheme, although more complex to implement. They still plan to standardize other PQC signatures. Just before this choice was published, after some delay, one of the 2020 finalist signatures PQC, Rainbow, was broken by IBM Zurich researchers at the first security level SL1

²⁷⁷⁶ See [NIST Post-Quantum Cryptography - A Hardware Evaluation Study](#), 2019 (16 pages), [Status Report on the First Round of the NIST Post-Quantum Cryptography Standardization Process](#), 2019 (27 pages) and [Recent Developments in Post Quantum Cryptography](#) by Tsuyoshi Takagi, November 2018 (38 slides).

²⁷⁷⁷ See [PQC Standardization Process: Third Round Candidate Announcement](#), July 2020.

²⁷⁷⁸ The Bit-flipping Key Encapsulation (BIKE) was codeveloped by Intel. It’s a public key based encryption. Decoding can be done with 1.3 million operations at 110 MHz on an Intel Arria 10 FPGA in 12 ms.

²⁷⁷⁹ See [Memorandum on Improving the Cybersecurity of National Security, Department of Defense, and Intelligence Community Systems](#), January 2022.

²⁷⁸⁰ See [NIST Announces First Four Quantum-Resistant Cryptographic Algorithms](#), NIST, July 2022.

are AWS, Cisco, Crypto4A Technologies, Cryptosense, InfoSec Global, ISARA Corporation, Microsoft, Samsung SDS, SandboxAQ, Thales and VMware. These players will provide deployment recommendations and their own software and services solutions. Simultaneously, the CISA (Cybersecurity and Infrastructure Security Agency), a US federal agency within the DHS (Department of Homeland Security) announced the creation of a PQC initiative to assist other federal agencies in the deployment of PQCs. Not surprisingly, many PQC and other security vendors are already providing NIST compliant solutions! They provide some encapsulation mechanisms for third-party and/or open source PQCs in their cybersecurity management tools.

In September 2022, the NSA released its Commercial National Security Algorithm Suite 2.0 (CNSA 2.0) Cybersecurity Advisory (CSA) recommending the deployment of PQC solutions for NSS, to notify organizations of future quantum resistant (QR) algorithms requirements for National Security Systems (NSS), the Federal networks distributing classified information. CNSA 2.0 mandates the use of CRYSTALS-Kyber and CRYSTALS-Dilithium for key creation and digital signatures²⁷⁸³.

- **2023:** new vulnerabilities were discovered for PQCs. It deals with code based McEliece cryptosystems²⁷⁸⁴, lattice-based cryptography potential attacks by coherent Ising machines²⁷⁸⁵ and side channel attack on CRYSTAL Dilithium and CRYSTAL Kyber which requires some access to the hardware²⁷⁸⁶. These various papers have not yet worried the PQC community as far as observed. In August 2023, NIST published draft standards for 3 of the 4 candidates selected in July 2022 (22 pages).
- **2025:** NIST's target date for finalizing PQC standards (Figure 654). Deployments of these standards would begin with the rapid deployment of commercial solutions supporting these standards. Fast, for the simple reason that the candidates are often in the standardization consortia. Some of them are already testing their solutions.

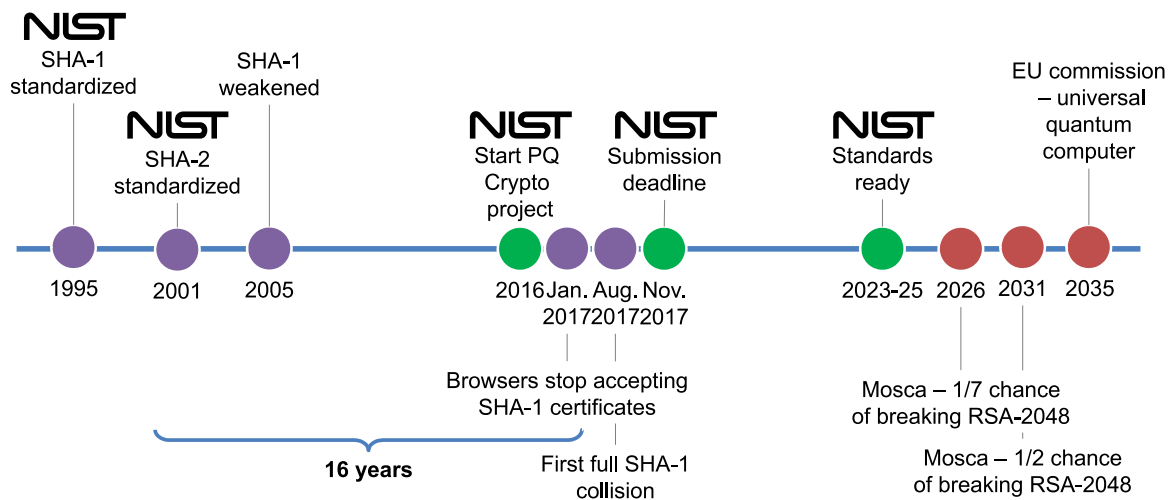


Figure 654: NISQ PQC standardization planning as of 2019.

Source: [Introduction to post-quantum cryptography and learning with errors](#), Douglas Stebila, 2018 (106 slides).

²⁷⁸³ See [Announcing the Commercial National Security Algorithm Suite 2.0](#), NSA, September 2022 (10 pages).

²⁷⁸⁴ See [A new approach based on quadratic forms to attack the McEliece cryptosystem](#) by Alain Couvreur, Rocco Mora and Jean-Pierre Tillich, June 2023 (61 pages).

²⁷⁸⁵ See [Quantum algorithmic solutions to the shortest vector problem on simulated coherent Ising machines](#) by Edmund Dable-Heath et al, April 2023 (15 pages).

²⁷⁸⁶ See [Exploiting Intermediate Value Leakage in Dilithium: A Template-Based Approach](#) by Alexandre Berzati et al, Thales, January-July 2023 (23 pages) and [Breaking a Fifth-Order Masked Implementation of CRYSTALS-Kyber by Copy-Paste](#) by Elena Dubrova, Kalle Ngo and Joel Gärtner, Royal Institute of Technology, Sweden, March 2023 (22 pages).

There are five distinct categories of PQC standards, as follows. I will not be able to technically describe them all except for the first category²⁷⁸⁷. In the last part of this section on cryptography, we will mention the case of some startups that are positioned in this market.

Table 2 - Comparison on encryption schemes (RSA decryption = 1, size in bits, k security strength)

Algorithm	KeyGen (time compared to RSA decrypt)	Decryption (time compared to RSA decrypt)	Encryption (time compared to RSA decrypt)	PubKey (key size in bits to achieve 128 bits of security)	PrivateKey (key size in bits to achieve 128 bits of security)	Cipher text (size of resulting cipher text)	Time Scaling	Key Scaling
NTRU	5	0.05	0.05	4939	1398	4939	k^2	k
McEliece	2	0.5	0.01	1537536	64861	2860	k^2	k^2
Quasi-Cyclic MDPC McEliece	5	0.5	0.1	9857	19714	19714	k^2	k
RSA	50	1	0.01	3072	24,576	3072	k^6	k^3
DH	0.2	0.2	0.2	3072	3238	3072	k^4	k^3
ECDH	0.05	0.05	0.05	256	256	512	k^2	k

Note: in key scaling, the factor log k is omitted.

Figure 655: Comparison of key size of various encryption schemes. Source: [Quantum Safe Cryptography and Security; An introduction, benefits, enablers and challenges](#), ETSI, 2015 (64 pages).

Established companies are not left out. **IBM** announced in August 2019 a system for archiving information on magnetic bank that integrates post-quantum cryptography²⁷⁸⁸ (Figure 656). They use encryption based on Euclidean networks. As it is usually long-term storage, it is necessary to keep the decryption software for the same length of time to avoid ending up with a pile of data that cannot be reused. IBM is also involved in the three consortia that responded to the NIST call for proposals. **Kudelski Security** (Switzerland) is also interested in PQC.

In September 2023 was created the **PQC Coalition** with Microsoft, IBM Quantum, MITRE, PQShield, SandboxAQ and the University of Waterloo with the goal to fasten the standardization, and improve the adoption of PQC in commercial and open source technologies.

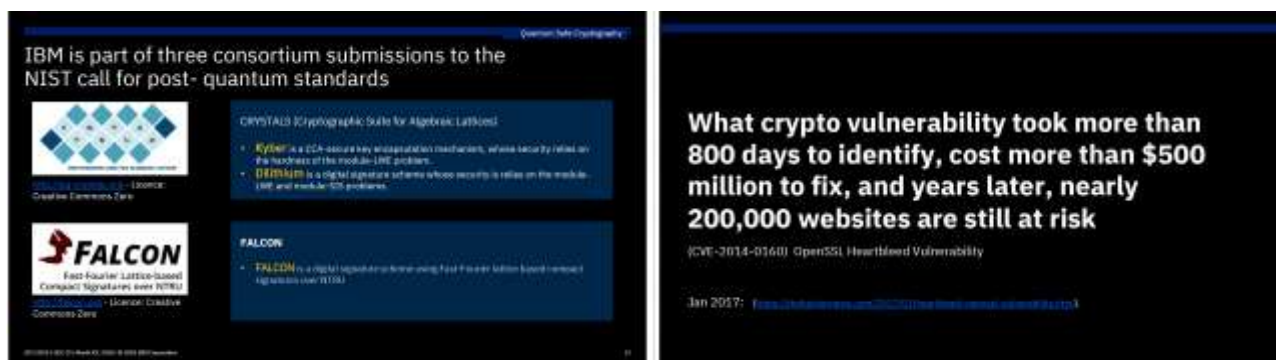


Figure 656: IBM's stance on cybersecurity. They bet on the right horse given their slides in 2019 presented 3 of the 4 2022 NIST finalists! Source: IBM.

²⁷⁸⁷ See in particular [A Guide to Post-Quantum Cryptography](#) by Ben Perez, October 2018.

²⁷⁸⁸ See [IBM's quantum-resistant magnetic tape storage is not actually snake oil](#) by Kevin Coldewey in TechCrunch, August 2019.

Code-based cryptography

This cryptographic system invented in 1978 by **Robert McEliece**, long before Shor's algorithm, has since resisted all cryptanalysis attacks, either classical or designed with quantum algorithms. It is the oldest of the PQC codes which was even a PQC before its time. The method consists in multiplying the data to be encrypted, represented as binary vectors (of length k), by a public and static matrix with more columns than rows ($k \times n$), aka a "binary Goppa code" (Figure 657).

This multiplication generates a vector larger than the original vector (with n bits). We then add a binary vector which adds random errors to the result but of constant value (vector z in schema with a given number of 1s). It is described as a "uniformly random word of weight t ". It is a series of random bits containing a fixed number " t " of 1s called a [Hamming weight](#). The public key sent by the receiver to the transmitter is the matrix \hat{G} and this number of errors t .

The three matrices having created \hat{G} constitute the private key. This matrix \hat{G} is the multiplication of three matrices called SGP for "non Singular", "generator matrix / Goppa code" and "Permutation matrix". The message decoding uses inverses of matrix S, P and G. This is explained in this diagram. The G matrix is by designed crafted to remove the " t " errors introduced in the encryption phase.

code-based cryptography

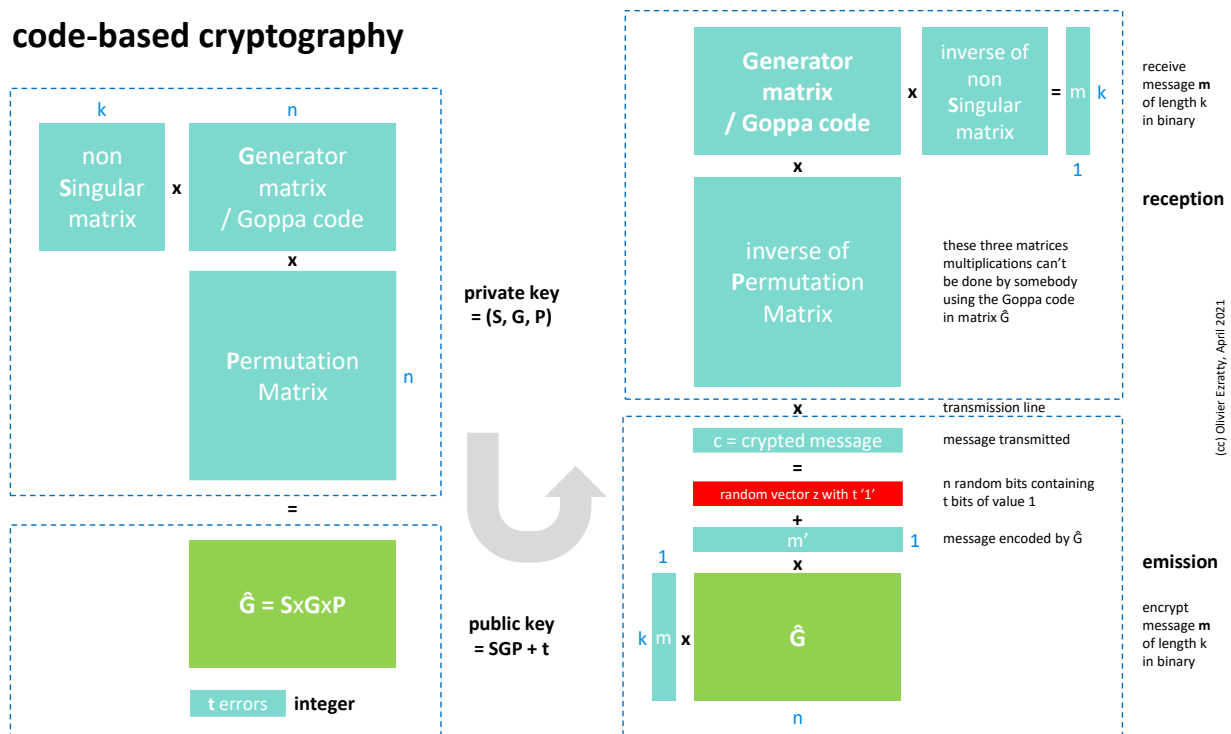


Figure 657: how a code-based PQC key generation works. It is all about mixing and matching many non-square matrices. (cc) Olivier Ezratty, from various sources. 2021.

This system generates public keys one hundred times larger than with RSA, of the order of 80 KB. It generates new vulnerabilities if you reduce their size.

The advantage of the PQC category is its good encryption and decryption speed. It can even be accelerated by using a dedicated FPGA chip²⁷⁸⁹.

²⁷⁸⁹ As seen in [Code-Based Cryptography for FPGAs](#) by Ruben Niederhagen, 2018 (73 slides).

Breaking this kind of encryption is an NP-Hard problem that is currently inaccessible to quantum computing, even though to resist quantum computing it would still require a fairly large key of at least 1 MB²⁷⁹⁰.

Lattice-based cryptography or Euclidean networks

The technique was proposed in 1996 by Miklos Ajtai, a researcher at IBM, and implemented in a public key system in 2005 by Oded Regev with its LWE (Learning With Errors) system and improved since then by many researchers.

The associated literature is inaccessible for non-specialists. It is not easy to understand how this encryption method works despite the elegance of the diagrams that present the notion of Euclidean network like the one in Figure 658²⁷⁹¹. Basically, it is a matrix of dots that allows to locate points according to their coordinates according to a mark of different vectors between the public and private keys.

An error is added to the coordinates generated with the public key vector. Only the coordinate vectors of the private key can be used to retrieve the coordinate of the encrypted value. Initially, it suffered from performance problems, but effective solutions appeared such as [NTRU](#), created in 1998 by Jeffrey Hoffstein, Jill Pipher and Joseph Silverman. The method advantage is to use small public keys. Its decryption is an NP-complete problem inaccessible to quantum computing. On the other hand, it is a method protected by many patents, so it is proprietary and potentially expensive²⁷⁹².

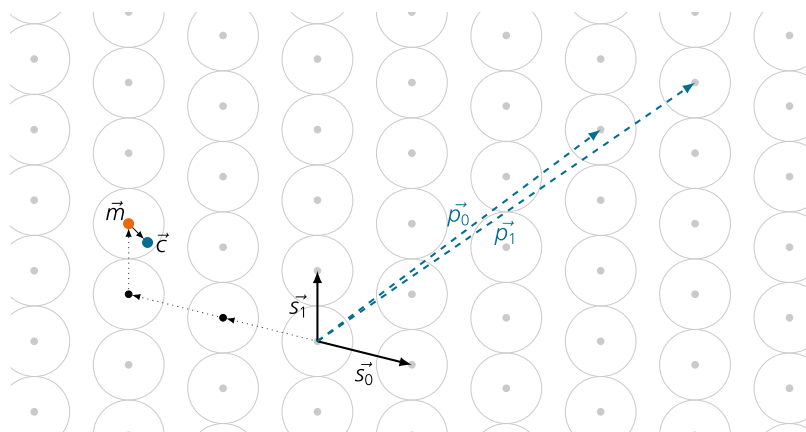


Figure 3.2: Example for lattice-based encryption in a two-dimensional lattice: The secret, well-formed base is $\{\vec{s}_0, \vec{s}_1\}$; the public, "scrambled" base is $\{\vec{p}_0, \vec{p}_1\}$. The sender uses $\{\vec{p}_0, \vec{p}_1\}$ to map the message to a lattice point \vec{m} and adds an error vector to obtain the point \vec{c} . The point \vec{c} is closer to \vec{m} than to any other lattice point. Therefore, the receiver can use the well-formed secret base $\{\vec{s}_0, \vec{s}_1\}$ to easily recover \vec{m} (dotted vectors); this is a hard computation for an attacker who only has the scrambled base $\{\vec{p}_0, \vec{p}_1\}$. For a secure scheme, the dimension of the lattice must be much higher than 2 as in this example.

Figure 658: Euclidean network key generation. Source: [Practical Post-Quantum Cryptography](#) by Ruben Niederhagen and Michael Waidner, 2017 (31 pages).

The PQC **New Hope** solution (CECPQ1) which was tested in 2016 for a few months by **Google** in Chrome and is based on Ring-LWE is in this class of methods. Since 2019, they have moved to CECPQ2 which includes a variant of the HRSS key exchange system that is among the bidders in the NIST competition and the selected in the last wave in the NTRU project²⁷⁹³.

In France, a team from the IRISA-EMSEC laboratory is developing a cryptographic solution based on these Lattice base systems, also named Euclidean networks.

²⁷⁹⁰ The resistance of this method to attacks is documented in [Code-Based Cryptography](#) by Tanja Lange, 2016 (38 slides). For more information, see also [Code Based Cryptography](#) by Alain Couvreur, 2018 (122 slides) and [Some Notes on Code-Based Cryptography](#), a thesis by Carl Löndahl, 2014 (192 pages).

²⁷⁹¹ See [Practical Post-Quantum Cryptography](#) by Ruben Niederhagen and Michael Waidner, 2017 (31 pages).

²⁷⁹² For more information, see the thesis [Lattice-based cryptography: a practical implementation](#) by Michael Rose, 2011 (103 pages), [Lattice-based Cryptography](#) by Daniele Micciancio and Oded Regev, 2008 (33 pages) and the slightly more pedagogical but still incomprehensible [Overview of Lattice based Cryptography from Geometric](#) by Leo Ducas, 2017 (53 slides).

²⁷⁹³ See [Experimenting with Post-Quantum Cryptography](#) by Matt Braithwaite, July 2016 and then [Google starts CECPQ2, a new postquantum key exchange for TLS](#), January 2019.

Damien Stehlé is another specialist of the domain, doing research at ENS Lyon. He participated to the creation of CRYSTALS-Kyber, a finalist in 2020 and 2022 of NIST's PQC competition.

Isogeny-based cryptography

This variant of elliptic curves is even less easy to grasp than all the above. It is a "*morphism of super-imposed group and finite kernel between two elliptic curves*". Piece of cake! The system was proposed in 2006 by Alexander Rostovtsev and Anton Stolbunov and then broken by quantum cryptanalysis by Andrew Childs, David Jao and Vladimir Soukharev. This led David Jao and Luca De Feo (Inria) to propose in 2011 the use of "super-singular" curves to correct this flaw²⁷⁹⁴.

This cryptography is used in Supersingular isogeny Diffie–Hellman key exchange (SIDH).

Software publisher **Cloudflare** has released an open source security solution based on isogenies, CIRCL (Cloudflare Interoperable Reusable Cryptographic Library). It is published on GitHub. Their SIKE key encapsulation solution has been submitted to NIST.

In January 2019, they were among the 17 finalist candidates for public key encryption or key creation solutions²⁷⁹⁵. In 2022, it was broken using a single computer for one hour to 21 hours depending on the key size (from SIKEp434 to SIKEp751).

Hash-based signatures

This post-quantum cryptography other method also pre-dates the very notion of quantum computer imagined by Richard Feynman in 1982. It is based on the work of **Leslie Lamport** of the SRI in 1979 and her single-use hash-based "signatures". The method was then improved by using hash trees also called Merkle trees to sign several messages (Figure 659). It is based on public keys of reduced size, down to 1 kbits.

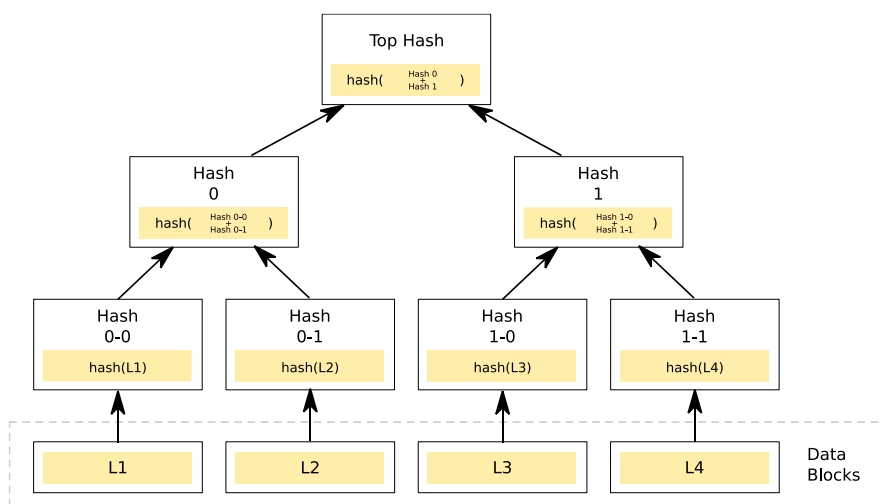


Figure 659: source: [Merkle Tree](#), Wikipedia.

This method is mainly used for electronic signature²⁷⁹⁶.

Multivariate polynomial cryptography

This last group of methods is reminiscent of error correction codes. The public key is a multiplication of several matrices, two of which are linear and one quadratic (with squared values), the three separate

²⁷⁹⁴ More on this with [20 years of isogeny-based cryptography](#) by Luca De Feo, 2017 (84 slides), [An introduction to supersingular isogeny-based cryptography](#) by Craig Costello (Microsoft Research), 2017 (78 slides), [Isogeny Graphs in Cryptography](#) by Luca De Feo, 2018 (73 slides) and [An introduction to isogeny-based crypto](#) by Chloe Martindale, 2017 (78 slides).

²⁷⁹⁵ See [Cloudflare wants to protect the internet from quantum computing](#), June 2019 and [Introducing CIRCL: An Advanced Cryptographic Library](#), June 2019.

²⁷⁹⁶ If you are well versed in mathematics and cryptography, see [Hash-based Signatures: An Outline for a New Standard](#) (12 pages), [Design and implementation of a post-quantum hash-based cryptographic signature scheme](#) by Guillaume Endignoux, 2017 (102 pages) and [SPHINCS: practical stateless hash-based signatures](#), 2015 (30 pages).

matrices constituting the private key used to reconstruct the encrypted message. As a result, the keys are extremely large (Figure 660).

Code breaking these keys is an NP-Hard problem, out of reach of quantum computing. The method dates from 2009 and was obviously then declined in several variants. The public keys are quite large, up to 130 KB (with the HFEBBoost variant)²⁷⁹⁷. This encryption method is also rather used for electronic signatures.

The Rainbow PQC signature selected by NIST in 2020 as a finalist and broken in March 2022 was in that category.

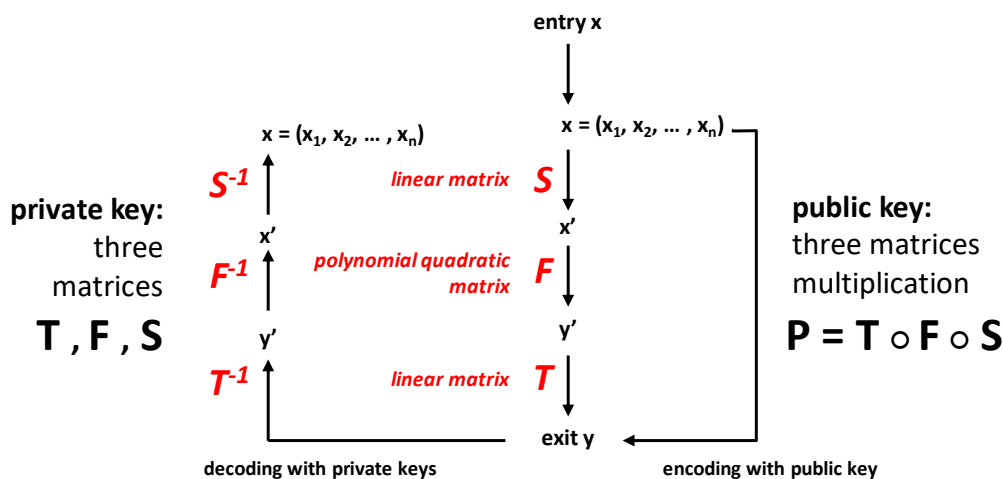


Figure 660: multivariate polynomial cryptography. Source: (cc) Olivier Ezratty, reconstructed from other sources.

We could imagine that QKD (physical protection of key distribution) could be combined with PQC (logical protection of encryption against quantum computer decryption). Actually, not really. QKD is rather dedicated to symmetric keys that assume protection of physical communication between correspondents, whereas PQC relies on public keys that do not need to be protected by QKD because their interception (without QKD) would already be useless to hackers.

However, QKD for key exchange can be combined with PQC for authentication and data encryption. QKD requires authentication, which can be provided upstream by PQC. On the other hand, QKD can be redundant with PQC used for key exchange²⁷⁹⁸.

PQC and blockchains

PQC quantum resistant keys and signatures can be used to protect the whereabouts of blockchains and cryptocurrencies. Many proposals exist and quantum resistant blockchains have already been launched²⁷⁹⁹.

²⁷⁹⁷ Note the contribution of Jacques Stern from the ENS "Post-quantum multivariate-quadratic public key schemes" at PQCRYPTO 2006.

²⁷⁹⁸ To learn more about PQC, see in particular [Post-quantum cryptography - dealing with the fallout of physics success](#) by Daniel Bernstein and Tanja Lange, 2017 (20 pages).

²⁷⁹⁹ See [From Portfolio Optimization to Quantum Blockchain and Security: A Systematic Review of Quantum Computing in Finance](#) by Abha Naik et al, June 2023 (64 pages).

Such a proposal was made in 2023 by LACChain, Quantinuum and Tecnologico de Monterrey. LACChain is a blockchain infrastructure from the Innovation Lab of the South America Inter-American Development Bank IDB Lab that is built using an Ethereum client Hyperledger Besu²⁸⁰⁰. The PQC layer is added on top of the existing blockchain, including Ethereum. It is using Falcon-512 public keys to generate X.509 certificates, Falcon being one of the five PQC selected by NIST in July 2022. It will use the Quantinuum Quantum Origin centralized entropy source that runs on quantum computers.



BTQ Technologies (2021, Taiwan, Canada) is a startup created by Olivier Roussy Newton (CEO) that proposes to secure blockchains with PQC.

Their product line contains PQScale (an efficient quantum resistant blockchain scaling technique based on Falcon signatures) and Kenting, with specialized hardware for zero-knowledge provers. The company has also patented a method at the USPTO to “*secure transmission of confidential information between entities using private cryptographic keys generated from a random vector shared between the entities*”. The company is also proposing to use coarse-grained boson sampling, or CGBS, to implement a proof-of-work scheme for blockchain consensus²⁸⁰¹. The hardware still has to be developed or selected!

In October 2023, they established a partnership with ITRI in Taiwan for the creation of a security chip using their QCIM (Quantum Computation in Memory) technology for managing key generation and computing using Crystal-Kyber that is being standardized by NIST.



ChainMaker (China), *aka* Chang’an Chain, launched in 2021 a 96 core chip that supported 100,000 transactions per second (TPS) in parallel for signature verification and smart contracts processing.

They now support 240 million transactions per second with a 1,000 server cluster. In 2023, they added a PQC to their open sourced Blockchain solution, that was codeveloped with Tsinghua University, Beihang University, Tencent and Baidu.

PQC energy consumption

The broad deployment of PQC solutions across the board will cover various platforms including your regular laptops and smartphones, on top of server and cloud infrastructures. Given the larger related keys that are more complicated to create and reassemble, we could expect that PQC will have its own additional energetic footprint. It indeed seems that high-security levels digital signatures like Falcon PQC costs 65x more than classical signatures generation. On laptop, the energy uptick goes from x37 to x47²⁸⁰². The energy uptick is about the same with elliptic curve PQC²⁸⁰³. Comparisons of energetic footprint have also be done for FPGAs implementing various breeds of PQCs²⁸⁰⁴.

Should we worry about this? It depends on the usage frequency of these PQC to generate keys. They depend on the use case but we can suspect that a relatively small share of usage time on consumer devices is dedicated to keys generation.

²⁸⁰⁰ See [Quantum-resistance in blockchain networks](#) by Marcos Allende et al, Nature Scientific Reports, April 2023 (23 pages).

²⁸⁰¹ See [Proof-of-work consensus by quantum sampling](#) by Deepesh Singh, Peter P. Rohde, Gavin K. Brennen et al, May 2023 (21 pages).

²⁸⁰² See [Mobile Energy Requirements of the Upcoming NIST Post-Quantum Cryptography Standards](#) by Markku-Juhani O. Saarinen, PQShield, April 2020 (8 pages).

²⁸⁰³ See [Energy Efficiency Analysis of Elliptic Curve Based Cryptosystems](#) by Tanushree Banerjee; M. Anwar Hasan et al, IEEE, 2018.

²⁸⁰⁴ See [FPGA Energy Consumption of Post-Quantum Cryptography](#) by Luke Beckwith, Jens-Peter Kaps and Kris Gaj, Georges Mason University, 2022 (10 pages).

Quantum computing cryptography

Quantum cryptography usually refers to the creation of shared symmetric cryptography keys using Quantum Key Distribution (QKD). But a narrow emerging field can play a similar role with using quantum computers to generate cryptographic keys.

Proposals to use quantum computers have been made to generate AES-128 keys in 2018 and quantum one-time pads as early as in 2000. The more recent Quantum Permutation Pad (QPP) has been experimented on IBM QPUs to provide 256 bits of entropy²⁸⁰⁵.

Quantum homomorphic cryptography

Homomorphic cryptography consists in encrypting data that can then pass through a conventional processing in encrypted mode and give an encrypted result that will be decipherable at the end of the processing.

In machine learning and deep learning, this mode of encryption makes it possible to distribute training and inference processing of learning machine models in the cloud without the hacking of the transmitted data revealing the data content that feeds the model or inferences.

The disadvantage of this method is that it does not work with all learning machine models and is very expensive in terms of machine time for data encryption and decryption as well as computation.

Quantum homomorphic encryption is a similar approach for encoding data that will feed a quantum computer in the cloud and then decode the result of the processing. It could help distribute variational algorithms over the cloud^{2806 2807}.

It is also one of the tools for implementing so-called "blind computing" in the cloud, where servers cannot understand and interpret the data they process.

Various algorithms for encrypting quantum gate control programs have been proposed but are not yet commonly used²⁸⁰⁸. Some of the keys can be quantum-transmitted like a QKD. This is one of the conditions to be sure that the server part cannot interpret the processing it performs²⁸⁰⁹.

Quantum telecommunications

QKD-based quantum cryptography is just one application of quantum telecommunications²⁸¹⁰. Quantum telecommunications and quantum networks are about using entanglement resources in various use cases.

Distributed quantum computing, following the example of classical distributed computing architectures that exist on the Internet, in data centers and within supercomputers. Connecting quantum computers is not an easy task. It is not about inputs/outputs or memory and storage sharing like with classical scale-out architectures. It should indeed be possible to convert the qubit state of these

²⁸⁰⁵ See [Quantum Encryption of superposition states with Quantum Permutation Pad in IBM Quantum Computers](#) by Maria Perepechaenko and Randy Kuang, Quantropi, January 2023 (28 pages).

²⁸⁰⁶ See [Eberhard limit for photon-counting Bell tests and its utility in quantum key distribution](#) by Thomas McDermott et al, November 2022 (13 pages).

²⁸⁰⁷ See [Delegated variational quantum algorithms based on quantum homomorphic encryption](#) by Qin Li et al, January 2023 (13 pages).

²⁸⁰⁸ See [Classical Homomorphic Encryption for Quantum Circuits](#) by Urmila Mahadev, 2018 (7 pages), [Quantum Fully Homomorphic Encryption With Verification](#), 2017 (30 pages and slides, 28 slides), [Quantum Homomorphic Encryption: A Survey](#), 2017 (11 pages) et [Quantum homomorphic encryption for circuits of low T-gate complexity](#) by Anne Broadbent et Stacey Jeffery, 2015 (35 pages).

²⁸⁰⁹ As indicated in [On the implausibility of classical client blind quantum computing](#) by Scott Aaronson, Elham Kashefi et al, 2017 (43 pages).

²⁸¹⁰ See the excellent [Quantum internet: A vision for the road ahead](#) by Stephanie Wehner et al, October 2018 (11 pages).

machines into quantum states of photons - usually in the infrared range at 1,550 nm - for optical transmission. Apart from the photon-based systems case, qubits are most often stored in electrons spins or atoms energy states. Hence the numerous efforts to convert these qubits states into transmissible photons, which themselves are not sent from one point to the other but establishing a durable entangled connection between the distance devices and their qubits²⁸¹¹. About the relationship with inter-QPU connectivity and data-transfer speed? Could these connections enable faster data-transfer than classical data links? Well, yes and no. Quantum telecommunications are not about transmitting information faster than light²⁸¹². If it is about transmitting classical data, an inter-QPU or quantum telecom link won't even make things faster. Inter-QPU connectivity is mainly about creating a (much) larger QPU than the separate QPUs. The main resources are entanglement and gate teleportation²⁸¹³. When you have two interconnected QPUs of N qubit each, the Hilbert space managed by the interconnected QPUs has a size of 2^{2N} complex numbers whereas the isolated QPUs handle only $2 * 2^N = 2^{N+1}$ complex numbers.

But in the end, when reading out the qubits in these isolated or consolidated QPUs, you don't capture more than 2N classical bits. Teleportation may be useful to teleport at a very fast rate an entangled state from one location to another or to create two qubit gates across distant QPUs using the gate teleportation technique²⁸¹⁴. Let's say that while the data is quantum, interconnect and teleportation can bring some speedup advantage. This could be the case when connecting quantum sensors and quantum computers.

Still, some researchers are studying distributed quantum computing architectures that are not based on creating a large virtual QPU but rely more on partitioning QPU tasks²⁸¹⁵.

Blind and verifiable delegated computing is a variation of the distributed quantum computing scenario. It involves a small quantum computer that would delegate some tasks to a larger one in a secured manner²⁸¹⁶. This is the concept of "blind computing" associated to the BFK protocol created in 2009 by Anne Broadbent, Joe Fitzsimons and Elham Kashefi²⁸¹⁷. The principle consists in preparing computation in a quantum way at the starting point and sending it by a quantum link by teleportation to the remote quantum computer. It is a bit the quantum equivalent of the homomorphic encryption used in distributed machine learning^{2818 2819}.

²⁸¹¹ See [Distributed Quantum Computing: A path to large scale quantum computing](#) by Stephen DiAdamo, August 2021.

²⁸¹² Let's remind at least two key explanations: first, entanglement and nonlocality is about having a correlation between two distant quantum objects values when measured sequentially, but this value is random by essence. You can't set one quantum value at one end (Alice) and then measure it at the other location (Bob's). You just decide to measure random values at both end that happen to be correlated. On a more practical reason, the teleportation algorithm that can send a qubit state to another location with using entanglement needs two classical communications links. So, we're stuck with the speed of light. See [No, We Still Can't Use Quantum Entanglement To Communicate Faster Than Light](#) by Ethan Siegel, February 2020.

²⁸¹³ See [S-QGPU: Shared Quantum Gate Processing Unit for Distributed Quantum Computing](#) by Shengwang Du et al, September 2023 (8 pages) which makes a proposal to mutualize gate teleportation resources.

²⁸¹⁴ See [Near-Term Distributed Quantum Computation using Mean-Field Corrections and Auxiliary Qubits](#) by Abigail McClain Gomez et al, Nvidia and Harvard, September 2023 (44 pages).

²⁸¹⁵ See [Towards Distributed Quantum Computing by Qubit and Gate Graph Partitioning Techniques](#) by Marc Grau Davis, Joaquin Chung, Dirk Englund and Rajkumar Kettimuthu, MIT, Doe Argonne and Brookhaven Labs, October 2023 (7 pages).

²⁸¹⁶ See [Equivalence in delegated quantum computing](#) by Fabian Wiesner, Jens Eisert and Anna Pappa, June 2022 (43 pages).

²⁸¹⁷ See [Universal blind quantum computation](#) by Anne Broadbent, Joseph Fitzsimons and Elham Kashefi, 2008 (20 pages) and the [associated presentation](#) (25 slides), [Blind quantum computing can always be made verifiable](#) by Tomoyuki Morimae, 2018 (5 pages), [Experimental Blind Quantum Computing for a Classical Client](#), 2017 (5 pages) and [Blind Quantum Computation](#) by Charles Herder (5 pages).

²⁸¹⁸ See [Applying the Quantum Error-correcting Codes for Fault-tolerant Blind Quantum Computation](#) by Qiang Zhao and John C.S. Lui, January 2023 (13 pages).

²⁸¹⁹ See [Verifiable blind quantum computing with trapped ions and single photons](#) by P. Drmota, Elham Kashefi et al, May 2023 (15 pages).

Quantum electronic signatures authenticating classic messages. They are transferable to third parties, non-repudiable and non-forgable.

Quantum computing cryptography to generate symmetric keys including quantum permutation pads.

Distributed quantum sensing which could be useful when it makes sense to consolidate quantum states from various quantum sensors to improve their precision²⁸²⁰, like with telescopes interferometry, and to protect their content²⁸²¹. It could also add the connection between quantum computers and sensors with quantum data coming out of sensors being directly used as a vector state by a quantum computer, enabling faster data loading than with going through some costly classical data loading.

Clock synchronization which has been tested in the early 2000s and is useful for telecommunication networks and GPS operations²⁸²².

Anonymous data transmissions, allowing two nodes in a quantum network to communicate with each other without one node being able to identify the other node and also without the other nodes not involved in the protocol being able to identify the sender and the recipient. The communications leave no trace and are therefore not auditable. This replaces traditional anonymization proxies. It can be used as a basis for distributed processing, coupling this with classical or quantum data encryption. It is a means of ensuring the anonymization of the transmission of data such as survey or health data.

Quantum Secure Direct Communication (QSDC) which is a keyless quantum communication approach where secure information is directly sent from Alice to Bob without using QKD protocols and data encryption/decryption cycles, first proposed in 2002^{2823 2824}. It could operate with discrete and continuous variables optical quantum communications and not necessarily require classical communication channels like with QKD²⁸²⁵. Data is sent as quantum states prepared by Alice with various properties of photons (polarization or others), sent through an optical fiber or free space quantum channel, and received and measured by Bob. Like with QKD, any eavesdropping attempts by an Eve would disturb the transmitted quantum states and would be detected by Bob.

Quantum money that applies a concept of Stephen Wiesner (1942-2021, Israeli) from 1970, and improved in 1983. It is based on tokens of verifiable integrity that can only be used once²⁸²⁶.

Quantum pseudotelepathy, a quantum entanglement conceptual use case where different users perform entangled particles measurements in a coordinated way, which yield correlated results which look like telepathic communication between them but are not^{2827 2828}. Thought experiments of

²⁸²⁰ See one example of quantum sensors interconnect proposal in [An elementary quantum network of entangled optical atomic clocks](#) by B. C. Nichol et al, Nature, [November 2021](#)-September 2022.

²⁸²¹ See one example with [Distributed quantum sensing with optical lattices](#) by Jose Carlos Pelayo, Karol Gietka and Thomas Busch, Okinawa Institute of Science and Technology Graduate University, August 2022 (7 pages).

²⁸²² See [Distant clock synchronization using entangled photon pairs](#) by Alejandra Valencia et al, 2004 (10 pages).

²⁸²³ See [Secure communication with a publicly known key](#) by Almut Beige et al, November 2001-May 2002 (14 pages).

²⁸²⁴ See [Two-step quantum direct communication protocol using the Einstein-Podolsky-Rosen pair block](#) by Fu-Guo Deng, Gui Lu Long, and Xiao-Shu Liu, 2003, PRA (8 pages).

²⁸²⁵ See [Practical quantum secure direct communication with squeezed states](#) by Iris Paparella et al, June 2023 (18 pages).

²⁸²⁶ A recent proposal of quantum money co-authored by Peter Shor is in [Publicly verifiable quantum money from random lattices](#) by Andrey Boris Khesin, Jonathan Z. Lu and Peter Shor, July 2022 (15 pages). It's still highly theoretical.

²⁸²⁷ See [The cost of exactly simulating quantum entanglement with classical communication](#) by Gilles Brassard, Richer Cleve and Alain Tapp, 1999 (9 pages).

²⁸²⁸ See [Quantum Pseudo-Telepathy](#) by Gilles Brassard, Anne Broadbent and Alain Tapp, 2004 (31 pages).

pseudotelepathy are implemented with guessing games like the nonlocal version of Mermin-Peres magic square game, with Alice and Bob cooperatively filling in a 3×3 magic square²⁸²⁹.

Temporal entanglement, that can be created between different quantum states in quantum networks that have distinct time intervals. It is a feature of quantum networks using memory-based repeaters and entanglement swapping where the future state of the system depends on its current and past states, due to the delays of entanglement distribution²⁸³⁰.

Quantum position verification protocols use QKD is used to use a geographical location as a credential to implement various cryptographic protocols²⁸³¹.

Detecting Extra-Terrestrial life. Well, sort of. That's the plan from SETI who wants to analyze "quantum communications" coming from exoplanets, which would bear some differentiated signature. One can wonder how such communications could be sorted out from the planet's star random photon streams, but who knows²⁸³².

In that section, we will first look at the various ways to interconnect quantum computers at the physical level. So far, there are three known approaches to connect quantum computers: microwaves, photons and shuttling electrons or ions. In that space, there's a clear difference in photon-based solutions which could scale at a large level, leveraging fiber optics telecommunication infrastructures and other options (microwave, shuttling electrons or ions) which are by design "on premise" and won't rely on telecommunications infrastructures²⁸³³.

Then, we'll look at quantum Internet and telecommunications architectures on a global basis and some related software aspects.

Microwaves interconnect

This type of QPUs interconnect is adapted to qubits that are driven by microwaves, so in order of priority, superconducting, silicon spin and to some extent trapped ions and cold atoms qubits. So far, it has been investigated mostly with superconducting qubits. This technology is adapted to relatively short range connectivity, on a same-site basis, and could have a high efficiency.

Superconducting qubits belong to the field of circuit quantum electrodynamics (cQED) and are driven by microwave pulses. Microwaves are used for qubit readout, so we know how to convert the state of a qubit into microwaves, which are in the 4-8 GHz range. These microwaves can also be used to establish short distance entanglement between pairs of qubits of different QPUs.

The first way to implement this is to connect qubit chips next to the other in chiplets. This was tested by NIST and is planned to be adopted by IBM²⁸³⁴. In 2023, a joint China and USA team tested a short range connection between five superconducting qubit chips using low-loss aluminum cables with relatively good fidelities (as shown in Figure 661)²⁸³⁵.

²⁸²⁹ See [Experimental Demonstration of Quantum Pseudotelepathy](#) by Jia-Min Xu et al, August 2022 (11 pages).

²⁸³⁰ See [Fundamental Limitations on Communication over a Quantum Network](#) by Junjing Xing et al, June 2023 (78 pages).

²⁸³¹ See [Single-qubit loss-tolerant quantum position verification protocol secure against entangled attackers](#) by Llorenç Escolà-Farràs et al, December 2022 (33 pages).

²⁸³² See [We could detect alien civilizations through their interstellar quantum communication](#) by Matt Williams, April 2021 referring to [Searching for interstellar quantum communications](#) by Michael Hippke, April 2021 (14 pages).

²⁸³³ See [Development of Quantum InterConnects for Next-Generation Information Technologies](#) by David Awschalom, Sophia E. Economou, Dirk Englund, Liang Jiang, Mikhail D. Lukin, Christopher Monroe, Jelena Vučković, Ronald Walsworth et al, 2019 (31 pages) which positions well different QPU interconnect technologies.

²⁸³⁴ See [Modeling Short-Range Microwave Networks to Scale Superconducting Quantum Computation](#) by Nicholas LaRacuenta et al, NIST, January 2022-January 2023 (23 pages).

²⁸³⁵ See [Low-loss interconnects for modular superconducting quantum processors](#) by Jingjing Niu et al, February 2023 (28 pages).

Longer distance connections are also tested. It was first realized by an international team led by the University of Chicago in 2020 with two nodes of three superconducting qubits, each arranged as an entangled GHZ state. They managed this entanglement with microwaves over a distance of one meter on a cryogenic niobium-titanium coax cable. The entanglement transmission was done with a fidelity of 65% and 91% for a single qubit transmission²⁸³⁶.

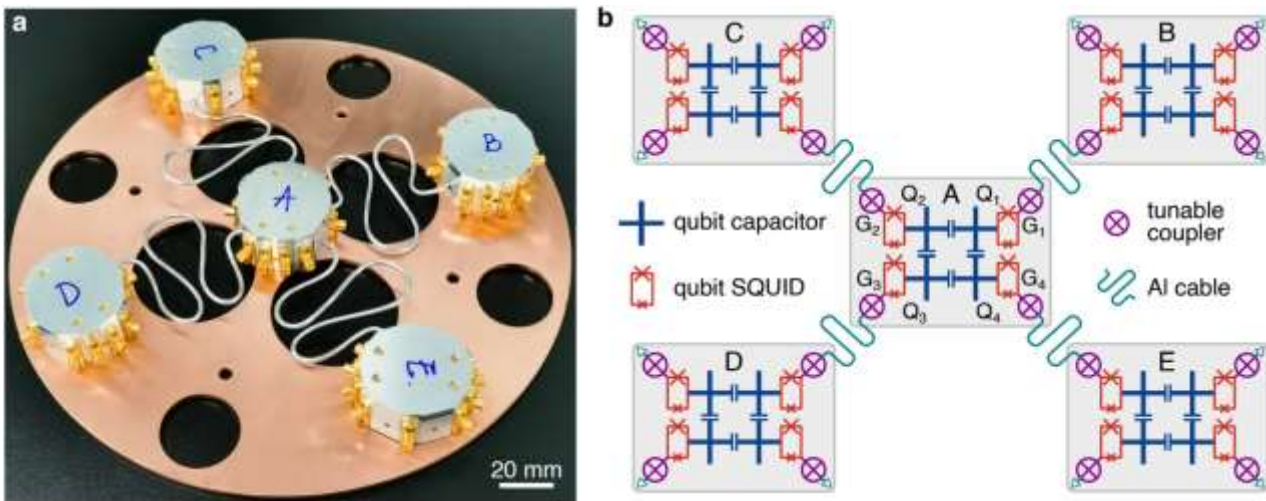


Figure 661: Source: [Low-loss interconnects for modular superconducting quantum processors](#) by Jingjing Niu et al, February 2023 (28 pages).

Later in 2020, an ETH Zurich and University of Sherbrooke team led by Andreas Wallraff connected several superconducting units using²⁸³⁷. The two processing units were separated by a 5-meter cryogenic link (pictured in Figure 662). A similar experiment with a Bell test was later done in 2022 over 30 m²⁸³⁸. Similar distances were experimented by a team led by Technische Universität München VTT in 2023²⁸³⁹.



Figure 662 above and below, ETH Zurich 5-meter cryogenic microwave link. Source: [Microwave Quantum Link between Superconducting Circuits Housed in Spatially Separated Cryogenic Systems](#) by Paul Magnard, Alexandre Blais, Andreas Wallraff et al, PRL, December 2020 (13 pages).

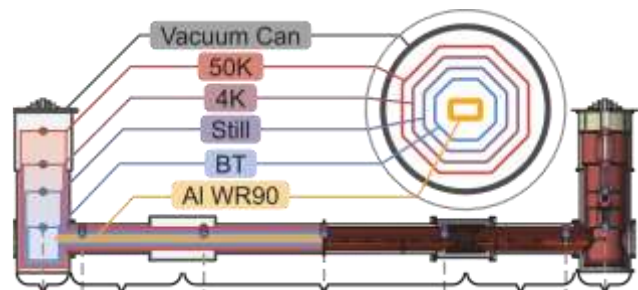


Figure 663: source: [Experimental quantum teleportation of propagating microwaves](#) by K. G. Fedorov et al, December 2021 (7 pages).

²⁸³⁶ See [Deterministic multi-qubit entanglement in a quantum network](#) by Youpeng Zhong, Audrey Bienfait (ENS Lyon), et al, November 2020 on arXiv and February 2021 in Nature (38 pages).

²⁸³⁷ See [Microwave Quantum Link between Superconducting Circuits Housed in Spatially Separated Cryogenic Systems](#) by Paul Magnard, Alexandre Blais, Andreas Wallraff et al, PRL, December 2020 (13 pages). Paul Magnard now works for Alice&Bob.

²⁸³⁸ See [Loophole-free Bell inequality violation with superconducting circuits](#) by Simon Storz, Andreas Wallraff, Alexandre Blais et al, Nature, May 2023 (8 pages).

²⁸³⁹ See [Cryogenic microwave link for quantum local area networks](#) by M. Renger et al, Technische Universität München, VTT, Oxford Instruments, Rohde & Schwartz, August 2023 (25 pages).

A China team extended the record to 64 m, enabling deterministic quantum state teleportation and quantum gates across the link with $94.2 \pm 0.6\%$ fidelity for EPR pairs²⁸⁴⁰. It is interesting but wouldn't scale well with a large number of such connections.

In an experiment published in 2021, a team from the TUM (Munich), RIKEN (Japan) and Aalto University (Finland) tested a microwave entangling connection of 45 cm between two superconducting qubits. They used two microwave parametric amplifiers (JPA) to create a pair of entangled and squeezed microwave photons²⁸⁴¹ (schema in Figure 663). The resulting teleportation fidelity was 69%. Still not enough to be of practical use.

Now, what is needed is way more sophisticated. Connecting different qubit chips would require connecting at least one qubit of nearby chips to each other. This would create a limited connectivity between the chips.

The example using a simple hexagonal qubit topology typical of IBM's superconducting chips would require the connections in red in Figure 664. But this is for 27 qubit chips, not thousand qubit chips²⁸⁴²!

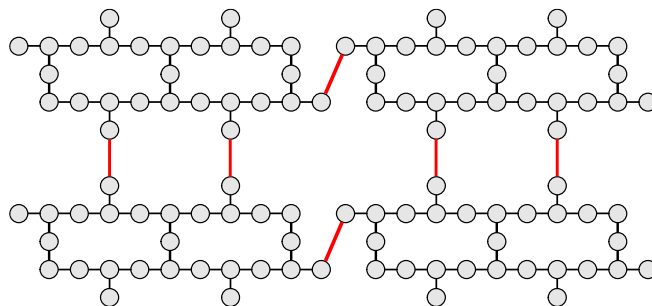


Figure 664: Source: [Short-Range Microwave Networks to Scale Superconducting Quantum Computation](#) by Nicholas LaRacuente et al, January 2022 (22 pages).

That's also what a team from the Universities of Pittsburgh and Illinois with ENS Paris proposed in 2021, using a microwave router and a SWAP gate to connect several chips²⁸⁴³ (Figure 665).

Another way would be the creation of more complicated many-to-many connectivity. If you have for example two superconducting chips ala Google Sycamore with, let's say, $N \times N$ qubits, you will first need to create N connections between the edge of the first chip and the edge of the nearby second chip. Then, with entanglement sharing, you will have to make sure you can create two-qubit gates with these nearby connected qubits²⁸⁴⁴.

What gate would be mandatory to enable a real scale-out? At least SWAP gates^{2845 2846}.

²⁸⁴⁰ See [Deterministic quantum teleportation between distant superconducting chips](#) by Jiawei Qiu et al, February 2023 (33 pages).

²⁸⁴¹ See [Experimental quantum teleportation of propagating microwaves](#) by K. G. Fedorov et al, December 2021 (7 pages).

²⁸⁴² See [Short-Range Microwave Networks to Scale Superconducting Quantum Computation](#) by Nicholas LaRacuente et al, January 2022 (22 pages).

²⁸⁴³ See also [A modular quantum computer based on a quantum state router](#) by Chao Zhou, Matthieu Praquin et al, Universities of Pittsburgh and Illinois and ENS Paris, September 2021 (11 pages). With Praquin from ENS Paris. About linking transmon qubits with microwaves, starting with implementing SWAP gates between 4 single-qubit modules with relatively slow gates (750 ns). Quote: "For atomic scale qubits communicating using optical frequency states, it is infeasible to couple photons into a communication channel with very high efficiency. This loss of information precludes light from simply being transferred from module to module, instead one must herald instances in which transmission is successful". This doesn't bode well for photons interconnect.

²⁸⁴⁴ See [Quantum transfer of interacting qubits](#) by Tony J. G. Apollaro et al, May 2022 (24 pages) which addresses this point of N qubits connectivity between nearby chipsets.

²⁸⁴⁵ See [A modular quantum computer based on a quantum state router](#) by Chao Zhou et al, April 2022 (21 pages) with all-to-all couplings among four independent quantum modules of superconducting qubits. They handle full- i SWAP time of 760 ns and average inter-module gate fidelity of 97%.

²⁸⁴⁶ and [Co-Designed Architectures for Modular Superconducting Quantum Computers](#) by Evan McKinney et al, University of Pittsburgh, May 2022 (14 pages) which uses a superconducting nonlinear asymmetric inductive element (SNAIL) modulator and \sqrt{i} SWAP gates.

You'd need to adopt a full stack approach, from the qubits, the QPUs interconnect and all related software concerns²⁸⁴⁷.

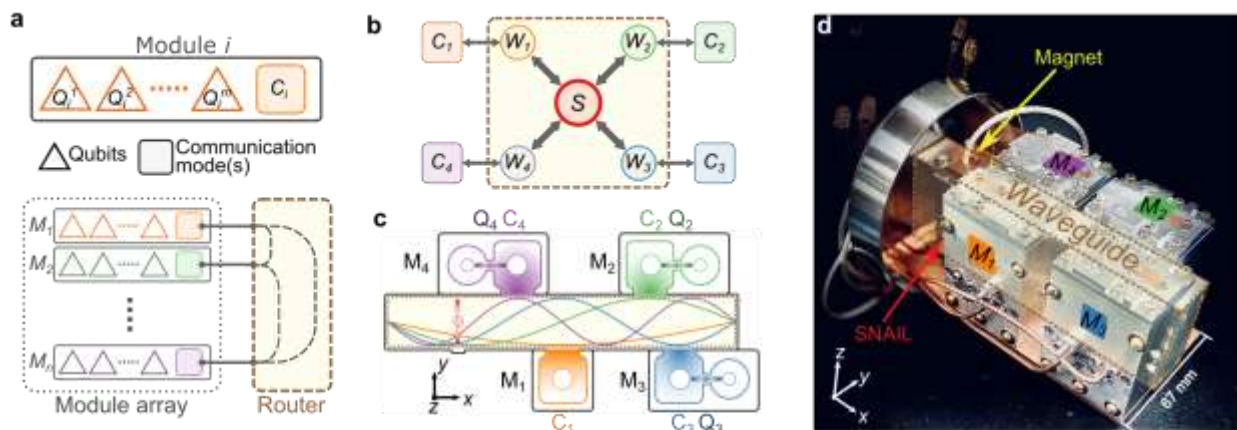


Figure 1. Schematic representation and picture of the modular quantum computer device (a) Basic structure of our modular quantum computer, in which a number of quantum modules are connected via their communication modes to a quantum state router. (b) Coupling scheme between the router and four communication modes. The brown dashed square represent the router with four waveguide modes ($W_1 - W_4$) and a SNAIL (S). Each waveguide mode is dispersively coupled to a single communication cavity mode ($C_1 - C_4$). (c) Schematic drawing of the full system consisting four modules and the central quantum state router. The colored curves inside the router represent the E (electric) field distribution of the first four waveguide $TE_{10,n}$ ($n = 1, 2, 3, 4$) eigenmodes. The SNAIL chip (represented in red) is placed at a location where it couples to all the waveguide modes being used. Each module (for M_2 to M_4) consists of a qubit ($Q_2 - Q_4$), a communication cavity ($C_2 - C_4$) and a readout cavity (for module M_1 the qubit has been omitted). (d) Photograph of the assembled device.

Figure 665: Source: [A modular quantum computer based on a quantum state router](#) by Chao Zhou, Matthieu Praquin et al, Universities of Pittsburgh and Illinois and ENS Paris, September 2021 (11 pages).

Various other superconducting qubit to other quantum states have been reported, like:

- Photonic coupling between superconducting qubits within the chip²⁸⁴⁸.
- Microwave photons and optical light photons conversion²⁸⁴⁹ or entanglement²⁸⁵⁰.
- Opto-Electro-Mechanical Modulator (OEMM) for RF-to-optical coupling²⁸⁵¹.
- Coupling between cold atoms and a superconducting qubit resonator^{2852 2853}.

Microwaves-based interconnect is also investigated to create quantum link between electron spin-based qubits²⁸⁵⁴.

²⁸⁴⁷ See [Will Quantum Computers Scale Without Inter-Chip Comms? A Structured Design Exploration to the Monolithic vs Distributed Architectures Quest](#) by Santiago Rodrigo et al, 2020 (6 pages) which makes some fully-stack architecture proposals. See also [Towards a distributed quantum computing ecosystem](#) by Daniele Cuomo et al, University of Naples, Italy, March 2020 (6 pages).

²⁸⁴⁸ See [Dynamically Reconfigurable Photon Exchange in a Superconducting Quantum Processor](#) by Brian Marinelli, Irfan Siddiqi et al, MIT Lincoln Lab, Berkeley, Anyon Computing and LBNL, March 2023 (22 pages).

²⁸⁴⁹ See [Continuous wideband microwave-to-optical converter based on room-temperature Rydberg atoms](#) by Sebastian Borówka et al, Nature Photonics, October 2023 (12 pages).

²⁸⁵⁰ See [Entangling microwaves with optical light](#) by Rishabh Sahu et al, TU Wien, January 2023 (28 pages).

²⁸⁵¹ See [Low Noise Opto-Electro-Mechanical Modulator for RF-to-Optical Transduction in Quantum Communications](#) by Michele Bonaldi et al, July 2023 (14 pages).

²⁸⁵² See [Continuous wideband microwave-to-optical converter based on room-temperature Rydberg atoms](#) by Sebastian Borówka et al, February 2023 (11 pages).

²⁸⁵³ See [Quantum-enabled millimetre wave to optical transduction using neutral atoms](#) by Aishwarya Kumar et al, Nature, March 2023 (28 pages), [arXiv](#).

²⁸⁵⁴ See [Resonant microwave-mediated interactions between distant electron spins](#) by F. Borjans, Jason Petta et al, Nature, December 2019 (6 pages) and [Strong coupling between a photon and a hole spin in silicon](#) by Cécile X. Yu, Simon Zihlmann, José C. Abadillo-Uriel, Vincent P. Michal, Nils Rambal, Heimanu Niebojewski, Thomas Bedecarrats, Maud Vinet, Etienne Dumur, Michele Filippone, Benoit Bertrand, Silvano De Franceschi, Yann-Michel Niquet and Romain Maurand, June 2022 (6 pages).

In August 2021, **AMD** published a patent designed to handle a local scale-out capacity for quantum computers, with a teleportation-based multi-SIMD architecture (shown in Figure 666). SIMD stands for “Single Instruction Multiple Data” and is heavily used in parallel classical hardware architectures like vector processors or tensor processors and GPUs. Here, teleportation would be used to handle coordination between several quantum processing units and reduce both the number of qubits and quantum gates needed to run an algorithm. Unfortunately, this patent doesn’t describe in any way a real quantum process, contains no physics, no mathematics, no compiling trick, no timing analysis and nothing about teleportation implementation and about any quantum algorithm parallelization. It also mentions a “global memory” like if creating qubits memory was some standard off-the-shelf technology. On top of that, none of the patent holders seem to have a quantum computing background and they never published any quantum-related paper visible on arXiv²⁸⁵⁵.

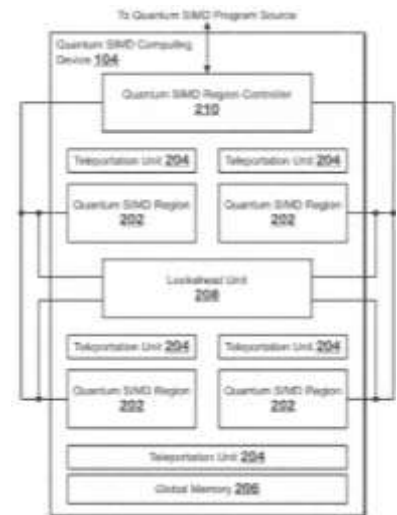


Figure 666: AMD's weird patent.

This has the flavor of a PR-driven approach that only a few scientists can fact-check, if not of a patent-troll. And it unfortunately worked²⁸⁵⁶!

In June 2022, **Huawei** also published a patent in China numbered [CN114613758A](#) related to the production of quantum computing chips and their scale-out, shown in Figure 667. It describes M subchips of N qubits²⁸⁵⁷. In the provided schematics, you can see four qubits subchips (20), four coupling structures (30) and a central one with no connectivity with the others that is the cavity mode suppression structure of undetermined nature, shape and form (40). The asserted benefit from this architecture is resilience to manufacturing defects more than a scale-in architecture. These have undetermined internal structures and connections, nor any physical or experimental data attached. This wouldn’t pass any scientific paper peer-reviewing process! This also looks like a patent troll.

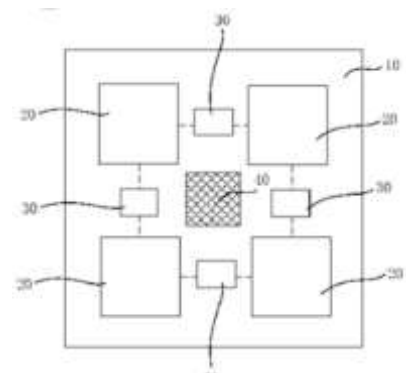


Figure 667: Huawei also weird patent.

Photonic interconnect

The most generic way to interconnect QPU, particularly over arbitrary distance, would be with photons and fiber optics. It requires a couple things like creating deterministic or heralded sources of entangled photons connecting qubits, qubits-to-photon or microwave-to-photon quantum state conversion^{2858 2859}, photons conversions to telecoms wavelengths using for example trapped ions or

²⁸⁵⁵ See [New AMD Patent Proposes Teleportation to Make Quantum Computing More Efficient](#) by Francisco Pires, August 2021.

²⁸⁵⁶ See for example [AMD patent reveals revolutionary teleportation-based quantum computer](#) by Bogdan Solca, Notebook Check, August 2021.

²⁸⁵⁷ See [Huawei publishes patents related to Quantum chips and Quantum computers](#) by Amit, Huawei, June 2022.

²⁸⁵⁸ See [Large-bandwidth Transduction Between an Optical Single Quantum Dot Molecule and a Superconducting Resonator](#) by Yuta Tsuchimoto, Andreas Wallraff, Martin Kroner et al, PRX Quantum, 2022 (13 pages).

²⁸⁵⁹ See [Coherent control of a superconducting qubit using light](#) by Hana K. Warner, Liang Jiang et al, Harvard, Rigetti, Hyperlight Corporation, Caltech, MIT and University of Chicago, October 2023 (23 pages).

nonlinear crystals, aka QFC for Quantum Frequency Conversion^{2860 2861 2862} and, most of the time, some form of quantum memory for synchronization purpose.

It seems better adapted to either photon qubits (which don't need any conversion) and qubits that are controlled by photons in the visible or near visible spectrum like cold atoms, trapped ions and NV centers²⁸⁶³. Other types of qubits require some conversion, usually between the microwave and visible/IR photo regimes to enable photon mediated remote entanglement²⁸⁶⁴.

An experiment of distant entanglement between atoms in two neutral atoms QPUs was achieved²⁸⁶⁵. Trapped ions can also be interconnected with photons. It is the main scale-out plan for startups like IonQ^{2866 2867}. A European team succeeded in interconnecting trapped ions with photons over a distance of 230 m in 2022²⁸⁶⁸. Silicon qubits use the spin of one or two electrons. Spin-to-charge and charge-to-photon conversions can then be performed.

At some point, as presented in Figure 668, interconnect architectures may someday mix various techniques, with short-range interconnect techniques using microwaves and longer range techniques based on photons entanglement.

Some photon-based interconnect experiments have also been done with silicon spin qubits²⁸⁶⁹. Another option to interconnect superconducting qubits is to entangle them first with NV centers spin qubits which themselves are then easier to interconnect with photons²⁸⁷⁰. Another one is to couple a SiV vacancies electron spin acting as a communication qubit to a ²⁹Si nuclear spin acting as a memory qubit²⁸⁷¹.

Other researchers are looking for ways to encode quantum information differently in transmitted photons. Instead of using a classical polarization encoding, researchers from Caltech experimented quantum teleportation of time-bin qubits (with "time of arrival" encoding) using a standard telecommunication wavelength of 1,536.5 nm with an average success superior to 90%²⁸⁷².

²⁸⁶⁰ See [Low noise quantum frequency conversion of photons from a trapped barium ion to the telecom O-band](#) by Uday Saha et al, University of Maryland, May 2023 (16 pages).

²⁸⁶¹ See [Quantum frequency conversion of memory-compatible single photons from 606 nm to the telecom C-band](#) by Nicolas Maring, Dario Lago-Rivera et al, IFCO, 2021 (7 pages).

²⁸⁶² See [Low-noise quantum frequency conversion in a monolithic bulk ppKTP cavity](#) by Felix Mann et al, April 2023 (7 pages) which is about converting NV center 637 nm photon to telecom wavelengths using a Periodically poled potassium titanyl phosphate (ppKTP) based on KTiOPO₄, a nonlinear optical crystal.

²⁸⁶³ In 2021, a team from Qutech and TU Delft connected three NV centers qubits quantumly in an entangled GHZ state, beyond the traditional two nodes existing experiments. See [Realization of a multi-node quantum network of remote solid-state qubits](#) by Matteo Pompil, Sophie Hermans, Stephanie Wehner et al, February 2021 (28 pages).

²⁸⁶⁴ See [Tutorial: Remote entanglement protocols for stationary qubits with photonic interfaces](#) by Hans K.C. Beukers, Dirk Englund, Ronald Hanson et al, QuTech and MIT, October 2023 (27 pages).

²⁸⁶⁵ See [Quantum networks with neutral atom processing nodes](#) by Jacob P. Covey et al, April 2023 (13 pages).

²⁸⁶⁶ See [Large Scale Modular Quantum Computer Architecture with Atomic Memory and Photonic Interconnects](#) by Chris Monroe, July 2013 (16 pages).

²⁸⁶⁷ See [A high-fidelity quantum matter-link between ion-trap microchip modules](#) by M. Akhtar et al, Nature, March 2022 (8 pages).

²⁸⁶⁸ See [Entanglement of trapped ion qubits separated by 230 meters](#) by V. Krutyanskiy, Nicolas Sangouard, Tracy Northup, August 2022 (22 pages) with a fidelity of 88% but a very low success rate of 4×10^{-5} .

²⁸⁶⁹ See for example [First chip-to-chip quantum teleportation harnessing silicon photonic chip fabrication](#) by the University of Bristol, December 2019 which refers to [Chip-to-chip quantum teleportation and multi-photon entanglement in silicon](#) by Daniel Llewellyn et al, 2019 (48 pages). And the exaggerated version in [The first "quantum teleportation" between two computer chips](#) by Valentin Cimini, December 2019.

²⁸⁷⁰ See [Anisotropic rare-earth spin ensemble strongly coupled to a superconducting resonator](#) by S. Probst et al, 2021 (7 pages).

²⁸⁷¹ See [Robust multi-qubit quantum network node with integrated error detection](#) by Pieter-Jan Stas, Mikhail D. Lukin et al, Harvard, July 2022 (24 pages).

²⁸⁷² See [Teleportation Systems Toward a Quantum Internet](#) by Raju Valivarthi et al, Caltech, 2020 (16 pages).

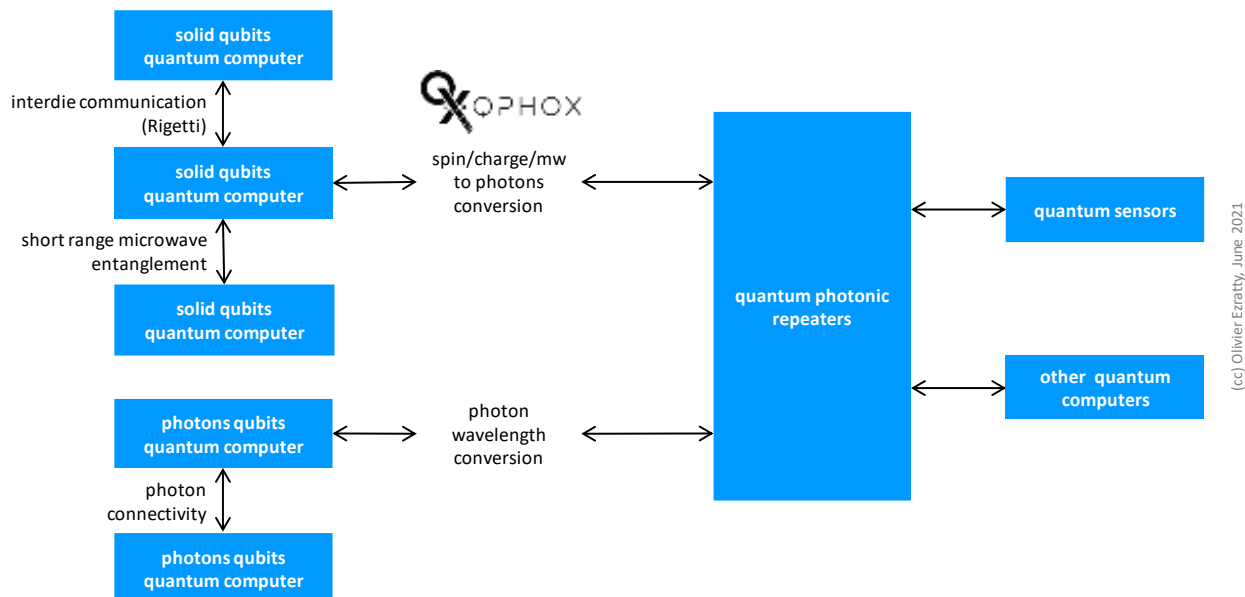


Figure 668: various interconnect architectures. (cc) Olivier Ezratty, 2022.

At last, tests were done of various heterogenous conversions between DV (direct variable) and CV (continuous variable) qubits in an all-optical setup²⁸⁷³ and to implement a photon to atom SWAP gate²⁸⁷⁴.



Given it is still the dominant architecture, superconducting to photons connectivity is an intense field of research. In that case, microwaves are converted to another frequency range while keeping the quantum state.

This conversion can be done with opto-electromechanical systems²⁸⁷⁵ ²⁸⁷⁶. TU Delft researchers led by Simon Gröblacher experimentally achieved this in 2018, at 20 mK, close to superconducting qubits operating temperature²⁸⁷⁷ (Figure 669).

This led to the creation of **QPhoX** (2021, the Netherlands, 12.5M€) by Simon Gröblacher, a startup seed funded by Quantonation. The research project turned into a “quantum modem for the quantum Internet”²⁸⁷⁸. Although QPhoX is a startup, it seems still operating in a field a fundamental and experimental research²⁸⁷⁹. In September 2022, the startup announced a partnership with IQM to scale-out superconducting qubit quantum computers. The company had a staff of 20 as of January 2024.

²⁸⁷³ See [A quantum-bit encoding converter](#) by Tom Darras, Julien Laurat et al, November 2022 (15 pages).

²⁸⁷⁴ See [Demonstration of deterministic SWAP gate between superconducting and frequency-encoded microwave-photon qubits](#) by Kazuki Koshino et al, February 2023 (14 pages).

²⁸⁷⁵ See also [A quantum microwave-to-optical transducer](#) by Thibaut Jacqmin of LKB, 2019 (17 slides) which describes opto-electromechanical mechanisms for state conversion of superconducting qubits into transportable photons on optical fibers.

²⁸⁷⁶ See [Optomechanical quantum teleportation](#) by Niccolò Fiaschi, Simon Gröblacher et al, April 2021-November 2022 (14 pages).

²⁸⁷⁷ See [New horizons for connecting future quantum computers into a quantum network](#), October 2019 which references [Microwave-to-optics conversion using a mechanical oscillator in its quantum ground state](#) by Moritz Forsch et al, 2019 (11 pages).

²⁸⁷⁸ See [The widely anticipated quantum internet breakthrough is finally here](#) by Maija Palmer, May 2021 and [A perspective on hybrid quantum opto- and electromechanical systems](#) by Yiwen Chua and Simon Gröblacher, 2020 (7 pages). Simon Gröblacher also created Nenso Solutions, a quantum technology consulting company.

²⁸⁷⁹ See [Optomechanical quantum teleportation](#) by Niccolò Fiaschi, Simon Gröblacher et al, Nature, October 2021 (9 pages), [Coherent feedback in optomechanical systems in the sideband-unresolved regime](#) by Jingkun Guo and Simon Gröblacher, June 2022 (12 pages), [An integrated microwave-to-optics interface for scalable quantum computing](#) by Matthew J. Weaver, Simon Gröblacher, Robert Stockill et al, QphoX, Nature Nanotechnology, October 2022-October 2023 (14 pages) and [Ultra-low-noise Microwave to Optics Conversion in Gallium Phosphide](#) by Robert Stockill, Simon Gröblacher et al, July 2021-November 2022 (14 pages).

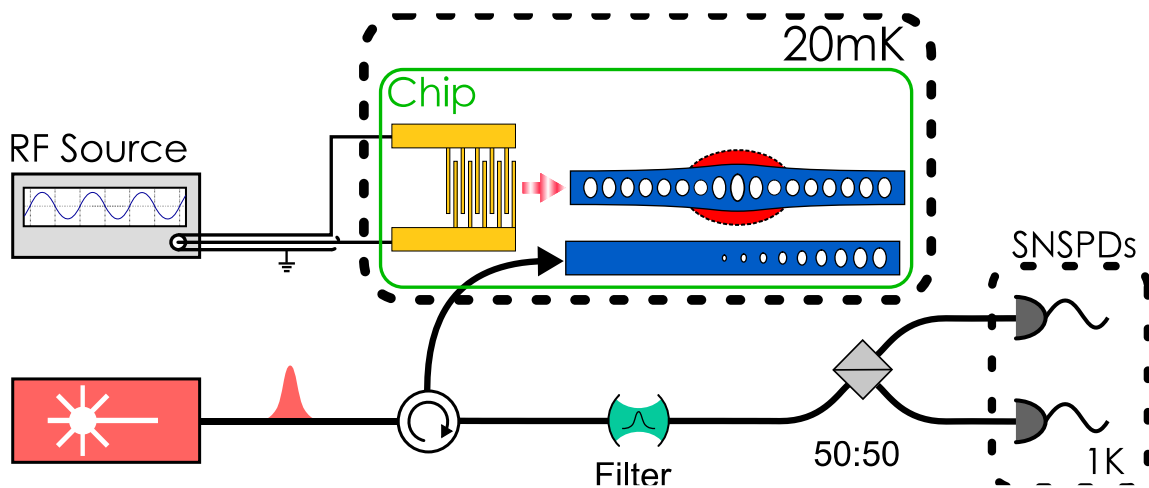


Figure 669: Source: [Microwave-to-optics conversion using a mechanical oscillator in its quantum ground state](#) by Moritz Forsch et al, 2019 (11 pages).

NEXT GENERATION QUANTUM

Next Generation Quantum (2019, USA) is CUNY university spin-off created by Shaina Raklyar (CEO) and German Kolmakov (CTO) developing commercial quantum computing applications and a hardware and software solution interconnecting multiple quantum computers to create quantum computer clusters.

They plan to manage this connection with photons and to use cavity polaritons, photons dressed with charges in a semiconductor optical microcavity that are sensitive to electric fields.

Welinq

Welinq (2022, France, 5M€) is a startup created by Tom Darras (CEO), Jean Lautier-Gaud (COO), Julien Laurat and Eleni Diamanti (both scientific advisors).

It is a spin-off from two laboratories from Sorbonne Université: the Laboratoire Kastler Brossel and the Laboratoire d'Informatique de Sorbonne Université.

They develop a unique full stack (hardware and software) quantum link solution to interconnect quantum processors to enable the scale up of quantum computing. Their quantum links are based on world record cold atom quantum memories (Figure 670). They enable the efficient interconnection of quantum processors to increase their computational power and the implementation of world's first quantum repeaters to enable secure access to quantum computing at a distance.

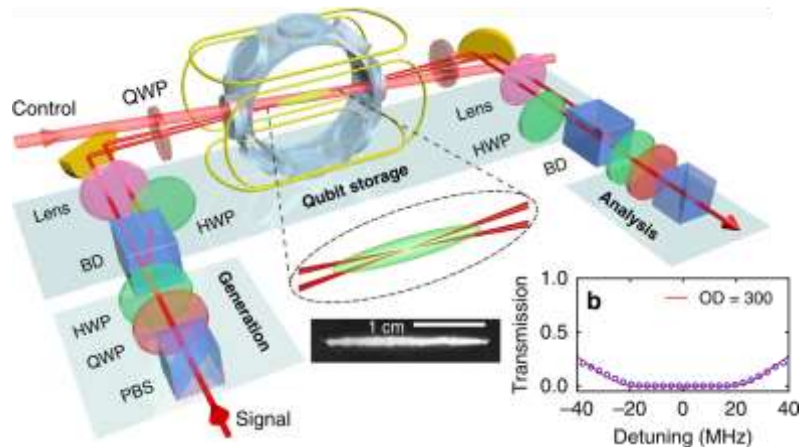


Figure 670: Source: [Highly-efficient quantum memory for polarization qubits in a spatially-multiplexed cold atomic ensemble](#) by Pierre Vernaz-Gris, Julien Laurat et al, Nature Communications, 2018 (6 pages)

Their first product, called *QDrive*, is a robust, compact, and transportable highly efficient quantum memory which will be deployed in quantum computing infrastructures to perform first proof of concepts with providers of quantum computing. Their memory technology is based on an elongated quasi-2D magneto-optical trap of alkali atoms cooled at a temperature close to 20 μ K.

It enables the on-demand (i.e., the storage time is adjustable by the user) and efficient storage of photonic qubits and entangled states with a world record efficiency of 90%, qubit fidelity above 99% and a storage time of 15 μs ²⁸⁸⁰. This is becoming a real commercial product.

In September 2022, Weling announced a partnership with ixBlue (now Exail) for the procurement of lasers adapted to their needs.

In the quantum memory realm, researchers in China succeeded in 2019 to entangle two rubidium atom ensembles quantum memories via entangled photons at a distance of 50 km²⁸⁸¹. But ensemble atoms are not perfect quantum objects for creating multi-qubit memories.

Other efforts are undertaken to connect heterogeneous quantum networks with hybrid entanglement swapping between DV and CV photonic systems²⁸⁸². More classically, qubits can be distantly connected through a photonic link, as MPQ researchers in Germany did show in 2021²⁸⁸³.



memQ (2022, USA, \$2M) is creating some solid-state quantum repeater and memory targeting quantum Internet use cases²⁸⁸⁴. The Chicago-based startup was seed funded by Quantonation, Exposition Ventures, and the George Schultz Innovation Fund.



Bohr Quantum Technology (2022, USA) is a stealth startup working on a quantum interconnect system based on some Caltech and Fermilab research. It is supposed to enable quantum computing scale-out architectures with interconnecting QPUs and/or quantum memories.

The company was created by Paul Dabbar (CEO, a former Under Secretary for Science of the DoE who oversaw DoE research labs during the whole Trump administration) and Conner Prochaska (Chief of Strategic Partnerships, also coming from the DoE). No CTO or Chief Scientist? Bad omen. Their LinkedIn profiles tout that the company “*has developed and built the world’s first commercial ready quantum networking system*”.



Entangled Networks (2020, Canada) is a startup developing a set of protocols and software for multi-QPU environment (multi-qubit gates implementation across distributed QPUs, performance optimization).

The hardware part requires optical quantum interconnect solutions including a high-resolution optical collection system and a low loss Bell state analyzer. The company was created by Aharon Brodutch (CEO) and Ilia Khait (CTO), two Israeli researchers established in Toronto. It was acquired by IonQ in January 2023.

²⁸⁸⁰ See [Highly-efficient quantum memory for polarization qubits in a spatially-multiplexed cold atomic ensemble](#) by Pierre Vernaz-Gris, Julien Laurat et al, Nature Communications, 2018 (6 pages) and [Connecting heterogeneous quantum networks by hybrid entanglement swapping](#) by G. Guccione, Tom Darras, Julien Laurat et al, April 2021 (15 pages) where they describe a higher-level interconnect architecture based on their technology.

²⁸⁸¹ See [New Record: Researchers have entangled quantum memory over 50 kilometers](#) by Stéphanie Schmidt, February 2020. The feat comes from Hefei’s Jian-Wei Pan laboratory in China. This refers to the article published in Nature: [Entanglement of two quantum memories via fibers over dozens of kilometers](#) by Jian-Wei Pan et al, February 2020 and previously on arXiv in March 2019: [Entanglement of two quantum memories via metropolitan-scale fibers](#) (19 pages).

²⁸⁸² See [Quantum Networking Demonstrated for First Time](#) par Dhananjay Khadilkar, November 2018, referencing [Connecting heterogeneous quantum networks by hybrid entanglement swapping](#) by Giovanni Guccione, Tom Darras et al, May 2020 (7 pages).

²⁸⁸³ See [Quantum systems learn joint computing - MPQ researchers realize the first quantum-logic computer operation between two separate quantum modules in different laboratories](#), February 2021.

²⁸⁸⁴ See [A perspective on the pathway to a scalable quantum internet using rare-earth ions](#) by Robert M. Pettit et al, MemQ, April 2023 (31 pages).

Electrons and ions shuttling

Electrons shuttling is a technique envisioned to enable interconnection of silicon spin qubits²⁸⁸⁵. It would have a very short range.

QUASAR is a semiconductor-based project using shuttling electrons with a QuBus (pictured next), a quantum bus to transport electrons and their quantum information over distances of 10 μm . The partners are Infineon, HQS, Fraunhofer (IAF, IPMS), Leibnitz Association (IHP, IKZ) and the Universities of Regensburg and Konstanz. The project will run until 2025 to create 25 coupled qubits. The resulting computer is to be deployed at JUNIQ.

Jülich is also participating to the European Flagship QLSI project driven by CEA-Leti in France. QUASAR got 7.5M€ funding from BMBF. The resulting computer is to be deployed at JUNIQ. Jülich is also participating to the European Flagship QLSI project driven by CEA-Leti in France. QUASAR got a 7.5M€ funding from BMBF²⁸⁸⁶ (Figure 671).

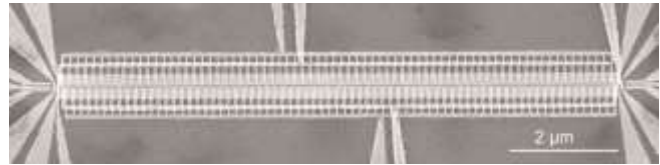


Figure 671: an electron shuttling waveguide.

Source: [Quanten-Shuttle zum Quantenprozessor "Made in Germany" gestartet](#), Jülich, February 2021.

Ion shuttling is an interconnect technique that we already quickly described with IonQ and Quantinuum.

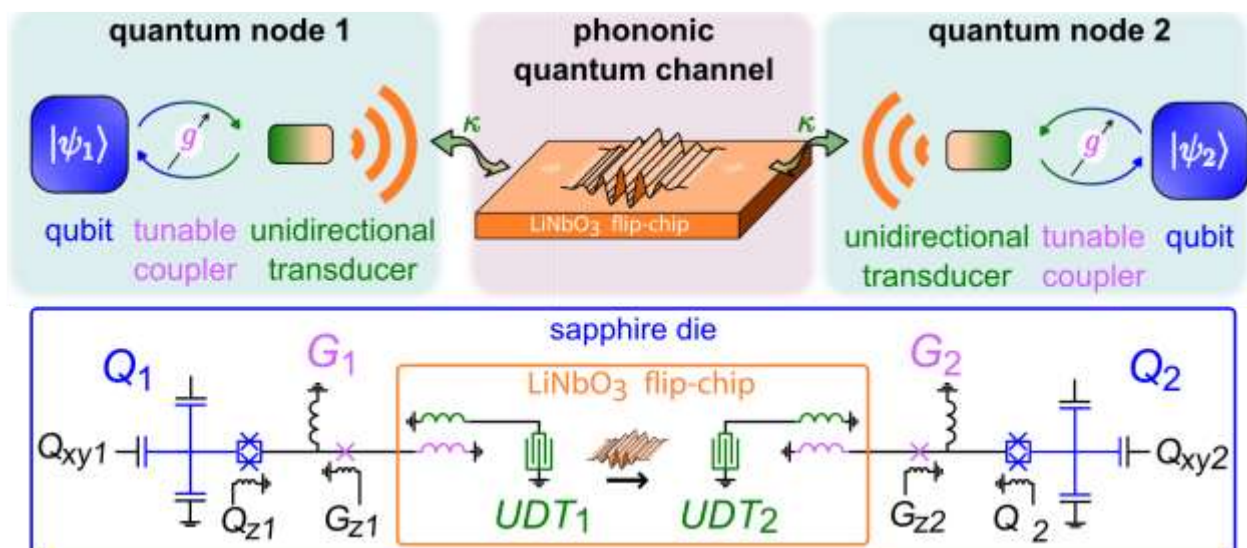


Figure 672: source: [Quantum Communication with itinerant surface acoustic wave phonons](#) by E. Dumur, Audrey Bienfait, et al, University of Chicago and ENS Lyon, December 2021 (5 pages).

At last, let's mention another interconnect technique, that ties superconducting qubits together with phononic communication using surface acoustic waves with the advantage that it fits into a solid-state circuit²⁸⁸⁷ (Figure 672).

²⁸⁸⁵ See [Multicore Quantum Computing](#) by Hamza Jnane, Simon Benjamin et al, Quantum Motion, January 2022 (24 pages) which deals with interconnecting silicon based QPUs with microwaves or electrons shuttling.

²⁸⁸⁶ See [Quanten-Shuttle zum Quantenprozessor "Made in Germany" gestartet](#), Jülich, February 2021.

²⁸⁸⁷ See [Quantum Communication with itinerant surface acoustic wave phonons](#) by E. Dumur, Audrey Bienfait, et al, University of Chicago and ENS Lyon, December 2021 (5 pages).

Infrastructures and architecture

Many key areas must make progress to enable the deployment of quantum telecommunications networks: protocols^{2888 2889}, repeaters^{2890 2891}, switches and routers^{2892 2893 2894}, quantum memories²⁸⁹⁵, distributed quantum error correction schemes²⁸⁹⁶, compilers and other various methods and software tools to distribute processing over several QPUs^{2897 2898 2899 2900 2901 2902}, and even distributed databases²⁹⁰³, and at last benchmarking techniques²⁹⁰⁴. All these components bear their own complicated scientific and technological challenges^{2905 2906}.

Communications bandwidth is already a huge challenge! For example, teleportation rates are currently quite slow. A recent record obtained in China deals with a teleportation rate of 7.1 qubits per second²⁹⁰⁷. That is far from enabling massive usages. Entanglement resources allocations will become the equivalent of classical bandwidth allocation²⁹⁰⁸.

²⁸⁸⁸ Let's mention the Quantum Protocol Zoo initiative launched by LIP6 and VeriQloud which inventories about 56 quantum telecommunication and cryptography protocols. See [Protocol Library](#).

²⁸⁸⁹ See [Benchmarking of Quantum Protocols](#) by Chin-Te Liao, Elham Kashefi et al, July 2022 (16 pages).

²⁸⁹⁰ See [Adaptive bandwidth management for entanglement distribution in quantum networks](#) by Navin B. Lingaraju et al, 2021 (5 pages).

²⁸⁹¹ See [Telecom-heralded entanglement between multimode solid-state quantum memories](#) by Dario Lago-Rivera et al, Nature, IFCO, June 2021 (7 pages).

²⁸⁹² See [Development of Quantum InterConnects \(QoICs\) for Next-Generation Information Technologies](#) by David Awschalom et al, 2019 (31 pages) and [Quantum Switch for the Quantum Internet: Noiseless Communications Through Noisy Channels](#), 2020 (14 pages).

²⁸⁹³ See [Quantum Routing for Emerging Quantum Networks](#) by Wenbo Shi and Robert Malaney, UNSW, November 2022 (6 pages).

²⁸⁹⁴ See [A Quantum Router Architecture for High-Fidelity Entanglement Flows in Quantum Networks](#) by Yuan Lee, Dirk Englund et al, May 2020-October 2022 (16 pages).

²⁸⁹⁵ See this general overview of quantum memories used in quantum networks: [Optical Quantum Memory and its Applications in Quantum Communication Systems](#) by Lijun Ma et al of NIST, 2020 (13 pages). The schema of this page on the Quantum Internet is derived from it. See also [Towards real-world quantum networks: a review](#) by Shi-Hai Wei et al, January 2022 (71 pages) that discusses the links between quantum computing resources and quantum memories.

²⁸⁹⁶ See [Quantum teleportation of physical qubits into logical code spaces](#) by Yi-Han Luo, William J. Munro, Anton Zeilinger, Jian-Wei Pan et al, July 2021 (5 pages).

²⁸⁹⁷ See [Optimized compiler for Distributed Quantum Computing](#) by Daniele Cuomo et al, December 2021 (15 pages) and [Distributed Shor's algorithm](#) by Ligang Xiao, July 2022 (15 pages).

²⁸⁹⁸ See [Mapping quantum algorithms to multi-core quantum computing architectures](#) by Anabel Ovide et al, March 2023 (5 pages).

²⁸⁹⁹ See [Mapping quantum circuits to modular architectures with QUBO](#) by Medina Bandic et al, May 2023 (12 pages).

²⁹⁰⁰ See [A Modular Quantum Compilation Framework for Distributed Quantum Computing](#) by Davide Ferrari et al, May 2023 (13 pages).

²⁹⁰¹ See [Software for Massively Parallel Quantum Computing](#) by Thien Nguyen et al, Quantum Brilliance, November-December 2022 (21 pages).

²⁹⁰² See [D-NISQ: A reference model for Distributed Noisy Intermediate-Scale Quantum computers](#) by Giovanni Acampora et al, Information Fusion, January 2023.

²⁹⁰³ See [SupercheQ: Quantum Advantage for Distributed Databases](#) by P. Gokhale et al, December 2022 (16 pages).

²⁹⁰⁴ See [Quantum Network Utility: A Framework for Benchmarking Quantum Networks](#) by Yuan Lee, Dirk Englund et al, MIT, October 2022 (23 pages).

²⁹⁰⁵ See the review [The Quantum Internet: A Hardware Review](#) by Rohit K. Ramakrishnan et al, June 2022-June 2023 (38 pages).

²⁹⁰⁶ See the review paper [Entanglement-Assisted Quantum Networks: Mechanics, Enabling Technologies, Challenges, and Research Directions](#) by Zhonghui Li et al, July 2023 (58 pages).

²⁹⁰⁷ See [Hertz-rate metropolitan quantum teleportation](#) by Si Shen et al, Nature Light Science & Application, 2023 (9 pages).

²⁹⁰⁸ See [Elastic Entangled Pair and Qubit Resource Management in Quantum Cloud Computing](#) by Rakpong Kaewpuang et al, July 2023 (30 pages).

From the architecture standpoint, we'll probably see evolving schemes in a Russian dolls fashion, with point-to-point interconnection between parties, then, metropolitan level connectivity with evolving network layouts²⁹⁰⁹, then, with longer distance connectivity, potentially using satellites, more global connectivity, creating what could be called a global quantum Internet. It will require that these systems not only enable easy point to point communications between different parties but also to make it interoperable with shared protocols, addressing²⁹¹⁰ and naming standards.

Resources will also have to be evaluated on how to build these networks, including assessing their potential cost and economical value²⁹¹¹.

At last, in the ambitious **DARPA QuANET** (Quantum Augmented Network) project that was launched with a RFP in June 2023²⁹¹², a 51-month project, DARPA is asking bidders to propose architecture and technology solutions to merge entanglement distribution and regular fiber optics lines for various applications involving quantum sensors and quantum computers. The constraints are that no QKD should be proposed nor any repeaters. They want qNIC (quantum network cards) able to handle both classical and quantum communications. It looks like being a very low TRL project.

Quantum Physical Unclonable Functions

qPUF are not the most talked about quantum technologies. It is at the crossroads of quantum cryptography, QRNGs, embedded systems and sensors. Generically, Physical Unclonable Functions (PUF) are systems containing a piece of classical hardware that contain some unique signature related to the random aspect of matter and physical disorder²⁹¹³. This unique signature can't be reproduced. It can also be dynamically generated and always be different²⁹¹⁴.

A PUF is implemented as a unique function and is hard to physically and logically clone. They operate on a challenge/response basis: a challenge is fed into the PUF, which generates a unique binary response coming from the hardware module, which is based on its unique material imperfections.

The physical imperfections used in PUF are manifold: reflection of optical materials, random scattering of light, ring oscillators, coating materials capacitance up to some random characteristics of electronic components like SRAM and DRAM memories. The most common PUFs are using silicon IC and their various defects and variations that are even greater as their integration nodes become smaller, now down to 5 nm.

The generated binary strings are used as keys or identifiers in cryptography systems and as anti-counterfeiting systems. These can also serve as generic true random number generators, either standalone or combined with other entropy sources. But these security systems are not perfect and

²⁹⁰⁹ In the network layout domain, a team led by British and Austrian researchers established an any-to-any quantum communication link with 8 network nodes using dense wavelength division multiplexers (DWDM) and a single source of polarization-entangled photon pairs. See [A trusted node-free eight-user metropolitan quantum communication network](#) by Siddarth Koduru Joshi et al, September 2020 (9 pages) and the subsequent work [Flexible entanglement-distribution network with an AlGaAs chip for secure communications](#) by Félicien Appas, Eleni Diamanti, Sara Ducci et al, NPJ Quantum Information, July 2021 (12 pages).

²⁹¹⁰ See [Quantum Internet Addressing](#) by Angela Sara Cacciapuoti et al, June 2023 (7 pages).

²⁹¹¹ See [Quantum City: simulation of a practical near-term metropolitan quantum network](#) by Raja Yehia, Simon Neves, Eleni Diamanti and Iordanis Kerenidis, Sorbonne Université LIP6 and Université Paris Cité IRIF, November 2022 (28 pages) which contains a simulation of a metropolitan quantum network including estimates for entanglement-based networking. The authors propose a star-type network topology using Qconnector nodes and Qlient endpoint nodes. The model estimates the impact of noise in key rates. It is using the open source NetSquid simulation tool that was developed at QuTech in the Netherlands.

²⁹¹² See [A Network Security Revolution Enhanced by Quantum Communication](#), Darpa, June 2023. "Quantum interconnects such as quantum repeaters, switches, and routers are not in scope for the program". Good luck!

²⁹¹³ See [Physical One-Way Functions](#) by Papu Srinivasa Ravikanth, 2001 (154 pages) and [Physically Unclonable Functions - a Study on the State of the Art and Future Research Directions](#) by Roel Maes and Ingrid Verbauwhede, 2010 (36 pages).

²⁹¹⁴ See the review paper [Comparison of Quantum PUF models](#) by Vladlen Galetsky et al, TUM, August-November 2022 (6 pages).

are prone to various attacks²⁹¹⁵, done with various methods including machine learning, side attacks and even, potentially, quantum computing²⁹¹⁶.

qPUFs are quantum equivalents of PUF that are based on quantum states and their physical unclonability. There's even a variation with Quantum read-out of PUF (QR-PUF) which reads-out quantumly a non-quantum physical disorder in a physical device. These qPUFs are better than classical PUFs but their resistance to forgery depends on their detailed level of unforgeability, which can be “existential” and “selective”^{2917 2918}.

What is the physical form of qPUFs? It can be based on photonic features and polarized prepared devices and multiple scattering medium.



Quantum Base (2014, UK, \$1.1M) offers various quantum product authentication solutions such as the Q-ID Optical, an optically readable "atomic" fingerprint solution that uses Physically Unclonable Functions (PUFs) in the form of physical tags that cannot be copied at the atomic scale level²⁹¹⁹ (Figure 673).

The tag exploits a thin 2D layer of graphene that contains unique irregularities at the atomic scale that cannot be cloned. These irregularities would be amplified by unspecified quantum phenomena. Moreover, these tags can be dynamically activated and deactivated.

The project stems from the work of Lancaster University of Robert Young who is the co-founder of the startup. The whole is integrated in a home-made random number generator (Q-RAND) based on a semiconductor diode, which can be integrated in a chip (video)²⁹²⁰. They also propose the Q-ID Electronic, a unique identifier generator.

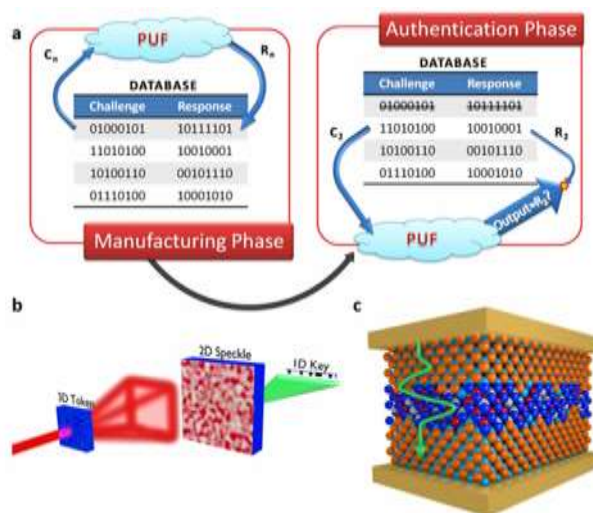


Figure 673: a qPUF made with photon and a scattering media. Source: [Using Quantum Confinement to Uniquely Identify Devices](#) by Robert Young et al, 2015 (8 pages).

²⁹¹⁵ A side-channel attack collects information from a security system or influence its execution in an indirect manner, by collecting in a stealth way some data on hardware operations (quantity of data processed in a computer, heating, amount of gas in a car tank). Side-channels may be power dissipation, operations timing, system temperature, acoustic, radio or optical emissions or a mix of these.

²⁹¹⁶ Samsung Galaxy S10 launched in 2019 contains an Exynos 9820 chipset with PUF technology, for crypto wallets, associated with Samsung Knox, a built-in storage hardware for security keys used with Blockchain services and cryptocurrencies like Ethereum. According to Samsung, the Exynos “PUF generates an unclonable key for data encryption by using the unique physical characteristics of each chip” but this characteristic is not specified. Looks like this PUF was replaced in some subsequent Samsung smartphones by a QRNG coming from IDQ.

²⁹¹⁷ See [Quantum Physical Unclonable Functions: Possibilities and Impossibilities](#) by Myrto Arapinis, Elham Kashefi et al, June 2021 (32 pages) and [A Unified Framework For Quantum Unforgeability](#) by Mina Doosti, Mahshid Delavar, Elham Kashefi and Myrto Arapinis, March 2021 (47 pages), all from the University of Edinburgh and CNRS LIP6 Paris.

²⁹¹⁸ See also [On the Connection Between Quantum Pseudorandomness and Quantum Hardware Assumptions](#) by Mina Doosti, Elham Kashefi et al, March 2022 (33 pages) which deals with the conditions of unforgeability in relation to quantum pseudorandomness

²⁹¹⁹ This is documented in the USPTO patent US10148435B2 [Quantum Physical Unclonable Function](#) filed in 2015 (11 pages) and validated in 2018. It evokes a semiconductor component based on gallium arsenide, aluminum and antimony that generates a random spectral response that differs from one component to another. The process is described in [Using Quantum Confinement to Uniquely Identify Devices](#) by Robert Young et al, 2015 (8 pages).

²⁹²⁰ The *resonant-tunnelling diode* (RTD) process is documented in [Resonant-Tunnelling Diodes as PUF Building Blocks](#), by Ibrahim Ethem Bagci et al, 2018 (6 pages).

Vendors

Let's now review the startups in this vast sector of activity of quantum and post-quantum cryptography, trying to describe the nature of their offer and their differentiation when the information is publicly available (Figure 674, Figure 675)! I have only kept startups offering technology solutions and not integrated consulting and integration companies. Note that on the market size side, the market for quantum and post-quantum cryptography is modest for the moment. A 2017 report estimated it at \$2.5B by 2022²⁹²¹. However, it is expected to gain momentum from this period onward, following the finalization of standardization by NIST and ETSI.

In addition to startups, commercial offers in quantum and post-quantum cryptography are also proposed or about to be proposed by various large IT players such as **Battelle**, **Infineon**, **Raytheon**, **IBM**²⁹²², **Eviden/Atos**, **Gemalto** (part of Thales group), **Cisco**²⁹²³, **Infineon**²⁹²⁴, **Microsoft**²⁹²⁵, **Intel**²⁹²⁶, **NEC**, **Huawei**²⁹²⁷, **KT** and **Samsung**.

Even **Amazon** announced in 2022 the creation of its own quantum networking center in Boston and a partnership with Harvard University²⁹²⁸.

IBM created a set of PQC protocols and participated to the NIST PQC competition. They were finalists of round 3 of the NIST selection in July 2020 for both lattice-based CRYSTALS-KYBER (secure key encapsulation mechanism) and CRYSTALS-DILITHIUM (secure digital signature). These were developed in partnership with **ENS Lyon** (France), **Ruhr-Universität Bochum** and **Radboud University** (Germany). These PQC solutions are embedded in an IBM TS1160 tape drive system with a modified firmware in combination with symmetric AES-256 encryption. It enables secured long-term data storage. In November 2020, IBM also announced it would integrate these protocols in its cloud offering.

Microsoft also works on PQC algorithms. It includes FrodoKEM and SIKE which are PQC based key exchanges protocols. Then, qTesla and Picnic, PQC based signatures protocols.

Let's also mention **Toshiba**'s ambitions in QKD deployments, announced in October 2020. They are deploying a QKD based network for **NICT** (National Institute of Information and Communications Technology) in Japan, on top of a similar deployment undertaken with BT and their Openreach network in the UK in 2020 and demonstrations done with **Verizon** and **Quantum Xchange**.

²⁹²¹ See [New CIR Report States Quantum Encryption Market To Reach \\$2.5 Billion Revenues By 2022: Mobile Systems Will Ultimately Dominate](#), 2017.

²⁹²² See [IBM's Cryptography Bill of Materials to speed up quantum-safe assessment](#) by Alessandro Curioni and Michael Osborne, IBM, December 2022.

²⁹²³ Cisco's Quantum Research is led by Alireza Shabani with three full time researchers. The company is even organizing a yearly event, [Cisco Quantum Summit](#).

²⁹²⁴ With its Optiga TPM SLB 9672, a hardware trusted module supporting AES and SHA2-384 encryptions that are quantum resistant.

²⁹²⁵ See the [Microsoft site](#) that describes their activity in PQC. In December 2022, Microsoft acquired Lumenisity, a UK startup developing a hollow core fiber (HCF) that can be useful to transmit QKD signals and improve key rates. It was tested late 2021 by British Telecom. See also [Distribution of telecom Time-Bin Entangled Photons through a 7.7 km Hollow-Core Fiber](#) by Michael Antesberger et al, August 2023 (9 pages).

²⁹²⁶ Intel participated to the creation of the BIKE PQC PKI that was preselected in 2020 by NIST but is not so far a finalist, per the 2022 4 selected PQCs, including only one PKI. Intel PQC research is done at their Crypto Frontiers Research Center that was launched in 2021. This collaborative effort with Universities is plan to last only until 2024. See [Intel Labs Establishes Crypto Frontiers Research Center](#), 2021.

²⁹²⁷ See [Continuous-Variable Quantum Key Distribution with Gaussian Modulation, the Theory of Practical Implementations](#), 2018 (71 pages). The Huawei team working on the QKD is partly located in their research center in Dusseldorf.

²⁹²⁸ See [Announcing the AWS Center for Quantum Networking](#) by Denis Sukachev and Mihir Bhaskar, June 2022 and [Announcing a research alliance between AWS and Harvard University](#) by Antia Lamas-Linares, Mihir Bhaskar, and Denis Sukachev, September 2022.

Their hardware offer includes the “Multiplexed QKD system” which can transmit QKDs at a key rate of 40 kb/s over 70 km, and high-speed data on the same fiber.

The “Long Distance QKD System” has similar features with a key rate of 300 kb/s and a range of up to 120 km but requiring two fibers. These BB84 solutions are manufactured in Cambridge, UK and fit in a 3U 19” rack format. They are also working to miniaturize their QKD appliances²⁹²⁹.



Figure 674: the big map you were expecting on QKD vendors. (cc) Olivier Ezratty, 2023.



Figure 675: and another one on PQC vendors. (cc) Olivier Ezratty, 2023.

ABCMintFoundation (2017, Switzerland) created by Jin Liu and Jintai Ding is tasked with creating a quantum resistant Blockchain using a Rainbow Multivariable Polynomial Signature Scheme. It is a community driven open source project. It uses keys that can be as large as 1.7MB.

²⁹²⁹ See [A Hybrid Integrated Quantum Key Distribution Transceiver Chip](#) by Joseph A. Dolphin et al, Tosbina, August 2023 (13 pages).



Abelian (2022, USA) is providing a Blockchain infrastructure enabling “gold 2.0” that is based on a lattice PQC.

It secures financial transactions in smart contracts and so-called DeFI (decentralized finance based on a Blockchain). It even deals with the Metaverse and Web3 applications. The company is organized as a foundation and its founders are anonymous²⁹³⁰.



AegiQ (2019, UK, \$4.3M) is developing quantum cryptography systems based on III-V single-photon source semiconductors. It was created by Max Sich (CEO), Scott Dufferwiel (CTO) and Andrii Iamshanov (CFO) as a spin-off of the University of Sheffield. They plan to equip telecommunication data centers for their fiber optical infrastructures upgrades to QKD. They are also building a satellite-based QKD offering.

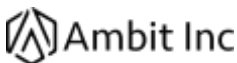


AgilePQ (2014, USA) provides a software platform for "post-quantum" security of communication between connected objects and the cloud, such as drones.

It includes AgilePQ C-code, a piece of software that runs on connected object microcontrollers and consumes little power, and AgilePQ DEFEND, an adaptive size-based key generation system. DEFEND generates codes that are harder to break than AES 256 and with 429 orders of magnitude difference. Specifically, we go from a key space of 10 to the power of 77 to $8 \cdot 10$ to the power of 506 (factor of 256)²⁹³¹. The system that is patented seems to be a variant of linear random codes but with keys of reasonable size. It has been standardized at NIST and interfaces with SCADA (Supervisory control and data acquisition) control and supervision systems. The company is a Microsoft Azure partner.



Agnostiq Inc (2018, Canada, \$8.9M) is a Toronto startup created by Oktay Goktas coming out of the Creative Destruction Lab accelerator in Toronto. They offer Covalent Cloud, a Python-based workflow management tool to submit and scale jobs on hybrid quantum computers, cloud privacy and quantum obfuscation tools and pre-built applications in the finance sector for portfolio optimization and options pricing. It supports all classical AWS cloud services.



American Binary or **Ambit** (2019, USA) sells PQC solutions to governments, enterprise customers and consumer products companies, including a VPN.



Anametric (2017, USA, \$1.9M), formerly bra-ket science, is a startup that wants to create information storage systems in qubits operating at room temperature. It seems they are focused on quantum telecommunication systems.



Alternatio (2016, Poland) develops a post-quantum cryptography IP core to be integrated in chips for the industry and connected objects.



ArQit (2016, UK, \$70M) is developing QuantumCloud, a cloud-distributed symmetric keys mixing keys generation in local agents. It was supposed to support key distribution via low earth orbit satellites and QKD.

²⁹³⁰ See [Abelian \(ABEL\) – A Quantum-Resistant Cryptocurrency Balancing Privacy and Accountability](#) by Alice, Bob, Eve, and λ, February 2022 (140 pages).

²⁹³¹ See [AgilePQ DEFEND Cryptographic Tests](#) (11 pages).

They claimed, through a patent, that they could implement terrestrial QKD without trusted nodes or repeaters, which was debunked by an international team of researchers²⁹³².

In May 2021, the company announced a funding round of \$400M using an IPO through a special purpose acquisition company like IonQ, this time with Centricus Acquisition Corp. As a result, the company published in May 2022, a revenue of \$12.3M for H2 2021 with an operating loss of \$14.3M, with \$5,3M in H1 2022, compared to a loss of \$5.5M in H2 2020. They also published a “myth busting” presentation²⁹³³. In December 2022, they announced that they were abandoning the satellite QKD market. We can now consider that this company is selling some quantum safe software solution that is not relying per se on PQC.



BLAKFX (2017, USA) develop quantum resistant software solutions around their Helix22 SDK that provides five layers of symmetric keys protections for end-user to end-user communications (AES1, TwoFish, AES2, ThreeFish, Snow3G). With sufficiently long keys, symmetric keys are quantum resistant.



BraneCell Systems (2015, Cambridge Massachusetts and Dusseldorf, \$1.8M) is a startup launched by Wassim Estephan and Christopher Papile.

It started to develop a cold atom based QPU²⁹³⁴! They have filed a few patents, including USPTO patent 9607271, validated in March 2017. They however later pivoted on creating an atom-based repeater.



CAS QuantumNet (2017, China, \$230M) *aka* Guoke Quantum is a quantum key operation services company that offers its Q-NET BOX quantum security mobile private network communication equipment. It secures the backbone of LTE telecom networks with QKD.



Ciena (1992, USA) is an equipment manufacturer in the field of optical telecommunications. They integrate IDQ's offers in their solutions, and, their optical random key generators.

Although they do not yet have a structured QKD offering, they are very interested in standardizing it. In particular, they are participating in the Quantum Alliance Initiative launched in 2018 in the USA by the Hudson Institute, a conservative think tank, which is working towards this goal and creating proposed standards for QKD and QRNG (quantum random number generation).



Craft Prospect (2017, UK) is a space engineering company that is providing satellite cubesat based QKD technology as part of the Amplified Quantum Key Distribution (AQKD) project funded by Innovate UK.

²⁹³² See [Long-range QKD without trusted nodes is not possible with current technology](#) by Bruno Huttner, Romain Alléaume, Philippe Grangier, Hugo Zbinden et al, npj, September 2022 (5 pages).

²⁹³³ See [Arqit Myth Busters](#) by Arqit, 2022 (10 pages). I'd say OK with most myths, but not for their assessment of the quantum computing threat on classical security which, like all cybersecurity vendors, they tend to exaggerate.

²⁹³⁴ Their communication is cryptic to say the least, as [BraneCell Systems Presents Distributed Quantum Information Processing for Future Cities](#), April 2018 and a partnership announced with the US government service provider, AST, in July 2018 in [AST and BraneCell Announce Their Partnership to Improve Critical Government Functions Through the Power of Quantum Computing](#). They do not provide any technical or popularization information about their solution, qubits and error rates. They were also aiming for an ICO that would have been the first of its kind for a quantum computing startup. Their main goal was to create a secure communication system. They target the financial, energy, health, chemical and public sectors. A Quantum Theranos? At the very least, we have the right to doubt.



Crypta Labs (2013, UK, \$300K) develops post-quantum encryption solutions adapted to connected objects. In particular, they propose quantum random number generators labelled Quantum Optics Module (QOM) that can be integrated into a cell phone (such as IDQ) and also work in space. The QRNG uses a LED or laser light source and a camera sensor. They are working with the University of Bristol as well as with Blueshift Memory.



Crypto4A Technologies (2016, Canada) offers an encryption solution based on a random number generation.

It includes a 19-inch QAOS format appliance server for generating entropy random numbers (without specifying the technology used) and another that generates quantum safe PQC encryption, the QxEdge Hardware Security Module (HSM). The PQC generation module is called QASM (Quantum Assured Security Module), which duplicates the quantum development language of the same name.

It is based on quantum safe hash-based signatures (HBS). These appliances are equipped with four Intel Core i7 chips, 16 GB of memory and 256 GB of SSD and run on a hardened version of Linux. They support algorithms certified by the NSA in the USA ("suite B") and future NIST PQC standards (Figure 676).



Figure 676: CryptoAA QRNG based HSM products.



CryptoExperts (2008, France) develops homomorphic encryption and post-quantum cryptography, and also offers services based on these technologies.



Cryptolab (2013, USA/Italy, \$800K) is a startup created by Massimo Bertacchini (CEO), Alessandro Passerini and Tiziana Landi (software engineers) that develops cryptographic solutions supporting AES-256 bit to secure data, particularly medical data.

They are testing a new solution that “allows transmitting a message directly via quantum channel” which may mean a lot of things like being a QSDC. They are also working on a way to unlock a device using brain waves signatures.



CryptoNext Security (2019, France, 11M€) is a startup that develops a post-quantum cryptography solution. They were founded by Ludovic Perret (CPO, ex Inria, who left the company in 2022) and Jean-Charles Faugères (CTO, ex LIP6 Sorbonne) with Florent Grosmaître as CEO.

Their software solution is developed in C language and assembler for performance reasons. It combines multivariate polynomials and hashing. Their solution can be integrated into RSA/ECC schemes by hybridization. CryptoNext is also one of the French teams who submitted a PQC proposal to the NIST which has been selected as an alternative candidate in 2020’s round 2, GeMSS, which consolidates contributions from CryptoNext, Inria, Orange, University of Versailles and Sorbonne Université.

PQC standardization processors are used in practice by many organizations such as ISO, ITU (X509), IETF (TLS) and ETSI (algorithms). Their PQC should be integrated into R3's CORDA blockchain solution for banks. Note that China is also organizing a competition with a faster selection schedule than the NIST one. CryptoNext equips French special forces with their PQC, running on secure mobiles using Android. In 2023, they announced a technology partnership with Quandela which provides them their device-independent Entropy QRNG source, to feed their PQC solution.



Crypto Quantique (2016, UK, \$8M) is a startup offering a cryptography solution to secure communication with connected objects targeting various markets ranging from automotive to finance. It uses a chip that is installed in the object. It is a "quantum processor" in silicon technology that is used to generate a unique identification key for the object, which is tamper-proof and tamper-proof. It probably exploits photonics with a random number generator similar to the Swiss IDQ technologies.

Their technology is called Quantum Driven Physically Unclonable Function (QD-PUF) but they do not explain how it works or what encryption model is used²⁹³⁵. The founders are of Iranian, Italian and Greek origins, a beautiful patchwork. In July 2022, they announced that their platform was supporting the only selected PKI by NIST the same month, CRYSTALS-Kyber.



CyferAll (2021, France) is selling a messaging and communication platform embedding CRYSTALS-Dilithium and CRYSTALS-Kyber PQC end-to-end cryptography, working in memory. The offer contains D8Alock (for SaaS) and D8Ashield (to encrypt local mass storage).



Cyph (2014, USA, \$1M) sells PQC solutions. The company was created by Ryan Lester and Joshua Boehm, two engineers from SpaceX. Mars not interesting anymore?



Dencrypt (2013, Denmark) is a cybersecurity software provider protecting smartphone communications. They are working on creating PQC based solutions in partnership with the Technical University of Denmark (DTU).



evolutionQ (2015, Canada, \$5.5M) is a startup that stands out especially for the pedigree of its creator, Michele Mosca, a specialist in post-quantum cryptography known for his Mosca scale to assess the risk of quantum computing on classical cybersecurity.

He is also the founder of the Institute for Quantum Computing at the University of Waterloo in Canada. The company provides what is known as "service equipped" to support companies in the adoption of post-quantum and quantum cryptography. It begins with a six-phase Quantum Risk Assessment product²⁹³⁶. Is it really a product? It looks more like a methodology to be implemented with consultants. The rest is of the same cream with integration and training services to evolve the company's cryptographic systems.

In July 2022, SandboxAQ announced a strategic partnership with evolutionQ including some funding in a series A round. It will help complement SandboxAQ's PQC offering with evolutionQ's QKD software platform, BasejumpQDN.



Flipscloud (2013, Taiwan) creates "quantum level" encryption software targeting IoT, cloud services and the big data market. It seems it is using some unspecified PQC and AES 256 bits keys. Software runs on embedded systems using Arm cores and Imagination CPUs.



fragmentiX (2018, Austria) offers a secure data storage management system that uses the technique of fragmentation and distribution of data on different physical media. All this is supplied in the form of appliances.

²⁹³⁵ See [Physically Unclonable Functions: a Study on the State of the Art and Future Research Directions](#) by Roel Maes and Ingrid Verbauwhede (36 pages) and [Quantum readout of Physical Unclonable Functions](#) by B. Skoric (21 pages).

²⁹³⁶ It is documented in [A Methodology for Quantum Risk Assessment](#), published in 2017.

The distributed data is of course encrypted, but in a classical way. This is another way to create data protection that is resistant to Shor's algorithm. It is not the only company positioned in this niche.

They combined their appliances with QKD equipment from IDQ and Toshiba that was available at AIT. The theoretical proposal comes from researchers of TU Darmstadt in Germany and it has already been implemented a couple of years ago in Tokyo.



GoQuantum (2018, Chile) is willing to provide “a post-quantum secure data transmission solutions through quantum-based hardware and radio link layer encryption.”. Translation: it’s using PQC encryption algorithms with a photonic based QRNG for key generation.



HaQien (2019, India) designs post-quantum cryptography (PQC) solutions. But it is not quite clear because they also seem to use a random number generator to create classical keys.



HEaAN CryptoLab (2017, South-Korea) is specialized in the development of homomorphic encryption technology.

They have their own PQC solution supporting NIST PQC finalists on top of supporting Korean’s RLizard key encapsulating mechanism to embed PQC in devices and HiMQ, a PQC NIST candidate that was not selected in the 2020 round. They helped LG U+ develop its own PQC for its optical transmission equipment. Their CSO Damien Stehlé, formerly from ENS Lyon, was a key contributor to the development of CRYSTALS-Dilithium and CRYSTALS-Kyber, two of the 4 finalists of the PQC NIST competition in July 2022.



Hub Security (2017, Israel, \$55M) sells quantum secure FPGA based Hardware Security Module (HSM). These HSM modules contain QRNGs and support quantum-resistant algorithms acceleration in hardware (PQC).



IDQ (ID Quantique) (2001, Switzerland, \$74.6M) is one of the oldest companies in the sector, cofounded by Swiss researcher Nicolas Gisin, a specialist in photonics and quantum entanglement. In 2023, the company had more than 120 employees.

The company offers a complete range of random number generators and QKD management systems as well as a high-efficiency (>95%) superconducting nanowire single photon detector (SNSPDs) as well as single-photon avalanche detectors (SPADs). These photon detectors are controlled by the ID1000 Time Controller Series introduced in January 2022.

Its Quantis random number generator, already described at the beginning of this section, is complemented by Cerberis, a QKD solution to protect the generation of encryption keys in a 6U rack and Centauris, a range of encryption servers supporting 100 GBits/s optical links (Figure 677).

This FPGA-based server currently supports elliptic curve-based systems as well as AES-256, pending the standardization of PQC (post-quantum-crypto) protocols. As of 2022, IDQ’s Cerberis XG (enterprise market) and XGR (research market, supporting OpenQKD) Series was the fourth generation of this product line in a 1U form factor for both ends supporting various network topologies (ring, hub and spoke, meshed). It supports a 1 GHz key generation rate and includes a QRNG system for photon basis readout selection.



Figure 677: IDQ's QKD offering.

IDQ's QKD offer is notably deployed in Korea to protect the 5G backbone of the operator SK Telecom. They are also partnering with Toshiba in Cambridge and in the OpenQKD project.

IDQ has two expansion plans. One deals with getting involved in satellite QKD, with their participation to the Eagle-1 EU and ESA sponsored initiative, for which they will provide their QRNG solution. The other one deals with creating a set of products supporting entanglement distribution and the quantum Internet. They are working on a SNSPD (superconducting single photon detectors) using 14 subpixels and nanowires arrays. It has a high system detection efficiency (SDE) of 90% in the telecom O-band²⁹³⁷. IDQ also integrates its QKD with **PacketLight** (Israel) fiber transport network.

Since the beginning of 2018, the Korean group SKT Invest is the Corporate Venture branch of **SK Telecom** invested \$65M in what was modestly [presented as a partnership](#) while it is actually a majority 51% ownership. Deutsche Telekom is still an investor in the company.



Keequant (2017-2020, Germany, \$1.7M), formerly InfiniQuant, is a spin-off from the Max Planck Institute for the Science of Light with 14 employees as of November 2022. They develop CV-QKD solutions for telecom operators.

They work on miniaturizing their QKD systems in miniaturized pluggable QKD+PQC hybrid boards costing less than 10K€. The startup is also working on a quantum random number generator.



Icarus Quantum (2023, USA) is a startup created by Poolad Imany (CEO) that develops quantum dot based quantum light generators coming out of NIST research labs. They generate deterministic entangled photons, probably using a frequency comb.



Infotecs (1991, Russia) is a cybersecurity specialist historically specialized in VPN creation. It has developed a PQC solution in 2016, with an awkward communication that could make it look like QKD²⁹³⁸.

But they develop many QKD solutions. In 2018, they launched their "ViPNet Quantum Phone", using their ViPNet VPN (ViPNet Client and ViPNet Connect) and a hardware QKD solution developed at Moscow University. What they call a "phone" is in fact a PC with an external box with a fiber optic link connecting it to a QKD key server²⁹³⁹.



ISARA (2015, Canada, \$27M) develops post-quantum encryption software solutions and PQC implementation consulting with "ISARA Radiate Security Solution Suite" which provides public keys and encryption algorithms.

They are visibly based on hash trees and combine PQC (post-quantum crypto) and traditional PKI (public-key infrastructure)²⁹⁴⁰. One of their investors is the [Quantum Valley Investments fund](#), managed by Mike Lazaridis, co-founder of Blackberry RIM. He reinvested his Blackberry-related fortune in the development of the Canadian scientific and entrepreneurial ecosystem, particularly in quantum, where he has invested a total of \$450M²⁹⁴¹.



KETS Quantum Security (2016, UK, £5.1M) develops a quantum random number generator (QRNG) and a QKD quantum key generator, all integrated in a single component miniaturized photonic and packaged in PCI cards.

²⁹³⁷ See [GHz detection rates and dynamic photon-number resolution with superconducting nanowire arrays](#) by Giovanni V. Resta et al, University of Geneva and IDQ, March-June 2023 (28 pages).

²⁹³⁸ See [Infotecs At The Forefront Of Quantum Cryptography](#), 2017.

²⁹³⁹ See [Infotecs has presented its ViPNet Quantum Phone](#), January 2018.

²⁹⁴⁰ This is documented in the white paper [Enabling Quantum-Safe Migration with Crypto-Agile Certificates](#), 2018 (7 pages).

²⁹⁴¹ See [The Co-Inventor of BlackBerry Is Building Canada's Quantum Brain Trust](#), Bloomberg, 2018.

All this is combined with a consulting activity for the deployment of the solutions. The company was founded by photonics researchers from the University of Bristol. They target the financial and public sector markets. They are prototyping UAVs with Airbus for QKD implementation in military or public security applications, with Airbus Defense. Their QKD chip can also equip Cubesat-type micro-satellites.



Ki3 Photonics (Canada) is a spin-off of the National Institute of Scientific Research on energy, materials and telecommunications from Montreal created by Yoann Jestin (CEO) and Piotr Rozgtockki (CTO)

It develops compact and energy efficient QKD hardware solutions to ease its deployment over standard telecommunications links with using signals multiplexing using frequency combs.

Knot Communications / Artedys (France) wants to launch a network of satellites to operate some sort of quantum blockchain satellite phone. They plan to launch a satellite between 2024 and 2027. This looks a little farfetched.



levelQuantum (2023, Italy) was created by Magdalena Stobińska (CEO), also a professor of quantum information at the University of Warsaw and Adam Buraczewski (CTO).

The company creates a QKD operating over satellite connections using a new DI-QKD (device independent, entanglement based) protocol protecting communication over long distance using twin-field light encoding and scaling, using SPDC based photon sources²⁹⁴². It works on long distance in terrestrial and satellite mode with good key rates of 10^3 to 10^4 bits/sec for satellite and 10^7 bits per second on ground communication²⁹⁴³. The company is focused on satellite QKD, having created a communication hub hooked to a small telescope. terminal. It works on daylight using infrared in the 600 nm to 800 nm range. They target all satellite orbits (LEO, MEO and GEO for low, middle, and geostationary). The satellite part is developed by **Beyond Gravity** (Switzerland) handling photon swapping without the need for some quantum memory^{2944 2945}.



LQUOM (2020, Japan, \$3M) is creating and selling various MDI-QKD quantum communication systems and quantum repeaters. It supports entanglement based BBM92 QKD on dual-bands telecom on a range of 50 km²⁹⁴⁶.



LuxQuanta (2021, Spain) is a spin-off of ICFO led by Vanesa Diaz (CEO). It created NOVA LQ, a CV-QKD solution for distributing secure keys in metropolitan networks using existing optical fiber links and supporting distances up to 40 km. It is available in AWS's marketplace and integrated with AWS Elastic Cloud Compute (EC2) instances hosted in AWS Edge devices.

LuxQuanta also deployed a 30 km pilot project in Spain in 2022. In 2023, it got the support from the EU as part of the QUARTER consortium (Quantum Cryptography Technology for Europe), which was awarded a grant of 7M€ as part of the EuroQCI initiative.

²⁹⁴² See [Quantum interference enables constant-time quantum information processing](#) by Magdalena Stobińska et al, Science Advances, July 2019 (38 pages).

²⁹⁴³ See [Proposal for the distribution of multiphoton entanglement with optimal rate-distance scaling](#) by Monika E. Mycroft, Thomas McDermott, Adam Buraczewski and Magdalena Stobińska, PRA, January 2023 (29 pages).

²⁹⁴⁴ See [Quantum-enhanced interferometry with large heralded photon-number states](#) by G. S. Thekkadath et al, npj Quantum Information, October 2020 (14 pages).

²⁹⁴⁵ See [Overcoming the rate–distance limit of quantum key distribution without quantum repeaters](#) by M. Lucamarini et al, Nature, 2018 (8 pages).

²⁹⁴⁶ See [Nonlinear improvement of measurement-device-independent quantum key distribution using multimode quantum memory](#) by Yusuke Mizutani and Tomoyuki Horikiri, Yokohama National University and LQUOM, June 2023 (18 pages).



MagiQ (1999, USA, \$7.5M) is a startup that initially started in 2003 with the creation of a QKD system. For about ten years, this company seems to have repositioned itself in the US service and defense industry. They have developed the Agile Interference Mitigation System (AIMS), a system for reducing electromagnetic communication interference.



MtPelerin (2018, Switzerland) is a startup specialized in the management of crypto assets via a dedicated mobile application ("Bridge Wallet"). They have created a quantum safe with IDQ, "The Quantum Vault", which is based on IDC's random number generator and QKD system.



NodeQ (2021, UK) is a software and service company dedicated to the deployment of quantum cryptography and telecommunications solutions. It was created by Stefano Pirandola and Samuel L. Braunstein. Stefano Pirandola pioneered continuous variable quantum cryptography, routing strategies on quantum networks using arbitrary topology, quantum repeaters, entanglement distillation and quantum computing optimization.

After working as a MIT researcher, he became a professor of quantum computing at the University of York (UK). Samuel L. Braunstein also worked on quantum teleportation with continuous variables and quantum teleportation networks.

He also worked in quantum sensing and introduced the first bosonic model for universal quantum computing with Seth Lloyd in 1998²⁹⁴⁷. Both created the hybrid quantum Internet concept, association direct and continuous variables²⁹⁴⁸.



NuCrypt (2003, USA) develops optical technologies for quantum communications and metrology, including entangled photon sources, optical pulse generators, single photon detectors, polarization analyzers and associated software.



Nu Quantum (2018, UK, \$12.8M) is a spin-off from the University of Cambridge developing QKD optical links and satellite systems using proprietary single-photon components. They also created their own source of single photons and have some ambition to create a photon-based quantum computer and photonic QPU interconnect of their own. The startup is co-founded and directed by Carmen Palacios-Berraquero.



Origone (2014, UK) develops cryptography solutions based on D-Wave computers. It targets the defense market as well as the railway industry. Their quantitative/post-quantum cryptography activity is an evolution of a traditional cybersecurity business.



Patero (2018, Germany) is a software PQC software and service vendor addressing the national security, critical infrastructures and supply chain markets.

It is bound to protect customers after "Q Day", the (elusive and very long term) moment when some quantum computer will break existing public-key based cryptography. It covers various parts of the IT stack: gateways, virtual cloud and edge computing. The company was cofounded by Henning Schiel who is their CTO.

²⁹⁴⁷ See [Quantum computation over continuous variables](#) by Seth Lloyd and Samuel L. Braunstein, 1998 (9 pages).

²⁹⁴⁸ See [Physics: Unite to build a quantum Internet](#) by Stefano Pirandola and Samuel L. Braunstein, Nature, 2016 (3 pages).



Post-Quantum or PQ Solutions (2009, UK, \$10.4M) is a startup initially created under the name SRD Wireless that created the secure PQ Chat messaging using the random linear codes invented by Robert McEliece.

The company was renamed as Post-Quantum or PQ Solutions Limited in 2014, or PQ Group. They offer a line of security products integrating post-quantum crypto algorithms. One of the co-founders, Martin Tomlinson, has developed the Tomlinson-Harashima pre-encoding, which corrects interference in telecommunication signals and various error correction codes. Their products also include PQ Guard, a post-quantum encryption system. Their CEO, Andersen Cheng is also the CEO of **Nomidio** (2020, UK), a provider of quantum-proof identity solutions, the Nomidio Private Identity Cloud.



PQSecure Technologies (2017, USA) is a provider of isogeny-based PQC solutions. It is a spin-off from the University of Florida Atlantic launched by Reza Azarderakhsh. Their SIKE algorithm is a finalist in the NIST PQC call for proposals.



PQShield (2018, UK, \$26.9M) is Oxford University spin-off that develops PQC solutions, including HSM (hardware security modules).

They participate to several finalist teams in the PQC competition launched by NIST including the CRYSTALS-Kyber PKI and CRYSTALS-Dilithium's signature that were selected in July 2022. They have developed a licensed SoC (system on chip) that integrates their in-house Euclidian networks based PQC. Bosch is one of their first customers. In May 2023, they announced a partnership with Tata Consultancy Services as well as with the side-channel attacks analysis and testing tools vendor eShard.



Qaisec (2019, Bulgaria) develops cryptographic solutions targeting the AI, finance and telecommunications sectors. They seem to offer first a security audit service and then cryptography solutions that use quantum random number generators for keys. They are also creating a PQC-based blockchain.



QANPlatform (2019, Estonia) was cofounded by Johann Polecsak (CTO) and is providing a quantum-proof Blockchain relying on a Lattice-based PQC (CRYSTALS-Dilithium) implemented in the RUST programming language.



QuantLR (2018, Israel) is the developer of an affordable QKD solution that is supposed to reduce the cost of QKD deployment by 90%. In February 2023, it was launched as LoQomo 1, with a 2U appliance form factor.

The startup was cofounded by Hagai Eisenberg, a professor at Hebrew University of Jerusalem. When looking at a recent paper he coauthored²⁹⁴⁹, you get an idea of what they may be doing. It consists in using a high-dimensional QKD architecture that can work on existing binary QKD hardware on distances of up to 40 km, thanks to using some time-bin encoding programmed on a FPGA component.

They also partner with a telecom equipment manufacturer, **PacketLight Networks** (2000, \$18M), also based in Israel, which provides optical fiber WDM (wavelength-division multiplexing) equipment. They also tested their solution with **Medone**, an Israeli datacenter service provider. In a sense, the startup's go-to-market is original, relying on Israeli local players when many Israeli startups usually directly go and reach international players and partners, particularly in the USA.

²⁹⁴⁹ See [Fast and Simple One-Way High-Dimensional Quantum Key Distribution](#) by Kfir Sulimany, Hagai Eisenberg, Michael Ben-Or et al, May 2021 (7 pages).



Qabacus (2019, USA) is developing quantum computing and cryptography technologies and a complete cyber-security software stack.



Qasky (2016, China, \$7.6M) *aka* Wentian Quantum commercializes research coming out of the Chinese Academy of Sciences. Funding comes from Wuhu Construction and Investment Ltd and the China University of Science and Technology.

They offer solutions for post-quantum crypto, QKD and photonics components. Their name is derived from CAS Key laboratory, CAS = China Academy of Sciences.



Q-Bird (2022, the Netherlands) is a spin-out of QuTech created by Remon Berrevoets (Research), Ingrid Romijn (Business Development), Joshua Slater (CTO) and Joël Abrahams (Software). It develops a QKD solution for the quantum Internet supporting multipoint-to-multipoint connectivity. Their first customer is the Port of Rotterdam.



QCi (Quantum Computing Inc) which develops photonic quantum computing solutions, is also in the PQC business. It got an exclusive right on various security related patents from Steven Institute of Technology to implement QKD distribution.



QEYnet (2016, Canada, \$7M) is developing a QKD quantum cryptography satellite network. Funding for the startup comes from the Canadian government.



QNu Labs (2016, India, \$5.3M) develops QKD-based solutions. They also offer their own quantum random number generator and are also working on the creation of a QKD solution operating on Li-Fi, W-Fi that uses the frequencies of visible light.



Qrate Quantum Communications (2015, Russia) sells QRate Key Distributor, a BB84 protocol-based QKD quantum key distribution solution in a 4U rack with a range of up to 100 km²⁹⁵⁰.

They also market a single-photon avalanche diode detector (SPAD) operating at 1,550 nm and a quantum random number generator (QRNG).

QSpace Technologies (2017, Russia, \$1M) is a developer of QKD satellites that is building a CubeSat with a QKD system transmitter, to be launch in 2023. It is a spin-off from the Russian Quantum Center, itself coming out of QRate in 2021.



QTI (2020, Italy) is a startup cofounded by Tommaso Occhipinti (CEO). It engineers, develops, and produces reconfigurable QKD hardware solutions, the Quell-X family products supporting BB84 keys operating in the microwave C-band and in the optical O-band. It supports 2 kBits/s key rate.



Qtlabs (2013, Austria) is a company providing ground stations for satellite QKD distribution, the Optical Ground Station 400 and 800 as well as prepare and satellite measure and entanglement based photon sources.

²⁹⁵⁰ See [Preparing a commercial quantum key distribution system for certification against implementation loopholes](#) by Vadim Makarov et al, Russian Quantum Center, University of Waterloo, Qrate et al, October 2023 (33 pages) about the way this prepare-and-measure QKD can be certified.



QuantiCor Security (2017, Germany) develops PQC solutions, particularly for Blockchain applications and connected objects, via offerings with Quantum-Multisign and Quantum IDEncrypt.

That they are supposed to be cheaper than traditional PKIs. They come from TU Darmstadt and target the healthcare market in particular.



Quantum Blockchains (2018, Poland) wants to create a quantum resilient blockchain based on QKD. That's an interesting long-term bet given the infrastructure required to make it happen at a large scale.



Quantum Bridge (2019, Canada, \$600K) is a startup created by Mattia Montagna (CEO) and Hoi-Kwong Lo (CTO) that provides a proprietary symmetric key distribution solution labelled DSKE (Distribution of symmetric key exchange) based on QKD. The offer contains Quantum Bridge KME, Security Hub, Black Phone (a mobile application that uses pre-shared symmetric keys) and a Client SDK.



Quantum Collective (2021, the Netherlands) is a European company created by Fabien Bouhier, Sebastien Le Goff and Floris Drupsteen that provides post-quantum security solutions. They name this "Quantum Security Solutions" but it's classical quantum-resilient security covering PKI, VPN and eMail security.



QuantumCTek (2009, China) is a provider of end-to-end quantum cryptography solutions: QKD, QKD repeaters, optical routers. The company is a spin-off of Hefei National Laboratory for Physical Science at Micro-scale (HFNL) and the University of Science and Technology of China (USTC).

It lived or lives with many other names: Anhui Quantum Communication Technology, National Shield Quantum, Guodun Quantum, Anhui GuoDun quantum Cloud Data Technology, Xinjiang GuoDun Quantum Information Technology, on top of its holding subsidiary Shandong Guoxun quantum core technology Co. The company was created by Peng Chengzhi and Zhao Yong with the help from Jian-Wei Pan.

They are behind the creation in 2014 of the "Quantum-Safe Security Working Group" with ID Quantique and Battelle, which promotes PQC. As we saw above, they have deployed the 2000 km QKD-protected link between Shanghai and Beijing. They ran an IPO (Initial Public Offering) in China in July 2020. They also develop their homegrown QRNG solution that seem to fit into a SIM card.



Quantum Impenetrable (2018, UK) is a Scottish startup that develops a security module (HSM) using a quantum random number generator and resistant to quantum key-breaking algorithms.



Quantum Xchange (2016, USA, \$23.5M) distributes Phio Trusted Xchange, a key distribution system supporting both PQC and QKD.

They partner with the telecom infrastructure operator Zayo Group, from which they operate their dark fibers and use ID Quantique's QKD solutions. They began by deploying a 1,000-kilometer QKD network from Boston to Washington via New York and New Jersey²⁹⁵¹. Since 2021, they also partner with **Cisco** for the support of the Cisco Secure Key Integration Protocol implemented in enterprise

²⁹⁵¹ See [Quantum Xchange Breaks Final Barriers to Make Quantum Key Distribution \(QKD\) Commercially Viable with the Launch of Phio TX](#), September 2019.

routers, for the non-quantum part of their hybrid key distribution architecture. In 2022, they announced a partnership with **Thales** for the delivery of security keys with Thales High Speed Encryptors (HSEs) that supports QRNGs, QKDs and PQCs²⁹⁵².



Quantum eMotion (2007, Canada), formerly Quantum Numbers Corp, develops a cryptographic system based on a quantum random number generator (branded QNG2) and targets in particular mobile uses. It mainly communicates on the filing of an associated patent (Figure 678).

Let's hope it won't be a patent troller! The company seems to be licensing its technology to electronic component designers. It exploits research work from the Department of Physics at the University of Sherbrooke in Quebec. One of the patents relates to the generation of random numbers based on the random noise generated by some electron tunneling effect through a potential barrier²⁹⁵³. The QRNG speed reaches 1 Gbits/s and fits in USB key form factor. The company is listed on the Canadian Venture Exchange (CVE). The company expect to release a Blockchain using their QRNG in 2023.

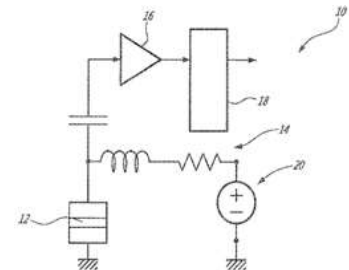


Figure 678: a patented QRNG.



Quantum Trilogy (2016, USA) created a secure communications solution based on applications (including for mail and voice communication) protected by an unspecified encryption, a QRNG to create real entropy in generated keys and servers that are protected at some level by a QKD.



QuBalt (2015, Germany) is a startup established between Germany and Latvia that develops solutions for post-quantum cryptography (PQC) and quantum algorithms.



Qubit Reset (2018, USA) develops quantum repeaters for QKD arrays. The company was founded by two Argentinians based in Miami. It is not listed in the Crunchbase and does not seem to have raised any funds, which seems to be a bad omen.



Qubitekk (2012, USA, \$5M) is a supplier of photon and entangled photon sources for second generation QKD deployments. In December 2022, it was deployed by EPB Quantum Network, a quantum networking branch of EPB, a Tennessee based energy utility and fiber optics telecom operator. This network target end-user companies and researchers and can be viewed as a testbed for benchmarking²⁹⁵⁴.



QuDoor (2016, China, \$7.8M) aka **Qike Quantum**, aka **Quantum Door**, aka **Guokai Quantum Technology** designs various products for QKD distribution, a trapped ion quantum processor supposed to reach someday 100 qubits (Tiansuan 1), a single photon source and a laser-based vibration quantum sensor.

QuDoor's cofounder and R&D track record include a commercial QKD system (2003), a waveform generator (2007), ion trapping (2012), quantum computing sensing (2015) and ion-phonon-photon entanglement function (2018).

²⁹⁵² See [Quantum Xchange Collaborates with Thales to Enable Quantum-Safe Key Delivery Across Any Distance, Over Any Network Media](#), November 2021.

²⁹⁵³ I found the complete PDF of USPTO patent 10437559 on <https://www.pat2pdf.org/>.

²⁹⁵⁴ See [Architecture of a First-Generation Commercial Network](#) by Duncan Earl et al, Qubitekk, November 2022 (11 pages).



Quintessence Labs (2006, Australia, \$49.3M) proposes a quantum random number generator and a QKD system. They use the CV-QKD technique which allows the use of existing fiber optic infrastructures of very high-speed telecom operators.



Qulabs (2018, India) is a jack-of-all-trade typical startup in India, created by Nixon Patel (CEO). It works in many fields like with the development of quantum inspired machine learning algorithms, building quantum memory storage (using their own software simulation tools) and at last, quantum secure direct communication (QSDC) sending quantum data without encryption or keys and quantum conference protocols (QCKA). At last, they also developed a blind quantum computing simulator.



Qunnect (2017, USA, \$12.4M) is a spin-off from Stony Brook University of Long Island created by Mehdi Namazi, Eden Figueroa, Noel Goddard and Mael Flament, Quantonation being one of their investors²⁹⁵⁵. Qunnect is developing a quantum product suite that enables long range quantum entanglement distribution protecting against photons loss.

Their repeaters are based on a quantum memory operating at room temperature, using warm rubidium vapor and without any requirement for vacuum- and/or cryogenic- support²⁹⁵⁶. This memory provides 100s of μ s of coherence time. They also develop their multi-laser multi-wavelength locking references and Qu-Source, a SFWM-based generated of entangled pairs of photons (Figure 679).

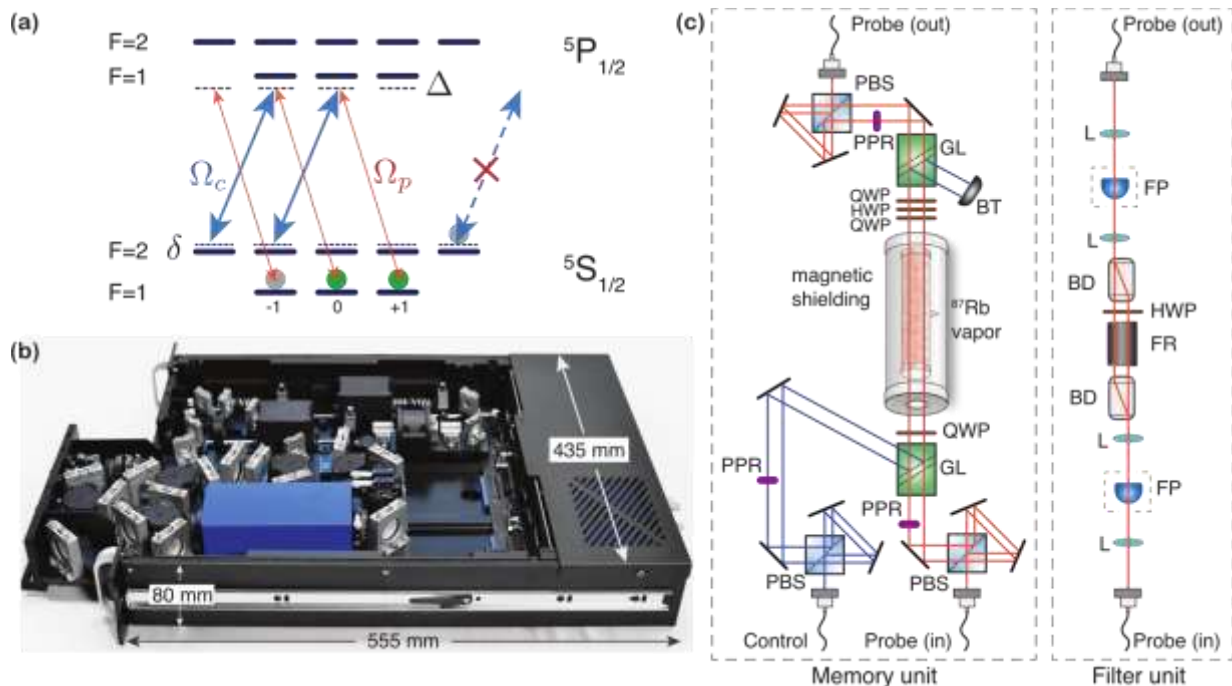


Figure 679: Qunnect repeater architecture. Source: [Field-deployable Quantum Memory for Quantum Networking](#) by Yang Wang, Alexander N. Craddock, Rourke Sekelsky, Mael Flament and Mehdi Namazi, May 2022 (16 pages).

²⁹⁵⁵ They received \$1.5 million of funding in April 2020 from the US Department of Energy under the Small Business Innovation Research Awards (SBIR) program. See [Qunnect receives \\$1.5M award from the DoE - Swiss Quantum Hub](#), April 2020.

²⁹⁵⁶ See [Field-deployable Quantum Memory for Quantum Networking](#) by Yang Wang, Alexander N. Craddock, Rourke Sekelsky, Mael Flament and Mehdi Namazi, May 2022 (16 pages). See also an explanation video, [Quantum Memories for long distance quantum networking](#) (3:40mn) and [Quantum Repeaters](#) which explains how it is deployed.

In May 2022, the company got two SBIR awards from the US DoE for \$1.85M to fund the development and commercialization of their quantum repeater product suite. In October 2022, the startup got a series A funding of \$8M led by Airbus Ventures Qconnect officially announces its Series A financing of over \$8 million. The round was led by Airbus Ventures with Quantonation, SandboxAQ, NY Ventures, Impact Science Ventures and Motus Ventures as other investors.

The company partners with various technology vendors like Exail, Welinq, Toptica, Q-CTRL, ColdQuanta and Single Quantum. It announced in 2023 the deployment of a new fiber loop expanding its existing quantum networking testbed GothamQ, from Brooklyn to Manhattan, connecting New York University to the Navy Yard.



QuSecure (2019, USA, \$1.7M) develops a secure blockchain solution that is resilient to quantum code breaking.

It seems that they are also developing a Blockchain that would be secured via QKD, and Blockchain security testing protocols. The startup is also doing cybersecurity consulting and, in particular, audits for the deployment of PQC. It was founded by Rebecca Krauthamer, who also founded the **Quantum Thought** startup mentioned above. In 2022, they were awarded a SBIR Phase III contract to become, surprisingly, the sole-source provider of PQC for over a dozen US federal agencies with their QuProtect solution. QuProtect is distributed by Arrow since 2023.



Ravel Technologies (2018, France) offers Ravel Homomorphic Encryption, a post-quantum and homomorphic encryption solution. The company was founded by Mehdi Sabeg.



SandboxAQ (2022, USA, \$500M) is a spin-out of Alphabet's Google AI that has a large breadth of activities, mostly around quantum related software applications and PQC software solutions.

Their first product offering is a multifunction Security Suite supporting PQC cryptography. They were selected in July 2022 as one of the 12 NIST partners to help the industry in the PQC migration path. In June 2023, the company was awarded a PQC contract for the US Defense Information Systems Agency (DISA) from the DoD, in partnership with Microsoft and Deloitte & Touche. In August 2023, they released Sandwich, an open source library designed to use other cryptography libraries, including PQCs to be standardized by NIST²⁹⁵⁷. It is accessible in Python, Rust and with the Go programming language.

The company also works on various quantum algorithms and on classical machine learning tools to exploit content from quantum medical image sensors. The company's CEO is Jack Hidary, a serial entrepreneur and book writer ("Quantum Computing: An Applied Approach") and its chairman is Eric Schmidt. In 2022, they made a strategic investment in evolutionQ and acquired Cryptosense (2013, France, \$5.7M).



Secure-IC (2010, France) is the leader of the RISQ project, which aims to create a French post-quantum crypto solution.

The company develops security hardware and software solutions that are used to evaluate the robustness of security solutions. The company is a spin-off from the Institut Mines-Télécom.



SECQAI (2021, UK) is a quantum cybersecurity company with a very broad goal to "provide world leading technologies to organisations of all sizes".

More precisely, they're in to "bringing together their own quantum and AI tech to create disruptive data and security products and services for organisations looking to gain a commercial advantage".

²⁹⁵⁷ See [Introducing Sandwich and the Journey Toward Modern Cryptography Management](#), SandboxAQ, August 2023.

The company was created by Rahul Tyagi, Dave Worrall and Martin Rudd. Rahul Tyagi developed a patented room temperature QRNG when he was the CEO of LyfGen. The patent USPTO 10606561 was filed in August 2018 and validated in March 2020. It is based on using slits-based diffraction and scattering entropy.



Smarts Quanttelecom (1991, Russia) proposes a quantum cryptography solution based on CV-QKD which exploits standard fibers of telecom operators.

Smarts was until 2015 a Russian mobile telecom operator. It has since become a telecom services operator with an offer of secure telecom links and data center and cloud services. Their QKD solution comes from Quanttelecom, a subsidiary of Smarts, developed jointly with the ITMO University of Saint Petersburg.



Sonora Gold and Silver Corp (2019, Canada) acquired in June 2021 a newly created startup, BTQ, that works on creating some quantum-safe Bitcoin solutions. BTQ was created in March 2021 in Lichtenstein.



SpeQtral Quantum Technologies (2017, Singapore), formerly S-Fifteen Space Systems, specializes in the distribution of QKD via satellite. They promote the work of the University of Singapore in the design of CubeSat-type pico-satellites for QKD key distribution.

They started in 2022 to work with Thales Alenia Space to test in 2025 a QKD distribution between their SpeQtral-1 satellites and Thales Alenia Space ground stations. In 2023, SpeQtral announced a partnership with RHEA System Luxembourg to build a QKD link between Singapore and Europe.



SSH Communications Security (1995, Finland, 14.1M€) is a cybersecurity company selling cybersecurity and SSH solutions. They sell NQX, a PQC-ready encryption solution among other cybersecurity solutions. In 2022, they released Tectia Quantum Safe Edition, a PQC protected SSH solution that protects remote access, file transfers and tunneling connections against the future quantum threat.



Surrey Satellite Technology or SSTL (1985, UK) wants to deploy a QKD-based quantum communications satellite built by Airbus Defense & Space (they are part of the Airbus group). The project is conducted in partnership with [Eutelsat](#) and ESA. The launch of the satellite was planned for 2020.



Synergy Quantum (2019, Switzerland) is a post-quantum encryption product and service startup that also supports data storage in a facility located in a former military bunker in the Swiss Alps.

They target governments, financial services, healthcare, smart Cities, energy, and telecom sectors. The company is run by Jay Oberai (CEO), Arun K. Pati (Chief Scientific Officer), Mayank Sharma (VP Engineering), Vipin Kumar Rathi (VP Technology Architecture) and Manu Khullar (Chief Operating Officer). Any non-Indian there? Yes, with John Paukulis (CMO, USA) and Sasha Lazarevic (Head of Government Partnerships) and Jake Hwang (Head of Business Development and Investor Relations). It launched in 2022 a joint venture with the Quantum Technology Hub of the Indian Government. They seem to also offer some services in the QKD realm, including some that are provided as part of this deal in India.

Taqbit Labs (2018, India) sell solutions for QKD. Their website and communication are so vague that it's impossible to understand whether they sell third party QKD products with some integration service of develop QKD hardware products of their own, and if so, in what category given most vendors don't reinvent the wheel to become full-stack vendors.

Terra Quantum (Switzerland) is also working on QKD. In 2023, it announced a world record for long-distance QKD operating with optical-fiber cables over 1,032 kilometers at a (relatively) high key rate of 34 bits per second²⁹⁵⁸.



ThinkQuantum (2021, Italy) is a spin-off of the University of Padua which develops QKD and QRNG solutions for simple fiber optics deployments as well as for free space and satellite QKD.



Ultimaco (1983, Germany) sells lattice based PQC embedded in Hardware Security Modules (HSMs). This solution is based on Picnic, one of the alternate PQC digital signature candidates selected by the third round of the NIST PQC challenge in July 2020.



VeriCloud (2017, France) is a startup created by Elham Kashefi, and Marc Kaplan (France) and Joshua Nunn (UK). It is specialized in the creation of quantum software solutions adapted to quantum telecommunications for both QKD and distributed quantum processing.

Their offer is based on the Qline, a software solution that enables the deployment of a multi-point quantum network with a lower cost in hardware infrastructure (Figure 680). With this architecture, nodes that are very expensive can be replaced by simple modulators that are much more affordable. The operation is based on a kind of "time-sharing" of the line²⁹⁵⁹. This lowers the hardware addition by about two thirds on a typical installation below with two intermediate stations in the network. At both ends of the line there is on one side a laser and modulator-based photon generator and on the other side a single photon detector, the most expensive part of the equipment ranging from 20K€ to 100K€. The solution is deployable on networks totaling 100 to 200 km.

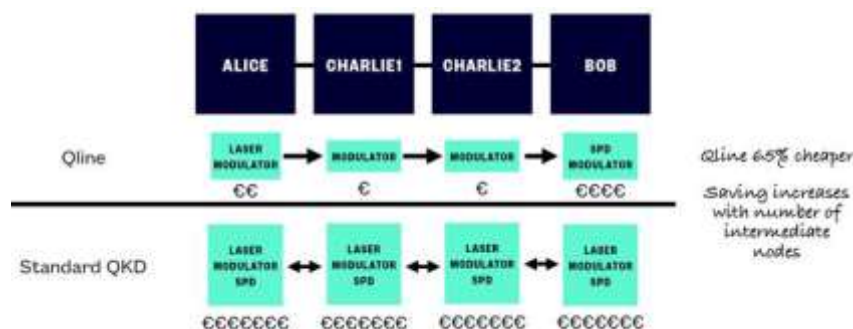


Figure 680: VeriCloud qline architecture. Source: VeriCloud.

The first application is QKD quantum key distribution. They can interoperate with classical QKD networks. Initially, secure file transfer and instant messaging are targeted as applications associated with QKD. The system can also be used to generate disposable masks²⁹⁶⁰.

The VeriCloud solution is also relevant for securing data storage. It has also been tested at a small scale for blind computing architecture²⁹⁶¹.

²⁹⁵⁸ See [Forty Thousand Kilometers Under Quantum Protection](#) by N. S. Kirsanov et al, Terra Quantum, January 2023 (17 pages).

²⁹⁵⁹ See [Establishing shared secret keys on quantum line networks: protocol and security](#) by Mina Doosti, Lucas Hanouz, Anne Marin, Elham Kashefi, Marc Kaplan, April 2023 (23 pages).

²⁹⁶⁰ See [How to build quantum communication networks at a small scale](#) by Marc Kaplan from VeriCloud, May 2020.

²⁹⁶¹ See [Multi-client distributed blind quantum computation with the Qline architecture](#) by Beatrice Polacchi, Marc Kaplan, Fabio Sciarrino, Elham Kashefi et al, Nature Communications, June-November 2023 (27 pages).



WIS@key Semiconductor (1999, Switzerland, \$256M) is a cybersecurity, AI, Blockchain, and IoT company that developed QUASARS (QUAntum resistant Secure ARchitectures project), a RISC V platform base security solution supporting PQC cryptography.

Sealsq is a subsidiary from WiSeKey which develops PKI and Post-Quantum technology hardware and software solutions.



Xiphera (2017, Finland, 480K€) is providing hardware-based security solutions, including their PQC based xQlave product family IP cores that can be used in FPGA and ASIC circuit designs. It supports CRYSTALS-Kyber and CRYSTALS-Dilithium.



XT Quantech (2017, China) specializes in CV-QKD distribution equipment after initially focusing on DV-QKD solutions. The CV-QKD is essential because it can coexist in the fiber links of telecom operators.

They offer server appliances for QKD key encoding and decoding gateways. Its full name is Shanghai Xuntai Information Technology Co. The company also sells a QRNG, their XT-QRNG100 that is certified in ... China.



ZY4 (2014, Canada) develops post-quantum cryptography solutions based on their in-house concept of the Shannon Event Horizon which would be a new class of PKI and random number generation²⁹⁶².

²⁹⁶² See their white paper [Introducing the Shannon Event Horizon](#), 2019 (20 pages).

Quantum telecommunications and cryptography key takeaways

- Quantum computing poses a theoretical threat to many existing cryptography systems, particularly those using public key distribution in asymmetric cryptography. This is due to Peter Shor's integer factoring algorithm that could efficiently break RSA public encryption keys in the far distant future. But other algorithms than Shor are creating various threats, including for symmetric key distributions. However, these threats are usually exaggerated, particularly by security solutions vendors.
- As a result, two breeds of solutions have been elaborated that use either mathematical or physical protection. The first one is based on quantum key distribution, requiring a photonic transmission channel (terrestrial, free-to-air, satellite or fiber-based), and using either prepare-and-measure key transmission or quantum entanglement resources for the next generation adapted to the quantum Internet connecting quantum computers and sensors together. Beware of a common misconception: these solutions are not based on quantum computers. Quantum computers are not (yet) making cryptography safer although some solutions are proposed to secure data transmission, but, interestingly, without any encryption in the classical meaning.
- The second option is to create classical cryptographic protocols generating public encryption keys that are not breakable by quantum computers. The USA NIST launched in 2016 an international competition to standardize a set of post-quantum cryptography (PQC) protocols. Four finalists were selected as NIST standard in July 2022, one for a public key interface (PKI) and three for signatures and they are now draft standards. They are currently a draft standard. Solutions deployments should happen next and be done way before the quantum computing menace will materialize, if it does some day. NIST may select other PQC solutions in the future. PQC solutions are popping up in various fields like to secure blockchains and Internet of things (IoT). However, PQC safety should not be taken for granted as side attack channels and other workaround seem to be discovered by some cryptanalysts.
- Quantum random numbers generation is/will be used for classical cryptography, and quantum cryptography. It provides sources of both random and non-deterministic numbers used in cryptography systems. It has other used cases when randomness is mandatory in classical computing like with lotteries and various simulation tools.
- Quantum telecommunications can also use quantum entanglement to enable communications between quantum computers and/or quantum sensors. Distributed quantum computing has two potential benefits: scale quantum computing beyond the capacity of individual quantum computers and enable safe communications between quantum computers. Distributed quantum sensing can enable better accuracy sensing.
- Quantum Physical Unclonable Functions are cryptographic solutions used to authenticate physical objects in an unfalsifiable quantum way. It is, however, still an immature technology.
- There are already many startups in the QKD and PQC scene. Deployments have already started worldwide, particularly in China with both landline fiber and satellite links. Europe is also experimenting quantum communication networks.

Quantum sensing

Quantum sensing is about the various precision measurement solutions that rely on second generation quantum technologies and go beyond the limits of classical measurements systems. It also often allows non-invasive measurements to be carried out on various solid or organic materials. The main physical values measured are time, distances, gravity, magnetism, temperature, and electromagnetic spectrum analysis.

Quantum sensing use-cases and market

Many applications use these technologies like radars, sonars, very high sensitivity microphones or the field of imaging in general and particularly in medical imaging²⁹⁶³ (Figure 681).

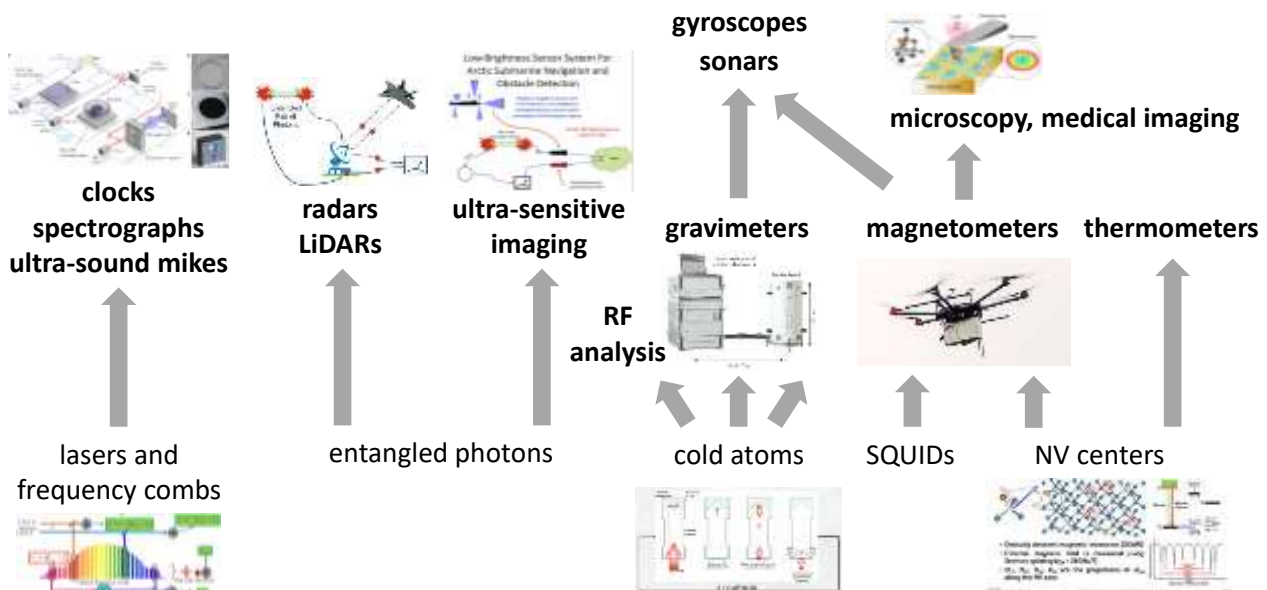


Figure 681: a map of various quantum sensing basic technologies and use cases. (cc) Olivier Ezratty, 2021-2023.

Some of these technologies have commonalities with the various qubit types we have already explored in detail. This is particularly the case for cold atoms, NV centers and superconducting qubits. Precision magnetometers use NV centers as well as SQUIDs (Superconducting Quantum Interference Device), which also measure the direction of current in superconducting flux-type qubits and are used by D-Wave in quantum annealers. Besides a couple exceptions like Inflektion, most quantum sensors vendors are pure players in the sensing space (Figure 684) or classical sensors vendors who extend their product range with quantum sensors.

Many of these quantum measurement technologies make extensive use of photonic tools, either directly based on photons (lasers, frequency combs, entangled photons) or exploiting cold atoms and even NV centers, whose quantum state of interest is then evaluated by measuring their fluorescence.

²⁹⁶³ See [Quantum Sensing Use Cases 2022](#), SRI for QED-C, September 2022 (36 pages), a report on quantum sensors which makes an interesting inventory of use cases and market readiness, with an eye on national security issues. It is focused on four types of sensors, for time, inertial, magnetic field and electric field measurement. It doesn't cover other sensors categories reviewed in this part like frequency monitoring sensors, quantum radars (which may be mythical objects), quantum pressure sensors, quantum chemical sensors and quantum thermometers.

Some of these technologies are already commercially viable and continue to progress steadily. It is still a niche market made of many sub-niche markets, evaluated at around \$1B and expected to double in a decade. The two largest applications markets are transportation and medical imaging (Figure 682, Figure 683).

But these forecasts may become wrong since some use cases might at some point become mainstream and drive more market growth. This is the case of GPS without satellite links using micro-magnetometers. It could for example someday equip many classical and autonomous vehicles.

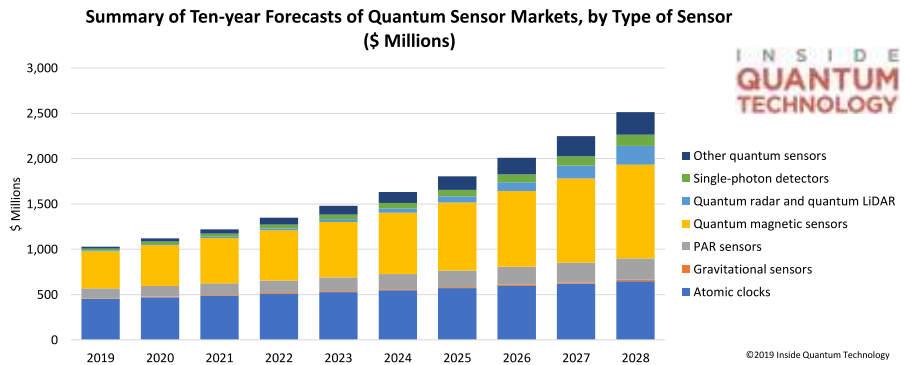


Figure 682: Source: [Quantum Sensors: Ten Year Market Projections](#) by Lawrence Gasman, 2019 (7 slides).

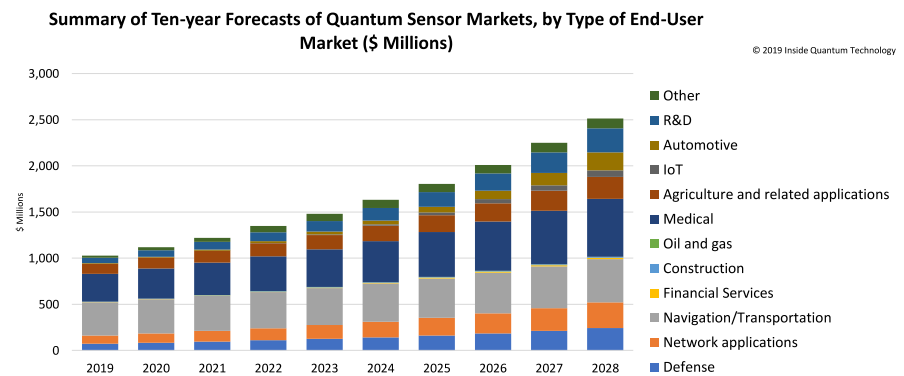


Figure 683: Source: [Quantum Sensors: Ten Year Market Projections](#) by Lawrence Gasman, 2019 (7 slides).

atomic clocks

- TELEDYNE O2V
- Microsemi
- SAFRAN
- QUANTIX
- LA

optical sensing

- OXFORD HIGHQ
- Twinleaf
- Qubic
- QUPIN
- entanglement
- DEVICES
- zeropoint motion

NV centers

- THALES
- FieldLine
- SBtech
- chipiron
- qutools
- Southwest Sciences
- kwan-tek
- SENSORIX
- cerca
- NVISION
- ODMR
- Qnami
- ODT
- BOSCH
- QUANTUM DIAMONDS
- SANDBOX AQ

SQUIDs

- THALES
- supracon
- HYPRES
- other
- MAG Health

cold atoms

- exail
- GEM
- THALES
- ATOMIONICS
- OK Quantum
- NOMAD
- Delta.g
- RYDBERG
- AQUARK TECHNOLOGIES

enabling

- HYPERLIGHT
- TMD
- Vescent

NV center diamonds

- elementsix
- LUCIGEM
- LakeDiamond
- DIAMFAB
- GREAT LAKES CRYSTAL TECHNOLOGIES
- DRSAY PHYSICS
- IZABRE
- ADAMAS CRYSTAL
- THE BOLLER
- CYMARIS LABS
- BIKANTA
- Diatope
- STAR CRYDELECTRONICS
- THALES mini-cryostats
- AO Sense
- TMD
- RYDBERG

Figure 684: and now ladies and gentlemen, here is the magnificent market map for quantum sensing, including some of their enabling technologies. (cc) Olivier Ezratty, 2023-2024.

Various other markets are relevant for quantum sensing: the energy and utilities sector²⁹⁶⁴, telecoms, space and astrophysics research²⁹⁶⁵, high-energy particles physics research²⁹⁶⁶ ²⁹⁶⁷, civil engineering, manufacturing industries using many sensors like for quality control and non-destructive testing and control, and of course, the aerospace and defense.

International System of Measurement

Sensing cannot be discussed without being connected to the **International System for Measurement** (or International System of Units, aka SI). It was recast after a unanimous vote on the Versailles Metre Treaty signed at the 26th General Conference on Weights and Measures (CGPM) in November 2018²⁹⁶⁸. Its implementation started on May 20, 2019.

The new 2019 SI updates the definition of the kilogram, ampere, kelvin and mole. It is built around seven fixed constants: a number of hyperfine transitions of cesium 133, the speed of light in vacuum²⁹⁶⁹, the Planck constant, the elementary charge of an electron, the Boltzmann constant, the Avogadro number or constant and the luminous efficiency. From these constants are derived the seven basic units of the system: kilogram, meter, second²⁹⁷⁰, ampere, kelvin, mole and candela (Figure 685).

It no longer relies on materials that are degrading over time, such as the standard kilogram kept at the BIPM in Saint-Cloud, or on the triple point of water (gel) which defined the kelvin, and which depended on its isotopic composition.

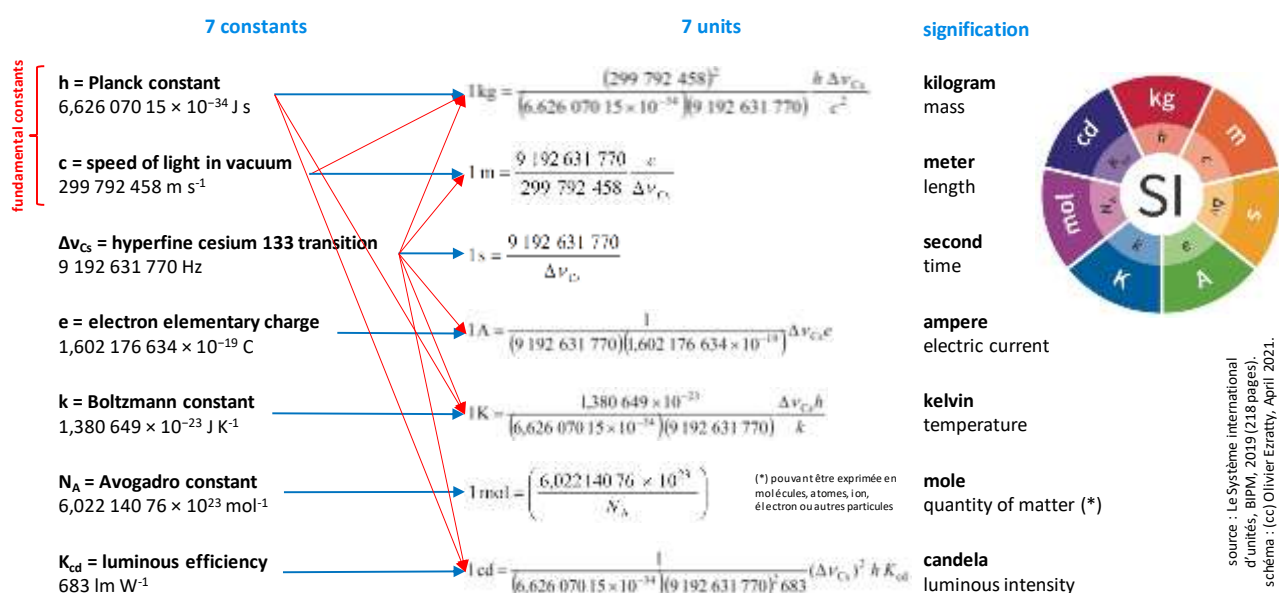


Figure 685: reconstruction of the SI constants, units and their signification. Source: (cc) Olivier Ezratty, 2021.

²⁹⁶⁴ See [Quantum Sensing for Energy Applications: Review and Perspective](#) by Scott E Crawford, Roman Shugayev, Hari P. Paudel and Ping Lu, June 2021 (33 pages).

²⁹⁶⁵ See [Quantum Communication, Sensing and Measurement in Space](#) by Baris I. Erkmen et al, 2012 (136 pages).

²⁹⁶⁶ See the review paper [Quantum Sensors for High Energy Physics](#) by Aaron Chou et al, November 2023 (63 pages).

²⁹⁶⁷ See [Snowmass 2021: Quantum Sensors for HEP Science -- Interferometers, Mechanics, Traps, and Clocks](#) by Daniel Carney et al, March 2022 (29 pages)

²⁹⁶⁸ See [The International System of Units \(SI\)](#), NIST, 2019 (13 pages) and [The International System of Units](#), BIPM, 2019 (218 pages).

²⁹⁶⁹ The definition of the speed of light at 299 792 458 m s⁻¹ dates from 1983.

²⁹⁷⁰ The second was defined with 9 192 631 770 periods of the hyperfine transition of cesium 133 at a temperature close to 0K since the 13th CGPM of 1967. Previously, it was a fraction of the solar day, which was not stable.

The mole was previously defined on the basis of 0.012 kg of ^{12}C ²⁹⁷¹. The standard meter, which is kept in the Archives in Paris, was no longer the reference since 1960. All other units of measurement such as hertz, joule, coulomb, lumen or watt are derived from constants and base units. This measurement system is branded as being "quantum" because it is based on the measurement of fundamental phenomena that bring us back to quanta, in particular for the definition of the second, which uses quantized energy transitions in the cesium atom, and that of the kilogram, which uses the Planck constant, itself a foundation of quantum physics.

Numerous quantum physics works related to these evolutions of the international measurement system, notably at NIST, have a link with the commercial devices discussed in this section.

Quantum sensing taxonomy

Reusing a definition found on C.L. Degen et al's 2017 review paper²⁹⁷², quantum sensing describes the use of quantum systems, quantum properties and phenomena to measure physical quantities. The first quantum sensors were SQUID magnetometers, atomic vapors, and atomic clocks. Then, the field was expanded to cover magnetic and electric fields, time and electromagnetic waves frequencies, mechanical rotations, temperature and pressure quantum measurement.

New "second generation" sensors work at the single-atom and spin level and may use quantum entanglement as a resource for increasing sensitivity.

Quantum sensing can use either or the following phenomenon corresponding to type I, II and III quantum sensors:

- **Type I:** using a quantum object to measure a physical quantity, characterized by quantized energy levels and a non-classical state, like a squeezed state, that is not entangled with the receiver.
- **Type II:** transmits a classical state that is not entangled with the receiver and use a quantum-enhanced detection technique in the receiver using, for example, quantum coherence, wave-like spatial or temporal superposition states to measure a physical quantity.
- **Type III:** using quantum entanglement to improve the sensitivity or precision of measurement. It is sometimes labelled as "quantum metrology", "quantum-enhanced sensing" or "second generation quantum sensing".

The difference between quantum sensing and quantum metrology is not that clear in the scientific literature. Quantum metrology is used for devices measuring units or fundamental constants such as an atomic clock or an atom interferometer measuring the fine structure constant, or constants that were used to create the last SI²⁹⁷³. It can relate to the study of quantum-based precision measurements and quantum sensing using entanglement as seen in the above type I/II/III taxonomy.

The table in Figure 686 lists several types of known quantum sensors with their type, the physical nature of the measuring object ("qubit nature") and the measured physical quantities. For example, charged systems like trapped ions are sensitive to electrical fields while spin-based systems mainly respond to magnetic fields. Some quantum sensors may respond to several physical parameters or measure indirectly some physical quantity, which is the case for quantum thermometry with NV centers. Most of the time, quantum sensing exploits changes in the transition frequency or the transition rate in response to an external signal.

²⁹⁷¹ With the new SI, one gram of matter contains N_A multiplied by the number of nucleons (protons and neutrons) of the element in question (atom, molecule). This comes from the fact that in an atom, the majority of the weight is in the atom nucleus. Electrons have a mass equivalent to 1/1836 times that of a single nucleon.

²⁹⁷² See [Quantum sensing](#) by C. L. Degen, F. Reinhard and P. Cappellaro, June 2017 (45 pages).

²⁹⁷³ See [What is the difference between quantum sensing and quantum metrology?](#), 2020.

sensor type		qubit nature	type I	type II	type III	rotation	acceleration	force	pressure	displacement	time	frequency	refractive index	magnetic field	electric field	voltage	temperature	mass
neutral atoms	atomic vapor	atomic spin	X	X	X						X	X		X				
	cold atom clouds	atomic spin	X	X			X				X	X		X				
Rydberg atoms		Rydberg states	X	X											X			
trapped ions		electronic state	X	X	X				X		X	X						
		vibrational mode	X						X							X		
solid state	spin ensembles	NMR		X										X				
		NV/SiC center ensembles		X		X				X				X	X		X	
	single spins	P donor in Si		X										X				
		quantum dot		X	X									X	X			
		single NV center		X		X				X				X	X		X	
superconducting circuits	SQUIDs	supercurrent	X	X										X				
	flux qubits	circulating current		X										X				
	charge qubits	charge eigenstates		X											X			
single electron transistor		charge eigenstates	X												X			
optomechanics		phonons	X				X	X						X		X		
interferometer		photons, atoms		X	X	X				X			X					

(cc) Olivier Erratty, 2022-2024, based on Quantum sensing by C. L. Degen, F. Reinhard and P. Cappellaro, June 2017

Figure 686: quantum sensing taxonomy. Source: table reconstructed and updated from [Quantum sensing](#) by C. L. Degen, F. Reinhard and P. Cappellaro, June 2017 (45 pages).

The rest of this quantum sensing part is mostly organized along the first row and its green/blue measured values: gravity, time, magnetism, temperature, radiofrequencies and then to higher-level applications like imaging, radars and lidars and chemical sensors.

Quantum sensors are a bit paradoxical: after a measurement of a quantum sensing qubit, the only information you retrieve is a single classical bit (0 or 1). So how to you get a floating number with a large precision? The answer is simple for the most basic cases: you make many measurements and average their results. But there are other subtleties. With NV centers sensors, you create a spin resonance spectrum with repeat measurements and the shape of the resulting curve enables you to determine the detected magnetic field by computing the distance between two curve peaks. It is an indirect measurement.

A quantum sensor measurement precision will depend on several parameters: the sampling rate (how many measurements are made with the same sensors or similar sensors in parallel), the sensor noise and the sensor sensitivity.

Which brings us to define some key concepts related to quantum measurement precision with more details. Quantum sensing has its own semantic zoology with measurements, estimators, estimations, precisions, variances, statistics, limits, bounds and the likes. I try here to clarify some of the quantum sensing lingua, given there are many inconsistencies in the related literature.

Quantum Fisher Information (QFI) is a fundamental limit of precision in quantum measurements which are subject to intrinsic limitations due to quantum uncertainty²⁹⁷⁴. It quantifies how well a parameter of interest can be estimated in a quantum system and the level of multipartite entanglement in use. Measuring it can help qualify the quality of multipartite entanglement with computing qubits²⁹⁷⁵. Some techniques like quantum error mitigation can be used to reach that limit in quantum sensing²⁹⁷⁶. QFI is the quantum variation of classical Fisher Information (FI).

²⁹⁷⁴ See [Variational Quantum Metrology with Loschmidt Echo](#) by Ran Liu et al, China, November 2022 (20 pages).

²⁹⁷⁵ See [Estimation of the Quantum Fisher Information on a quantum processor](#) by Vittorio Vitale, Cyril Branciard, Benoît Vermersch et al, August 2023 (24 pages).

²⁹⁷⁶ See [Quantum-Error-Mitigation Circuit Groups for Noisy Quantum Metrology](#) by Yusuke Hama et al, March-April 2023 (42 pages).

Cramér Rao Limit (CRL) is a theoretical lower bound on the variance of any unbiased estimator for a parameter in a statistical model. It gives the best possible precision achievable when estimating a parameter based on a set of single or multiple measurements. It is applicable in classical and quantum statistical contexts.

Cramér Rao Bound (CRB) refers to the actual minimum variance attainable by any unbiased estimator. The CRB is related to the Fisher Information as shown in the generic formulae in Figure 687. Running simultaneous estimation of multiple parameters in an experiment involves the QFI matrix (QFIM). The inverse of this matrix yields the quantum Cramér–Rao bound (QCRB), a lower bound on the uncertainty of any unbiased estimator of the parameters.

Shot-Noise Limit (SNL) is the type of noise due to the discrete nature of certain physical processes, such as the counting of photons or the detection of particles, associated with the statistical fluctuations in the number of these discrete events. SNL refers to the minimum uncertainty or variance in measurements that occurs when shot noise dominates the overall noise in a particular measurement setup. It has an influence on the Quantum Fisher Information of a quantum measurement and on the various ways to reach or exceed the Standard Quantum and the Heisenberg limits in sensing precision.

Standard Quantum Limit (SQL) is a limit on the precision of quantum measurements when implemented using classical light without entanglement or squeezing. Its cause is the Heisenberg uncertainty principle, which imposes a fundamental limit on the simultaneous precision of complementary observables. The best precision possible scales as $1/\sqrt{T}$, with T being the number of times the preparation and measurement process is done. An SQL is a special case of CRB.

Heisenberg Limit (HL) is the limit on the precision of quantum measurement when using certain complementary quantum observables can be simultaneously measured. It is obtained with using non-classical states of light and nonstandard measurements, like photon squeezed states (used in the LIGO interferometer experiment), entanglement of multiple similar quantum objects or quantum interferences. It can lower the precision below the Standard Quantum Limit, with a better scaling of $1/N$, N being the number of objects used in the measurement²⁹⁷⁷. This corresponds to Type III quantum sensing when entanglement is at play. Since entanglement is never perfect and has its own noise, it is argued by some quantum physicists that the Heisenberg limit is practically hard to reach^{2978 2979}. An HL is another special case of CRB.

Beyond Heisenberg Limit (BHL) corresponds to sensing situations when the obtained precision is better than the Heisenberg Limit. It usually consists in using various combinations of photon squeezing, entanglement and interferences as well as quantum signal processing techniques^{2980 2981}. It could help scale precision up to $1/N^2$ and even $1/2^N$ ^{2982 2983}. But some are arguing that quantum squeezing cannot practically beat the standard quantum limit²⁹⁸⁴.

²⁹⁷⁷ In many documents, the T in the Standard Quantum Limit seems to be confused with the N in the Heisenberg limit while these are not at the same metric. This is well explained in [General optimality of the Heisenberg limit in quantum metrology](#) by Marcin Zwierz, Carlos A. Pérez-Delgado and Pieter Kok, PRL, 2010 (4 pages).

²⁹⁷⁸ See [Quantum metrology and its noisy effects](#) by Lin Jiao et al, Lanzhou University, July 2023 (22 pages).

²⁹⁷⁹ See the thesis [Heisenberg Limit beyond Quantum Fisher Information](#) by Wojciech Górecki, April 2023 (103 pages).

²⁹⁸⁰ See [Beyond Heisenberg Limit Quantum Metrology through Quantum Signal Processing](#) by Yulong Dong et al, September 2022 (54 pages).

²⁹⁸¹ See [Sub-SQL electronic field sensing by simultaneously using quantum entanglements and squeezings](#) by X. N. Feng et al, August 2023 (10 pages).

²⁹⁸² See [Generalized Limits for Single-Parameter Quantum Estimation](#) by Sergio Boixo, Steven T. Flammia, Carlton M. Caves, and JM Geremia, PRL, 2007 (4 pages).

²⁹⁸³ See [Exponentially Enhanced Quantum Metrology](#) by S. M. Roy and Samuel L. Braunstein, PRL, 2008 (4 pages).

²⁹⁸⁴ See [Quantum squeezing cannot beat the standard quantum limit](#) by Liam P. McGuinness, June-July 2023 (25 pages).

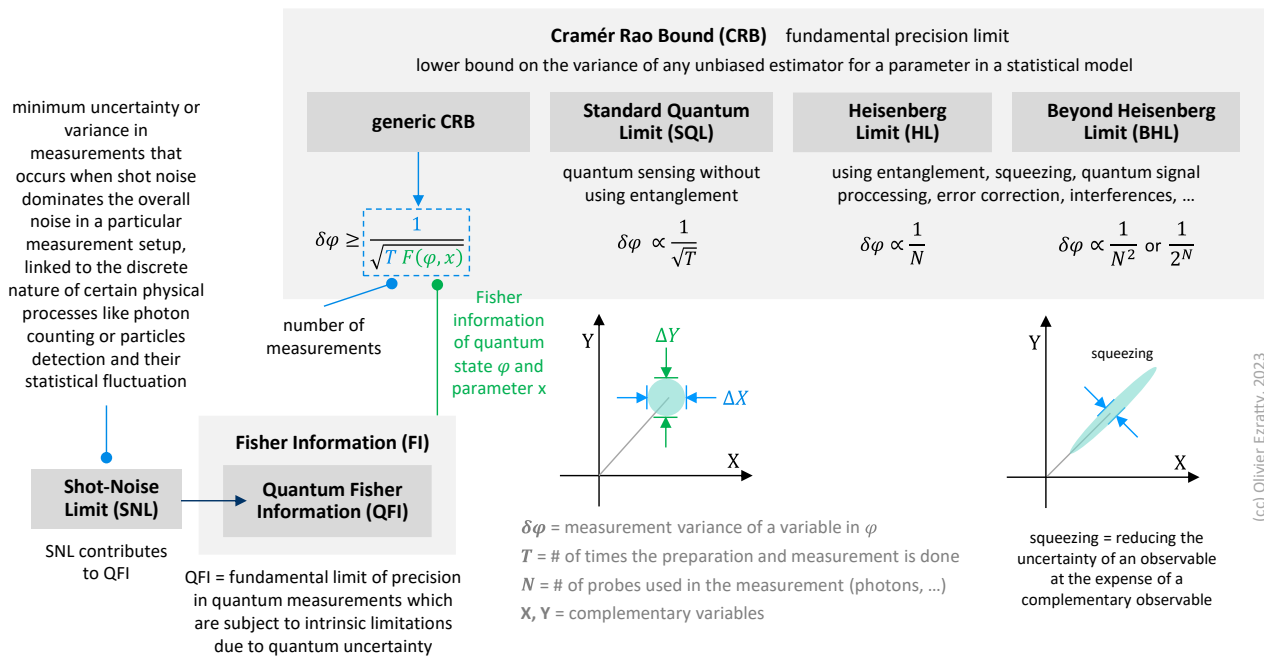


Figure 687: mapping of the various quantum measurements limits. (cc) Olivier Ezratty, 2023.

Let's also mention a developing field: quantumly networked sensors. This networking could have several benefits like connecting ensembles of quantum sensors to collectively improve their sensitivity^{2985 2986}, to connect them to some quantum computers to help these directly capture some quantum data and accelerate the processing of sensed data, and, to separate in a trusted way the state preparation, parameter encoding, measurement and data collection tasks²⁹⁸⁷.

Quantum gravimeters, gyroscopes and accelerometers

Quantum gravimeters measure gravity with a very high accuracy. These are useful in many scenarios: in seismic detectors and volcanoes monitoring, for precision autonomous navigation complementing GPS in airplanes, ships, submarines, and drones, for gravity field mapping, for detecting subterranean holes before undergoing constructions, for detecting groundwater, ice mass change, for oil and mineral exploration (well, to be restrained) and for the detection of gravitational waves in astronomy. One talked about use case is the detection of nuclear submarines, which would destabilize or neutralize nuclear deterrence used by nuclear countries owning these submarines, but its practicality is still questioned²⁹⁸⁸.

There are two categories of gravimeters. Absolute gravimeters measure the gravity per se measuring the free trajectory of a test mass in vacuum, and now, with cold atoms, their interferences. Relative gravimeters measure the variation of gravity over space and also time. They are usually calibrated using absolute gravimeters. The most precise relative gravimeters are superconducting based, but are not considered as quantum gravimeters.

²⁹⁸⁵ See [Distributed quantum sensing with a mode-entangled network of spin-squeezed atomic states](#) by Benjamin K. Malia, Mikhail Lukin, Ronald L. Walsworth et al, May 2022 (7 pages) and [Quantum Logic Enhanced Sensing in Solid-State Spin Ensembles](#) by Nithya Arunkumar, Ronald L. Walsworth et al, March 2022 (7 pages).

²⁹⁸⁶ See [Parallel Quantum-Enhanced Sensing](#) by Mohammadjavad Dowran et al, University of Oklahoma, Oak Ridge National Laboratory, November 2023 (12 pages).

²⁹⁸⁷ See [Quantum Metrology with Delegated Tasks](#) by Nathan Shettell and Damian Markham, December 2021 (20 pages).

²⁹⁸⁸ An airborne array of SQUIDs magnetometry detection of submarine was supposedly prototyped in China in 2017. It requires cooling but that's not a big deal for such a use case. See [China's quantum submarine detector could seal South China Sea](#) by David Hambling, New Scientist, 2017. Found in [Quantum Technology and Submarine Near-Invulnerability](#) by Katarzyna Kubiak, European Leadership Network, December 2020 (18 pages).

The quantum measurement of gravity is generally performed with cold atom interferometers (CAI), taking advantage of the wave-particle of cold atoms²⁹⁸⁹. The technique has been developed since 1991 and perfected since then²⁹⁹⁰. The principle consists in creating a source of cold atoms free falling in suspension, generally rubidium, preparing their state with lasers, then passing them through a three-stages laser-controlled atom interferometer and then analyzing the results.

In the USA, NIST and NOAA in partnership with Institute for Applied Geodesy (IFAG), Germany, developed the FG5 absolute gravimeter that was tested starting in 1993. It was using a free falling rubidium atoms vacuum chamber and an interferometer. Stanford created a cold atom gyroscope in 2006 which led to the creation of AOSense. In France, SYRTE developed a six-axis inertial sensor using two magneto-optical-traps (MOTs), also in 2006.

In June 2023, the **UK Royal Navy** conducted a trial of a cold atom quantum navigation system avoiding the use of GPS to determine a vessel's location anywhere on earth. The system that was tested in a Qinetiq NavyPOD container placed on deck of the 500 tons experimental ship XV Patrick Blackett was designed by physicists from the Centre for Quantum Engineering, Science and Technology (QuEST) at the Imperial College in London. It could also potentially be used by submarines.

A related field is gradiometry, which measures horizontal or vertical gravity gradients. It is used for the measurement of the variations or anomalies in the Earth's gravity field with creating gravity maps over the earth to either improve geopositioning or to detect changing underground features over time. It requires specific settings and techniques to reduce noise and vibrations within the gravimeter²⁹⁹¹. ONERA launched gradiometry experiments in 2009 (GIRAFE project) and in 2014-2016 (GIRAFE2)²⁹⁹². It will be tested by the French Navy in a surface vessel in 2023 and deployed on 4 vessels by 2026/2027. The goal is to create a map of underneath the oceans.

Related sensing fields are rotation measurement and gyroscopes which are implementing it. Quantum gyroscopes can be implemented with optical interferometry^{2993 2994} and, surprisingly, with superfluid ⁴He²⁹⁹⁵.

The figures of merits of quantum gravimeters are their **sensitivity** (smallest detectable change in gravity, measured in m/s² or cgs gals, for centimeter-gram-seconds, in reference to Galileo), **accuracy** (measurement uncertainty in reference to an absolute standard, is a %) and **stability**. Operational figure of merits are weight, size and warm-up time (which can last one hour). Best-in-class cold atom absolute gravimeters have a sensitivity of 10⁻⁹ m/s². Interesting miniaturization designs are also proposed, although they lead to a lower sensitivity measurement²⁹⁹⁶.

²⁹⁸⁹ See [Experimental gravitation and geophysics with matter wave sensors](#) by Philippe Bouyer, LP2N, 2018 (234 slides).

²⁹⁹⁰ See [Atomic Interferometry Using Stimulated Raman Transitions](#) by Mark Kasevich and Steven Chu, PRL, July 1991 (4 pages) and [Young double-slit experiment with atoms: A simple atom interferometer](#), from Olivier Carnal and Jürgen Mlynek, 1991 (6 pages) which describes a Young's double-slit interferometry experiment with helium atoms. See also [Experimental gravitation and geophysics with matter wave sensors](#), LP2N, 2018 (234 slides).

²⁹⁹¹ See recent advances with [Quantum sensing for gravity cartography](#) by Ben Stray, Kai Bongs et al, Nature, February 2022 (14 pages), [Position fixing with cold atom gravity gradiometers](#) by Alexander M. Phillips, April 2022 (10 pages) and [Circulating pulse cavity enhancement as a method for extreme momentum transfer atom interferometry](#) by Rustin Nourshargh, Kai Bongs et al, December 2021 (9 pages).

²⁹⁹² See [ONERA invents with SHOM the "atomic" precision gravity mapping](#), February 2016. SHOM is the Hydrographic and Oceanographic Service of the French Navy.

²⁹⁹³ See [Quantum optical gyroscope](#) by Lin Jiao and Jun-Hong An, January 2022 (7 pages).

²⁹⁹⁴ See [Nonlinear Multi-Resonant Cavity Quantum Photonics Gyroscopes Quantum Light Navigation](#) by Mengdi Sun et al, Virginia Tech, July 2023 (17 pages).

²⁹⁹⁵ See [Superfluid helium-4 whistles just the right tune](#) by Robert Sanders, UC Berkeley, 2005

²⁹⁹⁶ See [A Compact Cold-Atom Interferometer with a High Data-Rate Grating Magneto-Optical Trap and a Photonic-Integrated-Circuit-Compatible Laser System](#) by Jongmin Lee, July 2021-September 2022 (21 pages). It uses a compact titanium vacuum package with a grating chip inside a tetrahedral grating magneto-optical trap (GMOT) using a single cooling beam. The sensitivity is 2x10⁻⁶.

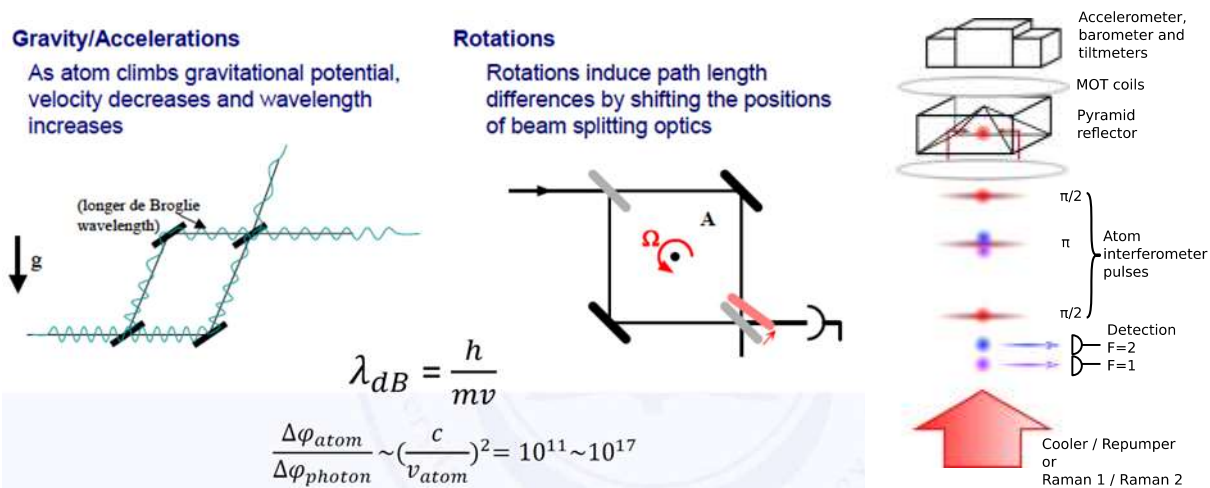


Figure 688: how cold atom interferometry works to measure both gravity, accelerations and rotations. Source: [Compact and Portable Atom Gravimeter](#) by Shuai Chen, University of Science and Technology of China, June 2019 (22 slides) and [Muquans](#).

Other cold atom use cases include magnetic field measurement in earth monitoring and temperature measurement. Hybrid sensors can associate electrostatic and cold atom acceleration sensors. Cold atom interferometry will even be used for gravitational waves detection in the MIGA experiment being setup in France²⁹⁹⁷.

Here are the various vendors also positioned in this market, given many are still in the product development phase and don't have yet a commercial offering.



AOSense (2004, USA) creates and sells quantum gyroscopes, commercial optical clocks and develop a quantum gravimeter. It also provides instrumentation equipment with cold atom generators and laser frequency comb generators

They collaborate with IonQ for their quantum computers based on trapped ions. It is a spin-out from Stanford and a pioneer in the sector who is now highly diversified.



M Squared (2006, UK, \$56M) has been developing a cold atom quantum gravimeter for a long time but withdrew from this market and focused back on its original lasers business covering the spectrum from 200 nm to 4,000 nm. These lasers are used in industry and in optical clocks.

Still, in November 2022, M Squared announced it was entering the neutral atoms quantum computing market with its Maxwell system as part of a collaborative UK government funded project. Maxwell is supposed to be a "state of the art breakthrough system" but with undisclosed characteristics.



exail (2000, France), formerly **iXblue Photonics** is a small business specialized in the design and manufacture of inertial and sonar systems, lithium niobate optical modulators, microwave amplifiers and modulator bias controllers for the control of Mach-Zehnder interferometers.

Their components are manufactured at their site in Lannion, Brittany and at Besancon. They are involved with the LP2N of Bordeaux in the creation of Ixatom, a quantum inertial sensor based on cold rubidium atoms²⁹⁹⁸. iXblue Photonics was the result of the acquisition of two companies: **iXFiber** in 2011, a specialist in passive optical components (FBG fiber grating filters, Fiber Bragg Gratings) and then, **Phonline Technologies** in 2013, a spin-off from Femto-ST created in 2000 in Besancon. In May

²⁹⁹⁷ See [A gravity antenna based on quantum technologies: MIGA](#) by B. Canuel, Philippe Bouyer et al, April 2022 (4 pages) and [Exploring gravity with the MIGA large scale atom interferometer](#) by B. Canuel, Philippe Bouyer et al, Nature Scientific Reports, 2018 (23 pages).

²⁹⁹⁸ See [iXAtom - LP2N and iXblue Cold Atoms joint laboratory](#).

2021, iXblue then acquired **Muquans** (quantum absolute gravimeters, created in 2011 in Bordeaux, France) and **Kylia** (a photonic equipment specialist, with its polarizers, delay line interferometers and multiplexers/multiplexers). In March 2022, Groupe Gorgé made the acquisition of iXblue Photonics to merge it with its subsidiary of **ECA Group**, a security, defense, and industry security technologies provider. It became **exail** in November 2022.

Muquans is based at the Institut d'Optique in Bordeaux. Their absolute quantum gravimeters are commercial products targeting, for example, the detection of cavities in construction, oil exploration and the monitoring of volcanoes such as Etna in Italy²⁹⁹⁹.

Here is how their absolute quantum gravimeter and other similar neutral atom-based quantum gravimeters work. The usual description looks like the image in Figure 689 from Muquans.

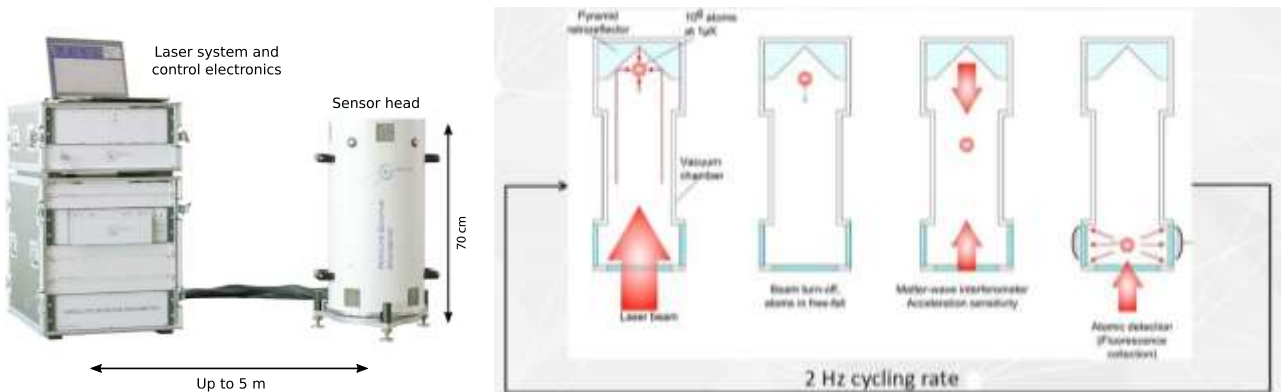


Figure 689: how atom interferometry works. All laser beams come from the bottom of the device. Source: Muquans.

We can decompose the quantum gravimetry steps in six parts.

① **Heating source**: a heated source at the top of the system prepares a small cloud of about 10^6 atoms of rubidium (^{87}Rb). The source of the atoms also contains an accelerometer that corrects the phase of the lasers in real time. It is prepared with a 2D MOT.

② **Magneto-optical trap**: a 3D MOT as shown in Figure 690 is used to confine and cool the prepared source of atoms at $1\mu\text{K}$ using three pairs of counter-propagating laser beams in three orthogonal directions, applying the Doppler effect, and two anti-Helmholtz coils which magnetically trap the atoms³⁰⁰⁰.

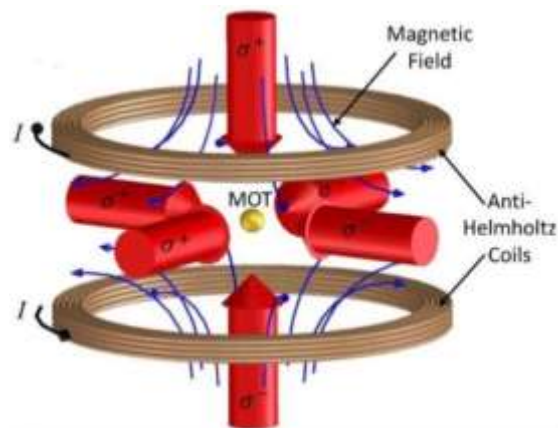


Figure 690: a typical Magneto-Optical Trap used to cool and confine neutral atoms. Source: [Cold atom interferometry sensors physics and technologies](#) by Martino Travagnin, 2020 (47 pages).

③ **Inverted pyramid retroreflection**: an inverted mirrors-based pyramid sits around the MOT and orient the prepared atom cloud downward in the instrument as shown in Figure 691.

④ **State preparation**: a laser beam coming from the bottom controls the atom cloud position. It is switched off and the cloud starts to freefall.

²⁹⁹⁹ See [Detecting Volcano-Related Underground Mass Changes With a Quantum Gravimeter](#) by Laura Antoni-Micollier, Bruno Desruelle et al, June 2022 (9 pages).

³⁰⁰⁰ The Muquans process is documented in [Gravity measurements below \$10^{-9}\text{g}\$ with a transportable absolute quantum gravimeter](#), 2018 (12 pages) and highlighted in [Digging Into Quantum Sensors](#) by Stewart Wills in Optics & Photonics, September 2019.

⑤ **Atom interferometer:** in its freefall, the atom cloud is exposed by two counter propagating vertical lasers pulses in three successive steps each generating a Raman transition with different durations and polarizations creating the equivalent of $\pi/2$, $-\pi$ and $-\pi/2$ gates (H, X and H)³⁰⁰¹. The first step has the effect of a coherent beam splitter and creates two streams of atoms in ground and excited state whose proportion depends on the ambient gravity. The second step has the effect of two mirrors like in an optical interferometer and inverse the population of ground and excited states. The third step focuses the two atom beams and creates a coherent beam mixing. Each step modifies the phase of the atom matter wave.

⑥ **Detection:** one or two other high precision lasers excite the two streams of atoms exiting the interferometer, generating a fluorescence effect that is detected by two sets of four broadband photodiodes using different frequencies. These diodes enable the measurement of the proportion of atoms in each interferometer output (excited/non excited). Their proportion will help compute the phase difference accumulated by the two atom streams, which itself will help calculate the ambient gravity. The process is repeated twice per second and a classical computer averages the results. Their gravimeters have a precision of 10^{-9} m/s².

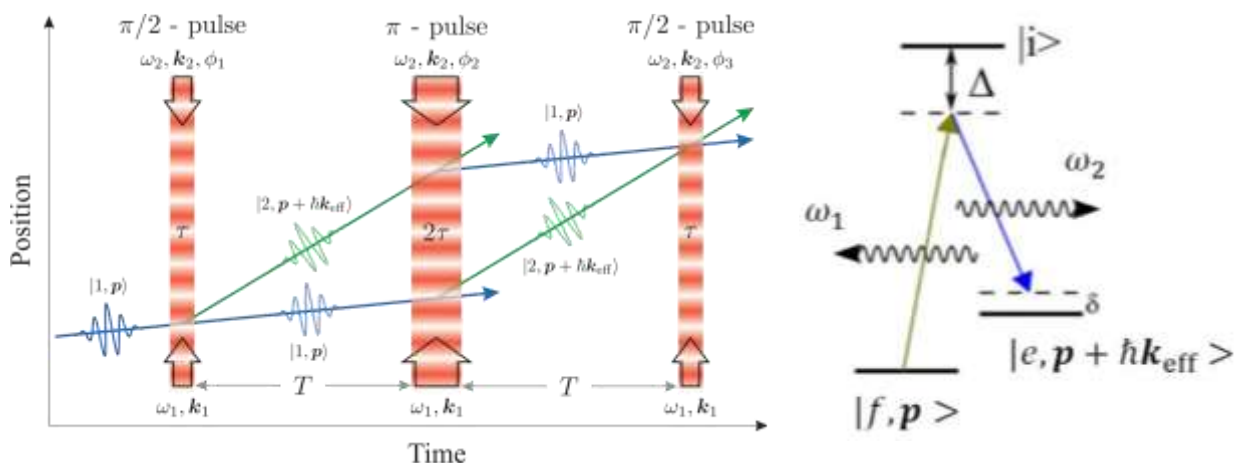


Figure 691: the three steps of cold atoms interferometry used in a gravimeter. The figure is somewhat confusing since the position axis (Z) goes up as the atom falls. So, it is inverted. Otherwise, how would you measure atoms at the bottom of the gravimeter? Two counterpropagating lasers are used, one coming from the top at frequency ω_1 and a wave vector k_1 and one from the bottom at ω_2 and a wave vector k_2 to create a double-photon Raman transition that will modify displacement for a share of the atoms that depends on the gravity. The diagram on the right shows the Raman transitions created by lasers with pulses ω_1 and ω_2 . f corresponds to the fundamental or ground state, e to the excited state. p is the atom momentum and its difference in the excited state is $\hbar k_{eff} = \hbar(k_1 - k_2)$. The width of the laser pulse τ (about 10 ms) corresponds to its duration which generates a superposition like a Hadamard gate in gate-based computing in step 1 and 3, and a population inversion in step 2 with a duration of 2τ . Meaning, the excited atoms (green lines) are turned in ground state atoms (blue line) and vice-versa, and also inverting their vertical velocity. If the lasers were used continuously, they would create a Rabi oscillation creating continuous change in the proposition of atoms in the ground and excited state over a couple ms. Sources: [Mobile and remote inertial sensing with atom interferometers](#) by B. Barrett et al, November 2013- August 2014 (63 pages) and [Cold atom interferometry sensors physics and technologies](#) by Martino Travagnin, 2020 (47 pages).

Exail is involved in the ESA's NAVISP program which plans to provide a supplementary navigation solution using gradiometry. The company is also developing a 3-axis quantum inertial sensor. The control of cold atoms has other applications³⁰⁰². For example, Muquans participates in the European flagship project **Quantum Internet Alliance** to create hardware to extend the reach of QKD systems and with the French startup **Pasqal** which creates quantum processors based on cold atoms.

³⁰⁰¹ Double-photon Raman cooling uses two lasers. One excites the atoms to reach a high excited state and the other de-excites the atom to bring it down to a higher excited state than the initial state. This technique also contributes to cool atoms below a micro-Kelvin.

³⁰⁰² See [Fifteen years of cold matter on the atom chip promise, realizations, and prospects](#) by Mark Keil, Ron Folman et al, 2019 (46 pages) which makes a good inventory of scientific applications of cold atoms and [Micro-fabricated components for cold atom sensors](#) by J. P. McGilligan et al, Review of Scientific Instruments, September 2022 (28 pages).

THALES

Thales Research & Technology (France) is developing miniaturized cold atom accelerometer, gyrometer and clock designed to be embedded. The whole with a "BEC on chip" component (for "Bose Einstein condensates on chip") in collaboration with the Charles Fabry laboratory of the Institut d'Optique (LCFIO). Atoms are vaporized in a glass cage glued to the chip, in which a good vacuum has been created. They are laser-cooled and trapped by a magnetic field and controlled by electromagnetic fields. This research project started around 2014 (Figure 692).



Figure 692: a Thales BEC on chip.

Photo credit: Ecliptique - Laurent Thion.

ATOMIONICS **Atomionics** (2018, Singapore, \$2.5M) is currently developing Gravio, a cold atoms interferometry based sensor measuring acceleration, rotations and gravity variations.

It can be used for navigation and resource exploration. It can also be used as an underground GPS.

Other laboratories are working on the same technology, such as the **Leibniz University** of Hannover³⁰⁰³.

The Chinese are also in this field, but without having gone so far in miniaturization³⁰⁰⁴ (Figure 688).



aQuark Technologies (2020, UK) is a spin-off from the University of Southampton developing small vacuum chambers and simpler atoms trap system avoiding the use of a MOT (magneto-optical trap) thanks to coupling several lasers with slightly different frequencies. In October 2023, they demonstrated a lightweight 10 kg airborne solution of their system.



Nomad Atomics (2018, Australia, \$10M) develops compact cold atom-based quantum gravimeters and accelerometers. The company was launched by Kyle Hardman, Christian Freier and Paul Wigley, respectively researcher and post-docs at the Australian National University.



Innoseis (2020, the Netherlands) was created by Mark Beker and Johannes van den Brand (who worked on gravitational waves detections instruments like those from LIGO), from Maastricht University. They develop MEMS based quantum gravimeters targeting seismic surveying.



Zero Point Motion (2020, UK, £2.58M) is a quantum optical inertial sensors company created by Ying Lia Li (Imperial College and University College London).

Their hybrid sensors use quantum photonics and cavity opto-mechanics to read the motion of MEMS masses. The product is being developed at the Quantum Technologies Innovation Centre at Bristol University with commercialization to start in 2024.



Delta G (2023, UK, £1.5M) is a spinout from the UK Quantum Technology Hub Sensors and Timing at the University of Birmingham. Created by Peter Stirling (CEO), Andrew Lamb (CTO) and Michael Holynski (CSO).

³⁰⁰³ See [Gravity measured using a Bose-Einstein condensate on a chip](#) by Hamish Johnston, 2016 mentioning the work of Ernst Rasel of the Leibniz University of Hannover who refers to [Atom interferometry and its applications](#) by S. Abend et al, 2020 (48 pages).

³⁰⁰⁴ See [Compact and Portable Atom Gravimeter](#) by Shuai Chen, 2019 (22 slides).

It develops cold atom sensors applied to gravity gradiometry, targeting use cases in construction, archaeology and for the discovery of hidden natural resources³⁰⁰⁵.



OK Quantum (2022, USA) or Oklahoma Quantum is a startup created by Saesun Kim (CEO) and Shan Zhong (Chief Scientist) who both come from the Center for Quantum Research and Technology (CQRT) of the University of Oklahoma. They design and manufacture cold atom based quantum inertial sensors. Given their web site, they don't sell it yet.



Vector Atomic (2021, USA) is a startup created by Jamil Abo-Shaeer (CEO), a former project manager at DARPA. It is developing with Honeywell Aerospace an atomic clock based navigation sensor that avoids the use of GPS. It was funded by Defense Innovation Unit of the US DoD.

Rafael Advanced Defense Systems (Israel) also has a department creating quantum sensing solutions, mainly gravitation sensors, with the Weizmann Institute of Science.

Microg LaCoste (1939, USA) develops absolute quantum gravimeters based on interferometry and free fall dropped mirrors, using a rubidium based atomic clock.

Draper Labs (1932, USA) also designs cold atoms sensors, mostly, gravimeters and accelerometers for navigation systems.

Trumpf (Germany) develops cold-atoms and VCSEL (lasers) based gyroscopes for satellites as part of the QYRO project funded by the German government and along with its subsidiary Q.ANT.

Wideblue (2006, UK) creates MEMS gravimeters. It is a consulting and engineering company.

Quantum accelerometers are also investigated to equip autonomous or assisted drive vehicles. German equipment manufacturer **Bosch** announced in February 2022 the creation its own quantum gyroscope for this purpose, aka IMU for inertial measurement unit as part of its new Bosch Quantum Sensing Unit, an internal startup led by Katrin Kobe and with a team of 15 people.

Finally, let's also mention a very special category of microgravimeters: the LIGO microgravimeters that are used to evaluate gravitational waves. They are based on optical interferometers of very high precision but of a size incompatible with all other imaginable uses³⁰⁰⁶.

Quantum clocks

Atomic clocks used in GPS provide resilience for navigation systems when standard satellite GPS signals are unavailable. They are also used in telecommunication infrastructure for the Internet and mobile communications, particularly with high-speed broadband landline and mobile infrastructures. Many industry sectors also rely on precision time measurement, like the financial sector and utilities power grids. Fundamental research and astrophysics also heavily rely on precision clocks.

Time measurement steadily progressed since the first mechanical clocks used between the 14th and 19th centuries. The quartz clocks which appeared between the two World Wars were based on the piezoelectric effect demonstrated by Pierre and Jacques Curie in 1880. With a frequency of 2^{15} Hz, time is measured using frequency dividers, with a drift of a few hundred microseconds per day.

The first cesium atomic clocks came out in the 1950s. Using a frequency around 9 GHz, they provide a time measurement accuracy ranging from 10^{-13} up to 10^{-16} with recent generations.

³⁰⁰⁵ See [Quantum sensing for gravity cartography](#) by Ben Stray, Andrew Lamb, Kai Bongs et al, Nature, February 2021 (14 pages).

³⁰⁰⁶ See [Advanced LIGO Just Got More Advanced Thanks To An All-New Quantum Enhancement](#) by Ethan Siegel, December 2019. And a description of the quantum squeezing technique used in the latest version of LIGO: [NIST Team Supersizes 'Quantum Squeezing' to Measure Ultrasmall Motion](#), 2019.

The second is defined since 1967 as the duration of 9,192,631,770 periods of the radiation corresponding to the transition between the two "hyperfine" levels of the fundamental electronic state of cesium 133. The recent variants of these clocks are "fountain clocks". They operate at very low temperature, with laser cooling bringing the atoms at 1 μ K, way much colder than superconducting qubits that are at 15 mK but is however easier to obtain than with a dilution refrigerator. A frequency oscillator generates a transition between two levels of cesium energy. The frequency is locked with a servo loop.

The precise measurement of frequencies has many applications: time measurement, synchronization of various devices on the Internet, even if only servers or scientific instruments, synchronization of moving objects to measure their position, astronomy (like with exoplanets and gravitational waves detection), absorption or emission precision spectroscopy, fiber optic transmissions and the generation of radio waves of arbitrary shape (Figure 693).

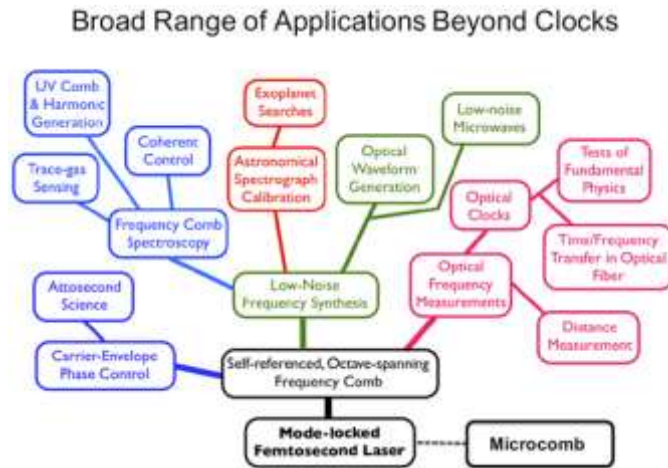


Figure 693: femto lasers use cases in quantum sensing.

However, a better accuracy may be needed, thus the need for quantum clocks³⁰⁰⁷. For about 20 years, time measurement was implemented with optical measurement of frequencies and time³⁰⁰⁸ (Figure 694).

The measurement of atomic vibrations can be replaced by the measurement of light waves generated by lasers and at 10^{15} Hz. It allows a gain in accuracy of five orders of magnitude (10^5). It was demonstrated in 2000 to generate an accuracy of a femtosecond. This earned the Nobel prize in Physics in 2005 to **Theodor Hänsch** (1941, German) and **John Hall** (1934, American).

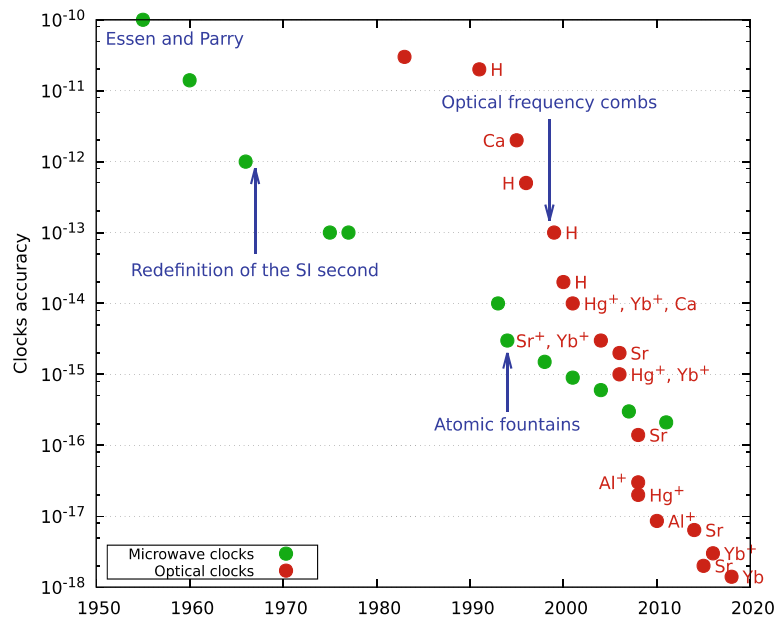


Figure 694: how quantum clocks accuracy evolved over time. Source: [Chronometric Geodesy: Methods and Applications](#) by Pacome Delva, Heiner Denker and Guillaume Lion, 2019 (61 pages).

³⁰⁰⁷ See [Time and Quantum Clocks: a review of recent developments](#) by M. Basil Altaie et al, 28 April 2022 (39 pages) and [Quantum clocks are more precise than classical ones](#) by Mischa P. Woods et al, February 2022 (75 pages).

³⁰⁰⁸ This is well explained in [Basics of atomic clocks](#) by Andrei Derevianko, University of Nevada, 2021 (77 slides).

In the USA, the **Chip Scale Atomic Clock (CSAC)** program funded by DARPA with NIST participation³⁰⁰⁹ led to the creation of highly compact vapor-cells cesium based atomic clocks manufactured by Microchip (mentioned later, with a size of 1.6"x1.4"x0.45") after a decade of work starting in 2000 and \$100M spent. It generates pulses of 4,596.3 MHz with a frequency tuning resolution of $1 \times 10^{-12} \text{s}$ ³⁰¹⁰ (Figure 695).



Figure 695: a CSAC chip.

Atomic clocks use microwave frequency transitions while the new generation of quantum clocks are based on higher electromagnetic wave frequencies in the optical spectrum. They use the technique of frequency combs. Since these frequencies are higher, these clocks can have a better precision, with three orders of magnitude gain compared to classical atomic clocks.

Frequency combs were discovered with the first mode-locked lasers by Logan Hargrove in 1964³⁰¹¹. Before optical combs, light frequency harmonic generators were used with a combination of several lasers in complicated setups. To measure light high frequencies, these clocks use optical frequency combs, which subdivided optical (high) frequencies into microwave (lower) frequencies for frequency measurement and timekeeping. It uses blocked-mode lasers that generate very short pulses, which can be as short as a few femtoseconds.

The frequency decomposition of this kind of signal gives a Gaussian-shaped frequency comb with each tooth regularly spaced at a frequency equivalent to that of the laser pulse. This is related to the fact that the length of the laser cavity is a multiple of the length of the electromagnetic waves emitted by the laser. The greater the multiple, the greater the frequency generated.

The frequency spectrum resembles a Gaussian curve. Its envelope is equal to the envelope of the spectrum of an isolated pulse, which is continuous. The width of the frequency spectrum covered can be narrow, a few nm in wavelength, or cover the entire visible spectrum, thus a few hundred nm.

A calculation is used to determine the very high frequencies of the frequency comb (f_n). It uses several parameters: the reference frequency f_{rep} of the laser pulses which is of the order of 250 MHz to 1GHz, n , the number of frequencies detected via spectroscopy (there can be hundreds of thousands) and the emission phase of the blocked mode laser which is added to each pulse and generates the frequency offset f_0 , which is evaluated with a method described below and which is also of a lower order than GHz (Figure 696).

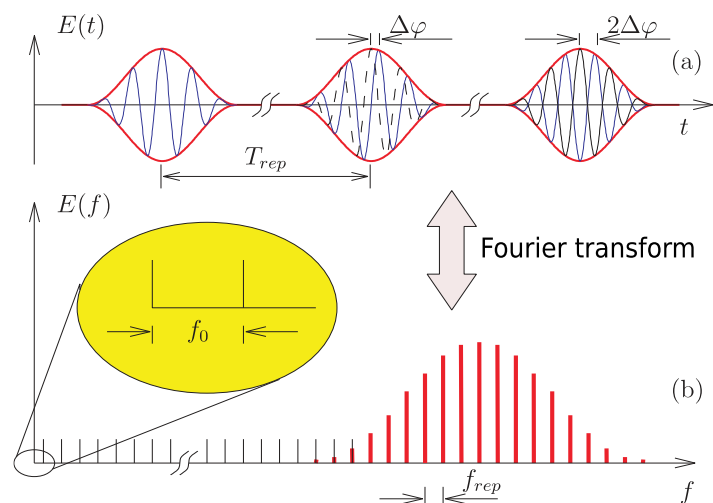


Figure 696: how a frequency comb works. Source: [Ultra-short light pulses for frequency metrology](#), CNRS (6 pages).

³⁰⁰⁹ See [MEMS Atomic Clocks](#) by Svenja Knappe, NIST, Comprehensive Microsystems, 2008 (45 pages).

³⁰¹⁰ CSAC are just one type of atoms chipsets, which have a broader spectrum of use cases in inertial sensing and electromagnetic field sensing. See [Fifteen Years of Cold Matter on the Atom Chip: Promise, Realizations, and Prospects](#) by Mark Keil, Ron Folman et al, 2016 (44 pages).

³⁰¹¹ See [Nobel Lecture: Defining and measuring optical frequencies](#) by John Hall, 2006 (17 pages) and [Light rules: frequency combs](#) by Steven Cundiff, Jun Ye and John Hall in Pour la Science, 2008 (8 pages). John Hall describes frequency combs as the intersection of four initially independent fields of research: ultra-stable lasers, fast pulse lasers, nonlinear optical materials, and precision laser spectroscopy. This is a reflection of quantum computing and its many scientific and technological sources.

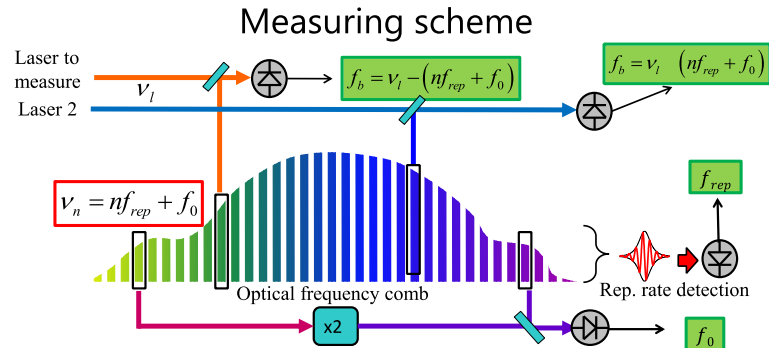
The measurement of radio frequencies in the MHz/GHz wave range results in the measurement of frequencies in 10s and 100s of THz to the nearest Hz. The system thus acts as a frequency multiplier. The measurement of light frequencies is impossible with traditional electronics because of the frequencies used, which are several tens or hundreds of tera-Hertz.

These calibrated frequency combs are also used to measure a frequency difference with this standard³⁰¹².

The frequency comb covers an octave, from one frequency (n) up to its double ($2n$) (Figure 697). The evaluation of f_0 is done by extracting the frequency f_n , and doubling it with a crystal. By adding this frequency doubled with f_{2n} , we obtain a beat at the frequency of f_0 .

$$2(f_0 + n \times f_{rep}) - (f_0 + 2n \times f_{rep}) = f_0$$

This is called **heterodyne detection**. The frequency comb becomes a kind of graduated ruler which is then used to position a frequency to be measured relative to the ruler. With that, you can build a new generation atomic clock³⁰¹³!



If we know n (and we are sure of the signs in the equations),
 → the system is mathematically well determined

In practice, we may

- impose values to the different f with phase lock loops (multiplier scheme : ϕ -lock f_{rep} , divider scheme: ϕ -lock f_b) (narrow line...)
- measure them with frequency counters
- and/or use clever tricks (exemple : $f_b \otimes f_0 \rightarrow \text{BPF} \rightarrow \nu_l - n f_{rep} - f_0 + f_0 = \nu_l - n f_{rep}$)

Figure 697: frequency comb and heterodyne detection. Source: [Optical frequency combs and optical frequency measurements](#) by Yann Le Coq, 2014 (38 slides), slide 11.

The readout of spectroscopy results using frequency combs can use CCD or CMOS cameras depending on the frequencies used in or around visible light³⁰¹⁴. This measurement accuracy evolves with the use of lasers using a high pulse frequency.

To date, the record for the accuracy of an atomic clock using spectroscopy is that of **NIST**. It is built with some aluminum ion associated with a magnesium anion. The aluminum ion is excited by two ytterbium lasers. Measurement is carried out using a quantum logic spectroscopy which is using the frequency combs, shown in Figure 698 (left)³⁰¹⁵. The clock reaches an accuracy of 10^{-18} seconds, a drift of one second per 33 billion years, 2.5 times the age of the Universe³⁰¹⁶.

In this market for optical quantum clocks, many research laboratories produce their own equipment. These are usually based on titanium-sapphire with pulses of a few femtoseconds (10^{-15} to 10^{-14} seconds).

³⁰¹² See [Phase Coherent Vacuum-Ultraviolet to Radio Frequency Comparison with a Mode-Locked Laser](#) by J. Reichert et al, 2005 (5 pages), [Direct Link between Microwave and Optical Frequencies with a 300 THz Femtosecond Laser Comb](#) by Scott Diddams et al, 2000 (4 pages), [Fundamentals of frequency combs What they are and how they work](#) by Scott Diddams (46 slides), [Optical frequency combs and optical frequency measurements](#) by Yann Le Coq, 2014 (38 slides) and [Chip-scale Optical Atomic Clocks and Integrated Photonics](#) by Matthew Hummon, NIST, 2018 (35 slides).

³⁰¹³ This is explained in [Optical Atomic Clocks](#) by Andrew Ludlow, Martin Boyd, Jun Ye, E. Peil and P.O. Schmidt, 2015 (65 pages) and [Optical atomic clocks](#) by N. Poli et al, 2014 (70 pages). See also [Photonic integration of an optical atomic clock](#) by Z. L. Newman et al, November 2018 (12 pages).

³⁰¹⁴ See [Frequency comb spectroscopy](#) by Nathalie Picqué and Theodor Hänsch, 2019 (27 pages) which describes the many methods and use cases of frequency comb based spectroscopy.

³⁰¹⁵ See this explanation: [Quantum Logic for Precision Spectroscopy](#) by Piet Schmidt et al, 2009 (6 pages).

³⁰¹⁶ See [²⁷Al⁺ Quantum-Logic Clock with a Systematic Uncertainty below 10⁻¹⁸](#), 2019 (6 pages).

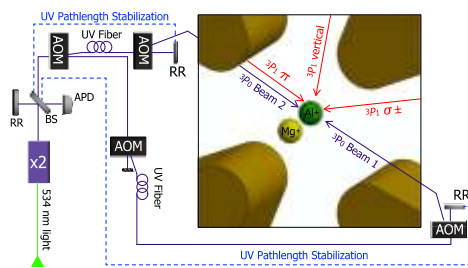


FIG. 1. Simplified schematic of the quantum-logic clock experimental setup. A frequency-quadrupled Yb-doped fiber laser is locked to the $^1S_0 \leftrightarrow ^3P_0$ transition ($\lambda \approx 267$ nm) by alternating the probe direction between two counterpropagating laser beams (shown in violet). An enlarged view of the trapping region is shown on the right. Three nominally orthogonal beams used for micromotion measurements are shown in red. Acousto-optic modulator (AOM), beam splitter (BS), retro-reflector (RR), frequency doubling stage (x2).

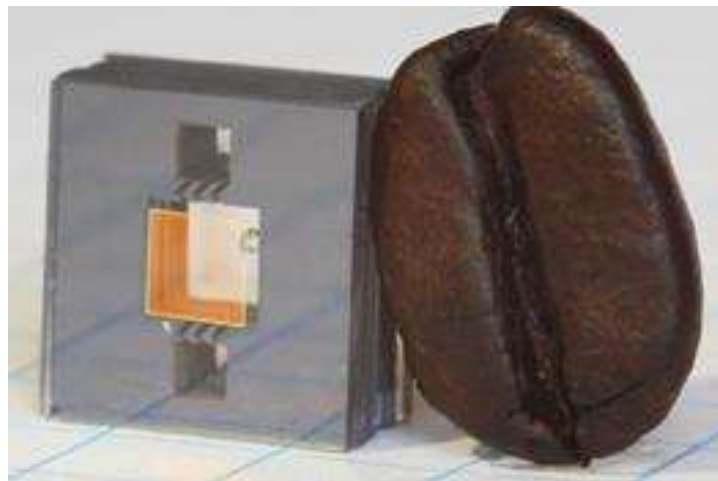


Figure 698: Source: (right) Illustration source: [²⁷AI[†] Quantum-Logic Clock with a Systematic Uncertainty below \$10^{-18}\$](#) , 2019 (6 pages).

NIST is also working on an atomic clock that would fit into a component the size of a coffee bean, using a double frequency comb and rubidium gas (in Figure 698, right). The whole thing consumes only 275 mW. This project was co-funded by DARPA³⁰¹⁷. However, for the moment, the precision obtained is not yet satisfactory for any industrialization.

One of the projects of the European Quantum Flagship, **iqClock** (the Netherlands, €10M), also aims to create very high-precision, portable quantum clocks. The consortium brings together six universities and six private partners including Teledyne EV (USA), Toptica (Germany), NKT Photonics (Denmark), AckTar (Israel) and Chronos (UK).

Optical clocks can be used for time synchronization between distant parties.

In 2022, China physicists led by Jian-Wei Pan (USTC) transferred time and frequency information over a 113 km in free space. They were using an optical clock having three components: atom samples with energy transitions operating at a stable reference frequency in optical frequencies, a feedback system that “locks” the output of the local oscillator laser to this reference frequency and a very precise measurement of the frequency of the laser using optical frequency comb (OFC). The researchers demonstrated time-frequency dissemination between such a feedback system and an OFC separated by 113 km using two ground optical telescopes³⁰¹⁸. After 10,000 seconds, the clock’s frequency instability was less than 4×10^{-19} , representing one second for 100 billion years. It opens the path for satellite-to-ground time-frequency dissemination. The China team now plans to extend this test to synchronize satellites at medium and geostationary orbits, and low-earth orbit satellites with ground stations. It could have various applications in metrology, navigation and positioning and in the search for dark matter, redefining fundamental constants and testing relativity.

These synchronization systems could even benefit from entanglement, which can yield a quantum advantage in atomic clock synchronization over lossy satellite-to-satellite channels³⁰¹⁹.

Let’s now look at some vendors in high-precision quantum time measurement.



In the private sector, **Teledyne** sells Minac (cesium atomic clock), T-CSAC (also cesium, integrated in a chip) and Synchronicity (ytterbium-based).

³⁰¹⁷ The project is documented in [Architecture for the photonic integration of an optical atomic clock](#), 2019 (6 pages).

³⁰¹⁸ See [Free-space dissemination of time and frequency with \$10^{-19}\$ instability over 113 km](#) by Qi Shen, Jian-Wei Pan et al, Nature, October 2022 (42 pages).

³⁰¹⁹ See [LEO Clock Synchronization with Entangled Light](#) by Ronakraj Gosalia et al, NASA, Northrop Grumman and UNSW, May 2023 (6 pages).

UK aircraft carrier HMS Prince of Wales has been fitted with the world's first atomic clock of its kind to help ensure pinpoint accuracy wherever she goes provided by BP and Teledyne e2v.



MicroSemi (1960, USA) sells its Quantum SA.45s, a miniaturized chip-scale atomic clock (CSAC). Among other use cases, it can be used in portable IED (improvised explosive devices) jammers. The company is a subsidiary of MicroChip Technology (1989, USA).



HyperLight Corp (2018, USA), based in Cambridge, near Boston, develops nanophotonic integrated circuits such as frequency combs or resonators that are used in quantum sensing.



QuantX Lab (2016, Australia), formerly Cryoclock, develops sapphire-based cryogenic oscillators. The company was co-founded by John Hartnett. Applications include trapped ion quantum processors and atomic clocks.



Safran acquired **Orolia** (2005, France) in July 2022 and **Syrlinks** (2011, France) in November 2022. Orolia creates atomic clocks with cesium, or based on rubidium oscillators. They mainly target the aerospace industry and provide the Galileo GNSS service.

Syrlinks develops miniature atomic clocks based on MEMS and cesium for embedded applications. Their MMAC is 40 x 35 x 22 mm and consumes less than 0.3 W. With Thales, and with the help of CNRS (SYRTE lab) Syrlinks is developing Chronos, new quantum clocks for civil and military applications with error inferior to 1 second per tens of thousands of years. It will enable geolocalization when GNSS like GPS and Galileo are not available.



TMD (1969, UK) sells microwave amplifiers. They also develop atomic clocks and instrumentation for the manipulation of cold atoms.



VectorAtomic (2018, USA) markets rubidium atomic clocks for quantum inertial navigation systems that can then avoid using GPS.



Vescent Photonics (2002, USA) offers optical frequency comb generators for use in atomic clocks. They also master the laser-based technique used for controlling cold. They are based in Colorado.

In June 2022, **Infleqtion** was announcing it was working for the US Navy with **LocatorX** (USA) to create an atomic clock using the Solid-state Miniature Atomic Clock (SMAC) technology created by LocatorX under license of Oxford University³⁰²⁰. The system is using fullerene molecules (C60) doped with nitrogen. It is not relying on cold atoms, the core technology mastered by ColdQuanta. It seems the two vendors are combining lightweight atomic clocks and more precise ones using cold atoms.

In January 2023, **GLOphotonics** (France) got a CES Innovation award for its Photonic Microcell Atomic Clock (PMCAC), a stylus form-factor atomic clock. I'm not sure what is the consumer use case for such a product (Figure 699).

³⁰²⁰ See [ColdQuanta and LocatorX Partner to Build Next Generation of Atomic Clocks](#) by ColdQuanta, June 2022.



Figure 699: GLOphotonics Photonic Microcell Atomic Clock (PMCAC) that fits into a relatively large stylus form factor package.
Source: GLOphotonics. January 2023.

Finally, let us mention again **Muquans**, which also uses its cold atoms expertise to sell an atomic clock, the MuClock, designed in partnership with the LP2N laboratory in Bordeaux and the LNE-SYRTE. It is positioned as an alternative to cesium atomic clocks. The instrument weighs 135 kg and consumes 200W.

Quantum magnetometers

Quantum magnetometers are used to detect small variations or levels of magnetism with high spatial accuracy. There are many use cases: navigation, mineral exploration, current detection, magnetocardiography, magnetoencephalography, orientation of drones and autonomous vehicles in tunnels where GPS does not work³⁰²¹, sonar, detection of moving metal objects such as vehicles and cellular imaging³⁰²².

Different techniques are available for high-precision magnetometry including Bose condensates and **atomic spins in vapors**^{3023 3024 3025}, **SQUIDs** (superconducting effect with a Josephson junction as in superconducting qubits³⁰²⁶), **NV-centers** solid-state systems, particularly using optically detected magnetic resonance (**ODMR**), with a sensitivity (or noise) usually ranging from 10^{-9} to $10^{-15} T/\sqrt{Hz}$ and decreasing as the signal frequency increases, and even **SiC-vacancies** (silicon vacancies in silicon carbide)³⁰²⁷ (Figure 700 left).

Measuring magnetism with NV centers exploit the variation of the spin resonance spectrum in the diamond cavity, which depends on the ambient magnetic field (see Figure 700 right on spin resonance spectrum). The distance between the two fluorescent light pulses (Y) generated is measured as a function of the electromagnetic excitation frequency used (X)³⁰²⁸.

³⁰²¹ A UAV solution using GPS in a tunnel is proposed by the startup Hovering Solutions (Spain).

³⁰²² See [Nitrogen-vacancy centers in diamond for nanoscale magnetic resonance imaging applications](#) by Alberto Boretti et al, 2019 (24 pages).

³⁰²³ See the Rydberg atom technique described in [Quantum sensing using circular Rydberg states](#) by Rémi Richaud, LKB, November 2018 (41 slides).

³⁰²⁴ See the thesis [Rubidium vapors in high magnetic fields](#) by Stefano Scotto, November 2017 (168 pages). See also [Brief Review of Quantum Magnetometers](#) by Ivan Hrvoic and Greg M. Hollyer, GEM Systems, not dated (15 pages).

³⁰²⁵ See [Atomic magnetometers and their application in industry](#) by Xuanyao Bai et al, Frontiers Physics, June 2023 (20 pages).

³⁰²⁶ See this presentation of SQUID applications: [SQUID Fundamentals and Applications](#) by Robin Cantor, 2017 (48 slides).

³⁰²⁷ See [Fiber-integrated silicon carbide silicon vacancy-based magnetometer](#) by Wei-Ke Quan et al, CAS and Sichuan University, August 2022 (13 pages) which describes a proposal of silicon carbide vacancy-based room temperature ODMR magnetometer using a fiber for results measurements.

³⁰²⁸ After optical magnification, fluorescence can be analyzed by a CCD image sensor.

The spins preparation is performed with a laser and its modification with 3 GHz microwave pulses. NV-center based magnetometers can use large unordered ensembles of NV centers³⁰²⁹ or individual NV centers³⁰³⁰.

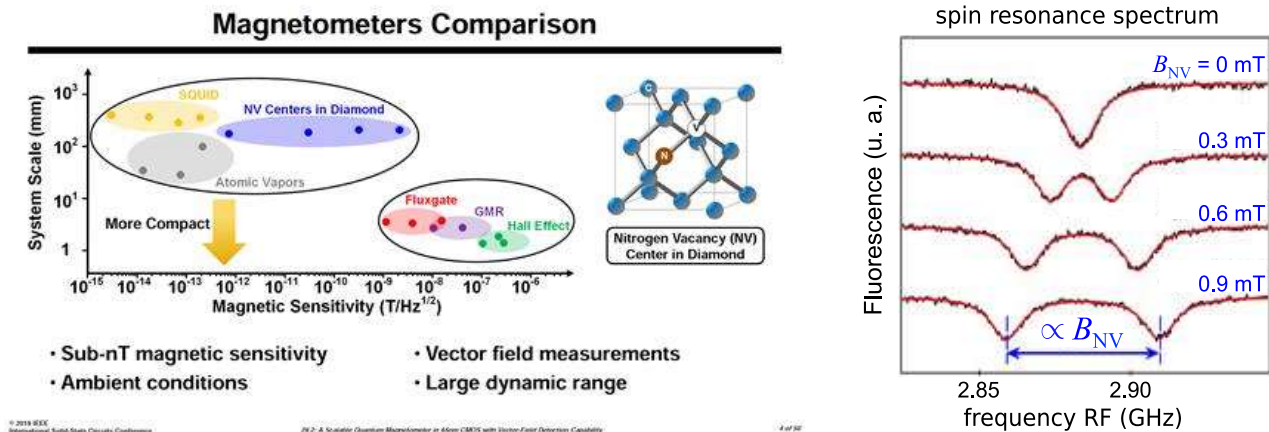


Figure 700: NV center magnetometry principle using spin resonance spectrum analysis. The two energy gaps enable the evaluation of the current magnetic field. Sources: [A Scalable Quantum Magnetometer in 65nm CMOS with Vector-Field Detection Capability](#) by Mohamed Ibrahim from MIT 2019 (51 slides) and [NV Diamond Centers: from material to applications](#) by Jean-François Roch, Collège de France, 2015 (52 slides).

The accuracy of magnetism measurement can reach a pico-Tesla, billions of times less than terrestrial magnetism³⁰³¹. NV centers provide a lesser precision than cold atoms, but their use is more practical because the instrument is easier to miniaturize and most of them work at ambient temperature³⁰³². Scanning probes magnetometers use a diamond nanocrystal containing a single cavity and a nitrogen atom, which ensures the accuracy of the measurement. The probe can be moved in space and used to analyze the magnetism of a material in 2D (Figure 701).

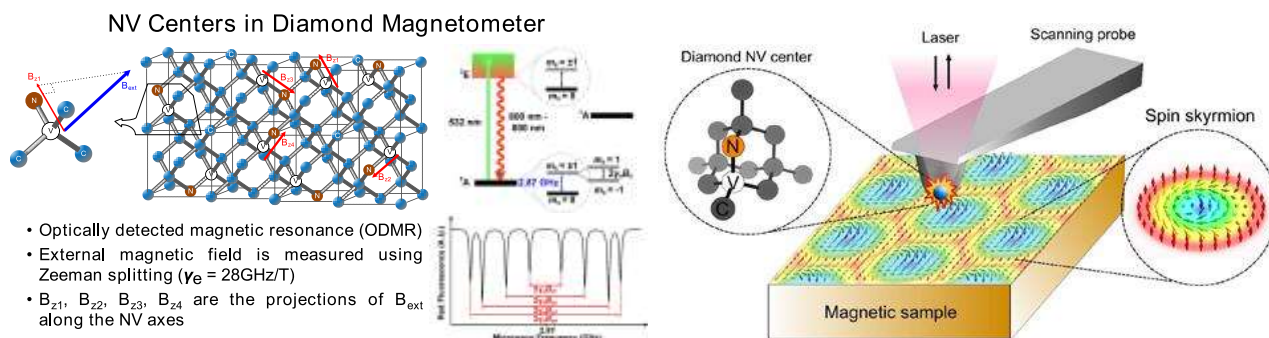


Figure 701: NV centers used in ODMR for medical imaging of materials inspection. Sources: [A Scalable Quantum Magnetometer in 65nm CMOS with Vector-Field Detection Capability](#) by Mohamed Ibrahim from MIT 2019 (51 slides) and [Probing and imaging nanoscale magnetism with scanning magnetometers based on diamond quantum defects](#), 2016 (35 slides).

³⁰²⁹ See for example [Picotesla magnetometry of microwave fields with diamond sensors](#) by Zhecheng Wang et al, June 2022 (7 pages).

³⁰³⁰ See for example [Scanning gradiometry with a single spin quantum magnetometer](#) by W. S. Huxter et al, 2022 (9 pages).

³⁰³¹ The accuracy of magnetometry with NV centers is evaluated with the formula $1\mu\text{T}/\sqrt{\text{Hz}}$. See [Picotesla magnetometry of microwave fields with diamond sensors](#) by Zhecheng Wang et al, August 2022 (7 pages) which describe a heterodyne measurement technique enabling picotesla precision.

³⁰³² See [A Scalable Quantum Magnetometer in 65nm CMOS with Vector-Field Detection Capability](#) by Mohamed Ibrahim from MIT 2019 (51 slides) which describes a miniaturization process of a quantum magnetometer combining a 65 nm CMOS circuit manufactured by TSMC and a diamond NV-center based system.

The NV-centers technique appeared in 2009. It is notably developed in France by **Thales**³⁰³³.

Laboratories in Bristol, the University of Ulm in Germany and Microsoft are working on the use of NV Centers techniques coupled with machine learning and Bayesian inference methods to correct the noise found at higher temperatures³⁰³⁴.

Quantum magnetometry can also rely on mixed optomechanics-photonics systems, like in a 2022 proposal from a China research team. It couples a thin SiN mechanical membrane to Terfenol-D rods³⁰³⁵ with a height that is sensitive to a static magnetic field. The membrane position modifies the phase of a laser-originated photon that is reflected in a cavity containing the membrane. The magnetic field is converted in the photon phase which is measured with homodyne detection using a local oscillator. The sensitivity of this sensor could be excellent, reaching 10^{-15} to $10^{-17} T/\sqrt{Hz}$ ³⁰³⁶ (Figure 702).

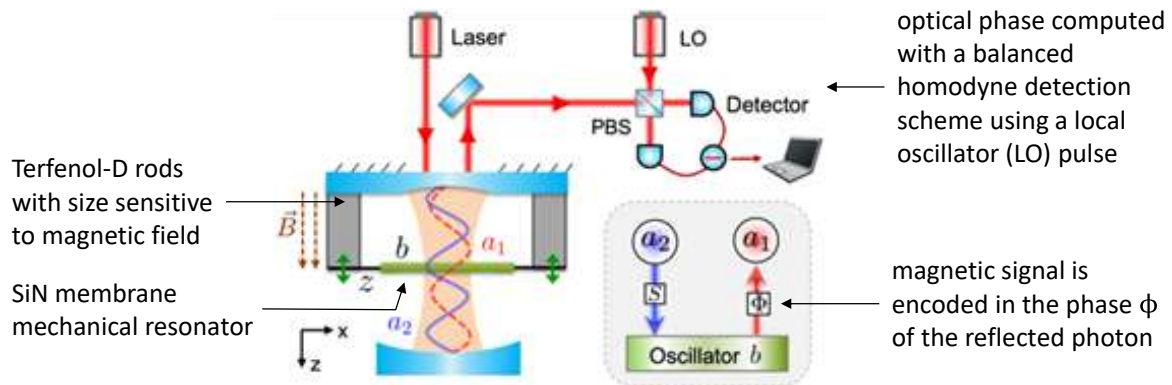


Figure 702: Source: [Quantum Magnetometer with Dual-Coupling Optomechanics](#) by Gui-Lei Zhu et al, May 2022 (7 pages).

Different technical approaches are developed to improve NV magnetometry, like with using the nuclear spin of the NV center nitrogen atom to drive sensing with an optical control, which can enable compact sensing in magnetometry and gyroscopic applications³⁰³⁷, using ultrathin NV center layers less than 20 nm below the surface of an ultrapure diamond³⁰³⁸ and using graphitic electrodes without the need of any metallic deposition on the diamond surface, thereby simplifying the sensor fabrication³⁰³⁹.

³⁰³³ ASTERIQS (France, €9.7M) or "Advancing Science and Technology through diamond Quantum Sensing" is a European Quantum Flagship project launched in 2018 and led by Thales, which is expected to advance techniques for measuring magnetic, electric, temperature and pressure fields. There are many applications, such as sensors for vehicle battery monitoring, high-resolution sensors for nuclear medical imaging (NMR, nuclear magnetic resonance) or for creating radio frequency spectrum analyzers. The Swiss startup Qnami is involved in the project and provides artificial diamonds.

³⁰³⁴ See [Magnetic-Field Learning Using a Single Electronic Spin in Diamond with One-Photon Readout at Room Temperature](#) by Raffaele Santagati et al, 2018 (18 pages).

³⁰³⁵ Terfenol-D is a magnetostrictive material made from an $Tb_xDy_{1-x}Fe_2$ ($x \approx 0.3$) alloy. Its name comes from terbium, iron (Fe), Naval Ordnance Laboratory (NOL, who developed the material in the 1970s), and D for dysprosium. The material is used to produce sonar systems.

³⁰³⁶ See [Quantum Magnetometer with Dual-Coupling Optomechanics](#) by Gui-Lei Zhu et al, May 2022 (7 pages).

³⁰³⁷ See [All-Optical Nuclear Quantum Sensing using Nitrogen-Vacancy Centers in Diamond](#) by Beat Bürgler et al, University of Basel, LSPM Université Sorbonne Paris Nord and Chimie ParisTech PSL, December 2022 (16 pages).

³⁰³⁸ See [Diamond-based optical vector magnetometer](#) by Charlie Oncebay Segura and Sérgio Ricardo Muniz1, Universidade de Sao Paulo, September 2022 (13 pages).

³⁰³⁹ See [Efficient and all-carbon electrical readout of a NV based quantum sensor](#) by Guillaume Villaret, Jean-François Roch, Thierry Debuisschert et al, December 2022 (11 pages).

Quantum magnetometry has some fancy use cases. One is for astrophysics and the search for dark matter using atomic magnetometers³⁰⁴⁰, NV center magnetometers³⁰⁴¹ and even transmon qubits³⁰⁴². Another amazing use case for NV center magnetometry is the precise measurement of battery charge and discharge³⁰⁴³.

Let's now look at some vendors in the quantum magnetometry space.

QDM.IO (2021, USA) is creating an NV center based microscope. It comes out of the Quantum Catalyzer from the University of Maryland.



Qubic (2019, Canada) is a startup from the Institut Quantique from the University of Sherbrooke in Quebec that is working on microwaves-based quantum sensing tools for sensing, imaging and communications. It is led by Jérôme Bourassa.



Qutools (2005, Germany) offers its quNV quantum magnetometer kit, based on diamond NV-centers as its name suggests. It fits in a 3U rack (Figure 703). They also sell an interferometer for interferometric displacement measurement.



Figure 703: a quantum magnetometer from qutools.

Also in Germany, the University of Stuttgart is working with the Fraunhofer Institute to transfer NV-centered magnetometry technology as part of the **QMag**³⁰⁴⁴ project.



Supracon (2001, Germany) manufactures magnetometers based on SQUIDs (Superconducting Quantum Interference Devices). It is a spin-off of the Leibnitz Institute of Photonics in Jena. It sells its sensors to astrophysics research laboratories and for geophysics prospection.



Great Lakes Crystal Technologies (2019, USA) is a supplier of diamonds for use in NV center applications, especially for quantum magnetometers. It is a spin-off from the University of Michigan and Fraunhofer USA.



FieldLine Inc (2020, USA) develops NV centers quantum sensing systems, particularly for medical brain imaging and non-destructive materials testing.



Q-Sensorix (2019, USA) develops NV centers magnetometer-based gyroscopes, launched by Alexey Akimov, Vladimir Shalaev and Yuri Lebedev. These are alumni of the University of Buffalo in New York State.



SandboxAQ (2022, USA) tested in May 2023 its airborne quantum sensor-based magnetic anomaly navigation system with the US Air Force aboard a C-17 GlobeMaster III transport aircraft.

³⁰⁴⁰ See [Search for dark photons with synchronized quantum sensor network](#) by Min Jiang et al, May 2023 (13 pages). It is using 15 atomic magnetometers, which are synchronized with the Global Positioning System (GPS) and are situated on the edges of two meter-scale shielded rooms, serving as a powerful tool to search for dark photons.

³⁰⁴¹ See [Light Dark Matter Search with Nitrogen-Vacancy Centers in Diamonds](#) by So Chigusa et al, February 2023 (6 pages).

³⁰⁴² See [Detection of hidden photon dark matter using the direct excitation of transmon qubits](#) by Shion Chen et al, University of Tokyo, December 2022 (7 pages).

³⁰⁴³ See [High-precision robust monitoring of charge/discharge current over a wide dynamic range for electric vehicle batteries using diamond quantum sensors](#) by Yuji Hatano et al, Nature Scientific Reports, September 2022 (10 pages).

³⁰⁴⁴ See [Quantum Magnetometers for Industrial Applications](#), April 2019.

This Assured Positioning, Navigation, and Timing (APNT) solution is designed to complement classical GPS to provide uninterrupted navigation when GPS is unavailable or intentionally denied or spoofed by enemies. The system collects data from NV sensors and uses machine learning to filter out the ambient noise generated by the airplane. The benefits of the system are manifold. The Earth's magnetic field cannot be jammed. It can be detected in any weather condition, and it works passively.



Twinleaf (2007, USA) develops precision magnetometers based on alkali metal lasers. The company is headed by Elisabeth Foley, a specialist in the field, and Thomas Kornack (CSO), both Princeton alumni.



Cerca Magnetics (2018, UK) is a spin-out from the UK Sensors and Timing Quantum Technology Hub at the University of Nottingham. It develops a wearable brain scanner magnetoencephalography (MEG) system, avoiding the use of cryogeny like heavy MRI scanners.

It uses optically pumped magnetometers measuring weak magnetic fields. These are made with a laser illuminating a small glass cell containing a pressured gas of rubidium or cesium. A diode detects the transmitted light that depends on the local magnetic field perpendicular to the laser beam³⁰⁴⁵. The technology is competing with SQUIDs based MEGs.



CIQTEK (2016, China, \$15M) manufactures quantum sensors targeting quantum computation, healthcare, food safety, chemistry and material science markets. These sensors are NV center magnetometers.

The company based in Hefei is also named Guoyi Quantum. It was created with the support of Jiangfeng Du (1969) and is led by Yu He, a student of his at the USTC.

At last, the **Ivar Giaever Geomagnetic Laboratory (IGGL)** in Norway also uses SQUIDs to detect underground magnetism for paleomagnetic applications, to measure the magnetic remanence of ancient rocks. Using SQUIDs, their magnetometer must be cooled to 4K with a pulsed tube³⁰⁴⁶.



GEM Systems (1980, Canada) is selling quantum magnetometers using optically pumped potassium (K-Mag).



ODMR Technologies (2015, USA) is a stealth spin-off from Berkeley which designs a magnetic resonance spectroscopic analysis system based on NV centers.



Elta Systems (1967, Israel) is a subsidiary from the IAI consortium. The company develops various electromagnetic sensors and radars for defense and intelligence.

They develop quantum magnetic sensors in collaboration with Israeli research groups and industry partners. These sensors can help detect IEDs (improvised explosive devices, unexploded ordinance, geophysical structures, vehicles and ships). They also work on quantum optical magnetometry and sub-pico-Tesla atomic magnetometers which can be used in medical imaging (MEG).



kwan-tek (2020, France), formerly Wainvam-E, is providing a set of NV centers magnetometry solutions for materials nondestructive inspection (corrosion and cracks detection), and for objects detection and navigation in the industry and defense markets.

³⁰⁴⁵ See [Optically pumped magnetometers: From quantum origins to multi-channel magnetoencephalography](#) by Tim M. Tierney et al, 2019 (12 pages).

³⁰⁴⁶ See [Instruments for Paleomagnetic Measurements WSGI \(2G\) Model 755 Superconducting Rock Magnetometer \(SRM\)](#).

Quantum thermometers

NV centers have another use: temperature measurement with an accuracy of a few mK and with a very high spatial resolution, all with highly miniaturized sensors. It is currently the most powerful temperature measurement technology for these different dimensions^{3047 3048}. It allows, for example, to determine the temperature within living cells and organisms with a sub-mm precision^{3049 3050} (Figure 704).

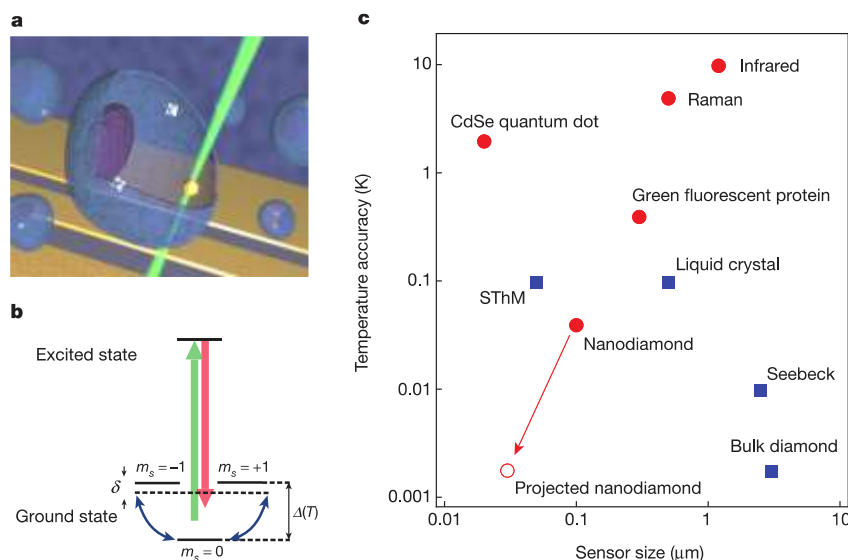


Figure 1 | Nitrogen–vacancy-based nanoscale thermometry. a, Schematic image depicting nanodiamonds (grey diamonds) and a gold nanoparticle (yellow sphere) within a living cell (central blue object; others are similar) with coplanar waveguide (yellow stripes) in the background. The controlled application of local heat is achieved by laser illumination of the gold nanoparticle, and nanoscale thermometry is achieved by precision spectroscopy of the nitrogen–vacancy spins in the nanodiamonds. b, Simplified nitrogen–vacancy level diagram showing a ground-state spin triplet and an

excited state. At zero magnetic field, the $|\pm 1\rangle$ sublevels are split from the $|0\rangle$ state by a temperature-dependent zero field splitting $\Delta(T)$. Pulsed microwave radiation is applied (detuning, δ) to perform Ramsey-type spectroscopy. c, Comparison of sensor sizes and temperature accuracies for the nitrogen–vacancy quantum thermometer and other reported techniques. Red circles indicate methods that are biologically compatible. The open red circle indicates the ultimate expected accuracy for our measurement technique in solution (Methods).

Figure 704: Source: [Nanometre-scale thermometry in a living cell](#), 2013 (6 pages).

Quantum thermometry also has applications in very low temperatures measurement, such as within cryostats and physics experiments. Quantum thermometers sensitivity is assessed in $K/\sqrt{\text{Hz}}$ meaning it increases with the number and frequency of measurements.

How are these NV center quantum thermometers working? Several methods are used like spin-based thermometry with ODMR (optically detected magnetic resonance) spectrum measurement using microwave excitation. The diamond containing NV centers can be attached to a fiber³⁰⁵¹. There are even hybrid thermometers associating NV centers and more classical magnetic nanoparticle thermometers³⁰⁵².

³⁰⁴⁷ See [High sensitivity silicon carbide divacancy-based thermometer](#) by Qin-Yue Luo et al, China, January 2023 (13 pages).

³⁰⁴⁸ See [Temperature sensing using nitrogen-vacancy centers with multiple-poly crystal directions based on Zeeman splitting](#) by Li Xing et al, National Institute of Metrology, Beijing, December 2022 (13 pages).

³⁰⁴⁹ See [Nanometre-scale thermometry in a living cell](#), 2013 (6 pages) and [Real-time nanodiamond thermometry probing in vivo thermogenic responses](#) by Masazumi Fujiwara et al, September 2020 (10 pages).

³⁰⁵⁰ See [Simultaneous nanorheometry and nanothermometry using intracellular diamond quantum sensors](#) by Qiushi Gu et al, University of Cambridge, June 2023 (28 pages).

³⁰⁵¹ See [Temperature dependence of nitrogen-vacancy center ensembles in diamond based on an optical fiber](#) by Ke-Chen Ouyang et al, November 2021 (17 pages).

³⁰⁵² See [Ultra-sensitive hybrid diamond nanothermometer](#) by Chu-Feng Liu and al, 2019-2021 (9 pages)

It uses the fact that the zero-field splitting frequencies are linearly dependent on the ambient temperature. All-optical methods use the correlation between the NV center ZPL (zero-phonon lines) and temperature³⁰⁵³.

There are solutions for temperature measurement in biological matter by fluorescence that are based on quantum dots³⁰⁵⁴.

In 2017, NIST produced a quantum photonics thermometer of very small size for optically measuring the surface temperature of metals. However, the picture does not show the control electronics associated with the sensor³⁰⁵⁵ (Figure 705).

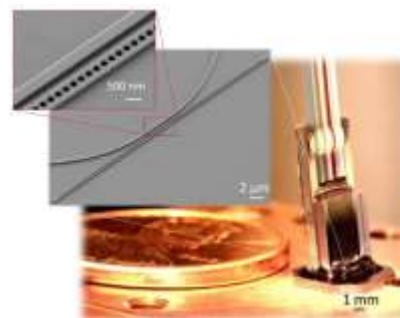


Figure 705: quantum photonic thermometer from NIST.



Southwest Sciences (1985, USA) develops optical temperature sensors based on NV centers for use in cryogenic systems. The company was founded by Alan C. Stanton and Joel A. Silver.

Quantum frequencies sensing

Radio frequency analysis is an old matter, but it is also progressing thanks to quantum technologies often associating optronics with cold atoms. Wideband frequency quantum sensing can be implemented with neutral atoms and NV centers.

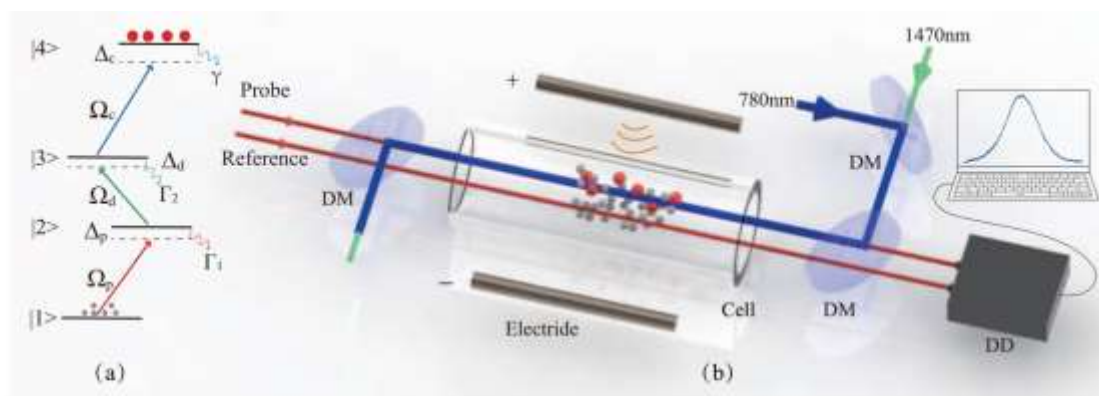


Figure 1. (a) Ladder-type four-level atomic energy diagram consisting of a ground state $|1\rangle$, two low-lying excited states $|2\rangle$ and $|3\rangle$, and a Rydberg state $|4\rangle$. An 852-nm probe light drives the transition $|1\rangle = |6S_{1/2}, F = 4\rangle \rightarrow |2\rangle = |6P_{3/2}, F = 5\rangle$, a 1470-nm dressing light couples the transition $|2\rangle = |6P_{3/2}, F = 5\rangle \rightarrow |3\rangle = |7S_{1/2}, F = 4\rangle$, and a 780-nm coupling light drives the transition $|3\rangle = |7S_{1/2}, F = 4\rangle \rightarrow |4\rangle = |55P_{3/2}\rangle$ of cesium atoms. (b) Overview of the experimental setup. The probe light and the reference light propagate in parallel through a Cs vapor cell. The probe light (red) overlaps the counter-propagating coupling light (blue) and dressing light (green) to form an EIT configuration. The transmission difference between the probe and reference lights is detected by a differentiating photodetector. Two electrode rods are placed parallel to each other on both sides of the vapor cell 4 cm apart. Labels: DM - dichroic mirror; DD - differentiating photodetector.

Figure 706: how neutral atoms are used to measure electromagnetic waves frequencies spectrum in a highly sensitive solution developed in China, using a hot vapor cell of cesium atoms excited by lasers in their Rydberg states. The grey electrodes are connected to an RF antenna. Source: [Highly sensitive measurement of a MHz RF electric field with a Rydberg atom sensor](#) by Bang Liu et al, June 2022 (7 pages).

Neutral atom-based sensors paired with optical readout using coherent spectroscopy can analyze electromagnetic waves frequencies from direct current (0 Hz) to the THz range. This is due to their so-called high-energy Rydberg states which can help measure high-frequency electro-magnetic waves

³⁰⁵³ See the review paper [Diamond quantum thermometry from foundations to applications](#) by Masazumi Fujiwara and Yutaka Shikano, April-September 2021 (24 pages).

³⁰⁵⁴ See [Intracellular thermometry with fluorescent sensors for thermal biology](#) by Kohki Okabe et al, 2018 (15 pages).

³⁰⁵⁵ See [Thermodynamic miniaturized sensors and standards and the quantum SI](#) by Gregory F. Strouse, 2016 (39 slides).

thanks to their strong dipole. It can help reduce the size of various antennas, improve radio frequency filtering and extend the range between mobile communications cellular towers. This sort of broadband spectrum analysis can have multiple use cases, particularly in the military and intelligence sectors. These systems don't necessarily showcase high-precision and can be used as "heads-up" spectrum analysis tools before more specialized tools are used for specific parts of the electromagnetic spectrum. But some progress is made to improve these neutral atom-based electromagnetic spectrography system, noticeably in the MHz bands³⁰⁵⁶ (Figure 706) and for creating isotropic (covering all directions) antennas³⁰⁵⁷.

A quantum sensor based on alkaline Rydberg atoms can analyze the radio spectrum from 1 kHz to 100 GHz³⁰⁵⁸. Other quantum sensors can analyze radio waves in the 1 THz band, that is intermediate between infrared and microwaves bands, with potential applications in the measurement of thickness of thin layers of heterogeneous materials³⁰⁵⁹ (Figure 707).

NV centers sensors can also help run RF signals spectral analysis, from 0 to 40 GHz with the advantage of being more lightweight than most neutral atoms sensors. NV centers sensors can even be arranged in sensor arrays enabling both a wide-band spectrum coverage and a high-precision analysis of a target band³⁰⁶⁰.

Some pure optics techniques can be used to implement frequency sensing in the THz range³⁰⁶¹.

And surprisingly, it can also work, in a different fashion, to create quantum optical microphones with the benefit to improve the quality of AI-based speech recognition³⁰⁶².



Rydberg Technologies (2015, USA) provides cesium or rubidium specimens for cold atom-based radio frequency sensing solutions.

They sell Rydberg lasers, a Rydberg atoms-based radio-frequency probe, a RFMS (Rydberg Field Measurement System) covering the 1MHz-100 GHz frequency range, and Rydberg vapor cells³⁰⁶³. Their technology is also integrated in AM and FM radio-frequency receivers as well as in radars. It enables long range radio communication. Their roadmap shows how far they are going with miniaturizing their device and reducing its power consumption (Figure 708).

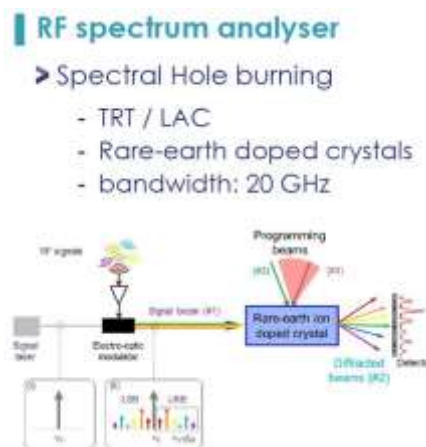


Figure 707: RF spectrum analyzer with rare-earth doped crystals. Source TBD.

³⁰⁵⁶ See [Highly sensitive measurement of a MHz RF electric field with a Rydberg atom sensor](#) by Bang Liu et al, June 2022 (7 pages) and [Quantum sensing of weak radio-frequency signals by pulsed Mollow absorption spectroscopy](#) by T. Joas et al, 2017 (6 pages).

³⁰⁵⁷ See [An isotropic antenna based on Rydberg atoms](#) by Shaoxin Yuan et al, Shanxi University, China, September 2023 (13 pages).

³⁰⁵⁸ See [Highly sensitive measurement of a MHz RF electric field with a Rydberg atom sensor](#) by Bang Liu et al, June 2022 (7 pages) and [Quantum sensing of weak radio-frequency signals by pulsed Mollow absorption spectroscopy](#) by T. Joas et al, 2017 (6 pages). See also [Assessment of Rydberg atoms for wideband electric field sensing](#) by David H Meyer et al, January 2020 (16 pages). See also another less impressive performance from the same lab and published later: [Waveguide-Coupled Rydberg Spectrum Analyzer from 0 to 20 GHz](#) by David H. Meyer, 2021 (10 pages).

³⁰⁵⁹ See [Researchers demonstrate first terahertz quantum sensing](#), March 2020, which refers to [Terahertz quantum sensing](#) by Mirco Kutas et al, 2020 (9 pages).

³⁰⁶⁰ See [Sensing of Arbitrary-Frequency Fields Using a Quantum Mixer](#) by Guoqing Wang et al, MIT, PRX, June 2022 (22 pages).

³⁰⁶¹ See [Terahertz quantum sensing](#) by Mirco Kutas et al, March 2020 (8 pages).

³⁰⁶² See [A Quantum Optical Microphone in the Audio Band](#) by Raphael Nold, Jörg Wrachtrup et al, April 2022 (7 pages).

³⁰⁶³ See [A vapor-cell atomic sensor for radio-frequency field detection using a polarization-selective field enhancement resonator](#) by D. A. Anderson et al, 2018 (11 pages).

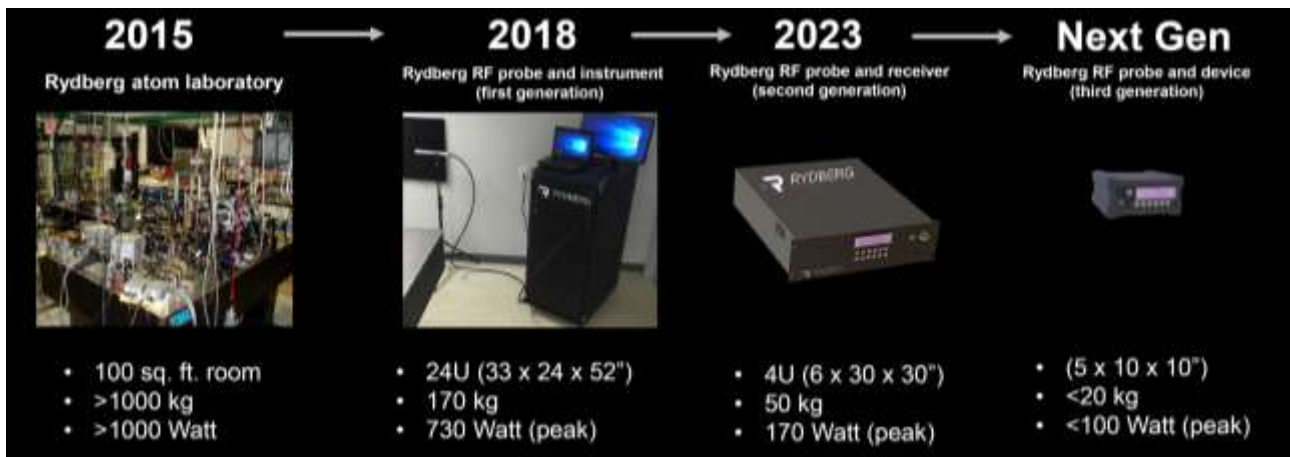


Figure 708: Rydberg Technologies miniaturization roadmap as presented at the Optica Conference in Rueil Malmaison in November 2022. Source: Rydberg Technologies. Added in 2023.

Thales is developing a real-time radiofrequency spectral analyzer *aka* a Quantum Diamond Signal Analyzer (Q-DiSA) with a bandwidth of 10 MHz to 25 GHz and a frequency resolution of 1 MHz, based on NV centers³⁰⁶⁴. The frequency adjustment is done with controlling the distance of the NV center with a small 1.3 cm magnetic sphere. The system is using a 532 nm laser and a CMOS sensor.

At last, we should mention **quantum antennas** where some non-classical phenomenon can occur like the creation of squeezed states³⁰⁶⁵. It is an emerging field that can address particular needs, like field shaping, quantum radars, quantum imaging and creating antennas for THz electromagnetic fields using quantum dots³⁰⁶⁶. Since 2022, **BAE Systems** (UK) is developing quantum antennas on behalf of DARPA.

Quantum imaging

Quantum sensing is enlarging the scope of what is possible to do in imaging, at both the microscale and nanoscale levels, noticeably for biology and non-destructive material inspection. These new tools are based on various techniques that we'll cover here: **SQUIDs**, *aka* superconducting qubits³⁰⁶⁷, **NV-centers** based magnetometry to implement NMR spectroscopy which tend to dominate the market nowadays thanks to their space resolution and readout precision, and **OPMs**, *aka* optical-pumped magnetometers which are mainly used for neuron imaging (MEG, magnetoencephalography). We'll also have a look at some mysterious "ghost imaging" systems that take pictures of objects with a single pixel sensor and other special quantum sensors.

SQUIDs are classically used in MRI systems which require helium-4 based cryogeny. They are also implemented in various specific use cases like in sub-mm astronomy and infrared (IR) imaging. One such imager with 10,000 pixels is embedded in the NIRSpec near-infrared telescope in the JWST (James-Webb Space Telescope) that is operating since July 2022³⁰⁶⁸.

³⁰⁶⁴ See [A quantum radio frequency signal analyzer based on nitrogen vacancy centers in diamond](#) by Simone Magaletti, Ludovic Mayer, Jean-François Roch and Thierry Debuisschert, Nature Communications, February-July 2022 (8 pages).

³⁰⁶⁵ See the review paper [Quantum Antennas](#) by Gregory Ya. Slepyan, Svetlana Vlasenko and Dmitri Mogilevtsev, June 2022 (70 pages).

³⁰⁶⁶ See [Generating tunable terahertz radiation with a novel quantum dot photoconductive antenna](#) by Andrei Gorodetsky, Ksenia A. Fedorova, Natalia Bazieva and Edik U. Rafailov, Aston University Birmingham, 2016.

³⁰⁶⁷ See [Magnetometry of neurons using a superconducting qubit](#) by Hiraku Toida et al, NTT Research Labs, June 2022 (6 pages).

³⁰⁶⁸ Seen in [Micromachined Quantum Circuits](#) by Teresa Brecht, 2017 (271 pages).

NV-centers imagers can be used to analyze organic molecules with excellent spatial resolution. It makes use of electron spin resonance spectroscopy (ESR) at cryogenic temperature which allows us to examine atoms and molecules at the level of their electron spin. This enables NMR (nuclear magnetic resonance) detection³⁰⁶⁹. The technique is usually integrated in scanning tunneling microscopes as well as in atomic force microscopes (AFM). The electron spin of the examined materials is excited by a magnetic field and microwaves.

NV-center imaging has many other variations like QDMTM (quantum-enhanced diamond molecular tension microscopy) which could quantify the integrin-based cell adhesive forces³⁰⁷⁰. The NV-center technique also allows the examination of a hard disk and semiconductors defects with a probe equipped with a single NV-center as shown in Figure 709 and Figure 711. It is also used for the characterization (quality control) of integrated circuits working with millimeter frequencies such as in 5G³⁰⁷¹. Others are working on NV centers-based microscopy of living cells³⁰⁷².

There is even an application to qualify malaria patients by analyzing hemozoin nanocrystals appearing in red blood cells affected by the disease parasite³⁰⁷³. These techniques are used with confocal microscopy. This generates images with a very shallow depth of field of about 400 nm, creating optical sections of the sample to analyze. By modifying the position of the depth focal plane, a series of images are created which are then assembled to generate a 3D view of the analyzed sample. The light source is reflected or obtained by fluorescence in reaction to a laser beam. The result is a Confocal Laser Scanning Microscope (CLSM). NV-centers can also improve the accuracy of adaptive optics, which are used in astronomy³⁰⁷⁴. NV center based microscopy can also analyze the time evolution of magnetic fields³⁰⁷⁵.

Imaging can also exploit an array of small NV centers that provide much better resolution than imaging systems based on SQUIDs magnetometers. The example in Figure 713 shows its architecture³⁰⁷⁶. The second was made to study bacteria that contain magnetic microelements. In other cases, magnetic markers can be used to attach themselves to the cells to be detected, typically in oncology. NV centers could also be used in heart monitoring using magnetocardiography. It was tested on rats in Japan, as shown in Figure 710³⁰⁷⁷.

³⁰⁶⁹ See [Advances in nano- and microscale NMR spectroscopy using diamond quantum sensors](#) by Robin D. Allert et al, May 2022 (42 pages).

³⁰⁷⁰ See [Quantum-Enhanced Diamond Molecular Tension Microscopy for Quantifying Cellular Forces](#) by Feng Xu, Jörg Wrachtrup, Qiang Wei, Zhiqin Chu et al, June 2023 (51 pages).

³⁰⁷¹ See [Microwave Device Characterization Using a Widefield Diamond Microscope](#), 2018 (10 pages) which involves in particular the LSPM of Paris.

³⁰⁷² See [A fluorescent nanodiamond foundation for quantum sensing in cells](#), 2018 (147 pages) which discusses microscopy of living cells.

³⁰⁷³ See [Diamond magnetic microscopy of malarial hemozoin nanocrystals](#) by Ilja Fescenko et al, September 2018 (17 pages),

³⁰⁷⁴ See [Nanodiamonds enable adaptive-optics enhanced, super-resolution, two-photon excitation microscopy](#), 2019 (7 pages).

³⁰⁷⁵ See [Quantum Diamond Microscope for Dynamic Imaging of Magnetic Fields](#) by Jiashen Tang, Ronald L. Walsworth et al, University of Maryland and MIT, September 2023 (18 pages).

³⁰⁷⁶ See [Enhanced widefield quantum sensing with nitrogen-vacancy ensembles using diamond nanopillar arrays](#) by D. J. McCloskey, 2019 (7 pages). The NV centers matrices are 100 μm wide. The illustration comes from other work published in 2013, cited in the conference [Magnetic imaging using NV-diamond: techniques & applications](#) by Ronald Walsworth, 2015 (51 min). Notably [Optical magnetic imaging of living cells](#), Le Sage et al, Nature, 2013 (11 pages). See also [Principles and Techniques of the Quantum Diamond Microscope](#) by Edlyn V. Levine et al, 2019 (47 pages) and [Atomic Scale Magnetic Sensing and Imaging Based on Diamond NV Centers](#) by Myeongwon Lee et al, 2019 (17 pages).

³⁰⁷⁷ See [Millimetre-scale magnetocardiography of living rats with thoracotomy](#) by Keigo Arai et al, Nature Communications Physics, August 2022 (10 pages).

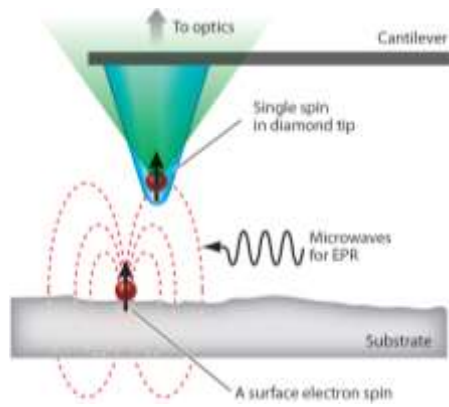


Figure 709: a typical NV center in a diamond tip for various imaging applications. Source: [Nitrogen-Vacancy Centers in Diamond: Nanoscale Sensors for Physics and Biology](#) by Romana Schirhagl, Kevin Chang, Michael Loretz and Christian L. Degen, ETH Zurich, 2014 (27 pages).

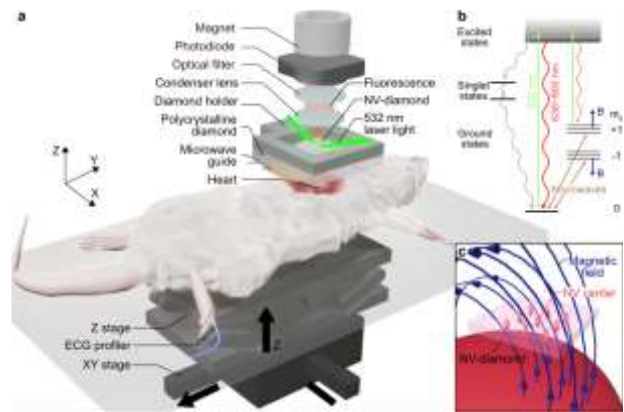


Figure 710: NV center based magnetocardiography experiment on rats. Source: [Millimetre-scale magnetocardiography of living rats with thoracotomy](#) by Keigo Arai et al, Nature Communications Physics, August 2022 (10 pages).

The European Quantum Flagship includes **MetaboliQs** (Germany, €6.7M), a diamond-based nuclear magnetic resonance cardiac medical imaging project. It also detects atrial fibrillation, a common cardiac pathology, with a rubidium-based atomic magnetometer³⁰⁷⁸. Another Flagship project, **PhoG** (United Kingdom, €2.6M) or [Sub-Poissonian Photon Gun by Coherent Diffusive Photonics](#), is about creating stable light sources for various applications, particularly in quantum sensing. It involves researchers from Belarus, Germany and Switzerland.

Other vacancies like color centers in hexagonal boron nitride (hBN) in 2D layered structure have a similar broad spectrum of applications to measure static magnetic fields, magnetic noise, temperature, strain, nuclear spins, paramagnetic spins in liquids and RF signals³⁰⁷⁹.

Optically pumped magnetometers (OPMs) are scalar-type quantum sensors enabling the measurement of very weak magnetic fields and based on the Zeeman effect³⁰⁸⁰. These sensors have emerged in the 1970s and expanded since the 2000s thanks to a better sensitivity, on par with SQUIDs.

One of their main use cases is MEG (magnetoencephalography) to examine brain activity³⁰⁸¹ but it can also be used for materials inspections³⁰⁸². OPMs are competing with MRI and NMR imaging systems. They are more lightweight, can be wearable, and don't require any cryogeny like with MRIs that are based on SQUIDs.

OPMs can for example help track some neurodegenerative diseases like dementia, Alzheimer's and Parkinson's with tracking patients' brain waves and how their change over time³⁰⁸³. OPMs principle of operation is rather simple. A small laser beam which can be a vertical-cavity surface emitting lasers (VCSEL) illuminates a heated alkali atoms vapor (rubidium, cesium or potassium) trapped in a millimeter-scale glass cell whose size determines the sensor spatial resolution.

³⁰⁷⁸ See [New quantum technology could help diagnose and treat heart condition](#), March 2020.

³⁰⁷⁹ See the review paper [Quantum sensing and imaging with spin defects in hexagonal boron nitride](#) by Sumukh Vaidya et al, Purdue University, February 2023 (21 pages).

³⁰⁸⁰ See the review paper [Optical magnetometry](#) by Dmitry Budker and Michael Romalis, Berkeley, Nature Physics, 2007 (8 pages).

³⁰⁸¹ See [Optically pumped magnetometers: From quantum origins to multi-channel magnetoencephalography](#) by Tim M. Tierney et al, 2019 (11 pages).

³⁰⁸² See [Optically Pumped Magnetometer Measuring Fatigue-Induced Damage in Steel](#) by Peter A. Koss et al, 2022 (11 pages).

³⁰⁸³ See [Improved spatio-temporal measurements of visually evoked fields using optically-pumped magnetometers](#) by Aikaterini Giallopsou et al, Nature Scientific Reports, November 2021 (11 pages).

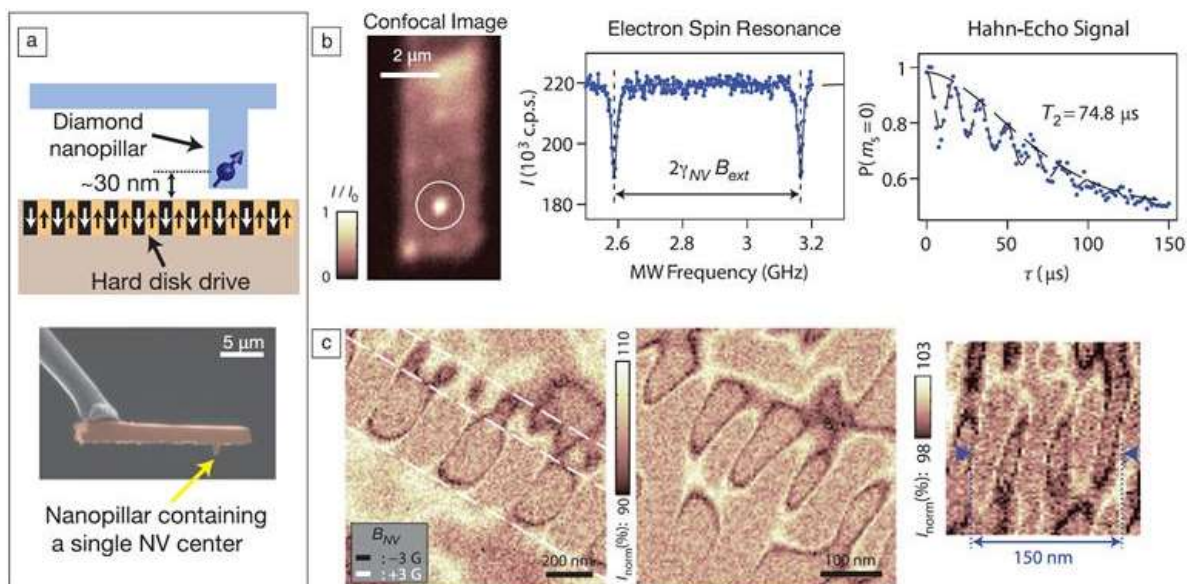


Figure 4. (a) Schematic of a monolithic diamond nanopillar probe (top) and representative SEM image of the nanopillar probe (bottom). (b) Characteristics of a nanopillar probe device. Confocal image of the device (left) clearly shows a localized fluorescence spot from a single NV center at the position of the nanopillar. Electron spin resonance (middle) was acquired with an enhanced fluorescence of 220,000 photons/sec. The coherence time of the measured Hahn-echo signal (right) is 74.8 μs , an order of magnitude longer than a typical Hahn-echo coherence time of commercial diamond nanocrystals ($\sim 5 \mu\text{s}$). (c) Magnetic images of a hard disk drive acquired by the nanopillar probe. Alternating magnetic bits were imaged with varying sizes down to 25 nm (right), indicating the distance between a single NV center at the probe and the hard disk sample is roughly within 25 nm. Adapted with permission from Reference 19. © 2012 Nature Publishing Group.

Figure 711: Source: [Nitrogen-Vacancy Centers in Diamond: Nanoscale Sensors for Physics and Biology](#) by Romana Schirhagl, Kevin Chang, Michael Loretz and Christian L. Degen, ETH Zurich, 2014 (27 pages).

The atoms nuclear and electron spin are influenced by the ambient magnetic field, which changes the vapor optical properties that will absorb more or less light depending on the probed magnetic field. Light is then measured by a photodetector after traversing a polarizing beam splitter³⁰⁸⁴ (Figure 712).

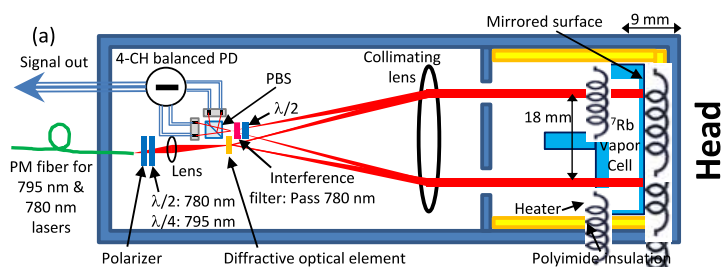


Figure 712: Source: [Four-channel optically pumped atomic magnetometer for magnetoencephalography](#) by Anthony P. Colombo et al, 2016 (15 pages).

Other quantum optical imaging techniques using **laser interferometry** make it possible to examine molecules at the atomic level in their environment and not in a vacuum and cryogenic cold³⁰⁸⁵.

The China laboratory of Jian-Wei Pan has developed a camera that analyzes the reflection of a single photon per pixel on the object to be observed. This is associated with algorithms filtering out the noise. Imaging is done in the infrared at 1,550 nm and with polarized photons. This could be integrated in observation satellites³⁰⁸⁶.

Superconducting nanowire single-photon detectors (SNSPDs) can also be assembled in arrays to create infrared multi-pixel imagers³⁰⁸⁷.

³⁰⁸⁴ See [Four-channel optically pumped atomic magnetometer for magnetoencephalography](#) by Anthony P. Colombo et al, 2016 (15 pages).

³⁰⁸⁵ See [An Entanglement-Enhanced Microscope](#) by Takafumi Ono, Ryo Okamoto, Shigeki Takeuchi, 2014 (8 pages).

³⁰⁸⁶ See [A new camera can photograph you from 45 kilometers away](#), May 2019 which refers to [Single-photon computational 3D imaging at 45 km](#) by Zheng-Ping Li et al, April 2019 (22 pages). And the presentation [Single Photon LiDAR](#) by Feihu Xu, June 2019 (25 slides).

³⁰⁸⁷ See [A 64-pixel mid-infrared single-photon imager based on superconducting nanowire detectors](#) by Benedikt Hampel et al, September 2023 (8 pages).

There is also a broad field of imaging that can be implemented with free electrons illumination and nanophotonics, but it is at best in type I quantum sensors³⁰⁸⁸.

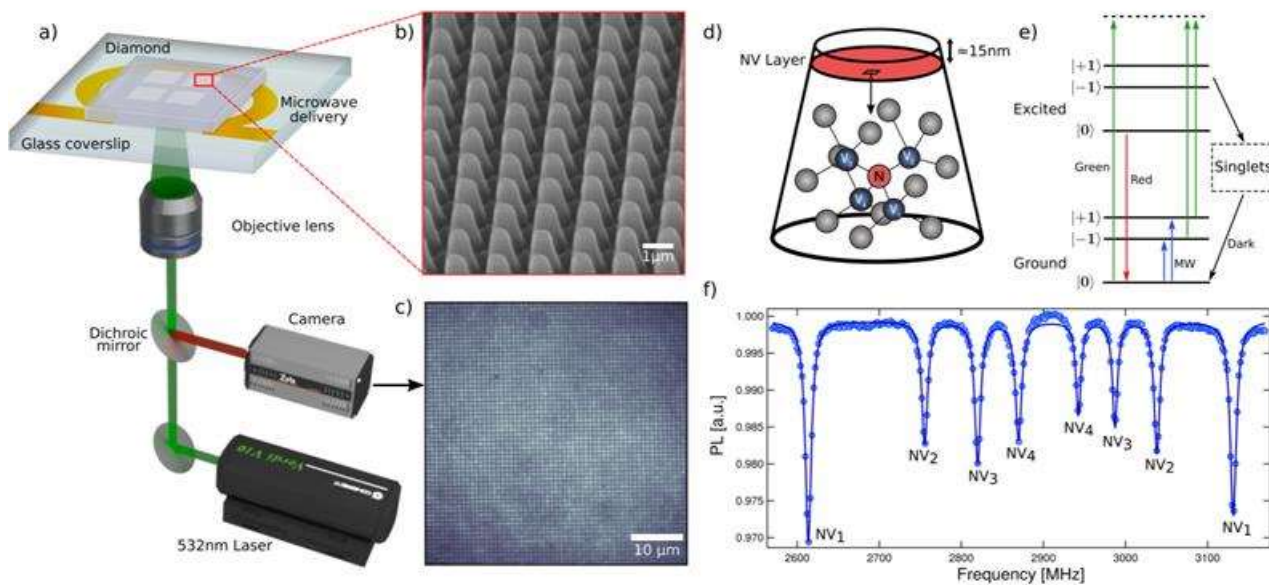


Figure 713: a widefield array of NV centers to improve their sensitivity, developed in Australia. Source: [Enhanced widefield quantum sensing with nitrogen-vacancy ensembles using diamond nanopillar arrays](#) by D. J. McCloskey, 2019 (7 pages).



QLM Technology (UK, \$14.64M) developed a “Quantum Gas Imaging Lidar”, a quantum magnetometer solution that detects methane leaks in pipelines up to 100 meters away. The measuring system weighing a few kg can be embarked in a large drone flying at 50 km/h. They use a laser that illuminates a gaseous medium of variable opacity and a photodetector.

IDQ is involved in the creation of the solution at the LiDAR level. Their solution will be embedded in “Schlumberger End-to-end Emissions Solutions” (SEES), a product line that detects and eliminates oil and gas industry’s polluting methane and flaring emissions. Their “Quantum Gas Imaging Lidar” will be embedded in “Schlumberger End-to-end Emissions Solutions” (SEES), a product line that detects and eliminates oil and gas industry’s polluting methane and flaring emissions (Figure 714).



Figure 714: an airborne LIDAR to detect gas leaks.



Chipiron (2020, France) develops a portable and helium-free 2D and 3D MRI system using stacked SQUIDs quantum detectors (superconducting / Josephson effect based). The startup created by Dimitri Labat and Evan Kervella is first targeting osteoporosis and brain diagnosis. The product is to be sold by 2024³⁰⁸⁹.



QDTI (2012, USA) is the only known startup initially engaged in the development of a quantum computer based on NV Centers. Created by a team from Harvard University, it is logically based in Boston.

³⁰⁸⁸ See the review paper [Free-electron-light interactions in nanophotonics](#) by Charles Roques-Carmes, August 2022 (34 pages). Astrahl (2022, USA) is a startup created out of the MIT which creates nanophotonics imaging systems based on free electrons scintillation. See [A framework for scintillation in nanophotonics](#) by Charles Roques-Carmes et al, Science, February 2022 (14 pages).

³⁰⁸⁹ See [Chipiron Ultra-low field MRI with SQUID detection](#) by Dimitri Labat, February 2022 (13 pages).



SeeDevices (2017, USA) develops a quantum imaging system, the PAT-PD (Photon Assisted Tunneling Photo Detector), which exceeds the performance of traditional CMOS imagers.

This imager contains photosites using the tunneling effect that can detect single photons in a wide range of wavelengths from near infrared (1,800 nm) to ultraviolet (up to UVA1, at 350 nm). This can be used for seeing in the dark and for medical imaging, like for detecting blood vessels in the infrared range (Figure 715).

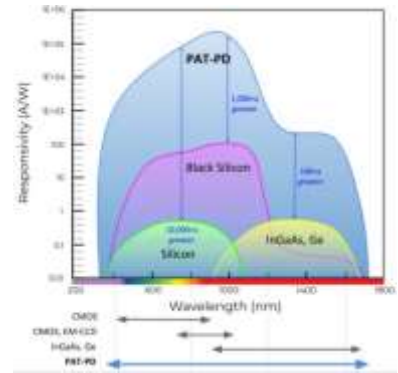


Figure 715: SeeDevice covered wavelengths.

The startup is now focused mainly on medical imaging systems also using these NV centers, with the creation of precision magnetometers combined with MRI and immunological tests.



Nvision Imaging (2015, Germany) is developing an NV centers-based MRI medical imaging solution.



SBQuantum (2019, Canada) also known as SBTech and Shine Bright Technologies develops NV centers-based quantum magnetometers. They target the automotive market but are also working on integrating their technology into Cubesat-type satellites. It is also a startup coming from Institut Quantique (University of Sherbrooke).

They have developed a tri-axial version of their system that measures magnetism in the three X, Y and Z axis. Research on this product was funded by the NIH (National Health Institute). The product is mainly targeting magnetoencephalography (MEG) brain imaging.



Mag4Health (2021, France) is a spin-off from CEA-Leti who develops a helium optically pumped magnetometer-based magnetoencephalography (MEG) system, working at room temperature³⁰⁹⁰.

It is using quantum sensors that were developed at CEA-Leti. These record the brain's electromagnetic activity in real time, helping neuronal diseases diagnosis. Mag4Health MEGs are much lighter (about 150 kg) than classical systems using large superconducting magnets (5 tons).



EuQlid (2023, USA) is a startup coming out of the Quantum Catalyzer (Q-Cat) in Maryland. They are combining large field-of-view a quantum diamond microscope (QDM) and some neural network image analysis to enable non-invasive imaging of integrated circuits.



Qurv (Spain) is a spin-off of ICFO that offers wide-spectrum quantum dots based image sensors covering the visible and short-wave infrared range.



QuSpin (2012, USA) is proposing an optical magnetometer (OPM) for neuroimaging.



Quantum Diamonds (Germany, 7M€) is a spin-off from TUM (Technical University of Munich) that produces NV center based non-destructive inspection tools.



Qnami (2017, Switzerland, \$7.3M) is a spin-off from the Quantum Metrology Research Laboratory at the University of Basel.

³⁰⁹⁰ See [Performance Analysis of Optically Pumped 4He Magnetometers vs. Conventional SQUIDS: From Adult to Infant Head Models](#) by Saeed Zahran et al, Mag4Health, Inserm and CEA, April 2022 (18 pages).

Among other things, they produce artificial diamonds for various photonics applications. They targeted first the quantum sensing market with their Quantilever MX nanodiamonds probes (Figure 716). They then launched in 2019 the ProteusQ range of NV center confocal microscopes, used to analyze ferromagnetic materials, based on the Quantilever probe. Quantonation and Runa capital are among their investors. And one of the co-founders and the CEO, Mathieu Munsch, came from Grenoble Phelma and worked at the CEA in Grenoble and did his PhD at CNRS Institut Néel.

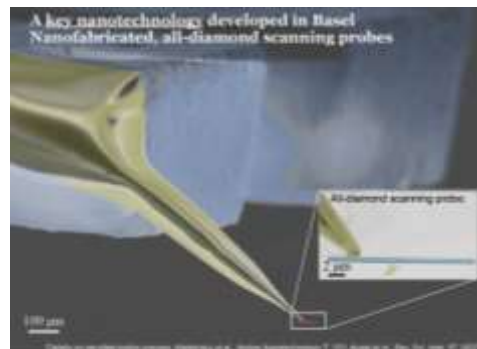


Figure 716: Qnami NV center based imaging system.



Siloton (2020, UK, £470K) is developing optical coherence tomography (OCT) solutions for the assessment of age-related macular degeneration.

The company is the first investment from the Quantum Exponential Group launched by Steven Metcalfe. Their chip devices are designed by VLC Photonics in Spain and manufactured by Ligentec in Switzerland. OCT uses low-coherence light to capture micrometer-resolution, 2- and 3-dimensional images from within optical scattering media like the retina. It is also used in nondestructive testing (NDT) in the industry. It makes use of low-coherence interferometry with near-infrared light that easily penetrates the inspected medium. It probably belongs to Type I quantum sensing.



Quantum Computing Inc (USA, aka QCi) announced in July 2023 its Quantum Photonic Vibrometer (QCi QPV-1.0), a photonic based remote vibration detection, sensing, and inspection instrument.

It can detect highly obscured and non-line-of-sight objects like landmines, implement non-destructive material control and also detect voices in noisy environments. It measures surface vibrations with counting the number of individual photons that are reflected as the surface slightly moves or tilts.



Quantum imaging could also use the curious technique of **ghost imaging** or quantum phantom imaging (Figure 717). It exists in many variations. The first one used a generator of infrared photons in 1995³⁰⁹¹. One half of the photons illuminates the object and the other half a photo sensor, by crossing an optical delay line³⁰⁹². The photons illuminating the object are entangled with those illuminating the camera, which has not seen the object at all! The obtained image is very noisy and requires some appropriate processing.

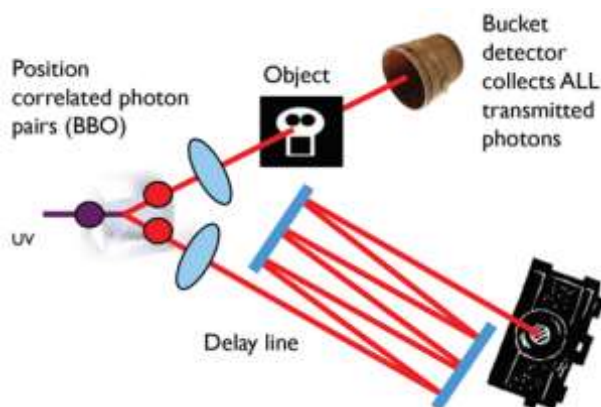


Figure 717: ghost imaging principle. Source: [An introduction to ghost imaging: quantum and classical](#) by Miles Padgett and Robert Boyd, 2016 (10 pages)

³⁰⁹¹ See [Optical imaging by means of two-photon quantum entanglement](#) by Yanhua Shih et al, 1995 (4 pages), University of Maryland. And [Observation of two-photon 'ghost' interference and diffraction](#) by Yanhua Shih, 1995 (4 pages).

³⁰⁹² See [An introduction to ghost imaging: quantum and classical](#) by Miles Padgett and Robert Boyd, 2016 (10 pages) provides a good overview of the subject. See also [Quantum Ghost Image Identification with Correlated Photon Pairs](#), 2010 (4 pages).

What is the purpose of this? Mainly to analyze objects with a very low photon number to avoid that they modify the object to be analyzed. This can be interesting in microbiology³⁰⁹³. The analyzed objects are seemingly always very small³⁰⁹⁴.

Other non-quantum techniques use a single-pixel color imager that uses 1,300 structured lights per second to illuminate the object for a few seconds, with up to one million iterations. The sensor prototyped at the University of Glasgow in 2013 contains four photodiodes positioned at different locations³⁰⁹⁵. This makes it possible to generate a 3D view of the object (Figure 718).

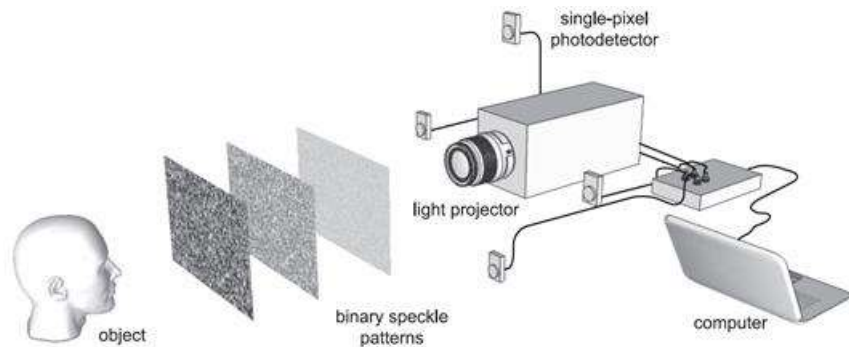


Fig. 1. Experimental setup used for 3D surface reconstructions. The light projector illuminates the object (head) with computer-generated random binary speckle patterns. The light reflected from the object is collected on four spatially separated single-pixel photodetectors. The signals from the photodetectors are measured and used to reconstruct a computational image for each photodetector.

Figure 718: Source: [3D Computational Imaging with Single-Pixel Detectors](#), 2013 (4 pages).

Finally, quantum imaging can also rely on the illumination of the object by entangled microwaves, using the principle of quantum radar that we will see in a following section. It is interesting for analyzing objects with low reflectivity, which would be useful in medical imaging as well as for creating short-range radars³⁰⁹⁶ (Figure 719). Entangled photon can also be used to create holograms, as recently discovered by a team of physicists from the University of Glasgow³⁰⁹⁷.

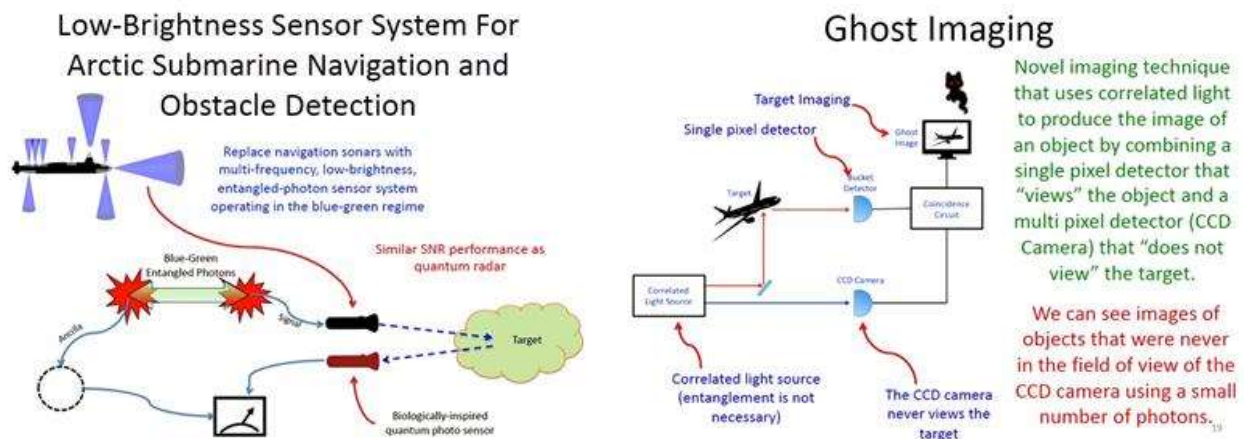


Figure 719: another ghost imaging concept. Source: [The Future of Quantum Sensing & Communications](#) by Marco Lanzagorta of the US Naval Research Laboratory (USA), September 2018 (37 minutes).

Another envisaged technique is a system coupling a camera that does not see the object to be captured and a single pixel sensor that sees the object.

³⁰⁹³ See [The Dawn of Quantum Biophotonics](#) by Dmitri Voronine et al, 2016 (30 pages).

³⁰⁹⁴ See this panorama of many ghost imaging methods: [The promise of quantum imaging](#) by Robert Boyd, 2016 (53 slides).

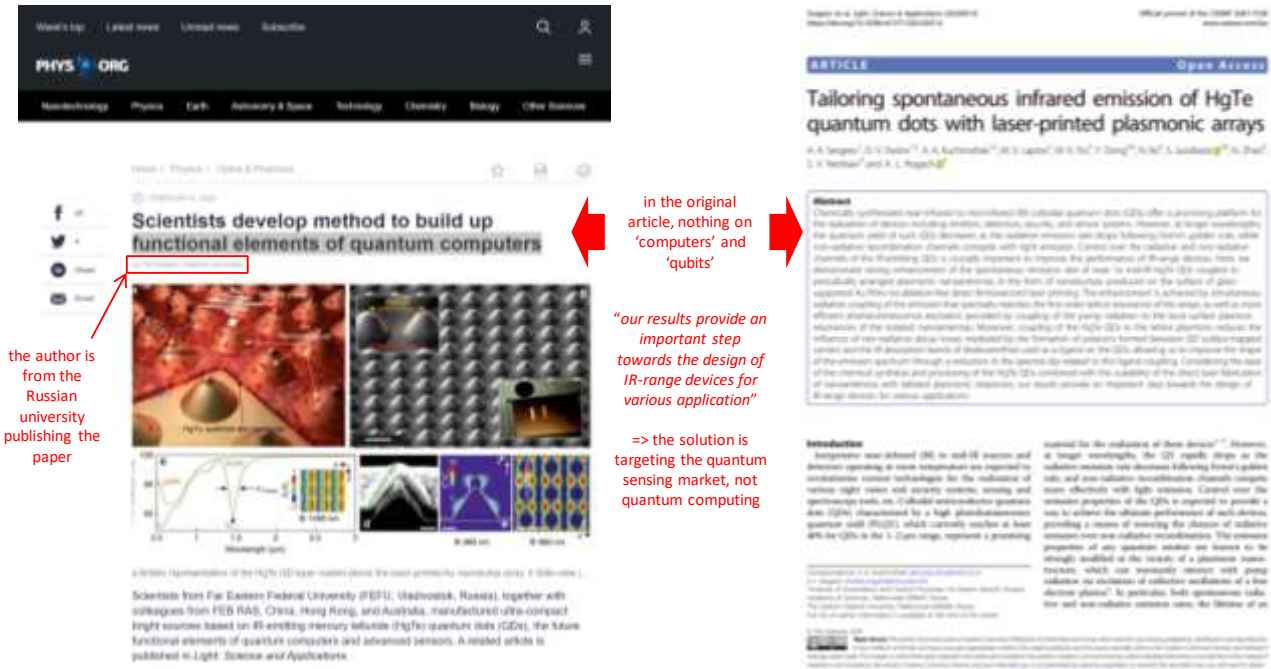
³⁰⁹⁵ See [Fast full-color computational imaging with single-pixel detectors](#) by Stephen Welsh et al, 2013 (7 pages). Also seen in [3D Computational Imaging with Single-Pixel Detectors](#), 2013 (4 pages) which extends this to the capture of 3D objects using four single-pixel sensors. The video projector creates patterns that illuminate the object and alternate with its negative. See finally [Imaging with a small number of photons](#) by Peter Morris et al, 2014 (9 pages) and [Quantum-inspired computational imaging](#), 2019 (9 pages).

³⁰⁹⁶ See [Experimental Microwave Quantum Illumination](#) by S. Barzanjeh, S. Pirandola et al, August 2019.

³⁰⁹⁷ See [Polarization entanglement-enabled quantum holography](#) by Hugo Defienne et al, Nature, 2021 (31 pages).

This kind of technique can be based on the entanglement of photons or of twister pairs of photons in the visible between the two sensors³⁰⁹⁸.

Note that the topic of quantum imaging can sometimes be confusing. This is eloquent with this promotion of a particular type of quantum dot, confused with some fancy quantum computing technique (Figure 720). And here, it was not a problem with some journalist since the "wrong" article comes from the laboratory promoting the research results³⁰⁹⁹.



the author is from the Russian university publishing the paper

in the original article, nothing on 'computers' and 'qubits'

"our results provide an important step towards the design of IR-range devices for various application"

=> the solution is targeting the quantum sensing market, not quantum computing

Figure 720: another example of how some research works gets hype to an incredible extent. Source: [Scientists develop method to build up functional elements of quantum computers](#) by Far Eastern Federal University, February 2020 and [Tailoring spontaneous infrared emission of HgTe quantum dots with laser-printed plasmonic arrays](#) by A. A. Sergeev et al, 2020 (10 pages).

There are many other quantum imaging applications being developed in research labs:

- **Superconducting SNSPD cameras**, the record being a 400,000 pixel camera from NIST with a factor of 400 improvement over the previous state-of-the-art³¹⁰⁰. It can be used for instance in astrophysics.
- **Entanglement based microscopy** with quantum microscopy by coincidence (QMC) which enables super resolution imaging at the Heisenberg limit with better contrast-to-noise ratios (CNRs) than existing wide-field quantum imaging methods³¹⁰¹.
- **Thermal light based quantum sensing** using a sub-threshold diode laser with a spectral density exceeding that of SPDC sources by approximately 10 orders of magnitude³¹⁰².

³⁰⁹⁸ See [An introduction to ghost imaging](#) by Miles John Padgett and Robert W. Boyd, 2017 (11 pages) and [Quantum imaging exploiting twisted photon pairs](#) by Dianzhen Cui et al, June 2022 (6 pages).

³⁰⁹⁹ See [Scientists develop method to build up functional elements of quantum computers](#) by Far Eastern Federal University, February 2020, which refers to [Tailoring spontaneous infrared emission of HgTe quantum dots with laser-printed plasmonic arrays](#) by A.A. Sergeev et al, 2020 (10 pages). Quantum dot seems to be more suited for night vision than for quantum computing. It is not a source of single photons. And the words "computer" and "qubit" are absent in the article.

³¹⁰⁰ See [A superconducting-nanowire single-photon camera with 400.000 pixels](#) by Bakhrom G. Oripov et al, NIST and JPL, June 2023 (19 pages).

³¹⁰¹ See [Quantum Microscopy of Cells at the Heisenberg Limit](#) by Zhe He et al, Nature Communications, April 2023 (8 pages).

³¹⁰² See [Practical Quantum Sensing with Thermal Light](#) by Peng Kian Tan et al, CQT and NUS, March 2023 (5 pages).

- **Super-resolution imaging** using interferometry in the microwave regime for passive remote sensing, like with satellites detecting the soil moisture, ocean salinity and ground temperature³¹⁰³.
- **Light-field microscopy (LFM)** with volumetric information being captured simultaneously with using the position and angular momentum of the light illuminating a scene. It has a depth of field of $\sim 500 \mu\text{m}$, 3 times better than the latest LFM designs or >100 times what can be obtained with conventional microscopes³¹⁰⁴.
- **Underwater LiDAR** using single-photon CMOS detection arrays (SPADs) directly interfaced to a GPU for real-time image reconstruction, but with a range of only 3 meters³¹⁰⁵.

Quantum pressure sensors

Quantum sensing also works with pressure measurement. Most pressure sensors are type I, not using superposition or entanglement features. They are used to measure pressure in specific conditions.

We have for example very thin ultra-high sensitivity pressure sensors used in medical monitoring³¹⁰⁶, for the measurement of low pressures using light interacting with helium gas and pressure dependent refractive index of helium³¹⁰⁷, various optomechanical quantum sensors³¹⁰⁸, high-pressures measurement up to 4 GPa using the shift of the optical spectra of quantum-wells made of III/V GaAs/AlGaAs materials³¹⁰⁹, with quantum dots used to measure pressure in liquids³¹¹⁰, and with using NV, SiV and GeV color centers to measure ultra-high pressure up to 180 GPa^{3111 3112}. These sensors can be placed either in the diamond anvil tip or in nano-diamonds embedded in the analyzed medium³¹¹³.

Quantum radars and LiDARs

Quantum radars are very slowly emerging from research. The idea initially came from Seth Lloyd from the MIT in 2008 when he devised the concept of quantum illumination³¹¹⁴. The idea initially relied on photons in the visible spectrum, and in three different ways:

³¹⁰³ See [Super-Resolution Imaging with Multiparameter Quantum Metrology in Passive Remote Sensing](#) by Emre Köse et al, Universität Tübingen, January 2023 (12 pages).

³¹⁰⁴ See [Quantum correlation light-field microscope with extreme depth of field](#) by Yingwen Zhang et al, December 2022 (14 pages).

³¹⁰⁵ See [Submerged single-photon LiDAR imaging sensor used for real-time 3D scene reconstruction in scattering underwater environments](#) by Aurora Maccarone et al, Optica Express, 2023 (19 pages).

³¹⁰⁶ See [Quantum effect-based flexible and transparent pressure sensors with ultrahigh sensitivity and sensing density](#) by Lan Shi et al, Nature Communications, 2020 (9 pages) that is based on thin films and spin-coating with carbon spheres dispersed in polydimethylsiloxane.

³¹⁰⁷ See [Quantum-Based Photonic Sensors for Pressure, Vacuum, and Temperature Measurements: A Vision of the Future with NIST on a Chip](#) by J Hendricks et al, NIST, 2021 (4 pages).

³¹⁰⁸ See the review paper [Progress of optomechanical micro/nano sensors: a review](#) by Xinmiao Liu et al, Singapore, 2021 (40 pages).

³¹⁰⁹ See [Quantum-well pressure sensors](#) by Witold Trzeciakowski, 1994.

³¹¹⁰ See [Quantum dots to probe temperature and pressure in highly confined liquids](#) by Sayed M. B. Albahrani et al, RSC Advances, 2018 (12 pages).

³¹¹¹ See [Optical properties of SiV and GeV color centers in nanodiamonds under hydrostatic pressures up to 180 GPa](#) by Baptiste Vindolet, Jocelyn Achard, Alexandre Tallaire, Jean-François Roch et al, ENS, September 2022 (7 pages).

³¹¹² See [NV center magnetometry up to 130 GPa as if at ambient pressure](#) by Antoine Hilberer, Jean-François Roch et al, January 2023 (5 pages).

³¹¹³ See [Spectroscopy Study on NV Sensors in Diamond-based High-pressure Devices](#) by Kin On Ho, Jörg Wrachtrup, Sen Yang et al, January 2023 (15 pages).

³¹¹⁴ See [Quantum Radars and Lidars - Concepts, realizations, and perspectives](#) by Gregory Slepyan et al, June 2022 (21 pages) and [Study on Quantum Radar Technology Developments and Design Consideration for its integration](#) by Manoj Mathews, Rowan University in New Jersey, May 2022 (8 pages) are relatively up-to-date theoretical papers on quantum radars.

- The radar emits classical photons in the visible spectrum and receives the photon reflected by the target. This does not work very well because of clouds and light noise surrounding the object.
- Radar emits photons but uses quantum photo-sensitive sensors to improve its performance. It does not work better enough.
- The radar prepares pairs of entangled photons. One is sent to the target and reflected and the other remains in the radar. The reflected photon is compared with the idler one using various techniques (Figure 721 and ref. in Figure 723).

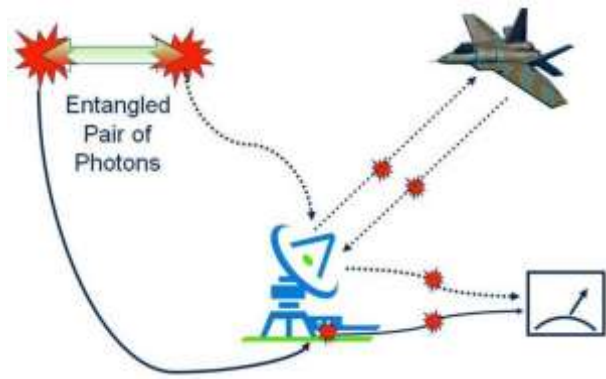


Figure 721: the principle of quantum radar. Source: [Quantum Radar](#) by Marco Lanzagorta, 2012 (141 pages).

As they have a common past, it is possible to sort the photons received by the radar to keep only the photons reflected by the target³¹¹⁵.

It is in fact a variant of the third way which is more seriously studied³¹¹⁶. It consists in converting the photons sent to the target into a radio wave or microwave photon, while preserving their quantum state. A conversion of the same kind takes place for the photon remaining in the radar (Figure 723). This allows the electromagnetic waves to traverse bad weather, which photons in the visible spectrum cannot do. Microwaves could also be directly generated without being converted from visible entangled photons, using for example JPAs (Josephson Parametric Amplifiers) or TWPAs (traveling wave parametric amplifiers).

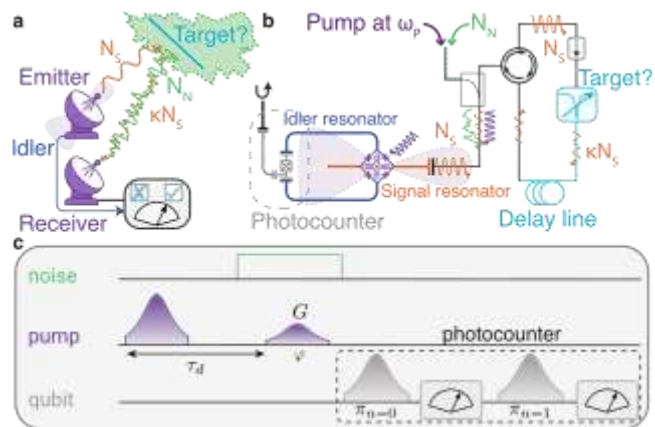


Figure 722: the superconducting circuitry based microwave quantum radar proposed by ENS Lyon, using a delay line. Source: [Quantum Advantage in Microwave Quantum Radar](#) by Réouven Assouly et al, *Nature Physics*, November 2022-June 2023 (13 pages).

This last solution was experimented by a French team from ENS Lyon in 2022/2023, as shown in Figure 722, using direct microwave photon counting and providing a 20% quantum advantage over classical methods³¹¹⁷.

These techniques are expected to improve the accuracy of traditional radars and to improve its resistance to noise, interference and jamming. This kind of radar could theoretically detect stealth aircraft, modulo the fact that their flat reflective surfaces reduce their radar signature whatever the radar frequency³¹¹⁸.

³¹¹⁵ See [Gaussian beam quantum radar protocol](#) by Lorenzo Maccone et al, September 2023 (6 pages).

³¹¹⁶ Another scenario proposes to use microwaves entanglement and a dual-receptor scheme to improve the angular detection of a target, in [Entanglement-assisted multi-aperture pulse-compression radar for angle resolving detection](#) by Bo-Han Wu et al, University of Arizona, Jul 2022 (18 pages).

³¹¹⁷ See [Demonstration of Quantum Advantage in Microwave Quantum Radar](#) by Réouven Assouly, R. Dassonneville, Théau Peronnin, Audrey Bienfait and Benjamin Huard, *Nature Physics*, November 2022-June 2023 (13 pages). It is using two entangled microwave modes with a delay line to detect targets with an improve signal to noise ratio.

³¹¹⁸ See [Can quantum mechanics improve radar technology?](#) by Giacomo Sorelli and Nicolas Treps, November 2020. Which was maybe inspired by [Quantum Flashlight Pierces the Darkness With a Few Percent as Many Photons](#) by Adrian Cho, 2020.

The first concepts saw the light of day in 2015³¹¹⁹.

China is very interested in this technology and is working hard on it to be able to detect American stealth fighters or bombers like the F-22 and B-2.

They announced a successful test of their first quantum radar in 2016, which was to become a prototype in 2018, produced by the government company **China Electronics Technology Group**³¹²⁰, with a range exceeding 100 km. But it is obviously hard to verify their claim.

Other labs and companies are developing such radars, such as the **Institute for Quantum Computing** at the University of Waterloo in Canada³¹²¹. This project is funded by the Canadian Department of Defense for \$2.7M.

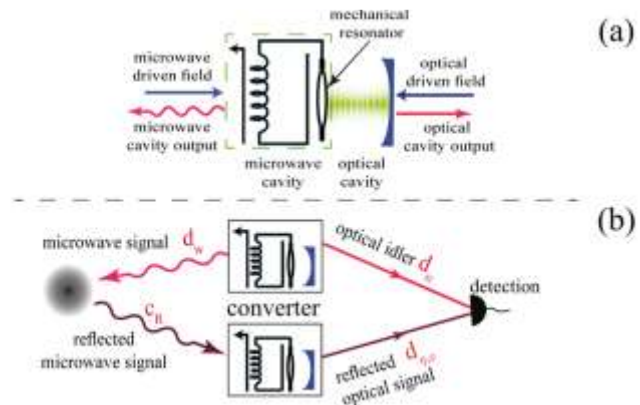


Figure 723: converting radar RF waves to/from photons. Source: the review paper [Advances in Quantum Radar and Quantum LiDAR](#) by Ricardo Gallego Torromé and Shabir Barzanjeh et al, October 2023 (19 pages).

There are also some similar projects in Austria at the Institute of Science and Technology in Klosterneuburg. In the USA, **Lockheed Martin** is also invested in this emerging field. Specialists such as Marco Lanzagorta of the US Naval Research Laboratory believe that QKD satellites launched by the Chinese like Micius would have military applications of this type³¹²². In Europe, the Quantum Flagship **QMICS** is dedicated to creating quantum microwave technologies operating at the single photon level that could help build quantum radars. **Guoyao Quantum Radar Technology** (2017, China) is a startup coming out of Jian-Wei Pan's Hefei's research lab that is developing a quantum radar. It has a related patent³¹²³.

Quantum radars are still very theoretical devices³¹²⁴ that are currently plagued by photon losses, noise and various detection issues, whether they operate in the visible or microwave domains^{3125 3126 3127}.

This technology could however be used in **LiDARs** to verify that the inbound photons correspond to those emitted by its own laser, avoiding unwanted optical interference from other LiDARs and frequently using interferometry³¹²⁸.

³¹¹⁹ See [Focus: Quantum Mechanics Could Improve Radar](#), 2015, [Microwave Quantum Illumination](#) by Shabir Barzanjeh et al, 2015 (5 pages) and [Enhanced Sensitivity of Photodetection via Quantum Illumination](#) by Seth Lloyd, 2018 (4 pages).

³¹²⁰ See [China's claim of developing "quantum radar" for detecting stealth planes: beyond skepticism](#) by Ashish Gupta, 2016 (4 pages) and [The US and China are in a quantum arms race that will transform warfare](#) by Martin Giles, MIT Technology Review, January 2019. Some scientists, "under the radar", find that quantum radars features are overstated.

³¹²¹ See [Quantum radar will expose stealth aircraft](#), April 2018.

³¹²² See [The Future of Quantum Sensing & Communications](#) by Marco Lanzagorta of the US Naval Research Laboratory (USA), September 2018 (37 minutes). He is the author of the book [Quantum Radar](#) by Marco Lanzagorta, 2012 (141 pages) which has been translated into Chinese by China, and officially bought the rights.

³¹²³ See [Atmospheric boundary layer detection method based on hybrid laser radar](#), 2019.

³¹²⁴ Like for example in [Quantum-Enhanced Doppler Radar/Lidar](#) by Maximilian Reichert et al, March 2022 (23 pages).

³¹²⁵ See [Detecting a target with quantum entanglement](#) by Giacomo Sorelli, Nicolas Treps, Frédéric Grosshans and Fabrice Boust, May 2020 (30 pages).

³¹²⁶ See [The short weird life and potential afterlife of quantum radar](#) by Adrian Cho, Science, September 2020.

³¹²⁷ See [Quantum Illumination and Quantum Radar: A Brief Overview](#) by Athena Karsa, Stefano Pirandola et al, October 2023 (13 pages).

³¹²⁸ See [Super-resolution and super-sensitivity of quantum LiDAR with multi-photon state and binary outcome photon counting measurement](#) by Priyanka Sharma et al, September 2023 (21 pages).

Without malicious interference, this will be very useful when many autonomous vehicles equipped with LiDARs will have to coexist on the road³¹²⁹. Quantum LiDARs can also have an improved resolution³¹³⁰ and be used in meteorologic monitoring³¹³¹.

Single-photon LiDARs could be used for remote wind detection at high resolution. It has been developed in China since 2014 and is used in transportable radars, including UAVs^{3132 3133 3134} (Figure 724).



Figure 724: Source: [Single Photon LiDAR](#) by Feihu Xu, June 2019 (25 slides).

European researchers are also working on quantum-enhanced Doppler LiDARs^{3135 3136}. Quantum LiDARs are however limited by their photon sources, thus the proposal for quantum inspired LiDARs which don't have such limitations³¹³⁷. "Quantum inspired" is thus not limited to computing.

In a domain close to radar, **quantum sonar** could also emerge, so to speak. They use photons in the blue-green zone of the visible spectrum and would be usable for navigation in the Arctic Ocean. It would be a kind of quantum LiDAR. These systems could also implement optical communication with submarines via satellite, to replace radio waves that do not penetrate well underwater and are exploitable for very low-speed links.

On the other hand, one day, it may be necessary to find countermeasures against "quantum" coatings that allow the infrared signature of objects to be removed or reduced³¹³⁸.

Quantum technologies can also be used for other tasks like for analyze classical radar data³¹³⁹ or revealing spoofing of classical radars thanks to the analysis of quantum noise³¹⁴⁰.

³¹²⁹ This approach has been studied since at least 2009. See [Quantum Lidar - Remote Sensing at the Ultimate Limit](#), 2009 (97 pages).

³¹³⁰ See [Two-photon interference LiDAR imaging](#) by Robbie Murray and Ashley Lyons, 2022 (7 pages).

³¹³¹ See [Analysis of Observation Performance of a Mobile Coherent Doppler Wind Lidar Using DBS Scanning Mode](#) by Debao Dong et al, Journal of Physics, 2020 (7 pages).

³¹³² See [Single-Photon Lidar for atmospheric detection](#) by Haiyun Xia et al, June 2019 (22 slides).

³¹³³ See [Quantum LiDAR with Frequency Modulated Continuous Wave](#) by Ming-Da Huang et al, China, July 2023 (21 pages).

³¹³⁴ See [Quantum secured LiDAR with Gaussian modulated coherent states](#) by Dong Wang et al, August 2023 (10 pages).

³¹³⁵ See [Quantum-enhanced Doppler lidar](#) by Maximilian Reichert et al, npj Quantum Information, 2022 (9 pages).

³¹³⁶ See [Demonstration of quantum-enhanced range finding robust against classical jamming](#) by Mateusz P. Mrozowski et al, University of Strathclyde, July 2023 (10 pages).

³¹³⁷ See [Compact All-Fiber Quantum-Inspired LiDAR with > 100dB Noise Rejection and Single Photon Sensitivity](#) by Han Liu et al, University of Toronto, July 2023 (10 pages).

³¹³⁸ See [Camouflage made of quantum material could hide you from infrared cameras](#) by Kayla Wiles, December 2019 which refers to [Temperature-independent thermal radiation](#) by Alireza Shahsaf et al, September 2019 (17 pages).

³¹³⁹ See [Synthetic Aperture Radar Image Segmentation with Quantum Annealing](#) by Timothe Presles et al, Thales, May 2023 (13 pages).

³¹⁴⁰ See [Revealing spoofing of classical radar using quantum noise](#) by Jonathan N. Blakely, Shawn D. Pethel and Kurt Jacobs, US Army, July 2023 (24 pages).

Quantum chemical sensors

Quantum sensing is also applicable with chemical sensors used to analyze the chemical composition of various materials and substances. It is commonly used with optical interferometers³¹⁴¹.

Many such solutions could use NV centers, like:

- The detection of paramagnetic species in biological samples using a fiber equipped with an NV center detection probe³¹⁴².
- Concentration sensors using NV center to detect electrochemical signals emerging from an electrolyte solution and using the inhomogeneous dephasing rate of the electron spin of the NV center ($1/T_2^*$) as a signal³¹⁴³. It is still theoretical work.
- Another theoretical NV center sensor, dedicated to the fast, cheap and low error (<1%) detection of the covid virus in biological samples. The NV sensor would be coated with cationic polymers such as polyethyleneimine (PEI), which can form reversible complexes with viral complementary DNA sequences. The detection is fairly indirect. A complicated biological reaction creates a RNA compound which diffuses in the solution, increasing the distance between magnetic molecules and the nanodiamond. The NV centers then senses less magnetic noise and has a longer T_1 time, which turns into a larger fluorescence intensity³¹⁴⁴.
- Various quantum sensing techniques, again, including NV centers, could help detect various breed of organic molecules³¹⁴⁵.

The University of Glasgow has developed and sells under license **IndiPIX**, an improved and simplified ambient temperature mid-wave infrared (MWIR) imager using indium antimonide (InSb) photodiodes on gallium arsenide (GaAs) transistors. It can detect outdoor gas leaks and plumes, mitigating explosion risks and reduce environmental impact³¹⁴⁶.

Ultracold chemical reactions could be used in cold atom sensors to detect very weak signals like in dark matter detection³¹⁴⁷.



Oxford HighQ (2017, UK) is a spin-off from the University of Oxford developing chemical and nanoparticles sensors using optical microcavities.



Entanglement Technologies (2010, USA) is a spin-off of Stanford and Caltech.

³¹⁴¹ See [Quantum Optical Technologies for Metrology, Sensing, and Imaging](#) by Jonathan Dowling, 2014 (20 slides) and [12 pages, Advanced Micro- and Nano-Gas Sensor Technology: A Review](#) by Haleh Nazemi et al, 2019 (23 pages).

³¹⁴² See [Nanodiamonds based optical-fiber quantum probe for magnetic field and biological sensing](#) by Yaofei Chen et al, February 2022 (21 pages).

³¹⁴³ See [Sensing electrochemical signals using a nitrogen-vacancy center in diamond](#) by Hossein T. Dinani et al, February 2021 (17 pages).

³¹⁴⁴ See [SARS-CoV-2 Quantum Sensor Based on Nitrogen-Vacancy Centers in Diamond](#) by Changhao L et al, University of Waterloo and MIT, December 2021 (14 pages).

³¹⁴⁵ See [A molecular approach to quantum sensing](#) by Chung-Jui Yu et al, April 2021 (12 pages).

³¹⁴⁶ See [IndiPIX: Paving the way towards compact, portable, and cost-effective mid-wave infrared systems imaging systems](#), University of Glasgow (7 pages).

³¹⁴⁷ See [Quantum metrology with ultracold chemical reactions](#) by Seong-Ho Shinn et al, August 2022 (28 pages).

It sells the AROMA (Autonomous Rugged Optical Multigas Analyzer) quantum gas detector that uses lasers and optical resonators similar to those used to detect gravitational waves in the LIGO, with a spectroscopy technique (CRDS: Cavity Ring-Down Spectroscopy). It allows the detection of dangerous gases in industry, especially in the extraction of fossil fuels (Figure 725). They were funded by EDF, via their Environmental Defense Fund.



Figure 725: Entanglement Technologies AROMA.

Quantum NEMS and MEMS

Nano or micro electromechanical structures are widely used in long-connected objects, such as accelerometers. They use many quantum phenomena, notably photonics-based, with mechanical resonators whose motion is analyzed by lasers and diodes.



At the heart of a new NIST portable pressure sensor is a dual cavity for laser measurements that is only 2.5 cm long.

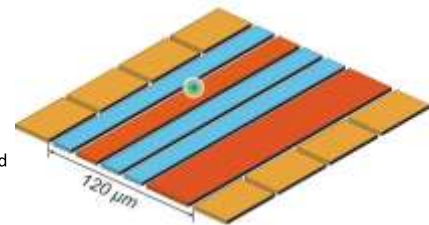
Figure 726: quantum pressure sensors and quantum motion sensors. Sources: [FLOC Takes Flight: First Portable Prototype of Photonic Pressure Sensor](#), February 2019 and [Quantum Information Science & NIST - Advancing QIS Technologies for Economic Impact](#), 2019 (39 slides).

Reversible Quantum Squeezing

NIST

Improving Measurement of Ultrasmall Motions

- 7X more precise than previous methods
- A single magnesium is manipulated in an ion trap made with sapphire base and gold electrodes
- Boost sensitivity in quantum sensors & speed up process for quantum entanglement



<https://www.nist.gov/news-events/news/2019/06/nist-team-supersizes-quantum-squeezing-measure-ultrasmall-motion>

27

They are found in quantum pressure sensors³¹⁴⁸ and motion detectors, both from NIST (in Figure 726³¹⁴⁹). Other sensors are used to detect electrical resistance, temperature, mass and force, vacuum or voltage³¹⁵⁰.

Finally, let's mention the European Quantum Flagship project **macQsimal** (Switzerland, €10.2M) or "Miniature Atomic vapor-Cells Quantum devices for SensIng and Metrology Applications", for the creation of quantum sensors aimed at the market of autonomous vehicle piloting and for medical imaging. This includes the creation of atomic clocks, gyroscopes, magnetometers, imaging systems using microwaves and electromagnetic fields in the tera-Hertz waves as well as gas detectors. In short, a fairly generalist approach. It is based on the use of cold atom vapor integrated in MEMS, a technique that Thales is also using.

³¹⁴⁸ See [FLOC Takes Flight: First Portable Prototype of Photonic Pressure Sensor](#), February 2019.

³¹⁴⁹ See [Quantum Information Science & NIST - Advancing QIS Technologies for Economic Impact](#), 2019 (39 slides).

³¹⁵⁰ See [Quantum electro-mechanics: a new quantum technology](#) by Konrad Lehnert from NIST JILA lab (47 slides), [From micro to nano-optomechanical systems: light interacting with mechanical resonators](#) by Ivan Favero (45 slides) and [Progress of optomechanical micro-nano sensors a review](#), by Xinmiao Liu et al, 2021 (40 pages).

Quantum sensing key takeaways

- Quantum sensing is the most mature and overlooked market of quantum technologies, one potential reason being its fragmentation and currently limited broad scale use cases.
- Quantum sensing enables better precision measurement of nearly any physical parameter: time, distance, temperature, movement, acceleration, pressure and gravity, magnetism, light frequency, radio spectrum and matter chemical composition.
- Quantum sensing has been extensively used to update the new international metric system put in place in 2019.
- Lasers and the frequency combs technique are used to measure time with extreme precision, beyond atomic cesium clocks. It is based on blocked-mode lasers generating very short pulses, aka femtosecond-lasers.
- The most used quantum sensing technology is based on NV centers. It helps measure variations of magnetism and has applications in many domains like in medical imaging and non-destructive control. Indirectly, measuring magnetism can help measure many other physical parameters like temperature and pressure.
- Another one is cold atoms based interferometry that is implemented in micro-gravimeters, accelerometers and inertial sensors. Cold atoms can also be used to analyze the radio frequency spectrum.
- China supposedly built some quantum radars using photons entanglement and up/down converts between visible photons and radar frequencies, but the real performance of these devices is questionable and is driving a lot of skepticism in the Western world. But the related research is still going on and quantum LiDARs seem to make progress.

page intentionally left blank.

page intentionally left blank.

The remainder of “Understanding Quantum Technologies” is in Volume 3.

It contains the following parts: algorithms, software tools, case studies, quantum technologies around the world, corporate adoption, quantum technologies and society, and quantum fake sciences, plus a glossary, table of figures and index for both documents using a continuous pagination numbering.

page intentionally left blank

back cover back page

Le Lab quantique



$|0\rangle$

$|1\rangle$